Spectroscopic Atlas of Atmospheric Microwindows in the Middle Infra-Red

2nd edition

Arndt Meier,
Geoffrey C. Toon, Curtis P. Rinsland,
Aaron Goldman and Frank Hase

IRF Technical Report 048
April 2004

ISSN 0284-1738

INSTITUTET FÖR RYMDFYSIK

Swedish Institute of Space Physics

Kiruna, Sweden

Spectroscopic Atlas of Atmospheric Microwindows in the Middle Infra-Red

2nd revised edition

Arndt Meier[1]
Swedish Institute of Space Physics, Box 812,
SE-981 28 Kiruna, Sweden

Geoffrey C. Toon
JPL Jet Propulsion Laboratory, 4800 Oak Grove Drive,
Pasadena, CA 91109, USA

Curtis P. Rinsland
NASA Langley Research Center, Mail Stop 401a,
Hampton, VA 23681-0001, USA

Aaron Goldman
Department of Physics, University of Denver,
Denver, CO 80208, USA

Frank Hase
Institut für Meteorologie und Klimaforschung,
Forschungszentrum Karlsruhe, PO Box 3640,
D-76021 Karlsruhe, Germany

IRF Technical Report 048
ISSN 0284-1738

Printed in Sweden
Swedish Institute of Space Physics
Kiruna, 2004

[1]Now at Wollongong University and ALS Ltd, Beaconsfield, NSW, Australia. Contact: arndt@uow.edu.au, arndt@apollolifesciences.com

Contents

1 Introduction

This second edition of the infrared microwindow atlas contains a collection of spectral microwindows commonly used or recently suggested for ground-based, high resolution, infrared solar absoption spectroscopy. These solar observations are aimed at quantifying the abundance of trace species in the terrestrial atmosphere. A microwindow is a narrow spectral interval that allows to observe a specific atmospheric absorber unambiguously. The width of a microwindow may vary but is typically between 0.1 and $5cm^{-1}$ wide, though wider windows may in some cases be used or multiple narrow windows may be combined in any particular retrieval.

The spectra and corresponding simulations shown in the figures are representing solar absorption spectra recorded in Arctic Scandinavia on 15/Mar/1997 (500 to $4370cm^{-1}$) and 01/Apr/1998 (3950 to $9000cm^{-1}$). The printed atlas discusses close to 250 microwindows.

Lively discussions at the annual meetings of the infrared working group of the Network for Detection of Stratospheric Change (NDSC) have demonstrated a continued high interest in an up-to-date reference work on commonly used microwindows in the field of infrared ground-based remote sensing. The present work attempts to summarise the collective knowledge that the NDSC community has on this topic. The work of many past and present experts in the field have contributed to this compilation and the authors wish to express their thanks to all of them.

At present, no recommendations on the optimum selection of microwindows for individual species are provided. That task is beyond the scope of the present work and also depends on the observation site and instrumental parameters. However, where inconsistencies between observation and simulations are striking, or in cases where common pitfalls have been reported, we provide comments to highlight potential problems.

Several microwindows have been noted previously in the literature, and we have included a list of references citing their use. We are aware that the current edition is still incomplete, and we encourage our readers to help us fill in the gaps, extend, and improve the atlas.

2 Data description

2.1 Description of the simulated and observed spectra presented

The main purpose of this atlas is to illustrate suitable absorption features for the quantitative analysis of ground-based solar infrared-spectra and to identify all significant, overlapping atmospheric and solar interferences. Thus, the main part of this atlas consists of an extensive set of figures that show the calculated absorptions of different atmospheric and solar species separately as well as an example of a fitted observed spectrum.

A microwindow is a narrow spectral interval, typically about one wavenumber wide, that allows the observation of the atmospheric absorption features of a particular molecular constituent. Ideally, this observation window is free from interferences of either solar or terrestrial origin. However, given that about one million absorption lines are known between 500 and 9000 cm^{-1}, chances are that there will be some interferences. The aim of this atlas is to illustrate the absorptions of any one molecule of interest along with all interfering signals in a particular microwindow under *"typical"* conditions. The experienced researcher may use that information as a base for judging the merits and uncertainties in retrieving total column amounts or volume mixing ratio profiles from any particular microwindow. It is often advisable to retrieve a target molecule by analysing multiple microwindows simultaneously as the combined information can help reduce the uncertainties introduced by interfering molecules significantly – if used skillfully.

The *a–priori* Volume Mixing Ratio (VMR) profiles used in all simulations are based on a Kiruna climatology incorporating several satellite derived monthly mean profiles. Some key parameters are listed in Table 2.1. Pressure and temperature profiles are based on local radio sonde data splined into NCEP data for altitudes above 30km. The supplemental DVD contains the model atmosphere, the a-priori profiles, a description of the underlying climatology data, the linelist and all other software used.

Table 2.2 (page 11) lists the microwindows discussed in the main section, ordered by the targeted absorption species arranged in alphanumerical order. Some details on the spectroscopic properties of the central absorption line of interest are provided. If no single line appears, but instead several features are present in the microwindow, the line position is marked with an asterisk '∗)' and the spectroscopic details given represent the parameters for the strongest line occurring in the target area. Explicit isotopic identifications are listed throughout. This information can be decoded from the index number (see below).

For each entry in Table 2.2 the reader finds a detailed description in the atlas with two figures each. The figures are ordered by wavenumber and the corresponding page is listed in the last column of Table 2.2. The spectroscopic data listed is quoted from the data base used (Appendix E). The index of the species (column 2) can be decoded from Table 2.3 (page 19) and reveals the molecule and its isotopic composition. The absorption strength is listed both in $cm/molec$ (from the spectroscopic linelist) and in effective absorption strength in percent total absorption in the line centre of the observed spectrum. The information content is this observed absorption strength divided by the total rms of the fit we achieved in our example retrieval. These last two numbers may vary considerably with site and observation conditions but are nevertheless a rough guide for a relative comparison of alternative retrieval windows for any one molecule. The temperature sensitivity column lists the change in retrieved Total Column Amount (TCA) for a +1 Kelvin perturbation in the assumed temperature profile in either the troposphere (0-12km) or the stratosphere and above (12-100km). A negative sign indicates that in an assumed warmer atmosphere the resulting TCA is underestimated. The temperatures were modified in the 205 layers FSCATM input temperature profile (*Meier et*

Table 2.1: Some characteristics of the a-priori Volume mixing ratio profiles assumed in the simulations for the contribution plots. The abundances of ClO, C_2H_4, H_2CO and NH_3 have deliberately been chosen higher than observed. These short-lived gases are normally very weak absorbers but can reach quite high levels under certain conditions (presence of polar stratospheric ice clouds, biomass burning, industrial processing, to name but a few). Appendix B presents some striking examples that justify this highlighting.

Molecule	TCA $molec/cm2$	VMR at 1.4km	VMR at 24.5km	Molecule	TCA $molec/cm2$	VMR at 1.4km	VMR at 24.5km
BRNO2	1.607e15	4.95e-13	1.03e-09	H2O	5.467e21	8.65e-04	5.02e-06
C2H2	5.568e15	6.07e-10	7.14e-16	H2O2	2.728e15	2.84e-10	2.79e-12
C2H4	1.899e15	1.46e-10	2.03e-14	H2S	3.027e14	1.50e-11	1.50e-11
C2H6	1.698e16	1.20e-09	1.69e-12	HBR	2.618e13	1.20e-12	1.67e-12
C3H8	9.856e15	6.00e-10	5.47e-12	HCL	2.965e15	1.23e-12	1.60e-09
CCL2F2	1.024e16	5.29e-10	1.69e-10	HCN	3.864e15	1.88e-10	1.21e-10
CCL3F	4.969e15	2.70e-10	3.63e-11	HCOOH	1.224e15	1.17e-10	8.41e-15
CCL4	1.988e15	1.11e-10	1.29e-12	HDO	5.468e21	8.65e-04	5.02e-06
CF4	2.525e15	1.51e-10	7.21e-11	HF	1.162e15	1.05e-12	6.68e-10
CFC113	1.649e13	8.81e-13	2.29e-13	HI	6.053e13	3.00e-12	3.00e-12
CH3BR	1.576e14	9.00e-12	8.39e-13	HNO3	1.838e16	2.78e-11	8.19e-09
CH3CCL3	1.491e15	8.00e-11	8.41e-12	HO2	1.102e14	6.48e-12	9.86e-12
CH3CL	1.058e16	6.04e-10	2.80e-11	HO2NO2	1.707e14	2.32e-12	1.18e-11
CH3D	3.292e19	1.80e-06	8.25e-07	HOCL	5.053e13	2.78e-13	1.94e-11
CH3F	7.500e12	4.00e-13	1.03e-13	HONO	6.291e12	4.04e-13	1.06e-12
CH3I	5.254e13	3.00e-12	2.80e-13	N2	1.576e25	7.81e-01	7.81e-01
CH4	3.292e19	1.80e-06	8.25e-07	N2O	5.992e18	3.14e-07	1.19e-07
CHCL2F	2.753e14	1.47e-11	6.74e-12	N2O5	5.653e13	3.51e-16	7.90e-11
CHF2CL	3.167e15	1.74e-10	6.11e-11	NH3	4.066e14	4.40e-11	1.17e-15
CLO	2.818e14	5.00e-15	2.17e-10	NO	2.232e15	9.56e-12	1.20e-09
CLONO2	1.887e15	1.03e-14	1.21e-09	NO2	3.485e15	1.75e-11	2.98e-09
CO	2.274e18	1.83e-07	1.37e-08	O2	4.090e24	2.03e-01	2.03e-01
CO2	7.420e21	3.69e-04	3.60e-04	O3	1.006e19	3.62e-08	3.80e-06
COCL2	4.179e14	2.24e-11	2.35e-12	O3667	1.082e19	3.62e-08	3.80e-06
COCLF	7.267e13	2.40e-13	3.19e-11	O3668	1.085e19	3.62e-08	3.80e-06
COF2	3.009e14	5.24e-13	2.08e-10	O3676	1.061e19	3.62e-08	3.80e-06
F134A	1.809e14	9.55e-12	5.38e-12	O3686	1.062e19	3.62e-08	3.80e-06
F141B	2.097e14	1.11e-11	6.24e-12	OCLO	2.018e13	1.00e-12	1.00e-12
F142B	2.016e14	1.07e-11	6.00e-12	OCS	8.370e15	4.31e-10	9.94e-12
H217O	5.467e21	8.65e-04	5.02e-06	OH	3.415e13	5.00e-14	1.18e-12
H218O	5.467e21	8.65e-04	5.02e-06	SF6	1.023e14	5.33e-12	3.16e-12
H2CO	5.000e15	4.37e-10	2.53e-11	SO2	4.792e15	2.91e-10	3.13e-11

al, 2003 & 2004); i.e. **before** the raytracing calculation was performed.

The first figure of each pair of figures is termed the contribution plot. It shows the contribution that each individual molecule makes to the total signal and compares the resulting sum with the observed spectrum. For the creation of the single species simulations an improved version of the simul109f code (see below) was used. The calculated absorptions represent the total column amounts according to the *a-priori* VMR profiles used and are uncertain by several percent. Wherever possible, the *a-priori* VMR–profile is scaled to match a total column amount known from previous analysis. However, for weak absorbers that we could not quantify reliably, like SO_2, CH_2O, SO_2, ClO, etc, the uncertainties are much larger.

There is to date no comprehensive treatment of solar interferences available for standard analysis software. To start with, there is no equivalent to the HITRAN linelist available for solar absorbers. Three strategies often employed are either to deweight all intervals featuring solar interferences, to subtract a matching extra-terrestrial solar spectrum, or to simulate the solar interferences in a separate module of the retrieval code. SFIT, for example, provides a simplified model based on the Mineart formulae for solar CO interferences. The elegant alternative of using an extra-terrestrial solar spectrum, or at least a very high altitude solar spectrum, is available to only a few instruments (ATMOS space mission, balloon instruments). Possible are also combinations of these approaches.

Appendix C takes a more in-depth view at simulating solar lines and describes the solar spectra and simulations used in this work. Whichever way you choose to tackle the solar interference problem, it is very useful to know whether a microwindow contains solar lines and of what nature these interferences are. Hence, each plot shows the solar component based on observed spectra as well as the often humble attempts of simulating them. The solar spectrum shown may be of different origin depending on the (limited) availability of observed solar spectra as indicated in the plots and tables:

Solar(A) ATMOS spectrum observed from space in 1989 (average over 20 spectra prepared by Kurucz). and available for the spectral interval 631 to $4700 cm^{-1}$.

Solar(D) Denver University solar OH simulations used for the spectral interval 500 to $631 cm^{-1}$

Solar(G) GGG/GFIT simulations based on ATMOS space & MK-IV balloon FTIR derived pseudolines and used for the spectral intervals 4700 to 6420 and 7584 to $8200 cm^{-1}$.

Solar(N) NOAO observations from the Kitt Peak observatory and used for the spectral intervals 6420 to 7584 and 8200 to $9000 cm^{-1}$.

The electronic supplement contains additional solar spectra including ATMOS spectra from 1994, the new solar simulations by Frank Hase, and the solar spectra based on the Minneart formulae. A number of solar features can be identified with the help of the solar atlas by *Geller* (1992). The simulated solar spectrum "Solar-sim" shown throughout the plots was created with the solar simulation model from the SFIT and simul109 packages using a combination of solar CO lines from the Minneart formulae, the (renormalised) solar OH linelist from the University of Denver and a number of pseudo-lines from Arndt Meier (derived from ATMOS observations). For details see Appendix C.

The second figure for each microwindow gives an example of a simulated spectrum fitted to the recorded spectrum as obtained with the SFIT2 algorithm (e.g. *Connor et al.,* 1998; *Rinsland et al.,* 2003; *Pougatchev et al.,* 1995). The lower part shows the observed spectrum *(solid line)* and the simulated spectrum *(dashed line, shifted vertically for clarity)*, while the upper part of the figure shows the residuals *(recorded minus simulated spectrum)*. Below the second figure there is a short table that describes the spectrum and the retrieval results. All species that have absorption lines in the spectral interval shown in the corresponding contribution plot are listed in the order of descending absorption strength.

The spectra presented in the main section of the atlas were recorded in Arctic Scandinavia at zenith angles close to 70^o. The instrument used is a commercial BRUKER 120-HR FTS and is located in Kiruna in northern Sweden (67.84^oN, 20.41^oE, 419 m above median sea level). It is operated by the *Institutet för Rymdfysik* (Swedish Institute for Space Physics) in cooperation with the *Forschungszentrum Karlsruhe* and the *University of Nagoya*. Note that typical spectra from a high altitude, a tropical, or a southern hemisphere site may look quite different. See Appendix A to get some ideas.

The middle infrared section features spectra recorded on 15/Mar/1997 with an optical resolution of $0.0035cm^{-1}$, (corresponding to $257.14cm$ maximum optical path difference or OPD) and using a boxcar apodisation function. The near infrared spectra were recorded on the 01/Apr/1998 at a resolution of $0.0075cm^{-1}$ ($120cm$ OPD) again using boxcar apodisation. The simulations shown in the main section of the atlas were carried out for a maximum optical path difference (OPD) of $257.14cm$ (middle–IR) and $120.0cm^{-1}$ (near–IR), a field of view between 1.91 and $4.06mrad$, and a perfect instrumental line shape (ILS) with boxcar apodisation, hence matching the observation conditions closely.

The spectroscopic data base used for the simulations is an updated and extended linelist based on the HITRAN 2000 linelist (*Rothman et al.,* 2003) with a number of updates and additions taken from various sources. For details see Appendix F. Please note that although considerable efforts were made to compile the best linelist available, it is definitely short of perfect.

The software employed to calculate the simulations is an extended and customised version of the Langley Spectral Simulation Code Sim109f that we refer to as sim109g-atlas. It incorporates numerous improvements adapted from the SFIT2 version 3.81 and a number of additions to its capabilities, simulation products and user interface (A. Meier, unpublished, 2003). All software used is available on the supplemental DVD as Windows or OS/2 executables. The source code is available on request from the main editor (for some 3rd party modules restrictions may apply).

The observed and simulated spectra in the electronic supplement are provided primarily in the Bruker OPUS-IR^{TM} data format. Dr Axel Keens from Bruker Optik GmbH, Rudolf-Plank-Str. 27, D-76275 Ettlingen, Germany, kindly provided permission to distribute their free viewer program for Microsoft Windows^{TM} operating systems. The copy included on the DVD is dated Aug 2003. Please check http://www.brukeroptics.com/downloads/index.html for the most recent version. Additionally, the electronic supplement contains spectra in the Bomem GRAMS^{TM} and the SFIT binary formats. The former may be viewed with either the Bruker viewer (provided) or with a native Bomem software (not provided). The SFIT spectra may be viewed with the somewhat antiquated DOS^{TM} program *'Specview'* (by A. Meier) included in the supplement. The *'Specview'* and *'Pbpview'* software are presently undergoing a major re-design and should become available soon as a modern cross-platform application.

All figures are plotted with the GNUPLOT V3.81 software (http://www.gnuplot.info, http://www.sci.muni.cz/m̃ikulik/gnuplot/)) and preparation of the plots is carried out with programs from the *'SFIT-Tools'* created by one of us (*A. Meier*). A subset of 60 microwindows had been published earlier in a similar form by *Meier* (1997) and additional details on the data preparation and software is found in that reference. The text and final layout was created with the free software LATEXin its VTex/2 distribution for OS/2 (MicroPress Inc.).

2.2 Overview over the microwindows studied

Table 2.2: *This table lists all 371 absorption lines that are discussed and illustrated in the main section of this work. The investigated species is listed in alphanumerical order in the first column followed by the molecular index that details its isotopic composition (see Table 2.3, page 19). ν_0 is the central line position. If multiple lines are present, the line position is marked with an asterisk '*)' and the line given represents the strongest line occurring in the targeted interval. The absorption strength is listed both in cm/molec at 296 K (quoted from the spectroscopic linelist) and in effective absorption strength in percent total absorption in the line centre (derived from the example observed Kiruna spectrum). The information content 'Info Cont.' is this observed absorption strength divided by the total rms of the fit we achieved in our example retrieval. These last two numbers may vary considerably with site and observation conditions. E''_{LST} is the lower state energy. The temperature sensitivity column 'T-depen' lists the change in retrieved Total Column Amount (TCA) for an increase of 1 Kelvin in the assumed temperature profile in either the troposphere (0-12km) or the stratosphere and above (12-100km). A negative sign indicates that the TCA retrieved decreases with a 1K increase in temperature. Note that the lower state energy allows to calculate the* theoretical *temperature dependency of the target line, while the 'T-depen' columns list the* observed *temperature dependency for a specific Kiruna spectrum; i.e. the latter include the effects from interfering lines. Detailed figures and additional information for each entry are found on the page given in the last column.*

chemical species	molec index	ν_0 in cm^{-1}	absorption strength $cm/molec$	%	Info Cont.	E''_{LST} cm^{-1}	T-depen [%/K] trop	strat	pa-ge
$BrNO_2$	641	787.1636*)	2.23e-22	1.6	5.4	88.2	+.019	-.241	41
$BrNO_2$	642	787.1769*)	2.25e-22	1.6	5.4	88.2	+.019	-.241	41
C_2H_2	401	766.7241	4.31e-19	4.8	14.3	282.3	-.874	+.022	27
C_2H_2	401	776.0810	2.67e-19	1.9	8.0	446.9	-.773	+.069	33
C_2H_2	401	3250.6624	2.02e-19	2.5	33.9	214.1	-.270	-.002	401
C_2H_2	401	3304.9655	2.46e-19	3.0	41.0	105.9	-1.14	-1.50	411
C_2H_4	391	941.8478	3.44e-20	<0.1	0.3	135.9	n.a.	n.a.	81
C_2H_4	391	947.1985	3.20e-20	<0.1	0.3	358.1	n.a.	n.a.	83
C_2H_4	391	950.0562	8.07e-20	<0.1	0.5	98.1	+1.59	+.203	85
C_2H_4	391	950.6498	7.08e-20	0.1	0.8	64.7	+1.59	+.203	85
C_2H_6	381	2976.7919*)	6.64e-21	17.2	150.5	121.5	+.221	-.025	367
C_2H_6	381	2983.3760*)	1.94e-20	26.8	224.4	105.4	+.040	+.012	369
C_2H_6	381	2986.7230*)	3.21e-20	25.4	133.4	87.5	+.338	-.027	371
CCl_2F_2	320	923.0600*)	2.44e-20	18.7	103.7	492.0	+.561	+.163	67
CCl_2F_2	320	1161.0400*)	6.27e-20	35.6	142.3	178.0	+.096	+.008	143
CCl_3F	330	846.0500*)	2.30e-20	8.0	20.8	505.0	+1.01	+.149	59
CCl_3F	330	846.9600*)	2.26e-20	8.0	20.8	468.0	+1.01	+.149	59
CCl_3F	330	848.9000*)	2.37e-20	8.0	20.8	388.0	+1.01	+.149	59
CCl_3F	330	850.0200*)	2.27e-20	8.0	20.8	374.0	+1.01	+.149	59
CF_4	310	1285.0350*)	1.67e-19	3.8	7.2	160.0	-2.17	-.529	175
CF_4	310	1285.3375*)	1.78e-19	3.8	7.2	215.0	-2.17	-.529	175
CF_4	310	1285.1075*)	1.04e-19	3.8	7.2	166.0	-2.17	-.529	175
CH_4	61	1202.4210	1.04e-21	39.4	264.7	1096.1	-2.23	-.314	153
CH_4	61	1204.0328	5.30e-22	26.1	212.8	1251.6	-2.55	-.268	155
CH_4	61	2600.2726	3.45e-22	35.1	175.0	219.9	-.194	-.028	291
CH_4	61	2651.0331	1.67e-22	25.2	237.2	31.4	+.405	+.035	299

chemical species	molec index	ν_0 in cm^{-1}	absorption strength $cm/molec$	%	Info Cont.	E''_{LST} cm^{-1}	T-depen [%/K] trop	strat	pa-ge
CH_4	61	2657.7116	1.54e-22	20.6	176.9	104.8	+.144	+.029	301
CH_4	61	2742.7428	2.35e-21	95.6	607.2	219.9	-.029	-.020	307
CH_4	61	2761.3523	1.82e-23	52.4	377.0	689.9	-.057	-.006	311
CH_4	61	2778.6428	5.22e-22	47.1	409.7	219.9	-.026	-.020	319
CH_4	61	2819.8338	6.10e-22	69.3	486.6	10.5	+.209	+.041	327
CH_4	61	2835.6763	1.89e-22	25.0	342.5	62.9	+.385	+.034	333
CH_4	61	2855.6328	6.88e-23	9.7	97.7	62.9	-.112	+.161	337
CH_4	61	2859.9876	8.71e-23	11.7	143.9	104.8	+.241	+.022	339
CH_4	61	2898.6953	9.77e-22	78.7	1051.6	157.1	+.214	+.003	349
CH_4	61	2903.8757	6.01e-22	54.6	734.4	219.9	-.087	-.019	351
CH_4	61	2923.6880	1.61e-22	14.1	198.7	293.2	-.582	+.086	357
CH_4	61	2941.4116	2.24e-22	17.7	128.7	470.9	-1.52	-.212	365
CH_4	61	4126.6561	1.50e-22	23.4	224.6	104.8	+.248	+.027	423
CH_4	61	4126.6724	7.04e-23	18.5	178.4	104.8	+.248	+.027	423
CH_4	61	4265.4212	4.95e-22	51.8	376.1	157.1	+.004	-.001	431
CH_4	61	4277.8105	3.29e-22	30.3	241.8	293.2	-.204	-.036	435
CH_4	61	4285.1555	2.77e-22	31.4	185.8	62.9	+.157	+.226	437
CH_4	61	4296.1496	2.59e-22	35.2	136.3	31.4	+.275	+.016	439
CH_4	61	5829.8684	2.76e-22	31.9	111.3	10.5	+.552	+.076	479
CH_4	61	5907.9194	5.51e-23	5.8	48.1	104.7	+.188	+.046	481
CH_4	61	5910.1250	1.30e-22	11.1	75.1	293.1	-.151	-.044	483
CH_4	61	5983.1942	2.72e-22	39.9	222.8	31.4	+.449	+.057	485
CH_4	61	6055.5279	3.04e-23	3.7	33.1	62.7	+.096	+.083	489
CH_4	61	6105.6261	3.41e-22	42.7	270.5	470.7	-.579	-.133	499
CH_4	62	1231.4358	7.28e-23	11.0	87.8	575.3	-.733	-.068	163
CH_4	62	1234.2262	1.82e-22	17.1	108.1	575.2	-1.05	-.129	167
CH_4	62	1234.2262	1.82e-22	17.1	142.0	575.3	-.957	-.133	169
CH_4	62	2924.8235	1.82e-23	3.7	59.5	157.1	-.358	+.076	359
CH_4	63	1199.4936	8.06e-24	1.4	4.3	116.4	-.107	-.101	151
CH_4	63	1199.9945	6.28e-24	1.5	4.6	251.3	-.107	-.101	151
CH_4	63	1204.3278	9.99e-24	2.0	16.5	328.2	-.623	-.462	155
CH_4	63	3061.4140	5.09e-23	5.6	62.1	89.9	-.069	+.029	387
CHF_2Cl	420	829.0551$^{*)}$	4.90e-20	3.8	13.8	169.0	+.004	-.006	49
ClO	181	830.6077	2.43e-21	<0.1	<0.5	72.5	N.A.	N.A.	51
ClO	181	833.2974	2.23e-21	<0.1	<0.5	47.7	N.A.	N.A.	53
ClO	181	834.6249	2.07e-21	<0.1	<0.5	37.2	N.A.	N.A.	55
$ClONO_2$	270	780.2200$^{*)}$	1.48e-20	4.1	14.3	164.2	+.066	+.435	35
CO	51	2111.5430	3.72e-19	100.0	220.8	138.4	+.606	+.106	207
CO	51	2111.5430	3.72e-19	100.0	220.8	138.4	+.606	+.106	207
CO	51	2158.2997	3.34e-19	99.8	571.8	23.1	+.128	-.047	217
CO	51	4274.7407	2.65e-21	20.0	129.9	23.1	+.135	+.016	433
CO	51	4285.0089	3.57e-21	23.7	140.5	80.7	+.508	+.080	437
CO	52	2057.8575	3.49e-21	17.8	96.0	202.1	-.425	-.249	203
CO	52	2069.6559	3.98e-21	32.6	172.3	102.9	+.135	+.064	205
CO_2	21	927.0083	5.22e-24	15.2	92.8	1966.2	-3.76	-1.10	69
CO_2	21	932.9604	9.91e-24	31.7	189.8	1800.1	-3.83	-1.03	73
CO_2	21	934.8945	1.18e-23	37.8	223.3	1751.0	-3.79	-.976	75
CO_2	21	936.8038	1.38e-23	44.6	284.1	1704.9	-3.71	-.928	77
CO_2	21	938.6882	1.58e-23	49.7	271.4	1662.0	-3.59	-.928	79
CO_2	21	942.3833	1.95e-23	62.5	390.9	1585.6	-3.47	-.849	81
CO_2	21	967.7075	1.79e-23	63.3	380.1	1416.3	-3.05	-.726	93

chemical species	molec index	ν_0 in cm^{-1}	absorption strength $cm/molec$	%	Info Cont.	E''_{LST} cm^{-1}	T-depen [%/K] trop	strat	pa-ge
CO_2	21	3161.6919	3.04e-25	8.6	111.5	273.9	-.361	-.052	389
CO_2	21	3204.7604	5.09e-25	13.8	194.6	316.8	-.439	-.093	395
CO_2	21	3315.7946	1.72e-24	37.6	440.2	362.8	-.591	-.148	417
CO_2	21	4887.6649	1.49e-23	95.6	373.5	994.2	-1.85	-.491	461
CO_2	21	4890.8190	5.13e-24	27.1	116.8	1244.2	-2.24	-.545	463
CO_2	21	4919.7575	3.37e-24	16.2	74.7	1559.4	-2.64	-.867	473
CO_2	21	6072.8428	7.41e-25	15.7	142.0	7.8	+.331	+.073	491
CO_2	21	6085.8833	1.98e-24	38.0	325.8	60.9	+.256	+.034	493
CO_2	21	6098.7790	1.20e-24	16.4	124.3	362.8	-.484	-.120	495
CO_2	21	6191.1724	3.23e-24	32.9	290.8	639.6	-1.01	-.295	501
CO_2	21	6254.6668	3.01e-24	27.4	201.8	704.3	-1.23	-.297	503
CO_2	21	6483.1375	1.38e-24	27.6	212.8	234.1	-.139	-.056	505
CO_2	21	6495.0753	1.52e-24	35.0	247.9	42.9	+.319	+.049	507
CO_2	22	4885.8159	2.02e-24	51.9	248.7	2.3	+.096	+.272	455
CO_2	22	4891.1846	4.92e-24	84.9	365.5	7.8	+.176	+.140	463
CO_2	22	4891.1846	4.92e-24	84.9	399.9	7.8	+.547	+.113	465
CO_2	22	4892.6575	6.61e-24	92.5	312.6	16.4	+.270	+.088	467
CO_2	22	4902.2035	9.74e-24	96.7	341.4	163.9	+.044	-.015	469
CO_2	22	4911.4478	3.09e-24	47.5	142.0	519.6	-.777	-.203	471
CO_2	23	2481.0844	1.74e-25	5.3	67.2	278.3	-1.17	-.787	253
CO_2	23	2481.0844	1.74e-25	5.8	48.6	278.3	-.084	-.058	255
CO_2	23	2486.1479	2.35e-25	7.6	53.9	154.6	-.950	-.699	257
CO_2	23	2487.5988	2.43e-25	9.9	12.2	125.9	-.897	-.605	259
CO_2	23	2489.0517	2.44e-25	9.3	159.7	100.1	-.152	+.035	261
CO_2	23	2489.7790	2.42e-25	10.0	174.4	88.3	-.152	+.035	261
CO_2	23	2492.6940	2.16e-25	9.5	166.7	48.6	+.074	-.084	263
CO_2	23	2517.1010	2.43e-25	9.5	221.1	170.1	-.032	-.017	265
CO_2	23	2523.0910	1.61e-25	5.4	95.2	320.2	-.662	-.109	269
CO_2	23	2523.8405	1.49e-25	4.9	95.2	342.3	-.662	-.109	269
CO_2	23	2626.6296	4.31e-25	17.1	155.0	100.1	+.098	+.007	297
CO_2	23	4879.8823	1.31e-24	24.8	114.6	342.3	-.576	-.207	451
CO_2	23	4883.5550	1.71e-24	40.3	146.4	258.4	-.339	-.070	453
CO_2	23	4886.2409	1.98e-24	47.5	196.0	203.2	-.236	+.004	457
CO_2	23	4887.1232	2.06e-24	49.6	254.0	186.3	+.060	-.012	459
CO_2	23	4890.5864	2.27e-24	56.2	242.0	125.9	+.001	+.157	463
CO_2	23	4891.4358	2.28e-24	59.3	279.1	112.7	-1.14	-.466	465
CO_2	23	4892.2786	2.28e-24	56.8	192.0	100.1	+.183	+.050	467
CO_2	23	4902.6309	6.83e-25	24.4	86.1	4.4	+.373	+.066	469
CO_2	23	4911.1863	1.84e-24	52.8	157.8	26.5	+.377	+.082	471
CO_2	23	4919.9492	2.14e-24	52.7	243.1	186.3	+.132	+.022	473
CO_2	23	4922.2122	1.76e-24	42.5	155.5	258.4	-.162	-.001	475
CO_2	24	4920.1675	3.52e-25	12.3	56.9	209.0	-.503	-.054	473
CO_2	24	4921.9862	3.80e-25	14.7	53.6	174.9	-.214	-.002	475
COF_2	361	1230.9436*)	2.58e-20	0.3	2.7	171.7	-.031	-.437	165
COF_2	361	1233.9731*)	3.13e-20	0.5	4.3	102.8	-.254	-.451	169
COF_2	361	1234.4356*)	2.79e-20	0.5	4.0	92.5	-.254	-.451	169
COF_2	361	1951.5865*)	3.62e-20	0.9	7.7	63.4	-.019	-.082	187
COF_2	361	1951.9479*)	3.70e-20	0.8	6.9	70.6	-.019	-.082	187
COF_2	361	1952.6658*)	3.79e-20	0.9	8.9	86.3	-.022	-.317	189
H_2CO	201	2759.8456	4.23e-20	0.5	4.1	120.9	-.758	+.423	309
H_2CO	201	2761.1500	4.48e-20	0.7	4.9	113.7	-.770	+4.10	311
H_2CO	201	2761.4941	4.19e-20	1.4	10.2	161.2	-.770	+4.10	311

chemical species	molec index	ν_0 in cm^{-1}	absorption strength $cm/molec$	%	Info Cont.	E''_{LST} cm^{-1}	T-depen [%/K] trop	strat	pa-ge
H_2CO	201	2763.4963	4.44e-20	0.3	3.7	92.6	-.028	-.289	313
H_2CO	201	2765.8454	4.23e-20	0.1	1.1	73.8	-.940	-.147	315
H_2CO	201	2778.5112	5.40e-20	1.5	12.8	240.8	-1.61	-.361	319
H_2CO	201	2780.9519	1.21e-20	1.0	8.0	329.0	-1.70	+.332	321
H_2CO	201	2869.8555	4.28e-20	0.3	4.7	190.8	-.225	+.060	341
H_2CO	201	2869.8895	2.84e-20	0.2	3.4	92.6	-.225	+.060	341
H_2O	11	825.1627	6.58e-24	35.9	135.6	586.5	-.808	+.003	47
H_2O	11	841.9028	2.45e-24	12.4	38.2	552.9	-.822	-.002	57
H_2O	11	849.5795	2.48e-23	66.6	213.5	1293.0	-2.26	-.007	61
H_2O	11	948.2629	1.80e-23	50.8	299.7	1327.1	-2.32	-.007	83
H_2O	11	953.3674	4.80e-24	18.0	108.0	1962.5	-3.25	-.003	89
H_2O	11	1959.6324	6.21e-24	29.3	135.2	446.5	-.599	+.128	191
H_2O	11	2144.8085	6.70e-24	13.5	55.2	1742.3	-1.53	-.005	209
H_2O	11	2819.4470	6.38e-24	24.3	170.4	782.4	-1.38	-.019	327
H_2O	11	2930.6506	6.74e-24	25.8	107.8	1255.9	-2.37	-.014	363
H_2O	11	3061.2280	1.94e-23	62.3	333.5	1201.9	-2.22	-.015	385
H_2O	11	3163.8269	1.78e-23	78.7	171.0	136.2	-.146	-.009	391
H_2O	11	3164.1851	1.06e-23	51.4	111.5	709.6	-.146	-.009	391
H_2O	11	3189.8770	1.77e-24	6.7	56.8	1059.6	-1.95	-.018	393
H_2O	11	3249.4719	1.58e-23	52.1	403.2	982.9	-1.77	-.013	399
H_2O	11	3315.0430	1.40e-23	28.0	172.9	1477.3	-2.92	-.015	415
H_2O	11	4169.0640	1.06e-24	5.2	67.9	508.8	-.920	-.020	429
H_2O	11	4556.5540	3.77e-24	33.2	138.5	300.4	-.090	-.030	441
H_2O	11	4598.7110	3.69e-24	38.4	192.1	222.1	+.180	-.040	443
H_2O	11	4699.7500	6.47e-24	56.9	251.5	23.8	+.542	-.017	445
H_2O	11	5652.5550	2.95e-24	24.8	46.6	224.8	+.347	+.044	477
H_2O	11	6011.4866	6.14e-25	7.8	36.1	586.2	-1.13	-.013	487
H_2O	11	6099.2974	4.91e-25	5.5	34.9	136.8	+.056	-.008	497
H_2O	11	6700.0889	1.13e-23	67.1	216.4	300.4	-.118	-.020	509
H_2O	12	787.6918	3.15e-25	1.7	7.0	1074.8	-2.01	+.163	43
H_2O	12	1205.0796	8.88e-25	2.9	27.4	1279.8	-3.42	-.118	157
H_2O	12	3019.8270	1.58e-24	9.7	53.7	445.3	-.868	+.026	373
H_2O	12	3165.1010	2.79e-24	25.0	54.2	23.8	+.482	-.034	391
H_2O	12	3205.4120	2.01e-24	16.0	165.5	172.9	+.222	-.006	397
H_2O	12	3299.3070	1.29e-24	8.8	122.2	79.0	+.024	+.019	407
H_2O	13	3249.9380	1.96e-25	1.6	12.7	224.3	+.213	-.004	399
HCl	151	2727.7819	1.12e-19	5.6	65.0	583.0	-.052	-1.22	305
HCl	151	2775.7612	2.88e-19	17.8	185.7	312.7	-.060	-.617	317
HCl	151	2821.5684	4.16e-19	27.6	251.2	125.2	+.035	+.017	331
HCl	151	2843.6243	3.69e-19	27.9	264.0	62.6	-.050	+.169	335
HCl	151	2925.8967	4.19e-19	31.1	355.9	20.9	-.025	+.303	361
HCl	152	2819.5605	1.33e-19	9.6	123.8	125.0	-.029	-.077	329
HCl	152	2904.1110	7.55e-20	6.8	92.1	0.0	-.119	+.320	351
HCl	152	2923.7322	1.34e-19	11.3	159.3	20.8	-.933	-.095	357
HCN	281	3268.2229	2.08e-19	1.3	20.3	310.3	-.537	-.122	403
HCN	281	3287.2483	3.23e-19	3.0	48.6	106.4	-.216	+.005	405
HCN	281	3299.5273	2.35e-19	2.0	34.6	29.6	-.278	+.055	409
HCN	281	3305.5440	1.30e-19	1.0	17.9	8.9	-1.38	+.167	413
$HCOOH$	461	1104.9481*)	7.90e-21	0.7	3.5	24.4	+.317	-.096	137
$HCOOH$	461	1105.0248*)	9.89e-21	0.9	4.2	42.9	+.317	-.096	137
$HCOOH$	461	1105.0691*)	5.66e-21	0.6	3.0	129.0	+.317	-.096	137

chemical species	molec index	ν_0 in cm^{-1}	absorption strength $cm/molec$	%	Info Cont.	E''_{LST} cm^{-1}	T-depen [%/K] trop	strat	pa-ge
HDO	491	1193.5135	5.70e-21	23.6	237.9	872.8	-1.62	+.004	149
HDO	491	1206.0199	3.07e-24	29.0	152.8	709.2	-1.06	-.016	159
HDO	491	1324.8088	1.22e-23	49.8	49.5	265.2	-.079	+.054	177
HDO	491	2612.5400	3.34e-24	13.9	106.6	490.4	-.847	-.023	293
HDO	491	2621.7310	5.33e-24	22.8	162.4	403.1	-.476	-.002	295
HDO	491	2622.1060	5.47e-24	23.2	165.3	362.5	-.476	-.002	295
HDO	491	2657.3300	5.38e-24	22.7	194.8	221.8	-.111	+.017	301
HDO	491	2660.5120	5.47e-24	24.7	222.1	217.0	+.066	-.005	303
HDO	491	2855.8740	8.78e-25	5.5	51.7	116.5	-.610	+.019	337
HDO	491	2855.9300	7.45e-25	5.5	55.4	743.1	-.610	+.019	337
HDO	491	4130.3200	5.46e-25	2.1	24.2	15.5	-.422	-.094	425
HDO	491	4144.4940	7.28e-25	4.3	68.3	46.2	+.073	-.034	427
HF	141	4038.9625	2.37e-18	64.1	292.4	41.1	-.785	-.549	419
HF	141	4109.9363	1.59e-18	38.4	360.5	246.4	-.338	-.706	421
HNO_3	121	868.1036*)	9.19e-21	11.2	38.7	120.0	+.026	+.387	63
HNO_3	121	869.4279*)	1.16e-20	12.0	38.7	110.3	+.026	+.387	63
HNO_3	121	872.9373*)	8.38e-21	11.1	39.9	35.1	+.002	+.537	65
HNO_3	121	874.2321*)	8.24e-21	9.8	39.9	29.9	+.002	+.537	65
HNO_3	121	1325.3160*)	1.53e-20	12.5	12.4	317.3	-.029	+.341	177
HO_2NO_2	251	802.5797*)	1.53e-22	0.9	3.3	171.3	-11.7	-11.4	45
N_2	411	2403.5650	3.31e-28	31.6	126.1	143.2	-.037	-.022	233
N_2	411	2411.1274	1.55e-28	15.7	90.4	179.0	-.111	-.037	235
N_2	411	2418.6520	2.83e-28	27.6	196.9	218.8	-.315	-.076	237
N_2O	41	1163.1315	3.15e-21	49.9	407.6	17.6	+.483	+.112	145
N_2O	41	1183.5154	5.70e-21	69.4	682.1	128.2	+.118	-.006	147
N_2O	41	1202.0263	1.22e-21	11.5	77.3	620.6	-1.42	-.145	153
N_2O	41	2168.7416	1.28e-20	33.1	378.1	1242.9	-2.92	-.376	221
N_2O	41	2184.4585	3.25e-20	92.2	1128.4	906.2	-2.00	-.261	223
N_2O	41	2184.5118	3.26e-20	83.3	1020.1	905.6	-2.00	-.261	223
N_2O	41	2186.0020	1.63e-19	100.0	733.3	653.2	-1.29	-.185	225
N_2O	41	2188.1894	2.12e-19	100.0	280.9	588.8	-1.07	-.109	227
N_2O	41	2190.4950	4.61e-20	99.8	525.7	782.4	-.662	-.097	229
N_2O	41	2194.5897	4.13e-19	100.0	444.0	415.5	-.953	-.072	231
N_2O	41	2442.2769	4.18e-21	52.1	418.5	231.2	-.193	-.055	239
N_2O	41	2444.0304	4.57e-21	58.3	366.4	193.6	-.024	-.028	241
N_2O	41	2444.9041	4.73e-21	59.4	373.5	176.0	-.024	-.028	241
N_2O	41	2446.6458	4.98e-21	63.9	725.8	143.3	+.144	+.099	243
N_2O	41	2447.5139	5.05e-21	63.7	531.0	128.2	+.233	+.000	245
N_2O	41	2454.3923	4.12e-21	58.9	639.3	37.7	+.500	+.040	247
N_2O	41	2464.5001	1.63e-21	28.4	242.5	2.5	+.570	+.041	249
N_2O	41	2465.3312	2.15e-21	36.2	309.2	5.0	+.570	+.041	249
N_2O	41	2471.0986	4.87e-21	65.7	508.9	46.1	+.283	+.008	251
N_2O	41	2471.9152	5.08e-21	66.6	516.2	55.3	+.283	+.008	251
N_2O	41	2479.9719	4.84e-21	59.6	762.6	193.5	-.059	-.075	253
N_2O	41	2480.7660	4.64e-21	56.6	724.0	212.0	-.059	-.075	253
N_2O	41	2481.5578	4.41e-21	53.2	447.3	231.2	-.038	-.035	255
N_2O	41	2482.3474	4.18e-21	51.2	430.3	251.3	-.038	-.035	255
N_2O	41	2486.2595	2.93e-21	37.9	268.5	364.4	-.422	-.034	257
N_2O	41	2487.0346	2.69e-21	32.5	39.8	389.5	-.585	-.081	259
N_2O	41	2487.8070	2.45e-21	36.9	45.3	415.5	-.585	-.081	259
N_2O	41	2492.3848	1.28e-21	12.0	211.5	588.8	-1.21	-.252	263
N_2O	41	2523.4799	2.99e-21	22.6	399.5	721.0	-1.43	-.193	269

chemical species	molec index	ν_0 in cm^{-1}	absorption strength $cm/molec$	%	Info Cont.	E''_{LST} cm^{-1}	T-depen [%/K] trop	strat	pa-ge
N_2O	41	2540.3611	1.63e-20	93.4	1705.0	272.3	-.252	-.058	275
N_2O	41	2551.9157	2.20e-20	99.1	1199.0	76.3	+.286	-.018	283
N_2O	41	2806.3157	7.71e-22	14.3	164.7	37.7	+.382	+.028	325
N_2O	41	4711.4532	6.20e-22	11.2	99.6	176.0	+.036	-.012	449
N_2O	41	4708.0752	5.43e-22	9.4	75.7	231.2	-.205	-.027	447
N_2O	42	2146.5160	1.15e-21	12.5	213.1	469.9	-.922	-.112	211
N_2O	42	2149.6423	1.54e-21	19.4	143.6	389.5	-.489	-.108	213
N_2O	42	2153.7194	2.13e-21	29.8	208.7	294.0	-.487	-.127	215
N_2O	42	2157.6919	2.69e-21	39.4	225.8	212.0	-.521	-.035	217
N_2O	42	2160.6023	3.00e-21	45.9	364.2	159.2	-.335	-.027	219
N_2O	42	2185.6697	2.89e-21	36.3	266.0	37.7	+3.71	+.869	225
N_2O	42	2187.9431	3.30e-21	38.2	107.2	65.4	+.485	+.030	227
N_2O	42	2188.6875	3.37e-21	43.7	122.7	76.2	+.485	+.030	227
N_2O	42	2190.8805	3.41e-21	46.6	245.5	114.0	+.567	+.003	229
N_2O	42	2195.0847	2.88e-21	34.8	154.4	212.0	-1.32	+.073	231
N_2O	42	2560.3820	6.81e-23	1.0	19.7	37.7	-.118	+.029	285
N_2O	42	2562.6282	7.74e-23	0.4	9.3	65.4	-.211	-.076	287
N_2O	42	2566.2273	7.91e-23	1.1	20.3	128.2	-.130	-.003	289
N_2O	43	1250.4709	4.30e-22	6.0	45.7	223.4	-.566	-.010	171
N_2O	43	1255.6967	5.16e-22	7.5	54.3	123.9	-.443	-.038	173
N_2O	43	2187.8459	3.27e-21	41.9	117.3	110.1	-.008	+.084	227
N_2O	43	2188.7560	3.27e-21	51.7	145.3	97.2	-.008	+.084	227
N_2O	43	2194.9397	2.43e-21	29.9	132.7	29.1	+.154	+.225	231
N_2O	43	2517.1892	6.60e-23	1.5	33.7	170.0	-.238	-.017	265
N_2O	43	2521.7504	7.07e-23	1.3	35.7	97.2	-.410	-.031	267
N_2O	43	2527.0261	5.71e-23	0.7	20.5	36.4	-.367	-.012	271
N_2O	43	2529.5827	4.19e-23	0.9	26.1	17.0	-.373	-.003	273
N_2O	43	2543.7733	7.06e-23	0.8	24.6	53.4	-.947	-.163	277
N_2O	43	2549.4462	7.24e-23	0.9	16.1	153.8	-.263	-.032	279
N_2O	43	2551.4732	6.50e-23	0.7	17.5	204.8	-.400	-.060	281
N_2O	44	1227.9559	2.51e-22	4.6	37.6	218.3	-.213	-.035	161
N_2O	44	1231.3564	2.89e-22	8.4	66.8	150.3	-.568	+.031	163
N_2O	44	1232.1995	2.95e-22	6.6	66.8	135.3	-.568	+.031	163
N_2O	44	1233.8772	3.01e-22	5.4	56.6	107.6	-.862	-.039	167
N_2O	44	1234.7118	3.00e-22	9.0	56.6	94.9	-.862	-.039	167
NH_3	111	929.8981	2.68e-19	0.4	2.5	140.2	+5.12	+.611	71
NH_3	111	951.7762	1.51e-19	<0.1	0.4	0.8	+.750	+1.28	87
NH_3	111	965.3539	4.69e-19	0.2	0.5	283.6	+1.55	-.847	91
NH_3	111	967.3463	5.68e-19	0.5	3.0	85.9	n.a.	n.a.	93
NO	81	1900.0706	2.32e-20	12.3	60.6	80.2	-.035	+.114	181
NO	81	1900.0816	2.32e-20	12.3	60.6	80.3	-.035	+.114	181
NO	81	1903.1335	2.31e-20	11.1	49.0	105.4	-.018	+.017	183
NO	81	1912.7947	1.03e-20	7.0	29.8	326.0	-.022	-.443	185
NO_2	101	1598.0059	9.10e-20	12.4	1334.7	207.9	-.155	-.075	179
NO_2	101	2881.6114	3.11e-21	0.4	5.4	321.4	-.050	-.356	343
NO_2	101	2881.9236	4.28e-21	0.6	9.3	277.8	-.050	-.356	343
NO_2	101	2882.2739	3.94e-21	0.5	6.7	284.1	-.050	-.356	343
NO_2	101	2887.6673	4.90e-21	0.7	12.0	190.6	-.122	-.089	345
NO_2	101	2890.3238	5.89e-21	0.9	12.7	134.9	-.050	+.004	347
NO_2	101	2914.6434	6.02e-21	0.8	12.8	46.4	-.102	+.282	353
NO_2	101	2914.6520	5.70e-21	0.8	11.7	54.6	-.102	+.282	353
NO_2	101	2922.6261	5.05e-21	0.3	5.1	237.1	+.099	-.300	355

chemical species	molec index	ν_0 in cm^{-1}	absorption strength $cm/molec$	%	Info Cont.	E''_{LST} cm^{-1}	T-depen [%/K] trop	strat	pa-ge
NO_2	101	2922.6327	4.84e-21	0.4	5.8	237.1	+.099	-.300	355
NO_2	101	2922.7015	5.17e-21	0.7	10.6	233.9	+.099	-.300	355
NO_2	101	2924.7844	3.90e-21	0.7	11.9	321.8	-1.01	-.924	359
NO_2	101	2924.7917	3.76e-21	0.6	9.9	349.1	-1.01	-.924	359
O_3	31	773.2868	3.77e-22	65.1	253.6	290.3	-.213	-1.15	29
O_3	31	773.3117	3.61e-22	59.4	253.6	343.4	-.213	-1.15	29
O_3	31	774.8417	3.31e-22	53.3	272.3	376.2	-.184	-.872	31
O_3	31	774.8853	3.62e-22	60.7	272.3	307.9	-.184	-.872	31
O_3	31	781.1807	2.97e-22	50.6	198.0	357.5	-.315	-.521	37
O_3	31	782.7720	2.83e-22	41.6	186.8	376.8	-.150	-.437	39
O_3	31	975.1705	1.74e-22	6.9	36.5	1484.3	-.409	-3.50	95
O_3	31	976.5119	1.57e-22	5.5	28.2	1495.0	-.341	-3.35	97
O_3	31	977.6600	3.10e-22	11.4	57.8	1357.0	-.284	-3.22	99
O_3	31	978.9563	5.53e-22	28.0	141.3	1234.1	-.667	-2.63	101
O_3	31	980.4040	6.73e-22	34.7	161.6	1190.5	-.727	-2.52	103
O_3	31	981.4870	1.83e-22	20.7	96.0	1404.3	-.656	-2.83	105
O_3	31	982.7663	4.36e-22	19.9	94.6	1272.9	-.710	-2.77	107
O_3	31	983.8910	6.19e-22	30.0	119.5	1204.3	-2.50	-2.45	109
O_3	31	984.6918	1.18e-21	58.7	236.7	1064.3	-.672	-2.17	111
O_3	31	986.1021	1.42e-21	70.6	255.8	1023.8	-.668	-2.13	113
O_3	31	987.4795	1.42e-21	69.1	236.0	1020.0	-.631	-2.03	115
O_3	31	988.5468	8.98e-22	44.8	169.2	1101.2	-.704	-2.27	117
O_3	31	989.8539	1.31e-21	70.8	240.9	1028.4	-.682	-2.12	119
O_3	31	990.2736	2.37e-21	90.1	284.9	907.0	-.614	-1.89	121
O_3	31	991.1447	1.26e-21	61.5	213.7	1023.1	-.657	-2.05	123
O_3	31	992.1168	1.89e-21	41.0	244.2	952.0	-.623	-1.84	125
O_3	31	993.7116	1.73e-21	74.5	188.9	948.2	-.661	-1.87	127
O_3	31	1002.7062	1.04e-21	57.0	179.4	945.2	-.412	-1.43	127
O_3	31	1043.4030	5.47e-22	28.4	82.6	1097.1	+2.34	+1.95	131
O_3	31	1044.0916	7.15e-22	55.5	153.0	1046.3	+.099	-.142	133
O_3	31	1090.4761	5.00e-22	67.2	454.7	385.7	-.102	-.092	135
O_3	31	1104.8375	3.63e-22	60.0	301.6	281.8	-.073	-.160	137
O_3	31	1146.4714	3.95e-22	55.6	467.8	372.4	-.148	-.386	139
O_3	31	1161.2893	3.35e-22	54.8	218.8	289.1	-.221	-.313	143
O_3	31	1163.4222	2.57e-22	46.7	381.7	253.9	-.114	-.109	145
O_3	31	2759.7801	2.71e-23	4.4	33.7	269.2	-.182	-.219	309
O_3	31	2781.7734	3.20e-23	9.3	94.9	8.4	-.093	+.327	323
O_3	31	3019.6297	3.29e-22	34.6	191.0	226.5	-.521	+.067	373
O_3	31	3023.3887	1.96e-22	30.2	103.3	241.1	-.149	+.125	375
O_3	31	3023.4442	3.39e-22	47.4	162.4	191.7	-.149	+.125	375
O_3	31	3023.5052	2.43e-22	36.6	125.3	222.0	-.149	+.125	375
O_3	31	3023.7434	3.55e-22	50.7	281.1	183.4	-.054	+.286	377
O_3	31	3023.8041	9.84e-23	15.4	85.7	287.9	-.054	+.286	377

chemical species	molec index	ν_0 in cm^{-1}	absorption strength $cm/molec$	%	Info Cont.	E''_{LST} cm^{-1}	T-depen [%/K] trop	strat	pa-ge
O_3	31	3026.7651	3.96e-22	55.0	326.5	141.1	-.194	+.174	379
O_3	31	3026.8615	3.34e-22	50.2	298.0	156.9	-.194	+.174	379
O_3	31	3039.9866	1.31e-22	34.6	249.8	158.8	+.015	+.235	381
O_3	31	3040.1108	2.00e-22	42.3	305.2	30.2	+.015	+.235	381
O_3	31	3045.1987	7.37e-23	16.0	155.3	340.7	-.020	+.357	383
O_3	31	3045.2951	6.96e-23	17.6	170.8	20.9	-.020	+.357	383
O_3	31	3161.4977	1.67e-23	2.6	33.5	260.4	-.162	-.228	389
O_3	32	1002.6060	4.04e-23	14.7	46.2	328.4	+.201	+.318	127
O_3	32	1043.4404	5.96e-23	16.1	46.9	230.4	-.302	-.101	131
O_3	32	1044.0128	4.60e-23	9.6	26.3	288.1	+.280	+1.01	133
O_3	32	1090.3638	1.76e-24	5.5	57.7	32.6	+.046	+.436	135
O_3	33	975.2838	2.30e-23	4.5	23.9	495.4	-.123	-.907	95
O_3	33	976.7864	2.84e-23	6.2	21.5	446.8	-.218	-.728	97
O_3	33	977.9250	3.10e-23	6.3	32.1	421.4	-.107	-.566	99
O_3	33	979.4801	3.80e-23	9.7	49.1	374.9	-.212	-.548	101
O_3	33	980.6024	4.12e-23	10.2	47.6	351.1	-.131	-.467	103
O_3	33	981.7107	4.46e-23	12.2	52.6	328.0	-.145	-.340	105
O_3	33	983.0755	4.46e-23	11.8	56.1	311.6	-.191	-.304	107
O_3	33	984.1683	4.54e-23	12.6	49.9	298.3	-.061	-.048	109
O_3	33	984.9790	5.48e-23	14.3	57.7	263.6	-.060	-.251	111
O_3	33	986.2977	5.10e-23	15.3	55.5	257.2	-.159	-.295	113
O_3	33	987.1014	6.10e-23	19.9	68.1	224.5	-.102	-.218	115
O_3	33	988.3912	5.58e-23	16.1	60.9	219.5	-.024	-.094	117
O_3	33	989.1177	5.14e-23	15.4	52.3	222.0	-.139	-.009	119
O_3	33	990.4487	5.94e-23	19.7	62.3	185.1	-.241	+.079	121
O_3	33	991.2137	7.04e-23	22.0	76.6	155.8	+.014	+.261	123
O_3	33	992.1759	7.22e-23	17.3	103.1	140.0	-.056	+.155	125
O_3	33	992.1764	5.44e-23	17.3	103.1	174.1	-.056	+.155	125
O_3	33	993.7910	4.56e-23	15.1	38.3	172.2	-.051	+.190	127
OCS	191	2045.5785	7.06e-19	10.4	67.2	285.1	-.531	-.030	193
OCS	191	2051.3313	1.01e-18	23.3	180.4	131.8	+.032	-.016	195
OCS	191	2053.1714	1.02e-18	18.6	71.9	93.7	+.005	-.154	197
OCS	191	2054.0778	1.00e-18	22.2	92.5	77.1	-.192	-.209	199
OCS	191	2054.5271	9.84e-19	26.6	110.7	69.4	-.192	-.209	199
OCS	191	2055.8606	9.08e-19	22.5	126.6	48.7	-1.31	-.524	201
SF_6	500	947.9300$^{*)}$	3.15e-19	1.5	9.1	241.0	+.542	+.178	83
SO_2	91	1156.9140$^{*)}$	3.40e-21	1.1	6.4	29.2	+5.55	+2.98	141
SO_2	91	1157.8785$^{*)}$	2.12e-21	1.1	2.5	29.2	+5.55	+2.98	141

2.3 The numerical encoding of molecules in spectroscopic linelists

Table 2.3: *This table gives an overview over all species known to the HITRAN2000 and ATMOS spectroscopic data bases. The first column gives the chemical name, the next two columns give the numerical encoding of that species in ATMOS and HITRAN2000 notation, respectively, splitted by its isotopic composition. The isotopic compositions listed in the fourth column denote the atomic masses of the atoms by their last digit ($^{12}C = 2$, $^{13}C = 3$, etc). The last column gives the natural isotopic abundances assumed in the data bases as quoted from HITRAN2000. The molecular masses of molecules not contained in HITRAN are taken from the FSCATM software (2003 edition) (Gallery et al., 1983, Goldman et al., 1999, Meier et al., 2003 & 2004) and are identical with the molecular masses used in SFIT2 V3.81. For more details see Rothman et al., (1998 and 2003) and http://www.hitran.com.*

Molecular indices of ATMOS and HITRAN agree for molecules 1 to 21, but differ for other molecules. In the cases of heavy water vapour, heavy methane and heavy ozone, ATMOS and SFIT allow two different notations. The alternative identifier is given in brackets. The larger of any set of two identifiers for the same isotopomer makes SFIT to treat that isotopomer as an independent species that can be retrieved independently of all remaining isotopomers of that molecule. Note also that some recently added isotopomers and molecules may not be supported by older versions of SFIT.

Species	**3-digit Indentifier Codes**			**Isotopic**	**Molecular**
	ATMOS	HITRAN	Isotopes	**Abundances**	**Mass m_r**
H_2O	11	11	161	.997317E-00	18.010565
	12 (511)	12	181	1.99983E-03	20.014811
	13 (512)	13	171	3.71884E-04	19.014780
	491 (14)	14	162	3.10693E-04	19.016740
	492 (15)	15	182	6.23003E-07	21.020985
	493 (16)	16	172	1.15853E-07	20.020956
CO_2	21	21	626	.984204E+00	43.989830
	22	22	636	1.10574E-02	44.993185
	23	23	628	3.94707E-03	45.994076
	24	24	627	7.33989E-04	44.994045
	25	25	638	4.43446E-05	46.997431
	26	26	637	8.24623E-06	45.997400
	27	27	828	3.95734E-06	47.998322
	28	28	728	1.47180E-06	46.998291
O_3	31	31	666	.992901E+00	47.984745
	32 (541)	32	668	3.98194E-03	49.988991
	33 (551)	33	686	1.99097E-03	49.988991
	34 (561)	34	667	7.40475E-04	48.988960
	35 (571)	35	676	3.70237E-04	48.988960

Species	3-digit Indentifier Codes			Isotopic	Molecular
	ATMOS	HITRAN	Isotopes	Abundances	Mass m_r
N_2O	41	41	446	.990333E+00	44.001062
	42	42	456	3.64093E-03	44.998096
	43	43	546	3.64093E-03	44.998096
	44	44	448	1.98582E-03	46.005308
	45	45	447	3.69280E-04	45.005278
CO	51	51	26	.986544E+00	27.994915
	52	52	36	1.10836E-02	28.998270
	53	53	28	1.97822E-03	29.999161
	54	54	27	3.67867E-04	28.999130
	55	55	38	2.22250E-05	31.002516
	56	56	37	4.13292E-06	30.002485
CH_4	61	61	211	.988274E+00	16.031300
	62	62	311	1.11031E-02	17.034655
	63 (531)	63	212	6.15751E-04	17.037475
O_2	71	71	66	.995262E+00	31.989830
	72	72	68	3.99141E-03	33.994076
	73	73	67	7.42235E-04	32.994045
NO	81	81	46	.993974E+00	29.997989
	82	82	56	3.65431E-03	30.995023
	83	83	48	1.99312E-03	32.002234
SO_2	91	91	626	.945678E+00	63.961901
	92	92	646	4.19503E-02	65.957695
NO_2	101	101	646	.991616E+00	45.992904
NH_3	111	111	4111	.995872E+00	17.026549
	112	112	5111	3.66129E-03	18.023583
HNO_3	121	121	146	.989110E+00	62.995644
OH	131	131	61	.997473E+00	17.002740
	132	132	81	2.00014E-03	19.006986
	133	133	62	1.55371E-04	18.008915
HF	141	141	19	.999844E+00	20.006229
HCl	151	151	15	.757587E+00	35.976678
	152	152	17	.242257E+00	37.973729
HBr	161	161	19	.506781E+00	79.926160
	162	162	11	.493063E+00	81.924115
HI	171	171	17	.999844E+00	127.912297
ClO	181	181	56	.755908E+00	50.963768
	182	182	76	.241720E+00	52.960819
OCS	191	191	622	.937395E+00	59.966986
	192	192	624	4.15828E-02	61.962780
	193	193	632	1.05315E-02	60.970341
	194	194	623	7.39908E-03	60.966371
	195	195	822	1.87967E-03	61.971231

Species	3-digit Indentifier Codes			Isotpoic	Molecular
	ATMOS	HITRAN	Isotopes	Abundances	Mass m_r
H_2CO	201	201	126	.986237E+00	30.010565
	202	202	136	1.10802E-02	31.013920
	203	203	128	1.97761E-03	32.014811
$HOCl$	211	211	165	.755790E+00	51.971593
	212	212	167	.241683E+00	53.968644
HO_2	221	331	166	.995107E+00	32.997655
H_2O_2	231	251	1661	.994952E+00	34.005480
$HONO$	241	--	1646	--	47.0
HO_2NO_2	251	--	--	--	79.0
N_2O_5	261	--	--	--	108.0
$ClONO_2$	271	351	5646	.749570E+00	96.956672
	272	352	7646	.239694E+00	98.953723
HCN	281	231	124	.985114E+00	27.010899
	282	232	134	1.10676E-02	28.014254
	283	233	125	3.62174E-03	28.007933
CH_3F (CFC-41)	291	--	--	--	34.0331
CH_3Cl	301	241	215	.748937E+00	49.992328
	302	242	217	.239491E+00	51.989379
CF_4 (CFC-14)	311	--	--	--	88.0046
CCl_2F_2 (CFC-12)	321	--	--	--	121.0
CCl_3F (CFC-11)	331	--	--	--	136.0
CH_3CCl_3	341	--	--	--	133.4047
CCl_4	351	--	--	--	153.823
COF_2	361	291	269	.986544E+00	65.991722
$COClF$	371	--	--	--	82.4618
C_2H_6	381	271	1221	.976990E+00	30.046950
C_2H_4	391	381	221	.977294E+00	28.031300
	392	382	231	2.19595E-02	29.034655
C_2H_2	401	261	1221	.977599E+00	26.015650
	402	262	1231	2.19663E-02	27.019005
N_2	411	221	44	.992687E+00	28.006147
CHF_2Cl (CFC-22)	421	--	--	--	86.0
$COCl_2$	431	--	--	--	98.0
$COCl_2$	432	--	--	--	102.0
CH_3Br	441	--	--	--	95.0
CH_3I	451	--	--	--	142.0
$HCOOH$	461	321	126	.983898E+00	46.005480
H_2S	471	311	121	.949884E+00	33.987721
	472	312	141	4.21369E-02	35.983515
	473	313	131	7.49766E-03	34.987105
$CHCl_2F$ (CFC-21)	481	--	--	--	44.0

Species	3-digit Indentifier Codes			Isotopic	Molecular
	ATMOS	HITRAN	Isotopes	Abundances	Mass m_r
HDO	491 (14)	14	162	3.10693E-04	19.016740
	492 (15)	15	182	6.23003E-07	21.020985
	493 (16)	16	172	1.15853E-07	20.020956
SF_6	501	301	29	.950180E+00	145.962492
$H_2{}^{18}O$	511 (12)	12	181	1.99983E-03	20.014811
$H_2{}^{17}O$	521 (13)	13	171	3.71884E-04	19.014780
CH_3D	531 (63)	63	212	6.15751E-04	17.037475
$^{16}O^{16}O^{18}O$	541 (32)	32	668	3.98194E-03	49.988991
$^{16}O^{18}O^{16}O$	551 (33)	33	686	1.99097E-03	49.988991
$^{16}O^{16}O^{17}O$	561 (34)	34	667	7.40475E-04	48.988960
$^{16}O^{17}O^{16}O$	571 (35)	35	676	3.70237E-04	48.988960
$OClO$	581	--	--	--	67.46
$F134A$ $(C_2H_2F_4)$	591	--	--	--	83.033
C_3H_8	601	--	--	--	44.0962
F142B $(C_2H_3ClF_2)$	611	--	--	--	100.4955
$CFC113$ $(C_2Cl_3F_3)$	621	--	--	--	187.3762
$F141B$ $(C_2H_3Cl_2F)$	631	--	--	--	116.9501
$BrNO_2$	641	--	9466	0.505579	125.0
	642	--	1466	0.491894	127.0
PH_3	--	281	1111	.999533E+00	33.997238
O	--	341	6	.997628E+00	15.994915
NO^+	--	361	46	.993974E+00	29.997989
$HOBr$	--	371	169	.505579E+00	95.921076
	--	372	161	.491894E+00	97.919027

In the spectral simulation program *Sim109g-atlas* used in the creation of this atlas, there is additional tentative support for the following species. Please note that the molecule index listed is not an official one but specific to this software and version.

Species	3-digit Indentifier Codes			Isotopic	Molecular
	sim109g	HITRAN	Isotopes	Abundance	Mass m_r
CH_3OH	651	--	--	--	32.042
$CO36$	661(52)	52	36	1.10836E-2	28.99827
CH_3COOH	671	--	--	--	60.0524
ACETONE (CH_3COCH_3)	681	--	--	--	58.0798
PAN $(C_2H_3NO_5)$	691	--	--	--	121.05

3 Main part: The illustrated microwindow atlas

On the following pages more than twohundredandfourty so-called *microwindows* are discussed in detail. Each microwindow is discussed over 2 pages. On the left side you find a page-filling illustration that we call the *contribution plot*. It shows an interval from a ground-based FTIR spectrum recorded at Kiruna at a solar zenith angle of 70^o labelled **'observed'**, a simulated spectrum matching the conditions of the observed spectrum that is the sum of all known molecular absorptions plus simulated solar interferences (labelled **'AllMol'**), and the simulations of each known absorber individually (the label is the name of the corresponding molecule). The spectra are shifted vertically so they can be destinguished. Simulated absorptions from individual molecules are plotted only if the maximum absorption in the interval shown exceeds 0.05%. Weaker species are included in the right-hand side table (discussed below) but not in the figure.

Molecules occur in a mixture of isotopic forms, also known as *isotopomers*. Any rare isotopomer is shown as a seperate species if its maximum absorption strength exceeds 0.5% in total absorption strength in the interval shown. Rare isotopomers are identified by the isotopic specifier **'(i#)'** after the molecule name, where # indicates the isotopic index as defined in Table 2.3 (page 19). Isotopic forms not shown separately are included in the simulation for the bulk isotopic form.

Solar interferences are illustrated through both "observed"[2] and simulated spectra. The "observed" solar spectrum is labelled **'Solar(A,D,G,** or **N)'**, indicating the **A**TMOS, **D**enver, **G**GG Mark IV, or the **N**OAO Kitt Peak data set, respectively. The *simulated* solar spectrum labelled "solar-sim" is based on Arndt Meier's compilation[3]. In some illustrations solar simulations from the Denver University OH linelist ('solar-DU') are provided as well to highlight some of the differences. Unfortunately, we did not manage to include the new solar simulations from Frank Hase into the contribution plots in time, but we encourage readers to study Appendix C and the electronic copy of the simulated solar spectrum on the DVD. Note that the ATMOS spectra were recorded at a 5 times lower spectral resolution than all other data discussed, resulting in notably broader lineshapes.

On the right hand side an illustrated retrieval example is presented. The title above the residuals plot provides

– σ the total standard deviation of the residuals achieved in the example fit,
– **970315s6.92** (or similar) the name of the recorded spectrum,
– φ the astronomical solar zenith angle in degrees,
– **FoV** the field of view (aperture diameter divided by the focal length) in *mrad*, and
– the **apodisation** function used in the Fourier Transform (typ. boxcar).

The table below the example fit specifies the target molecule and spectroscopic key parameters from the transition(s) of interest. The line position is marked with an asterisk '$*$)', if several significant and overlapping absorptions lines of the target molecule make up one absorption feature. In that case, the spectrocopic details given represent the parameters for the strongest line occuring in the region of interest.

The total column amount (TCA) obtained with the best known temperature profile is reported in absolute numbers. The number listed as *'information content'* is simply the ratio of the relative absorption depth of the target line (minus shoulder effects from any interfering absorptions) divided by the total rms of the residuals achieved in our example fit[4]. The larger

[2]This is not strictly true for all intervals as some gaps in the available material of solar spectra had to be filled with simulated data. For more details see section 2 and Appendix C.5.

[3]For more details see section 2 and Appendix C.5.

[4]these numbers are only rough guides and vary considerably with observation conditions.

the information content, the smaller the statistical retrieval errors are.

In order to obtain a realistic estimate of the temperature sensitivity of any particular retrieval, we prepared 3 temperature profiles: one that is to our knowledge the most accurate one, one that is 2 Kelvin warmer in the troposphere (all layers from 0 to 12km), and one that is warmer in the stratosphere and beyond (all layers from 12 to 100km). TCAs obtained using one of the alternative temperature profiles are reported in terms of relative differences from the corresponding TCAs obtained with the best known temperature profile. However, the differences found were divided by a factor of 2 such that the temperature sensitivities reported represent the effect of a 1 Kelvin (and not 2 Kelvin) perturbation. This provides a handy–to–use temperature sensitivity of the retrieved TCA per Kelvin temperature uncertainty in either the troposphere or stratosphere. A temperature sensitivity for any one transition can also be calculated directly from the corresponding lower state energy without the need for the more labourous perturbation calculations. However, the perturbation takes also into acount the effects from interfering absorptions and is thus of higher practical use.

Microwindows that contain interesting absorptions suitable for the retrieval of more than one molecule give details for the second most interesting molecule in round brackets after the correspondig data for the molecule of primary interest. A line position or lower state energy or temperature dependence (etc.) printed in brackets, corresponds to the molecule in brackets at the top of the table.

All molecules for which spectroscopic data is available in the interval discussed are listed in the bottom half of the table. Molecules are listed with their ATMOS molecular plus isotopic index[5] in the order of descending maximum absorption strength as simulated for the 70^o SZA Kiruna spectrum. Beware that the observed absorption depths vary considerably with atmospheric conditions and site location and are valid for this particular scenario from Kiruna only. However, the absorption strengths listed in percent may be useful for relative comparisons between different microwindows. Appendix A may also assist in estimating conditions at other popular FTIR observation sites.

[5]That is the molecular index used in the cfgl-type linelist or as used by the SFIT algorithms - see Table 2.3, page 19, for more details.

This page is intentionally blank.

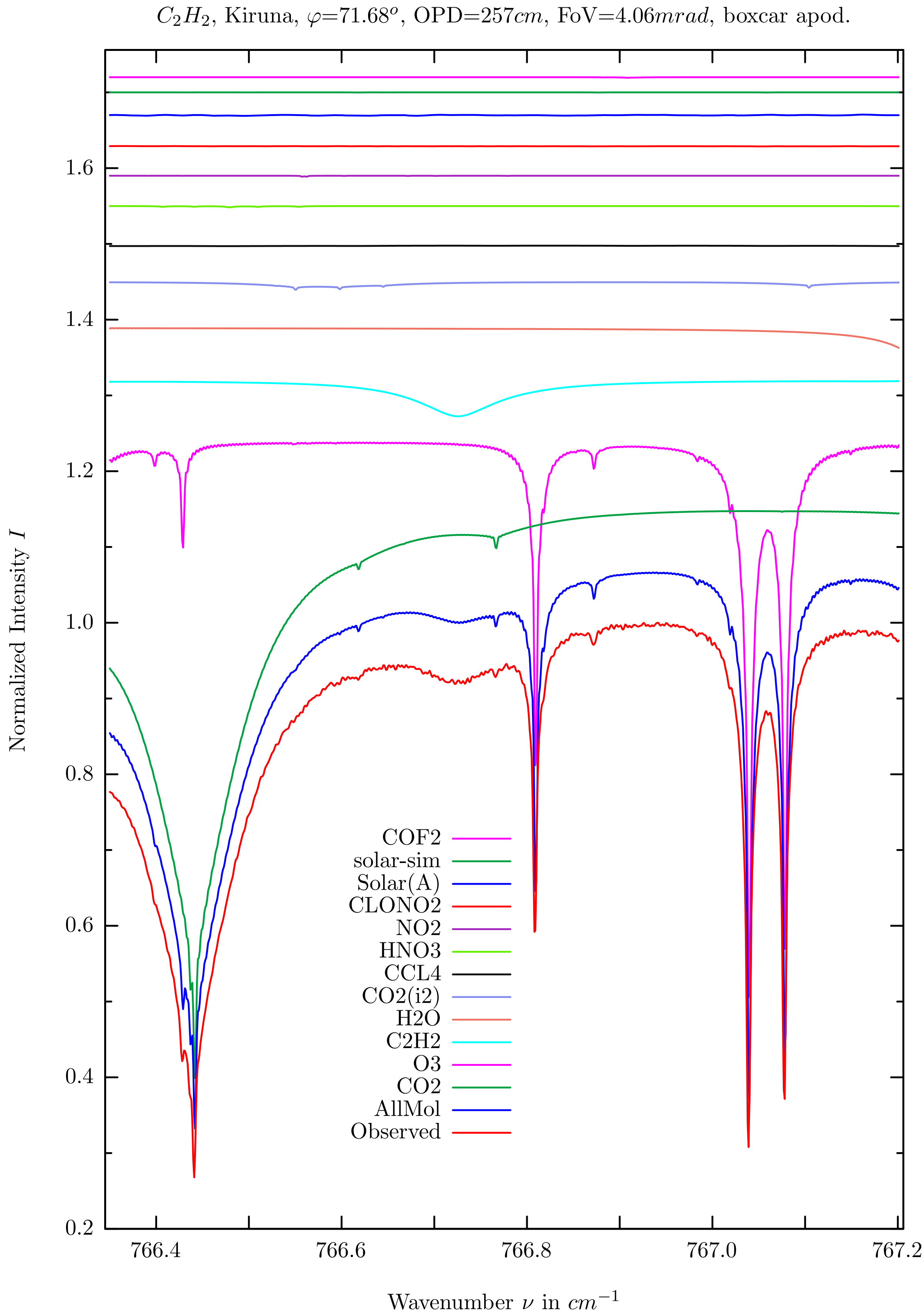

C_2H_2, Kiruna, φ=71.68^o, OPD=257cm, FoV=4.06$mrad$, boxcar apod.
Normalized Intensity I
Wavenumber ν in cm^{-1}
1.6
1.4
1.2
1.0
0.8
0.6
0.4
0.2
766.4
766.6
766.8
767.0
767.2
COF2
solar-sim
Solar(A)
CLONO2
NO2
HNO3
CCL4
CO2(i2)
H2O
C2H2
O3
CO2
AllMol
Observed

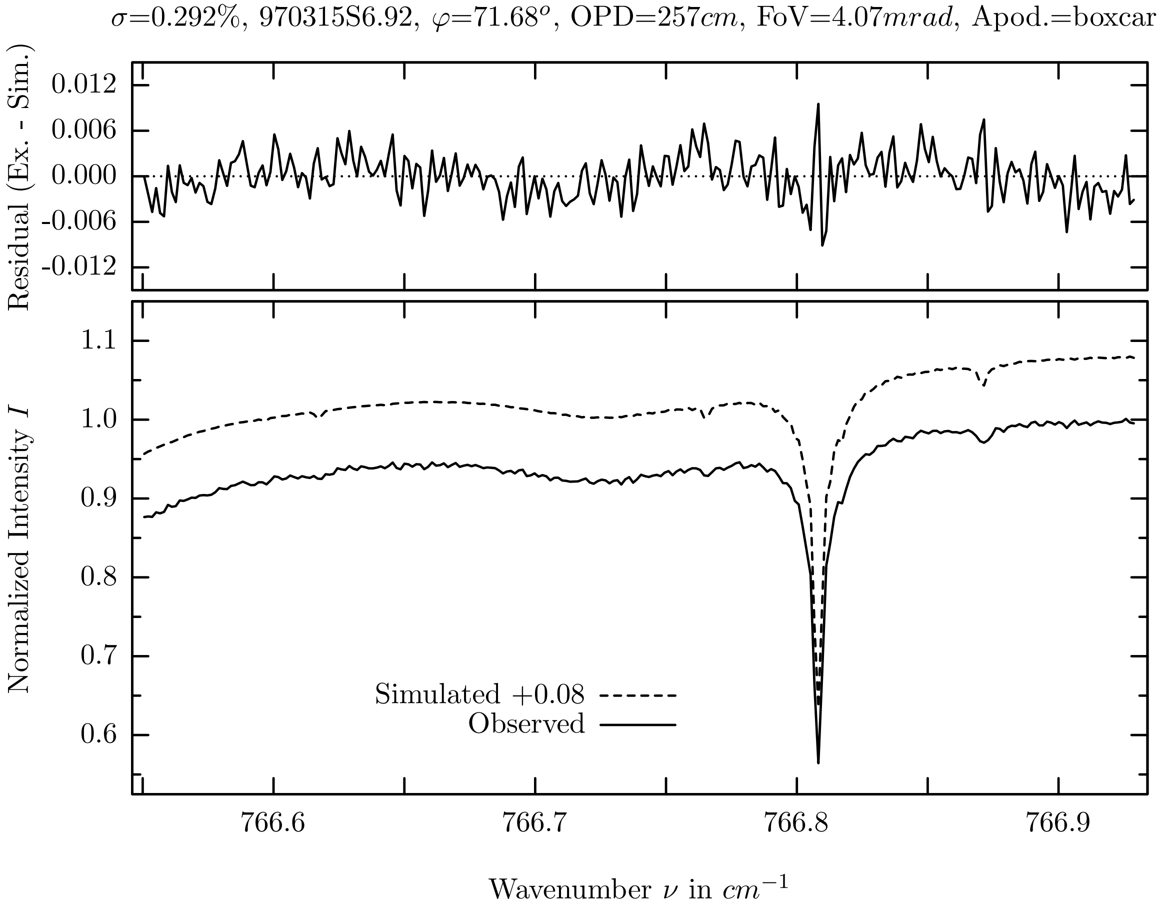

investigated species	:	C_2H_2
line position(s) ν_0	:	766.7241 cm^{-1}
lower state energy E''_{lst}	:	282.3 cm^{-1}
retrieved TCA, information content	:	7.65E+15 $molec/cm^2$, 14.3
temperature dependence of the TCA	:	-0.874%/K (trop), +0.022%/K (strat)
location, date, solar zenith angle	:	Kiruna, 15/Mar/1997, 71.68^o
spectral interval fitted	:	766.550 – 766.930 cm^{-1}

Molecule	iCode	Absorption	Molecule	iCode	Absorption
$CO2$	21	80.953%	$COF2$	361	0.069%
$O3$	31	79.328%	$C2H6$	381	0.016%
C2H2	401	4.757%	HCN	281	0.010%
$H2O$	11	2.836%	$CH3Cl$	301	0.008%
$CO2$	2**2**	1.181%	$NH3$	111	0.004%
$CCl4$	351	0.292%	$N2O5$	261	0.001%
$HNO3$	121	0.171%	$C2H4$	391	0.001%
$NO2$	101	0.147%	HDO	491	0.001%
$ClONO2$	271	0.134%	OH	131	<0.001%
Solar(A)	—	0.100%	ClO	18**2**	<0.001%
Solar-sim	—	<0.001%	$HO2$	221	<0.001%

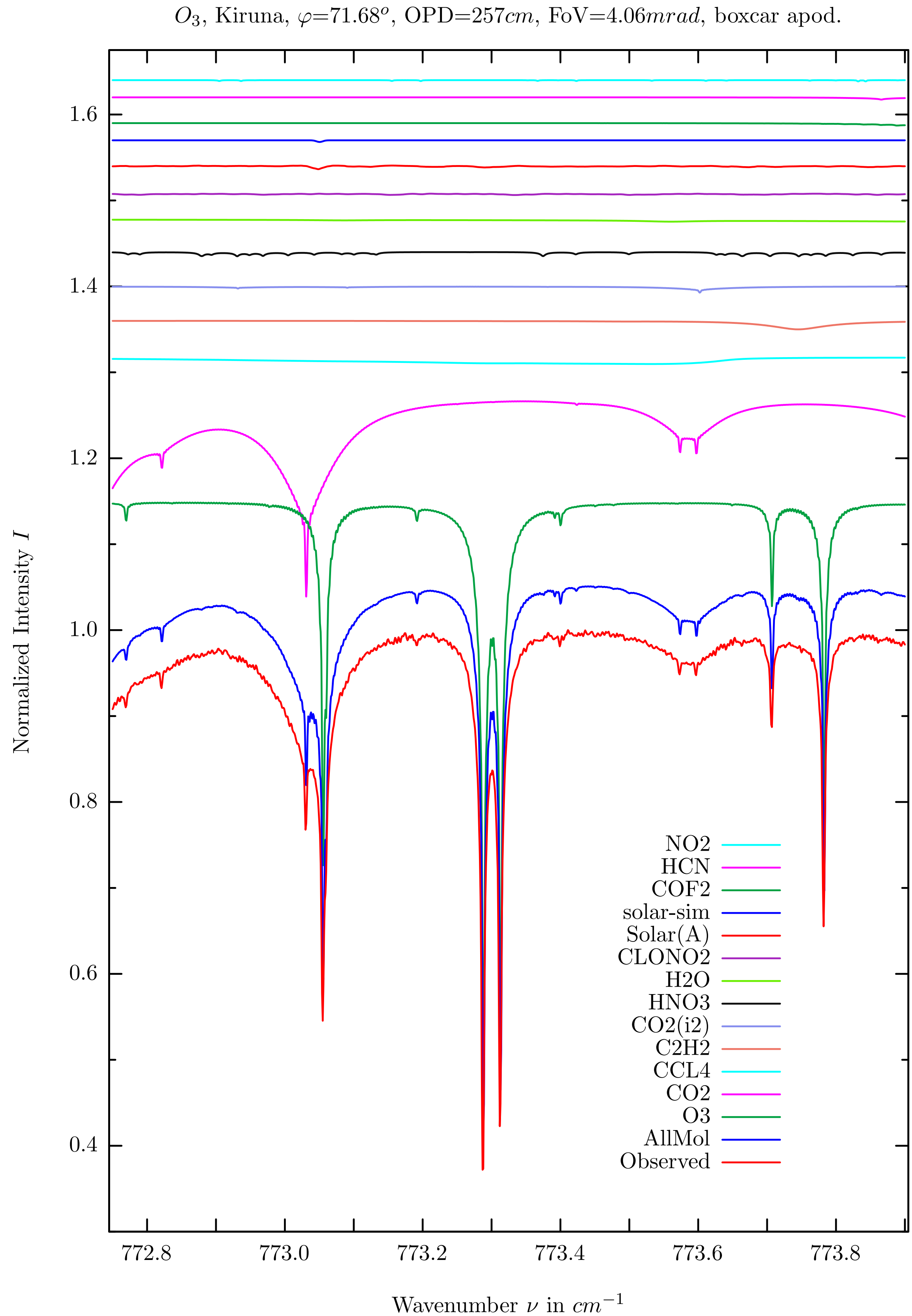
O_3, Kiruna, φ=71.68^o, OPD=257cm, FoV=4.06$mrad$, boxcar apod.
Normalized Intensity I
Wavenumber ν in cm^{-1}
NO2
HCN
COF2
solar-sim
Solar(A)
CLONO2
H2O
HNO3
CO2(i2)
C2H2
CCL4
CO2
O3
AllMol
Observed

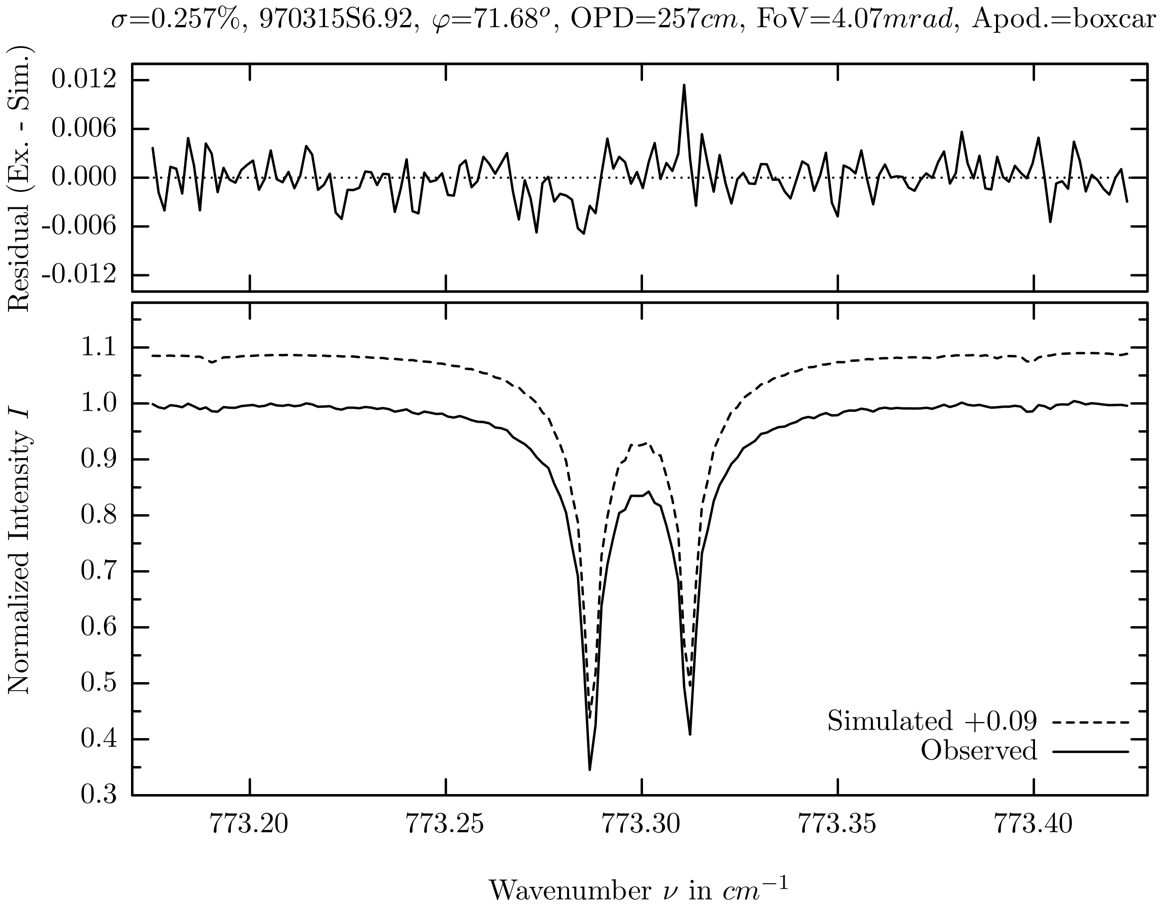

investigated species	:	O_3
line position(s) ν_0	:	773.2868, 773.3117 cm^{-1}
lower state energy E''_{lst}	:	290.3, 343.4 cm^{-1}
retrieved TCA, information content	:	9.53E+15 $molec/cm^2$, 253.6
temperature dependence of the TCA	:	-.213%/K (trop), -1.154%/K (strat)
location, date, solar zenith angle	:	Kiruna, 15/Mar/1997, 71.68^o
spectral interval fitted	:	773.175 – 773.425 cm^{-1}

Molecule	iCode	Absorption	Molecule	iCode	Absorption
O3	31	72.169%	$NO2$	101	0.173%
$CO2$	21	27.304%	$C2H6$	381	0.034%
$CCl4$	351	1.033%	$NH3$	111	0.001%
$C2H2$	401	1.001%	$N2O5$	261	0.001%
$CO2$	2**2**	0.815%	$C2H4$	391	0.001%
$HNO3$	121	0.520%	HDO	491	0.001%
$H2O$	11	0.464%	OH	131	<0.001%
$ClONO2$	271	0.370%	ClO	181	<0.001%
Solar(A)	—	0.358%	$HO2$	221	<0.001%
Solar-sim	—	0.196%	$CH3Cl$	301	<0.001%
$COF2$	361	0.285%	$CHF2Cl$	421	<0.001%
HCN	281	0.267%	$BrNO2$	641	<0.001%

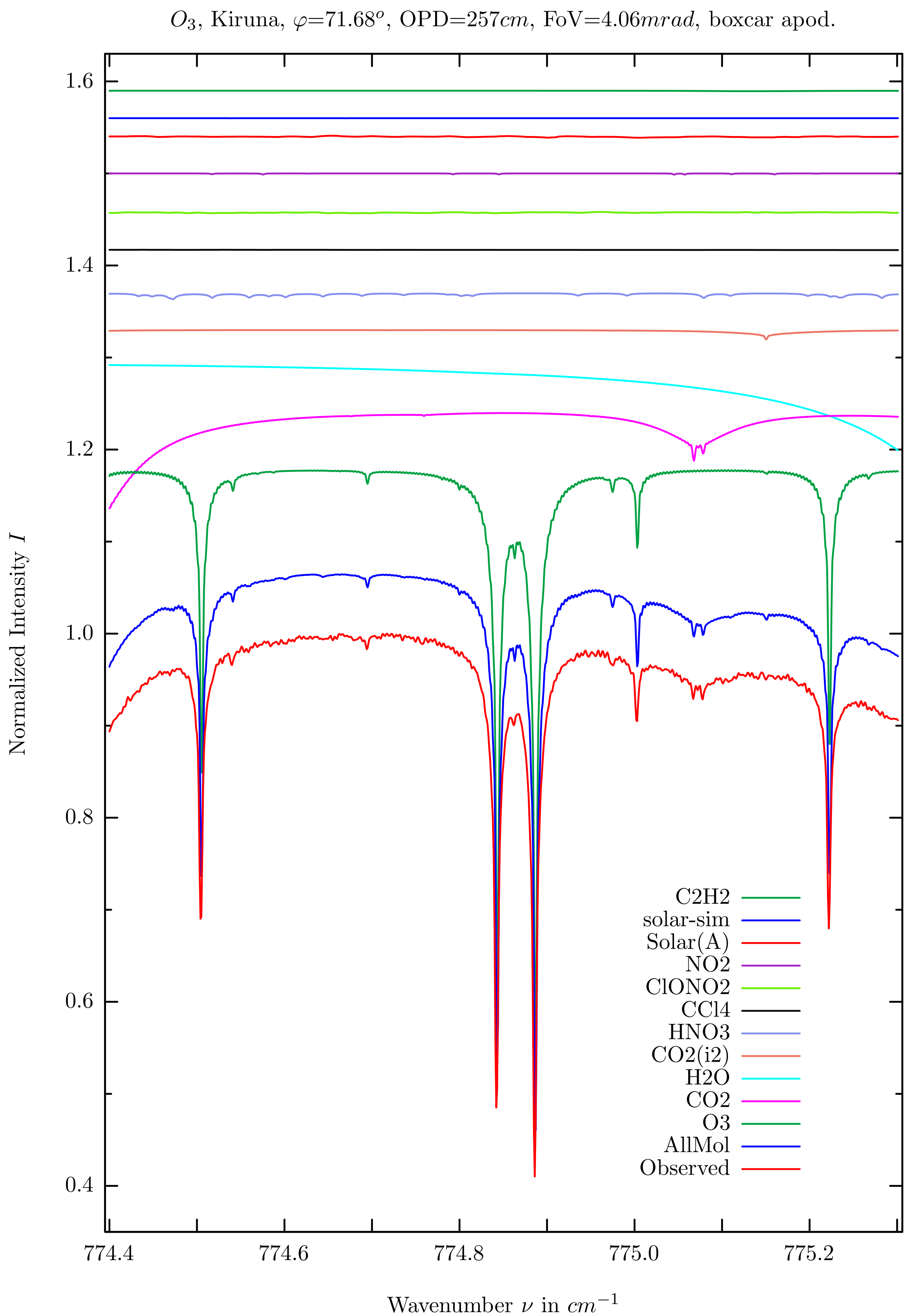

O_3, Kiruna, φ=71.68^o, OPD=257cm, FoV=4.06$mrad$, boxcar apod.
Normalized Intensity I
Wavenumber ν in cm^{-1}
1.6
1.4
1.2
1.0
0.8
0.6
0.4
774.4
774.6
774.8
775.0
775.2
C2H2
solar-sim
Solar(A)
NO2
ClONO2
CCl4
HNO3
CO2(i2)
H2O
CO2
O3
AllMol
Observed

σ=0.223%, 970315S6.92, φ=71.68^o, OPD=257cm, FoV=4.07$mrad$, Apod.=boxcar

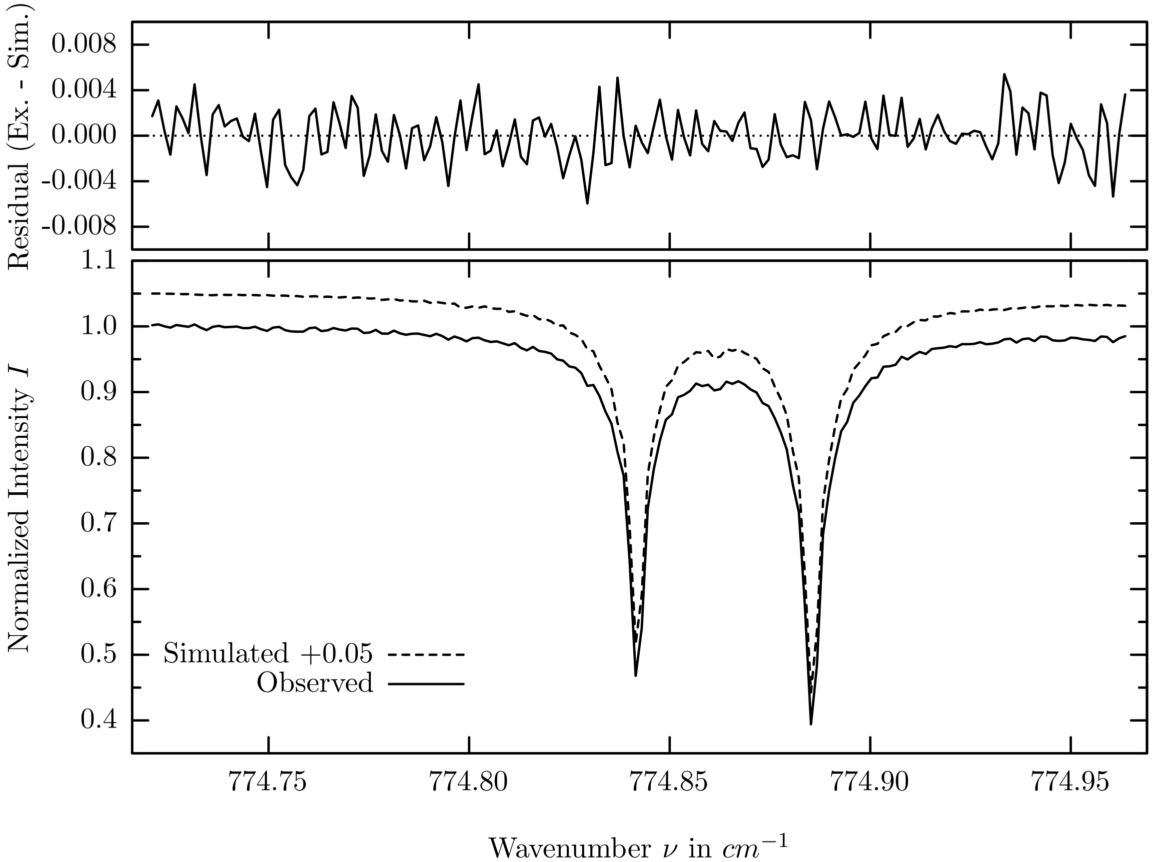

investigated species	:	O_3
line position(s) ν_0	:	774.8417, 774.8853 cm^{-1}
lower state energy E''_{lst}	:	376.2, 307.9 cm^{-1}
retrieved TCA, information content	:	1.09E+19 $molec/cm^2$, 272.3
temperature dependence of the TCA	:	-.184%/K (trop), -.872%/K (strat)
location, date, solar zenith angle	:	Kiruna, 15/Mar/97, 71.68^o
spectral interval fitted	:	774.720 – 774.965 cm^{-1}

Molecule	iCode	Absorption	Molecule	iCode	Absorption
O3	31	68.526%	$COF2$	361	0.025%
$CO2$	21	11.210%	$BrNO2$	641	0.008%
$H2O$	11	10.220%	HCN	281	0.002%
$CO2$	2**2**	1.184%	$NH3$	111	0.001%
$HNO3$	121	0.682%	$N2O5$	261	0.001%
$CCl4$	351	0.326%	$C2H4$	391	0.001%
$ClONO2$	271	0.324%	OH	131	<0.001%
$NO2$	101	0.155%	ClO	181	<0.001%
Solar(A)	—	0.120%	$HO2$	221	<0.001%
Solar-sim	—	0.001%	$CH3Cl$	301	<0.001%
Solar-DU	—	0.001%	$CHF2Cl$	421	<0.001%
$C2H2$	401	0.066%	HDO	491	<0.001%
$C2H6$	381	0.039%			

C_2H_2, Kiruna, φ=71.68^o, OPD=257cm, FoV=4.06$mrad$, boxcar apod.

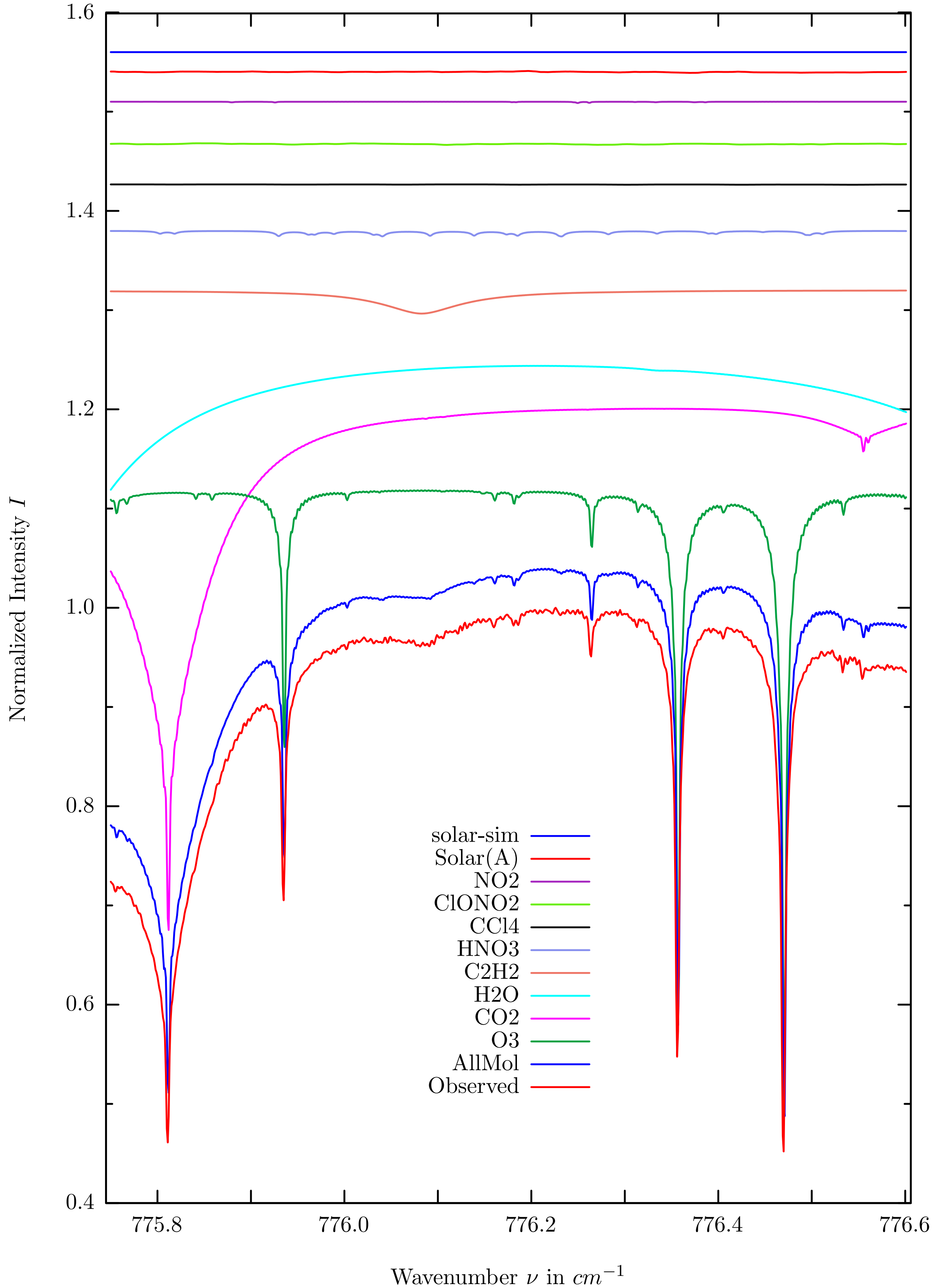

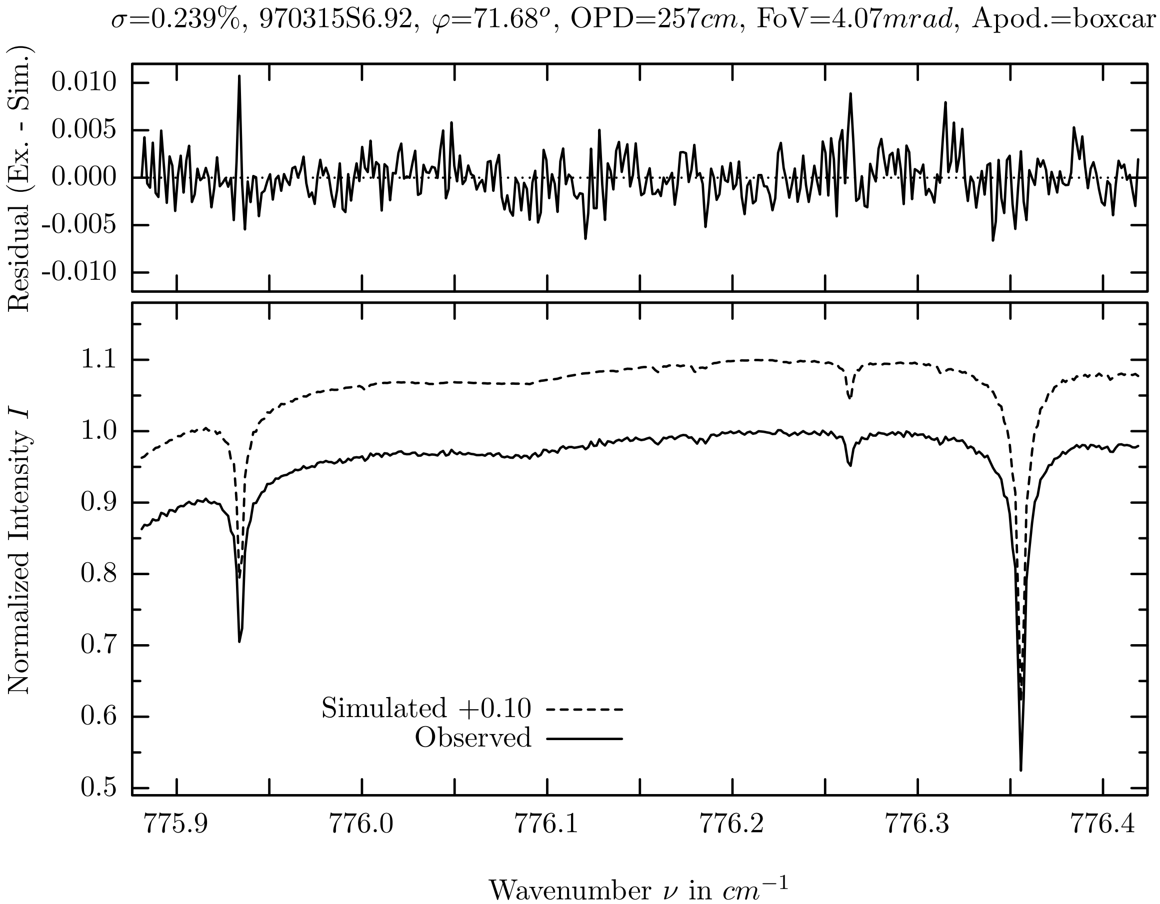

investigated species	:	C_2H_2
line position(s) ν_0	:	776.0810 cm^{-1}
lower state energy E''_{lst}	:	446.9 cm^{-1}
retrieved TCA, information content	:	7.90E+15 $molec/cm^2$, 8.0
temperature dependence of the TCA	:	-.773%/K (trop), +.069%/K (strat)
location, date, solar zenith angle	:	Kiruna, 15/Mar/97, 71.68^o
spectral interval fitted	:	775.880 – 776.420 cm^{-1}

Molecule	iCode	Absorption	Molecule	iCode	Absorption
$O3$	31	65.821%	$BrNO2$	641	0.035%
$CO2$	21	58.307%	$CHF2Cl$	421	0.020%
$H2O$	11	15.981%	$NH3$	111	0.017%
C2H2	401	2.349%	$COF2$	361	0.016%
$HNO3$	121	0.586%	HCN	281	0.013%
$CCl4$	351	0.365%	$C2H4$	391	0.001%
$ClONO2$	271	0.348%	OH	131	<0.001%
$NO2$	101	0.149%	ClO	181	<0.001%
Solar(A)	—	0.090%	$HO2$	221	<0.001%
Solar-sim	—	0.001%	$N2O5$	261	<0.001%
Solar-DU	—	0.001%	HDO	491	<0.001%
$C2H6$	381	0.043%			

$ClNO_3$, Kiruna, φ=71.68^o, OPD=257cm, FoV=4.06$mrad$, boxcar apod.

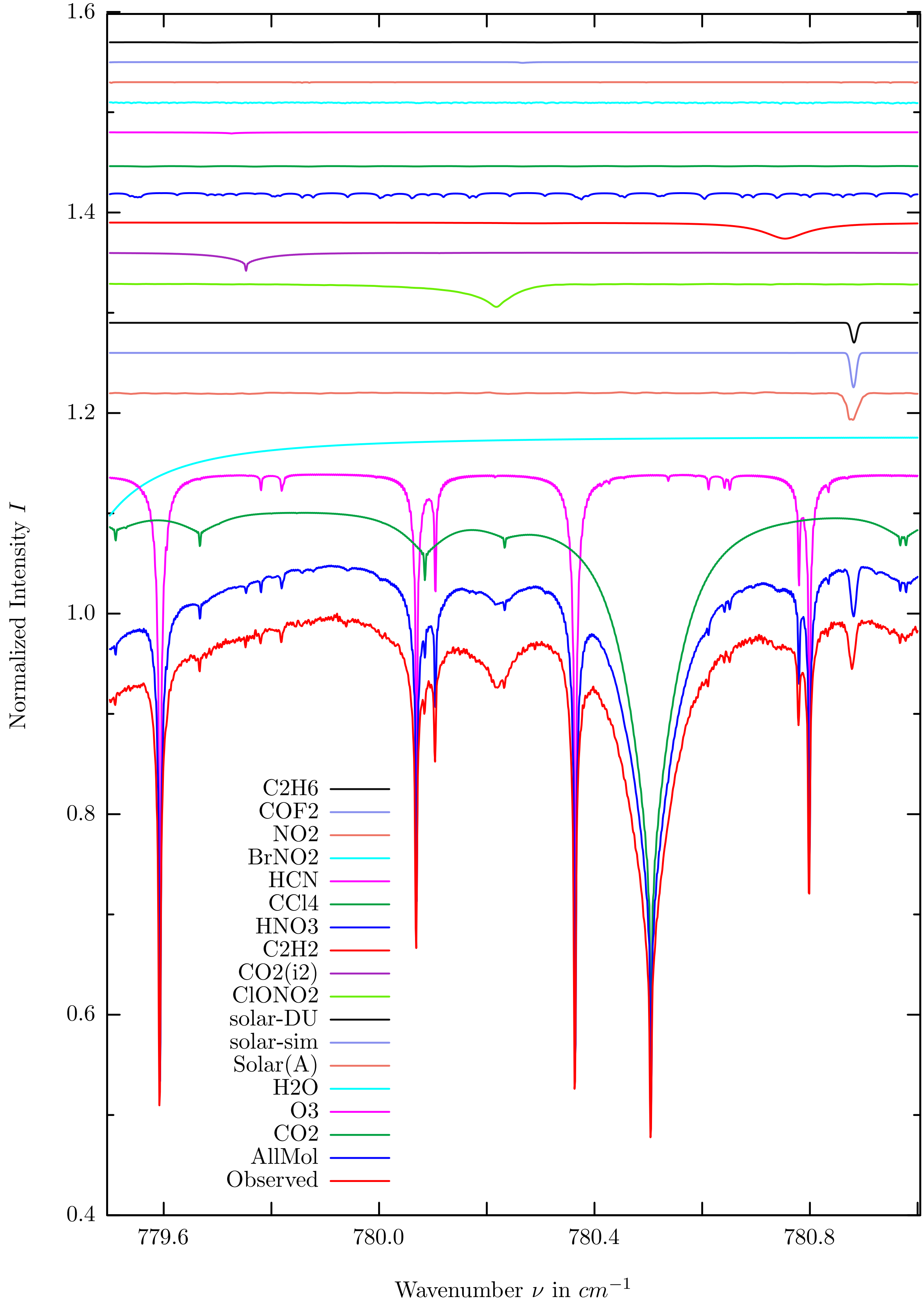

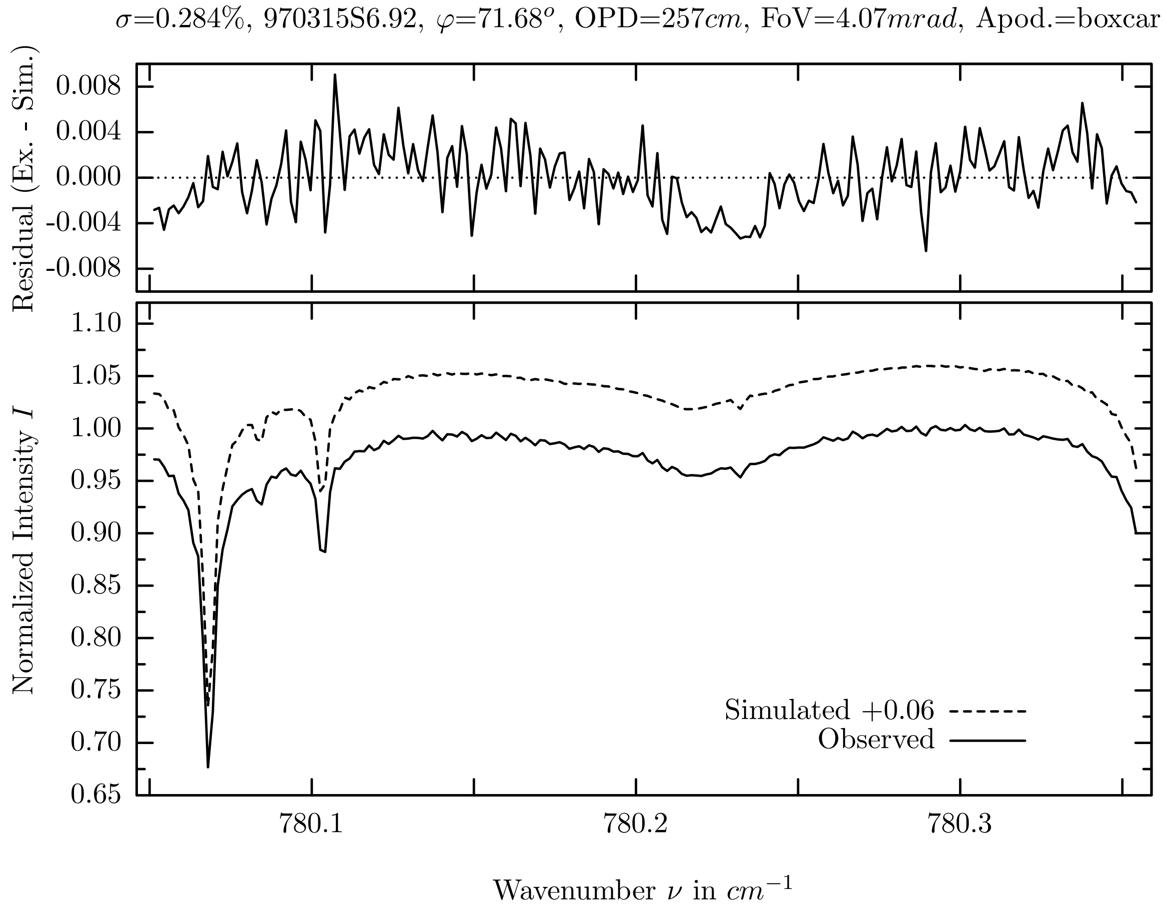

investigated species	:	$ClONO_2$
line position(s) ν_0	:	780.2200*) (pseudoline) cm^{-1}
lower state energy E''_{lst}	:	164.2 cm^{-1}
retrieved TCA, information content	:	4.10E+15 $molec/cm^2$, 14.3
temperature dependence of the TCA	:	+.066%/K (trop), +.435%/K (strat)
location, date, solar zenith angle	:	Kiruna, 15/Mar/97, 71.68^o
spectral interval fitted	:	780.050 – 780.355 cm^{-1}

Molecule	iCode	Absorption	Molecule	iCode	Absorption
$CO2$	21	61.624%	$NO2$	101	0.091%
$O3$	31	57.477%	$COF2$	361	0.077%
$H2O$	11	8.157%	$C2H6$	381	0.055%
Solar(A)	—	2.680%	$NH3$	111	0.044%
Solar-sim	—	3.452%	$CHF2Cl$	421	0.030%
Solar-DU	—	1.985%	ClO	181	0.001%
CLONO2	270	2.413%	$C2H4$	391	0.001%
$CO2$	2**2**	2.055%	OH	131	<0.001%
$C2H2$	401	1.602%	$HO2$	221	<0.001%
$HNO3$	121	0.717%	$N2O5$	261	<0.001%
$CCl4$	351	0.421%	HDO	491	<0.001%
HCN	281	0.123%	$CFC113$	621	<0.001%
$BrNO2$	641	0.123%			

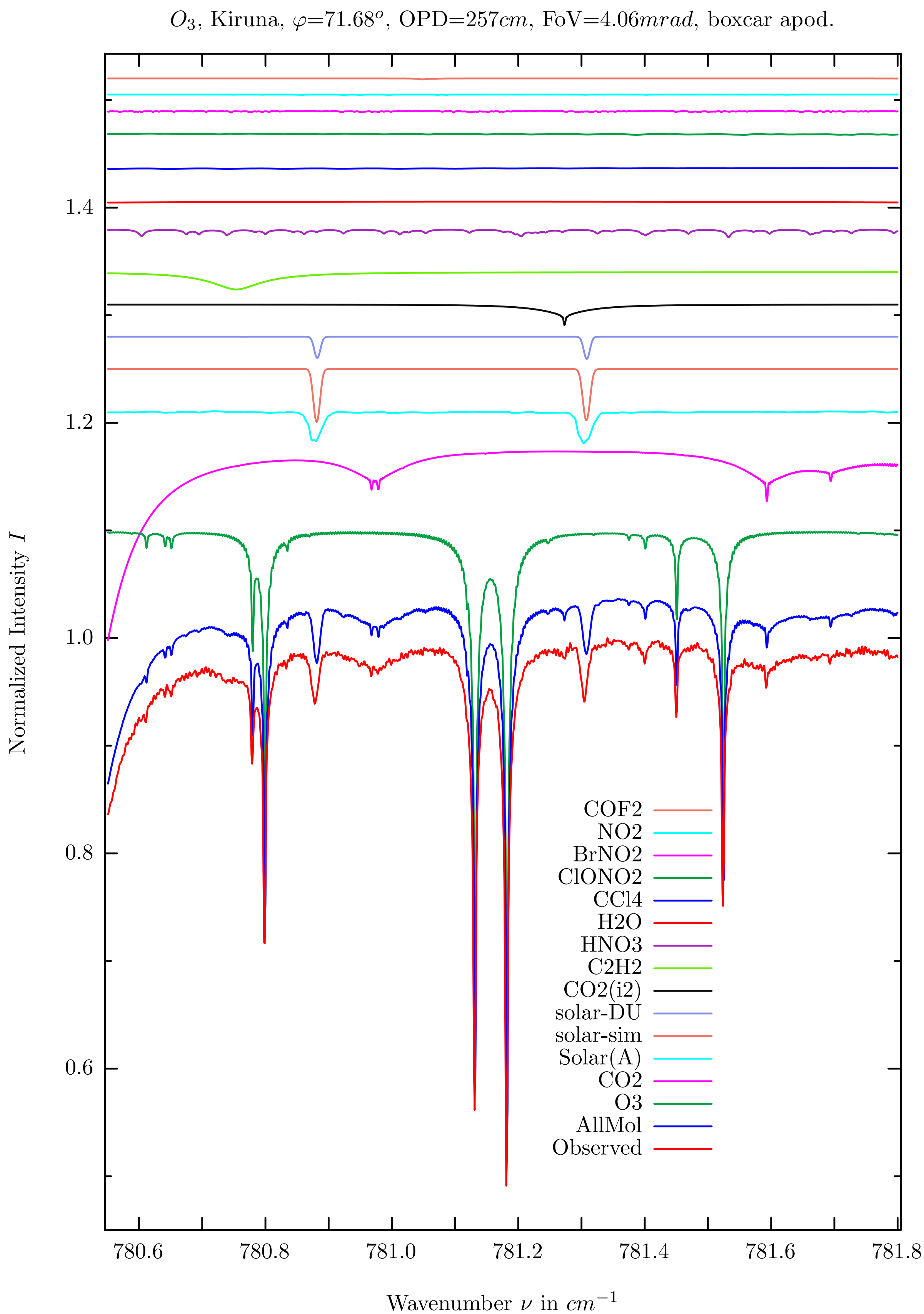
O_3, Kiruna, φ=71.68^o, OPD=257cm, FoV=4.06$mrad$, boxcar apod.
Normalized Intensity I
1.4
1.2
1.0
0.8
0.6
780.6
780.8
781.0
781.2
781.4
781.6
781.8
Wavenumber ν in cm^{-1}
COF2
NO2
BrNO2
ClONO2
CCl4
H2O
HNO3
C2H2
CO2(i2)
solar-DU
solar-sim
Solar(A)
CO2
O3
AllMol
Observed

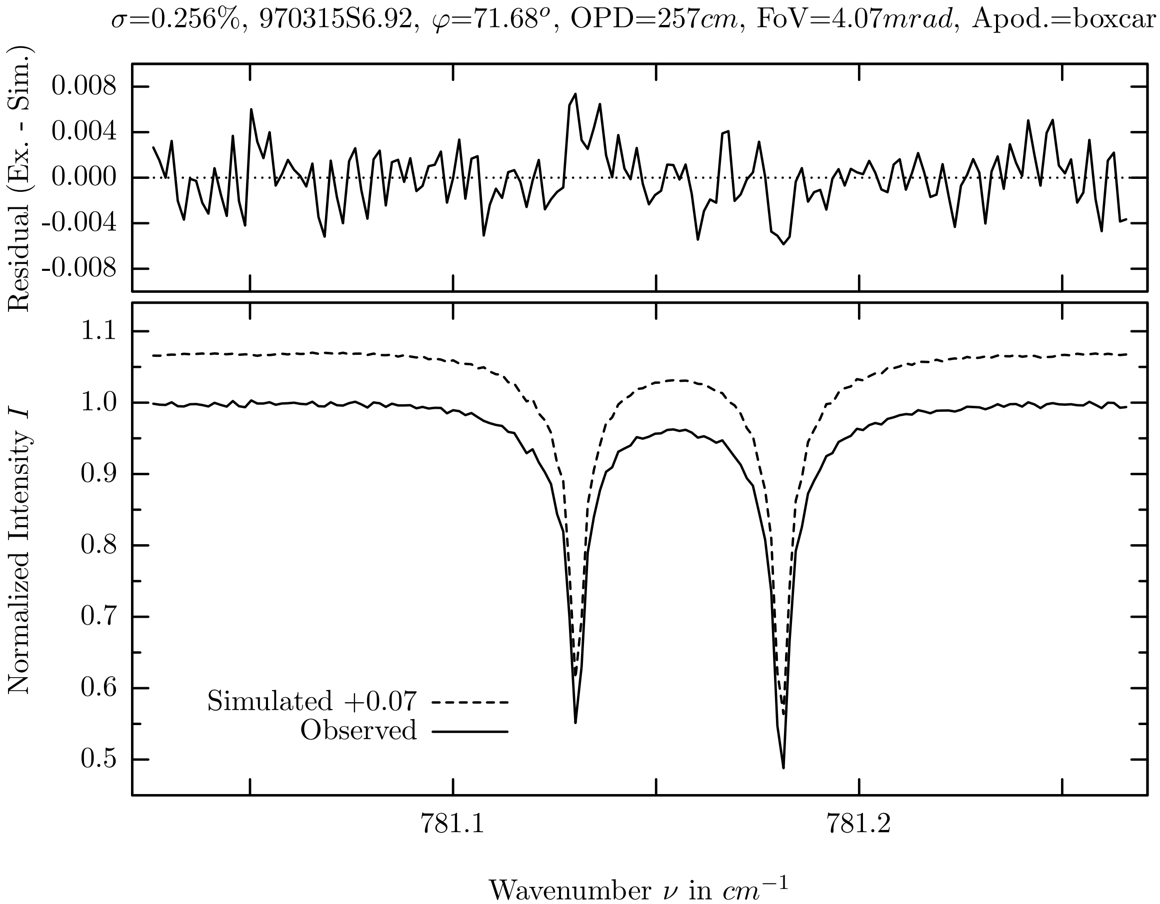

investigated species	:	O_3
line position(s) ν_0	:	781.1807 cm^{-1}
lower state energy E''_{lst}	:	357.5 cm^{-1}
retrieved TCA, information content	:	1.05E+19 $molec/cm^2$, 198.0
temperature dependence of the TCA	:	-.315%/K (trop), -.521%/K (strat)
location, date, solar zenith angle	:	Kiruna, 15/Mar/97, 71.68^o
spectral interval fitted	:	781.025 – 781.267 cm^{-1}

Molecule	iCode	Absorption	Molecule	iCode	Absorption
O3	31	58.870%	*COF*2	361	0.088%
*CO*2	21	17.871%	*C*2*H*6	381	0.049%
Solar(A)	—	2.897%	*NH*3	111	0.044%
Solar-sim	—	4.952%	*CHF*2*Cl*	421	0.034%
Solar-DU	—	2.071%	*HCN*	281	0.003%
*CO*2	2**2**	2.152%	*ClO*	181	0.001%
*C*2*H*2	401	1.602%	*C*2*H*4	391	0.001%
*HNO*3	121	0.751%	*OH*	131	<0.001%
*H*2*O*	11	0.530%	*HO*2	221	<0.001%
*CCl*4	351	0.396%	*N*2*O*5	261	<0.001%
*ClONO*2	271	0.244%	*HDO*	491	<0.001%
*BrNO*2	641	0.165%	*CFC*113	621	<0.001%
*NO*2	101	0.091%			

O_3, Kiruna, φ=71.68^o, OPD=257cm, FoV=4.06$mrad$, boxcar apod.

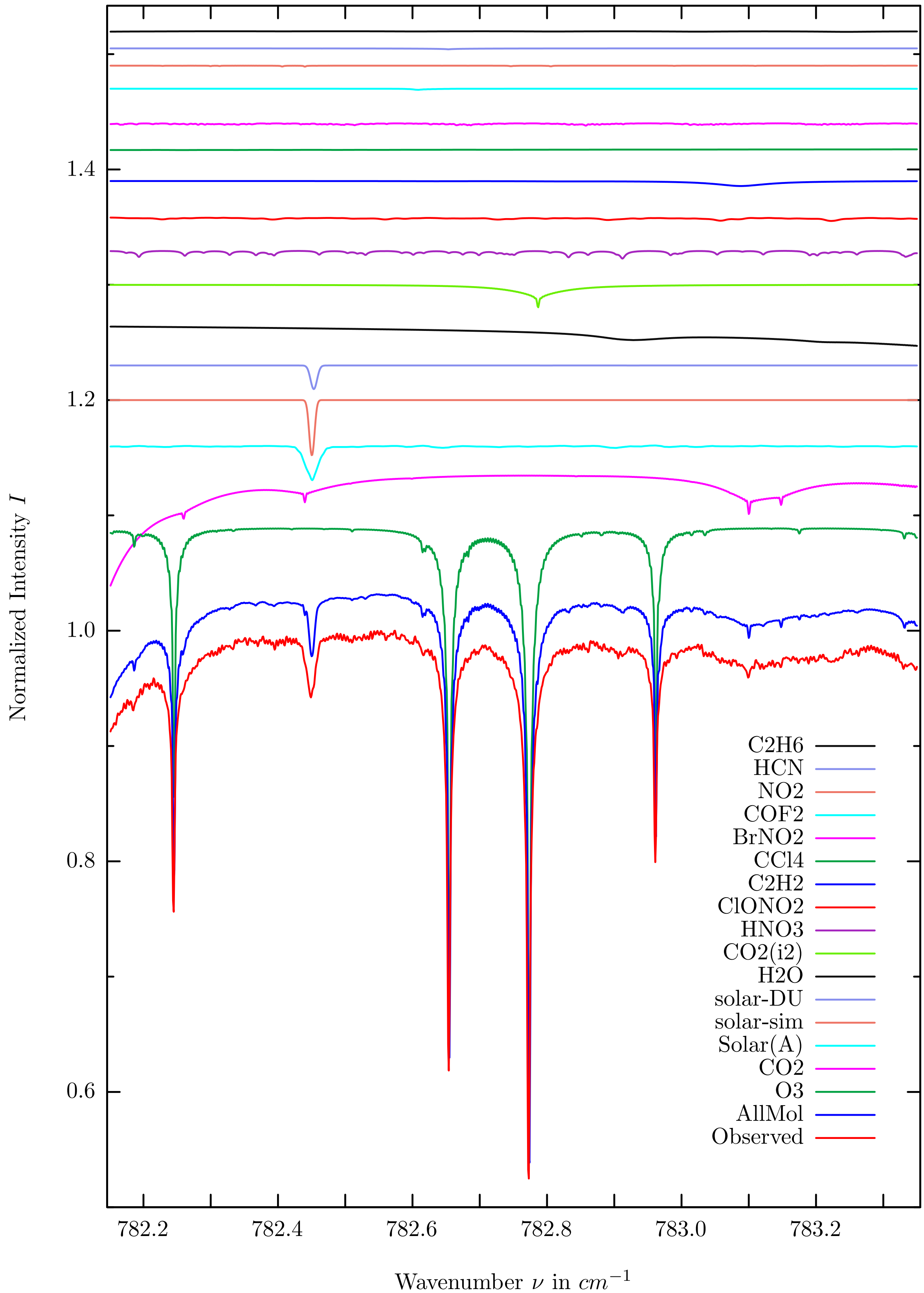

σ=0.270%, 970315S6.92, φ=71.68^o, OPD=257cm, FoV=4.07$mrad$, Apod.=boxcar

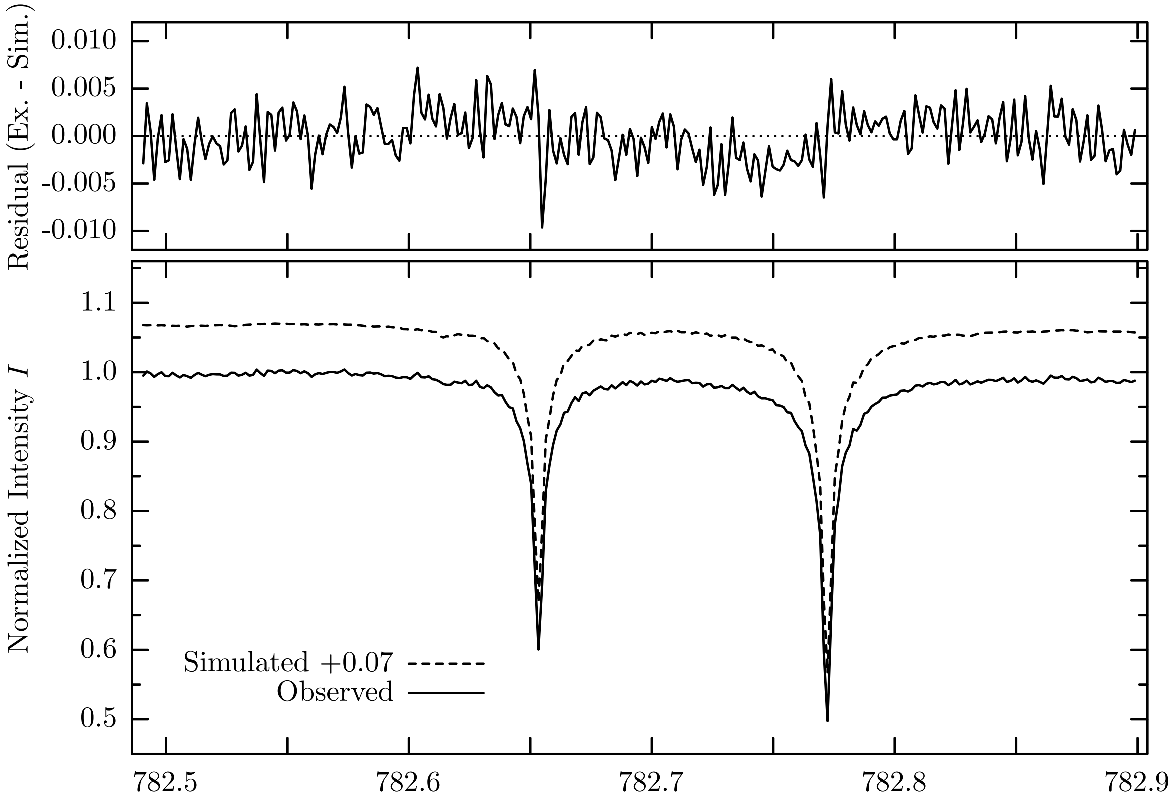

Wavenumber ν in cm^{-1}

investigated species	:	O_3
line position(s) ν_0	:	782.7720 cm^{-1}
lower state energy E''_{lst}	:	376.8 cm^{-1}
retrieved TCA, information content	:	1.03E+19 $molec/cm^2$, 186.8
temperature dependence of the TCA	:	-.150%/K (trop), -.437%/K (strat)
location, date, solar zenith angle	:	Kiruna, 15/Mar/97, 71.68^o
spectral interval fitted	:	782.490 – 782.900 cm^{-1}

Molecule	iCode	Absorption	Molecule	iCode	Absorption
O3	31	58.651%	$NO2$	101	0.096%
$CO2$	21	9.942%	HCN	281	0.083%
Solar(A)	—	2.949%	$C2H6$	381	0.066%
Solar-sim	—	4.834%	$CHF2Cl$	421	0.045%
Solar-DU	—	2.058%	$NH3$	111	0.001%
$H2O$	11	2.296%	ClO	181	0.001%
$CO2$	2**2**	2.190%	OH	131	<0.001%
$HNO3$	121	0.737%	$HO2$	221	<0.001%
$ClONO2$	271	0.465%	$N2O5$	261	<0.001%
$C2H2$	401	0.428%	$C2H4$	391	<0.001%
$CCl4$	351	0.318%	HDO	491	<0.001%
$BrNO2$	641	0.134%	$CFC113$	621	<0.001%
$COF2$	361	0.097%			

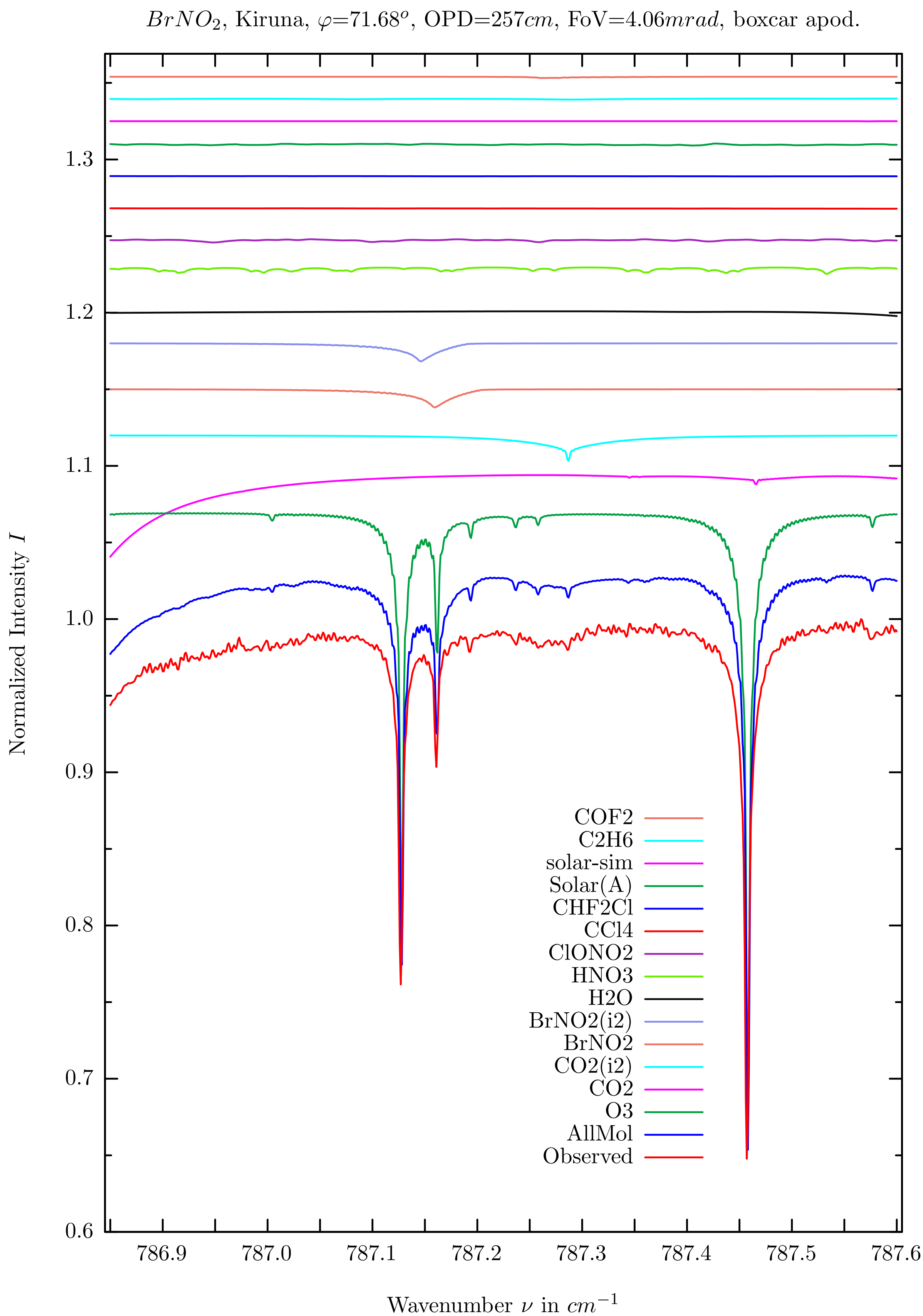

$BrNO_2$, Kiruna, φ=71.68^o, OPD=257cm, FoV=4.06$mrad$, boxcar apod.
Normalized Intensity I
Wavenumber ν in cm^{-1}
1.3
1.2
1.1
1.0
0.9
0.8
0.7
0.6
786.9
787.0
787.1
787.2
787.3
787.4
787.5
787.6
COF2
C2H6
solar-sim
Solar(A)
CHF2Cl
CCl4
ClONO2
HNO3
H2O
BrNO2(i2)
BrNO2
CO2(i2)
CO2
O3
AllMol
Observed

σ=0.304%, 970315S6.92, φ=71.68^o, OPD=257cm, FoV=4.07$mrad$, Apod.=boxcar

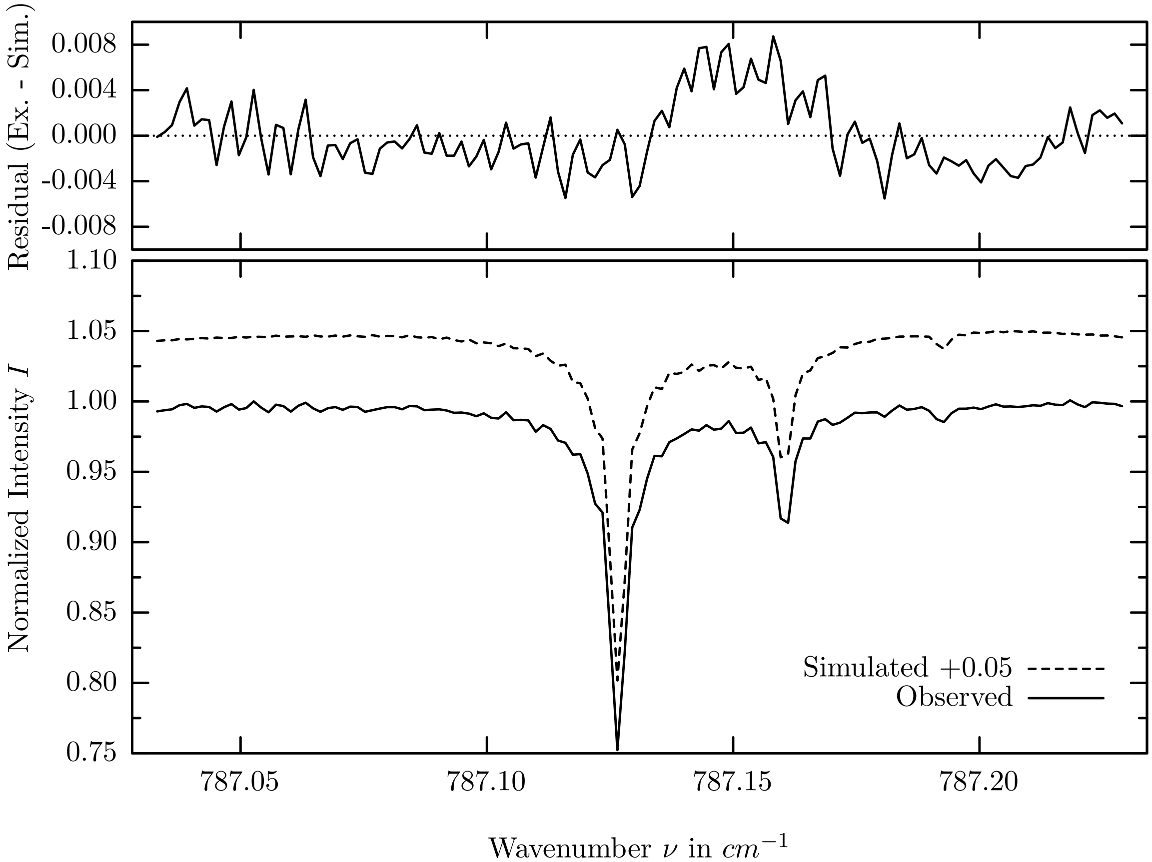

investigated species	:	$BrNO_2, BrNO_2(i2)$
line position(s) ν_0	:	787.1769*$^{)}$, 787.1636*$^{)}$ cm^{-1}
lower state energy E''_{lst}	:	88.2, 88.2 cm^{-1}
retrieved TCA, information content	:	1.31E+15 $molec/cm^2$, 5.4
temperature dependence of the TCA	:	+.019%/K (trop), -.241%/K (strat)
spectral interval fitted	:	787.033 – 787.230 cm^{-1}

Molecule	iCode	Absorption	Molecule	iCode	Absorption
$O3$	31	44.239%	$C2H6$	381	0.088%
$CO2$	21	5.844%	$COF2$	361	0.085%
$CO2$	2**2**	1.880%	$C2H2$	401	0.027%
BRNO2	641	1.200%	$NH3$	111	0.018%
BRNO2	64**2**	1.197%	$NO2$	101	0.013%
$H2O$	11	0.503%	HCN	281	0.003%
$HNO3$	121	0.477%	$C2H4$	391	0.001%
$ClONO2$	271	0.416%	$CFC113$	621	0.001%
$CCl4$	351	0.214%	OH	131	<0.001%
$CHF2Cl$	421	0.102%	ClO	181	<0.001%
Solar(A)	—	0.090%	$HO2$	221	<0.001%
Solar-sim	—	0.008%	HDO	491	<0.001%

Comment: Spectroscopic line data of $BrNO_2$ kindly provided by Johannes Orphal, University Pierre et Marie Curie, Paris, (email: johannes.orphal@ppm.u-psud.fr, not included on the DVD).

H_2O, Kiruna, φ=71.68^o, OPD=257cm, FoV=4.06$mrad$, boxcar apod.

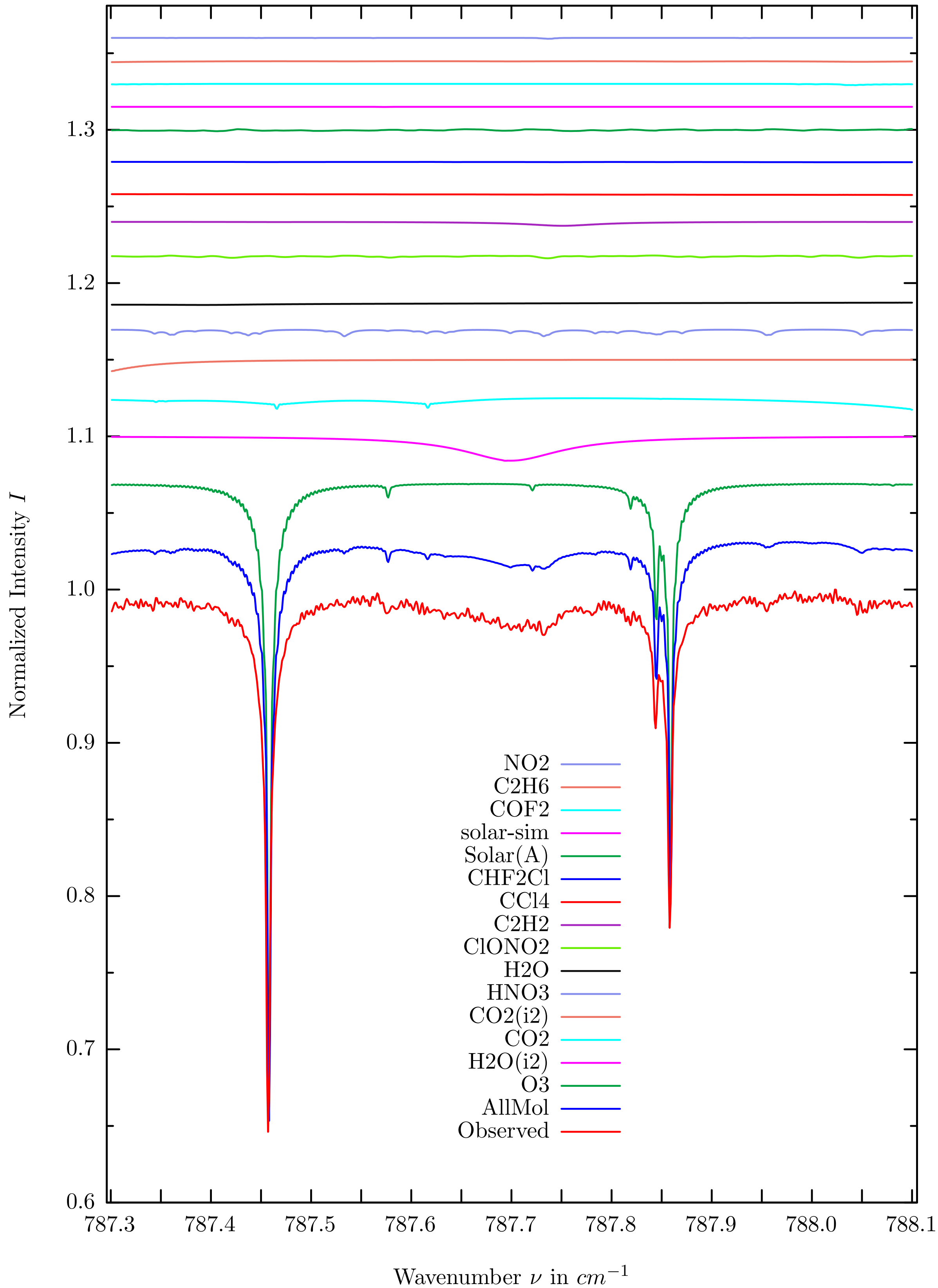

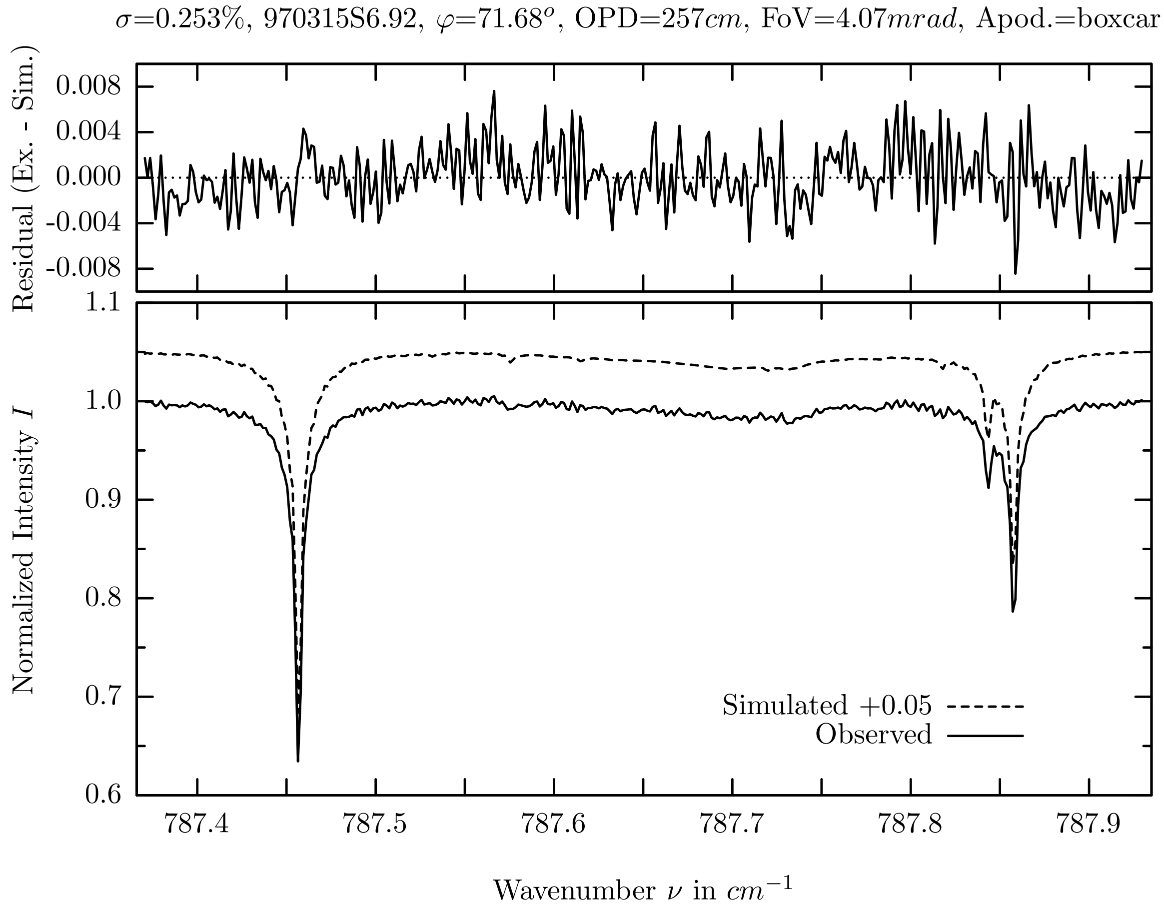

investigated species	:	$H_2O(i2 = H_2{}^{18}O)$
line position(s) ν_0	:	787.6918 cm^{-1}
lower state energy E''_{lst}	:	1074.8 cm^{-1}
retrieved TCA, information content	:	6.44E+21 $molec/cm^2$, 7.0
temperature dependence of the TCA	:	-2.009%/K (trop), +.163%/K (strat)
location, date, solar zenith angle	:	Kiruna, 15/Mar/97, 71.68^o
spectral interval fitted	:	787.370 – 787.930 cm^{-1}

Molecule	iCode	Absorption	Molecule	iCode	Absorption
$O3$	31	44.239%	$COF2$	361	0.088%
H2O	1**2**	1.597%	$C2H6$	381	0.082%
$CO2$	21	1.340%	$NO2$	101	0.060%
$CO2$	2**2**	0.739%	$BrNO2$	641	0.026%
$HNO3$	121	0.477%	$NH3$	111	0.024%
$H2O$	11	0.427%	HCN	281	0.003%
$ClONO2$	271	0.383%	$C2H4$	391	0.002%
$C2H2$	401	0.260%	$CFC113$	621	0.001%
$CCl4$	351	0.250%	OH	131	<0.001%
$CHF2Cl$	421	0.115%	ClO	181	<0.001%
Solar(A)	—	0.090%	$HO2$	221	<0.001%
Solar-sim	—	0.008%	HDO	491	<0.001%
Solar-DU	—	0.008%			

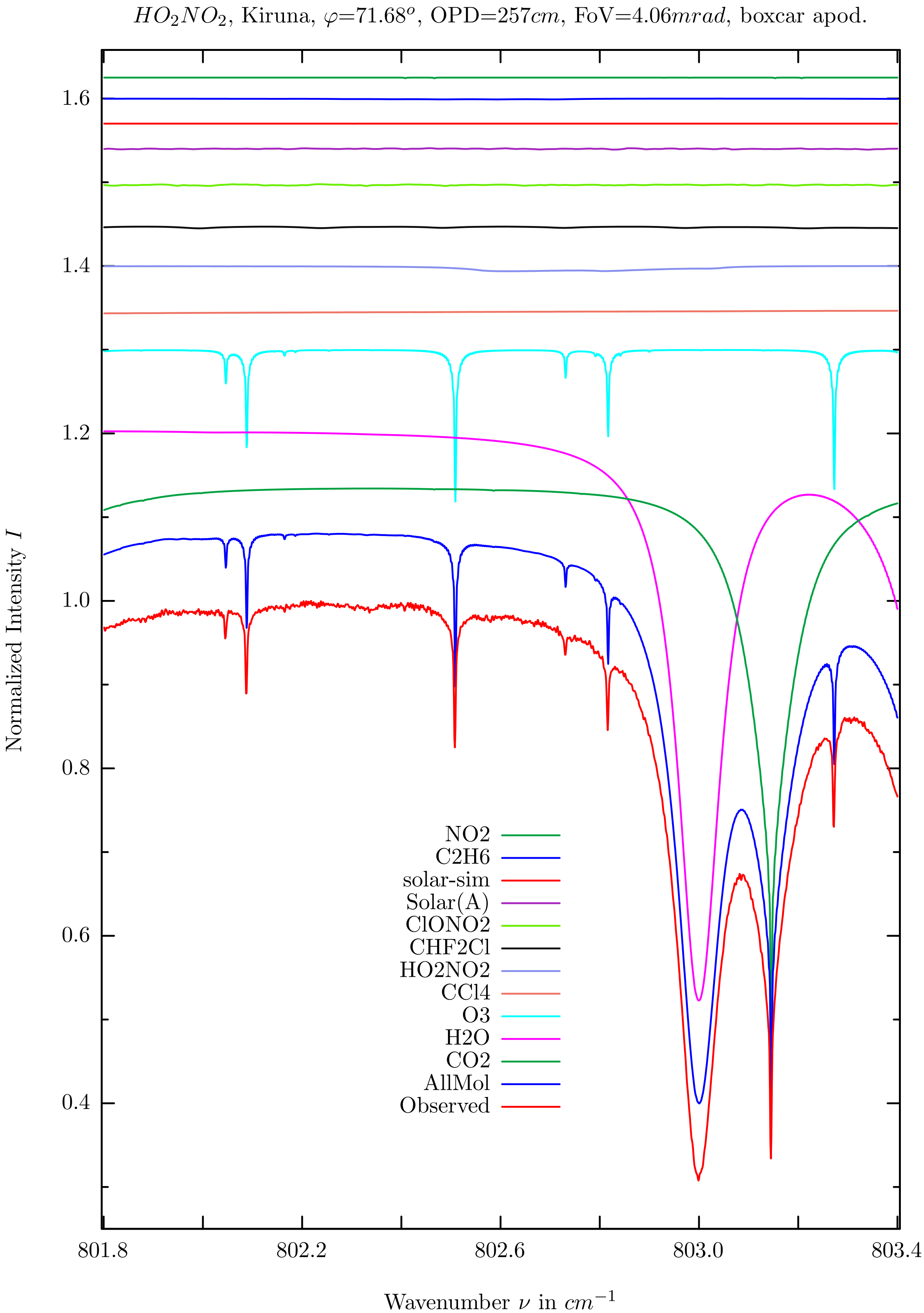
HO_2NO_2, Kiruna, φ=71.68^o, OPD=257cm, FoV=4.06$mrad$, boxcar apod.
Normalized Intensity I
Wavenumber ν in cm^{-1}
1.6
1.4
1.2
1.0
0.8
0.6
0.4
801.8
802.2
802.6
803.0
803.4
NO2
C2H6
solar-sim
Solar(A)
ClONO2
CHF2Cl
HO2NO2
CCl4
O3
H2O
CO2
AllMol
Observed

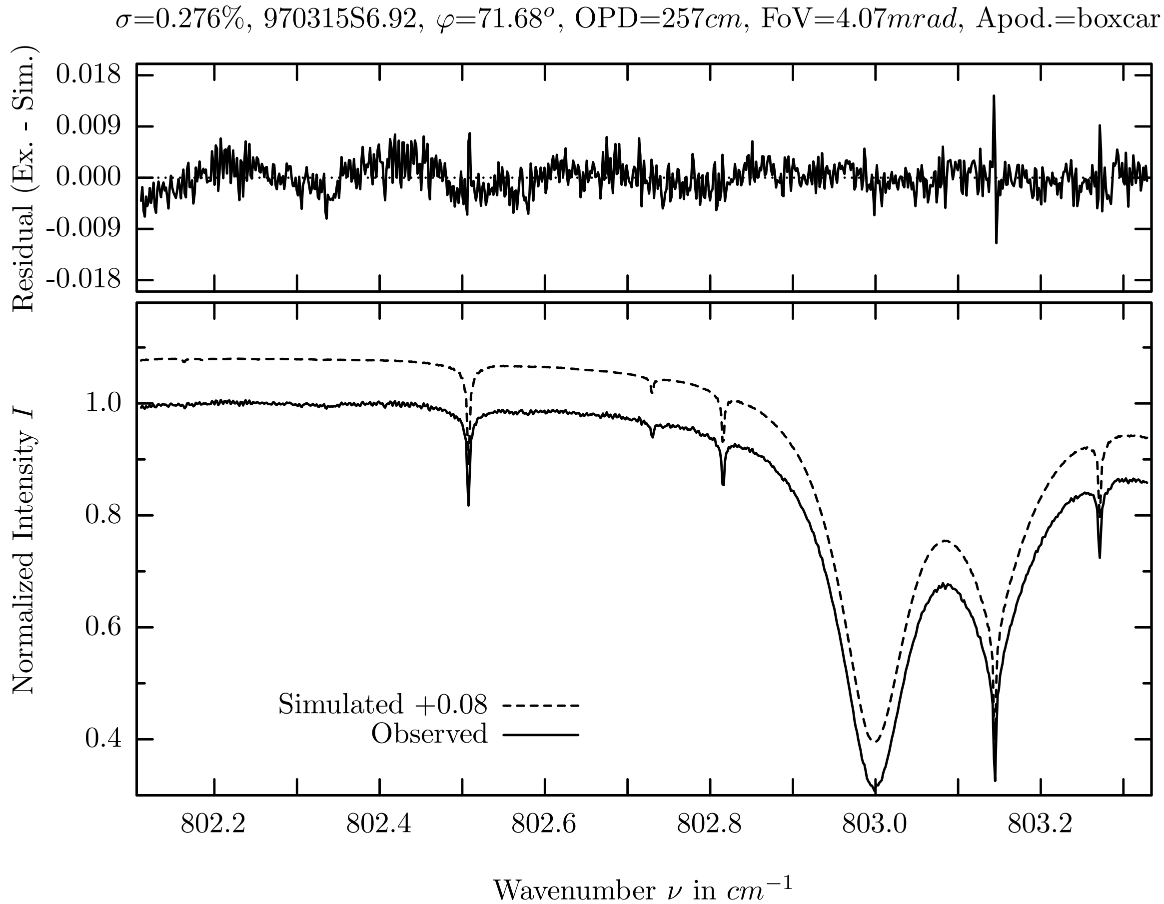

investigated species	:	HO_2NO_2
line position(s) ν_0	:	802.5797*) cm^{-1}
lower state energy E''_{lst}	:	171.3 cm^{-1}
retrieved TCA, information content	:	3.28E+14 $molec/cm^2$, 3.3
temperature dependence of the TCA	:	-11.659%/K (trop), -11.369%/K (strat)
location, date, solar zenith angle	:	Kiruna, 15/Mar/97, 71.68^o
spectral interval fitted	:	802.110 – 803.330 cm^{-1}

Molecule	iCode	Absorption	Molecule	iCode	Absorption
$CO2$	21	71.587%	$COF2$	361	0.017%
$H2O$	11	68.738%	ClO	181	0.007%
$O3$	31	21.533%	$C2H2$	401	0.007%
$CCl4$	351	0.660%	HCN	281	0.003%
HO2NO2	251	0.634%	$CFC113$	621	0.001%
$CHF2Cl$	421	0.505%	$NH3$	111	<0.001%
$ClONO2$	271	0.445%	OH	131	<0.001%
Solar(A)	—	0.110%	$HO2$	221	<0.001%
Solar-sim	—	0.002%	$CCl3F$	331	<0.001%
Solar-DU	—	0.007%	$C2H4$	391	<0.001%
$C2H6$	381	0.108%	HDO	491	<0.001%
$NO2$	101	0.097%	$BrNO2$	641	<0.001%
$HNO3$	121	0.047%			

H_2O, Kiruna, φ=71.68^o, OPD=257cm, FoV=4.06$mrad$, boxcar apod.

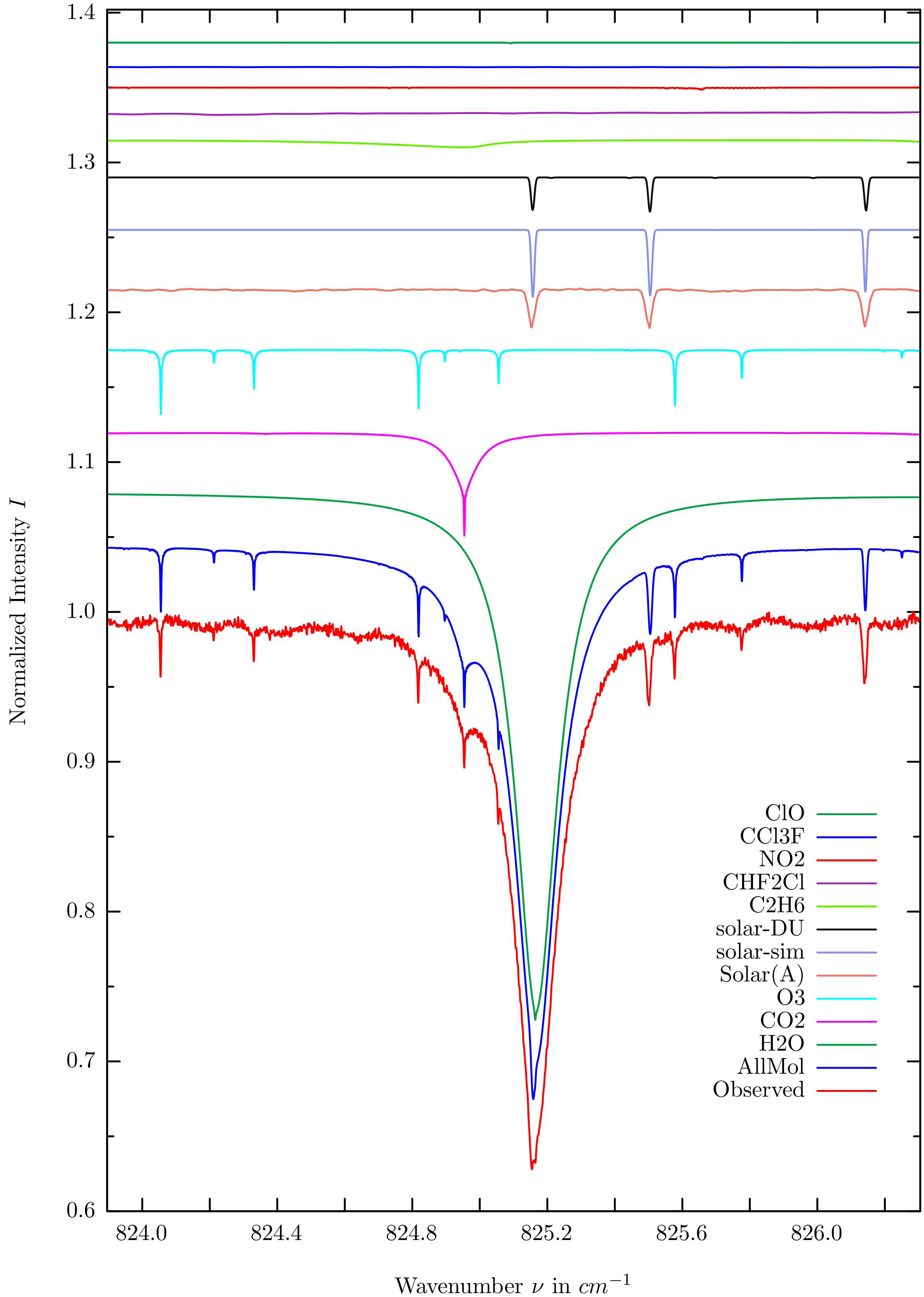

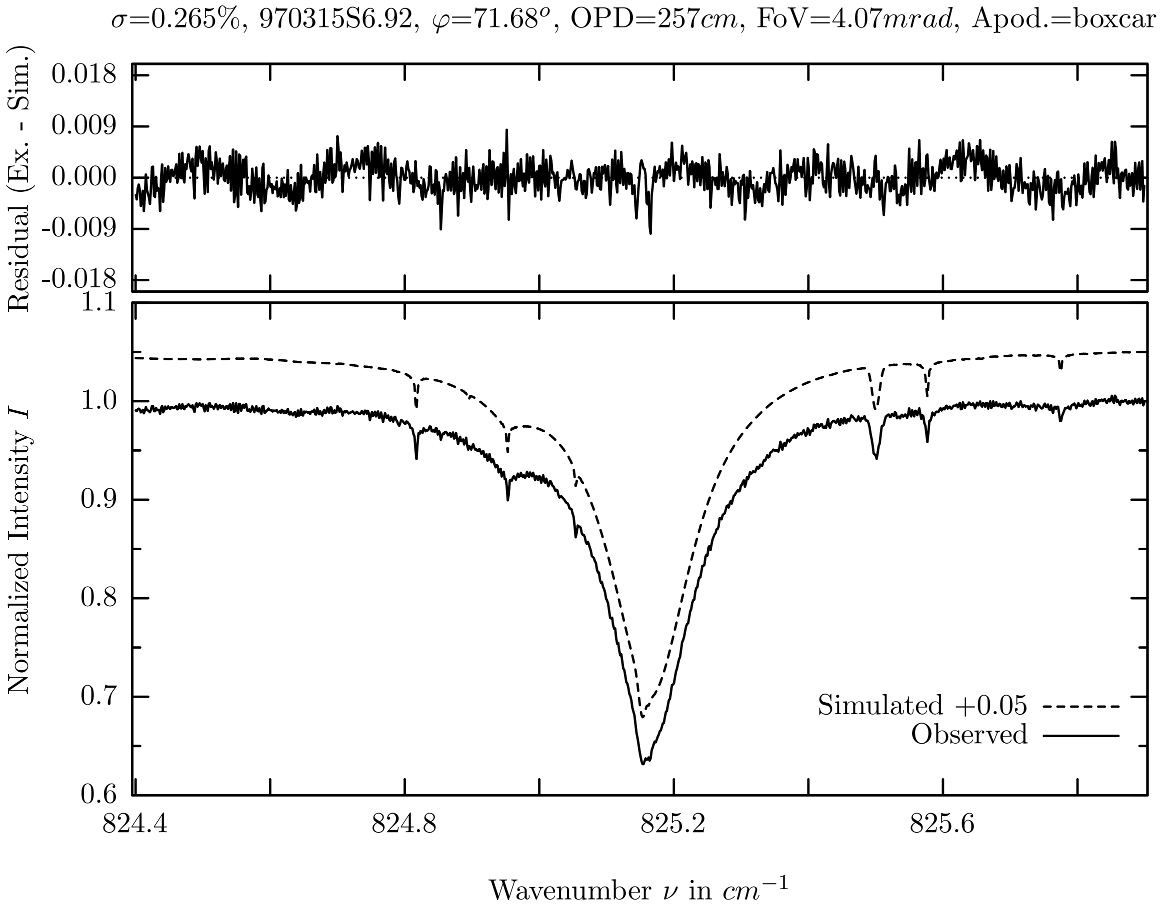

investigated species	:	H_2O
line position(s) ν_0	:	825.1627 cm^{-1}
lower state energy E''_{lst}	:	586.5 cm^{-1}
retrieved TCA, information content	:	5.55E+21 $molec/cm^2$, 135.6
temperature dependence of the TCA	:	-.808%/K (trop), +.003%/K (strat)
location, date, solar zenith angle	:	Kiruna, 15/Mar/97, 71.68^o
spectral interval fitted	:	824.400 – 825.900 cm^{-1}

Molecule	iCode	Absorption	Molecule	iCode	Absorption
H2O	11	35.296%	HDO	491	0.009%
$CO2$	21	7.910%	$NH3$	111	0.008%
$O3$	31	5.286%	$CFC113$	621	0.005%
Solar(A)	—	2.549%	$HNO3$	121	0.004%
Solar-sim	—	4.511%	OCS	191	0.004%
Solar-DU	—	2.292%	$COF2$	361	0.001%
$C2H6$	381	0.484%	$C2H4$	391	0.001%
$CHF2Cl$	421	0.326%	$C2H2$	401	0.001%
$NO2$	101	0.163%	$COCl2$	431	0.001%
$CCl3F$	331	0.153%	OH	131	<0.001%
ClO	181	0.066%	$N2O5$	261	<0.001%
$ClONO2$	271	0.032%	HCN	281	<0.001%

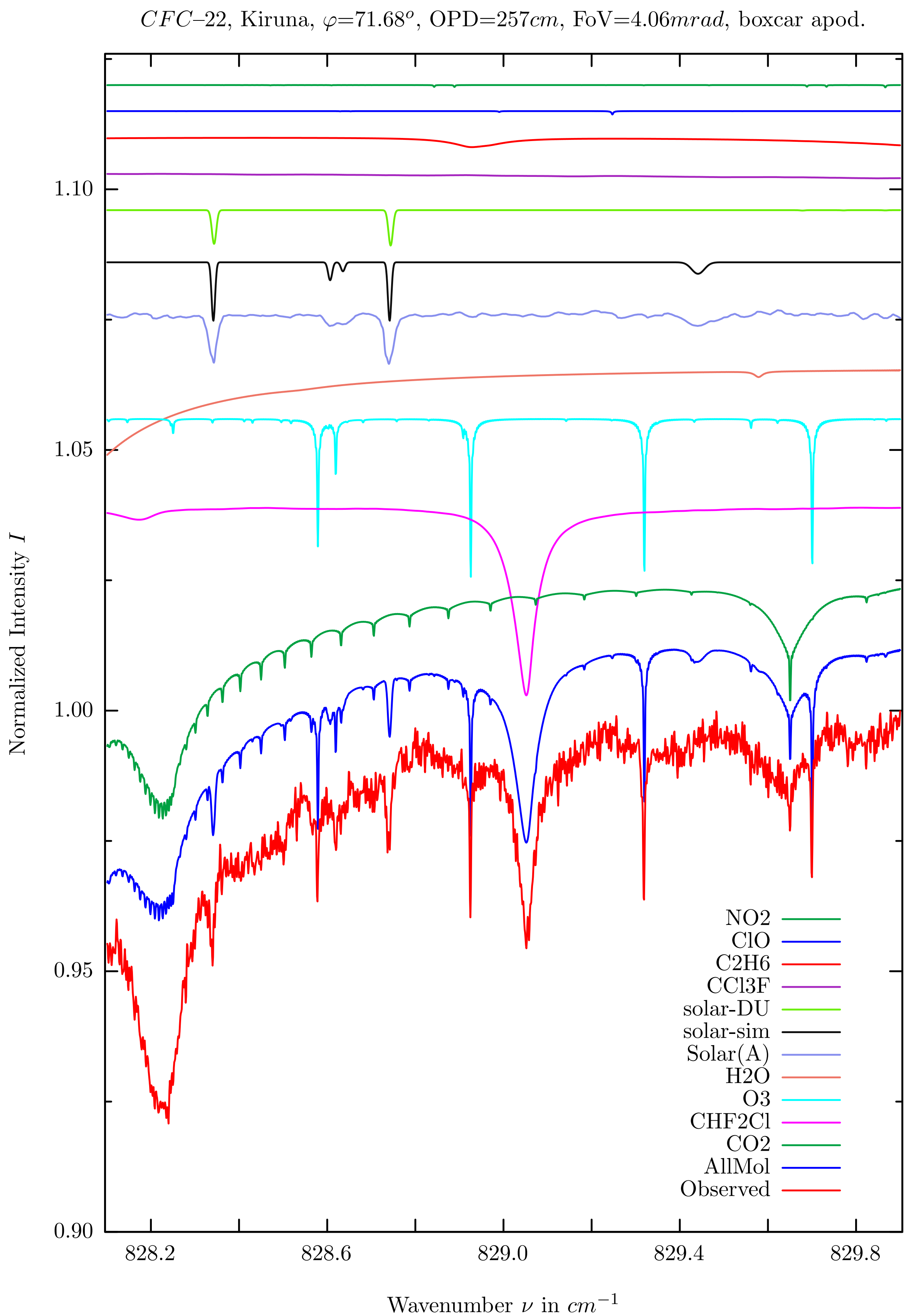
CFC–22, Kiruna, φ=71.68^o, OPD=257cm, FoV=4.06$mrad$, boxcar apod.
Normalized Intensity I
1.10
1.05
1.00
0.95
0.90
828.2
828.6
829.0
829.4
829.8
Wavenumber ν in cm^{-1}
NO2
ClO
C2H6
CCl3F
solar-DU
solar-sim
Solar(A)
H2O
O3
CHF2Cl
CO2
AllMol
Observed

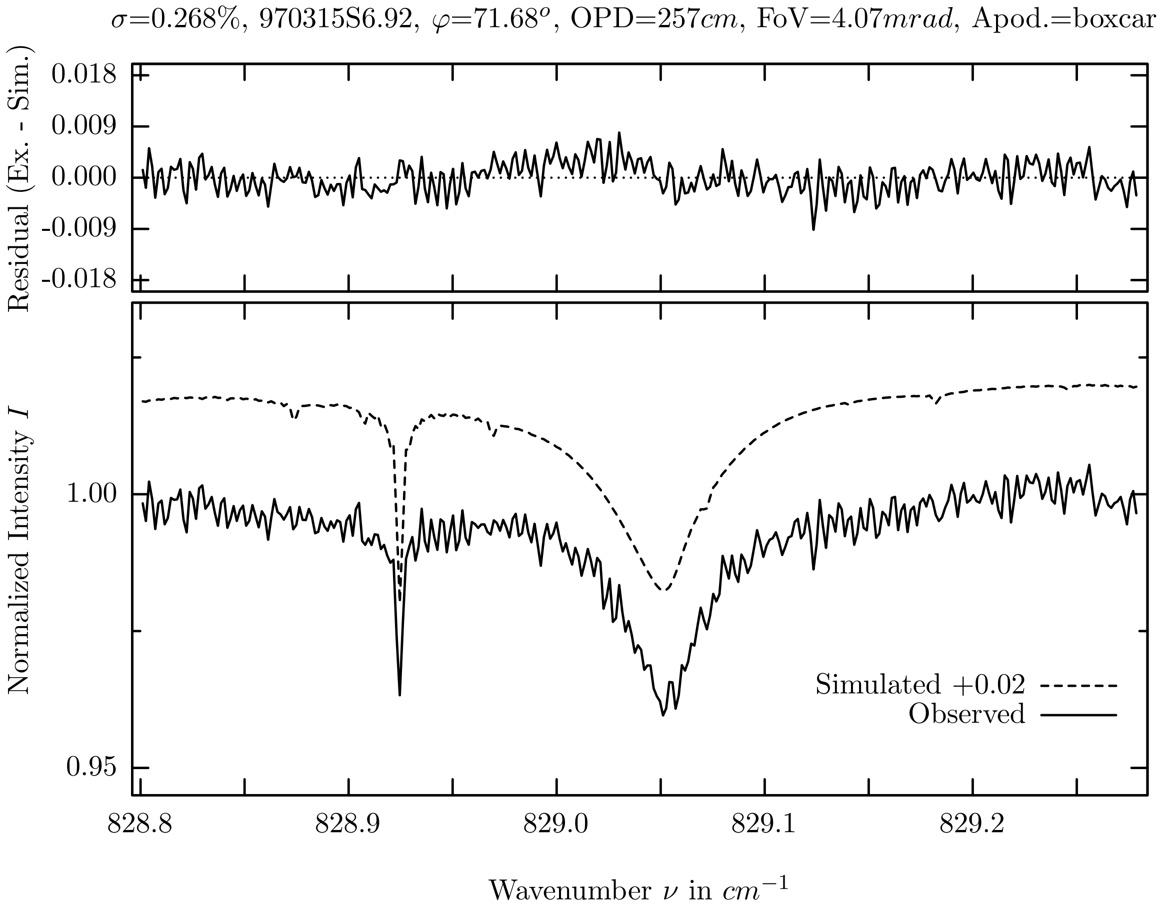

investigated species	:	CHF_2Cl(Freon22)
line position(s) ν_0	:	829.0551 cm^{-1}
lower state energy E''_{lst}	:	169.0 cm^{-1}
retrieved TCA, information content	:	2.65E+15 $molec/cm^2$, 13.8
temperature dependence of the TCA	:	+.004%/K (trop), -.006%/K (strat)
location, date, solar zenith angle	:	Kiruna, 15/Mar/97, 71.68^o
spectral interval fitted	:	828.800 – 829.280 cm^{-1}

Molecule	iCode	Absorption	Molecule	iCode	Absorption
$CO2$	21	4.690%	OCS	191	0.010%
CHF2Cl	421	3.709%	$NH3$	111	0.009%
$O3$	31	3.682%	$HNO3$	121	0.008%
$H2O$	11	1.685%	$COCl2$	431	0.005%
Solar(A)	—	0.950%	$C2H4$	391	0.001%
Solar-sim	—	1.131%	$C2H2$	401	0.001%
Solar-DU	—	0.683%	$CFC113$	621	0.001%
$CCl3F$	331	0.289%	OH	131	<0.001%
$C2H6$	381	0.191%	HCN	281	<0.001%
ClO	181	0.074%	$COF2$	361	<0.001%
$NO2$	101	0.054%	HDO	491	<0.001%
$ClONO2$	271	0.033%			

ClO, Kiruna, φ=71.68^o, OPD=257cm, FoV=4.06$mrad$, boxcar apod.

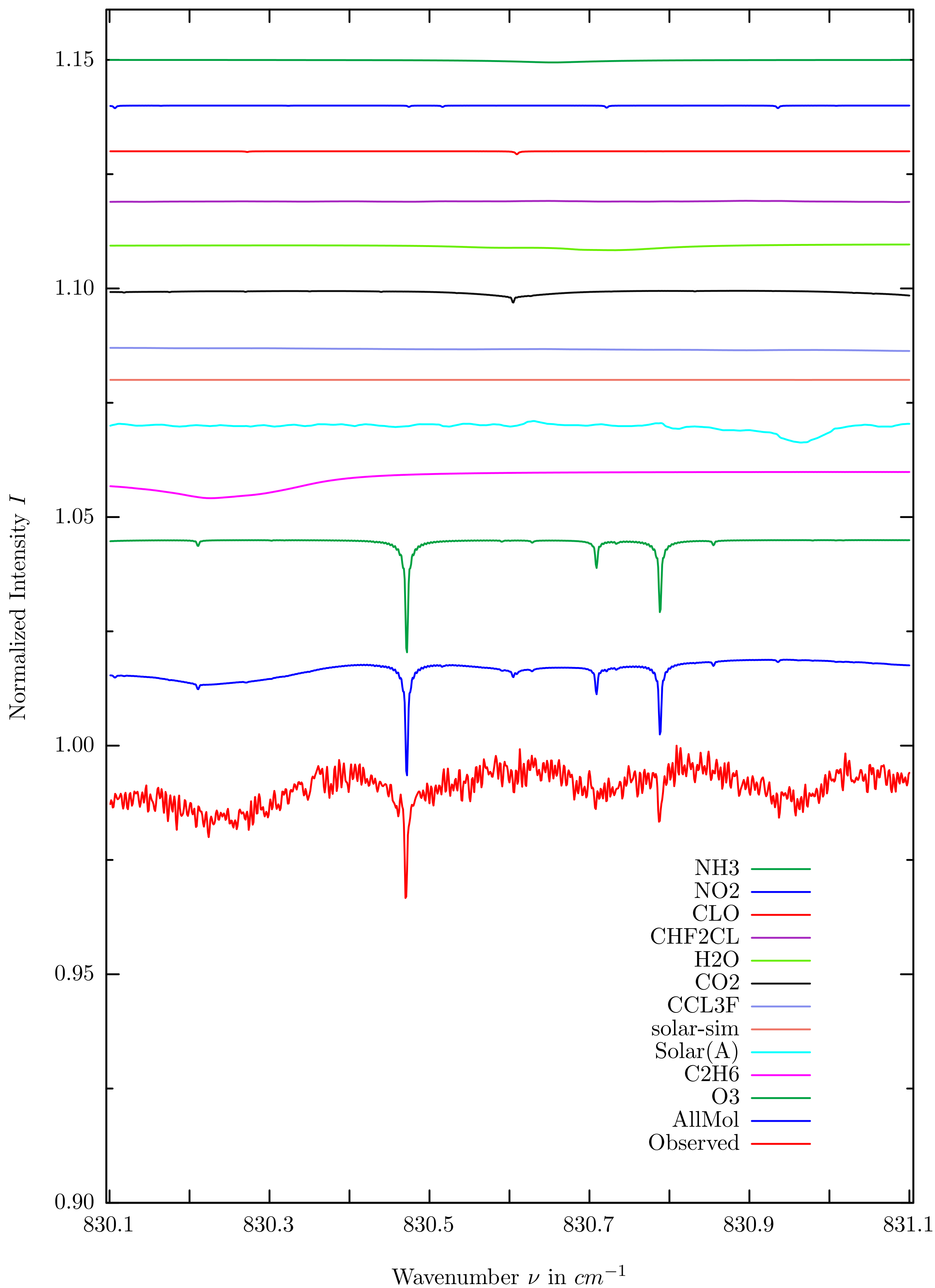

σ=0.233%, 970315S6.92, φ=71.68^o, OPD=257cm, FoV=4.07$mrad$, Apod.=boxcar

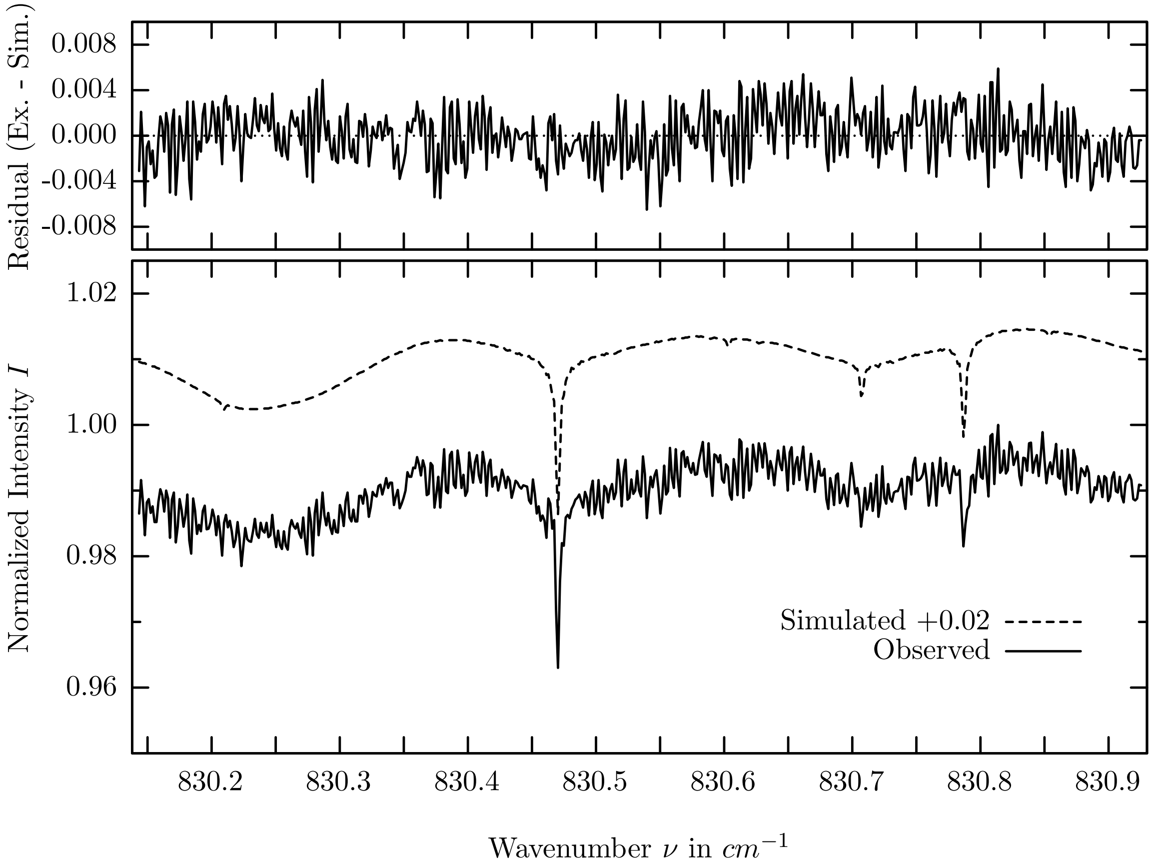

investigated species	:	ClO
line position(s) ν_0	:	830.6077 cm^{-1}
lower state energy E''_{lst}	:	72.5 cm^{-1}
retrieved TCA, information content	:	<1.00E+14 $molec/cm^2$, <0.5
temperature dependence of the TCA	:	N.A.%/K (trop), N.A.%/K (strat)
location, date, solar zenith angle	:	Kiruna, 15/Mar/97, 71.68^o
spectral interval fitted	:	830.142 – 830.926 cm^{-1}

Molecule	iCode	Absorption	Molecule	iCode	Absorption
$O3$	31	3.078%	$ClONO2$	271	0.034%
$C2H6$	381	0.587%	OCS	191	0.016%
Solar(A)	—	0.370%	$HNO3$	121	0.014%
Solar-sim	—	0.001%	$COCl2$	431	0.009%
$CCl3F$	331	0.367%	$C2H4$	391	0.001%
$CO2$	21	0.355%	$CFC113$	621	0.001%
$H2O$	11	0.163%	OH	131	<0.001%
$CHF2Cl$	421	0.109%	HCN	281	<0.001%
ClO	181	0.073%	$COF2$	361	<0.001%
$NO2$	101	0.065%	$C2H2$	401	<0.001%
$NH3$	111	0.056%	HDO	491	<0.001%

Comment: ClO is below the detection limit. Analysis further hampered by standing waves.

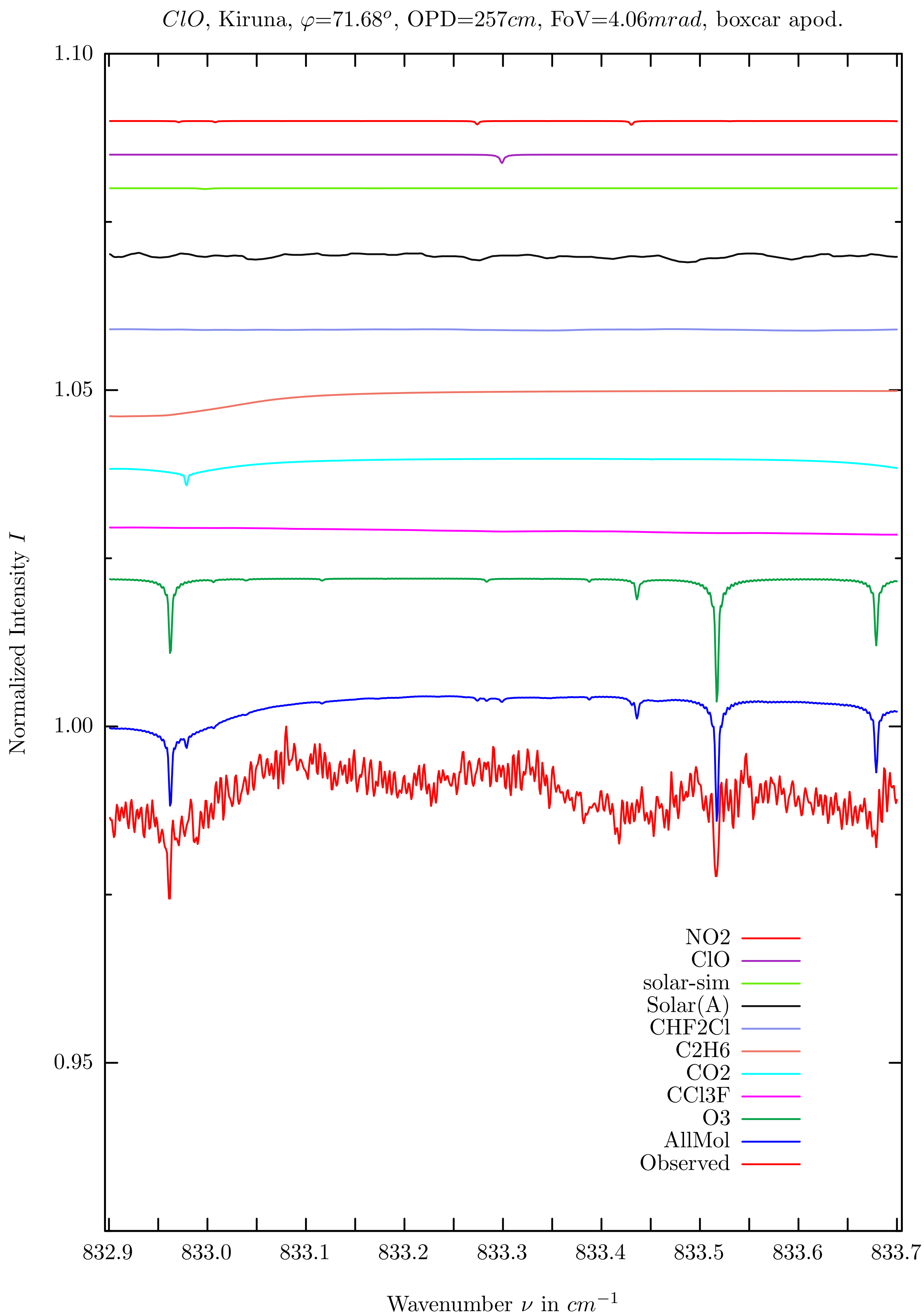
ClO, Kiruna, φ=71.68^o, OPD=257cm, FoV=4.06$mrad$, boxcar apod.
Normalized Intensity I
Wavenumber ν in cm^{-1}
1.10
1.05
1.00
0.95
832.9
833.0
833.1
833.2
833.3
833.4
833.5
833.6
833.7
NO2
ClO
solar-sim
Solar(A)
CHF2Cl
C2H6
CO2
CCl3F
O3
AllMol
Observed

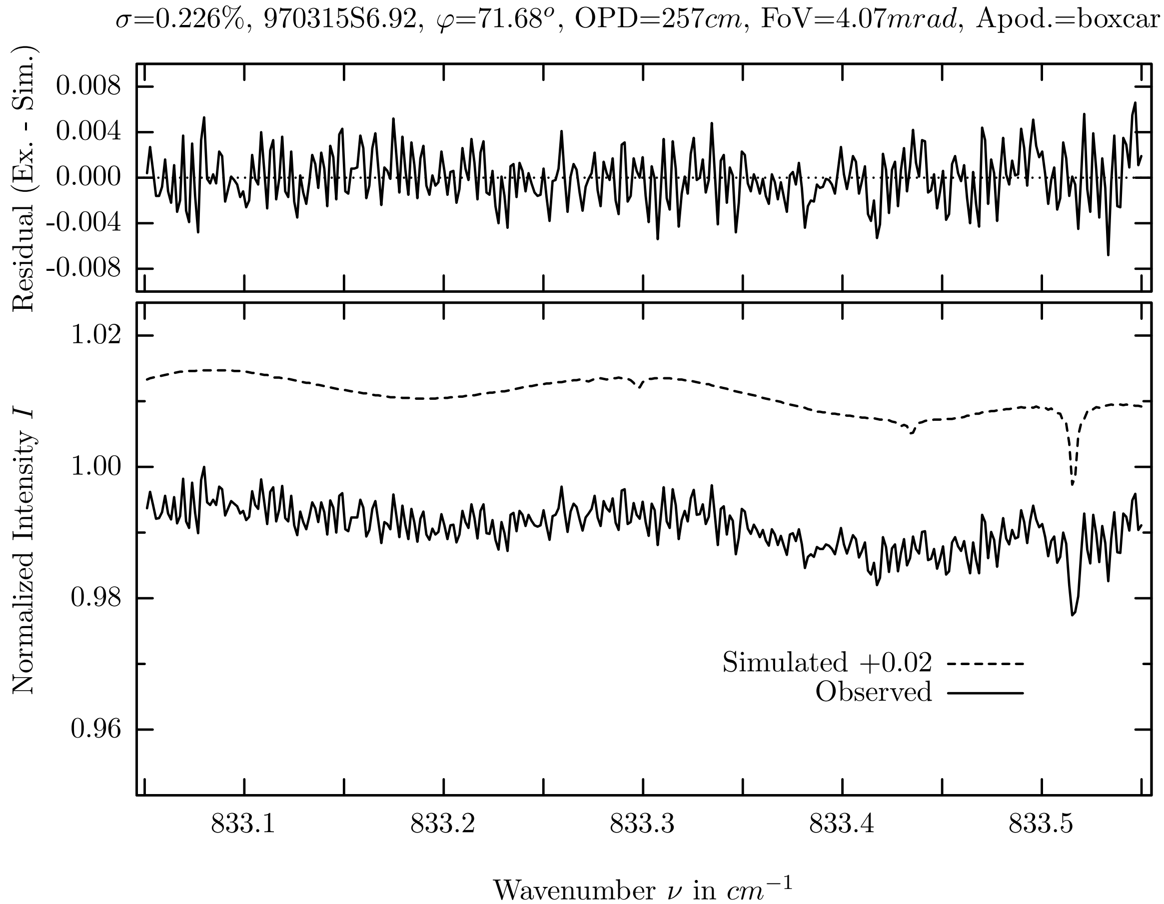

investigated species	:	*ClO*
line position(s) ν_0	:	833.2974 cm^{-1}
lower state energy E''_{lst}	:	47.7 cm^{-1}
retrieved TCA, information content	:	<1.00E+14 $molec/cm^2$, <0.5
temperature dependence of the TCA	:	N.A.%/K (trop), N.A.%/K (strat)
location, date, solar zenith angle	:	Kiruna, 15/Mar/97, 71.68^o
spectral interval fitted	:	833.050 – 833.550 cm^{-1}

Molecule	iCode	Absorption	Molecule	iCode	Absorption
O3	31	2.264%	*H2O*	11	0.029%
CCl3F	331	0.649%	*COCl2*	431	0.029%
CO2	21	0.471%	*HNO3*	121	0.018%
C2H6	381	0.392%	*NH3*	111	0.012%
CHF2Cl	421	0.117%	*C2H4*	391	0.001%
Solar(A)	—	0.100%	*CFC113*	621	0.001%
Solar-sim	—	0.011%	*OH*	131	<0.001%
Solar-DU	—	0.009%	*HO2*	221	<0.001%
CLO	181	0.071%	*HCN*	281	<0.001%
NO2	101	0.067%	*COF2*	361	<0.001%
OCS	191	0.034%	*C2H2*	401	<0.001%
ClONO2	271	0.031%	*HDO*	491	<0.001%

Comment: ClO is below the detection limit. Analysis further hampered by standing waves.

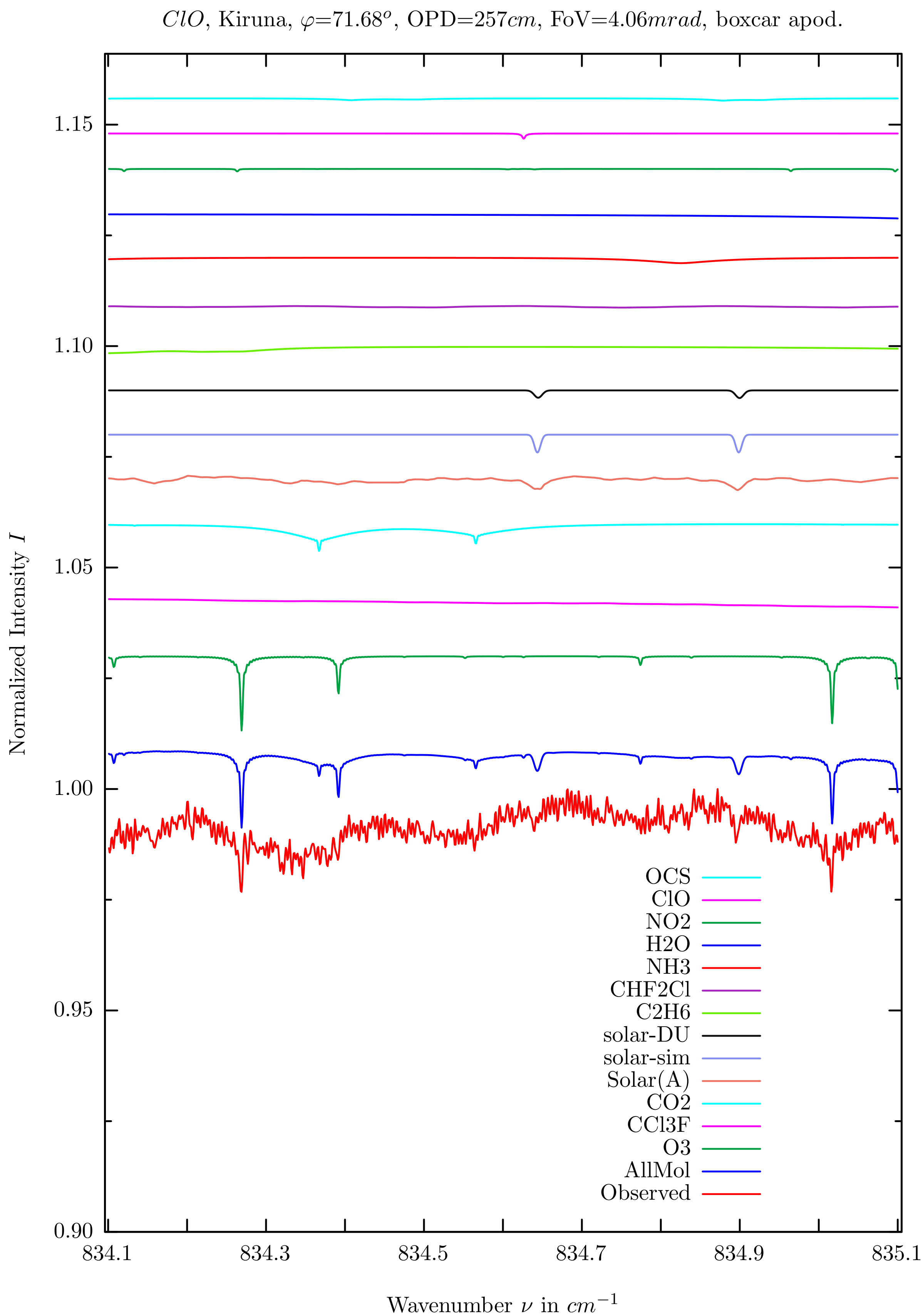

ClO, Kiruna, φ=71.68^o, OPD=257cm, FoV=4.06$mrad$, boxcar apod.
Normalized Intensity I
Wavenumber ν in cm^{-1}
1.15
1.10
1.05
1.00
0.95
0.90
834.1
834.3
834.5
834.7
834.9
835.1
OCS
ClO
NO2
H2O
NH3
CHF2Cl
C2H6
solar-DU
solar-sim
Solar(A)
CO2
CCl3F
O3
AllMol
Observed

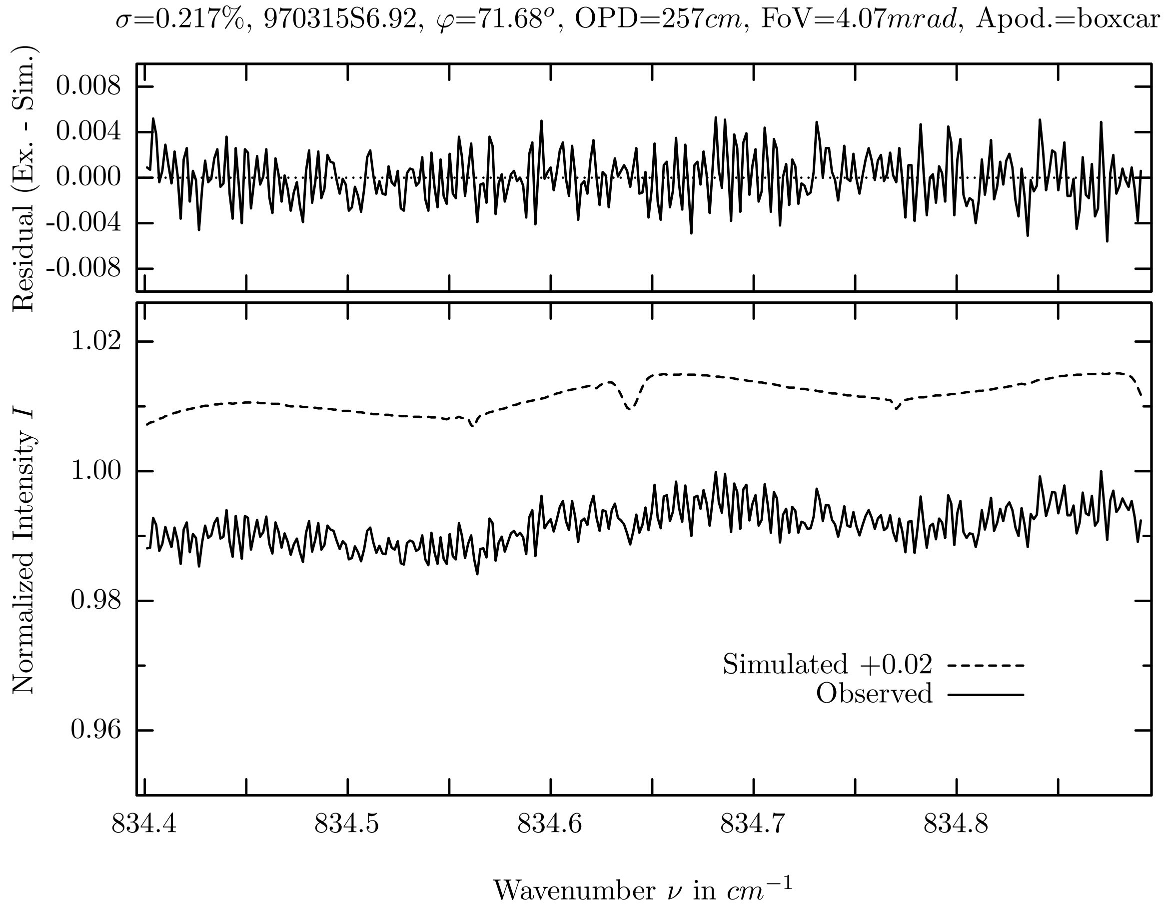

investigated species	:	ClO
line position(s) ν_0	:	834.6249 cm^{-1}
lower state energy E''_{lst}	:	37.2 cm^{-1}
retrieved TCA, information content	:	<1.00E+14 $molec/cm^2$, <0.5
temperature dependence of the TCA	:	N.A.%/K (trop), N.A.%/K (strat)
location, date, solar zenith angle	:	Kiruna, 15/Mar/97, 71.68^o
spectral interval fitted	:	834.400 – 834.892 cm^{-1}

Molecule	iCode	Absorption	Molecule	iCode	Absorption
$O3$	31	2.086%	OCS	191	0.052%
$CCl3F$	331	0.899%	$COCl2$	431	0.043%
$CO2$	21	0.714%	$ClONO2$	271	0.029%
Solar(A)	—	0.250%	$HNO3$	121	0.020%
Solar-sim	—	0.406%	HDO	491	0.009%
Solar-DU	—	0.174%	$C2H4$	391	0.002%
$C2H6$	381	0.159%	$CFC113$	621	0.001%
$CHF2Cl$	421	0.130%	OH	131	<0.001%
$NH3$	111	0.127%	$HO2$	221	<0.001%
$H2O$	11	0.118%	HCN	281	<0.001%
$NO2$	101	0.067%	$C2H2$	401	<0.001%
CLO	181	0.067%			

Comment: ClO is below the detection limit. Analysis further hampered by standing waves.

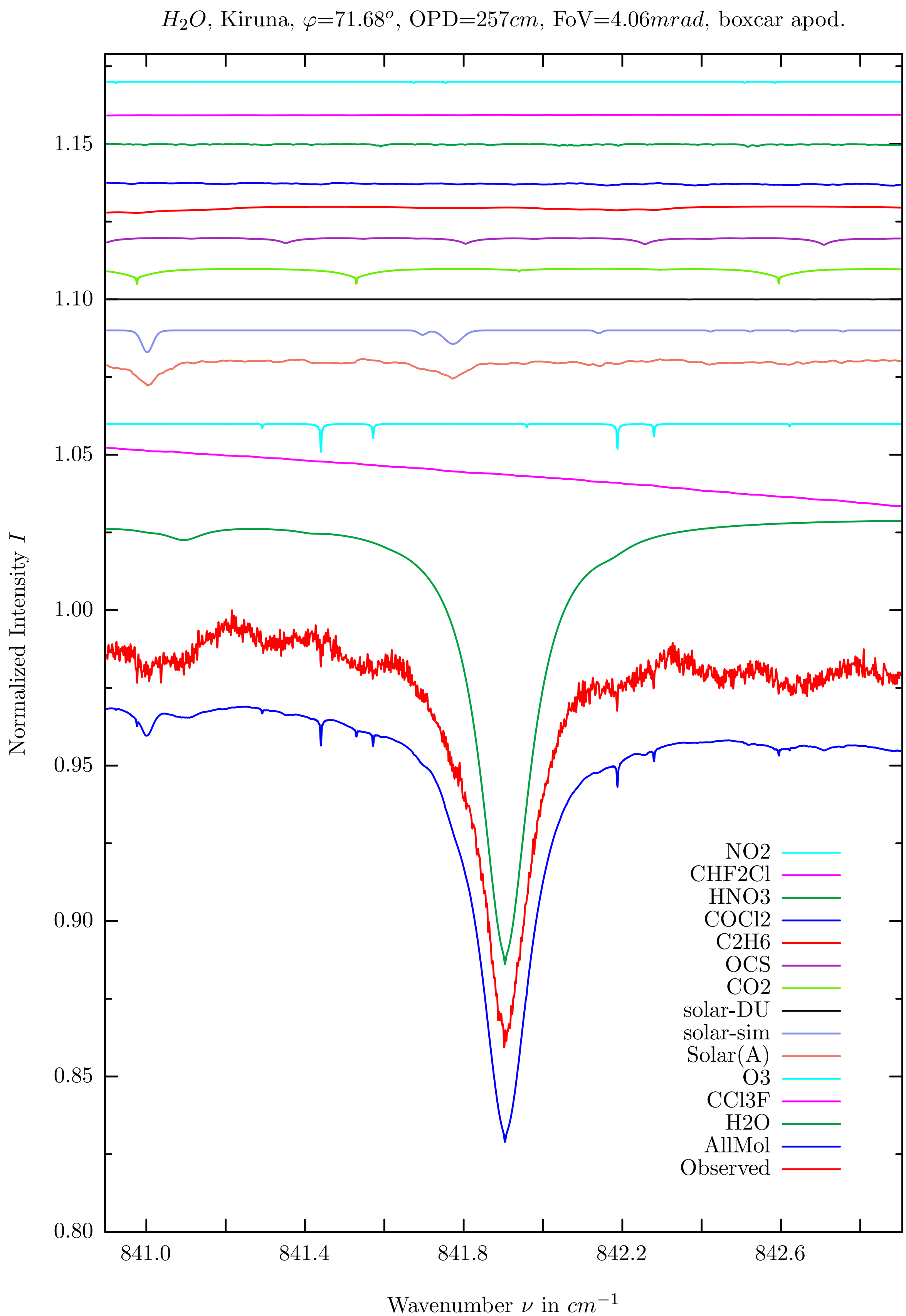

H_2O, Kiruna, φ=71.68^o, OPD=257cm, FoV=4.06$mrad$, boxcar apod.
Normalized Intensity I
Wavenumber ν in cm^{-1}
1.15
1.10
1.05
1.00
0.95
0.90
0.85
0.80
841.0
841.4
841.8
842.2
842.6
NO2
CHF2Cl
HNO3
COCl2
C2H6
OCS
CO2
solar-DU
solar-sim
Solar(A)
O3
CCl3F
H2O
AllMol
Observed

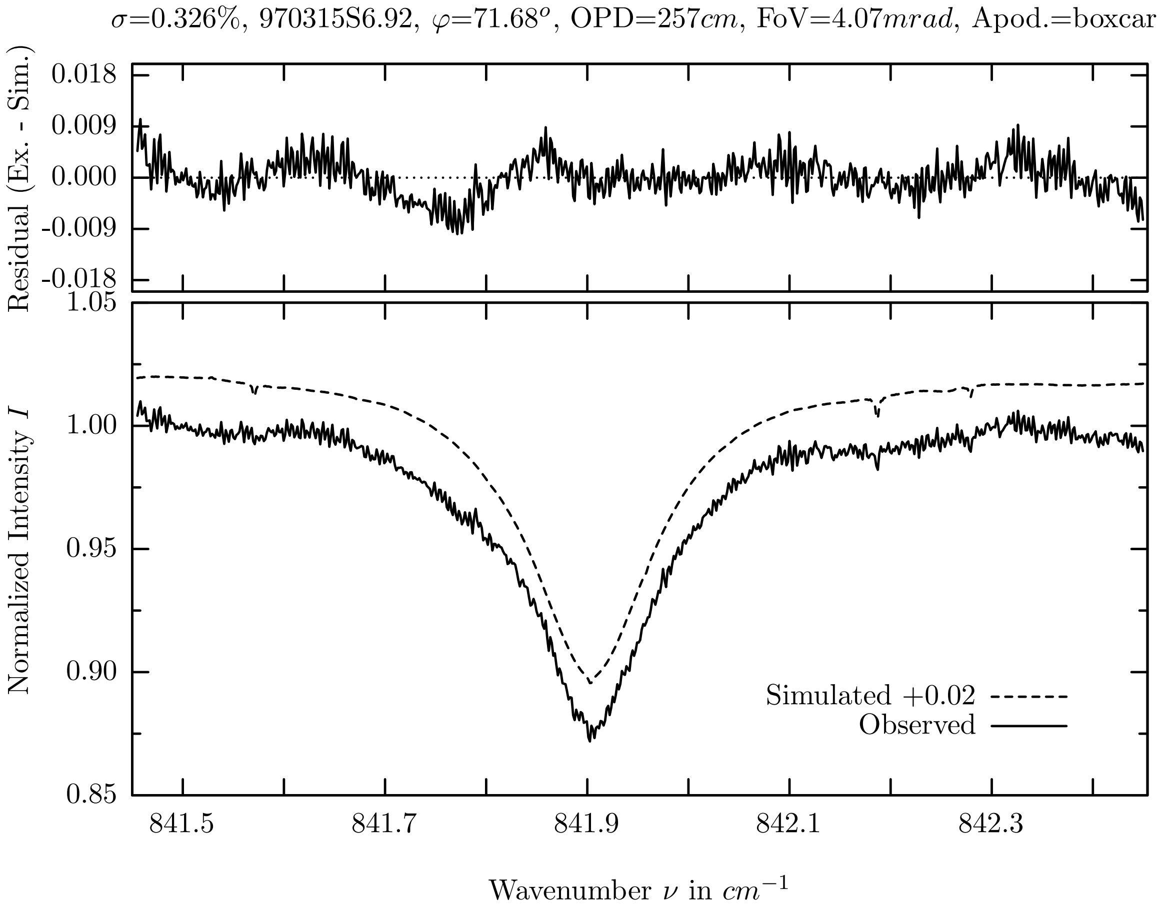

investigated species	:	H_2O
line position(s) ν_0	:	841.9028 cm^{-1}
lower state energy E''_{lst}	:	552.9 cm^{-1}
retrieved TCA, information content	:	4.80E+21 $molec/cm^2$, 38.2
temperature dependence of the TCA	:	-.822%/K (trop), -.002%/K (strat)
location, date, solar zenith angle	:	Kiruna, 15/Mar/97, 71.68^o
spectral interval fitted	:	841.455 – 842.450 cm^{-1}

Molecule	iCode	Absorption	Molecule	iCode	Absorption
H2O	11	14.412%	$NO2$	101	0.055%
$CCl3F$	331	4.848%	$ClONO2$	271	0.035%
$O3$	31	1.118%	ClO	181	0.019%
Solar(A)	—	0.770%	$C2H4$	391	0.003%
Solar-sim	—	0.703%	$NH3$	111	0.001%
Solar-DU	—	0.003%	$CFC113$	621	0.001%
$CO2$	21	0.598%	OH	131	<0.001%
OCS	191	0.240%	$HO2$	221	<0.001%
$C2H6$	381	0.221%	HCN	281	<0.001%
$COCl2$	431	0.221%	$CCl2F2$	321	<0.001%
$HNO3$	121	0.096%	$C2H2$	401	<0.001%
$CHF2Cl$	421	0.087%	HDO	491	<0.001%

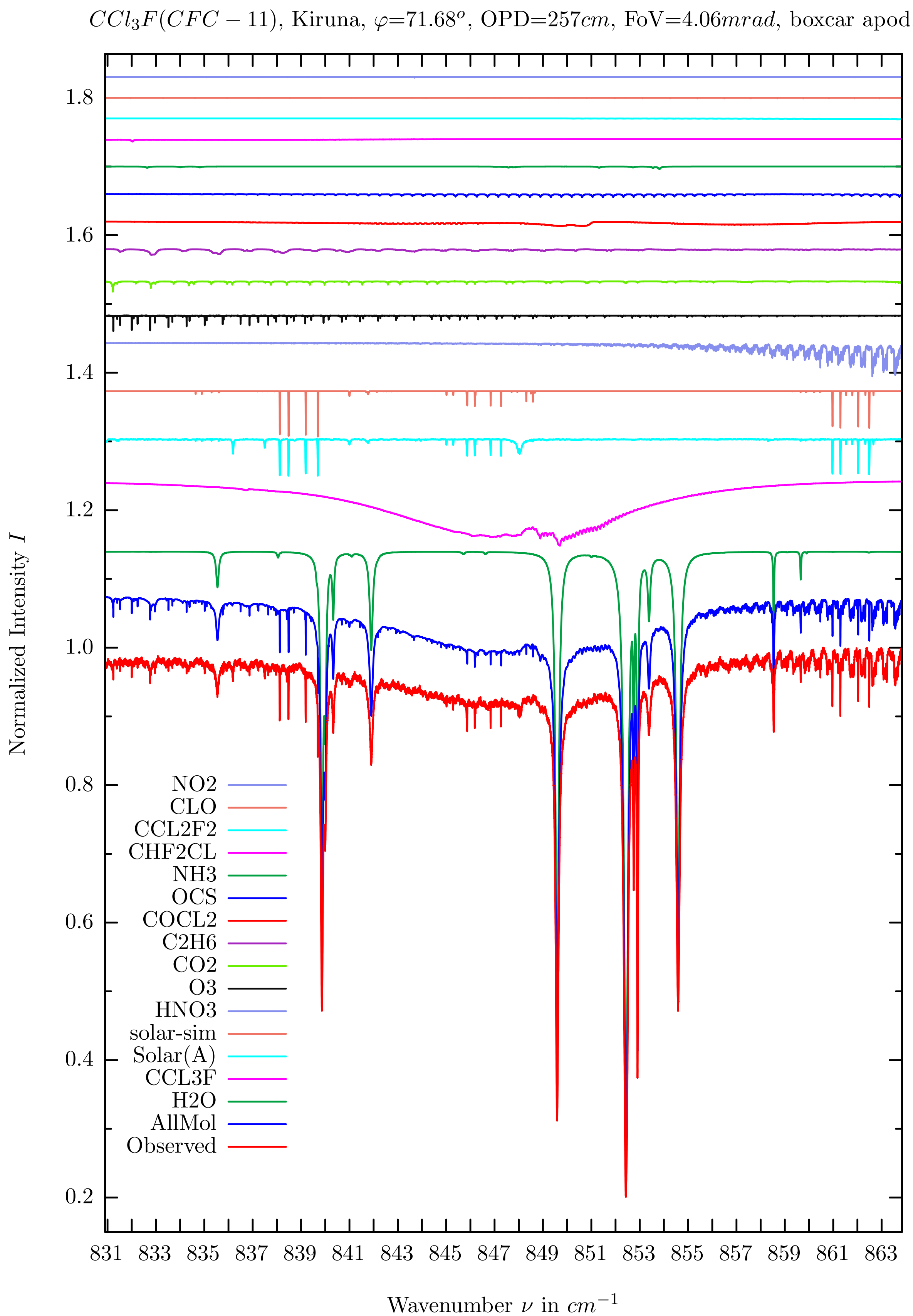
$CCl_3F(CFC-11)$, Kiruna, φ=71.68^o, OPD=257cm, FoV=4.06$mrad$, boxcar apod.
Normalized Intensity I
Wavenumber ν in cm^{-1}
NO2
CLO
CCL2F2
CHF2CL
NH3
OCS
COCL2
C2H6
CO2
O3
HNO3
solar-sim
Solar(A)
CCL3F
H2O
AllMol
Observed
1.8
1.6
1.4
1.2
1.0
0.8
0.6
0.4
0.2
831
833
835
837
839
841
843
845
847
849
851
853
855
857
859
861
863

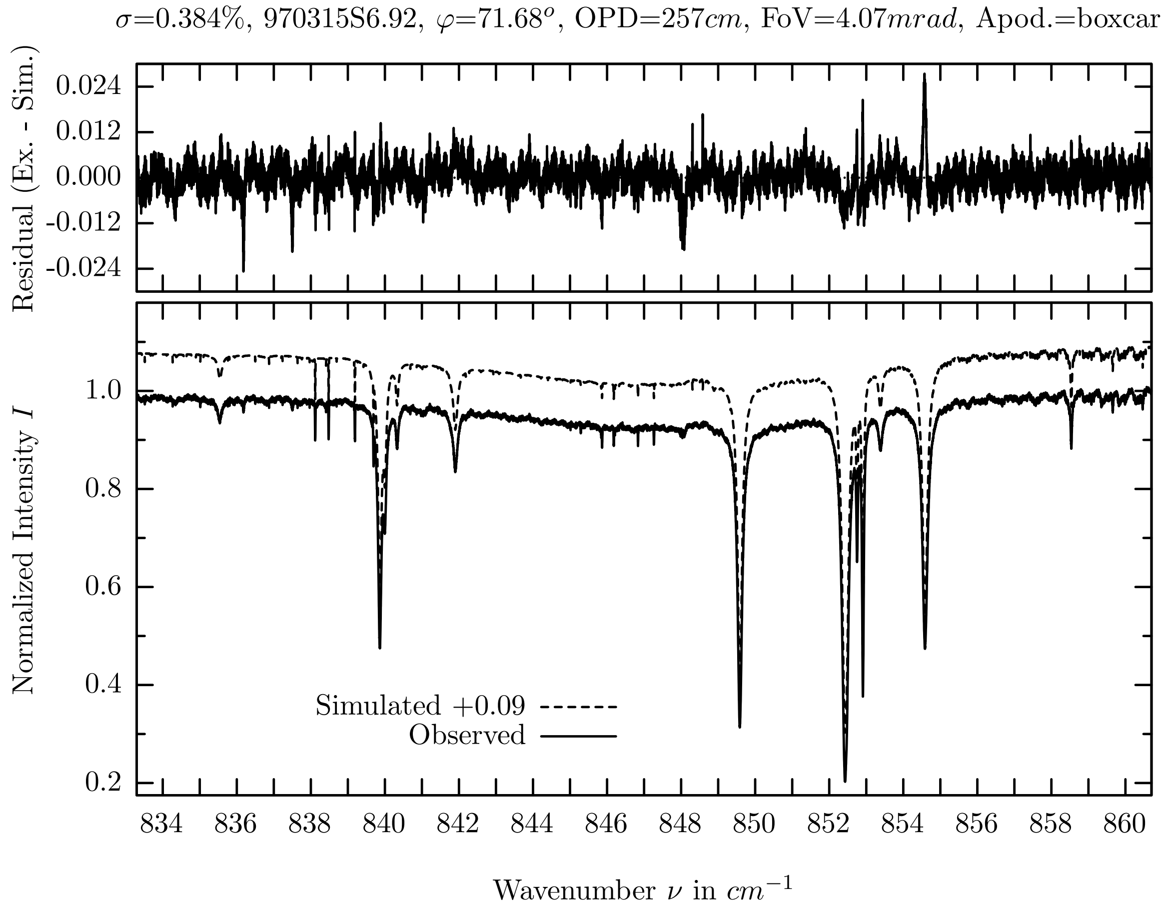

investigated species	:	CCl_3F (= CFC − 11)
line position(s) ν_0	:	846.050*), 846.960*), 848.900*), 850.020*) cm^{-1}
lower state energy E''_{lst}	:	typ. 359.0 to 505.0 cm^{-1}
retrieved TCA, information content	:	4.51E+15-01 $molec/cm^2$, 20.8
temperature dependence of the TCA	:	+1.007%/K (trop), +0.149%/K (strat)
location, date, solar zenith angle	:	Kiruna, 15/Mar/97, 71.68^o
spectral interval fitted	:	833.300 − 860.700 cm^{-1}

Molecule	iCode	Absorption	Molecule	iCode	Absorption
$H2O$	11	79.804%	$NH3$	111	0.363%
CCl3F	331	9.470%	$CHF2Cl$	421	0.361%
Solar(A)	—	5.289%	$CCl2F2$	321	0.149%
Solar-sim	—	6.643%	ClO	181	0.096%
$HNO3$	121	4.915%	$NO2$	101	0.073%
$O3$	31	2.703%	$ClONO2$	271	0.037%
$CO2$	21	1.741%	$C2H4$	391	0.022%
$COCl2$	431	0.640%	HDO	491	0.007%
$C2H6$	381	0.859%	$C2H2$	401	0.001%
OCS	191	0.467%	$CFC113$	621	0.001%
$CH4$, OH, $HO2$, $N2O5$, HCN, $COF2$, and $F142B$					<0.001%

Note: Analysis carried out with a custom-built SFIT2 version capable of simulating up to 65000 spectroscopic lines in a 30cm^{-1} wide interval.

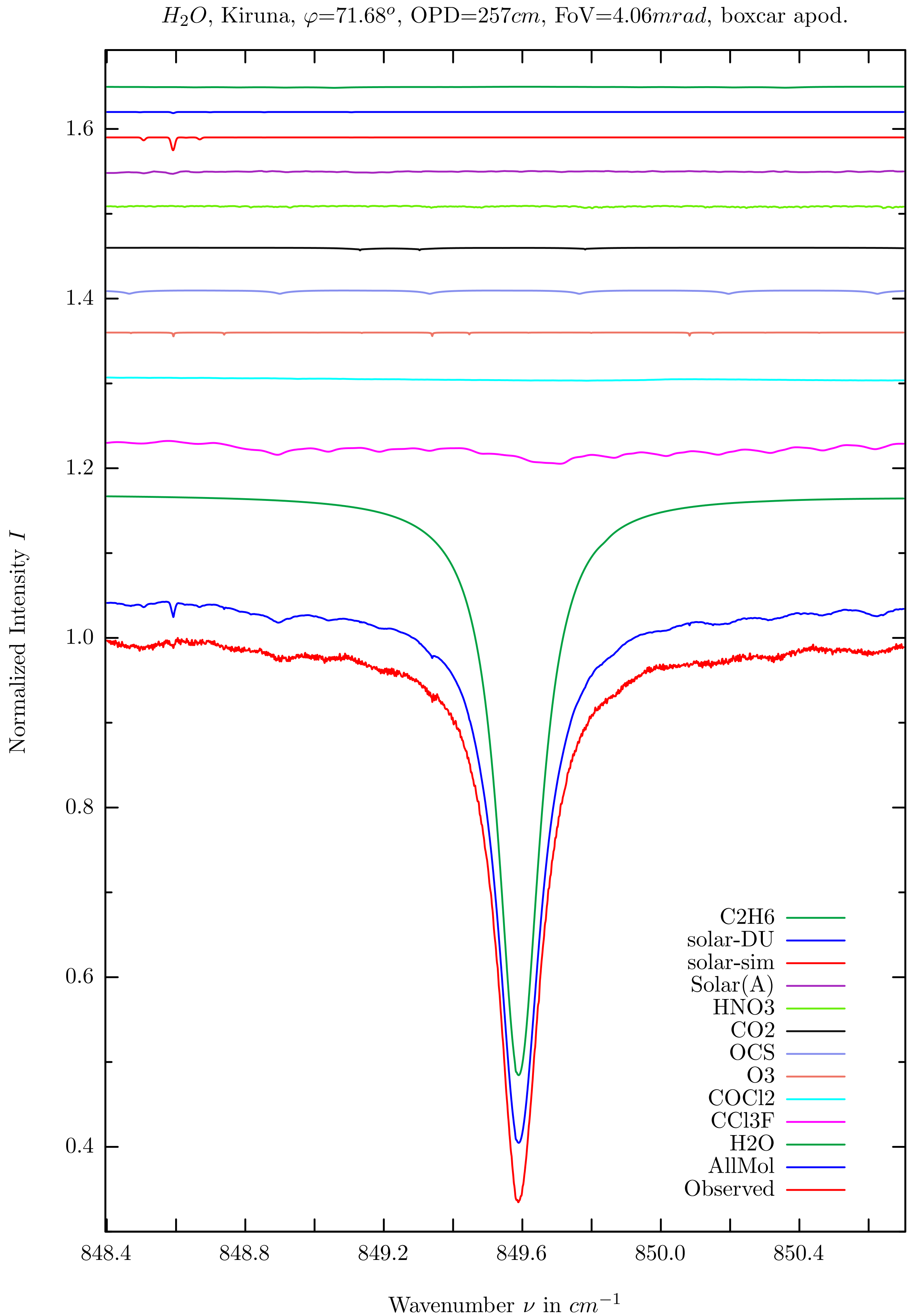
H_2O, Kiruna, φ=71.68^o, OPD=257cm, FoV=4.06$mrad$, boxcar apod.
Normalized Intensity I
Wavenumber ν in cm^{-1}
1.6
1.4
1.2
1.0
0.8
0.6
0.4
848.4
848.8
849.2
849.6
850.0
850.4
C2H6
solar-DU
solar-sim
Solar(A)
HNO3
CO2
OCS
O3
COCl2
CCl3F
H2O
AllMol
Observed

σ=0.312%, 970315S6.92, φ=71.68^o, OPD=257cm, FoV=4.07$mrad$, Apod.=boxcar

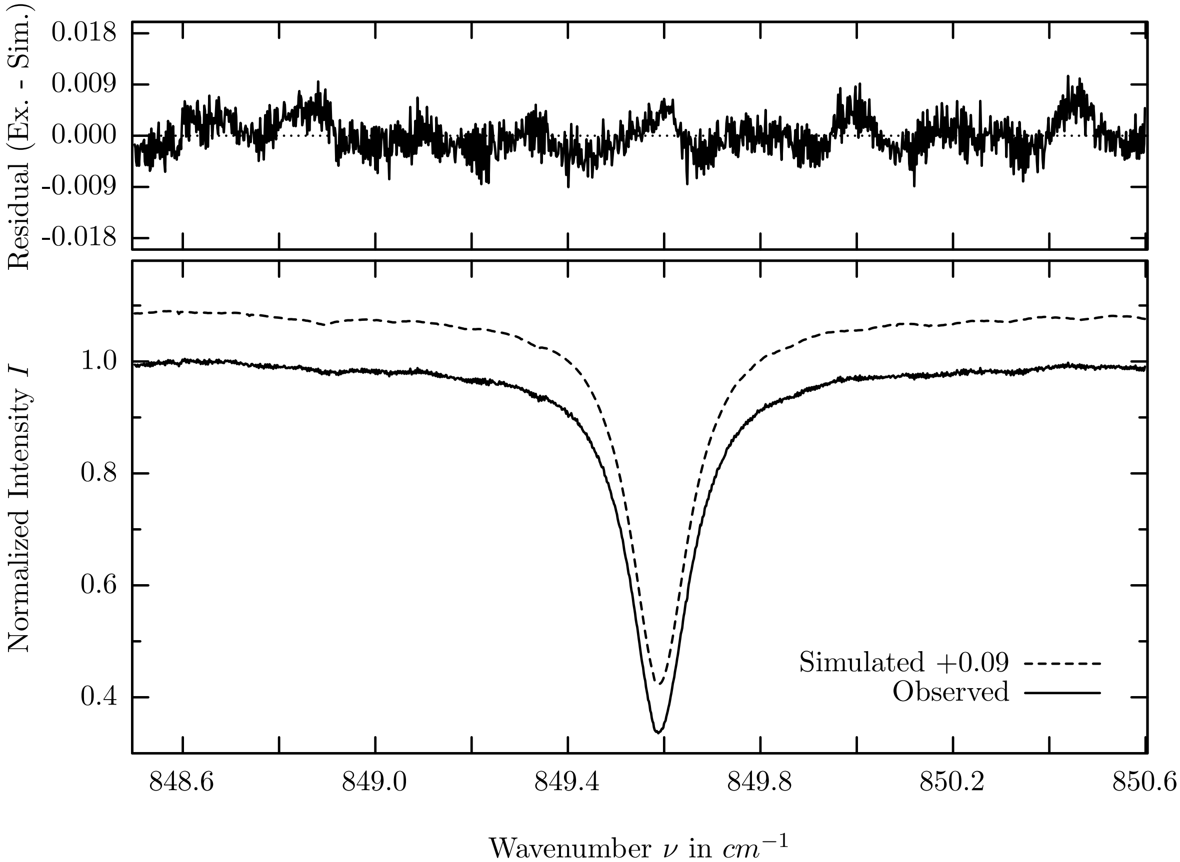

investigated species	:	H_2O
line position(s) ν_0	:	849.5795 cm^{-1}
lower state energy E''_{lst}	:	1293.0 cm^{-1}
retrieved TCA, information content	:	5.10E+21 $molec/cm^2$, 213.5
temperature dependence of the TCA	:	-2.257%/K (trop), -.007%/K (strat)
location, date, solar zenith angle	:	Kiruna, 15/Mar/97, 71.68^o
spectral interval fitted	:	848.500 – 850.600 cm^{-1}

Molecule	iCode	Absorption	Molecule	iCode	Absorption
H2O	11	68.553%	$CCl2F2$	321	0.035%
$CCl3F$	331	9.470%	$CHF2Cl$	421	0.021%
$COCl2$	431	0.640%	$ClONO2$	271	0.015%
$O3$	31	0.597%	$C2H4$	391	0.008%
OCS	191	0.437%	$NH3$	111	0.003%
$CO2$	21	0.372%	$CFC113$	621	0.001%
$HNO3$	121	0.350%	$CH4$	6**3**	<0.001%
Solar(A)	—	0.290%	OH	131	<0.001%
Solar-sim	—	1.525%	$HO2$	221	<0.001%
Solar-DU	—	0.133%	$N2O5$	261	<0.001%
$C2H6$	381	0.152%	HCN	281	<0.001%
ClO	181	0.049%	$C2H2$	401	<0.001%
$NO2$	101	0.048%			

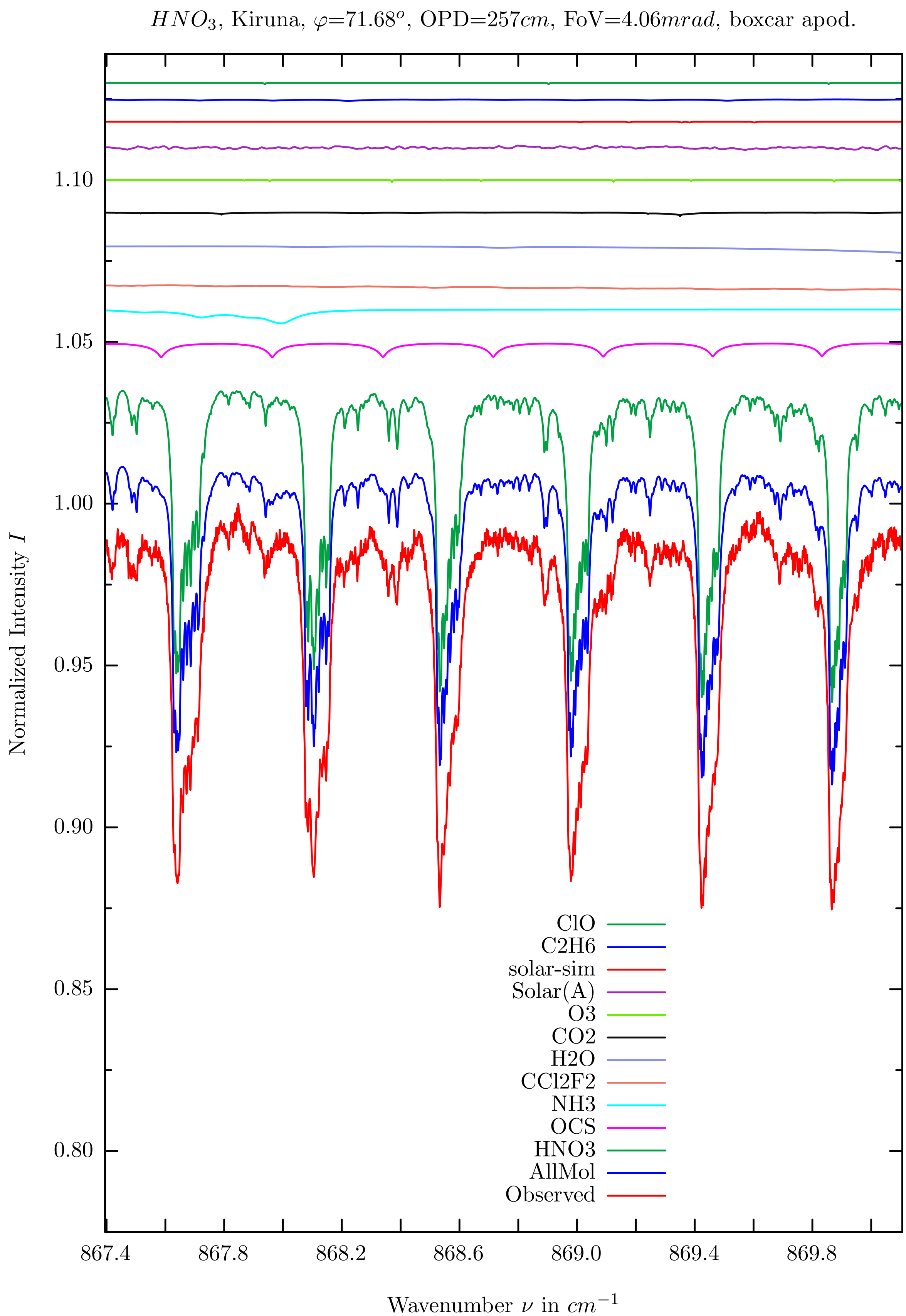
HNO_3, Kiruna, φ=71.68^o, OPD=257cm, FoV=4.06$mrad$, boxcar apod.
Normalized Intensity I
1.10
1.05
1.00
0.95
0.90
0.85
0.80
867.4
867.8
868.2
868.6
869.0
869.4
869.8
Wavenumber ν in cm^{-1}
ClO
C2H6
solar-sim
Solar(A)
O3
CO2
H2O
CCl2F2
NH3
OCS
HNO3
AllMol
Observed

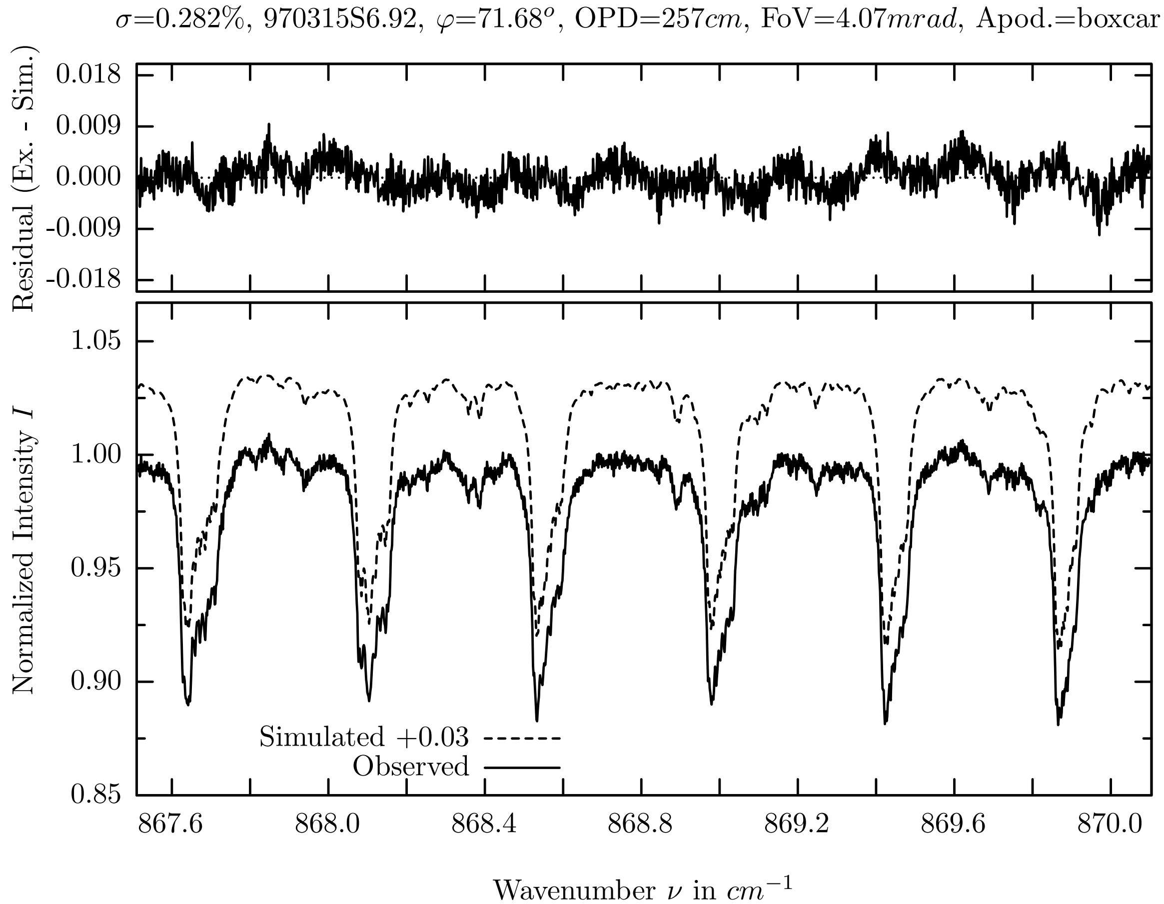

investigated species	:	HNO_3
line position(s) ν_0	:	868.104, 868.524, 868.970, 869.416$^{*)}$ cm^{-1}
lower state energy E''_{lst}	:	138.5, 130.3, 120.0, 110.3 cm^{-1}
retrieved TCA, information content	:	2.67E+16 $molec/cm^2$, 38.7 – 42.4
temperature dependence of the TCA	:	+.026%/K (trop), +.387%/K (strat)
spectral interval fitted	:	867.514 – 870.100 cm^{-1}

Molecule	iCode	Absorption	Molecule	iCode	Absorption
HNO3	121	10.354%	$CCl3F$	331	0.045%
OCS	191	0.473%	$NO2$	101	0.033%
$NH3$	111	0.428%	$C2H4$	391	0.031%
$CCl2F2$	321	0.391%	$ClONO2$	271	0.022%
$H2O$	11	0.247%	$COCl2$	431	0.003%
$CO2$	21	0.134%	$CFC113$	621	0.001%
$O3$	31	0.085%	$CH4$	6**3**	<0.001%
Solar(A)	—	0.072%	OH	131	<0.001%
Solar-sim	—	0.024%	$HO2$	221	<0.001%
Solar-DU	—	0.024%	$N2O5$	261	<0.001%
$C2H6$	381	0.054%	$C2H2$	401	<0.001%
ClO	181	0.051%	$F142B$	611	<0.001%

Beware of ammonia interferences (compare Figure B.10, page 556).

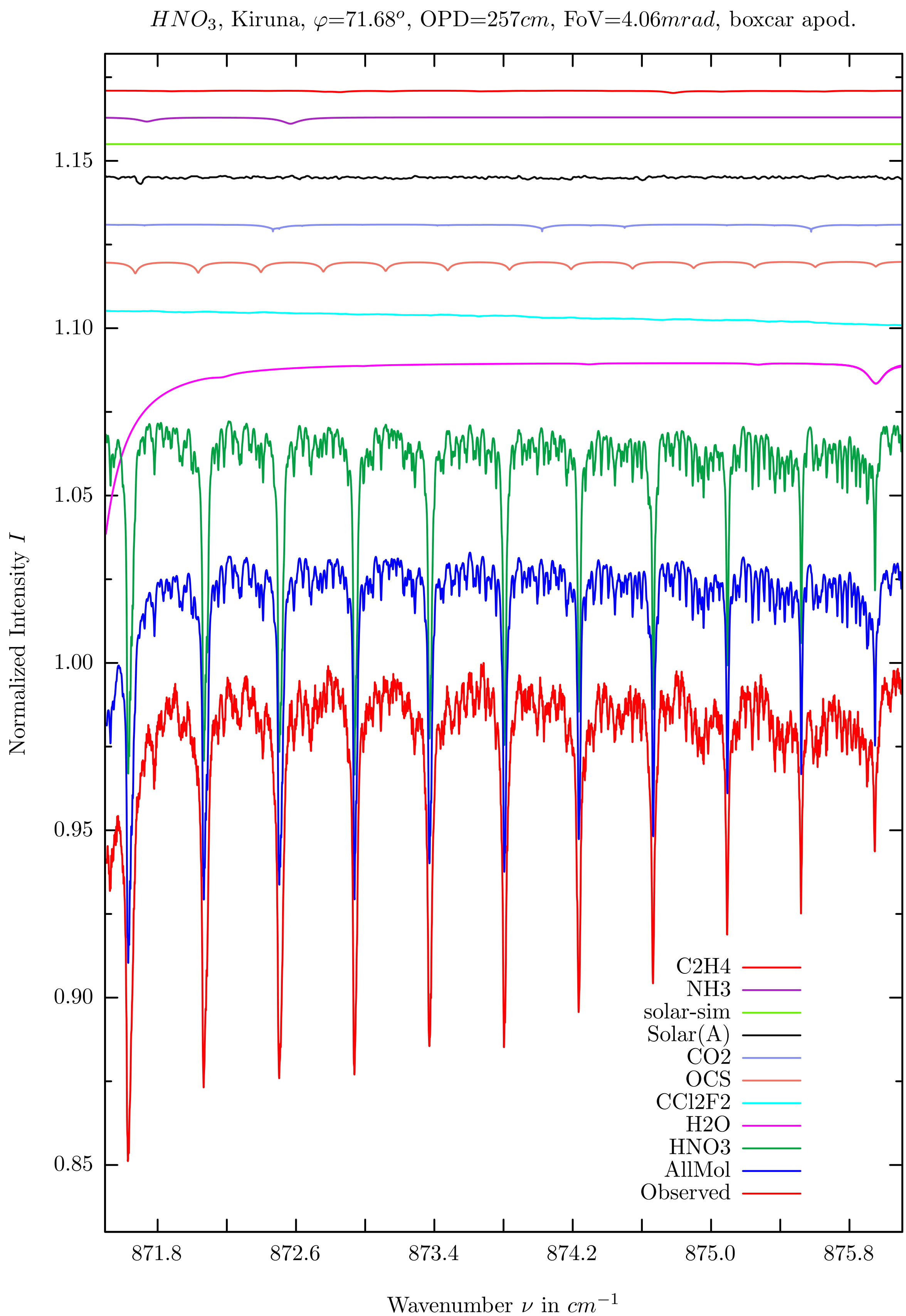

HNO_3, Kiruna, φ=71.68^o, OPD=257cm, FoV=4.06$mrad$, boxcar apod.
Normalized Intensity I
Wavenumber ν in cm^{-1}
1.15
1.10
1.05
1.00
0.95
0.90
0.85
871.8
872.6
873.4
874.2
875.0
875.8
C2H4
NH3
solar-sim
Solar(A)
CO2
OCS
CCl2F2
H2O
HNO3
AllMol
Observed

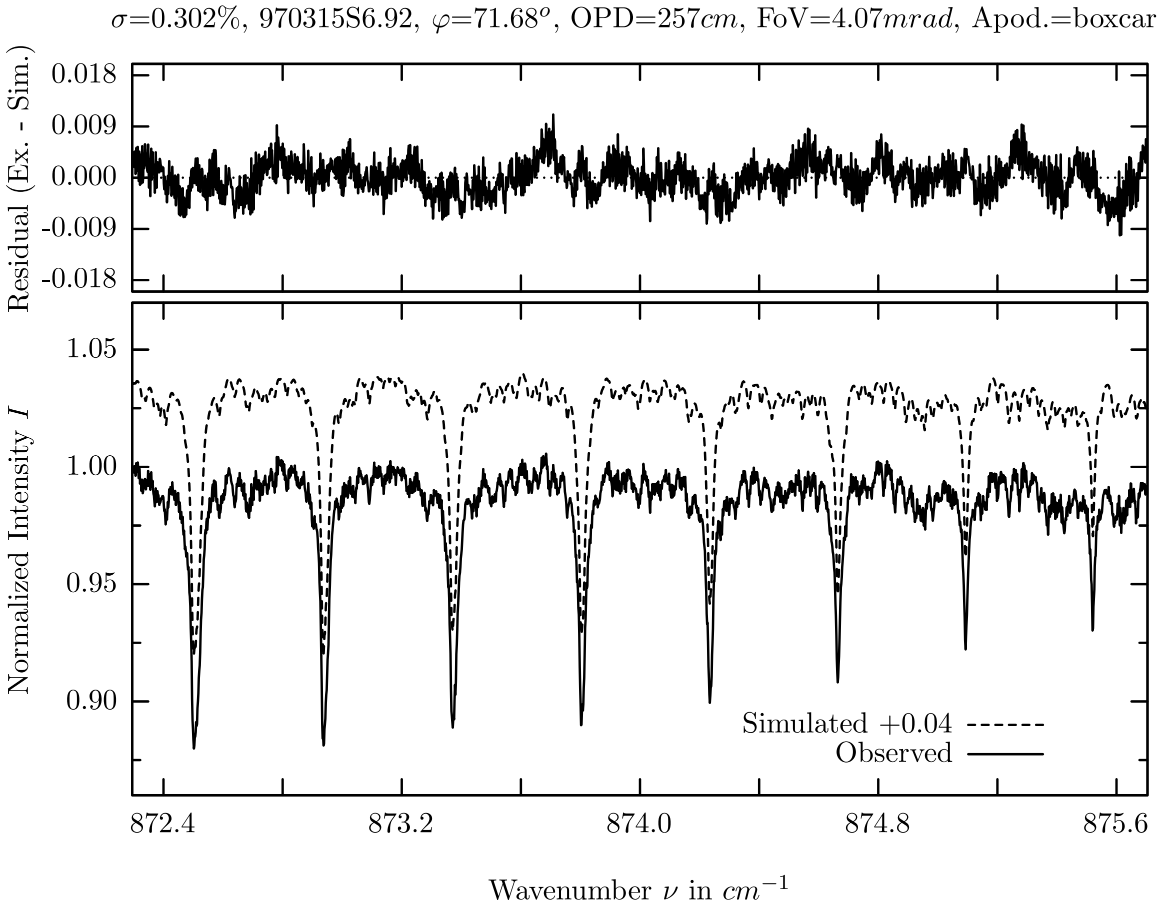

investigated species	:	HNO_3
line position(s) ν_0	:	872.937, 873.367, 873.800, 874.232*) cm^{-1}
lower state energy E''_{lst}	:	46.0, 40.7, 35.1, 29.9 cm^{-1}
retrieved TCA, information content	:	2.65E+16 $molec/cm^2$, 39.9 – 32.5
temperature dependence of the TCA	:	+.002%/K (trop), +.537%/K (strat)
location, date, solar zenith angle	:	Kiruna, 15/Mar/97, 71.68^o
spectral interval fitted	:	872.300 – 875.700 cm^{-1}

Molecule	iCode	Absorption	Molecule	iCode	Absorption
HNO3	121	11.513%	$NO2$	101	0.030%
$H2O$	11	5.102%	ClO	181	0.029%
$CCl2F2$	321	0.909%	$ClONO2$	271	0.021%
OCS	191	0.362%	$CCl3F$	331	0.016%
$CO2$	21	0.252%	$COCl2$	431	0.001%
Solar(A)	—	0.191%	$CFC113$	621	0.001%
Solar-sim	—	0.001%	$N2O$	41	<0.001%
Solar-DU	—	0.001%	$CH4$	6**3**	<0.001%
$NH3$	111	0.190%	OH	131	<0.001%
$C2H4$	391	0.071%	$HO2$	221	<0.001%
$O3$	31	0.048%	$C2H2$	401	<0.001%
$C2H6$	381	0.045%	$F142B$	611	<0.001%

CFC–12, Kiruna, φ=71.68^o, OPD=257cm, FoV=4.06$mrad$, boxcar apod.

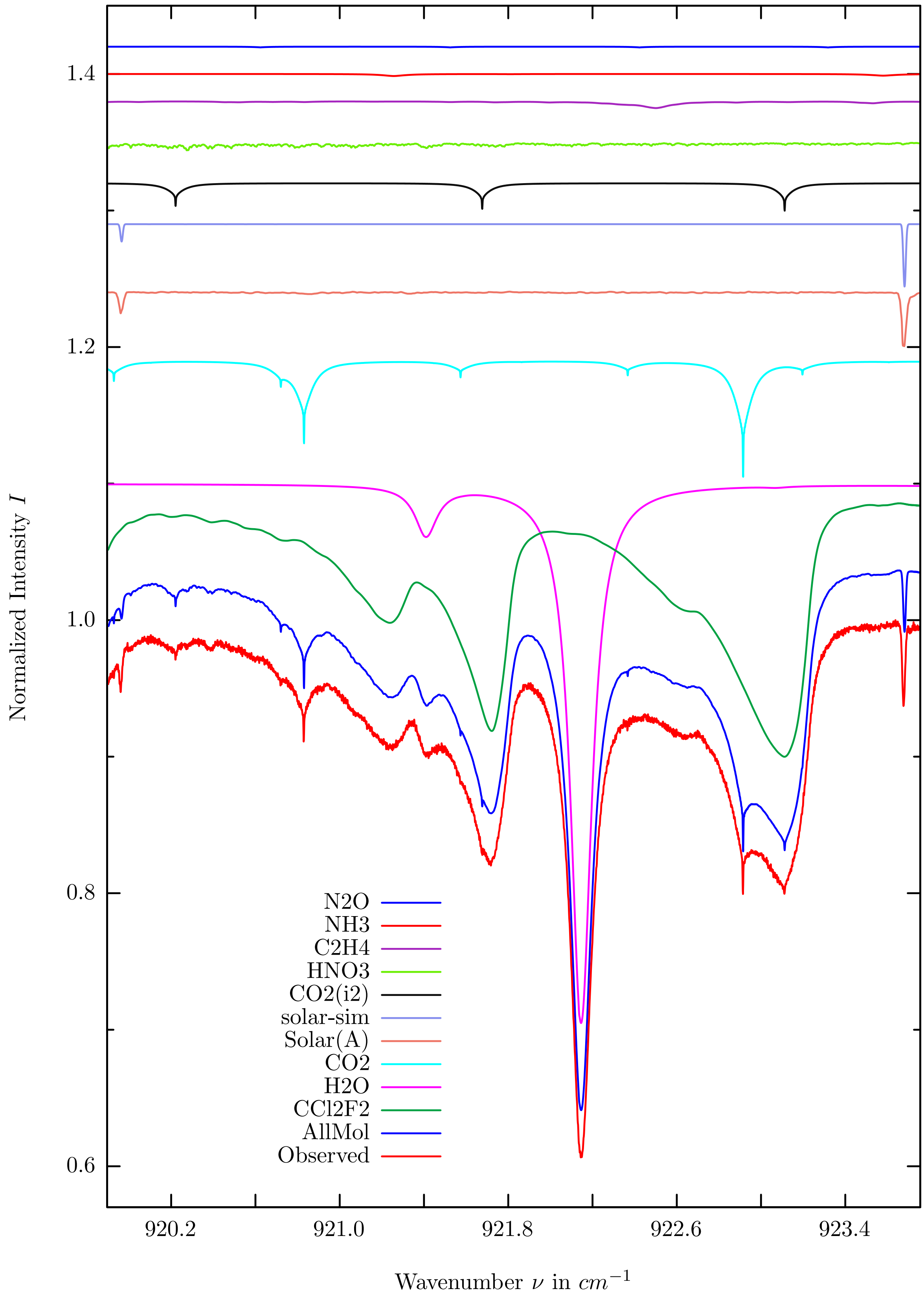

σ=0.180%, 970315S6.92, φ=71.68^o, OPD=257cm, FoV=4.07$mrad$, Apod.=boxcar

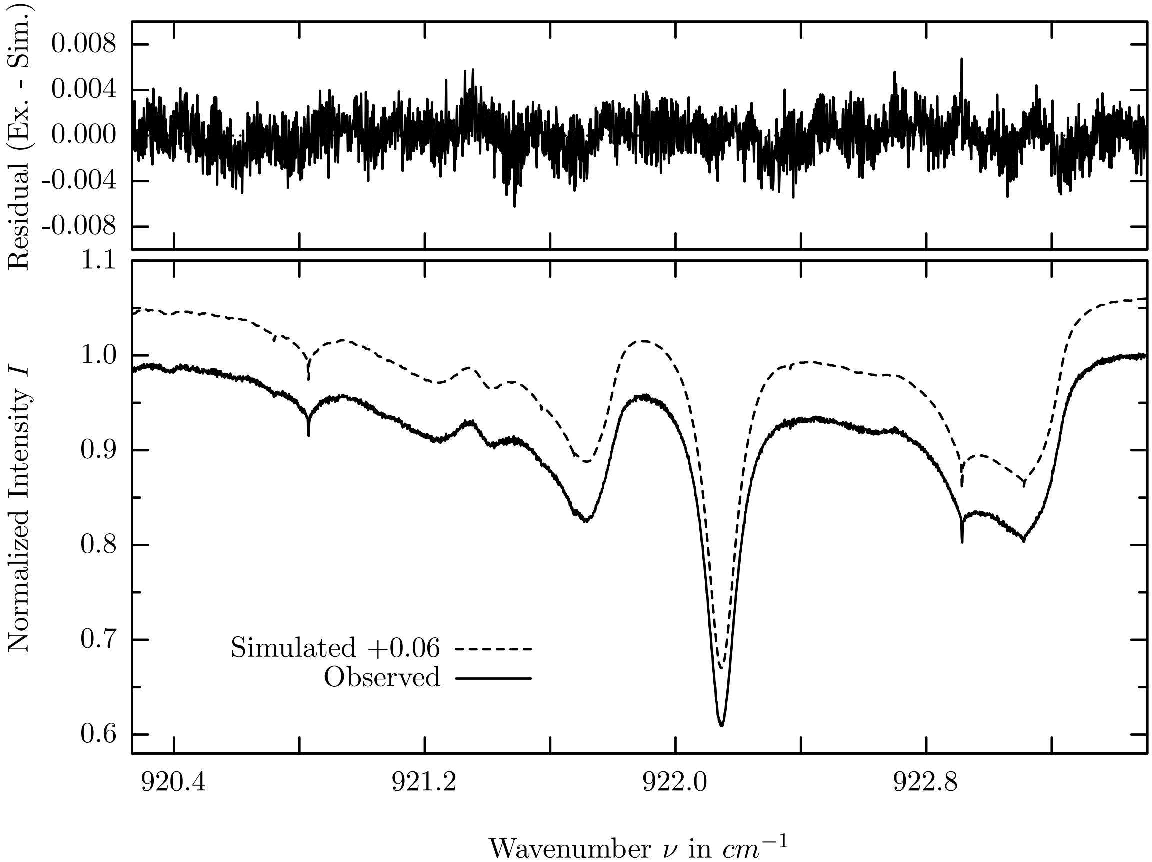

investigated species	:	CCl_2F_2(Freon12)
line position(s) ν_0	:	(921.180$^{*)}$), (921.710$^{*)}$), 923.060$^{*)}$ cm^{-1}
lower state energy E''_{lst}	:	492.0, 247.0, 219.0 cm^{-1}
retrieved TCA, information content	:	9.51E+15 $molec/cm^2$, 103.7
temperature dependence of the TCA	:	+0.561%/K (trop), +.163%/K (strat)
location, date, solar zenith angle	:	Kiruna, 15/Mar/97, 71.68^o
spectral interval fitted	:	920.270 – 923.500 cm^{-1}

Molecule	iCode	Absorption	Molecule	iCode	Absorption
$H2O$	11	39.513%	$O3$	31	0.019%
CCL2F2	321	21.509%	$F142B$	611	0.008%
$CO2$	21	9.505%	$NO2$	101	0.003%
Solar(A)	—	3.935%	$CFC113$	621	0.003%
Solar-sim	—	4.588%	$ClONO2$	271	0.001%
Solar-DU	—	4.588%	$CH4$	61	<0.001%
$CO2$	2**2**	2.236%	OH	131	<0.001%
$HNO3$	121	0.594%	$C2H6$	381	<0.001%
$C2H4$	391	0.497%	HDO	491	<0.001%
$NH3$	111	0.149%	$SF6$	501	<0.001%
$N2O$	41	0.059%			

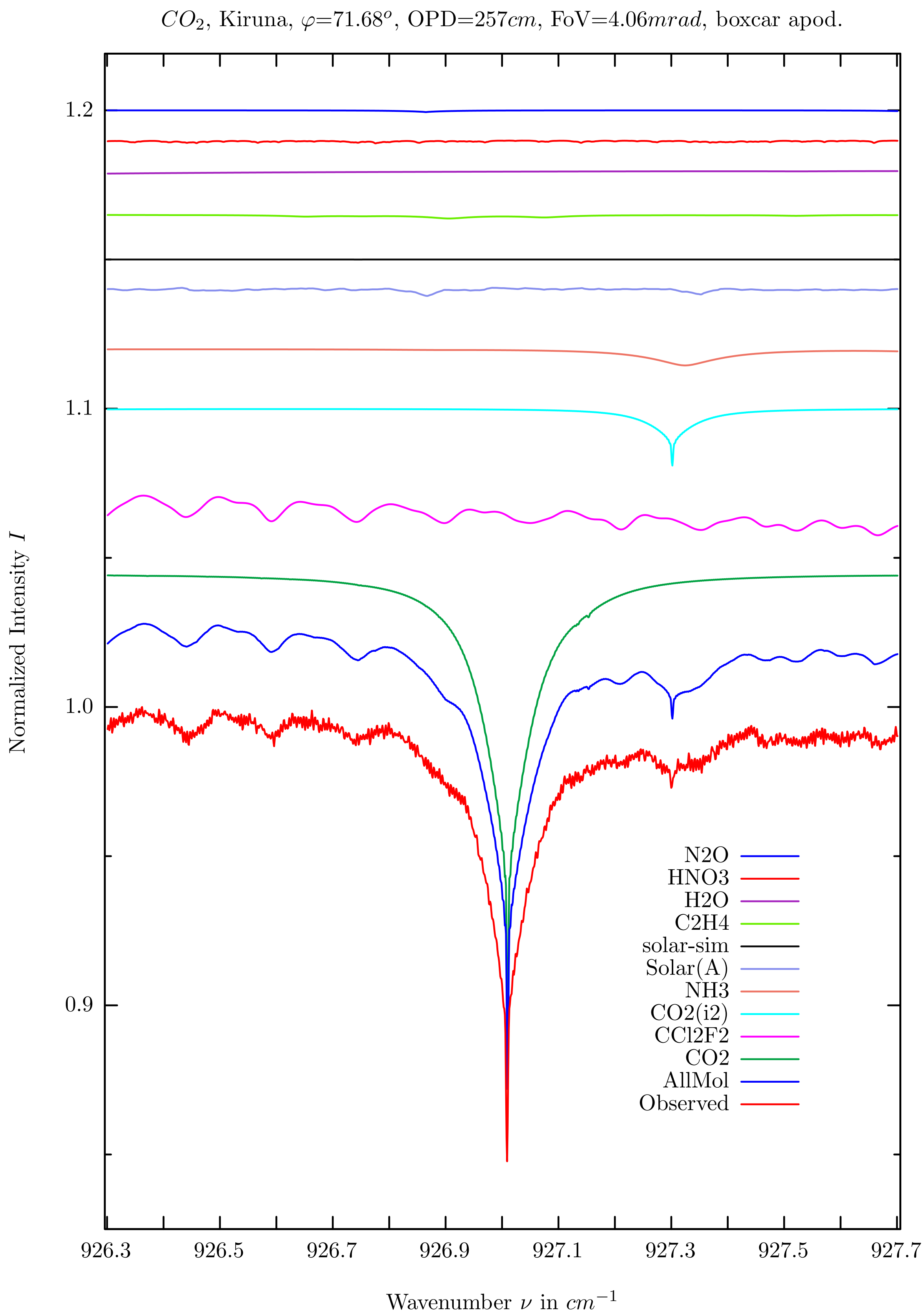

CO_2, Kiruna, φ=71.68^o, OPD=257cm, FoV=4.06$mrad$, boxcar apod.
Normalized Intensity I
Wavenumber ν in cm^{-1}
1.2
1.1
1.0
0.9
926.3
926.5
926.7
926.9
927.1
927.3
927.5
927.7
N2O
HNO3
H2O
C2H4
solar-sim
Solar(A)
NH3
CO2(i2)
CCl2F2
CO2
AllMol
Observed

σ=0.163%, 970315S6.92, φ=71.68^o, OPD=257cm, FoV=4.07$mrad$, Apod.=boxcar

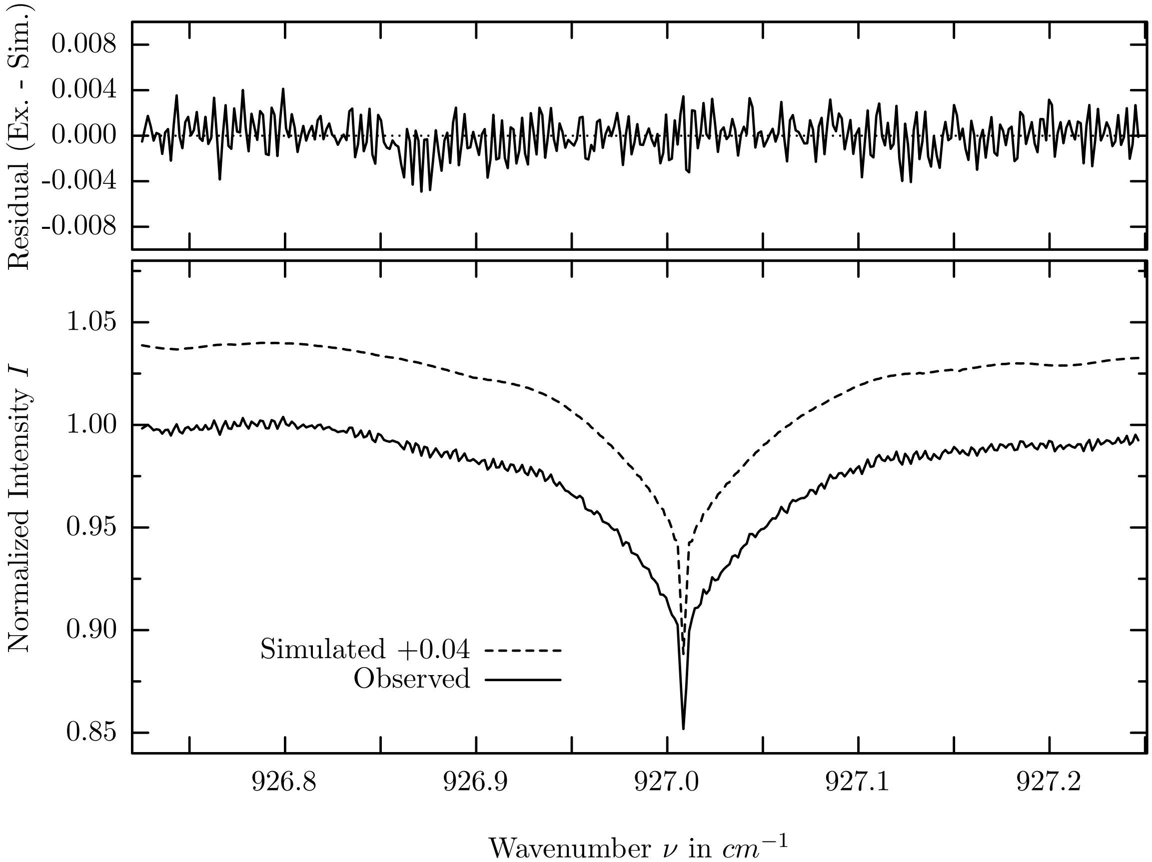

investigated species	:	CO_2
line position(s) ν_0	:	927.0083 cm^{-1}
lower state energy E''_{lst}	:	1966.2 cm^{-1}
retrieved TCA, information content	:	7.09E+21 $molec/cm^2$, 92.8
temperature dependence of the TCA	:	-3.757%/K (trop), -1.100%/K (strat)
location, date, solar zenith angle	:	Kiruna, 15/Mar/97, 71.68^o
spectral interval fitted	:	926.725 – 927.247 cm^{-1}

Molecule	iCode	Absorption	Molecule	iCode	Absorption
CO2	21	17.792%	$O3$	31	0.010%
$CCl2F2$	321	6.744%	HDO	491	0.008%
$CO2$	2**2**	2.119%	$NO2$	101	0.004%
$NH3$	111	0.549%	$CFC113$	621	0.002%
Solar(A)	—	0.221%	$CH4$	61	<0.001%
Solar-sim	—	0.001%	OH	131	<0.001%
Solar-DU	—	0.001%	$H2O2$	231	<0.001%
$C2H4$	391	0.125%	$ClONO2$	271	<0.001%
$H2O$	11	0.120%	$COF2$	361	<0.001%
$HNO3$	121	0.108%	$C2H6$	381	<0.001%
$N2O$	41	0.060%	$F142B$	611	<0.001%
$SF6$	501	0.027%			

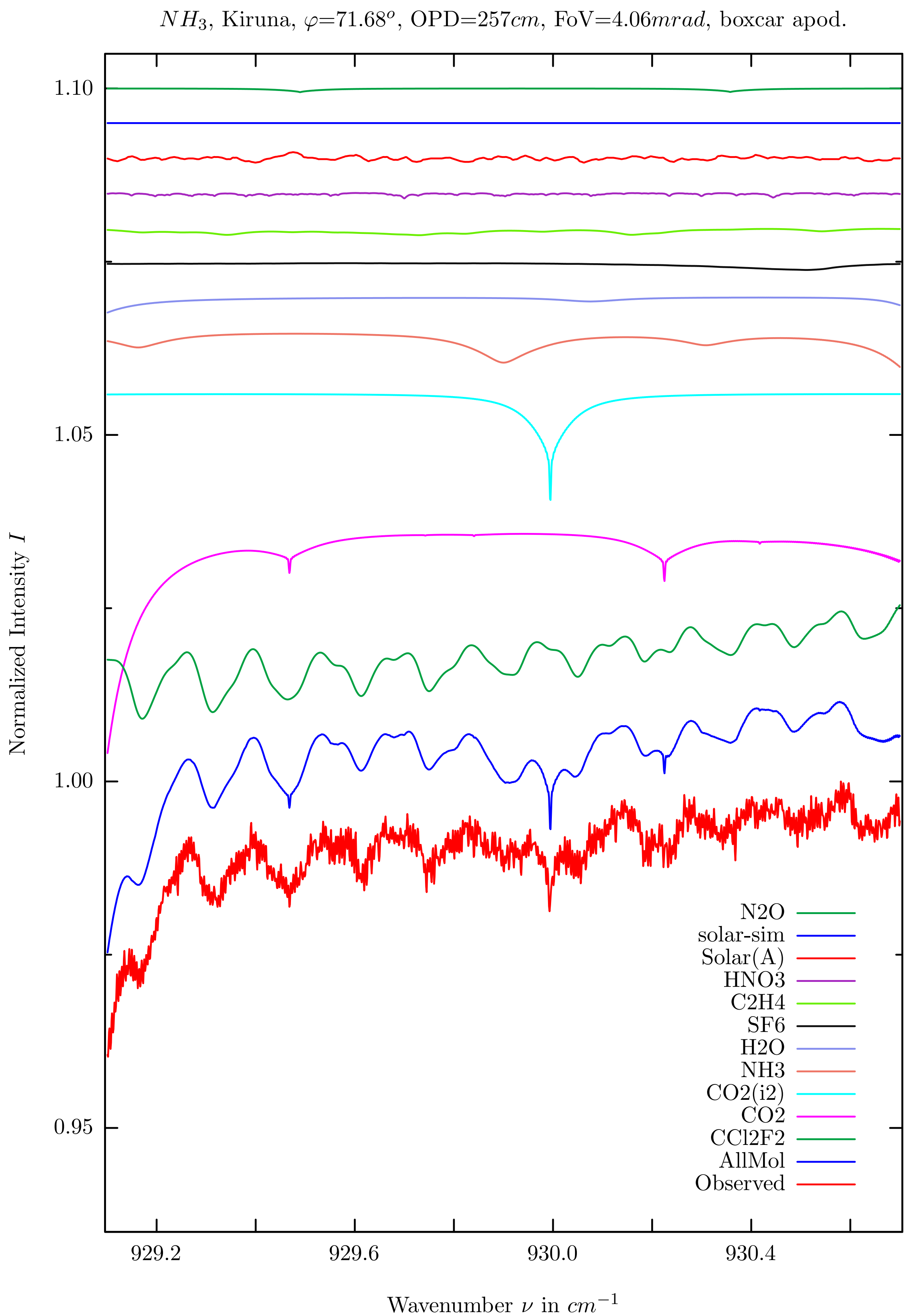

NH_3, Kiruna, φ=71.68^o, OPD=257cm, FoV=4.06$mrad$, boxcar apod.
1.10
1.05
1.00
0.95
Normalized Intensity I
929.2
929.6
930.0
930.4
Wavenumber ν in cm^{-1}
N2O
solar-sim
Solar(A)
HNO3
C2H4
SF6
H2O
NH3
CO2(i2)
CO2
CCl2F2
AllMol
Observed

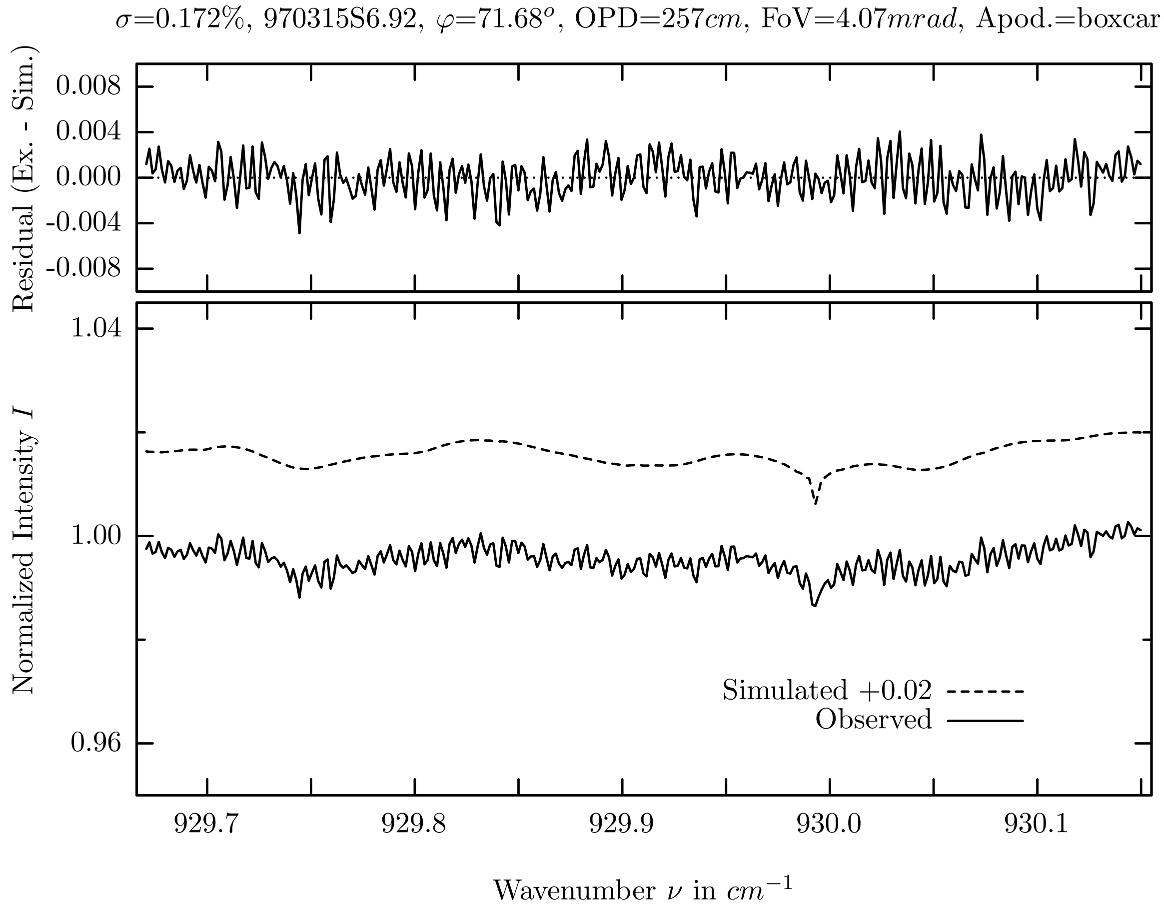

investigated species	:	NH_3
line position(s) ν_0	:	929.8981 cm^{-1}
lower state energy E''_{lst}	:	140.2 cm^{-1}
retrieved TCA, information content	:	1.46E+14 $molec/cm^2$, 2.5
temperature dependence of the TCA	:	+5.124%/K (trop), +.611%/K (strat)
location, date, solar zenith angle	:	Kiruna, 15/Mar/97, 71.68^o
spectral interval fitted	:	929.670 – 930.150 cm^{-1}

Molecule	iCode	Absorption	Molecule	iCode	Absorption
$CCl2F2$	321	7.295%	$O3$	31	0.011%
$CO2$	21	3.239%	$NO2$	101	0.004%
$CO2$	2**2**	1.758%	$CFC113$	621	0.001%
NH3	111	0.531%	$CH4$	61	<0.001%
$H2O$	11	0.232%	OH	131	<0.001%
$SF6$	501	0.119%	$H2O2$	231	<0.001%
$C2H4$	391	0.118%	$ClONO2$	271	<0.001%
$HNO3$	121	0.088%	$COF2$	361	<0.001%
Solar(A)	—	0.070%	$C2H6$	381	<0.001%
Solar-sim	—	<0.001%	HDO	491	<0.001%
Solar-DU	—	<0.001%	$F142B$	611	<0.001%
$N2O$	41	0.054%			

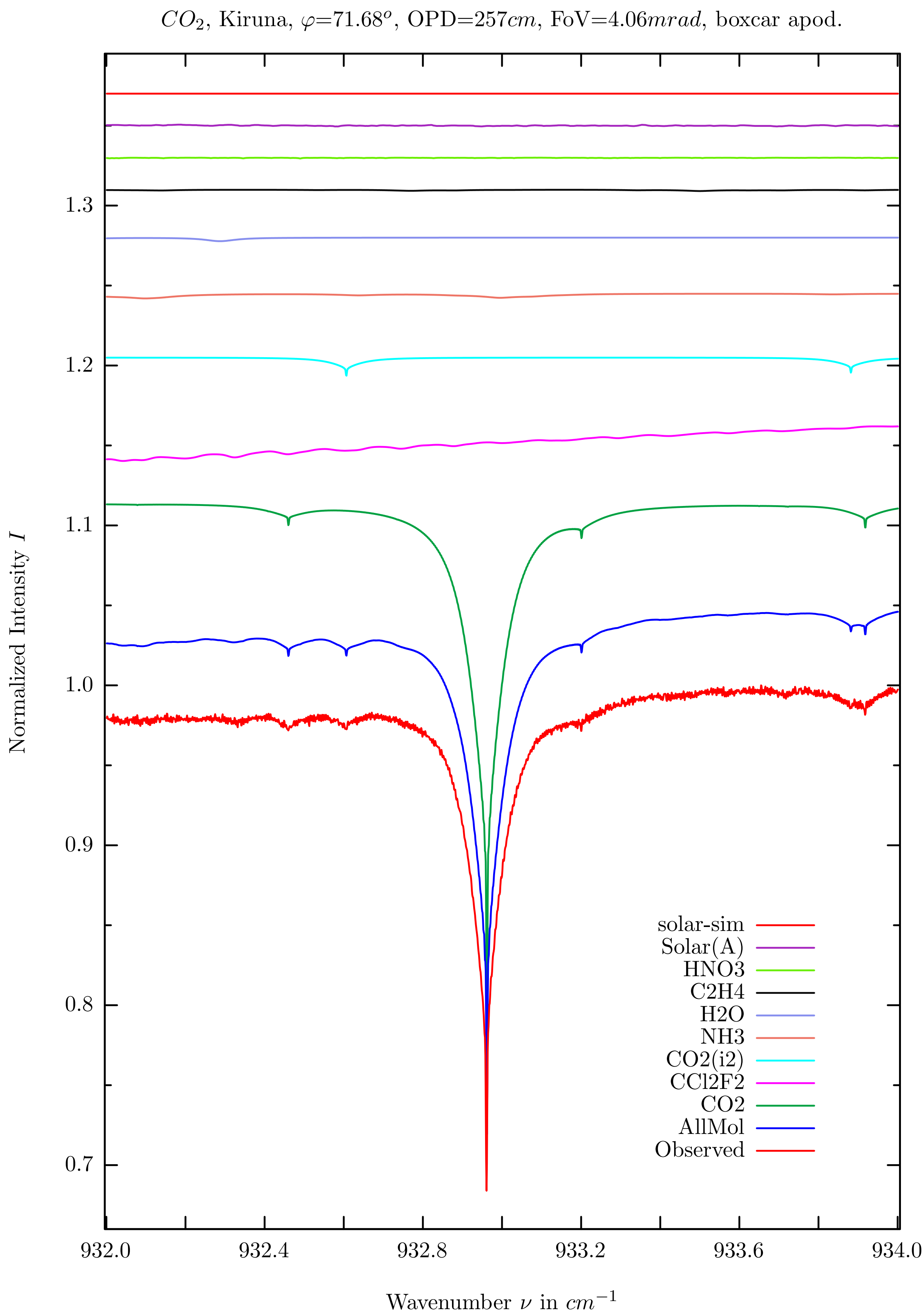

CO_2, Kiruna, φ=71.68^o, OPD=257cm, FoV=4.06$mrad$, boxcar apod.
Normalized Intensity I
Wavenumber ν in cm^{-1}
1.3
1.2
1.1
1.0
0.9
0.8
0.7
932.0
932.4
932.8
933.2
933.6
934.0
solar-sim
Solar(A)
HNO3
C2H4
H2O
NH3
CO2(i2)
CCl2F2
CO2
AllMol
Observed

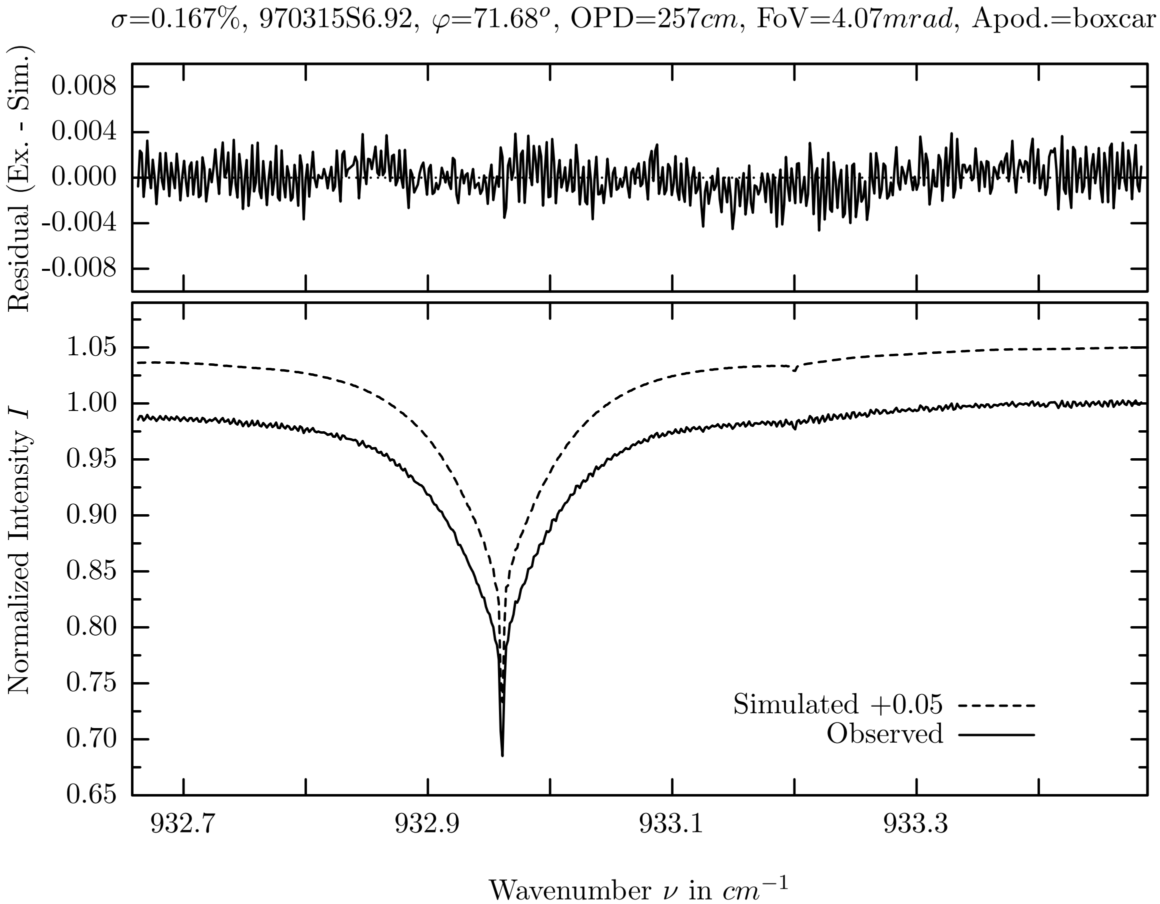

investigated species	:	CO_2
line position(s) ν_0	:	932.9604 cm^{-1}
lower state energy E''_{lst}	:	1800.1 cm^{-1}
retrieved TCA, information content	:	7.18E+21 $molec/cm^2$, 189.8
temperature dependence of the TCA	:	-3.834%/K (trop), -1.033%/K (strat)
location, date, solar zenith angle	:	Kiruna, 15/Mar/97, 71.68^o
spectral interval fitted	:	932.662 – 933.485 cm^{-1}

Molecule	iCode	Absorption	Molecule	iCode	Absorption
CO2	21	36.452%	$SF6$	501	0.030%
$CCl2F2$	321	4.469%	$O3$	31	0.027%
$CO2$	2**2**	1.287%	$NO2$	101	0.003%
$NH3$	111	0.306%	$COF2$	361	0.002%
$H2O$	11	0.226%	HDO	491	0.001%
$C2H4$	391	0.091%	$CFC113$	621	0.001%
$HNO3$	121	0.056%	$CH4$	61	<0.001%
Solar(A)	—	0.051%	OH	131	<0.001%
Solar-sim	—	0.001%	$H2O2$	231	<0.001%
Solar-DU	—	0.001%	$C2H6$	381	<0.001%
$N2O$	41	0.044%	$F142B$	611	<0.001%

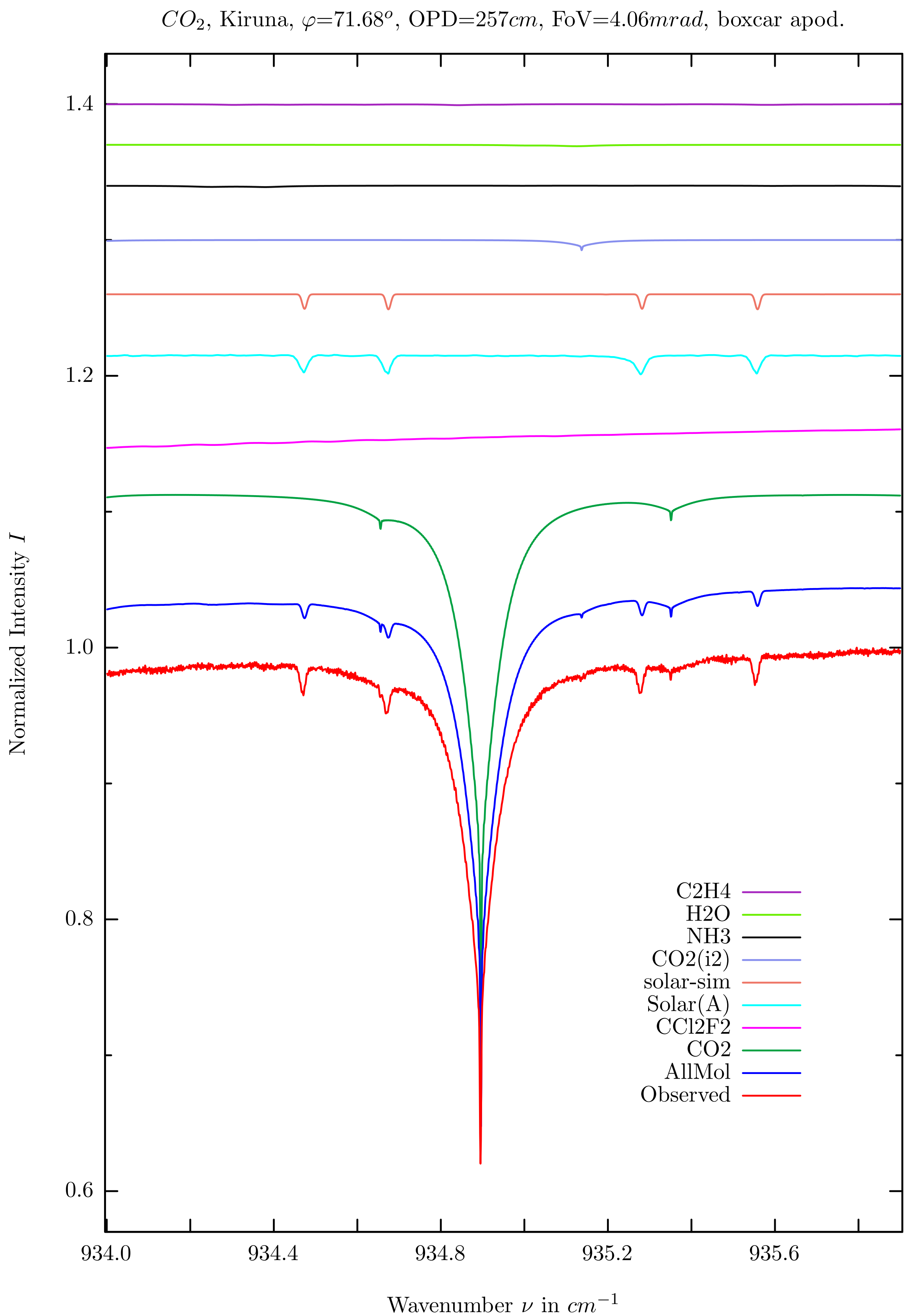
CO_2, Kiruna, φ=71.68^o, OPD=257cm, FoV=4.06$mrad$, boxcar apod.
Normalized Intensity I
Wavenumber ν in cm^{-1}
1.4
1.2
1.0
0.8
0.6
934.0
934.4
934.8
935.2
935.6
C2H4
H2O
NH3
CO2(i2)
solar-sim
Solar(A)
CCl2F2
CO2
AllMol
Observed

σ=0.169%, 970315S6.92, φ=71.68^o, OPD=257cm, FoV=4.07$mrad$, Apod.=boxcar

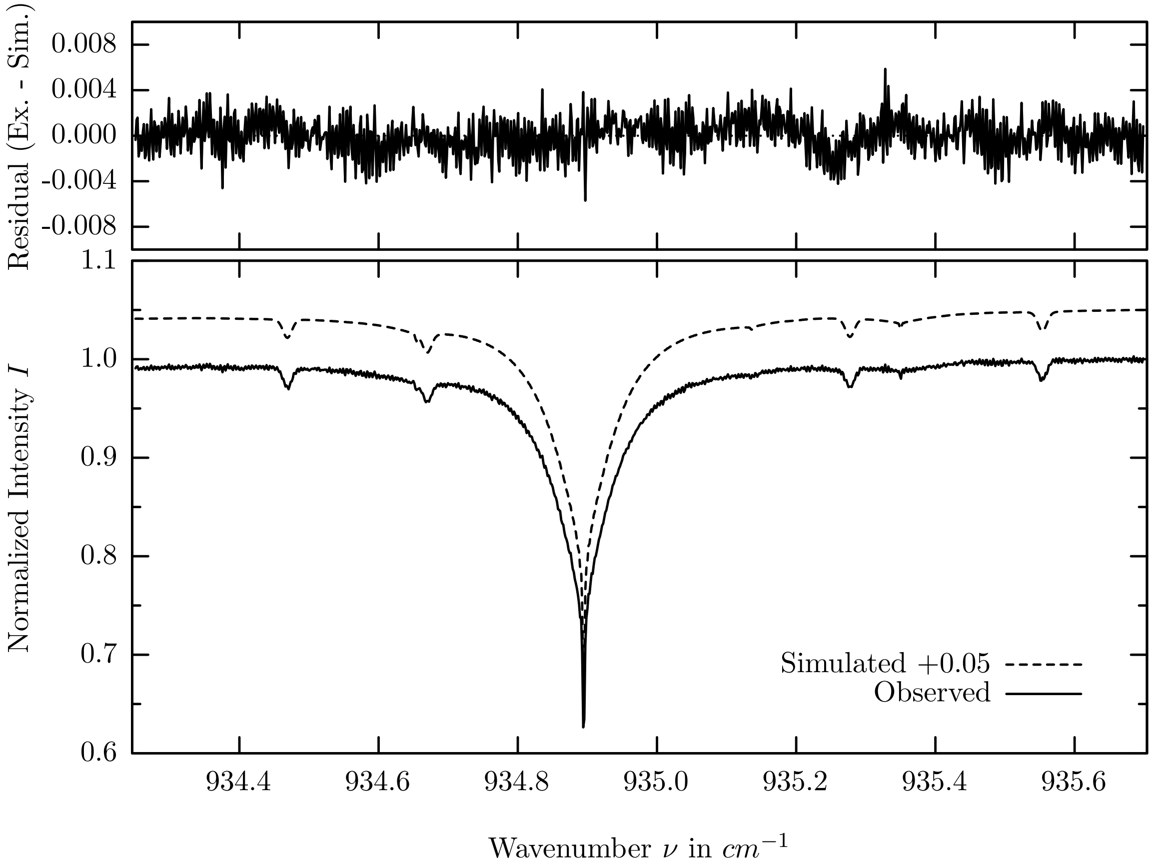

investigated species	:	CO_2
line position(s) ν_0	:	934.8945 cm^{-1}
lower state energy E''_{lst}	:	1751.0 cm^{-1}
retrieved TCA, information content	:	7.18E+21 $molec/cm^2$, 223.3
temperature dependence of the TCA	:	-3.785%/K (trop), -.976%/K (strat)
location, date, solar zenith angle	:	Kiruna, 15/Mar/97, 71.68^o
spectral interval fitted	:	934.250 – 935.700 cm^{-1}

Molecule	iCode	Absorption	Molecule	iCode	Absorption
CO2	21	43.683%	$SF6$	501	0.018%
$CCl2F2$	321	2.303%	$NO2$	101	0.003%
Solar(A)	—	1.388%	$COF2$	361	0.003%
Solar-sim	—	1.116%	$CFC113$	621	0.001%
Solar-DU	—	1.116%	$CH4$	61	<0.001%
$CO2$	2**2**	0.853%	OH	131	<0.001%
$NH3$	111	0.110%	$H2O2$	231	<0.001%
$H2O$	11	0.103%	$N2O5$	261	<0.001%
$C2H4$	391	0.081%	$C2H6$	381	<0.001%
$O3$	31	0.042%	HDO	491	<0.001%
$HNO3$	121	0.034%	$F142B$	611	<0.001%
$N2O$	41	0.029%			

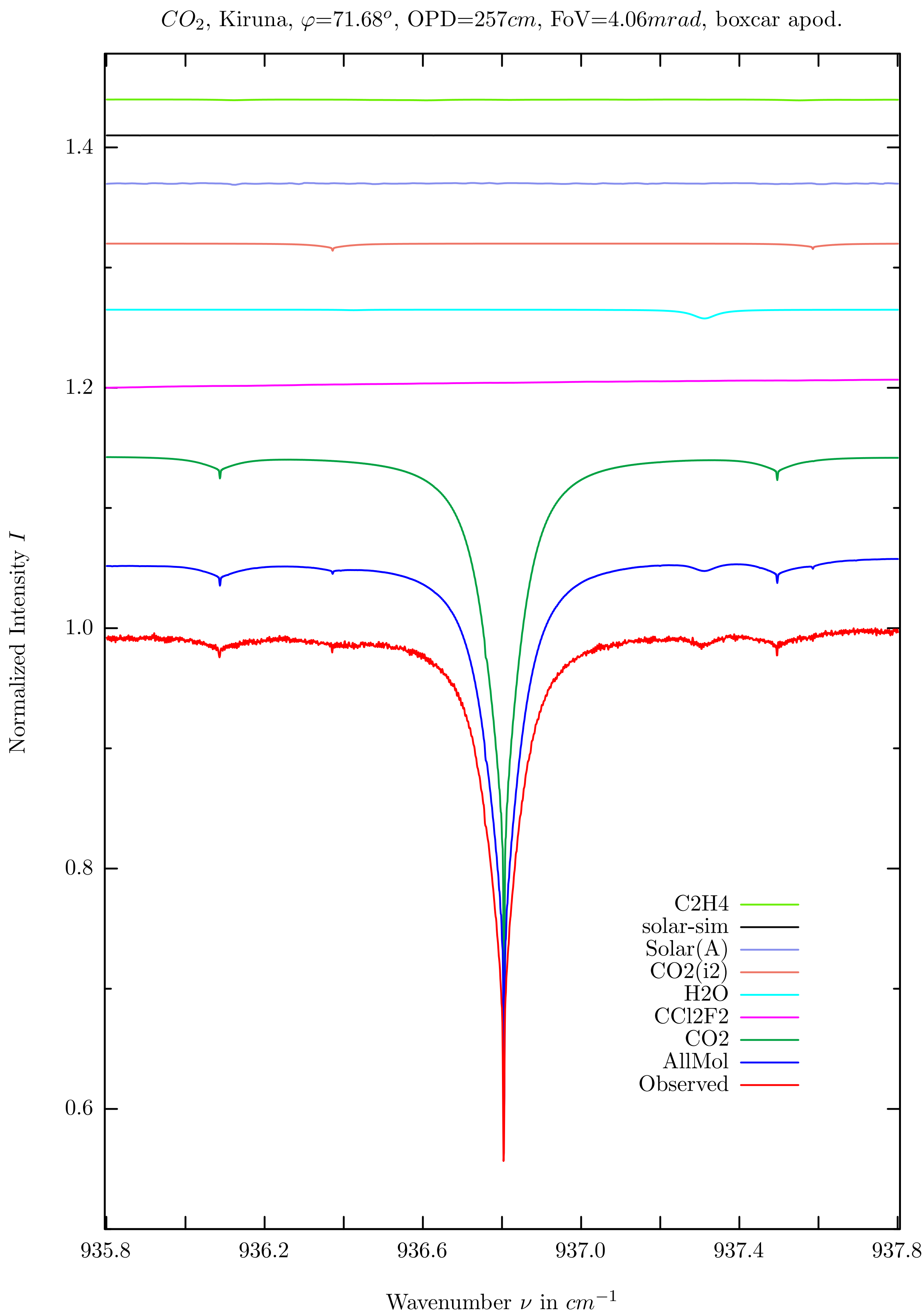
CO_2, Kiruna, φ=71.68^o, OPD=257cm, FoV=4.06$mrad$, boxcar apod.
Normalized Intensity I
1.4
1.2
1.0
0.8
0.6
935.8
936.2
936.6
937.0
937.4
937.8
Wavenumber ν in cm^{-1}
C2H4
solar-sim
Solar(A)
CO2(i2)
H2O
CCl2F2
CO2
AllMol
Observed

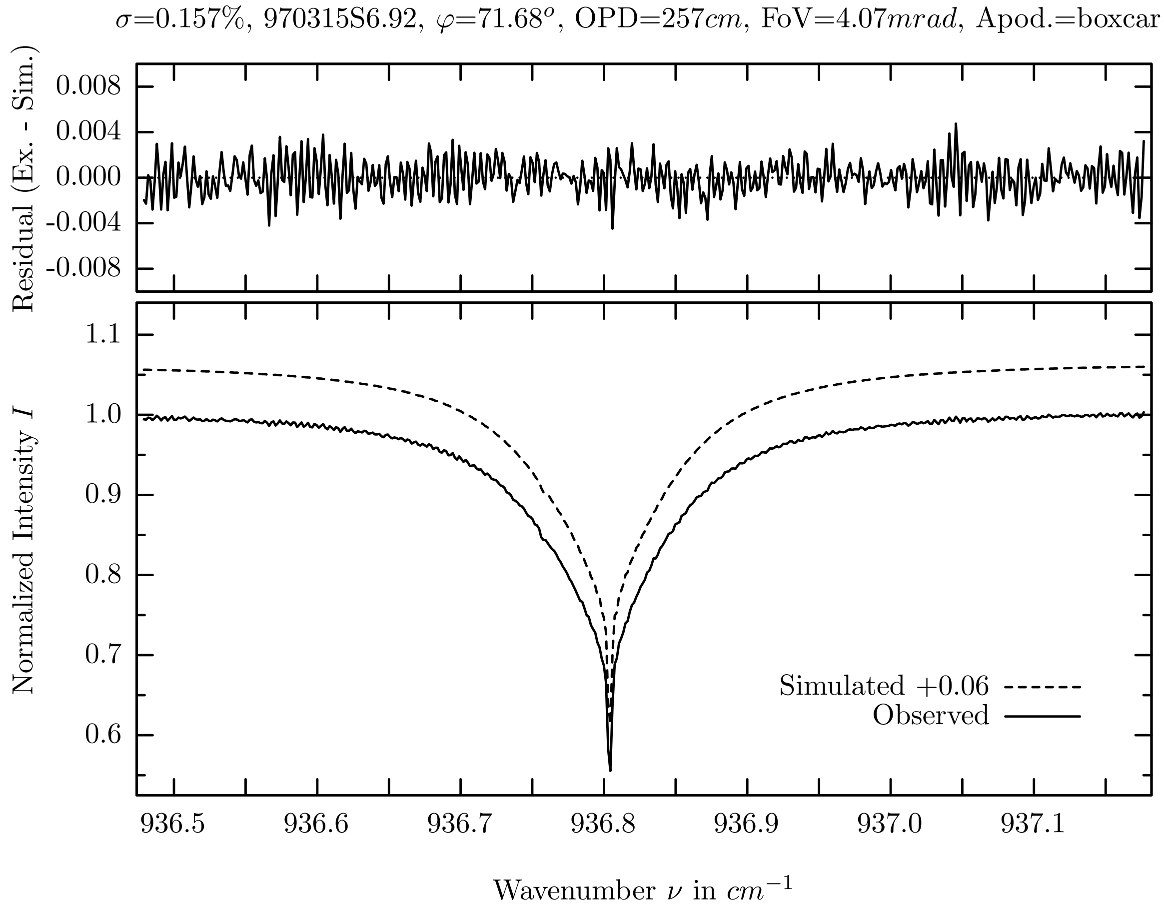

investigated species	:	CO_2
line position(s) ν_0	:	936.8038 cm^{-1}
lower state energy E''_{lst}	:	1704.9 cm^{-1}
retrieved TCA, information content	:	7.31E+21 $molec/cm^2$, 284.1
temperature dependence of the TCA	:	-3.710%/K (trop), -.928%/K (strat)
location, date, solar zenith angle	:	Kiruna, 15/Mar/97, 71.68^o
spectral interval fitted	:	936.478 – 937.178 cm^{-1}

Molecule	iCode	Absorption	Molecule	iCode	Absorption
CO2	21	50.336%	$N2O$	41	0.017%
$CCl2F2$	321	0.996%	$COF2$	361	0.011%
$H2O$	11	0.733%	$NO2$	101	0.002%
$CO2$	2**2**	0.676%	$CFC113$	621	0.001%
Solar(A)	—	0.111%	$CH4$	61	<0.001%
Solar-sim	—	0.003%	OH	131	<0.001%
Solar-DU	—	0.003%	$H2O2$	231	<0.001%
$C2H4$	391	0.086%	$N2O5$	261	<0.001%
$NH3$	111	0.049%	$C2H6$	381	<0.001%
$O3$	31	0.045%	HDO	491	<0.001%
$HNO3$	121	0.031%	$F142B$	611	<0.001%
$SF6$	501	0.020%			

CO_2, Kiruna, φ=71.68^o, OPD=257cm, FoV=4.06$mrad$, boxcar apod.

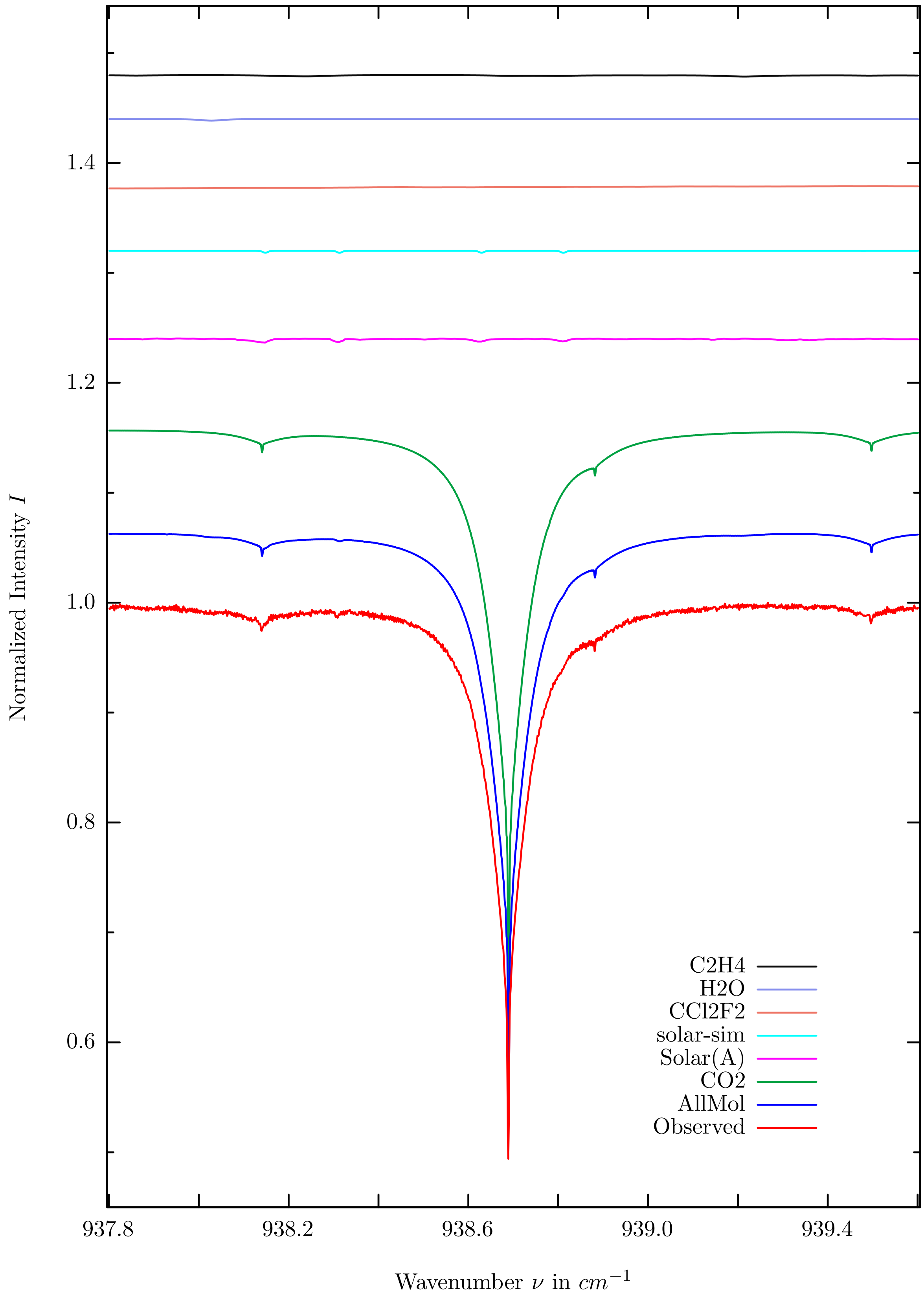

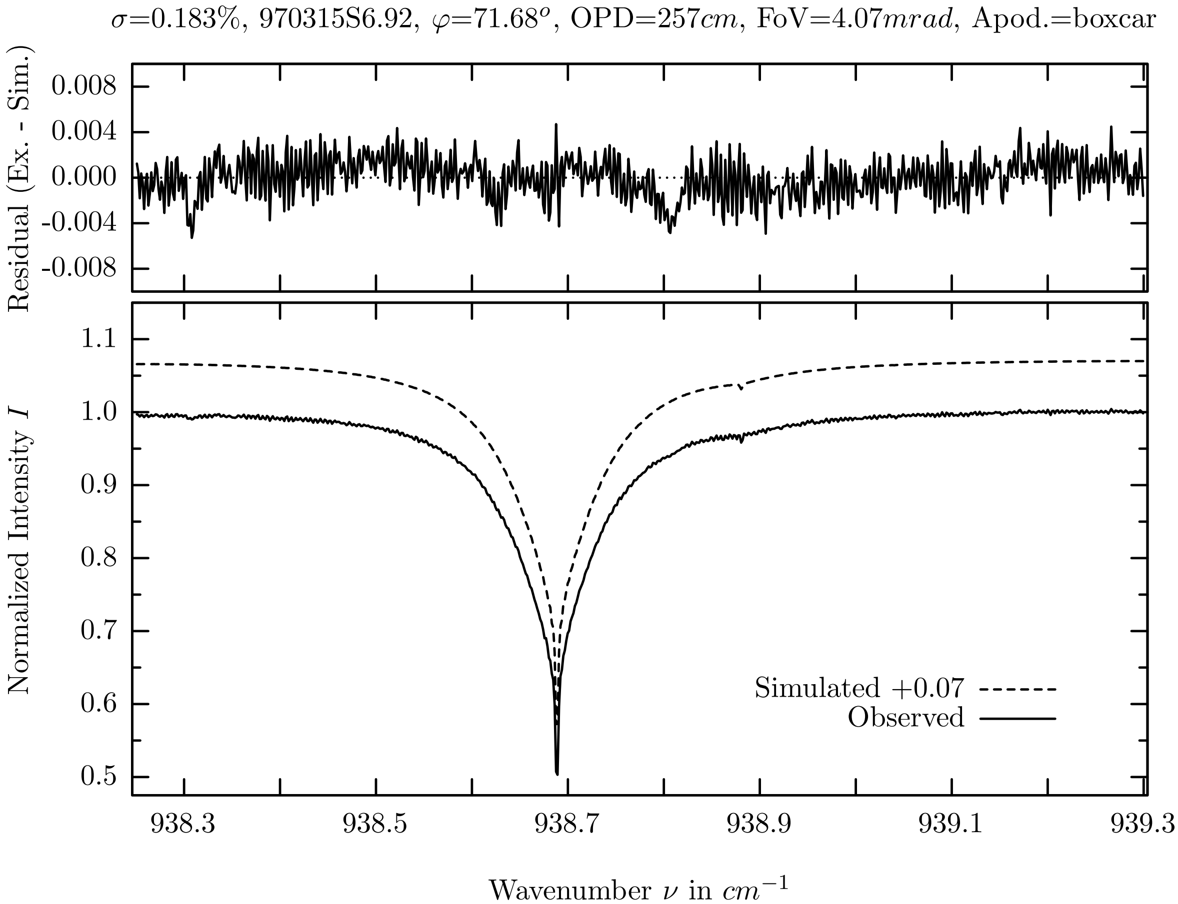

investigated species	:	CO_2
line position(s) ν_0	:	938.6882 cm^{-1}
lower state energy E''_{lst}	:	1662.0 cm^{-1}
retrieved TCA, information content	:	7.30E+21 $molec/cm^2$, 271.4
temperature dependence of the TCA	:	-3.585%/K (trop), -.928%/K (strat)
location, date, solar zenith angle	:	Kiruna, 15/Mar/97, 71.68^o
spectral interval fitted	:	938.250 – 939.300 cm^{-1}

Molecule	iCode	Absorption	Molecule	iCode	Absorption
CO2	21	56.721%	$N2O$	41	0.006%
Solar(A)	—	0.344%	$NH3$	111	0.006%
Solar-sim	—	0.178%	$NO2$	101	0.002%
Solar-DU	—	0.178%	HDO	491	0.001%
$CCl2F2$	321	0.327%	$CFC113$	621	0.001%
$H2O$	11	0.155%	$CH4$	61	<0.001%
$C2H4$	391	0.151%	OH	131	<0.001%
$SF6$	501	0.049%	$H2O2$	231	<0.001%
$O3$	31	0.039%	$N2O5$	261	<0.001%
$HNO3$	121	0.022%	$C2H6$	381	<0.001%
$COF2$	361	0.013%	$F142B$	611	<0.001%

CO_2, Kiruna, φ=71.68^o, OPD=257cm, FoV=4.06$mrad$, boxcar apod.

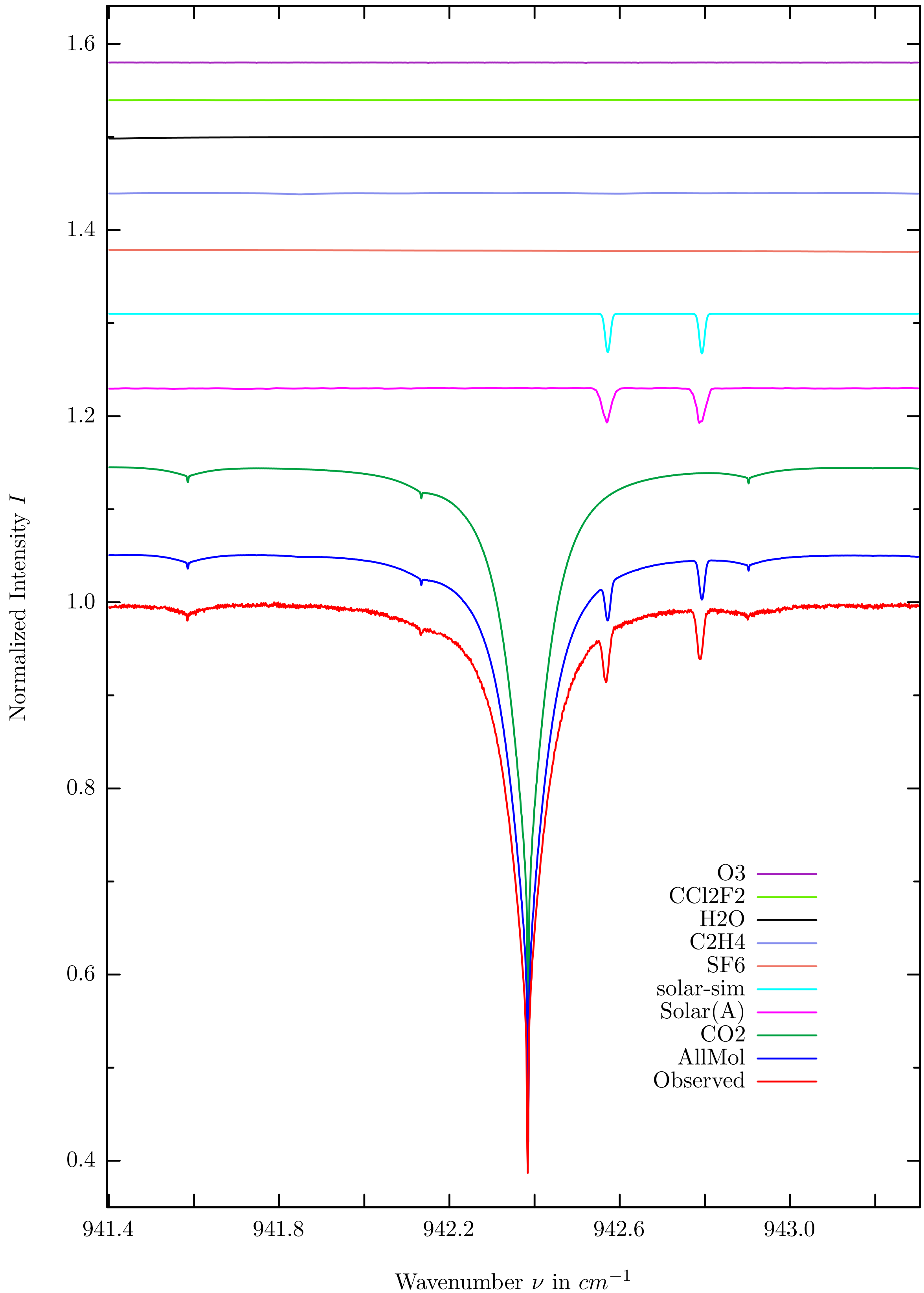

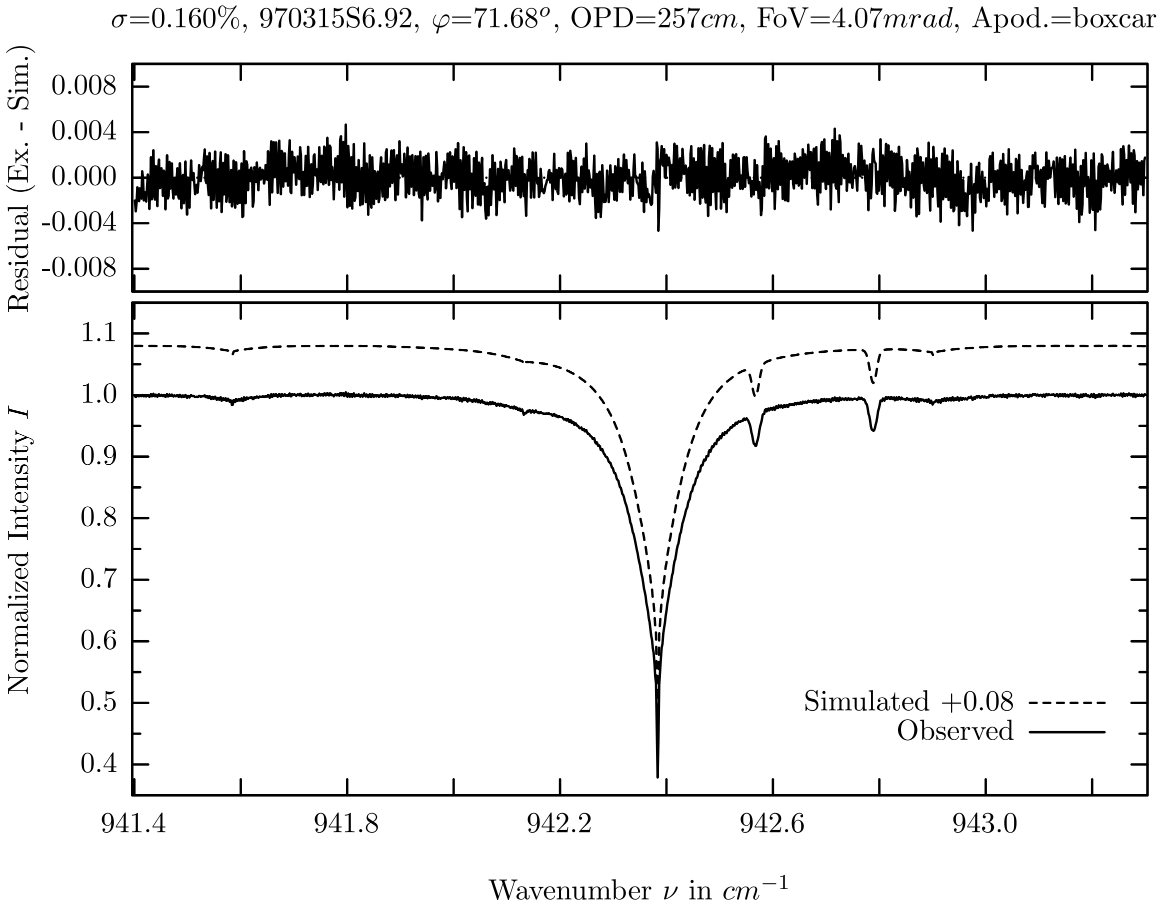

investigated species	:	$CO_2, (C_2H_4)$
line position(s) ν_0	:	942.3833, (941.8478) cm^{-1}
lower state energy E''_{lst}	:	1585.6, (135.9) cm^{-1}
retrieved TCA, information content	:	7.27E+21, (<1.0E+15) $molec/cm^2$, 390.9, (0.3)
temperature dependence of the TCA	:	-3.466, (n.a.)%/K (trop), -.849, (n.a.)%/K (strat)
location, date, solar zenith angle	:	Kiruna, 15/Mar/97, 71.68^o
spectral interval fitted	:	941.400 – 943.300 cm^{-1}

Molecule	iCode	Absorption	Molecule	iCode	Absorption
CO2	21	67.854%	HDO	491	0.011%
Solar(A)	—	3.717%	$HNO3$	121	0.008%
Solar-sim	—	4.284%	$NO2$	101	0.001%
Solar-DU	—	4.284%	$NH3$	111	0.001%
$SF6$	501	0.335%	$F142B$	611	0.001%
$C2H4$	391	0.176%	$CFC113$	621	0.001%
$H2O$	11	0.170%	$CH4$	61	<0.001%
$CCl2F2$	321	0.055%	OH	131	<0.001%
$O3$	31	0.051%	$H2O2$	231	<0.001%
$N2O$	41	0.029%	$N2O5$	261	<0.001%
$COF2$	361	0.027%			

SF_6, Kiruna, φ=71.68^o, OPD=257cm, FoV=4.06$mrad$, boxcar apod.

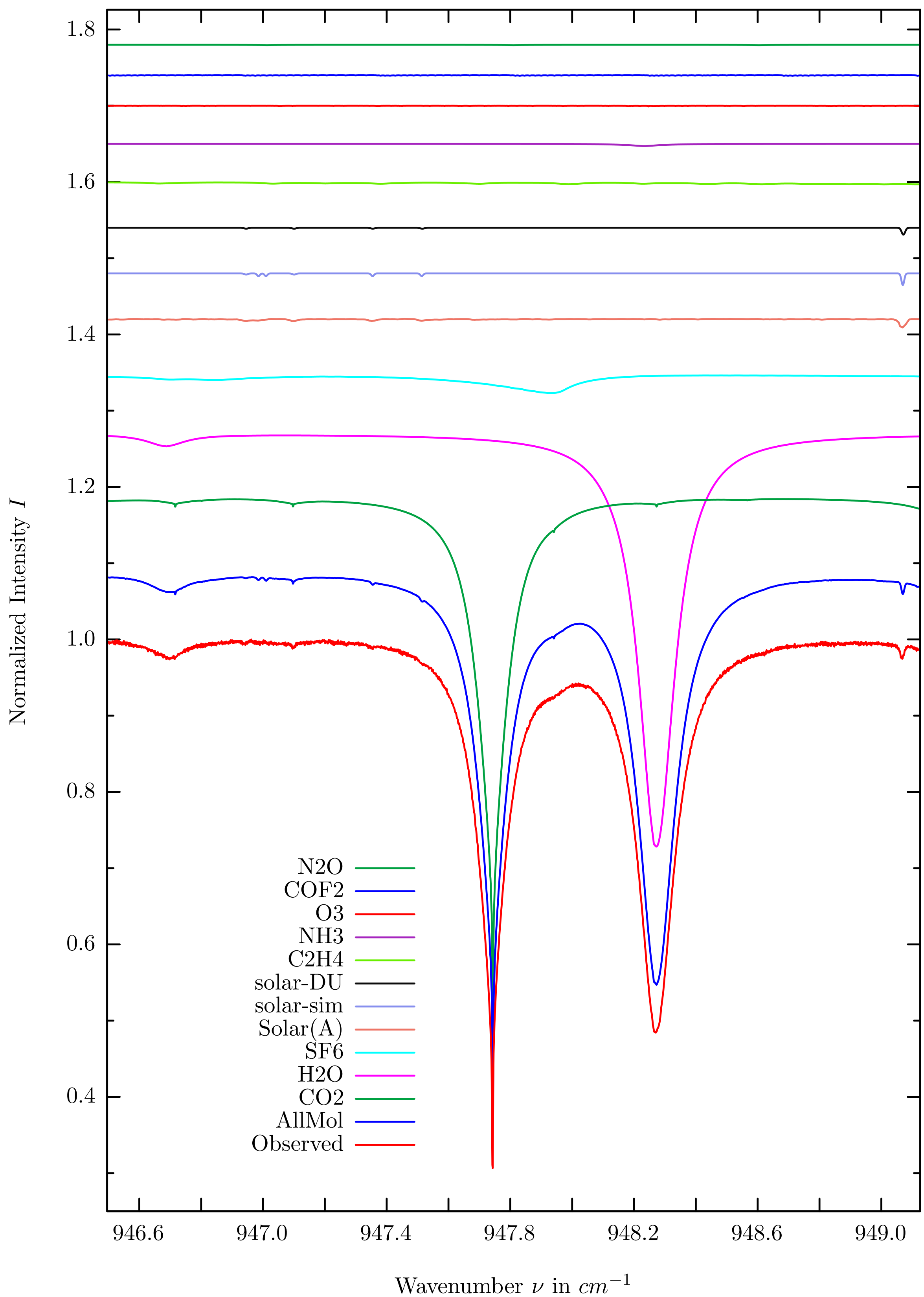

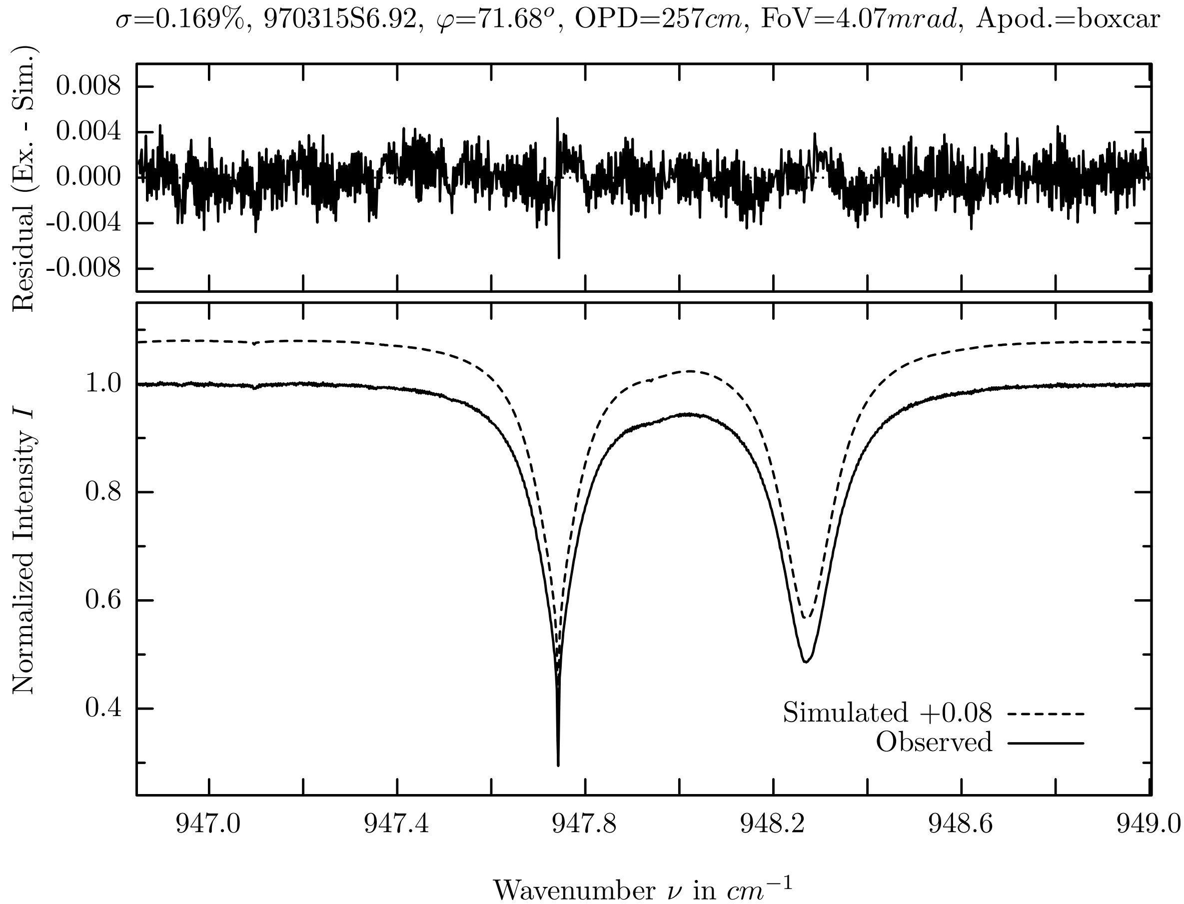

investigated species	:	$SF_6, (H_2O)$
line position(s) ν_0	:	947.9300, (948.2629) cm^{-1}
lower state energy E''_{lst}	:	241.0, (1327.1) cm^{-1}
retrieved TCA, information content	:	8.80E+13 (1.25E+15) $molec/cm^2$, 9.1, (0.3)
temperature dependence of the TCA	:	+.542 (-2.323)%/K (trop), +.178 (-.007)%/K (strat)
location, date, solar zenith angle	:	Kiruna, 15/Mar/97, 71.68^o
spectral interval fitted	:	946.850 – 949.000 cm^{-1}

Molecule	iCode	Absorption	Molecule	iCode	Absorption
$CO2$	21	76.183%	$CCl2F2$	321	0.025%
$H2O$	11	54.180%	$HNO3$	121	0.004%
SF6	501	2.698%	$F142B$	611	0.003%
Solar(A)	—	1.081%	$NO2$	101	0.002%
Solar-sim	—	1.533%	$CFC113$	621	0.001%
Solar-DU	—	0.918%	$CH4$	61	<0.001%
$C2H4$	391	0.307%	OH	131	<0.001%
$NH3$	111	0.289%	$H2O2$	231	<0.001%
$O3$	31	0.138%	$N2O5$	261	<0.001%
$COF2$	361	0.070%	HDO	491	<0.001%
$N2O$	41	0.061%			

Comment: Standing wave artefacts add substantial systematic uncertainties to the TCAs reported.

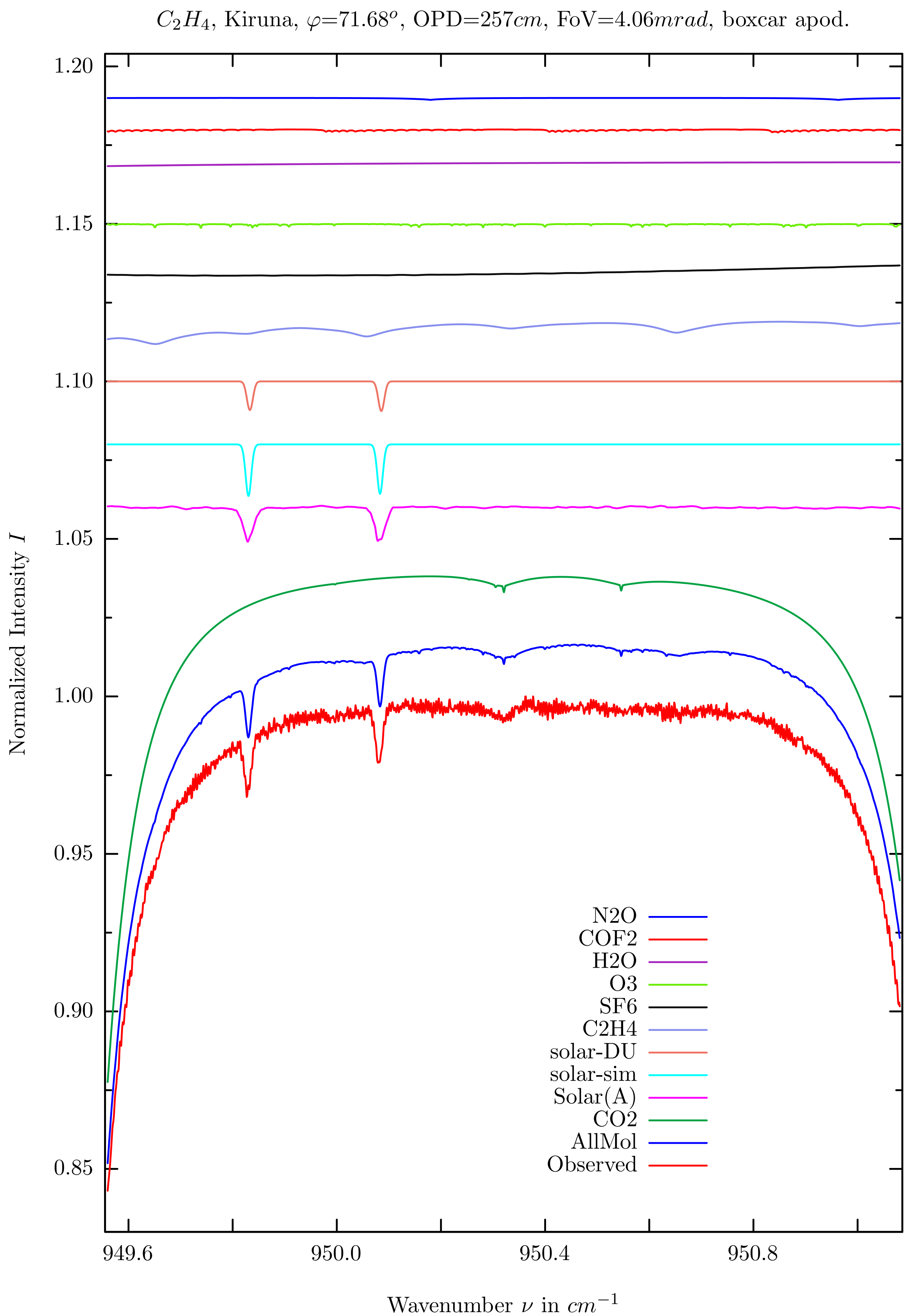
C_2H_4, Kiruna, φ=71.68^o, OPD=257cm, FoV=4.06$mrad$, boxcar apod.
1.20
1.15
1.10
1.05
1.00
0.95
0.90
0.85
Normalized Intensity I
949.6
950.0
950.4
950.8
Wavenumber ν in cm^{-1}
N2O
COF2
H2O
O3
SF6
C2H4
solar-DU
solar-sim
Solar(A)
CO2
AllMol
Observed

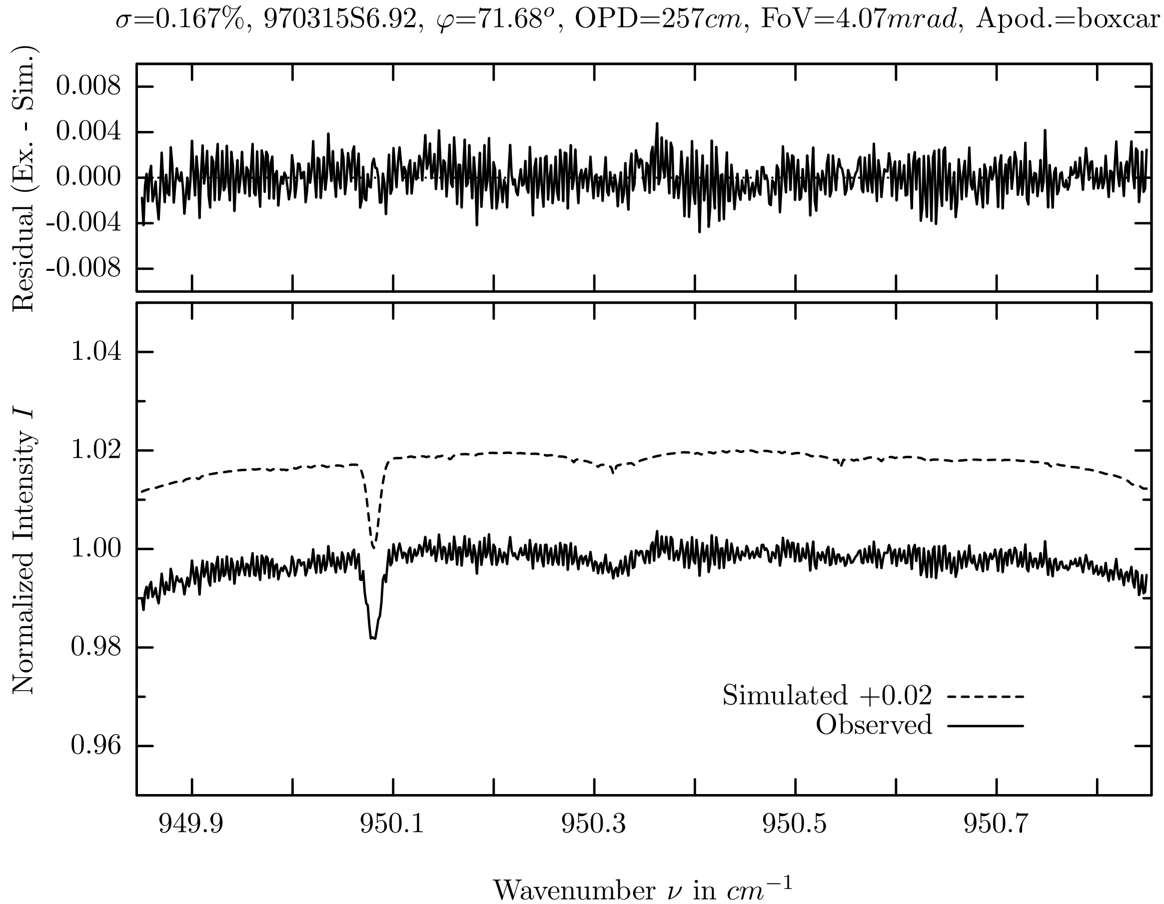

investigated species	:	C_2H_4
line position(s) ν_0	:	950.0562, 950.6498 cm^{-1}
lower state energy E''_{lst}	:	98.1, 64.7 cm^{-1}
retrieved TCA, information content	:	8.34E+14 $molec/cm^2$, 0.5, 0.8
temperature dependence of the TCA	:	+1.589%/K (trop), +.203%/K (strat)
location, date, solar zenith angle	:	Kiruna, 15/Mar/97, 71.68^o
spectral interval fitted	:	949.850 – 950.850 cm^{-1}

Molecule	iCode	Absorption	Molecule	iCode	Absorption
$CO2$	21	16.483%	$F142B$	611	0.005%
Solar(A)	—	1.091%	$NH3$	111	0.004%
Solar-sim	—	1.649%	$HNO3$	121	0.002%
Solar-DU	—	0.947%	$NO2$	101	0.001%
C2H4	391	0.814%	$CFC113$	621	0.001%
$SF6$	501	0.645%	$CH4$	61	<0.001%
$O3$	31	0.166%	OH	131	<0.001%
$H2O$	11	0.165%	$H2O2$	231	<0.001%
$COF2$	361	0.102%	$N2O5$	261	<0.001%
$N2O$	41	0.065%	HDO	491	<0.001%
$CCl2F2$	321	0.019%			

Comment: Standing wave artefacts add substantial systematic uncertainties to the TCAs reported.

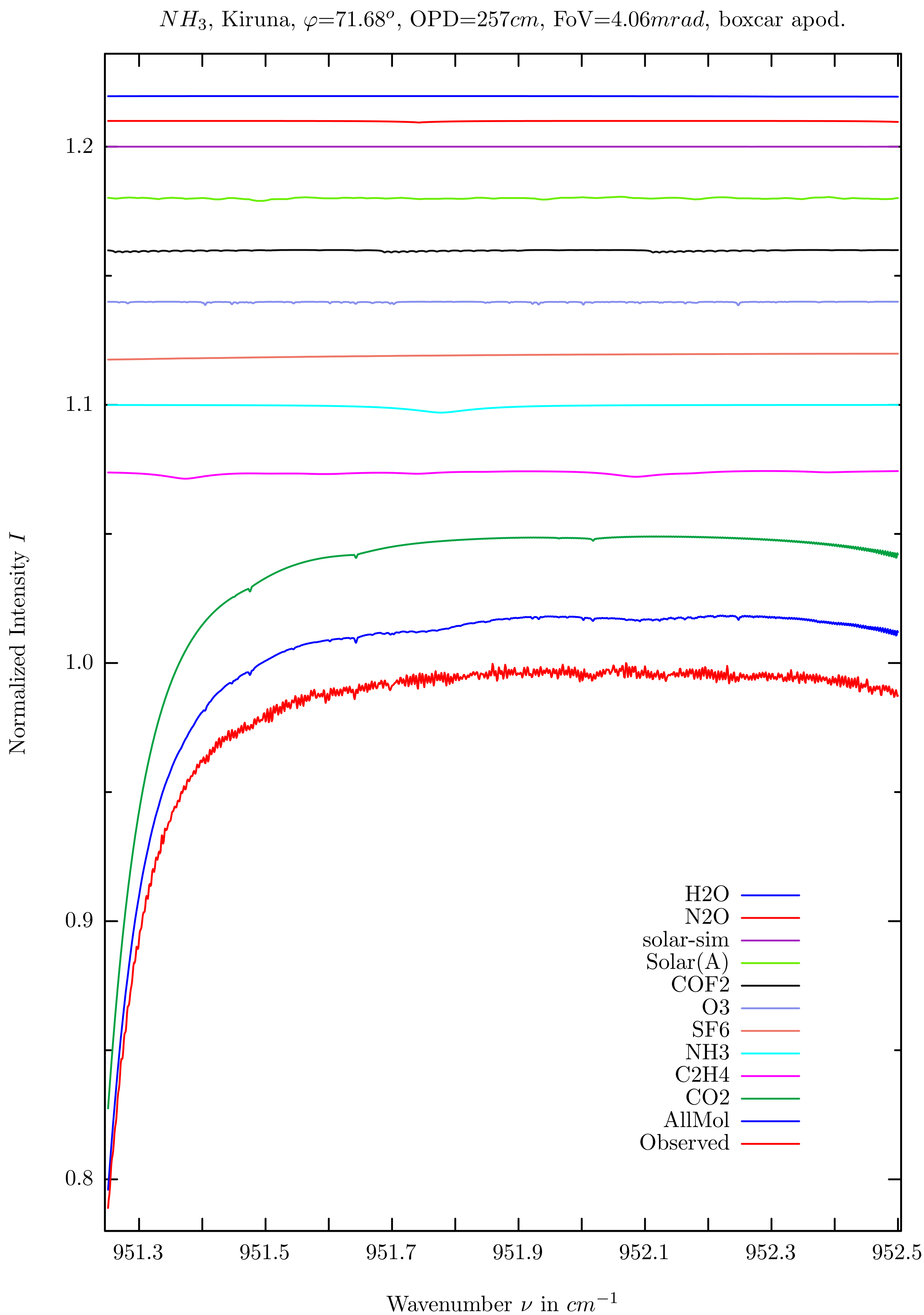
NH_3, Kiruna, φ=71.68^o, OPD=257cm, FoV=4.06$mrad$, boxcar apod.
Normalized Intensity I
Wavenumber ν in cm^{-1}
1.2
1.1
1.0
0.9
0.8
951.3
951.5
951.7
951.9
952.1
952.3
952.5
H2O
N2O
solar-sim
Solar(A)
COF2
O3
SF6
NH3
C2H4
CO2
AllMol
Observed

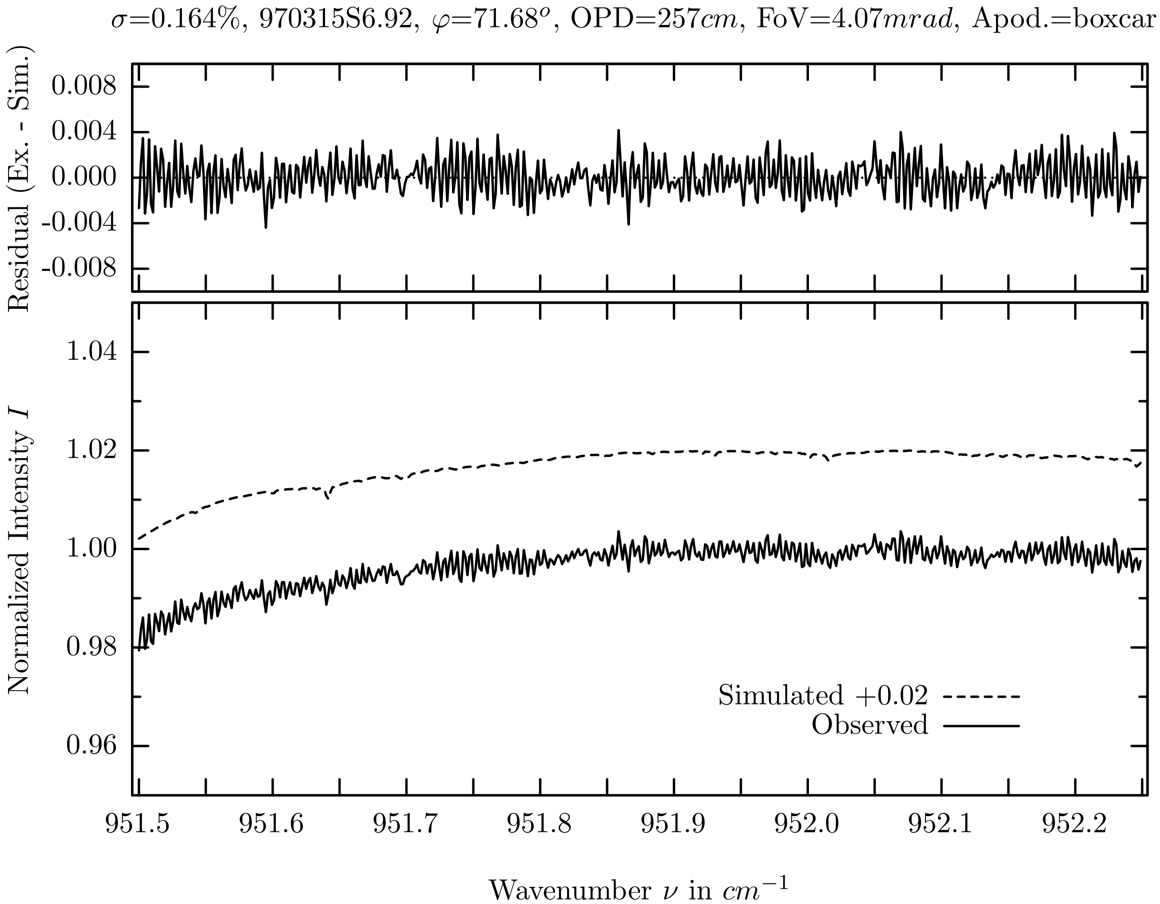

investigated species	:	NH_3
line position(s) ν_0	:	951.7762 cm^{-1}
lower state energy E''_{lst}	:	0.8 cm^{-1}
retrieved TCA, information content	:	3.86E+14 $molec/cm^2$, 0.4
temperature dependence of the TCA	:	+.750%/K (trop), +1.283%/K (strat)
location, date, solar zenith angle	:	Kiruna, 15/Mar/97, 71.68^o
spectral interval fitted	:	951.500 – 952.250 cm^{-1}

Molecule	iCode	Absorption	Molecule	iCode	Absorption
$CO2$	21	22.389%	$H2O$	11	0.064%
$C2H4$	391	0.361%	$F142B$	611	0.007%
NH3	111	0.300%	$NO2$	101	0.001%
$SF6$	501	0.247%	$HNO3$	121	0.001%
$O3$	31	0.171%	$CH4$	61	<0.001%
$COF2$	361	0.105%	OH	131	<0.001%
Solar(A)	—	0.101%	$H2O2$	231	<0.001%
Solar-sim	—	0.002%	$CCl2F2$	321	<0.001%
Solar-DU	—	0.002%	$HCOOH$	461	<0.001%
$N2O$	41	0.066%	$CFC113$	621	<0.001%

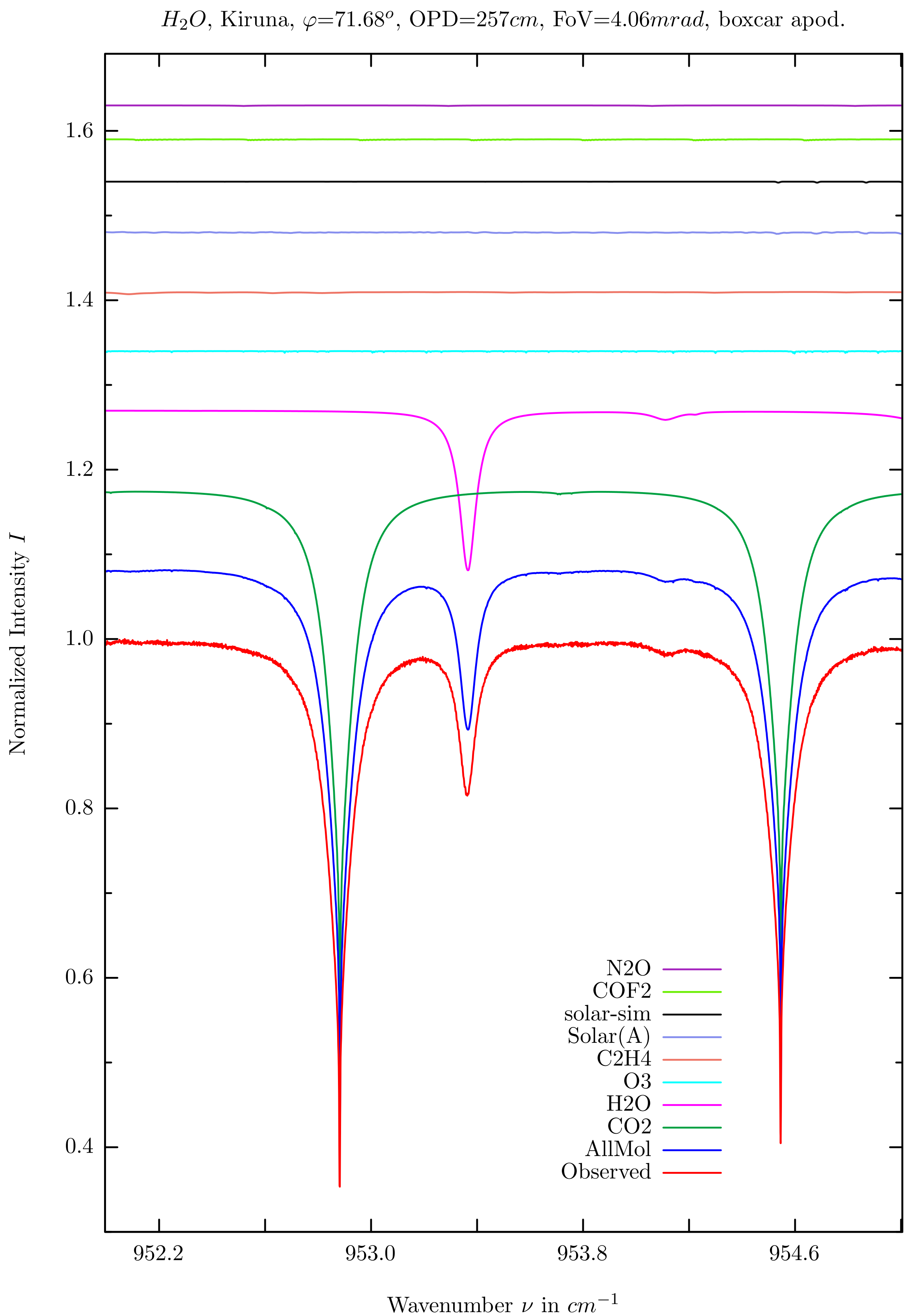

H_2O, Kiruna, φ=71.68^o, OPD=257cm, FoV=4.06$mrad$, boxcar apod.
Normalized Intensity I
1.6
1.4
1.2
1.0
0.8
0.6
0.4
952.2
953.0
953.8
954.6
Wavenumber ν in cm^{-1}
N2O
COF2
solar-sim
Solar(A)
C2H4
O3
H2O
CO2
AllMol
Observed

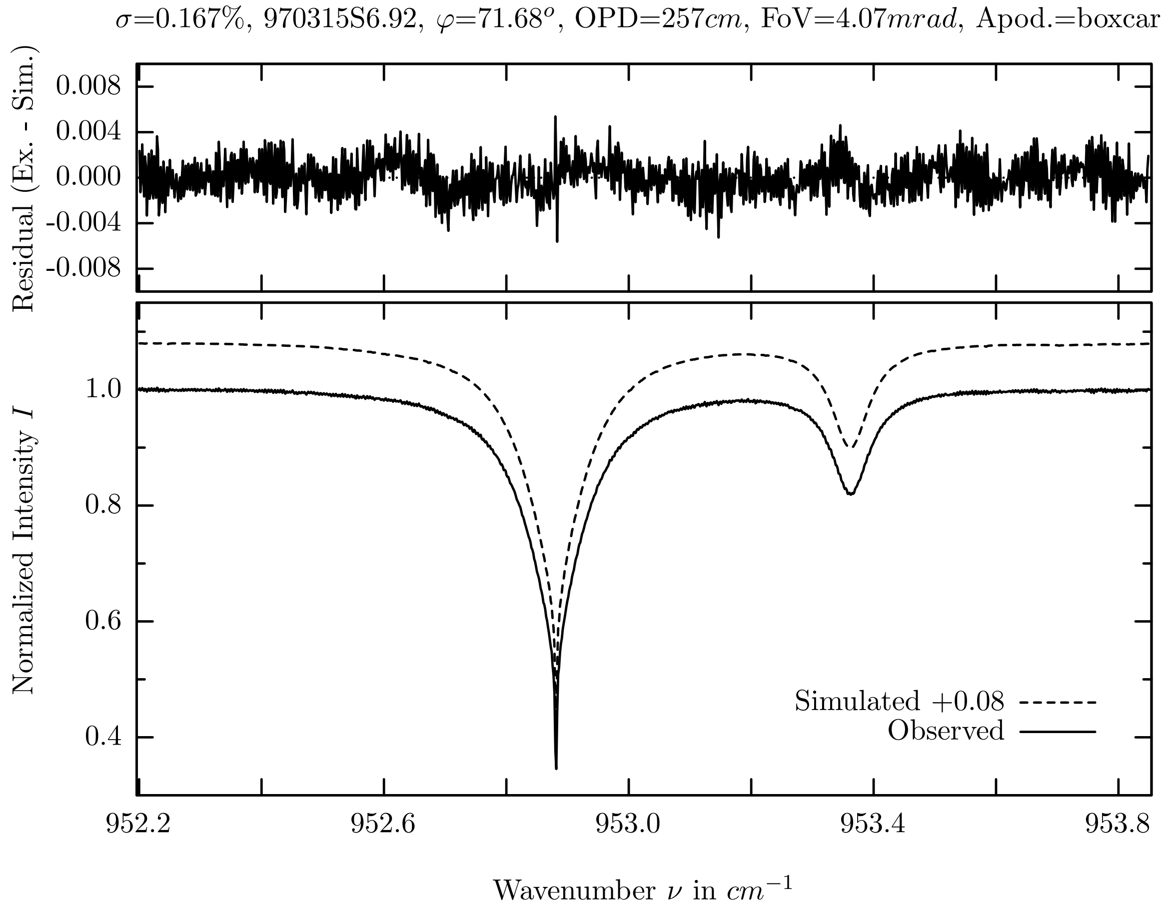

investigated species	:	H_2O
line position(s) ν_0	:	953.3674 cm^{-1}
lower state energy E''_{lst}	:	1962.5 cm^{-1}
retrieved TCA, information content	:	5.19E+21 $molec/cm^2$, 108.0
temperature dependence of the TCA	:	-3.249%/K (trop), -.003%/K (strat)
location, date, solar zenith angle	:	Kiruna, 15/Mar/97, 71.68^o
spectral interval fitted	:	952.200 – 953.850 cm^{-1}

Molecule	iCode	Absorption	Molecule	iCode	Absorption
$CO2$	21	71.637%	$F142B$	611	0.009%
H2O	11	18.886%	$NO2$	101	0.001%
$O3$	31	0.325%	$HNO3$	121	0.001%
$C2H4$	391	0.286%	$CH4$	61	<0.001%
Solar(A)	—	0.163%	OH	131	<0.001%
Solar-sim	—	0.115%	$H2O2$	231	<0.001%
Solar-DU	—	0.115%	$CCl2F2$	321	<0.001%
$COF2$	361	0.134%	$HCOOH$	461	<0.001%
$N2O$	41	0.065%	HDO	491	<0.001%
$SF6$	501	0.048%	$CFC113$	621	<0.001%
$NH3$	111	0.028%			

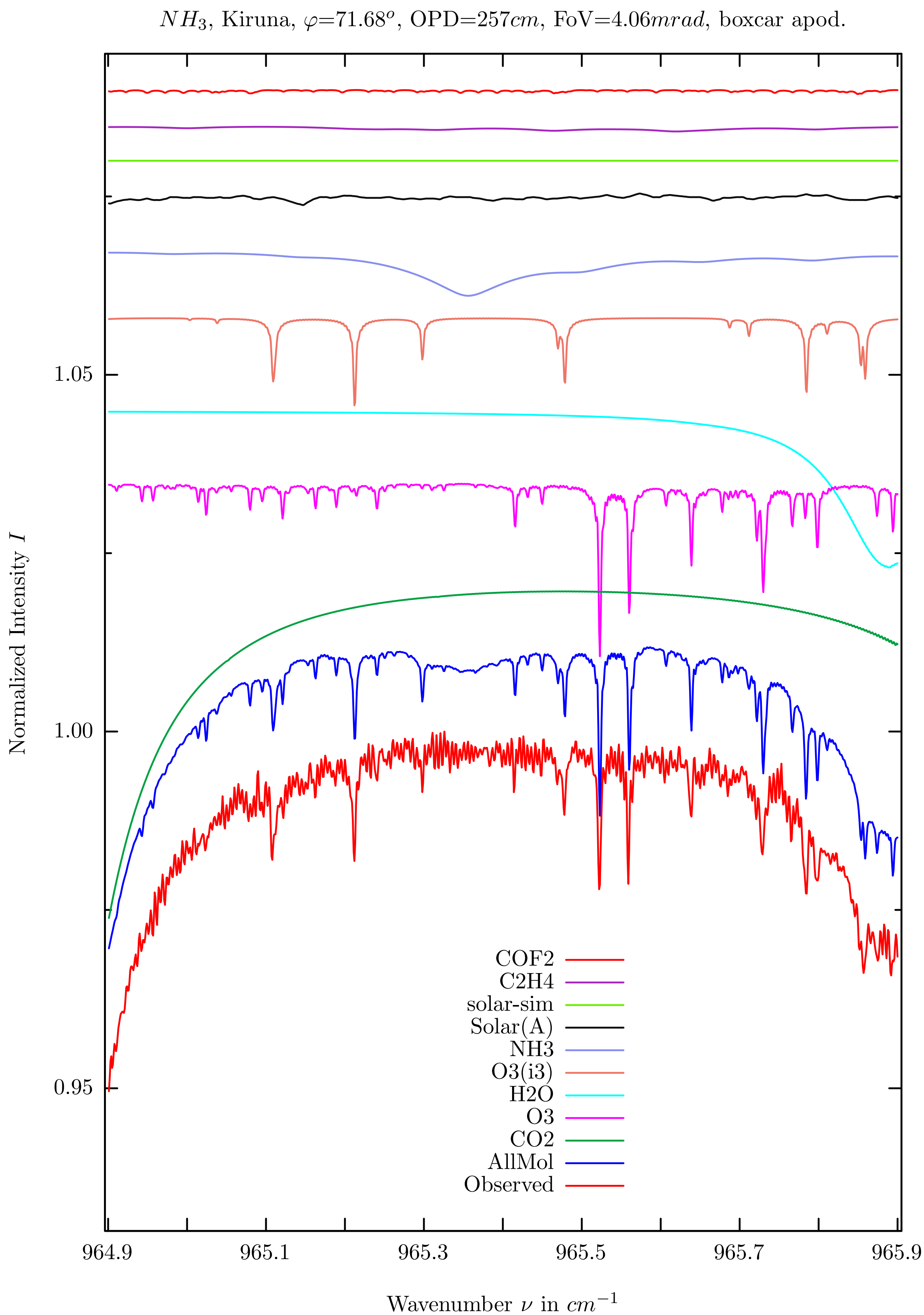

NH_3, Kiruna, φ=71.68^o, OPD=257cm, FoV=4.06$mrad$, boxcar apod.
Normalized Intensity I
1.05
1.00
0.95
964.9
965.1
965.3
965.5
965.7
965.9
Wavenumber ν in cm^{-1}
COF2
C2H4
solar-sim
Solar(A)
NH3
O3(i3)
H2O
O3
CO2
AllMol
Observed

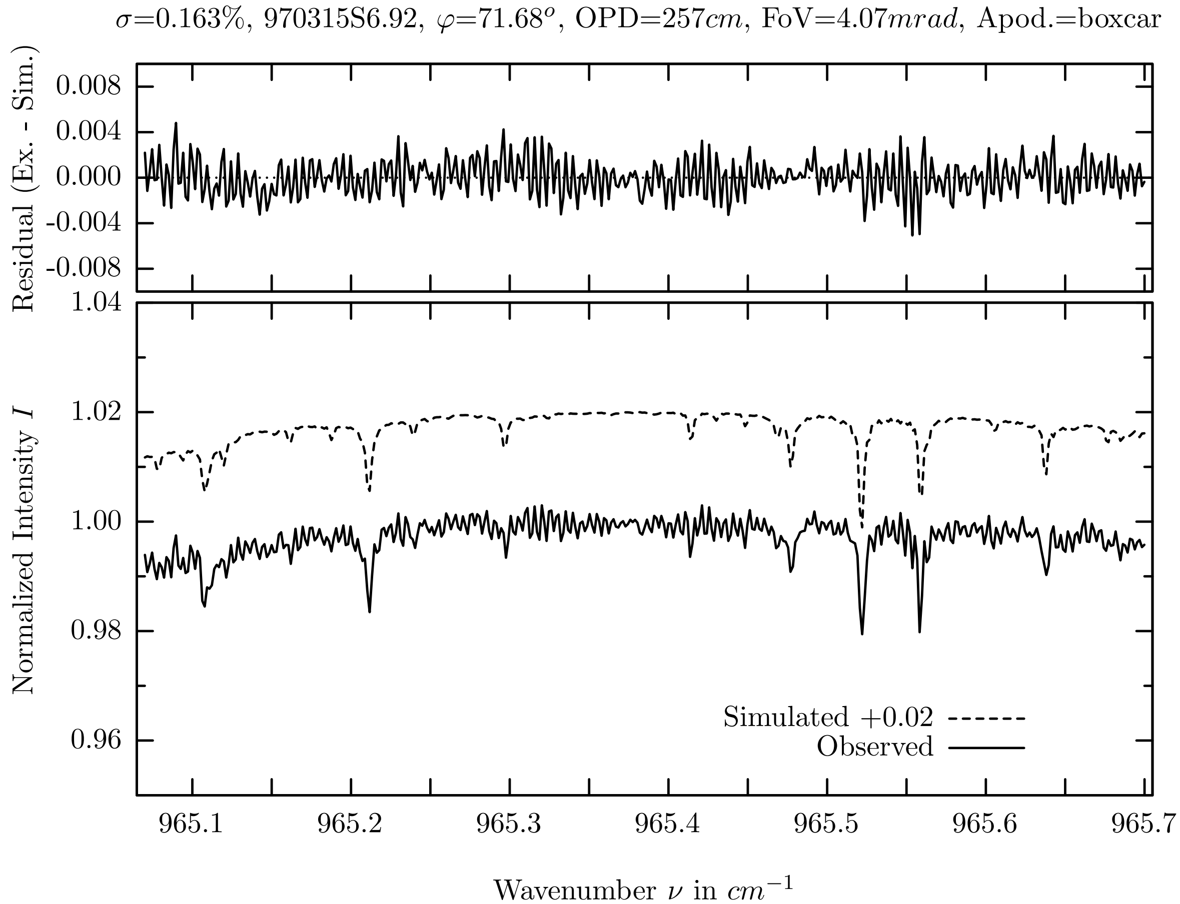

investigated species	:	NH_3
line position(s) ν_0	:	965.3539 cm^{-1}
lower state energy E''_{lst}	:	283.6 cm^{-1}
retrieved TCA, information content	:	1.77E+14 $molec/cm^2$, 0.5
temperature dependence of the TCA	:	+1.549%/K (trop), -.847%/K (strat)
location, date, solar zenith angle	:	Kiruna, 15/Mar/97, 71.68^o
spectral interval fitted	:	965.070 – 965.700 cm^{-1}

Molecule	iCode	Absorption	Molecule	iCode	Absorption
$CO2$	21	5.052%	HDO	491	0.012%
$O3$	31	3.043%	$CHF2Cl$	421	0.003%
$H2O$	11	2.204%	$ClONO2$	271	0.002%
$O3$	**33**	1.508%	$NO2$	101	0.001%
NH3	111	0.693%	$CCl3F$	331	0.001%
Solar(A)	—	0.121%	$CH4$	61	<0.001%
Solar-sim	—	<0.001%	$HNO3$	121	<0.001%
Solar-DU	—	<0.001%	OH	131	<0.001%
$C2H4$	391	0.090%	$H2O2$	231	<0.001%
$COF2$	361	0.068%	$HCOOH$	461	<0.001%
$F142B$	611	0.025%	$CFC113$	621	<0.001%
$N2O$	41	0.020%			

NH_3, Kiruna, φ=71.68^o, OPD=257cm, FoV=4.06$mrad$, boxcar apod.

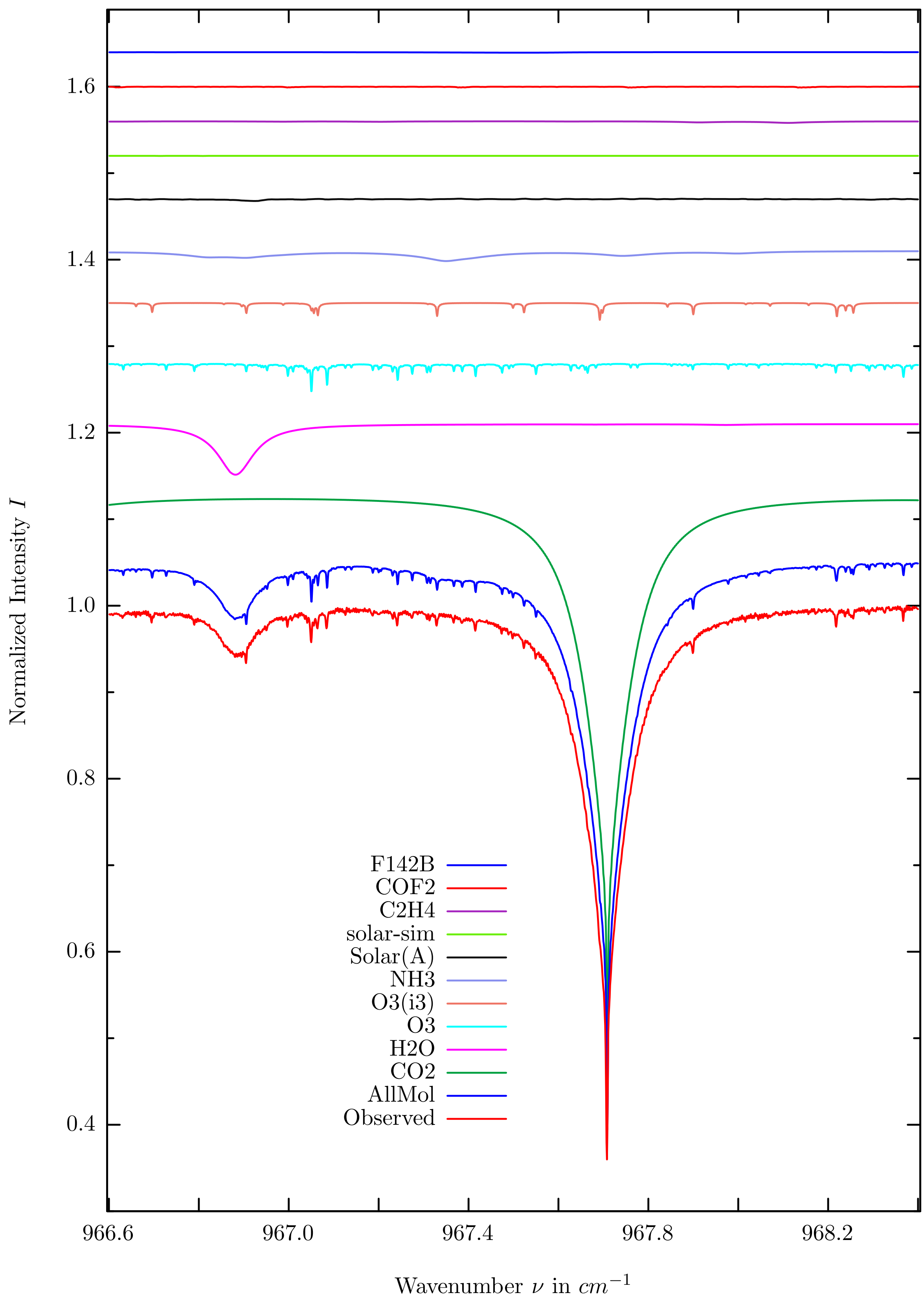

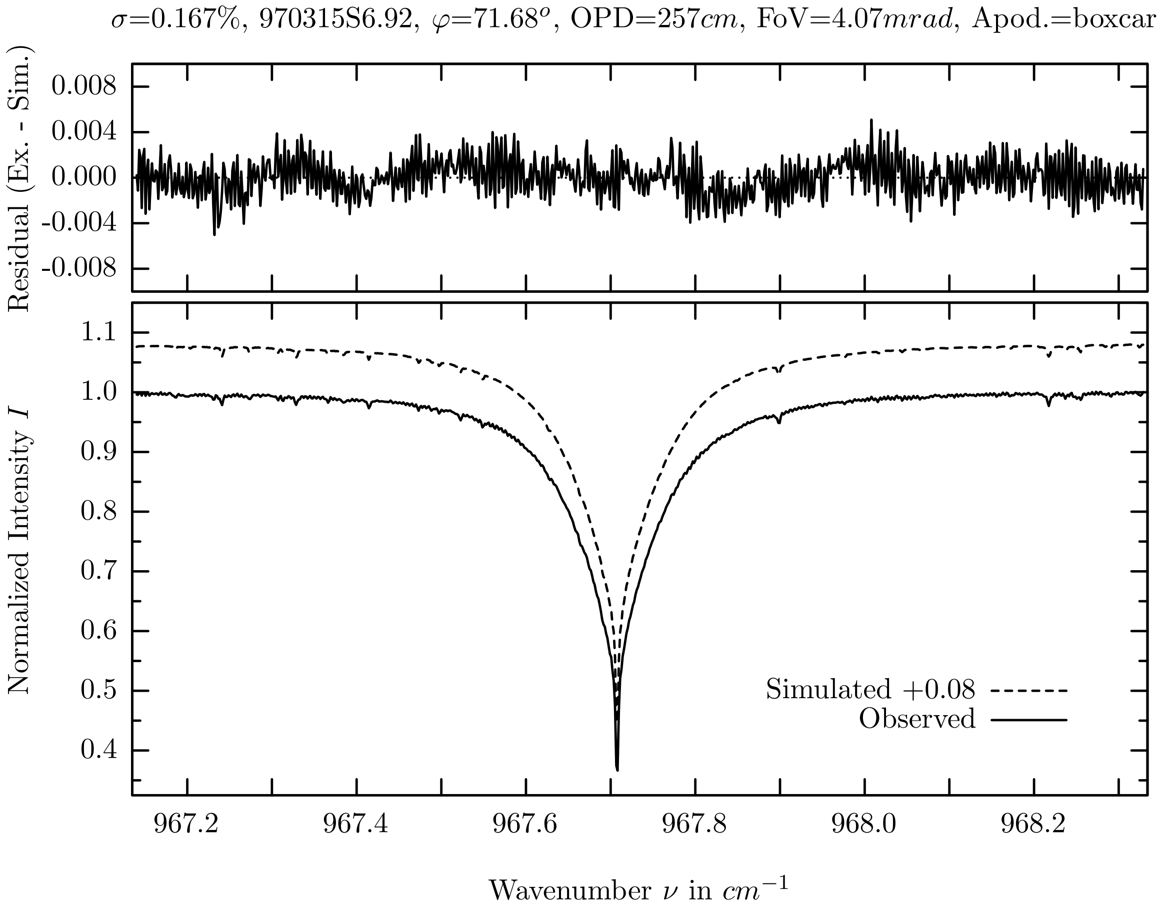

investigated species	:	$NH_3, (CO_2)$
line position(s) ν_0	:	967.3463, (967.7075) cm^{-1}
lower state energy E''_{lst}	:	85.9, (1416.3) cm^{-1}
retrieved TCA, information content	:	<1.0E+14, (7.31E+21) $molec/cm^2$, 3.0, (380.1)
temperature dependence of the TCA	:	n.a., (-3.047)%/K (trop), n.a., (-.726)%/K (strat)
location, date, solar zenith angle	:	Kiruna, 15/Mar/97, 71.68^o
spectral interval fitted	:	967.140 – 968.330 cm^{-1}

Molecule	iCode	Absorption	Molecule	iCode	Absorption
$CO2$	21	69.855%	$ClONO2$	271	0.003%
$H2O$	11	5.859%	$NO2$	101	0.001%
$O3$	31	4.197%	HDO	491	0.001%
$O3$	**33**	2.331%	$CH4$	61	<0.001%
NH3	111	1.164%	$HNO3$	121	<0.001%
Solar(A)	—	0.220%	OH	131	<0.001%
Solar-sim	—	0.012%	$H2O2$	231	<0.001%
Solar-DU	—	0.012%	$CCl3F$	331	<0.001%
$C2H4$	391	0.190%	$CHF2Cl$	421	<0.001%
$COF2$	361	0.112%	$HCOOH$	461	<0.001%
$F142B$	611	0.074%	$CFC113$	621	<0.001%
$N2O$	41	0.015%			

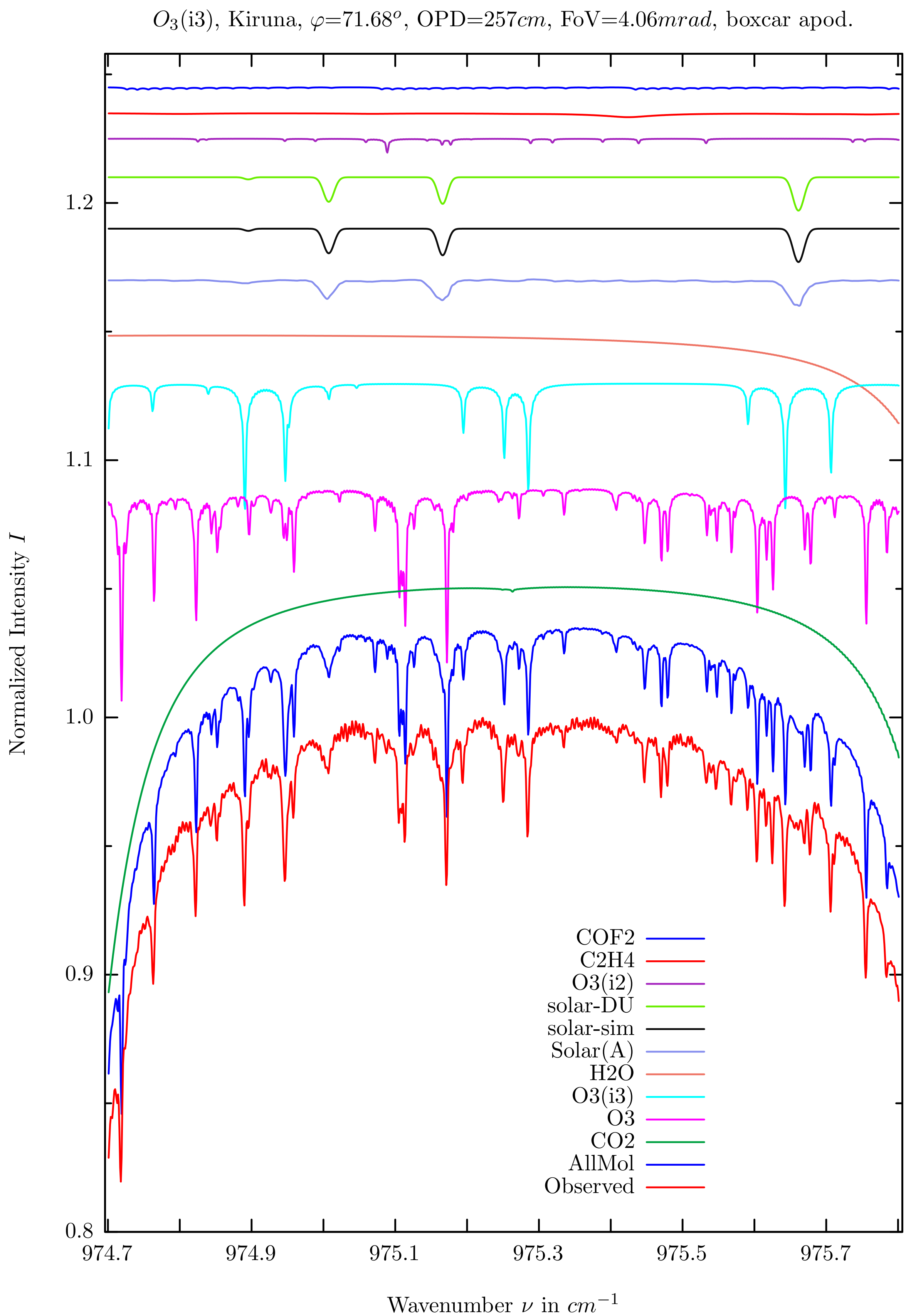
O_3(i3), Kiruna, φ=71.68^o, OPD=257cm, FoV=4.06$mrad$, boxcar apod.
Normalized Intensity I
Wavenumber ν in cm^{-1}
0.8
0.9
1.0
1.1
1.2
974.7
974.9
975.1
975.3
975.5
975.7
COF2
C2H4
O3(i2)
solar-DU
solar-sim
Solar(A)
H2O
O3(i3)
O3
CO2
AllMol
Observed

σ=0.188%, 970315S6.92, φ=17649704.00^o, OPD=257cm, FoV=4.07$mrad$, Apod.=boxcar

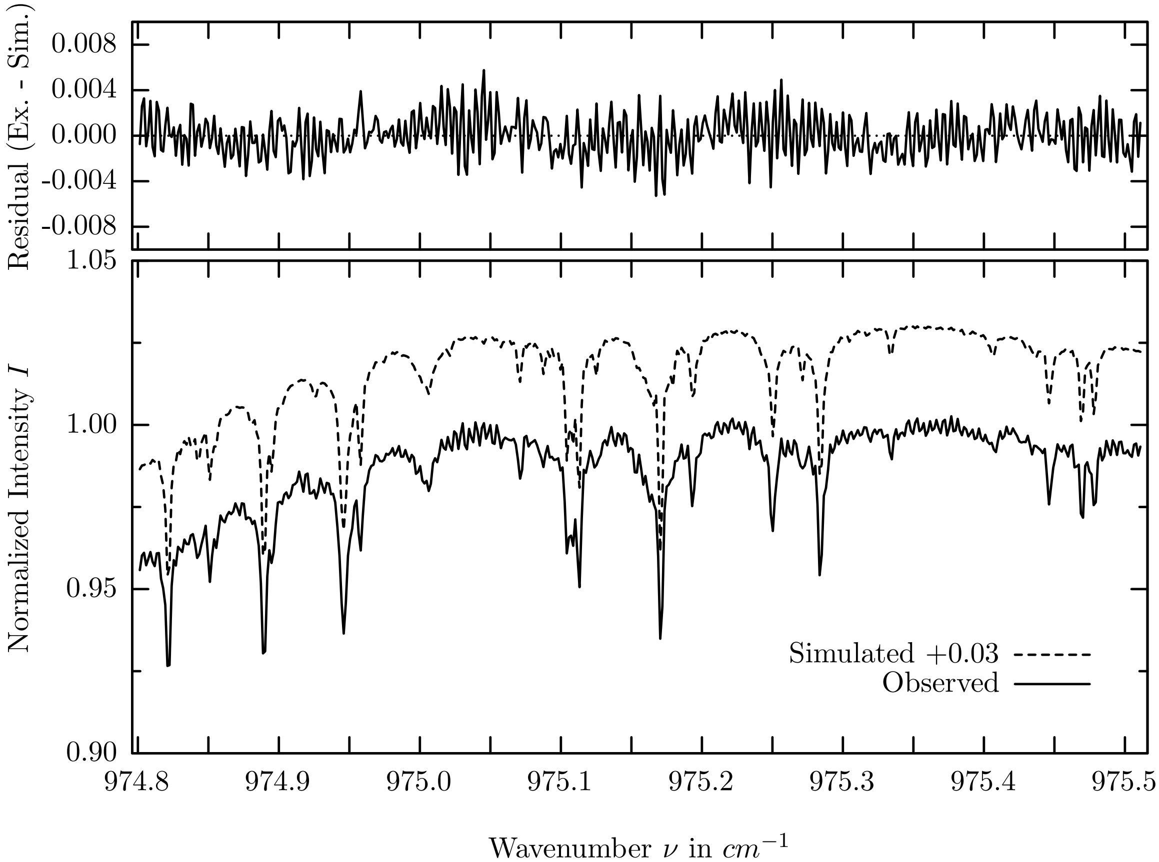

investigated species	:	$O_3(i3 = {}^{16}O\,{}^{18}O\,{}^{16}O), (O_3)$
line position(s) ν_0	:	975.2838, (975.1705) cm^{-1}
lower state energy E''_{lst}	:	495.4, (1484.3) cm^{-1}
retrieved TCA, information content	:	1.10E+19 (9.18E+19) $molec/cm^2$, 23.9, (36.5)
temperature dependence of the TCA	:	-.123 (-.409)%/K (trop), -.907 (-3.496)%/K (strat)
location, date, solar zenith angle	:	Kiruna, 15/Mar/97, 71.68^o
spectral interval fitted	:	974.800 – 975.512 cm^{-1}

Molecule	iCode	Absorption	Molecule	iCode	Absorption
$CO2$	21	16.411%	$ClONO2$	271	0.007%
$O3$	31	10.270%	$N2O$	41	0.002%
O3	**33**	5.860%	$CH4$	61	0.001%
$H2O$	11	3.617%	$NO2$	101	0.001%
Solar(A)	—	0.998%	$NH3$	111	0.001%
Solar-sim	—	1.301%	$CFC113$	621	0.001%
Solar-DU	—	0.650%	OH	131	<0.001%
$O3$	**32**	0.654%	$H2O2$	231	<0.001%
$C2H4$	391	0.165%	$HCOOH$	461	<0.001%
$COF2$	361	0.103%	HDO	491	<0.001%
$F142B$	611	0.012%			

O_3(i3), Kiruna, φ=71.68^o, OPD=257cm, FoV=4.06$mrad$, boxcar apod.

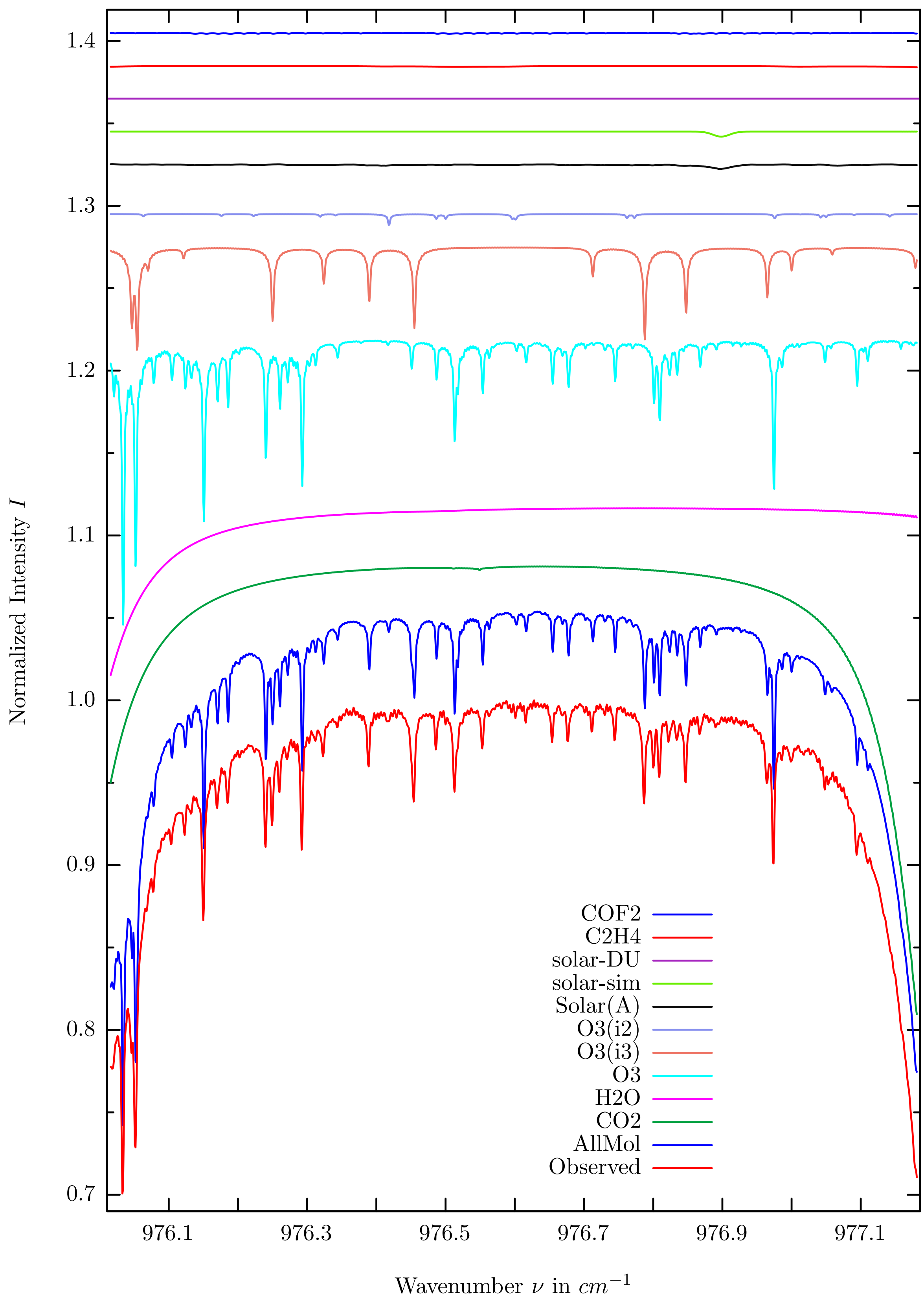

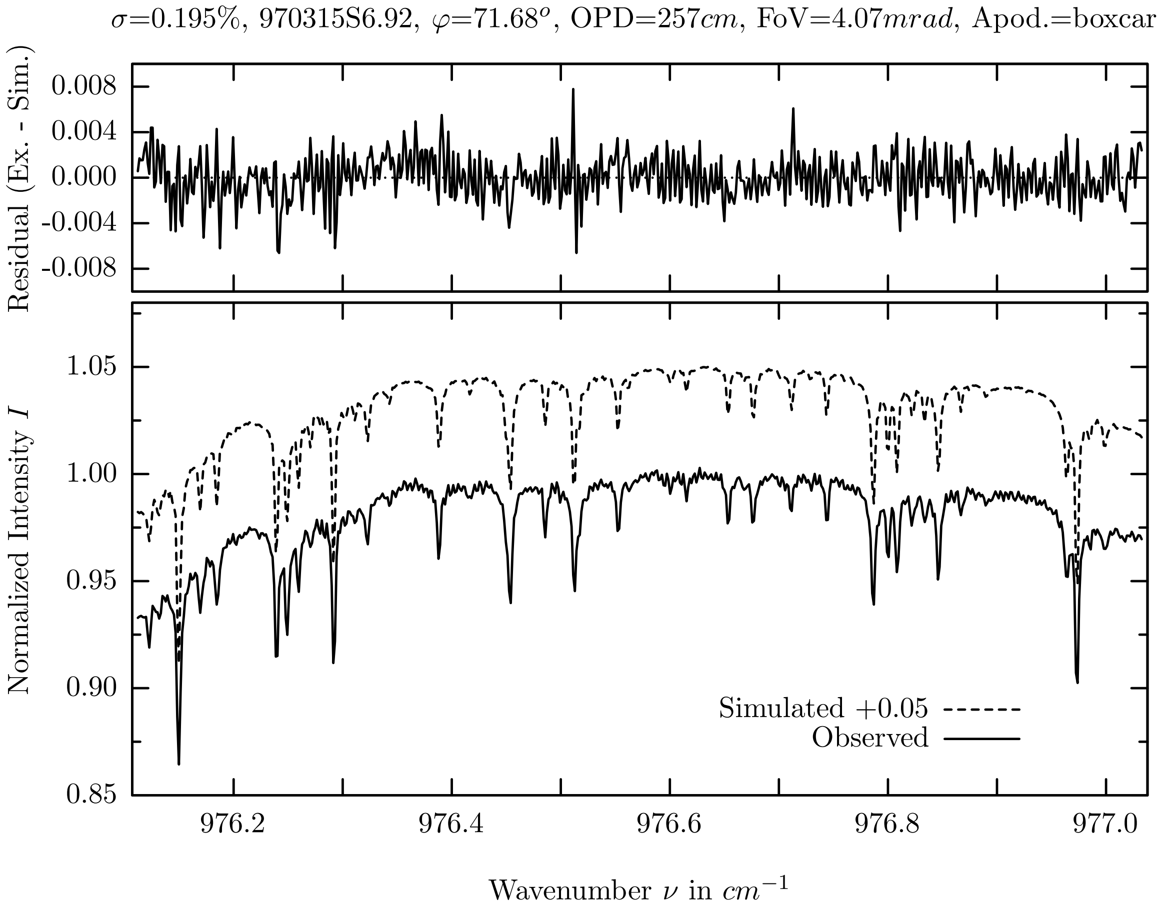

investigated species	:	$O_3(i3 = {}^{16}O\,{}^{18}O\,{}^{16}O), (O_3)$
line position(s) ν_0	:	976.7864, (976.5119) cm^{-1}
lower state energy E''_{lst}	:	446.8, (1495.0) cm^{-1}
retrieved TCA, information content	:	1.10E+19, (9.14E+18) $molec/cm^2$, 21.5, (28.2)
temperature dependence of the TCA	:	-.218, (-.341)%/K (trop), -.728, (-3.346)%/K (strat)
location, date, solar zenith angle	:	Kiruna, 15/Mar/97, 71.68^o
spectral interval fitted	:	976.112 – 977.033 cm^{-1}

Molecule	iCode	Absorption	Molecule	iCode	Absorption
$CO2$	21	28.468%	$ClONO2$	271	0.008%
$O3$	31	20.861%	$N2O$	41	0.002%
$H2O$	11	10.222%	$CH4$	61	0.001%
O3	**33**	7.330%	$NO2$	101	0.001%
$O3$	**32**	0.800%	$CFC113$	621	0.001%
Solar(A)	—	0.270%	$NH3$	111	<0.001%
Solar-sim	—	0.303%	OH	131	<0.001%
Solar-DU	—	<0.001%	$H2O2$	231	<0.001%
$C2H4$	391	0.092%	$N2O5$	261	<0.001%
$COF2$	361	0.084%	$HCOOH$	461	<0.001%
$F142B$	611	0.012%	HDO	491	<0.001%

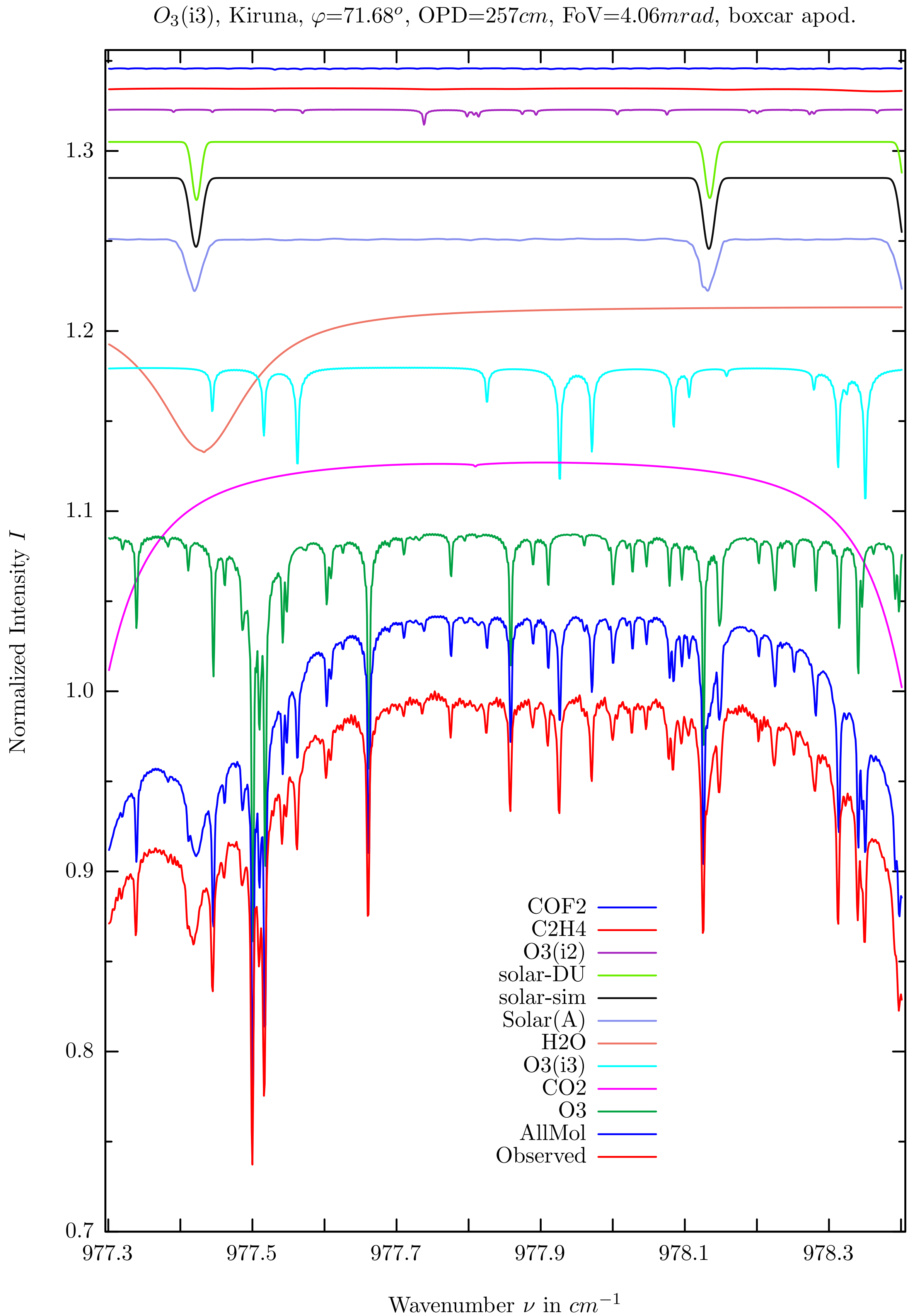

O_3(i3), Kiruna, φ=71.68^o, OPD=257cm, FoV=4.06$mrad$, boxcar apod.
Normalized Intensity I
Wavenumber ν in cm^{-1}
1.3
1.2
1.1
1.0
0.9
0.8
0.7
977.3
977.5
977.7
977.9
978.1
978.3
COF2
C2H4
O3(i2)
solar-DU
solar-sim
Solar(A)
H2O
O3(i3)
CO2
O3
AllMol
Observed

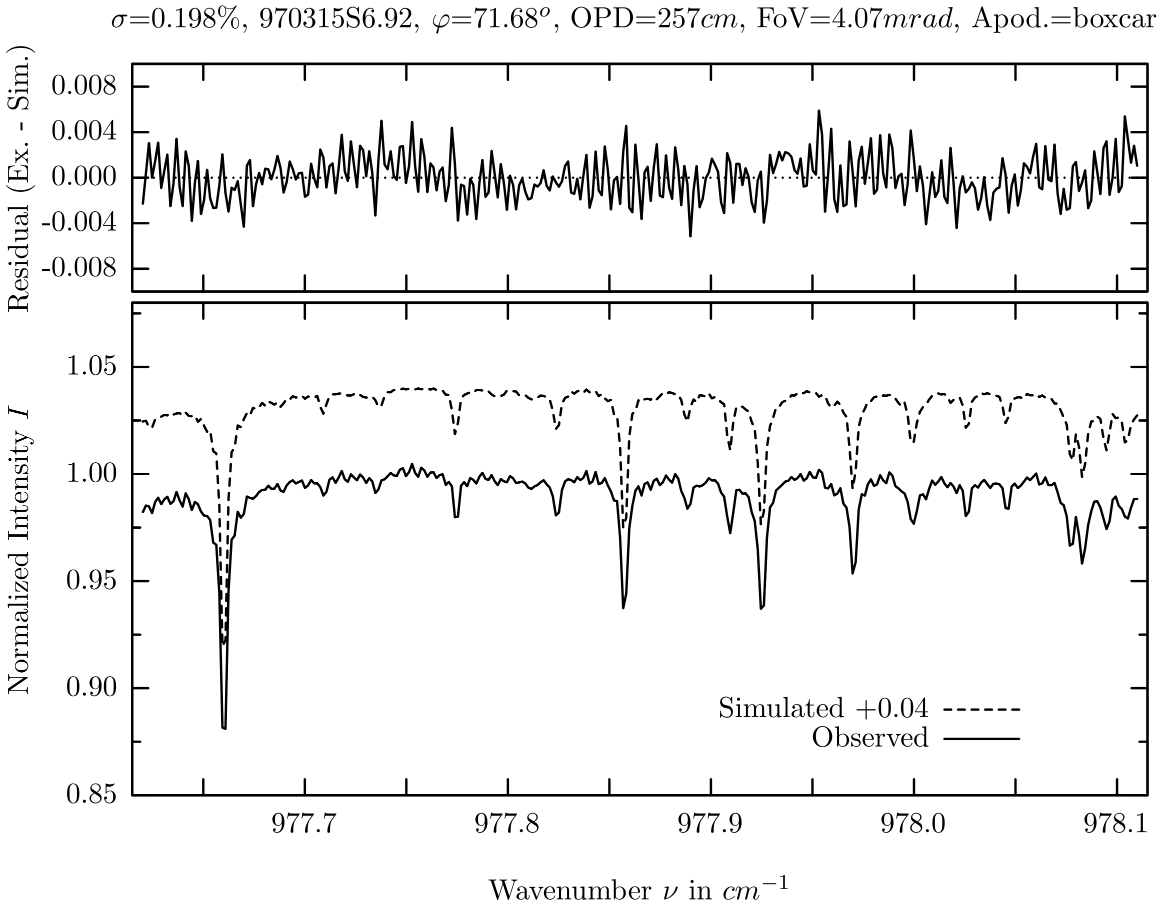

investigated species	:	$O_3(i3 = {}^{16}O\,{}^{18}O\,{}^{16}O), (O_3)$
line position(s) ν_0	:	977.9250, (977.6600) cm^{-1}
lower state energy E''_{lst}	:	421.4, (1357.0) cm^{-1}
retrieved TCA, information content	:	1.02E+19, (9.34E+18) $molec/cm^2$, 32.1, (57.8)
temperature dependence of the TCA	:	-.107, (-.284)%/K (trop), -.566, (-3.218)%/K (strat)
location, date, solar zenith angle	:	Kiruna, 15/Mar/97, 71.68^o
spectral interval fitted	:	977.620 – 978.110 cm^{-1}

Molecule	iCode	Absorption	Molecule	iCode	Absorption
$O3$	31	27.938%	$ClONO2$	271	0.009%
$CO2$	21	13.418%	$N2O$	41	0.001%
O3	**33**	8.818%	$CH4$	61	0.001%
$H2O$	11	8.136%	$NO2$	101	0.001%
Solar(A)	—	2.879%	HDO	491	0.001%
Solar-sim	—	3.953%	$CFC113$	621	0.001%
Solar-DU	—	3.244%	$NH3$	111	<0.001%
$O3$	**32**	1.000%	OH	131	<0.001%
$C2H4$	391	0.195%	$H2O2$	231	<0.001%
$COF2$	361	0.093%	$N2O5$	261	<0.001%
$F142B$	611	0.012%	$HCOOH$	461	<0.001%

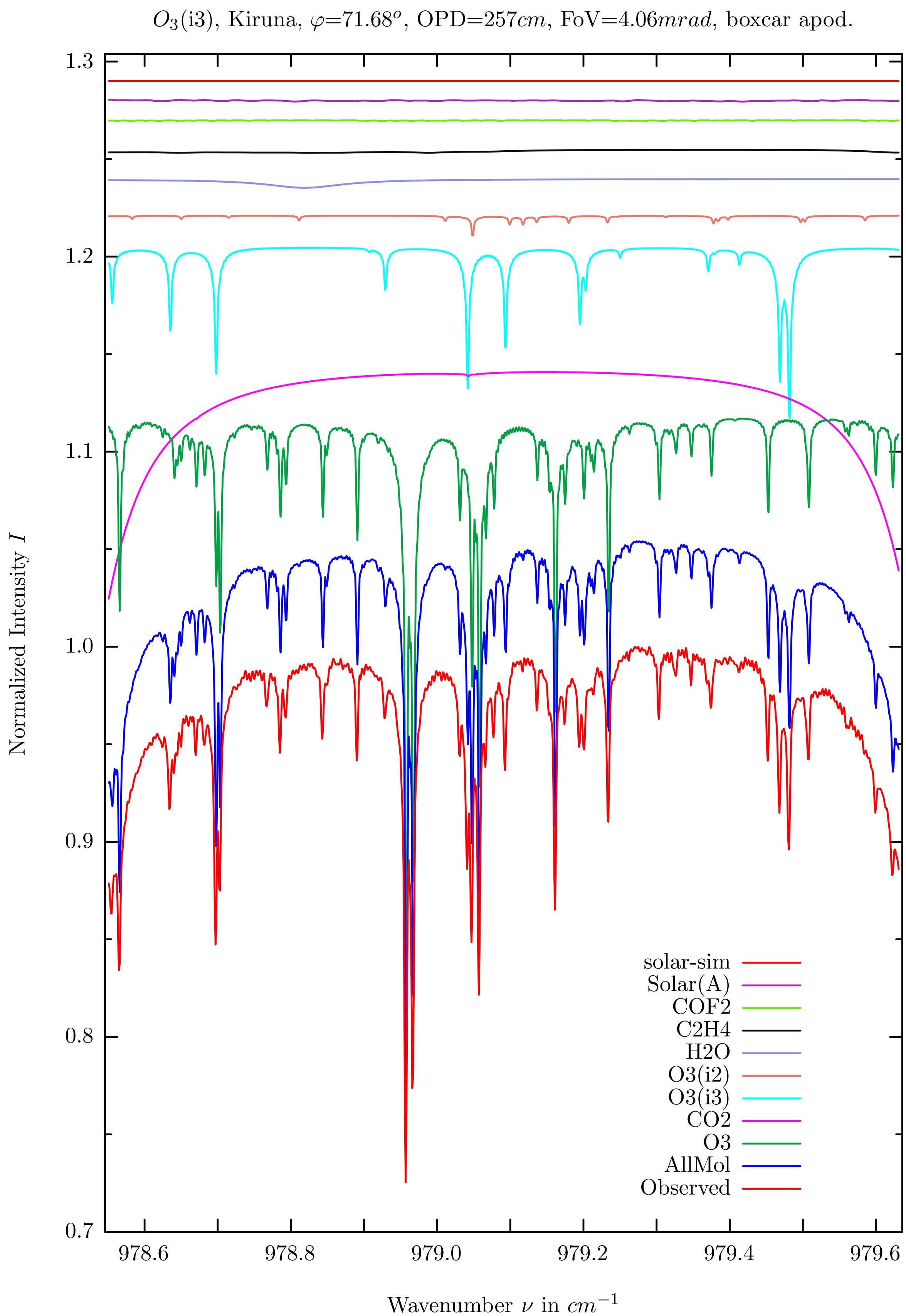
O_3(i3), Kiruna, φ=71.68^o, OPD=257cm, FoV=4.06$mrad$, boxcar apod.
Normalized Intensity I
Wavenumber ν in cm^{-1}
1.3
1.2
1.1
1.0
0.9
0.8
0.7
978.6
978.8
979.0
979.2
979.4
979.6
solar-sim
Solar(A)
COF2
C2H4
H2O
O3(i2)
O3(i3)
CO2
O3
AllMol
Observed

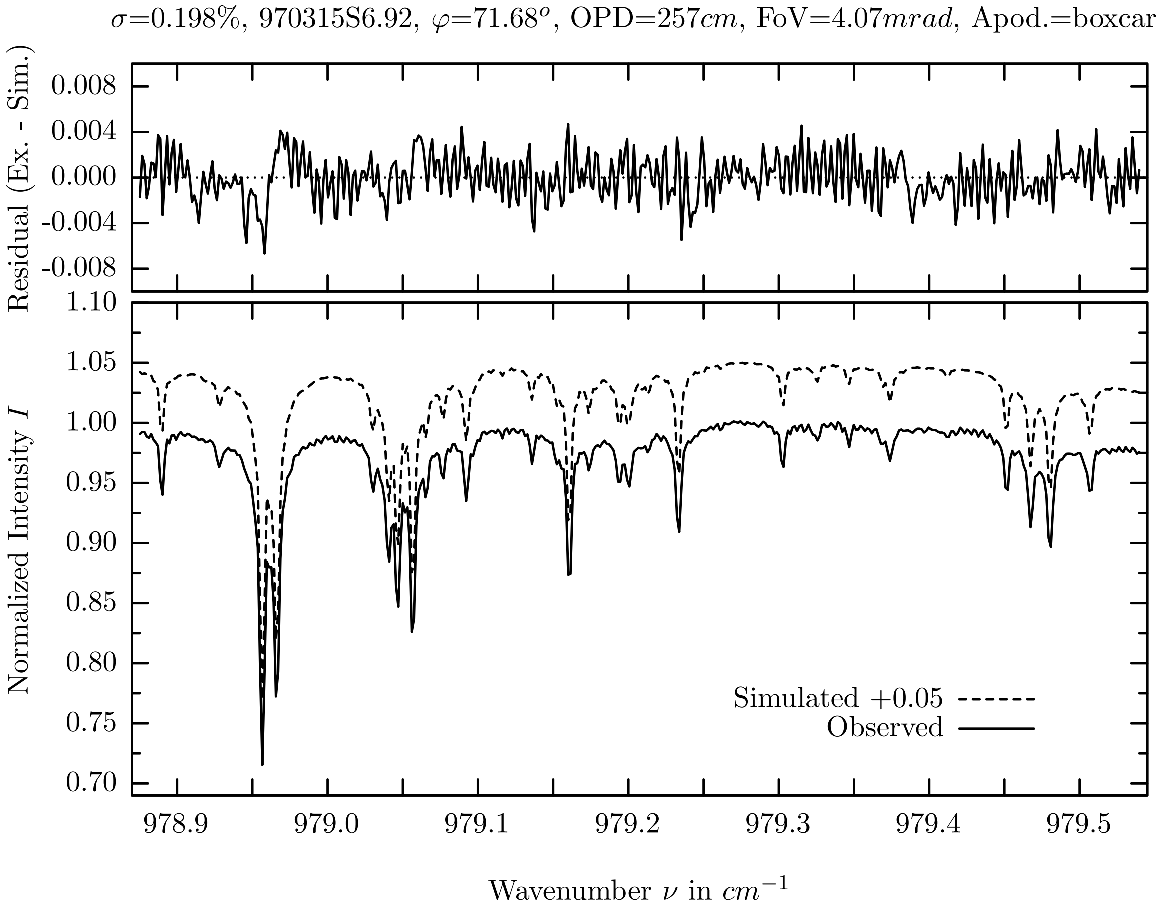

investigated species	:	$O_3(i3 = {}^{16}O\,{}^{18}O\,{}^{16}O), (O_3)$
line position(s) ν_0	:	979.4801, (978.9563) cm^{-1}
lower state energy E''_{lst}	:	374.9, (1234.1) cm^{-1}
retrieved TCA, information content	:	1.09E+19, (1.06E+19) $molec/cm^2$, 49.1, (141.3)
temperature dependence of the TCA	:	-.212, (-.667)%/K (trop), -.548, (-2.625)%/K (strat)
location, date, solar zenith angle	:	Kiruna, 15/Mar/97, 71.68^o
spectral interval fitted	:	978.875 – 979.540 cm^{-1}

Molecule	iCode	Absorption	Molecule	iCode	Absorption
$O3$	31	33.777%	$F142B$	611	0.011%
$CO2$	21	12.121%	$ClONO2$	271	0.010%
O3	**33**	10.313%	$N2O$	41	0.001%
$O3$	**32**	1.246%	$NO2$	101	0.001%
$H2O$	11	0.477%	$CFC113$	621	0.001%
$C2H4$	391	0.175%	$CH4$	61	<0.001%
$COF2$	361	0.067%	$NH3$	111	<0.001%
Solar(A)	—	0.051%	OH	131	<0.001%
Solar-sim	—	<0.001%	$H2O2$	231	<0.001%
Solar-DU	—	<0.001%	$N2O5$	261	<0.001%
HDO	491	0.031%	$HCOOH$	461	<0.001%

O_3(i3), Kiruna, φ=71.68^o, OPD=257cm, FoV=4.06$mrad$, boxcar apod.

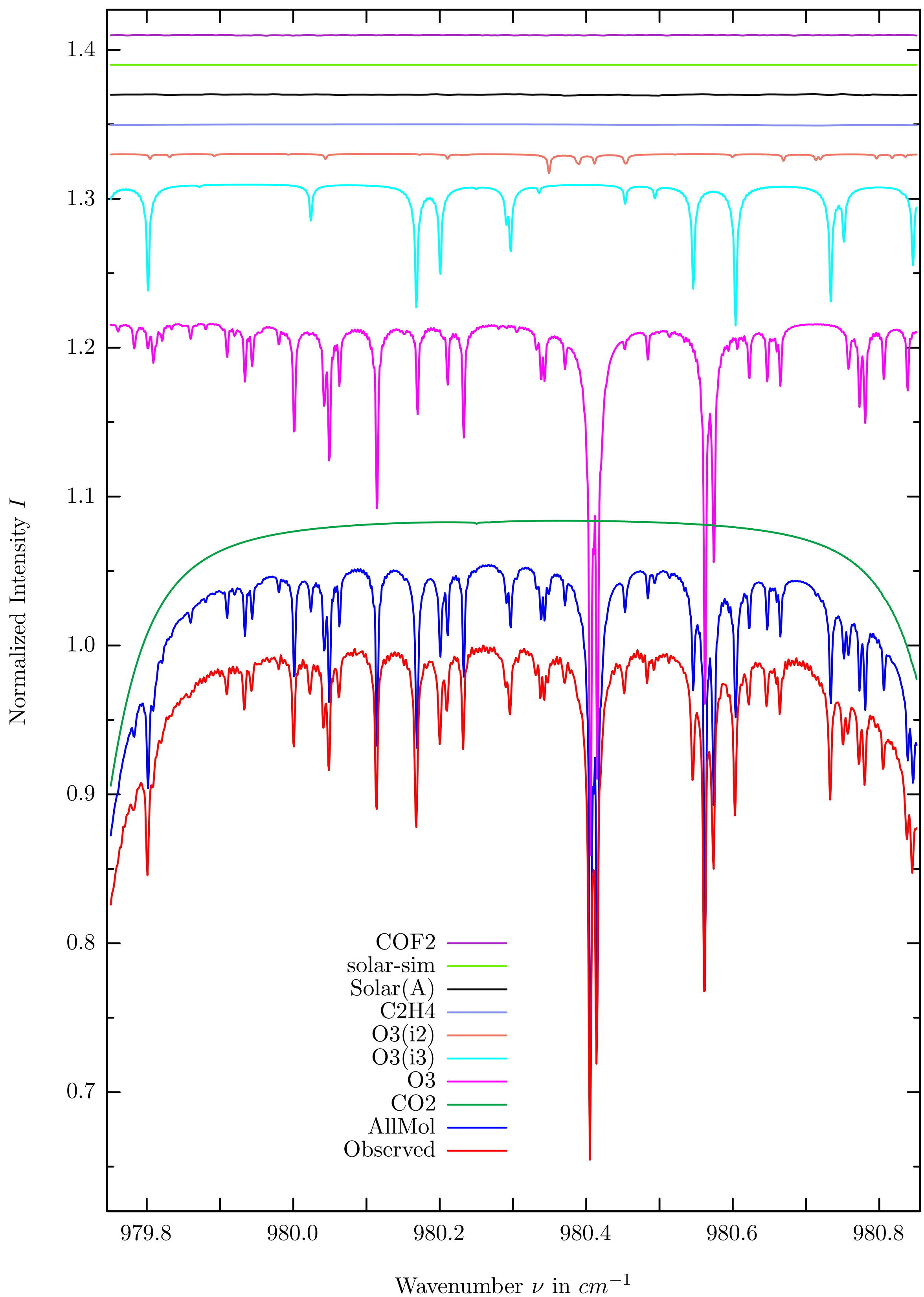

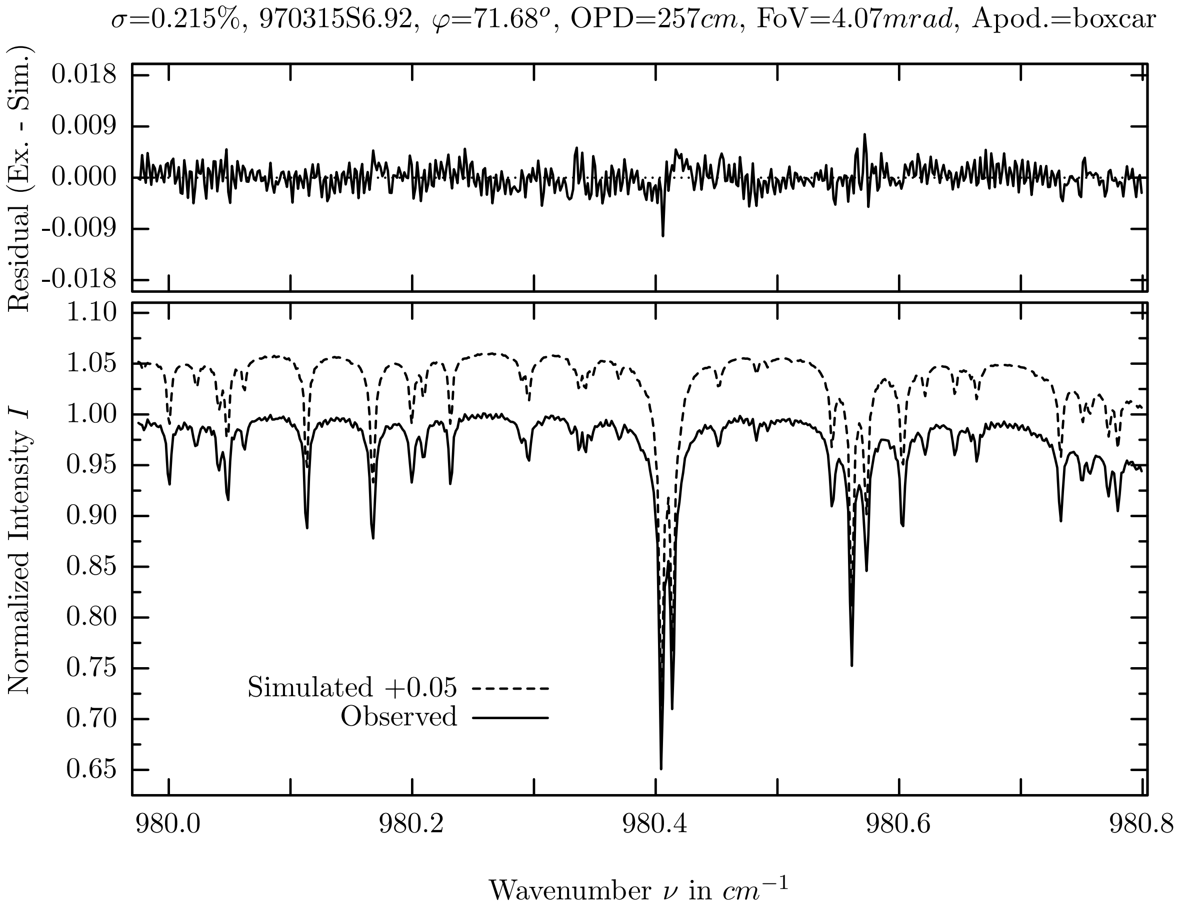

investigated species	:	$O_3(i3 = {}^{16}O\,{}^{18}O\,{}^{16}O), (O_3)$
line position(s) ν_0	:	980.6024, (980.4040) cm^{-1}
lower state energy E''_{lst}	:	351.1, (1190.5) cm^{-1}
retrieved TCA, information content	:	1.10E+19, (1.05E+19) $molec/cm^2$, 47.6, (161.6)
temperature dependence of the TCA	:	-.131, (-.727)%/K (trop), -.467, (-2.516)%/K (strat)
location, date, solar zenith angle	:	Kiruna, 15/Mar/97, 71.68^o
spectral interval fitted	:	979.975 – 980.800 cm^{-1}

Molecule	iCode	Absorption	Molecule	iCode	Absorption
$O3$	31	41.515%	$F142B$	611	0.009%
$CO2$	21	18.088%	HDO	491	0.002%
O3	**33**	10.999%	$N2O$	41	0.001%
$O3$	**32**	1.498%	$CH4$	61	0.001%
$C2H4$	391	0.081%	$NO2$	101	0.001%
Solar(A)	—	0.071%	$CFC113$	621	0.001%
Solar-sim	—	<0.001%	$NH3$	111	<0.001%
Solar-DU	—	<0.001%	OH	131	<0.001%
$COF2$	361	0.055%	$H2O2$	231	<0.001%
$H2O$	11	0.030%	$N2O5$	261	<0.001%
$ClONO2$	271	0.012%	$HCOOH$	461	<0.001%

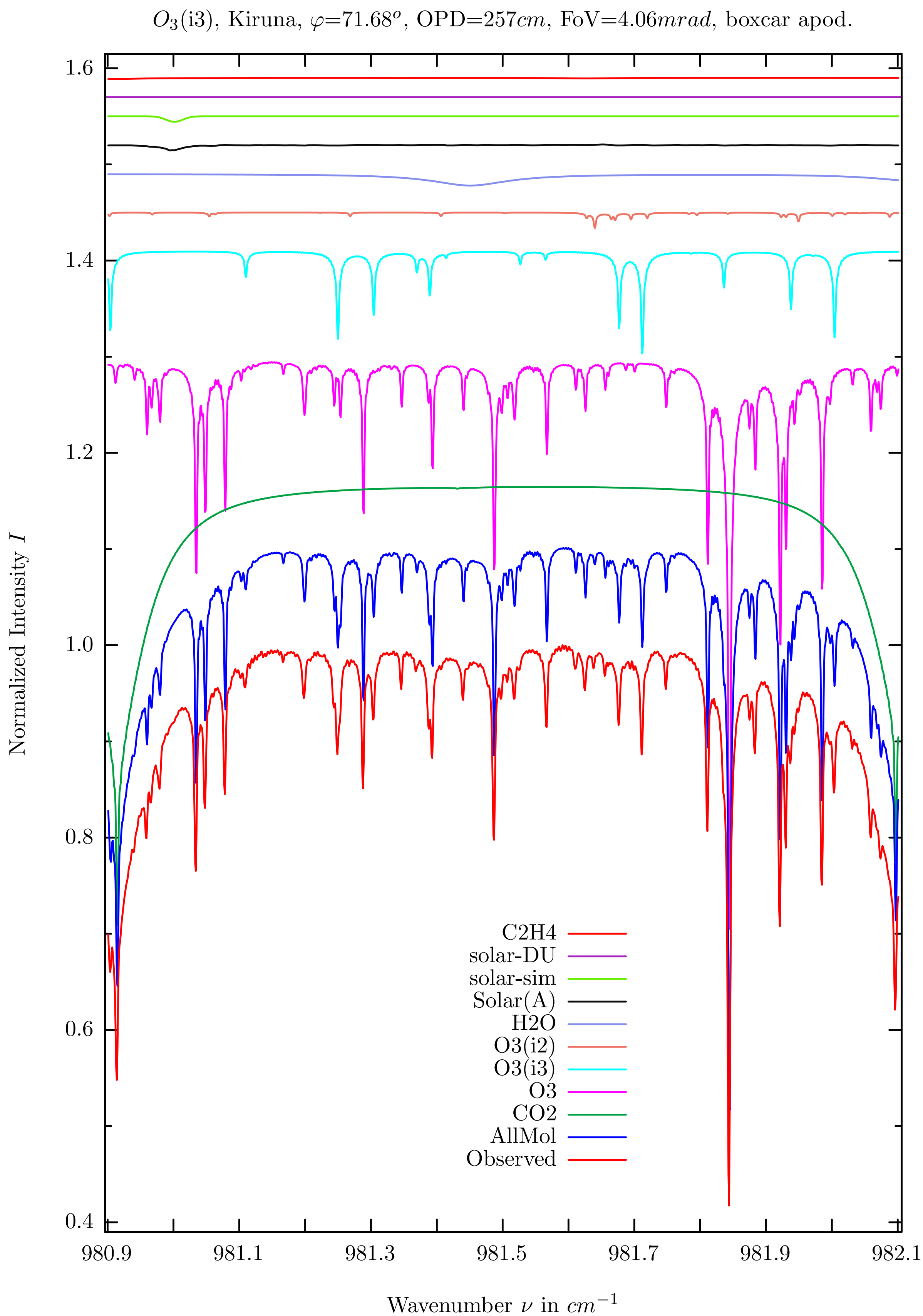
O_3(i3), Kiruna, φ=71.68^o, OPD=257cm, FoV=4.06$mrad$, boxcar apod.
Normalized Intensity I
1.6
1.4
1.2
1.0
0.8
0.6
0.4
980.9
981.1
981.3
981.5
981.7
981.9
982.1
Wavenumber ν in cm^{-1}
C2H4
solar-DU
solar-sim
Solar(A)
H2O
O3(i2)
O3(i3)
O3
CO2
AllMol
Observed

σ=0.216%, 970315S6.92, φ=71.68^o, OPD=257cm, FoV=4.07$mrad$, Apod.=boxcar

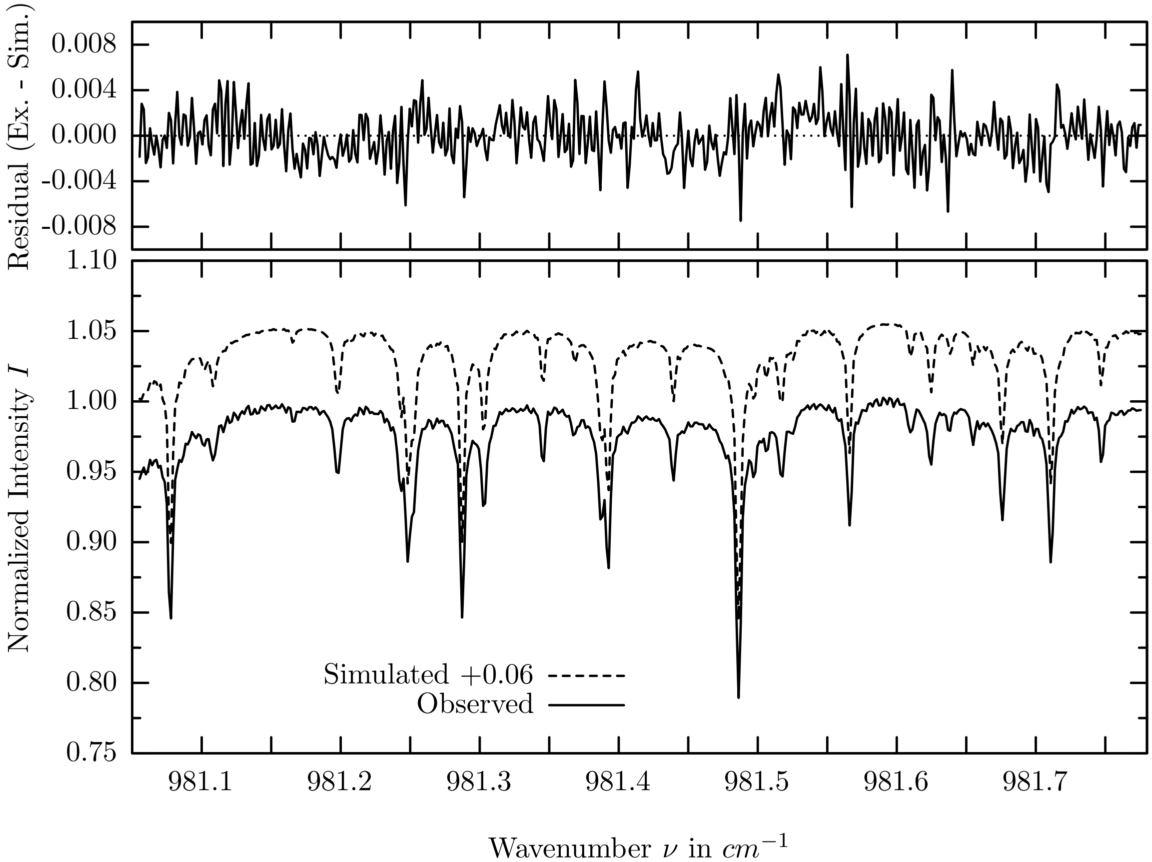

investigated species	:	$O_3(i3 = {}^{16}O\,{}^{18}O\,{}^{16}O), (O_3)$
line position(s) ν_0	:	981.7107, (981.4870) cm^{-1}
lower state energy E''_{lst}	:	328.0, (1404.3) cm^{-1}
retrieved TCA, information content	:	1.10E+19, (1.03E+19) $molec/cm^2$, 52.6, (96.0)
temperature dependence of the TCA	:	-.145, (-.656)%/K (trop), -.340, (-2.827)%/K (strat)
location, date, solar zenith angle	:	Kiruna, 15/Mar/97, 71.68^o
spectral interval fitted	:	981.055 – 981.777 cm^{-1}

Molecule	iCode	Absorption	Molecule	iCode	Absorption
$O3$	31	67.756%	$F142B$	611	0.008%
$CO2$	21	49.626%	$N2O$	41	0.001%
O3	**33**	12.223%	$NO2$	101	0.001%
$O3$	**32**	1.850%	$CFC113$	621	0.001%
$H2O$	11	1.215%	$CH4$	61	<0.001%
Solar(A)	—	0.539%	$NH3$	111	<0.001%
Solar-sim	—	0.577%	OH	131	<0.001%
Solar-DU	—	0.002%	$H2O2$	231	<0.001%
$C2H4$	391	0.132%	$N2O5$	261	<0.001%
$COF2$	361	0.040%	$HCOOH$	461	<0.001%
$ClONO2$	271	0.014%	HDO	491	<0.001%

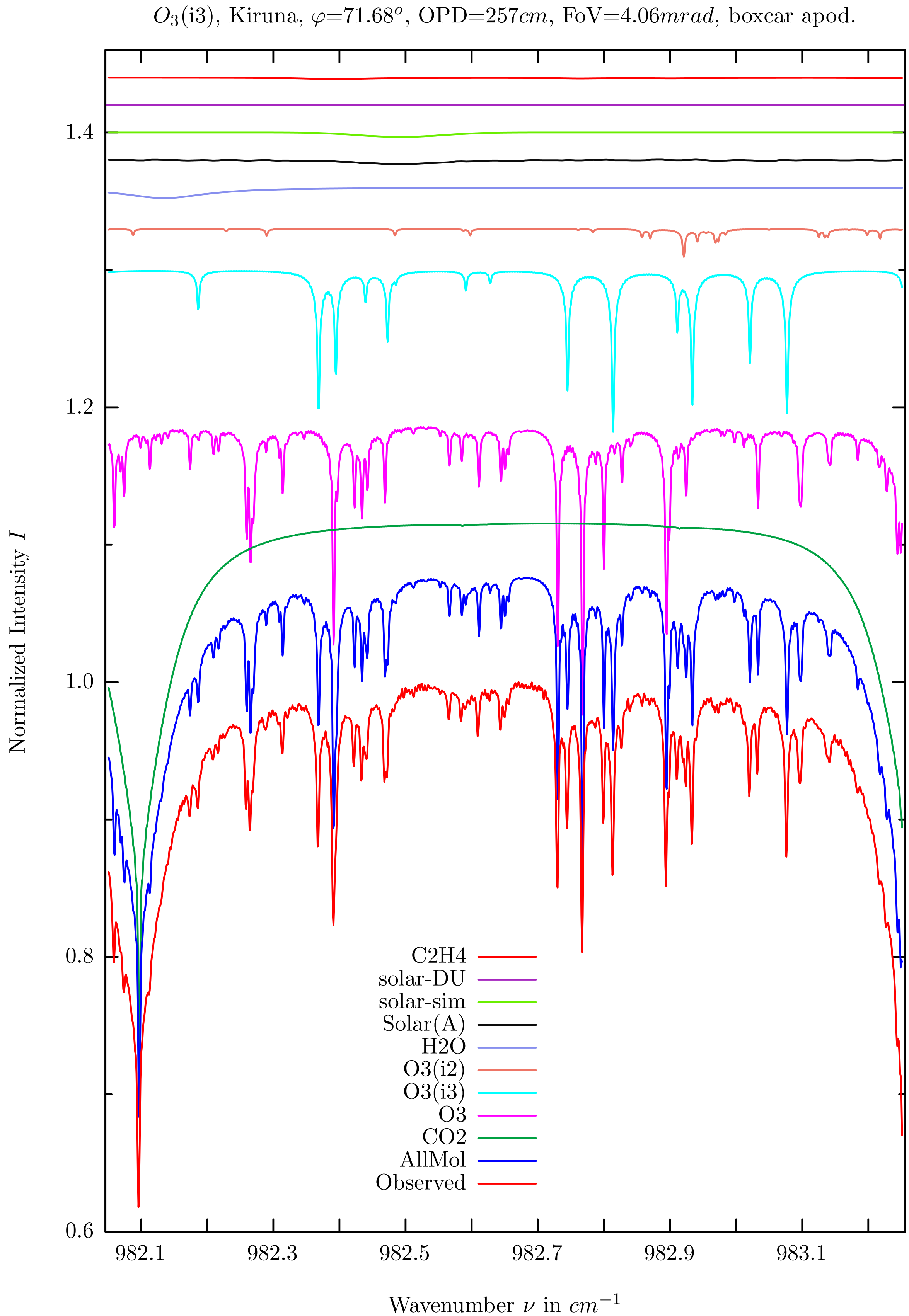

O_3(i3), Kiruna, φ=71.68^o, OPD=257cm, FoV=4.06$mrad$, boxcar apod.
Normalized Intensity I
1.4
1.2
1.0
0.8
0.6
982.1
982.3
982.5
982.7
982.9
983.1
Wavenumber ν in cm^{-1}
C2H4
solar-DU
solar-sim
Solar(A)
H2O
O3(i2)
O3(i3)
O3
CO2
AllMol
Observed

σ=0.210%, 970315S6.92, φ=71.68^o, OPD=257cm, FoV=4.07$mrad$, Apod.=boxcar

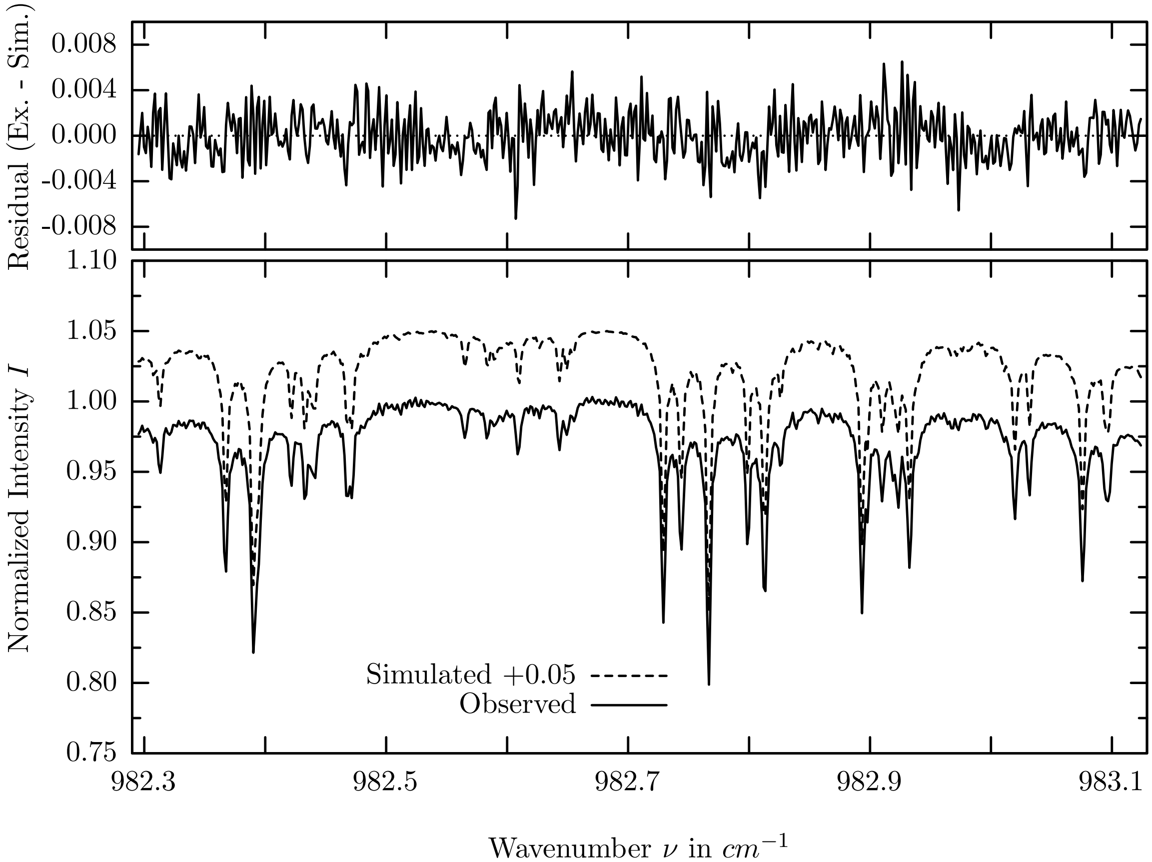

investigated species	:	$O_3(i3 = {}^{16}O\,{}^{18}O\,{}^{16}O), (O_3)$
line position(s) ν_0	:	983.0755, (982.7663) cm^{-1}
lower state energy E''_{lst}	:	311.6, (1272.9) cm^{-1}
retrieved TCA, information content	:	1.10E+19, (1.03E+19) $molec/cm^2$, 56.1, (94.6)
temperature dependence of the TCA	:	-.191, (-.710)%/K (trop), -.304, (-2.77)%/K (strat)
location, date, solar zenith angle	:	Kiruna, 15/Mar/97, 71.68^o
spectral interval fitted	:	982.295 – 983.125 cm^{-1}

Molecule	iCode	Absorption	Molecule	iCode	Absorption
$CO2$	21	42.825%	$F142B$	611	0.006%
$O3$	31	25.368%	$N2O$	41	0.001%
O3	**33**	13.612%	$NO2$	101	0.001%
$O3$	**32**	2.242%	$CFC113$	621	0.001%
$H2O$	11	0.794%	$CH4$	61	<0.001%
Solar(A)	—	0.311%	$NH3$	111	<0.001%
Solar-sim	—	0.330%	OH	131	<0.001%
Solar-DU	—	0.001%	$H2O2$	231	<0.001%
$C2H4$	391	0.130%	$N2O5$	261	<0.001%
$COF2$	361	0.031%	$HCOOH$	461	<0.001%
$ClONO2$	271	0.016%	HDO	491	<0.001%

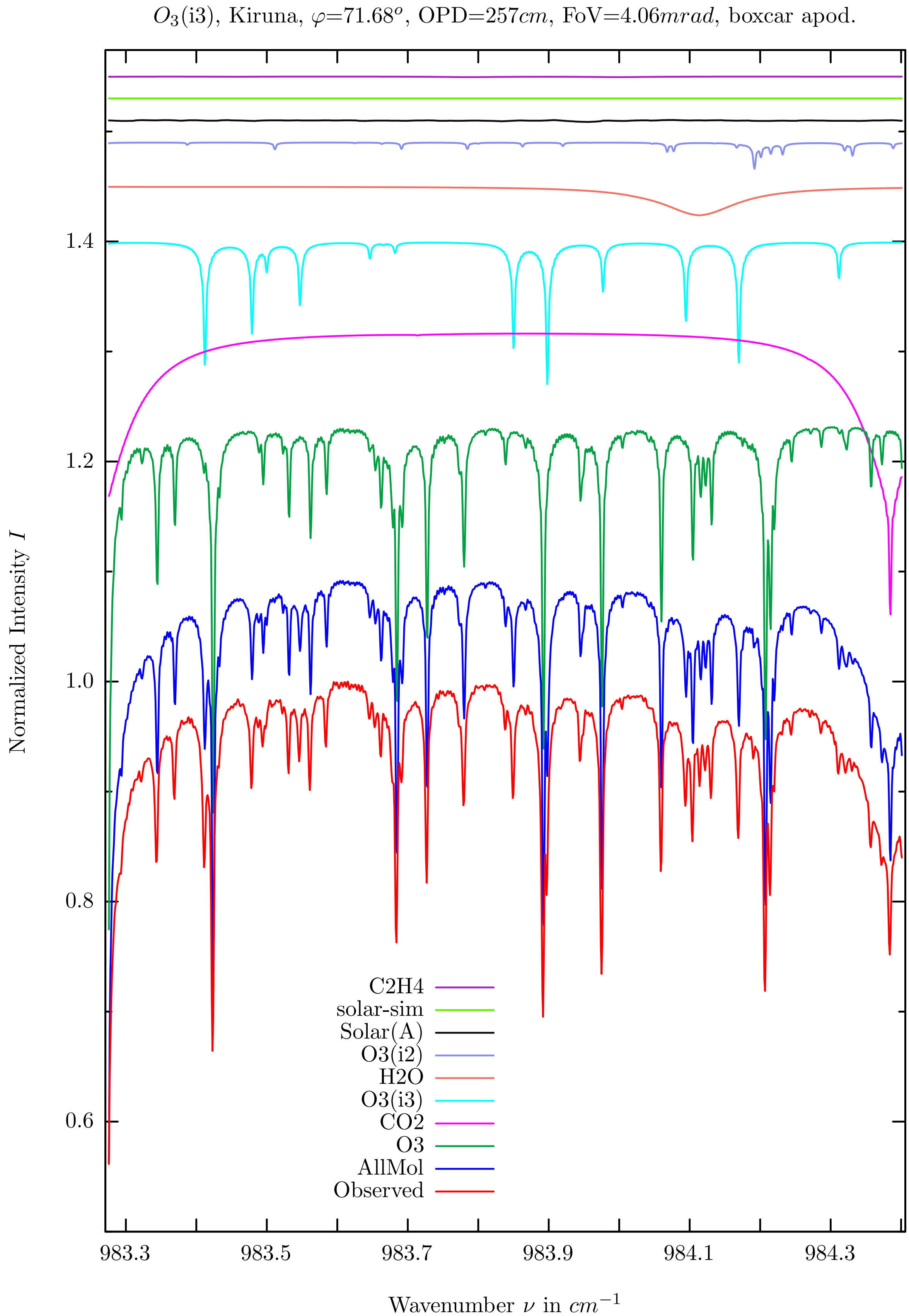

O_3(i3), Kiruna, φ=71.68^o, OPD=257cm, FoV=4.06$mrad$, boxcar apod.
Normalized Intensity I
1.4
1.2
1.0
0.8
0.6
C2H4
solar-sim
Solar(A)
O3(i2)
H2O
O3(i3)
CO2
O3
AllMol
Observed
983.3
983.5
983.7
983.9
984.1
984.3
Wavenumber ν in cm^{-1}

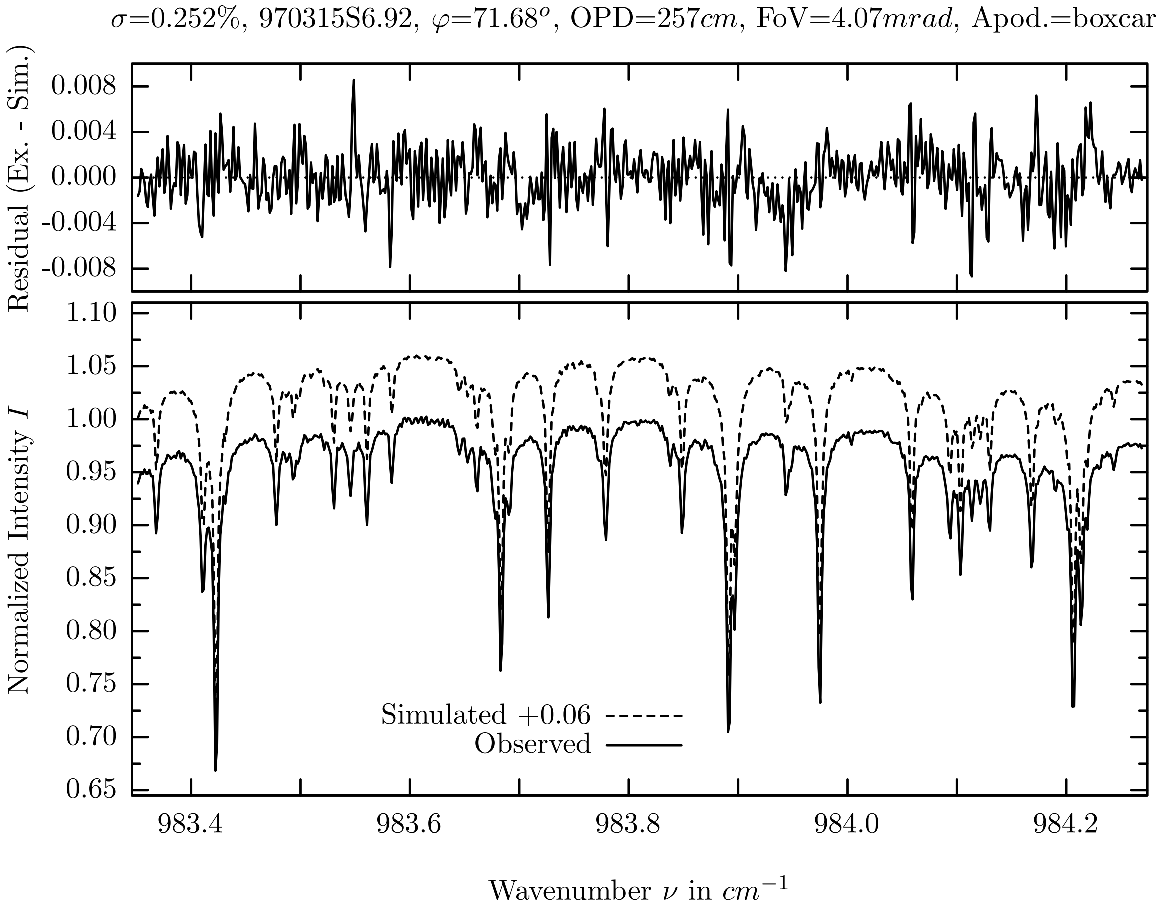

investigated species	:	$O_3(i3 = {}^{16}O\,{}^{18}O\,{}^{16}O), (O_3)$
line position(s) ν_0	:	984.1683, (983.8910) cm^{-1}
lower state energy E''_{lst}	:	298.3, (1204.3) cm^{-1}
retrieved TCA, information content	:	1.14E+19, (1.06E+19) $molec/cm^2$, 49.9, (119.5)
temperature dependence of the TCA	:	-.061, (-2.50)%/K (trop), -.048, (-2.45)%/K (strat)
location, date, solar zenith angle	:	Kiruna, 15/Mar/97, 71.68^o
spectral interval fitted	:	983.350 – 984.270 cm^{-1}

Molecule	iCode	Absorption	Molecule	iCode	Absorption
$O3$	31	42.126%	$F142B$	611	0.005%
$CO2$	21	28.267%	$NO2$	101	0.001%
O3	**33**	14.769%	HDO	491	0.001%
$H2O$	11	2.630%	$CFC113$	621	0.001%
$O3$	**32**	2.573%	$N2O$	41	<0.001%
Solar(A)	—	0.130%	$CH4$	61	<0.001%
Solar-sim	—	<0.001%	$NH3$	111	<0.001%
Solar-DU	—	<0.001%	OH	131	<0.001%
$C2H4$	391	0.064%	$H2O2$	231	<0.001%
$COF2$	361	0.030%	$N2O5$	261	<0.001%
$ClONO2$	271	0.018%	$HCOOH$	461	<0.001%

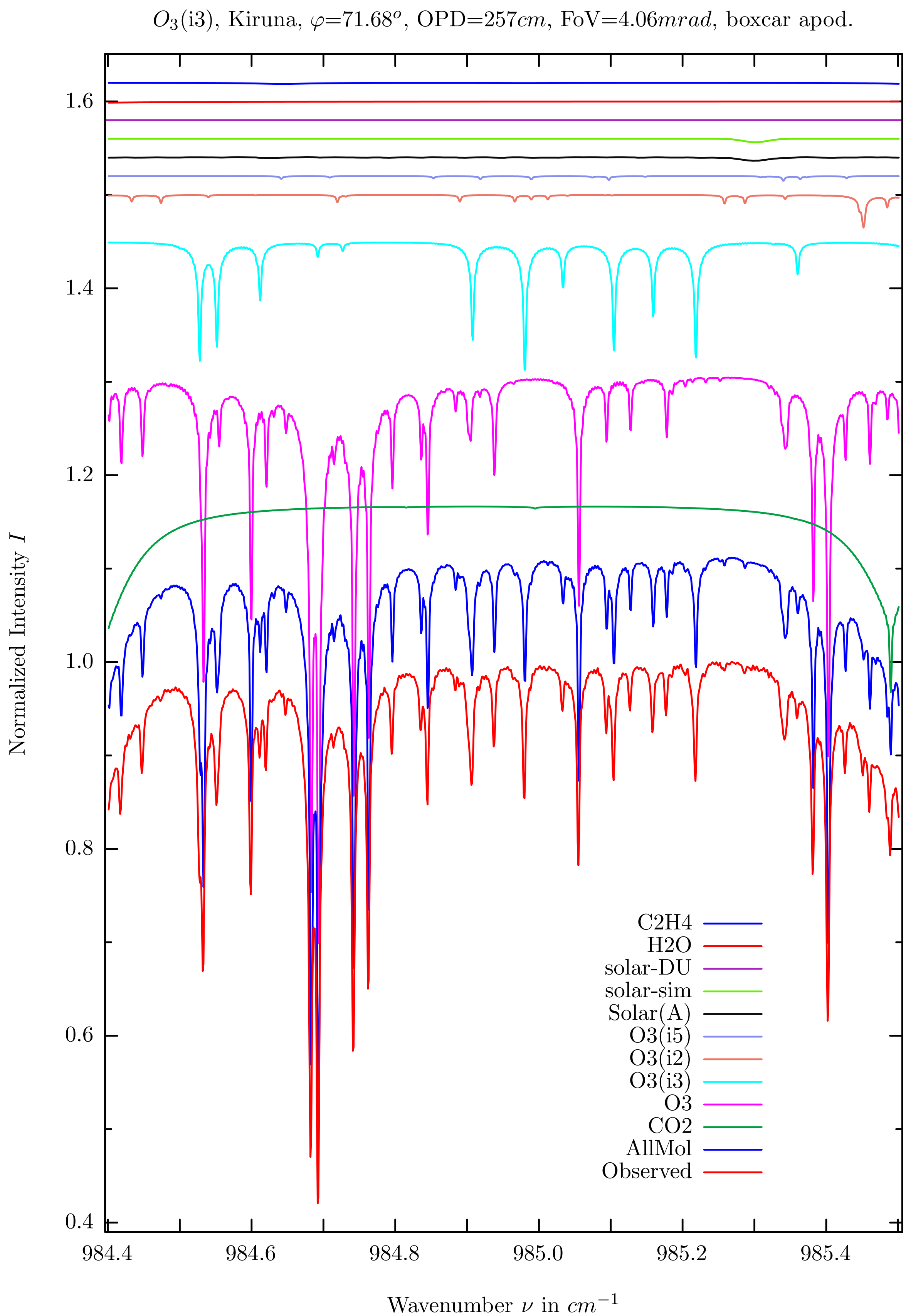

O_3(i3), Kiruna, φ=71.68^o, OPD=257cm, FoV=4.06$mrad$, boxcar apod.
1.6
1.4
1.2
1.0
0.8
0.6
0.4
Normalized Intensity I
984.4
984.6
984.8
985.0
985.2
985.4
Wavenumber ν in cm^{-1}
C2H4
H2O
solar-DU
solar-sim
Solar(A)
O3(i5)
O3(i2)
O3(i3)
O3
CO2
AllMol
Observed

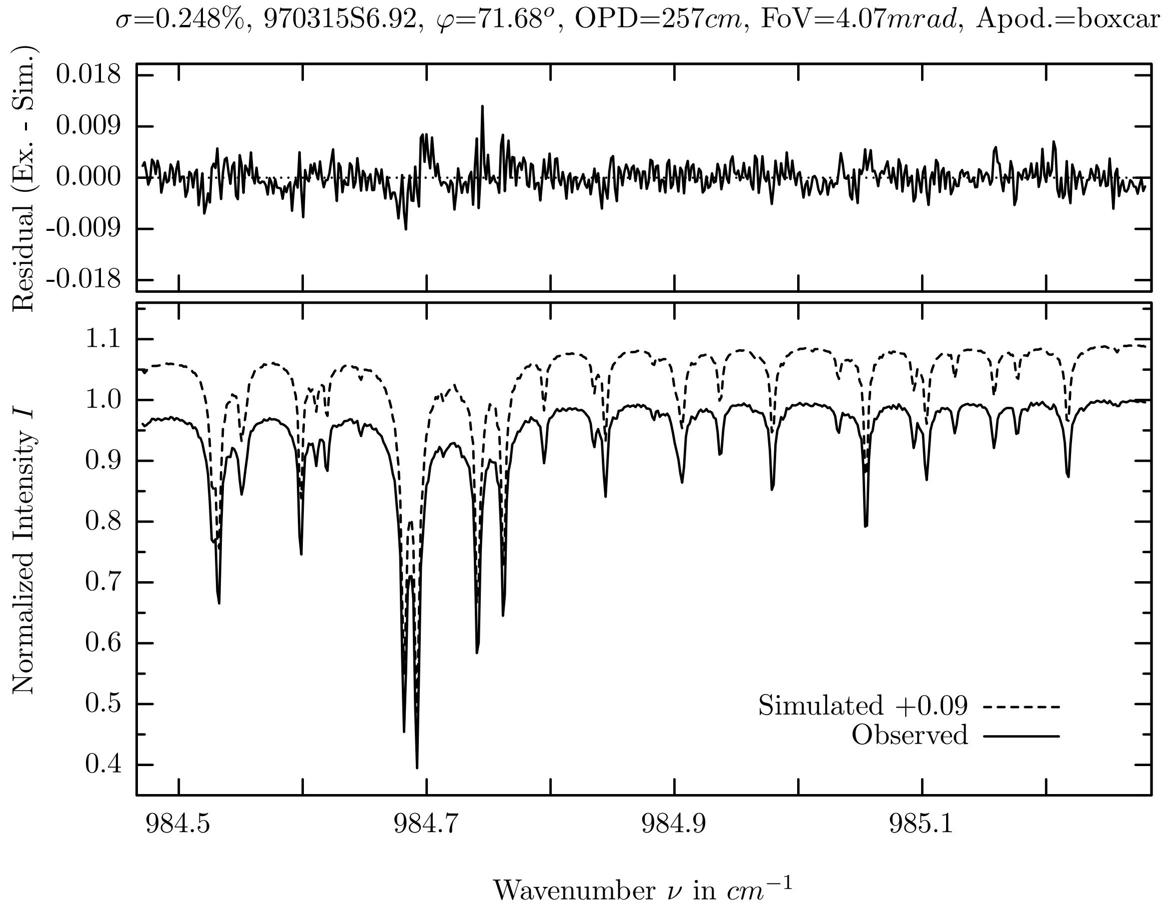

investigated species	:	$O_3(i3 = {}^{16}O\,{}^{18}O\,{}^{16}O), (O_3)$
line position(s) ν_0	:	984.9790, (984.6918) cm^{-1}
lower state energy E''_{lst}	:	263.6, (1064.3) cm^{-1}
retrieved TCA, information content	:	1.08E+19, (1.05E+19) $molec/cm^2$, 57.7, (236.7)
temperature dependence of the TCA	:	-.060, (-.672)%/K (trop), -.251, (-2.17)%/K (strat)
location, date, solar zenith angle	:	Kiruna, 15/Mar/97, 71.68^o
spectral interval fitted	:	984.470 – 985.280 cm^{-1}

Molecule	iCode	Absorption	Molecule	iCode	Absorption
$O3$	31	68.144%	$COF2$	361	0.018%
$CO2$	21	22.222%	$F142B$	611	0.004%
O3	**33**	16.327%	$NO2$	101	0.001%
$O3$	**32**	3.559%	$NH3$	111	0.001%
$O3$	**35**	0.591%	$CFC113$	621	0.001%
Solar(A)	—	0.351%	$N2O$	41	<0.001%
Solar-sim	—	0.369%	$CH4$	61	<0.001%
Solar-DU	—	0.001%	OH	131	<0.001%
$H2O$	11	0.130%	$H2O2$	231	<0.001%
$C2H4$	391	0.127%	$N2O5$	261	<0.001%
HDO	491	0.033%	$HCOOH$	461	<0.001%
$ClONO2$	271	0.018%			

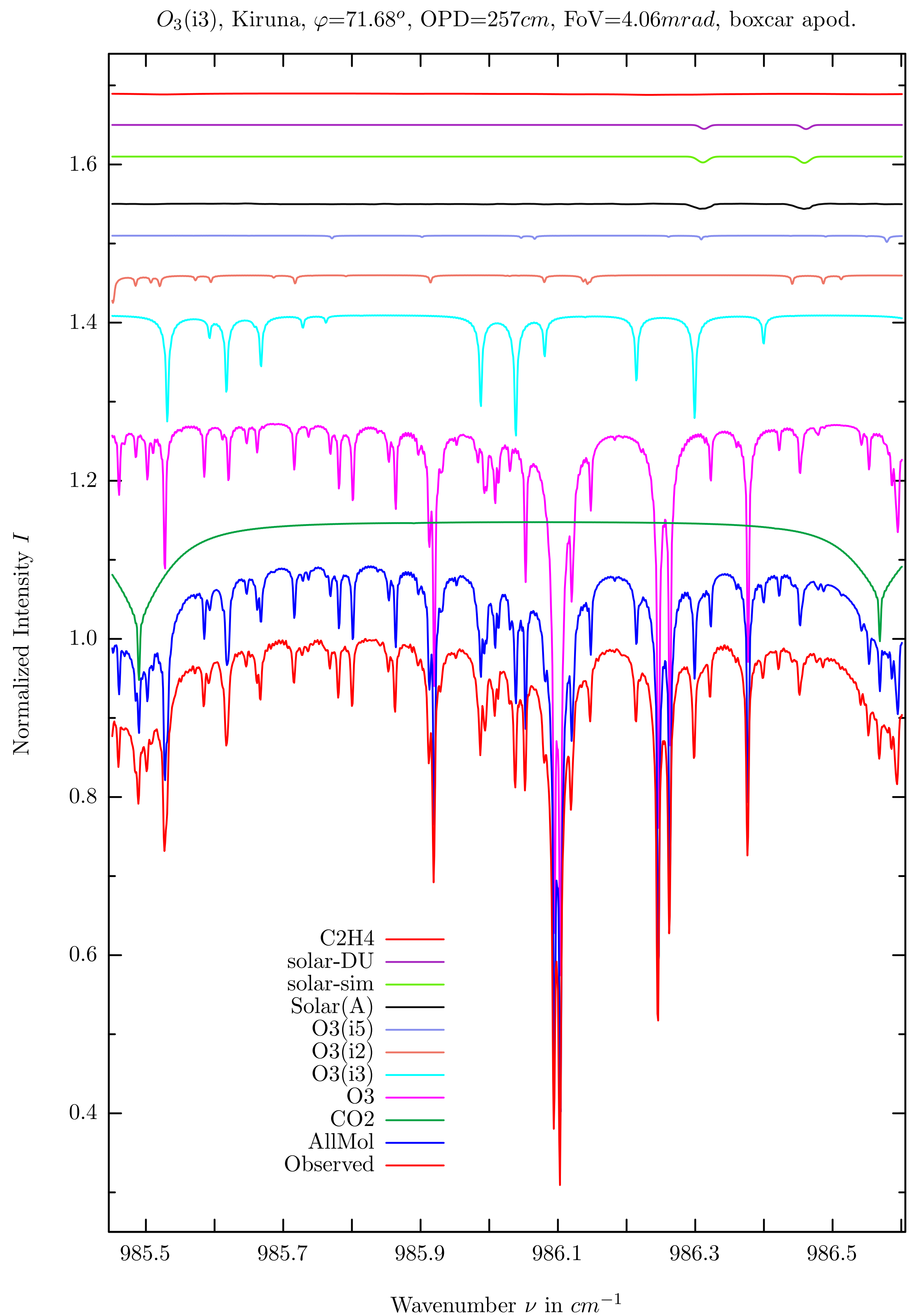

O_3(i3), Kiruna, φ=71.68^o, OPD=257cm, FoV=4.06$mrad$, boxcar apod.
Normalized Intensity I
Wavenumber ν in cm^{-1}
1.6
1.4
1.2
1.0
0.8
0.6
0.4
985.5
985.7
985.9
986.1
986.3
986.5
C2H4
solar-DU
solar-sim
Solar(A)
O3(i5)
O3(i2)
O3(i3)
O3
CO2
AllMol
Observed

σ=0.276%, 970315S6.92, φ=71.68^o, OPD=257cm, FoV=4.07$mrad$, Apod.=boxcar

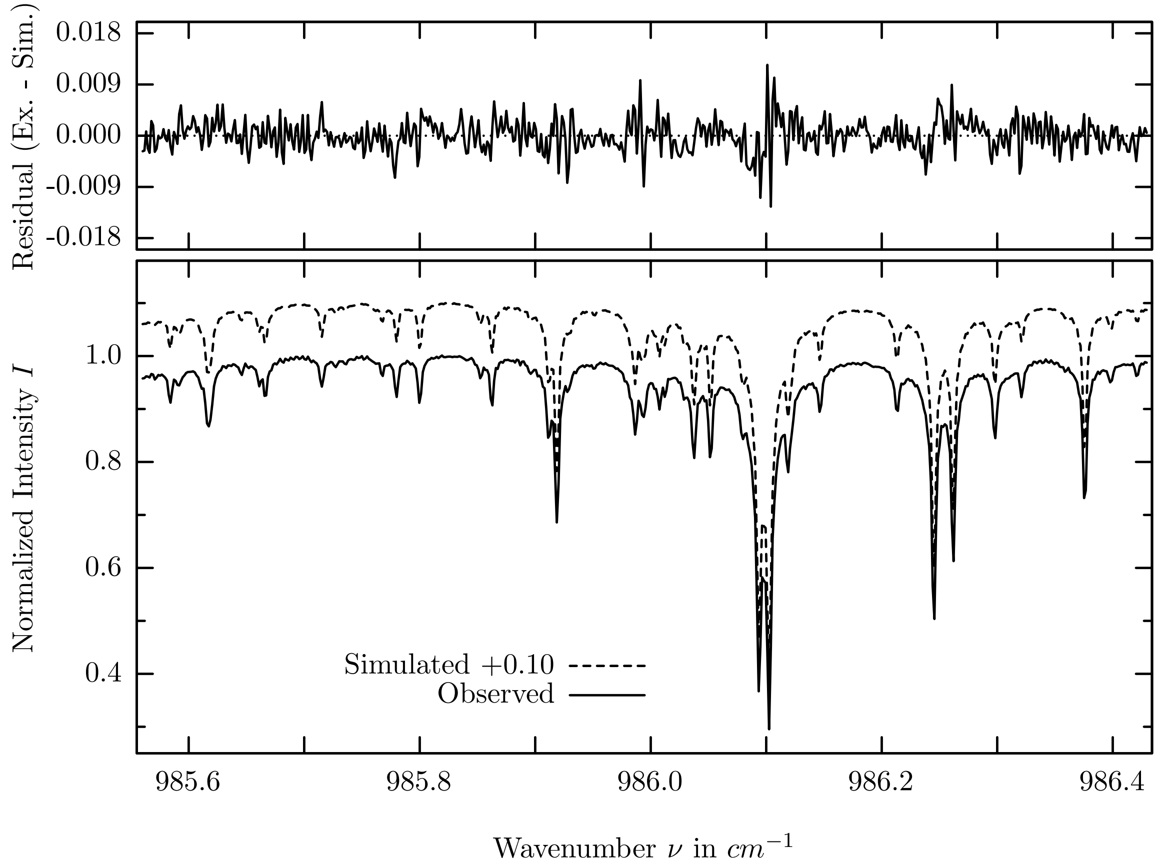

investigated species	:	$O_3(i3 = {}^{16}O\,{}^{18}O\,{}^{16}O), (O_3)$
line position(s) ν_0	:	986.2977, (986.1021) cm^{-1}
lower state energy E''_{lst}	:	257.2, (1023.8) cm^{-1}
retrieved TCA, information content	:	1.10E+19, (1.04E+19) $molec/cm^2$, 55.5, (255.8)
temperature dependence of the TCA	:	-.159, (-.668)%/K (trop), -.295, (-2.126)%/K (strat)
location, date, solar zenith angle	:	Kiruna, 15/Mar/97, 71.68^o
spectral interval fitted	:	985.560 – 986.430 cm^{-1}

Molecule	iCode	Absorption	Molecule	iCode	Absorption
$O3$	31	77.785%	$H2O$	11	0.008%
$CO2$	21	22.221%	$F142B$	611	0.003%
O3	**33**	17.465%	$NO2$	101	0.001%
$O3$	**32**	3.559%	$NH3$	111	0.001%
$O3$	**35**	0.865%	$N2O$	41	<0.001%
Solar(A)	—	0.619%	$CH4$	61	<0.001%
Solar-sim	—	0.808%	OH	131	<0.001%
Solar-DU	—	0.524%	$H2O2$	231	<0.001%
$C2H4$	391	0.199%	$N2O5$	261	<0.001%
HDO	491	0.028%	$HCOOH$	461	<0.001%
$ClONO2$	271	0.018%	$H2S$	471	<0.001%
$COF2$	361	0.016%	$CFC113$	621	<0.001%

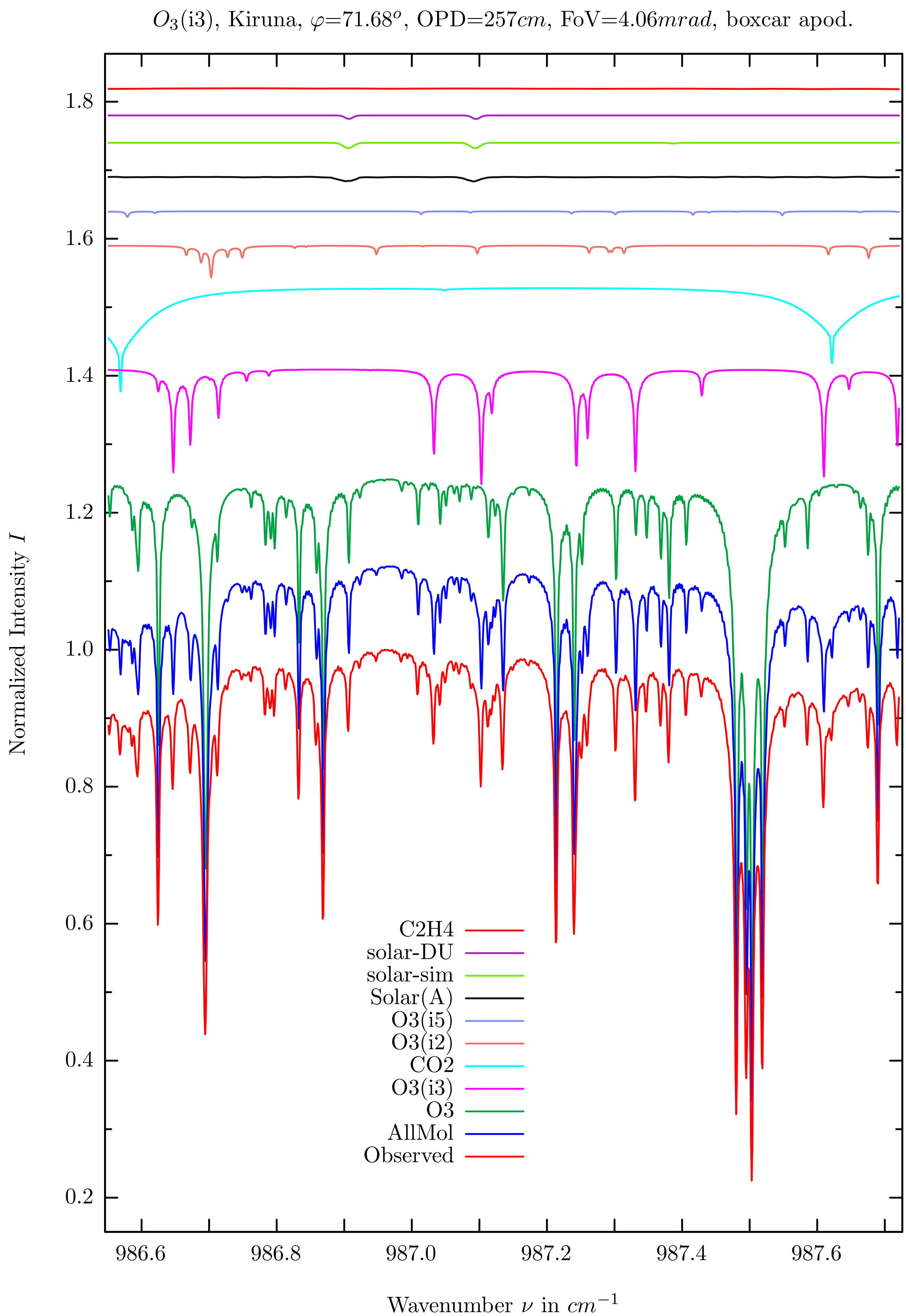
O_3(i3), Kiruna, φ=71.68^o, OPD=257cm, FoV=4.06$mrad$, boxcar apod.
Normalized Intensity I
Wavenumber ν in cm^{-1}
1.8
1.6
1.4
1.2
1.0
0.8
0.6
0.4
0.2
986.6
986.8
987.0
987.2
987.4
987.6
C2H4
solar-DU
solar-sim
Solar(A)
O3(i5)
O3(i2)
CO2
O3(i3)
O3
AllMol
Observed

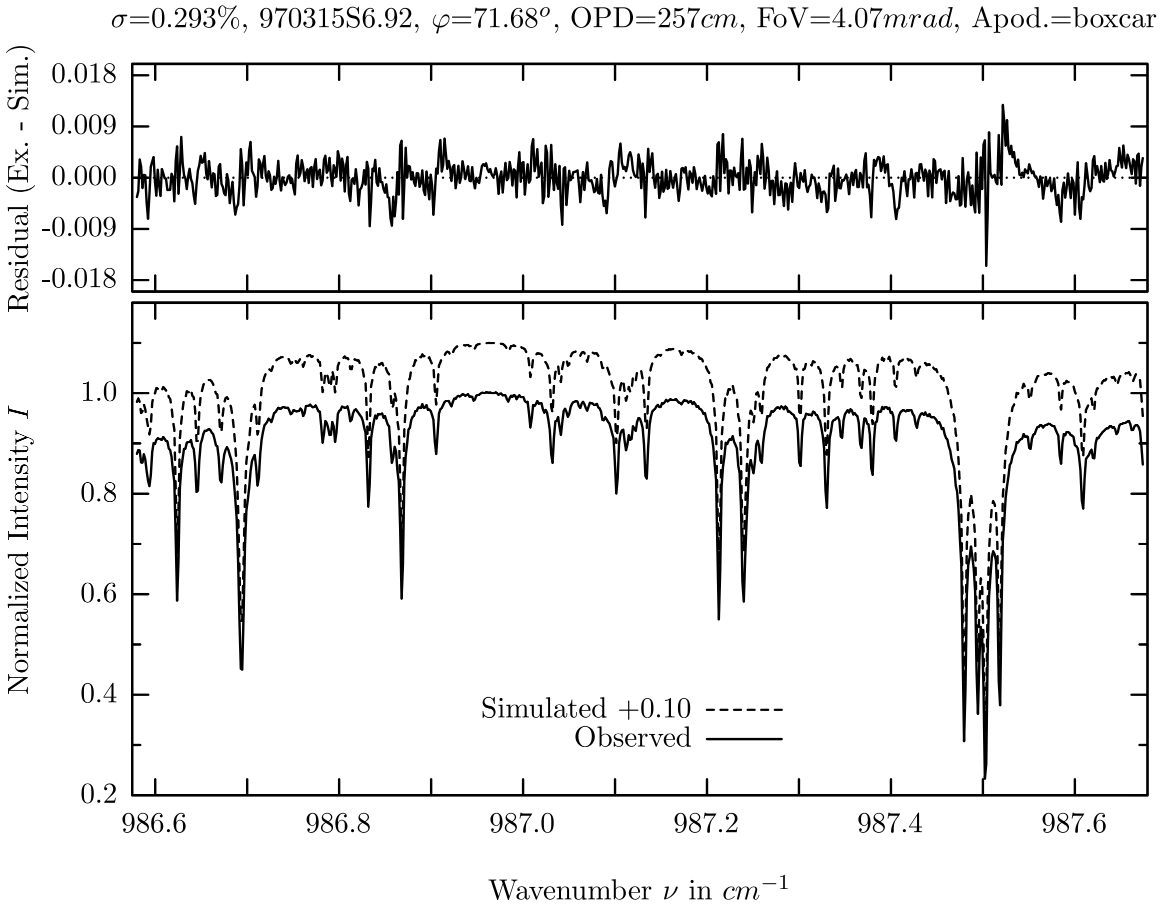

investigated species	:	$O_3(i3 = {}^{16}O\,{}^{18}O\,{}^{16}O), (O_3)$
line position(s) ν_0	:	987.1014, (987.4795) cm^{-1}
lower state energy E''_{lst}	:	224.5, (1020.0) cm^{-1}
retrieved TCA, information content	:	1.12E+19, (1.05E+19) $molec/cm^2$, 68.1, (236.0)
temperature dependence of the TCA	:	-.102, (-.631)%/K (trop), -.218, (-2.03)%/K (strat)
location, date, solar zenith angle	:	Kiruna, 15/Mar/97, 71.68^o
spectral interval fitted	:	986.580 – 987.675 cm^{-1}

Molecule	iCode	Absorption	Molecule	iCode	Absorption
$O3$	31	84.975%	$NH3$	111	0.002%
O3	**33**	19.162%	$F142B$	611	0.002%
$CO2$	21	16.927%	$NO2$	101	0.001%
$O3$	**32**	4.779%	HDO	491	0.001%
$O3$	**35**	0.865%	$N2O$	41	<0.001%
Solar(A)	—	0.638%	$CH4$	61	<0.001%
Solar-sim	—	0.783%	OH	131	<0.001%
Solar-DU	—	0.521%	$H2O2$	231	<0.001%
$C2H4$	391	0.172%	$N2O5$	261	<0.001%
$ClONO2$	271	0.019%	$HCOOH$	461	<0.001%
$COF2$	361	0.013%	$H2S$	471	<0.001%
$H2O$	11	0.012%	$CFC113$	621	<0.001%

O_3(i3), Kiruna, φ=71.68^o, OPD=257cm, FoV=4.06$mrad$, boxcar apod.

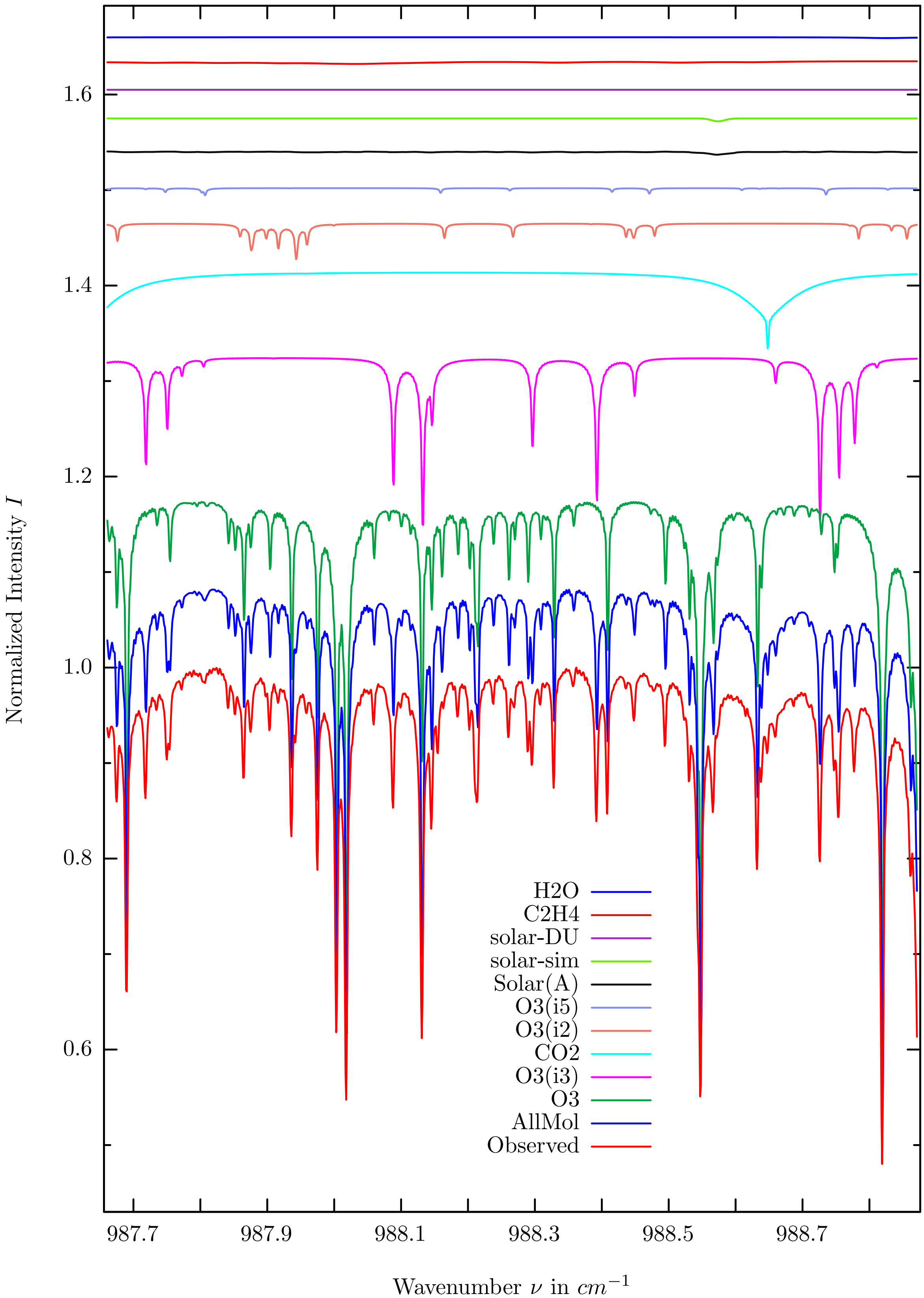

σ=0.265%, 970315S6.92, φ=71.68^o, OPD=257cm, FoV=4.07$mrad$, Apod.=boxcar

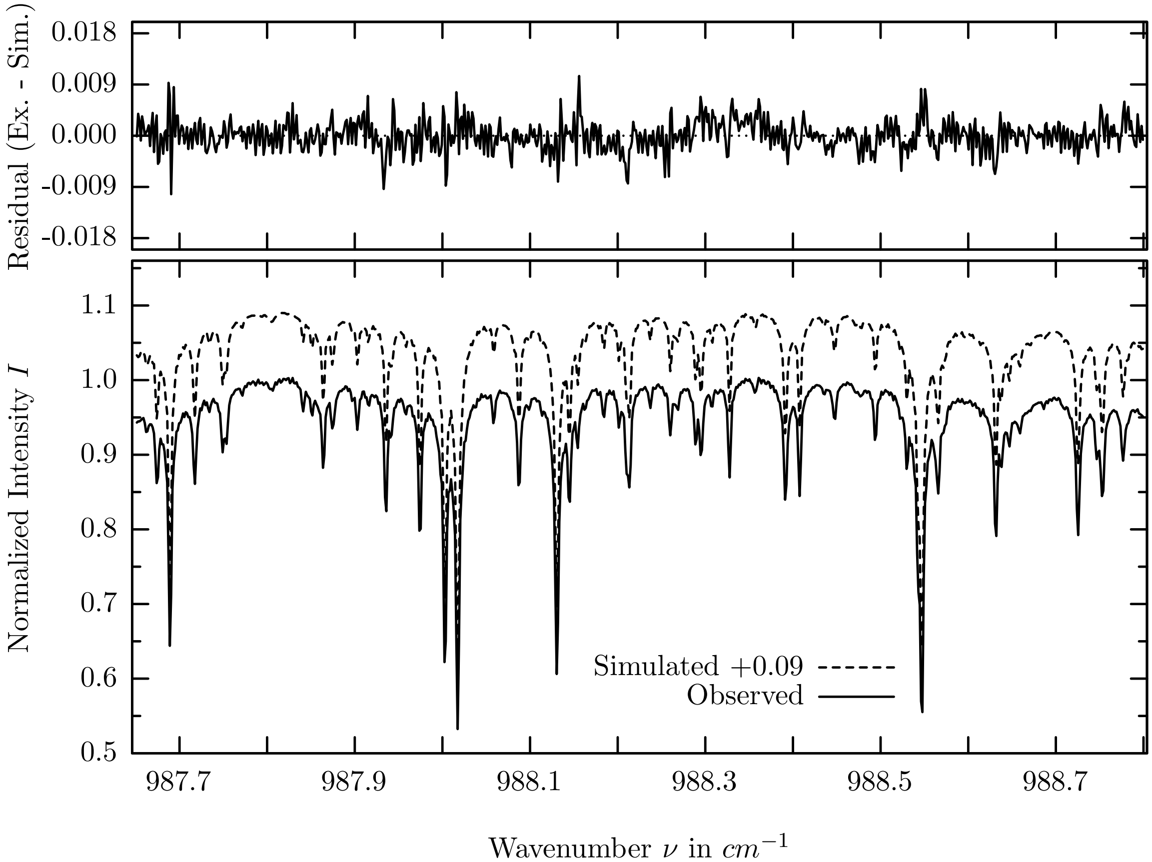

investigated species	:	$O_3(i3 = {}^{16}O\,{}^{18}O\,{}^{16}O), (O_3)$
line position(s) ν_0	:	988.3912, (988.5468) cm^{-1}
lower state energy E''_{lst}	:	219.5, (1101.2) cm^{-1}
retrieved TCA, information content	:	1.06E+19, (1.04E+19) $molec/cm^2$, 60.9, (169.2)
temperature dependence of the TCA	:	-.024, (-.704)%/K (trop), -.094, (-2.27)%/K (strat)
spectral interval fitted	:	987.650 – 988.800 cm^{-1}

Molecule	iCode	Absorption	Molecule	iCode	Absorption
$O3$	31	62.932%	$NO2$	101	0.001%
O3	**33**	20.583%	$F142B$	611	0.001%
$CO2$	21	8.996%	$N2O$	41	<0.001%
$O3$	**32**	3.796%	$CH4$	61	<0.001%
$O3$	**35**	0.868%	OH	131	<0.001%
Solar(A)	—	0.300%	OCS	19**3**	<0.001%
Solar-sim	—	0.299%	$H2O2$	231	<0.001%
Solar-DU	—	0.001%	$N2O5$	261	<0.001%
$C2H4$	391	0.296%	$HCOOH$	461	<0.001%
$H2O$	11	0.086%	$H2S$	471	<0.001%
$ClONO2$	271	0.022%	HDO	491	<0.001%
$COF2$	361	0.008%	$CFC113$	621	<0.001%
$NH3$	111	0.002%			

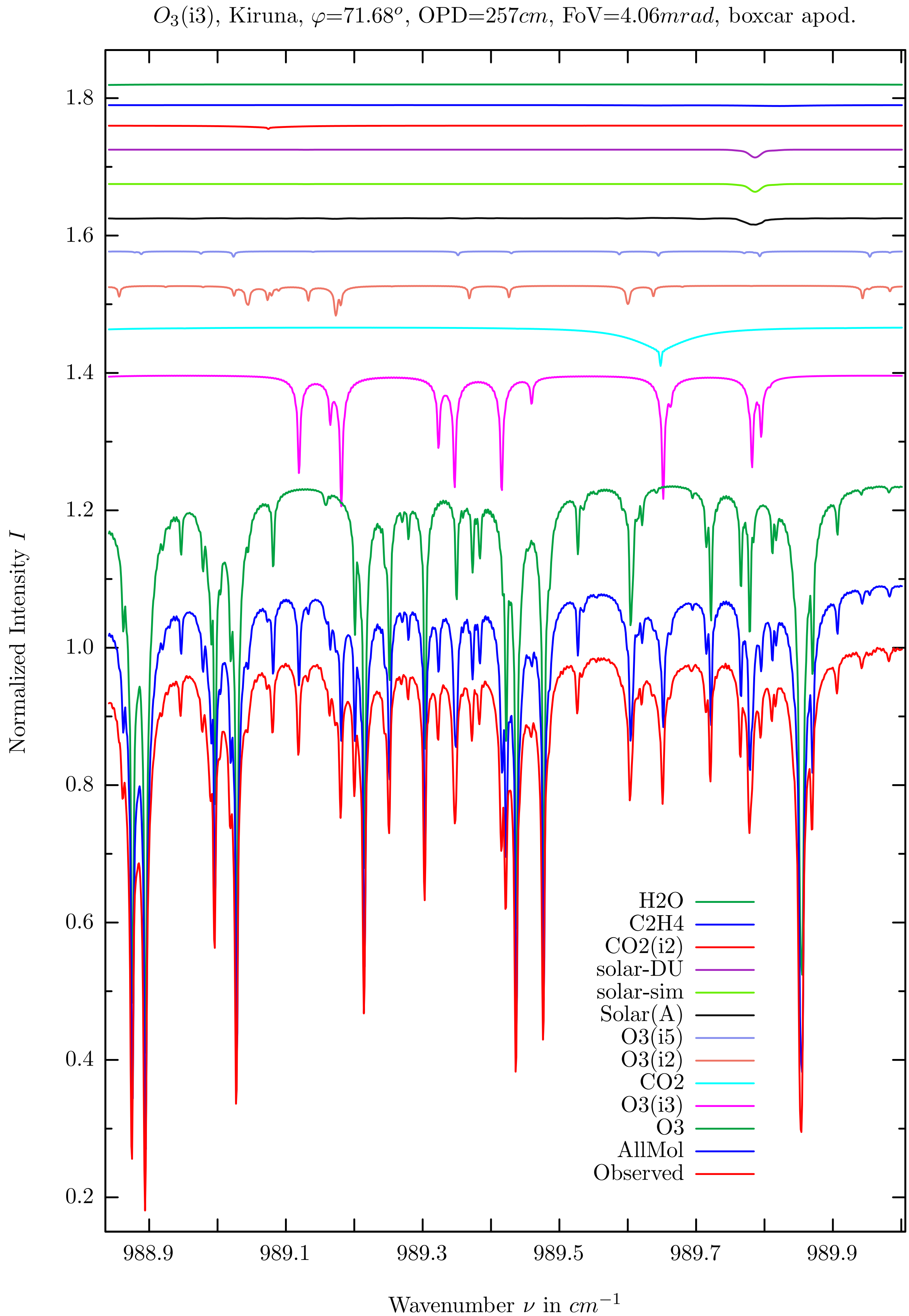
O_3(i3), Kiruna, φ=71.68^o, OPD=257cm, FoV=4.06$mrad$, boxcar apod.
Normalized Intensity I
Wavenumber ν in cm^{-1}
1.8
1.6
1.4
1.2
1.0
0.8
0.6
0.4
0.2
988.9
989.1
989.3
989.5
989.7
989.9
H2O
C2H4
CO2(i2)
solar-DU
solar-sim
Solar(A)
O3(i5)
O3(i2)
CO2
O3(i3)
O3
AllMol
Observed

σ=0.294%, 970315S6.92, φ=71.68^o, OPD=257cm, FoV=4.07$mrad$, Apod.=boxcar

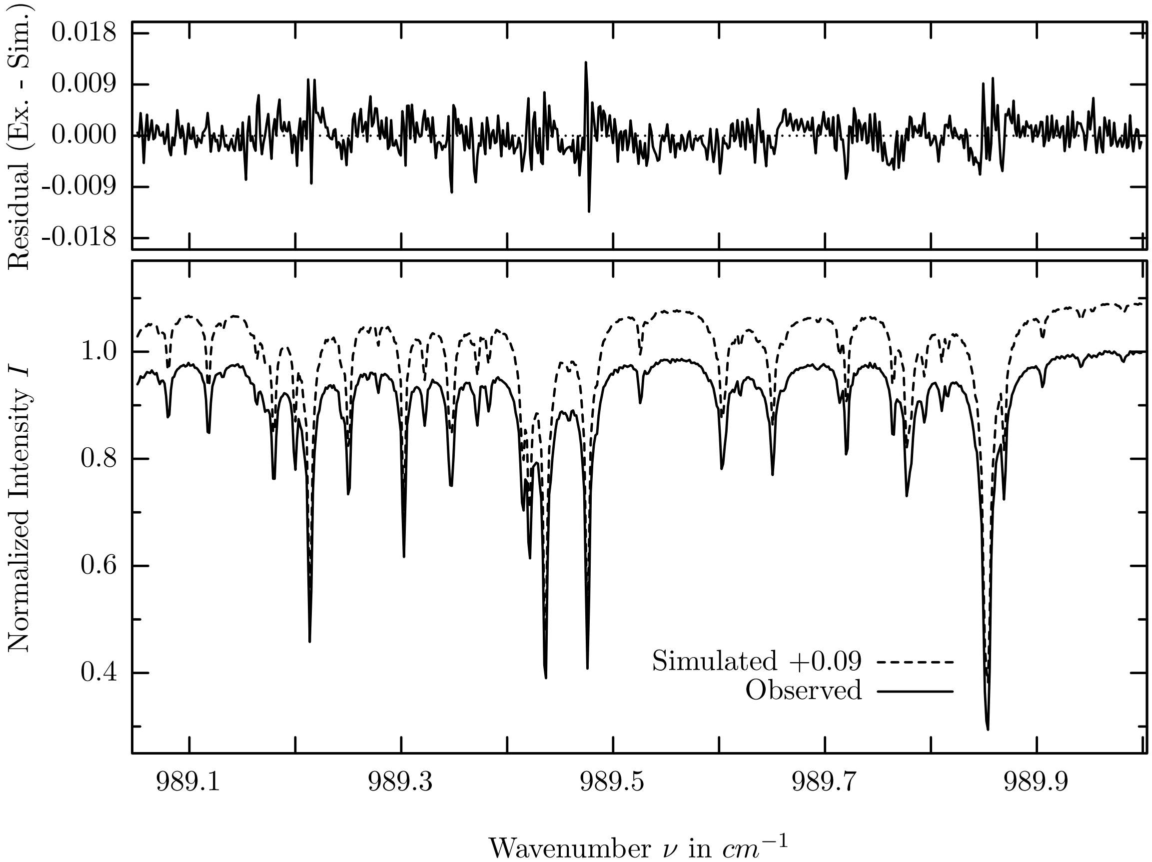

investigated species	:	$O_3(i3 = {}^{16}O\,{}^{18}O\,{}^{16}O), (O_3)$
line position(s) ν_0	:	989.1177, (989.8539) cm^{-1}
lower state energy E''_{lst}	:	222.0, (1028.4) cm^{-1}
retrieved TCA, information content	:	1.12E+19, (1.03E+19) $molec/cm^2$, 52.3, (240.9)
temperature dependence of the TCA	:	-.139, (-.682)%/K (trop), -.009, (-2.117)%/K (strat)
spectral interval fitted	:	989.050 – 990.000 cm^{-1}

Molecule	iCode	Absorption	Molecule	iCode	Absorption
$O3$	31	89.253%	$NO2$	101	0.001%
O3	**33**	21.646%	$NH3$	111	0.001%
$CO2$	21	6.361%	$F142B$	611	0.001%
$O3$	**32**	4.403%	$N2O$	41	<0.001%
$O3$	**35**	0.943%	$CH4$	61	<0.001%
Solar(A)	—	0.917%	OH	131	<0.001%
Solar-sim	—	1.137%	OCS	19**3**	<0.001%
Solar-DU	—	0.012%	$H2O2$	231	<0.001%
$CO2$	2**2**	0.539%	$N2O5$	261	<0.001%
$C2H4$	391	0.141%	$HCOOH$	461	<0.001%
$H2O$	11	0.076%	$H2S$	471	<0.001%
$ClONO2$	271	0.028%	HDO	491	<0.001%
$COF2$	361	0.006%	$CFC113$	621	<0.001%

O_3(i3), Kiruna, φ=71.68^o, OPD=257cm, FoV=4.06$mrad$, boxcar apod.

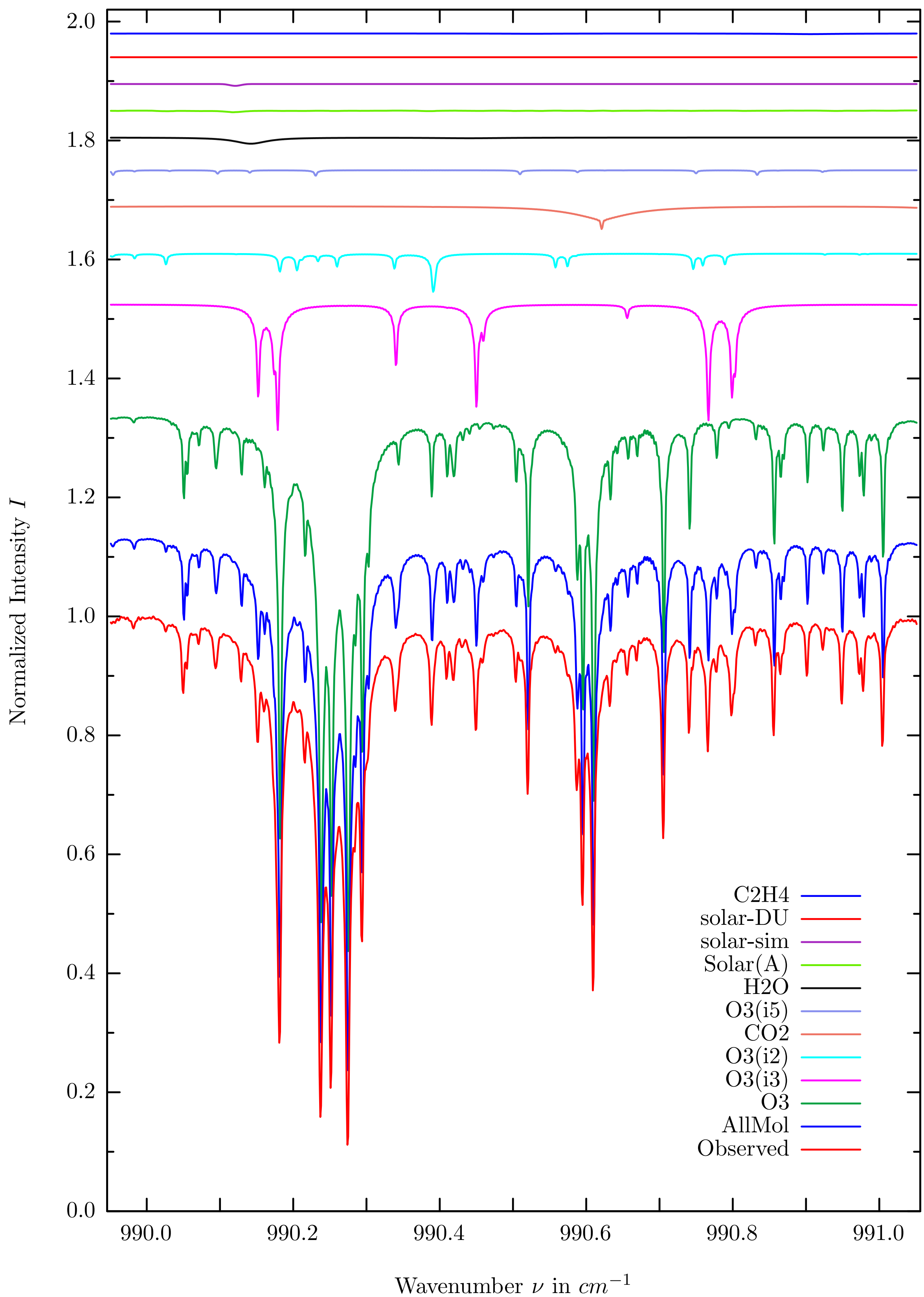

σ=0.316%, 970315S6.92, φ=71.68^o, OPD=257cm, FoV=4.07$mrad$, Apod.=boxcar

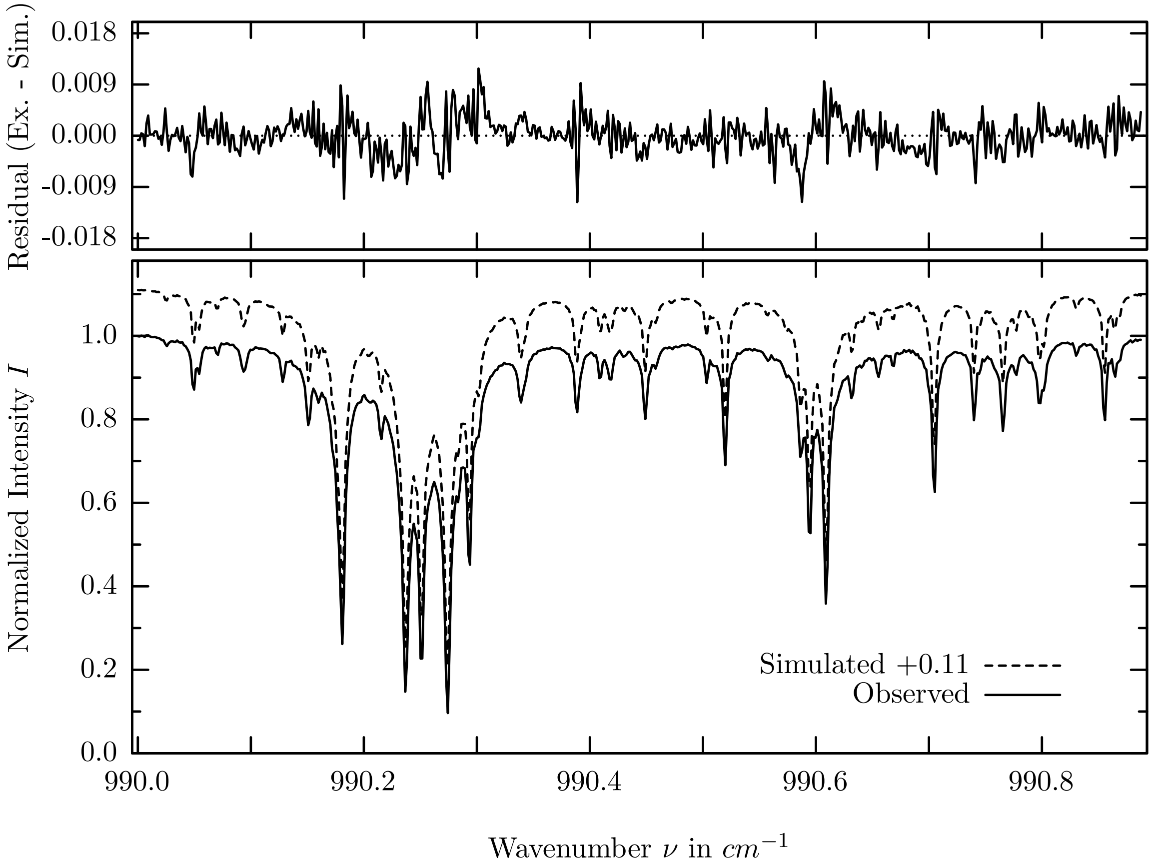

investigated species	:	$O_3(i3 = {}^{16}O\,{}^{18}O\,{}^{16}O), (O_3)$
line position(s) ν_0	:	990.4487, (990.2736) cm^{-1}
lower state energy E''_{lst}	:	185.1, (907.0) cm^{-1}
retrieved TCA, information content	:	1.08E+19, (1.04E+19) $molec/cm^2$, 62.3, (284.9)
temperature dependence of the TCA	:	-.241, (-.614)%/K (trop), +.079, (-1.89)%/K (strat)
spectral interval fitted	:	990.000 – 990.888 cm^{-1}

Molecule	iCode	Absorption	Molecule	iCode	Absorption
$O3$	31	94.685%	$NO2$	101	0.001%
O3	**33**	23.703%	HDO	491	0.001%
$O3$	**32**	7.038%	$F142B$	611	0.001%
$CO2$	21	4.337%	$N2O$	41	<0.001%
$O3$	**35**	1.088%	OH	131	<0.001%
$H2O$	11	1.037%	OCS	19**3**	<0.001%
Solar(A)	—	0.250%	$H2O2$	231	<0.001%
Solar-sim	—	0.308%	$N2O5$	261	<0.001%
Solar-DU	—	<0.001%	$COF2$	361	<0.001%
$C2H4$	391	0.114%	$HCOOH$	461	<0.001%
$ClONO2$	271	0.018%	$H2S$	471	<0.001%
$NH3$	111	0.004%	$CFC113$	621	<0.001%
$CH4$	61	0.001%			

O_3(i3), Kiruna, φ=71.68^o, OPD=257cm, FoV=4.06$mrad$, boxcar apod.

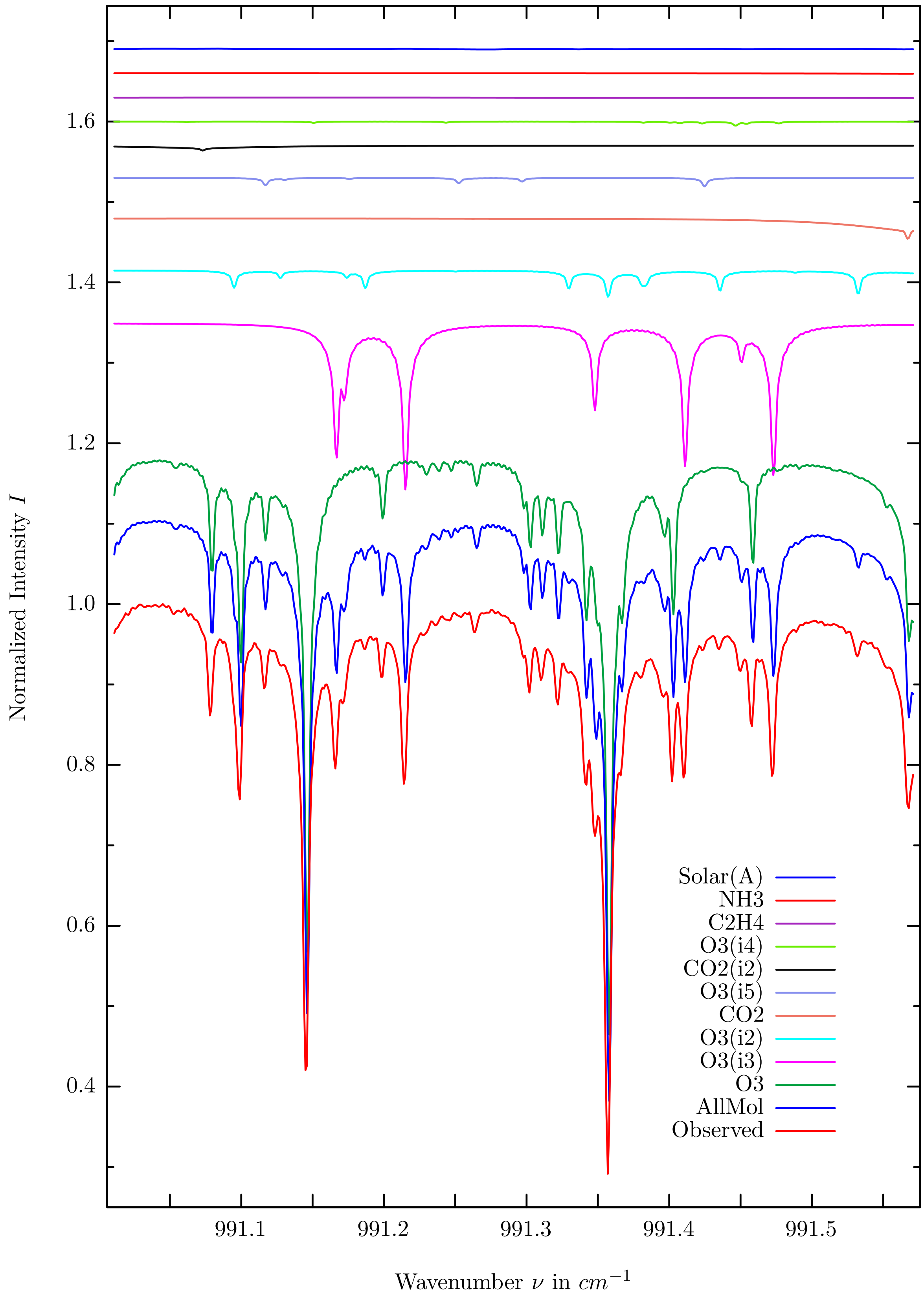

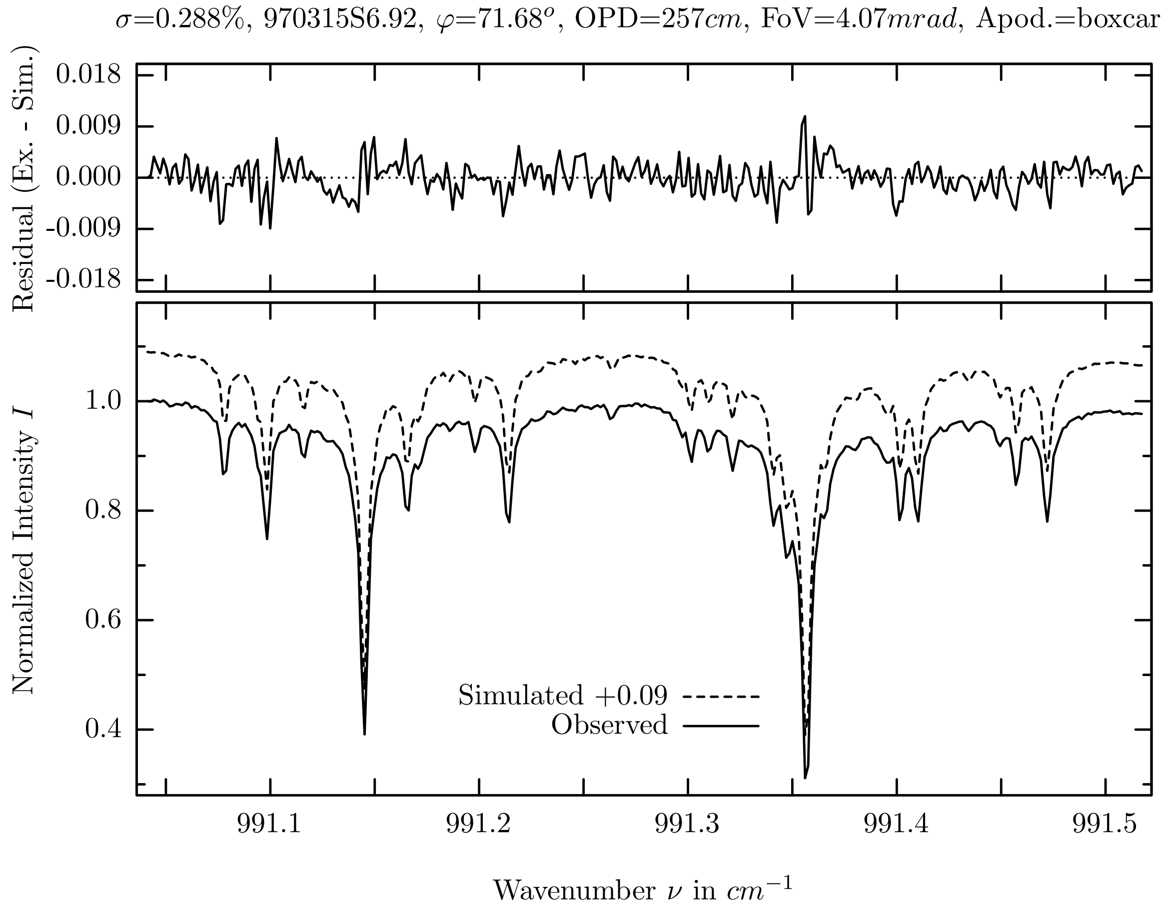

investigated species	:	$O_3(i3 = {}^{16}O\,{}^{18}O\,{}^{16}O), (O_3)$
line position(s) ν_0	:	991.2137, (991.1447) cm^{-1}
lower state energy E''_{lst}	:	155.8, (1023.1) cm^{-1}
retrieved TCA, information content	:	1.09E+19, (1.04E+19) $molec/cm^2$, 76.6, (213.7)
temperature dependence of the TCA	:	+.014, (-.657)%/K (trop), +.261, (-2.05)%/K (strat)
spectral interval fitted	:	991.040 – 991.518 cm^{-1}

Molecule	iCode	Absorption	Molecule	iCode	Absorption
$O3$	31	79.930%	HDO	491	0.002%
O3	**33**	23.302%	$CH4$	61	0.001%
$O3$	**32**	3.583%	$F142B$	611	0.001%
$CO2$	21	2.898%	$N2O$	41	<0.001%
$O3$	**35**	1.239%	$NO2$	101	<0.001%
$CO2$	2**2**	0.686%	OH	131	<0.001%
$O3$	**34**	0.556%	OCS	19**3**	<0.001%
$C2H4$	391	0.082%	$H2O2$	231	<0.001%
$NH3$	111	0.053%	$N2O5$	261	<0.001%
Solar(A)	—	0.041%	$COF2$	361	<0.001%
Solar-sim	—	<0.001%	$HCOOH$	461	<0.001%
$H2O$	11	0.019%	$H2S$	471	<0.001%
$ClONO2$	271	0.015%	$CFC113$	621	<0.001%

O_3(i3), Kiruna, φ=71.68^o, OPD=257cm, FoV=4.06$mrad$, boxcar apod.

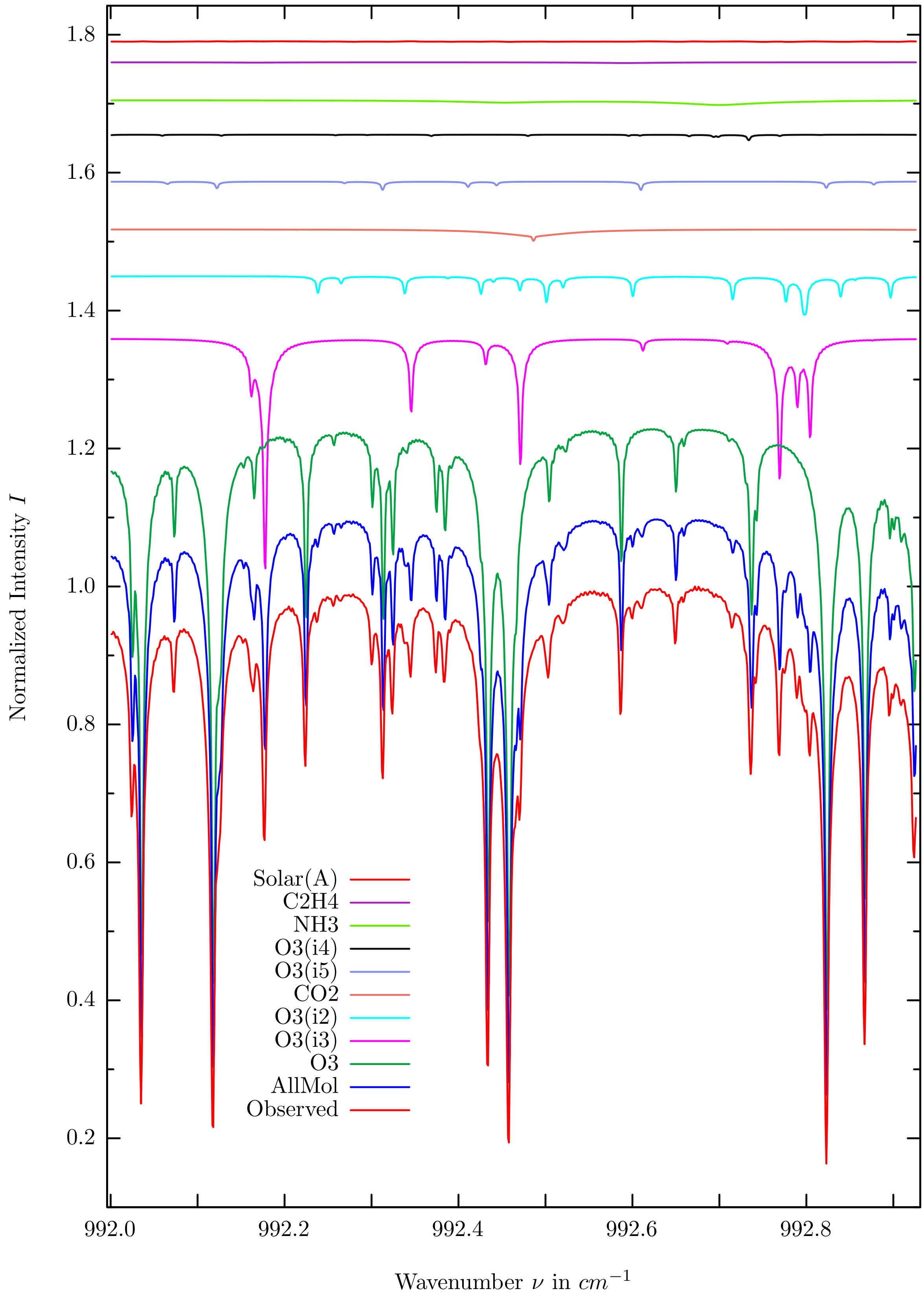

σ=0.335%, 970315S6.92, φ=71.68^o, OPD=257cm, FoV=4.07$mrad$, Apod.=boxcar

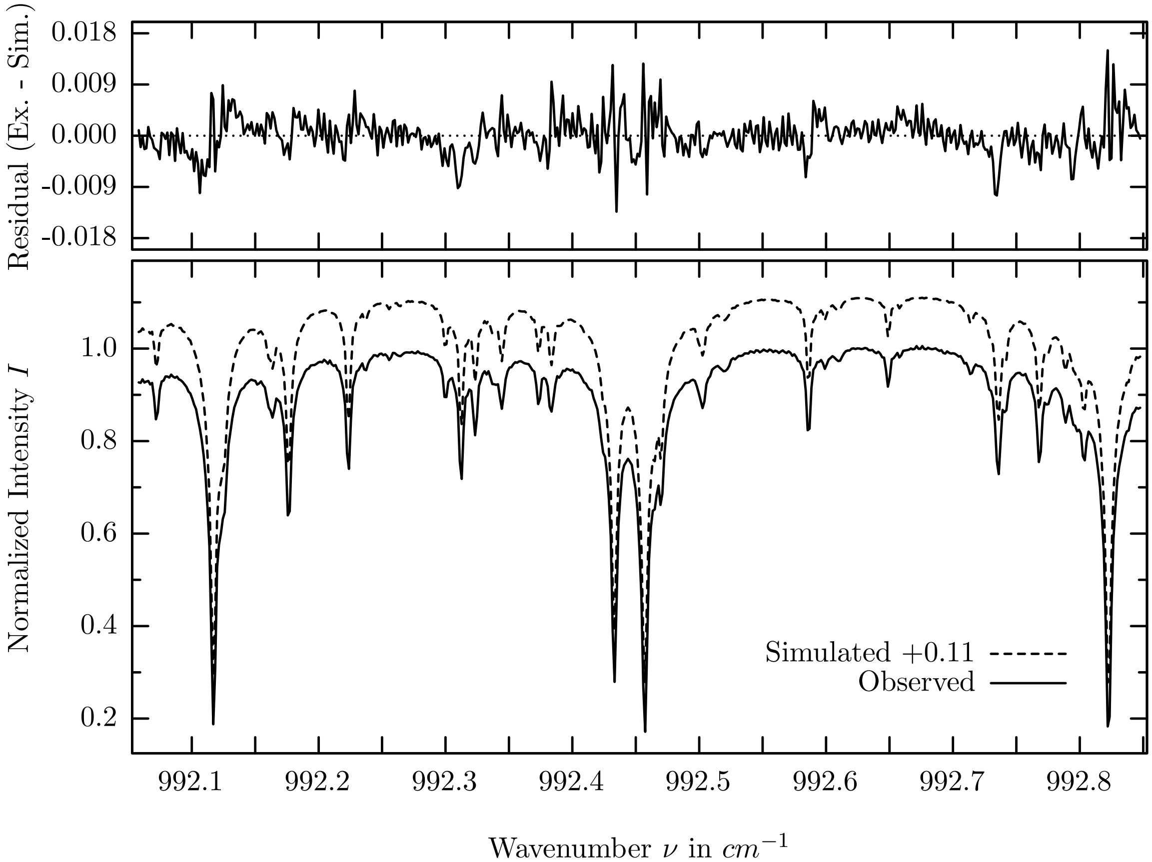

investigated species	:	$O_3(i3 = {}^{16}O\,{}^{18}O\,{}^{16}O), (O_3)$
line position(s) ν_0	:	992.1759, 992.1764, (992.1168) cm^{-1}
lower state energy E''_{lst}	:	140.0, 174.1, (952.0) cm^{-1}
retrieved TCA, information content	:	1.07E+19, (1.04E+19) $molec/cm^2$, 103.1, (244.2)
temperature dependence of the TCA	:	-.056, (-.623)%/K (trop), +.155, (-1.839)%/K (strat)
spectral interval fitted	:	992.058 – 992.849 cm^{-1}

Molecule	iCode	Absorption	Molecule	iCode	Absorption
$O3$	31	90.940%	HDO	491	0.003%
O3	**33**	37.522%	$CH4$	61	0.001%
$O3$	**32**	6.180%	$F142B$	611	0.001%
$CO2$	21	1.902%	$N2O$	41	<0.001%
$O3$	**35**	1.433%	$NO2$	101	<0.001%
$O3$	**34**	0.890%	OH	131	<0.001%
$NH3$	111	0.691%	OCS	19**3**	<0.001%
$C2H4$	391	0.110%	$H2O2$	231	<0.001%
Solar(A)	—	0.042%	$CCl2F2$	321	<0.001%
Solar-sim	—	0.002%	$COF2$	361	<0.001%
Solar-DU	—	0.002%	$HCOOH$	461	<0.001%
$ClONO2$	271	0.018%	$H2S$	471	<0.001%
$H2O$	11	0.004%	$CFC113$	621	<0.001%

O_3(i3), Kiruna, φ=71.68^o, OPD=257cm, FoV=4.06$mrad$, boxcar apod.

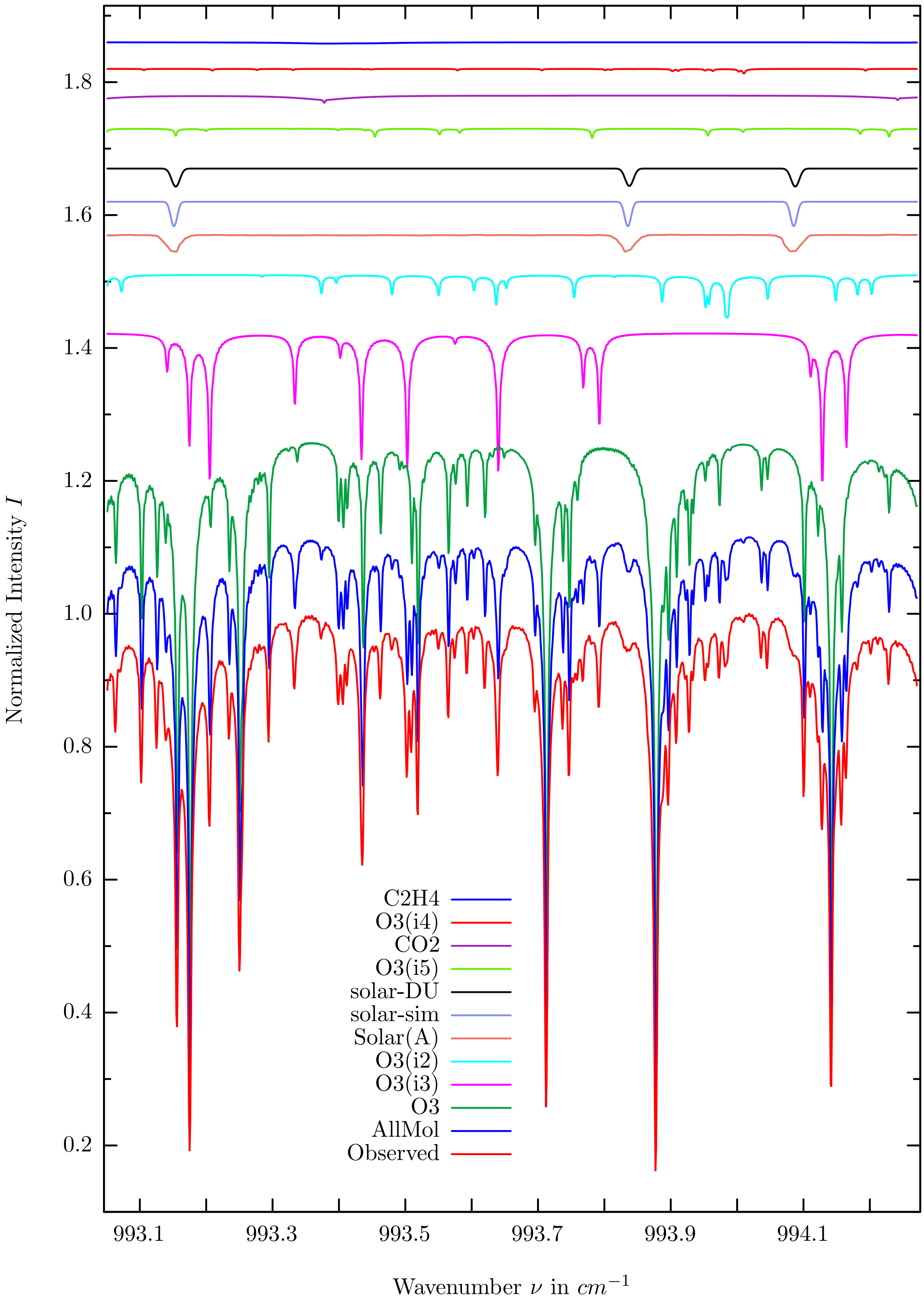

σ=0.394%, 970315S6.92, φ=71.68^o, OPD=257cm, FoV=4.07$mrad$, Apod.=boxcar

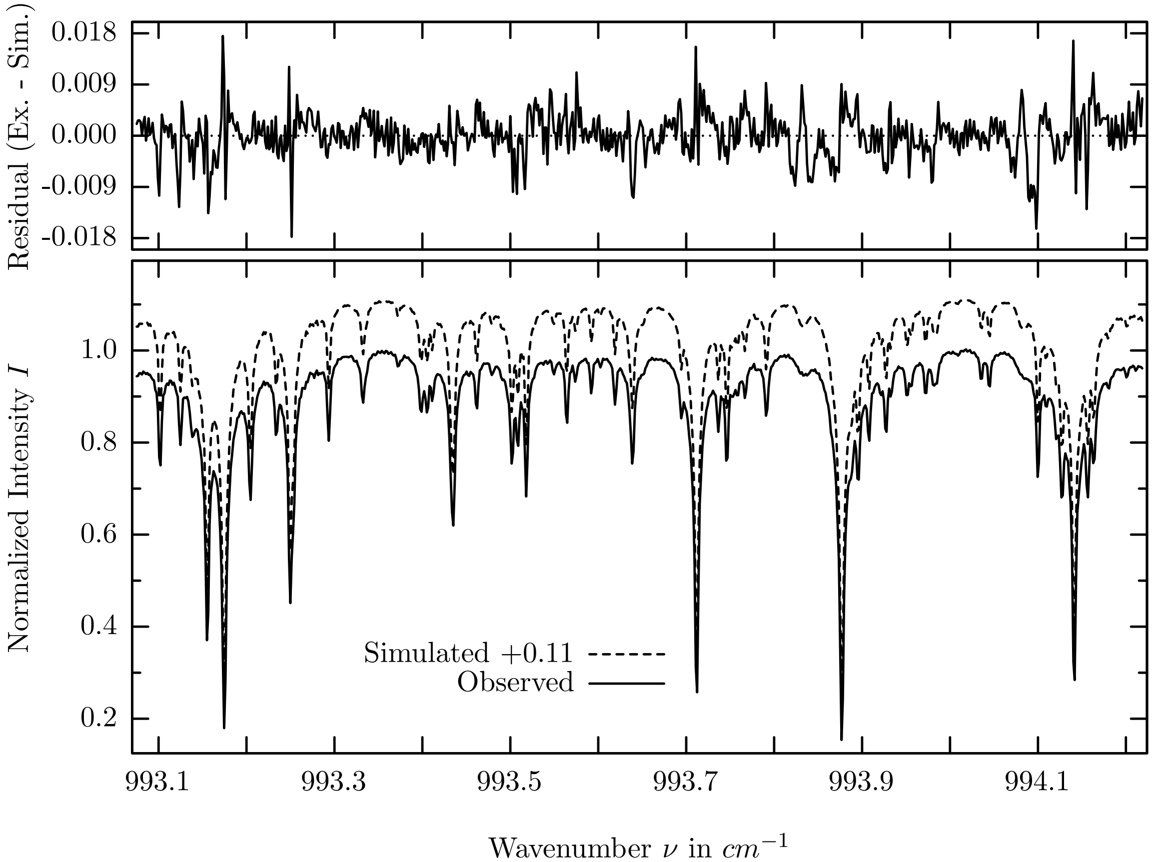

investigated species	:	$O_3(i3 = {}^{16}O\,{}^{18}O\,{}^{16}O), (O_3)$
line position(s) ν_0	:	993.7910, (993.7116) cm^{-1}
lower state energy E''_{lst}	:	172.2, (948.2) cm^{-1}
retrieved TCA, information content	:	1.08E+19, (1.04E+19) $molec/cm^2$, 38.3, (188.9)
temperature dependence of the TCA	:	-.051, (-.661)%/K (trop), +.190, (-1.87)%/K (strat)
spectral interval fitted	:	993.075 – 994.220 cm^{-1}

Molecule	iCode	Absorption	Molecule	iCode	Absorption
$O3$	31	91.457%	HDO	491	0.029%
O3	**33**	25.793%	$CH4$	61	0.001%
$O3$	**32**	7.215%	$F142B$	611	0.001%
Solar(A)	—	2.544%	$N2O$	41	<0.001%
Solar-sim	—	3.698%	$NO2$	101	<0.001%
Solar(A)	—	2.544%	OH	131	<0.001%
$O3$	**35**	1.650%	OCS	19**3**	<0.001%
$CO2$	21	1.238%	$H2O2$	231	<0.001%
$O3$	**34**	0.732%	$CCl2F2$	321	<0.001%
$C2H4$	391	0.194%	$COF2$	361	<0.001%
$ClONO2$	271	0.048%	$HCOOH$	461	<0.001%
$H2O$	11	0.036%	$H2S$	471	<0.001%
$NH3$	111	0.030%	$CFC113$	621	<0.001%

O_3(i2,i3), Kiruna, φ=71.68^o, OPD=257cm, FoV=4.06$mrad$, boxcar apod.

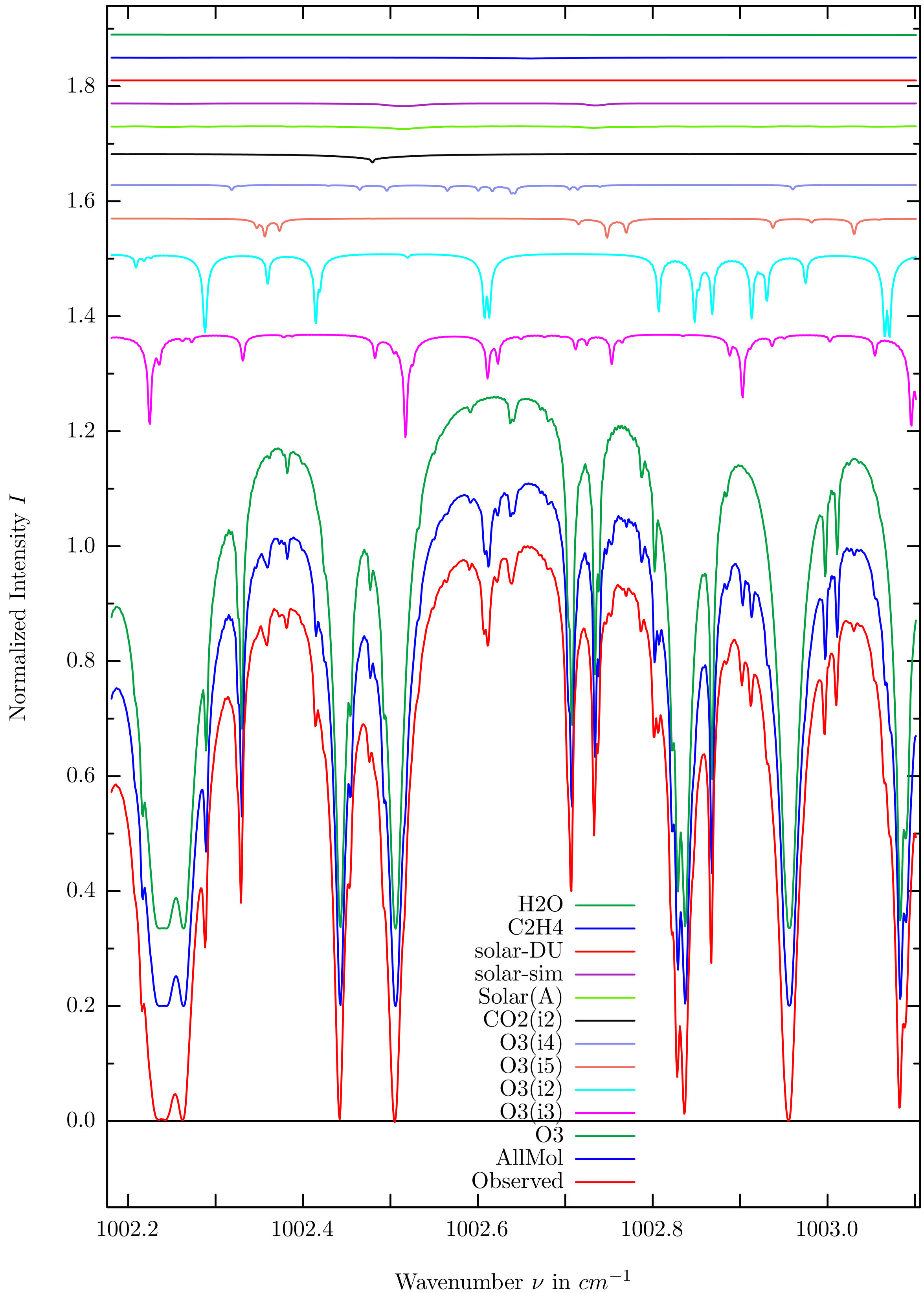

σ=0.318%, 970315S6.92, φ=71.68^o, OPD=257cm, FoV=4.07$mrad$, Apod.=boxcar

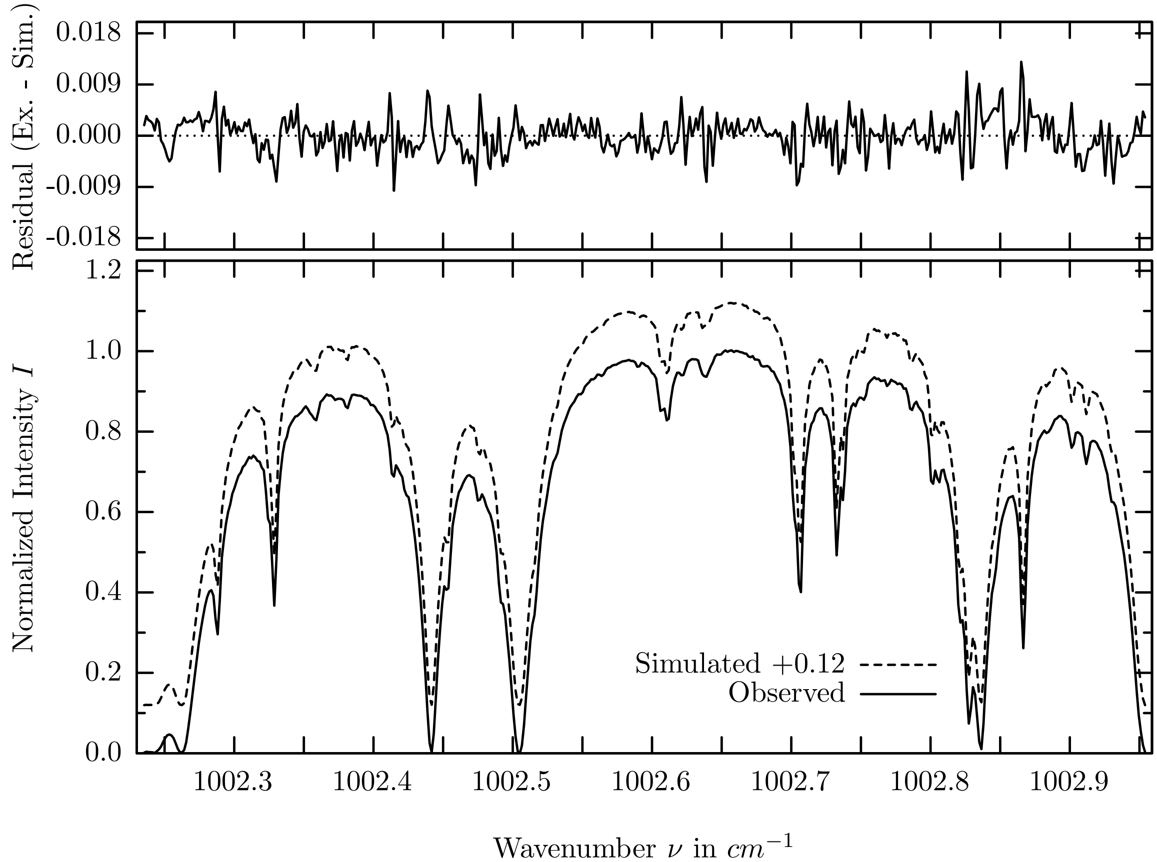

investigated species	:	$O_3(i2 = {}^{16}O\,{}^{16}O\,{}^{18}O), O_3(i3), (O_3)$
line position(s) ν_0	:	1002.6060, (1002.7062) cm^{-1}
lower state energy E''_{lst}	:	328.4, (945.2) cm^{-1}
retrieved TCA, information content	:	1.12E+19, (1.03E+19) $molec/cm^2$, 46.2, (179.4)
temperature dependence of the TCA	:	+.201, (-.412)%/K (trop), +.318, (-1.434)%/K (strat)
spectral interval fitted	:	1002.234 – 1002.956 cm^{-1}

Molecule	iCode	Absorption	Molecule	iCode	Absorption
$O3$	31	100.000%	$N2O$	41	0.001%
O3	**33**	20.278%	$NH3$	111	0.001%
O3	**32**	16.362%	OCS	19**3**	0.001%
$O3$	**35**	3.835%	$CH4$	61	<0.001%
$O3$	**34**	1.709%	$NO2$	101	<0.001%
$CO2$	2**2**	1.615%	OH	131	<0.001%
Solar(A)	—	0.434%	$H2O2$	231	<0.001%
Solar-sim	—	0.491%	$CCl2F2$	321	<0.001%
Solar-DU	—	0.001%	$HCOOH$	461	<0.001%
$C2H4$	391	0.180%	$H2S$	471	<0.001%
$H2O$	11	0.100%	HDO	491	<0.001%
$CO2$	21	0.043%	$F142B$	611	<0.001%
$ClONO2$	271	0.010%			

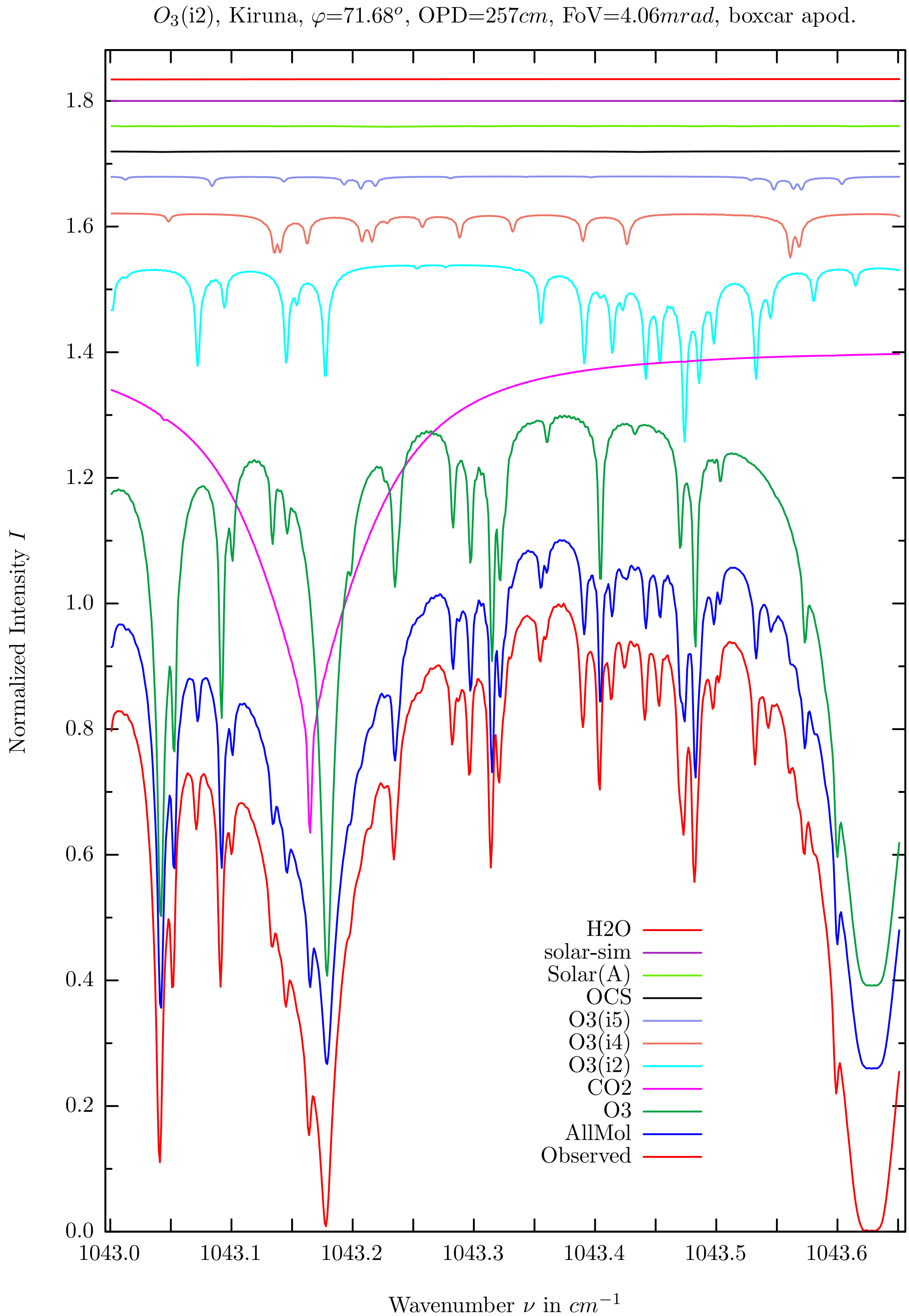

O_3(i2), Kiruna, φ=71.68^o, OPD=257cm, FoV=4.06$mrad$, boxcar apod.
Normalized Intensity I
Wavenumber ν in cm^{-1}
1.8
1.6
1.4
1.2
1.0
0.8
0.6
0.4
0.2
0.0
1043.0
1043.1
1043.2
1043.3
1043.4
1043.5
1043.6
H2O
solar-sim
Solar(A)
OCS
O3(i5)
O3(i4)
O3(i2)
CO2
O3
AllMol
Observed

σ=0.344%, 970315S6.92, φ=71.68^o, OPD=257cm, FoV=4.07$mrad$, Apod.=boxcar

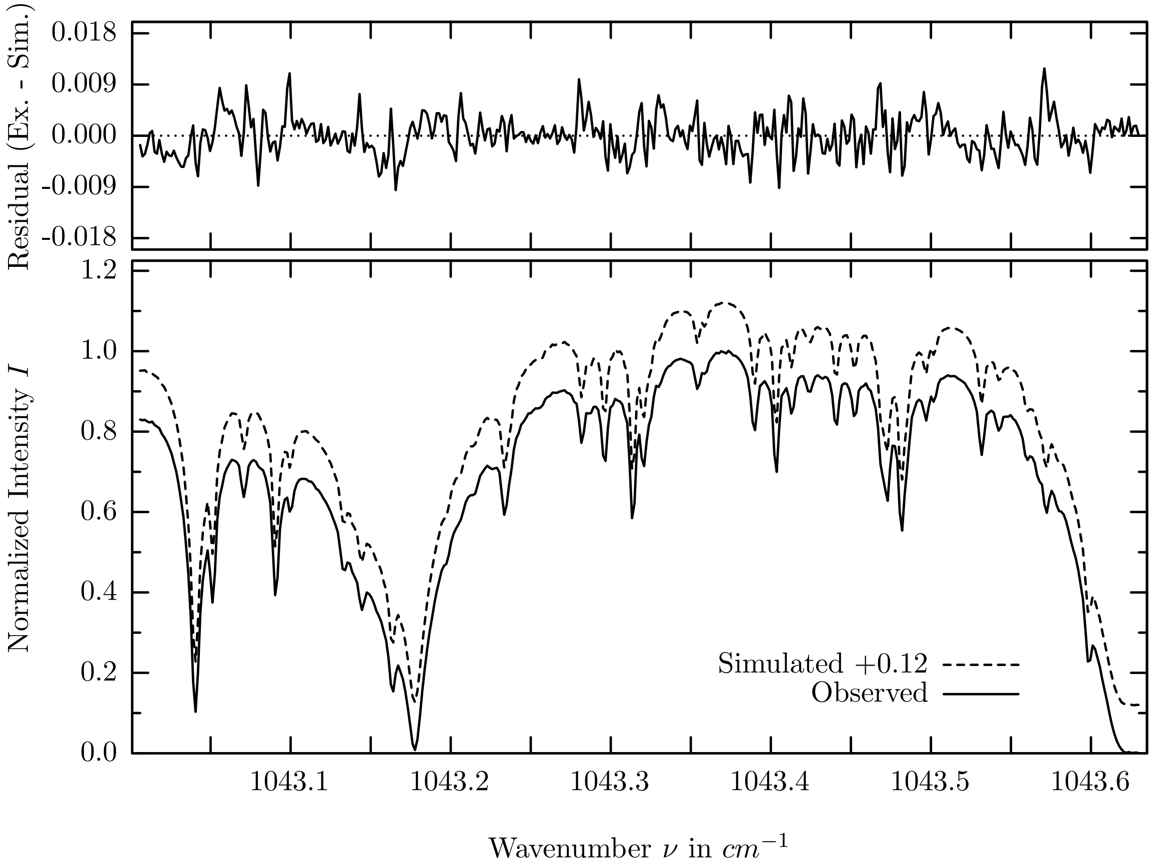

investigated species	:	$O_3(i2 = {}^{16}O\,{}^{16}O\,{}^{18}O), (O_3)$
line position(s) ν_0	:	1043.4404, (1043.4030) cm^{-1}
lower state energy E''_{lst}	:	230.4, (1097.1) cm^{-1}
retrieved TCA, information content	:	1.14E+19, (1.01E+19) $molec/cm^2$, 46.9, (82.6)
temperature dependence of the TCA	:	-.302, (+2.34)%/K (trop), -.101, (+1.95)%/K (strat)
location, date, solar zenith angle	:	Kiruna, 15/Mar/97, 71.68^o
spectral interval fitted	:	1043.005 – 1043.630 cm^{-1}

Molecule	iCode	Absorption	Molecule	iCode	Absorption
$O3$	31	100.000%	$NH3$	111	0.002%
$CO2$	21	80.375%	$HO2$	221	0.002%
O3	**32**	31.399%	$CH4$	61	0.001%
$O3$	**34**	7.946%	HDO	491	0.001%
$O3$	**35**	2.462%	$SO2$	91	<0.001%
OCS	191	0.117%	OH	131	<0.001%
Solar(A)	—	0.101%	$H2O2$	231	<0.001%
Solar-sim	—	<0.001%	$ClONO2$	271	<0.001%
$H2O$	11	0.083%	$CCl2F2$	321	<0.001%
$C2H4$	391	0.032%	$CCl3F$	331	<0.001%
$N2O$	41	0.022%	$H2S$	471	<0.001%
$HCOOH$	461	0.004%	$F142B$	611	<0.001%

O_3(i2), Kiruna, φ=71.68^o, OPD=257cm, FoV=4.06$mrad$, boxcar apod.

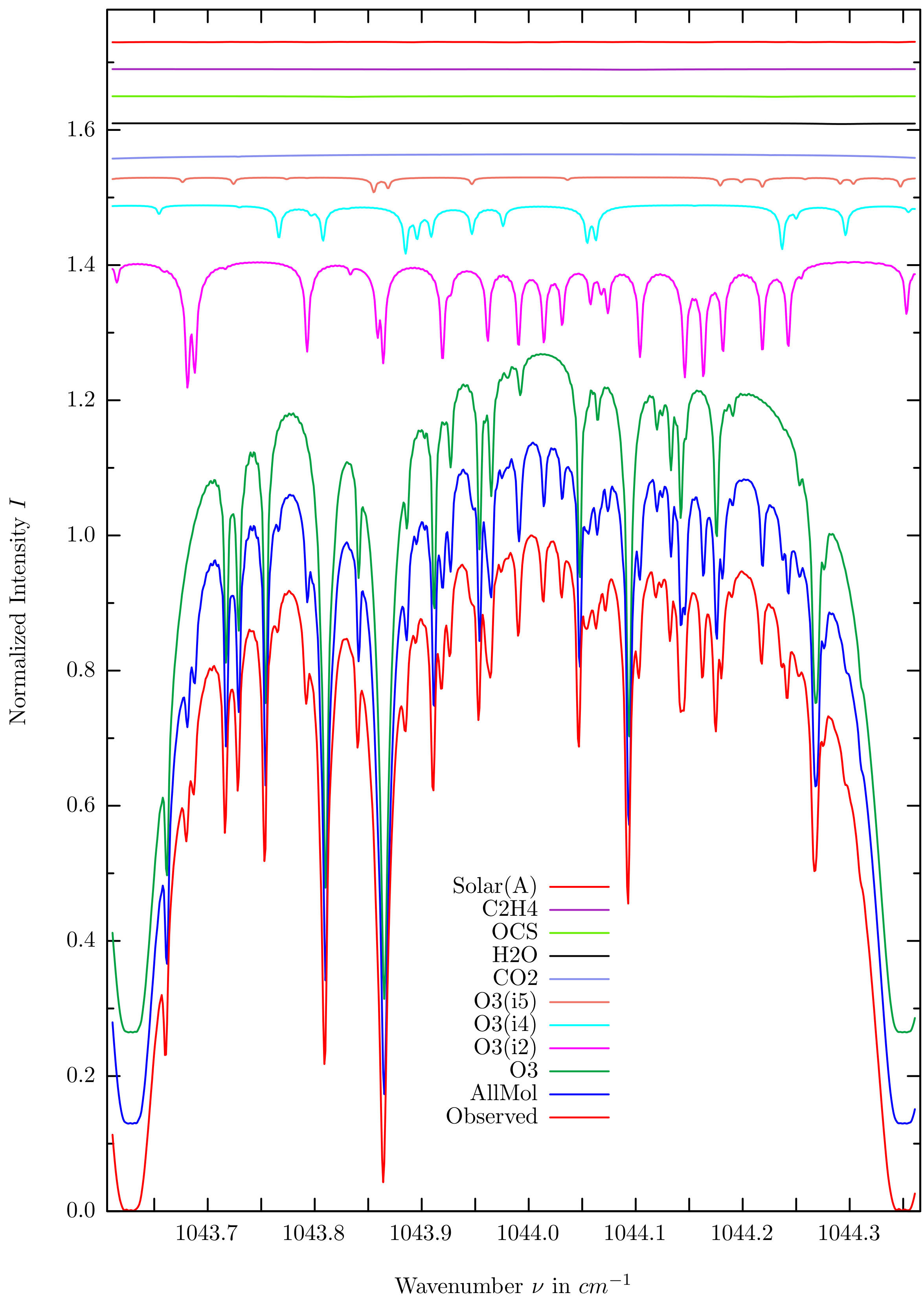

σ=0.363%, 970315S6.92, φ=71.68^o, OPD=257cm, FoV=4.07$mrad$, Apod.=boxcar

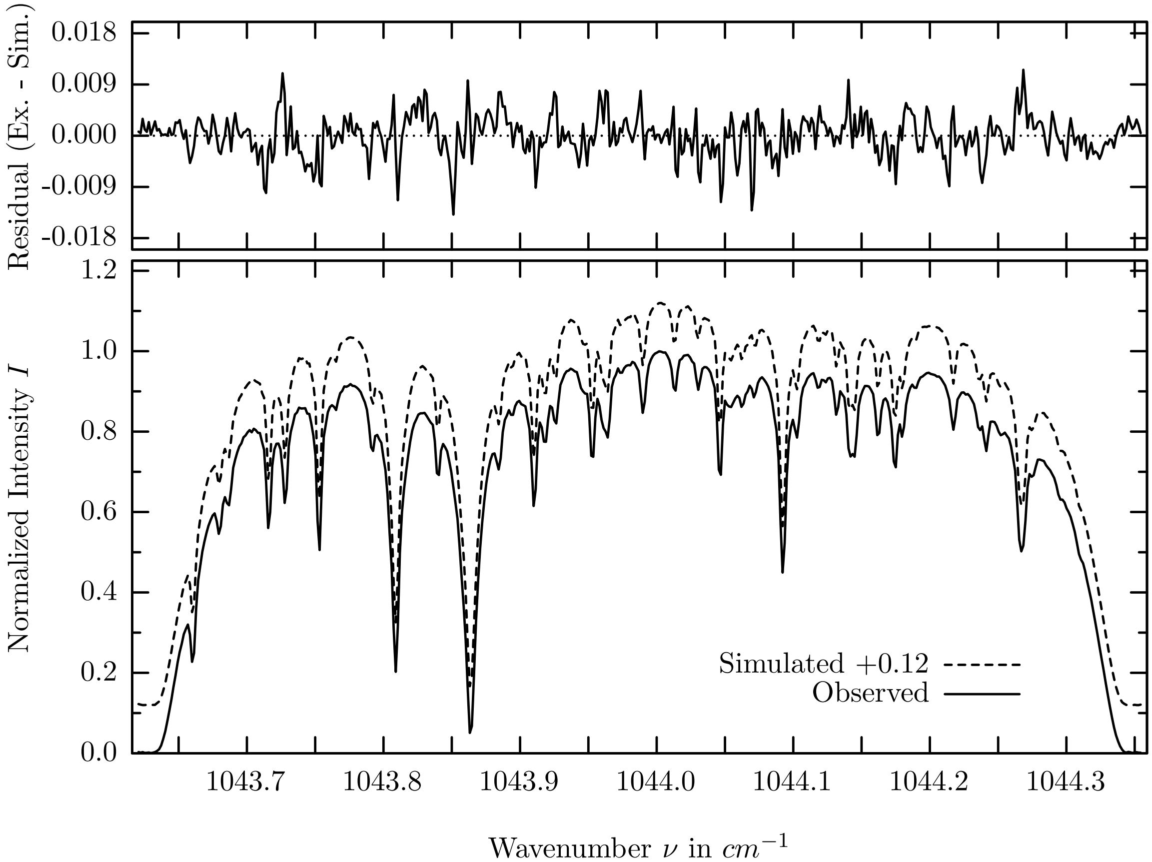

investigated species	:	$O_3(i2 = {}^{16}O\,{}^{16}O\,{}^{18}O), (O_3)$
line position(s) ν_0	:	1044.0128, (1044.0916) cm^{-1}
lower state energy E''_{lst}	:	288.1, (1046.3) cm^{-1}
retrieved TCA, information content	:	1.13E+19, (1.06E+19) $molec/cm^2$, 26.3, (153.0)
temperature dependence of the TCA	:	+.280, (+.099)%/K (trop), +1.007, (-.142)%/K (strat)
location, date, solar zenith angle	:	Kiruna, 15/Mar/97, 71.68^o
spectral interval fitted	:	1043.620 – 1044.355 cm^{-1}

Molecule	iCode	Absorption	Molecule	iCode	Absorption
$O3$	31	100.000%	$HO2$	221	0.003%
O3	**32**	21.646%	$NH3$	111	0.002%
$O3$	**34**	8.170%	$CH4$	61	0.001%
$O3$	**35**	2.548%	HDO	491	0.001%
$CO2$	21	1.181%	$SO2$	91	<0.001%
$H2O$	11	0.125%	OH	131	<0.001%
OCS	191	0.104%	$H2O2$	231	<0.001%
$C2H4$	391	0.085%	$ClONO2$	271	<0.001%
Solar(A)	—	0.031%	$CCl2F2$	321	<0.001%
Solar-sim	—	0.001%	$CCl3F$	331	<0.001%
$N2O$	41	0.022%	$H2S$	471	<0.001%
$HCOOH$	461	0.004%	$F142B$	611	<0.001%

O_3(i2), Kiruna, φ=71.68^o, OPD=257cm, FoV=4.06$mrad$, boxcar apod.

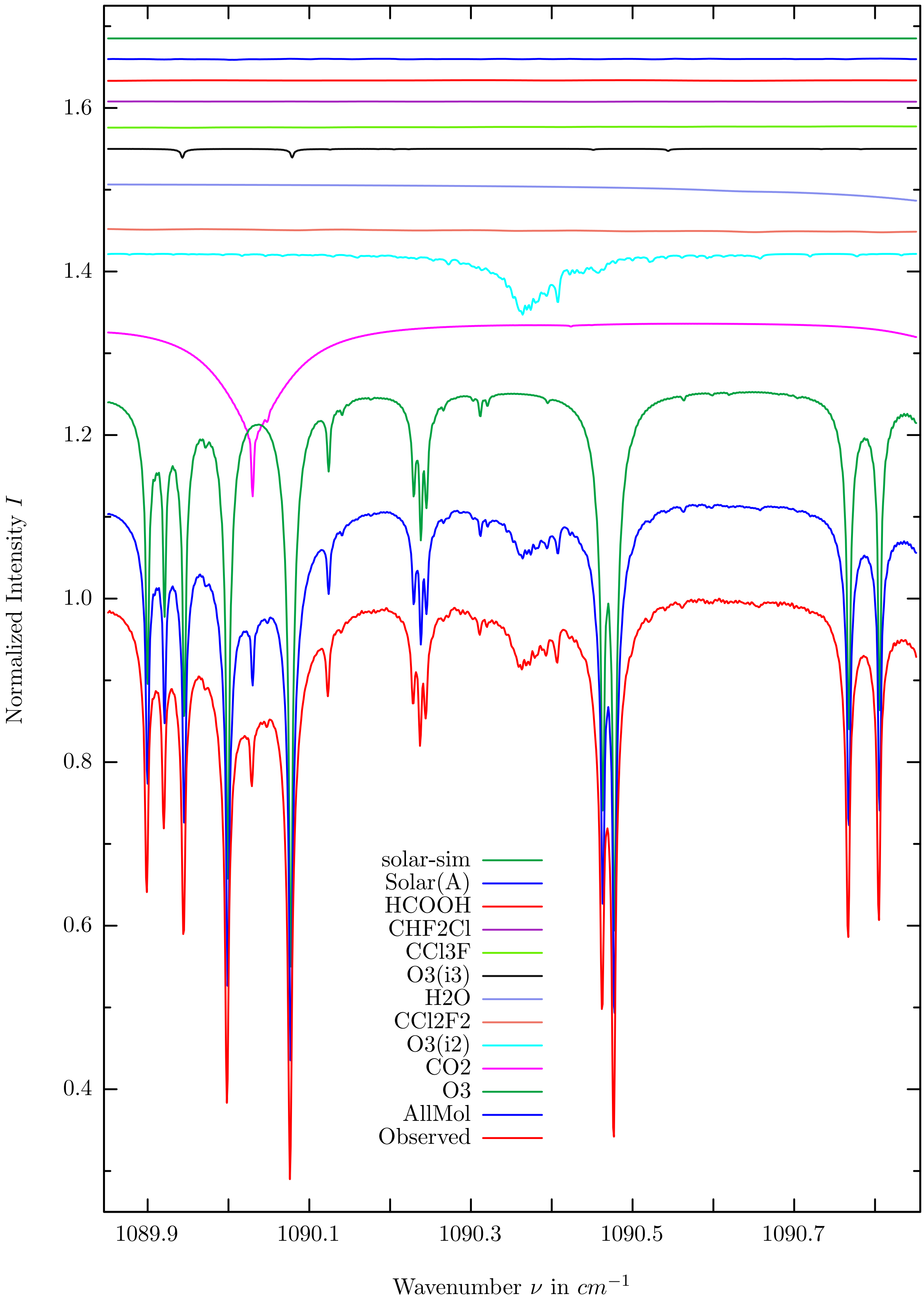

σ=0.148%, 970315S6.92, φ=71.68^o, OPD=257cm, FoV=4.07$mrad$, Apod.=boxcar

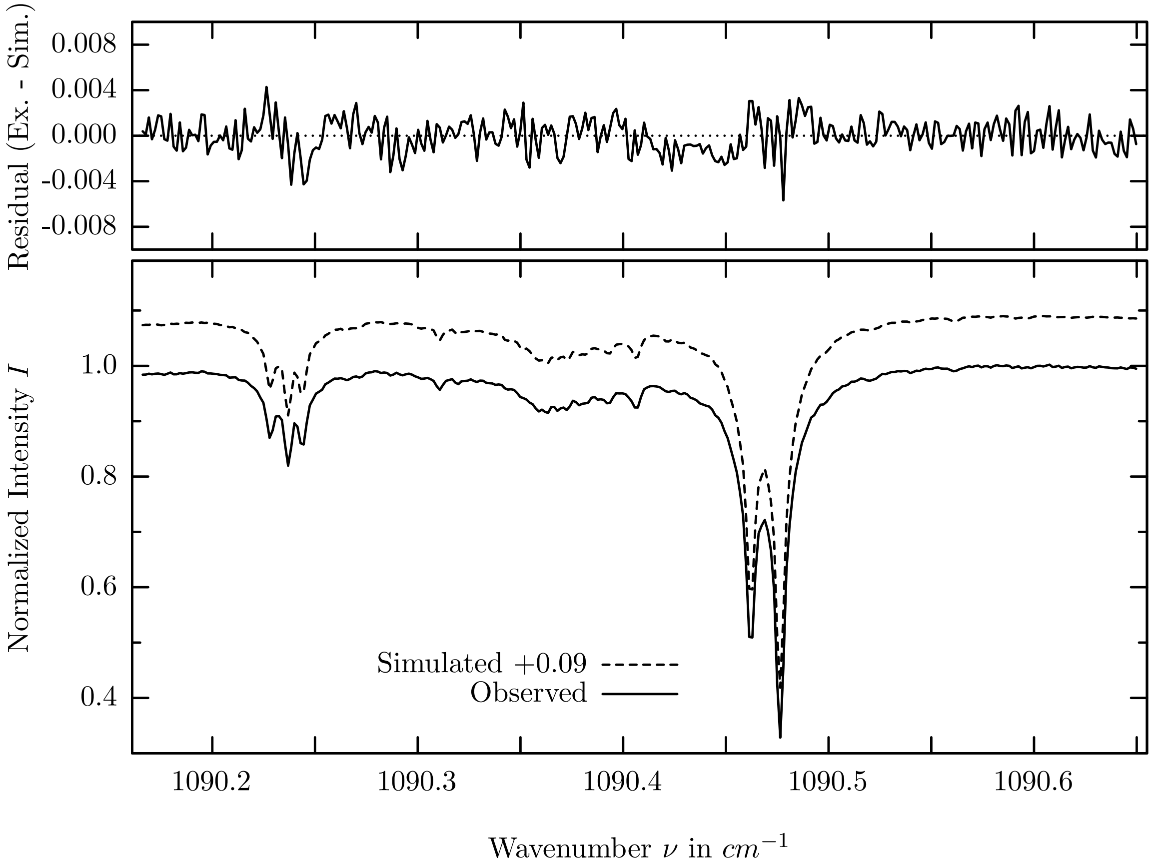

investigated species	:	$O_3(i2 = {}^{16}O\,{}^{16}O\,{}^{18}O), (O_3)$
line position(s) ν_0	:	1090.3638, (1090.4761) cm^{-1}
lower state energy E''_{lst}	:	32.6, (385.7) cm^{-1}
retrieved TCA, information content	:	1.20E+19, (1.03E+19) $molec/cm^2$, 57.7, (454.7)
temperature dependence of the TCA	:	+.046, (-.102)%/K (trop), +.436, (-.092)%/K (strat)
spectral interval fitted	:	1090.165 – 1090.650 cm^{-1}

Molecule	iCode	Absorption	Molecule	iCode	Absorption
$O3$	31	75.805%	$SO2$	91	0.009%
$CO2$	21	23.346%	$HO2$	221	0.006%
O3	**32**	7.579%	$F142B$	611	0.003%
$CCl2F2$	321	3.202%	$NH3$	111	0.002%
$H2O$	11	2.158%	$ClONO2$	271	0.001%
$O3$	3**3**	1.253%	$C2H4$	391	0.001%
$CCl3F$	331	0.919%	$N2O$	41	<0.001%
$CHF2Cl$	421	0.244%	$HNO3$	121	<0.001%
$HCOOH$	461	0.183%	OH	131	<0.001%
Solar(A)	—	0.112%	ClO	18**2**	<0.001%
Solar-sim	—	<0.001%	OCS	191	<0.001%
HDO	491	0.025%	$H2O2$	231	<0.001%
$CH4$	61	0.024%	$H2S$	471	<0.001%

$HCOOH$, Kiruna, φ=71.68^o, OPD=257cm, FoV=4.06$mrad$, boxcar apod.

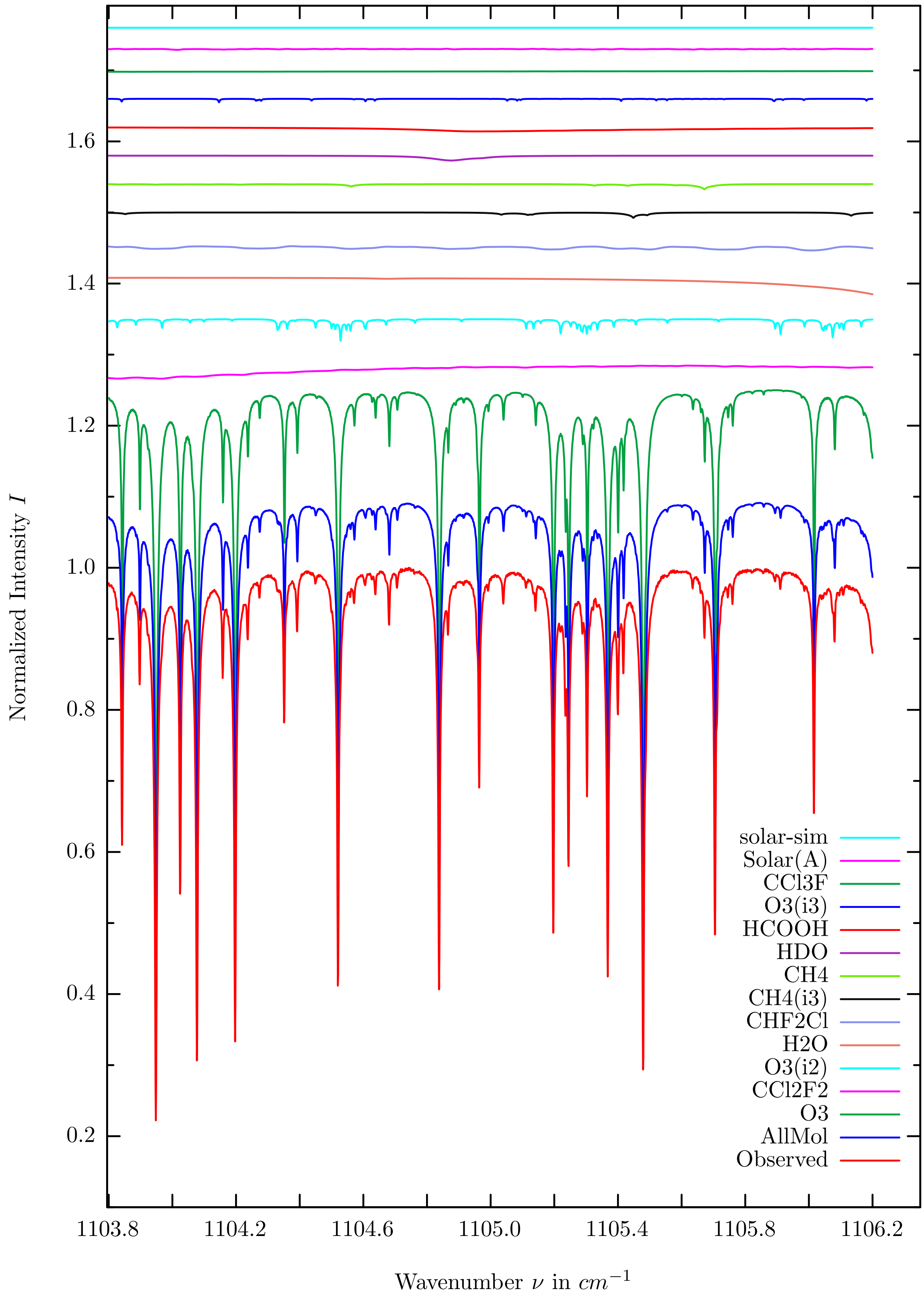

σ=0.199%, 970315S6.92, φ=71.68^o, OPD=257cm, FoV=4.07$mrad$, Apod.=boxcar

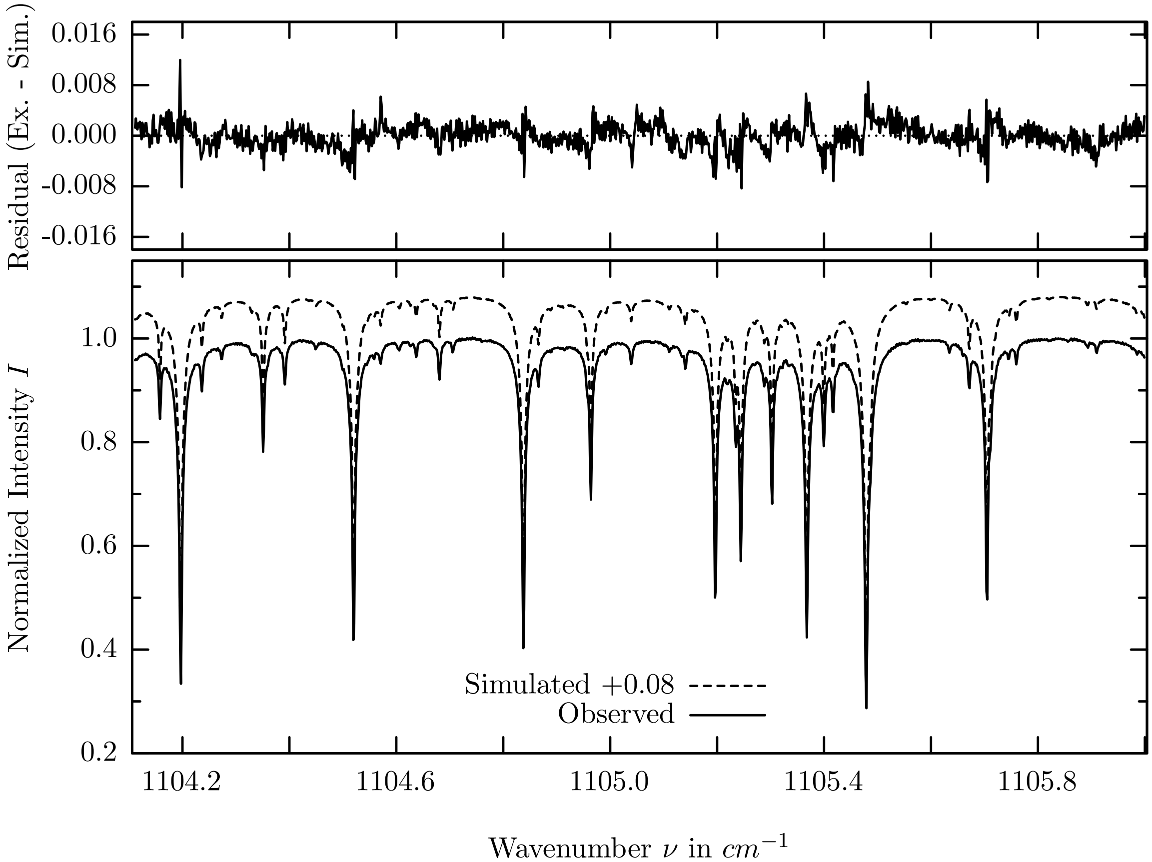

investigated species	:	$HCOOH, (O_3)$
line position(s) ν_0	:	1104.948$^{*)}$, 1105.025$^{*)}$, 1105.069$^{*)}$, (1104.8375) cm^{-1}
lower state energy E''_{lst}	:	24 to 129, (281.8) cm^{-1}
retrieved TCA, information content	:	3.06e15, (1.03e19) $molec/cm^2$, 3.5, 4.2, 3.0 (301.6)
temperature dependence of the TCA	:	+.317, (-.073)%/K (trop), -.096, (-.160)%/K (strat)
spectral interval fitted	:	1104.110 – 1106.000 cm^{-1}

Molecule	iCode	Absorption	Molecule	iCode	Absorption
$O3$	31	82.755%	$CO2$	21	0.040%
$CCl2F2$	321	5.895%	$SO2$	91	0.028%
$O3$	**32**	3.312%	$NH3$	111	0.028%
$H2O$	11	2.531%	$HO2$	221	0.012%
$CHF2Cl$	421	1.343%	$F142B$	611	0.012%
$CH4$	6**3**	0.766%	$ClONO2$	271	0.006%
$CH4$	61	0.756%	$C2H4$	391	0.004%
HDO	491	0.696%	$N2O$	41	0.001%
HCOOH	461	0.588%	$HNO3$	121	0.001%
$O3$	**33**	0.533%	$H2S$	471	0.001%
$CCl3F$	331	0.196%	ClO	181	<0.001%
Solar(A)	—	0.110%	$H2O2$	231	<0.001%
Solar-sim	—	0.001%	$N2O5$	261	<0.001%

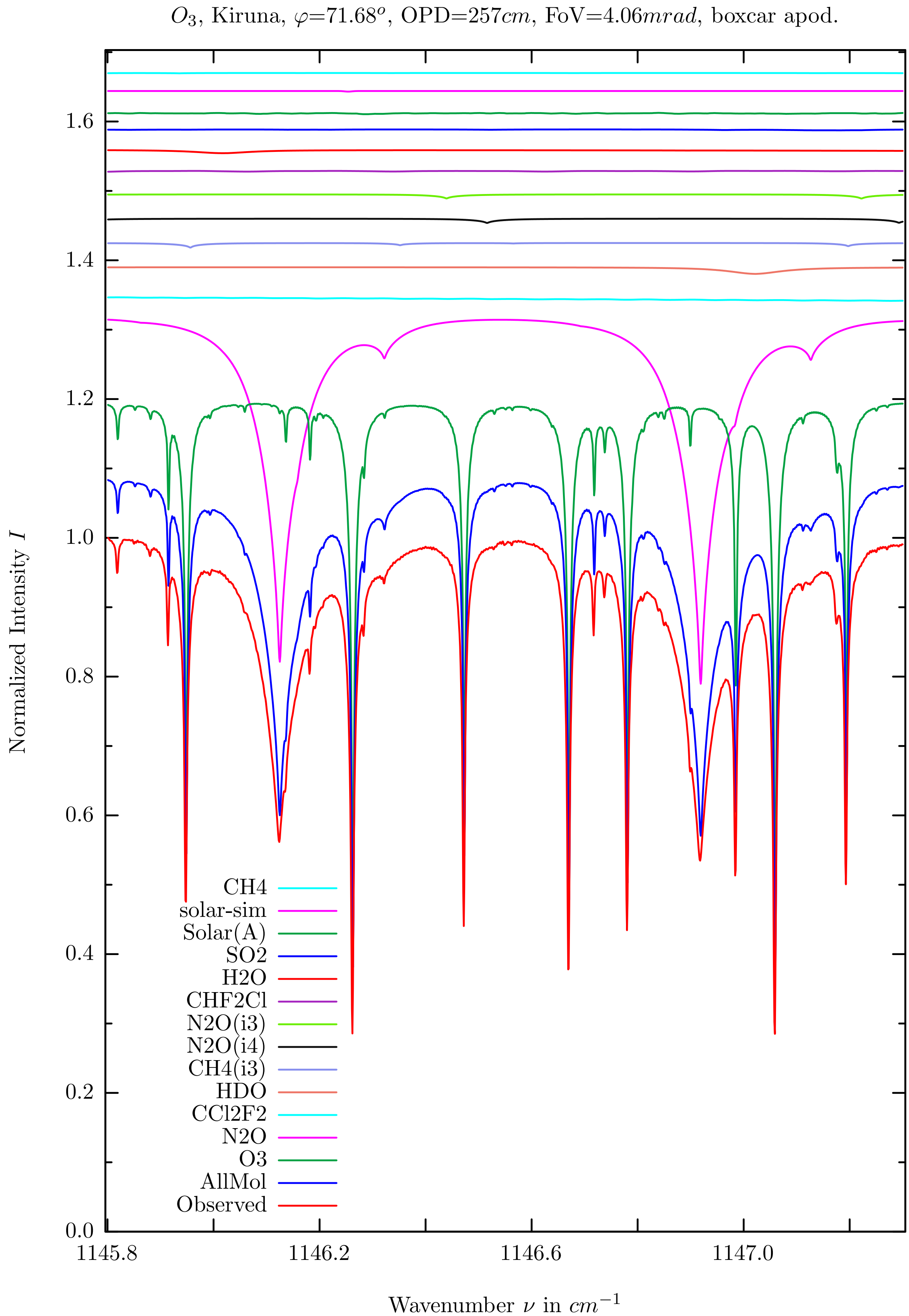
O_3, Kiruna, φ=71.68^o, OPD=257cm, FoV=4.06$mrad$, boxcar apod.
Normalized Intensity I
Wavenumber ν in cm^{-1}
0.0
0.2
0.4
0.6
0.8
1.0
1.2
1.4
1.6
1145.8
1146.2
1146.6
1147.0
CH4
solar-sim
Solar(A)
SO2
H2O
CHF2Cl
N2O(i3)
N2O(i4)
CH4(i3)
HDO
CCl2F2
N2O
O3
AllMol
Observed

σ=0.119%, 970315S6.92, φ=71.68^o, OPD=257cm, FoV=4.07$mrad$, Apod.=boxcar

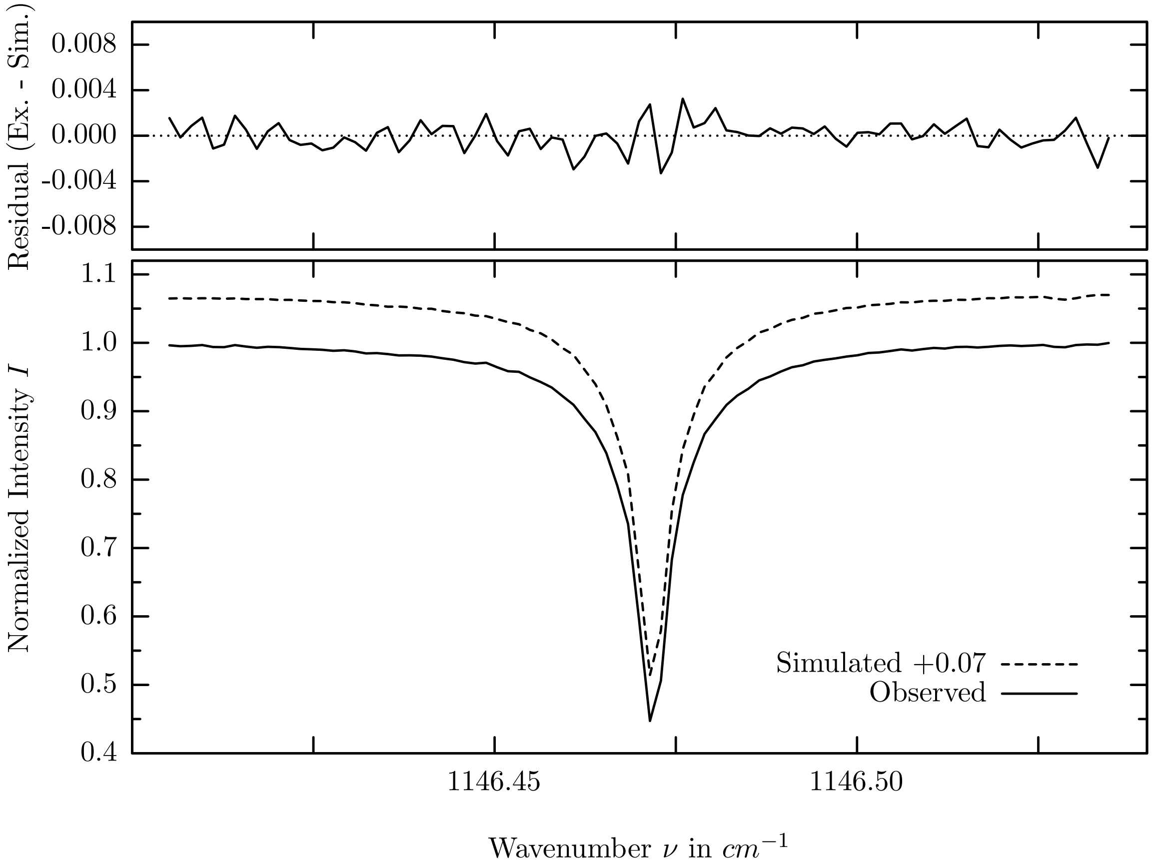

investigated species	:	O_3
line position(s) ν_0	:	1146.4714 cm^{-1}
lower state energy E''_{lst}	:	372.4 cm^{-1}
retrieved TCA, information content	:	1.01E+19 $molec/cm^2$, 467.8
temperature dependence of the TCA	:	-0.148%/K (trop), -0.386%/K (strat)
location, date, solar zenith angle	:	Kiruna, 15/Mar/97, 71.68^o
spectral interval fitted	:	1146.405 – 1146.535 cm^{-1}

Molecule	iCode	Absorption	Molecule	iCode	Absorption
O3	31	77.622%	$F142B$	611	0.038%
$N2O$	41	54.549%	$HCOOH$	461	0.011%
$CCl2F2$	321	2.144%	$HNO3$	121	0.002%
HDO	491	0.965%	$NH3$	111	0.001%
$CH4$	6**3**	0.671%	$C2H4$	391	0.001%
$N2O$	4**4**	0.625%	$NO2$	101	<0.001%
$N2O$	4**3**	0.601%	OH	131	<0.001%
$CHF2Cl$	421	0.232%	ClO	181	<0.001%
$H2O$	11	0.225%	$HO2$	221	<0.001%
$SO2$	91	0.173%	$H2O2$	231	<0.001%
Solar(A)	—	0.142%	$N2O5$	261	<0.001%
Solar-sim	—	0.085%	$H2S$	471	<0.001%
$CH4$	61	0.051%			

SO_2, Kiruna, φ=71.68^o, OPD=257cm, FoV=4.06$mrad$, boxcar apod.

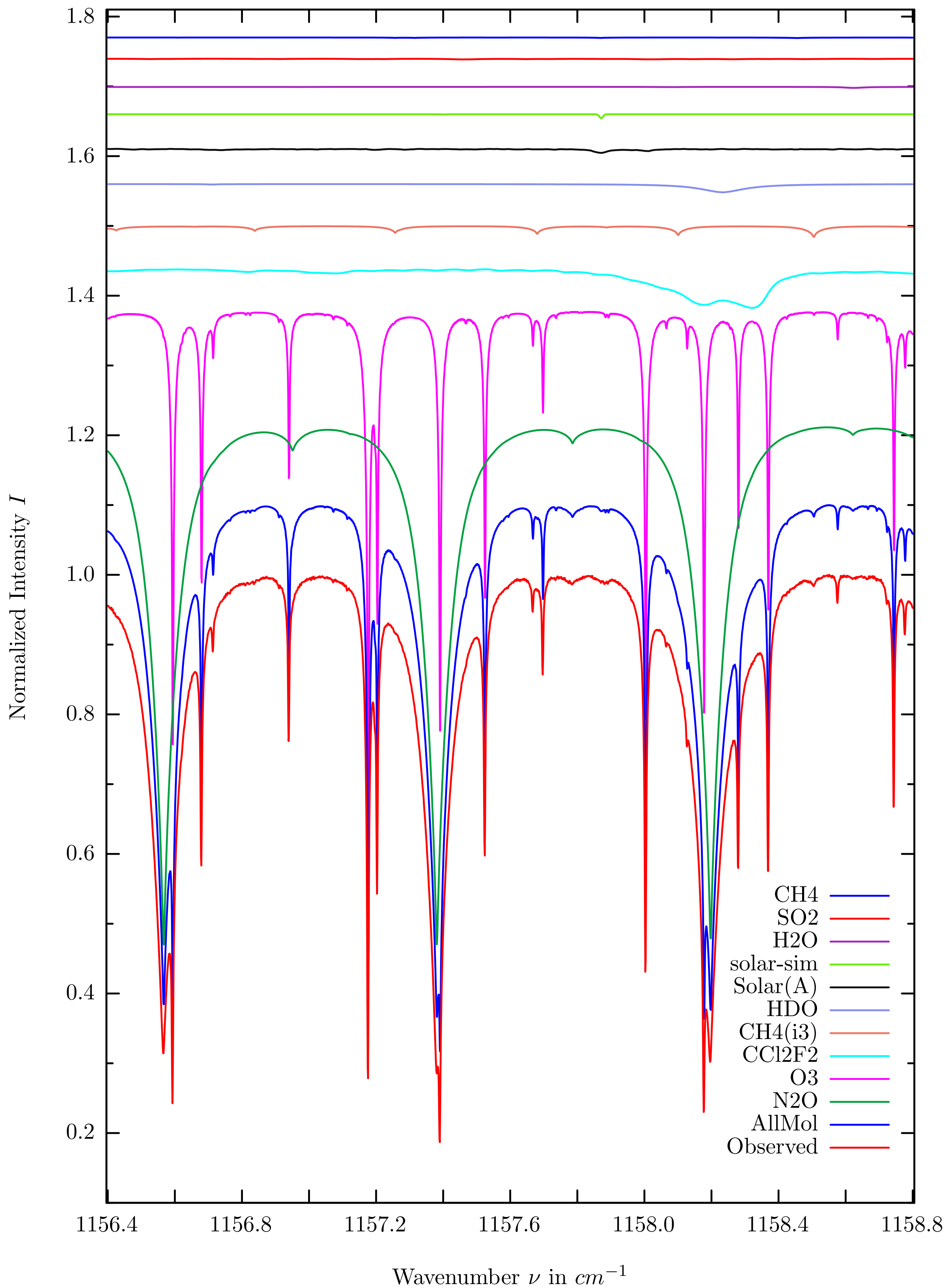

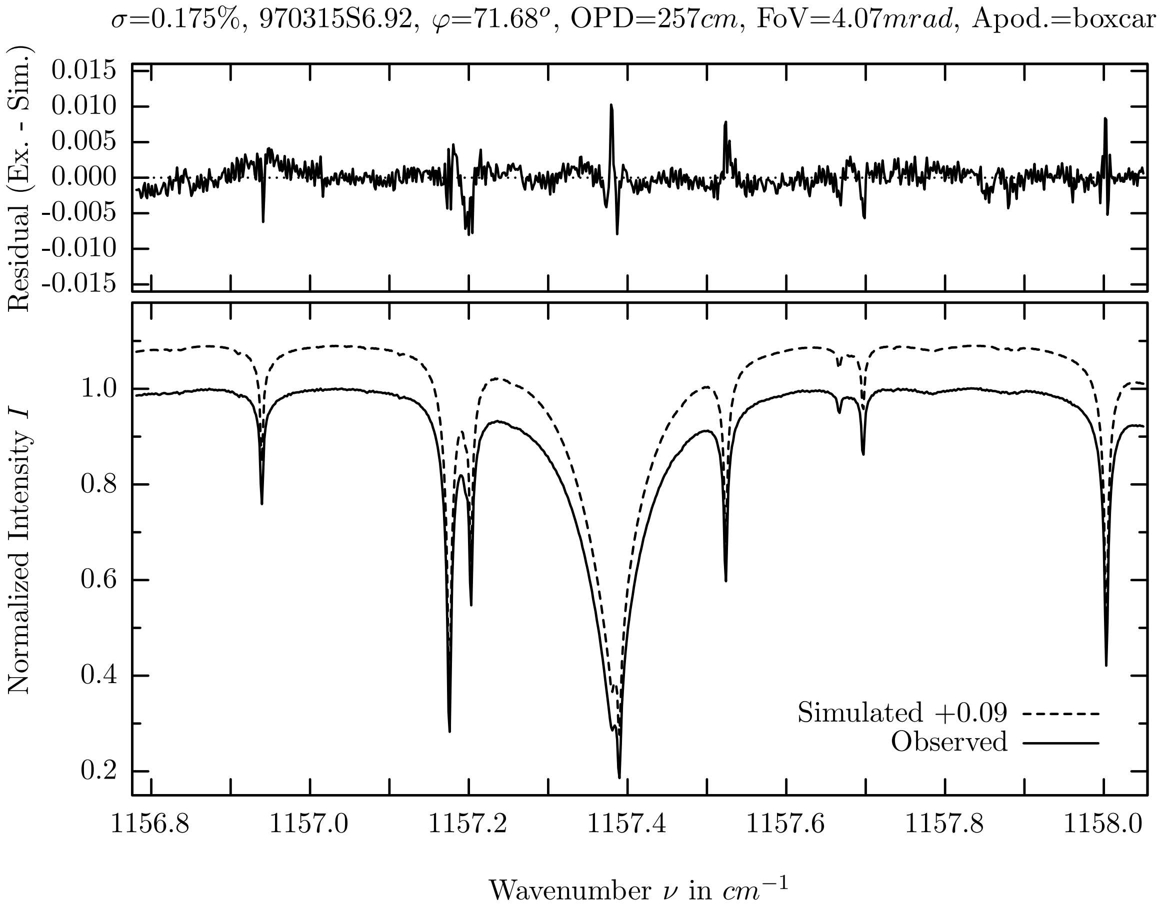

investigated species	:	SO_2
line position(s) ν_0	:	1156.9140$^{*)}$, 1157.8785$^{*)}$ cm^{-1}
lower state energy E''_{lst}	:	13.0 to 404.0 cm^{-1}
retrieved TCA, information content	:	1.06E+16 $molec/cm^2$, 6.4, 2.5
temperature dependence of the TCA	:	+5.552%/K (trop), +2.979%/K (strat)
location, date, solar zenith angle	:	Kiruna, 15/Mar/97, 71.68^o
spectral interval fitted	:	1156.780 – 1158.050 cm^{-1}

Molecule	iCode	Absorption	Molecule	iCode	Absorption
$O3$	31	79.185%	$HCOOH$	461	0.007%
$N2O$	41	77.579%	$F142B$	611	0.002%
$CCl2F2$	321	8.252%	$HNO3$	121	0.001%
$CH4$	6**3**	1.603%	$C2H4$	391	0.001%
HDO	491	1.204%	$H2S$	471	0.001%
Solar(A)	—	0.540%	$NO2$	101	<0.001%
Solar-sim	—	0.562%	OH	131	<0.001%
$H2O$	11	0.223%	ClO	181	<0.001%
SO2	91	0.142%	$H2O2$	231	<0.001%
$CH4$	61	0.080%	$N2O5$	261	<0.001%
$NH3$	111	0.033%	$CHF2Cl$	421	<0.001%

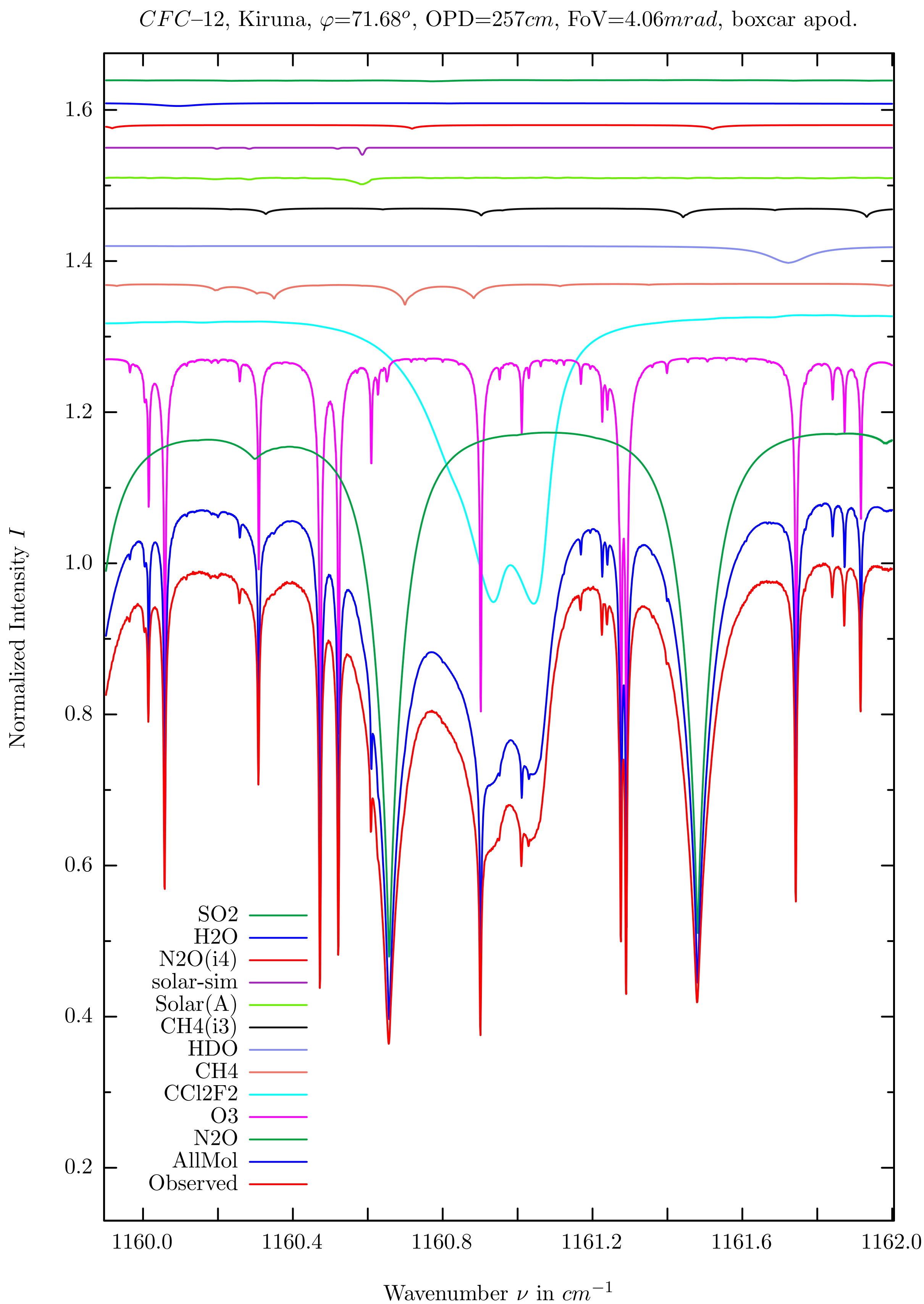
CFC–12, Kiruna, φ=71.68^o, OPD=257cm, FoV=4.06$mrad$, boxcar apod.
Normalized Intensity I
1.6
1.4
1.2
1.0
0.8
0.6
0.4
0.2
SO2
H2O
N2O(i4)
solar-sim
Solar(A)
CH4(i3)
HDO
CH4
CCl2F2
O3
N2O
AllMol
Observed
1160.0
1160.4
1160.8
1161.2
1161.6
1162.0
Wavenumber ν in cm^{-1}

σ=0.250%, 970315S6.92, φ=71.68^o, OPD=257cm, FoV=4.07$mrad$, Apod.=boxcar

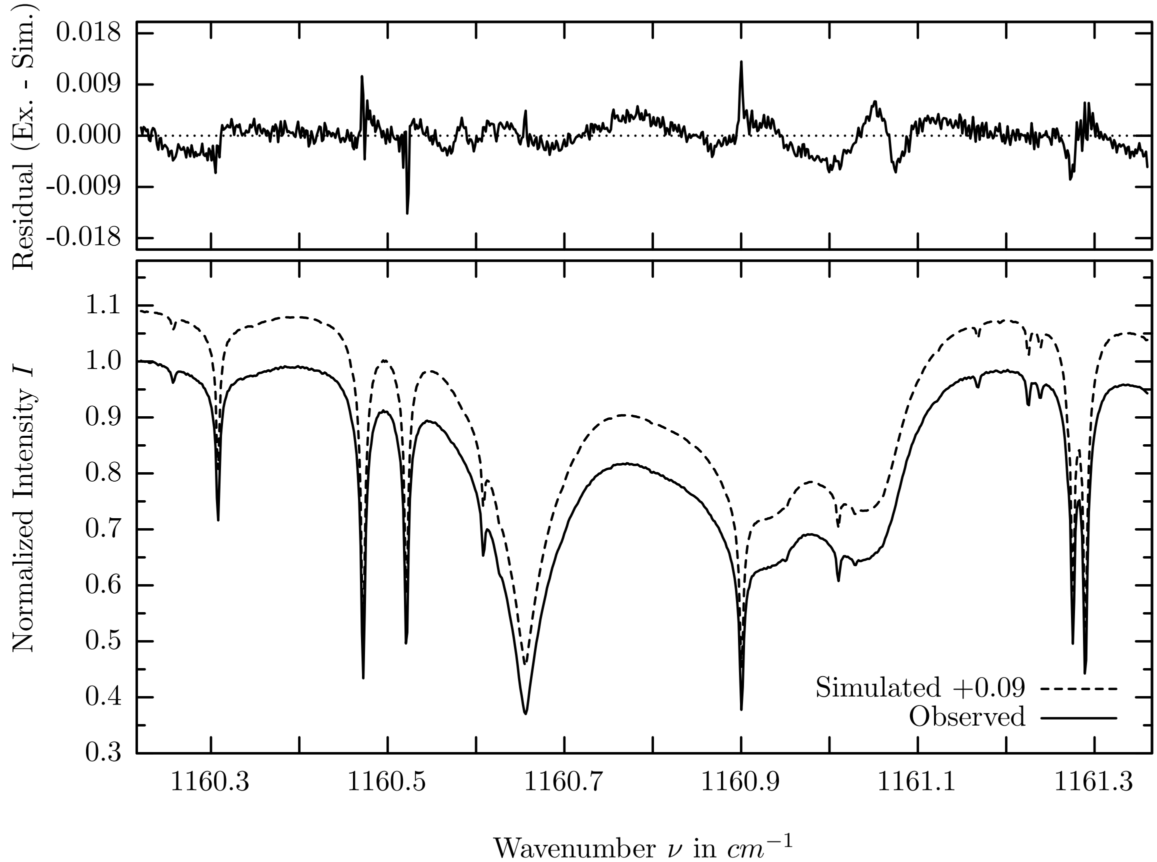

investigated species	:	CCl_2F_2(Freon12), (O_3)
line position(s) ν_0	:	1161.0400$^{*)}$, (1161.2893) cm^{-1}
lower state energy E''_{lst}	:	178.0, (289.1) cm^{-1}
retrieved TCA, information content	:	9.54E+15, (1.00E+19) $molec/cm^2$, 142.3, (218.8)
temperature dependence of the TCA	:	+.096, (-.221)%/K (trop), +.008, (-.313)%/K (strat)
location, date, solar zenith angle	:	Kiruna, 15/Mar/97, 71.68^o
spectral interval fitted	:	1160.220 – 1161.360 cm^{-1}

Molecule	iCode	Absorption	Molecule	iCode	Absorption
$N2O$	41	72.056%	$HCOOH$	461	0.007%
$O3$	31	63.694%	$NH3$	111	0.003%
CCL2F2	321	39.856%	$F142B$	611	0.002%
$CH4$	61	2.812%	$H2S$	471	0.001%
HDO	491	2.244%	$NO2$	101	<0.001%
$CH4$	6**3**	1.216%	$HNO3$	121	<0.001%
Solar(A)	—	0.828%	OH	131	<0.001%
Solar-sim	—	0.942%	ClO	181	<0.001%
$N2O$	4**4**	0.544%	$H2O2$	231	<0.001%
$H2O$	11	0.476%	$C2H4$	391	<0.001%
$SO2$	91	0.212%			

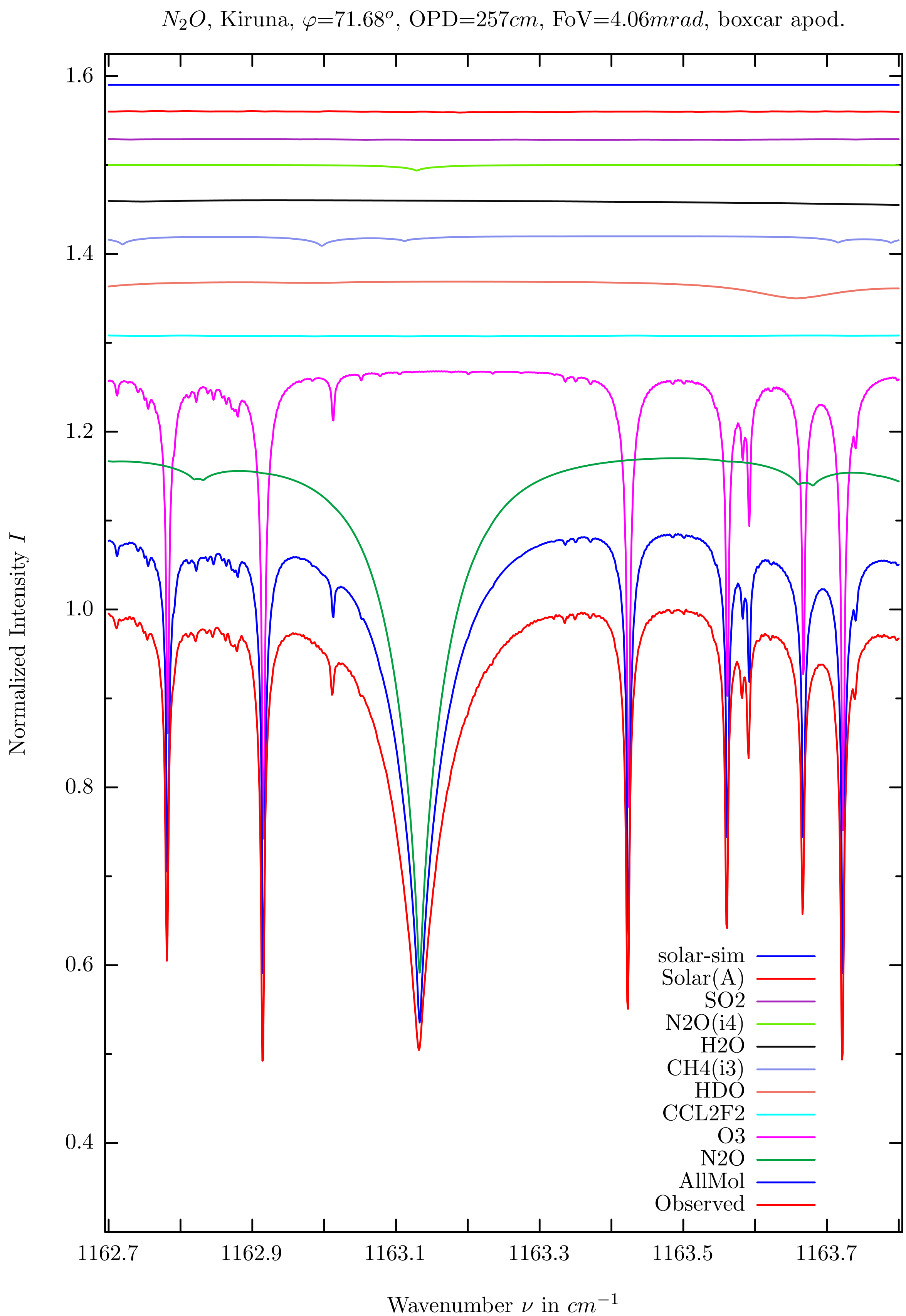

N_2O, Kiruna, φ=71.68^o, OPD=257cm, FoV=4.06$mrad$, boxcar apod.
Normalized Intensity I
Wavenumber ν in cm^{-1}
1.6
1.4
1.2
1.0
0.8
0.6
0.4
1162.7
1162.9
1163.1
1163.3
1163.5
1163.7
solar-sim
Solar(A)
SO2
N2O(i4)
H2O
CH4(i3)
HDO
CCL2F2
O3
N2O
AllMol
Observed

σ=0.122%, 970315S6.92, φ=71.68^o, OPD=257cm, FoV=4.07$mrad$, Apod.=boxcar

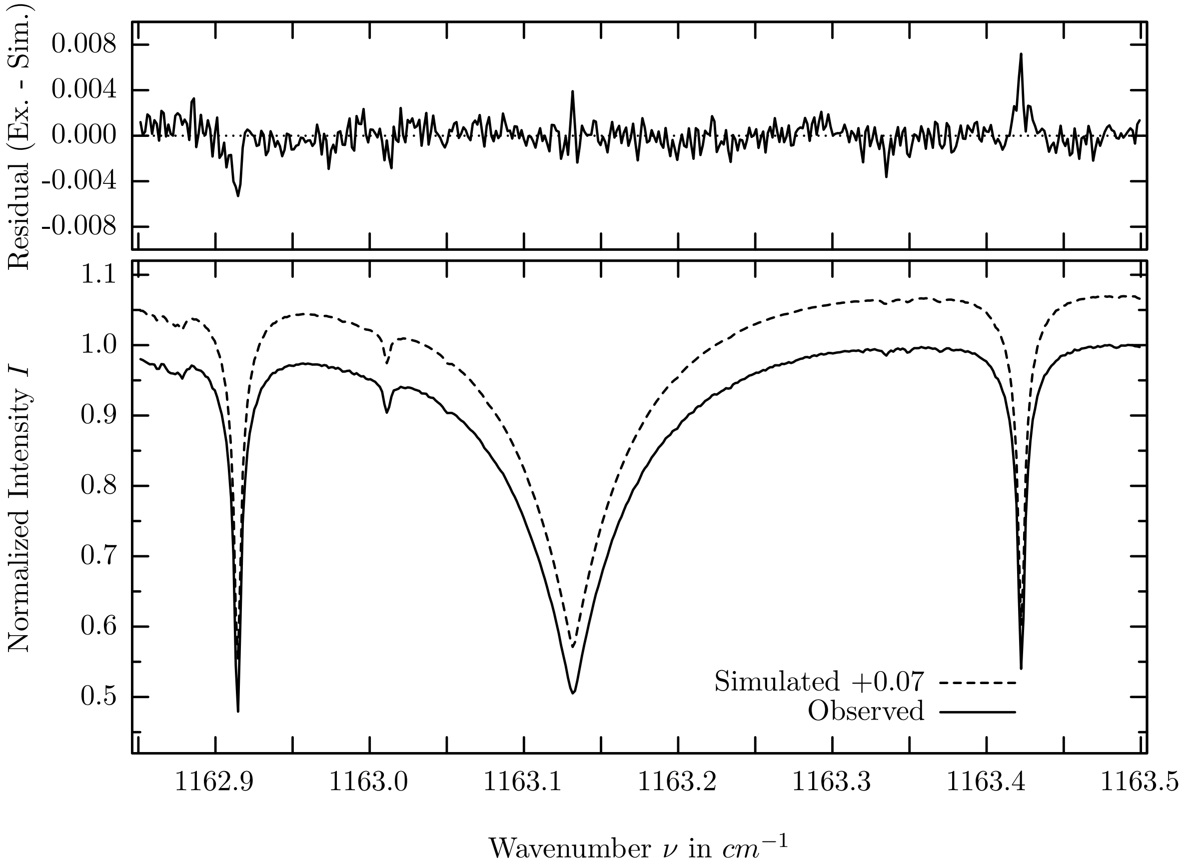

investigated species	:	$N_2O, (O_3)$
line position(s) ν_0	:	1163.1315, (1163.4222) cm^{-1}
lower state energy E''_{lst}	:	17.6, (253.9) cm^{-1}
retrieved TCA, information content	:	5.60E+18, (1.01E+19) $molec/cm^2$, 407.6, (381.7)
temperature dependence of the TCA	:	+.483, (-.114)%/K (trop), +.112, (-.109)%/K (strat)
location, date, solar zenith angle	:	Kiruna, 15/Mar/97, 71.68^o
spectral interval fitted	:	1162.850 – 1163.500 cm^{-1}

Molecule	iCode	Absorption	Molecule	iCode	Absorption
N2O	41	60.307%	$HCOOH$	461	0.005%
$O3$	31	59.257%	$HNO3$	121	0.002%
$CCl2F2$	321	2.279%	$F142B$	611	0.002%
HDO	491	2.014%	$NO2$	101	<0.001%
$CH4$	6**3**	1.096%	$NH3$	111	<0.001%
$H2O$	11	0.871%	OH	131	<0.001%
$N2O$	4**4**	0.640%	ClO	181	<0.001%
$SO2$	91	0.209%	$H2O2$	231	<0.001%
Solar(A)	—	0.110%	$C2H4$	391	<0.001%
Solar-sim	—	<0.001%	$H2S$	471	<0.001%
$CH4$	61	0.018%			

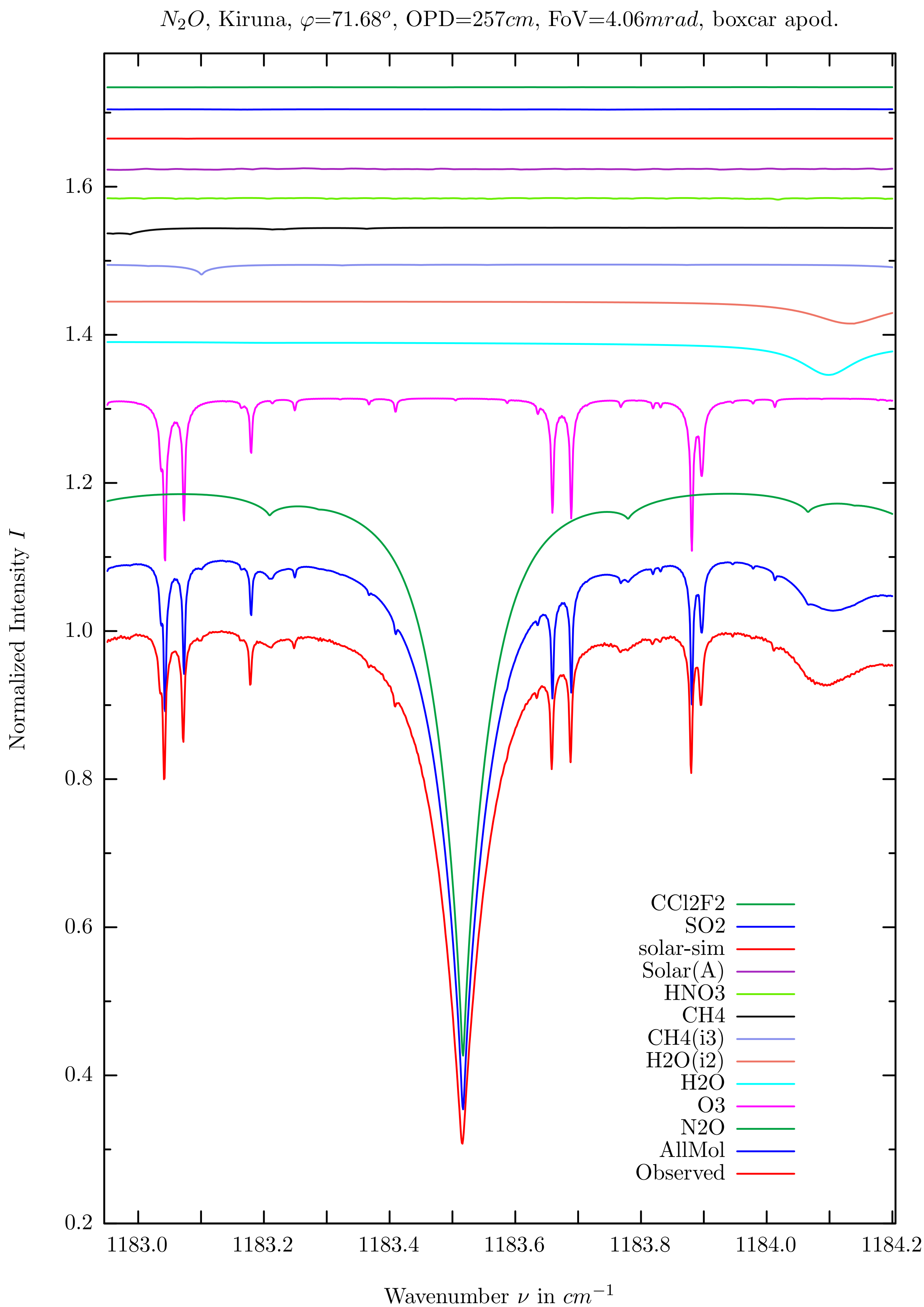

N_2O, Kiruna, φ=71.68^o, OPD=257cm, FoV=4.06$mrad$, boxcar apod.
Normalized Intensity I
Wavenumber ν in cm^{-1}
1.6
1.4
1.2
1.0
0.8
0.6
0.4
0.2
1183.0
1183.2
1183.4
1183.6
1183.8
1184.0
1184.2
CCl2F2
SO2
solar-sim
Solar(A)
HNO3
CH4
CH4(i3)
H2O(i2)
H2O
O3
N2O
AllMol
Observed

σ=0.102%, 970315S6.92, φ=71.68^o, OPD=257cm, FoV=4.07$mrad$, Apod.=boxcar

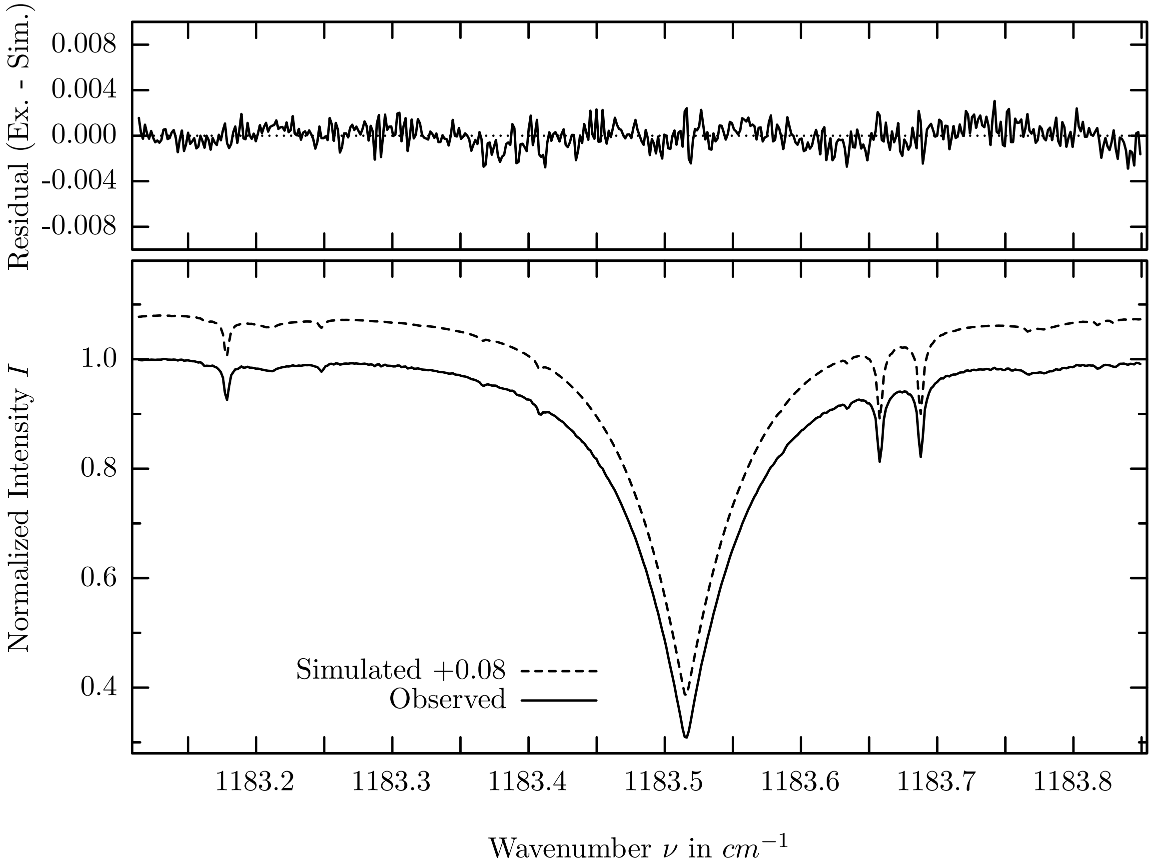

investigated species	:	N_2O
line position(s) ν_0	:	1183.5154 cm^{-1}
lower state energy E''_{lst}	:	128.2 cm^{-1}
retrieved TCA, information content	:	5.59E+18 $molec/cm^2$, 682.1
temperature dependence of the TCA	:	+0.118%/K (trop), -0.006%/K (strat)
location, date, solar zenith angle	:	Kiruna, 15/Mar/97, 71.68^o
spectral interval fitted	:	1183.113 – 1183.850 cm^{-1}

Molecule	iCode	Absorption	Molecule	iCode	Absorption
N2O	41	78.810%	$F142B$	611	0.035%
$O3$	31	25.283%	HDO	491	0.015%
$H2O$	11	4.912%	$HCOOH$	461	0.002%
$H2O$	1**2**	2.987%	$NH3$	111	0.001%
$CH4$	6**3**	1.381%	$H2O2$	231	0.001%
$CH4$	61	0.916%	$NO2$	101	<0.001%
$HNO3$	121	0.252%	OH	131	<0.001%
Solar(A)	—	0.230%	ClO	181	<0.001%
Solar-sim	—	0.016%	$HOCL$	211	<0.001%
$SO2$	91	0.090%	$COF2$	361	<0.001%
$CCl2F2$	321	0.081%	$H2S$	471	<0.001%

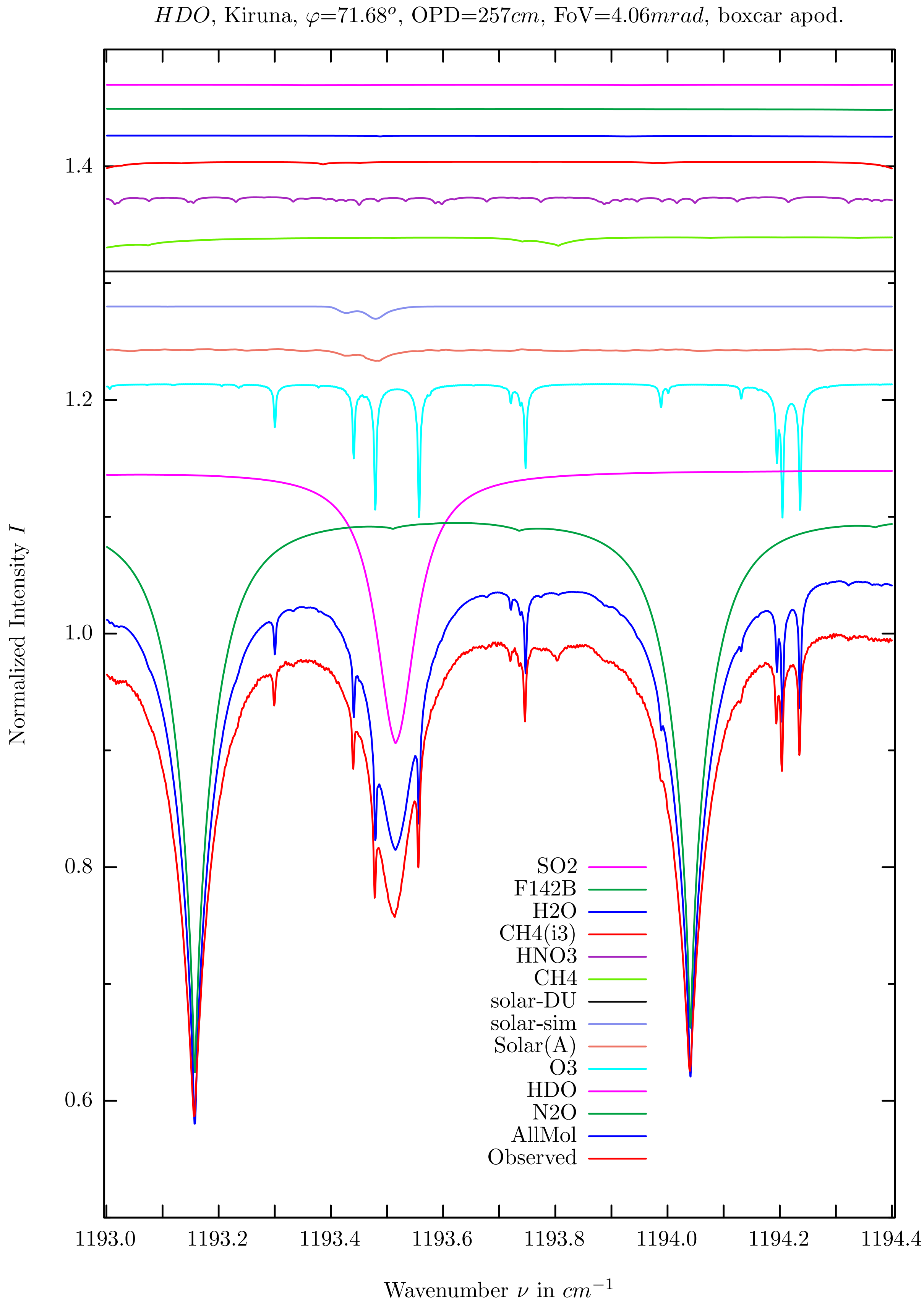

HDO, Kiruna, φ=71.68^o, OPD=257cm, FoV=4.06$mrad$, boxcar apod.
Normalized Intensity I
1.4
1.2
1.0
0.8
0.6
1193.0
1193.2
1193.4
1193.6
1193.8
1194.0
1194.2
1194.4
Wavenumber ν in cm^{-1}
SO2
F142B
H2O
CH4(i3)
HNO3
CH4
solar-DU
solar-sim
Solar(A)
O3
HDO
N2O
AllMol
Observed

σ=0.099%, 970315S6.92, φ=71.68^o, OPD=257cm, FoV=4.07$mrad$, Apod.=boxcar

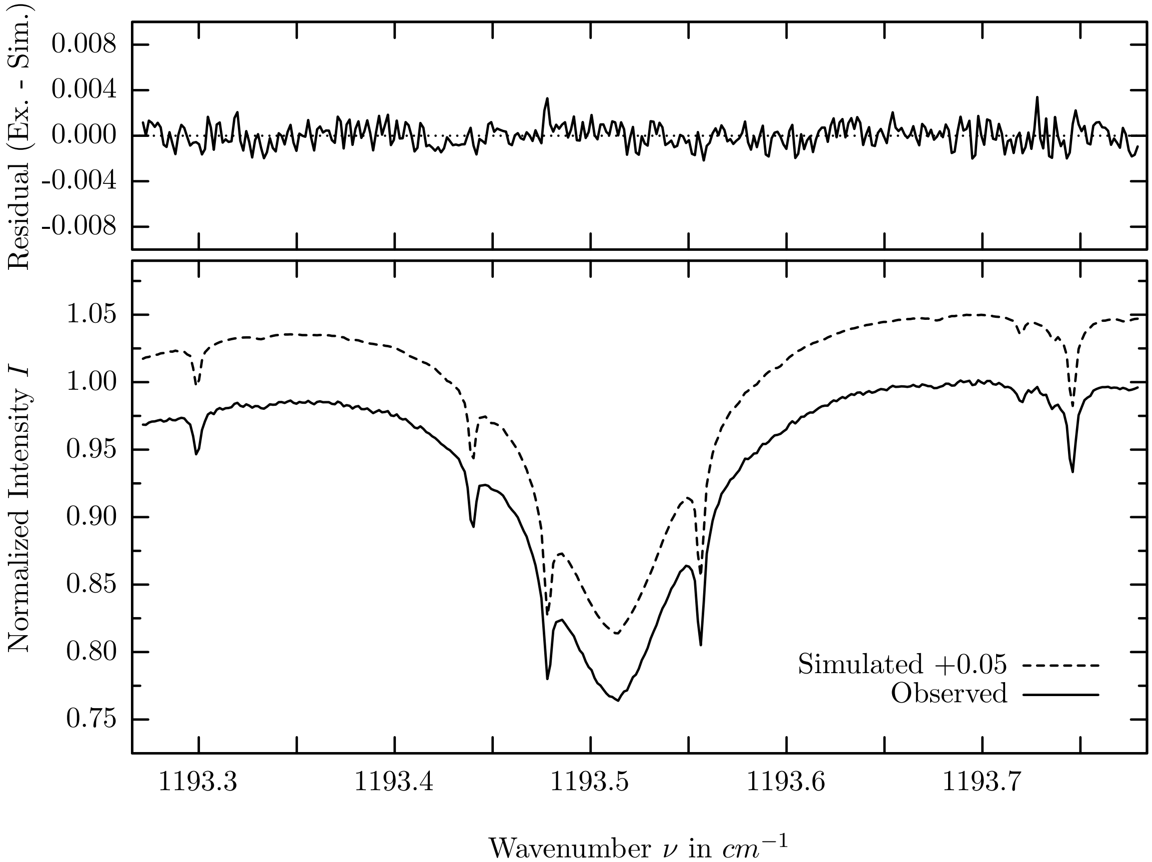

investigated species	:	HDO
line position(s) ν_0	:	1193.5135 cm^{-1}
lower state energy E''_{lst}	:	872.8 cm^{-1}
retrieved TCA, information content	:	4.28E+21 $molec/cm^2$, 237.9
temperature dependence of the TCA	:	-1.615%/K (trop), +0.004%/K (strat)
location, date, solar zenith angle	:	Kiruna, 15/Mar/97, 71.68^o
spectral interval fitted	:	1193.270 – 1193.780 cm^{-1}

Molecule	iCode	Absorption	Molecule	iCode	Absorption
$N2O$	41	48.729%	$CCl2F2$	321	0.039%
HDO	491	29.256%	$H2O2$	231	0.003%
$O3$	31	13.192%	$COF2$	361	0.002%
Solar(A)	—	1.053%	$NO2$	101	0.001%
Solar-sim	—	1.054%	$NH3$	111	0.001%
$CH4$	61	0.915%	$HOCL$	211	0.001%
$HNO3$	121	0.731%	$HCOOH$	461	0.001%
$CH4$	6**3**	0.633%	OH	131	<0.001%
$H2O$	11	0.452%	ClO	181	<0.001%
$F142B$	611	0.167%	$N2O5$	261	<0.001%
$SO2$	91	0.052%	$H2S$	471	<0.001%

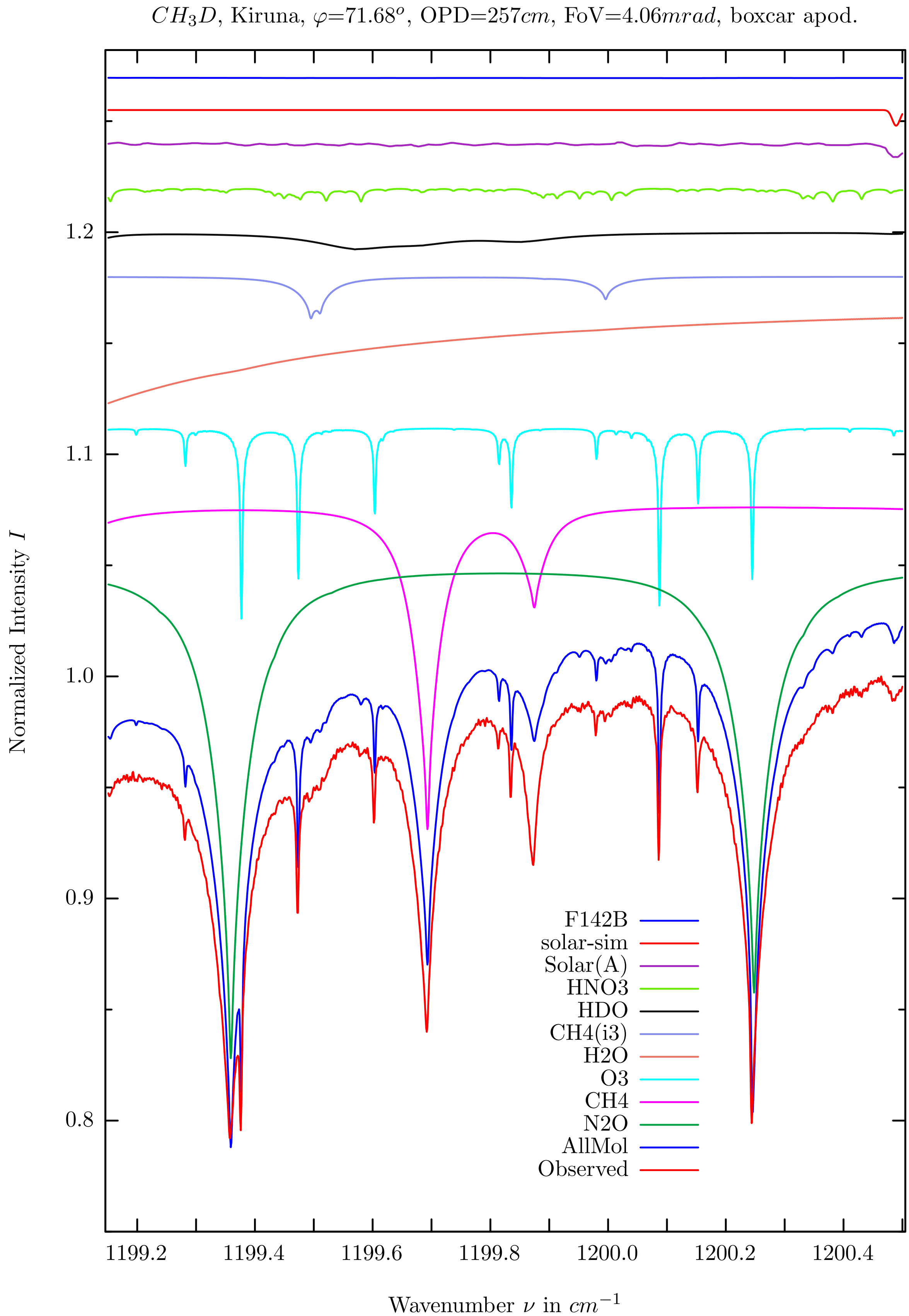
CH_3D, Kiruna, φ=71.68^o, OPD=257cm, FoV=4.06$mrad$, boxcar apod.
Normalized Intensity I
1.2
1.1
1.0
0.9
0.8
1199.2
1199.4
1199.6
1199.8
1200.0
1200.2
1200.4
Wavenumber ν in cm^{-1}
F142B
solar-sim
Solar(A)
HNO3
HDO
CH4(i3)
H2O
O3
CH4
N2O
AllMol
Observed

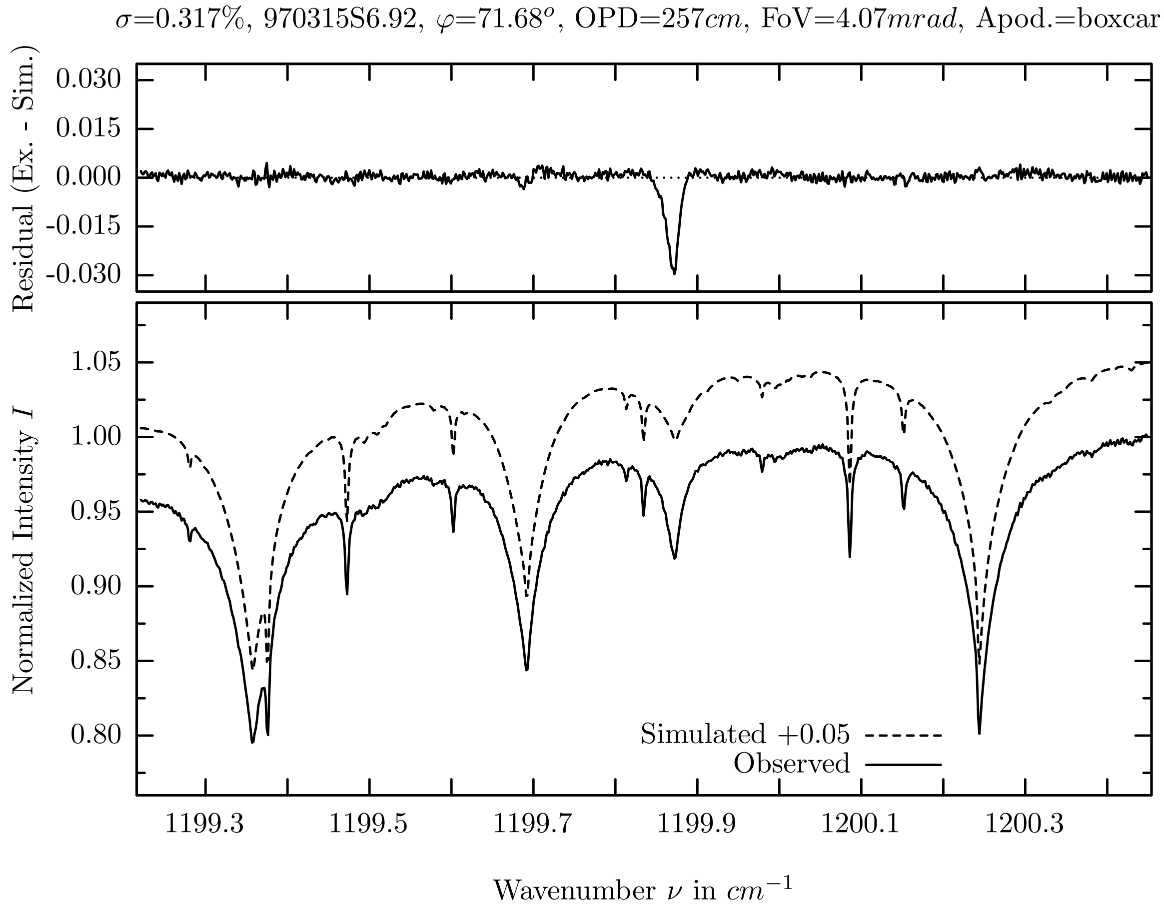

investigated species	:	$CH_3D(=CH_4(i3))$
line position(s) ν_0	:	1199.4936, 1199.9945 cm^{-1}
lower state energy E''_{lst}	:	116.4, 251.3 cm^{-1}
retrieved TCA, information content	:	4.01E+19 $molec/cm^2$, 4.3, 4.6
temperature dependence of the TCA	:	-0.107%/K (trop), -0.101%/K (strat)
location, date, solar zenith angle	:	Kiruna, 15/Mar/97, 71.68^o
spectral interval fitted	:	1199.220 – 1200.450 cm^{-1}

Molecule	iCode	Absorption	Molecule	iCode	Absorption
$N2O$	41	22.481%	$SO2$	91	0.038%
$CH4$	61	14.842%	$COF2$	361	0.007%
$O3$	31	9.964%	$H2O2$	231	0.006%
$H2O$	11	4.690%	$HOCL$	211	0.004%
CH3D	6**3**	1.909%	$NO2$	101	0.001%
HDO	491	0.773%	$NH3$	111	0.001%
$HNO3$	121	0.646%	$HCOOH$	461	0.001%
Solar(A)	—	0.617%	$H2S$	471	0.001%
Solar-sim	—	0.710%	OH	131	<0.001%
$F142B$	611	0.062%	ClO	181	<0.001%
$CCl2F2$	321	0.041%	$N2O5$	261	<0.001%

The spectroscopic line data of CH_4 at 1199.874cm^{-1} is inconsistent with observations.

CH_4, Kiruna, φ=71.68^o, OPD=257cm, FoV=4.06$mrad$, boxcar apod.

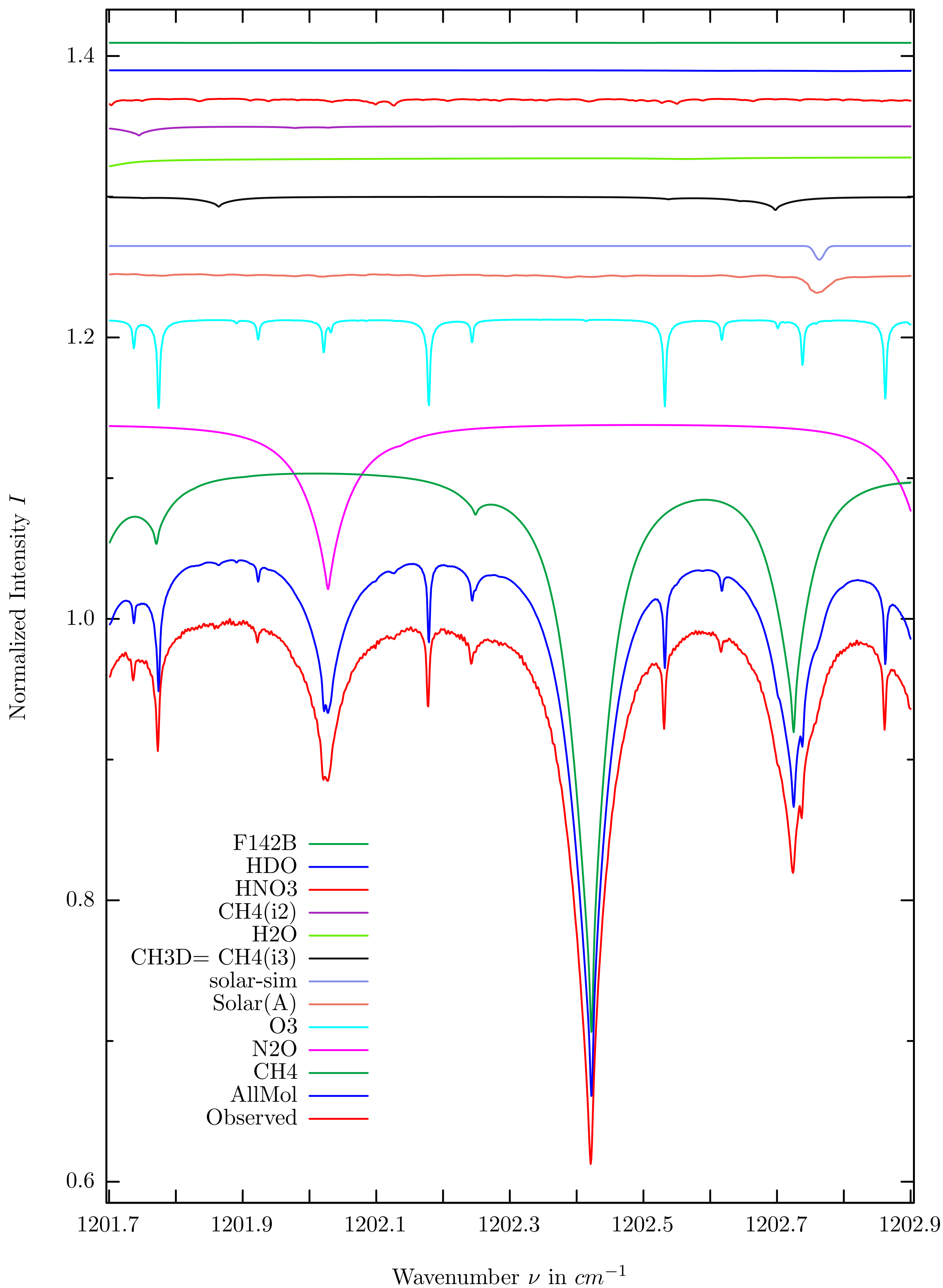

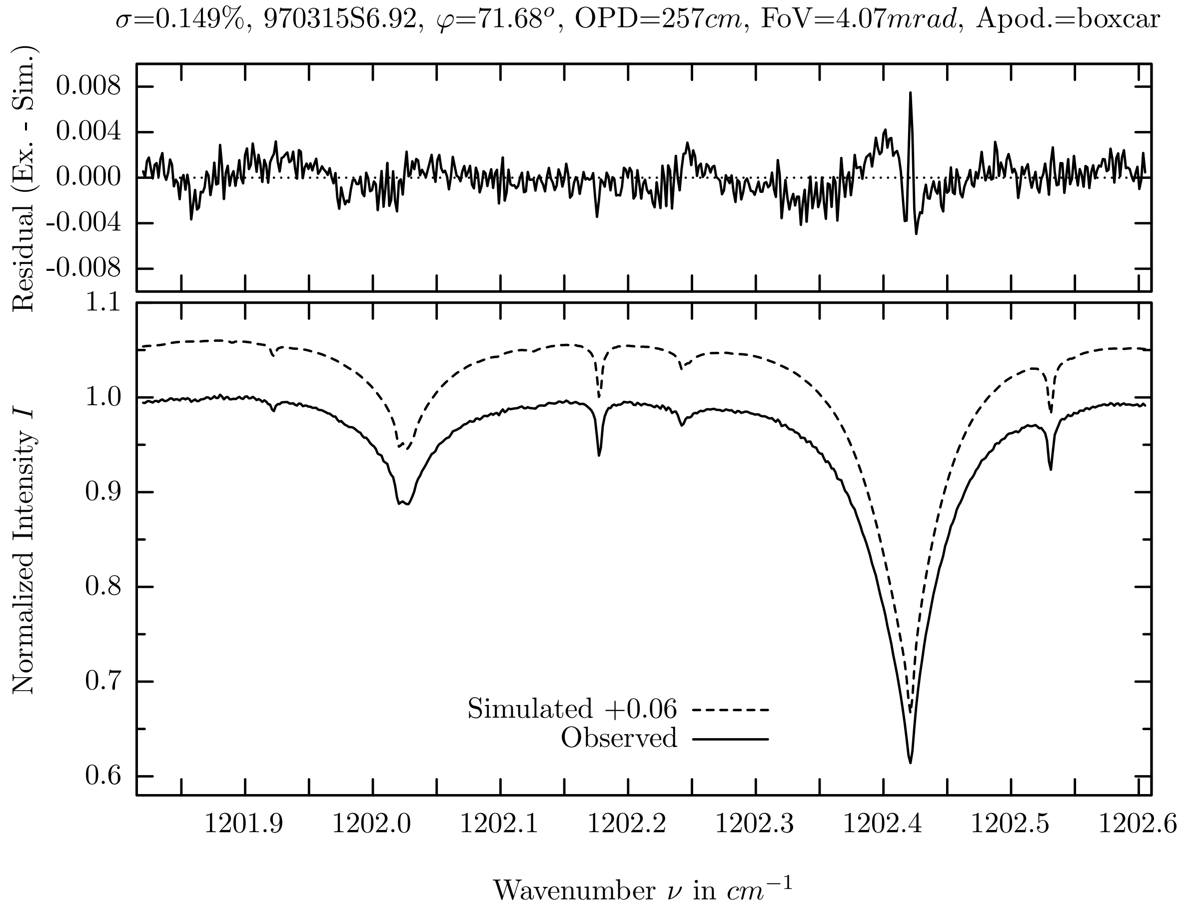

investigated species	:	$CH_4, (N_2O)$
line position(s) ν_0	:	1202.4210, (1202.0263) cm^{-1}
lower state energy E''_{lst}	:	1096.1, (620.6) cm^{-1}
retrieved TCA, information content	:	3.35E+19, (5.52E+18) $molec/cm^2$, 264.7, (77.3)
temperature dependence of the TCA	:	-2.228, (-1.42)%/K (trop), -.314, (-.145)%/K (strat)
location, date, solar zenith angle	:	Kiruna, 15/Mar/97, 71.68^o
spectral interval fitted	:	1201.820 – 1202.605 cm^{-1}

Molecule	iCode	Absorption	Molecule	iCode	Absorption
CH4	61	40.821%	*H2O2*	231	0.011%
N2O	41	11.979%	*COF2*	361	0.008%
O3	31	7.255%	*HOCL*	211	0.006%
Solar(A)	—	1.332%	*NO2*	101	0.001%
Solar-sim	—	0.983%	*N2O5*	261	0.001%
CH3D	531	0.961%	*H2S*	471	0.001%
H2O	11	0.821%	*CO2*	2**3**	<0.001%
CH4	6**2**	0.654%	*NH3*	111	<0.001%
HNO3	121	0.534%	*OH*	131	<0.001%
HDO	491	0.070%	*ClO*	181	<0.001%
F142B	611	0.070%	*CCl2F2*	321	<0.001%
SO2	91	0.030%	*HCOOH*	461	<0.001%

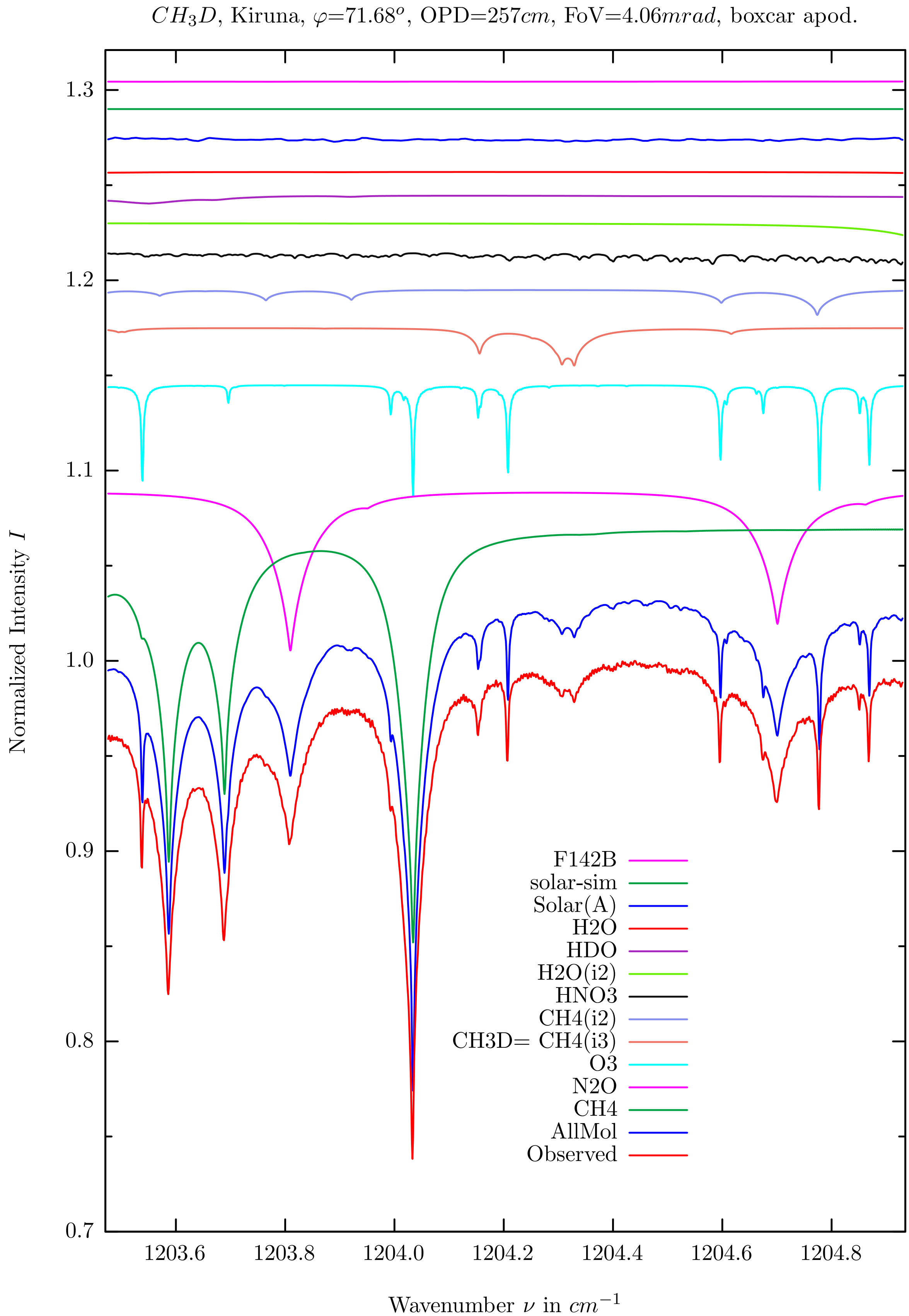

CH_3D, Kiruna, φ=71.68^o, OPD=257cm, FoV=4.06$mrad$, boxcar apod.
Normalized Intensity I
Wavenumber ν in cm^{-1}
1.3
1.2
1.1
1.0
0.9
0.8
0.7
1203.6
1203.8
1204.0
1204.2
1204.4
1204.6
1204.8
F142B
solar-sim
Solar(A)
H2O
HDO
H2O(i2)
HNO3
CH4(i2)
CH3D= CH4(i3)
O3
N2O
CH4
AllMol
Observed

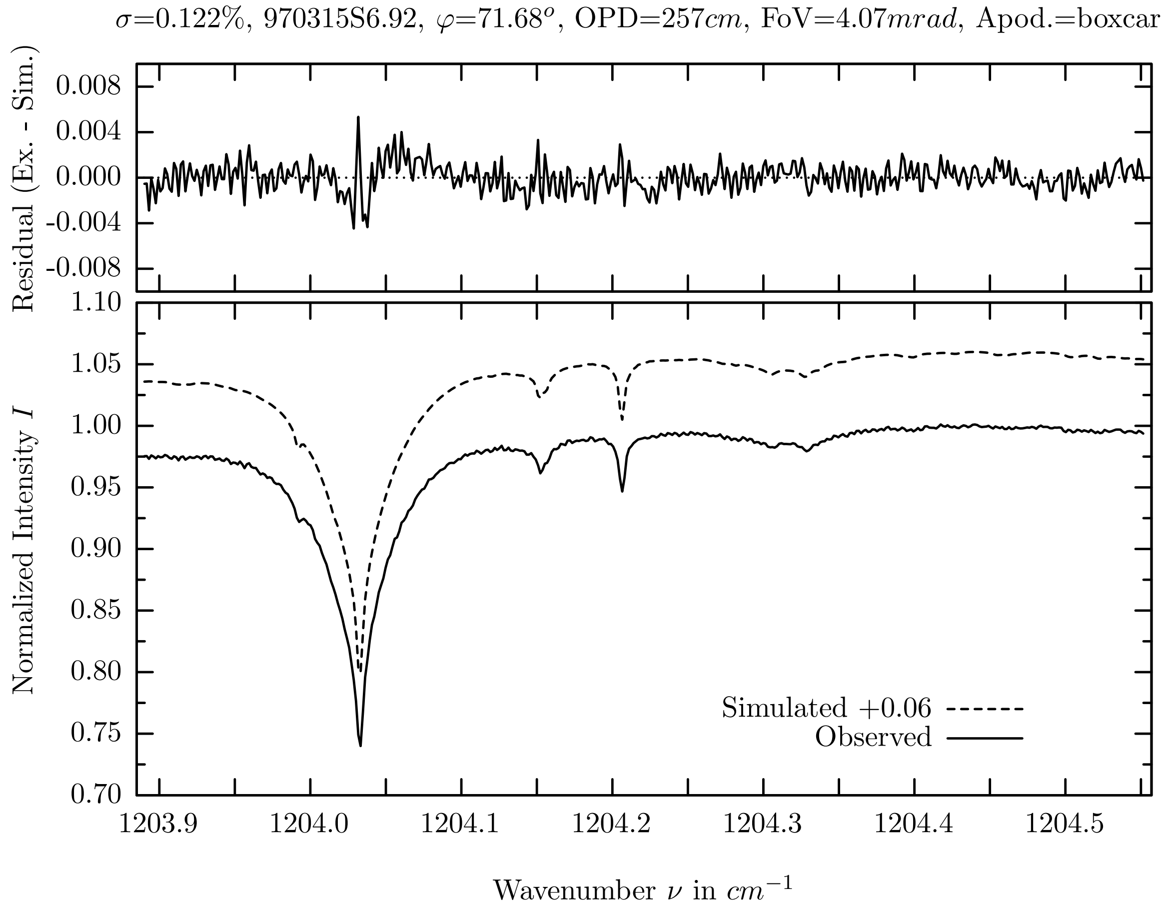

investigated species	:	$CH3D(=CH_4(i3)),(CH_4)$
line position(s) ν_0	:	1204.3278, (1204.0328) cm^{-1}
lower state energy E''_{lst}	:	328.2, (1251.6) cm^{-1}
retrieved TCA, information content	:	3.45E+19, (3.41E+19) $molec/cm^2$, 16.5, (212.8)
temperature dependence of the TCA	:	-.623, (-2.55)%/K (trop), -.462, (-.268)%/K (strat)
spectral interval fitted	:	1203.890 – 1204.553 cm^{-1}

Molecule	iCode	Absorption	Molecule	iCode	Absorption
$CH4$	61	22.066%	$COF2$	361	0.010%
$N2O$	41	8.536%	$HOCL$	211	0.009%
$O3$	31	6.689%	$H2O2$	231	0.009%
CH3D	6**3**	2.007%	$NO2$	101	0.001%
$CH4$	6**2**	1.344%	$NH3$	111	0.001%
$HNO3$	121	0.685%	$N2O5$	261	0.001%
$H2O$	1**2**	0.637%	$H2S$	471	0.001%
HDO	491	0.458%	$CO2$	2**3**	<0.001%
$H2O$	11	0.361%	OH	131	<0.001%
Solar(A)	—	0.220%	ClO	181	<0.001%
Solar-sim	—	<0.001%	$CCl2F2$	321	<0.001%
$F142B$	611	0.064%	$HCOOH$	461	<0.001%
$SO2$	91	0.029%			

$H_2\ ^{18}O$, Kiruna, φ=71.68^o, OPD=257cm, FoV=4.06$mrad$, boxcar apod.

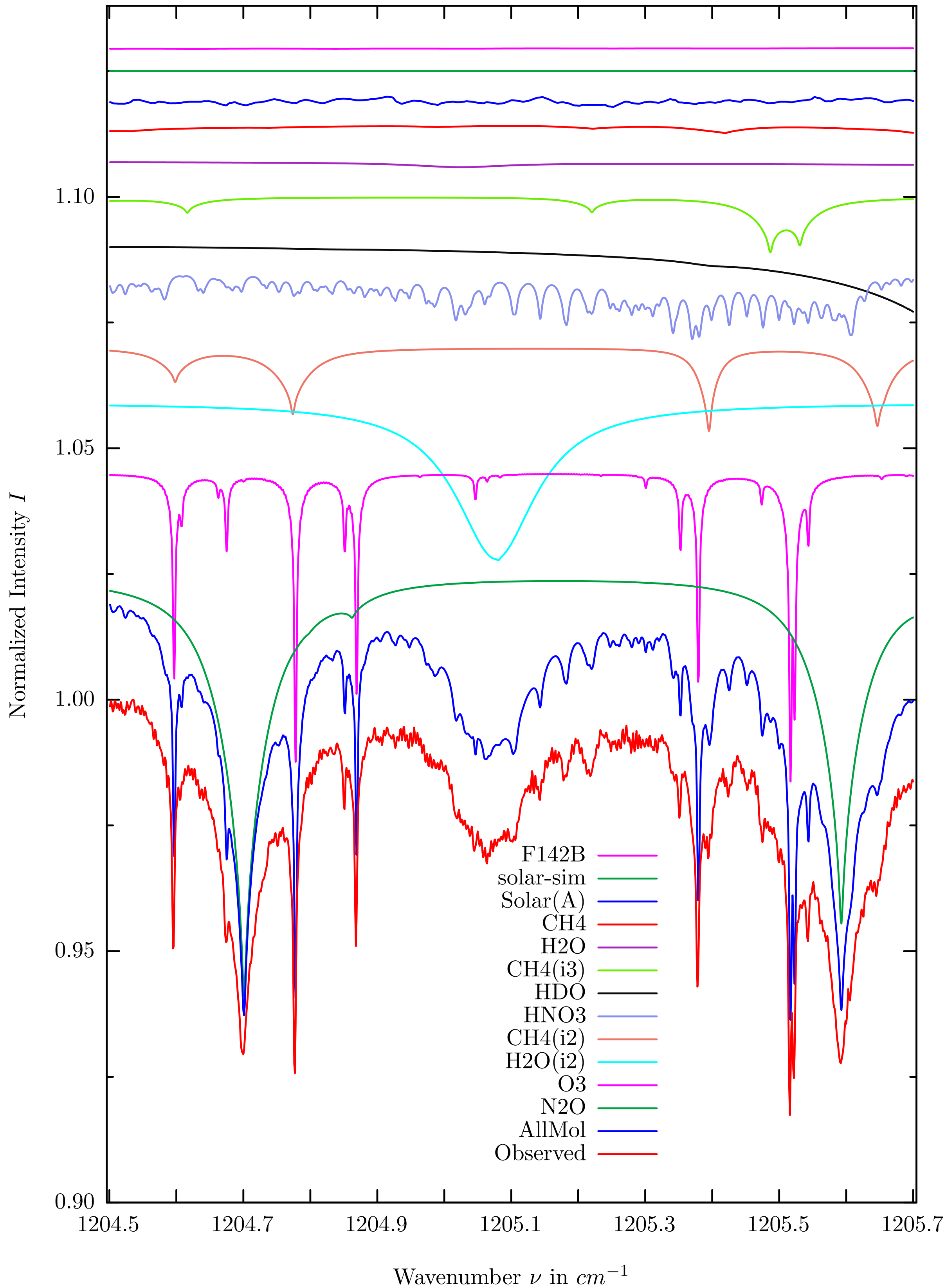

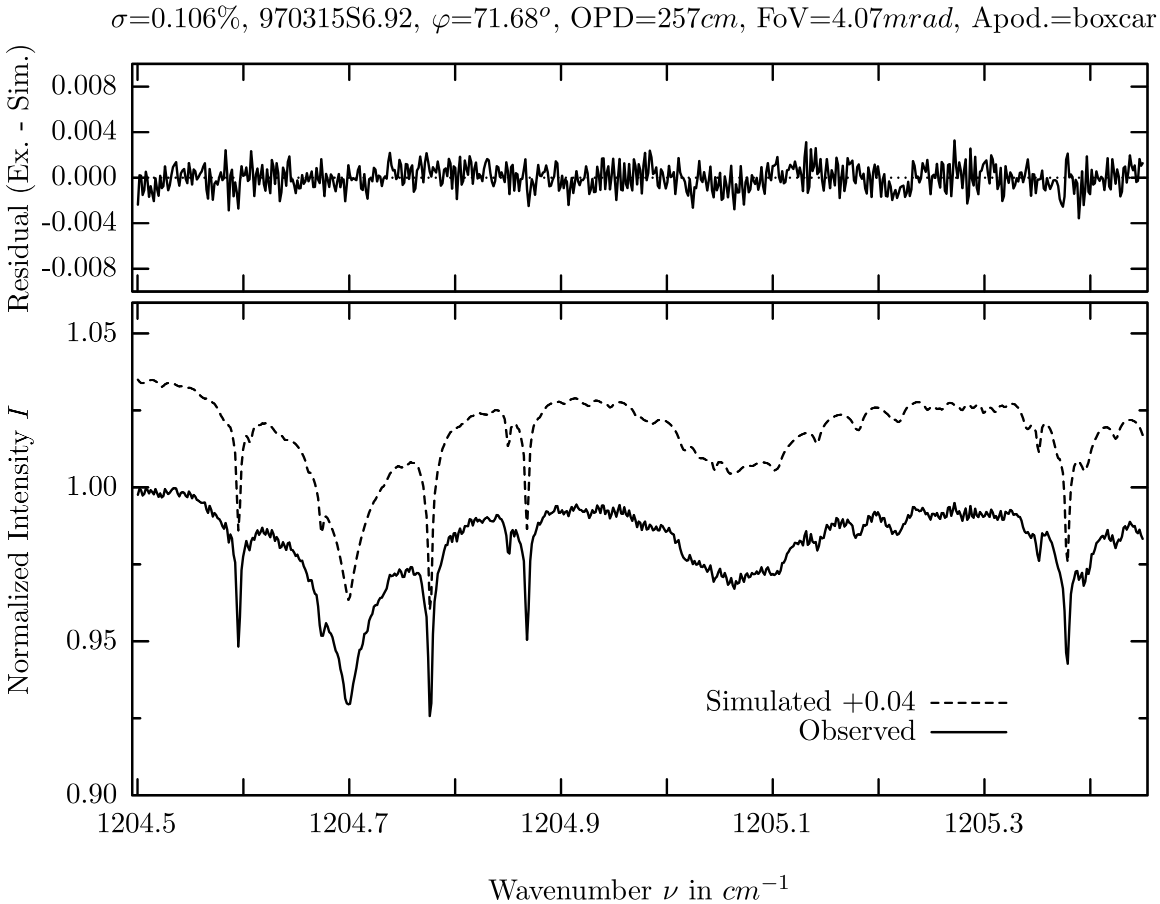

investigated species	:	$H_2{}^{18}O(= H_2O(i2))$
line position(s) ν_0	:	1205.0796 cm^{-1}
lower state energy E''_{lst}	:	1279.8 cm^{-1}
retrieved TCA, information content	:	5.14E+21 $molec/cm^2$, 27.4
temperature dependence of the TCA	:	-3.418%/K (trop), -0.118%/K (strat)
spectral interval fitted	:	1204.500 – 1205.450 cm^{-1}

Molecule	iCode	Absorption	Molecule	iCode	Absorption
$N2O$	41	8.499%	$H2O2$	231	0.014%
$O3$	31	6.998%	$COF2$	361	0.013%
H2O	1**2**	3.131%	$HOCL$	211	0.011%
$CH4$	6**2**	1.693%	$NO2$	101	0.001%
$HNO3$	121	1.450%	$NH3$	111	0.001%
HDO	491	1.400%	$N2O5$	261	0.001%
$CH4$	6**3**	1.121%	$H2S$	471	0.001%
$H2O$	11	0.412%	$CO2$	2**3**	<0.001%
$CH4$	61	0.240%	OH	131	<0.001%
Solar(A)	—	0.211%	ClO	181	<0.001%
Solar-sim	—	<0.001%	$CCl2F2$	321	<0.001%
$F142B$	611	0.057%	$HCOOH$	461	<0.001%
$SO2$	91	0.022%			

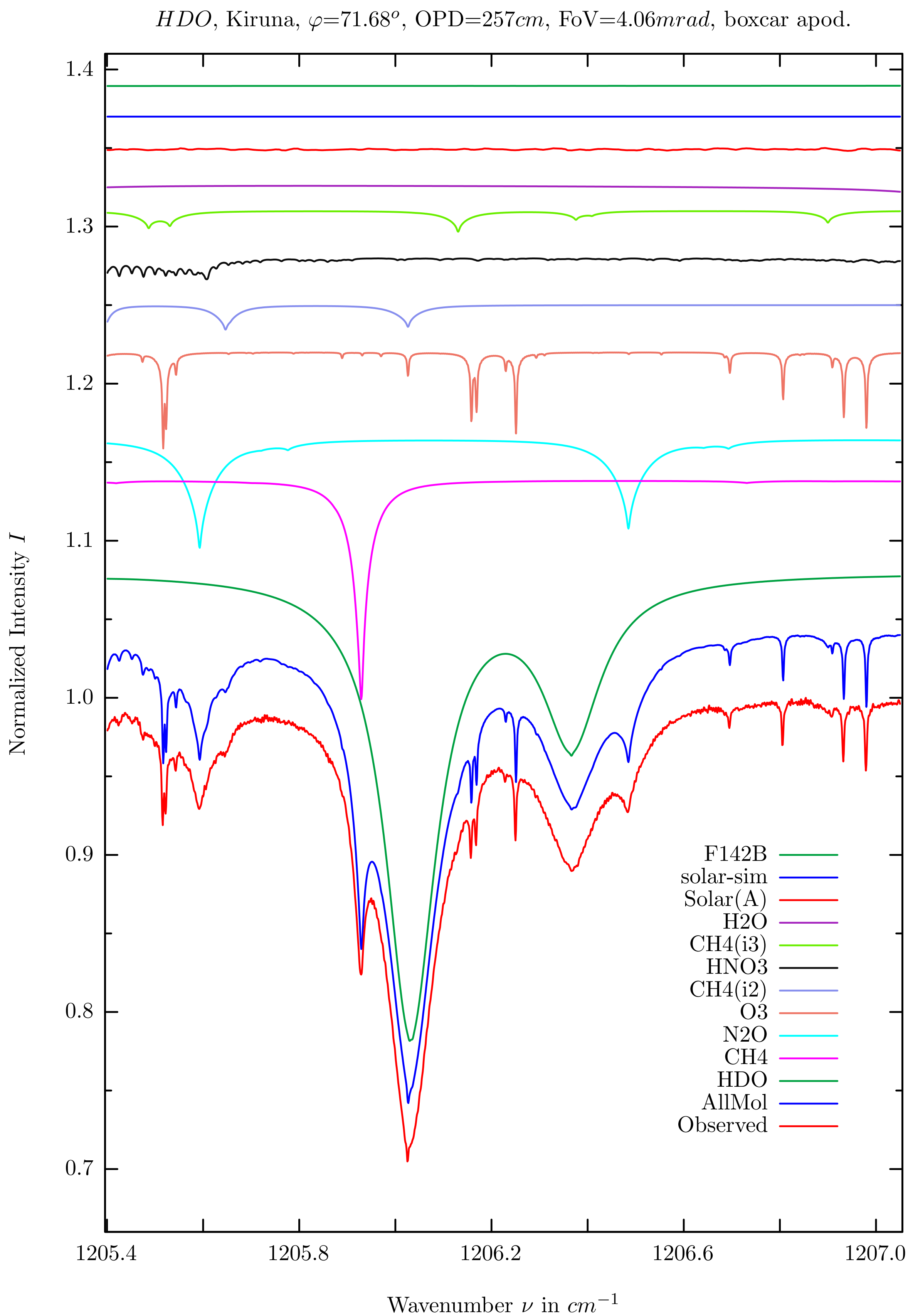

HDO, Kiruna, φ=71.68^o, OPD=257cm, FoV=4.06$mrad$, boxcar apod.
Normalized Intensity I
1.4
1.3
1.2
1.1
1.0
0.9
0.8
0.7
1205.4
1205.8
1206.2
1206.6
1207.0
Wavenumber ν in cm^{-1}
F142B
solar-sim
Solar(A)
H2O
CH4(i3)
HNO3
CH4(i2)
O3
N2O
CH4
HDO
AllMol
Observed

σ=0.190%, 970315S6.92, φ=71.68^o, OPD=257cm, FoV=4.07$mrad$, Apod.=boxcar

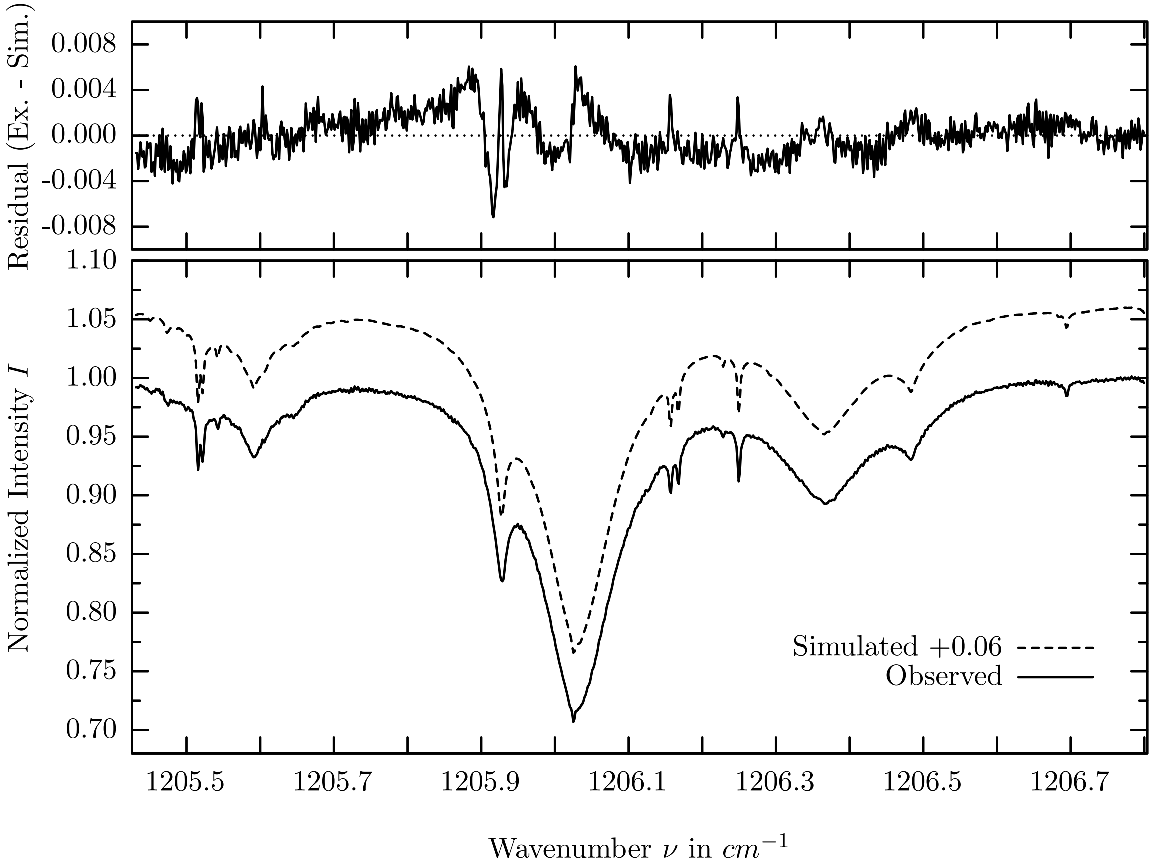

investigated species	:	HDO
line position(s) ν_0	:	1206.0199 cm^{-1}
lower state energy E''_{lst}	:	709.2 cm^{-1}
retrieved TCA, information content	:	4.36E+21 $molec/cm^2$, 152.8
temperature dependence of the TCA	:	-1.058%/K (trop), -0.016%/K (strat)
location, date, solar zenith angle	:	Kiruna, 15/Mar/97, 71.68^o
spectral interval fitted	:	1205.430 – 1206.800 cm^{-1}

Molecule	iCode	Absorption	Molecule	iCode	Absorption
HDO	491	33.932%	$H2O2$	231	0.019%
$CH4$	61	14.128%	$HOCL$	211	0.013%
$N2O$	41	7.037%	$NO2$	101	0.001%
$O3$	31	6.998%	$NH3$	111	0.001%
$CH4$	6**2**	1.582%	$N2O5$	261	0.001%
$HNO3$	121	1.358%	$H2S$	471	0.001%
$CH4$	6**3**	1.351%	$CO2$	2**3**	<0.001%
$H2O$	11	0.781%	OH	131	<0.001%
Solar(A)	—	0.180%	ClO	181	<0.001%
Solar-sim	—	<0.001%	$ClONO2$	271	<0.001%
$F142B$	611	0.051%	$CCl2F2$	321	<0.001%
$SO2$	91	0.025%	$HCOOH$	461	<0.001%
$COF2$	361	0.021%			

N_2O(i4), Kiruna, φ=71.68^o, OPD=257cm, FoV=4.06$mrad$, boxcar apod.

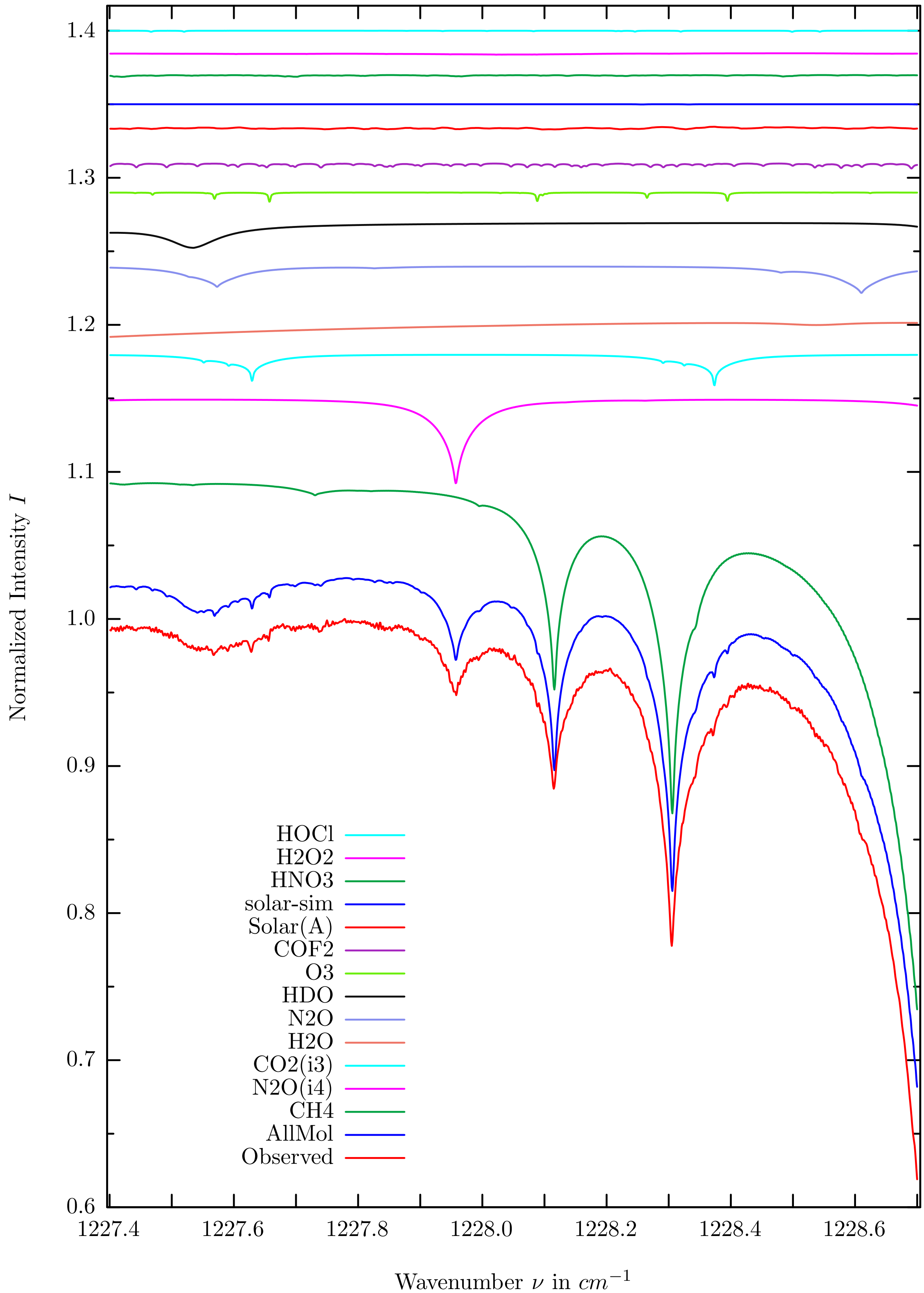

σ=0.123%, 970315S6.92, φ=71.68^o, OPD=257cm, FoV=4.07$mrad$, Apod.=boxcar

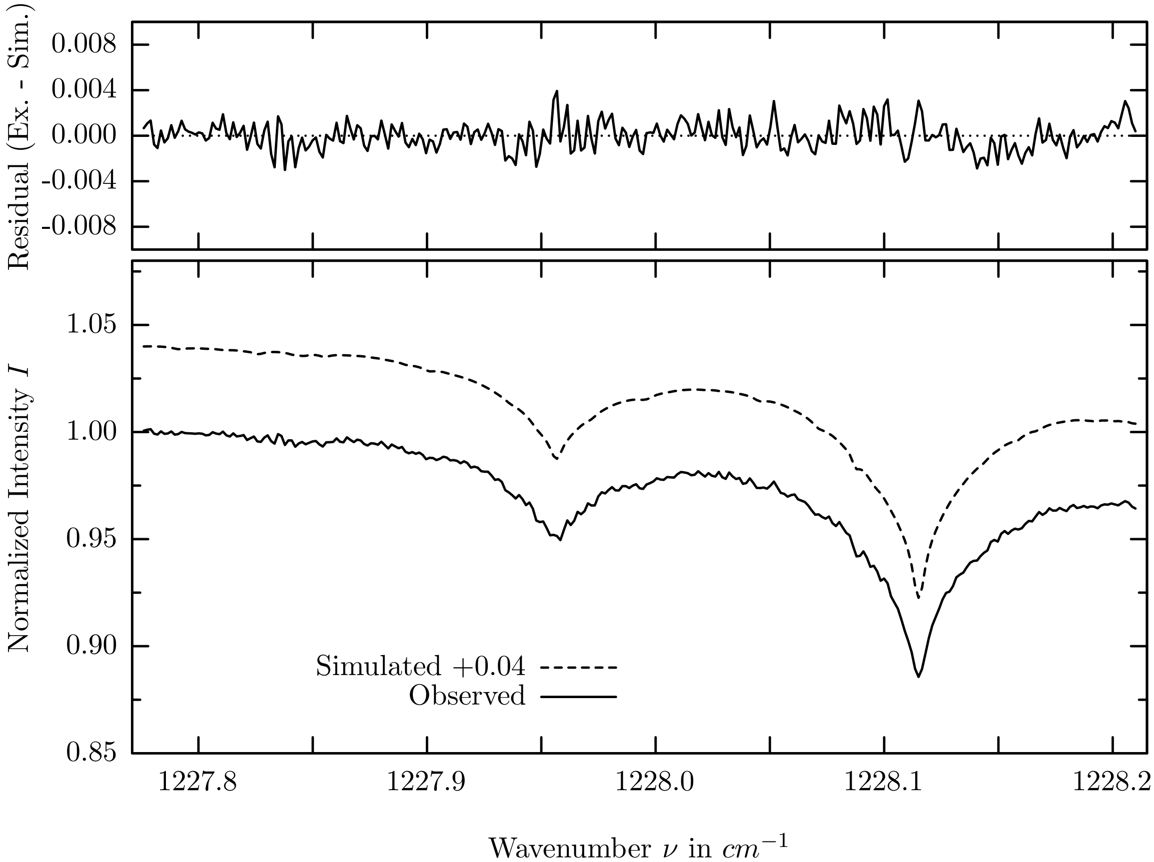

investigated species	:	$N_2O(i4)$
line position(s) ν_0	:	1227.9559 cm^{-1}
lower state energy E''_{lst}	:	218.3 cm^{-1}
retrieved TCA, information content	:	5.26E+18 $molec/cm^2$, 37.6
temperature dependence of the TCA	:	-0.213%/K (trop), -0.035%/K (strat)
location, date, solar zenith angle	:	Kiruna, 15/Mar/97, 71.68^o
spectral interval fitted	:	1227.775 – 1228.210 cm^{-1}

Molecule	iCode	Absorption	Molecule	iCode	Absorption
$CH4$	61	37.537%	$HOCL$	211	0.080%
N2O	4**4**	5.874%	$F142B$	611	0.019%
$CO2$	2**3**	2.276%	$ClONO2$	271	0.009%
$H2O$	11	2.118%	$N2O5$	261	0.004%
$N2O$	41	1.827%	$SO2$	91	0.003%
HDO	491	1.753%	$NO2$	101	0.001%
$O3$	31	0.763%	$H2S$	471	0.001%
$COF2$	361	0.386%	$NH3$	111	<0.001%
Solar(A)	—	0.212%	OH	131	<0.001%
Solar-sim	—	0.015%	$CHF2Cl$	421	<0.001%
$HNO3$	121	0.141%	$HCOOH$	461	<0.001%
$H2O2$	231	0.129%			

N_2O, Kiruna, φ=71.68^o, OPD=257cm, FoV=4.06$mrad$, boxcar apod.

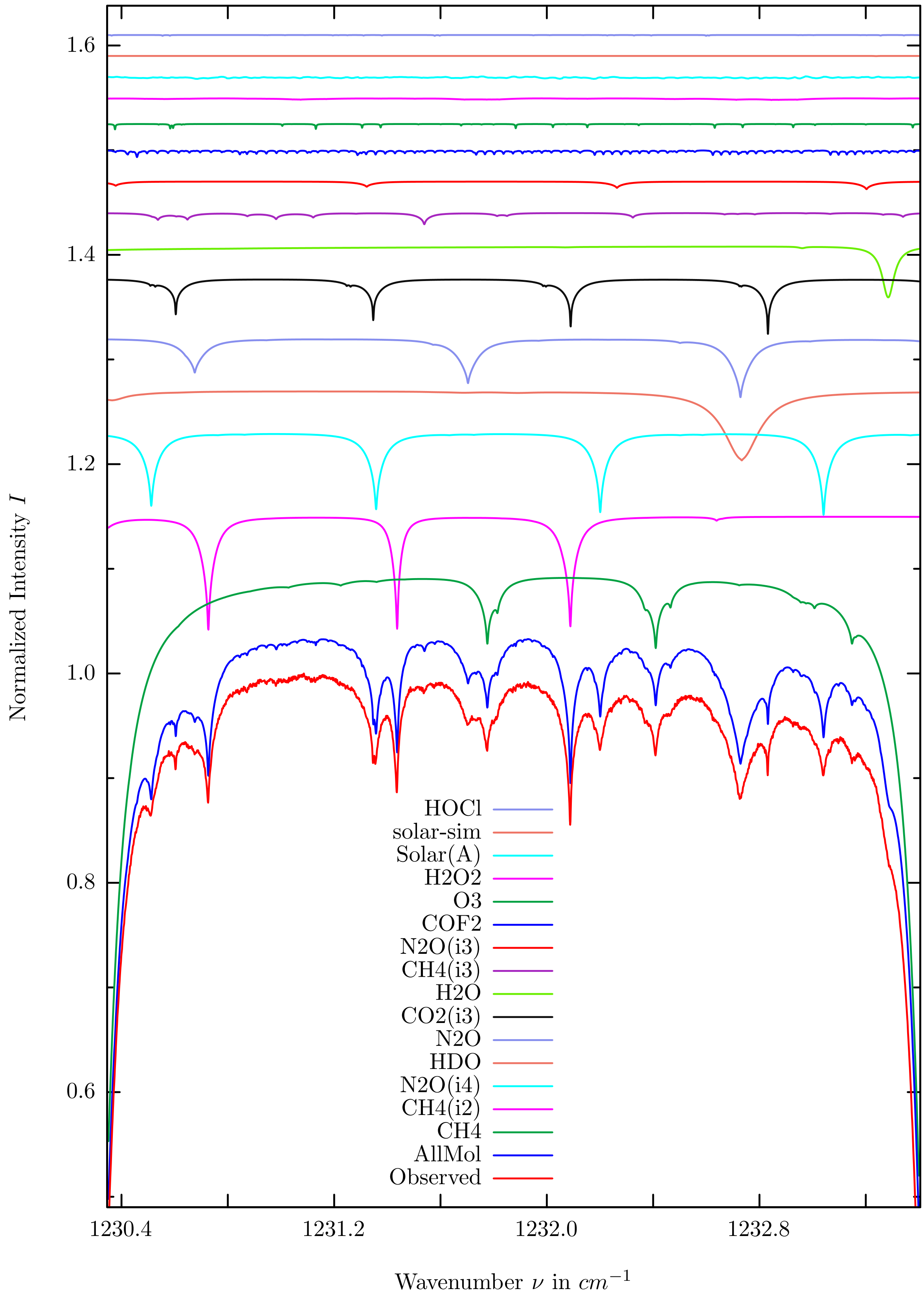

σ=0.125%, 970315S6.92, φ=71.68^o, OPD=257cm, FoV=4.07$mrad$, Apod.=boxcar

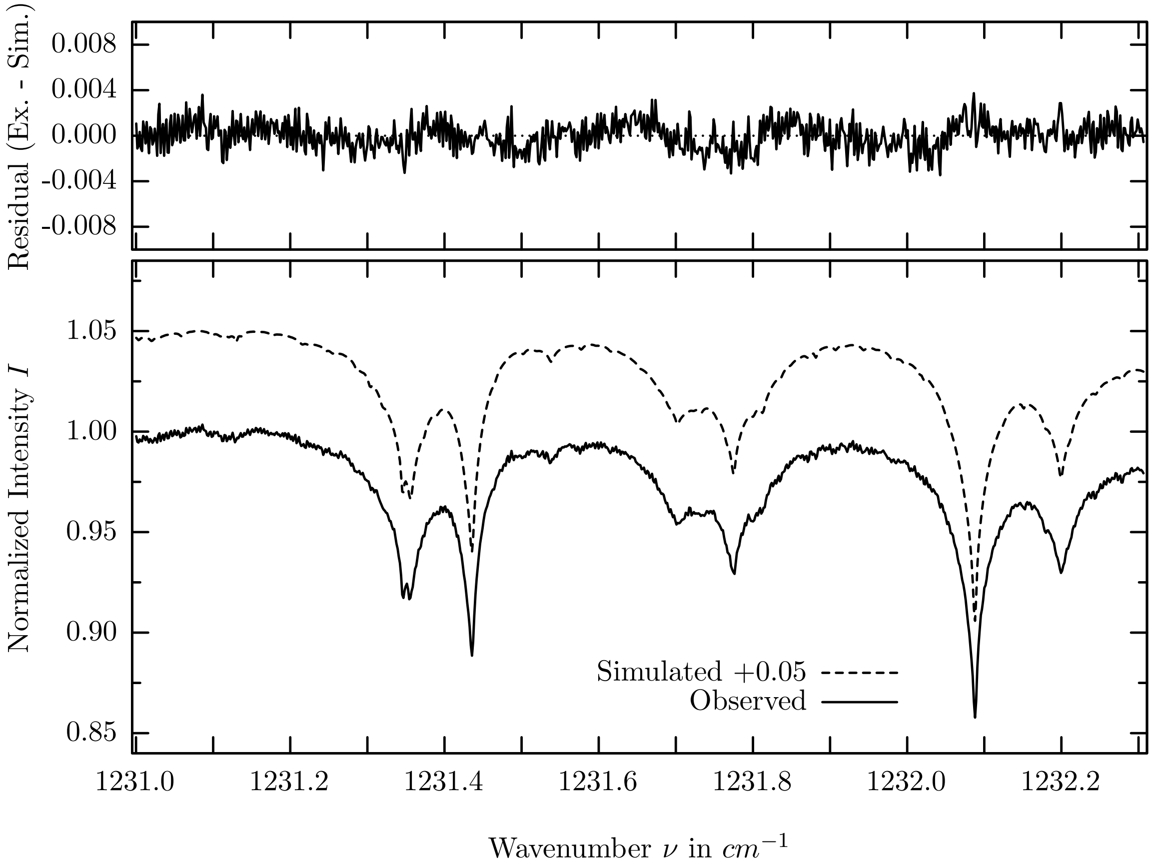

investigated species	:	$N_2O(i4), (CH_4(i2))$
line position(s) ν_0	:	1231.3564, 1232.1995, (1231.4358) cm^{-1}
lower state energy E''_{lst}	:	150.3, 135.3, (575.3) cm^{-1}
retrieved TCA, information content	:	5.89E+18, (3.23E+19) $molec/cm^2$, 66.8, (87.8)
temperature dependence of the TCA	:	-.568, (-.733)%/K (trop), +.031, (-.068)%/K (strat)
spectral interval fitted	:	1231.000 – 1232.307 cm^{-1}

Molecule	iCode	Absorption	Molecule	iCode	Absorption
$CH4$	61	59.745%	Solar-sim	—	0.014%
$CH4$	6**2**	11.002%	$HOCL$	211	0.086%
N2O	4**4**	7.961%	$HNO3$	121	0.035%
HDO	491	6.655%	$F142B$	611	0.023%
$N2O$	41	5.680%	$ClONO2$	271	0.014%
$CO2$	2**3**	5.611%	$N2O5$	261	0.011%
$H2O$	11	5.070%	$SO2$	91	0.002%
$CH4$	6**3**	1.100%	$NO2$	101	0.001%
$N2O$	4**3**	0.739%	$NH3$	111	0.001%
$COF2$	361	0.691%	$H2S$	471	0.001%
$O3$	31	0.630%	OH	131	<0.001%
$H2O2$	231	0.209%	$HCOOH$	461	<0.001%
Solar(A)	—	0.191%			

COF_2, Kiruna, φ=71.68^o, OPD=257cm, FoV=4.06$mrad$, boxcar apod.

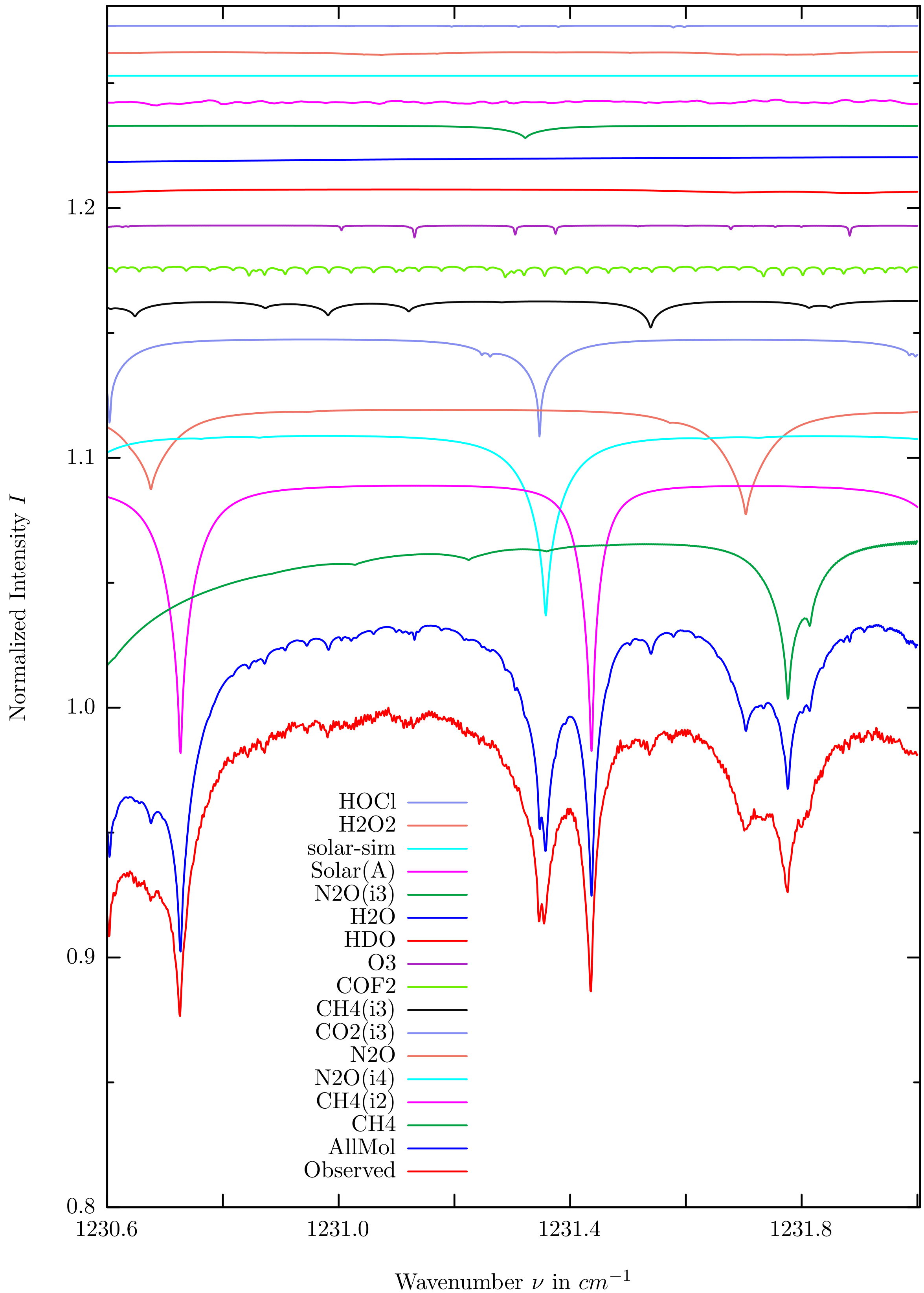

σ=0.111%, 970315S6.92, φ=71.68^o, OPD=257cm, FoV=4.07$mrad$, Apod.=boxcar

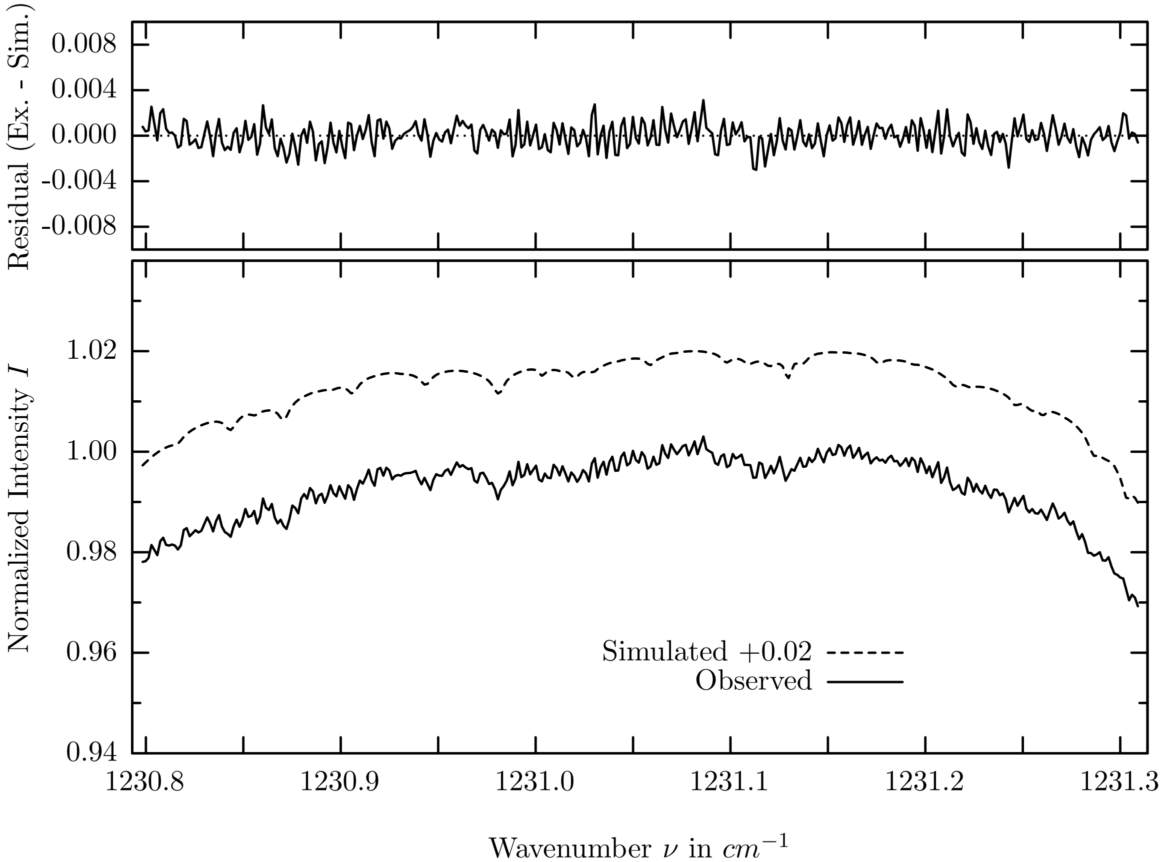

investigated species	:	COF_2
line position(s) ν_0	:	1230.9436*) cm^{-1}
lower state energy E''_{lst}	:	171.7 cm^{-1}
retrieved TCA, information content	:	3.05E+14 $molec/cm^2$, 2.7
temperature dependence of the TCA	:	-0.031%/K (trop), -0.437%/K (strat)
location, date, solar zenith angle	:	Kiruna, 15/Mar/97, 71.68^o
spectral interval fitted	:	1230.797 – 1231.310 cm^{-1}

Molecule	iCode	Absorption	Molecule	iCode	Absorption
$CH4$	61	21.149%	$H2O2$	231	0.179%
$CH4$	6**2**	11.002%	$HOCl$	211	0.086%
$N2O$	4**4**	7.422%	$HNO3$	121	0.034%
$N2O$	41	4.309%	$F142B$	611	0.021%
$CO2$	2**3**	4.209%	$ClONO2$	271	0.012%
$CH4$	6**3**	1.100%	$N2O5$	261	0.008%
COF2	361	0.691%	$SO2$	91	0.002%
$O3$	31	0.563%	$NO2$	101	0.001%
HDO	491	0.535%	$NH3$	111	0.001%
$H2O$	11	0.507%	$H2S$	471	0.001%
$N2O$	4**3**	0.500%	OH	131	<0.001%
Solar(A)	—	0.191%	$HCOOH$	461	<0.001%
Solar-sim	—	<0.001%			

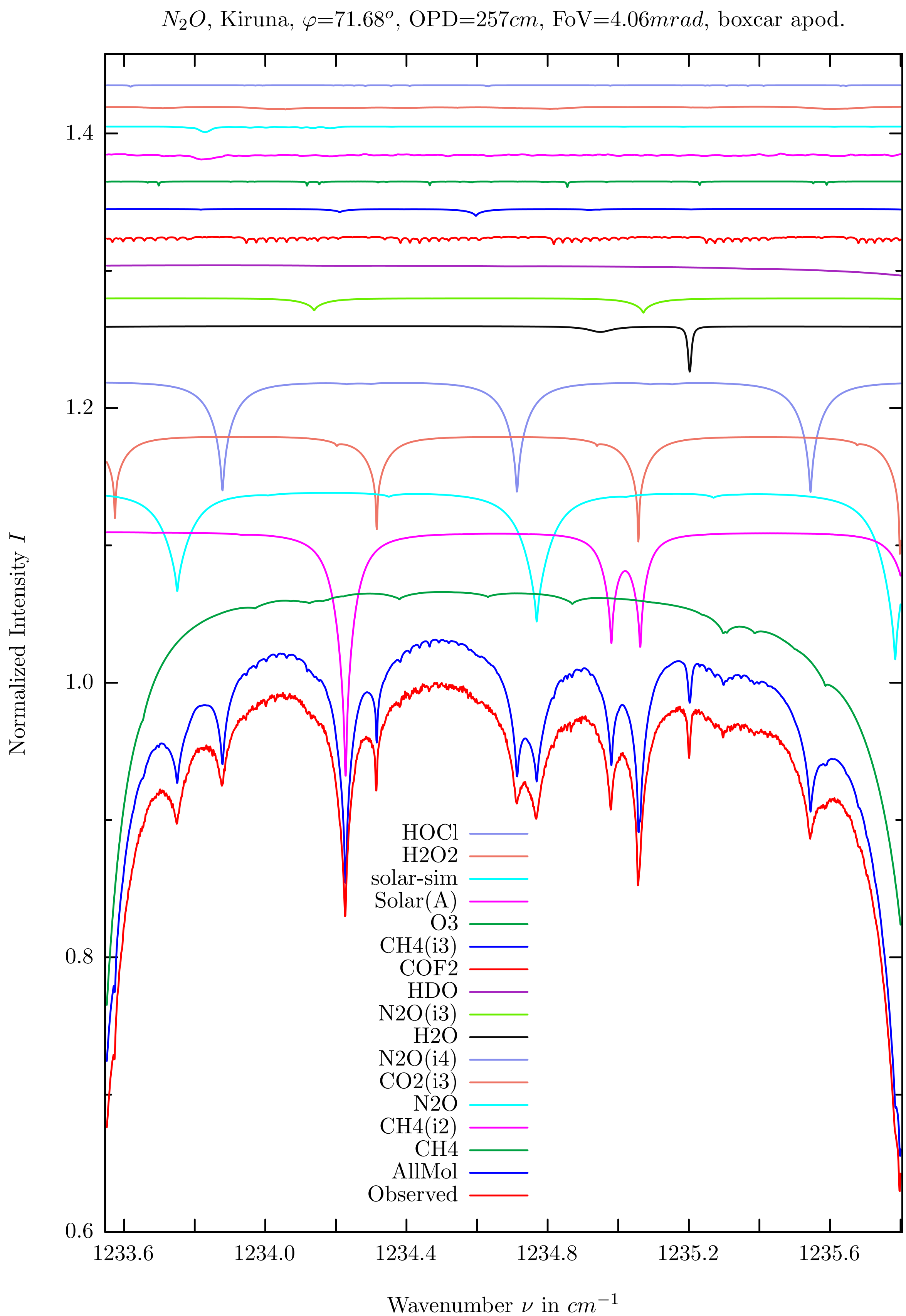
N_2O, Kiruna, φ=71.68^o, OPD=257cm, FoV=4.06$mrad$, boxcar apod.
Normalized Intensity I
Wavenumber ν in cm^{-1}
1.4
1.2
1.0
0.8
0.6
1233.6
1234.0
1234.4
1234.8
1235.2
1235.6
HOCl
H2O2
solar-sim
Solar(A)
O3
CH4(i3)
COF2
HDO
N2O(i3)
H2O
N2O(i4)
CO2(i3)
N2O
CH4(i2)
CH4
AllMol
Observed

σ=0.158%, 970315S6.92, φ=71.68^o, OPD=257cm, FoV=4.07$mrad$, Apod.=boxcar

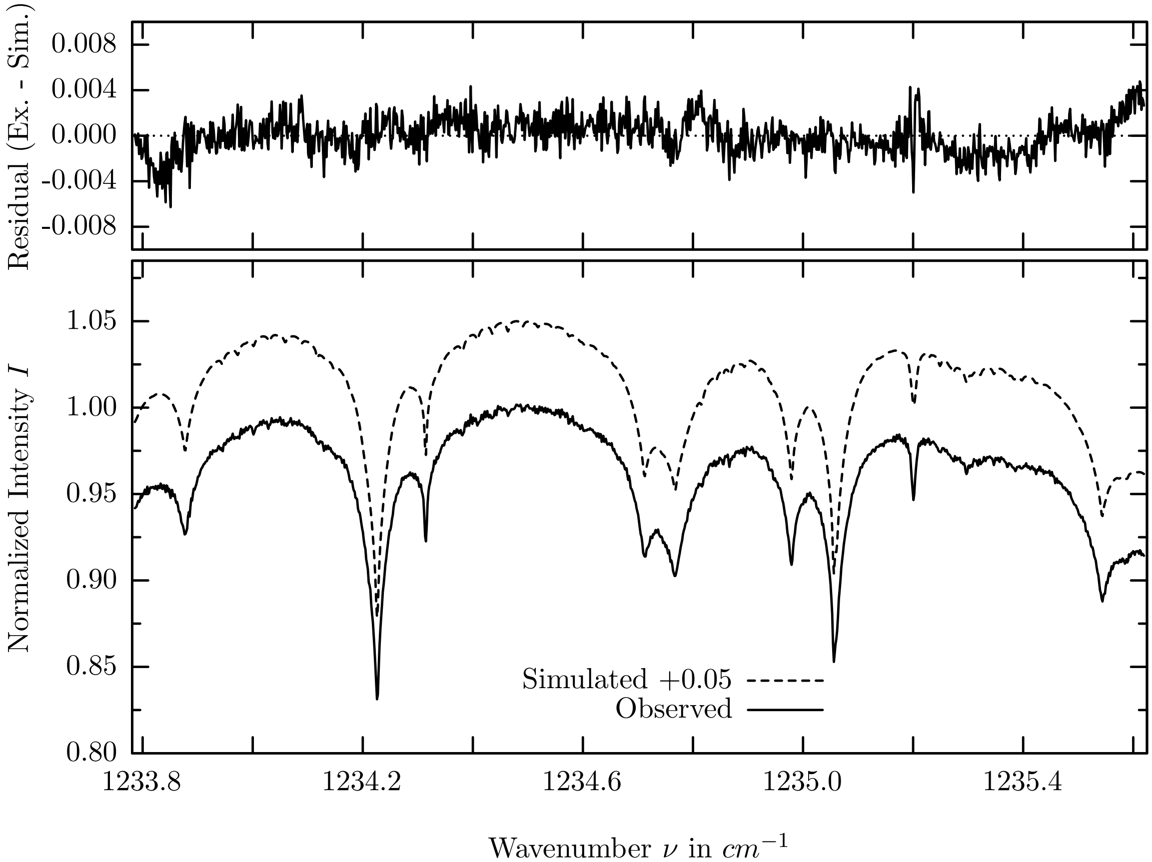

investigated species	:	$N_2O(i4), (CH_4(i2))$
line position(s) ν_0	:	1233.8772, 1234.7118, (1234.2262) cm^{-1}
lower state energy E''_{lst}	:	107.6, 94.9, (575.2) cm^{-1}
retrieved TCA, information content	:	5.66E+18, (3.21E+19) $molec/cm^2$, 56.6, (108.1)
temperature dependence of the TCA	:	-.862, (-1.05)%/K (trop), -.039, (-.129)%/K (strat)
location, date, solar zenith angle	:	Kiruna, 15/Mar/97, 71.68^o
spectral interval fitted	:	1233.785 – 1235.620 cm^{-1}

Molecule	iCode	Absorption	Molecule	iCode	Absorption
$CH4$	61	31.017%	$H2O2$	231	0.260%
$CH4$	6**2**	18.125%	$HOCL$	211	0.102%
$N2O$	41	12.447%	$F142B$	611	0.026%
$CO2$	2**3**	9.287%	$HNO3$	121	0.019%
N2O	4**4**	8.232%	$N2O5$	261	0.019%
$H2O$	11	3.388%	$ClONO2$	271	0.016%
$N2O$	4**3**	1.071%	$NO2$	101	0.002%
HDO	491	0.856%	$H2S$	471	0.002%
$COF2$	361	0.604%	$SO2$	91	0.001%
$CH4$	6**3**	0.510%	$NH3$	111	<0.001%
$O3$	31	0.452%	OH	131	<0.001%
Solar(A)	—	0.400%	$HCOOH$	461	<0.001%
Solar-sim	—	0.404%			

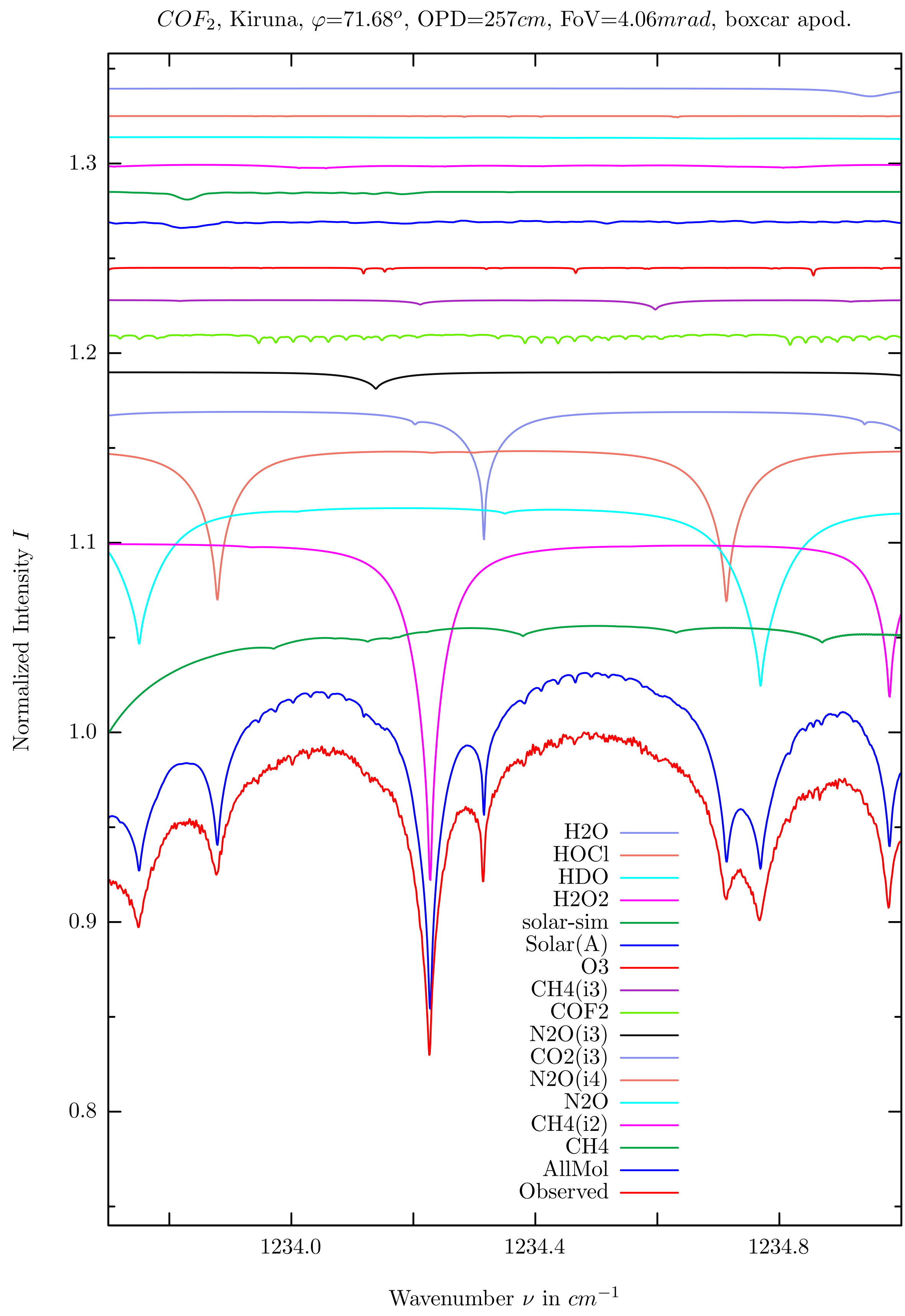

COF_2, Kiruna, φ=71.68^o, OPD=257cm, FoV=4.06$mrad$, boxcar apod.
Normalized Intensity I
Wavenumber ν in cm^{-1}
1.3
1.2
1.1
1.0
0.9
0.8
1234.0
1234.4
1234.8
H2O
HOCl
HDO
H2O2
solar-sim
Solar(A)
O3
CH4(i3)
COF2
N2O(i3)
CO2(i3)
N2O(i4)
N2O
CH4(i2)
CH4
AllMol
Observed

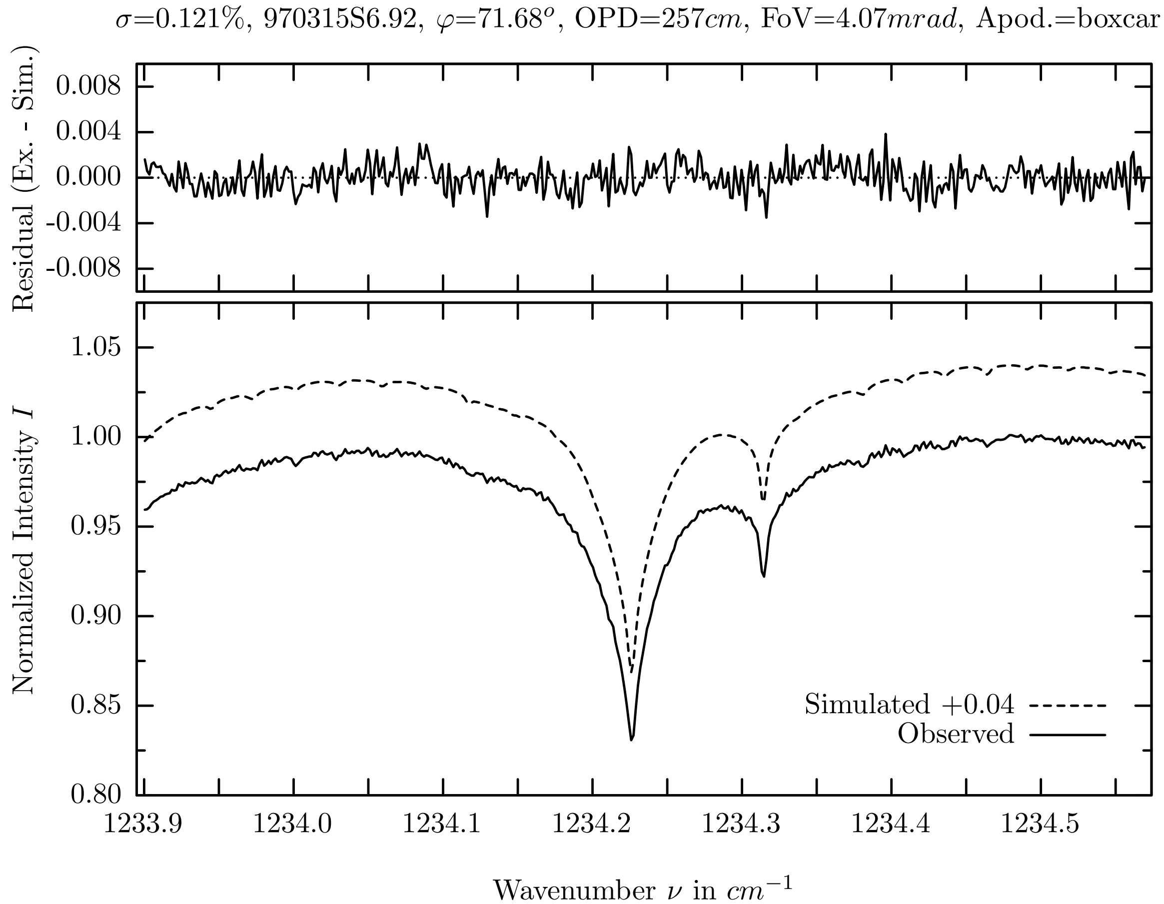

investigated species	:	$COF_2, (CH_4(i2))$
line position(s) ν_0	:	1233.9731$^{*)}$, 1234.4356$^{*)}$, (1234.2262) cm^{-1}
lower state energy E''_{lst}	:	102.8, 92.5, (575.3) cm^{-1}
retrieved TCA, information content	:	3.18E+14, (3.22E+19) $molec/cm^2$, 4.3, 4.0, (142.0)
temperature dependence of the TCA	:	-.254, (-.957)%/K (trop), -.451, (-.133)%/K (strat)
spectral interval fitted	:	1233.900 – 1234.570 cm^{-1}

Molecule	iCode	Absorption	Molecule	iCode	Absorption
$CH4$	61	31.012%	$HOCL$	211	0.102%
$CH4$	6**2**	18.125%	$H2O$	11	0.087%
$N2O$	41	9.660%	$F142B$	611	0.026%
$N2O$	4**4**	8.213%	$HNO3$	121	0.019%
$CO2$	2**3**	8.205%	$N2O5$	261	0.016%
$N2O$	4**3**	1.071%	$ClONO2$	271	0.016%
COF2	361	0.604%	$NO2$	101	0.002%
$CH4$	6**3**	0.510%	$H2S$	471	0.002%
$O3$	31	0.452%	$SO2$	91	0.001%
Solar(A)	—	0.400%	$NH3$	111	<0.001%
Solar-sim	—	0.404%	OH	131	<0.001%
$H2O2$	231	0.260%	$HCOOH$	461	<0.001%
HDO	491	0.243%			

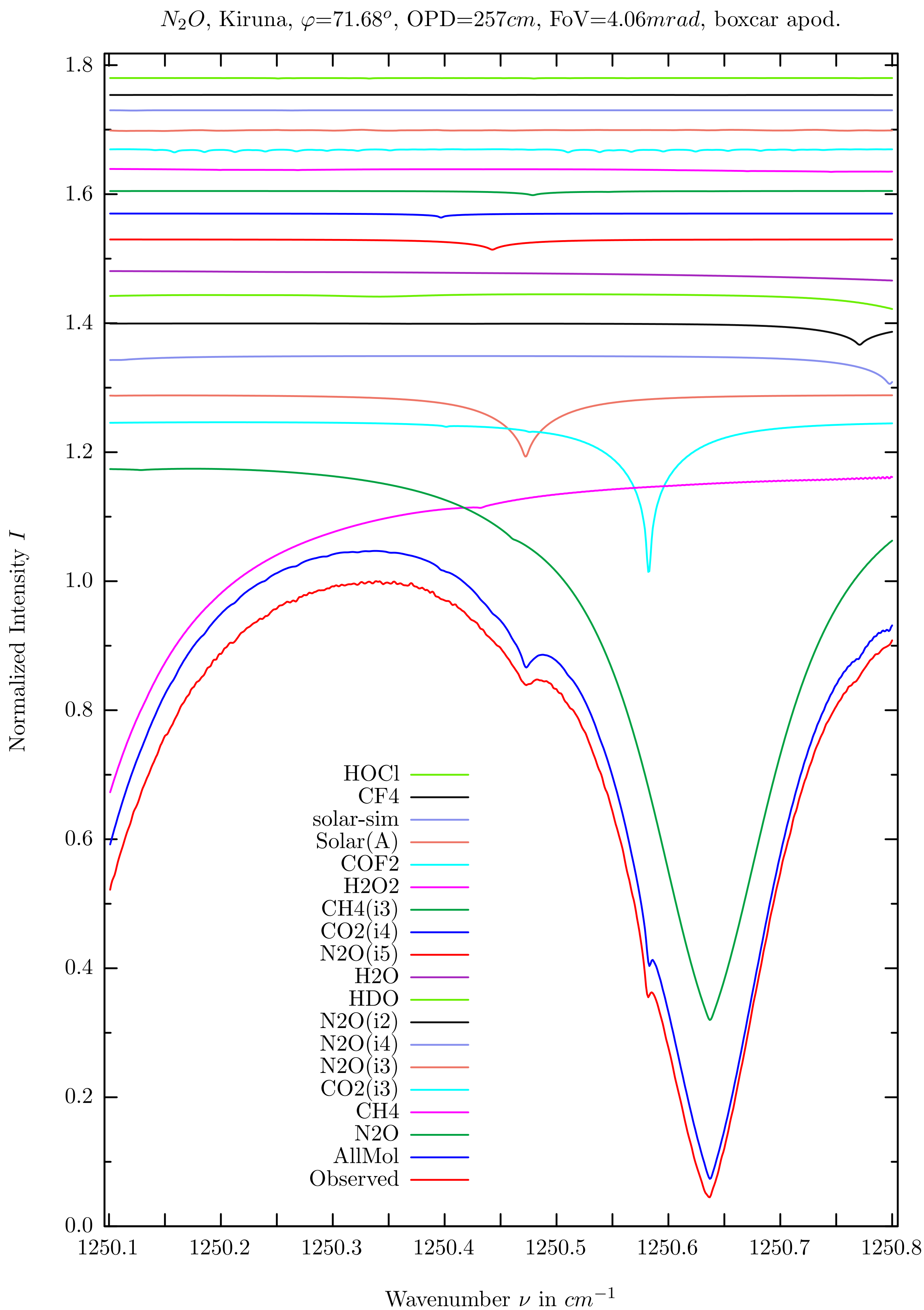

N_2O, Kiruna, φ=71.68^o, OPD=257cm, FoV=4.06$mrad$, boxcar apod.
Normalized Intensity I
0.0
0.2
0.4
0.6
0.8
1.0
1.2
1.4
1.6
1.8
1250.1
1250.2
1250.3
1250.4
1250.5
1250.6
1250.7
1250.8
Wavenumber ν in cm^{-1}
HOCl
CF4
solar-sim
Solar(A)
COF2
H2O2
CH4(i3)
CO2(i4)
N2O(i5)
H2O
HDO
N2O(i2)
N2O(i4)
N2O(i3)
CO2(i3)
CH4
N2O
AllMol
Observed

σ=0.129%, 970315S6.92, φ=71.68^o, OPD=257cm, FoV=4.07$mrad$, Apod.=boxcar

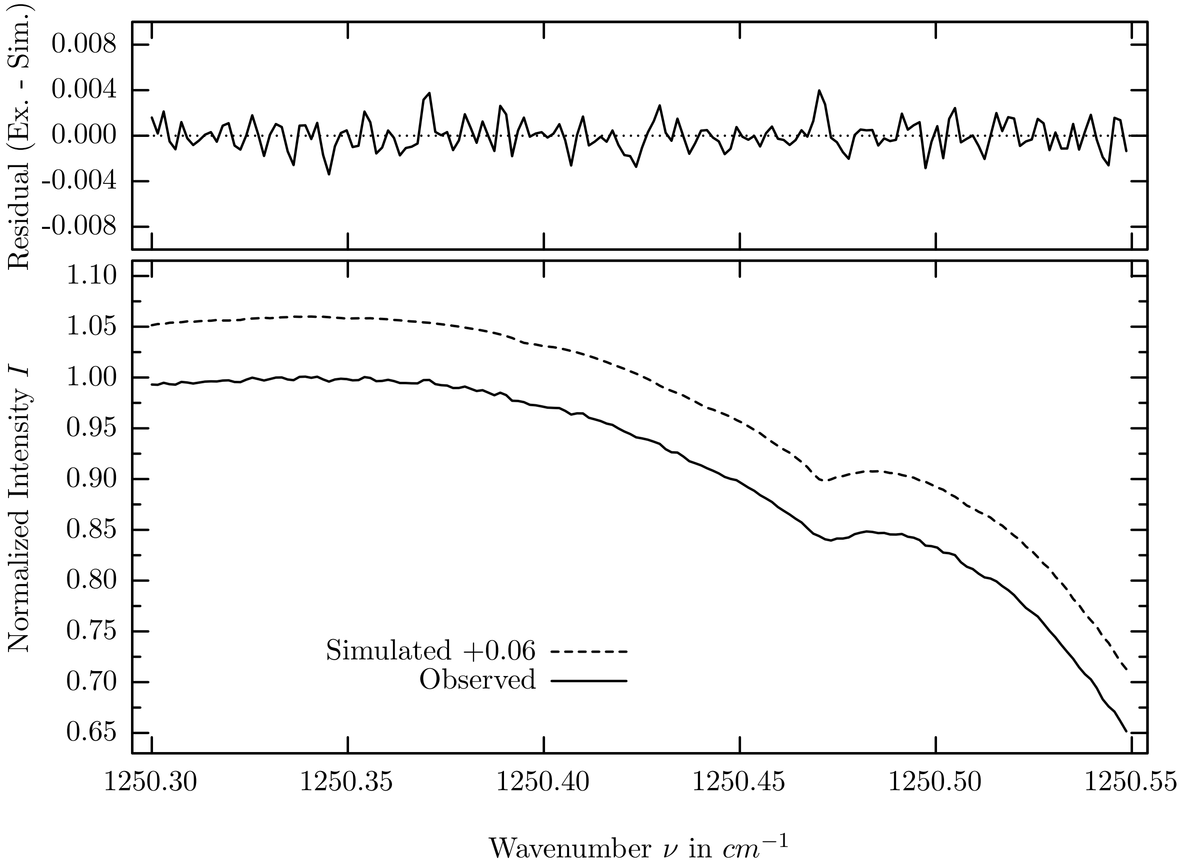

investigated species	:	$N_2O(i3)$
line position(s) ν_0	:	1250.4709 cm^{-1}
lower state energy E''_{lst}	:	223.4 cm^{-1}
retrieved TCA, information content	:	5.80E+18 $molec/cm^2$, 45.7
temperature dependence of the TCA	:	-0.566%/K (trop), -0.010%/K (strat)
spectral interval fitted	:	1250.300 – 1250.550 cm^{-1}

Molecule	iCode	Absorption	Molecule	iCode	Absorption
$N2O$	41	97.968%	Solar-sim	—	0.039%
$CH4$	61	52.076%	$CF4$	311	0.140%
$CO2$	**23**	25.071%	$HOCL$	211	0.088%
N2O	4**3**	9.845%	$O3$	31	0.046%
$N2O$	4**4**	4.465%	$HNO3$	121	0.040%
$N2O$	4**2**	3.406%	$N2O5$	261	0.034%
HDO	491	2.879%	$ClONO2$	271	0.006%
$H2O$	11	2.391%	$NO2$	101	0.003%
$N2O$	4**5**	1.626%	$F142B$	611	0.003%
$CO2$	**24**	0.671%	$C2H2$	401	0.002%
$CH4$	**63**	0.666%	$SO2$	91	0.001%
$H2O2$	231	0.556%	$NH3$	111	<0.001%
$COF2$	361	0.554%	OH	131	<0.001%
Solar(A)	—	0.210%	$H2S$	471	<0.001%

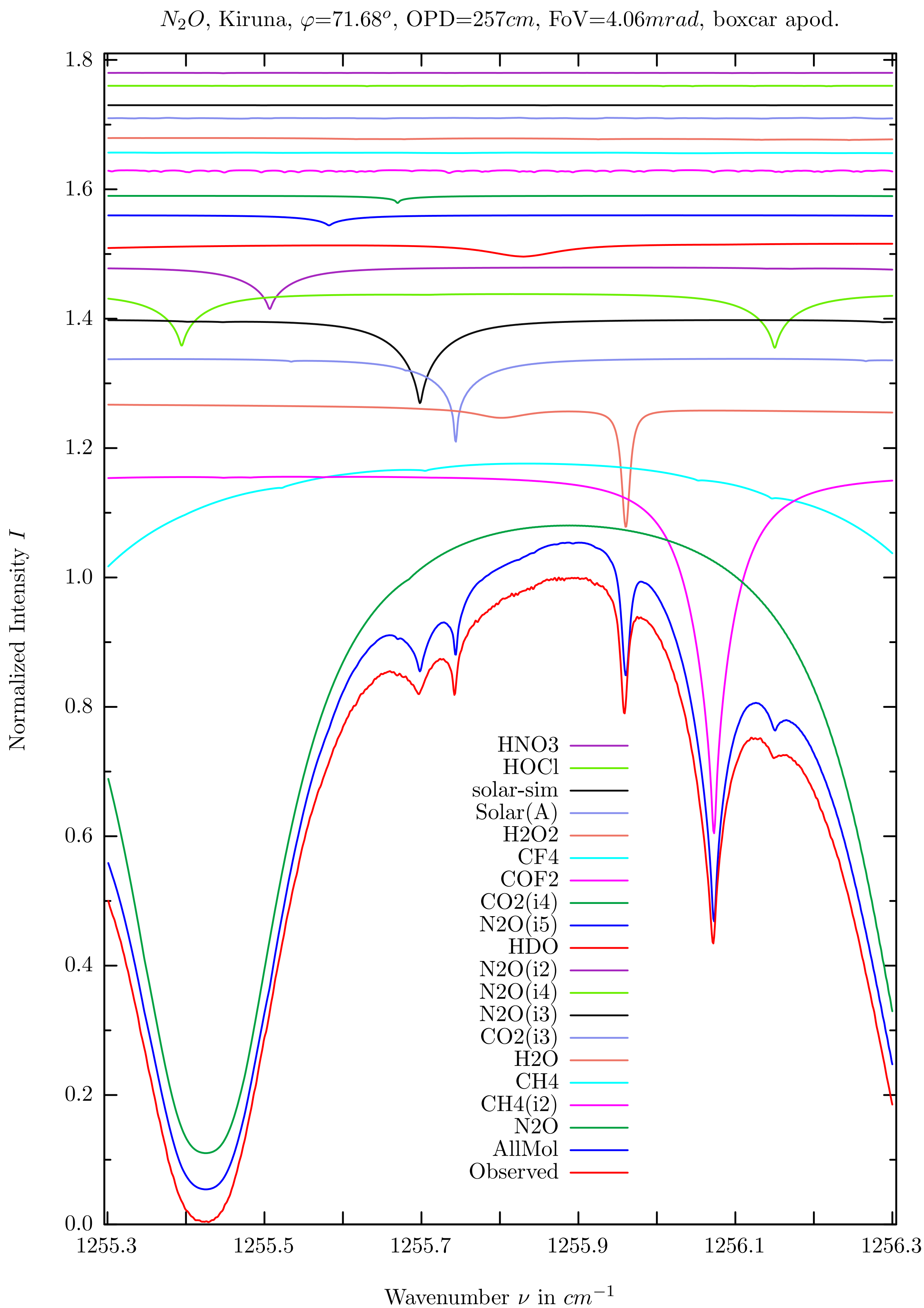

N_2O, Kiruna, φ=71.68^o, OPD=257cm, FoV=4.06$mrad$, boxcar apod.
Normalized Intensity I
Wavenumber ν in cm^{-1}
1.8
1.6
1.4
1.2
1.0
0.8
0.6
0.4
0.2
0.0
1255.3
1255.5
1255.7
1255.9
1256.1
1256.3
HNO3
HOCl
solar-sim
Solar(A)
H2O2
CF4
COF2
CO2(i4)
N2O(i5)
HDO
N2O(i2)
N2O(i4)
N2O(i3)
CO2(i3)
H2O
CH4
CH4(i2)
N2O
AllMol
Observed

σ=0.137%, 970315S6.92, φ=71.68^o, OPD=257cm, FoV=4.07$mrad$, Apod.=boxcar

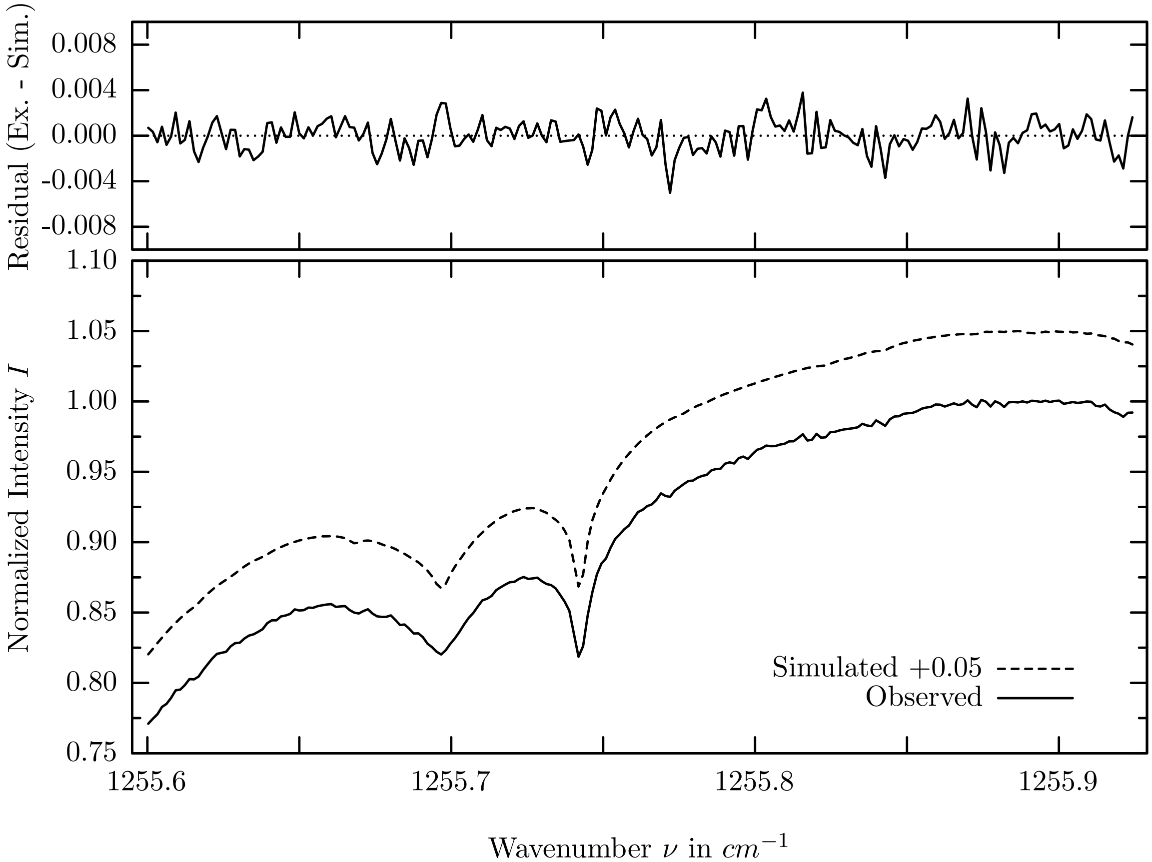

investigated species	:	$N_2O(i3)$
line position(s) ν_0	:	1255.6967 cm^{-1}
lower state energy E''_{lst}	:	123.9 cm^{-1}
retrieved TCA, information content	:	5.59E+18 $molec/cm^2$, 54.3
temperature dependence of the TCA	:	-0.443%/K (trop), -0.038%/K (strat)
spectral interval fitted	:	1255.600 – 1255.925 cm^{-1}

Molecule	iCode	Absorption	Molecule	iCode	Absorption
$N2O$	41	99.987%	Solar(A)	—	0.080%
$CH4$	6**2**	56.152%	Solar-sim	—	0.023%
$CH4$	61	24.156%	$HOCL$	211	0.074%
$H2O$	11	21.372%	$HNO3$	121	0.056%
$CO2$	2**3**	13.783%	$O3$	31	0.024%
N2O	4**3**	13.239%	$N2O5$	261	0.023%
$N2O$	4**4**	8.623%	$ClONO2$	271	0.005%
$N2O$	4**2**	6.605%	$NO2$	101	0.003%
HDO	491	2.404%	$C2H2$	401	0.001%
$N2O$	4**5**	1.601%	$F142B$	611	0.001%
$CO2$	2**4**	1.183%	$SO2$	91	<0.001%
$COF2$	361	0.480%	$NH3$	111	<0.001%
$CF4$	311	0.422%	OH	131	<0.001%
$H2O2$	231	0.397%	$H2S$	471	<0.001%

CF_4, Kiruna, φ=71.68^o, OPD=257cm, FoV=4.06$mrad$, boxcar apod.

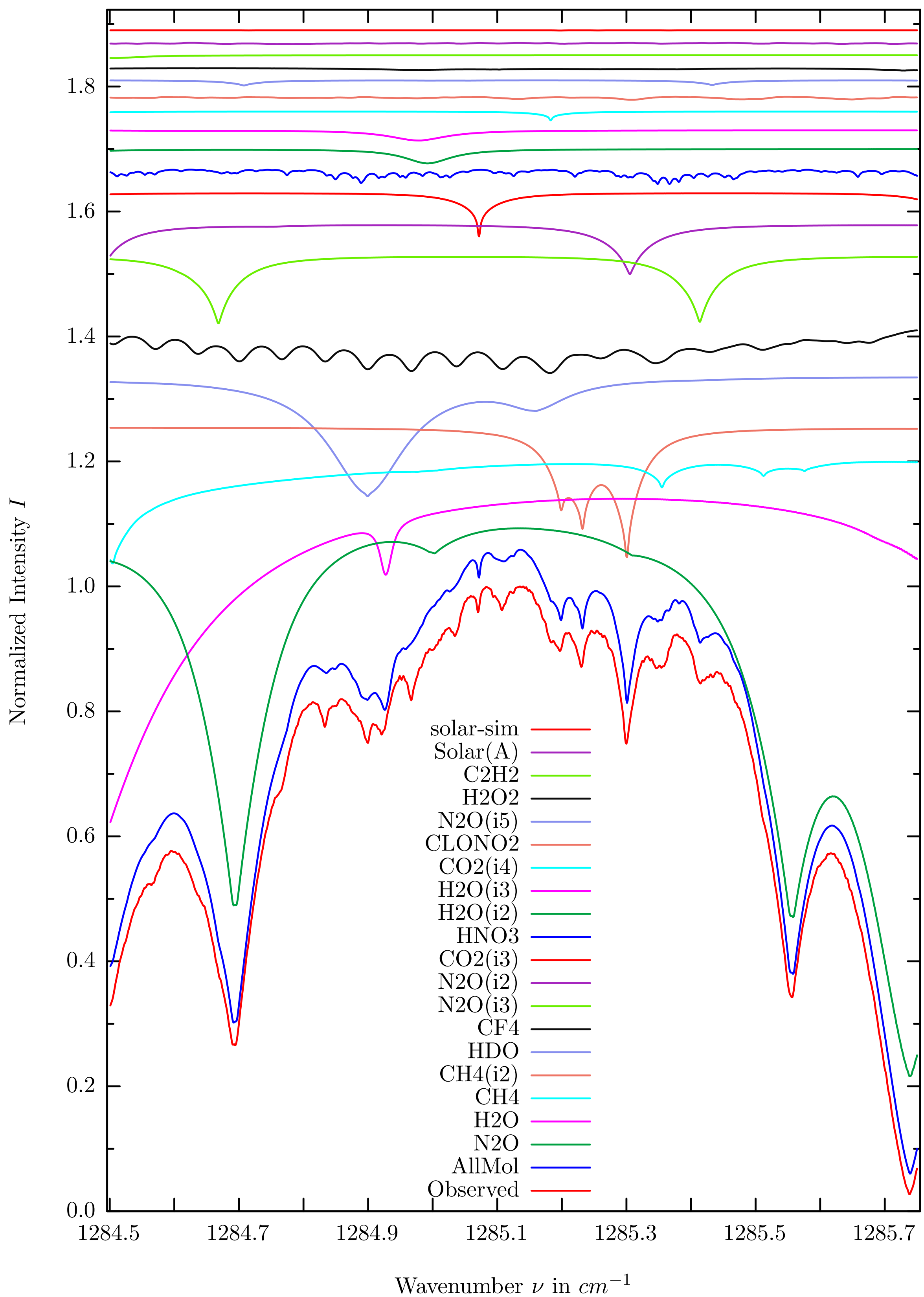

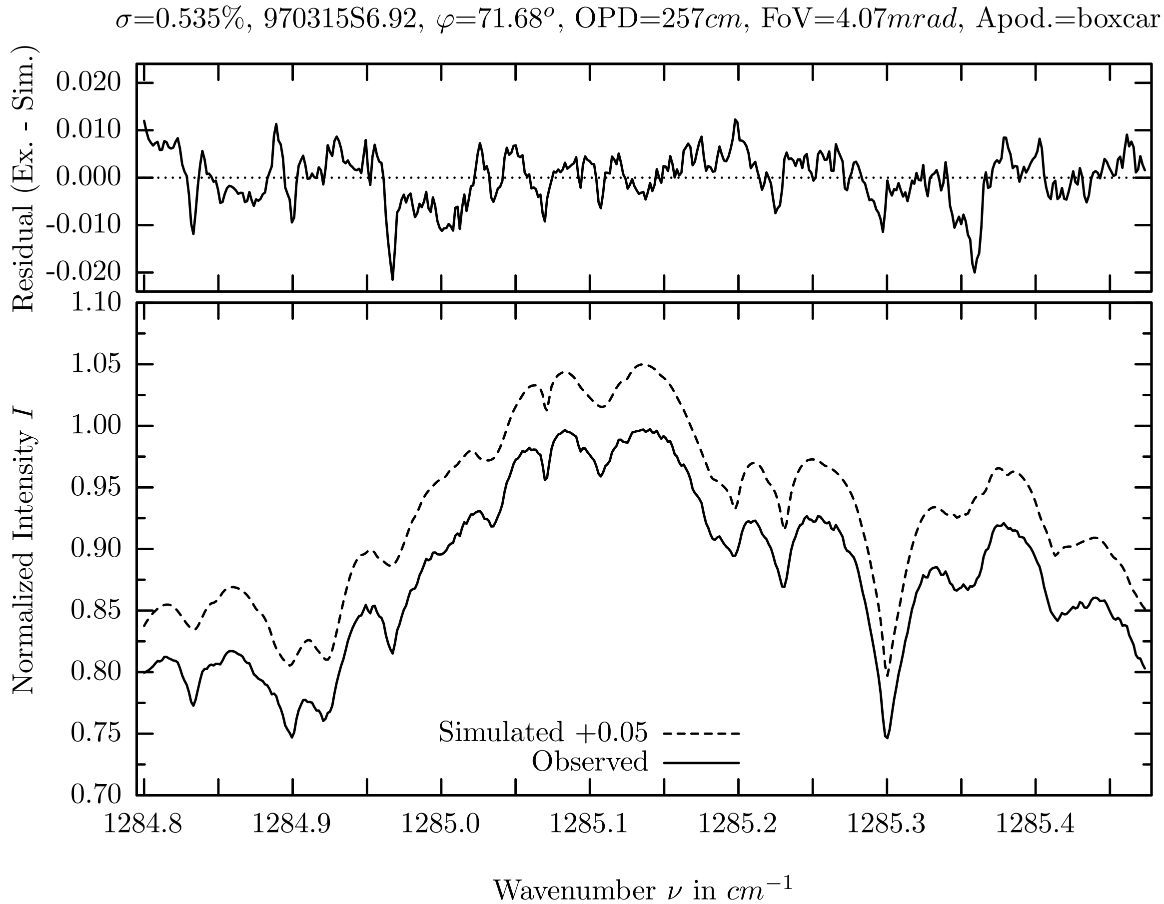

investigated species	:	$CF_4(= CFC - 14)$
line position(s) ν_0	:	1285.0350*), 1285.1075*), 1285.3375*) cm^{-1}
lower state energy E''_{lst}	:	typ. 114.0 to 281.0 cm^{-1}
retrieved TCA, information content	:	1.92E+15 $molec/cm^2$, 7.2
temperature dependence of the TCA	:	-2.173%/K (trop), -0.529%/K (strat)
location, date, solar zenith angle	:	Kiruna, 15/Mar/97, 71.68^o
spectral interval fitted	:	1284.800 – 1285.475 cm^{-1}

Molecule	iCode	Absorption	Molecule	iCode	Absorption
$N2O$	41	97.534%	$CO2$	2**4**	1.496%
$H2O$	11	61.429%	$CLONO2$	271	1.114%
$CH4$	61	24.437%	$N2O$	4**5**	0.838%
$CH4$	6**2**	21.200%	$H2O2$	231	0.446%
HDO	491	19.601%	$C2H2$	401	0.444%
CF4	311	17.860%	Solar(A)	—	0.231%
$N2O$	4**3**	11.027%	Solar-sim	—	0.043%
$N2O$	4**2**	8.106%	$NO2$	101	0.007%
$CO2$	**23**	7.434%	$COF2$	361	0.005%
$HNO3$	121	2.676%	$HOCL$	211	0.001%
$H2O$	1**2**	2.316%	$CHF2CL$	421	<0.001%
$H2O$	1**3**	1.642%	$H2S$, $NH3$, OH, $N2O5$		<0.001%

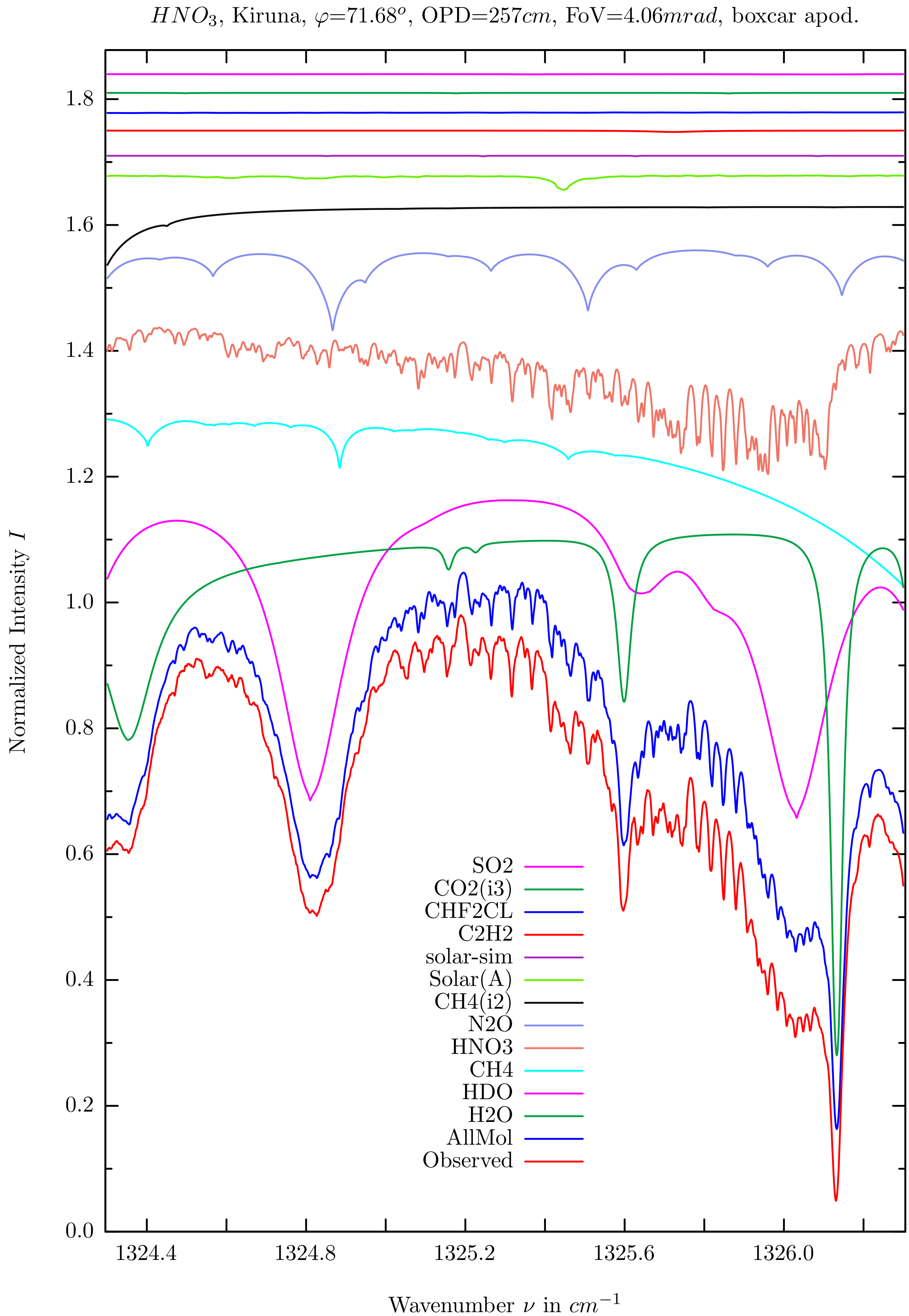
HNO_3, Kiruna, φ=71.68^o, OPD=257cm, FoV=4.06$mrad$, boxcar apod.
Normalized Intensity I
Wavenumber ν in cm^{-1}
1.8
1.6
1.4
1.2
1.0
0.8
0.6
0.4
0.2
0.0
1324.4
1324.8
1325.2
1325.6
1326.0
SO2
CO2(i3)
CHF2CL
C2H2
solar-sim
Solar(A)
CH4(i2)
N2O
HNO3
CH4
HDO
H2O
AllMol
Observed

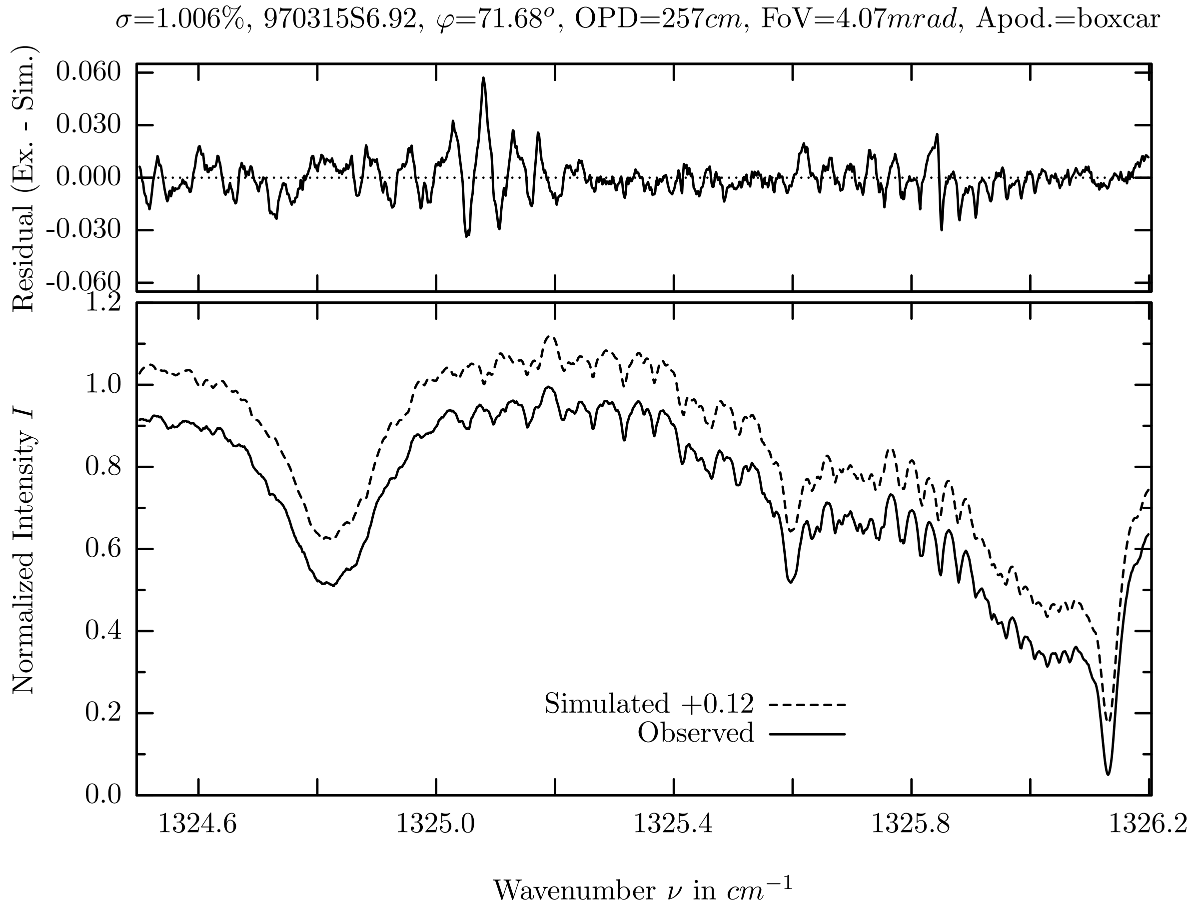

investigated species	:	$HNO_3, (HDO)$
line position(s) ν_0	:	1325.3160*), (1324.8088) cm^{-1}
lower state energy E''_{lst}	:	317.3, (265.2) cm^{-1}
retrieved TCA, information content	:	3.60E+16, (4.10E+21) $molec/cm^2$, 12.4, (49.5)
temperature dependence of the TCA	:	-.029, (-.079)%/K (trop), +.341, (+.054)%/K (strat)
spectral interval fitted	:	1324.500 − 1326.200 cm^{-1}

Molecule	iCode	Absorption	Molecule	iCode	Absorption
$H2O$	11	91.073%	$SO2$	91	0.067%
HDO	491	61.979%	$NO2$	101	0.015%
$CH4$	61	34.935%	$H2O2$	231	0.012%
HNO3	121	25.405%	$ClONO2$	271	0.011%
$N2O$	41	13.915%	$O3$	31	0.009%
$CH4$	6**2**	9.231%	HCN	281	0.001%
Solar(A)	—	2.409%	$H2S$	471	0.001%
Solar-sim	—	0.083%	$NH3$	111	<0.001%
$C2H2$	401	0.216%	OH	131	<0.001%
$CHF2Cl$	421	0.206%	$HO2$	221	<0.001%
$CO2$	2**3**	0.117%	$N2O5$	261	<0.001%

The spectroscopic line data is inconsistent with observations, in particular around 1325.1cm^{-1}.

NO_2, Kiruna, φ=71.68^o, OPD=257cm, FoV=4.06$mrad$, boxcar apod.

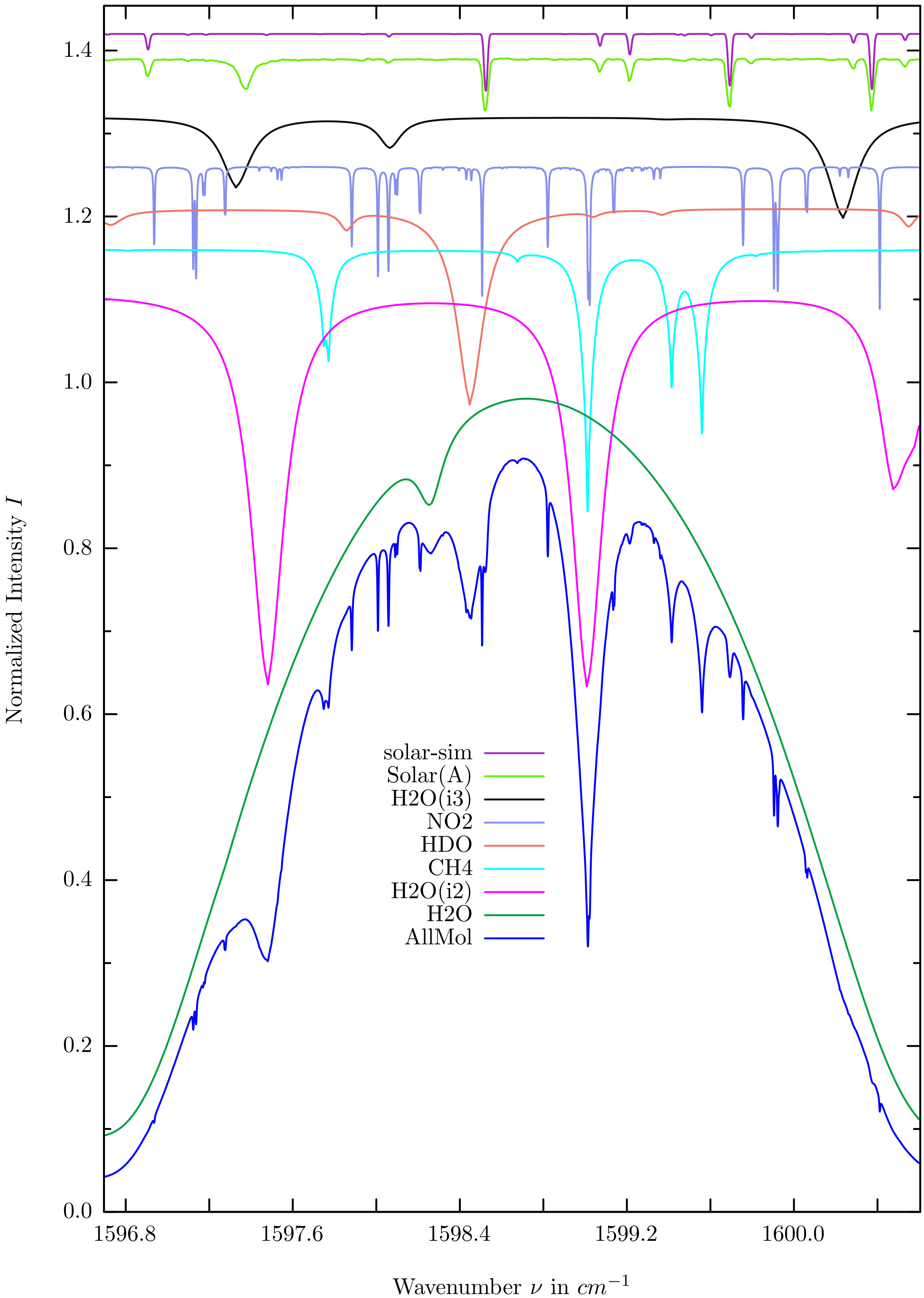

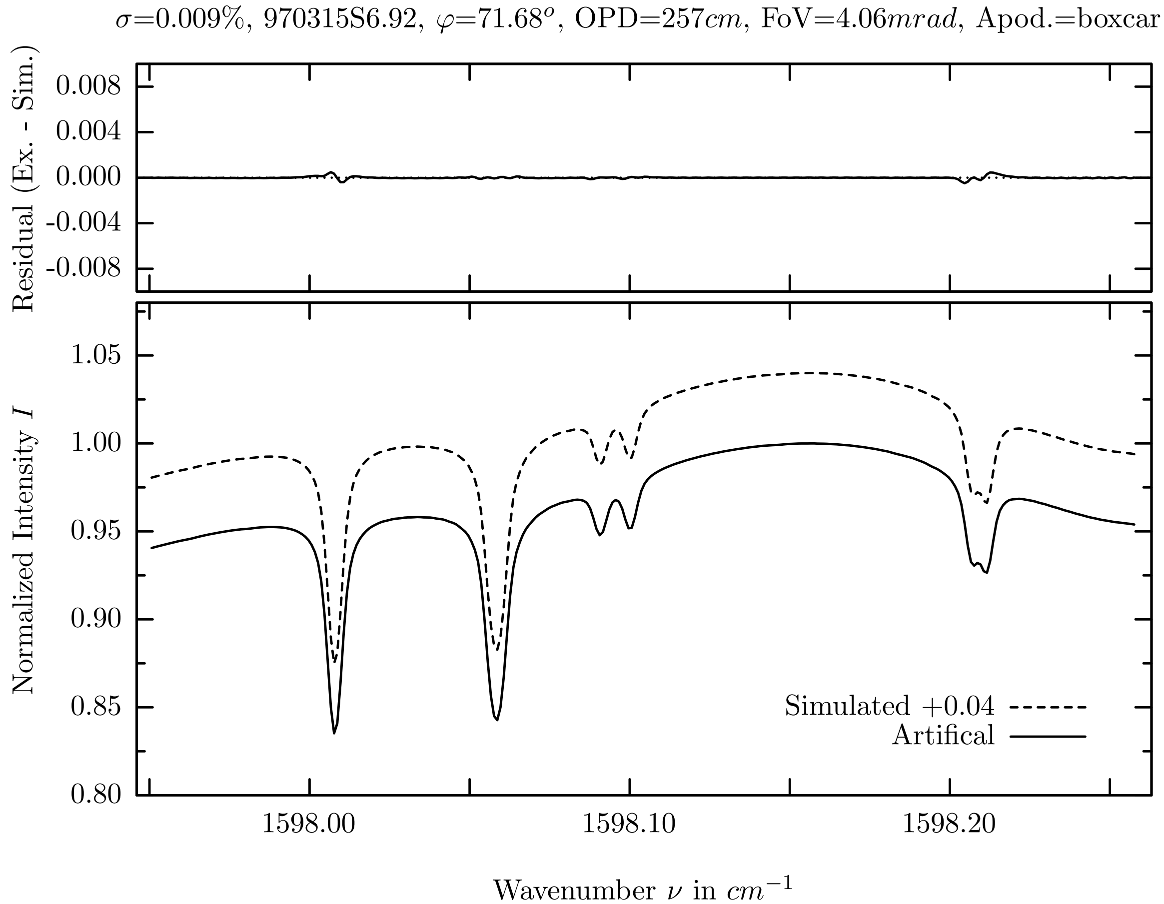

investigated species	:	NO_2
line position(s) ν_0	:	1598.0059, 1598.0557 cm^{-1}
lower state energy E''_{lst}	:	207.9, 199.7 cm^{-1}
retrieved TCA, information content	:	2.26E+15 $molec/cm^2$, 1334.7, 1347.3
temperature dependence of the TCA	:	-0.155%/K (trop), -0.075%/K (strat)
location, date, solar zenith angle	:	Kiruna, 15/Mar/97, 71.68^o
spectral interval fitted	:	1597.950 – 1598.258 cm^{-1}

Molecule	iCode	Absorption	Molecule	iCode	Absorption
H2O	11	99.880%	Solar-sim	—	6.903%
H2O	**12**	47.716%	*N2O*	41	0.017%
CH4	61	31.871%	*NH3*	111	0.015%
HDO	491	23.735%	*O2*	71	0.001%
NO2	101	19.296%	*NO*	81	<0.001%
H2O	**13**	12.201%	*OH*	131	<0.001%
Solar(A)	—	6.254%	*H2O2*	231	<0.001%

Note: This is a retrieval from a **theoretical** spectrum. Unfortunately no observations were available due to optical bandfilter restrictions.

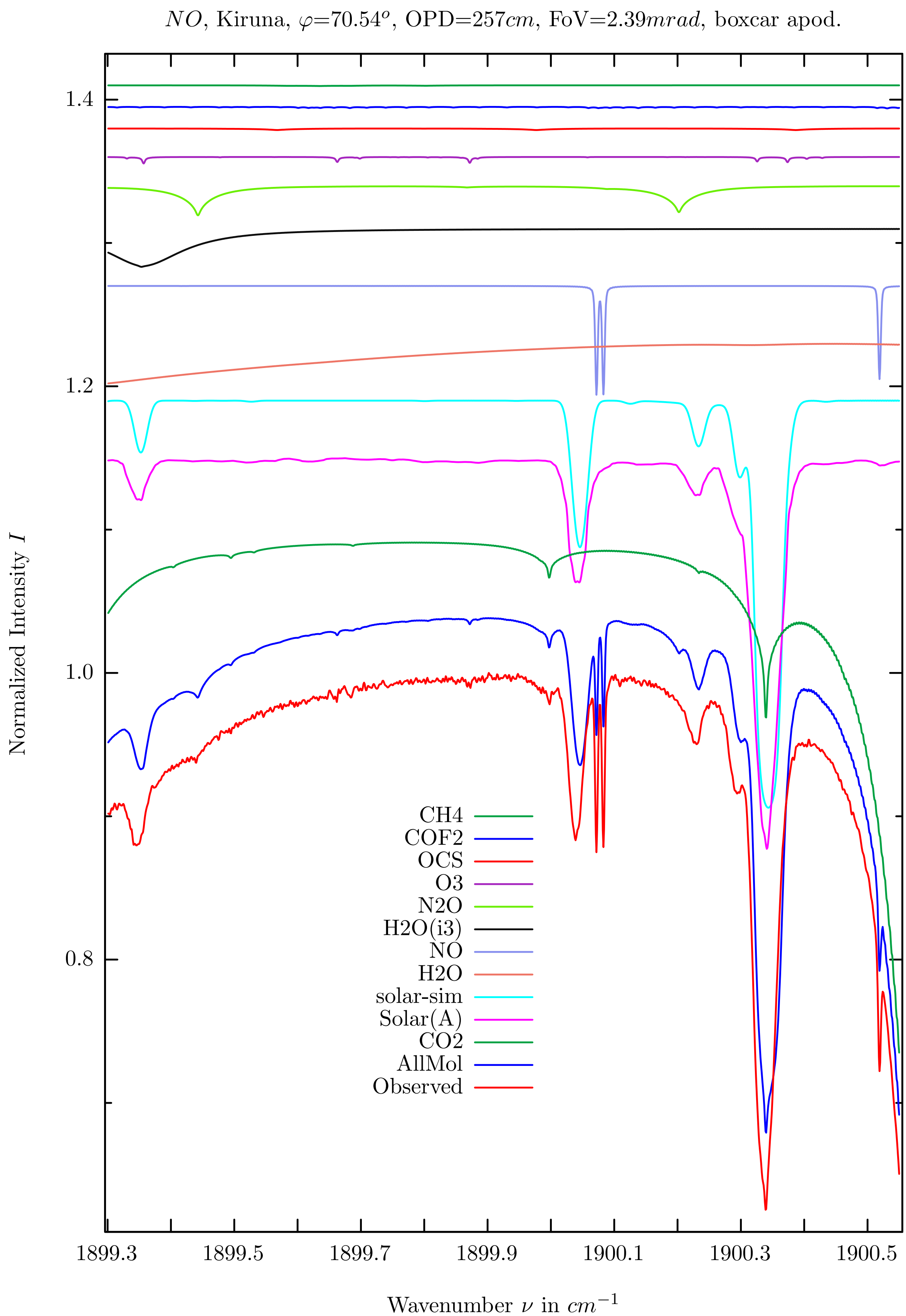

NO, Kiruna, φ=70.54°, OPD=257cm, FoV=2.39mrad, boxcar apod.
Normalized Intensity I
Wavenumber ν in cm⁻¹
1.4
1.2
1.0
0.8
1899.3
1899.5
1899.7
1899.9
1900.1
1900.3
1900.5
CH4
COF2
OCS
O3
N2O
H2O(i3)
NO
H2O
solar-sim
Solar(A)
CO2
AllMol
Observed

σ=0.202%, 970315S5.90, φ=70.54°, OPD=257cm, FoV=2.39mrad, Apod.=boxcar

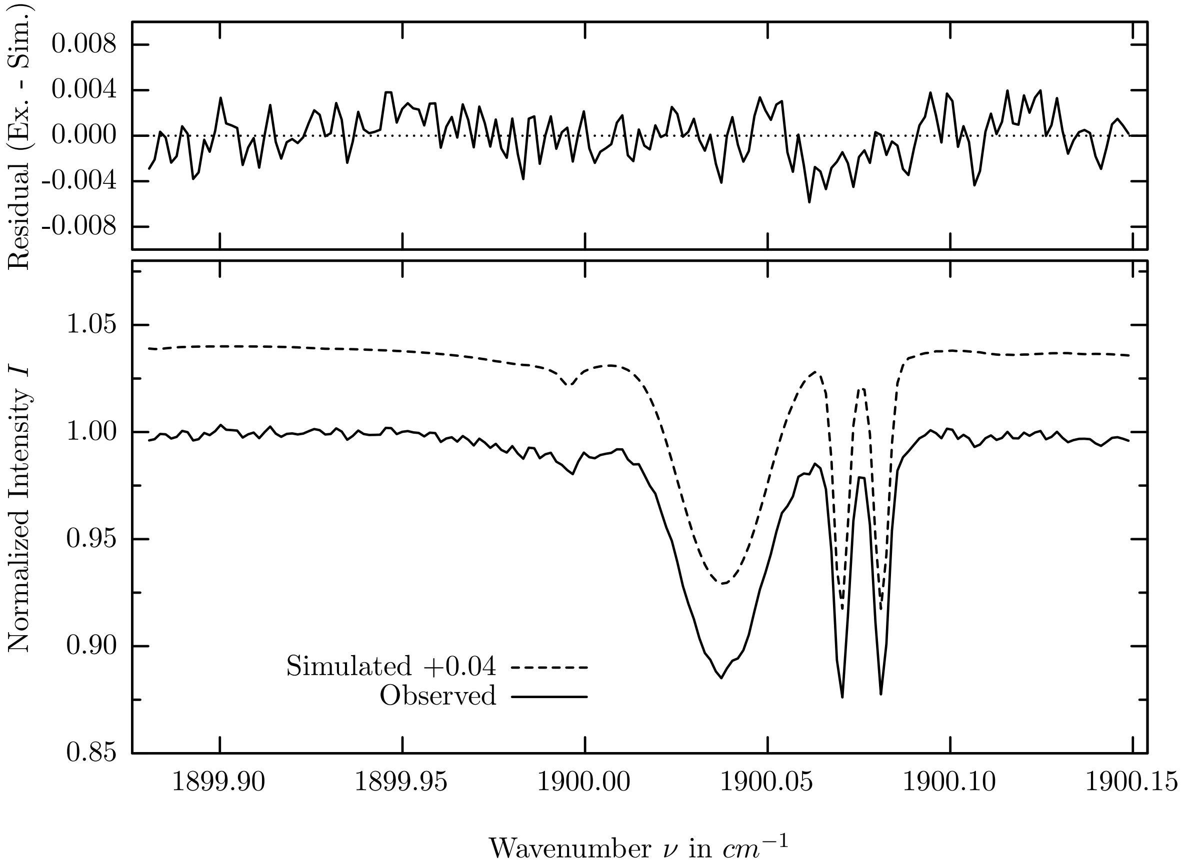

investigated species	:	NO
line position(s) ν_0	:	1900.0706*), 1900.0816*) cm^{-1}
lower state energy E''_{lst}	:	80.2, 80.3 cm^{-1}
retrieved TCA, information content	:	3.60E+15 $molec/cm^2$, 60.6
temperature dependence of the TCA	:	-0.035%/K (trop), +0.114%/K (strat)
location, date, solar zenith angle	:	Kiruna, 15/Mar/97, 70.54^o
spectral interval fitted	:	1899.880 – 1900.150 cm^{-1}

Molecule	iCode	Absorption	Molecule	iCode	Absorption
$CO2$	21	37.616%	$COF2$	361	0.110%
Solar(A)	—	27.271%	$CH4$	61	0.050%
Solar-sim	—	28.404%	$COCLF$	371	0.019%
$H2O$	11	16.641%	$C2H2$	401	0.001%
NO	81	7.790%	CO	51	<0.001%
$H2O$	1**3**	2.667%	$NH3$	111	<0.001%
$N2O$	41	2.081%	OH	131	<0.001%
$O3$	31	0.468%	HDO	491	<0.001%
OCS	191	0.122%			

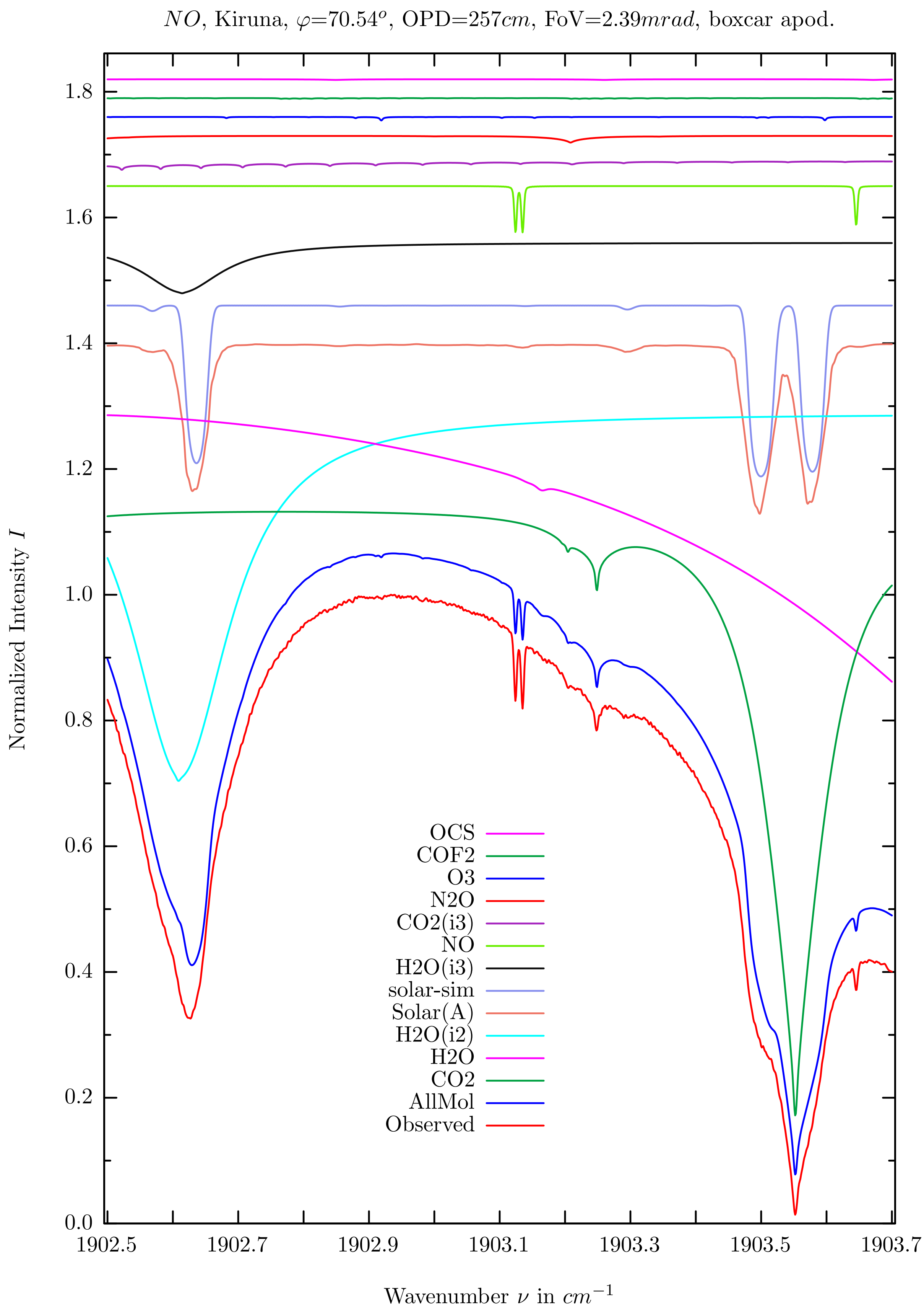

NO, Kiruna, φ=70.54^o, OPD=257cm, FoV=2.39$mrad$, boxcar apod.
Normalized Intensity I
Wavenumber ν in cm^{-1}
0.0
0.2
0.4
0.6
0.8
1.0
1.2
1.4
1.6
1.8
1902.5
1902.7
1902.9
1903.1
1903.3
1903.5
1903.7
OCS
COF2
O3
N2O
CO2(i3)
NO
H2O(i3)
solar-sim
Solar(A)
H2O(i2)
H2O
CO2
AllMol
Observed

σ=0.227%, 970315S5.90, φ=70.54^o, OPD=257cm, FoV=2.39$mrad$, Apod.=boxcar

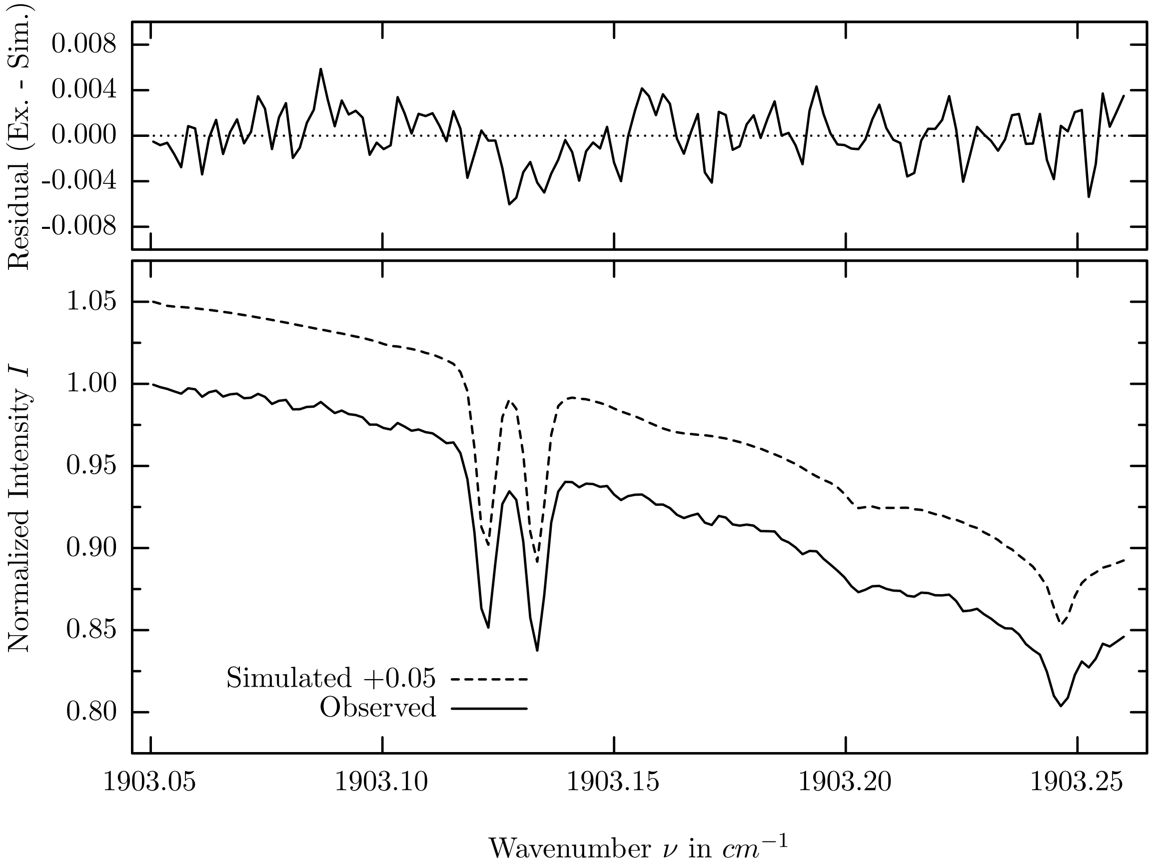

investigated species	:	NO
line position(s) ν_0	:	1903.1335$^{*)}$ cm^{-1}
lower state energy E''_{lst}	:	105.4 cm^{-1}
retrieved TCA, information content	:	3.52E+15 $molec/cm^2$, 49.0
temperature dependence of the TCA	:	-0.018%/K (trop), +0.017%/K (strat)
location, date, solar zenith angle	:	Kiruna, 15/Mar/97, 70.54^o
spectral interval fitted	:	1903.050 – 1903.260 cm^{-1}

Molecule	iCode	Absorption	Molecule	iCode	Absorption
$CO2$	21	97.391%	$COF2$	361	0.126%
$H2O$	11	68.030%	OCS	191	0.118%
$H2O$	1**2**	58.627%	$COCLF$	371	0.014%
Solar(A)	—	27.125%	$CH4$	61	0.001%
Solar-sim	—	27.188%	$C2H2$	401	0.001%
$H2O$	1**3**	8.048%	CO	51	<0.001%
NO	81	7.559%	$NH3$	111	<0.001%
$CO2$	2**3**	1.431%	OH	131	<0.001%
$N2O$	41	1.080%	HDO	491	<0.001%
$O3$	31	0.581%			

NO, Kiruna, φ=70.54^o, OPD=257cm, FoV=2.39$mrad$, boxcar apod.

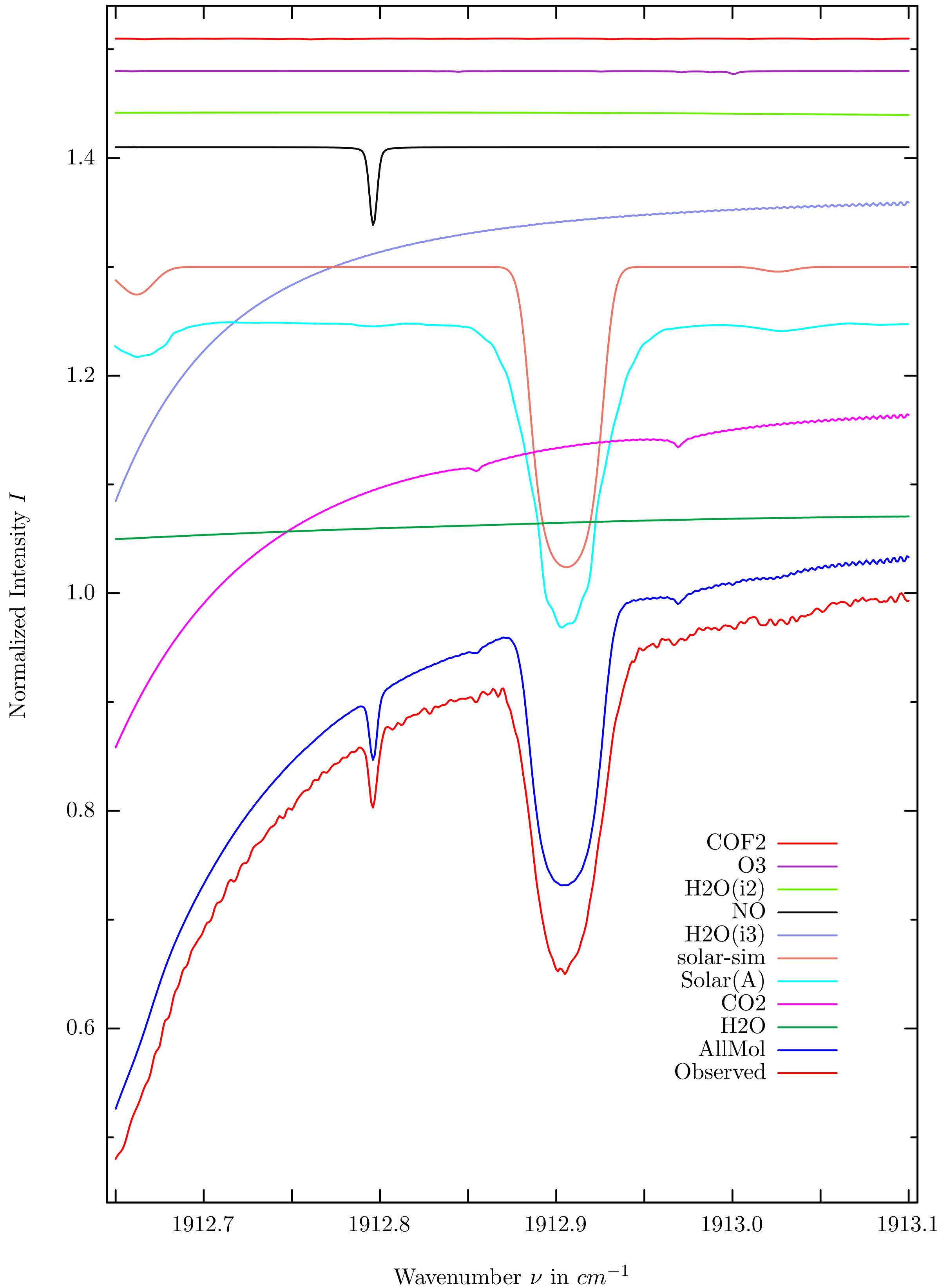

σ=0.235%, 970315S5.90, φ=70.54^o, OPD=257cm, FoV=2.39$mrad$, Apod.=boxcar

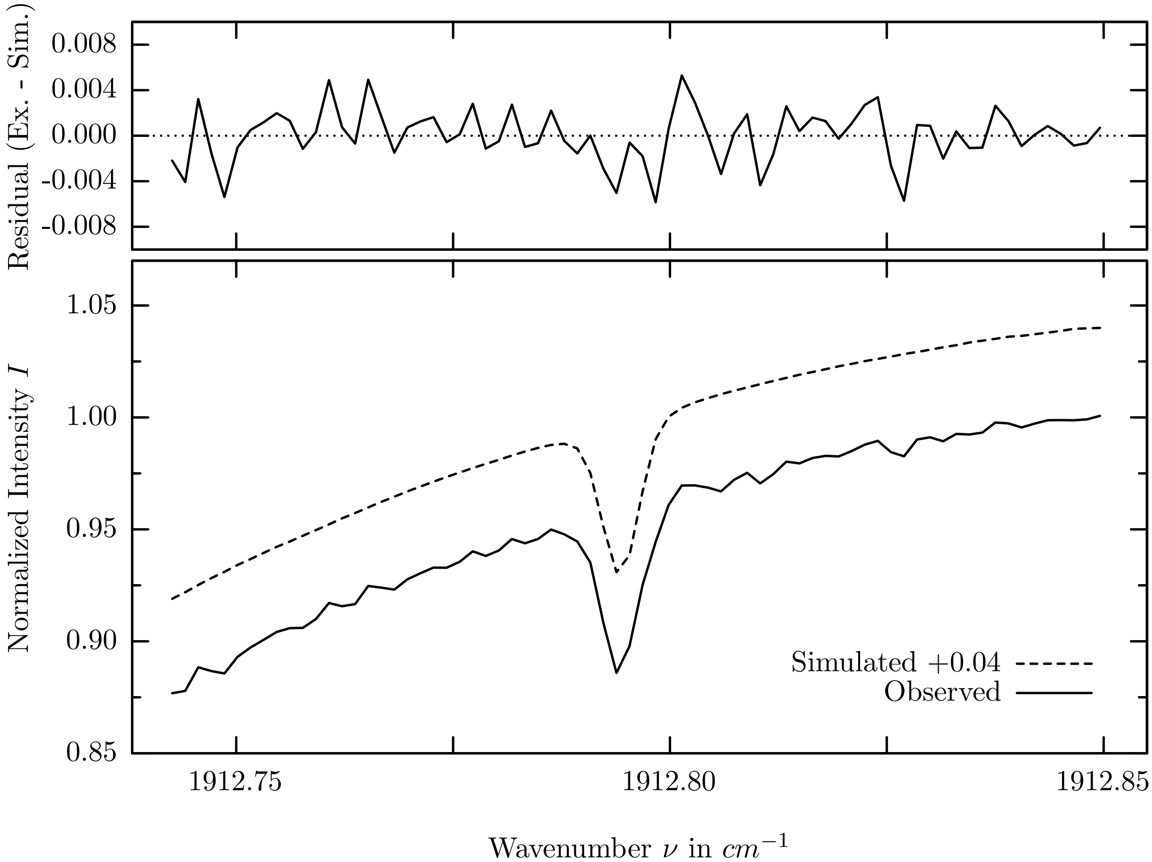

investigated species	:	NO
line position(s) ν_0	:	1912.7947$^{*)}$ cm^{-1}
lower state energy E''_{lst}	:	326.0 cm^{-1}
retrieved TCA, information content	:	3.56E+15 $molec/cm^2$, 29.8
temperature dependence of the TCA	:	-0.022%/K (trop), -0.443%/K (strat)
location, date, solar zenith angle	:	Kiruna, 15/Mar/97, 70.54^o
spectral interval fitted	:	1912.742 – 1912.850 cm^{-1}

Molecule	iCode	Absorption	Molecule	iCode	Absorption
$H2O$	11	52.022%	$N2O$	41	0.036%
$CO2$	21	33.804%	OCS	191	0.025%
Solar(A)	—	28.150%	$CH4$	61	0.005%
Solar-sim	—	27.606%	CO	51	<0.001%
$H2O$	1**3**	28.125%	$NH3$	111	<0.001%
NO	81	7.277%	OH	131	<0.001%
$H2O$	1**2**	1.057%	$COCLF$	371	<0.001%
$O3$	31	0.294%	$C2H2$	401	<0.001%
$COF2$	361	0.104%	HDO	491	<0.001%

COF_2, Kiruna, φ=70.54^o, OPD=257cm, FoV=2.39$mrad$, boxcar apod.

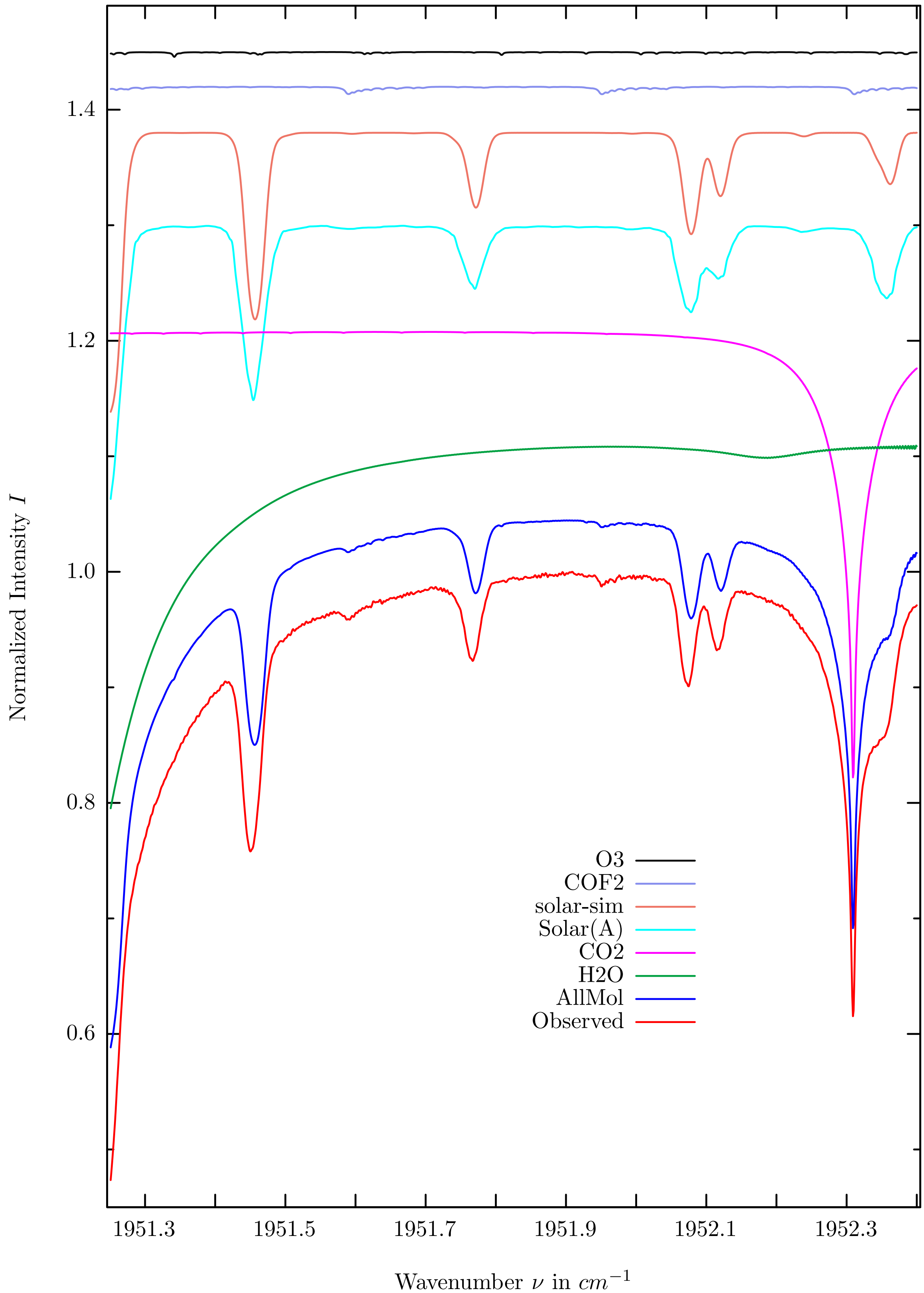

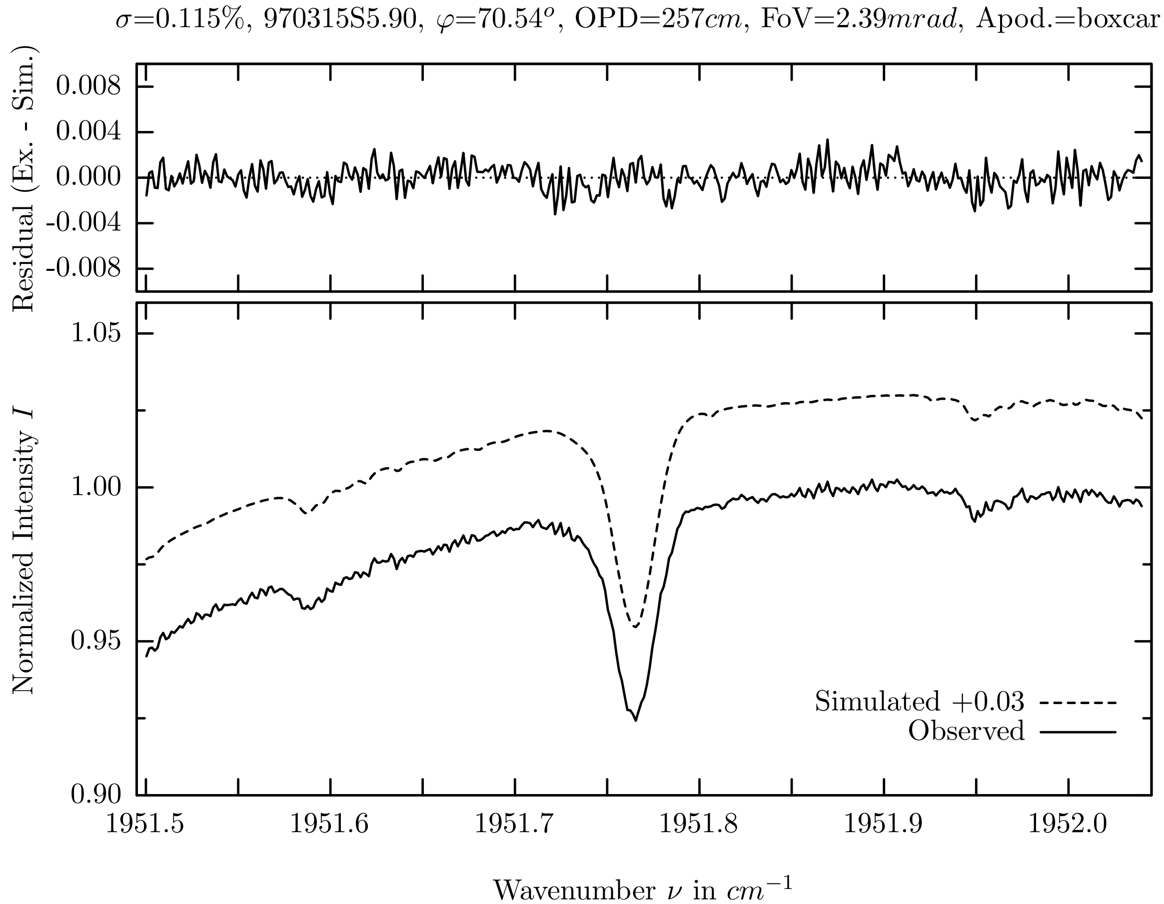

investigated species	:	COF_2
line position(s) ν_0	:	1951.5865*), 1951.9479*) cm^{-1}
lower state energy E''_{lst}	:	63.4, 70.6 cm^{-1}
retrieved TCA, information content	:	3.96E+14 $molec/cm^2$, 7.7, 6.9
temperature dependence of the TCA	:	-0.019%/K (trop), -0.082%/K (strat)
location, date, solar zenith angle	:	Kiruna, 15/Mar/97, 70.54^o
spectral interval fitted	:	1951.500 – 1952.040 cm^{-1}

Molecule	iCode	Absorption	Molecule	iCode	Absorption
$H2O$	11	40.130%	$N2O$	41	0.034%
$CO2$	21	39.278%	$CH4$	61	0.001%
Solar(A)	—	23.694%	$C2H2$	401	0.001%
Solar-sim	—	23.994%	CO	51	<0.001%
COF2	361	0.663%	$NH3$	111	<0.001%
$O3$	31	0.441%	OH	131	<0.001%
NO	81	0.043%	HI	171	<0.001%

COF_2, Kiruna, φ=70.54^o, OPD=257cm, FoV=2.39$mrad$, boxcar apod.

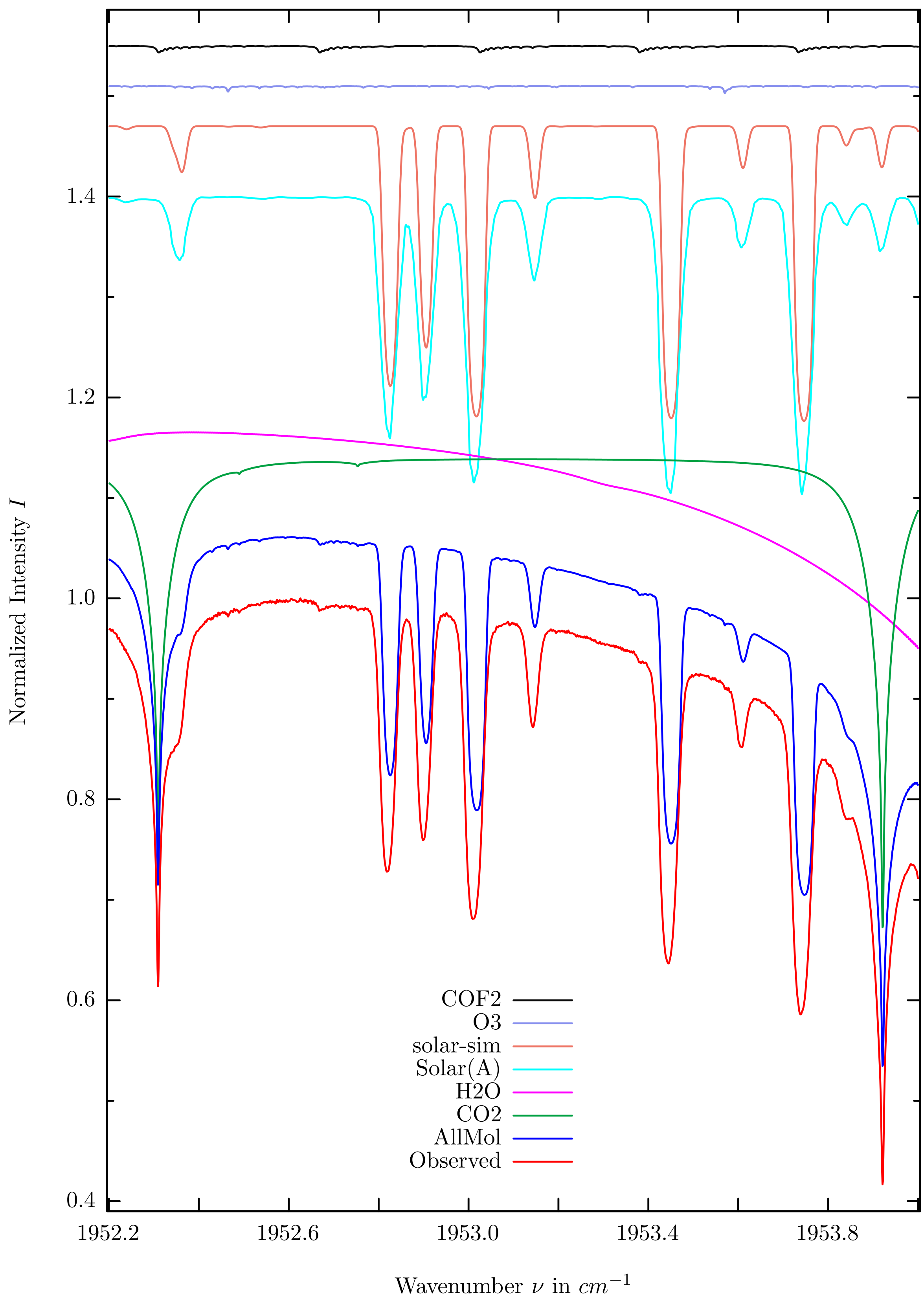

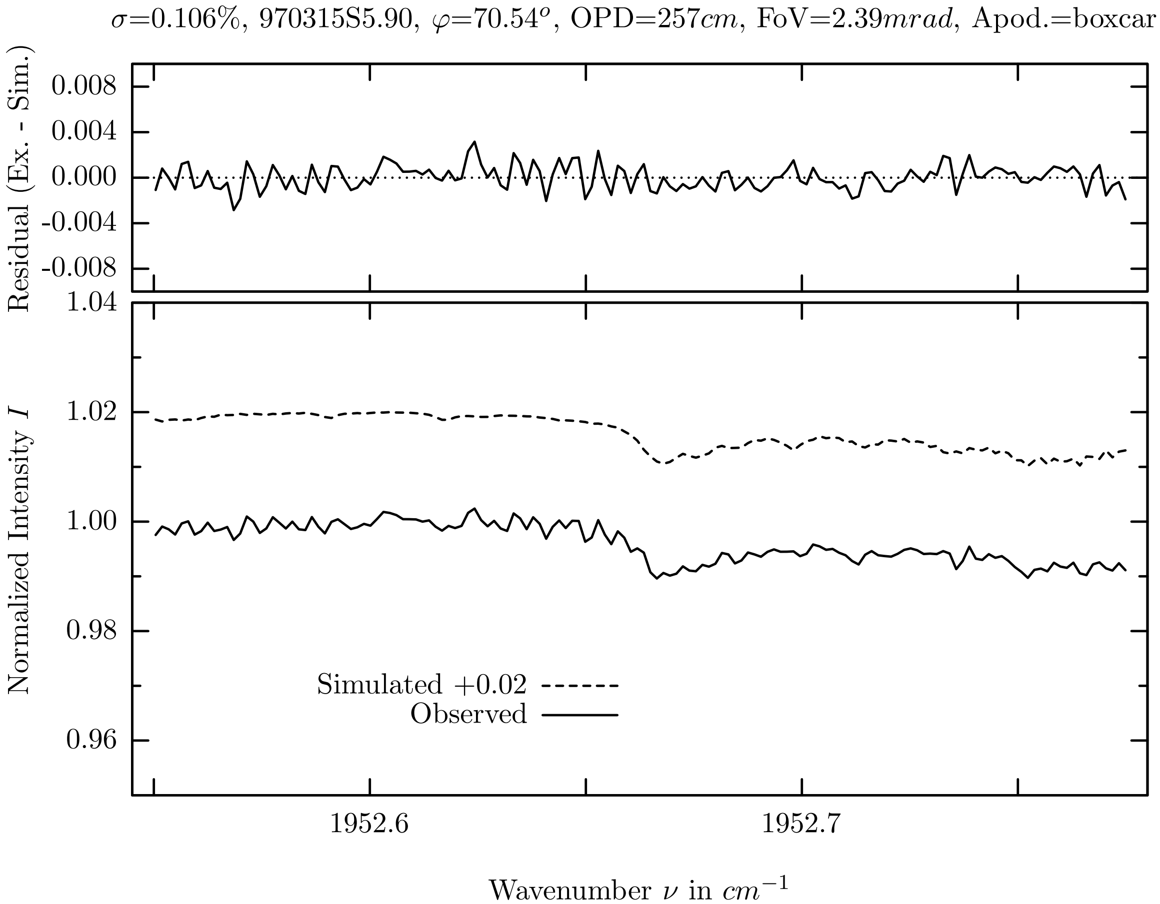

investigated species	:	COF_2
line position(s) ν_0	:	1952.6658*) cm^{-1}
lower state energy E''_{lst}	:	86.3 cm^{-1}
retrieved TCA, information content	:	3.39E+14 $molec/cm^2$, 8.9
temperature dependence of the TCA	:	-0.022%/K (trop), -0.317%/K (strat)
location, date, solar zenith angle	:	Kiruna, 15/Mar/97, 70.54^o
spectral interval fitted	:	1952.550 – 1952.775 cm^{-1}

Molecule	iCode	Absorption	Molecule	iCode	Absorption
CO2	21	47.427%	*CH4*	61	0.001%
H2O	11	30.773%	*C2H2*	401	0.001%
Solar(A)	—	29.621%	*CO*	51	<0.001%
Solar-sim	—	29.347%	*NH3*	111	<0.001%
O3	31	0.728%	*OH*	131	<0.001%
COF2	361	0.669%	*HI*	171	<0.001%
N2O	41	0.039%	*OCS*	19**3**	<0.001%
NO	81	0.017%			

H_2O, Kiruna, φ=70.54^o, OPD=257cm, FoV=2.39$mrad$, boxcar apod.

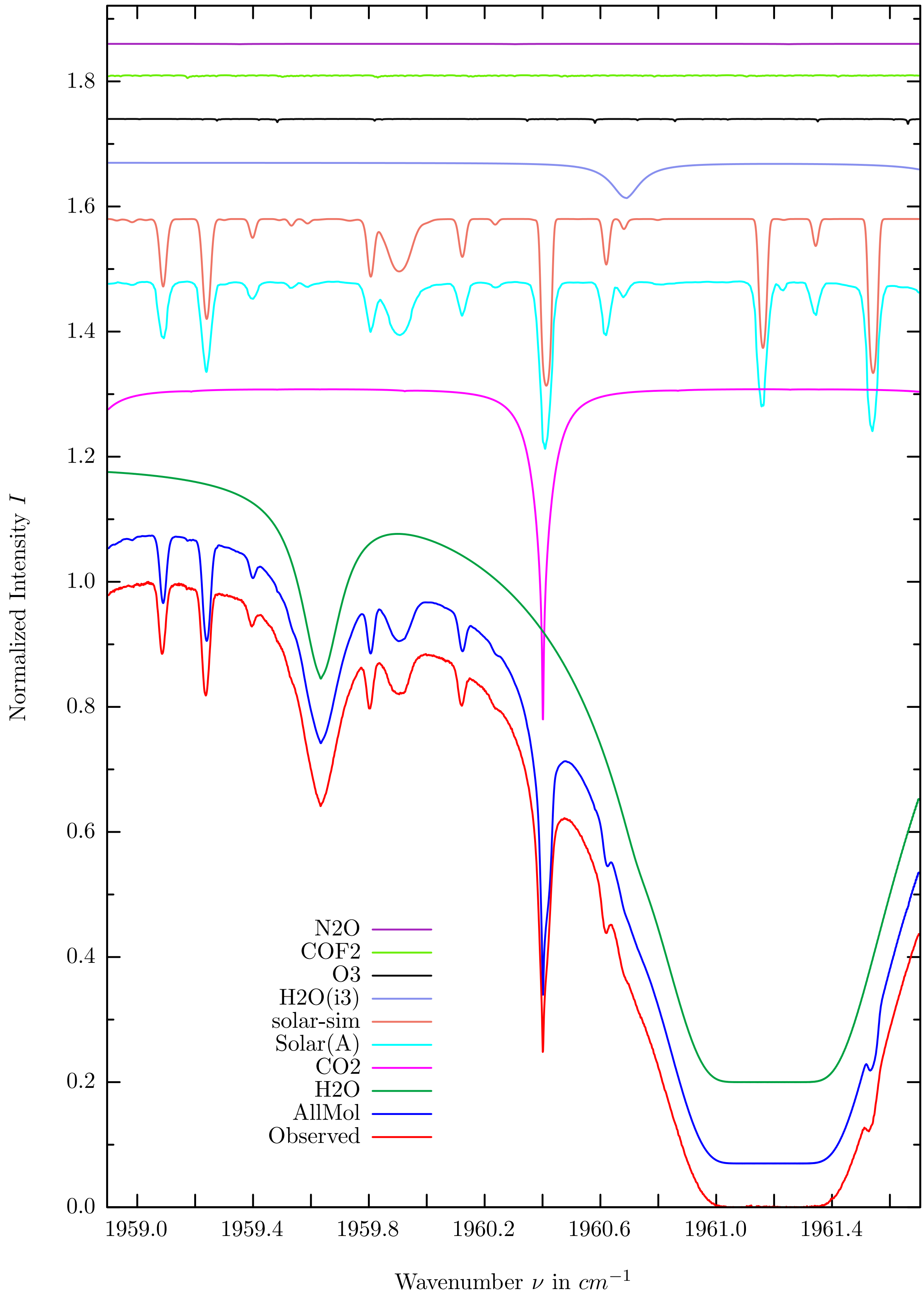

σ=0.217%, 970315S5.90, φ=70.54^o, OPD=257cm, FoV=2.39$mrad$, Apod.=boxcar

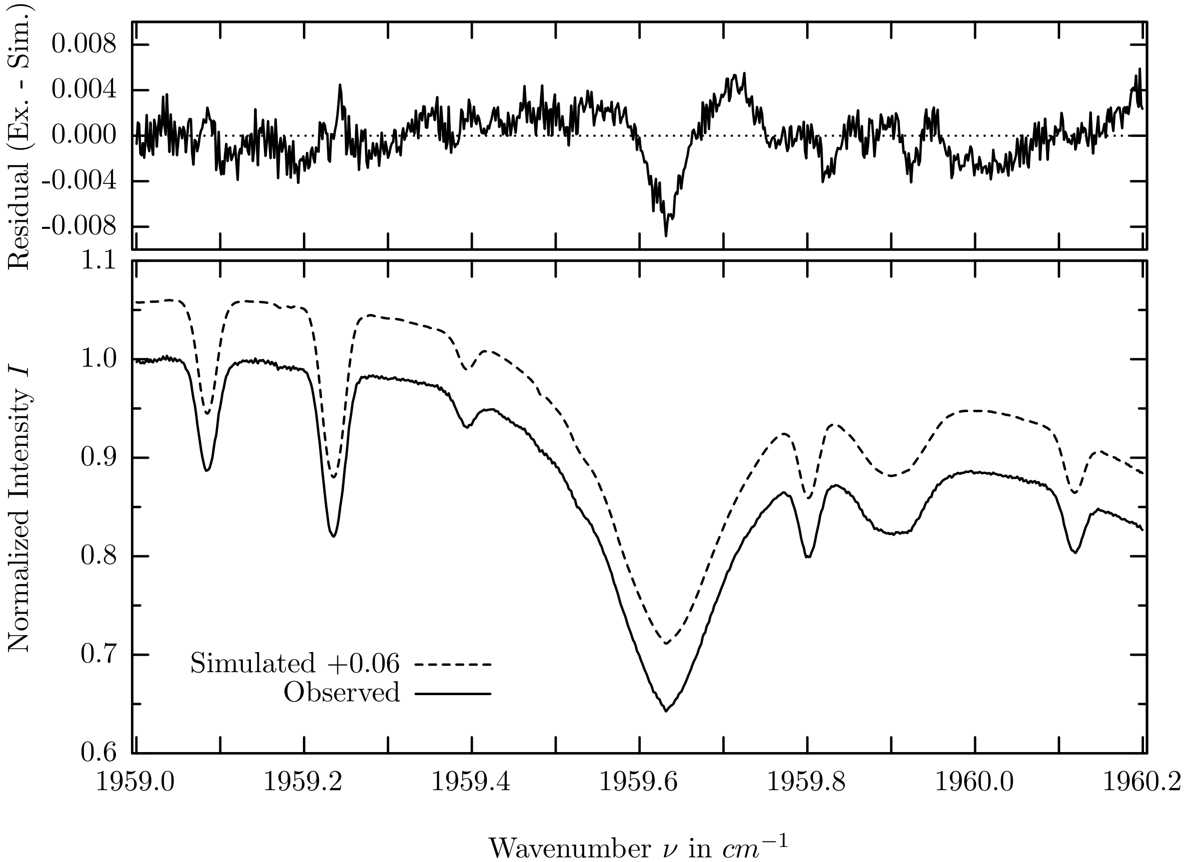

investigated species	:	H_2O
line position(s) ν_0	:	1959.6324 cm^{-1}
lower state energy E''_{lst}	:	446.5 cm^{-1}
retrieved TCA, information content	:	5.99E+21 $molec/cm^2$, 135.2
temperature dependence of the TCA	:	-0.599%/K (trop), +0.128%/K (strat)
location, date, solar zenith angle	:	Kiruna, 15/Mar/97, 70.54^o
spectral interval fitted	:	1959.000 – 1960.200 cm^{-1}

Molecule	iCode	Absorption	Molecule	iCode	Absorption
H2O	11	100.000%	*NO*	81	0.009%
CO2	21	53.800%	*CH4*	61	0.001%
Solar(A)	—	26.751%	*C2H2*	401	0.001%
Solar-sim	—	26.657%	*CO*	51	<0.001%
H2O	1**3**	5.655%	*NH3*	111	<0.001%
O3	31	0.831%	*OH*	131	<0.001%
COF2	361	0.472%	*HI*	171	<0.001%
N2O	41	0.050%	*OCS*	19**3**	<0.001%

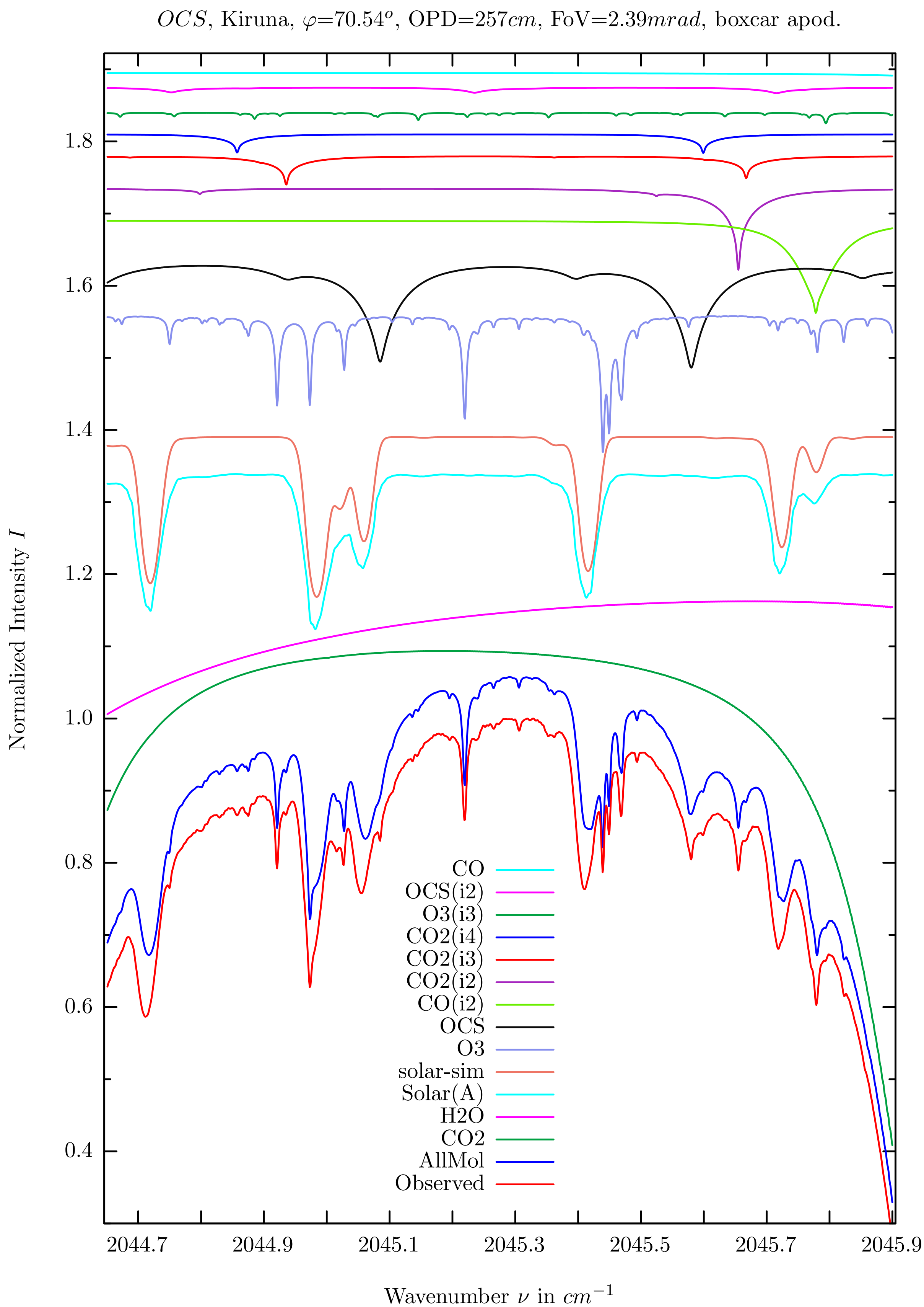

OCS, Kiruna, φ=70.54°, OPD=257cm, FoV=2.39mrad, boxcar apod.
Normalized Intensity I
Wavenumber ν in cm^-1
1.8
1.6
1.4
1.2
1.0
0.8
0.6
0.4
2044.7
2044.9
2045.1
2045.3
2045.5
2045.7
2045.9
CO
OCS(i2)
O3(i3)
CO2(i4)
CO2(i3)
CO2(i2)
CO(i2)
OCS
O3
solar-sim
Solar(A)
H2O
CO2
AllMol
Observed

σ=0.155%, 970315S5.90, φ=70.54^o, OPD=257cm, FoV=2.39$mrad$, Apod.=boxcar

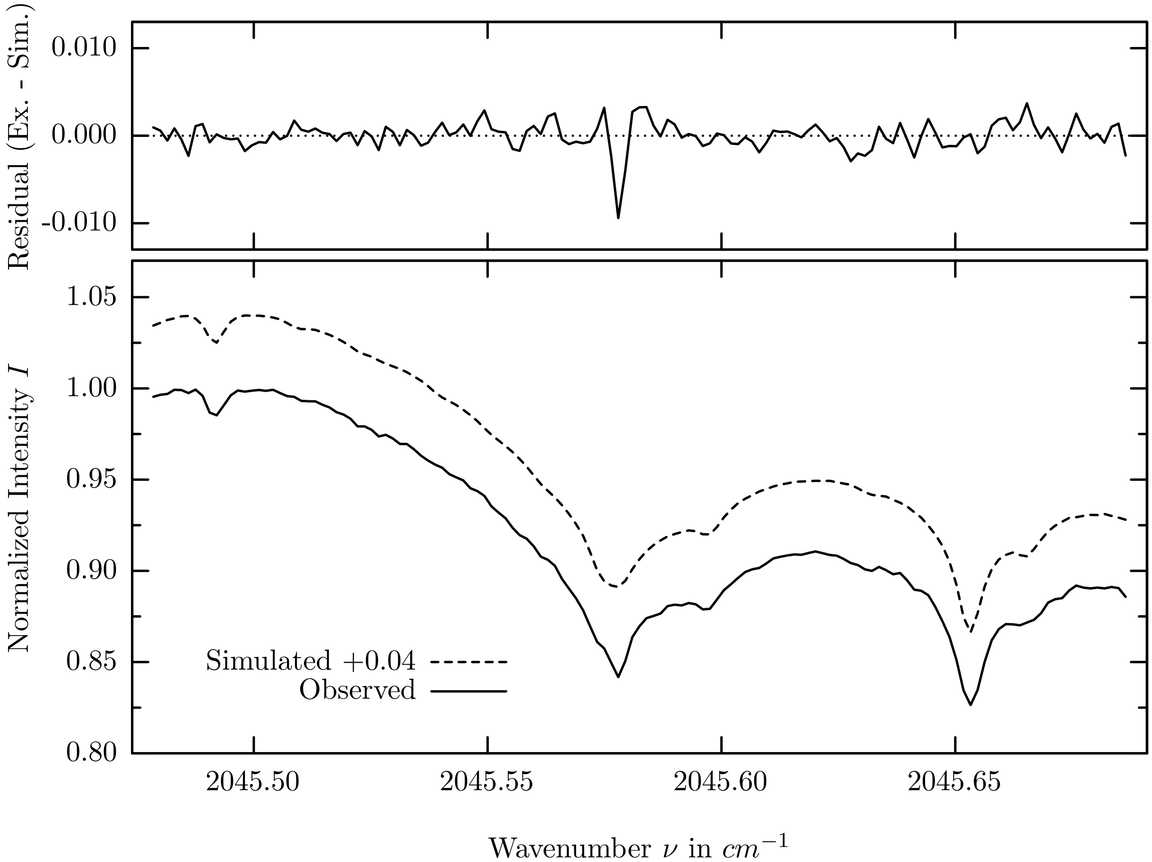

investigated species	:	OCS
line position(s) ν_0	:	2045.5785 cm^{-1}
lower state energy E''_{lst}	:	285.1 cm^{-1}
retrieved TCA, information content	:	9.87E+15 $molec/cm^2$, 67.2
temperature dependence of the TCA	:	-0.531%/K (trop), -0.030%/K (strat)
location, date, solar zenith angle	:	Kiruna, 15/Mar/97, 70.54^o
spectral interval fitted	:	2045.477 – 2045.687 cm^{-1}

Molecule	iCode	Absorption	Molecule	iCode	Absorption
$CO2$	21	74.621%	OCS	19**2**	0.821%
$H2O$	11	22.838%	CO	51	0.250%
Solar(A)	—	21.623%	$N2O$	41	<0.001%
Solar-sim	—	22.149%	$CH4$	61	<0.001%
$O3$	31	19.651%	NO	81	<0.001%
OCS	191	15.356%	$NH3$	111	<0.001%
CO	5**2**	12.825%	OH	131	<0.001%
$CO2$	**22**	11.402%	HI	171	<0.001%
$CO2$	**23**	4.051%	$C2H2$	401	<0.001%
$CO2$	**24**	2.628%	$N2$	411	<0.001%
$O3$	**33**	1.511%			

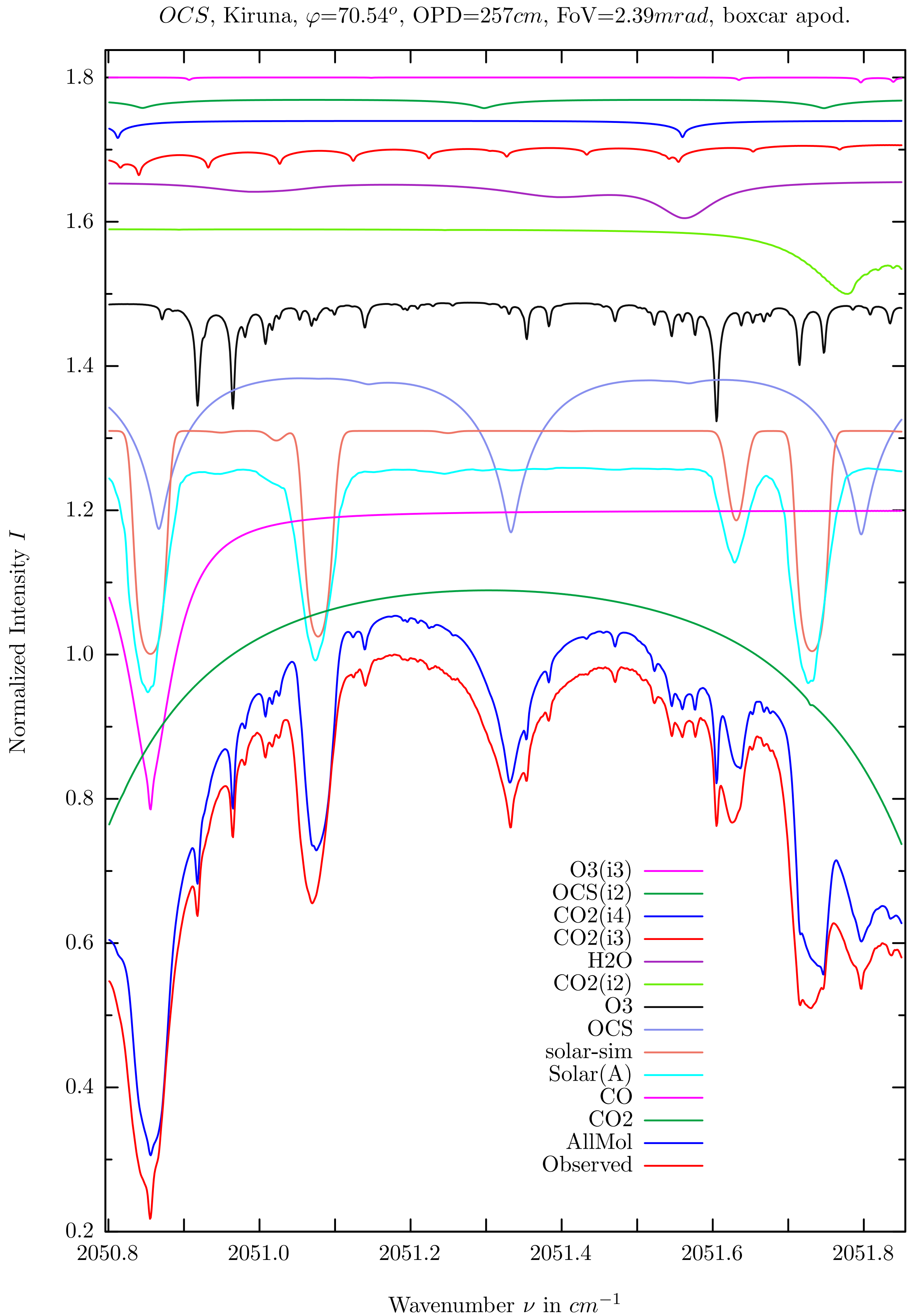
OCS, Kiruna, φ=70.54^o, OPD=257cm, FoV=2.39$mrad$, boxcar apod.
Normalized Intensity I
Wavenumber ν in cm^{-1}
1.8
1.6
1.4
1.2
1.0
0.8
0.6
0.4
0.2
2050.8
2051.0
2051.2
2051.4
2051.6
2051.8
O3(i3)
OCS(i2)
CO2(i4)
CO2(i3)
H2O
CO2(i2)
O3
OCS
solar-sim
Solar(A)
CO
CO2
AllMol
Observed

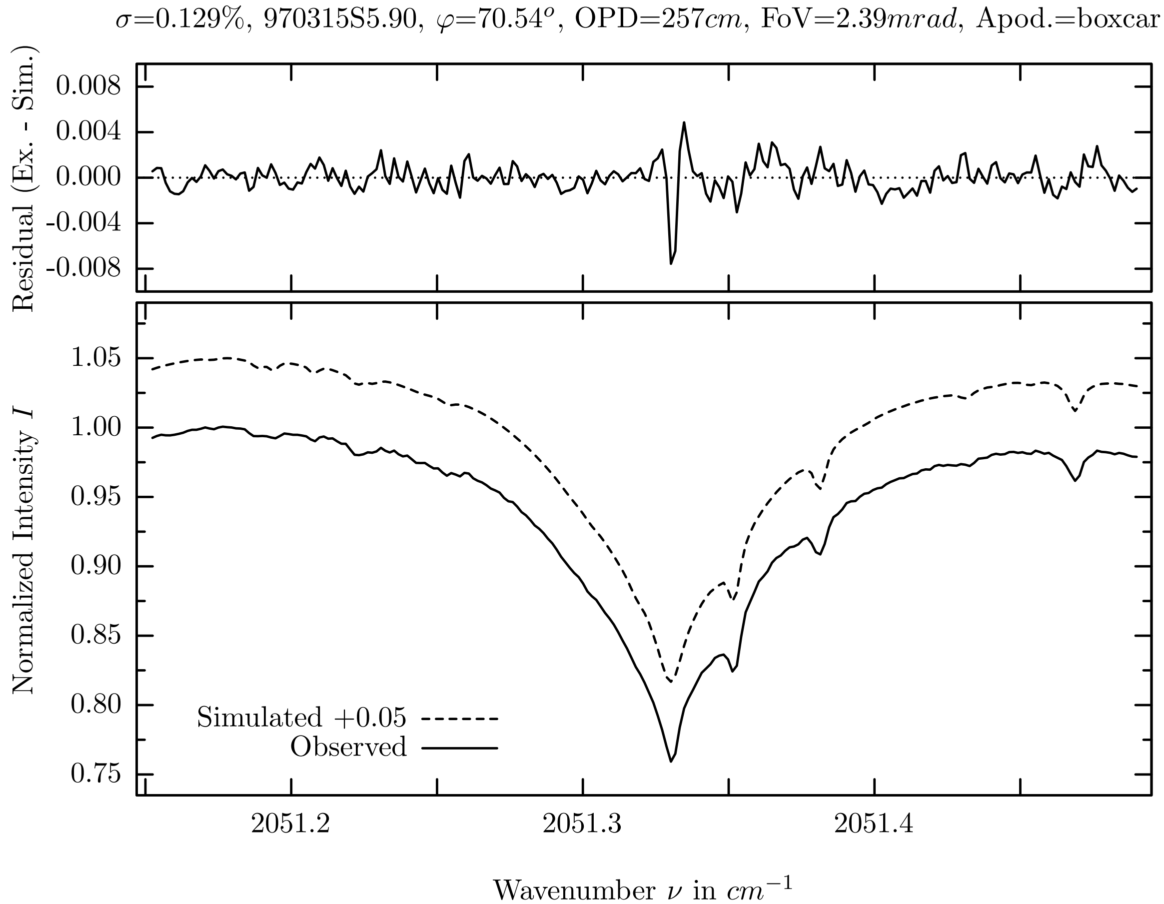

investigated species	:	OCS
line position(s) ν_0	:	2051.3313 cm^{-1}
lower state energy E''_{lst}	:	131.8 cm^{-1}
retrieved TCA, information content	:	9.55E+15 $molec/cm^2$, 180.4
temperature dependence of the TCA	:	+0.032%/K (trop), -0.016%/K (strat)
location, date, solar zenith angle	:	Kiruna, 15/Mar/97, 70.54^o
spectral interval fitted	:	2051.152 – 2051.490 cm^{-1}

Molecule	iCode	Absorption	Molecule	iCode	Absorption
$CO2$	21	44.347%	OCS	19**2**	1.256%
CO	51	41.604%	$O3$	**33**	0.713%
Solar(A)	—	31.227%	$N2O$	41	0.001%
Solar-sim	—	30.918%	$CH4$	61	<0.001%
OCS	191	24.354%	NO	81	<0.001%
$O3$	31	16.886%	$NH3$	111	<0.001%
$CO2$	2**2**	9.011%	OH	131	<0.001%
$H2O$	11	5.477%	HI	171	<0.001%
$CO2$	2**3**	4.579%	$C2H2$	401	<0.001%
$CO2$	2**4**	2.424%	$N2$	411	<0.001%

OCS, Kiruna, φ=70.54^o, OPD=257cm, FoV=2.39$mrad$, boxcar apod.

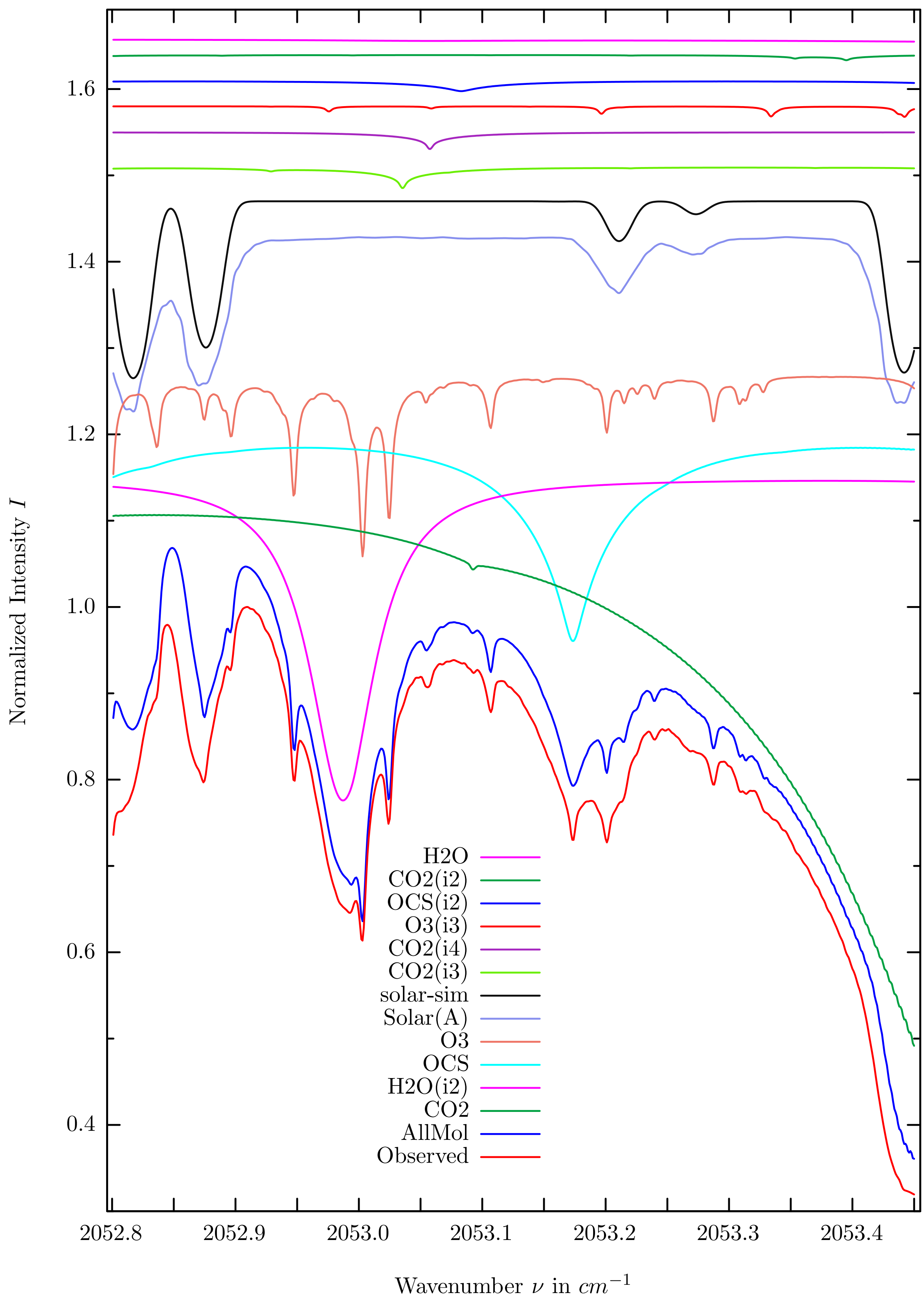

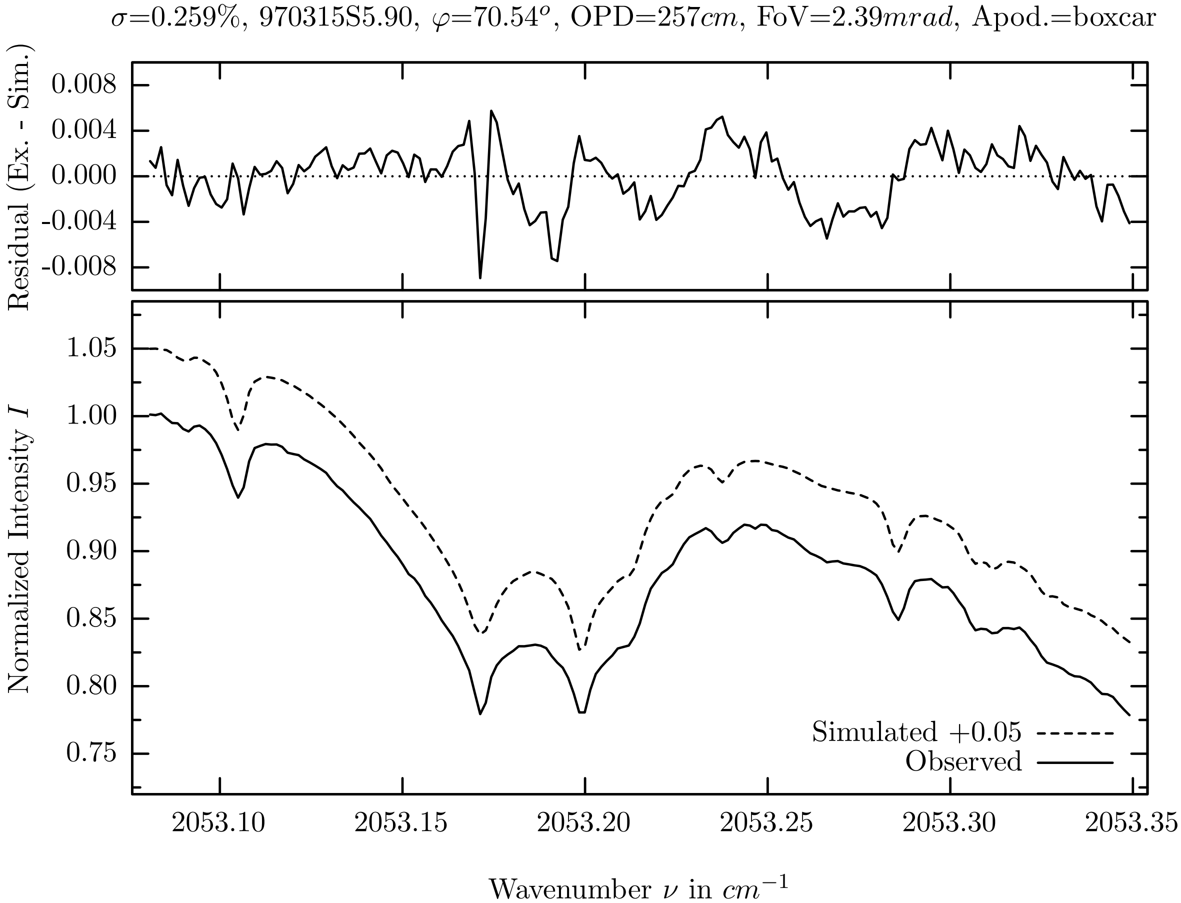

investigated species	:	OCS
line position(s) ν_0	:	2053.1714 cm^{-1}
lower state energy E''_{lst}	:	93.7 cm^{-1}
retrieved TCA, information content	:	1.04E+16 $molec/cm^2$, 71.9
temperature dependence of the TCA	:	+0.005%/K (trop), -0.154%/K (strat)
location, date, solar zenith angle	:	Kiruna, 15/Mar/97, 70.54^o
spectral interval fitted	:	2053.080 – 2053.350 cm^{-1}

Molecule	iCode	Absorption	Molecule	iCode	Absorption
$CO2$	21	70.424%	$H2O$	11	0.507%
$H2O$	1**2**	37.423%	CO	51	0.037%
OCS	191	24.961%	$N2O$	41	0.001%
$O3$	31	21.463%	$CH4$	61	<0.001%
Solar(A)	—	20.355%	NO	81	<0.001%
Solar-sim	—	20.504%	$NH3$	111	<0.001%
$CO2$	2**3**	2.511%	OH	131	<0.001%
$CO2$	2**4**	1.977%	HI	171	<0.001%
$O3$	3**3**	1.244%	$C2H2$	401	<0.001%
OCS	19**2**	1.242%	$N2$	411	<0.001%
$CO2$	2**2**	0.662%			

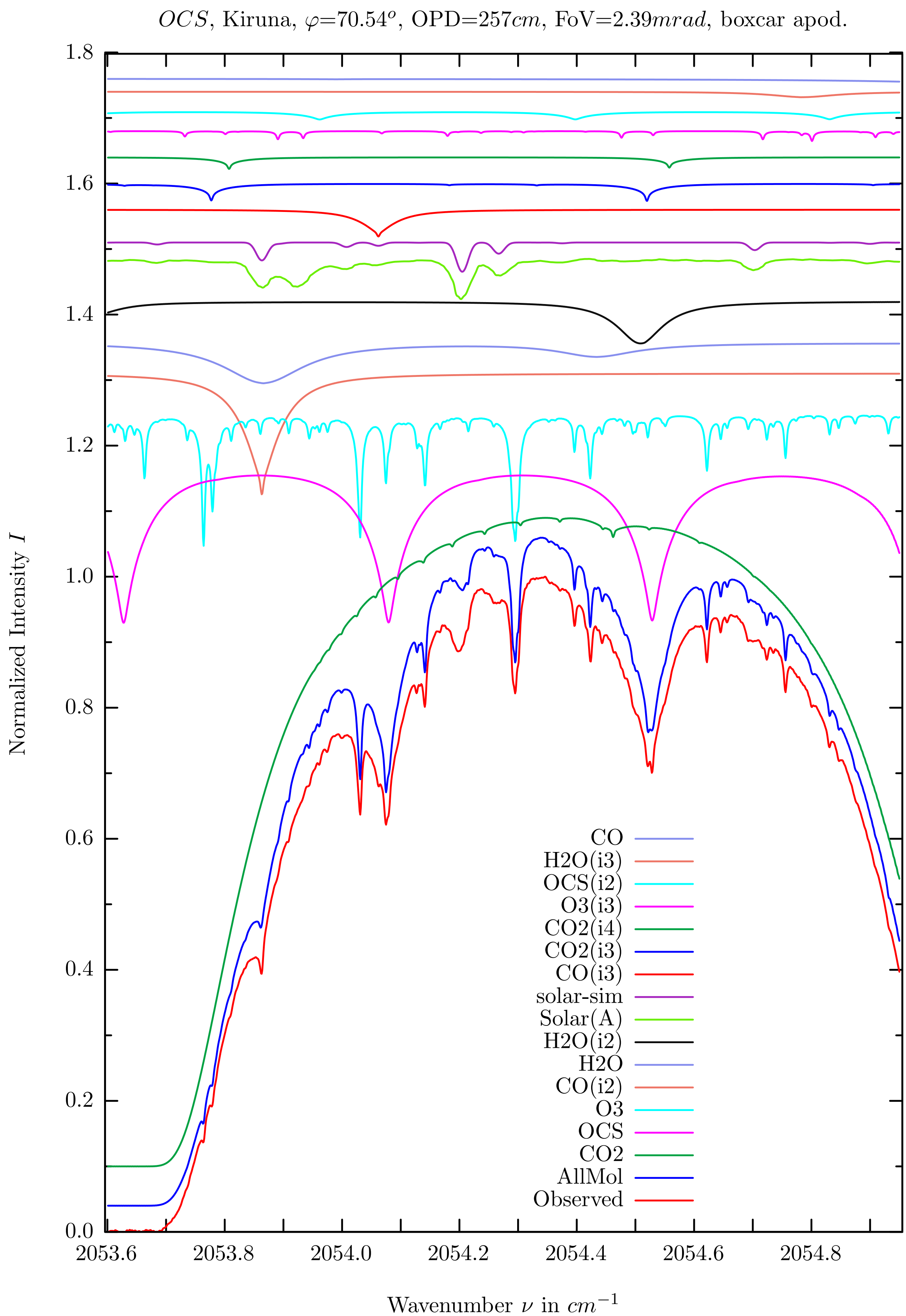

OCS, Kiruna, φ=70.54^o, OPD=257cm, FoV=2.39$mrad$, boxcar apod.
Normalized Intensity I
Wavenumber ν in cm^{-1}
0.0
0.2
0.4
0.6
0.8
1.0
1.2
1.4
1.6
1.8
2053.6
2053.8
2054.0
2054.2
2054.4
2054.6
2054.8
CO
H2O(i3)
OCS(i2)
O3(i3)
CO2(i4)
CO2(i3)
CO(i3)
solar-sim
Solar(A)
H2O(i2)
H2O
CO(i2)
O3
OCS
CO2
AllMol
Observed

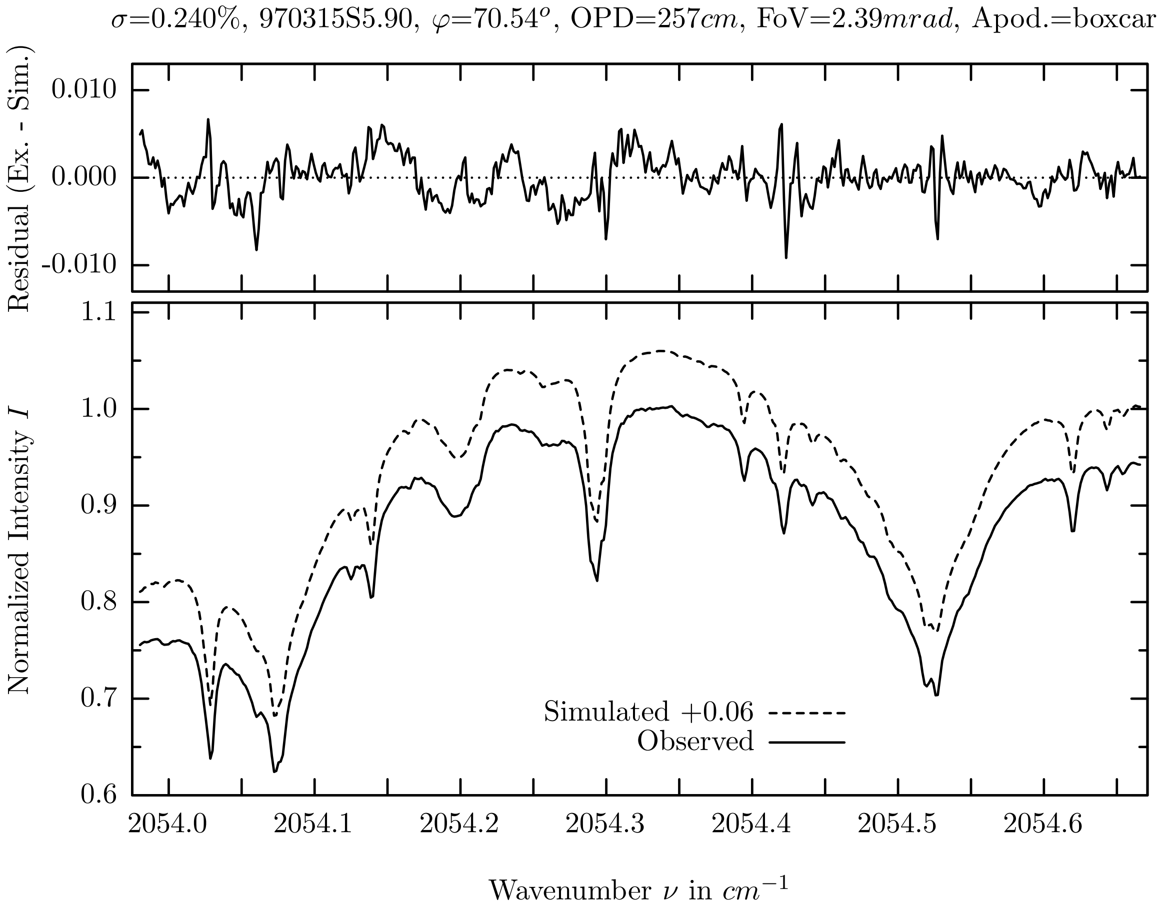

investigated species	:	OCS
line position(s) ν_0	:	2054.0778, 2054.5271 cm^{-1}
lower state energy E''_{lst}	:	77.1, 69.4 cm^{-1}
retrieved TCA, information content	:	8.56E+15 $molec/cm^2$, 92.5, 110.73
temperature dependence of the TCA	:	-0.192%/K (trop), -0.209%/K (strat)
location, date, solar zenith angle	:	Kiruna, 15/Mar/97, 70.54^o
spectral interval fitted	:	2053.980 – 2054.666 cm^{-1}

Molecule	iCode	Absorption	Molecule	iCode	Absorption
$CO2$	21	100.000%	OCS	19**2**	1.231%
OCS	191	25.044%	$H2O$	1**3**	0.829%
$O3$	31	20.615%	CO	51	0.457%
CO	5**2**	18.500%	$N2O$	41	0.001%
$H2O$	11	6.487%	NO	81	0.001%
$H2O$	1**2**	6.406%	$CH4$	61	<0.001%
Solar(A)	—	6.148%	$NH3$	111	<0.001%
Solar-sim	—	4.469%	OH	131	<0.001%
CO	5**3**	4.097%	HI	171	<0.001%
$CO2$	2**3**	2.690%	$C2H2$	401	<0.001%
$CO2$	2**4**	1.793%	$N2$	411	<0.001%
$O3$	3**3**	1.545%			

OCS, Kiruna, φ=70.54^o, OPD=257cm, FoV=2.39$mrad$, boxcar apod.

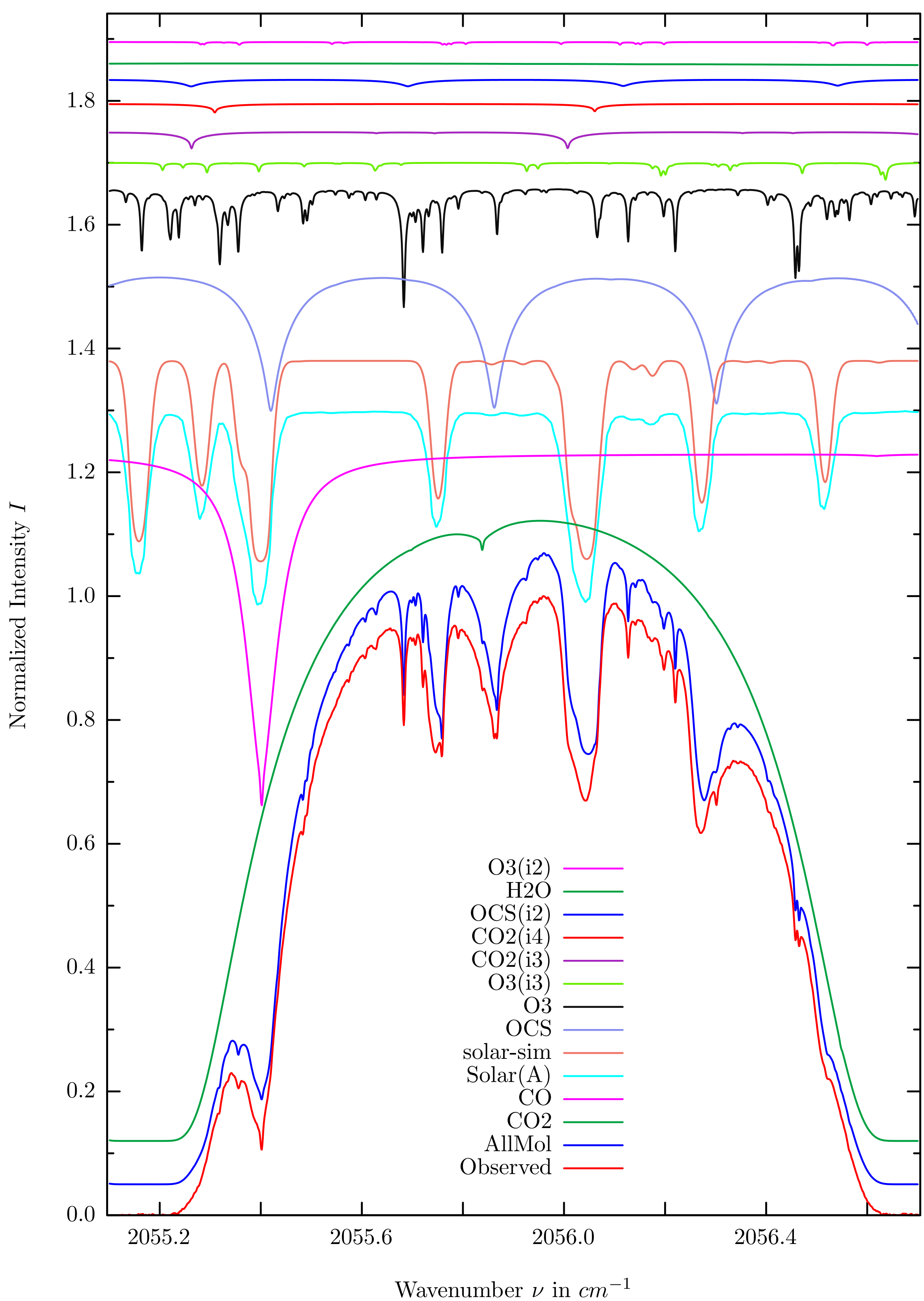

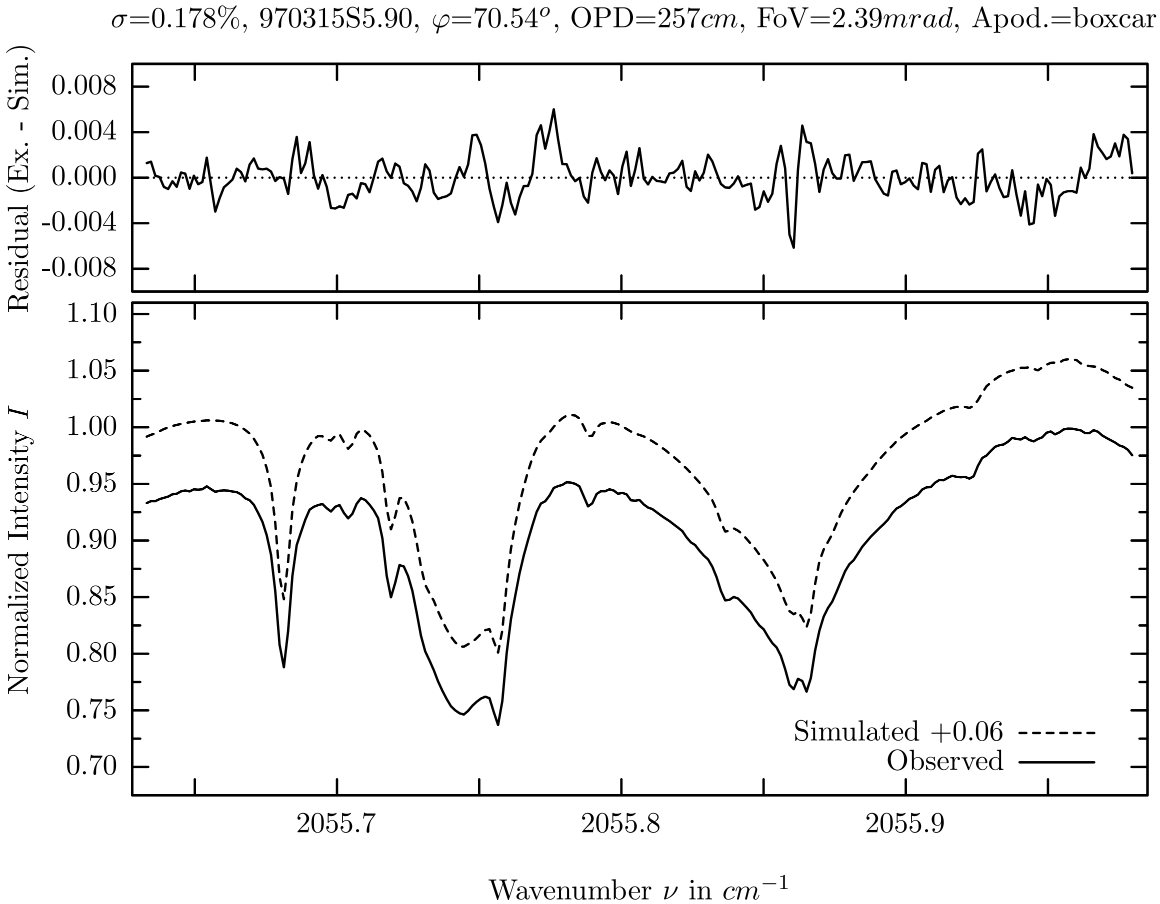

investigated species	:	OCS
line position(s) ν_0	:	2055.8606 cm^{-1}
lower state energy E''_{lst}	:	48.7 cm^{-1}
retrieved TCA, information content	:	9.38E+15 $molec/cm^2$, 126.6
temperature dependence of the TCA	:	-1.312%/K (trop), -0.524%/K (strat)
location, date, solar zenith angle	:	Kiruna, 15/Mar/97, 70.54^o
spectral interval fitted	:	2055.632 – 2055.980 cm^{-1}

Molecule	iCode	Absorption	Molecule	iCode	Absorption
$CO2$	21	100.000%	$H2O$	11	0.707%
CO	51	56.873%	$O3$	**32**	0.544%
Solar(A)	—	31.369%	$N2O$	41	0.001%
Solar-sim	—	32.386%	$CH4$	61	<0.001%
OCS	191	24.073%	NO	81	<0.001%
$O3$	31	19.668%	$NH3$	111	<0.001%
$O3$	**33**	2.776%	OH	131	<0.001%
$CO2$	2**3**	2.712%	HI	171	<0.001%
$CO2$	2**4**	1.397%	$C2H2$	401	<0.001%
OCS	19**2**	1.167%	$N2$	411	<0.001%

CO, Kiruna, φ=70.54^o, OPD=257cm, FoV=2.39$mrad$, boxcar apod.

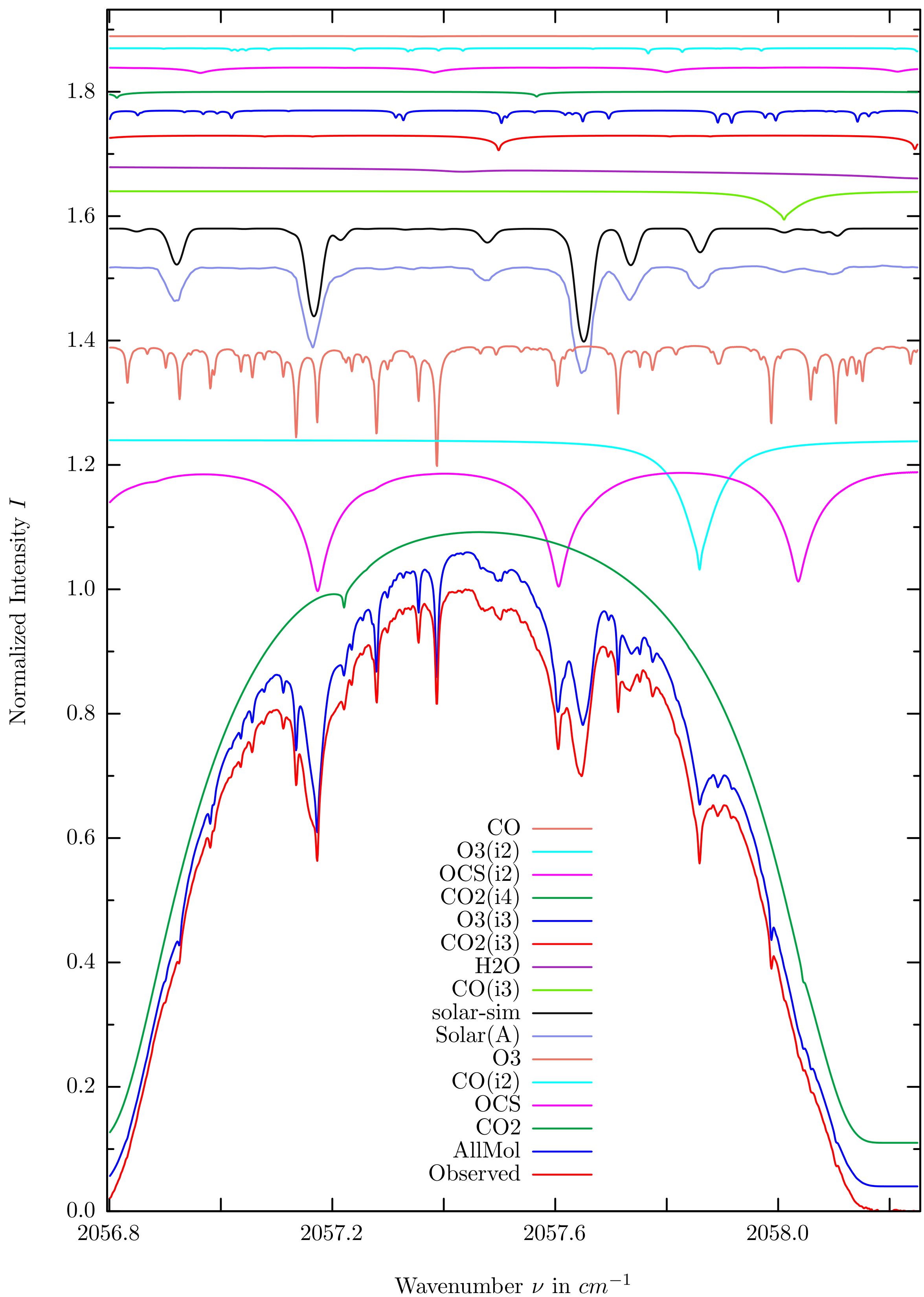

σ=0.186%, 970315S5.90, φ=70.54^o, OPD=257cm, FoV=2.39$mrad$, Apod.=boxcar

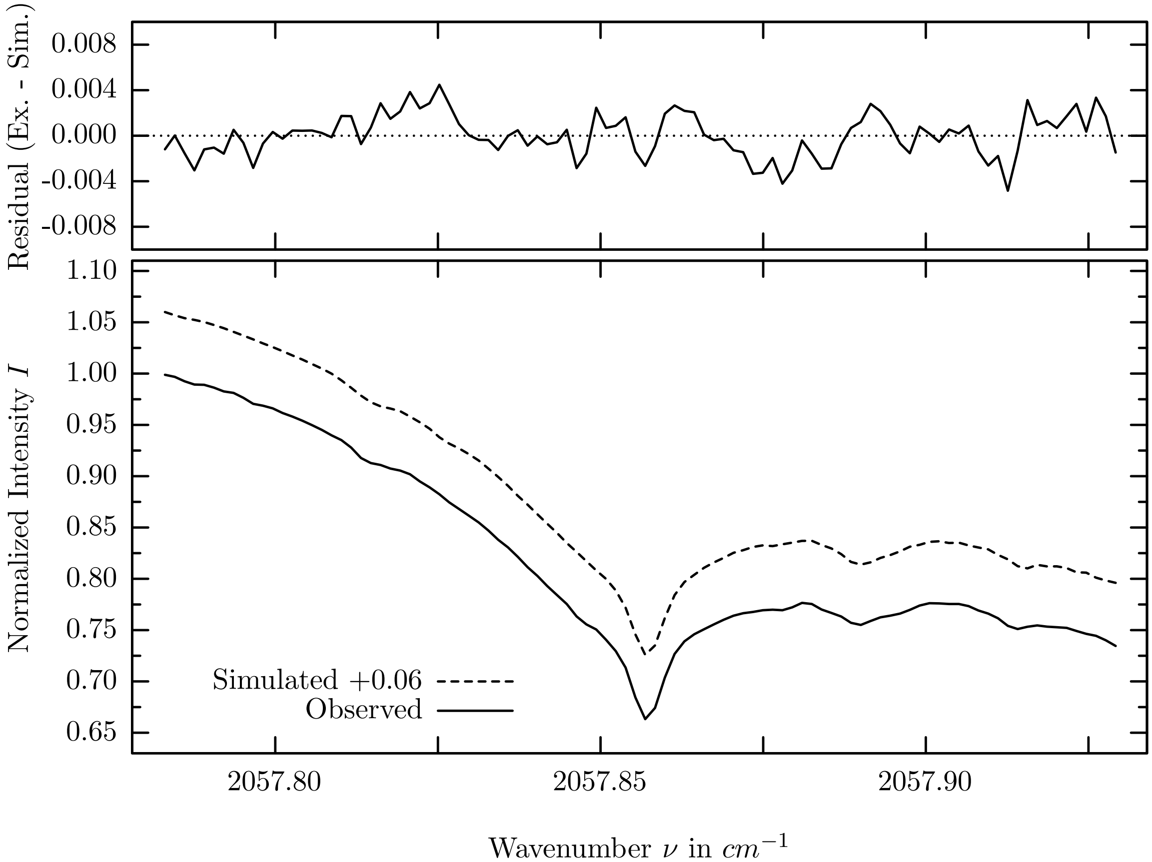

investigated species	:	$CO(i2)$
line position(s) ν_0	:	2057.8575 cm^{-1}
lower state energy E''_{lst}	:	202.1 cm^{-1}
retrieved TCA, information content	:	2.35E+18 $molec/cm^2$, 96.0
temperature dependence of the TCA	:	-0.425%/K (trop), -0.249%/K (strat)
location, date, solar zenith angle	:	Kiruna, 15/Mar/97, 70.54^o
spectral interval fitted	:	2057.783 – 2057.930 cm^{-1}

Molecule	iCode	Absorption	Molecule	iCode	Absorption
$CO2$	21	100.000%	OCS	19**2**	0.983%
OCS	191	21.286%	$O3$	**32**	0.877%
CO	5**2**	20.904%	CO	51	0.069%
$O3$	31	20.245%	$N2O$	41	0.001%
Solar(A)	—	17.241%	$CH4$	61	<0.001%
Solar-sim	—	18.188%	NO	81	<0.001%
CO	5**3**	4.595%	$NH3$	111	<0.001%
$H2O$	11	2.863%	OH	131	<0.001%
$CO2$	2**3**	2.451%	HI	171	<0.001%
$O3$	**33**	2.107%	$C2H2$	401	<0.001%
$CO2$	**24**	0.988%	$N2$	411	<0.001%

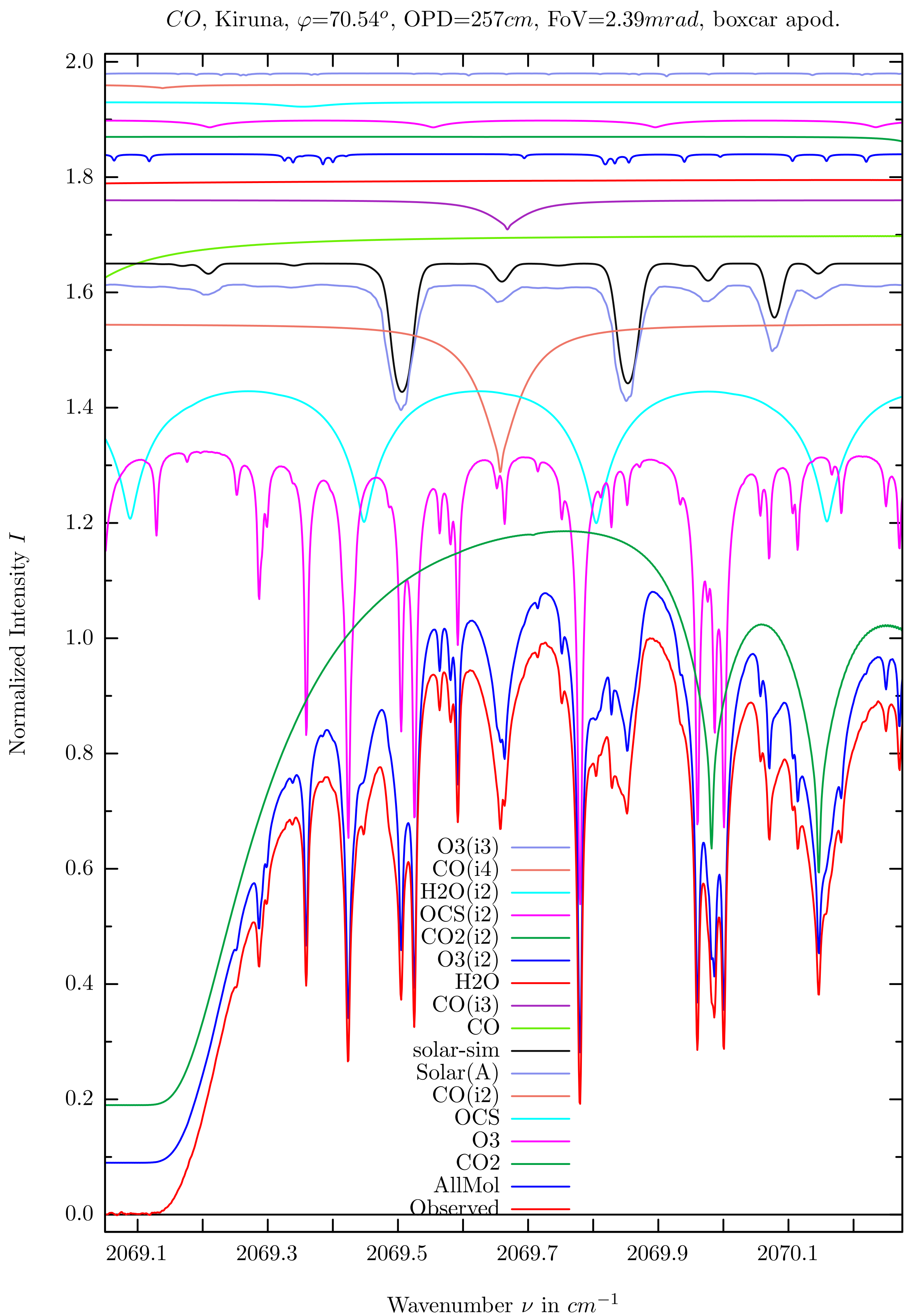

CO, Kiruna, φ=70.54^o, OPD=257cm, FoV=2.39$mrad$, boxcar apod.
Normalized Intensity I
0.0
0.2
0.4
0.6
0.8
1.0
1.2
1.4
1.6
1.8
2.0
2069.1
2069.3
2069.5
2069.7
2069.9
2070.1
Wavenumber ν in cm^{-1}
O3(i3)
CO(i4)
H2O(i2)
OCS(i2)
CO2(i2)
O3(i2)
H2O
CO(i3)
CO
solar-sim
Solar(A)
CO(i2)
OCS
O3
CO2
AllMol
Observed

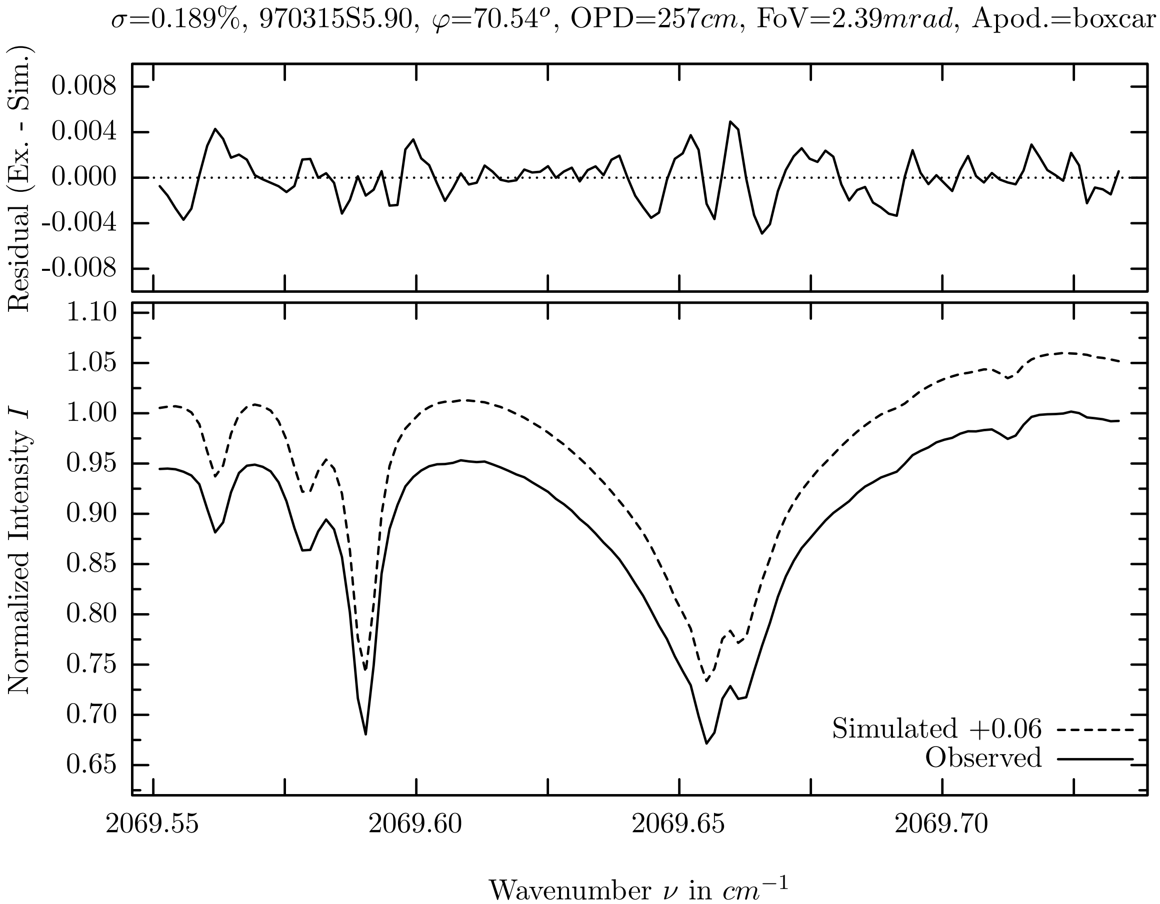

investigated species	:	$CO(i2)$
line position(s) ν_0	:	2069.6559 cm^{-1}
lower state energy E''_{lst}	:	102.9 cm^{-1}
retrieved TCA, information content	:	2.67E+18 $molec/cm^2$, 172.3
temperature dependence of the TCA	:	+0.135%/K (trop), +0.064%/K (strat)
location, date, solar zenith angle	:	Kiruna, 15/Mar/97, 70.54^o
spectral interval fitted	:	2069.550 – 2069.735 cm^{-1}

Molecule	iCode	Absorption	Molecule	iCode	Absorption
$CO2$	21	100.000%	$H2O$	1**2**	0.780%
$O3$	31	80.624%	CO	5**4**	0.562%
OCS	191	27.039%	$O3$	**33**	0.532%
CO	5**2**	25.796%	$N2O$	41	0.001%
Solar(A)	—	21.921%	$CH4$	61	<0.001%
Solar-sim	—	22.275%	NO	81	<0.001%
CO	51	7.310%	$NH3$	111	<0.001%
CO	5**3**	5.107%	OH	131	<0.001%
$H2O$	11	2.085%	HI	171	<0.001%
$O3$	**32**	1.831%	$C2H2$	401	<0.001%
$CO2$	**22**	1.402%	$N2$	411	<0.001%
OCS	19**2**	1.371%			

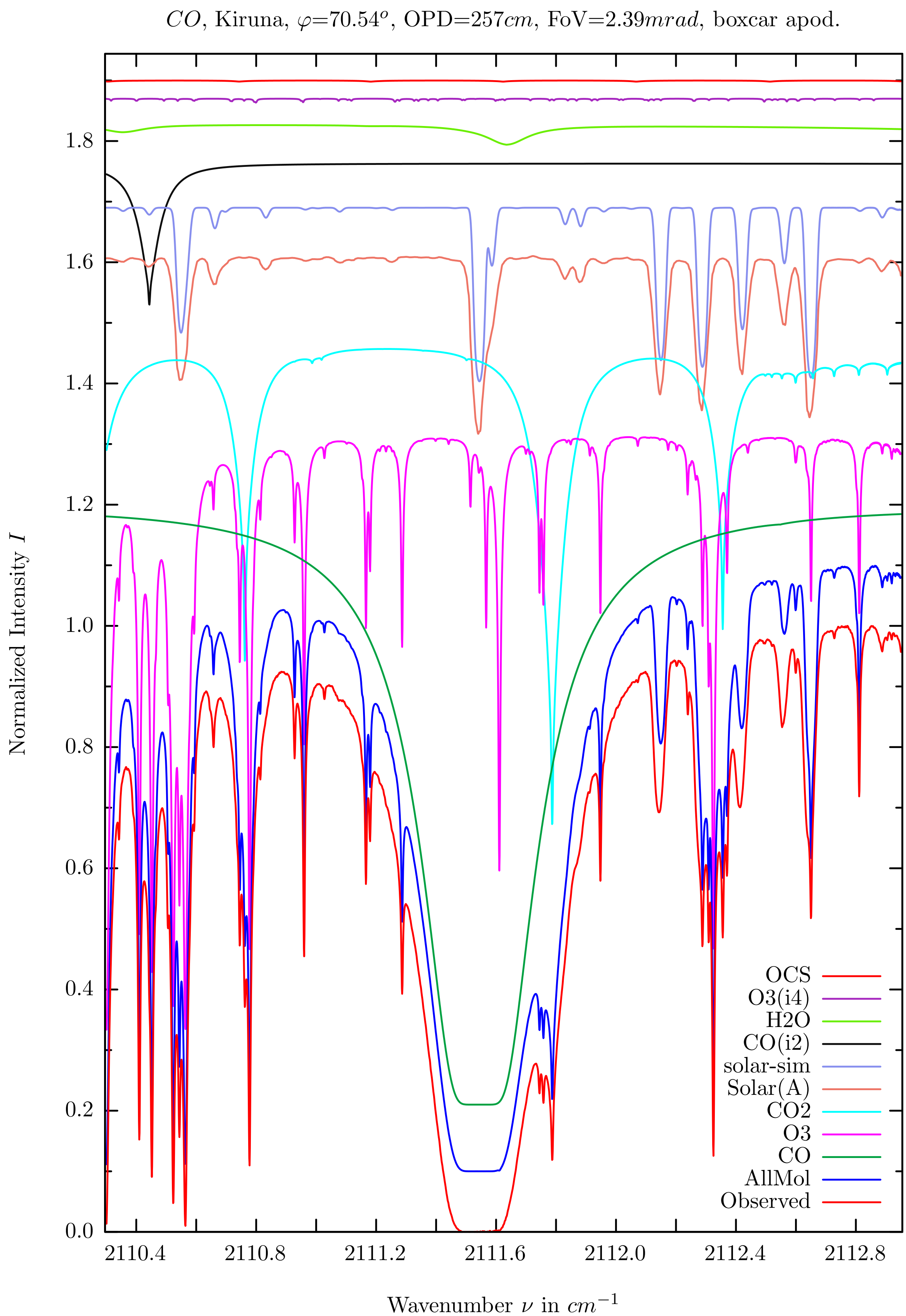
CO, Kiruna, φ=70.54^o, OPD=257cm, FoV=2.39$mrad$, boxcar apod.
Normalized Intensity I
Wavenumber ν in cm^{-1}
OCS
O3(i4)
H2O
CO(i2)
solar-sim
Solar(A)
CO2
O3
CO
AllMol
Observed
0.0
0.2
0.4
0.6
0.8
1.0
1.2
1.4
1.6
1.8
2110.4
2110.8
2111.2
2111.6
2112.0
2112.4
2112.8

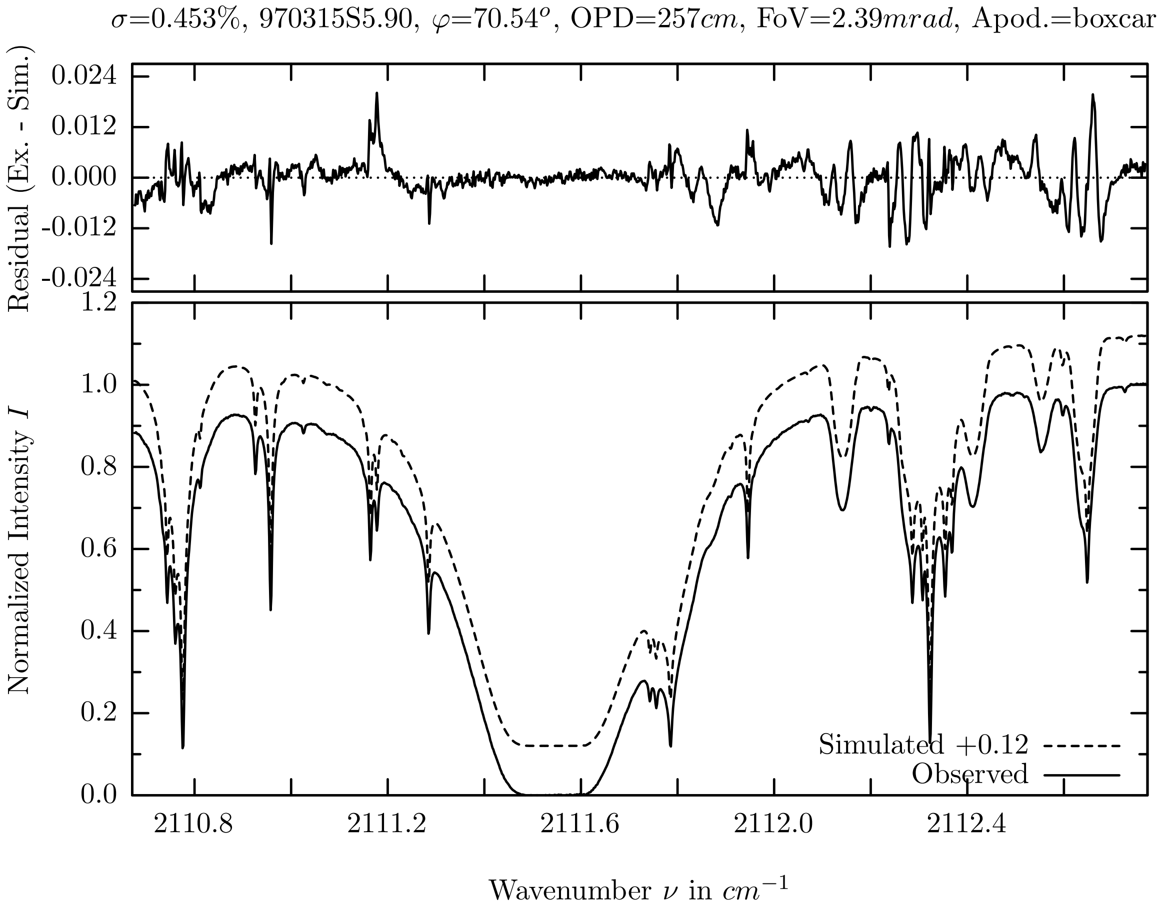

investigated species	:	CO
line position(s) ν_0	:	2111.5430 cm^{-1}
lower state energy E''_{lst}	:	138.4 cm^{-1}
retrieved TCA, information content	:	2.55E+18 $molec/cm^2$, 220.8
temperature dependence of the TCA	:	+0.606%/K (trop), +0.106%/K (strat)
location, date, solar zenith angle	:	Kiruna, 15/Mar/97, 70.54^o
spectral interval fitted	:	2110.675 – 2112.770 cm^{-1}

Molecule	iCode	Absorption	Molecule	iCode	Absorption
CO	51	100.000%	$C2H2$	401	0.001%
$O3$	31	98.595%	$N2O$	41	<0.001%
$CO2$	21	80.338%	$CH4$	61	<0.001%
Solar(A)	—	29.305%	NO	81	<0.001%
Solar-sim	—	28.660%	$NH3$	111	<0.001%
CO	5**2**	23.407%	OH	131	<0.001%
$H2O$	11	3.600%	HI	171	<0.001%
$O3$	**34**	0.661%	$N2$	411	<0.001%
OCS	191	0.193%			

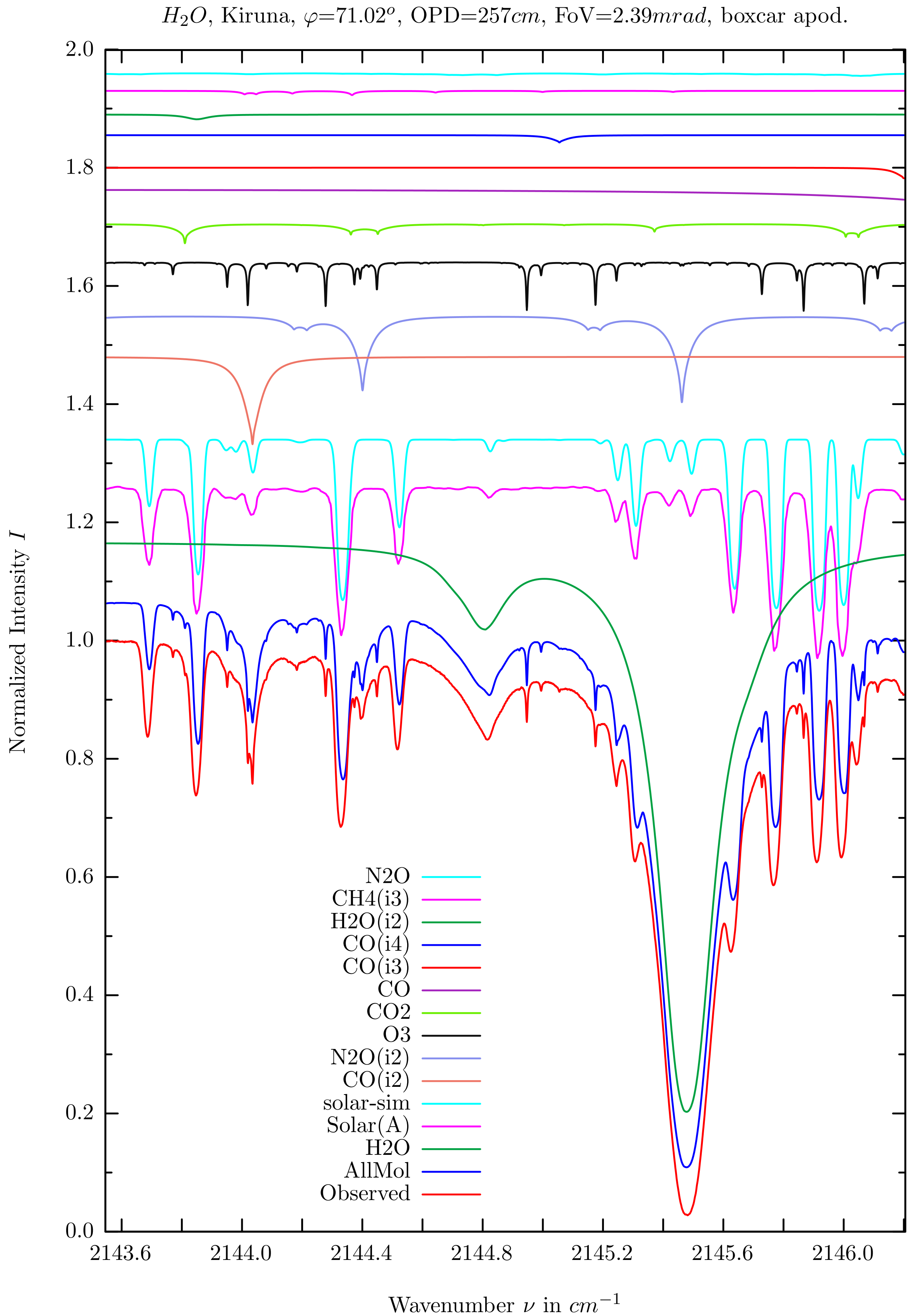
H_2O, Kiruna, φ=71.02^o, OPD=257cm, FoV=2.39$mrad$, boxcar apod.
Normalized Intensity I
Wavenumber ν in cm^{-1}
2.0
1.8
1.6
1.4
1.2
1.0
0.8
0.6
0.4
0.2
0.0
2143.6
2144.0
2144.4
2144.8
2145.2
2145.6
2146.0
N2O
CH4(i3)
H2O(i2)
CO(i4)
CO(i3)
CO
CO2
O3
N2O(i2)
CO(i2)
solar-sim
Solar(A)
H2O
AllMol
Observed

σ=0.245%, 970315S5.90, φ=70.54^o, OPD=257cm, FoV=2.39$mrad$, Apod.=boxcar

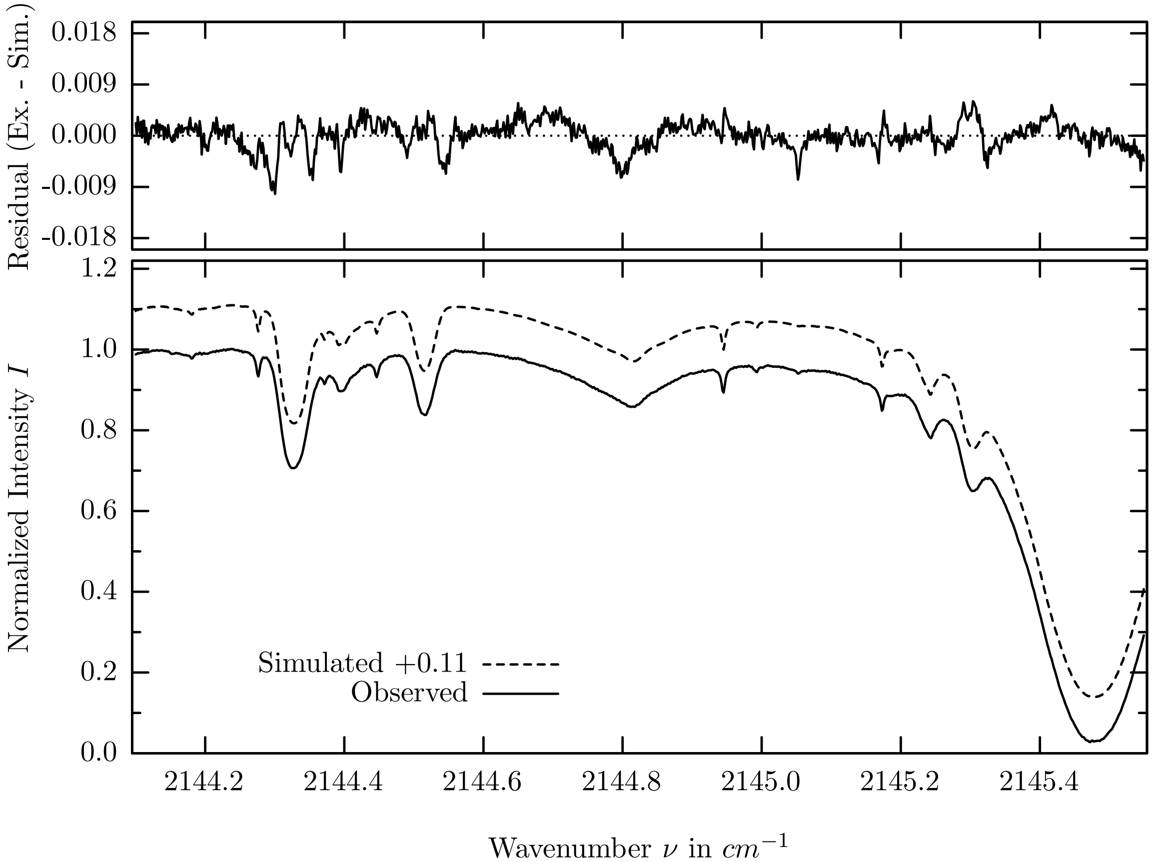

investigated species	:	H_2O
line position(s) ν_0	:	2144.8085 cm^{-1}
lower state energy E''_{lst}	:	1742.3 cm^{-1}
retrieved TCA, information content	:	5.47E+21 $molec/cm^2$, 55.2
temperature dependence of the TCA	:	-1.529%/K (trop), -0.005%/K (strat)
location, date, solar zenith angle	:	Kiruna, 15/Mar/97, 70.54^o
spectral interval fitted	:	2144.100 – 2145.550 cm^{-1}

Molecule	iCode	Absorption	Molecule	iCode	Absorption
H2O	11	96.728%	$N2O$	41	0.386%
Solar(A)	—	28.969%	OCS	191	0.001%
Solar-sim	—	28.967%	$C2H2$	401	0.001%
CO	5**2**	14.827%	$N2$	411	0.001%
$N2O$	4**2**	14.754%	$CH4$	61	<0.001%
$O3$	31	8.399%	NO	81	<0.001%
$CO2$	21	3.324%	$NH3$	111	<0.001%
CO	51	1.914%	OH	131	<0.001%
CO	5**3**	1.791%	HBr	161	<0.001%
CO	5**4**	1.233%	HI	171	<0.001%
$H2O$	1**2**	0.812%	$H2S$	471	<0.001%
$CH4$	6**3**	0.720%			

N_2O, Kiruna, φ=71.02^o, OPD=257cm, FoV=2.39$mrad$, boxcar apod.

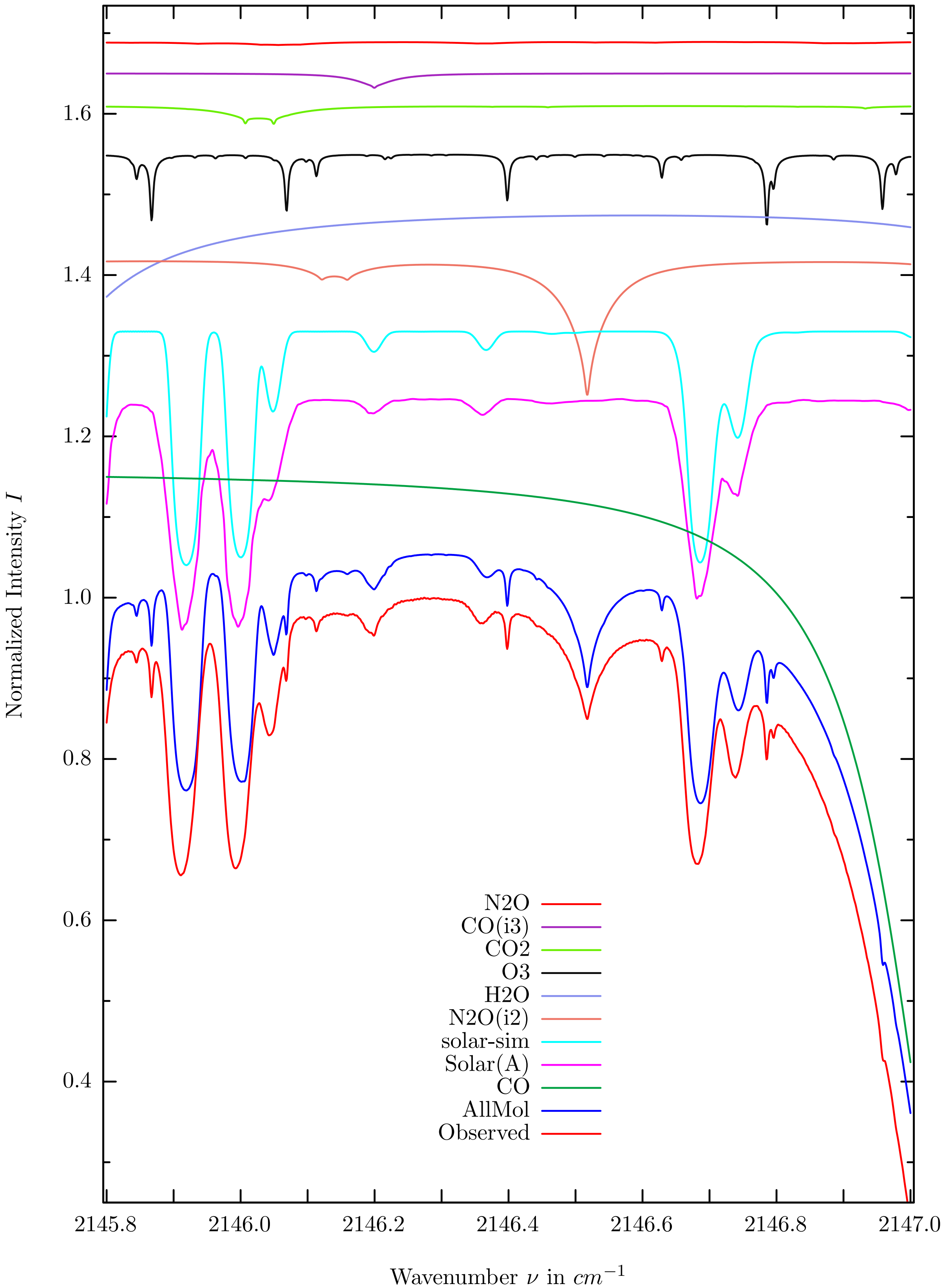

σ=0.058%, 970315S4.90, φ=71.02^o, OPD=257cm, FoV=2.39$mrad$, Apod.=boxcar

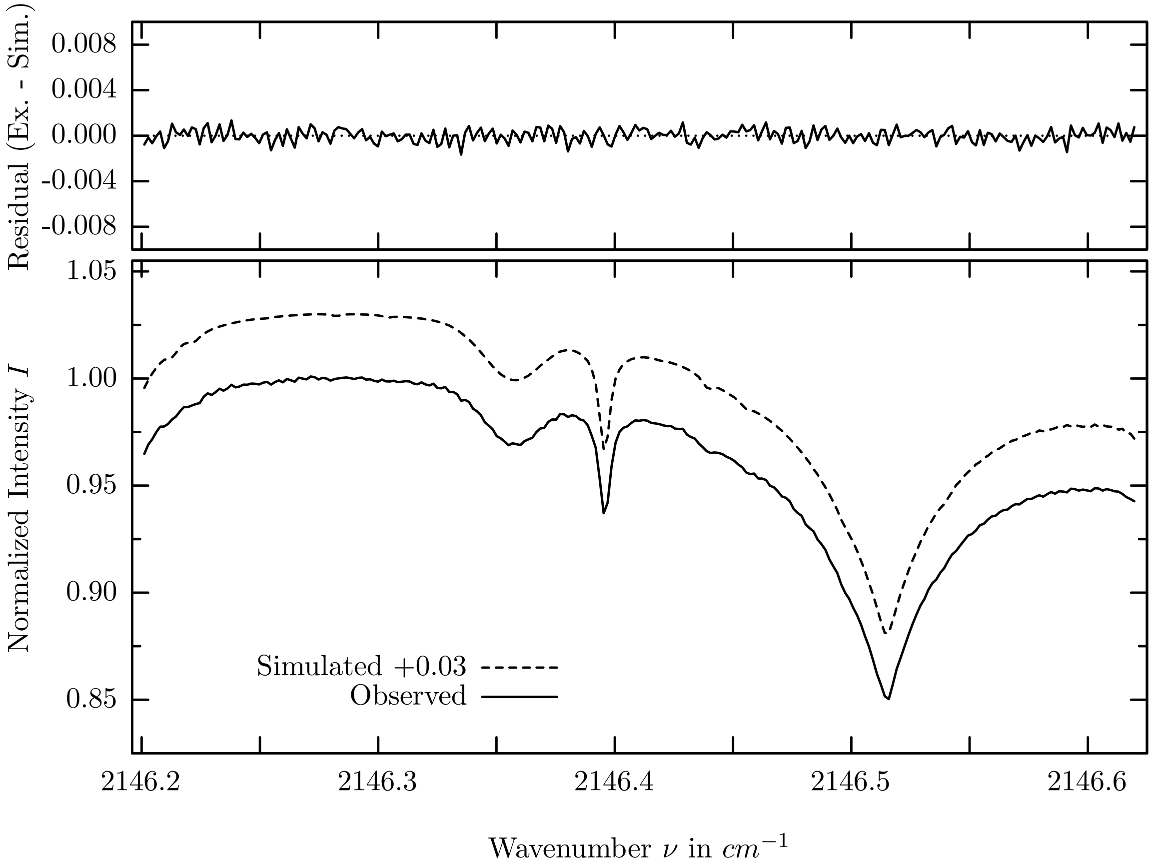

investigated species	:	$N_2O(i2)$
line position(s) ν_0	:	2146.5160 cm^{-1}
lower state energy E''_{lst}	:	469.9 cm^{-1}
retrieved TCA, information content	:	5.75E+18 $molec/cm^2$, 213.1
temperature dependence of the TCA	:	-0.922%/K (trop), -0.112%/K (strat)
location, date, solar zenith angle	:	Kiruna, 15/Mar/97, 71.02^o
spectral interval fitted	:	2146.200 – 2146.620 cm^{-1}

Molecule	iCode	Absorption	Molecule	iCode	Absorption
CO	51	74.656%	$C2H2$	401	0.001%
Solar(A)	—	28.969%	$CH4$	61	<0.001%
Solar-sim	—	28.967%	NO	81	<0.001%
N2O	4**2**	16.936%	$NH3$	111	<0.001%
$H2O$	11	11.621%	OH	131	<0.001%
$O3$	31	9.083%	HBr	161	<0.001%
$CO2$	21	2.279%	HI	171	<0.001%
CO	5**3**	1.791%	$N2$	411	<0.001%
$N2O$	41	0.387%	$H2S$	471	<0.001%
OCS	191	0.001%			

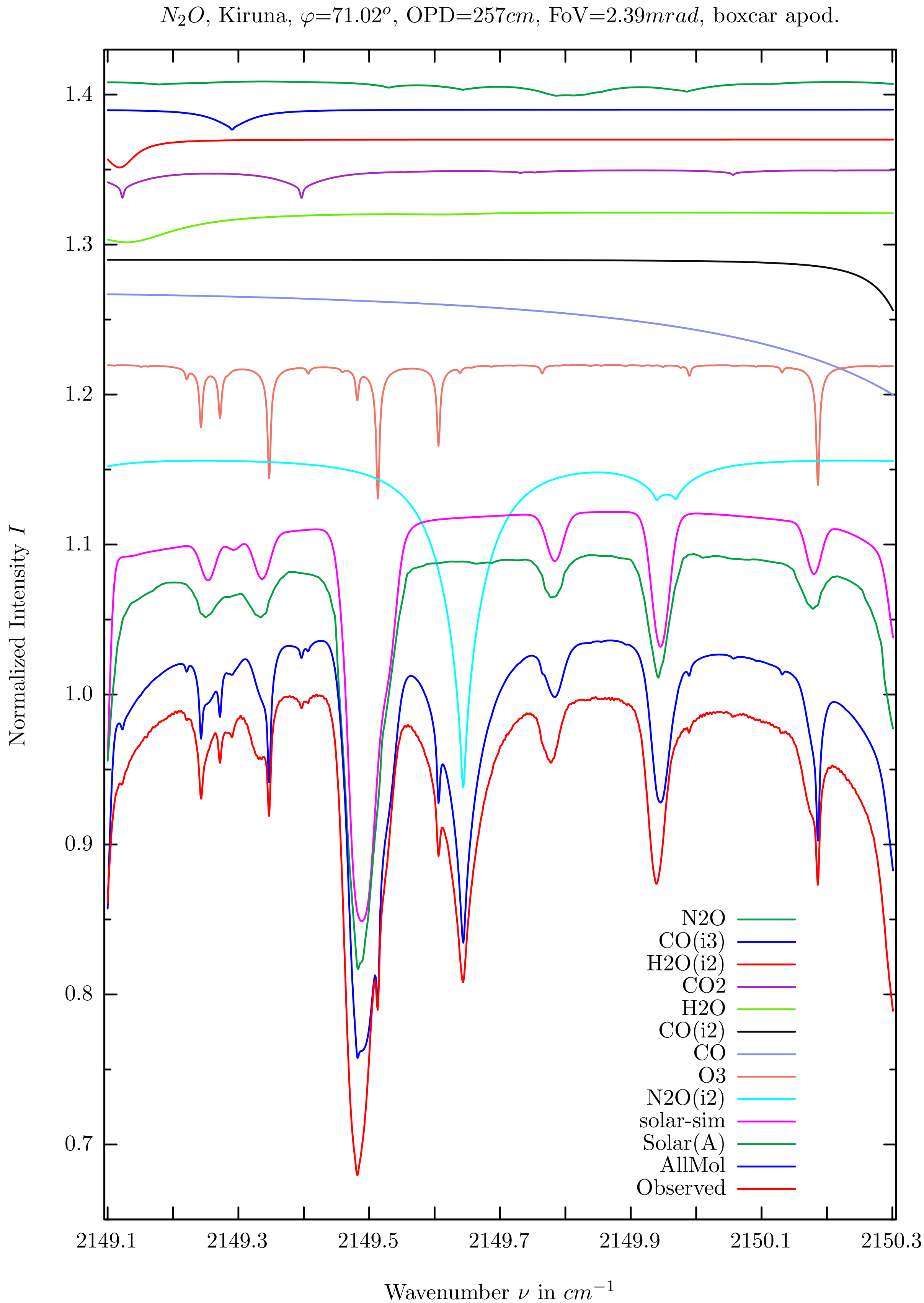
N_2O, Kiruna, φ=71.02^o, OPD=257cm, FoV=2.39$mrad$, boxcar apod.
Normalized Intensity I
Wavenumber ν in cm^{-1}
1.4
1.3
1.2
1.1
1.0
0.9
0.8
0.7
2149.1
2149.3
2149.5
2149.7
2149.9
2150.1
2150.3
N2O
CO(i3)
H2O(i2)
CO2
H2O
CO(i2)
CO
O3
N2O(i2)
solar-sim
Solar(A)
AllMol
Observed

σ=0.135%, 970315S4.90, φ=71.02^o, OPD=257cm, FoV=2.39$mrad$, Apod.=boxcar

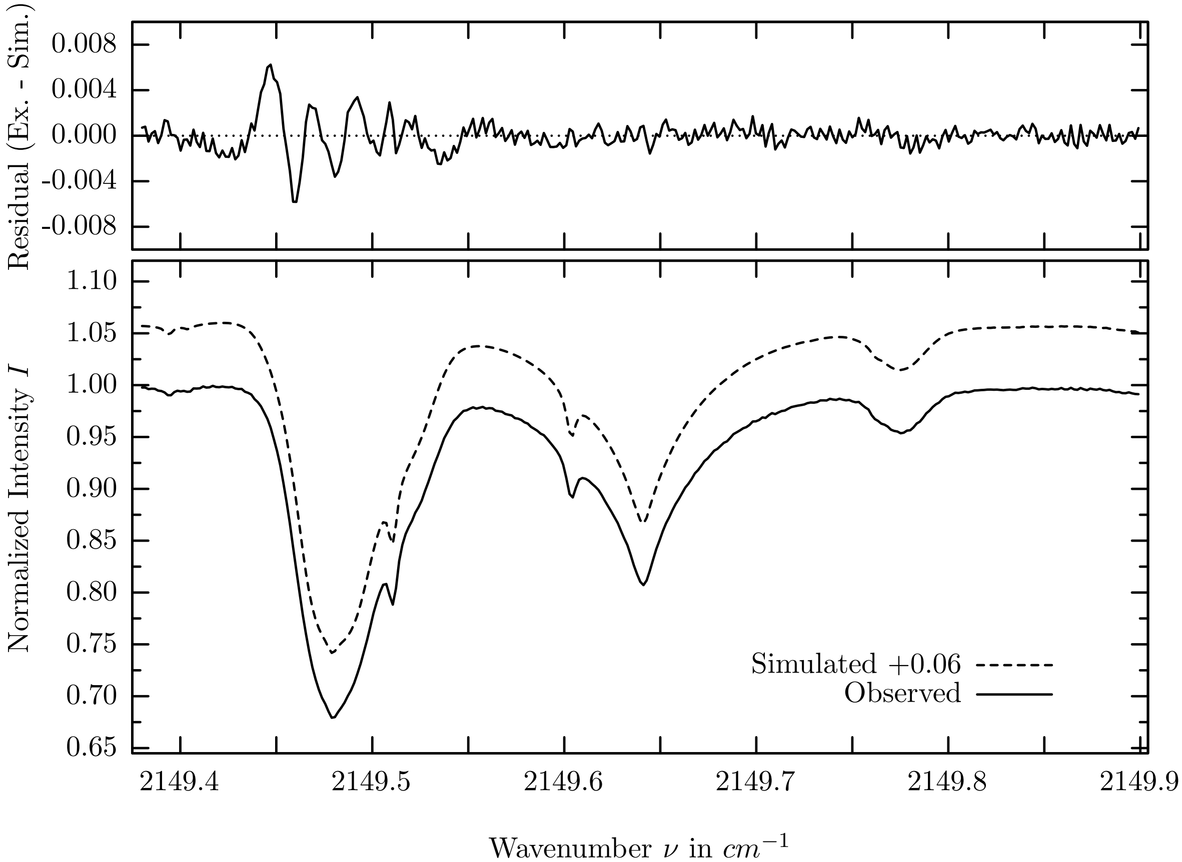

investigated species	:	$N_2O(i2)$
line position(s) ν_0	:	2149.6423 cm^{-1}
lower state energy E''_{lst}	:	389.5 cm^{-1}
retrieved TCA, information content	:	5.81E+18 $molec/cm^2$, 143.6
temperature dependence of the TCA	:	-0.489%/K (trop), -0.108%/K (strat)
location, date, solar zenith angle	:	Kiruna, 15/Mar/97, 71.02^o
spectral interval fitted	:	2149.380 – 2149.900 cm^{-1}

Molecule	iCode	Absorption	Molecule	iCode	Absorption
Solar(A)	—	29.305%	$CH4$	61	<0.001%
Solar-sim	—	28.120%	NO	81	<0.001%
N2O	4**2**	24.729%	$NH3$	111	<0.001%
$O3$	31	9.169%	OH	131	<0.001%
CO	51	8.058%	HBr	161	<0.001%
CO	5**2**	3.562%	HI	171	<0.001%
$H2O$	11	2.346%	OCS	191	<0.001%
$CO2$	21	1.916%	$C2H2$	401	<0.001%
$H2O$	1**2**	1.866%	$N2$	411	<0.001%
CO	5**3**	1.343%	$H2S$	471	<0.001%
$N2O$	41	0.933%			

N_2O, Kiruna, φ=71.02^o, OPD=257cm, FoV=2.39$mrad$, boxcar apod.

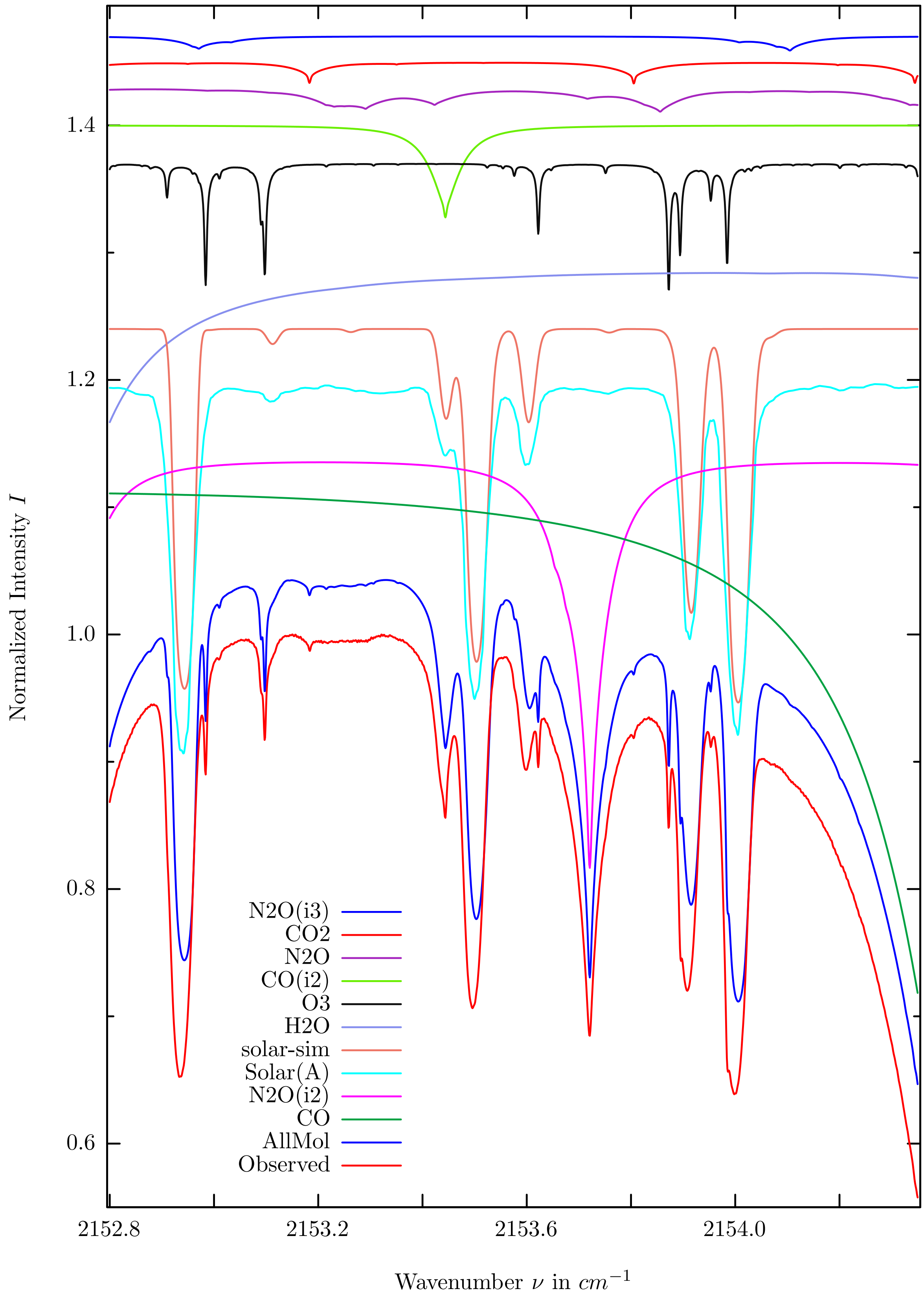

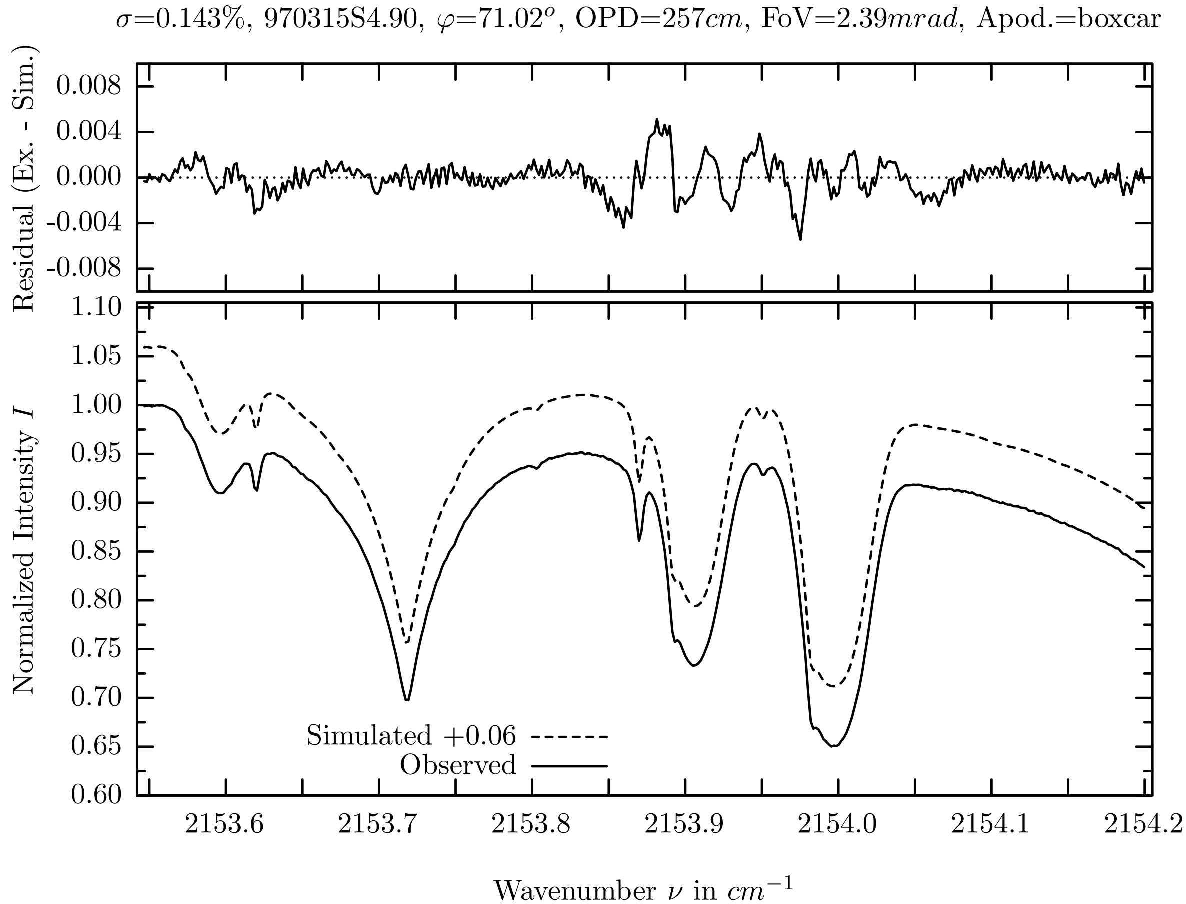

investigated species	:	$N_2O(i2)$
line position(s) ν_0	:	2153.7194 cm^{-1}
lower state energy E''_{lst}	:	294.0 cm^{-1}
retrieved TCA, information content	:	5.85E+18 $molec/cm^2$, 208.7
temperature dependence of the TCA	:	-0.487%/K (trop), -0.127%/K (strat)
location, date, solar zenith angle	:	Kiruna, 15/Mar/97, 71.02^o
spectral interval fitted	:	2153.546 – 2154.200 cm^{-1}

Molecule	iCode	Absorption	Molecule	iCode	Absorption
CO	51	41.643%	*C2H2*	401	0.001%
N2O	4**2**	37.262%	*N2*	411	0.001%
Solar(A)	—	29.344%	*CH4*	61	<0.001%
Solar-sim	—	29.350%	*NO*	81	<0.001%
H2O	11	12.230%	*NH3*	111	<0.001%
O3	31	10.316%	*OH*	131	<0.001%
CO	5**2**	7.254%	*HBr*	161	<0.001%
N2O	41	1.926%	*HI*	171	<0.001%
CO2	21	1.736%	*OCS*	191	<0.001%
N2O	4**3**	1.124%	*H2S*	471	<0.001%

CO, Kiruna, φ=70.54^o, OPD=257cm, FoV=2.39$mrad$, boxcar apod.

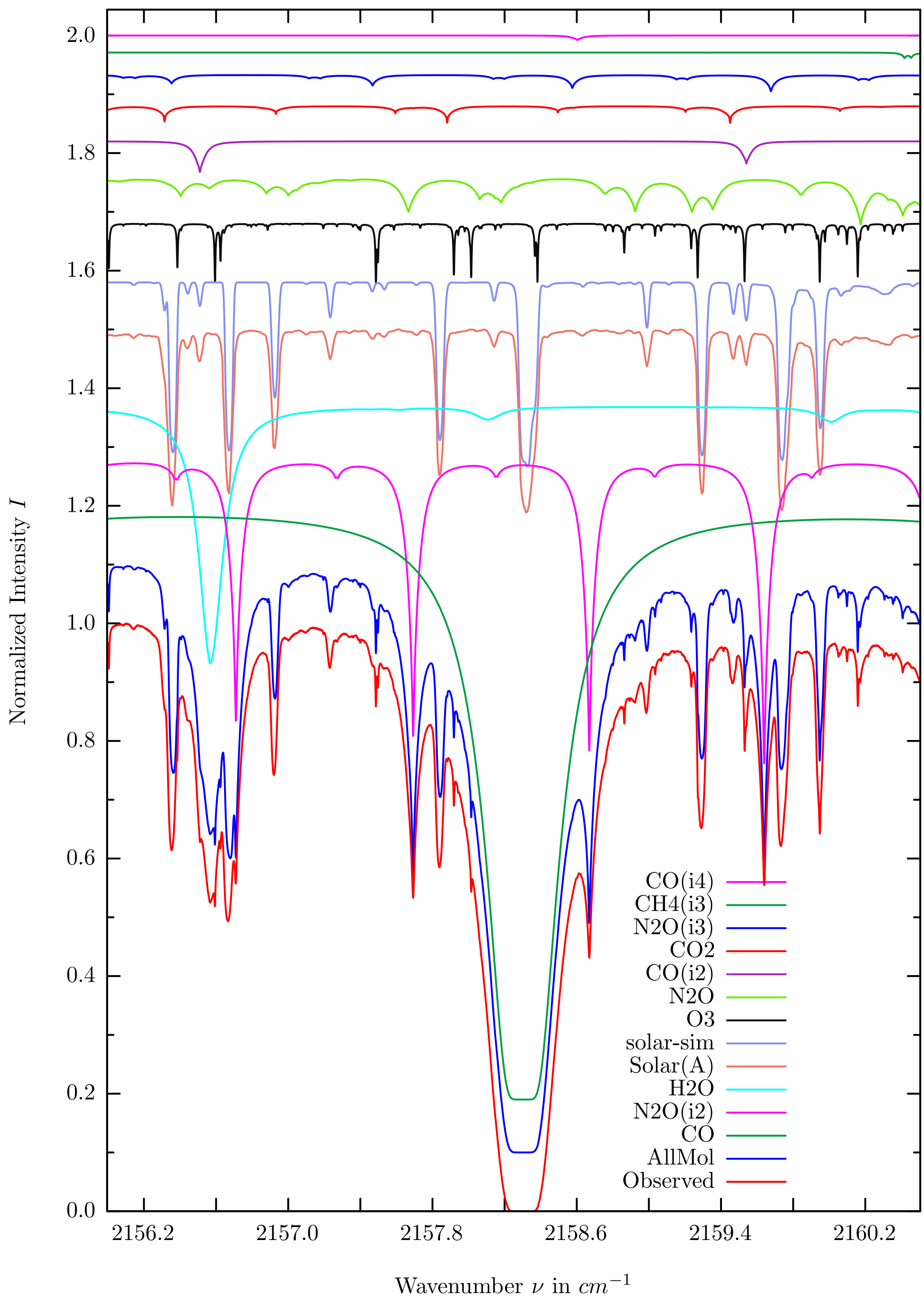

σ=0.175%, 970315S5.90, φ=70.54^o, OPD=257cm, FoV=2.39$mrad$, Apod.=boxcar

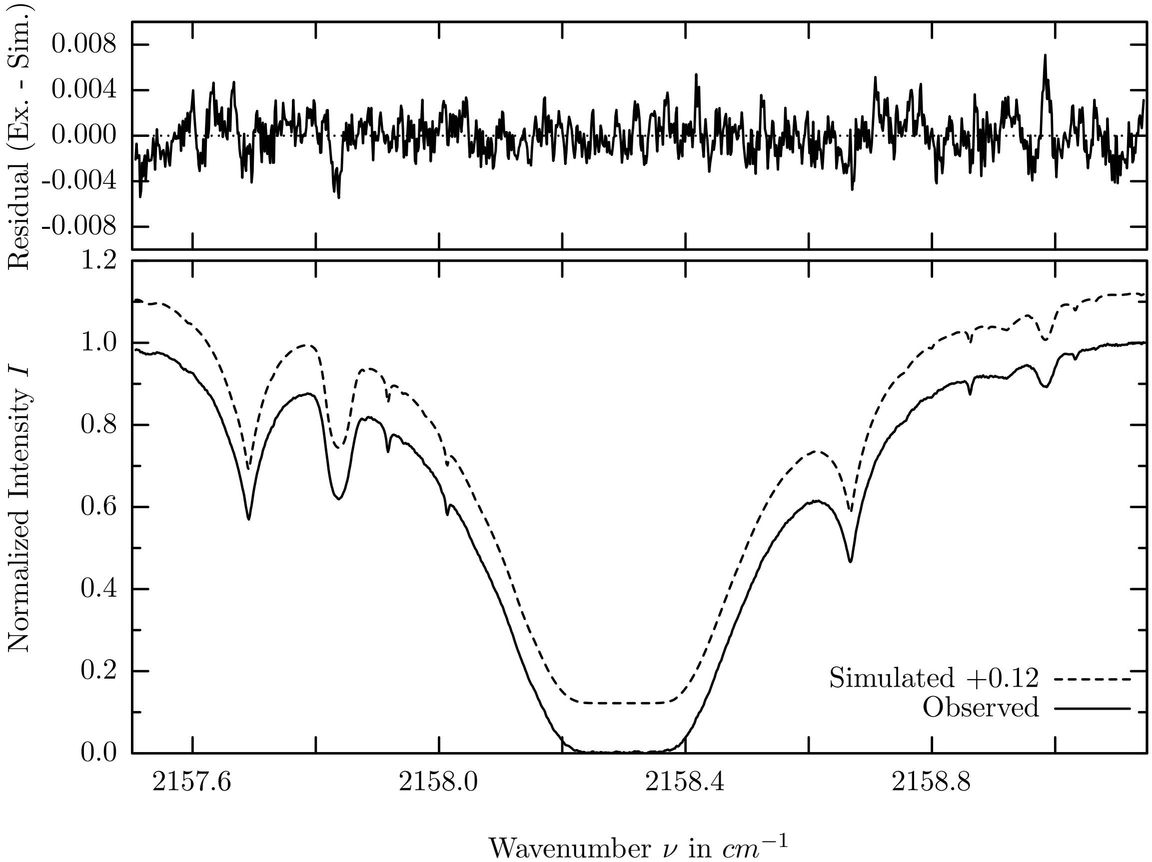

investigated species	:	$CO, (N_2O(i2))$
line position(s) ν_0	:	2158.2997, (2157.6919) cm^{-1}
lower state energy E''_{lst}	:	23.1, (212.0) cm^{-1}
retrieved TCA, information content	:	2.55E+18, (5.77E+18) $molec/cm^2$, 571.8, (225.8)
temperature dependence of the TCA	:	+.128, (-.521)%/K (trop), -.047, (-.035)%/K (strat)
location, date, solar zenith angle	:	Kiruna, 15/Mar/97, 70.54^o
spectral interval fitted	:	2157.507 – 2159.144 cm^{-1}

Molecule	iCode	Absorption	Molecule	iCode	Absorption
CO	51	100.000%	*CO*	5**4**	0.775%
N2O	4**2**	51.936%	*N2*	411	0.019%
H2O	11	43.783%	*C2H2*	401	0.001%
Solar(A)	—	31.109%	*CH4*	61	<0.001%
Solar-sim	—	31.308%	*NO*	81	<0.001%
O3	31	10.481%	*NH3*	111	<0.001%
N2O	41	8.152%	*OH*	131	<0.001%
CO	5**2**	5.228%	*HBr*	161	<0.001%
CO2	21	2.903%	*HI*	171	<0.001%
N2O	4**3**	2.782%	*OCS*	191	<0.001%
CH4	6**3**	0.936%	*H2S*	471	<0.001%

N_2O, Kiruna, φ=71.02^o, OPD=257cm, FoV=2.39$mrad$, boxcar apod.

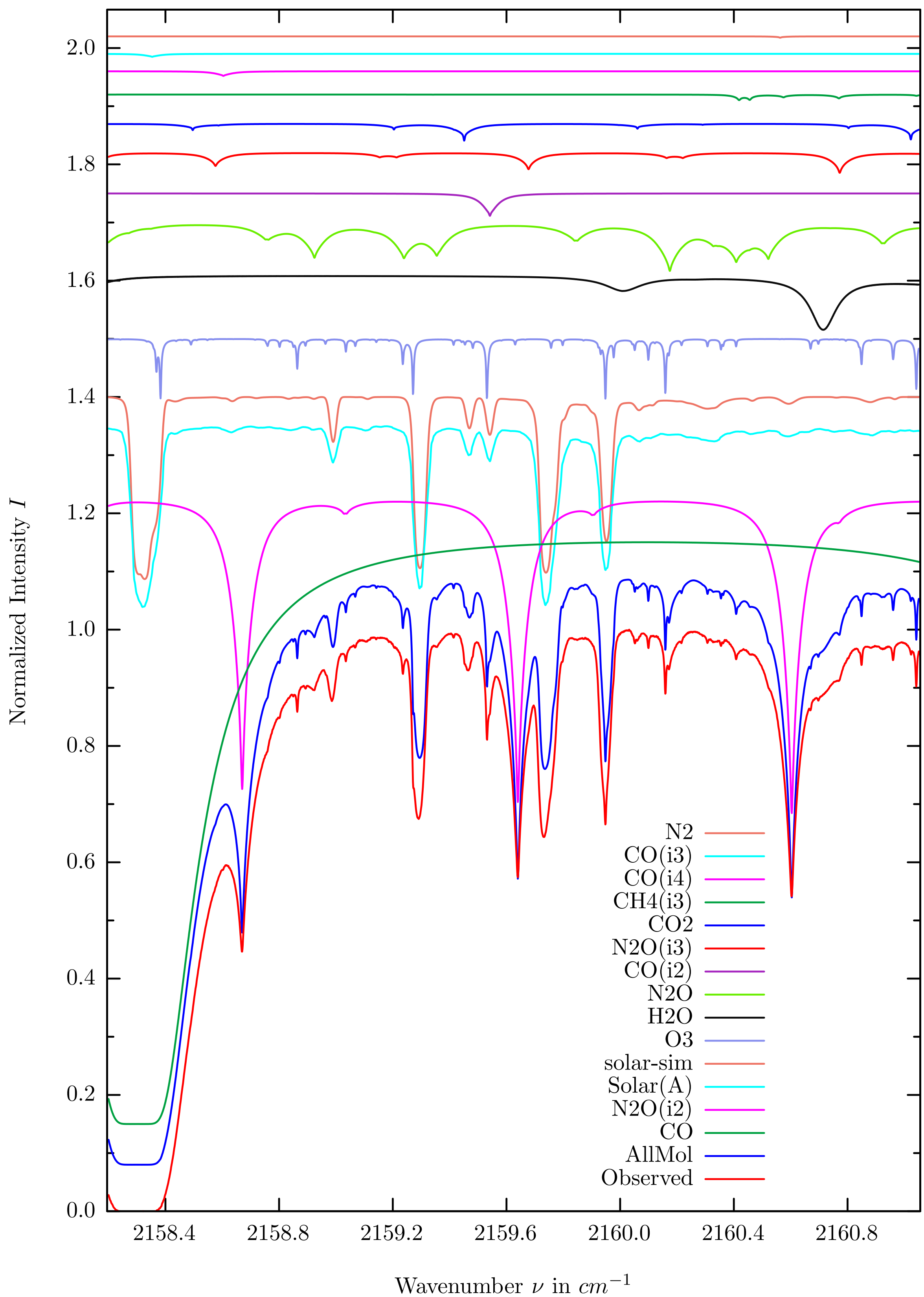

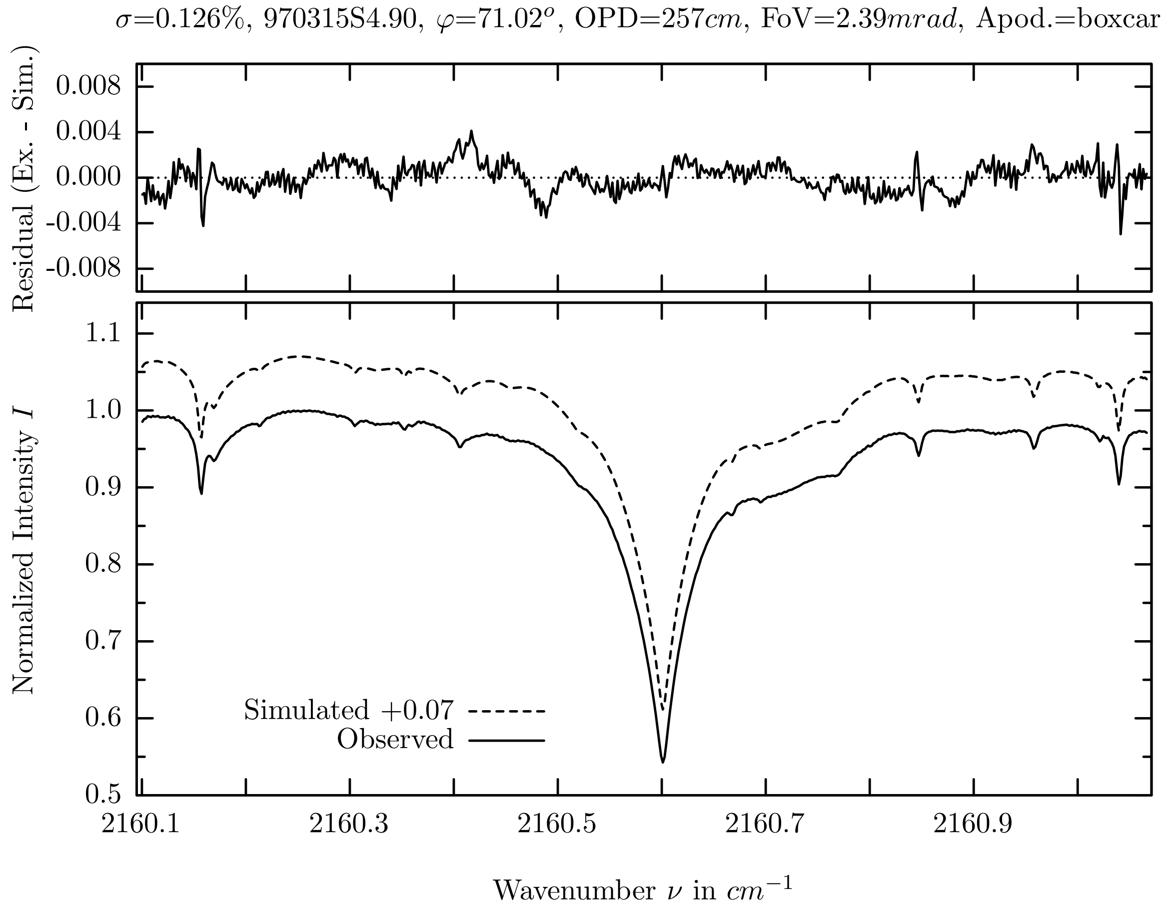

investigated species	:	$N_2O(i2)$
line position(s) ν_0	:	2160.6023 cm^{-1}
lower state energy E''_{lst}	:	159.2 cm^{-1}
retrieved TCA, information content	:	5.65E+18 $molec/cm^2$, 364.2
temperature dependence of the TCA	:	-0.335%/K (trop), -0.027%/K (strat)
location, date, solar zenith angle	:	Kiruna, 15/Mar/97, 71.02^o
spectral interval fitted	:	2160.100 – 2161.068 cm^{-1}

Molecule	iCode	Absorption	Molecule	iCode	Absorption
CO	51	100.000%	CO	5**4**	0.793%
N2O	4**2**	54.661%	CO	5**3**	0.510%
Solar(A)	—	31.109%	$N2$	411	0.224%
Solar-sim	—	31.308%	$C2H2$	401	0.001%
$O3$	31	10.543%	$CH4$	61	<0.001%
$H2O$	11	9.441%	NO	81	<0.001%
$N2O$	41	8.340%	$NH3$	111	<0.001%
CO	5**2**	3.861%	OH	131	<0.001%
$N2O$	4**3**	3.469%	HI	171	<0.001%
$CO2$	21	2.969%	OCS	191	<0.001%
$CH4$	6**3**	0.958%	$H2S$	471	<0.001%

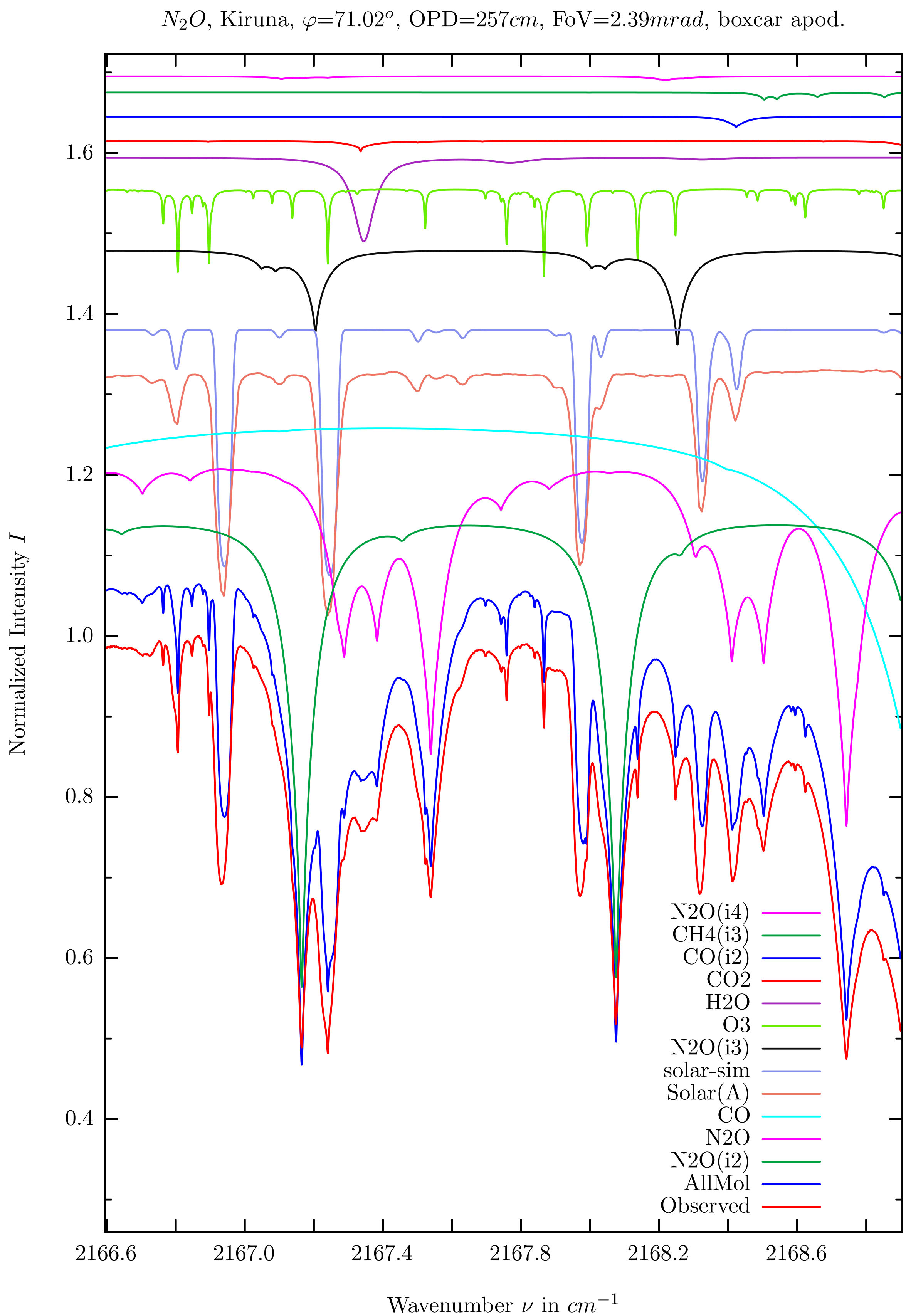
N_2O, Kiruna, φ=71.02^o, OPD=257cm, FoV=2.39$mrad$, boxcar apod.
Normalized Intensity I
Wavenumber ν in cm^{-1}
1.6
1.4
1.2
1.0
0.8
0.6
0.4
2166.6
2167.0
2167.4
2167.8
2168.2
2168.6
N2O(i4)
CH4(i3)
CO(i2)
CO2
H2O
O3
N2O(i3)
solar-sim
Solar(A)
CO
N2O
N2O(i2)
AllMol
Observed

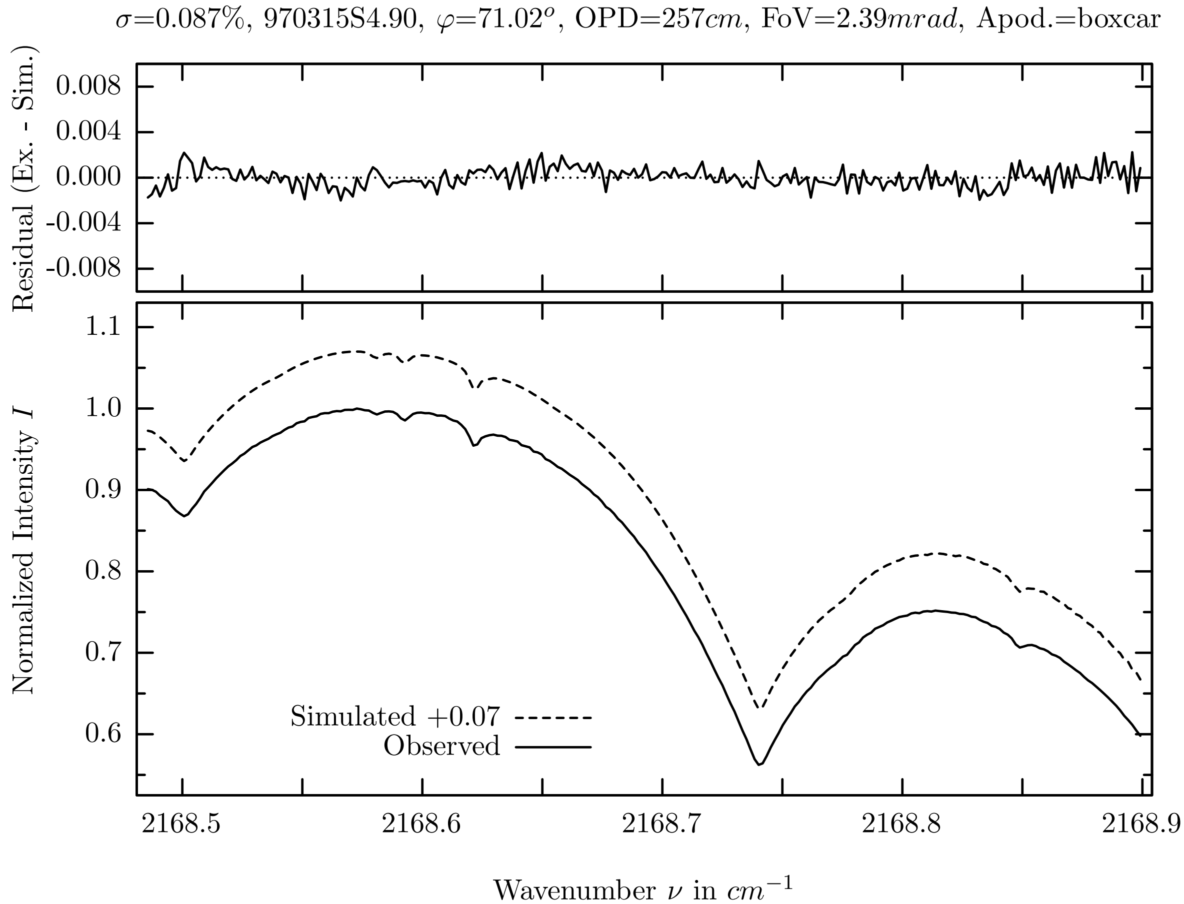

investigated species	:	N_2O
line position(s) ν_0	:	2168.7416 cm^{-1}
lower state energy E''_{lst}	:	1242.9 cm^{-1}
retrieved TCA, information content	:	5.53E+18 $molec/cm^2$, 378.1
temperature dependence of the TCA	:	-2.916%/K (trop), -0.376%/K (strat)
location, date, solar zenith angle	:	Kiruna, 15/Mar/97, 71.02^o
spectral interval fitted	:	2168.485 – 2168.900 cm^{-1}

Molecule	iCode	Absorption	Molecule	iCode	Absorption
N2O	4**2**	58.710%	*N2O*	4**4**	0.500%
N2O	41	46.641%	*N2*	411	0.006%
CO	51	40.873%	*CH4*	61	0.001%
Solar(A)	—	30.452%	*C2H2*	401	0.001%
Solar-sim	—	30.477%	*NO*	81	<0.001%
N2O	4**3**	11.881%	*NH3*	111	<0.001%
O3	31	11.055%	*OH*	131	<0.001%
H2O	11	10.492%	*HBr*	161	<0.001%
CO2	21	1.341%	*HI*	171	<0.001%
CO	5**2**	1.287%	*H2S*	471	<0.001%
CH4	6**3**	0.901%			

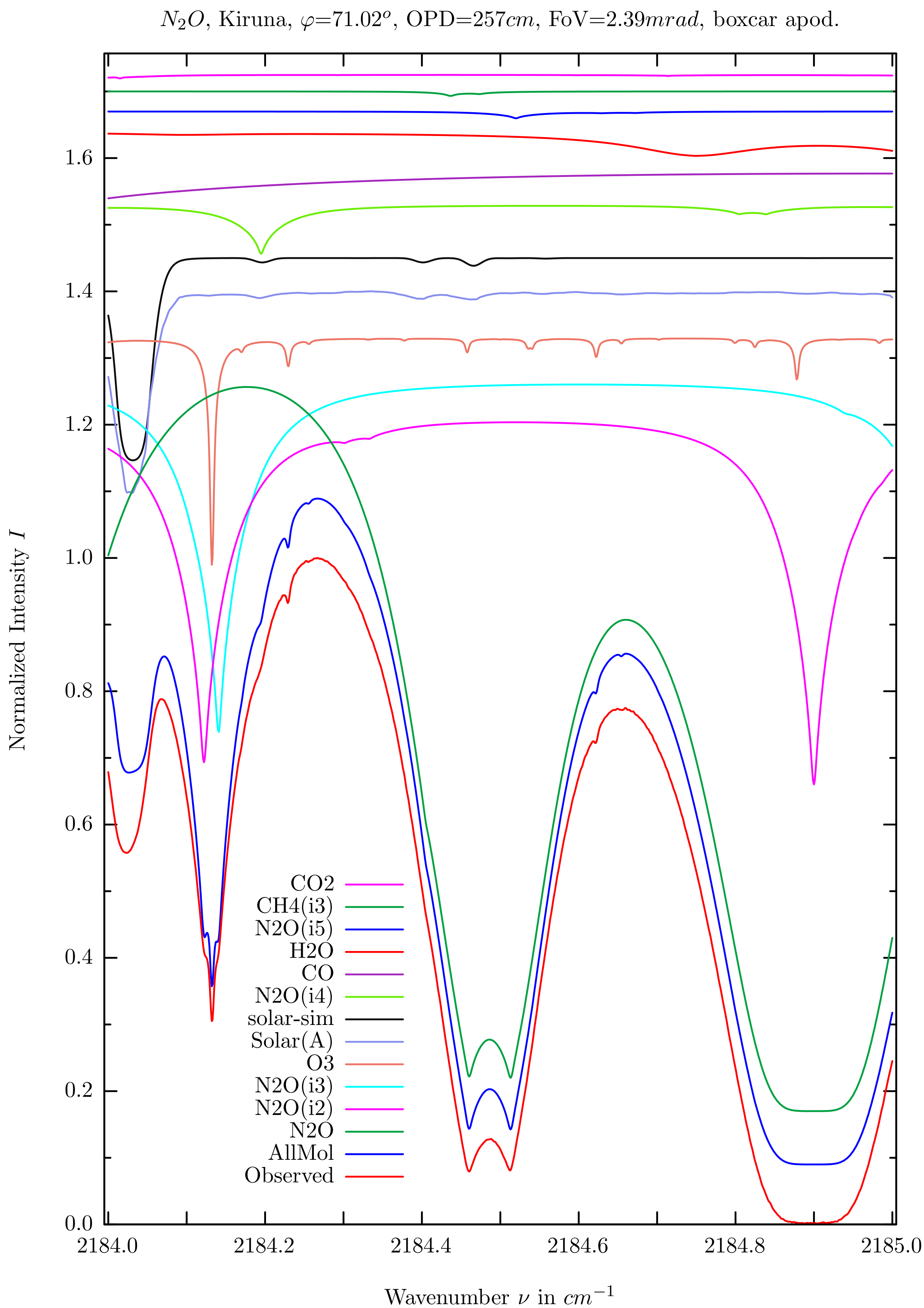

N_2O, Kiruna, φ=71.02^o, OPD=257cm, FoV=2.39$mrad$, boxcar apod.
Normalized Intensity I
Wavenumber ν in cm^{-1}
0.0
0.2
0.4
0.6
0.8
1.0
1.2
1.4
1.6
2184.0
2184.2
2184.4
2184.6
2184.8
2185.0
CO2
CH4(i3)
N2O(i5)
H2O
CO
N2O(i4)
solar-sim
Solar(A)
O3
N2O(i3)
N2O(i2)
N2O
AllMol
Observed

σ=0.082%, 970315S4.90, φ=71.02^o, OPD=257cm, FoV=2.39$mrad$, Apod.=boxcar

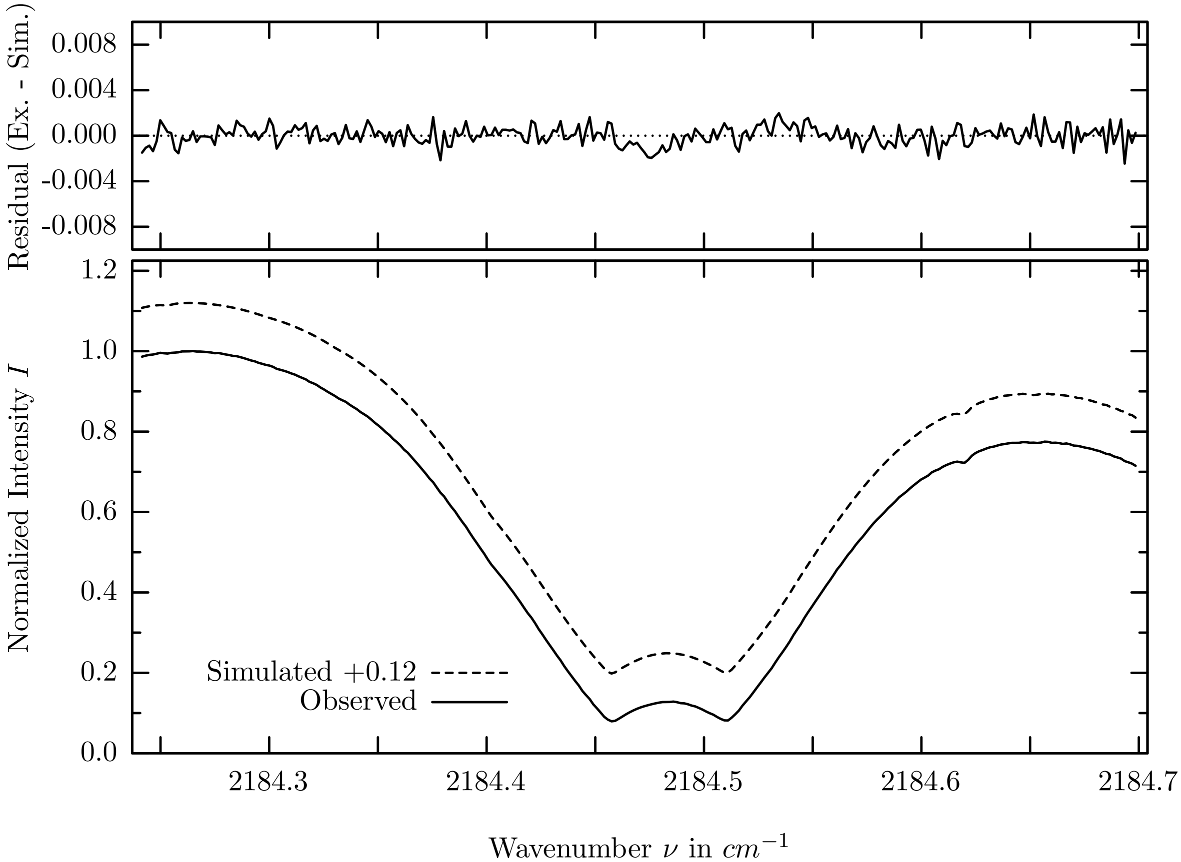

investigated species	:	N_2O
line position(s) ν_0	:	2184.4585, 2184.5118 cm^{-1}
lower state energy E''_{lst}	:	906.2, 905.6 cm^{-1}
retrieved TCA, information content	:	5.61E+18 $molec/cm^2$, 1128.4, 1020.1
temperature dependence of the TCA	:	-2.003%/K (trop), -0.261%/K (strat)
location, date, solar zenith angle	:	Kiruna, 15/Mar/97, 71.02^o
spectral interval fitted	:	2184.240 – 2184.700 cm^{-1}

Molecule	iCode	Absorption	Molecule	iCode	Absorption
N2O	41	100.000%	$CH4$	6**3**	0.676%
$N2O$	4**2**	56.094%	$CO2$	21	0.536%
$N2O$	4**3**	53.247%	$N2$	411	0.001%
$O3$	31	34.728%	$CH4$	61	<0.001%
Solar(A)	—	30.279%	NO	81	<0.001%
Solar-sim	—	30.353%	$NH3$	111	<0.001%
$N2O$	4**4**	7.383%	OH	131	<0.001%
CO	51	5.951%	HI	171	<0.001%
$H2O$	11	3.668%	$C2H2$	401	<0.001%
$N2O$	4**5**	1.034%	$H2S$	471	<0.001%

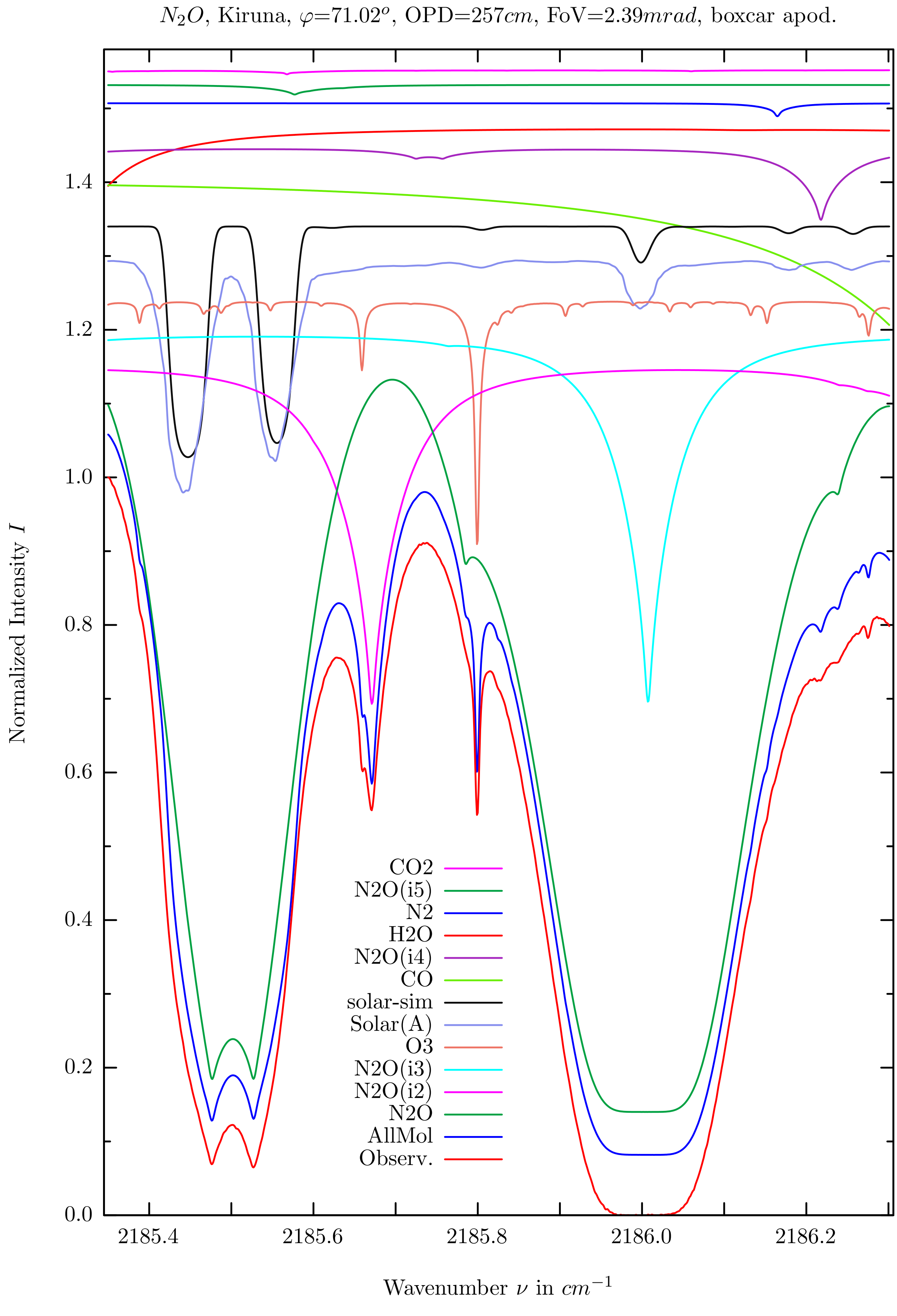

N_2O, Kiruna, φ=71.02^o, OPD=257cm, FoV=2.39$mrad$, boxcar apod.
Normalized Intensity I
Wavenumber ν in cm^{-1}
0.0
0.2
0.4
0.6
0.8
1.0
1.2
1.4
2185.4
2185.6
2185.8
2186.0
2186.2
CO2
N2O(i5)
N2
H2O
N2O(i4)
CO
solar-sim
Solar(A)
O3
N2O(i3)
N2O(i2)
N2O
AllMol
Observ.

σ=0.136%, 970315S4.90, φ=71.02^o, OPD=257cm, FoV=2.39$mrad$, Apod.=boxcar

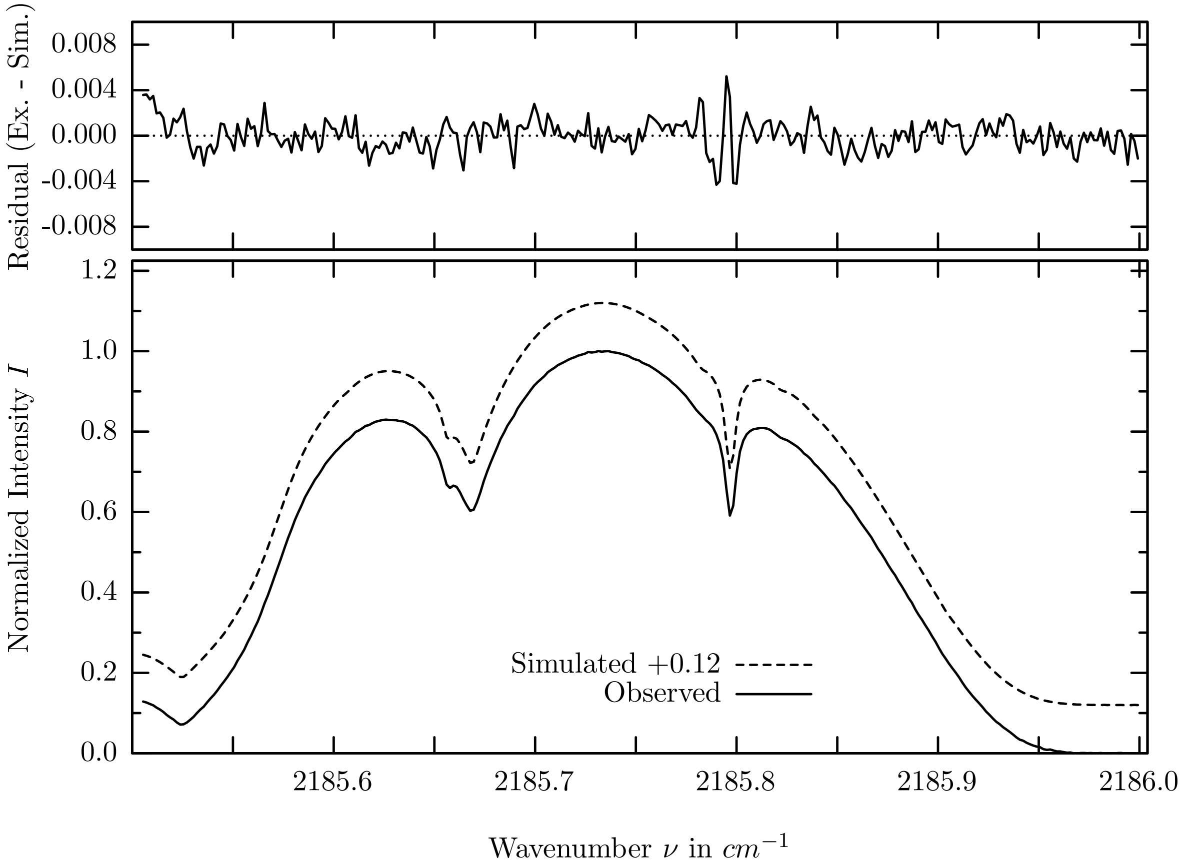

investigated species	:	$N_2O(i2), (N_2O)$
line position(s) ν_0	:	2185.6697, (2186.0020) cm^{-1}
lower state energy E''_{lst}	:	37.7, (653.2) cm^{-1}
retrieved TCA, information content	:	5.63E+18, (5.67E+18) $molec/cm^2$, 266.0, (733.3)
temperature dependence of the TCA	:	+3.707, (-1.286)%/K (trop), +.869, (-.185)%/K (strat)
location, date, solar zenith angle	:	Kiruna, 15/Mar/97, 71.02^o
spectral interval fitted	:	2185.505 – 2186.010 cm^{-1}

Molecule	iCode	Absorption	Molecule	iCode	Absorption
N2O	41	100.000%	*N2O*	4**5**	1.317%
N2O	4**2**	58.478%	*CO2*	21	0.579%
N2O	4**3**	56.200%	*CH4*	61	0.001%
O3	31	33.972%	*C2H2*	401	0.001%
Solar(A)	—	32.051%	*NO*	81	<0.001%
Solar-sim	—	31.262%	*NH3*	111	<0.001%
CO	51	21.766%	*OH*	131	<0.001%
N2O	4**4**	9.835%	*HBr*	161	<0.001%
H2O	11	8.075%	*HI*	171	<0.001%
N2	411	1.772%	*H2S*	471	<0.001%

N_2O, Kiruna, φ=71.02^o, OPD=257cm, FoV=2.39$mrad$, boxcar apod.

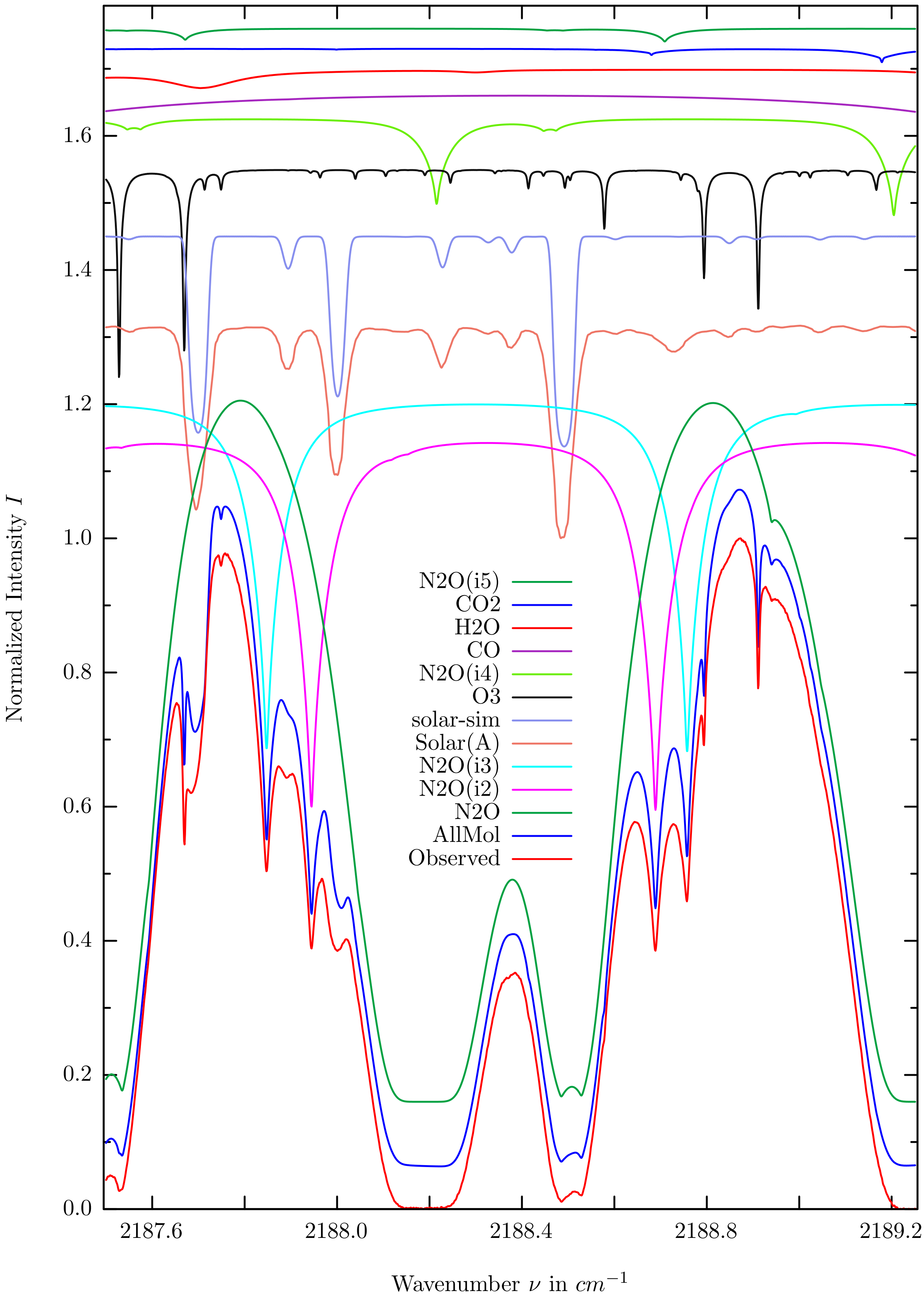

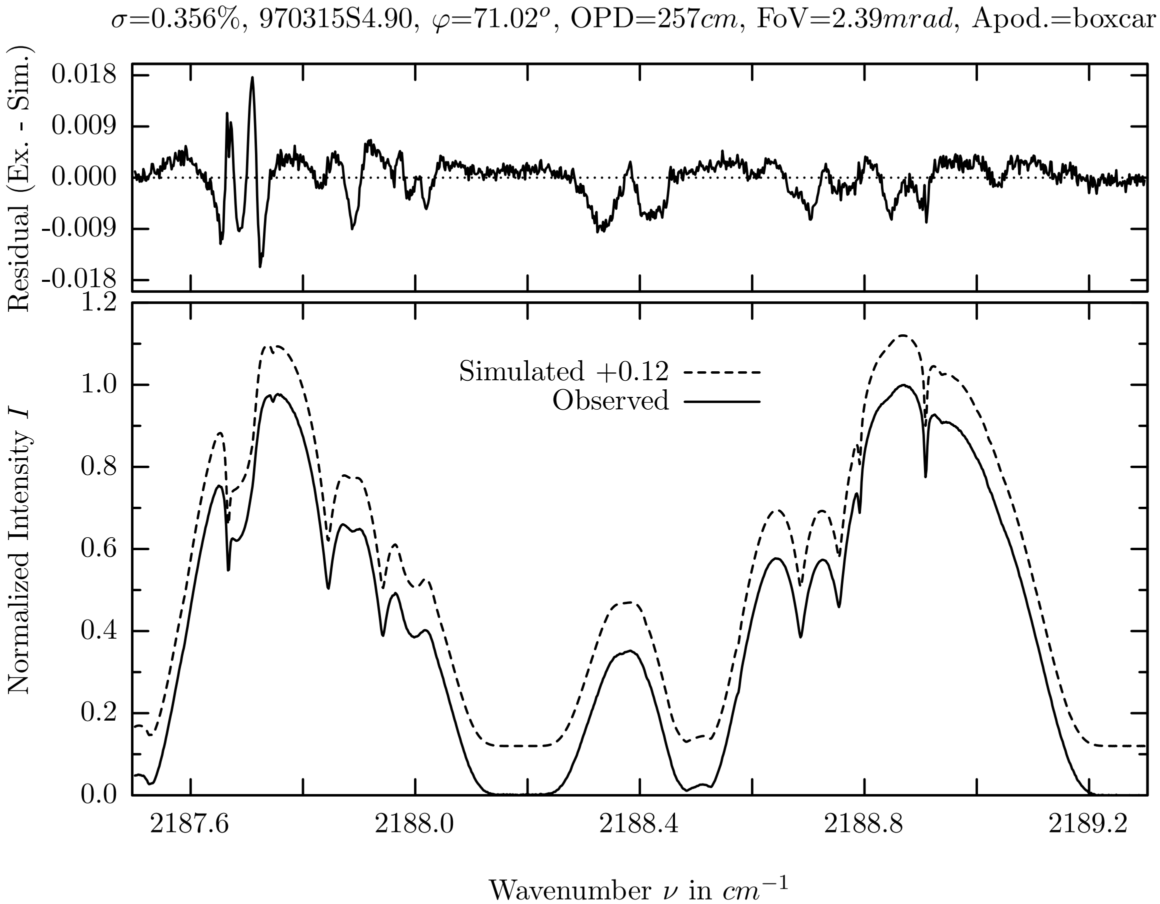

investigated species	:	$N_2O(i3), (N_2O)$
line position(s) ν_0	:	2187.8459, 2188.7560, (2188.1894) cm^{-1}
lower state energy E''_{lst}	:	110.1, 97.2, (588.8) cm^{-1}
retrieved TCA, information content	:	6.01e18, (5.68e18) $molec/cm^2$, 117.3, 145.27, (280.9)
temperature dependence of the TCA	:	-.008, (-1.068)%/K (trop), +.084, (-.109)%/K (strat)
investigated species, position	:	$N_2O(i2)$, 2187.9431, 2188.6875 cm^{-1}
lower state energy E''_{lst}	:	65.4, 76.2 cm^{-1}
retrieved TCA, information content	:	5.62E+18 $molec/cm^2$, 107.2, 122.7
temperature dependence of the TCA	:	+.485%/K (trop), +.030%/K (strat)

Molecule	iCode	Absorption	Molecule	iCode	Absorption
N2O	41	100.000%	*N2O*	4**5**	1.939%
N2O	4**2**	62.885%	*C2H2*	401	0.002%
N2O	4**3**	58.832%	*CH4*	61	0.001%
Solar(A)	—	31.970%	*N2*	411	0.001%
Solar-sim	—	31.316%	*NO*	81	<0.001%
O3	31	31.827%	*NH3*	111	<0.001%
N2O	4**4**	14.580%	*OH*	131	<0.001%
CO	51	4.438%	*HBr*	161	<0.001%
H2O	11	2.879%	*HI*	171	<0.001%
CO2	21	2.036%	*H2S*	471	<0.001%

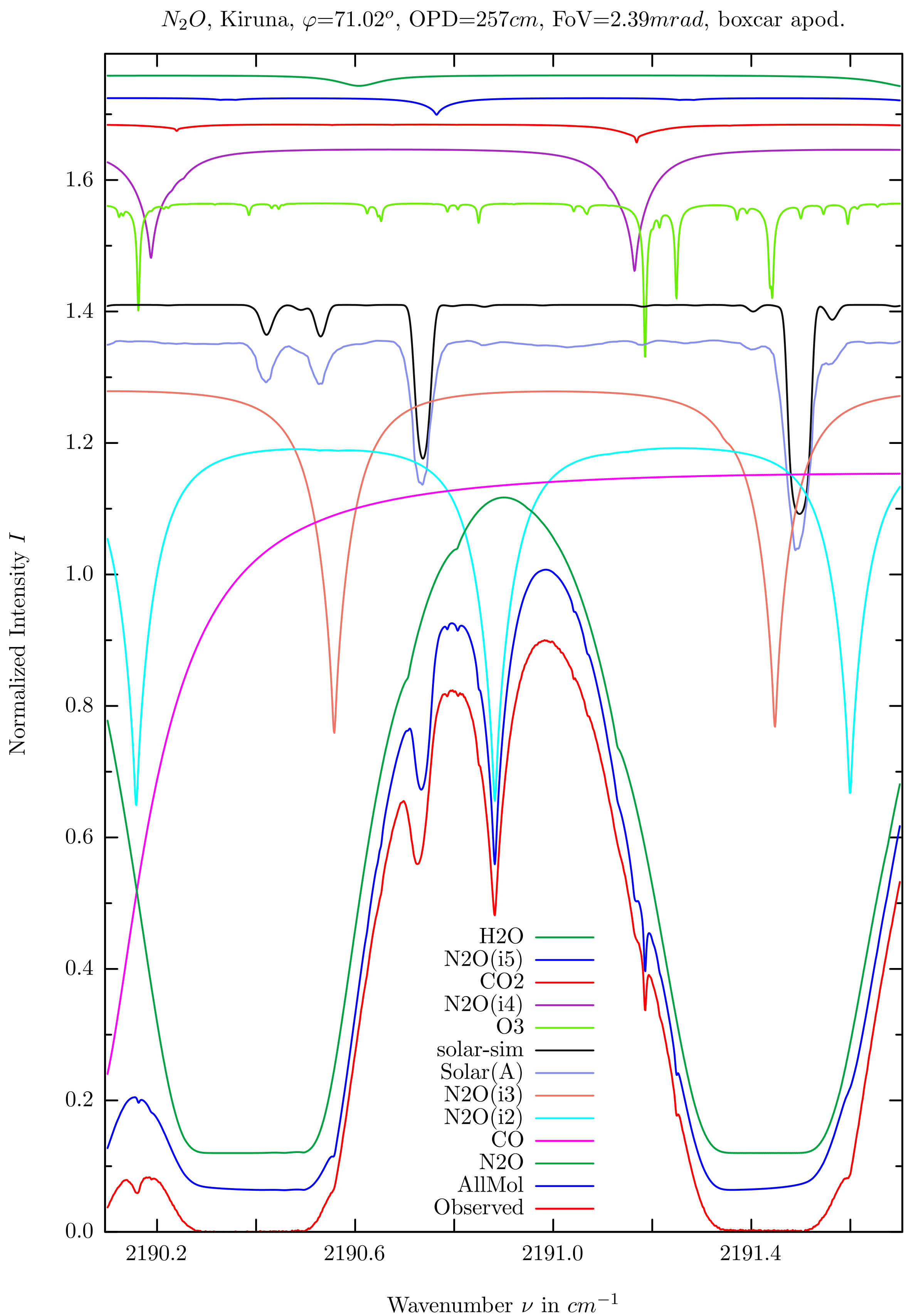

N_2O, Kiruna, φ=71.02^o, OPD=257cm, FoV=2.39$mrad$, boxcar apod.
Normalized Intensity I
Wavenumber ν in cm^{-1}
0.0
0.2
0.4
0.6
0.8
1.0
1.2
1.4
1.6
2190.2
2190.6
2191.0
2191.4
H2O
N2O(i5)
CO2
N2O(i4)
O3
solar-sim
Solar(A)
N2O(i3)
N2O(i2)
CO
N2O
AllMol
Observed

σ=0.190%, 970315S4.90, φ=71.02^o, OPD=257cm, FoV=2.39$mrad$, Apod.=boxcar

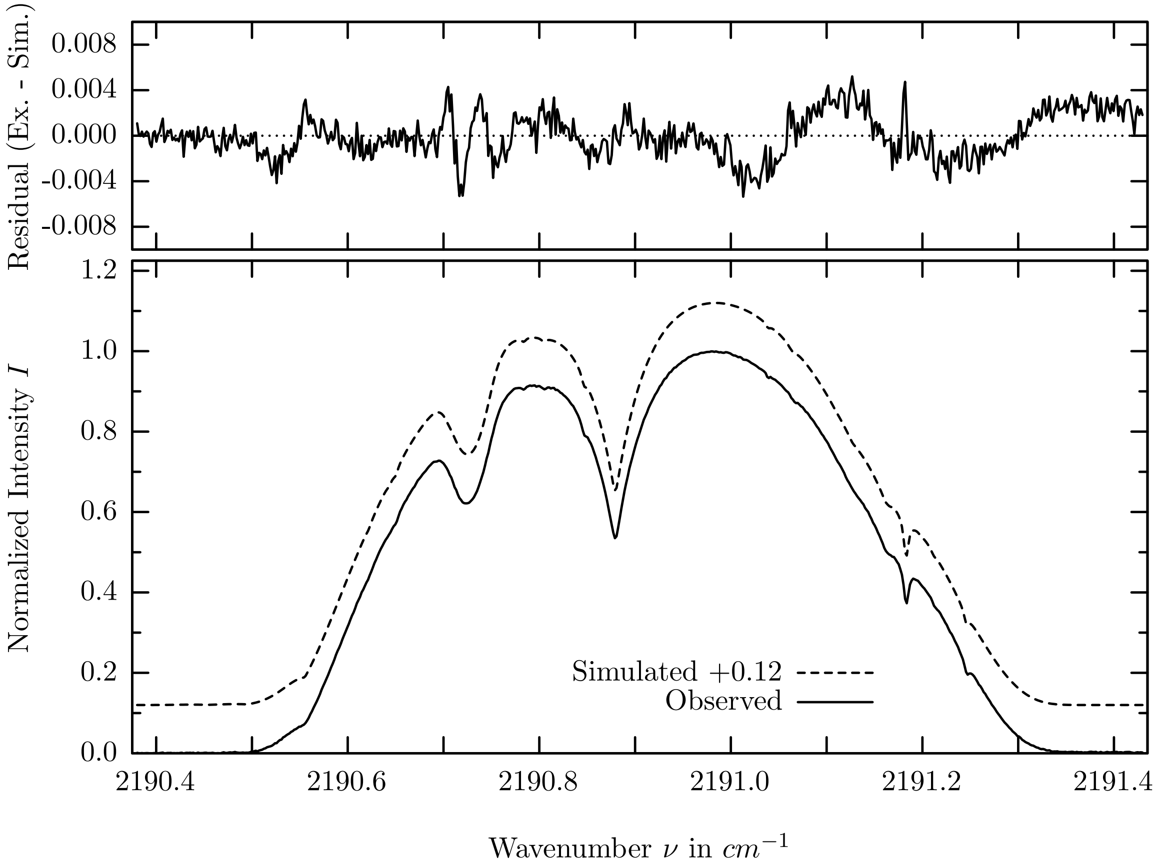

investigated species	:	$N_2O(i2), (N_2O)$
line position(s) ν_0	:	2190.8805, (2190.4950) cm^{-1}
lower state energy E''_{lst}	:	114.0, (782.4) cm^{-1}
retrieved TCA, information content	:	5.17E+18, (5.56E+18) $molec/cm^2$, 245.5, (525.7)
temperature dependence of the TCA	:	+.567, (-.662)%/K (trop), +.003, (-.097)%/K (strat)
location, date, solar zenith angle	:	Kiruna, 15/Mar/97, 71.02^o
spectral interval fitted	:	2190.380 – 2191.430 cm^{-1}

Molecule	iCode	Absorption	Molecule	iCode	Absorption
$N2O$	41	100.000%	$H2O$	11	1.744%
CO	51	92.617%	$CH4$	61	0.001%
N2O	4**2**	62.457%	$C2H2$	401	0.001%
$N2O$	4**3**	59.133%	NO	81	<0.001%
Solar(A)	—	32.310%	$NH3$	111	<0.001%
Solar-sim	—	31.798%	OH	131	<0.001%
$O3$	31	24.217%	HBr	161	<0.001%
$N2O$	4**4**	18.787%	HI	171	<0.001%
$CO2$	21	2.808%	$N2$	411	<0.001%
$N2O$	4**5**	2.581%	$H2S$	471	<0.001%

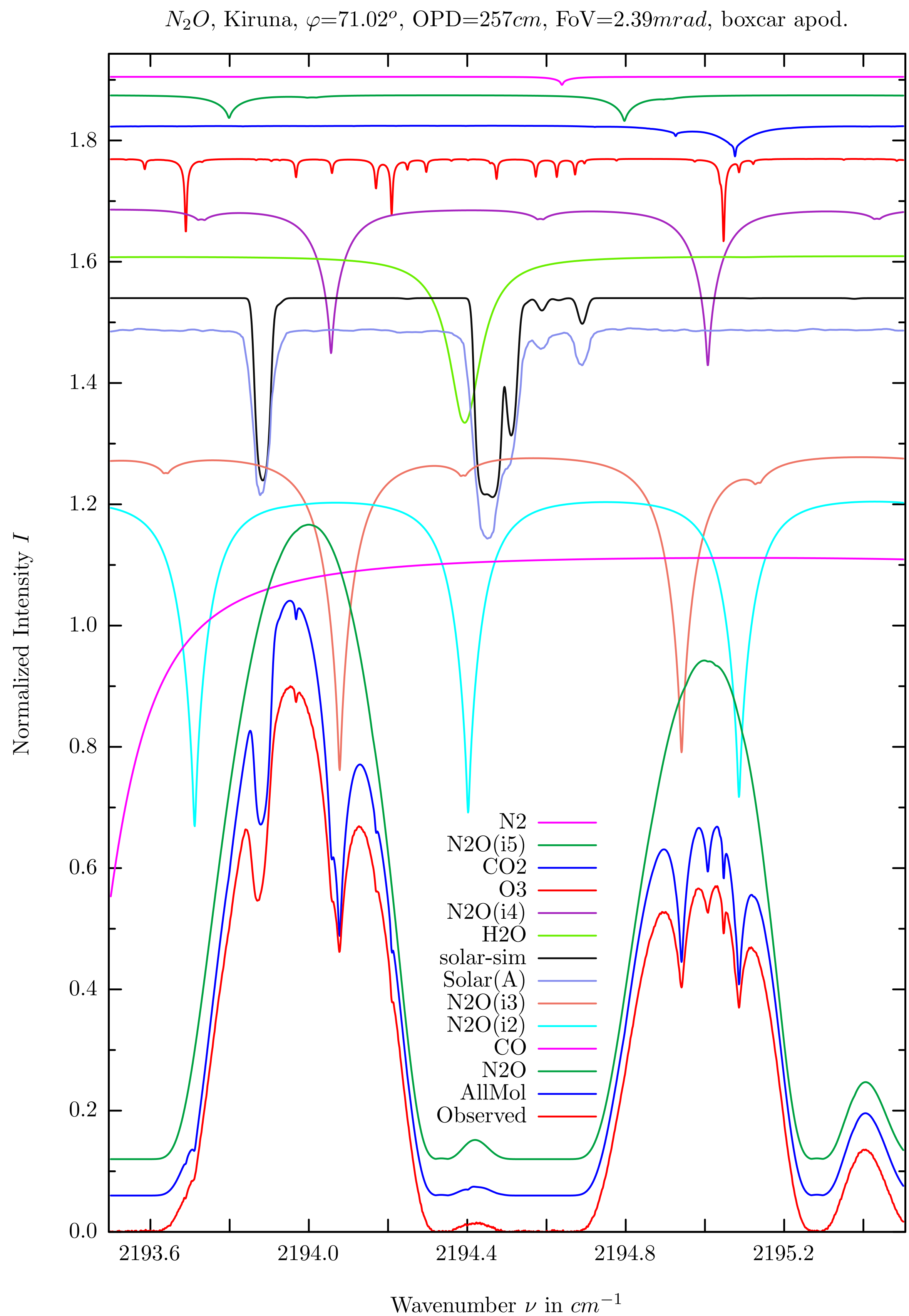

N_2O, Kiruna, φ=71.02^o, OPD=257cm, FoV=2.39$mrad$, boxcar apod.
Normalized Intensity I
Wavenumber ν in cm^{-1}
0.0
0.2
0.4
0.6
0.8
1.0
1.2
1.4
1.6
1.8
2193.6
2194.0
2194.4
2194.8
2195.2
N2
N2O(i5)
CO2
O3
N2O(i4)
H2O
solar-sim
Solar(A)
N2O(i3)
N2O(i2)
CO
N2O
AllMol
Observed

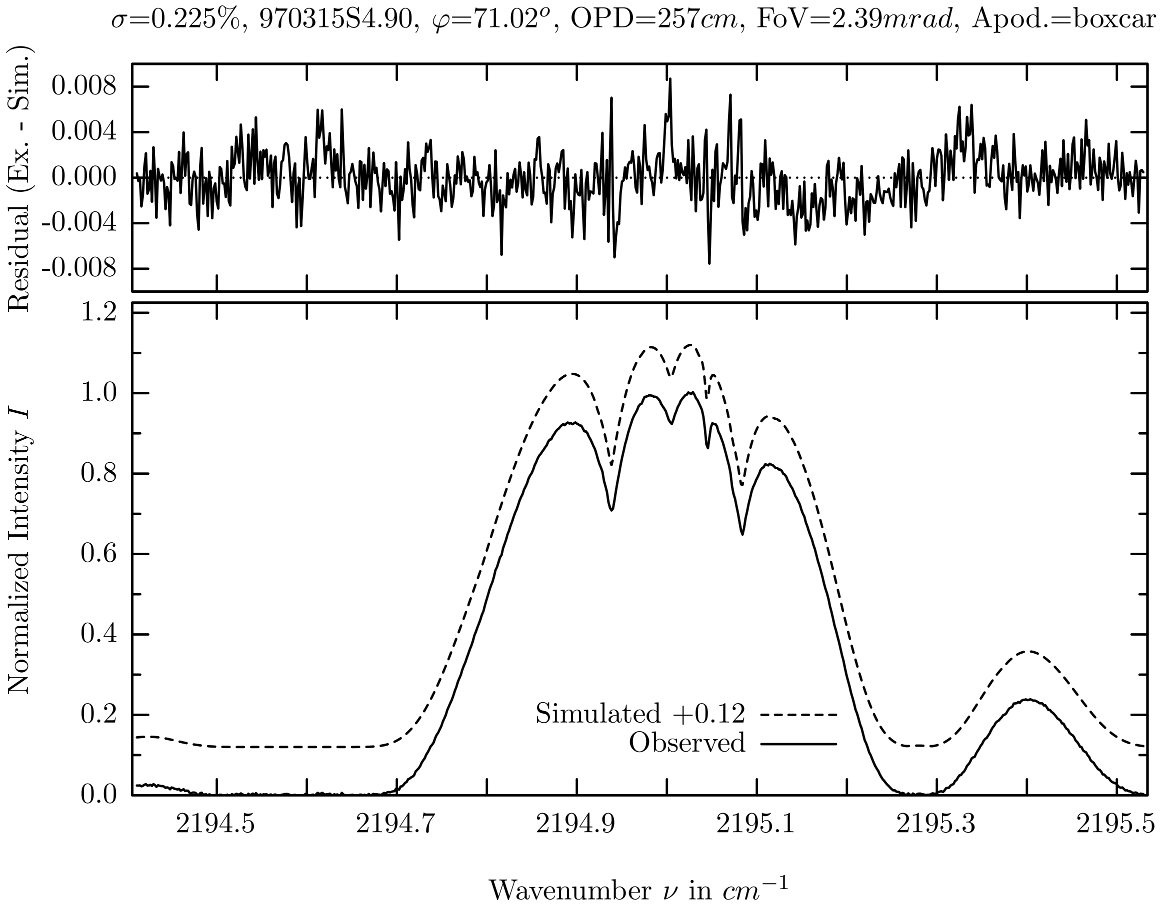

investigated species	:	$N_2O(i3), (N_2O)$
line position(s) ν_0	:	2194.9397, (2194.5897) cm^{-1}
lower state energy E''_{lst}	:	29.1, (212.0) cm^{-1}
retrieved TCA, information content	:	5.35e18, (5.73e18) $molec/cm^2$, 132.7, (444.0)
temperature dependence of the TCA	:	+.154, (-.953)%/K (trop), +.225, (-.072)%/K (strat)
investigated species, position	:	$N_2O(i2)$, 2195.0847 cm^{-1}
lower state energy E''_{lst}	:	415.5 cm^{-1}
retrieved TCA, information content	:	5.58e18 $molec/cm^2$, 154.4
temperature dependence of the TCA	:	-1.32%/K (trop), +0.073%/K (strat)

Molecule	iCode	Absorption	Molecule	iCode	Absorption
N2O	41	100.000%	*N2O*	4**5**	4.289%
CO	51	56.692%	*N2*	411	1.336%
N2O	4**2**	55.239%	*CH4*	61	0.001%
N2O	4**3**	52.955%	*C2H2*	401	0.001%
Solar(A)	—	34.656%	*NO*	81	<0.001%
Solar-sim	—	32.819%	*NH3*	111	<0.001%
H2O	11	27.559%	*OH*	131	<0.001%
N2O	4**4**	26.215%	*HBr*	161	<0.001%
O3	31	14.010%	*HI*	171	<0.001%
CO2	21	5.026%	*H2S*	471	<0.001%

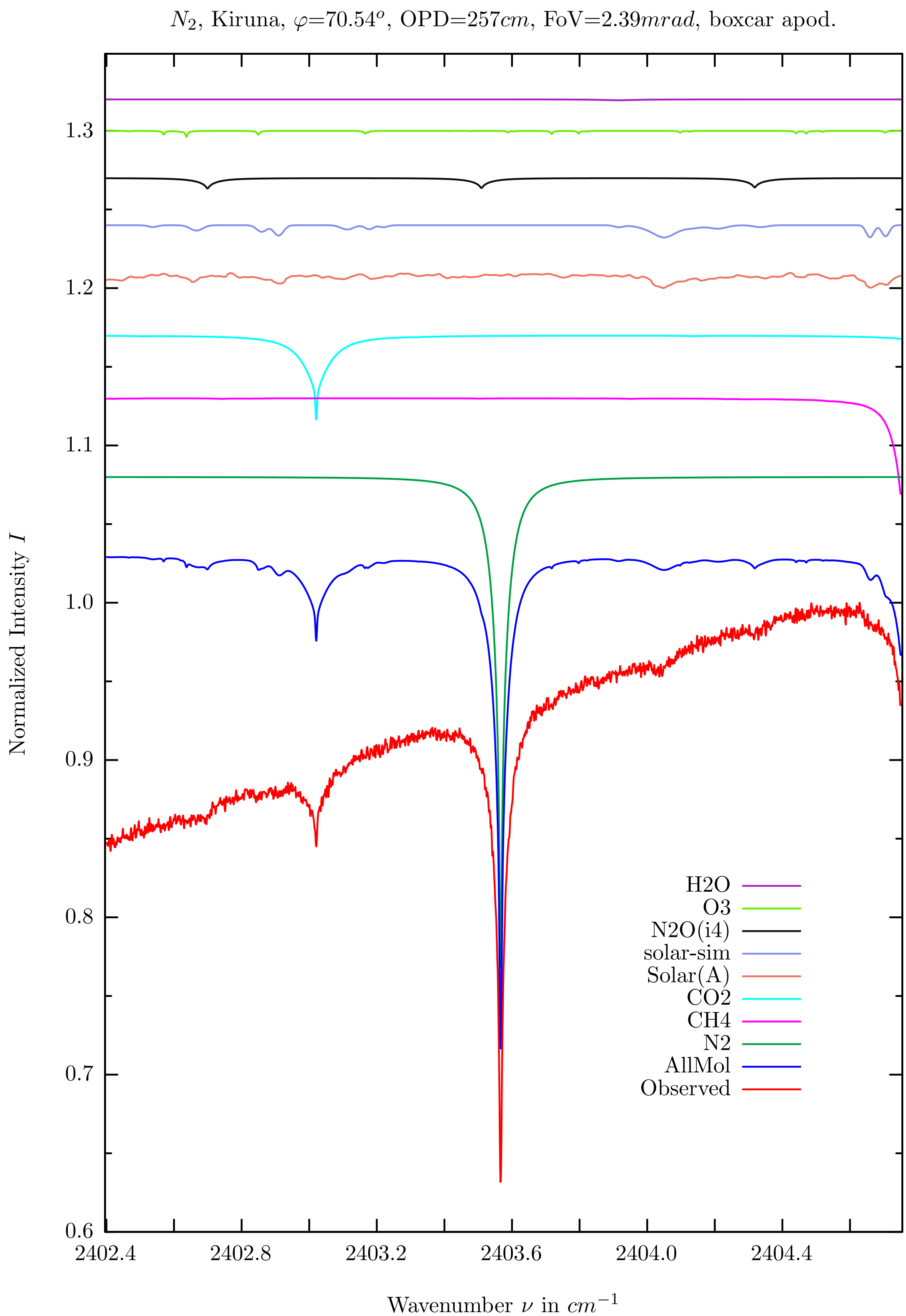

N_2, Kiruna, φ=70.54^o, OPD=257cm, FoV=2.39$mrad$, boxcar apod.
Normalized Intensity I
Wavenumber ν in cm^{-1}
1.3
1.2
1.1
1.0
0.9
0.8
0.7
0.6
2402.4
2402.8
2403.2
2403.6
2404.0
2404.4
H2O
O3
N2O(i4)
solar-sim
Solar(A)
CO2
CH4
N2
AllMol
Observed

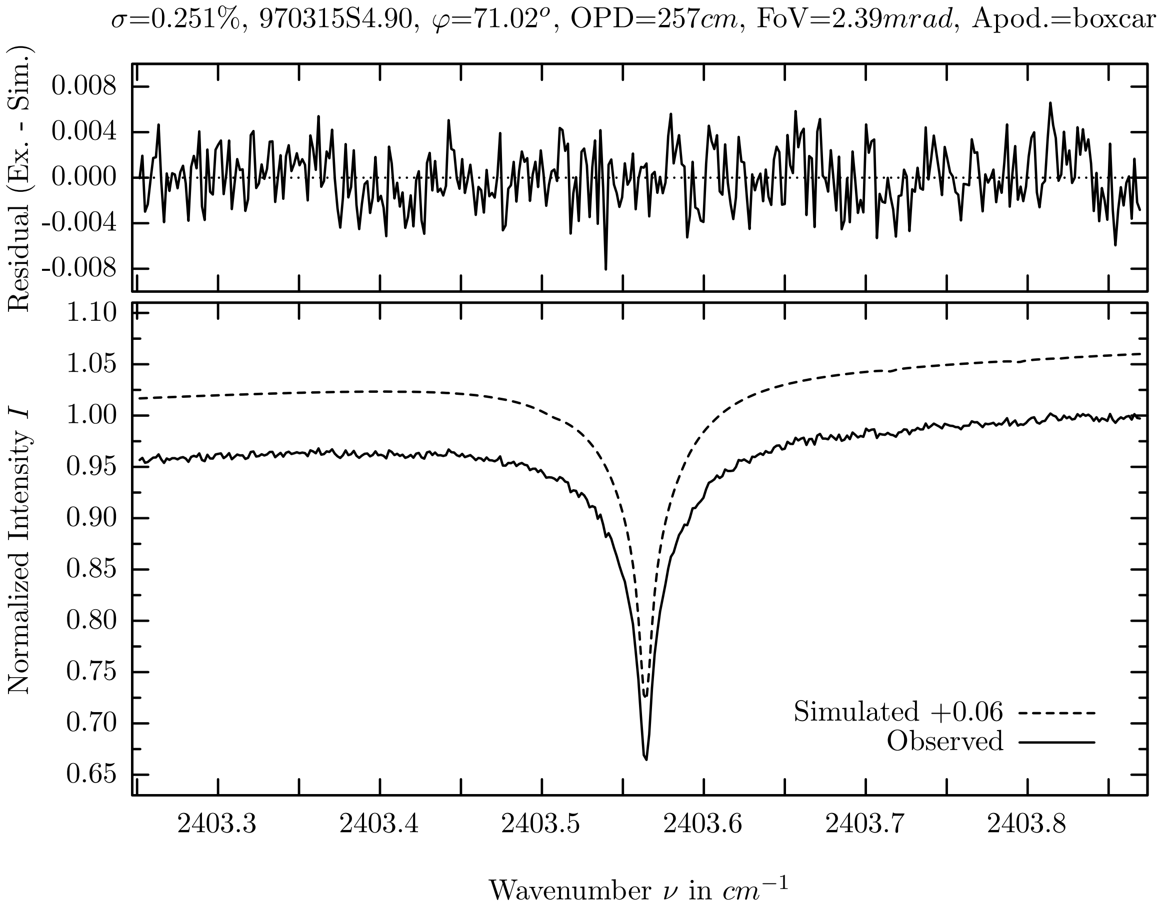

investigated species	:	N_2
line position(s) ν_0	:	2403.5650 cm^{-1}
lower state energy E''_{lst}	:	143.2 cm^{-1}
retrieved TCA, information content	:	1.63E+25 $molec/cm^2$, 126.1
temperature dependence of the TCA	:	-0.037%/K (trop), -0.022%/K (strat)
location, date, solar zenith angle	:	Kiruna, 15/Mar/97, 71.02^o
spectral interval fitted	:	2403.250 – 2403.870 cm^{-1}

Molecule	iCode	Absorption	Molecule	iCode	Absorption
N2	411	31.497%	$N2O$	41	0.020%
$CH4$	61	6.211%	$NH3$	111	<0.001%
$CO2$	21	5.409%	OH	131	<0.001%
Solar(A)	—	1.000%	HCl	151	<0.001%
Solar-sim	—	0.779%	HBr	161	<0.001%
$N2O$	44	0.669%	HI	171	<0.001%
$O3$	31	0.395%	$H2S$	471	<0.001%
$H2O$	11	0.056%	HDO	491	<0.001%

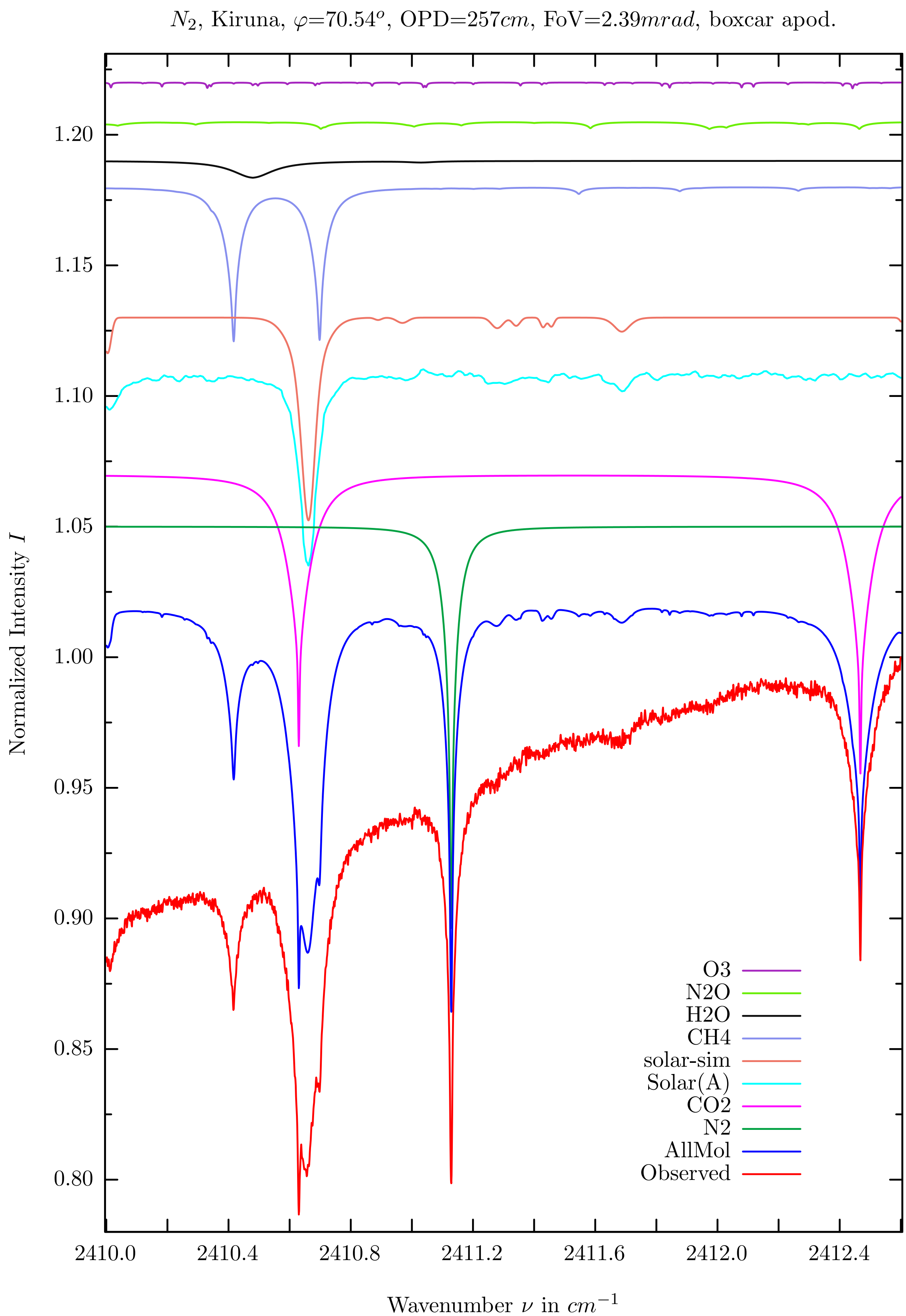
N_2, Kiruna, φ=70.54^o, OPD=257cm, FoV=2.39$mrad$, boxcar apod.
Normalized Intensity I
1.20
1.15
1.10
1.05
1.00
0.95
0.90
0.85
0.80
2410.0
2410.4
2410.8
2411.2
2411.6
2412.0
2412.4
Wavenumber ν in cm^{-1}
O3
N2O
H2O
CH4
solar-sim
Solar(A)
CO2
N2
AllMol
Observed

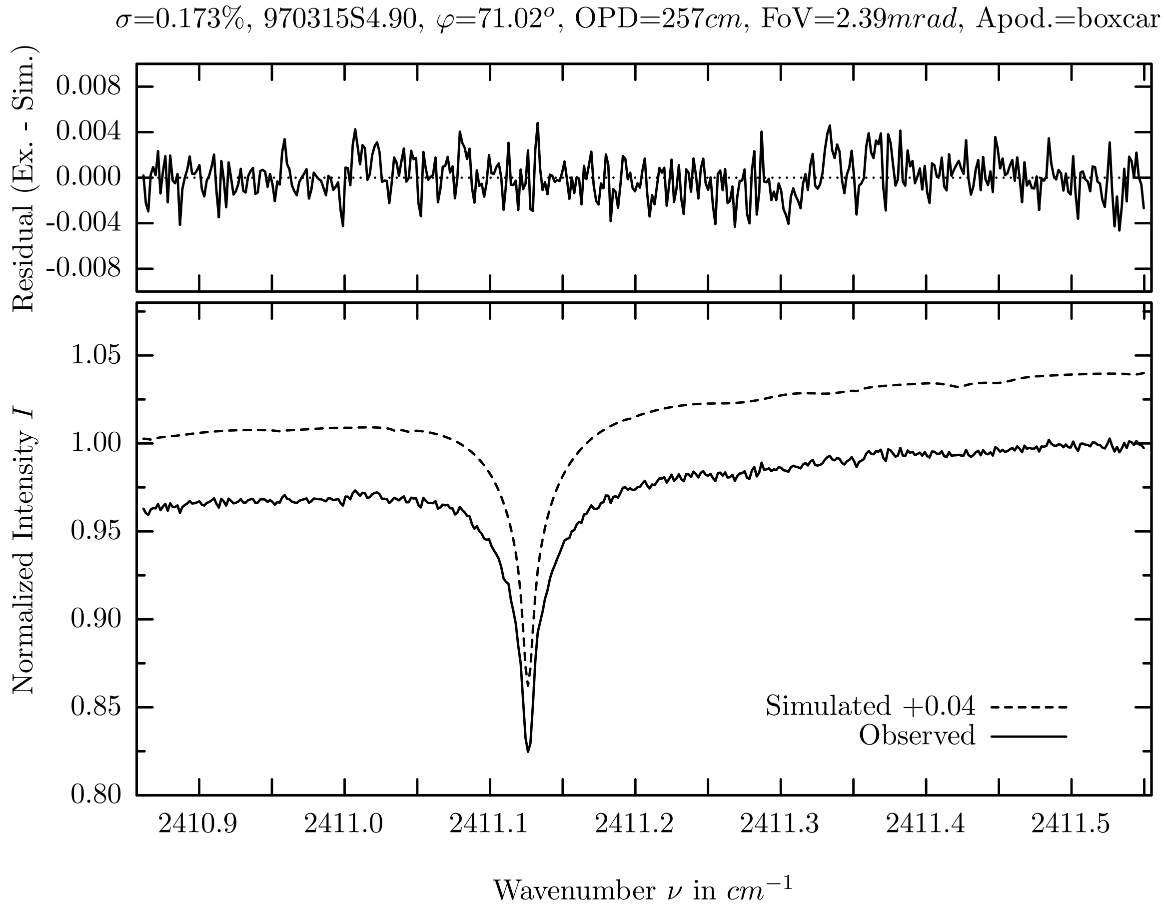

investigated species	:	N_2
line position(s) ν_0	:	2411.1274 cm^{-1}
lower state energy E''_{lst}	:	179.0 cm^{-1}
retrieved TCA, information content	:	1.62E+25 $molec/cm^2$, 90.4
temperature dependence of the TCA	:	-0.111%/K (trop), -0.037%/K (strat)
location, date, solar zenith angle	:	Kiruna, 15/Mar/97, 71.02^o
spectral interval fitted	:	2410.860 – 2411.550 cm^{-1}

Molecule	iCode	Absorption	Molecule	iCode	Absorption
N2	411	15.469%	$O3$	31	0.229%
$CO2$	21	11.567%	$NH3$	111	<0.001%
Solar(A)	—	7.490%	OH	131	<0.001%
Solar-sim	—	7.763%	HBr	161	<0.001%
$CH4$	61	5.922%	HI	171	<0.001%
$H2O$	11	0.645%	$H2S$	471	<0.001%
$N2O$	41	0.246%	HDO	491	<0.001%

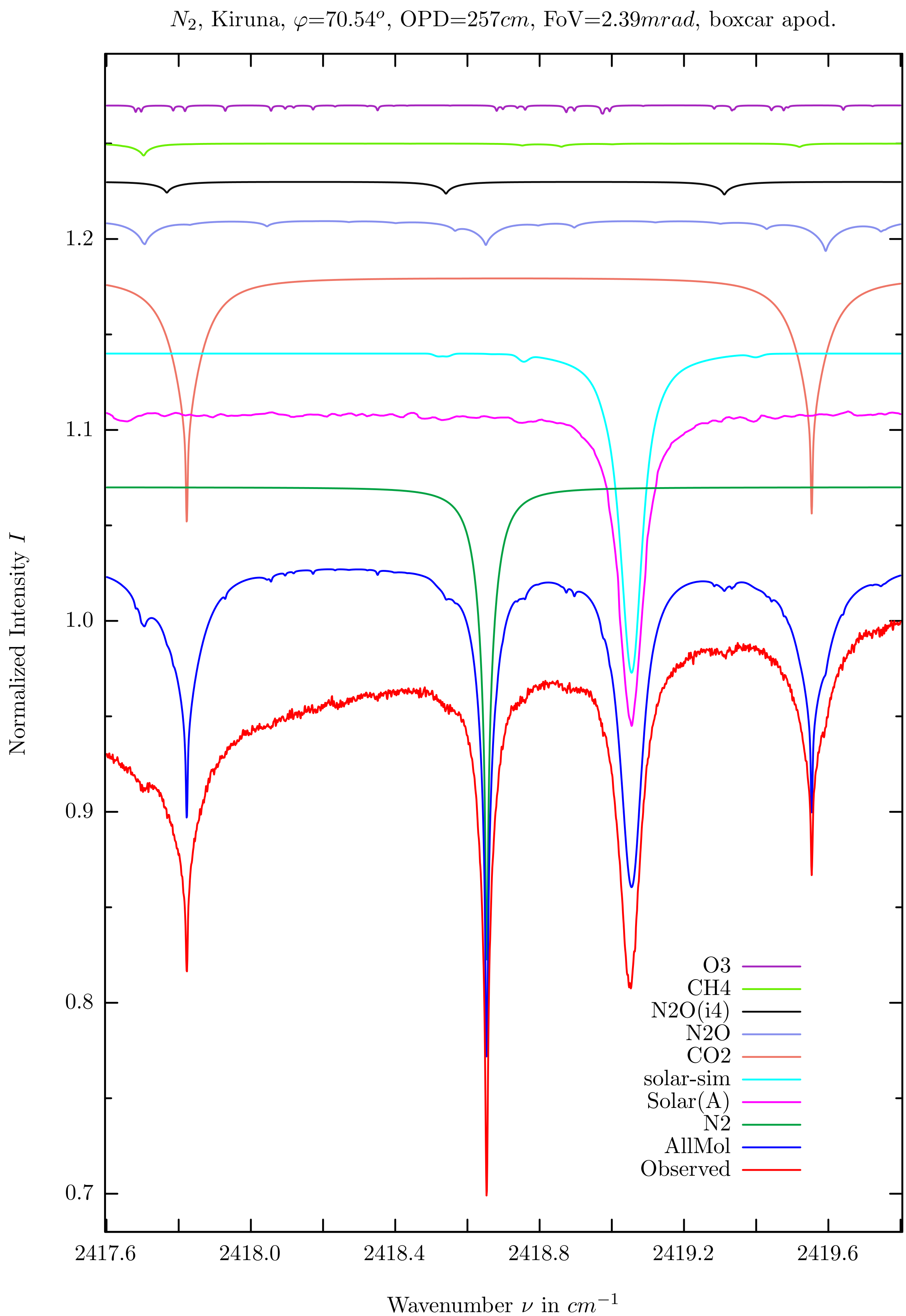

N_2, Kiruna, φ=70.54^o, OPD=257cm, FoV=2.39$mrad$, boxcar apod.
Normalized Intensity I
Wavenumber ν in cm^{-1}
1.2
1.1
1.0
0.9
0.8
0.7
2417.6
2418.0
2418.4
2418.8
2419.2
2419.6
O3
CH4
N2O(i4)
N2O
CO2
solar-sim
Solar(A)
N2
AllMol
Observed

σ=0.140%, 970315S4.90, φ=71.02^o, OPD=257cm, FoV=2.39$mrad$, Apod.=boxcar

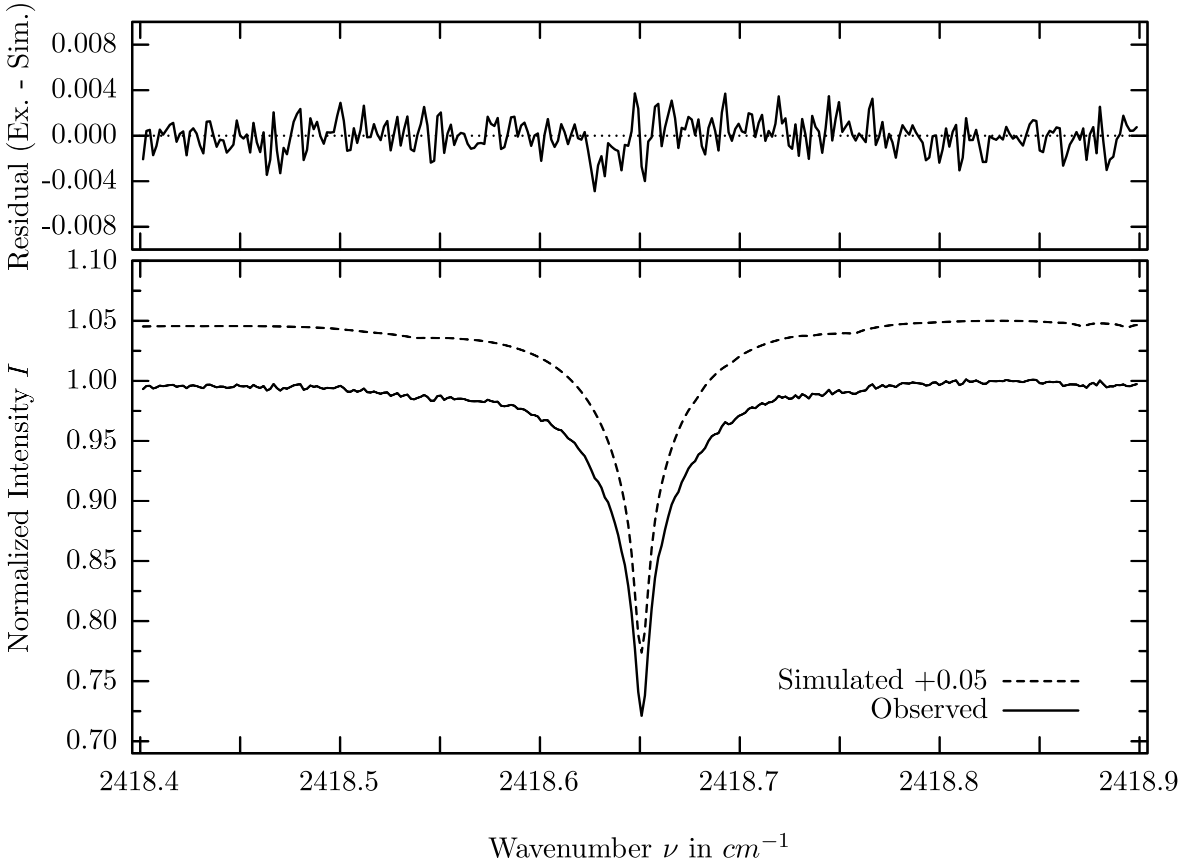

investigated species	:	N_2
line position(s) ν_0	:	2418.6520 cm^{-1}
lower state energy E''_{lst}	:	218.8 cm^{-1}
retrieved TCA, information content	:	1.65E+25 $molec/cm^2$, 196.9
temperature dependence of the TCA	:	-0.315%/K (trop), -0.076%/K (strat)
location, date, solar zenith angle	:	Kiruna, 15/Mar/97, 71.02^o
spectral interval fitted	:	2418.400 – 2418.900 cm^{-1}

Molecule	iCode	Absorption	Molecule	iCode	Absorption
N2	411	25.033%	$O3$	31	0.443%
Solar(A)	—	16.501%	$H2O$	11	0.046%
Solar-sim	—	16.719%	HDO	491	0.035%
$CO2$	21	13.004%	$NH3$	111	<0.001%
$N2O$	41	1.601%	OH	131	<0.001%
$N2O$	44	0.673%	HBr	161	<0.001%
$CH4$	61	0.629%	$H2S$	471	<0.001%

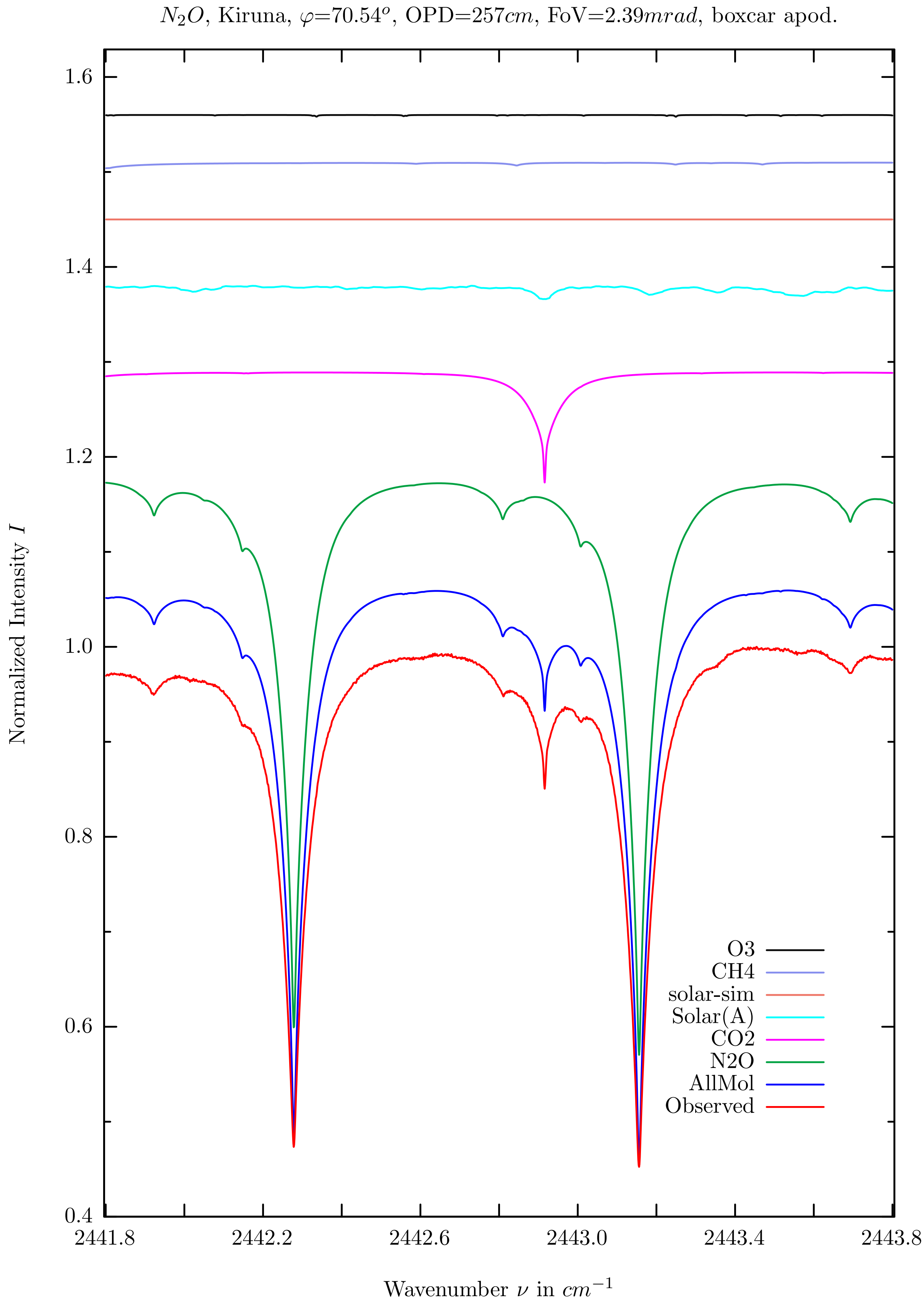

N_2O, Kiruna, φ=70.54^o, OPD=257cm, FoV=2.39$mrad$, boxcar apod.
Normalized Intensity I
Wavenumber ν in cm^{-1}
1.6
1.4
1.2
1.0
0.8
0.6
0.4
2441.8
2442.2
2442.6
2443.0
2443.4
2443.8
O3
CH4
solar-sim
Solar(A)
CO2
N2O
AllMol
Observed

σ=0.124%, 970315S4.90, φ=71.02^o, OPD=257cm, FoV=2.39$mrad$, Apod.=boxcar

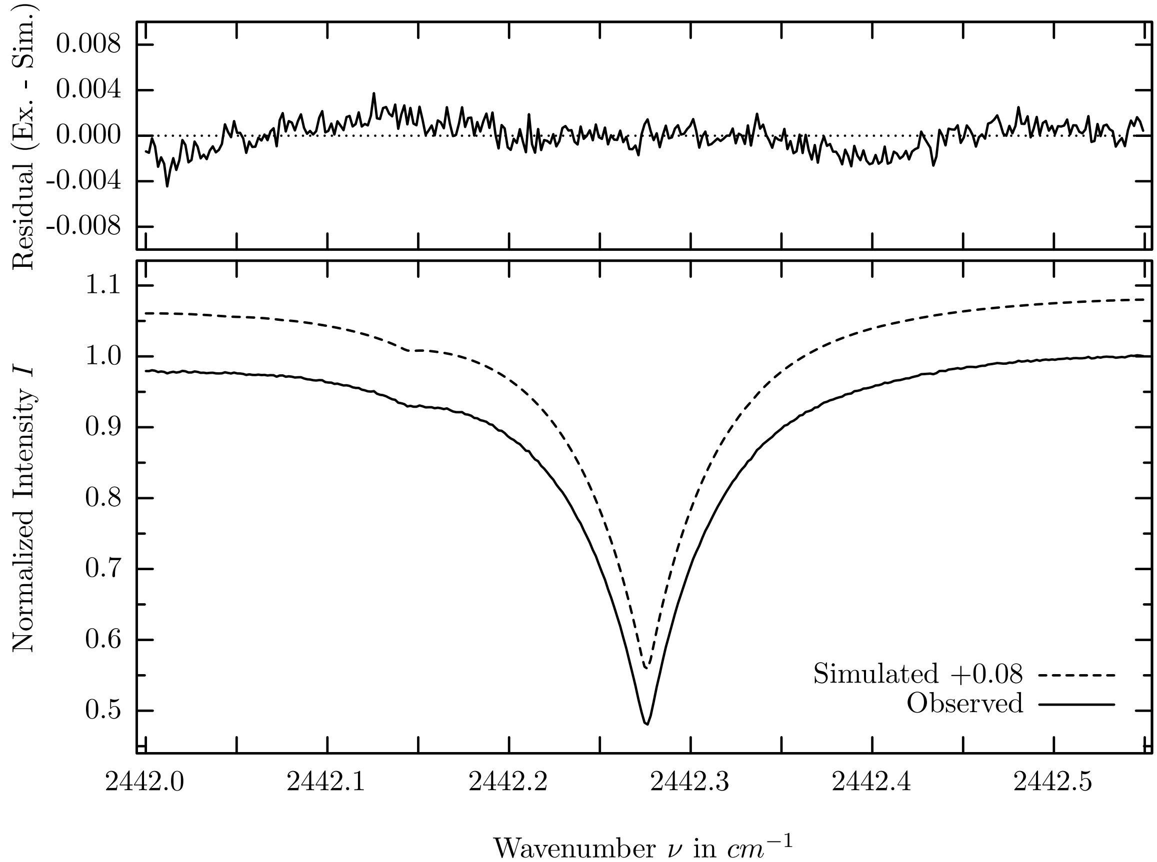

investigated species	:	N_2O
line position(s) ν_0	:	2442.2769 cm^{-1}
lower state energy E''_{lst}	:	231.2 cm^{-1}
retrieved TCA, information content	:	5.56E+18 $molec/cm^2$, 418.5
temperature dependence of the TCA	:	-0.193%/K (trop), -0.055%/K (strat)
location, date, solar zenith angle	:	Kiruna, 15/Mar/97, 71.02^o
spectral interval fitted	:	2442.000 – 2442.550 cm^{-1}

Molecule	iCode	Absorption	Molecule	iCode	Absorption
N2O	41	62.086%	$N2$	411	0.004%
$CO2$	21	11.795%	HDO	491	0.003%
Solar(A)	—	1.384%	$SO2$	91	<0.001%
Solar-sim	—	<0.001%	$NH3$	111	<0.001%
$CH4$	61	0.598%	OH	131	<0.001%
$O3$	31	0.186%	HBr	161	<0.001%
$H2O$	11	0.019%	$H2S$	471	<0.001%

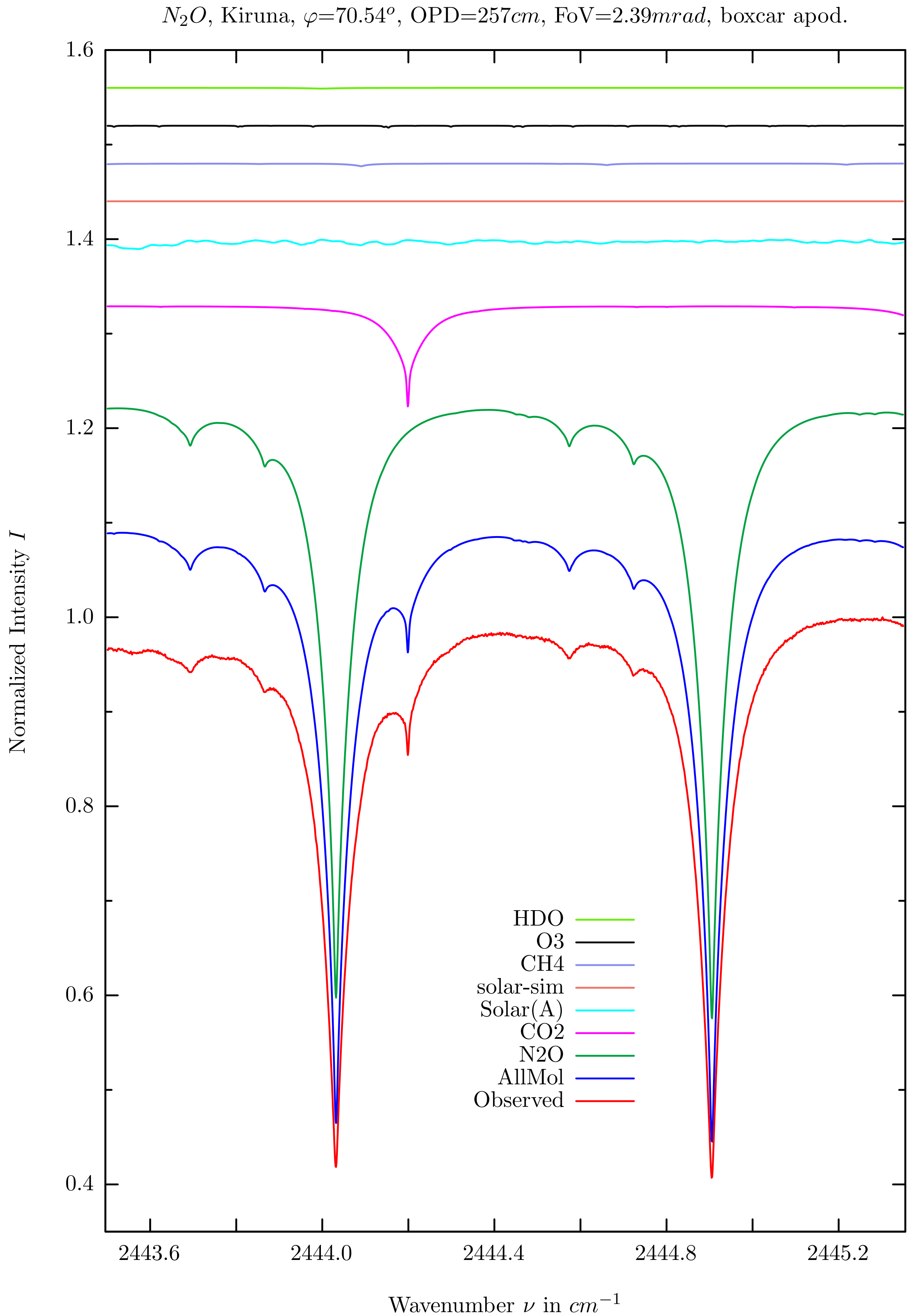

N_2O, Kiruna, φ=70.54^o, OPD=257cm, FoV=2.39$mrad$, boxcar apod.
1.6
1.4
1.2
1.0
0.8
0.6
0.4
Normalized Intensity I
2443.6
2444.0
2444.4
2444.8
2445.2
Wavenumber ν in cm^{-1}
HDO
O3
CH4
solar-sim
Solar(A)
CO2
N2O
AllMol
Observed

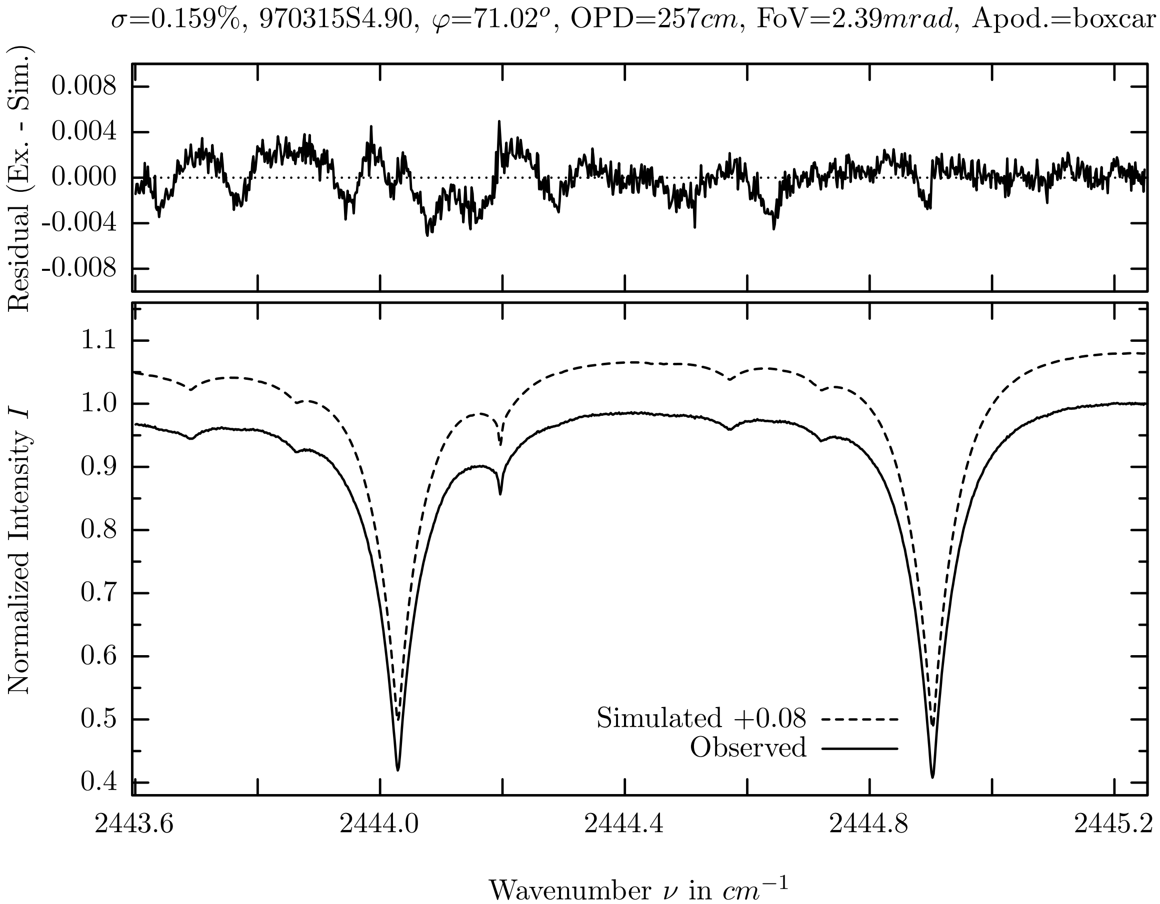

investigated species	:	N_2O
line position(s) ν_0	:	2444.0304, 2444.9041 cm^{-1}
lower state energy E''_{lst}	:	193.6, 176.0 cm^{-1}
retrieved TCA, information content	:	5.64E+18 $molec/cm^2$, 366.4, 373.5
temperature dependence of the TCA	:	-0.024%/K (trop), -0.028%/K (strat)
location, date, solar zenith angle	:	Kiruna, 15/Mar/97, 71.02^o
spectral interval fitted	:	2443.600 – 2445.250 cm^{-1}

Molecule	iCode	Absorption	Molecule	iCode	Absorption
N2O	41	66.628%	$H2O$	11	0.001%
$CO2$	21	10.803%	$N2$	411	0.001%
Solar(A)	—	1.051%	$SO2$	91	<0.001%
Solar-sim	—	<0.001%	$NH3$	111	<0.001%
$CH4$	61	0.289%	OH	131	<0.001%
$O3$	31	0.212%	HBr	161	<0.001%
HDO	491	0.076%	$H2S$	471	<0.001%

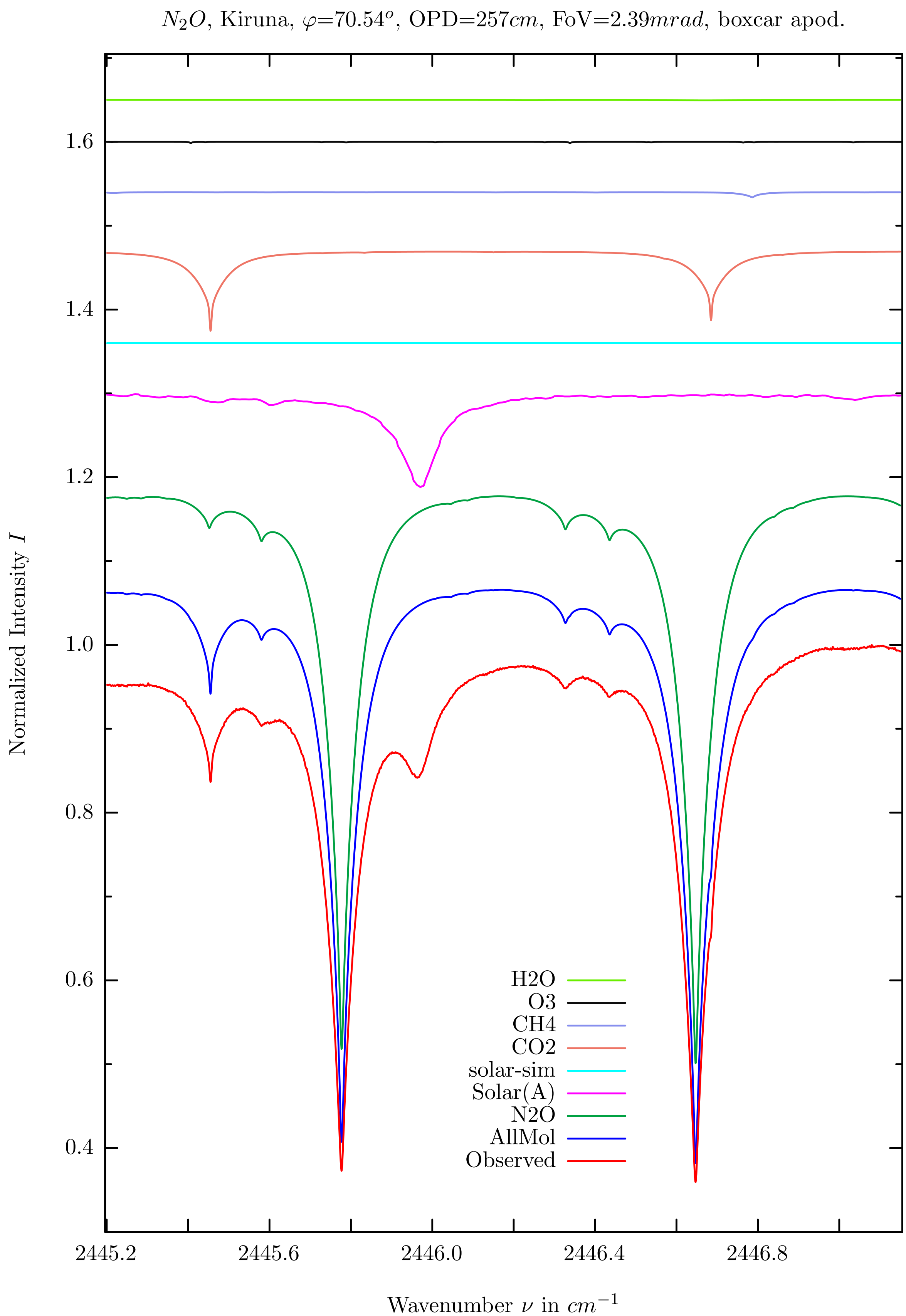

N_2O, Kiruna, φ=70.54^o, OPD=257cm, FoV=2.39$mrad$, boxcar apod.
Normalized Intensity I
Wavenumber ν in cm^{-1}
1.6
1.4
1.2
1.0
0.8
0.6
0.4
2445.2
2445.6
2446.0
2446.4
2446.8
H2O
O3
CH4
CO2
solar-sim
Solar(A)
N2O
AllMol
Observed

σ=0.088%, 970315S4.90, φ=71.02^o, OPD=257cm, FoV=2.39$mrad$, Apod.=boxcar

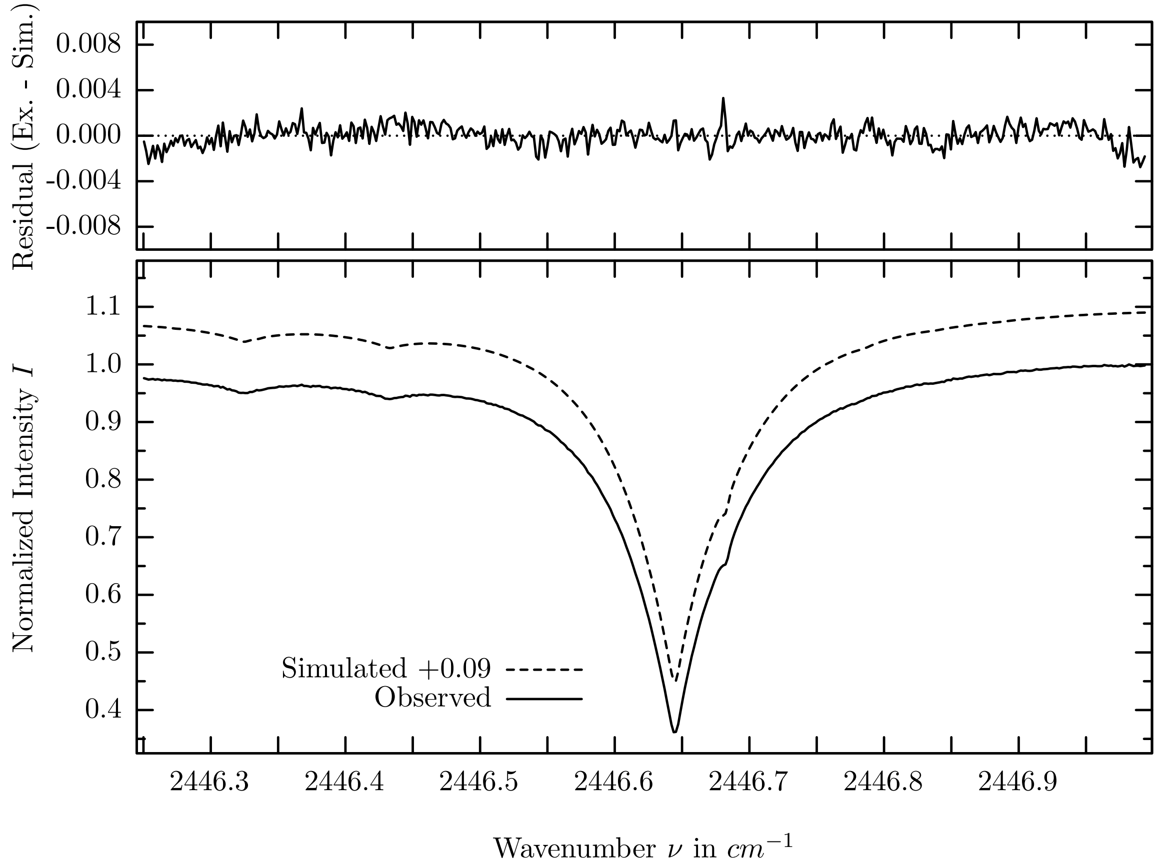

investigated species	:	N_2O
line position(s) ν_0	:	2446.6458 cm^{-1}
lower state energy E''_{lst}	:	143.3 cm^{-1}
retrieved TCA, information content	:	5.57E+18 $molec/cm^2$, 725.8
temperature dependence of the TCA	:	+0.144%/K (trop), +0.099%/K (strat)
location, date, solar zenith angle	:	Kiruna, 15/Mar/97, 71.02^o
spectral interval fitted	:	2446.250 – 2446.995 cm^{-1}

Molecule	iCode	Absorption	Molecule	iCode	Absorption
N2O	41	70.032%	$N2$	411	0.003%
Solar(A)	—	11.160%	$SO2$	91	<0.001%
Solar-sim	—	<0.001%	$NH3$	111	<0.001%
$CO2$	21	9.621%	OH	131	<0.001%
$CH4$	61	0.611%	HBr	161	<0.001%
$O3$	31	0.151%	$H2S$	471	<0.001%
$H2O$	11	0.060%	HDO	491	<0.001%

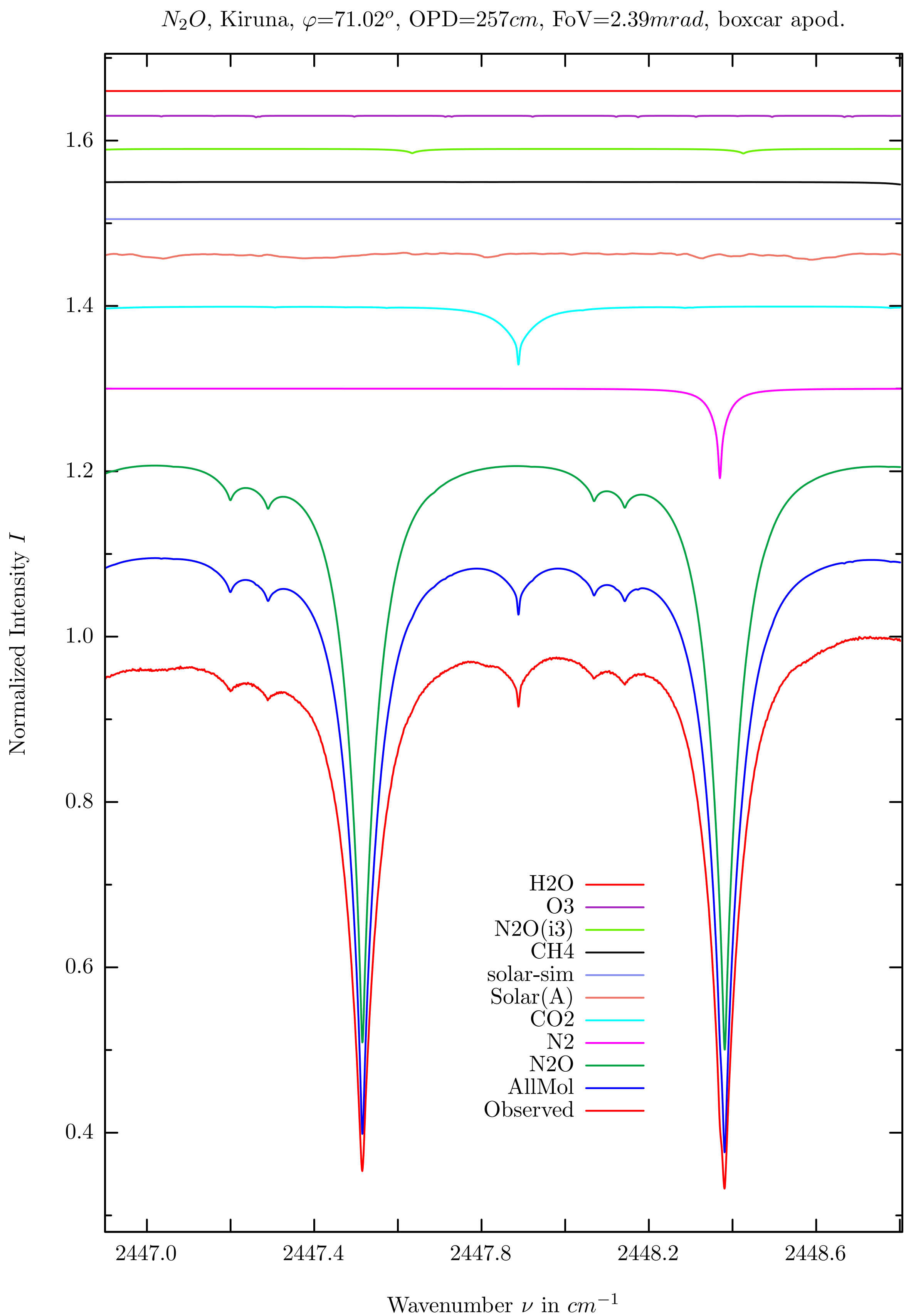
N_2O, Kiruna, φ=71.02^o, OPD=257cm, FoV=2.39$mrad$, boxcar apod.
Normalized Intensity I
Wavenumber ν in cm^{-1}
1.6
1.4
1.2
1.0
0.8
0.6
0.4
2447.0
2447.4
2447.8
2448.2
2448.6
H2O
O3
N2O(i3)
CH4
solar-sim
Solar(A)
CO2
N2
N2O
AllMol
Observed

σ=0.120%, 970315S4.90, φ=71.02^o, OPD=257cm, FoV=2.39$mrad$, Apod.=boxcar

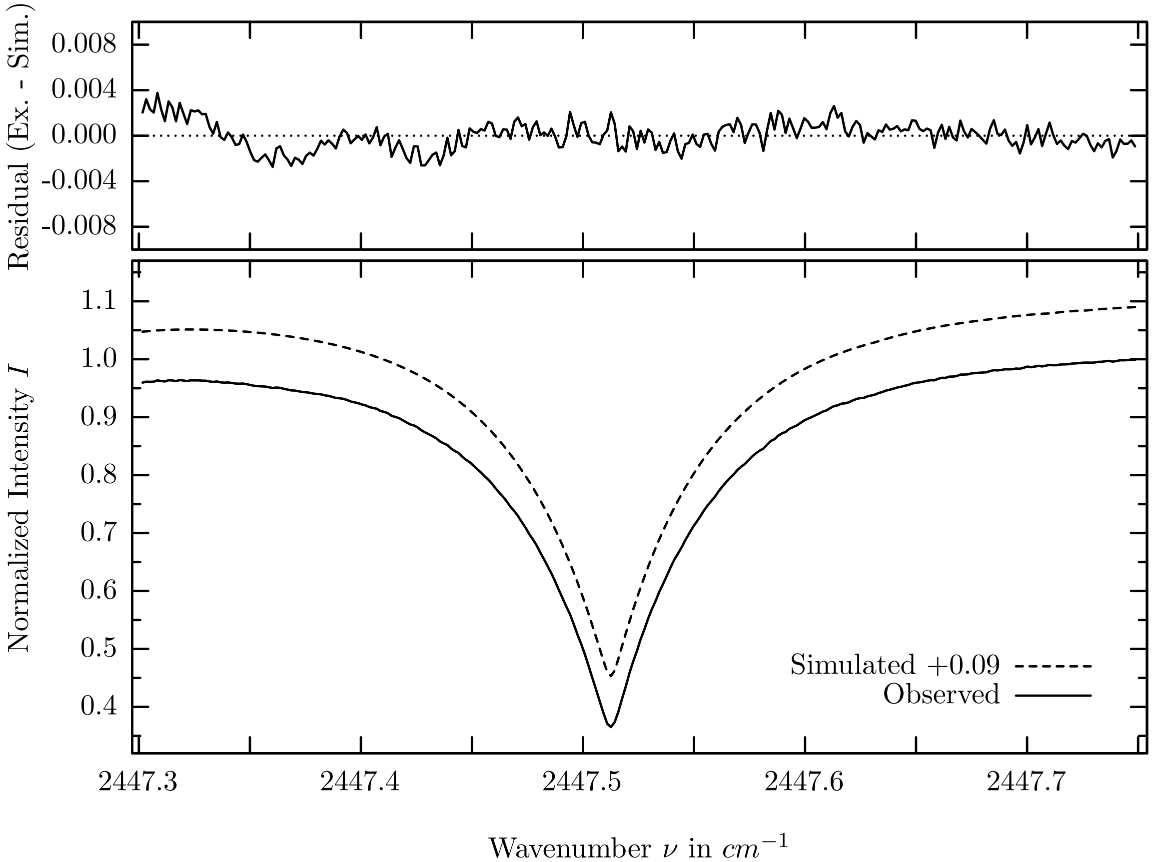

investigated species	:	N_2O
line position(s) ν_0	:	2447.5139 cm^{-1}
lower state energy E''_{lst}	:	128.2 cm^{-1}
retrieved TCA, information content	:	5.69E+18 $molec/cm^2$, 531.0
temperature dependence of the TCA	:	+0.233%/K (trop), +0.000%/K (strat)
location, date, solar zenith angle	:	Kiruna, 15/Mar/97, 71.02^o
spectral interval fitted	:	2447.300 – 2447.750 cm^{-1}

Molecule	iCode	Absorption	Molecule	iCode	Absorption
N2O	41	73.175%	$H2O$	11	0.062%
$N2$	411	10.908%	HDO	491	0.001%
$CO2$	21	8.528%	$SO2$	91	<0.001%
Solar(A)	—	0.911%	$NH3$	111	<0.001%
Solar-sim	—	<0.001%	OH	131	<0.001%
$CH4$	61	0.625%	HCl	15**2**	<0.001%
$N2O$	4**3**	0.557%	HBr	161	<0.001%
$O3$	31	0.183%	$H2S$	471	<0.001%

N_2O, Kiruna, φ=71.02^o, OPD=257cm, FoV=2.39$mrad$, boxcar apod.

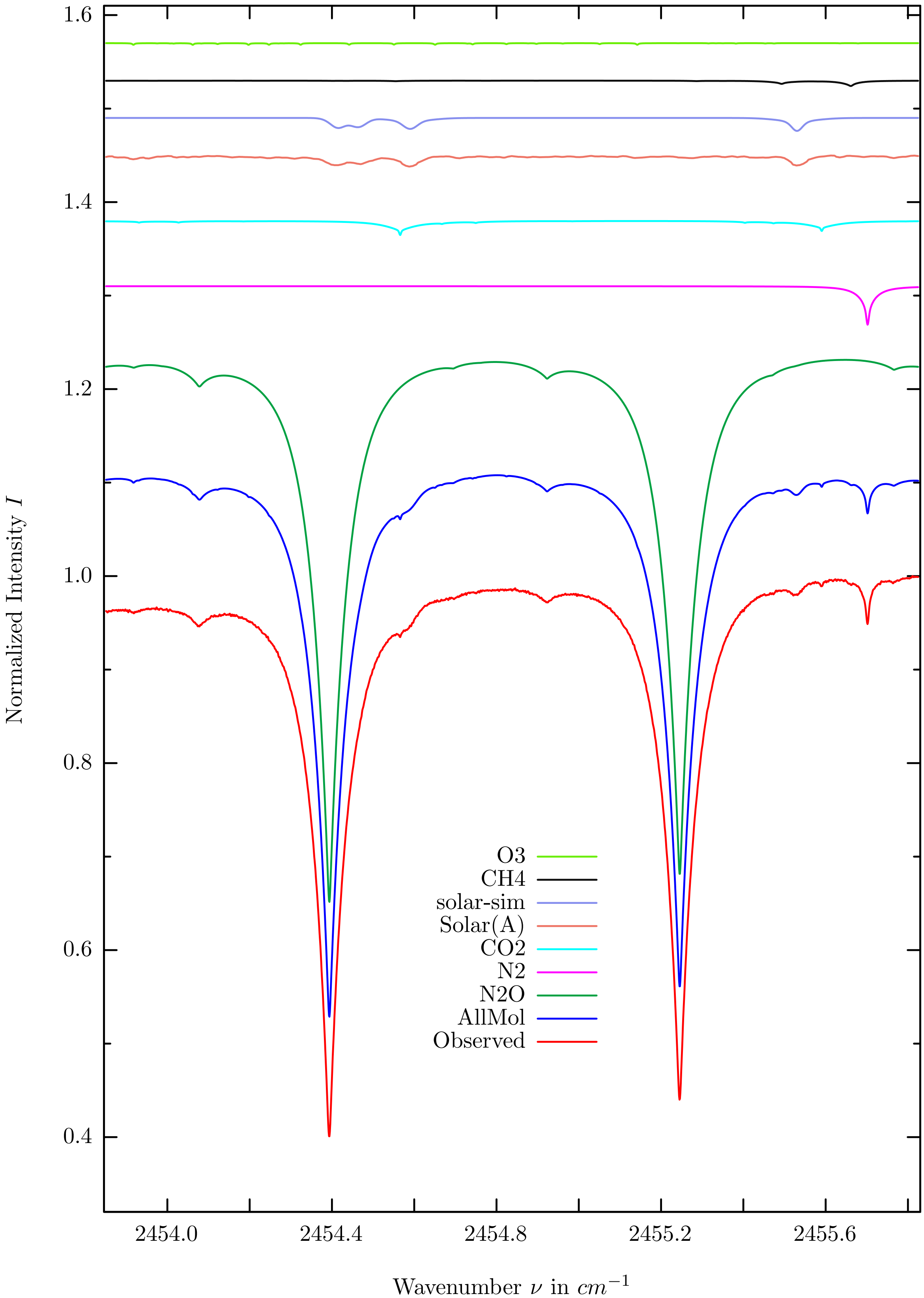

σ=0.092%, 970315S4.90, φ=71.02^o, OPD=257cm, FoV=2.39$mrad$, Apod.=boxcar

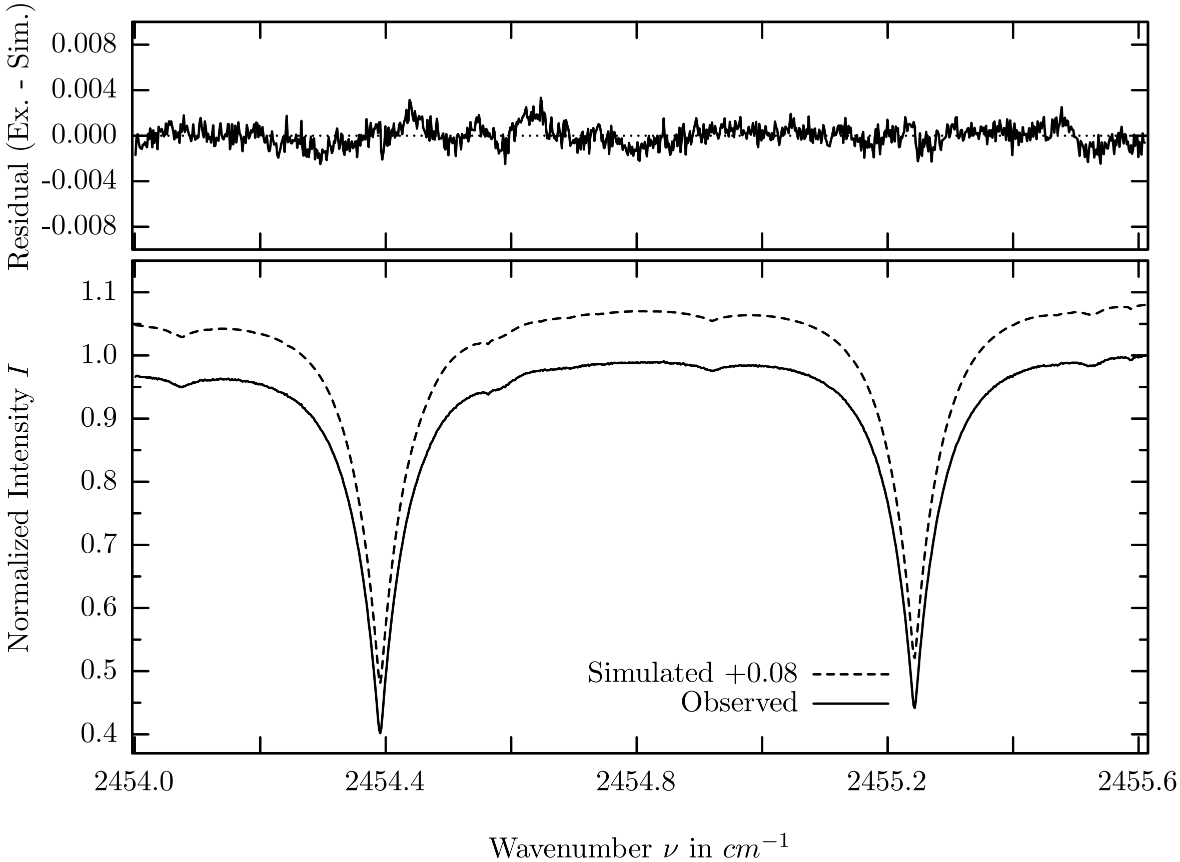

investigated species	:	N_2O
line position(s) ν_0	:	2454.3923, 2455.2441 cm^{-1}
lower state energy E''_{lst}	:	37.7, 30.2 cm^{-1}
retrieved TCA, information content	:	5.65E+18 $molec/cm^2$, 639.3, 607.3
temperature dependence of the TCA	:	+0.500%/K (trop), +0.040%/K (strat)
location, date, solar zenith angle	:	Kiruna, 15/Mar/97, 71.02^o
spectral interval fitted	:	2454.000 – 2455.610 cm^{-1}

Molecule	iCode	Absorption	Molecule	iCode	Absorption
N2O	41	59.946%	$H2O$	11	0.001%
$N2$	411	4.140%	$NH3$	111	0.001%
$CO2$	21	1.526%	$SO2$	91	<0.001%
Solar(A)	—	1.200%	OH	131	<0.001%
Solar-sim	—	1.387%	HCl	151	<0.001%
$CH4$	61	0.574%	HBr	161	<0.001%
$O3$	31	0.182%	$H2S$	471	<0.001%
HDO	491	0.023%			

N_2O, Kiruna, φ=70.54^o, OPD=257cm, FoV=2.39$mrad$, boxcar apod.

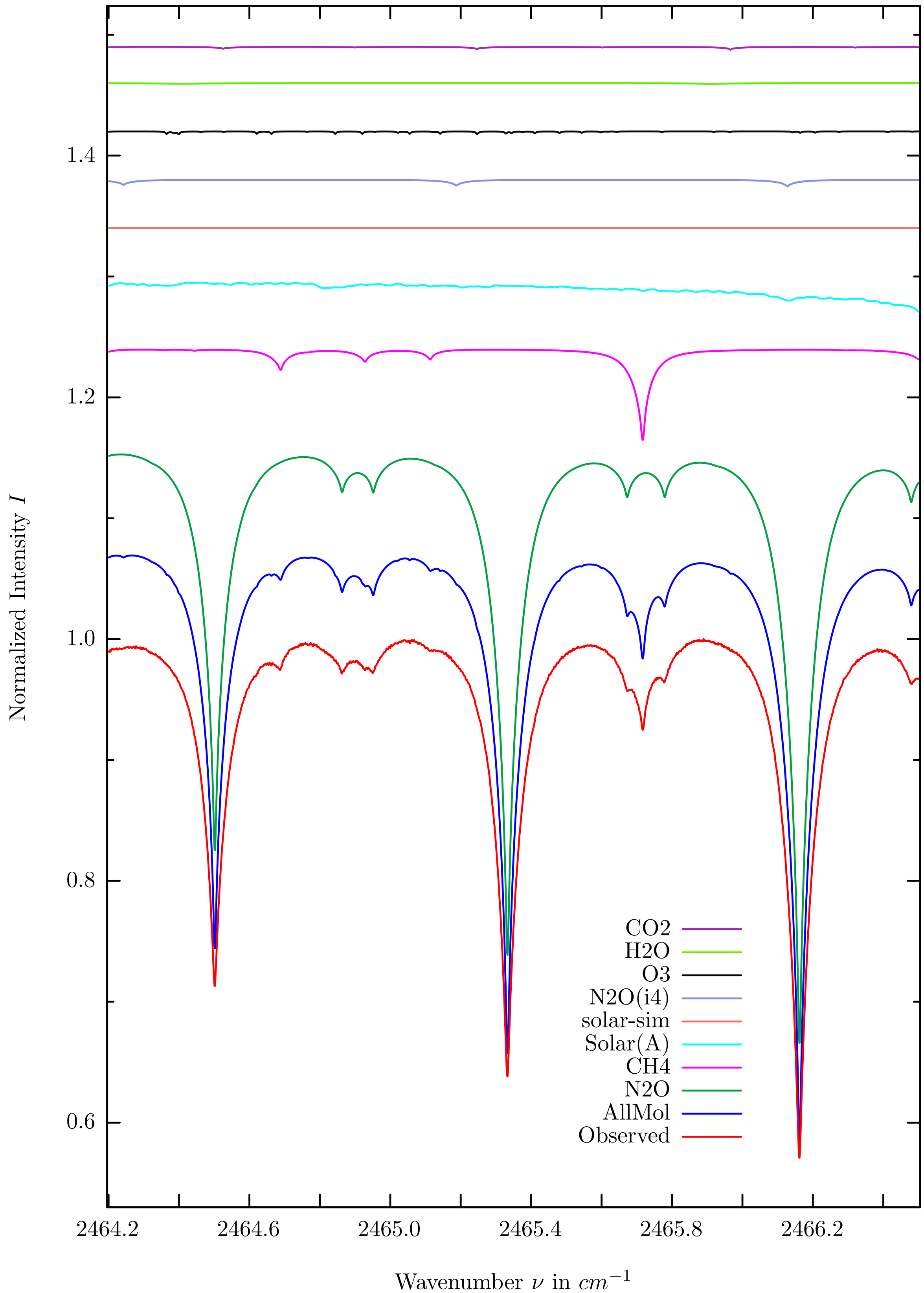

σ=0.117%, 970315S4.90, φ=71.02^o, OPD=257cm, FoV=2.39$mrad$, Apod.=boxcar

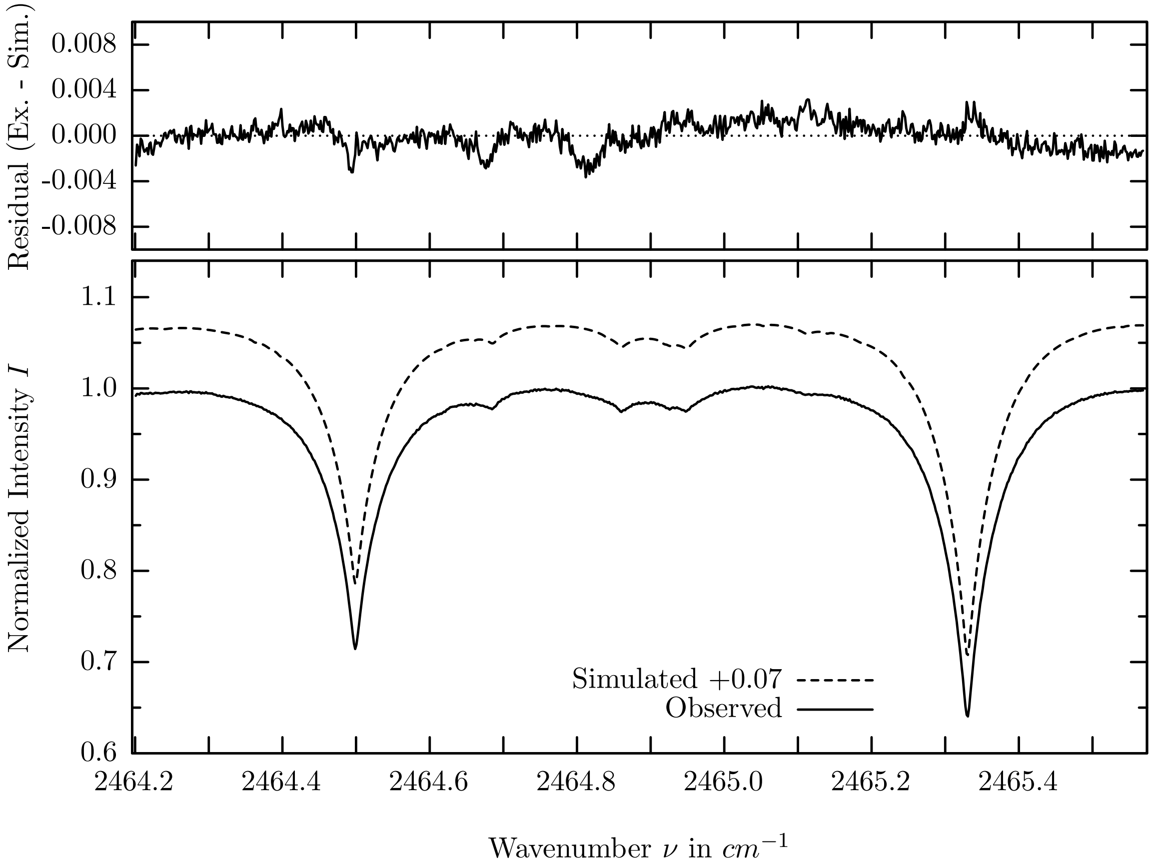

investigated species	:	N_2O
line position(s) ν_0	:	2464.5001, 2465.3312 cm^{-1}
lower state energy E''_{lst}	:	2.5, 5.0 cm^{-1}
retrieved TCA, information content	:	5.58E+18 $molec/cm^2$, 242.5, 309.2
temperature dependence of the TCA	:	+0.570%/K (trop), +0.041%/K (strat)
location, date, solar zenith angle	:	Kiruna, 15/Mar/97, 71.02^o
spectral interval fitted	:	2464.200 – 2465.570 cm^{-1}

Molecule	iCode	Absorption	Molecule	iCode	Absorption
N2O	41	50.505%	HDO	491	0.014%
$CH4$	61	7.548%	$SO2$	91	0.003%
Solar(A)	—	2.939%	$N2$	411	0.001%
Solar-sim	—	<0.001%	$NH3$	111	<0.001%
$N2O$	**44**	0.536%	OH	131	<0.001%
$O3$	31	0.239%	HCl	151	<0.001%
$H2O$	11	0.073%	HBr	161	<0.001%
$CO2$	21	0.062%	$H2S$	471	<0.001%

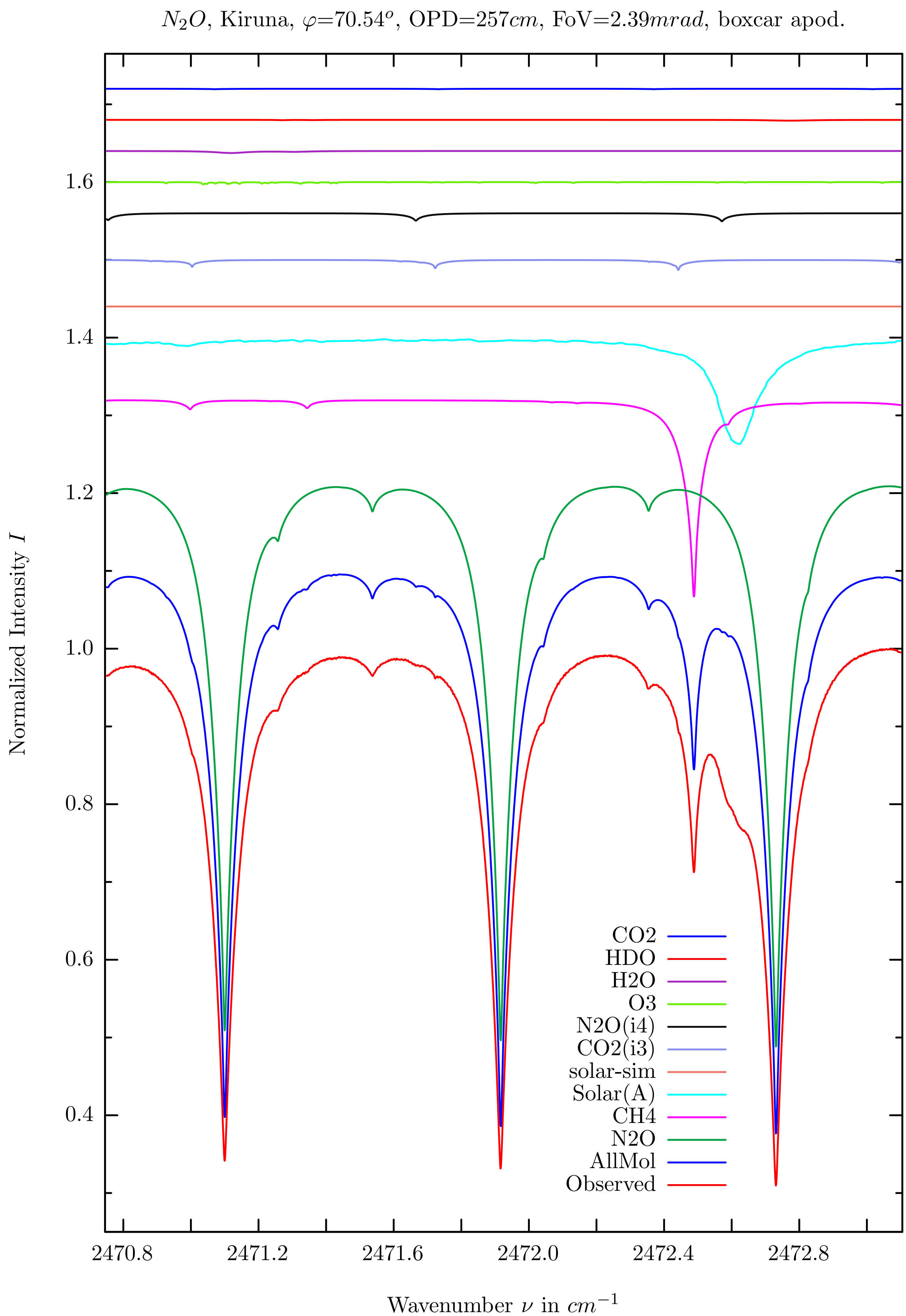
N_2O, Kiruna, φ=70.54^o, OPD=257cm, FoV=2.39$mrad$, boxcar apod.
Normalized Intensity I
Wavenumber ν in cm^{-1}
1.6
1.4
1.2
1.0
0.8
0.6
0.4
2470.8
2471.2
2471.6
2472.0
2472.4
2472.8
CO2
HDO
H2O
O3
N2O(i4)
CO2(i3)
solar-sim
Solar(A)
CH4
N2O
AllMol
Observed

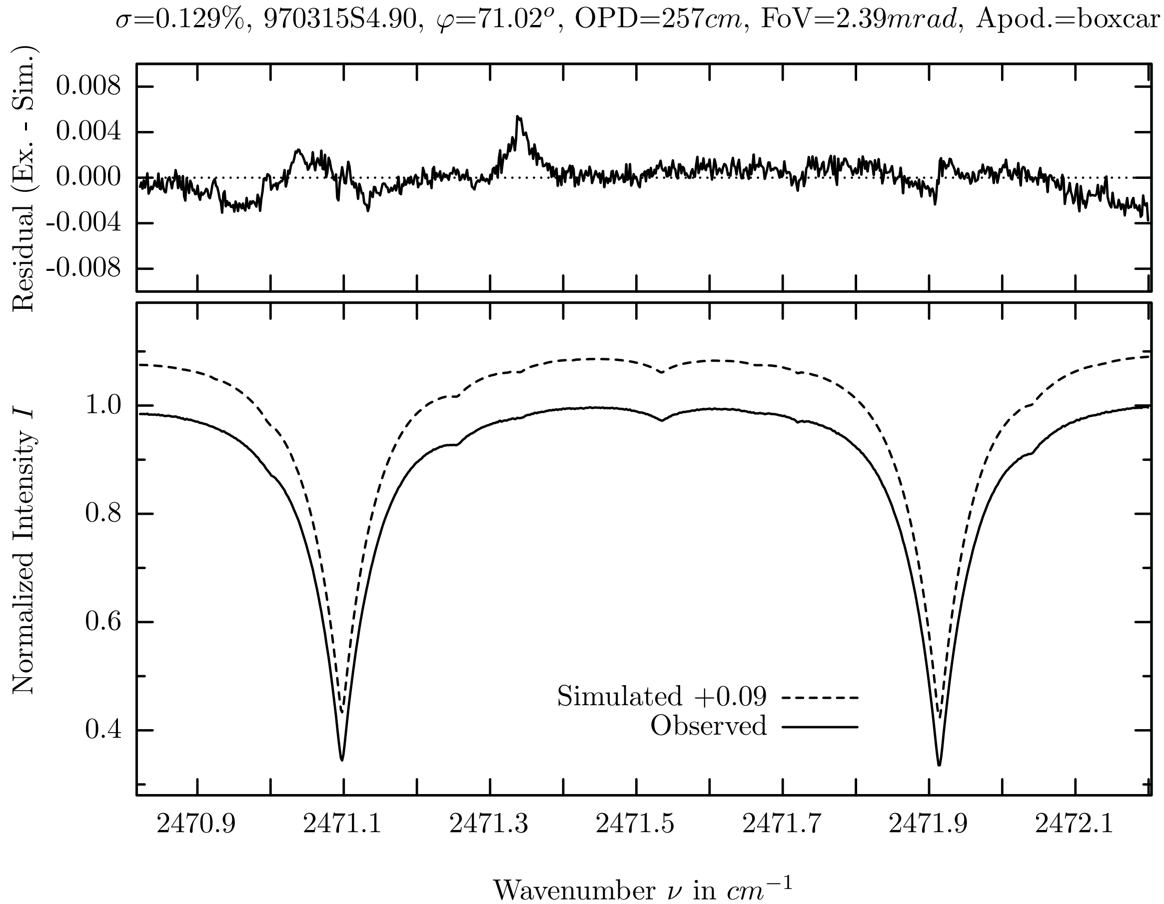

investigated species	:	N_2O
line position(s) ν_0	:	2471.0986, 2471.9152 cm^{-1}
lower state energy E''_{lst}	:	46.1, 55.3 cm^{-1}
retrieved TCA, information content	:	5.66E+18 $molec/cm^2$, 508.9, 516.2
temperature dependence of the TCA	:	+0.283%/K (trop), +0.008%/K (strat)
location, date, solar zenith angle	:	Kiruna, 15/Mar/97, 71.02^o
spectral interval fitted	:	2470.820 – 2472.200 cm^{-1}

Molecule	iCode	Absorption	Molecule	iCode	Absorption
N2O	41	75.357%	HDO	491	0.099%
$CH4$	61	25.379%	$CO2$	21	0.064%
Solar(A)	—	13.687%	$SO2$	91	0.009%
Solar-sim	—	<0.001%	HBr	161	0.009%
$CO2$	**23**	1.318%	$N2$	411	0.003%
$N2O$	**44**	1.044%	$NH3$	111	<0.001%
$O3$	31	0.307%	OH	131	<0.001%
$H2O$	11	0.264%	$H2S$	471	<0.001%

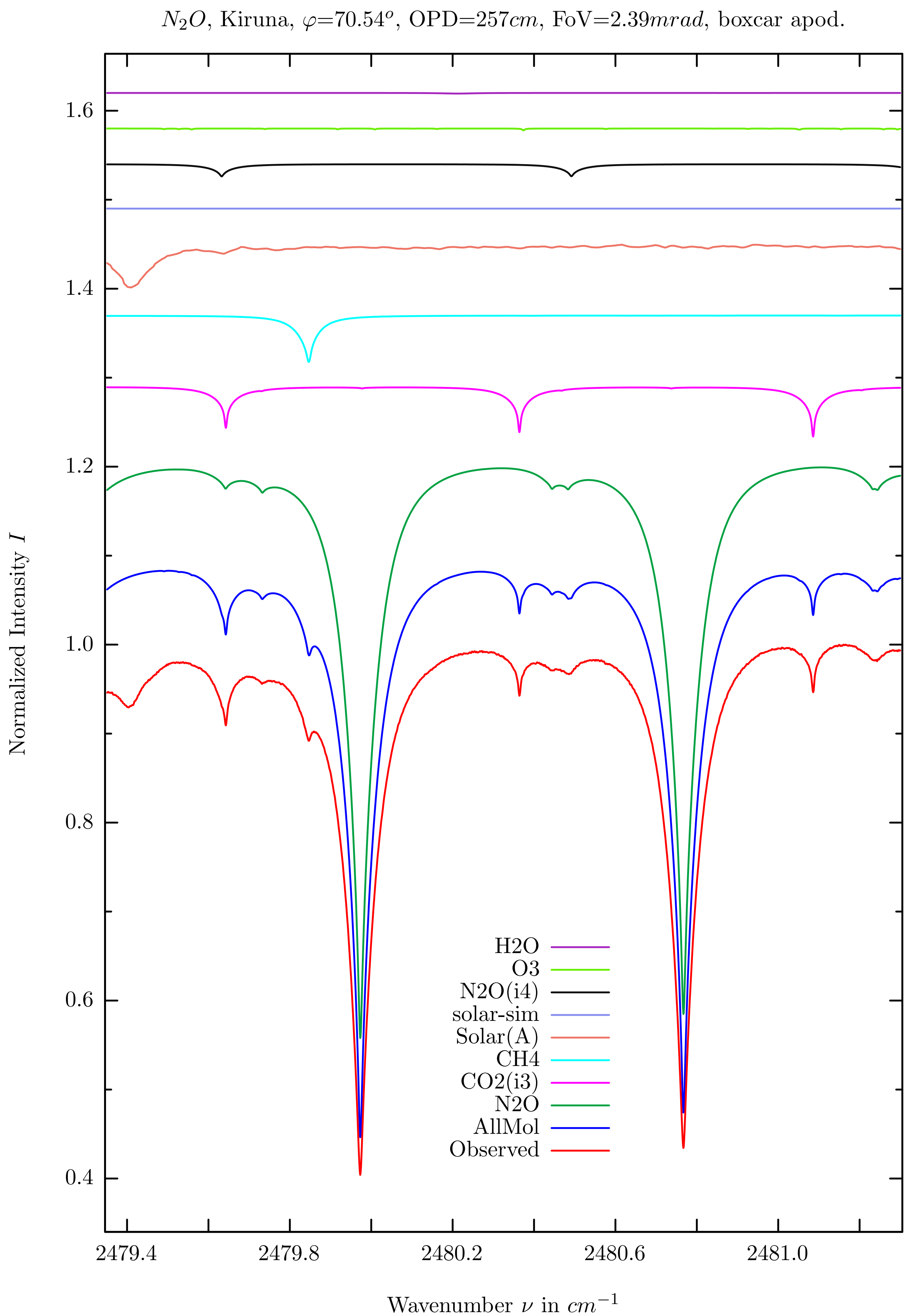
N_2O, Kiruna, φ=70.54^o, OPD=257cm, FoV=2.39$mrad$, boxcar apod.
Normalized Intensity I
Wavenumber ν in cm^{-1}
1.6
1.4
1.2
1.0
0.8
0.6
0.4
2479.4
2479.8
2480.2
2480.6
2481.0
H2O
O3
N2O(i4)
solar-sim
Solar(A)
CH4
CO2(i3)
N2O
AllMol
Observed

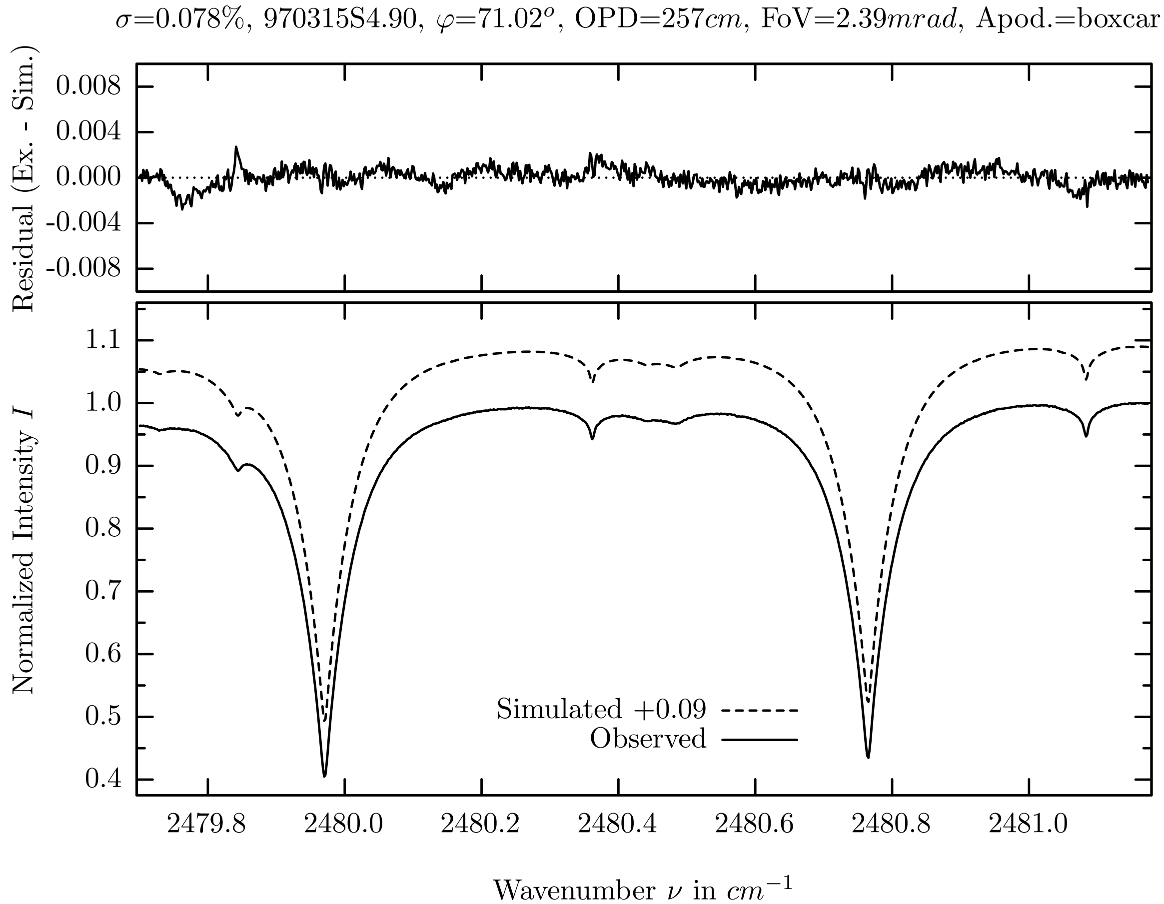

investigated species	:	$N_2O, (CO_2)$
line position(s) ν_0	:	2479.9719, 2480.7660, (2481.0844) cm^{-1}
lower state energy E''_{lst}	:	193.5, 212.0, (278.3) cm^{-1}
retrieved TCA, information content	:	5.64e18, (7.81e21) $molec/cm^2$, 762.6, 724.0, (67.2)
temperature dependence of the TCA	:	-.059, (-1.173)%/K (trop), -.075, (-.787)%/K (strat)
location, date, solar zenith angle	:	Kiruna, 15/Mar/97, 71.02^o
spectral interval fitted	:	2479.700 – 2481.175 cm^{-1}

Molecule	iCode	Absorption	Molecule	iCode	Absorption
N2O	41	66.363%	$CO2$	21	0.022%
$CO2$	2**3**	5.679%	$SO2$	91	0.022%
$CH4$	61	5.254%	$N2$	411	0.001%
Solar(A)	—	4.861%	$NH3$	111	<0.001%
Solar-sim	—	<0.001%	OH	131	<0.001%
$N2O$	4**4**	1.387%	HCl	151	<0.001%
$O3$	31	0.212%	HBr	161	<0.001%
$H2O$	11	0.073%	$H2S$	471	<0.001%
HDO	491	0.025%			

N_2O, Kiruna, φ=70.54^o, OPD=257cm, FoV=2.39$mrad$, boxcar apod.

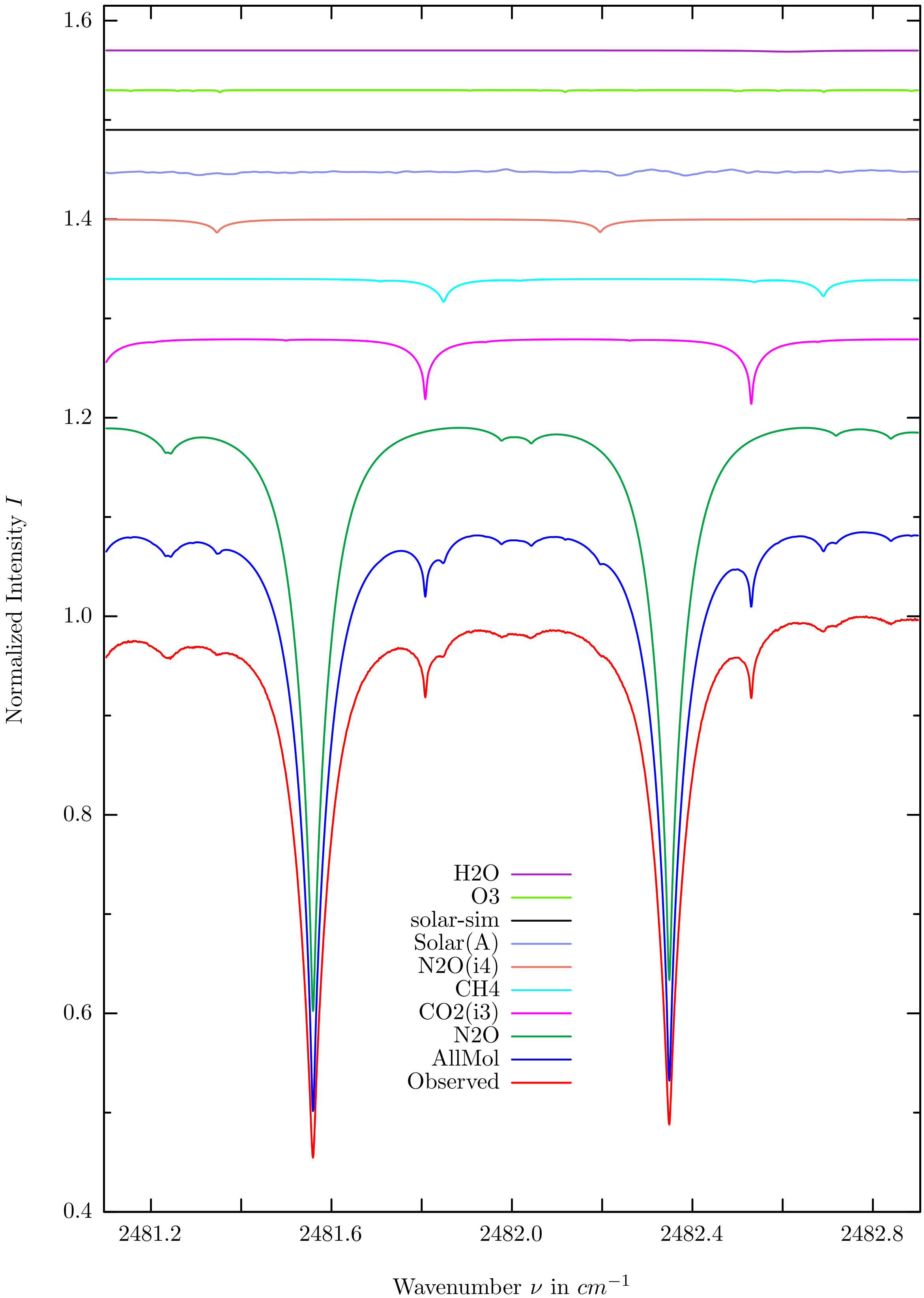

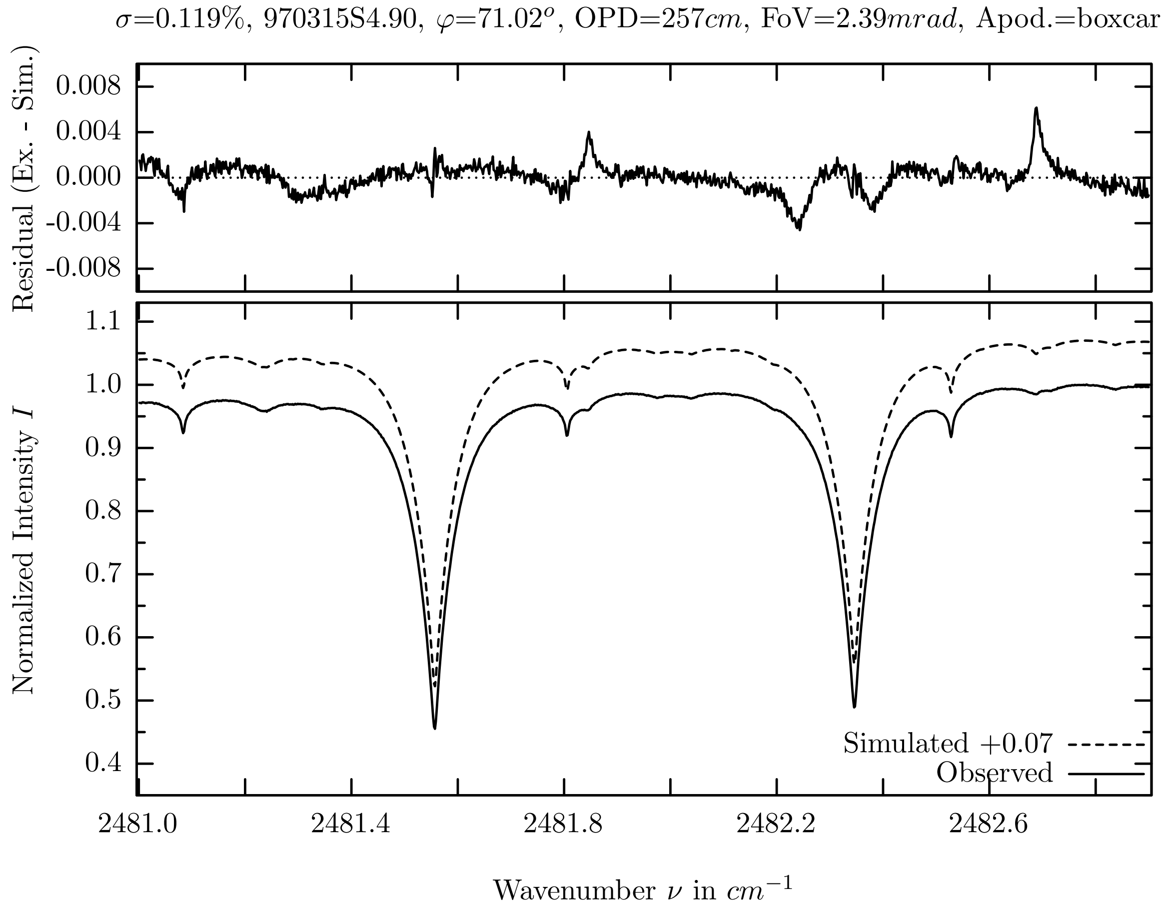

investigated species	:	$N_2O, (CO_2(i3))$
line position(s) ν_0	:	2481.5578, 2482.3474, (2481.0844) cm^{-1}
lower state energy E''_{lst}	:	231.2, 251.3, (278.3) cm^{-1}
retrieved TCA, information content	:	5.65e18, (7.36e21) $molec/cm^2$, 447.3, 430.3, (48.6)
temperature dependence of the TCA	:	-.038, (-.084)%/K (trop), -.035, (-.058)%/K (strat)
location, date, solar zenith angle	:	Kiruna, 15/Mar/97, 71.02^o
spectral interval fitted	:	2481.000 – 2482.900 cm^{-1}

Molecule	iCode	Absorption	Molecule	iCode	Absorption
N2O	41	60.915%	*CO2*	21	0.015%
CO2	2**3**	6.704%	*HDO*	491	0.005%
CH4	61	2.313%	*NH3*	111	<0.001%
N2O	4**4**	1.350%	*OH*	131	<0.001%
Solar(A)	—	0.610%	*HCl*	151	<0.001%
Solar-sim	—	<0.001%	*HBr*	161	<0.001%
O3	31	0.219%	*N2*	411	<0.001%
H2O	11	0.125%	*H2S*	471	<0.001%
SO2	91	0.031%			

N_2O, Kiruna, φ=70.54^o, OPD=257cm, FoV=2.39$mrad$, boxcar apod.

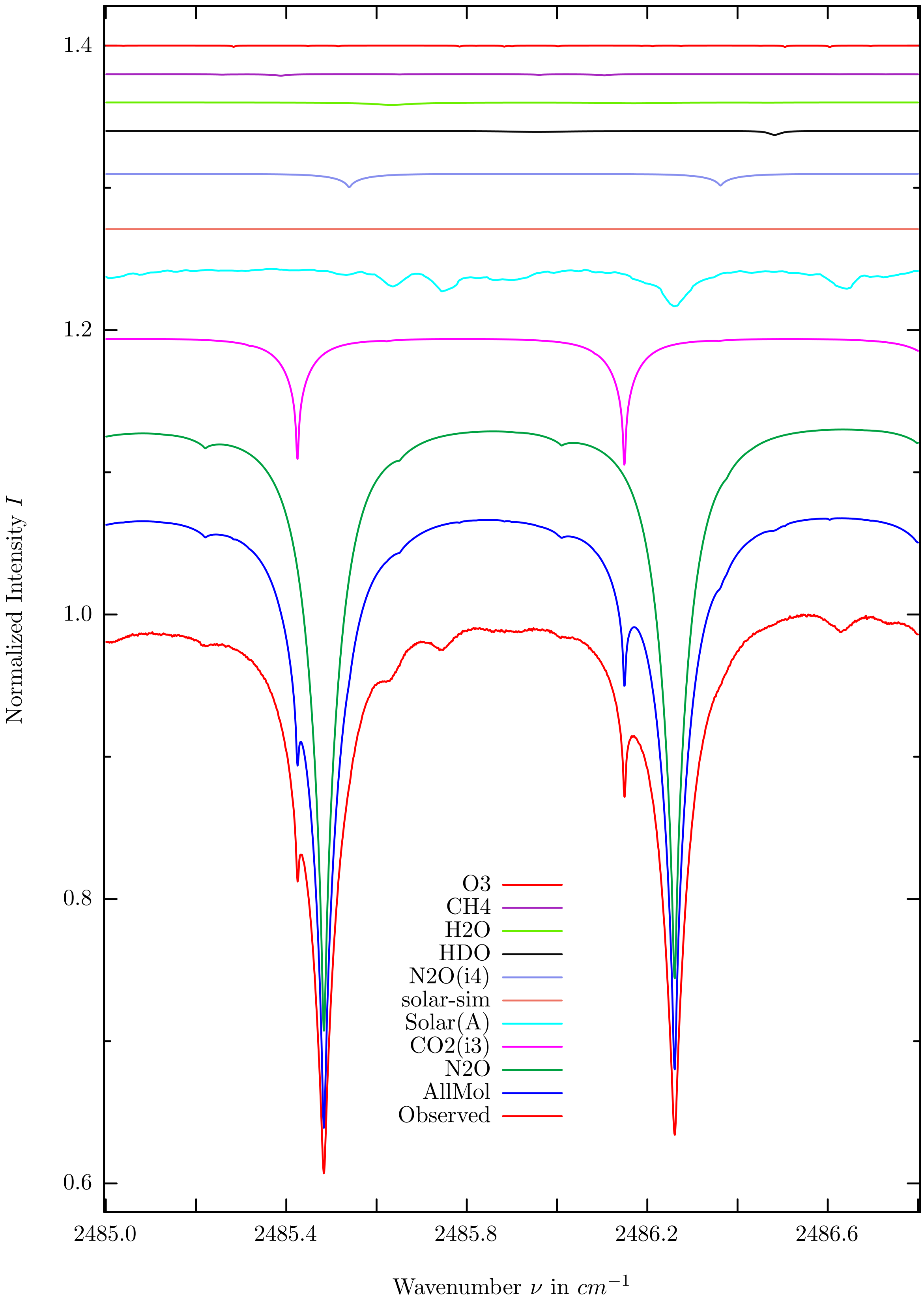

σ=0.141%, 970315S4.90, φ=71.02^o, OPD=257cm, FoV=2.39$mrad$, Apod.=boxcar

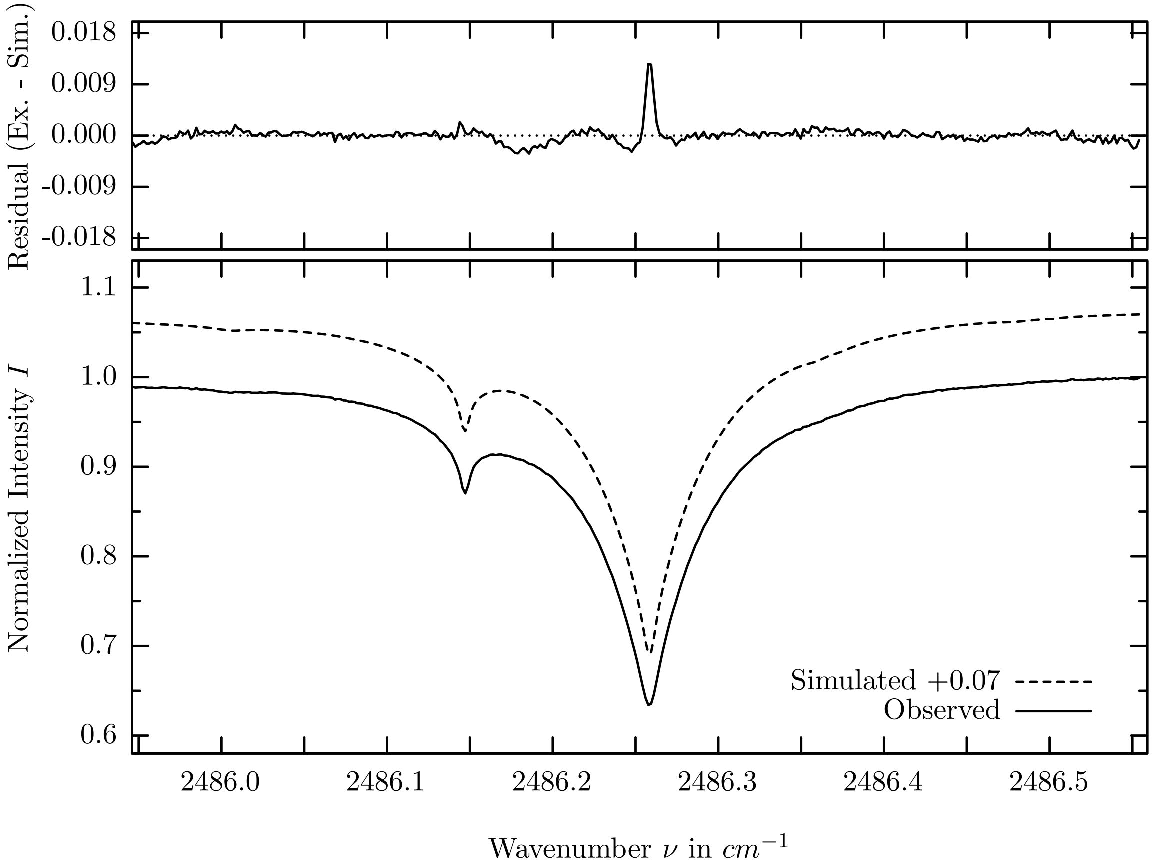

investigated species	:	$N_2O, (CO_2(i3))$
line position(s) ν_0	:	2486.2595, (2486.1479) cm^{-1}
lower state energy E''_{lst}	:	364.4, (154.6) cm^{-1}
retrieved TCA, information content	:	6.07E+18, (7.79E+21) $molec/cm^2$, 268.5, (53.9)
temperature dependence of the TCA	:	-.422, (-.950)%/K (trop), -.034, (-.699)%/K (strat)
location, date, solar zenith angle	:	Kiruna, 15/Mar/97, 71.02^o
spectral interval fitted	:	2485.940 – 2486.555 cm^{-1}

Molecule	iCode	Absorption	Molecule	iCode	Absorption
N2O	41	43.467%	$SO2$	91	0.037%
$CO2$	**23**	9.082%	$N2$	411	0.003%
Solar(A)	—	2.731%	$CO2$	21	0.001%
Solar-sim	—	<0.001%	$NH3$	111	<0.001%
$N2O$	4**4**	0.963%	OH	131	<0.001%
HDO	491	0.276%	HCl	151	<0.001%
$H2O$	11	0.167%	HBr	161	<0.001%
$CH4$	61	0.124%	$H2S$	471	<0.001%
$O3$	31	0.115%			

N_2O, Kiruna, φ=70.54^o, OPD=257cm, FoV=2.39$mrad$, boxcar apod.

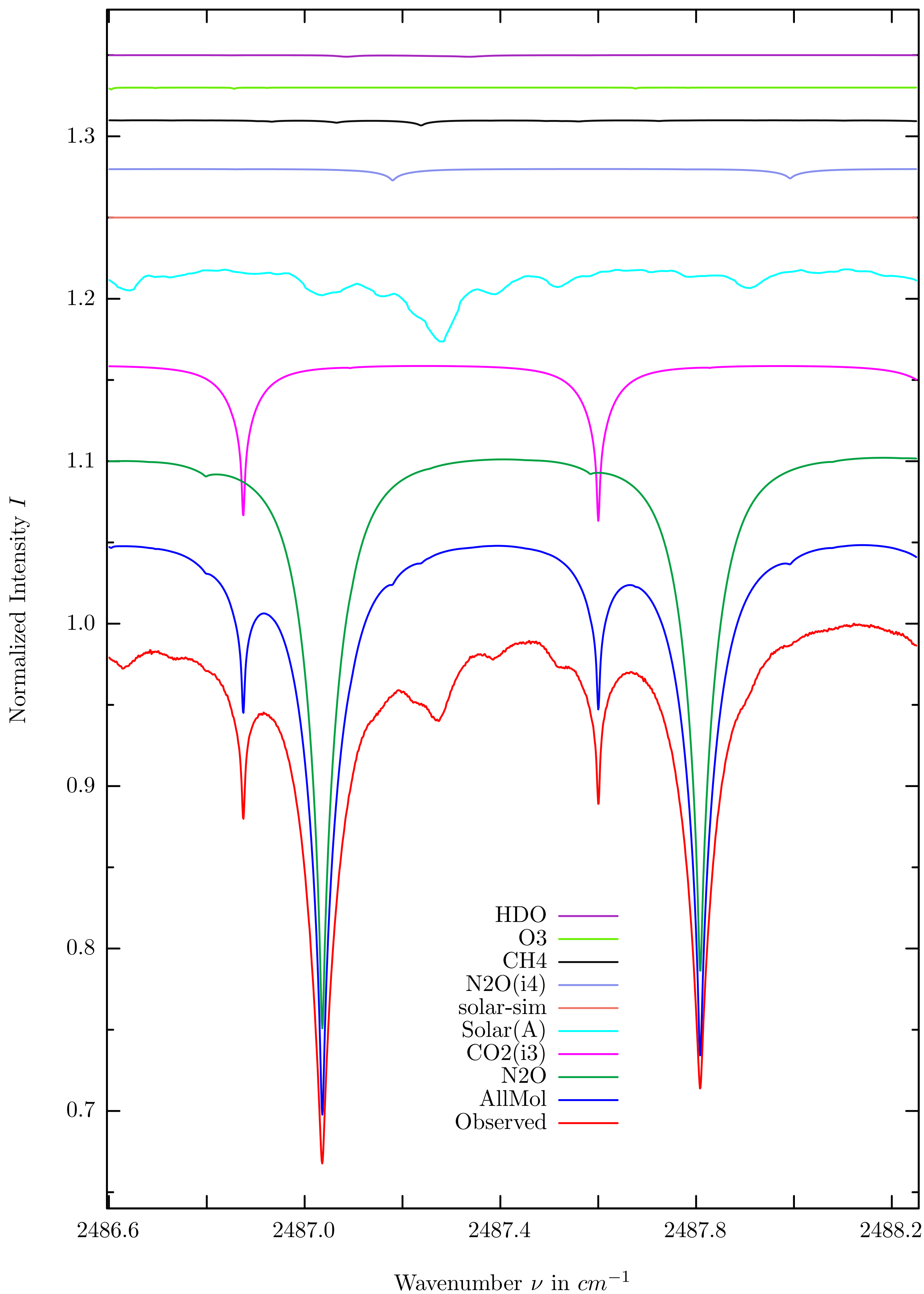

σ=0.815%, 970315S4.90, φ=71.02^o, OPD=257cm, FoV=2.39$mrad$, Apod.=boxcar

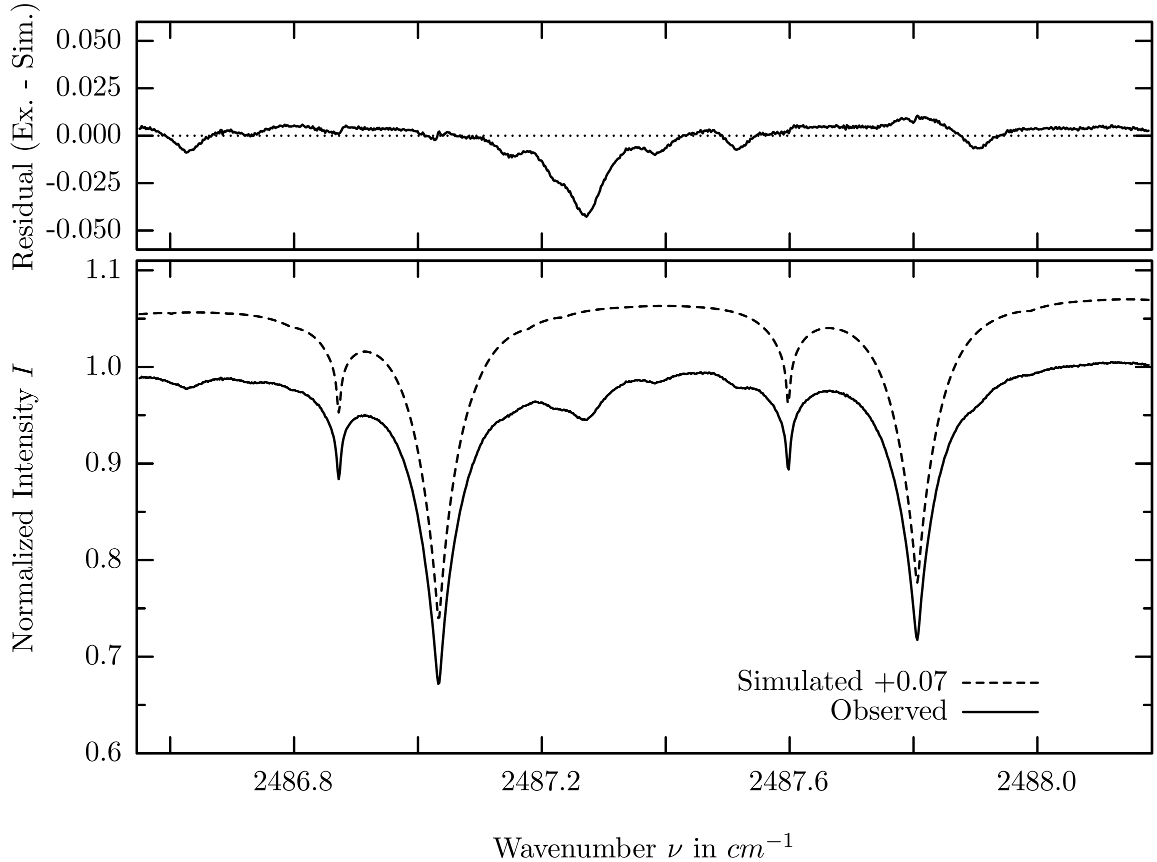

investigated species	:	$N_2O, (CO_2(i3))$
line position(s) ν_0	:	2487.0346, 2487.8070, (2487.5988) cm^{-1}
lower state energy E''_{lst}	:	389.5, 415.5, (125.9) cm^{-1}
retrieved TCA, information content	:	5.86e18, (7.43e21) $molec/cm^2$, 39.8, 45.3, (12.2)
temperature dependence of the TCA	:	-.585, (-.897)%/K (trop), -.081, (-.605)%/K (strat)
location, date, solar zenith angle	:	Kiruna, 15/Mar/97, 71.02^o
spectral interval fitted	:	2486.550 – 2488.180 cm^{-1}

Molecule	iCode	Absorption	Molecule	iCode	Absorption
N2O	41	36.012%	$H2O$	11	0.028%
$CO2$	**23**	9.764%	$NH3$	111	0.001%
Solar(A)	—	4.637%	$CO2$	21	<0.001%
Solar-sim	—	<0.001%	OH	131	<0.001%
$N2O$	4**4**	0.717%	HCl	151	<0.001%
$CH4$	61	0.328%	HBr	161	<0.001%
$O3$	31	0.115%	$N2$	411	<0.001%
HDO	491	0.101%	$H2S$	471	<0.001%
$SO2$	91	0.031%			

Comment: The lack of solar line data make this window a poor choice at present.

CO_2, Kiruna, φ=71.02^o, OPD=257cm, FoV=2.39$mrad$, boxcar apod.

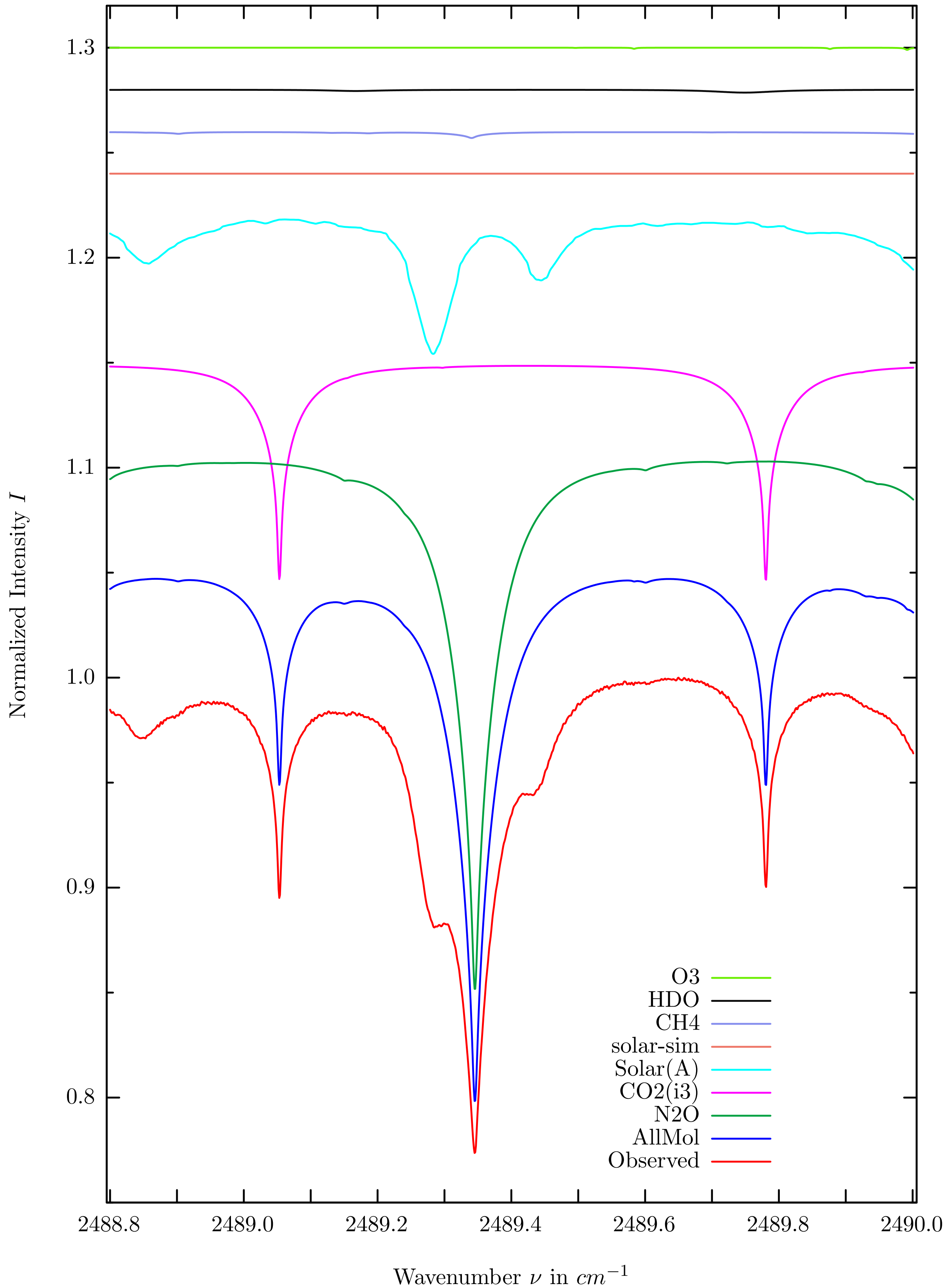

σ=0.057%, 970315S4.90, φ=71.02^o, OPD=257cm, FoV=2.39$mrad$, Apod.=boxcar

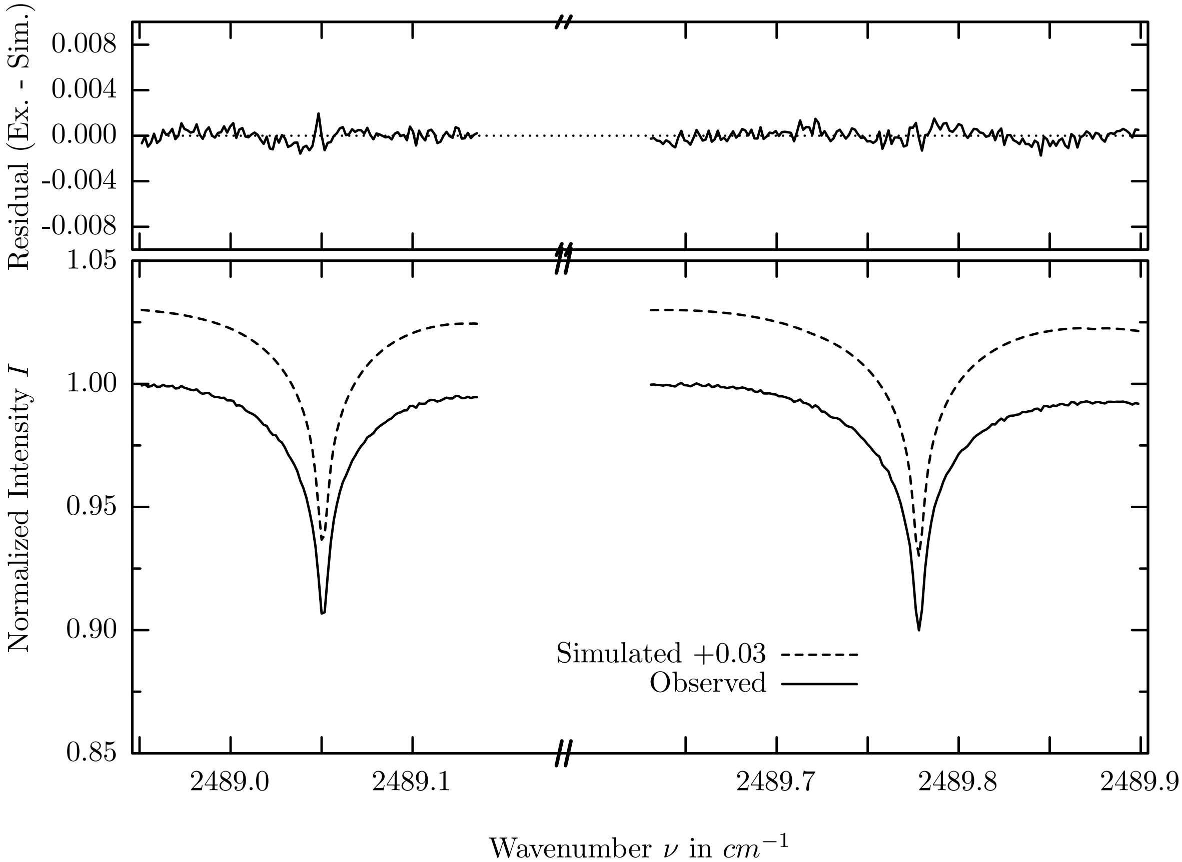

investigated species	:	$CO_2(i3)$
line position(s) ν_0	:	2489.0517, 2489.7790 cm^{-1}
lower state energy E''_{lst}	:	100.1, 88.3 cm^{-1}
retrieved TCA, information content	:	7.07E+21 $molec/cm^2$, 159.7, 174.4
temperature dependence of the TCA	:	-0.152%/K (trop), +0.035%/K (strat)
location, date, solar zenith angle	:	Kiruna, 15/Mar/97, 71.02^o
spectral interval fitted	:	2488.95 - 2489.137 & 2489.63 – 2489.90 cm^{-1}

Molecule	iCode	Absorption	Molecule	iCode	Absorption
$N2O$	41	25.956%	HBr	161	0.011%
CO2	**23**	10.497%	$H2O$	11	0.001%
Solar(A)	—	6.582%	$N2$	411	0.001%
Solar-sim	—	<0.001%	$CO2$	21	<0.001%
$CH4$	61	0.302%	$NH3$	111	<0.001%
HDO	491	0.138%	OH	131	<0.001%
$O3$	31	0.106%	HCl	151	<0.001%
$SO2$	91	0.028%	$H2S$	471	<0.001%

Comment: Simultaneous 2-microwindow fit

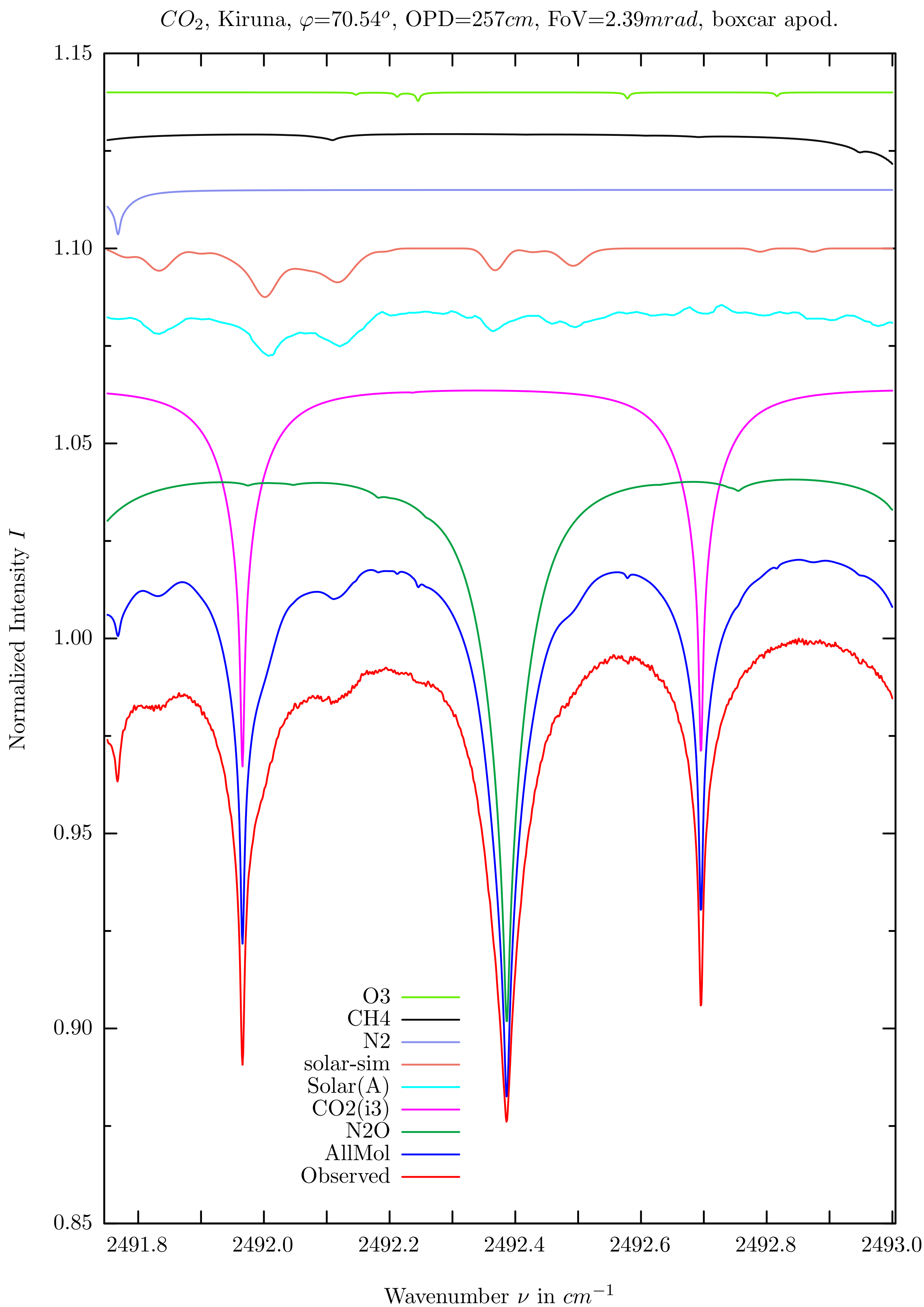
CO_2, Kiruna, φ=70.54^o, OPD=257cm, FoV=2.39$mrad$, boxcar apod.
1.15
1.10
1.05
1.00
0.95
0.90
0.85
Normalized Intensity I
2491.8
2492.0
2492.2
2492.4
2492.6
2492.8
2493.0
Wavenumber ν in cm^{-1}
O3
CH4
N2
solar-sim
Solar(A)
CO2(i3)
N2O
AllMol
Observed

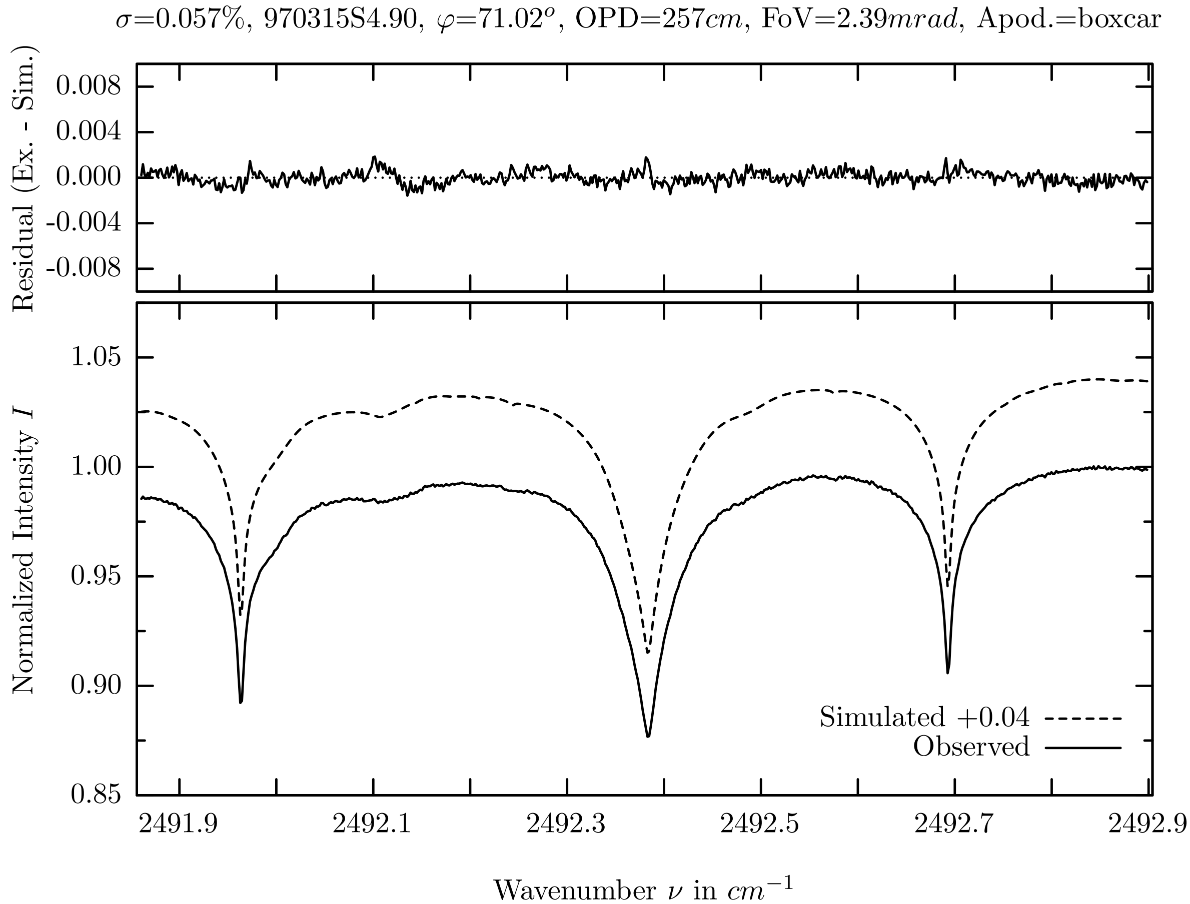

investigated species	:	$CO_2(i3),(N_2O)$
line position(s) ν_0	:	2492.6940, (2492.3848) cm^{-1}
lower state energy E''_{lst}	:	48.6, (588.8) cm^{-1}
retrieved TCA, information content	:	7.32E+21, (5.57E+18) $molec/cm^2$, 166.7, (211.5)
temperature dependence of the TCA	:	+.074, (-1.21)%/K (trop), -.084, (-.252)%/K (strat)
location, date, solar zenith angle	:	Kiruna, 15/Mar/97, 71.02^o
spectral interval fitted	:	2491.860 – 2492.900 cm^{-1}

Molecule	iCode	Absorption	Molecule	iCode	Absorption
$N2O$	41	14.381%	HDO	491	0.007%
CO2	**23**	9.870%	$H2O$	11	0.001%
Solar(A)	—	1.251%	$CO2$	21	<0.001%
Solar-sim	—	1.248%	$NH3$	111	<0.001%
$N2$	411	1.149%	OH	131	<0.001%
$CH4$	61	0.861%	HCl	151	<0.001%
$O3$	31	0.225%	HBr	161	<0.001%
$SO2$	91	0.023%	$H2S$	471	<0.001%

CO_2(i3), Kiruna, φ=71.02^o, OPD=257cm, FoV=2.39$mrad$, boxcar apod.

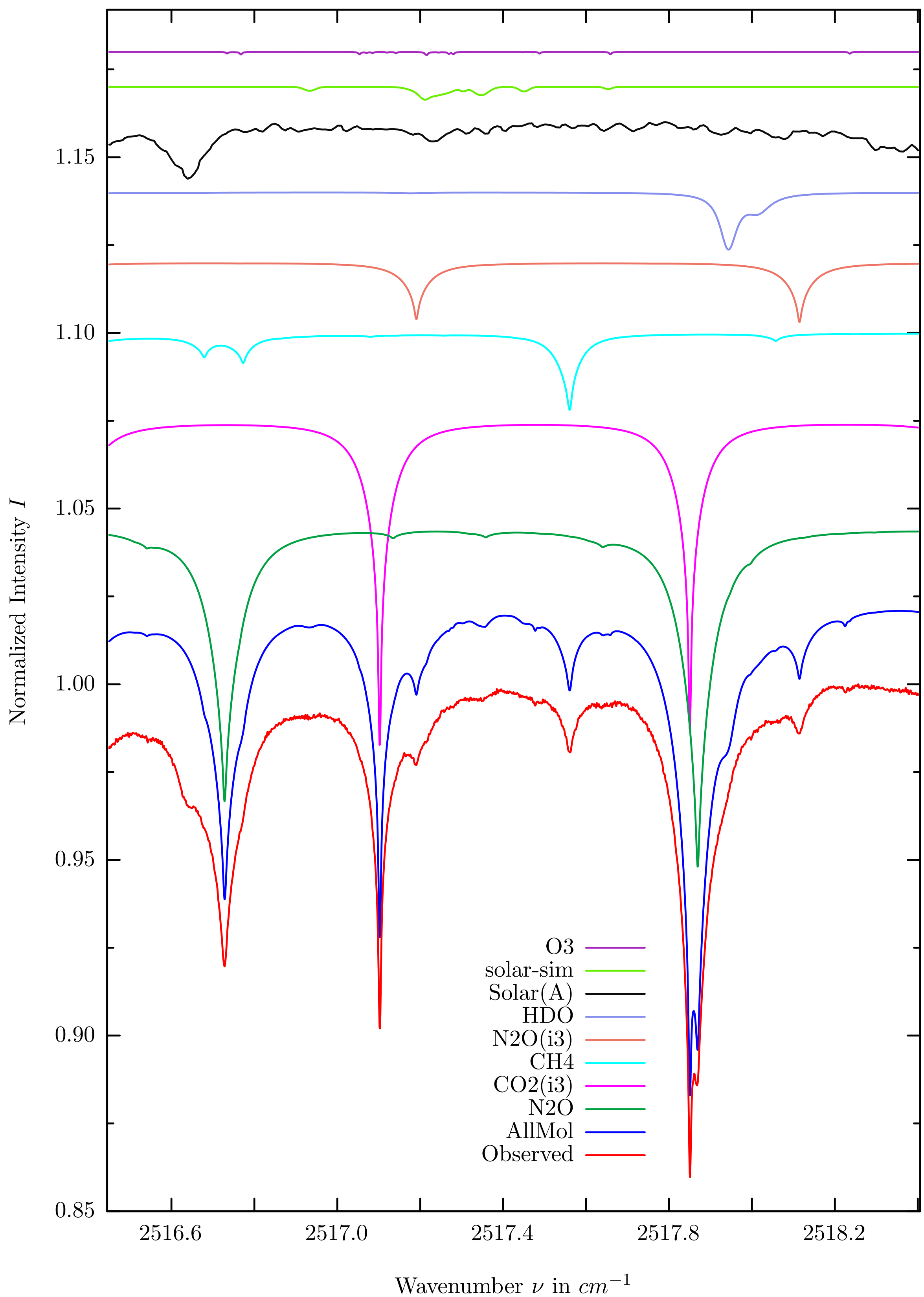

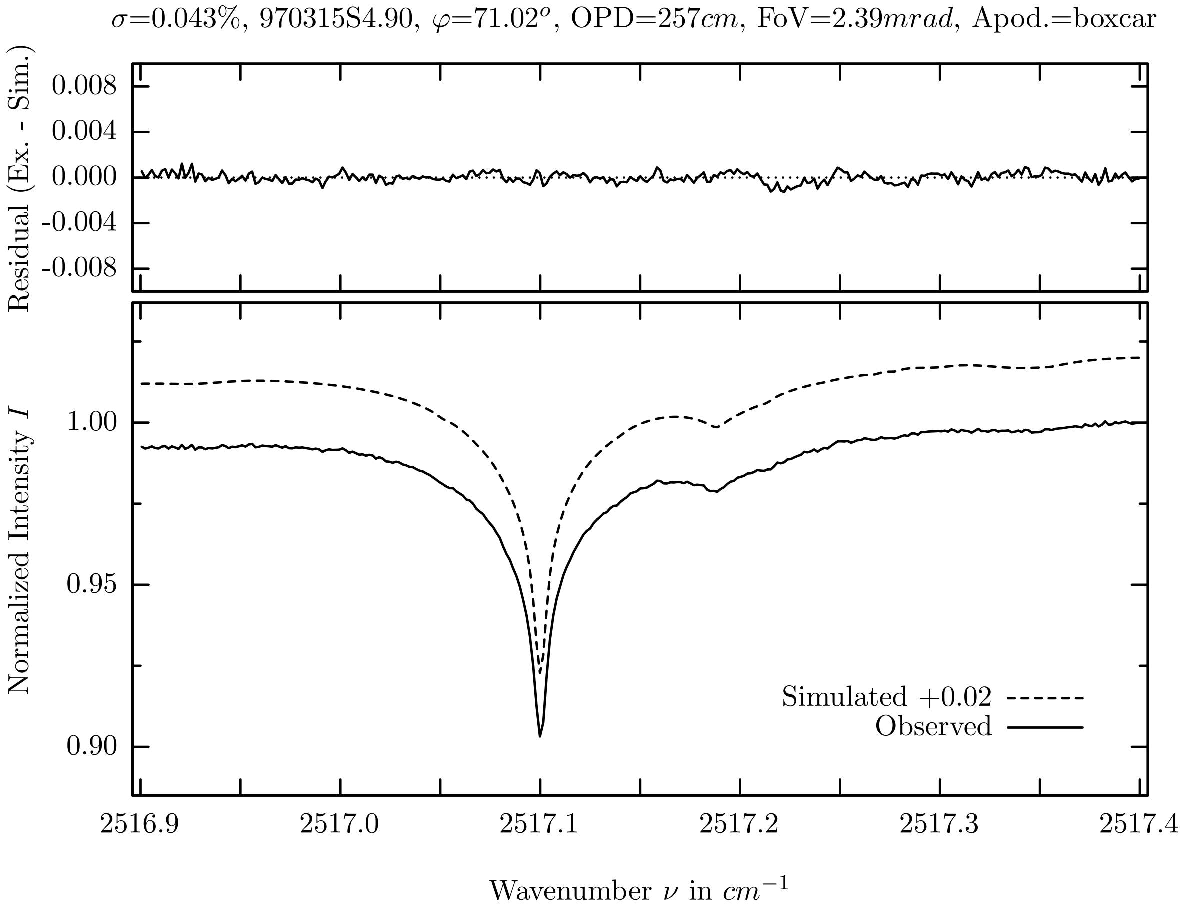

investigated species	:	$CO_2(i3), (N_2O(i3))$
line position(s) ν_0	:	2517.1010, (2517.1892) cm^{-1}
lower state energy E''_{lst}	:	170.1, (170.0) cm^{-1}
retrieved TCA, information content	:	7.44E+21, (5.72E+18) $molec/cm^2$, 221.1, (33.7)
temperature dependence of the TCA	:	-.032, (-.238)%/K (trop), -.017, (-.017)%/K (strat)
location, date, solar zenith angle	:	Kiruna, 15/Mar/97, 71.02^o
spectral interval fitted	:	2516.900 – 2517.400 cm^{-1}

Molecule	iCode	Absorption	Molecule	iCode	Absorption
$N2O$	41	9.695%	$H2O$	11	0.017%
CO2	**23**	9.380%	$NH3$	111	<0.001%
$CH4$	61	2.192%	OH	131	<0.001%
$N2O$	4**3**	1.702%	HCl	151	<0.001%
HDO	491	1.632%	HBr	161	<0.001%
Solar(A)	—	1.610%	OCS	191	<0.001%
solar-sim	—	0.363%	$N2$	411	<0.001%
$O3$	31	0.093%	$H2S$	471	<0.001%
$SO2$	91	0.018%			

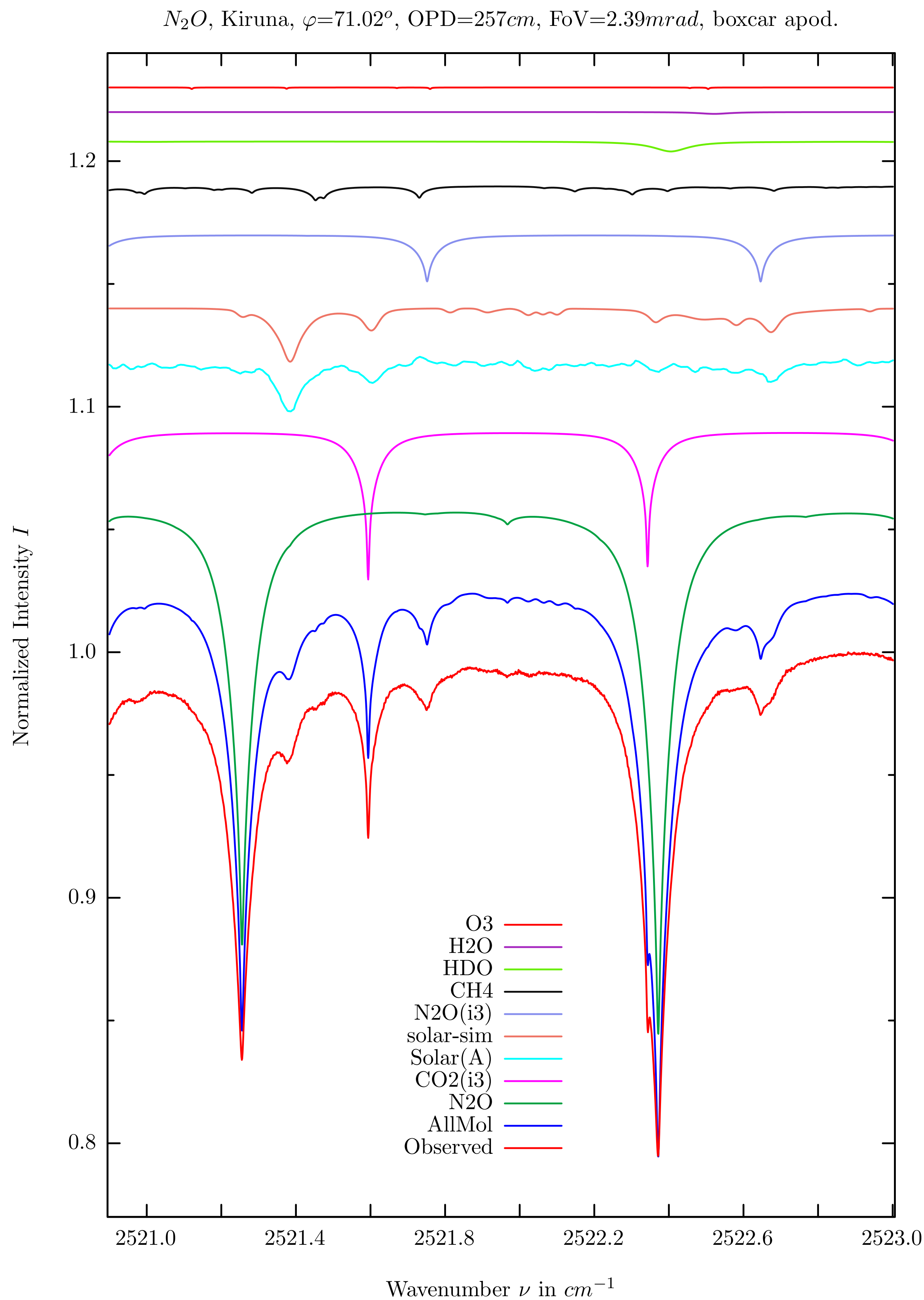

N_2O, Kiruna, φ=71.02^o, OPD=257cm, FoV=2.39$mrad$, boxcar apod.
Normalized Intensity I
Wavenumber ν in cm^{-1}
1.2
1.1
1.0
0.9
0.8
2521.0
2521.4
2521.8
2522.2
2522.6
2523.0
O3
H2O
HDO
CH4
N2O(i3)
solar-sim
Solar(A)
CO2(i3)
N2O
AllMol
Observed

σ=0.035%, 970315S4.90, φ=71.02^o, OPD=257cm, FoV=2.39$mrad$, Apod.=boxcar

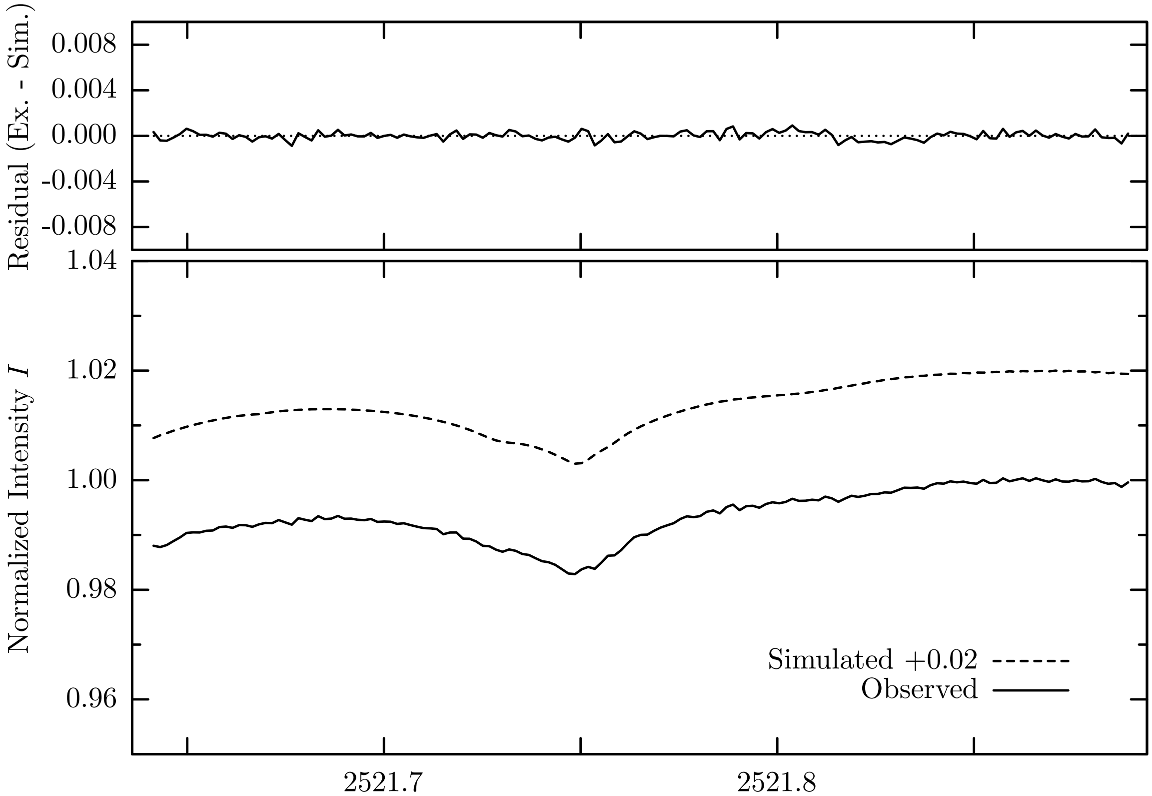

Wavenumber ν in cm^{-1}

investigated species	:	$N_2O(i3)$
line position(s) ν_0	:	2521.7504 cm^{-1}
lower state energy E''_{lst}	:	97.2 cm^{-1}
retrieved TCA, information content	:	5.61E+18 $molec/cm^2$, 35.7
temperature dependence of the TCA	:	-0.410%/K (trop), -0.031%/K (strat)
location, date, solar zenith angle	:	Kiruna, 15/Mar/97, 71.02^o
spectral interval fitted	:	2521.640 – 2521.890 cm^{-1}

Molecule	iCode	Absorption	Molecule	iCode	Absorption
$N2O$	41	21.622%	$SO2$	91	0.006%
$CO2$	2**3**	6.097%	$NH3$	111	<0.001%
Solar(A)	—	2.191%	OH	131	<0.001%
solar-sim	—	2.168%	HCl	151	<0.001%
N2O	4**3**	1.912%	HBr	161	<0.001%
$CH4$	61	0.588%	OCS	191	<0.001%
HDO	491	0.407%	$N2$	411	<0.001%
$H2O$	11	0.074%	$H2S$	471	<0.001%
$O3$	31	0.064%			

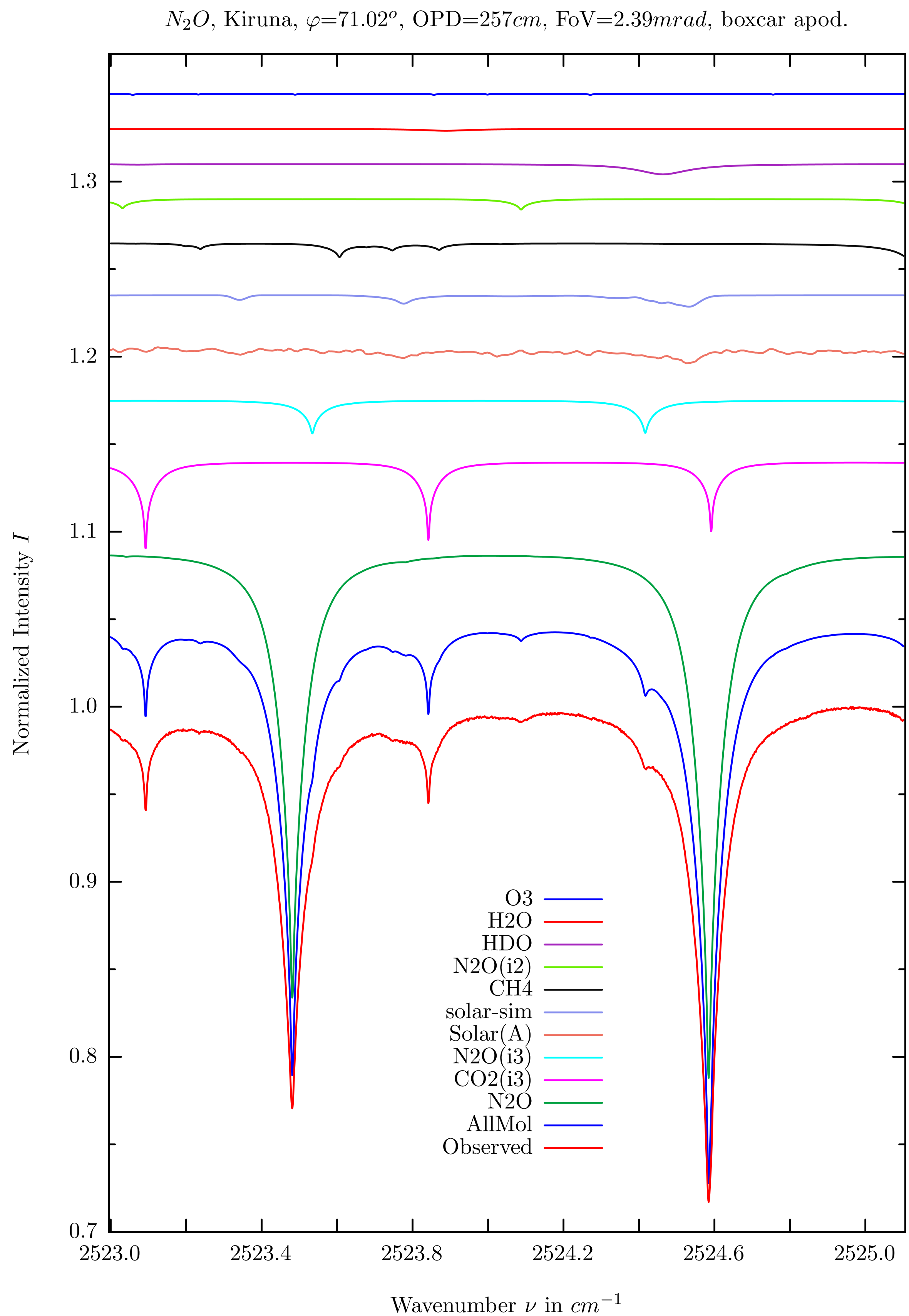
N_2O, Kiruna, φ=71.02^o, OPD=257cm, FoV=2.39$mrad$, boxcar apod.
Normalized Intensity I
1.3
1.2
1.1
1.0
0.9
0.8
0.7
2523.0
2523.4
2523.8
2524.2
2524.6
2525.0
Wavenumber ν in cm^{-1}
O3
H2O
HDO
N2O(i2)
CH4
solar-sim
Solar(A)
N2O(i3)
CO2(i3)
N2O
AllMol
Observed

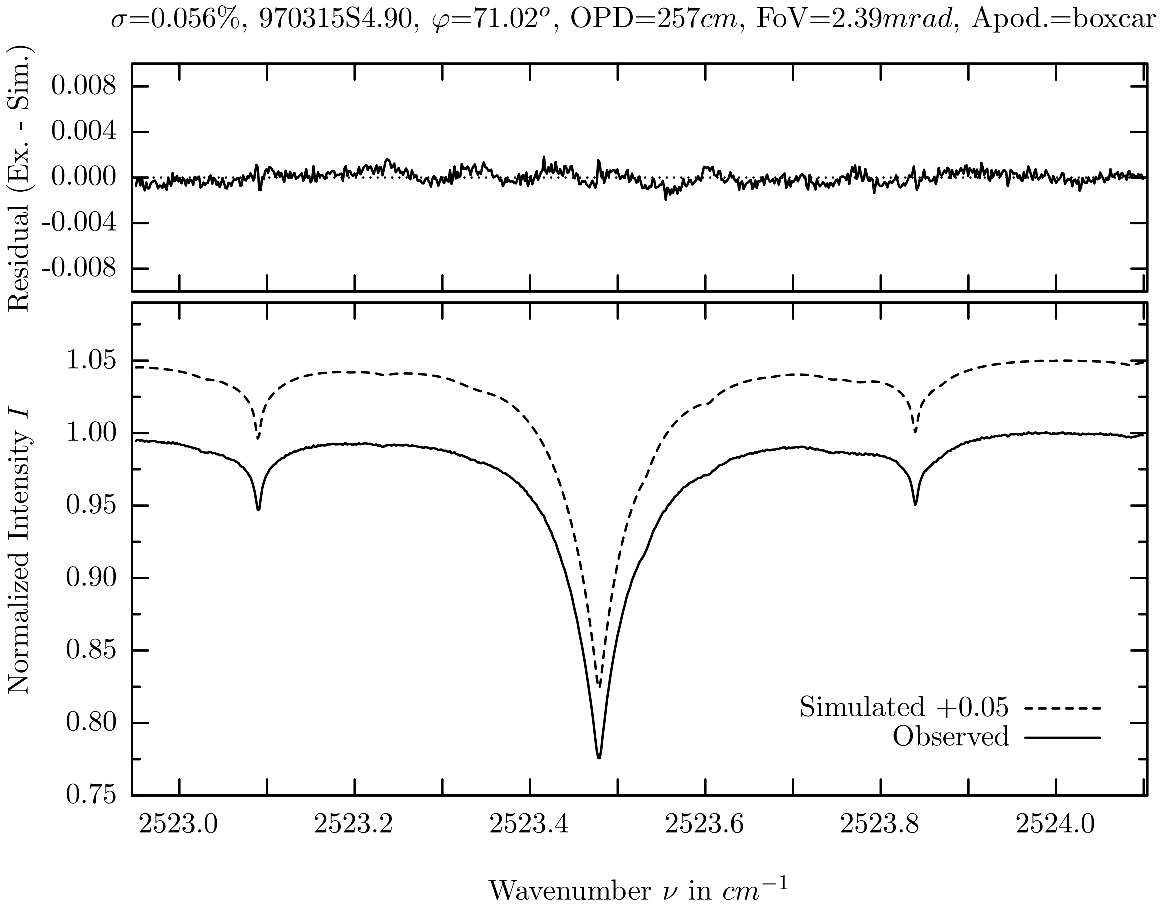

investigated species	:	$N_2O, (CO_2(i3))$
line position(s) ν_0	:	2523.4799, (2523.0910, 2523.8405) cm^{-1}
lower state energy E''_{lst}	:	721.0, (320.2, 342.3) cm^{-1}
retrieved TCA, information content	:	5.61E+18, (7.70E+21) $molec/cm^2$, 399.5, (95.2, 87.5)
temperature dependence of the TCA	:	-1.429, (-.662)%/K (trop), -.193, (-.109)%/K (strat)
location, date, solar zenith angle	:	Kiruna, 15/Mar/97, 71.02^o
spectral interval fitted	:	2522.950 – 2524.100 cm^{-1}

Molecule	iCode	Absorption	Molecule	iCode	Absorption
N2O	41	30.280%	*O3*	31	0.064%
CO2	2**3**	5.026%	*HBr*	161	0.009%
N2O	4**3**	1.900%	*SO2*	91	0.003%
Solar(A)	—	0.882%	*OCS*	191	0.001%
solar-sim	—	0.647%	*NH3*	111	<0.001%
CH4	61	0.800%	*OH*	131	<0.001%
N2O	4**2**	0.605%	*HCl*	151	<0.001%
HDO	491	0.591%	*N2*	411	<0.001%
H2O	11	0.099%	*H2S*	471	<0.001%

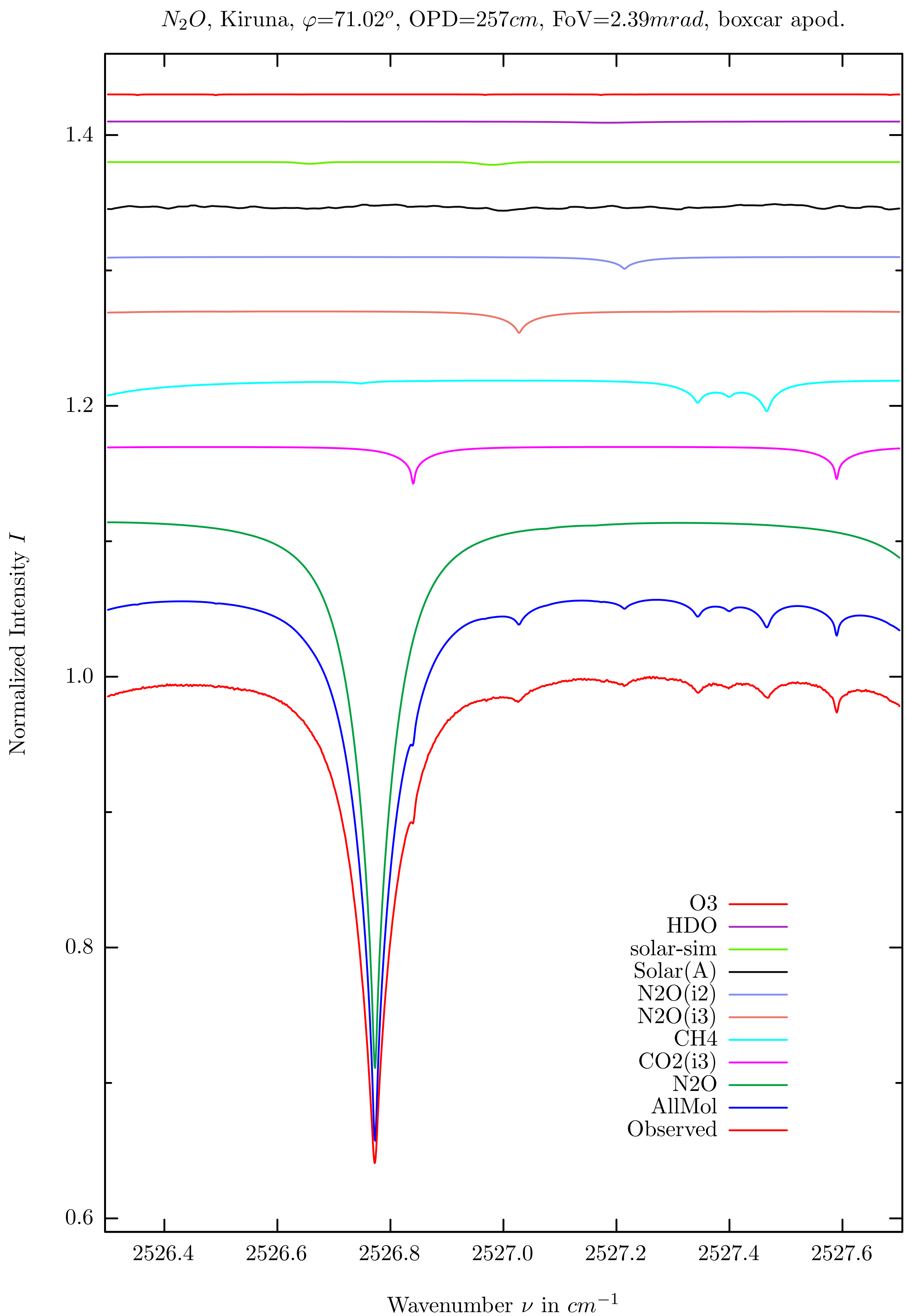
N_2O, Kiruna, φ=71.02^o, OPD=257cm, FoV=2.39$mrad$, boxcar apod.
Normalized Intensity I
Wavenumber ν in cm^{-1}
1.4
1.2
1.0
0.8
0.6
2526.4
2526.6
2526.8
2527.0
2527.2
2527.4
2527.6
O3
HDO
solar-sim
Solar(A)
N2O(i2)
N2O(i3)
CH4
CO2(i3)
N2O
AllMol
Observed

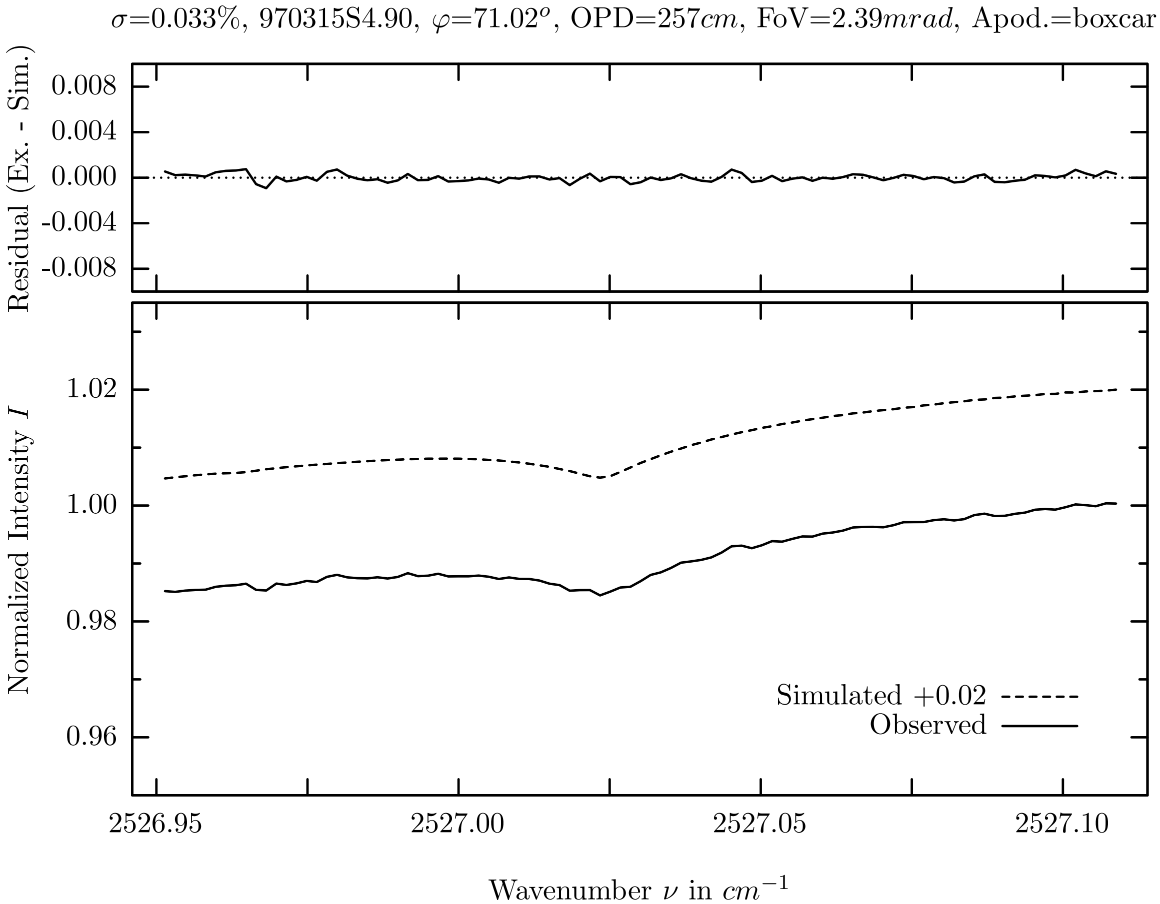

investigated species	:	$N_2O(i3)$
line position(s) ν_0	:	2527.0261 cm^{-1}
lower state energy E''_{lst}	:	36.4 cm^{-1}
retrieved TCA, information content	:	5.65E+18 $molec/cm^2$, 20.5
temperature dependence of the TCA	:	-0.367%/K (trop), -0.012%/K (strat)
location, date, solar zenith angle	:	Kiruna, 15/Mar/97, 71.02^o
spectral interval fitted	:	2526.950 – 2527.110 cm^{-1}

Molecule	iCode	Absorption	Molecule	iCode	Absorption
$N2O$	41	41.012%	$N2$	411	0.043%
$CO2$	2**3**	2.782%	$H2O$	11	0.001%
$CH4$	61	2.394%	$SO2$	91	0.001%
N2O	4**3**	1.614%	OCS	191	0.001%
$N2O$	4**2**	0.886%	$NH3$	111	<0.001%
Solar(A)	—	0.590%	OH	131	<0.001%
solar-sim	—	0.200%	HCl	151	<0.001%
HDO	491	0.092%	HBr	161	<0.001%
$O3$	31	0.055%	$H2S$	471	<0.001%

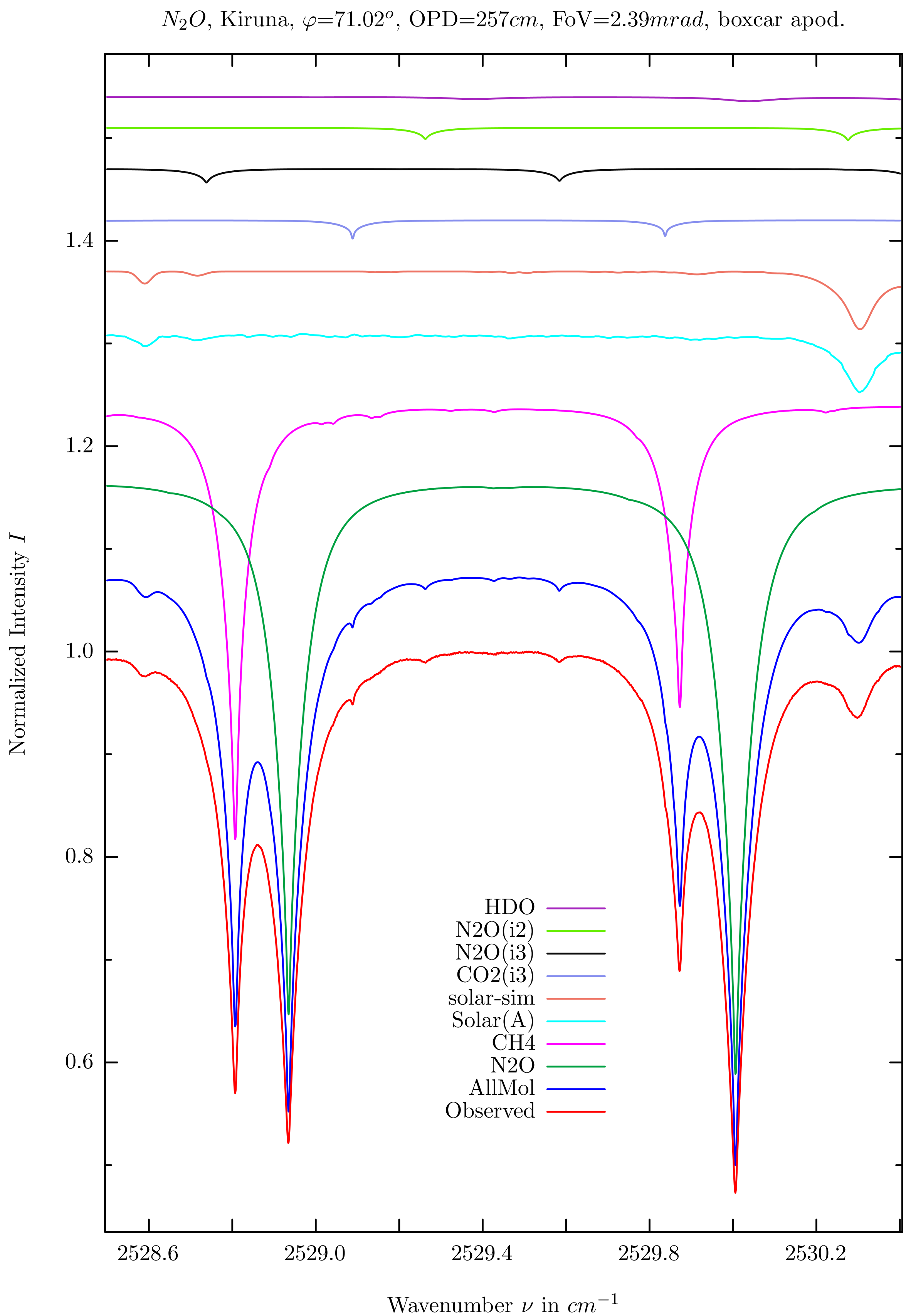

N_2O, Kiruna, φ=71.02^o, OPD=257cm, FoV=2.39$mrad$, boxcar apod.
Normalized Intensity I
1.4
1.2
1.0
0.8
0.6
HDO
N2O(i2)
N2O(i3)
CO2(i3)
solar-sim
Solar(A)
CH4
N2O
AllMol
Observed
2528.6
2529.0
2529.4
2529.8
2530.2
Wavenumber ν in cm^{-1}

σ=0.034%, 970315S4.90, φ=71.02^o, OPD=257cm, FoV=2.39$mrad$, Apod.=boxcar

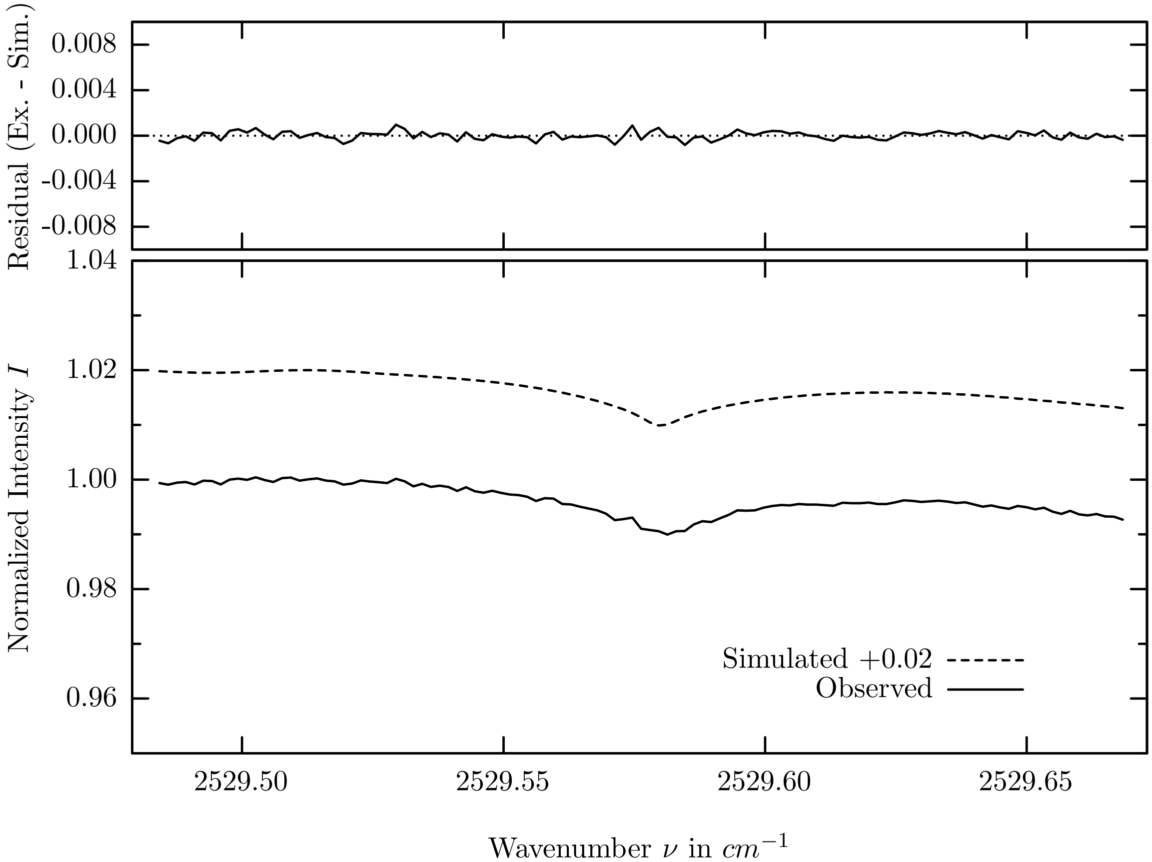

investigated species	:	$N_2O(i3)$
line position(s) ν_0	:	2529.5827 cm^{-1}
lower state energy E''_{lst}	:	17.0 cm^{-1}
retrieved TCA, information content	:	5.62E+18 $molec/cm^2$, 26.1
temperature dependence of the TCA	:	-0.373%/K (trop), -0.003%/K (strat)
location, date, solar zenith angle	:	Kiruna, 15/Mar/97, 71.02^o
spectral interval fitted	:	2529.483 – 2529.670 cm^{-1}

Molecule	iCode	Absorption	Molecule	iCode	Absorption
$N2O$	41	58.308%	$H2O$	11	0.009%
$CH4$	61	42.345%	OCS	191	0.001%
Solar(A)	—	5.759%	$SO2$	91	<0.001%
solar-sim	—	5.625%	$NH3$	111	<0.001%
$CO2$	2**3**	1.821%	OH	131	<0.001%
N2O	4**3**	1.343%	HBr	161	<0.001%
$N2O$	4**2**	1.209%	$N2$	411	<0.001%
HDO	491	0.419%	$H2S$	471	<0.001%
$O3$	31	0.044%			

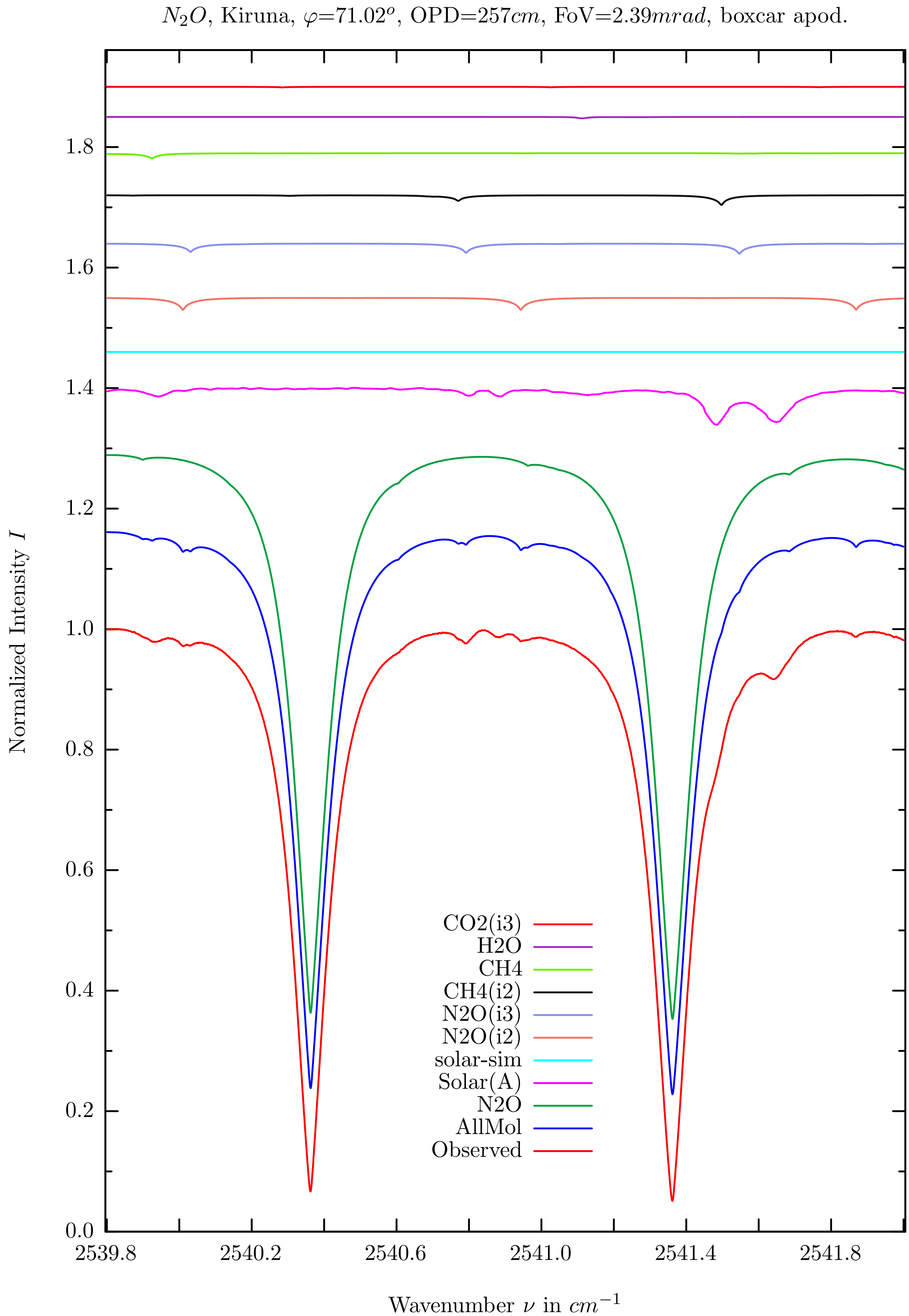
N_2O, Kiruna, φ=71.02^o, OPD=257cm, FoV=2.39$mrad$, boxcar apod.
Normalized Intensity I
Wavenumber ν in cm^{-1}
0.0
0.2
0.4
0.6
0.8
1.0
1.2
1.4
1.6
1.8
2539.8
2540.2
2540.6
2541.0
2541.4
2541.8
CO2(i3)
H2O
CH4
CH4(i2)
N2O(i3)
N2O(i2)
solar-sim
Solar(A)
N2O
AllMol
Observed

σ=0.055%, 970315S4.90, φ=71.02^o, OPD=257cm, FoV=2.39$mrad$, Apod.=boxcar

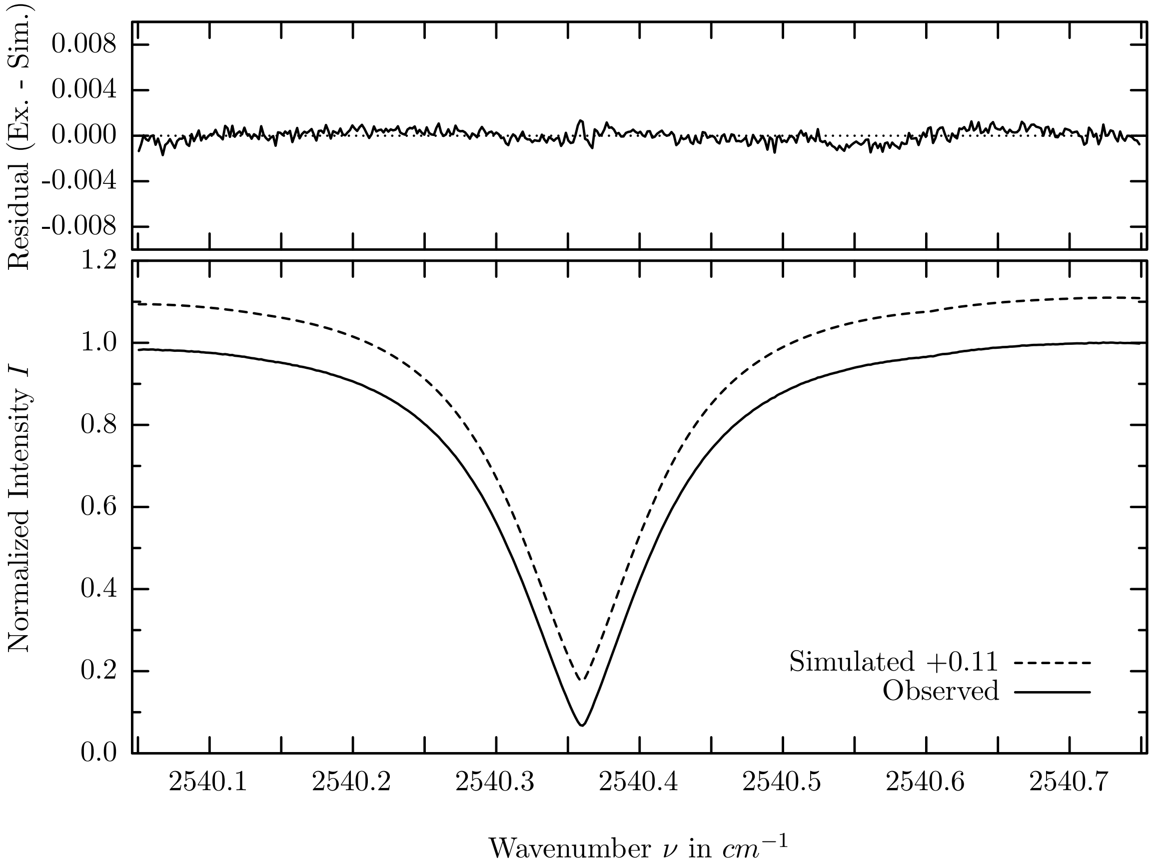

investigated species	:	N_2O
line position(s) ν_0	:	2540.3611 cm^{-1}
lower state energy E''_{lst}	:	272.3 cm^{-1}
retrieved TCA, information content	:	5.66E+18 $molec/cm^2$, 1705.0
temperature dependence of the TCA	:	-0.252%/K (trop), -0.058%/K (strat)
location, date, solar zenith angle	:	Kiruna, 15/Mar/97, 71.02^o
spectral interval fitted	:	2540.050 – 2540.750 cm^{-1}

Molecule	iCode	Absorption	Molecule	iCode	Absorption
N2O	41	97.234%	HDO	491	0.018%
Solar(A)	—	6.099%	$N2$	411	0.013%
solar-sim	—	<0.001%	OCS	191	0.003%
$N2O$	4**2**	2.014%	$SO2$	91	<0.001%
$N2O$	4**3**	1.704%	$NH3$	111	<0.001%
$CH4$	6**2**	1.591%	OH	131	<0.001%
$CH4$	61	0.872%	HCl	151	<0.001%
$H2O$	11	0.232%	HBr	161	<0.001%
$CO2$	2**3**	0.109%	$H2S$	471	<0.001%
$O3$	31	0.028%			

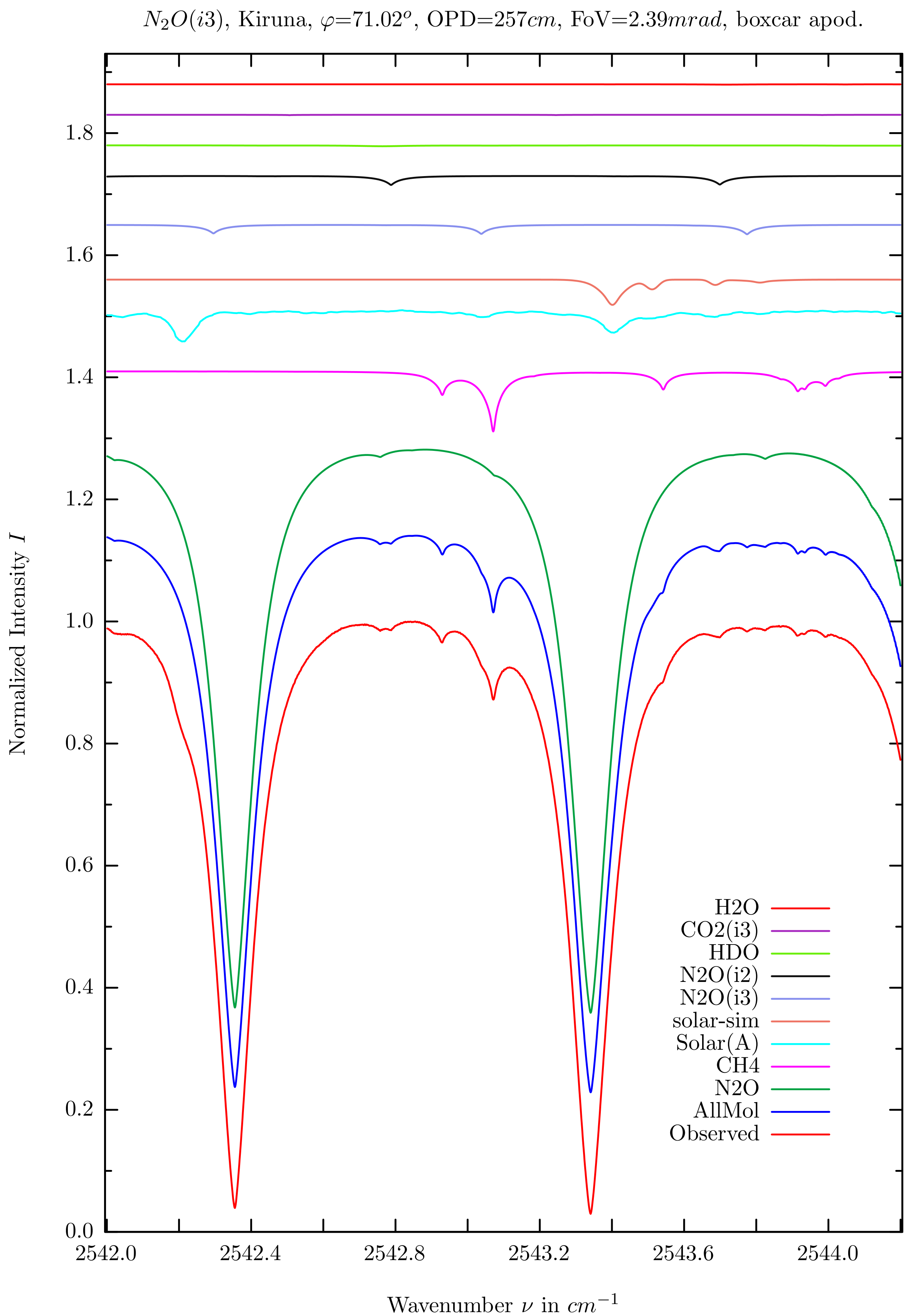

$N_2O(i3)$, Kiruna, φ=71.02^o, OPD=257cm, FoV=2.39$mrad$, boxcar apod.
Normalized Intensity I
Wavenumber ν in cm^{-1}
0.0
0.2
0.4
0.6
0.8
1.0
1.2
1.4
1.6
1.8
2542.0
2542.4
2542.8
2543.2
2543.6
2544.0
H2O
CO2(i3)
HDO
N2O(i2)
N2O(i3)
solar-sim
Solar(A)
CH4
N2O
AllMol
Observed

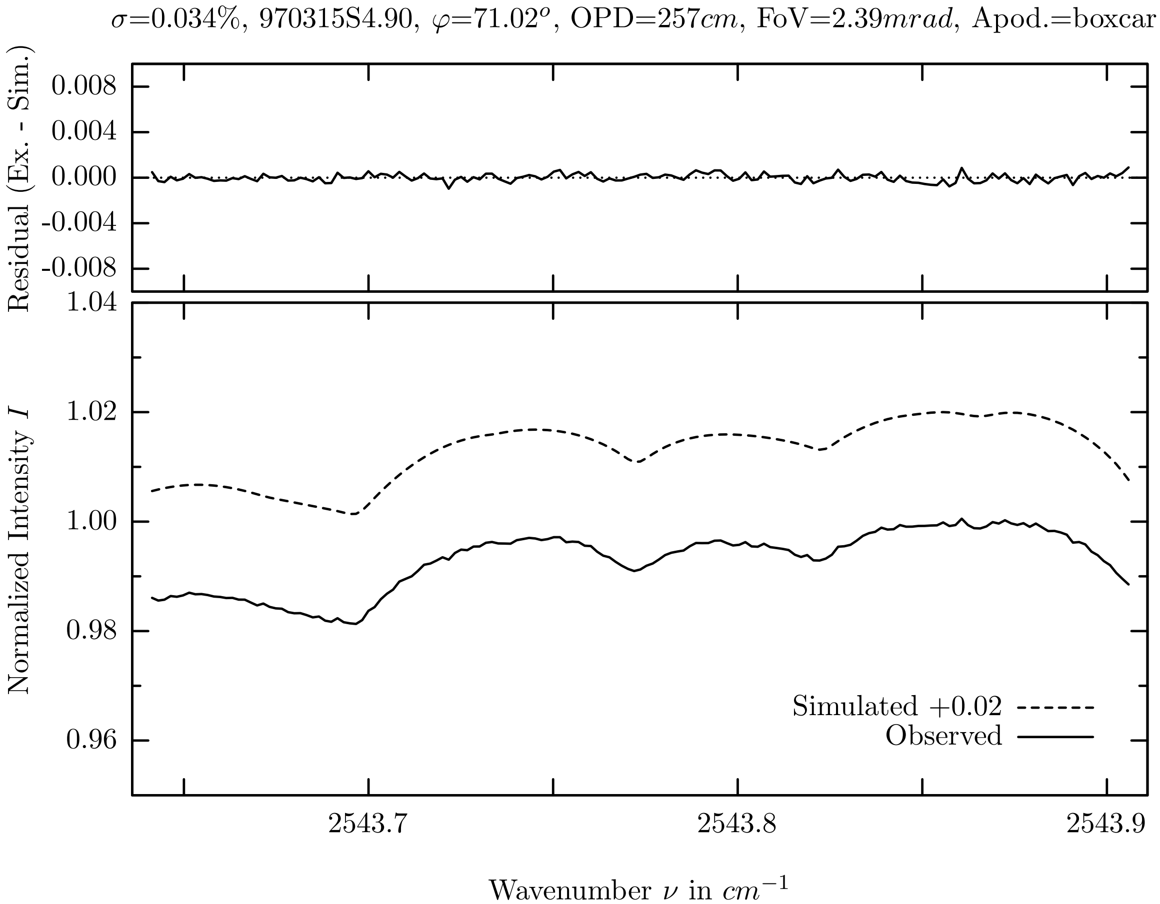

investigated species	:	$N_2O(i3)$
line position(s) ν_0	:	2543.7733 cm^{-1}
lower state energy E''_{lst}	:	53.4 cm^{-1}
retrieved TCA, information content	:	5.49E+18 $molec/cm^2$, 24.6
temperature dependence of the TCA	:	-0.947%/K (trop), -0.163%/K (strat)
location, date, solar zenith angle	:	Kiruna, 15/Mar/97, 71.02^o
spectral interval fitted	:	2543.640 – 2543.907 cm^{-1}

Molecule	iCode	Absorption	Molecule	iCode	Absorption
N2O	41	97.133%	*O3*	31	0.024%
CH4	61	9.890%	*HBr*	161	0.004%
Solar(A)	—	5.127%	*OCS*	191	0.004%
solar-sim	—	4.136%	*NH3*	111	<0.001%
N2O	4**3**	1.571%	*OH*	131	<0.001%
N2O	4**2**	1.491%	*HCl*	151	<0.001%
HDO	491	0.149%	*N2*	411	<0.001%
CO2	2**3**	0.055%	*H2S*	471	<0.001%
H2O	11	0.050%			

N_2O, Kiruna, φ=71.02^o, OPD=257cm, FoV=2.39$mrad$, boxcar apod.

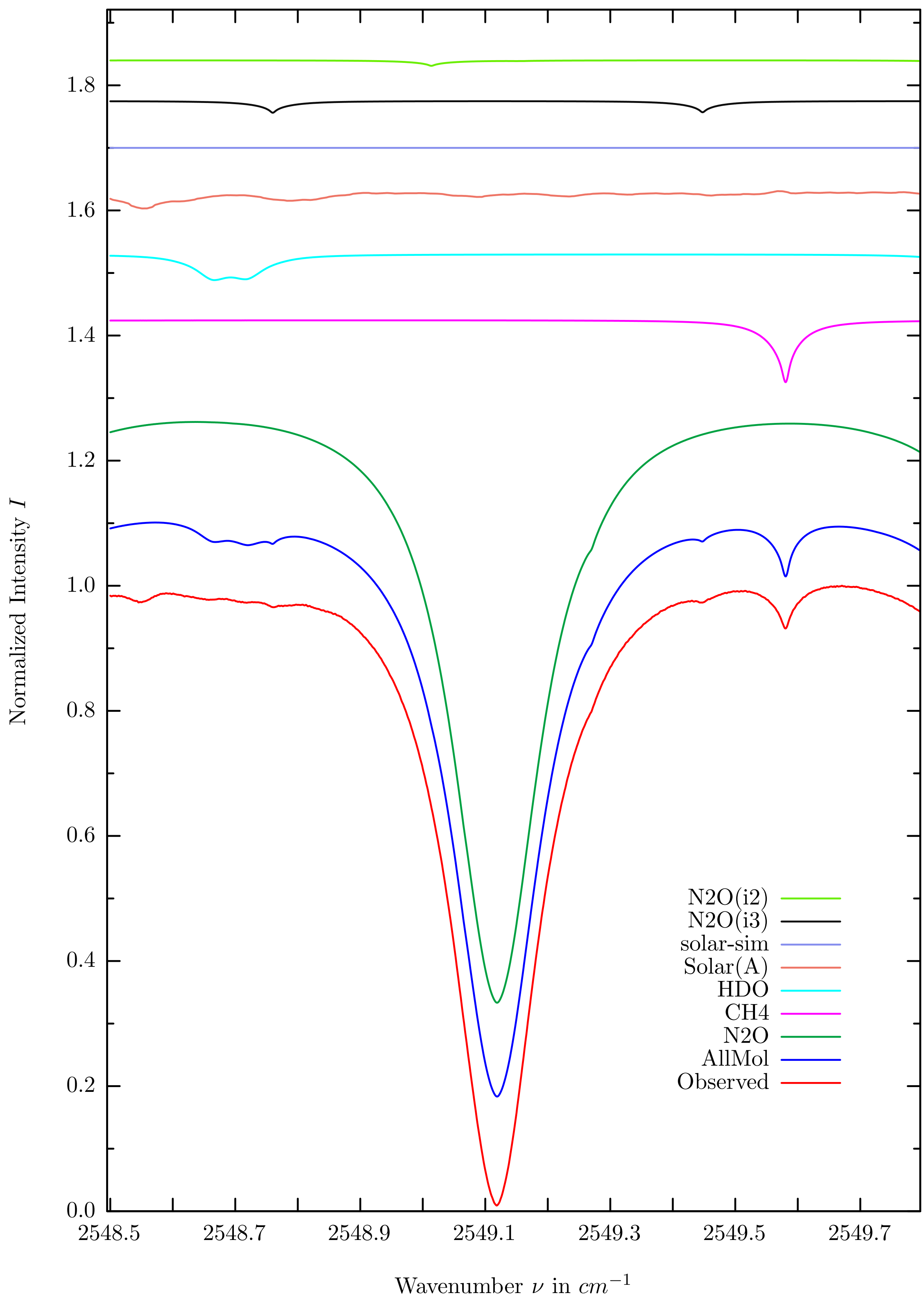

σ=0.057%, 970315S4.90, φ=71.02^o, OPD=257cm, FoV=2.39$mrad$, Apod.=boxcar

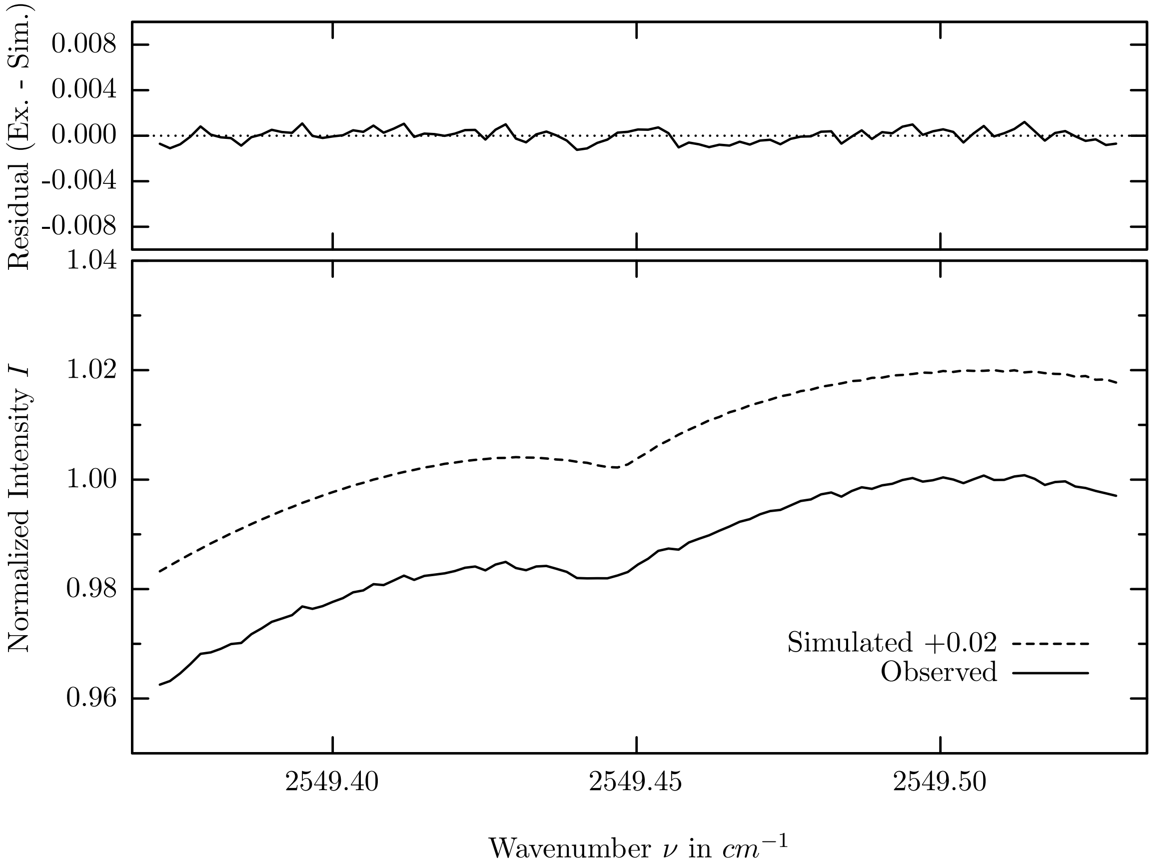

investigated species	:	$N_2O(i3)$
line position(s) ν_0	:	2549.4462 cm^{-1}
lower state energy E''_{lst}	:	153.8 cm^{-1}
retrieved TCA, information content	:	6.07E+18 $molec/cm^2$, 16.1
temperature dependence of the TCA	:	-0.263%/K (trop), -0.032%/K (strat)
location, date, solar zenith angle	:	Kiruna, 15/Mar/97, 71.02^o
spectral interval fitted	:	2549.370 – 2549.530 cm^{-1}

Molecule	iCode	Absorption	Molecule	iCode	Absorption
$N2O$	41	99.676%	$H2O$	11	0.001%
$CH4$	61	9.995%	$CO2$	2**3**	<0.001%
HDO	491	4.138%	$NH3$	111	<0.001%
Solar(A)	—	2.685%	OH	131	<0.001%
solar-sim	—	<0.001%	HCl	151	<0.001%
N2O	4**3**	1.892%	HBr	161	<0.001%
$N2O$	4**2**	0.885%	$N2$	411	<0.001%
$O3$	31	0.014%	$H2S$	471	<0.001%
OCS	191	0.004%			

N_2O, Kiruna, φ=71.02^o, OPD=257cm, FoV=2.39$mrad$, boxcar apod.

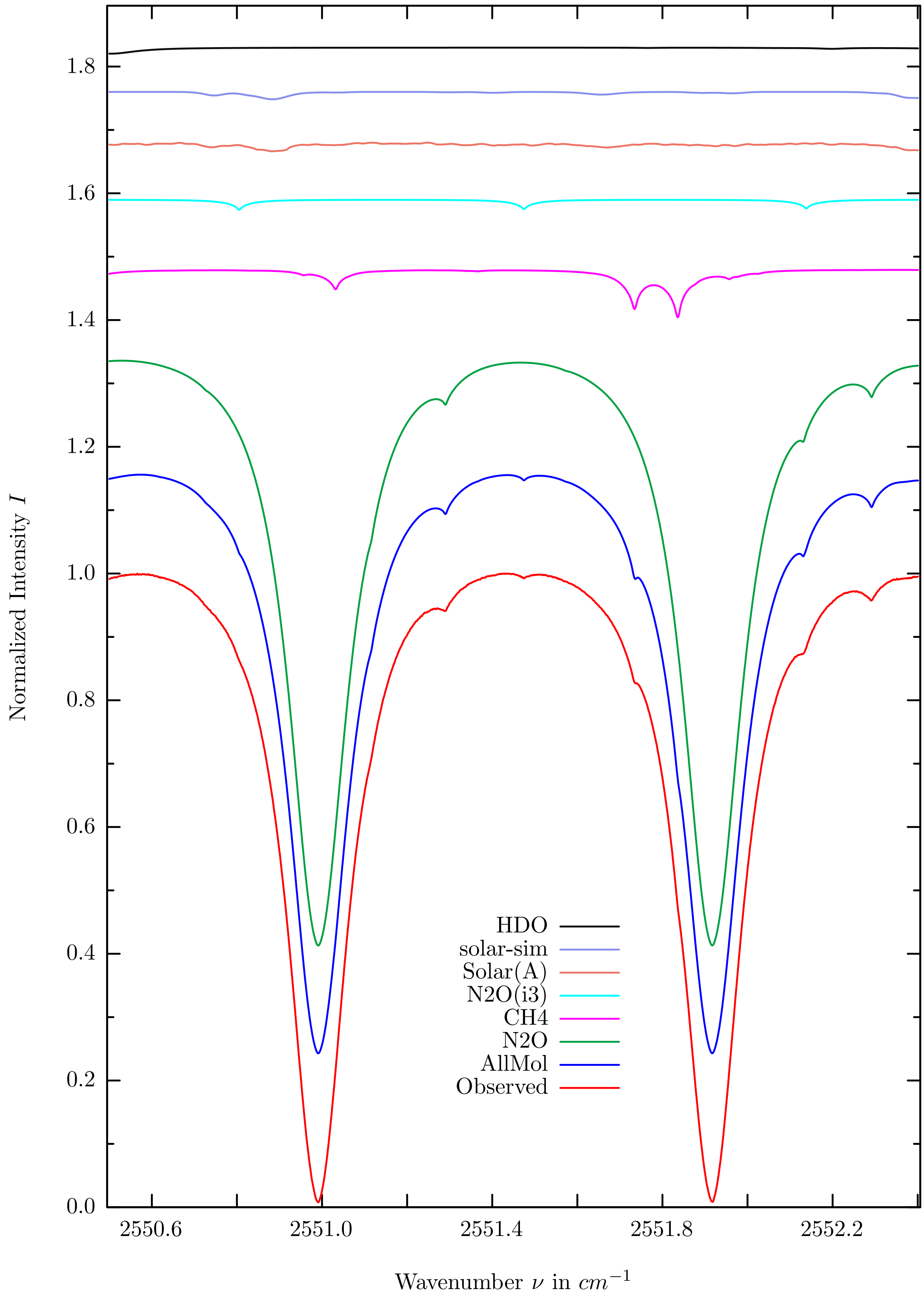

σ=0.038%, 970315S4.90, φ=71.02^o, OPD=257cm, FoV=2.39$mrad$, Apod.=boxcar

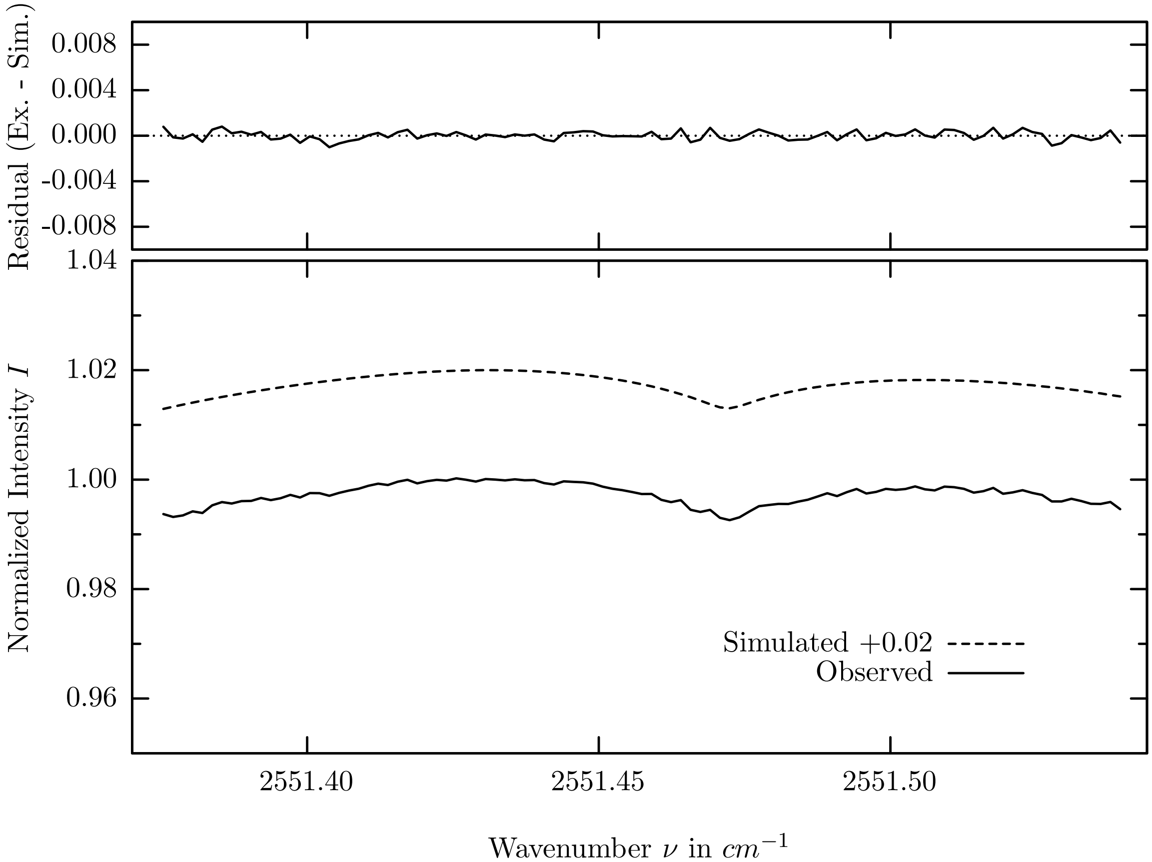

investigated species	:	$N_2O(i3)$
line position(s) ν_0	:	2551.4732 cm^{-1}
lower state energy E''_{lst}	:	204.8 cm^{-1}
retrieved TCA, information content	:	5.57E+18 $molec/cm^2$, 17.5
temperature dependence of the TCA	:	-0.400%/K (trop), -0.060%/K (strat)
location, date, solar zenith angle	:	Kiruna, 15/Mar/97, 71.02^o
spectral interval fitted	:	2551.375 – 2551.540 cm^{-1}

Molecule	iCode	Absorption	Molecule	iCode	Absorption
$N2O$	41	99.714%	OCS	191	0.003%
$CH4$	61	7.580%	$CO2$	**23**	<0.001%
N2O	4**3**	1.616%	$NH3$	111	<0.001%
Solar(A)	—	1.375%	OH	131	<0.001%
solar-sim	—	1.167%	HCl	151	<0.001%
HDO	491	0.968%	HBr	161	<0.001%
$O3$	31	0.013%	$N2$	411	<0.001%
$H2O$	11	0.010%	$H2S$	471	<0.001%

N_2O, Kiruna, φ=71.02^o, OPD=257cm, FoV=2.39$mrad$, boxcar apod.

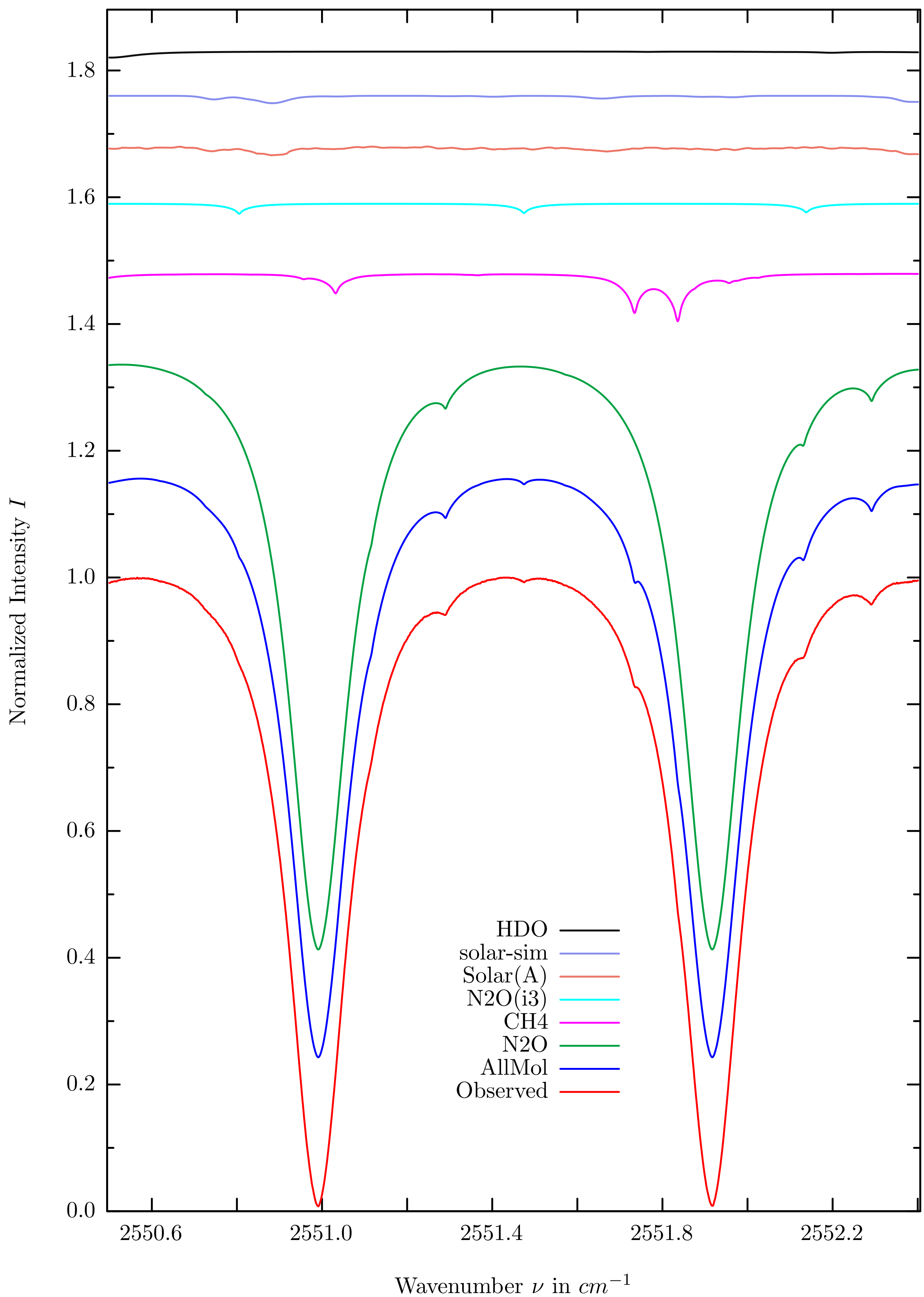

σ=0.083%, 970315S4.90, φ=71.02^o, OPD=257cm, FoV=2.39$mrad$, Apod.=boxcar

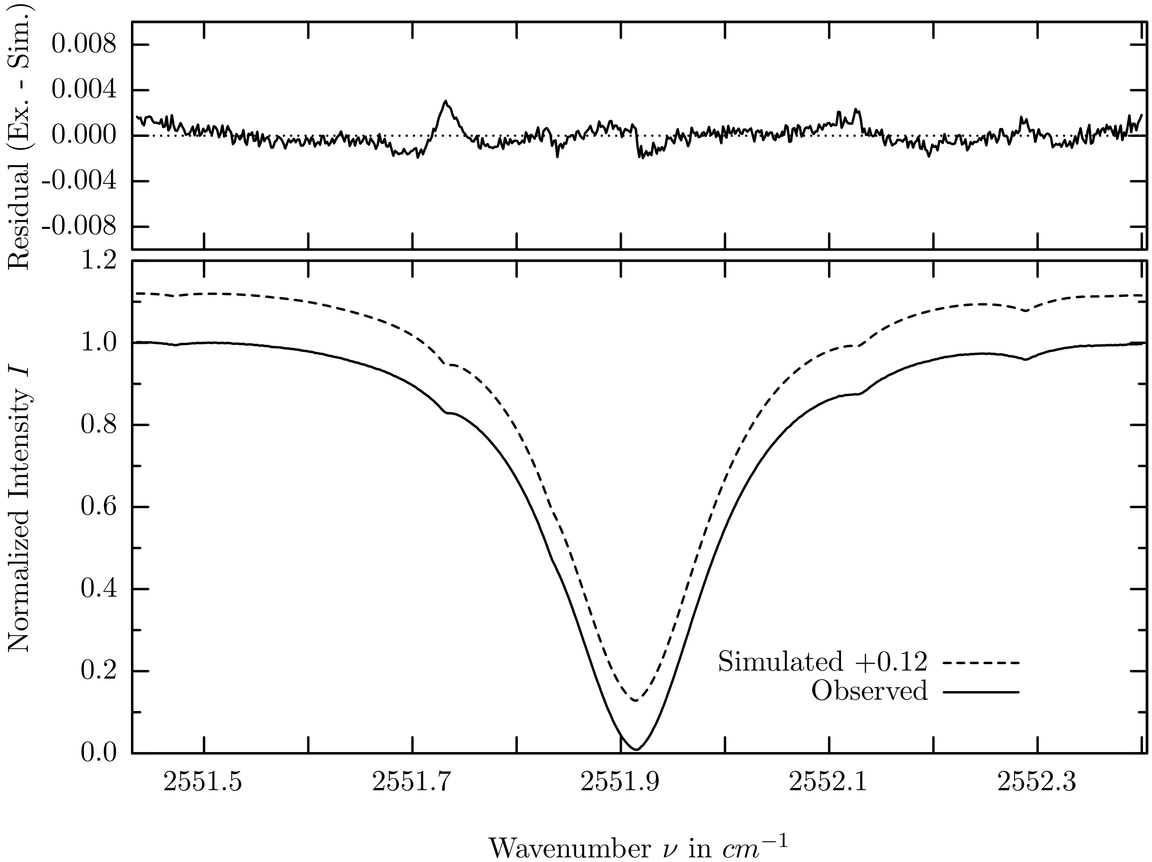

investigated species	:	N_2O
line position(s) ν_0	:	2551.9157 cm^{-1}
lower state energy E''_{lst}	:	76.3 cm^{-1}
retrieved TCA, information content	:	5.71E+18 $molec/cm^2$, 1199.0
temperature dependence of the TCA	:	+0.286%/K (trop), -0.018%/K (strat)
location, date, solar zenith angle	:	Kiruna, 15/Mar/97, 71.02^o
spectral interval fitted	:	2551.435 – 2552.400 cm^{-1}

Molecule	iCode	Absorption	Molecule	iCode	Absorption
N2O	41	99.714%	OCS	191	0.003%
$CH4$	61	7.580%	$CO2$	2**3**	<0.001%
$N2O$	4**3**	1.616%	$NH3$	111	<0.001%
Solar(A)	—	1.375%	OH	131	<0.001%
solar-sim	—	1.167%	HCl	151	<0.001%
HDO	491	0.968%	HBr	161	<0.001%
$O3$	31	0.013%	$N2$	411	<0.001%
$H2O$	11	0.010%	$H2S$	471	<0.001%

$N_2O(i2)$, Kiruna, φ=71.02^o, OPD=257cm, FoV=2.39$mrad$, boxcar apod.

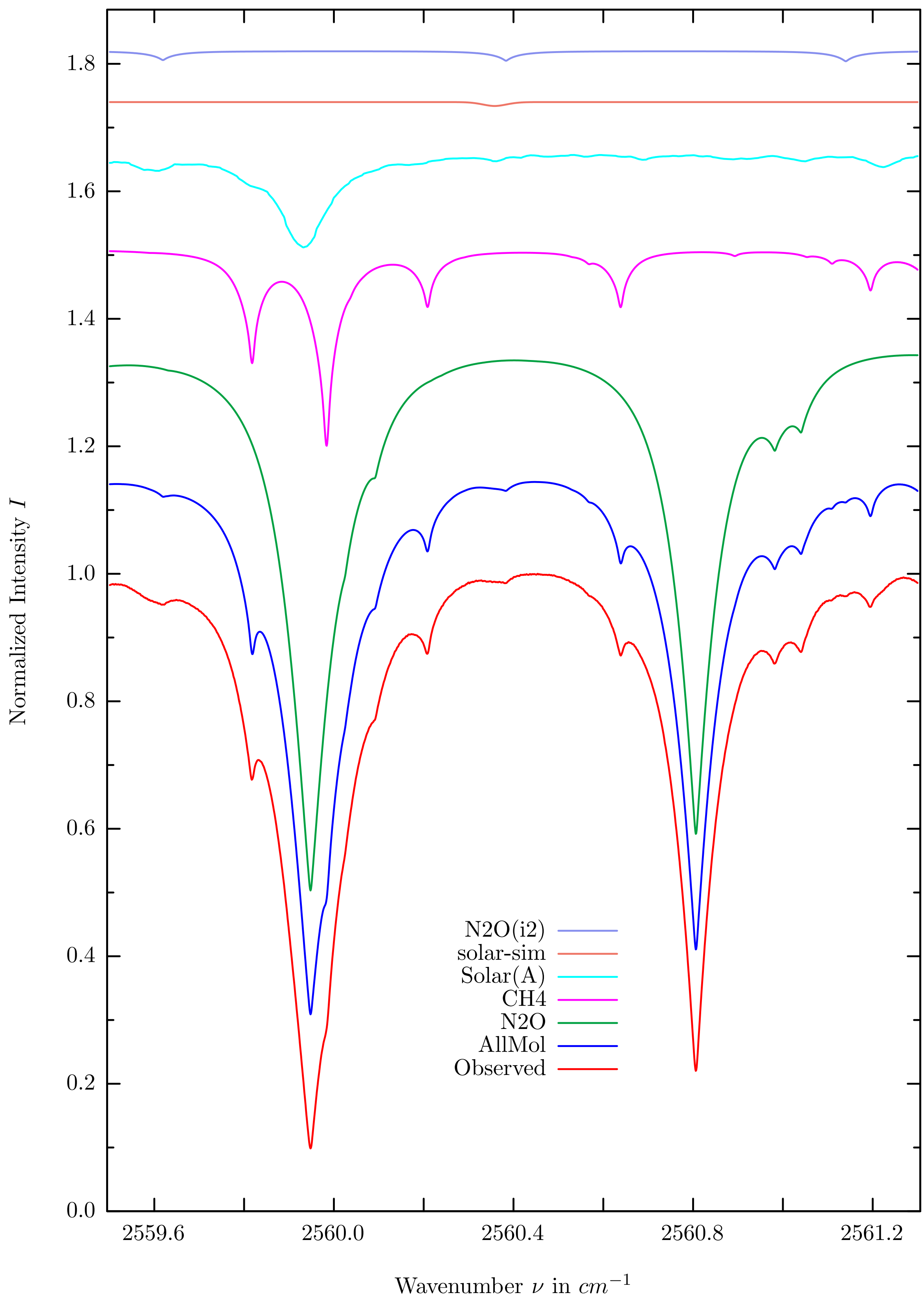

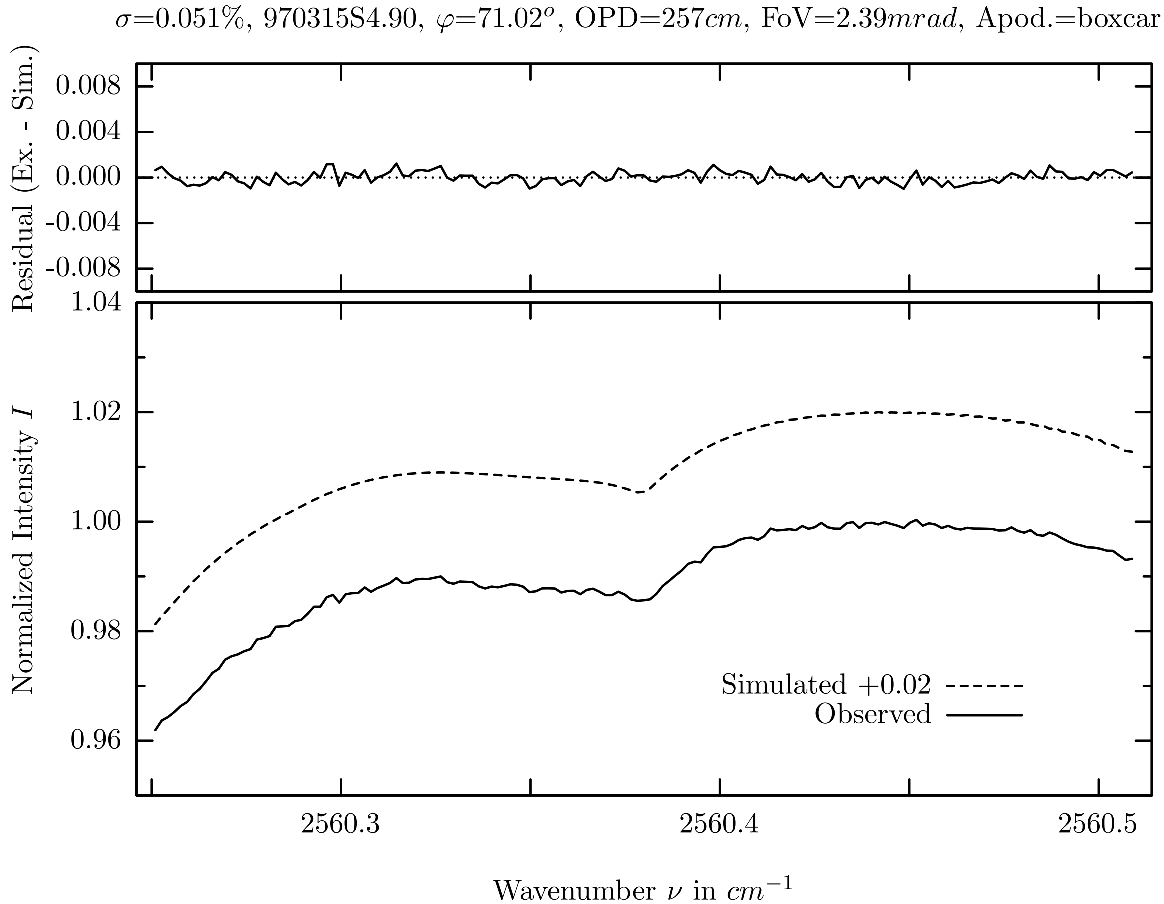

investigated species	:	N_2O
line position(s) ν_0	:	2560.3820 cm^{-1}
lower state energy E''_{lst}	:	37.7 cm^{-1}
retrieved TCA, information content	:	5.33E+18 $molec/cm^2$, 19.7
temperature dependence of the TCA	:	-0.118%/K (trop), +0.029%/K (strat)
location, date, solar zenith angle	:	Kiruna, 15/Mar/97, 71.02^o
spectral interval fitted	:	2560.250 – 2560.510 cm^{-1}

Molecule	iCode	Absorption	Molecule	iCode	Absorption
N2O	41	87.742%	*OCS*	191	0.004%
CH4	61	30.980%	*N2*	411	0.004%
Solar(A)	—	14.791%	*NH3*	111	<0.001%
solar-sim	—	0.613%	*OH*	131	<0.001%
N2O	4**2**	1.597%	*HCl*	151	<0.001%
HDO	491	0.038%	*HBr*	161	<0.001%
H2O	11	0.023%	*H2S*	471	<0.001%

N_2O, Kiruna, φ=71.02^o, OPD=257cm, FoV=2.39$mrad$, boxcar apod.

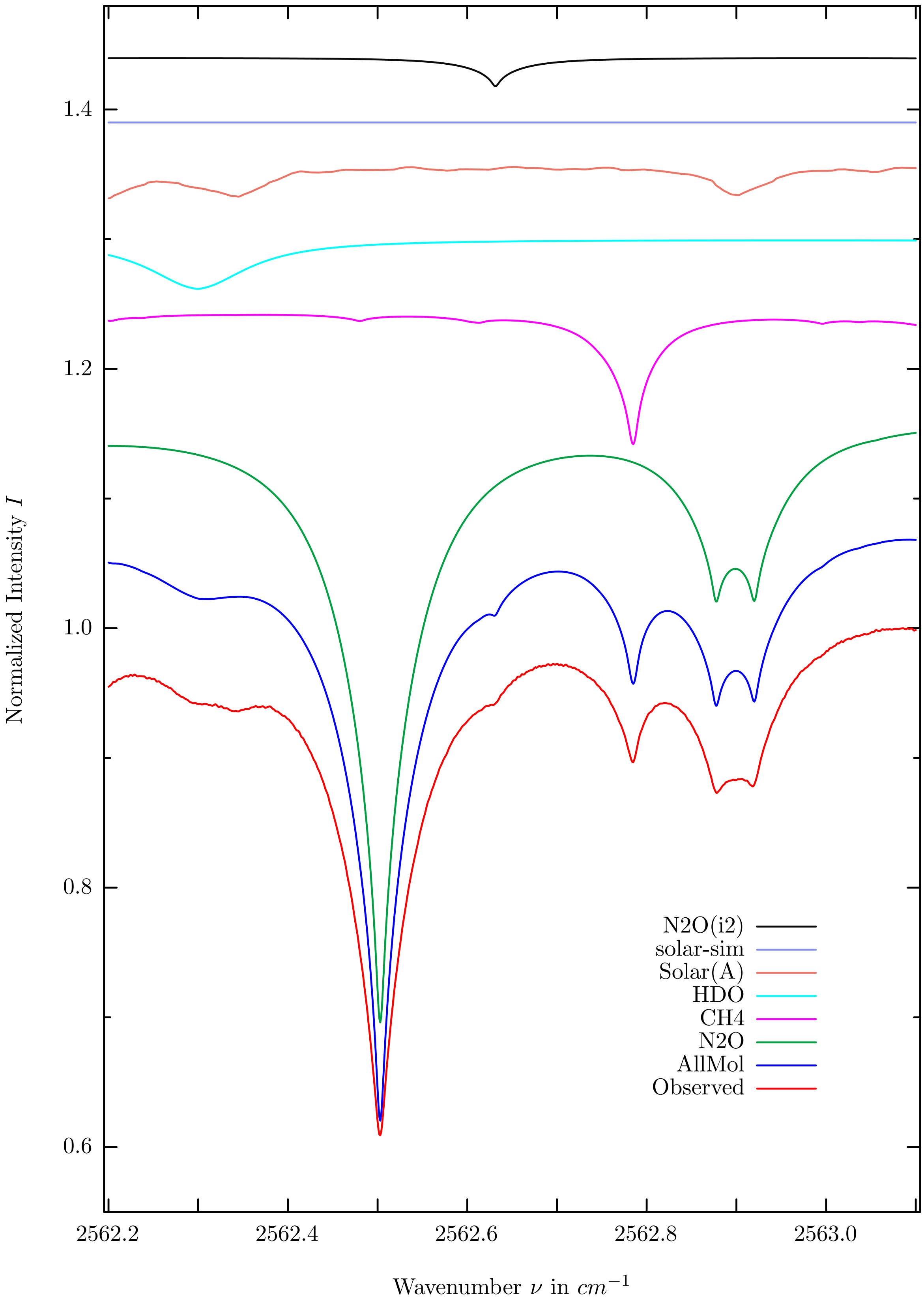

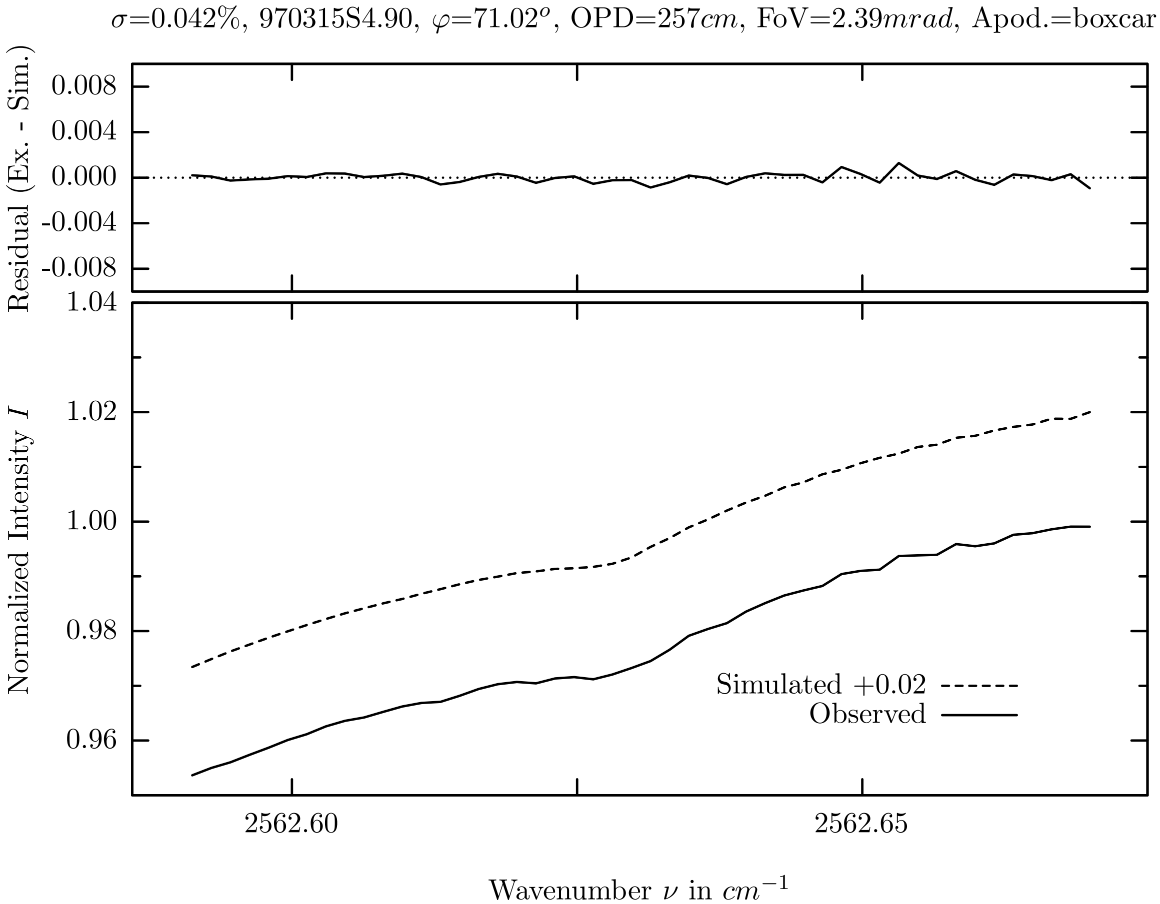

investigated species	:	$N_2O(i2)$
line position(s) ν_0	:	2562.6282 cm^{-1}
lower state energy E''_{lst}	:	65.4 cm^{-1}
retrieved TCA, information content	:	5.65E+18 $molec/cm^2$, 9.3
temperature dependence of the TCA	:	-0.211%/K (trop), -0.076%/K (strat)
location, date, solar zenith angle	:	Kiruna, 15/Mar/97, 71.02^o
spectral interval fitted	:	2562.590 – 2562.670 cm^{-1}

Molecule	iCode	Absorption	Molecule	iCode	Absorption
N2O	41	47.419%	*CO2*	2**3**	<0.001%
CH4	61	10.322%	*NH3*	111	<0.001%
HDO	491	3.836%	*OH*	131	<0.001%
Solar(A)	—	2.853%	*HCl*	151	<0.001%
solar-sim	—	<0.001%	*HBr*	161	<0.001%
N2O	4**2**	2.219%	*N2*	411	<0.001%
OCS	191	0.005%	*H2S*	471	<0.001%
H2O	11	0.002%			

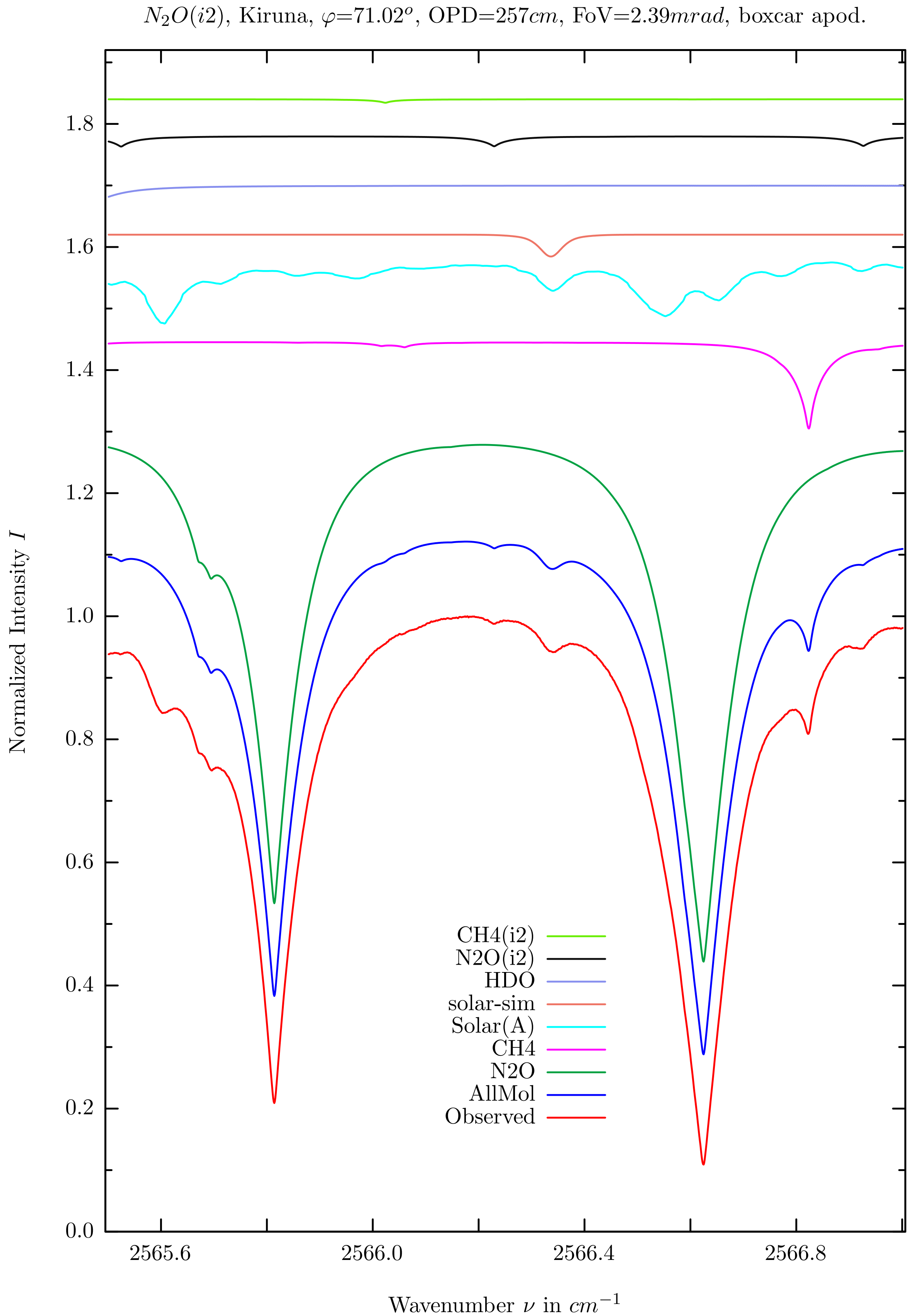

$N_2O(i2)$, Kiruna, φ=71.02^o, OPD=257cm, FoV=2.39$mrad$, boxcar apod.
Normalized Intensity I
Wavenumber ν in cm^{-1}
0.0
0.2
0.4
0.6
0.8
1.0
1.2
1.4
1.6
1.8
2565.6
2566.0
2566.4
2566.8
CH4(i2)
N2O(i2)
HDO
solar-sim
Solar(A)
CH4
N2O
AllMol
Observed

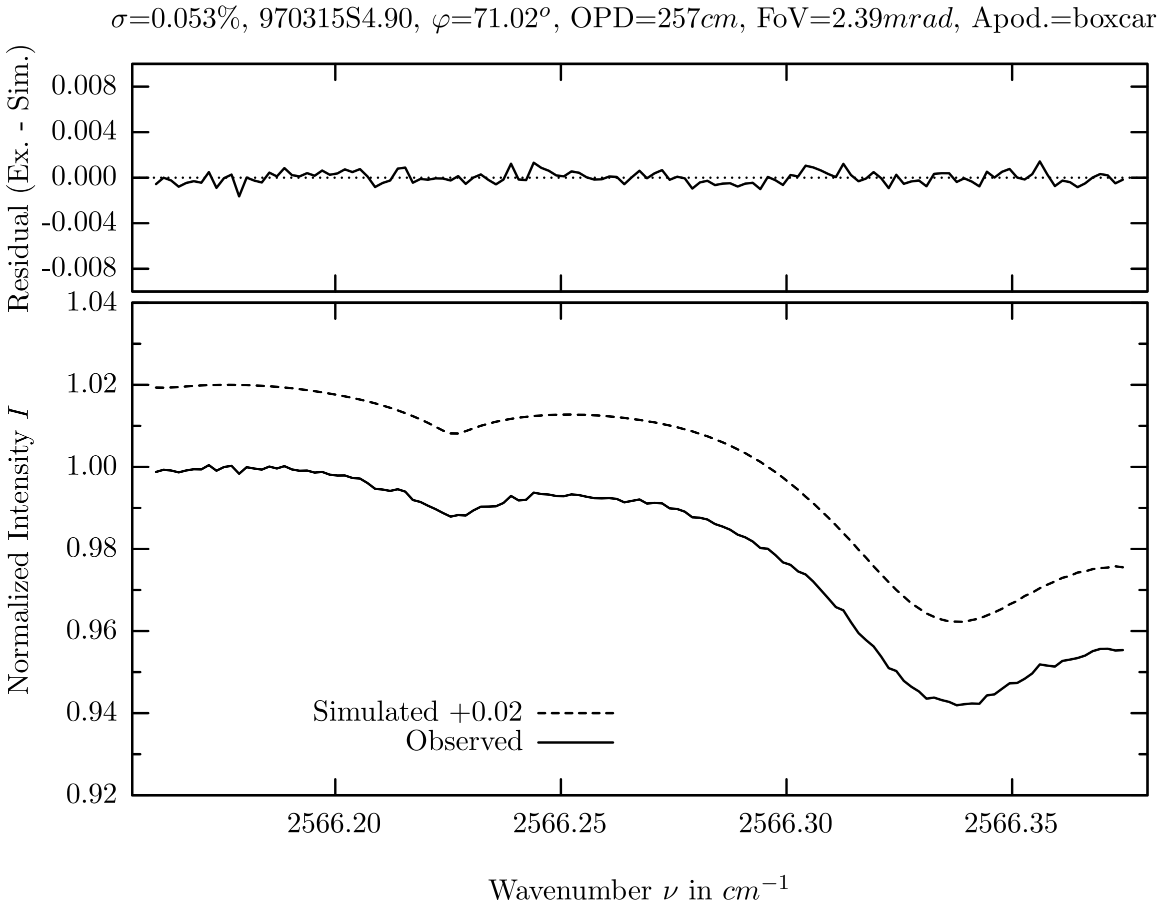

investigated species	:	$N_2O(i2)$
line position(s) ν_0	:	2566.2273 cm^{-1}
lower state energy E''_{lst}	:	128.2 cm^{-1}
retrieved TCA, information content	:	5.77E+18 $molec/cm^2$, 20.3
temperature dependence of the TCA	:	-0.130%/K (trop), -0.003%/K (strat)
location, date, solar zenith angle	:	Kiruna, 15/Mar/97, 71.02^o
spectral interval fitted	:	2566.160 – 2566.375 cm^{-1}

Molecule	iCode	Absorption	Molecule	iCode	Absorption
$N2O$	41	89.179%	OCS	191	0.005%
$CH4$	61	14.133%	$CO2$	2**3**	<0.001%
Solar(A)	—	10.436%	$NH3$	111	<0.001%
solar-sim	—	3.546%	OH	131	<0.001%
HDO	491	1.819%	HCl	151	<0.001%
N2O	4**2**	1.682%	HBr	161	<0.001%
$CH4$	6**2**	0.560%	$N2$	411	<0.001%
$H2O$	11	0.006%	$H2S$	471	<0.001%

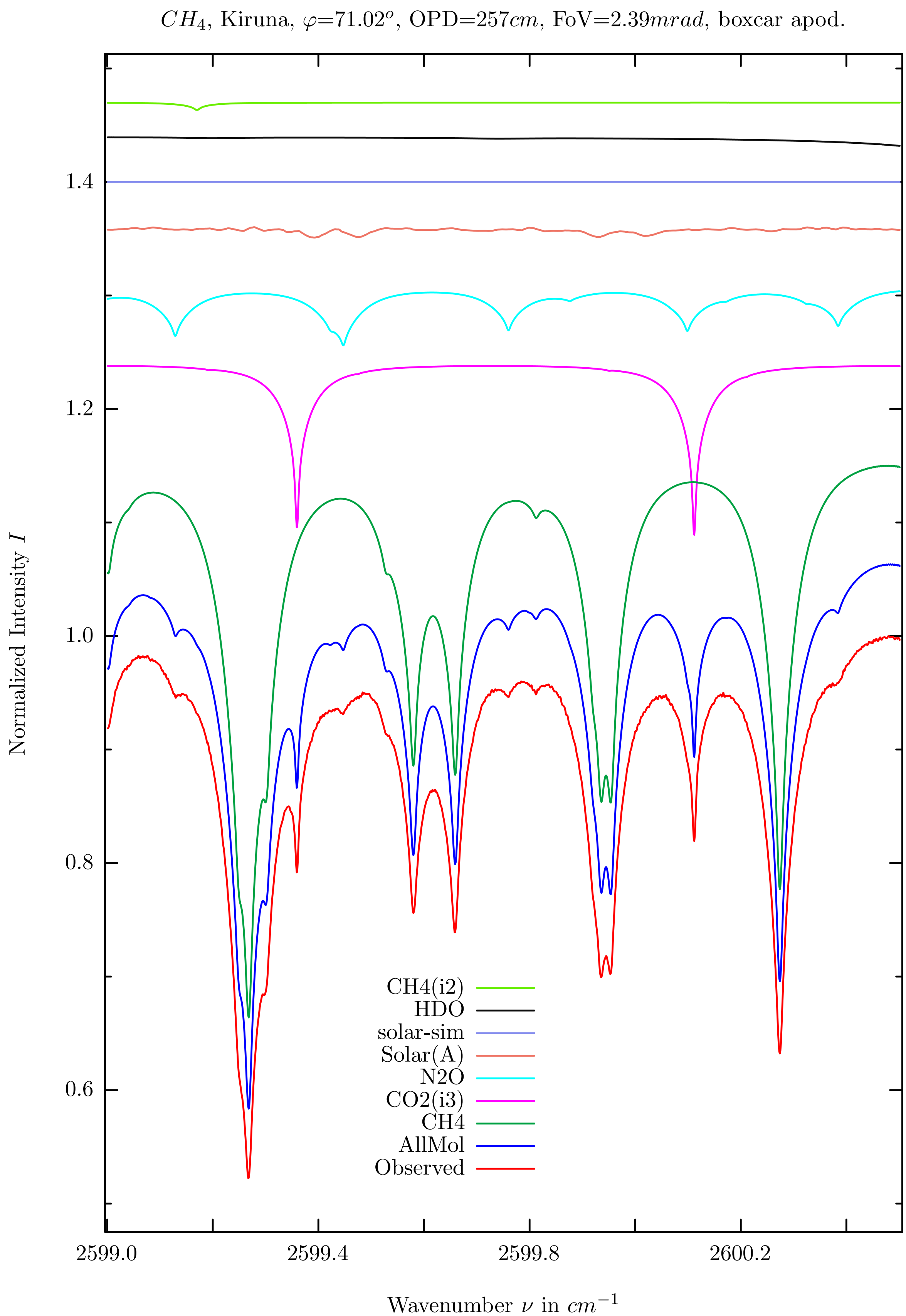
CH_4, Kiruna, φ=71.02^o, OPD=257cm, FoV=2.39$mrad$, boxcar apod.
Normalized Intensity I
Wavenumber ν in cm^{-1}
1.4
1.2
1.0
0.8
0.6
2599.0
2599.4
2599.8
2600.2
CH4(i2)
HDO
solar-sim
Solar(A)
N2O
CO2(i3)
CH4
AllMol
Observed

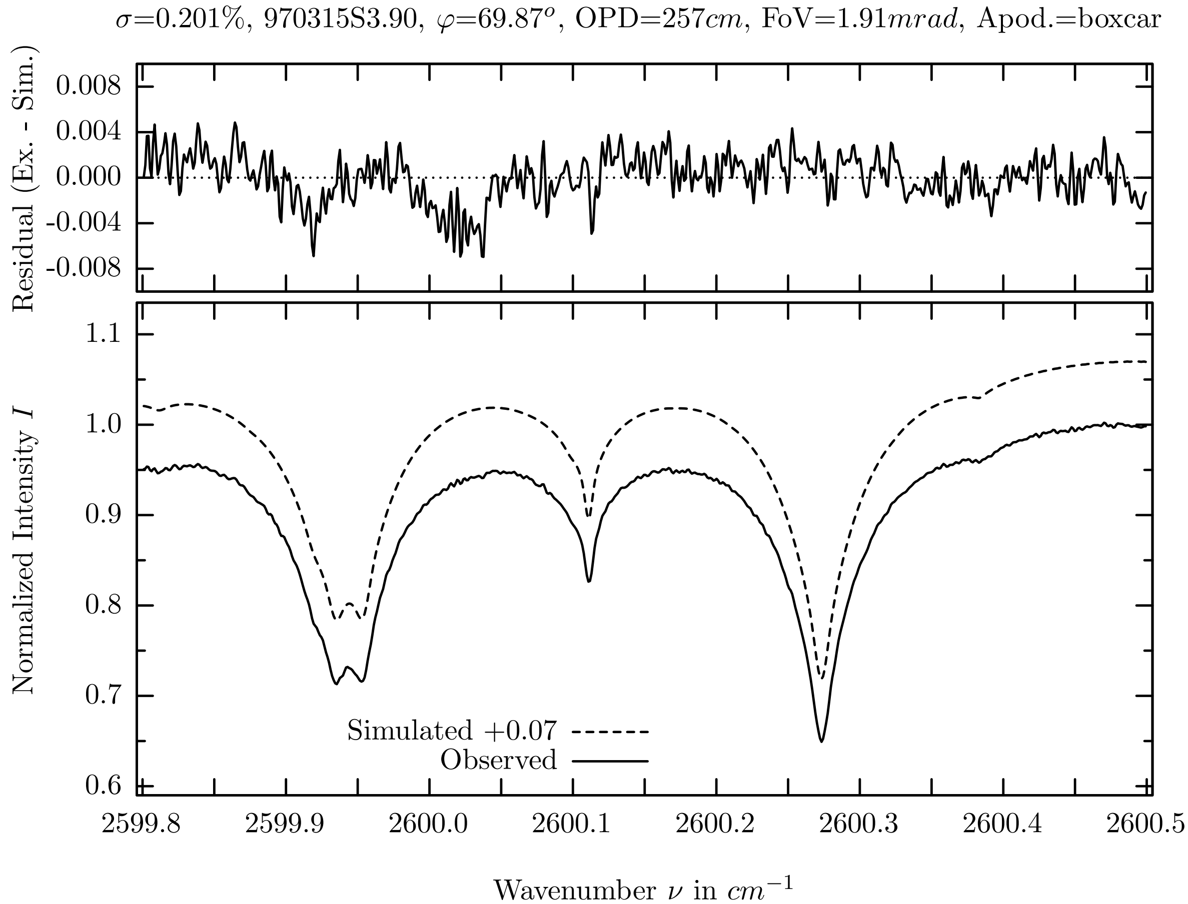

investigated species	:	CH_4
line position(s) ν_0	:	2600.2726 cm^{-1}
lower state energy E''_{lst}	:	219.9 cm^{-1}
retrieved TCA, information content	:	3.20E+19 $molec/cm^2$, 175.0
temperature dependence of the TCA	:	-0.194%/K (trop), -0.028%/K (strat)
location, date, solar zenith angle	:	Kiruna, 15/Mar/97, 69.87^o
spectral interval fitted	:	2599.800 – 2600.500 cm^{-1}

Molecule	iCode	Absorption	Molecule	iCode	Absorption
CH4	61	50.671%	*HCl*	151	0.016%
*CO*2	2**3**	15.215%	*SO*2	91	<0.001%
*N*2*O*	41	5.397%	*NH*3	111	<0.001%
Solar(A)	—	0.890%	*OH*	131	<0.001%
Solar-sim	—	<0.001%	*HBr*	161	<0.001%
HDO	491	0.817%	*OCS*	191	<0.001%
*CH*4	6**2**	0.654%	*N*2	411	<0.001%
*H*2*O*	11	0.038%	*H*2*S*	471	<0.001%

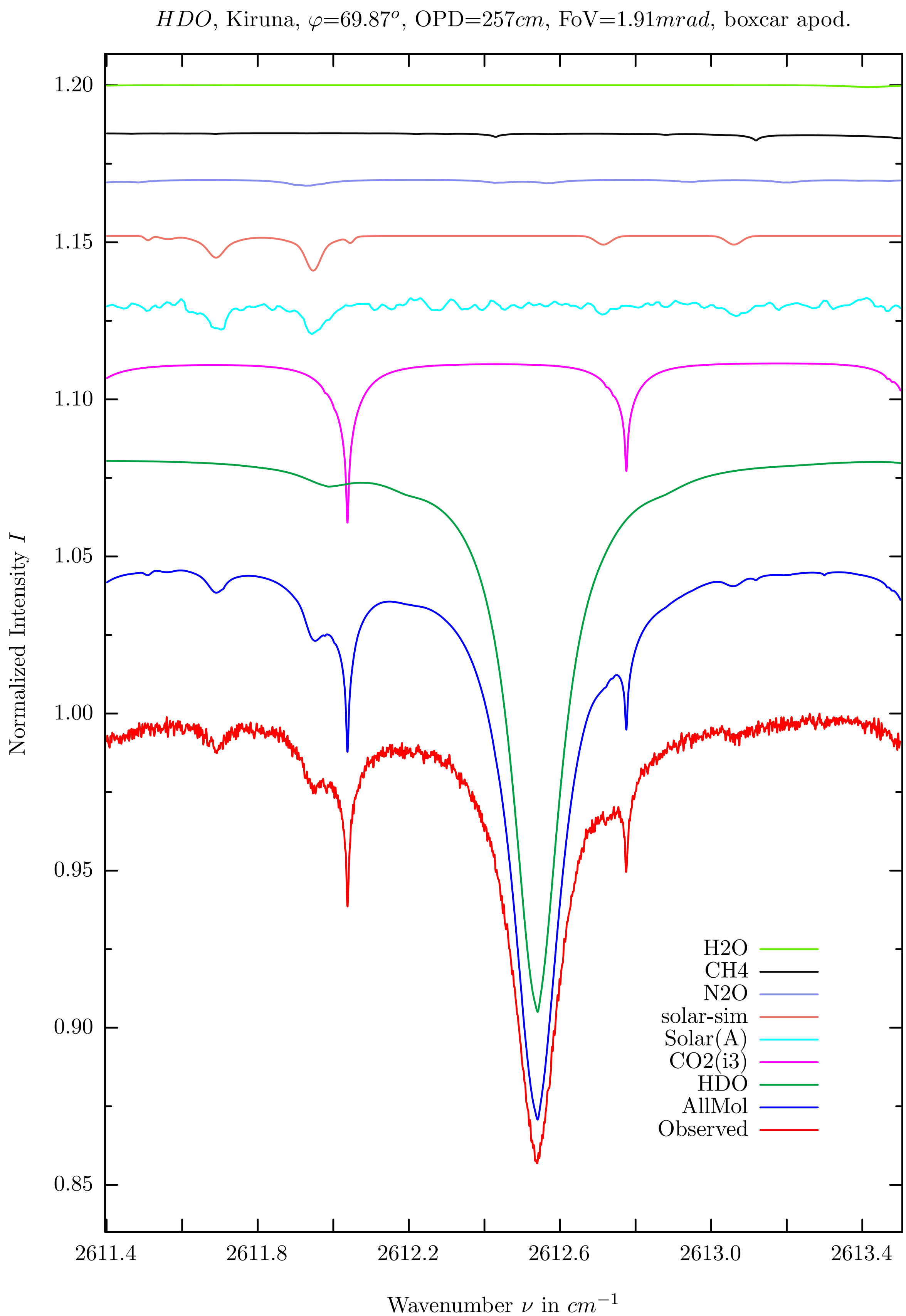
HDO, Kiruna, φ=69.87^o, OPD=257cm, FoV=1.91$mrad$, boxcar apod.
Normalized Intensity I
Wavenumber ν in cm^{-1}
1.20
1.15
1.10
1.05
1.00
0.95
0.90
0.85
2611.4
2611.8
2612.2
2612.6
2613.0
2613.4
H2O
CH4
N2O
solar-sim
Solar(A)
CO2(i3)
HDO
AllMol
Observed

σ=0.130%, 970315S3.90, φ=69.87^o, OPD=257cm, FoV=1.91$mrad$, Apod.=boxcar

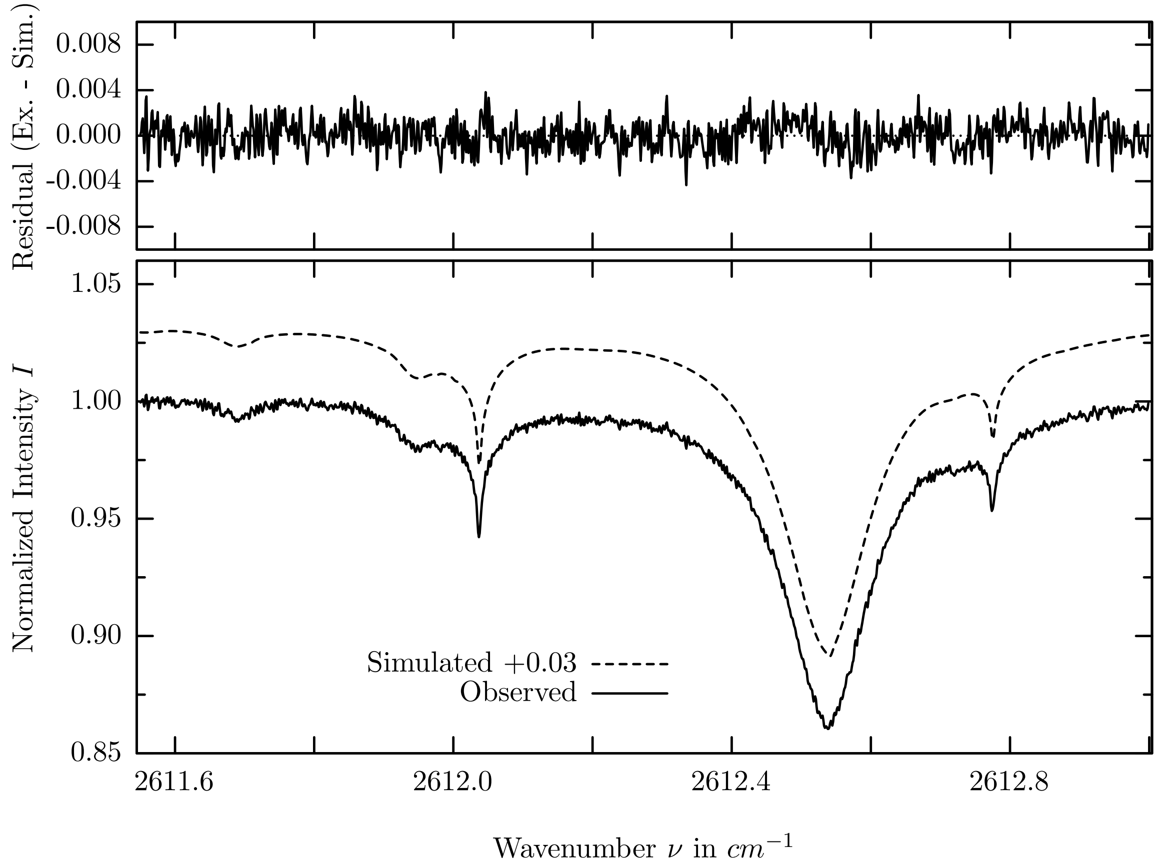

investigated species	:	HDO
line position(s) ν_0	:	2612.5400 cm^{-1}
lower state energy E''_{lst}	:	490.4 cm^{-1}
retrieved TCA, information content	:	4.18E+21 $molec/cm^2$, 106.6
temperature dependence of the TCA	:	-0.847%/K (trop), -0.023%/K (strat)
location, date, solar zenith angle	:	Kiruna, 15/Mar/97, 69.87^o
spectral interval fitted	:	2611.550 – 2612.999 cm^{-1}

Molecule	iCode	Absorption	Molecule	iCode	Absorption
HDO	491	17.700%	$SO2$	91	<0.001%
$CO2$	**23**	5.179%	$NH3$	111	<0.001%
Solar(A)	—	1.119%	OH	131	<0.001%
Solar-sim	—	1.104%	HCl	151	<0.001%
$N2O$	41	0.201%	HBr	161	<0.001%
$CH4$	61	0.186%	$N2$	411	<0.001%
$H2O$	11	0.065%	$H2S$	471	<0.001%
$O3$	31	<0.001%			

HDO, Kiruna, φ=69.87^o, OPD=257cm, FoV=1.91$mrad$, boxcar apod.

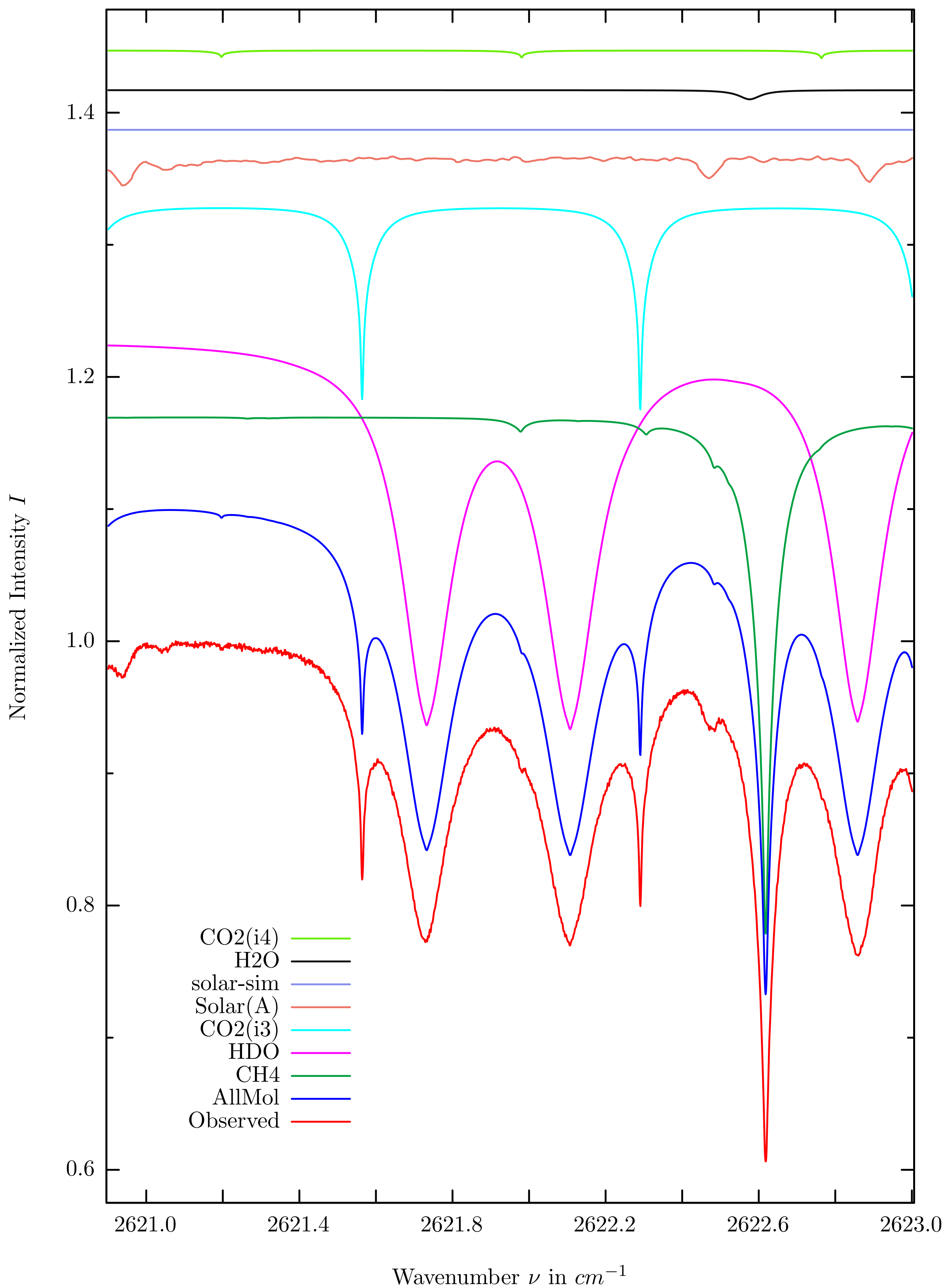

σ=0.140%, 970315S3.90, φ=69.87^o, OPD=257cm, FoV=1.91$mrad$, Apod.=boxcar

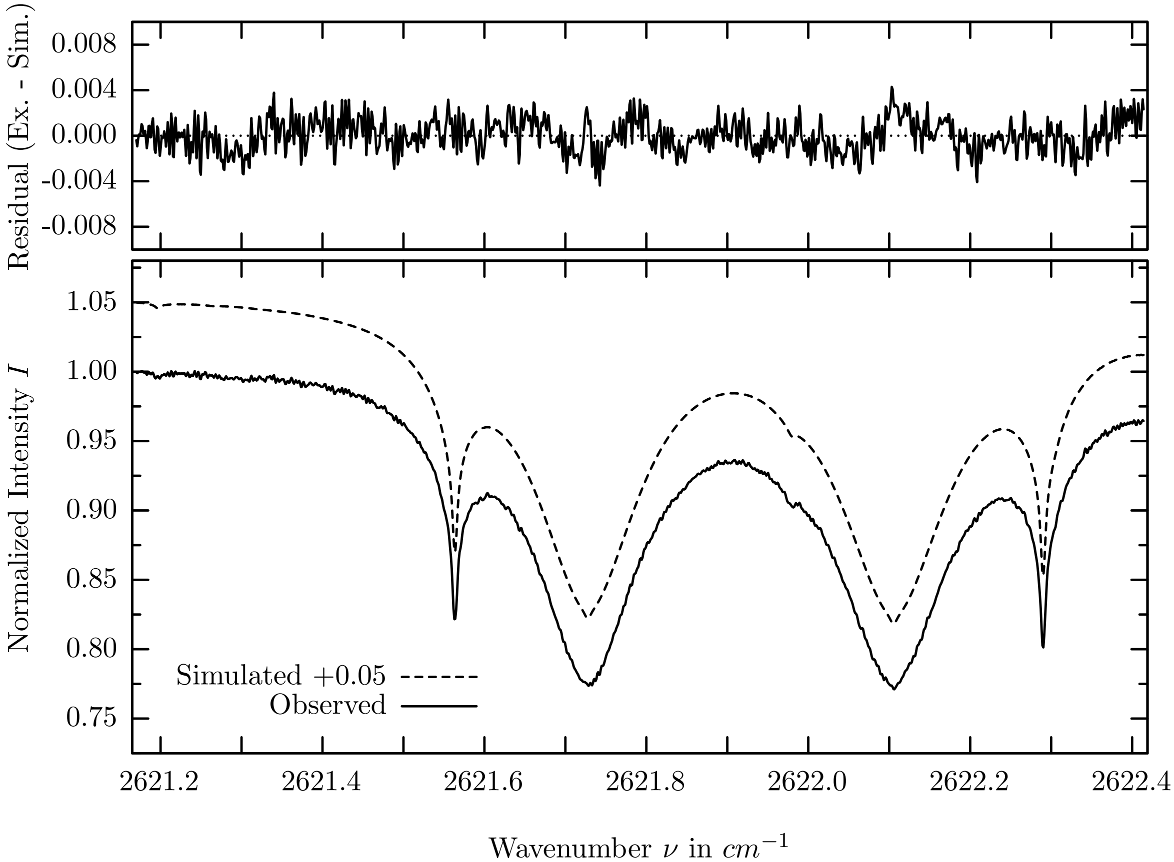

investigated species	:	HDO
line position(s) ν_0	:	2621.7310, 2622.1060 cm^{-1}
lower state energy E''_{lst}	:	403.1, 362.5 cm^{-1}
retrieved TCA, information content	:	4.13E+21 $molec/cm^2$, 162.4, 165.3
temperature dependence of the TCA	:	-0.476%/K (trop), -0.002%/K (strat)
location, date, solar zenith angle	:	Kiruna, 15/Mar/97, 69.87^o
spectral interval fitted	:	2621.170 – 2622.415 cm^{-1}

Molecule	iCode	Absorption	Molecule	iCode	Absorption
$CH4$	61	39.131%	$O3$	31	0.010%
HDO	491	29.663%	$N2O$	41	0.005%
$CO2$	2**3**	15.561%	$SO2$	91	<0.001%
Solar(A)	—	2.210%	$NH3$	111	<0.001%
Solar-sim	—	<0.001%	OH	131	<0.001%
$H2O$	11	0.692%	HCl	151	<0.001%
$CO2$	2**4**	0.572%	$N2$	411	<0.001%
HBr	161	0.013%	$H2S$	471	<0.001%

CO_2, Kiruna, φ=69.87^o, OPD=257cm, FoV=1.91$mrad$, boxcar apod.

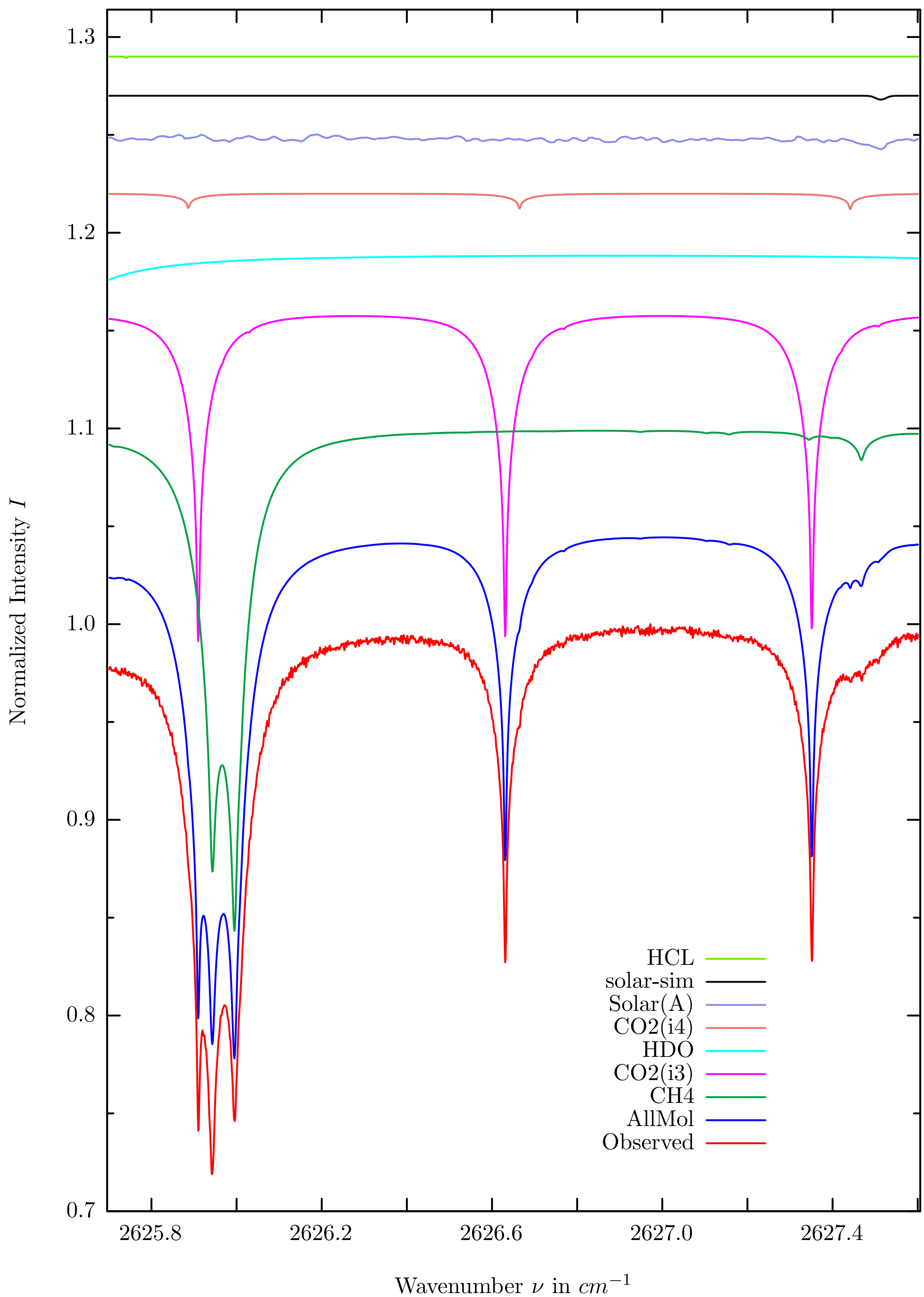

σ=0.110%, 970315S3.90, φ=69.87^o, OPD=257cm, FoV=1.91$mrad$, Apod.=boxcar

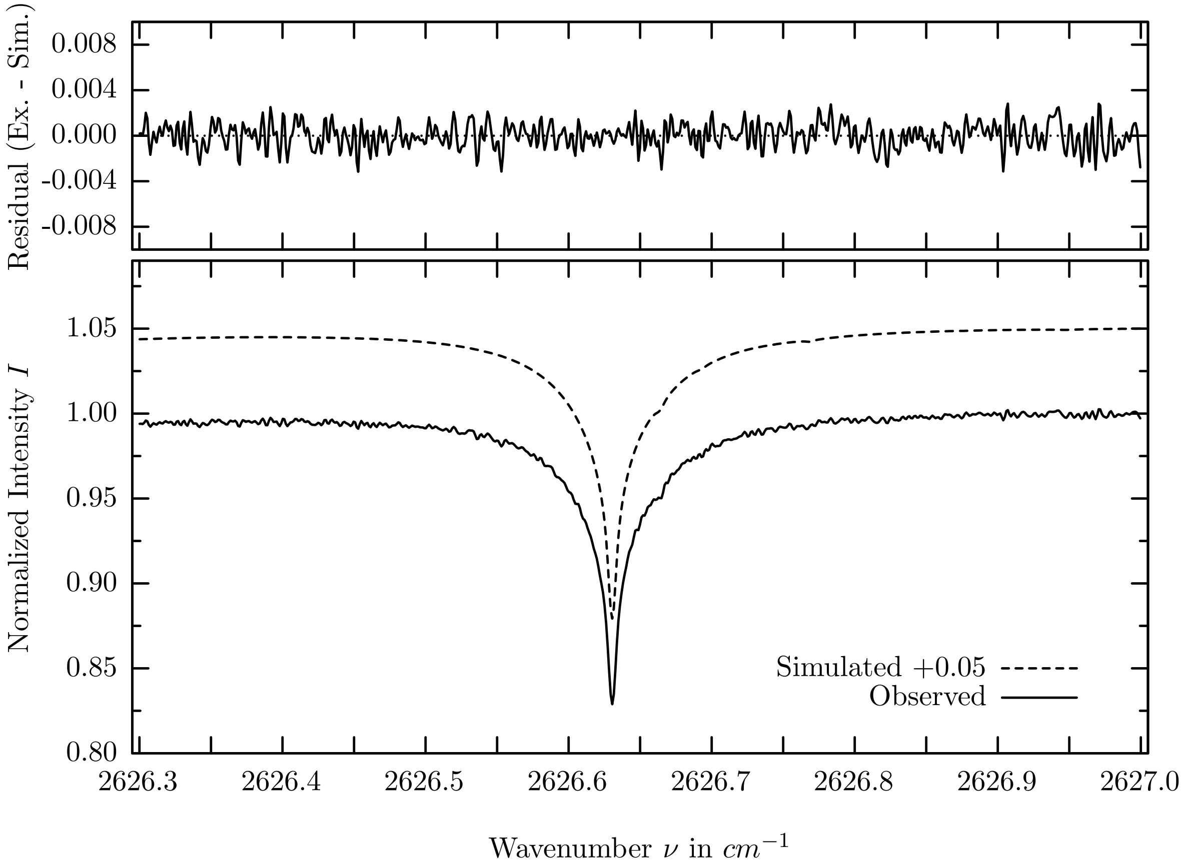

investigated species	:	$CO_2(i3)$
line position(s) ν_0	:	2626.6296 cm^{-1}
lower state energy E''_{lst}	:	100.1 cm^{-1}
retrieved TCA, information content	:	7.21E+21 $molec/cm^2$, 155.0
temperature dependence of the TCA	:	+0.098%/K (trop), +0.007%/K (strat)
location, date, solar zenith angle	:	Kiruna, 15/Mar/97, 69.87^o
spectral interval fitted	:	2626.300 – 2627.000 cm^{-1}

Molecule	iCode	Absorption	Molecule	iCode	Absorption
$CH4$	61	25.690%	$H2O$	11	0.003%
CO2	**23**	16.939%	$N2O$	41	0.001%
HDO	491	1.390%	$SO2$	91	<0.001%
$CO2$	**24**	0.800%	$NH3$	111	<0.001%
Solar(A)	—	0.730%	OH	131	<0.001%
Solar-sim	—	0.196%	HBr	161	<0.001%
HCl	151	0.066%	$N2$	411	<0.001%
$O3$	31	0.010%	$H2S$	471	<0.001%

CH_4, Kiruna, φ=69.87^o, OPD=257cm, FoV=1.91$mrad$, boxcar apod.

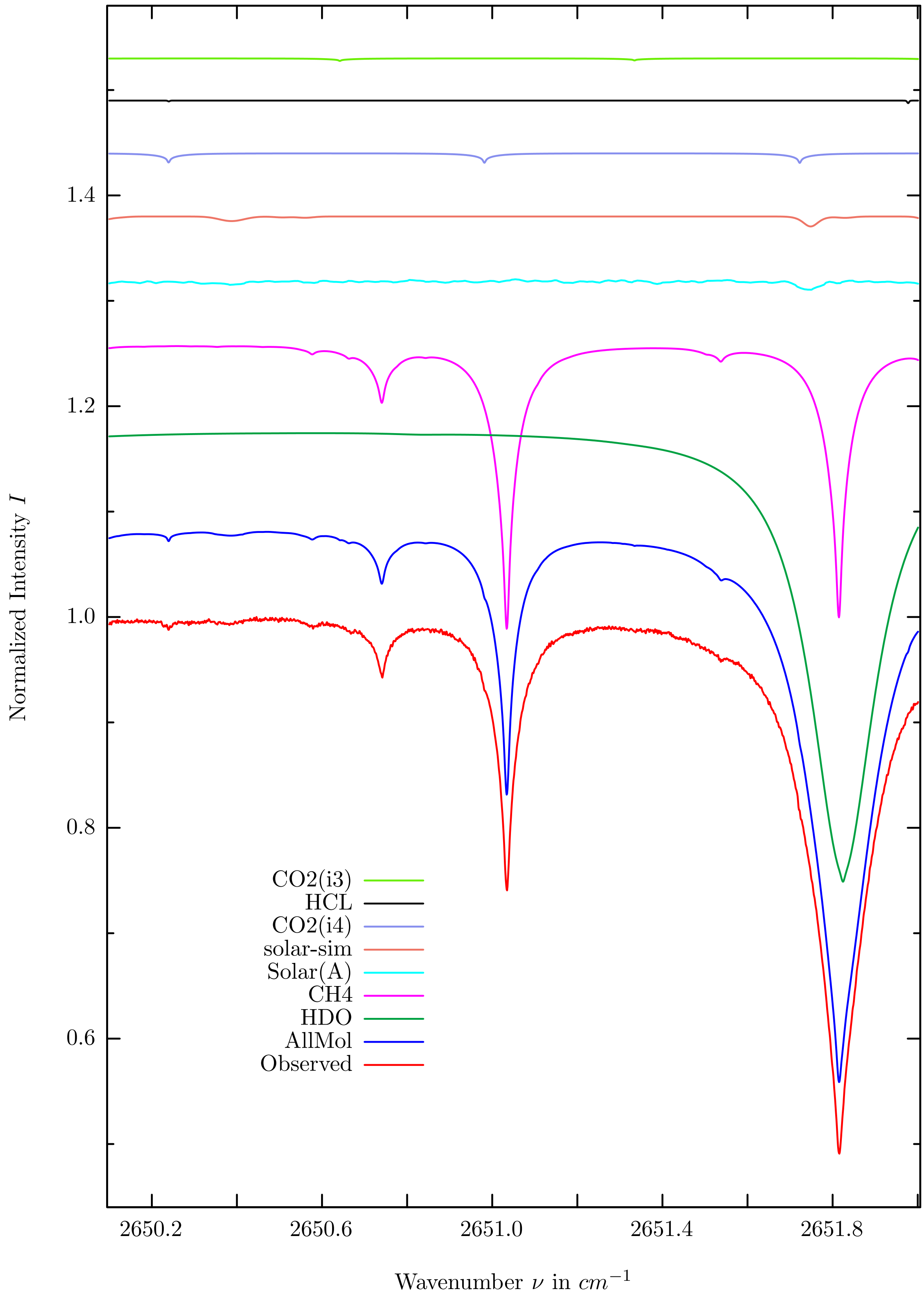

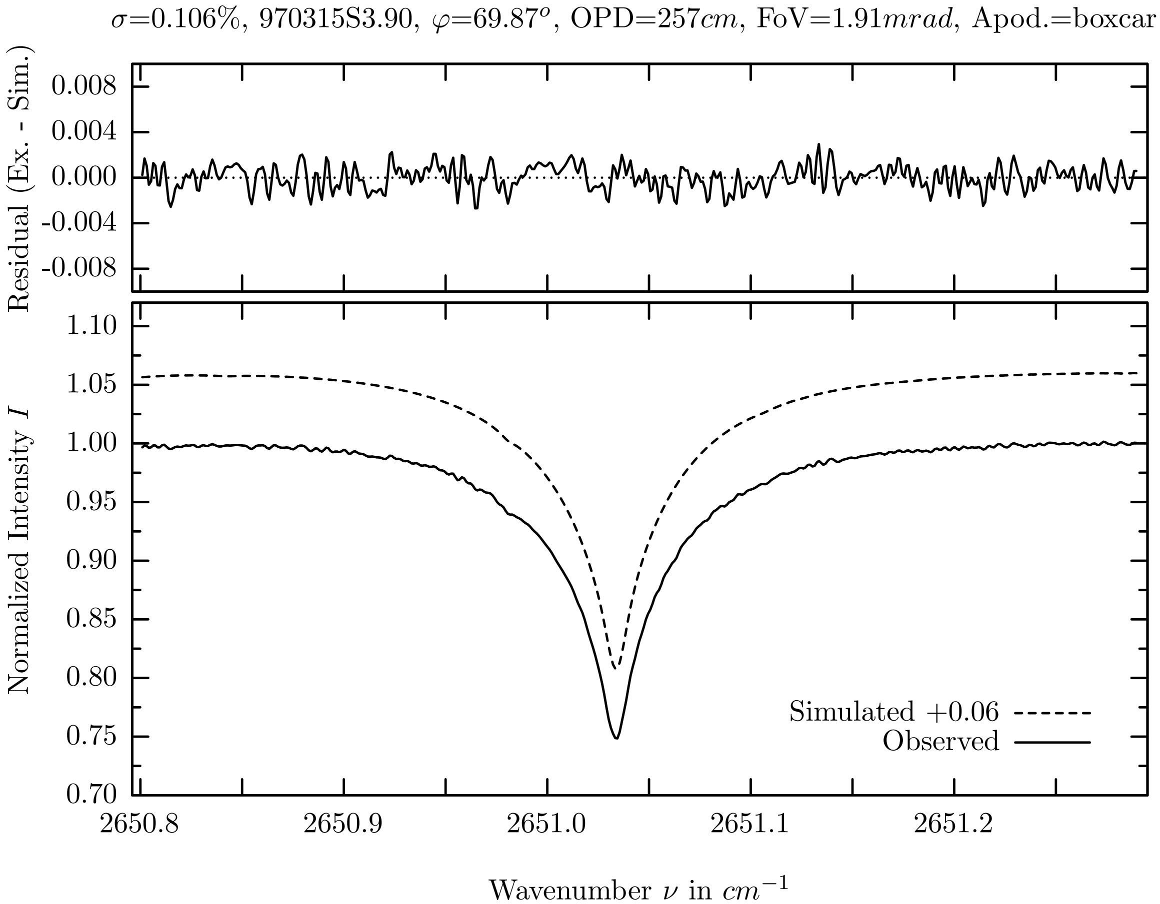

investigated species	:	CH_4
line position(s) ν_0	:	2651.0331 cm^{-1}
lower state energy E''_{lst}	:	31.4 cm^{-1}
retrieved TCA, information content	:	3.42E+19 $molec/cm^2$, 237.2
temperature dependence of the TCA	:	+0.405%/K (trop), +0.035%/K (strat)
location, date, solar zenith angle	:	Kiruna, 15/Mar/97, 69.87^o
spectral interval fitted	:	2650.800 – 2651.290 cm^{-1}

Molecule	iCode	Absorption	Molecule	iCode	Absorption
HDO	491	43.121%	*O*3	31	0.049%
CH4	61	27.146%	*H*2*O*	11	<0.001%
Solar(A)	—	0.947%	*SO*2	91	<0.001%
Solar-sim	—	0.942%	*NH*3	111	<0.001%
*CO*2	**24**	0.920%	*OH*	131	<0.001%
HCl	151	0.249%	*HBr*	161	<0.001%
*CO*2	2**3**	0.240%	*H*2*S*	471	<0.001%

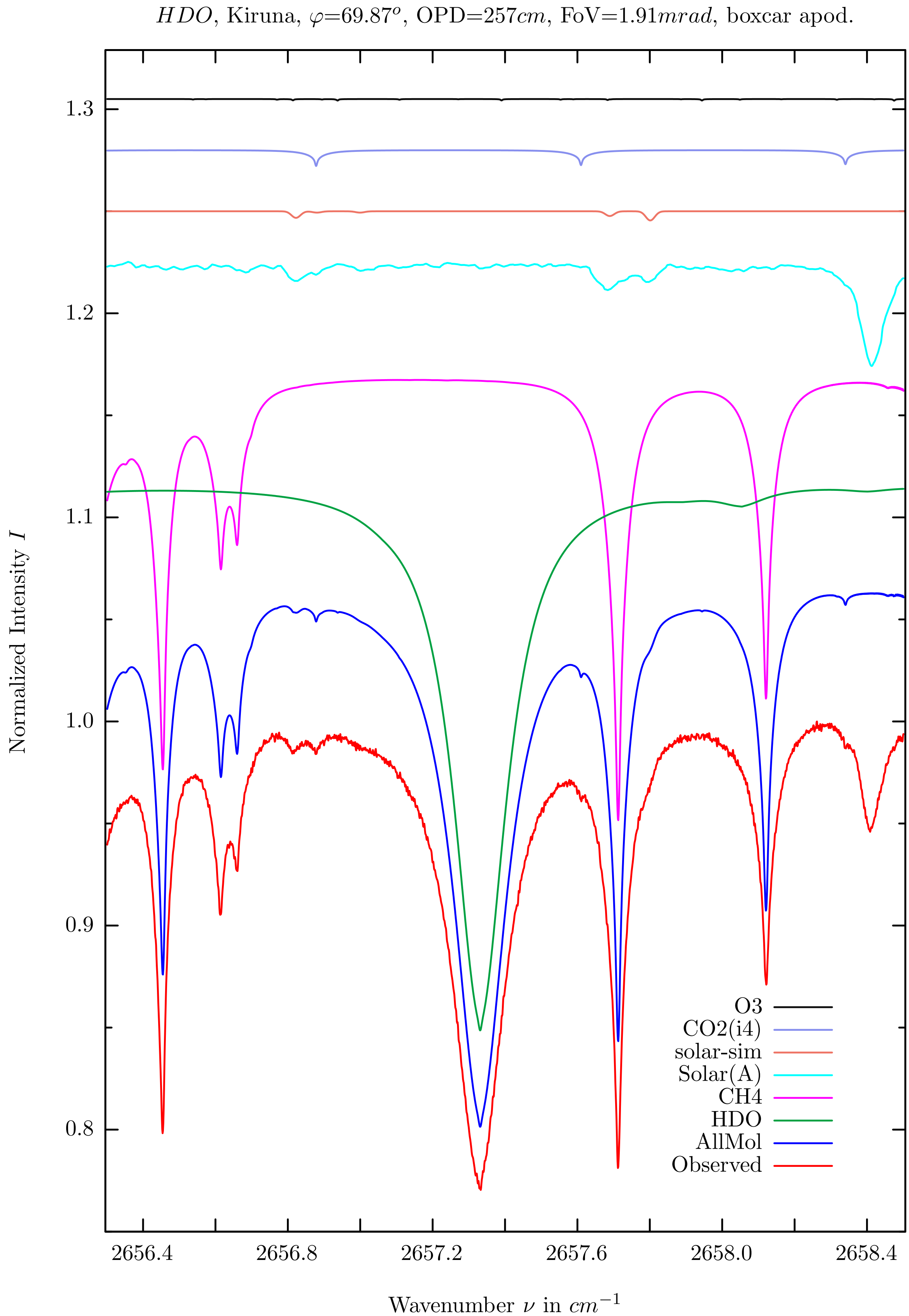

HDO, Kiruna, φ=69.87^o, OPD=257cm, FoV=1.91$mrad$, boxcar apod.
Normalized Intensity I
1.3
1.2
1.1
1.0
0.9
0.8
2656.4
2656.8
2657.2
2657.6
2658.0
2658.4
Wavenumber ν in cm^{-1}
O3
CO2(i4)
solar-sim
Solar(A)
CH4
HDO
AllMol
Observed

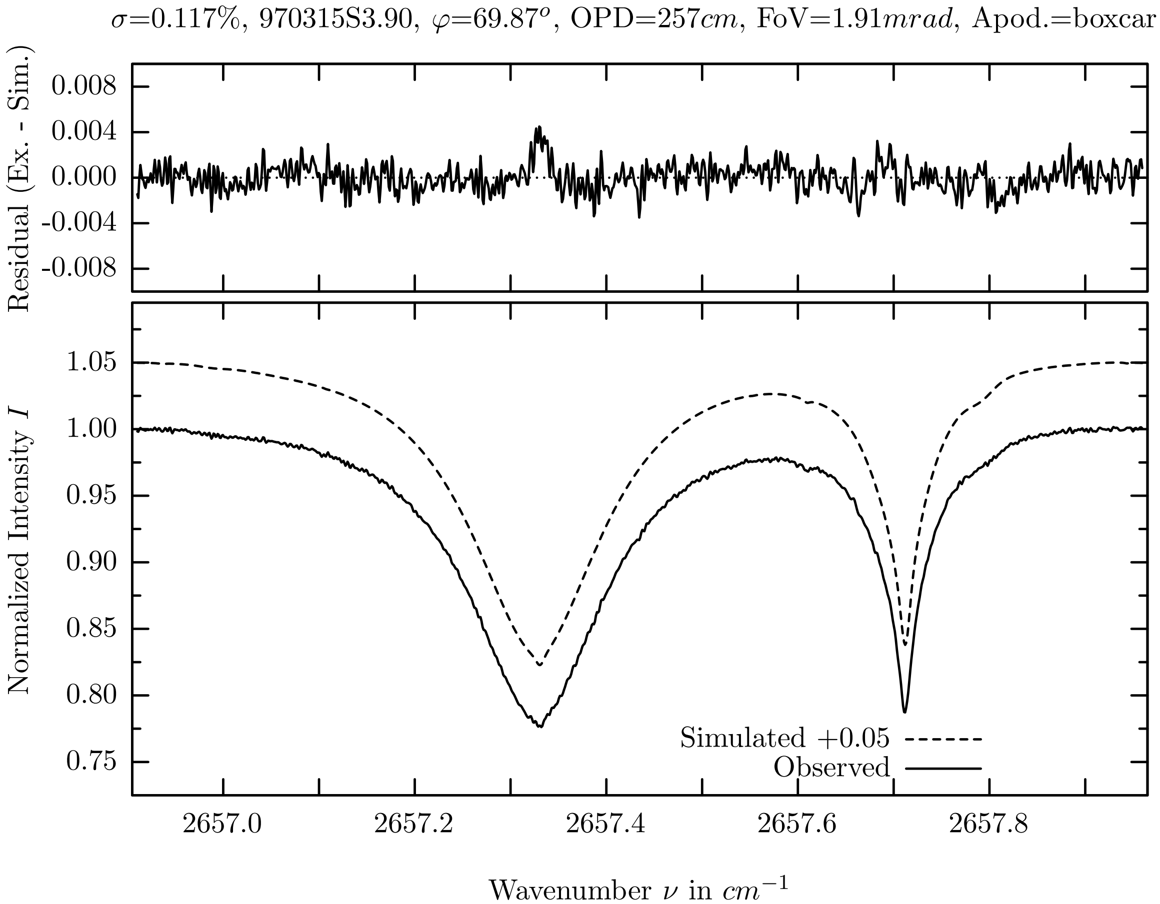

investigated species	:	$HDO, (CH_4)$
line position(s) ν_0	:	2657.3300, (2657.7116) cm^{-1}
lower state energy E''_{lst}	:	221.8, (104.8) cm^{-1}
retrieved TCA, information content	:	4.07E+21, (3.64E+19) $molec/cm^2$, 194.8, (176.9)
temperature dependence of the TCA	:	-.111, (+.144)%/K (trop), +.017, (+.029)%/K (strat)
location, date, solar zenith angle	:	Kiruna, 15/Mar/97, 69.87^o
spectral interval fitted	:	2656.910 – 2657.960 cm^{-1}

Molecule	iCode	Absorption	Molecule	iCode	Absorption
HDO	491	30.160%	$H2O$	11	0.001%
$CH4$	61	21.862%	$SO2$	91	<0.001%
Solar(A)	—	5.082%	$NH3$	111	<0.001%
Solar-sim	—	0.448%	OH	131	<0.001%
$CO2$	**24**	0.784%	HCl	151	<0.001%
$O3$	31	0.077%	HBr	161	<0.001%
$CO2$	**23**	0.028%	$H2S$	471	<0.001%

HDO, Kiruna, φ=69.87^o, OPD=257cm, FoV=1.91$mrad$, boxcar apod.

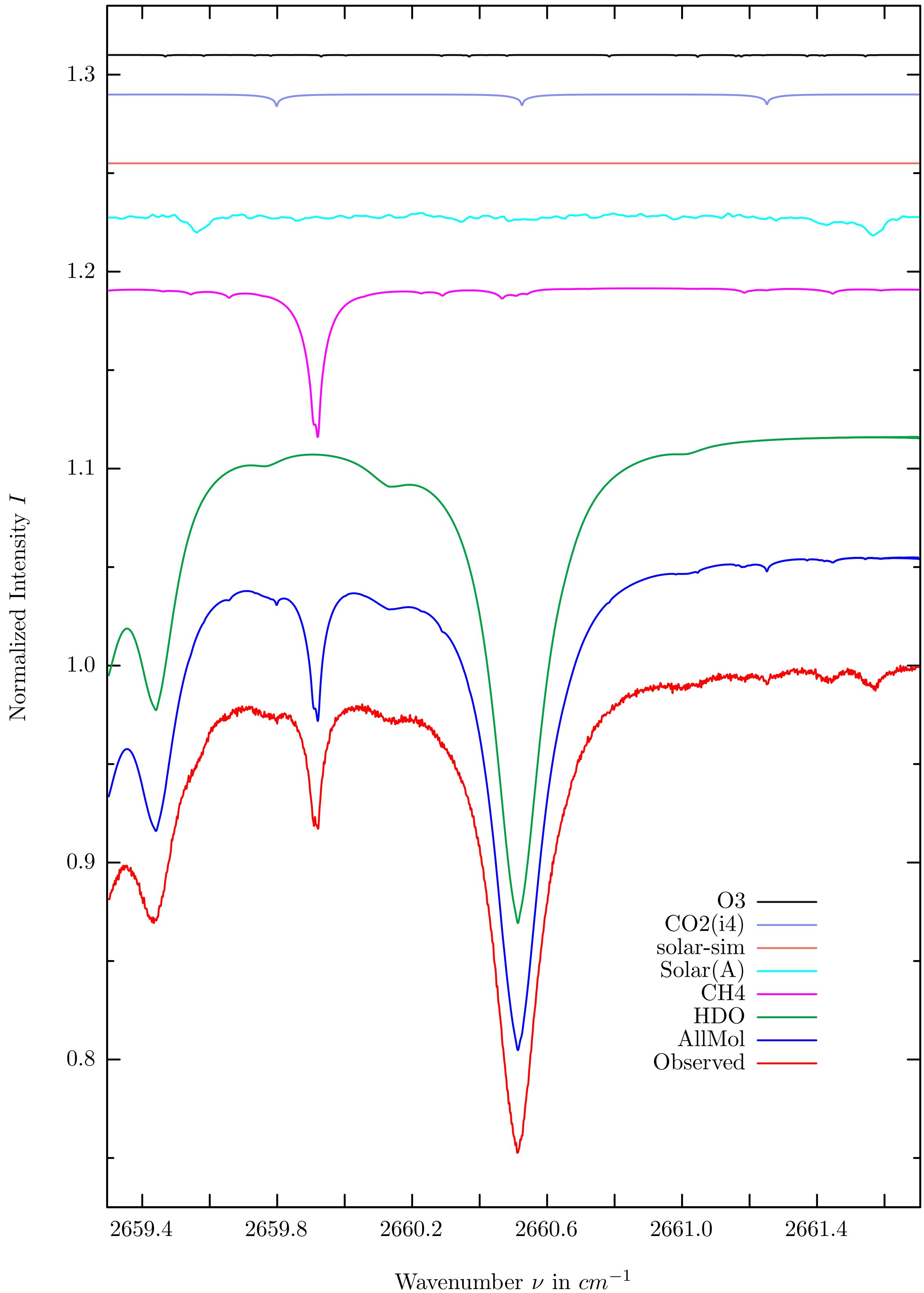

σ=0.111%, 970315S3.90, φ=69.87^o, OPD=257cm, FoV=1.91$mrad$, Apod.=boxcar

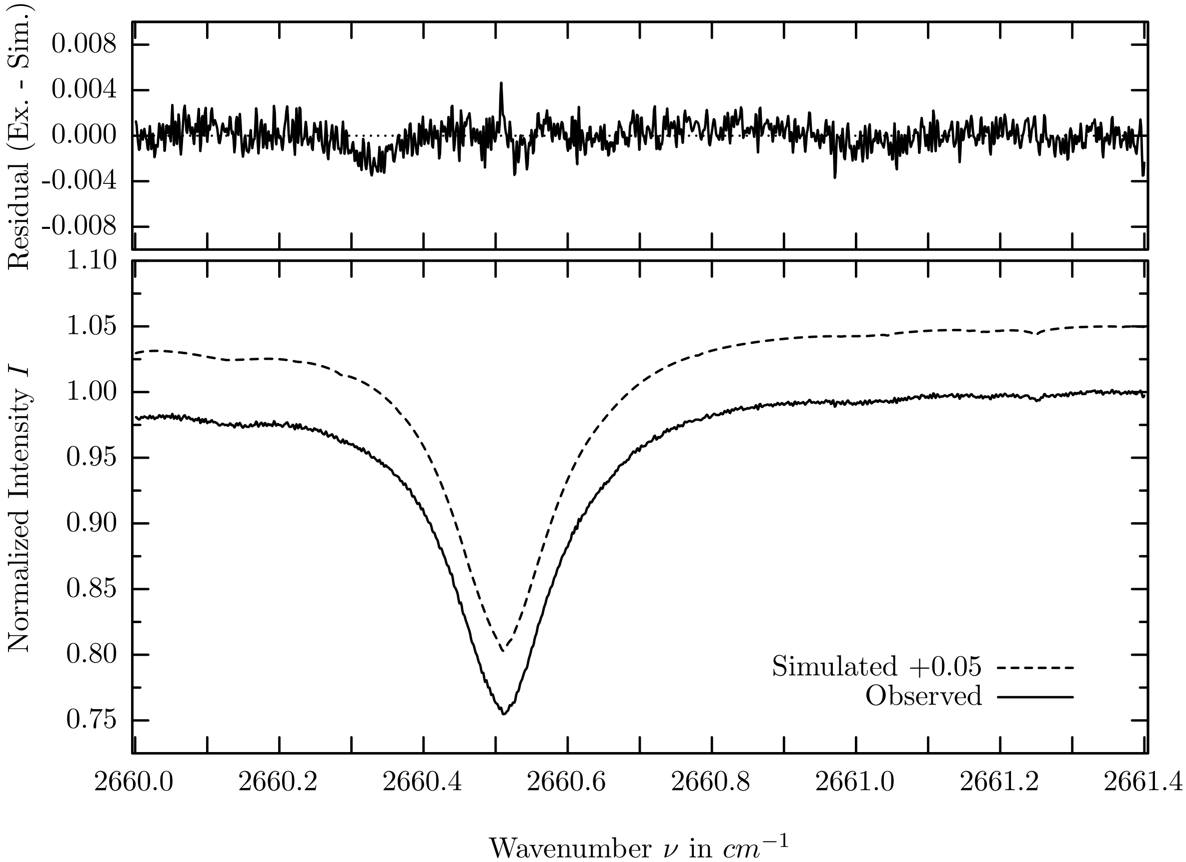

investigated species	:	HDO
line position(s) ν_0	:	2660.5120 cm^{-1}
lower state energy E''_{lst}	:	217.0 cm^{-1}
retrieved TCA, information content	:	4.17E+21 $molec/cm^2$, 222.1
temperature dependence of the TCA	:	+0.066%/K (trop), -0.005%/K (strat)
location, date, solar zenith angle	:	Kiruna, 15/Mar/97, 69.87^o
spectral interval fitted	:	2660.000 – 2661.400 cm^{-1}

Molecule	iCode	Absorption	Molecule	iCode	Absorption
HDO	491	31.354%	$CO2$	**23**	<0.001%
$CH4$	61	7.593%	$SO2$	91	<0.001%
Solar(A)	—	1.169%	$NH3$	111	<0.001%
Solar-sim	—	<0.001%	OH	131	<0.001%
$CO2$	**24**	0.605%	HCl	151	<0.001%
$O3$	31	0.102%	HBr	161	<0.001%
$H2O$	11	0.040%	$H2S$	471	<0.001%

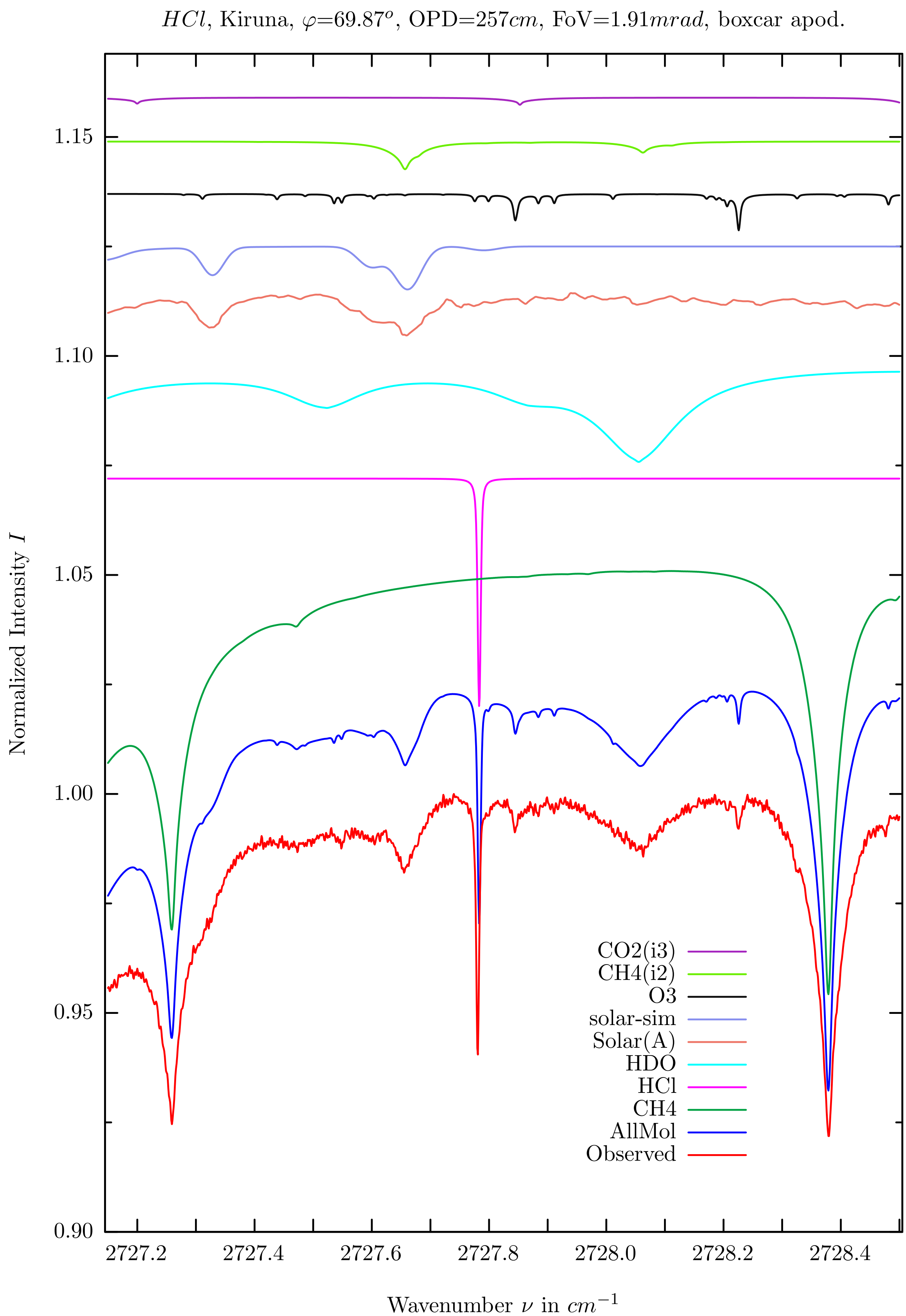
HCl, Kiruna, φ=69.87^o, OPD=257cm, FoV=1.91$mrad$, boxcar apod.
Normalized Intensity I
Wavenumber ν in cm^{-1}
1.15
1.10
1.05
1.00
0.95
0.90
2727.2
2727.4
2727.6
2727.8
2728.0
2728.2
2728.4
CO2(i3)
CH4(i2)
O3
solar-sim
Solar(A)
HDO
HCl
CH4
AllMol
Observed

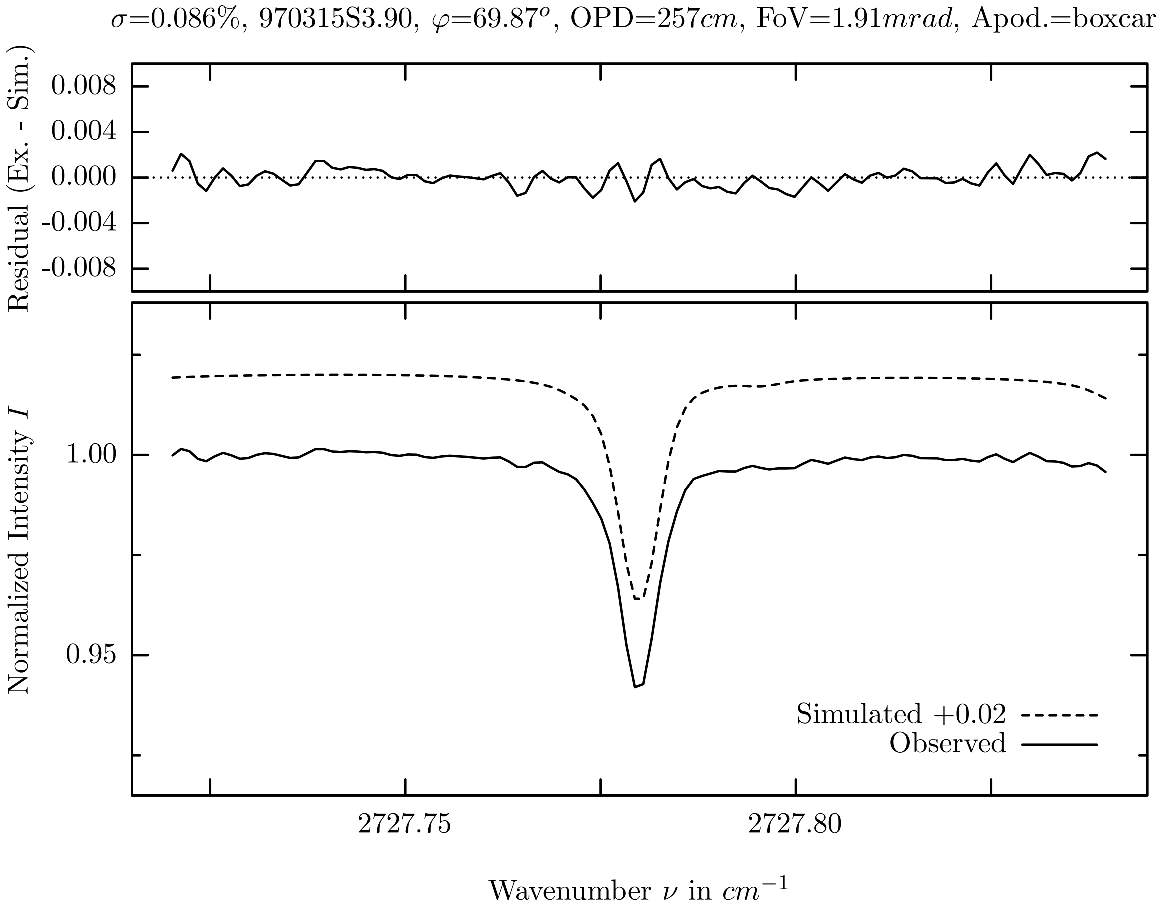

investigated species	:	HCl
line position(s) ν_0	:	2727.7819 cm^{-1}
lower state energy E''_{lst}	:	583.0 cm^{-1}
retrieved TCA, information content	:	3.25E+15 $molec/cm^2$, 65.0
temperature dependence of the TCA	:	-0.052%/K (trop), -1.221%/K (strat)
location, date, solar zenith angle	:	Kiruna, 15/Mar/97, 69.87^o
spectral interval fitted	:	2727.720 – 2727.840 cm^{-1}

Molecule	iCode	Absorption	Molecule	iCode	Absorption
$CH4$	61	10.284%	$H2O$	11	0.009%
HCl	151	5.252%	OCS	191	0.003%
HDO	491	2.419%	$N2O$	41	<0.001%
Solar(A)	—	1.031%	$SO2$	91	<0.001%
Solar-sim	—	0.981%	$NO2$	101	<0.001%
$O3$	31	0.838%	$NH3$	111	<0.001%
$CH4$	6**2**	0.637%	OH	131	<0.001%
$CO2$	2**3**	0.166%	HBr	161	<0.001%
$H2CO$	201	0.021%	$H2S$	471	<0.001%

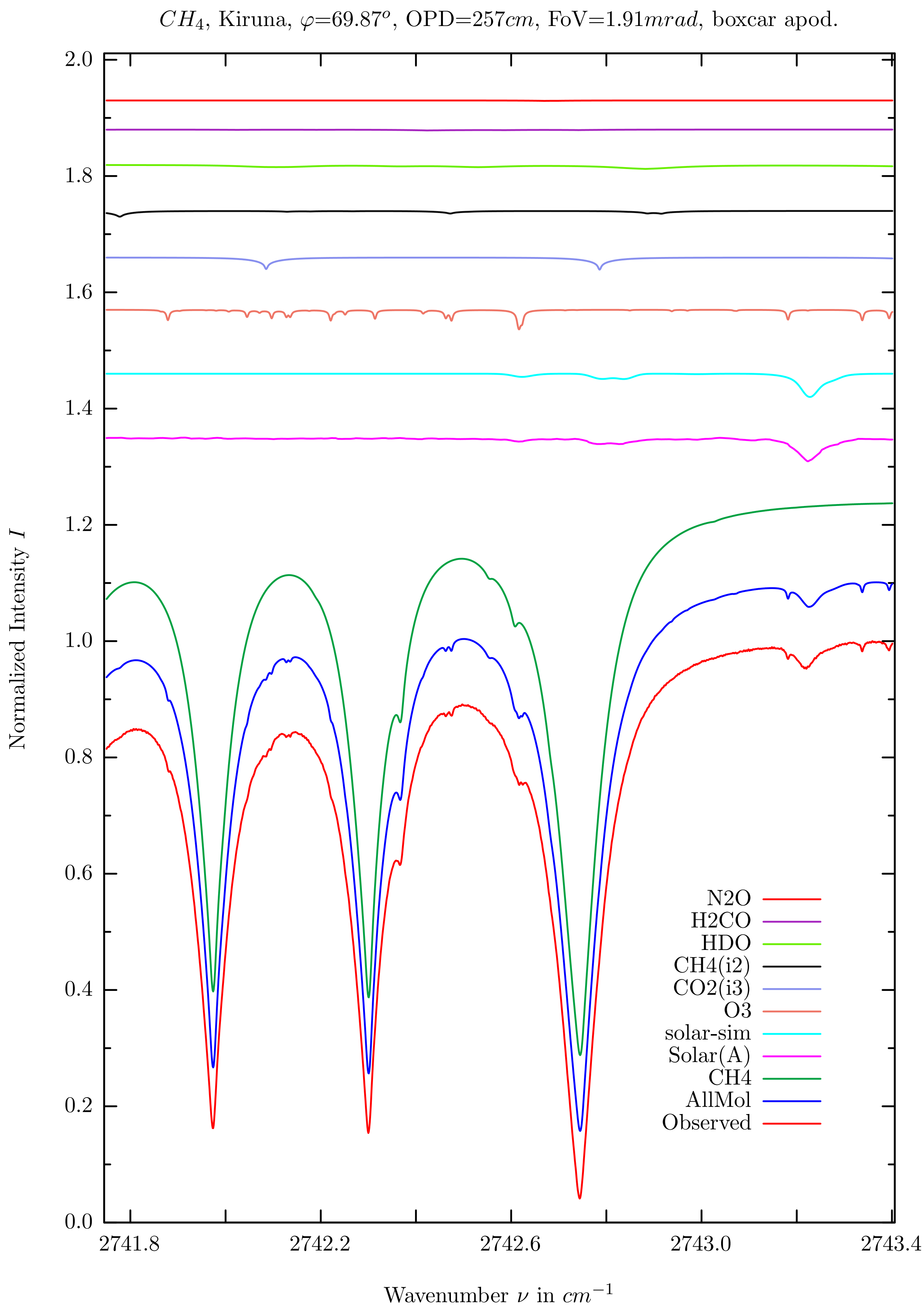

CH_4, Kiruna, φ=69.87^o, OPD=257cm, FoV=1.91$mrad$, boxcar apod.
Normalized Intensity I
Wavenumber ν in cm^{-1}
0.0
0.2
0.4
0.6
0.8
1.0
1.2
1.4
1.6
1.8
2.0
2741.8
2742.2
2742.6
2743.0
2743.4
N2O
H2CO
HDO
CH4(i2)
CO2(i3)
O3
solar-sim
Solar(A)
CH4
AllMol
Observed

σ=0.157%, 970315S3.90, φ=69.87^o, OPD=257cm, FoV=1.91$mrad$, Apod.=boxcar

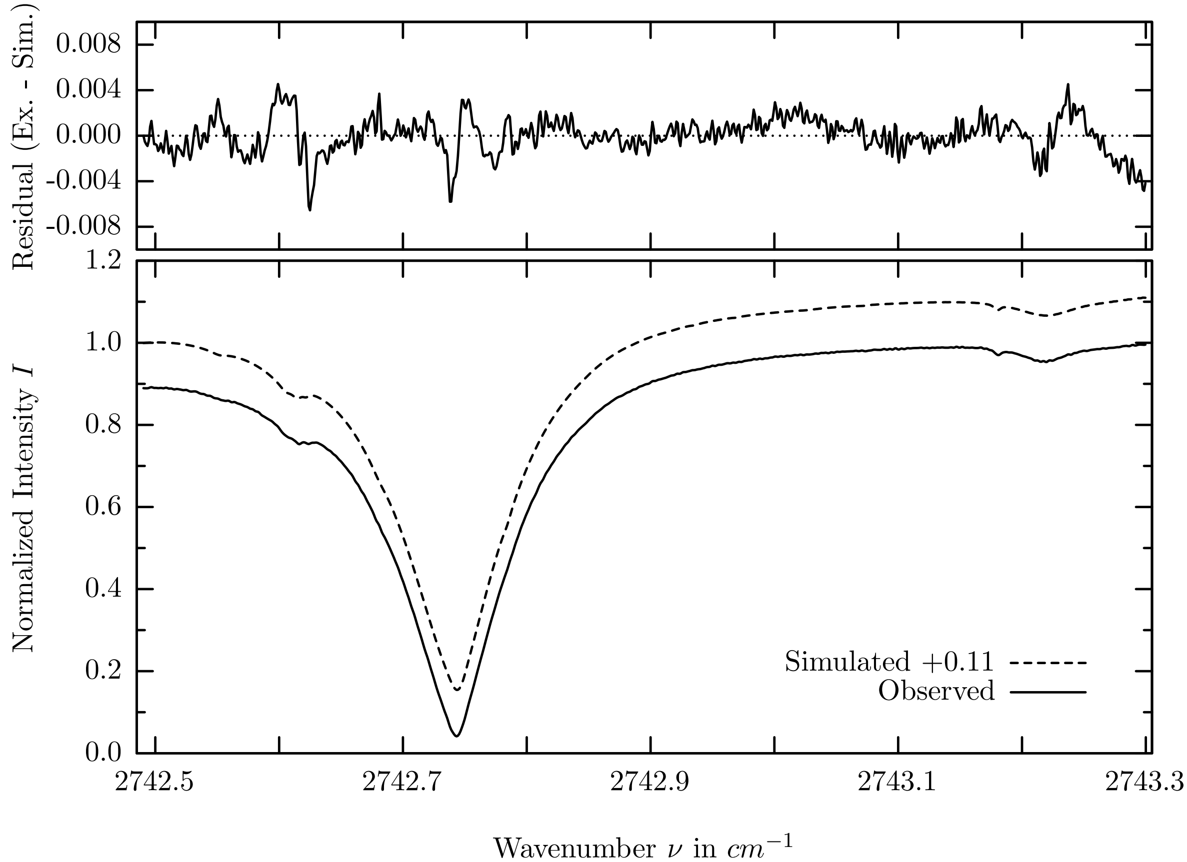

investigated species	:	CH_4
line position(s) ν_0	:	2742.7428 cm^{-1}
lower state energy E''_{lst}	:	219.9 cm^{-1}
retrieved TCA, information content	:	3.33E+19 $molec/cm^2$, 607.2
temperature dependence of the TCA	:	-0.029%/K (trop), -0.020%/K (strat)
location, date, solar zenith angle	:	Kiruna, 15/Mar/97, 69.87^o
spectral interval fitted	:	2742.490 – 2743.300 cm^{-1}

Molecule	iCode	Absorption	Molecule	iCode	Absorption
CH4	61	96.226%	$H2O$	11	0.021%
Solar(A)	—	4.056%	OCS	191	0.004%
Solar-sim	—	4.001%	$SO2$	91	<0.001%
$O3$	31	3.398%	$NO2$	101	<0.001%
$CO2$	2**3**	2.110%	$NH3$	111	<0.001%
$CH4$	6**2**	0.991%	OH	131	<0.001%
HDO	491	0.770%	HCl	151	<0.001%
$H2CO$	201	0.158%	HBr	161	<0.001%
$N2O$	41	0.074%	$H2S$	471	<0.001%

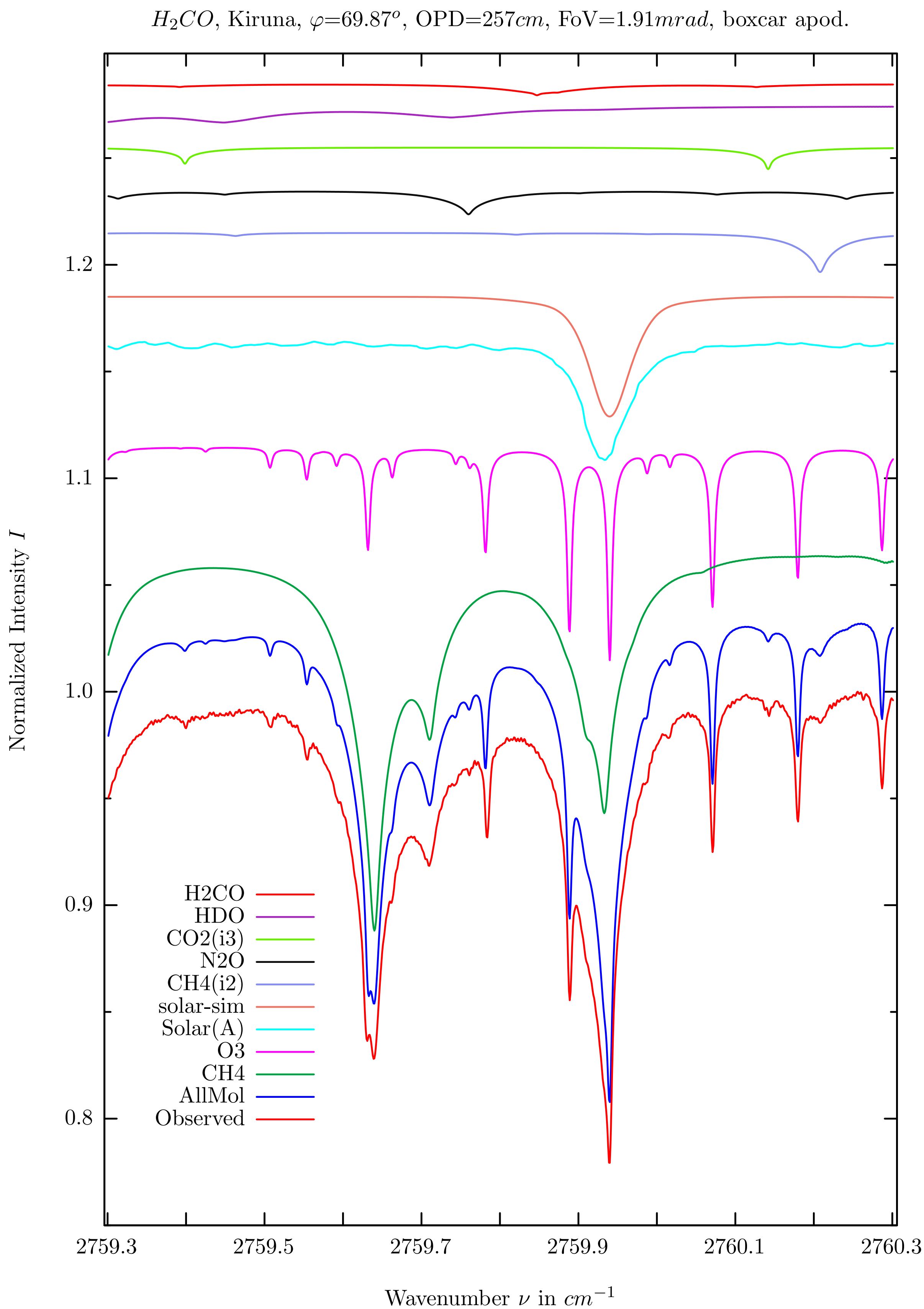
H_2CO, Kiruna, φ=69.87^o, OPD=257cm, FoV=1.91$mrad$, boxcar apod.
Normalized Intensity I
1.2
1.1
1.0
0.9
0.8
H2CO
HDO
CO2(i3)
N2O
CH4(i2)
solar-sim
Solar(A)
O3
CH4
AllMol
Observed
2759.3
2759.5
2759.7
2759.9
2760.1
2760.3
Wavenumber ν in cm^{-1}

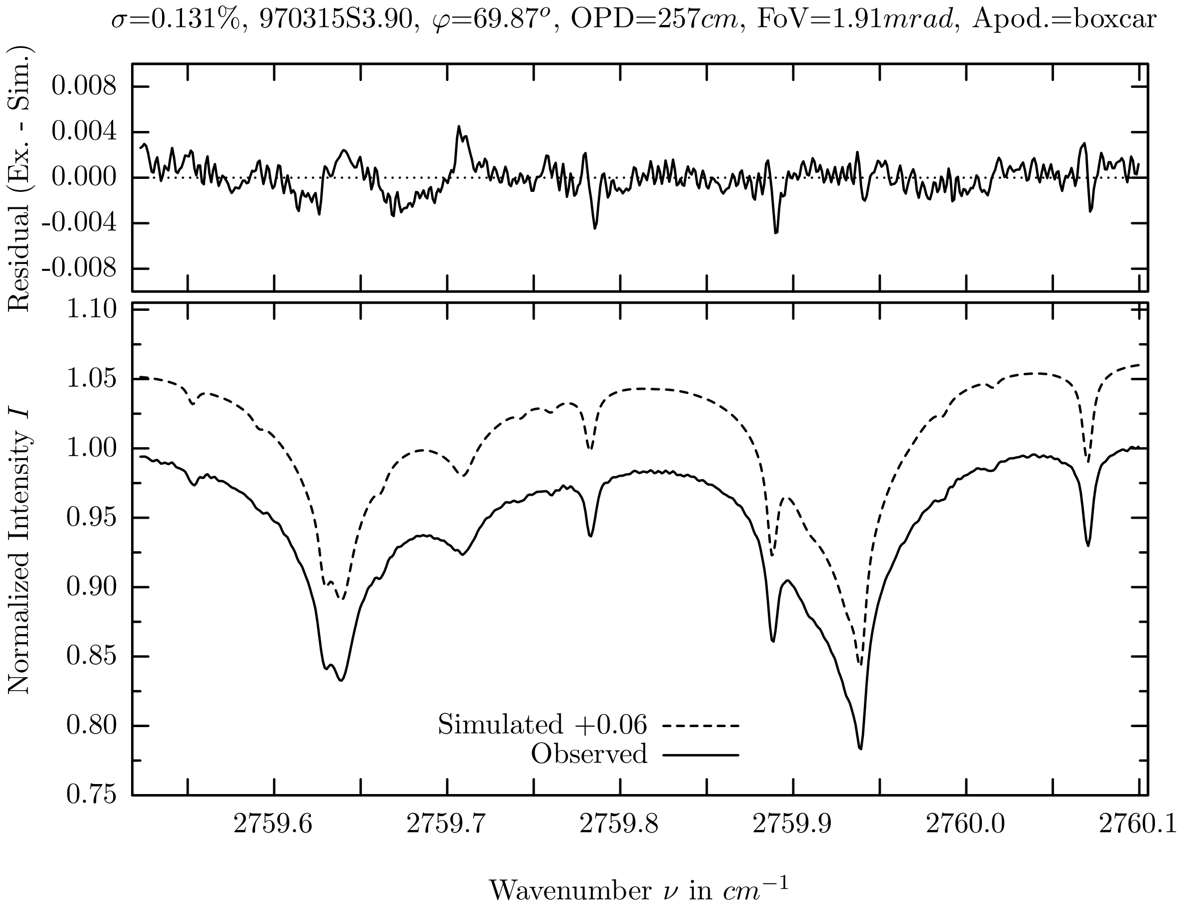

investigated species	:	$H_2CO, (O_3)$
line position(s) ν_0	:	2759.8456*), (2759.7801) cm^{-1}
lower state energy E''_{lst}	:	120.9, (269.2) cm^{-1}
retrieved TCA, information content	:	1.43E+15, (9.53E+18) $molec/cm^2$, 4.1, (33.7)
temperature dependence of the TCA	:	-.758, (-.182)%/K (trop), +.423, (-.219)%/K (strat)
location, date, solar zenith angle	:	Kiruna, 15/Mar/97, 69.87^o
spectral interval fitted	:	2759.522 – 2760.100 cm^{-1}

Molecule	iCode	Absorption	Molecule	iCode	Absorption
$CH4$	61	18.209%	$H2O$	11	0.025%
$O3$	31	10.110%	$SO2$	91	<0.001%
Solar(A)	—	5.644%	$NO2$	101	<0.001%
Solar-sim	—	5.608%	$NH3$	111	<0.001%
$CH4$	6**2**	1.843%	OH	131	<0.001%
$N2O$	41	1.125%	HCl	151	<0.001%
$CO2$	2**3**	1.022%	HBr	161	<0.001%
HDO	491	0.836%	OCS	191	<0.001%
H2CO	201	0.557%	$H2S$	471	<0.001%

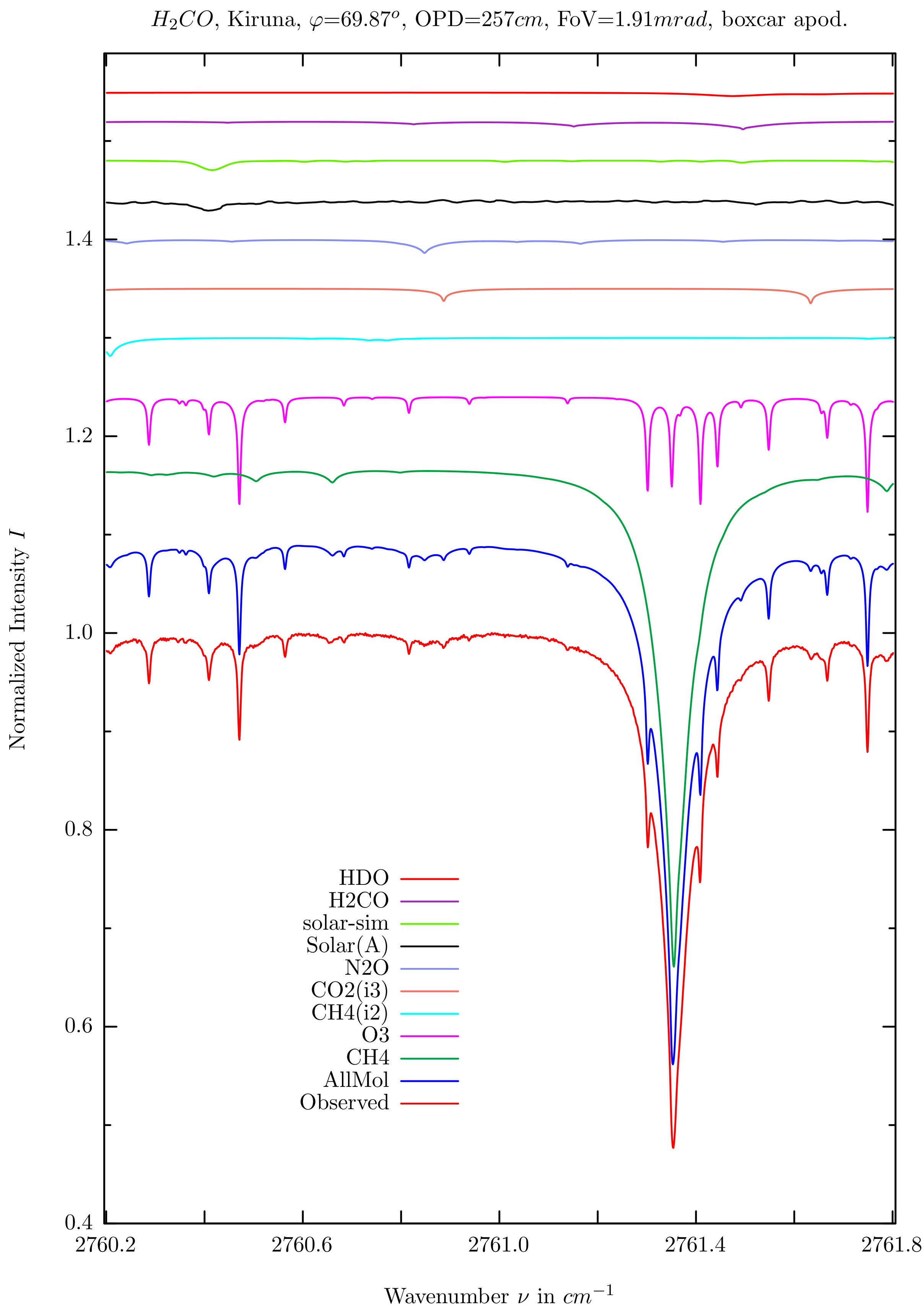

H_2CO, Kiruna, φ=69.87^o, OPD=257cm, FoV=1.91$mrad$, boxcar apod.
Normalized Intensity I
1.4
1.2
1.0
0.8
0.6
0.4
2760.2
2760.6
2761.0
2761.4
2761.8
Wavenumber ν in cm^{-1}
HDO
H2CO
solar-sim
Solar(A)
N2O
CO2(i3)
CH4(i2)
O3
CH4
AllMol
Observed

σ=0.139%, 970315S3.90, φ=69.87^o, OPD=257cm, FoV=1.91$mrad$, Apod.=boxcar

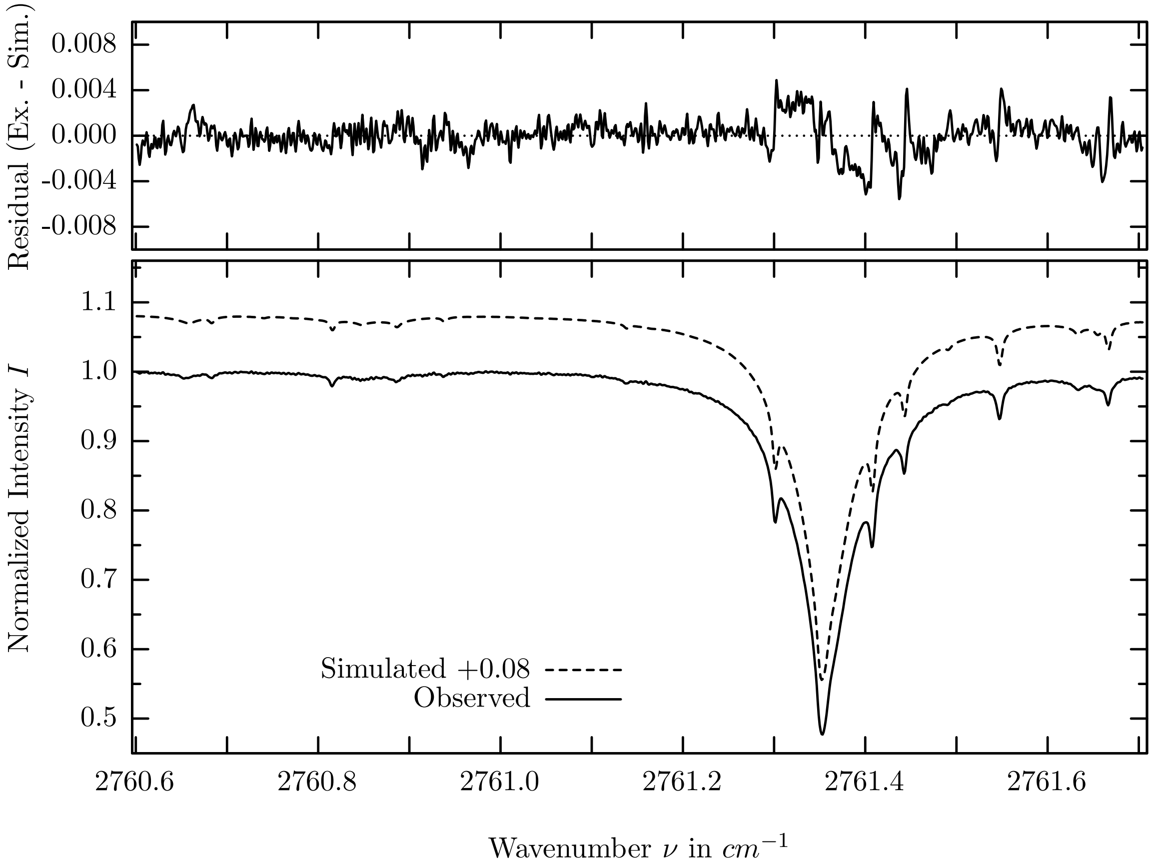

investigated species	:	$H_2CO, (CH_4)$
line position(s) ν_0	:	2761.1500*), 2761.4941*), (2761.3523) cm^{-1}
lower state energy E''_{lst}	:	113.7, 161.2, (689.9) cm^{-1}
retrieved TCA, information content	:	9.21e14, (3.33e19) $molec/cm^2$, 4.9, 10.2, (377.0)
temperature dependence of the TCA	:	-.770, (-.057)%/K (trop), +4.10, (-.006)%/K (strat)
location, date, solar zenith angle	:	Kiruna, 15/Mar/97, 69.87^o
spectral interval fitted	:	2760.600 – 2761.705 cm^{-1}

Molecule	iCode	Absorption	Molecule	iCode	Absorption
$CH4$	61	50.942%	$H2O$	11	0.025%
$O3$	31	11.785%	$SO2$	91	<0.001%
$CH4$	6**2**	1.843%	$NO2$	101	<0.001%
$CO2$	2**3**	1.506%	$NH3$	111	<0.001%
$N2O$	41	1.368%	OH	131	<0.001%
Solar(A)	—	1.080%	HCl	151	<0.001%
Solar-sim	—	0.957%	HBr	161	<0.001%
H2CO	201	0.815%	OCS	191	<0.001%
HDO	491	0.434%	$H2S$	471	<0.001%

H_2CO, Kiruna, φ=69.87^o, OPD=257cm, FoV=1.91$mrad$, boxcar apod.

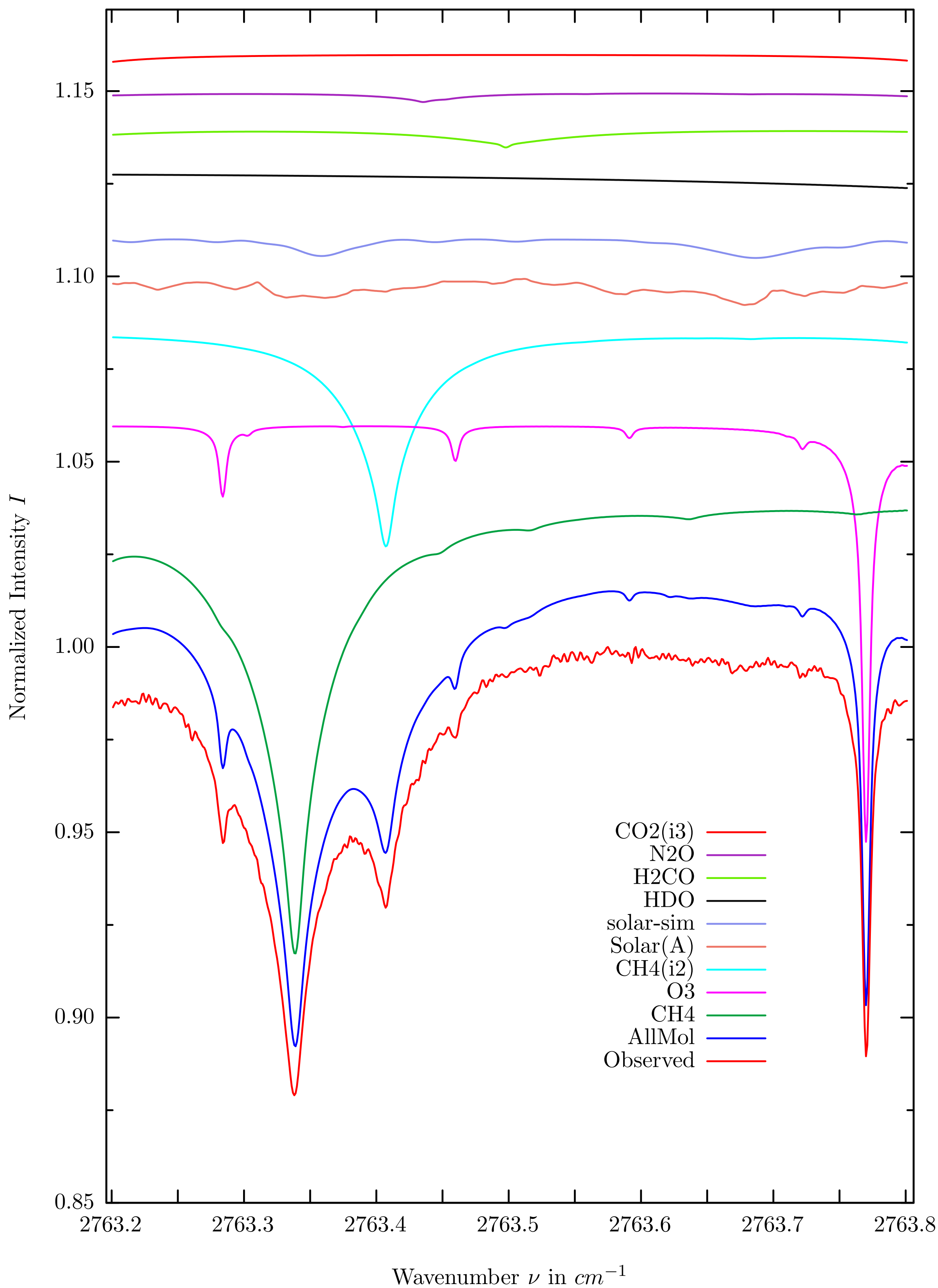

σ=0.092%, 970315S3.90, φ=69.87^o, OPD=257cm, FoV=1.91$mrad$, Apod.=boxcar

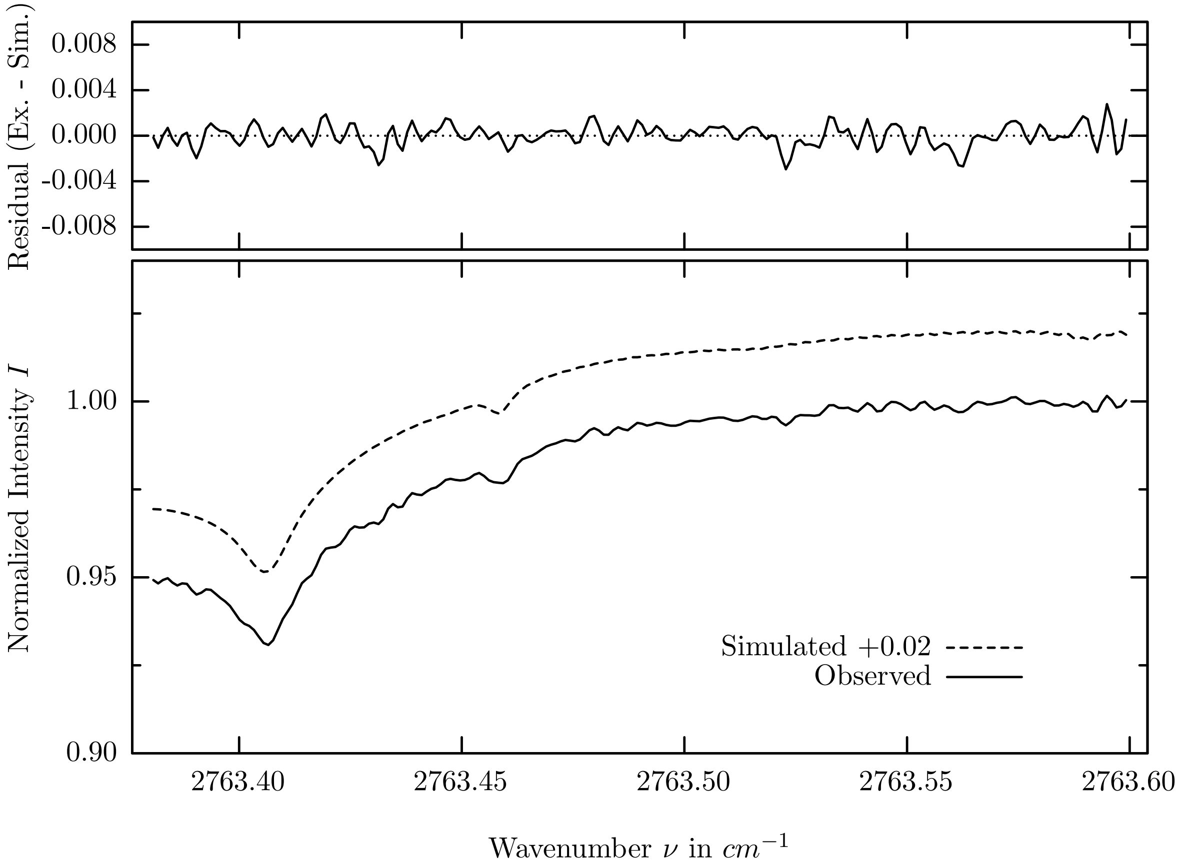

investigated species	:	H_2CO
line position(s) ν_0	:	2763.4963$^{*)}$ cm^{-1}
lower state energy E''_{lst}	:	92.6 cm^{-1}
retrieved TCA, information content	:	1.09E+15 $molec/cm^2$, 3.7
temperature dependence of the TCA	:	-0.028%/K (trop), -0.289%/K (strat)
location, date, solar zenith angle	:	Kiruna, 15/Mar/97, 69.87^o
spectral interval fitted	:	2763.380 – 2763.600 cm^{-1}

Molecule	iCode	Absorption	Molecule	iCode	Absorption
$CH4$	61	12.293%	$H2O$	11	0.001%
$O3$	31	11.358%	$SO2$	91	<0.001%
$CH4$	6**2**	5.793%	$NO2$	101	<0.001%
Solar(A)	—	0.771%	$NH3$	111	<0.001%
Solar-sim	—	0.503%	OH	131	<0.001%
HDO	491	0.618%	HCl	151	<0.001%
H2CO	201	0.522%	HBr	161	<0.001%
$N2O$	41	0.267%	OCS	191	<0.001%
$CO2$	2**3**	0.206%	$H2S$	471	<0.001%

H_2CO, Kiruna, φ=69.87^o, OPD=257cm, FoV=1.91$mrad$, boxcar apod.

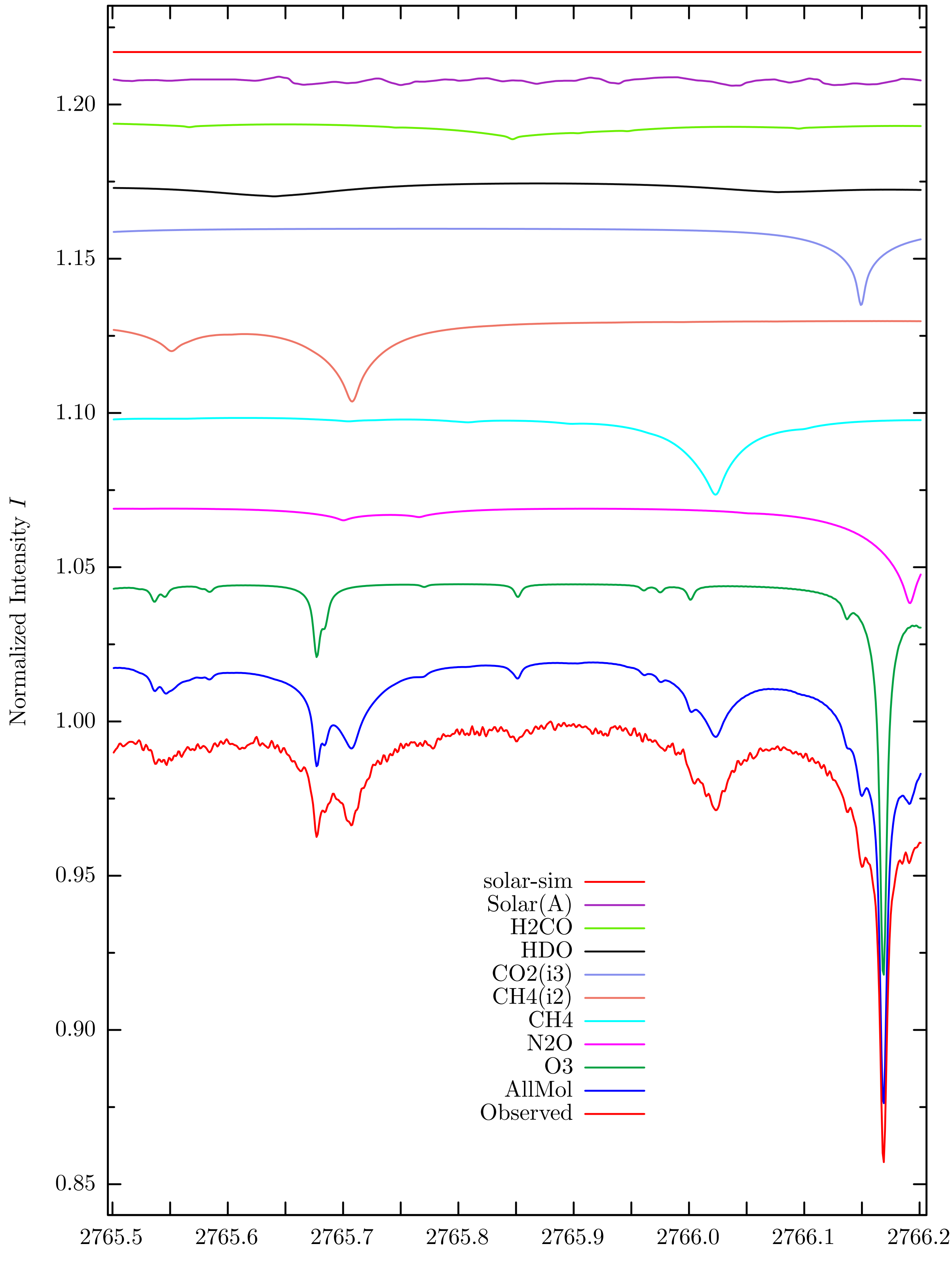

Wavenumber ν in cm^{-1}

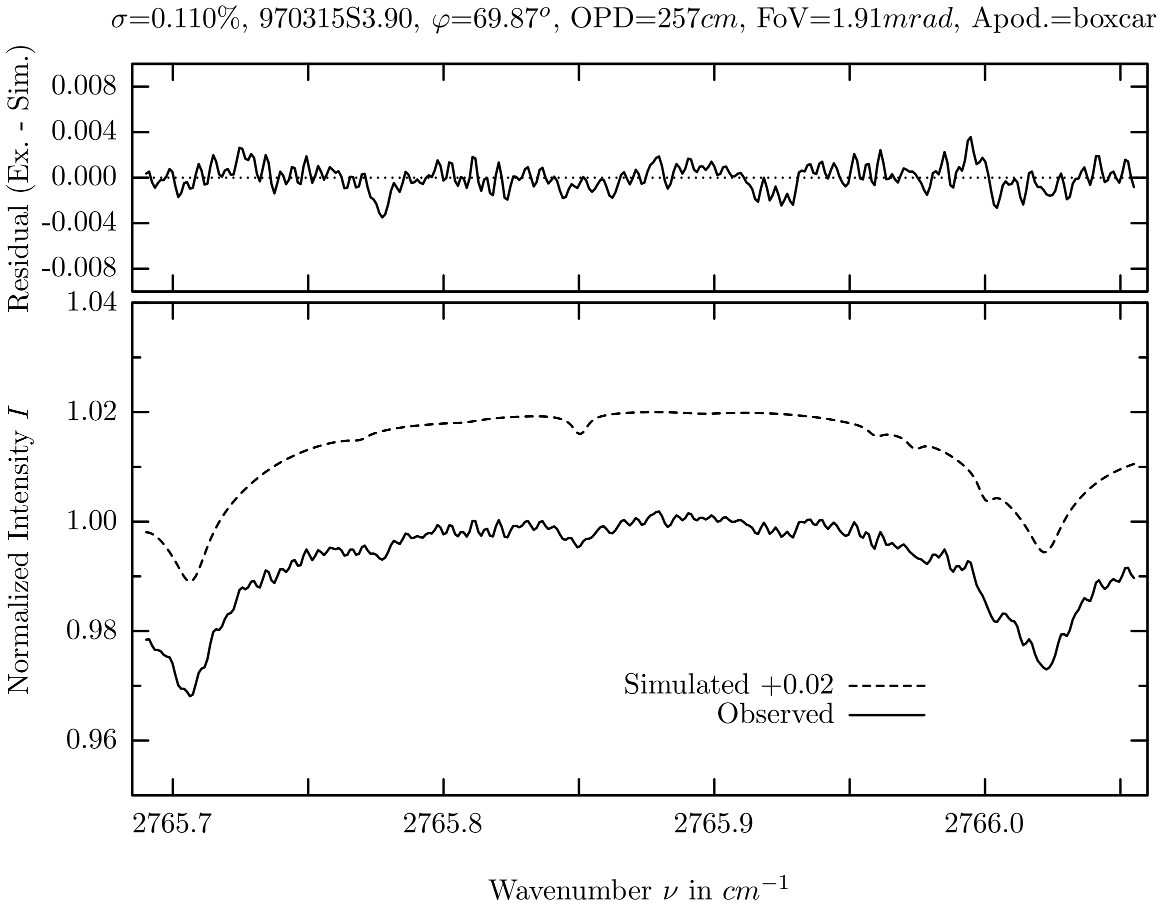

investigated species	:	H_2CO	
line position(s) ν_0	:	2765.8454$^{*)}$ cm^{-1}	
lower state energy E''_{lst}	:	73.8 cm^{-1}	
retrieved TCA, information content	:	1.22E+15 $molec/cm^2$, 1.1	
temperature dependence of the TCA	:	-0.940%/K (trop), -0.147%/K (strat)	
location, date, solar zenith angle	:	Kiruna, 15/Mar/97, 69.87^o	
spectral interval fitted	:	2765.690 – 2766.055 cm^{-1}	

Molecule	iCode	Absorption	Molecule	iCode	Absorption
O3	31	12.920%	*H2O*	11	0.001%
N2O	41	3.166%	*SO2*	91	<0.001%
CH4	61	2.652%	*NO2*	101	<0.001%
CH4	6**2**	2.633%	*NH3*	111	<0.001%
CO2	2**3**	2.516%	*OH*	131	<0.001%
HDO	491	0.979%	*HCl*	151	<0.001%
H2CO	201	0.627%	*HBr*	161	<0.001%
Solar(A)	—	0.391%	*H2S*	471	<0.001%
Solar-sim	—	<0.001%			

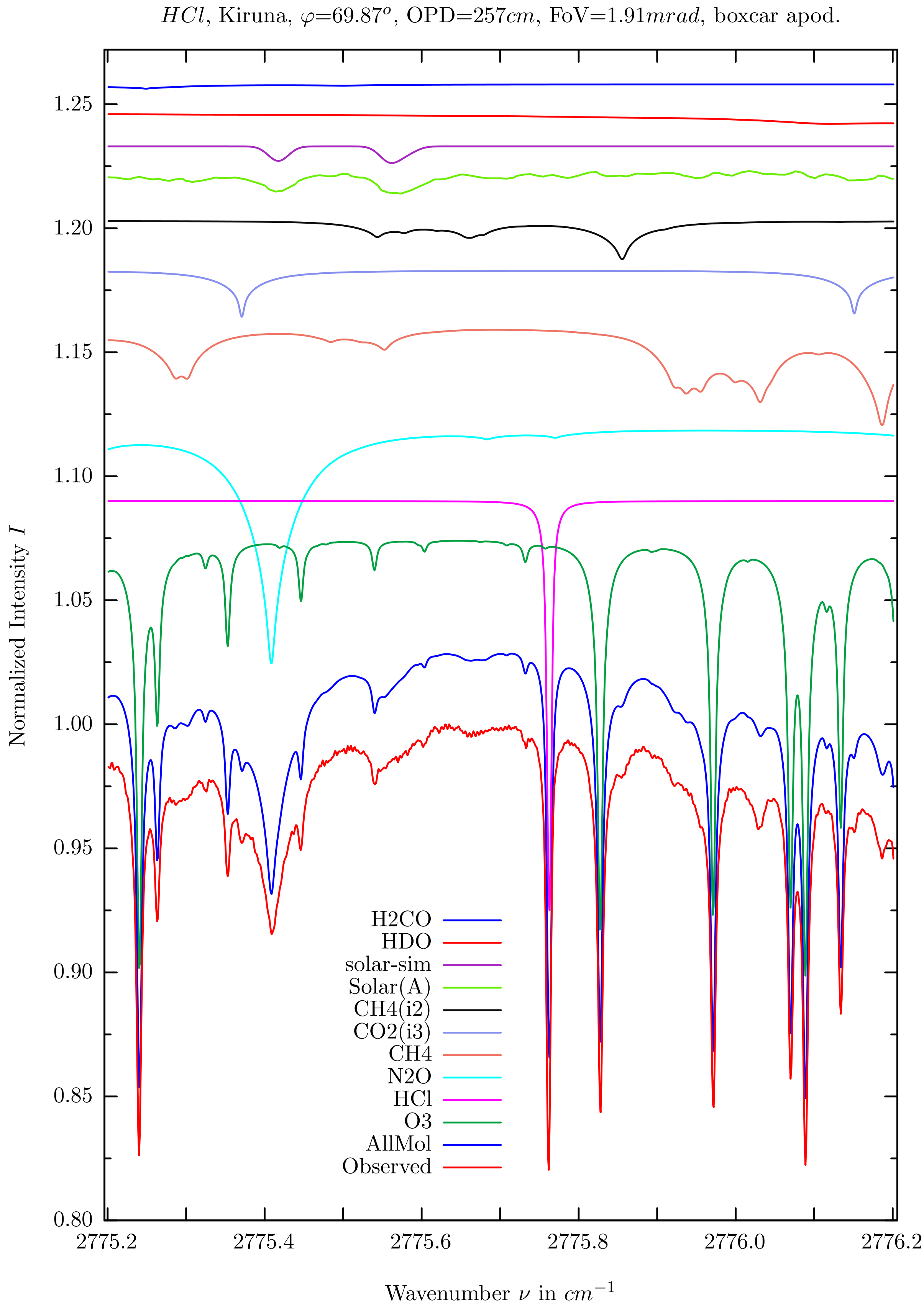

HCl, Kiruna, φ=69.87^o, OPD=257cm, FoV=1.91$mrad$, boxcar apod.
Normalized Intensity I
Wavenumber ν in cm^{-1}
1.25
1.20
1.15
1.10
1.05
1.00
0.95
0.90
0.85
0.80
2775.2
2775.4
2775.6
2775.8
2776.0
2776.2
H2CO
HDO
solar-sim
Solar(A)
CH4(i2)
CO2(i3)
CH4
N2O
HCl
O3
AllMol
Observed

σ=0.096%, 970315S3.90, φ=69.87^o, OPD=257cm, FoV=1.91$mrad$, Apod.=boxcar

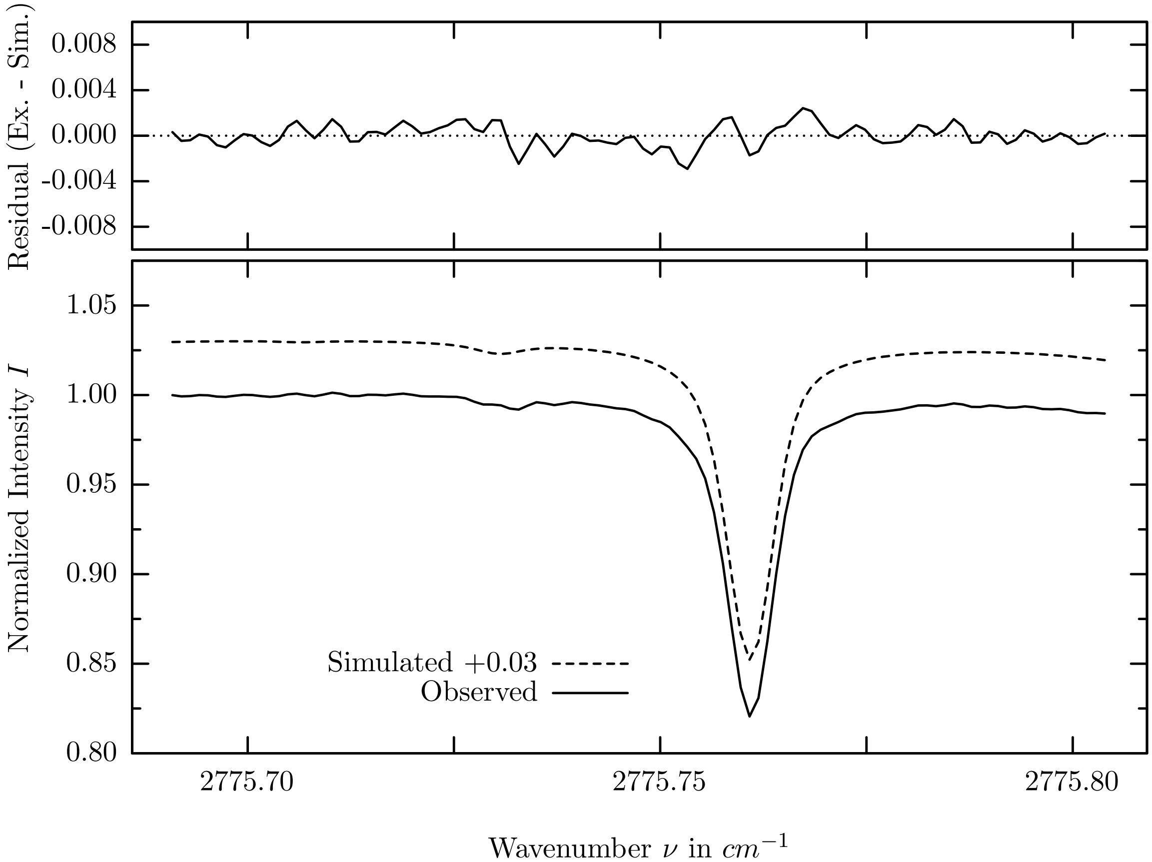

investigated species	:	HCl
line position(s) ν_0	:	2775.7612 cm^{-1}
lower state energy E''_{lst}	:	312.7 cm^{-1}
retrieved TCA, information content	:	3.07E+15 $molec/cm^2$, 185.7
temperature dependence of the TCA	:	-0.060%/K (trop), -0.617%/K (strat)
location, date, solar zenith angle	:	Kiruna, 15/Mar/97, 69.87^o
spectral interval fitted	:	2775.690 – 2775.804 cm^{-1}

Molecule	iCode	Absorption	Molecule	iCode	Absorption
$O3$	31	17.754%	$H2CO$	201	0.174%
HCl	151	16.755%	$H2O$	11	0.001%
$N2O$	41	9.579%	$SO2$	91	<0.001%
$CH4$	61	4.253%	$NO2$	101	<0.001%
$CO2$	2**3**	1.880%	$NH3$	111	<0.001%
$CH4$	6**2**	1.556%	OH	131	<0.001%
Solar(A)	—	0.901%	HBr	161	<0.001%
Solar-sim	—	0.674%	$H2S$	471	<0.001%
HDO	491	0.593%			

H_2CO, Kiruna, φ=69.87^o, OPD=257cm, FoV=1.91$mrad$, boxcar apod.

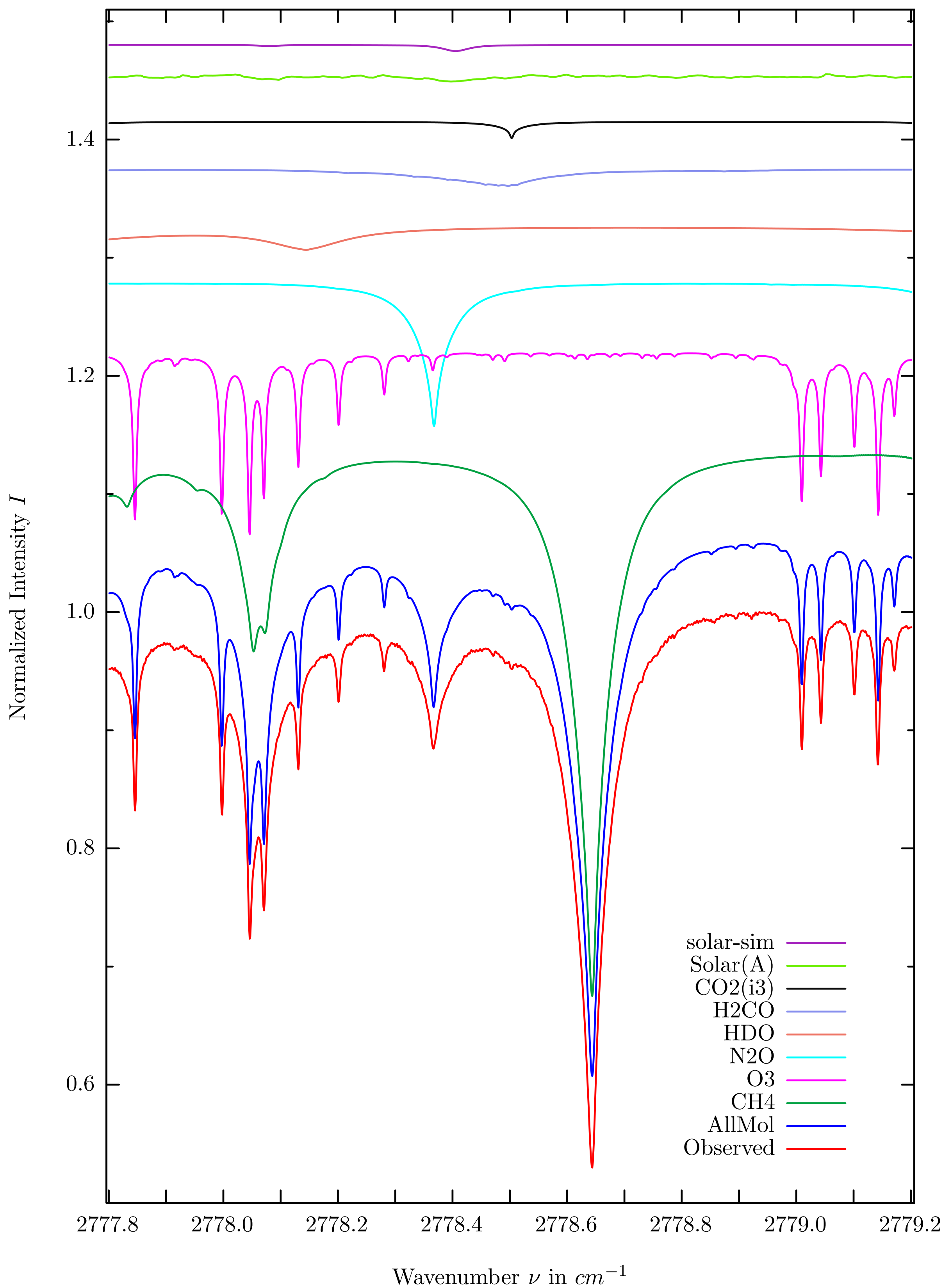

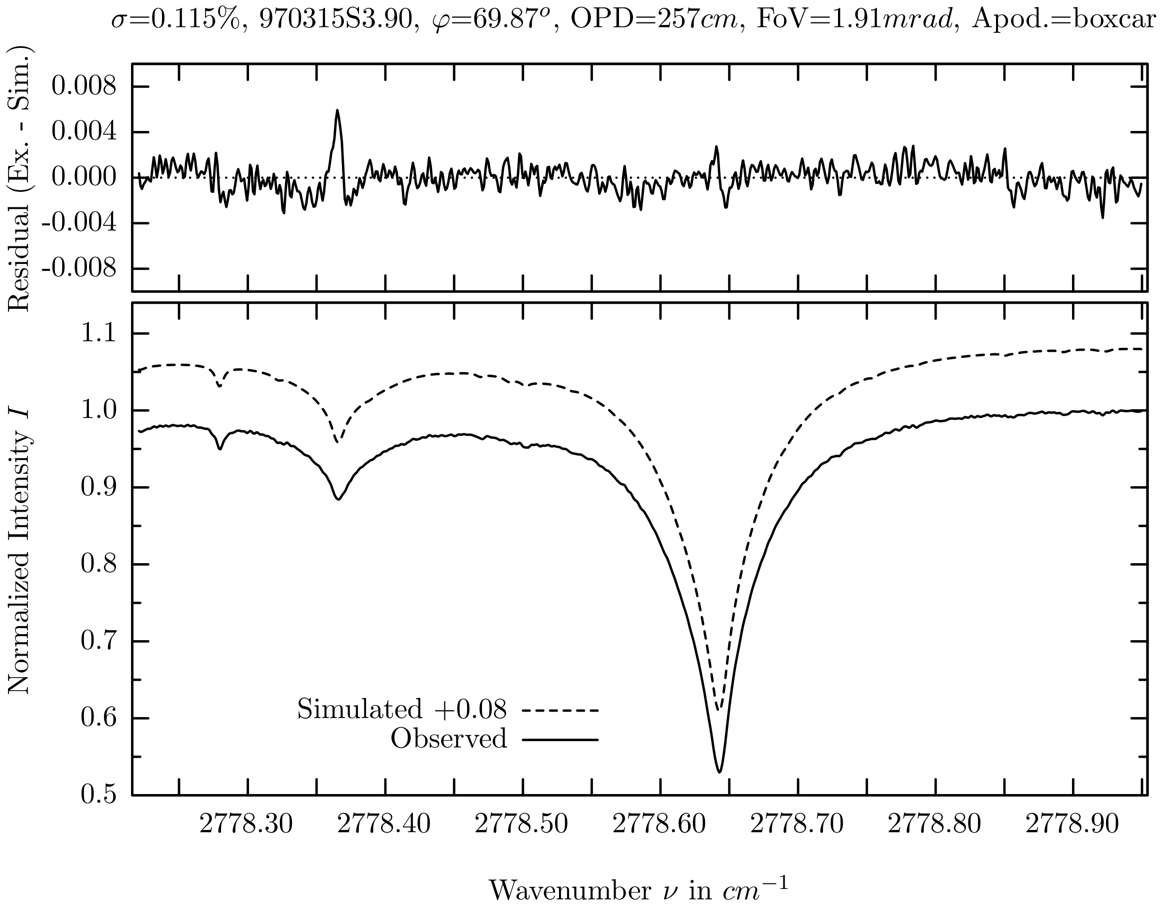

investigated species	:	$H_2CO, (CH_4)$
line position(s) ν_0	:	2778.5112*), (2778.6428) cm^{-1}
lower state energy E''_{lst}	:	240.8, (219.9) cm^{-1}
retrieved TCA, information content	:	1.43E+15, (3.29E+19) $molec/cm^2$, 12.8, (409.7)
temperature dependence of the TCA	:	-1.606, (-.026)%/K (trop), -.361, (-.020)%/K (strat)
location, date, solar zenith angle	:	Kiruna, 15/Mar/97, 69.87^o
spectral interval fitted	:	2778.220 – 2778.950 cm^{-1}

Molecule	iCode	Absorption	Molecule	iCode	Absorption
$CH4$	61	46.509%	$H2O$	11	0.018%
$O3$	31	15.555%	$SO2$	91	<0.001%
$N2O$	41	12.275%	$NO2$	101	<0.001%
HDO	491	2.352%	$NH3$	111	<0.001%
H2CO	201	1.440%	OH	131	<0.001%
$CO2$	2**3**	1.382%	HCl	151	<0.001%
Solar(A)	—	0.590%	HBr	161	<0.001%
Solar-sim	—	0.510%	$H2S$	471	<0.001%

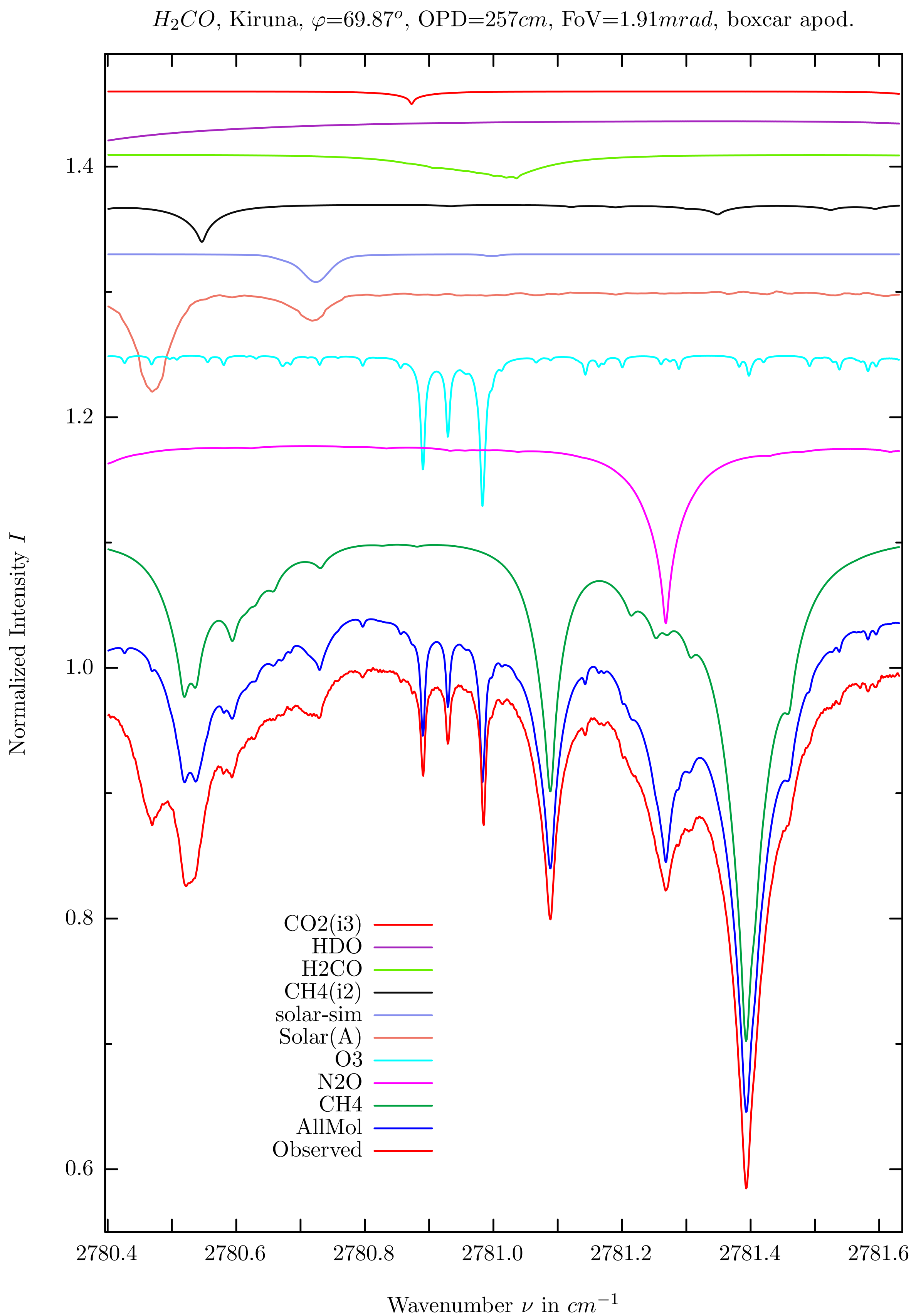
H_2CO, Kiruna, φ=69.87^o, OPD=257cm, FoV=1.91$mrad$, boxcar apod.
Normalized Intensity I
1.4
1.2
1.0
0.8
0.6
2780.4
2780.6
2780.8
2781.0
2781.2
2781.4
2781.6
Wavenumber ν in cm^{-1}
CO2(i3)
HDO
H2CO
CH4(i2)
solar-sim
Solar(A)
O3
N2O
CH4
AllMol
Observed

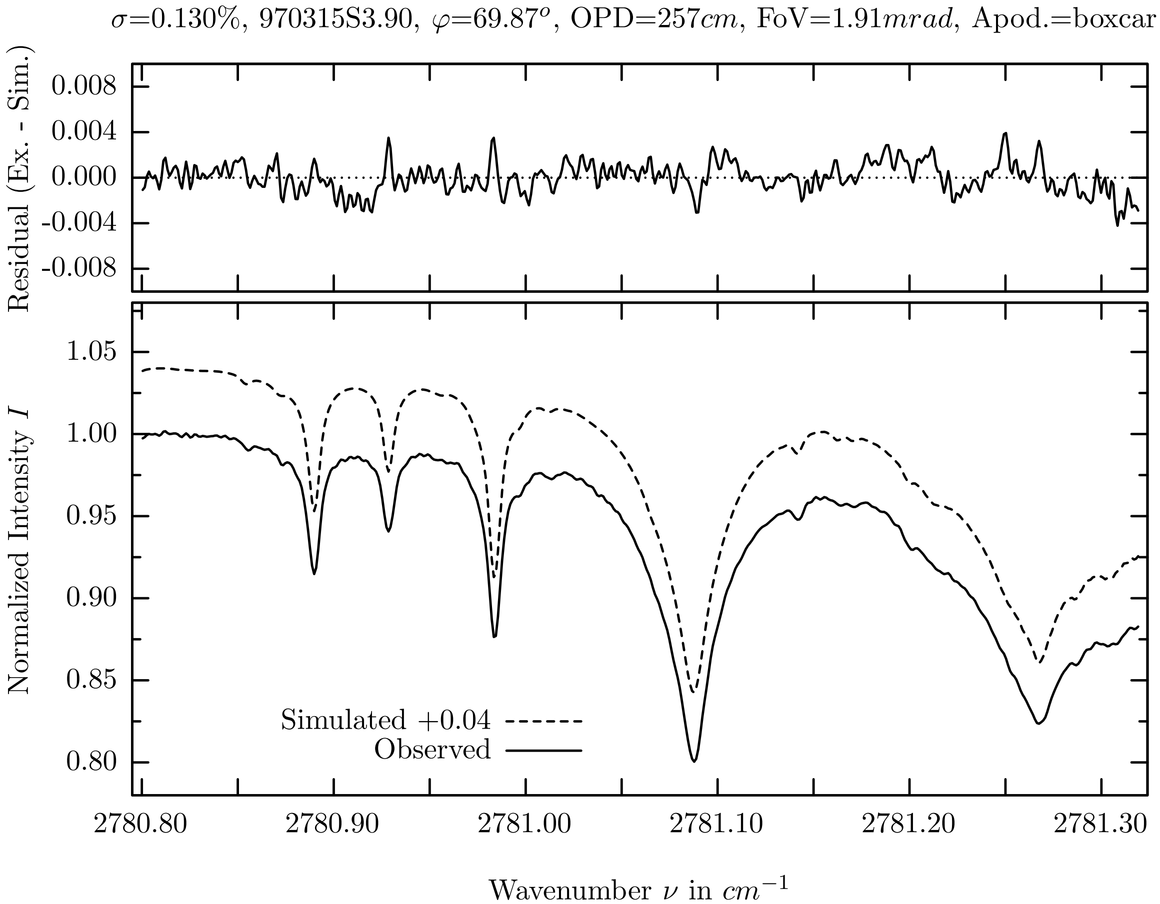

investigated species	:	H_2CO
line position(s) ν_0	:	2780.9519$^{*)}$ cm^{-1}
lower state energy E''_{lst}	:	329.0 cm^{-1}
retrieved TCA, information content	:	1.16E+15 $molec/cm^2$, 8.0
temperature dependence of the TCA	:	-1.702%/K (trop), +0.332%/K (strat)
location, date, solar zenith angle	:	Kiruna, 15/Mar/97, 69.87^o
spectral interval fitted	:	2780.800 – 2781.320 cm^{-1}

Molecule	iCode	Absorption	Molecule	iCode	Absorption
$CH4$	61	40.801%	$H2O$	11	0.017%
$N2O$	41	14.462%	$SO2$	91	<0.001%
$O3$	31	12.157%	$NO2$	101	<0.001%
Solar(A)	—	7.960%	$NH3$	111	<0.001%
Solar-sim	—	2.217%	OH	131	<0.001%
$CH4$	6**2**	3.011%	HCl	151	<0.001%
H2CO	201	1.944%	HBr	161	<0.001%
HDO	491	1.909%	$H2S$	471	<0.001%
$CO2$	2**3**	1.013%			

O_3, Kiruna, φ=69.87^o, OPD=257cm, FoV=1.91$mrad$, boxcar apod.

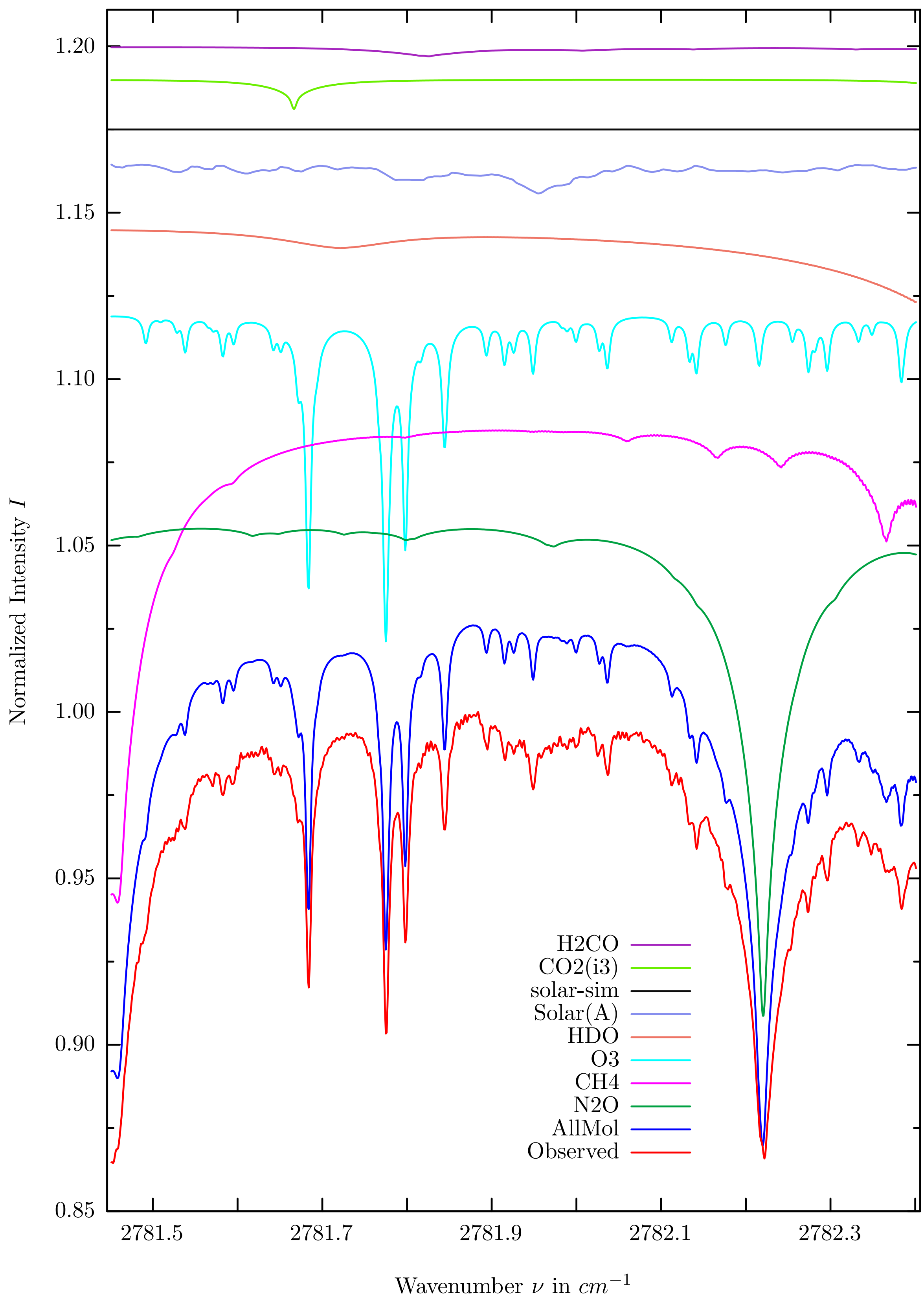

σ=0.098%, 970315S3.90, φ=69.87^o, OPD=257cm, FoV=1.91$mrad$, Apod.=boxcar

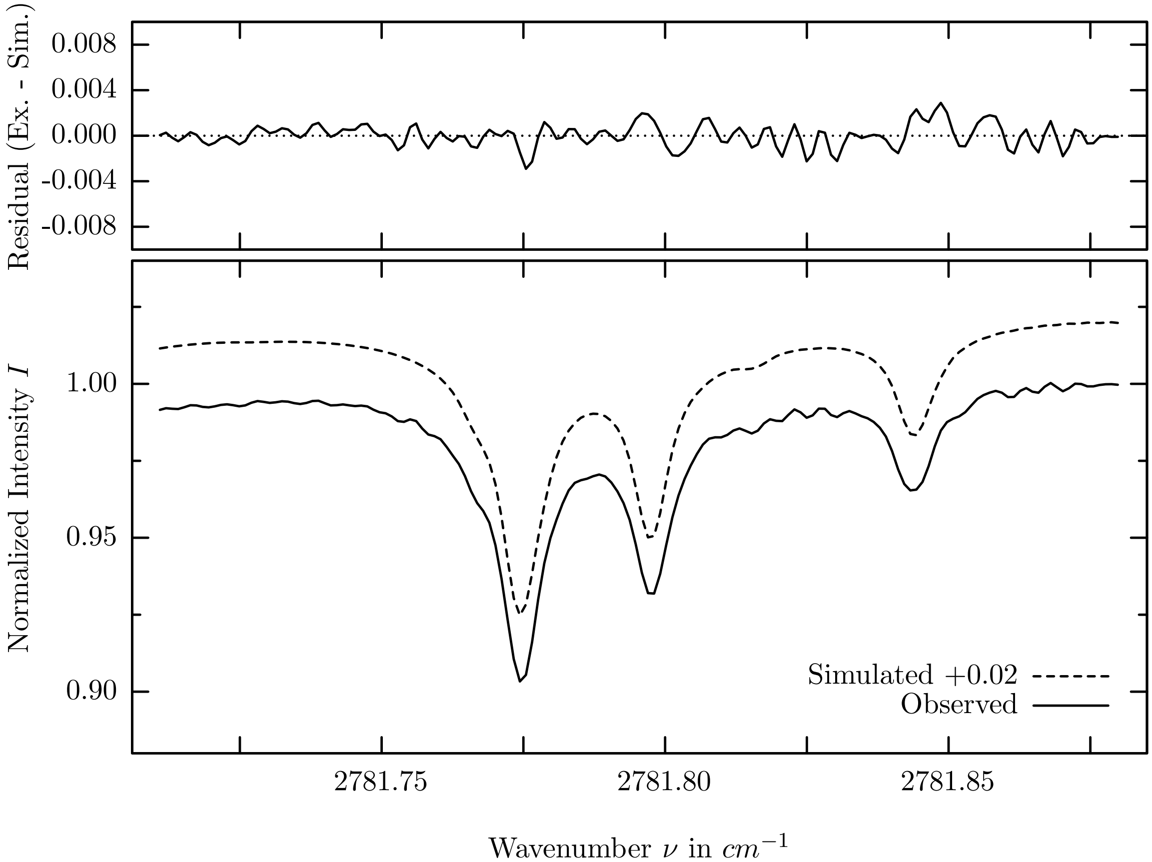

investigated species	:	O_3
line position(s) ν_0	:	2781.7734 cm^{-1}
lower state energy E''_{lst}	:	8.4 cm^{-1}
retrieved TCA, information content	:	1.02E+19 $molec/cm^2$, 94.9
temperature dependence of the TCA	:	-0.093%/K (trop), +0.327%/K (strat)
location, date, solar zenith angle	:	Kiruna, 15/Mar/97, 69.87^o
spectral interval fitted	:	2781.710 – 2781.880 cm^{-1}

Molecule	iCode	Absorption	Molecule	iCode	Absorption
$N2O$	41	15.187%	$H2O$	11	0.020%
$CH4$	61	14.615%	$SO2$	91	<0.001%
O3	31	9.946%	$NO2$	101	<0.001%
HDO	491	2.706%	$NH3$	111	<0.001%
Solar(A)	—	0.921%	OH	131	<0.001%
Solar-sim	—	<0.001%	HCl	151	<0.001%
$CO2$	2**3**	0.890%	HBr	161	<0.001%
$H2CO$	201	0.303%	$H2S$	471	<0.001%

N_2O, Kiruna, φ=69.87^o, OPD=257cm, FoV=1.91$mrad$, boxcar apod.

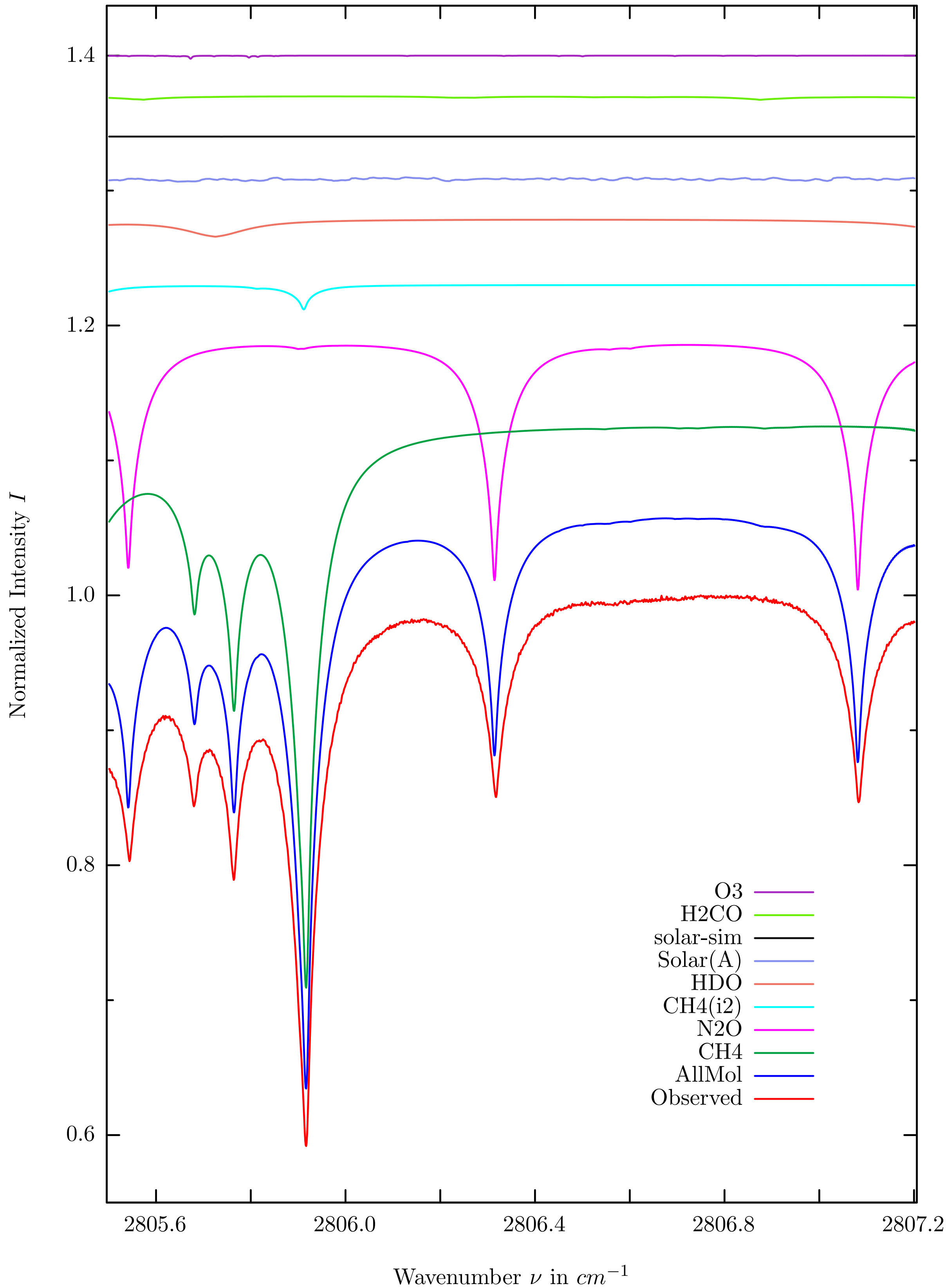

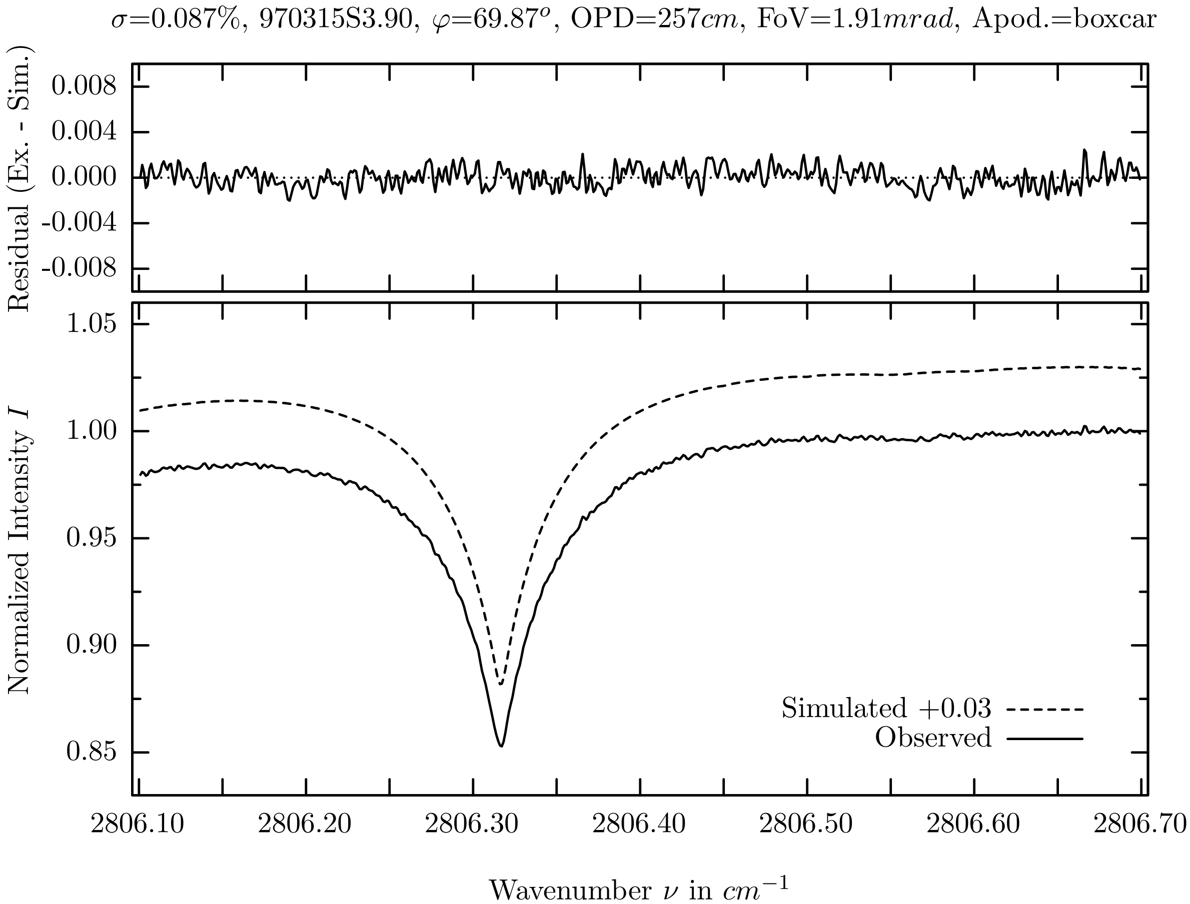

investigated species	:	N_2O
line position(s) ν_0	:	2806.3157 cm^{-1}
lower state energy E''_{lst}	:	37.7 cm^{-1}
retrieved TCA, information content	:	5.57E+18 $molec/cm^2$, 164.7
temperature dependence of the TCA	:	+0.382%/K (trop), +0.028%/K (strat)
location, date, solar zenith angle	:	Kiruna, 15/Mar/97, 69.87^o
spectral interval fitted	:	2806.100 – 2806.700 cm^{-1}

Molecule	iCode	Absorption	Molecule	iCode	Absorption
$CH4$	61	42.112%	$O3$	31	0.236%
N2O	41	18.640%	$H2O$	11	0.009%
$CH4$	6**2**	1.813%	$NO2$	101	<0.001%
HDO	491	1.418%	$NH3$	111	<0.001%
Solar(A)	—	0.341%	OH	131	<0.001%
Solar-sim	—	0.001%	HCl	151	<0.001%
$H2CO$	201	0.278%	$H2S$	471	<0.001%

H_2O, Kiruna, φ=69.87^o, OPD=257cm, FoV=1.91$mrad$, boxcar apod.

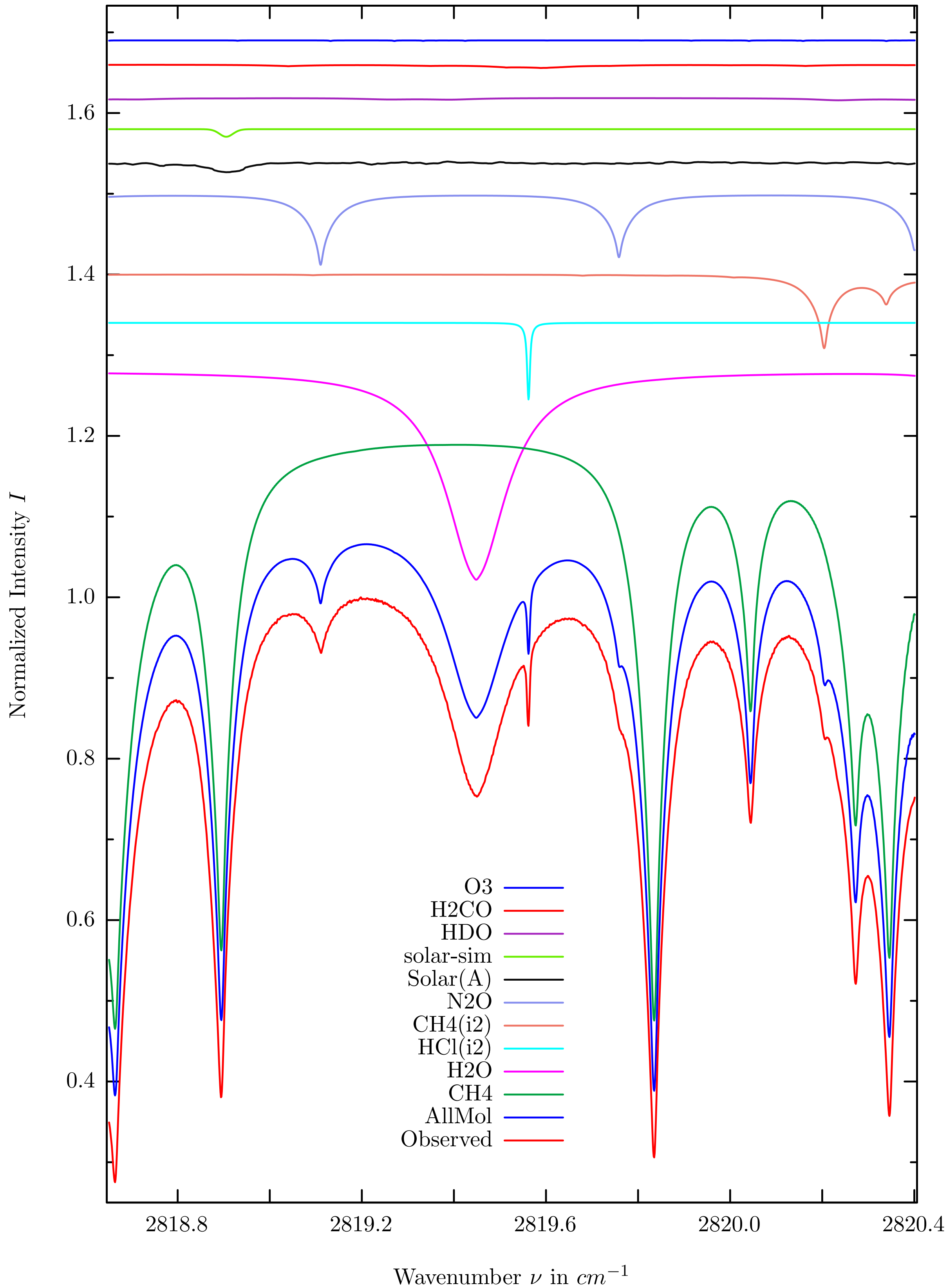

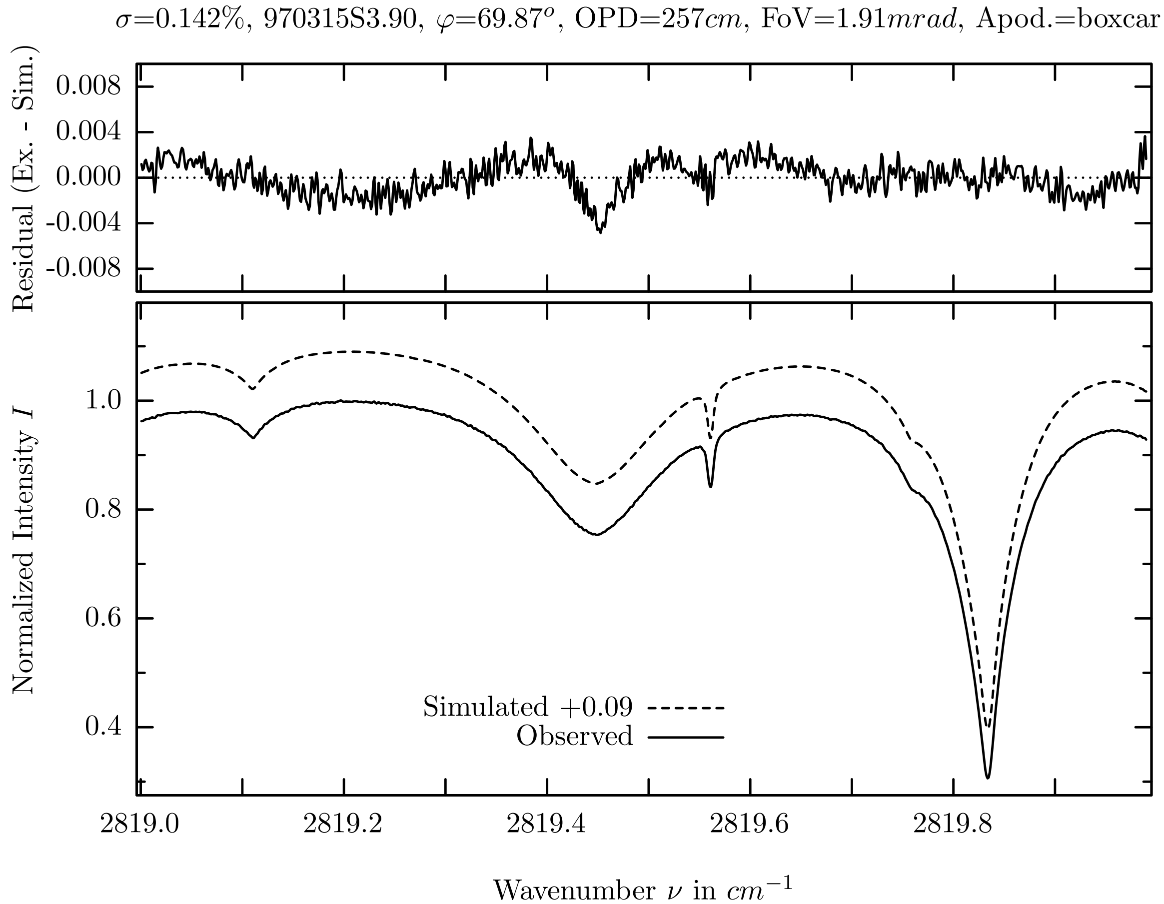

investigated species	:	$H_2O, (CH_4)$
line position(s) ν_0	:	2819.4470, (2819.8338) cm^{-1}
lower state energy E''_{lst}	:	782.4, (10.5) cm^{-1}
retrieved TCA, information content	:	5.82E+21, (3.38E+19) $molec/cm^2$, 170.4, (486.6)
temperature dependence of the TCA	:	-1.384, (+.209)%/K (trop), -.019, (+.041)%/K (strat)
location, date, solar zenith angle	:	Kiruna, 15/Mar/97, 69.87^o
spectral interval fitted	:	2819.000 – 2819.990 cm^{-1}

Molecule	iCode	Absorption	Molecule	iCode	Absorption
CH4	61	74.509%	*H2CO*	201	0.418%
H2O	11	25.829%	*O3*	31	0.077%
HCl	15**2**	9.564%	*HCl*	151	0.001%
CH4	6**2**	9.150%	*NO2*	101	<0.001%
N2O	41	8.835%	*NH3*	111	<0.001%
Solar(A)	—	1.331%	*OH*	131	<0.001%
Solar-sim	—	0.939%	*OCS*	19**3**	<0.001%
HDO	491	0.423%	*H2S*	471	<0.001%

HCl, Kiruna, φ=69.87^o, OPD=257cm, FoV=1.91$mrad$, boxcar apod.

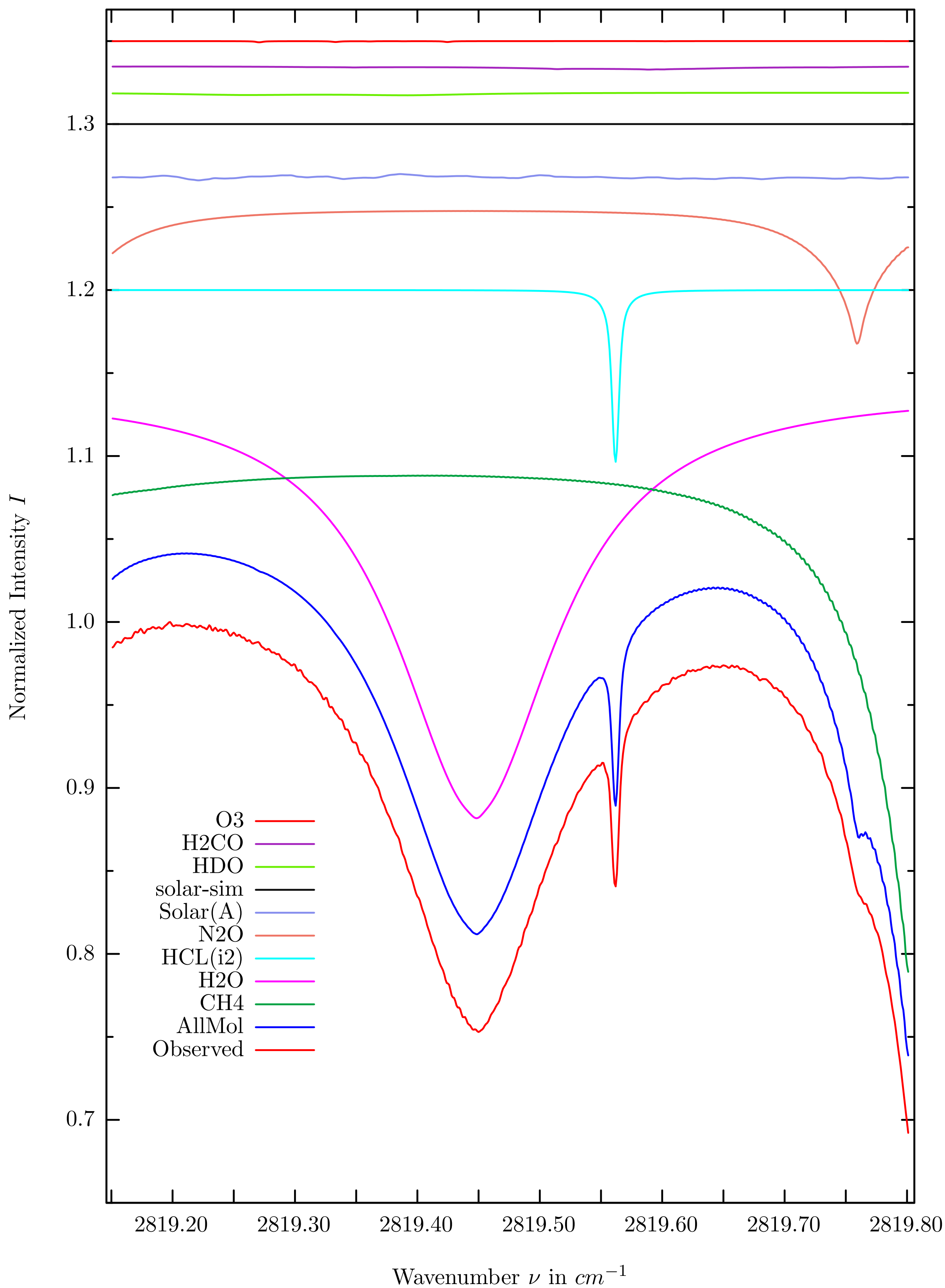

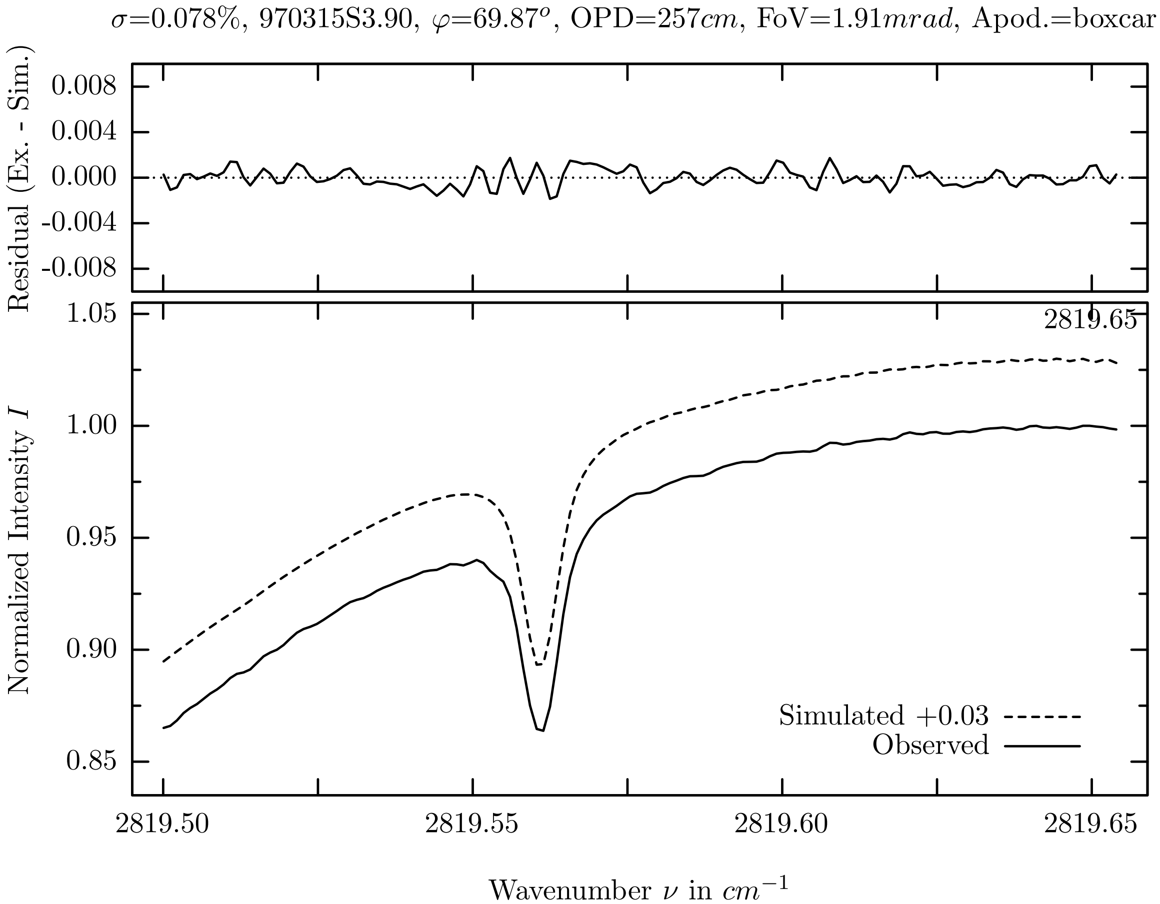

investigated species	:	HCl
line position(s) ν_0	:	2819.5605 cm^{-1}
lower state energy E''_{lst}	:	125.0 cm^{-1}
retrieved TCA, information content	:	3.10E+15 $molec/cm^2$, 123.8
temperature dependence of the TCA	:	-0.029%/K (trop), -0.077%/K (strat)
location, date, solar zenith angle	:	Kiruna, 15/Mar/97, 69.87^o
spectral interval fitted	:	2819.500 – 2819.655 cm^{-1}

Molecule	iCode	Absorption	Molecule	iCode	Absorption
$CH4$	61	32.993%	$O3$	31	0.072%
$H2O$	11	25.829%	HCl	151	0.001%
HCl	15**2**	9.564%	$NO2$	101	<0.001%
$N2O$	41	8.248%	$NH3$	111	<0.001%
Solar(A)	—	0.390%	OH	131	<0.001%
Solar-sim	—	<0.001%	OCS	19**3**	<0.001%
HDO	491	0.264%	$H2S$	471	<0.001%
$H2CO$	201	0.216%			

HCl, Kiruna, φ=69.87^o, OPD=257cm, FoV=1.91$mrad$, boxcar apod.

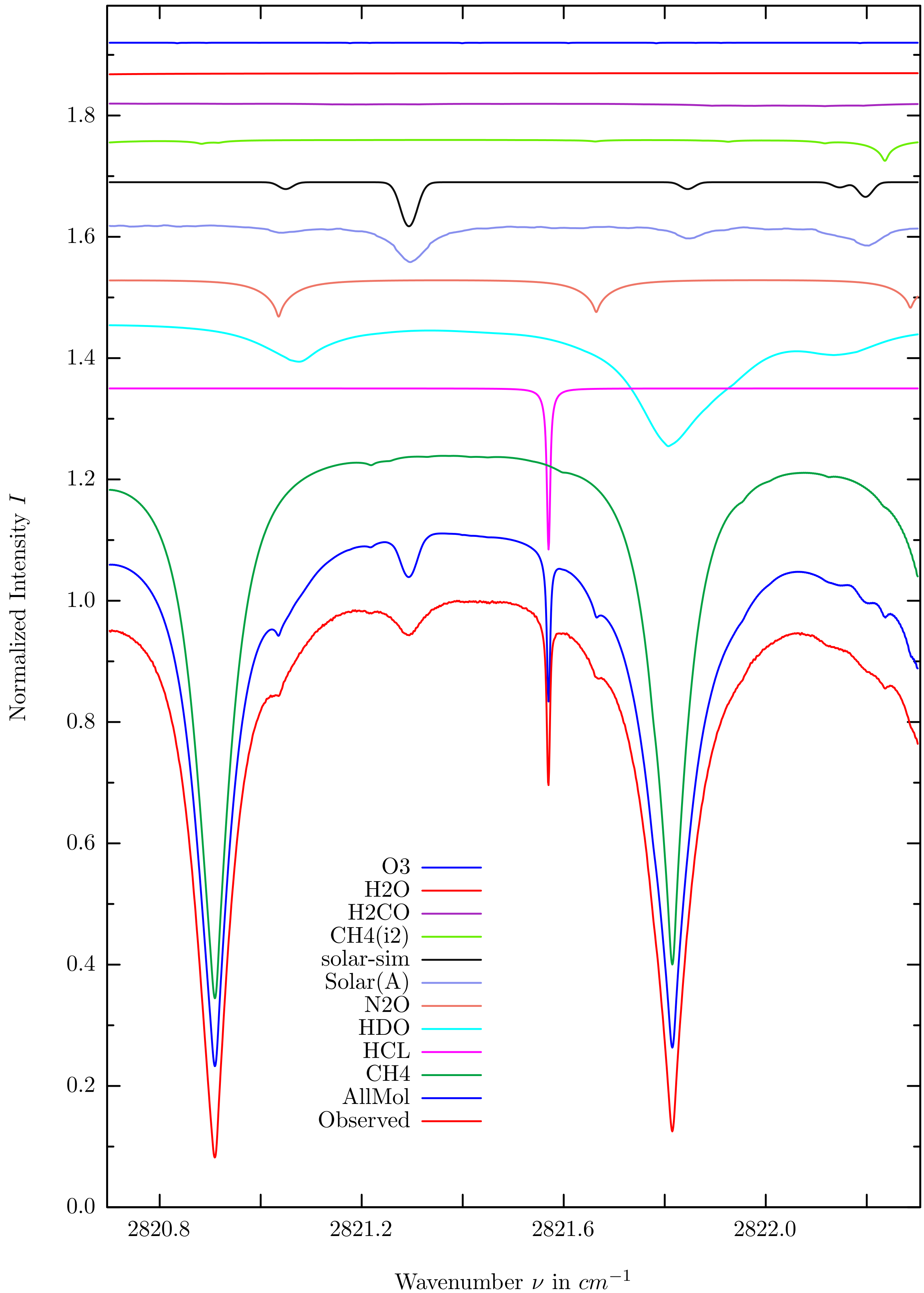

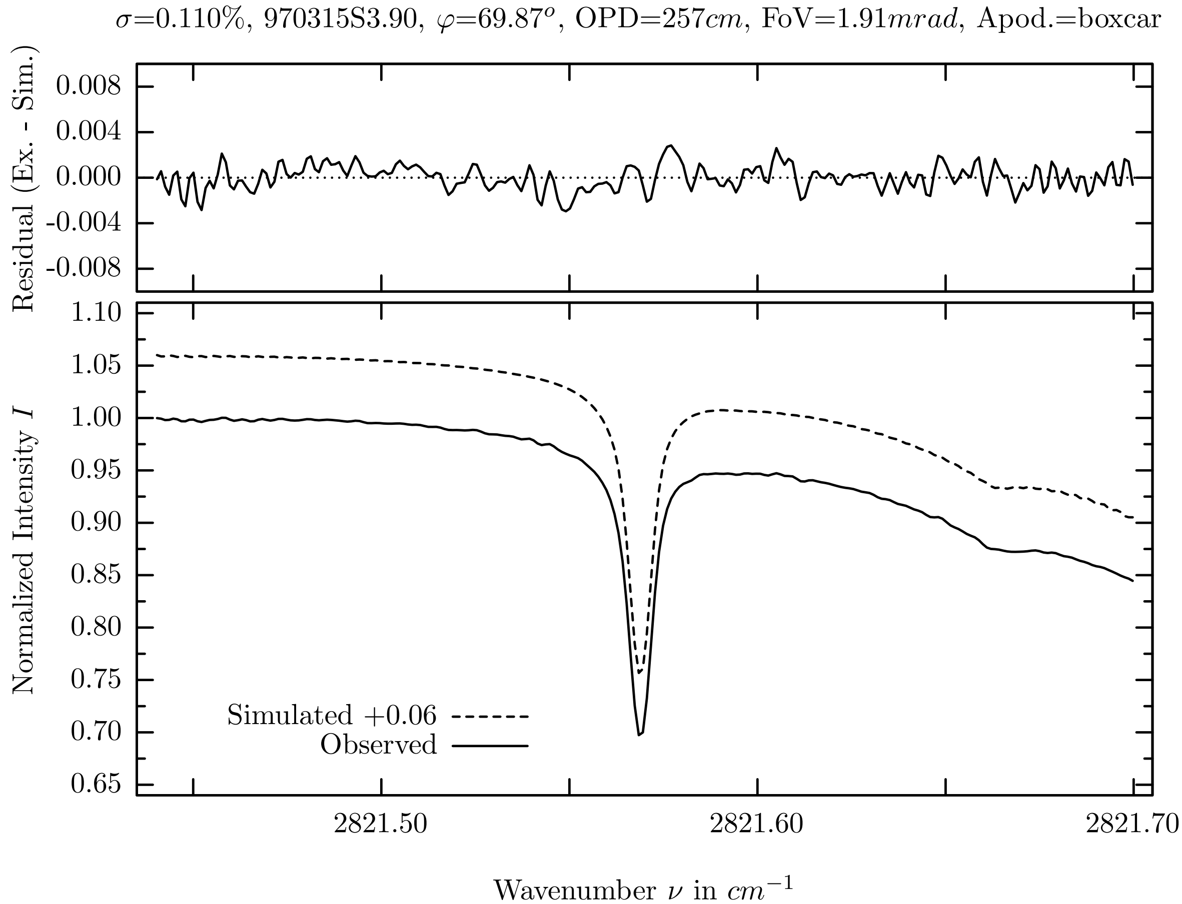

investigated species	:	HCl
line position(s) ν_0	:	2821.5684 cm^{-1}
lower state energy E''_{lst}	:	125.2 cm^{-1}
retrieved TCA, information content	:	3.16E+15 $molec/cm^2$, 251.2
temperature dependence of the TCA	:	+0.035%/K (trop), +0.017%/K (strat)
location, date, solar zenith angle	:	Kiruna, 15/Mar/97, 69.87^o
spectral interval fitted	:	2821.440 – 2821.700 cm^{-1}

Molecule	iCode	Absorption	Molecule	iCode	Absorption
$CH4$	61	92.592%	$H2O$	11	0.205%
HCl	151	26.735%	$O3$	31	0.087%
HDO	491	20.528%	$NO2$	101	<0.001%
$N2O$	41	6.182%	$NH3$	111	<0.001%
Solar(A)	—	6.170%	OH	131	<0.001%
Solar-sim	—	7.268%	OCS	19**3**	<0.001%
$CH4$	6**2**	3.480%	$H2S$	471	<0.001%
$H2CO$	201	0.453%			

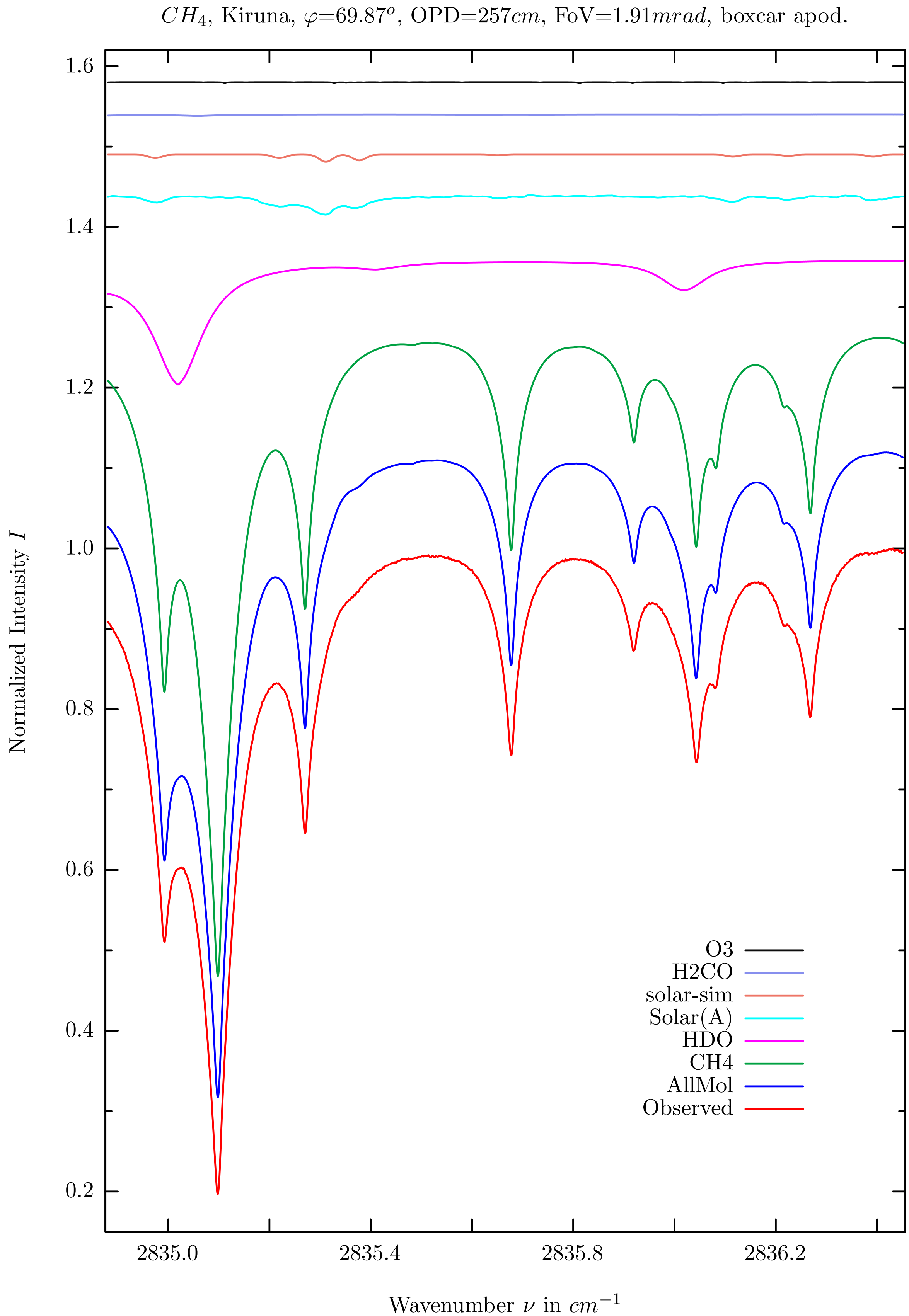
CH_4, Kiruna, φ=69.87^o, OPD=257cm, FoV=1.91$mrad$, boxcar apod.
Normalized Intensity I
Wavenumber ν in cm^{-1}
1.6
1.4
1.2
1.0
0.8
0.6
0.4
0.2
2835.0
2835.4
2835.8
2836.2
O3
H2CO
solar-sim
Solar(A)
HDO
CH4
AllMol
Observed

σ=0.073%, 970315S3.90, φ=69.87^o, OPD=257cm, FoV=1.91$mrad$, Apod.=boxcar

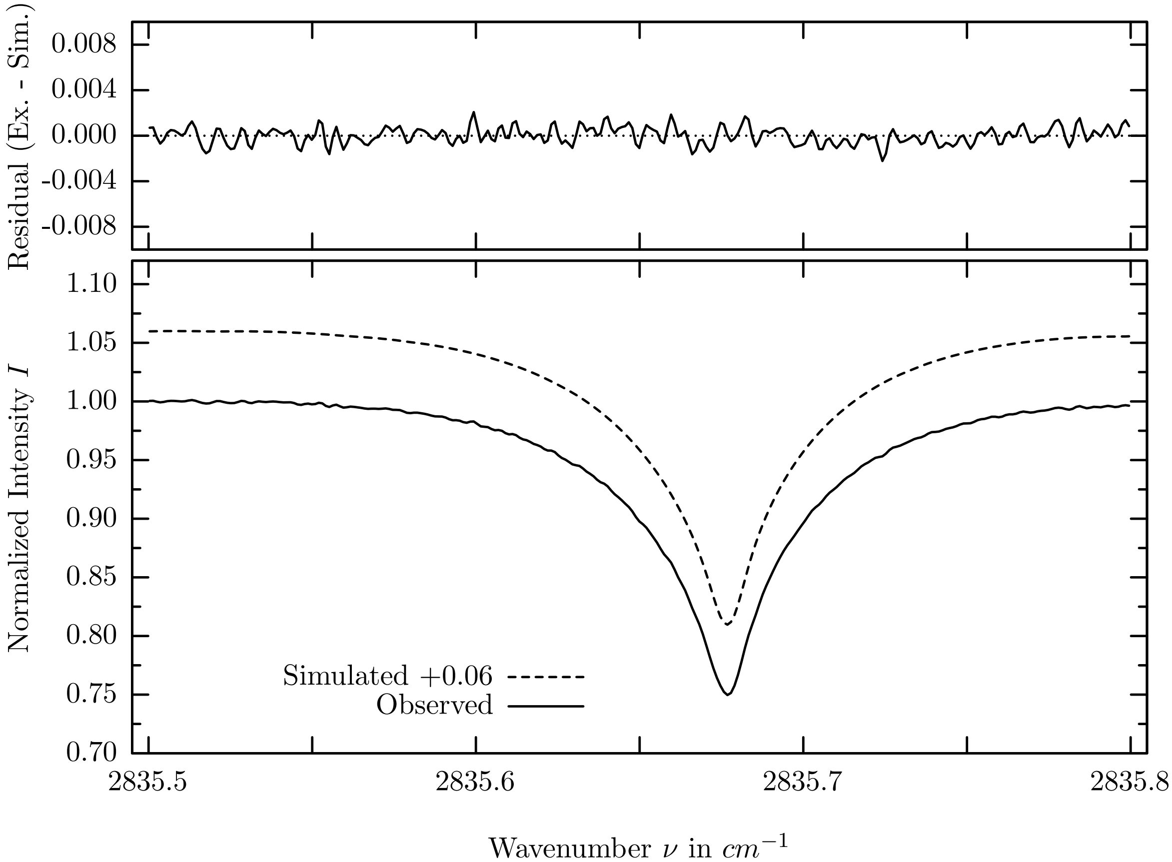

investigated species	:	CH_4
line position(s) ν_0	:	2835.6763 cm^{-1}
lower state energy E''_{lst}	:	62.9 cm^{-1}
retrieved TCA, information content	:	3.27E+19 $molec/cm^2$, 342.5
temperature dependence of the TCA	:	+0.385%/K (trop), +0.034%/K (strat)
location, date, solar zenith angle	:	Kiruna, 15/Mar/97, 69.87^o
spectral interval fitted	:	2835.500 – 2835.800 cm^{-1}

Molecule	iCode	Absorption	Molecule	iCode	Absorption
CH4	61	82.245%	$H2O$	11	0.006%
HDO	491	15.608%	$NO2$	101	0.001%
Solar(A)	—	2.464%	OCS	19**3**	0.001%
Solar-sim	—	0.888%	$NH3$	111	<0.001%
$H2CO$	201	0.181%	OH	131	<0.001%
$O3$	31	0.133%	HCl	151	<0.001%
$N2O$	41	0.028%	$H2S$	471	<0.001%

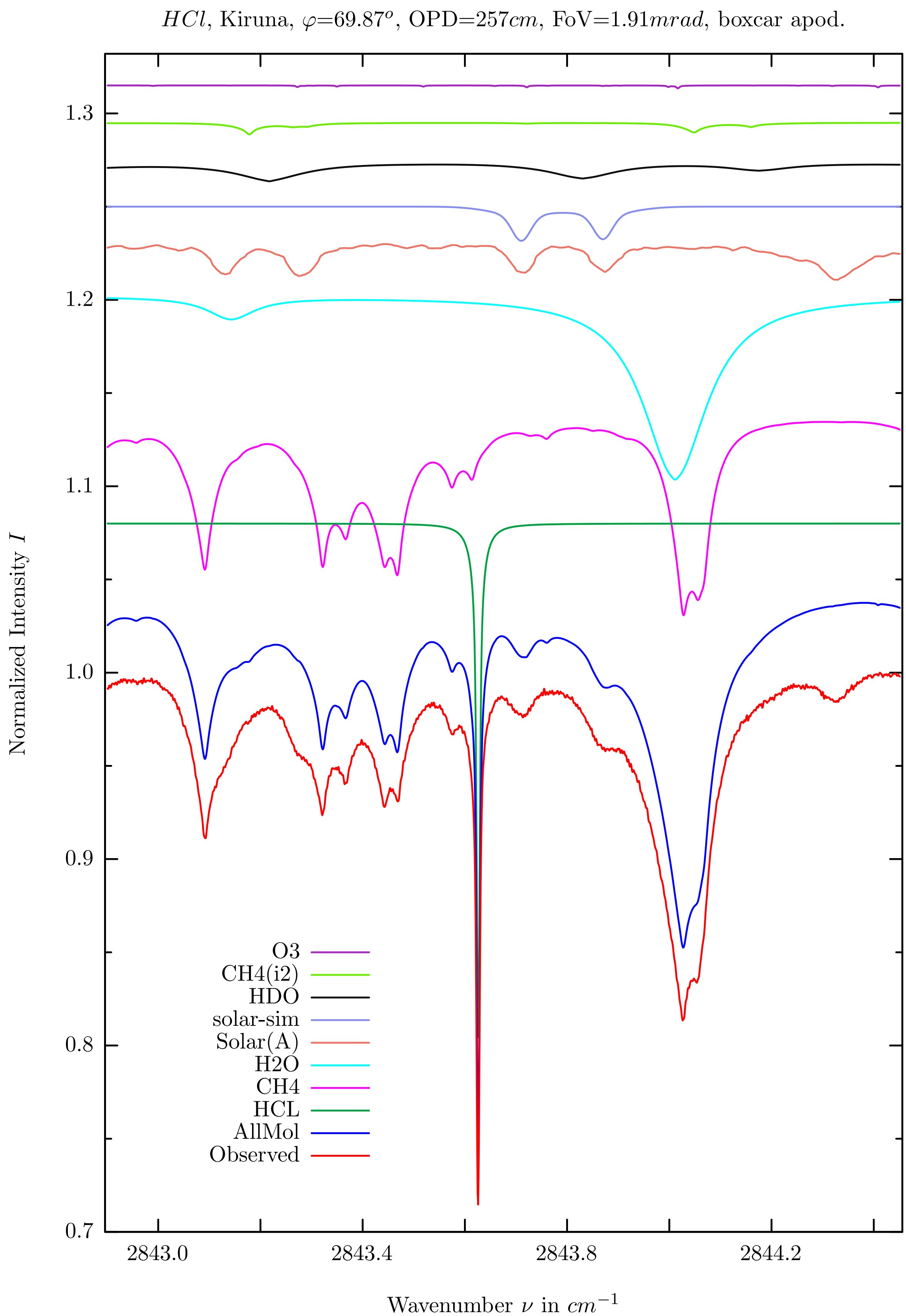

HCl, Kiruna, φ=69.87^o, OPD=257cm, FoV=1.91$mrad$, boxcar apod.
1.3
1.2
1.1
1.0
0.9
0.8
0.7
Normalized Intensity I
2843.0
2843.4
2843.8
2844.2
Wavenumber ν in cm^{-1}
O3
CH4(i2)
HDO
solar-sim
Solar(A)
H2O
CH4
HCL
AllMol
Observed

σ=0.106%, 970315S3.90, φ=69.87^o, OPD=257cm, FoV=1.91$mrad$, Apod.=boxcar

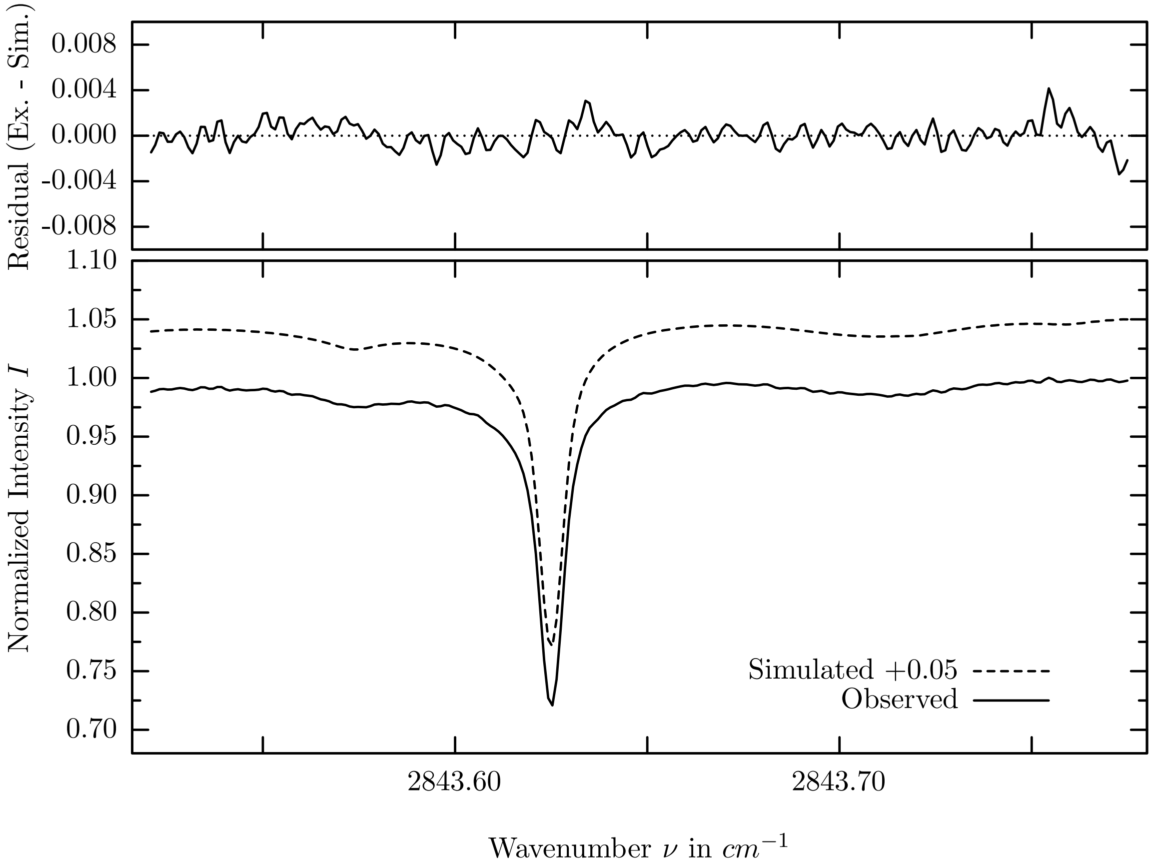

investigated species	:	HCl
line position(s) ν_0	:	2843.6243 cm^{-1}
lower state energy E''_{lst}	:	62.6 cm^{-1}
retrieved TCA, information content	:	3.11E+15 $molec/cm^2$, 264.0
temperature dependence of the TCA	:	-0.050%/K (trop), +0.169%/K (strat)
location, date, solar zenith angle	:	Kiruna, 15/Mar/97, 69.87^o
spectral interval fitted	:	2843.520 – 2843.775 cm^{-1}

Molecule	iCode	Absorption	Molecule	iCode	Absorption
HCL	151	27.724%	OCS	19**3**	0.003%
$CH4$	61	10.922%	$NO2$	101	0.001%
$H2O$	11	9.843%	$H2CO$	201	0.001%
Solar(A)	—	1.925%	$N2O$	41	<0.001%
Solar-sim	—	1.833%	$NH3$	111	<0.001%
HDO	491	1.139%	OH	131	<0.001%
$CH4$	6**2**	0.628%	$H2S$	471	<0.001%
$O3$	31	0.156%			

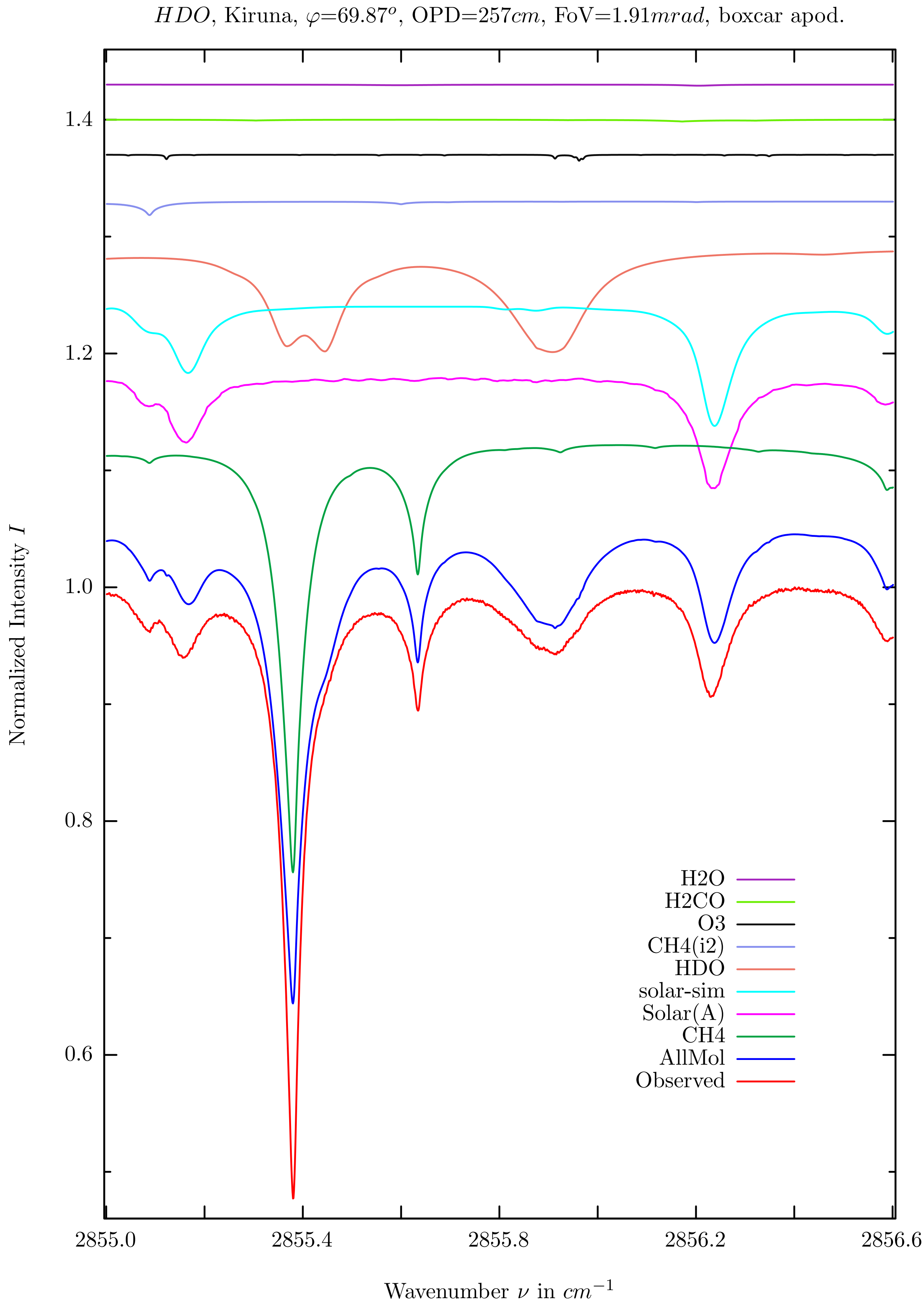

HDO, Kiruna, φ=69.87^o, OPD=257cm, FoV=1.91$mrad$, boxcar apod.
Normalized Intensity I
1.4
1.2
1.0
0.8
0.6
2855.0
2855.4
2855.8
2856.2
2856.6
Wavenumber ν in cm^{-1}
H2O
H2CO
O3
CH4(i2)
HDO
solar-sim
Solar(A)
CH4
AllMol
Observed

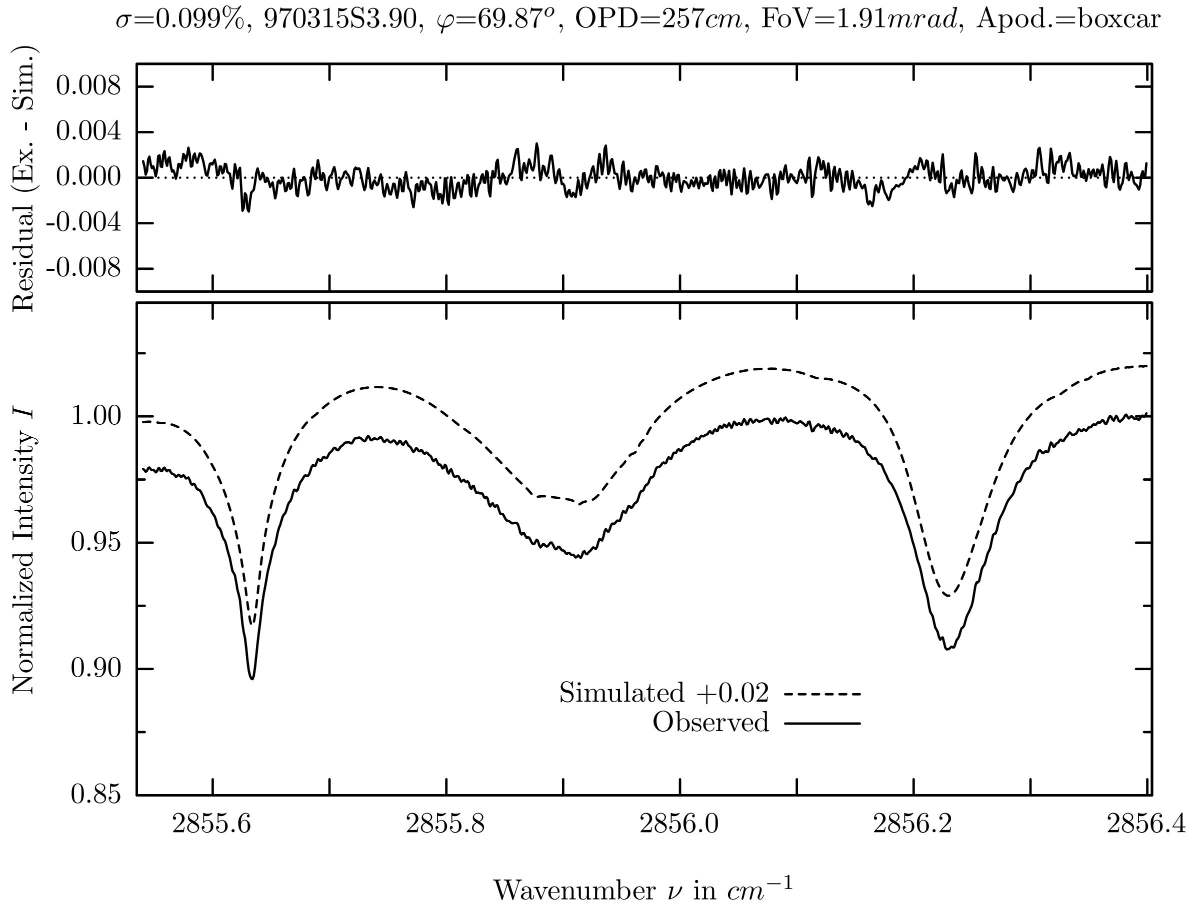

investigated species	:	$HDO, (CH_4)$
line position(s) ν_0	:	2855.8740, 2855.9300, (2855.6328) cm^{-1}
lower state energy E''_{lst}	:	116.5, 743.1, (62.9) cm^{-1}
retrieved TCA, information content	:	3.69E+21, (3.35E+19) $molec/cm^2$, 51.72, 55.4, (97.7)
temperature dependence of the TCA	:	-.610, (-.112)%/K (trop), +.019, (+.161)%/K (strat)
location, date, solar zenith angle	:	Kiruna, 15/Mar/97, 69.87^o
spectral interval fitted	:	2855.540 – 2856.400 cm^{-1}

Molecule	iCode	Absorption	Molecule	iCode	Absorption
$CH4$	61	37.385%	$H2O$	11	0.092%
Solar(A)	—	9.523%	$NO2$	101	0.020%
Solar-sim	—	10.199%	$NH3$	111	<0.001%
HDO	491	8.881%	OH	131	<0.001%
$CH4$	6**2**	1.165%	HCl	151	<0.001%
$O3$	31	0.515%	OCS	191	<0.001%
$H2CO$	201	0.157%	$H2S$	471	<0.001%

CH_4, Kiruna, φ=69.87^o, OPD=257cm, FoV=1.91$mrad$, boxcar apod.

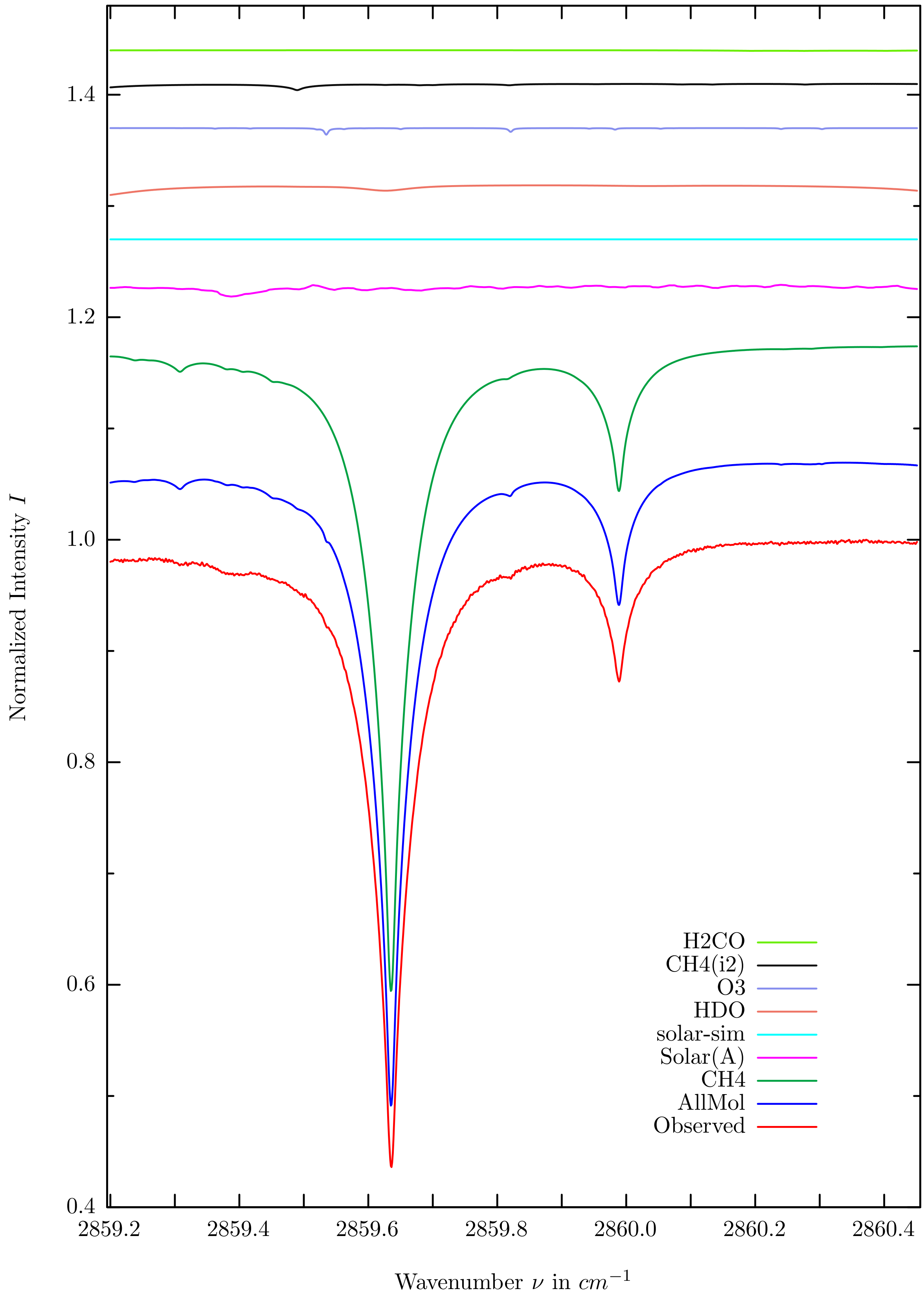

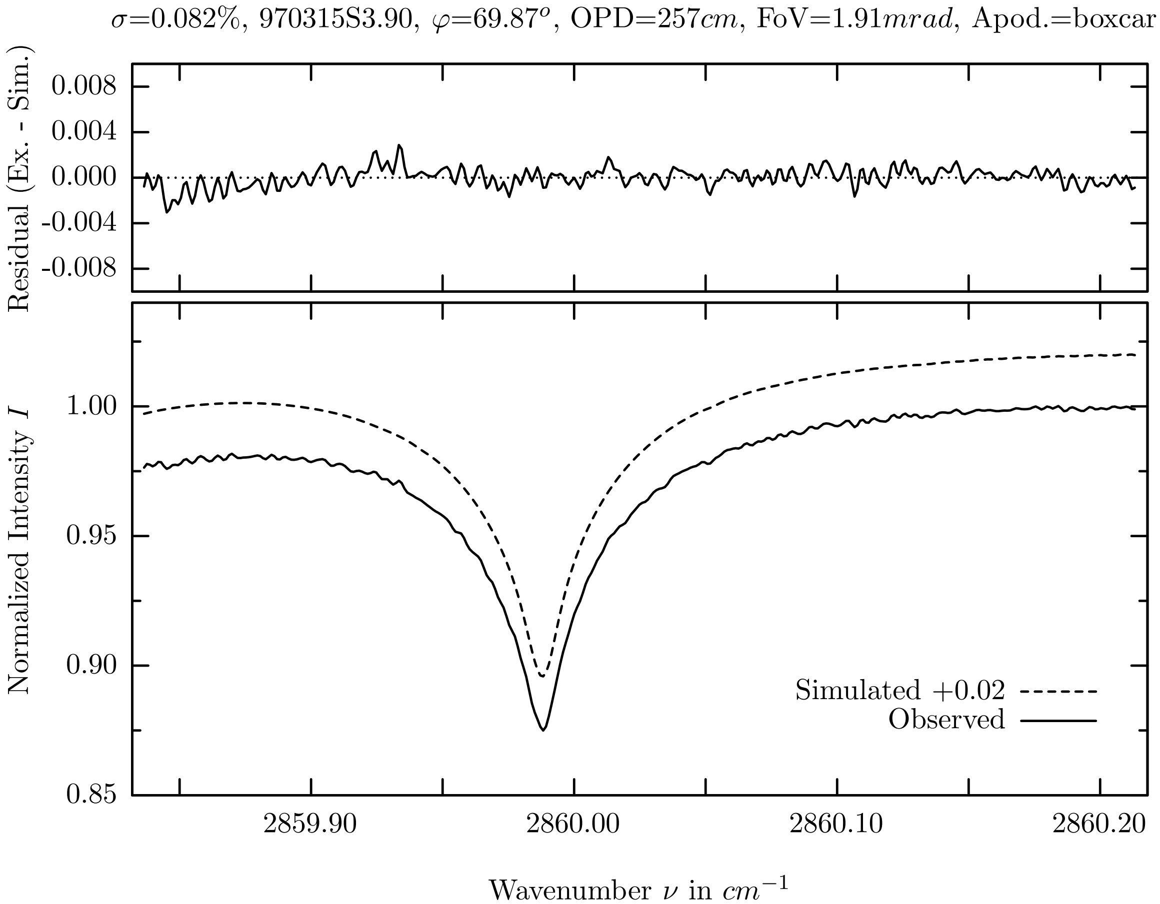

investigated species	:	CH_4
line position(s) ν_0	:	2859.9876 cm^{-1}
lower state energy E''_{lst}	:	104.8 cm^{-1}
retrieved TCA, information content	:	3.40E+19 $molec/cm^2$, 143.9
temperature dependence of the TCA	:	+0.241%/K (trop), +0.022%/K (strat)
location, date, solar zenith angle	:	Kiruna, 15/Mar/97, 69.87^o
spectral interval fitted	:	2859.836 – 2860.214 cm^{-1}

Molecule	iCode	Absorption	Molecule	iCode	Absorption
CH4	61	58.620%	$NO2$	101	0.035%
Solar(A)	—	1.140%	$H2O$	11	0.005%
Solar-sim	—	0.001%	$NH3$	111	<0.001%
HDO	491	1.002%	OH	131	<0.001%
$O3$	31	0.597%	HCl	151	<0.001%
$CH4$	6**2**	0.586%	OCS	191	<0.001%
$H2CO$	201	0.061%	$H2S$	471	<0.001%

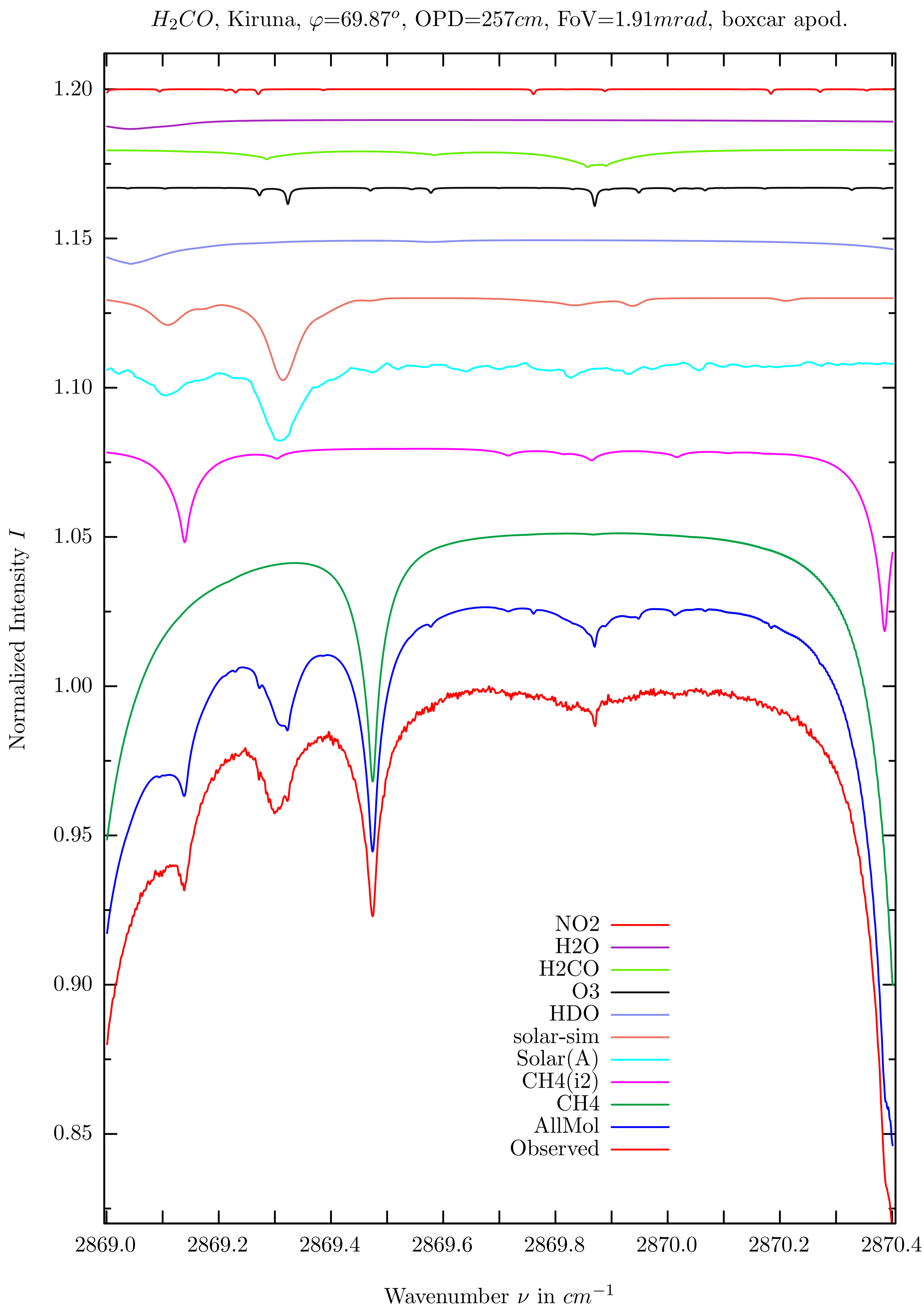

H_2CO, Kiruna, φ=69.87^o, OPD=257cm, FoV=1.91$mrad$, boxcar apod.
Normalized Intensity I
Wavenumber ν in cm^{-1}
1.20
1.15
1.10
1.05
1.00
0.95
0.90
0.85
2869.0
2869.2
2869.4
2869.6
2869.8
2870.0
2870.2
2870.4
NO2
H2O
H2CO
O3
HDO
solar-sim
Solar(A)
CH4(i2)
CH4
AllMol
Observed

σ=0.071%, 970315S3.90, φ=69.87^o, OPD=257cm, FoV=1.91$mrad$, Apod.=boxcar

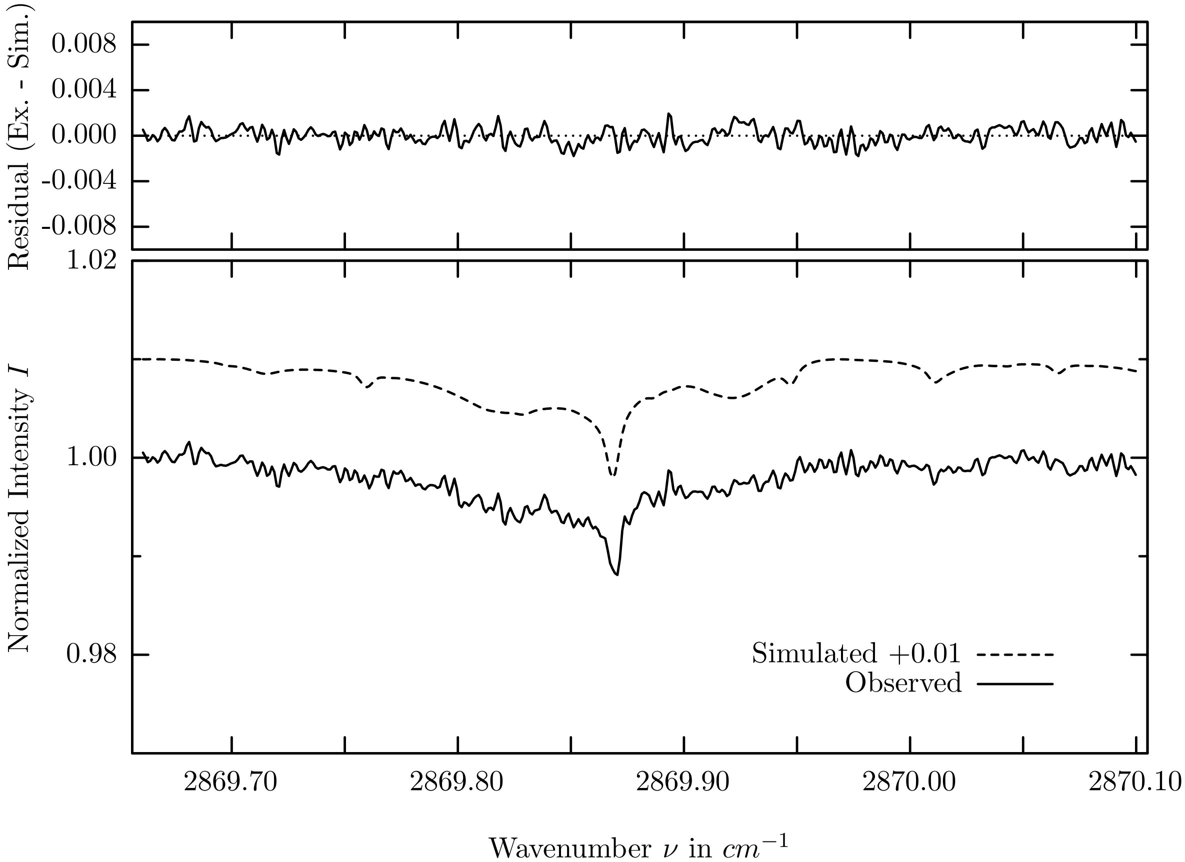

investigated species	:	H_2CO
line position(s) ν_0	:	2869.8555, (2869.8895) cm^{-1}
lower state energy E''_{lst}	:	190.8, (92.6) cm^{-1}
retrieved TCA, information content	:	1.24E+15 $molec/cm^2$, 4.7, 3.4
temperature dependence of the TCA	:	-0.225%/K (trop), +0.060%/K (strat)
location, date, solar zenith angle	:	Kiruna, 15/Mar/97, 69.87^o
spectral interval fitted	:	2869.660 – 2870.100 cm^{-1}

Molecule	iCode	Absorption	Molecule	iCode	Absorption
$CH4$	61	16.460%	$NO2$	101	0.168%
$CH4$	6**2**	6.167%	$N2O$	41	0.018%
Solar(A)	—	2.779%	OCS	191	0.001%
Solar-sim	—	2.748%	$NH3$	111	<0.001%
HDO	491	0.852%	OH	131	<0.001%
$O3$	31	0.620%	HCl	151	<0.001%
H2CO	201	0.610%	$H2S$	471	<0.001%
$H2O$	11	0.332%			

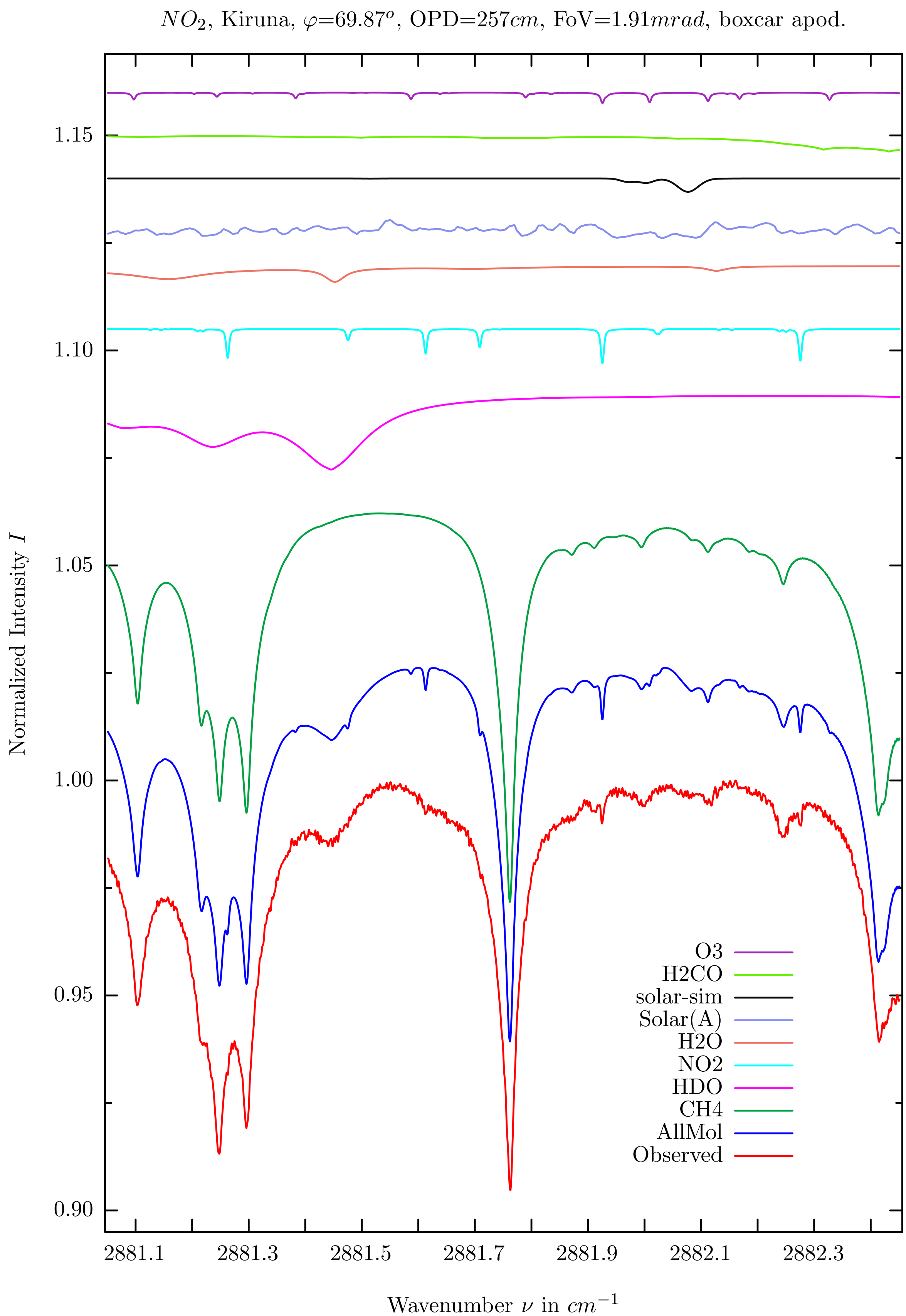
NO_2, Kiruna, φ=69.87^o, OPD=257cm, FoV=1.91$mrad$, boxcar apod.
Normalized Intensity I
1.15
1.10
1.05
1.00
0.95
0.90
2881.1
2881.3
2881.5
2881.7
2881.9
2882.1
2882.3
Wavenumber ν in cm^{-1}
O3
H2CO
solar-sim
Solar(A)
H2O
NO2
HDO
CH4
AllMol
Observed

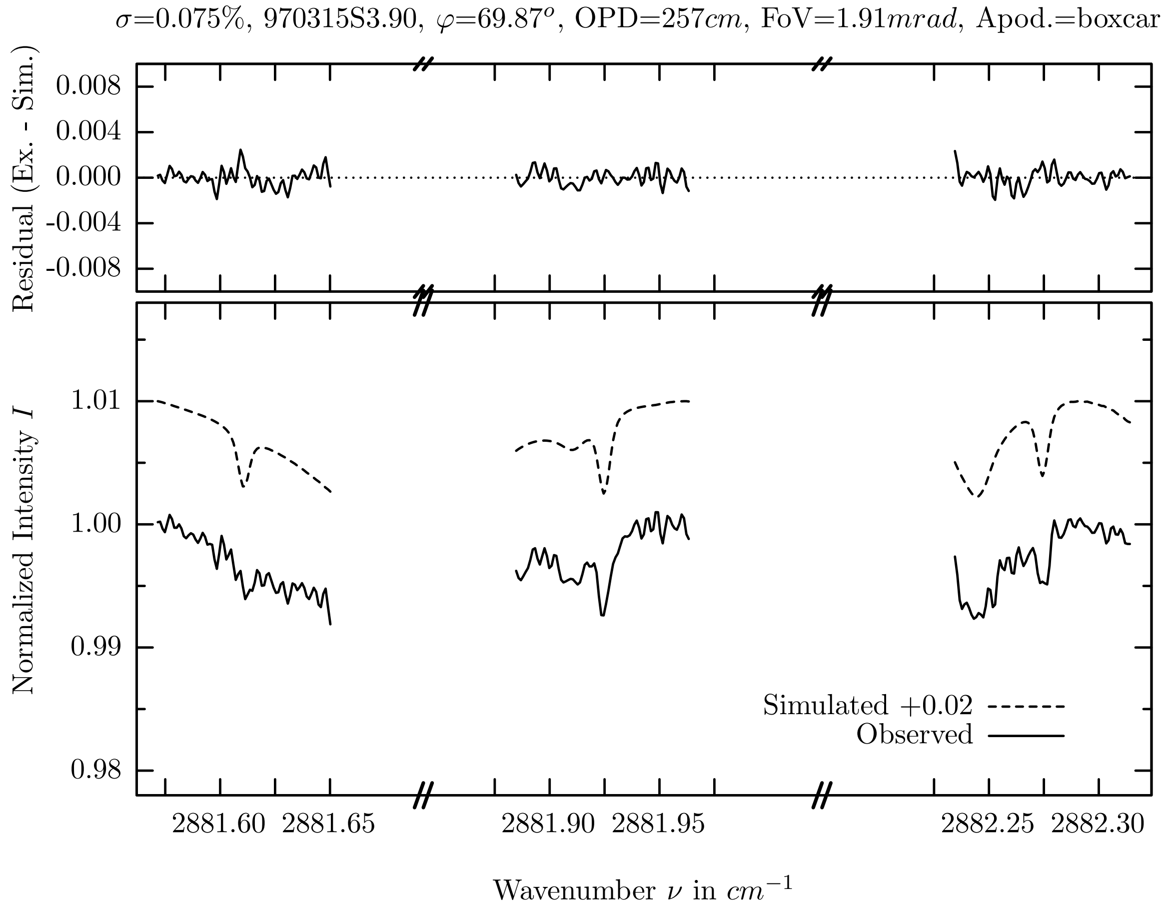

investigated species	:	NO_2
line position(s) ν_0	:	2881.6114, 2881.9236, 2882.2739 cm^{-1}
lower state energy E''_{lst}	:	321.4, 277.8, 284.1 cm^{-1}
retrieved TCA, information content	:	2.91E+15 $molec/cm^2$, 5.4, 9.3, 6.7
temperature dependence of the TCA	:	-0.050%/K (trop), -0.356%/K (strat)
location, date, solar zenith angle	:	Kiruna, 15/Mar/97, 69.87^o
spectral interval fitted	:	2881.571 – 2881.651, 2881.884 – 2881.964, cm^{-1}
spectral interval fitted	:	and 2882.234 – 2882.314 cm^{-1}

Molecule	iCode	Absorption	Molecule	iCode	Absorption
$CH4$	61	11.541%	$O3$	31	0.251%
HDO	491	1.966%	OCS	191	0.008%
NO2	101	0.815%	$NH3$	111	<0.001%
$H2O$	11	0.391%	OH	131	<0.001%
Solar(A)	—	0.390%	HCl	151	<0.001%
Solar-sim	—	0.310%	$H2S$	471	<0.001%
$H2CO$	201	0.374%			

Comment: Simultaneous 3-microwindow fit

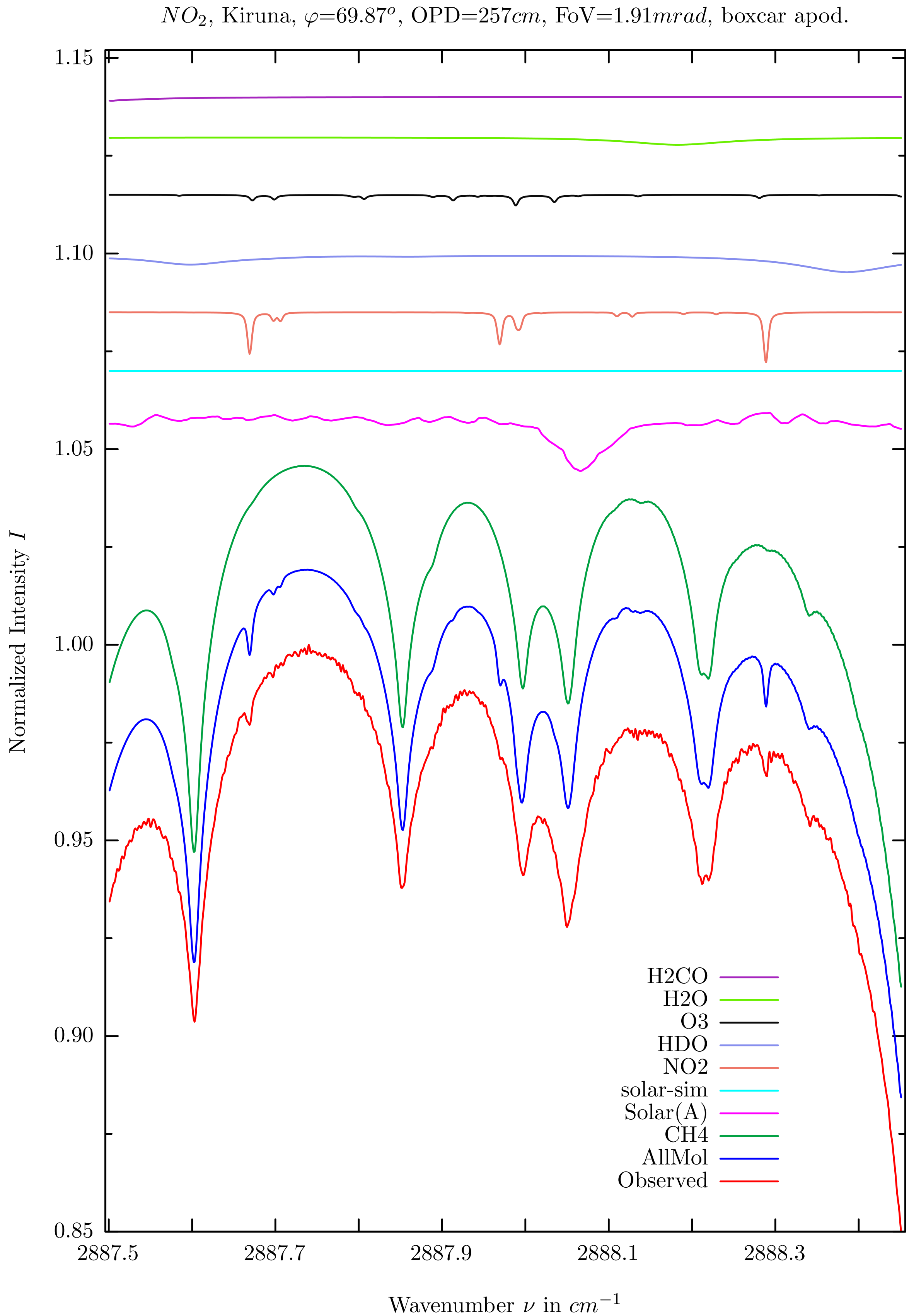

NO_2, Kiruna, φ=69.87^o, OPD=257cm, FoV=1.91$mrad$, boxcar apod.
1.15
1.10
1.05
1.00
0.95
0.90
0.85
Normalized Intensity I
2887.5
2887.7
2887.9
2888.1
2888.3
Wavenumber ν in cm^{-1}
H2CO
H2O
O3
HDO
NO2
solar-sim
Solar(A)
CH4
AllMol
Observed

σ=0.056%, 970315S3.90, φ=69.87^o, OPD=257cm, FoV=1.91$mrad$, Apod.=boxcar

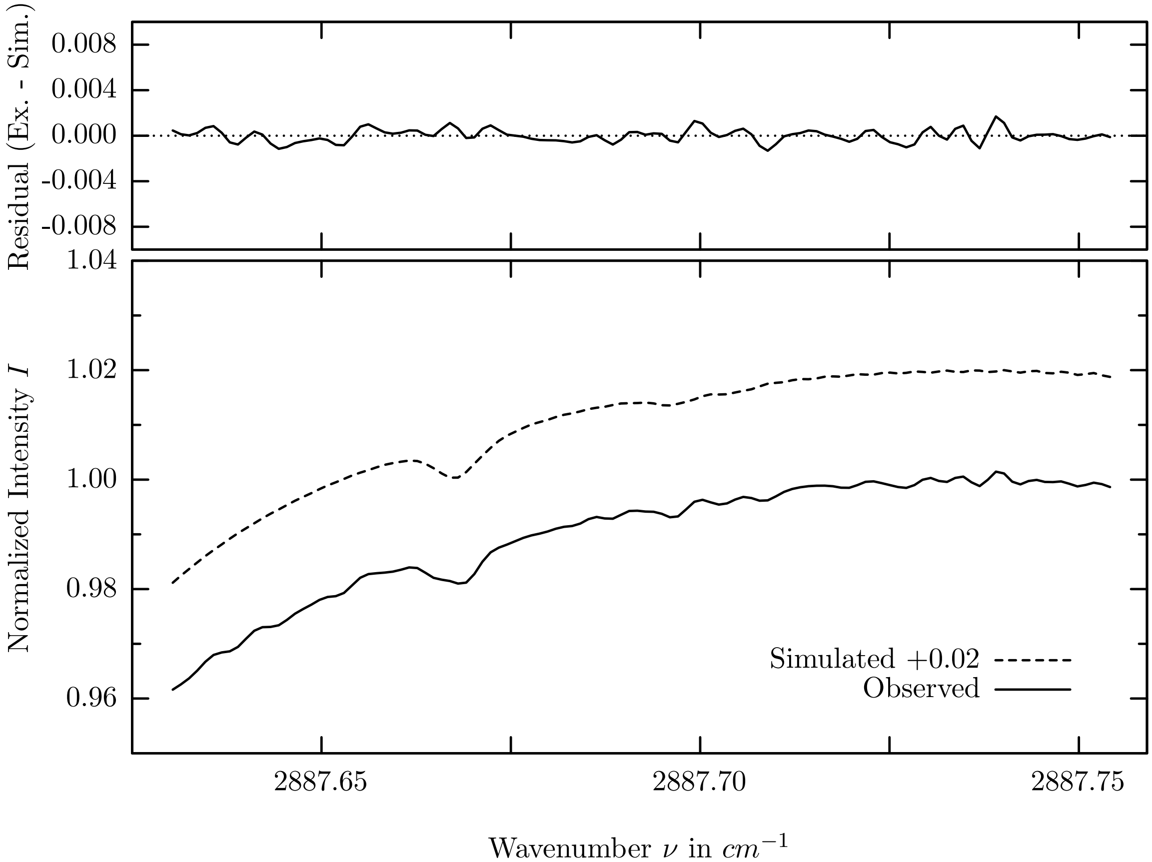

investigated species	:	NO_2
line position(s) ν_0	:	2887.6673, 2887.6679 cm^{-1}
lower state energy E''_{lst}	:	190.6, 190.6 cm^{-1}
retrieved TCA, information content	:	2.29E+15 $molec/cm^2$, 12.0
temperature dependence of the TCA	:	-0.122%/K (trop), -0.089%/K (strat)
location, date, solar zenith angle	:	Kiruna, 15/Mar/97, 69.87^o
spectral interval fitted	:	2887.630 – 2887.755 cm^{-1}

Molecule	iCode	Absorption	Molecule	iCode	Absorption
$CH4$	61	16.975%	$H2CO$	201	0.096%
Solar(A)	—	1.560%	OCS	191	0.032%
Solar-sim	—	0.002%	$NH3$	111	<0.001%
NO2	101	1.297%	OH	131	<0.001%
HDO	491	0.481%	HCl	151	<0.001%
$O3$	31	0.277%	$H2S$	471	<0.001%
$H2O$	11	0.220%			

NO_2, Kiruna, φ=69.87^o, OPD=257cm, FoV=1.91$mrad$, boxcar apod.

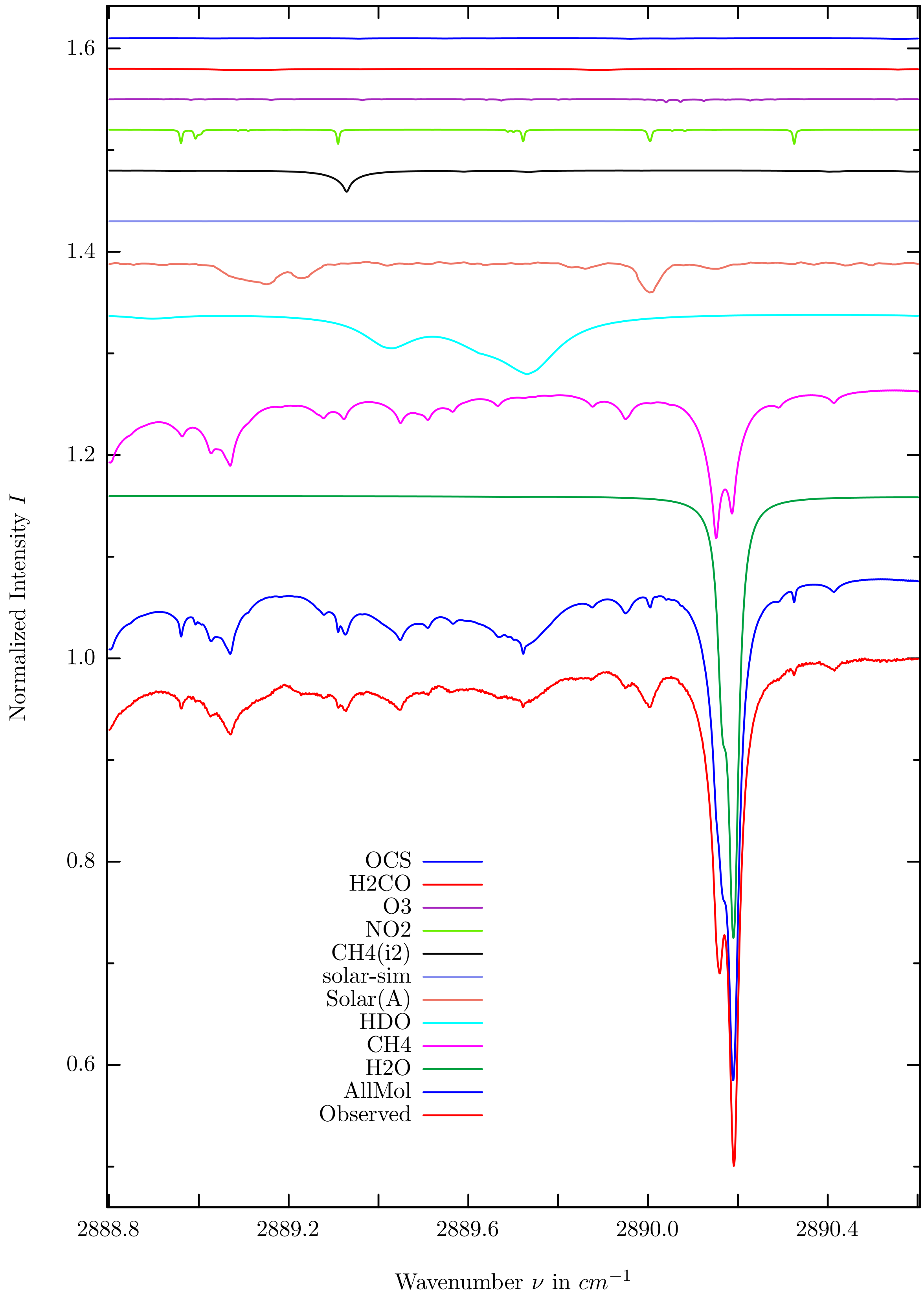

σ=0.067%, 970315S3.90, φ=69.87^o, OPD=257cm, FoV=1.91$mrad$, Apod.=boxcar

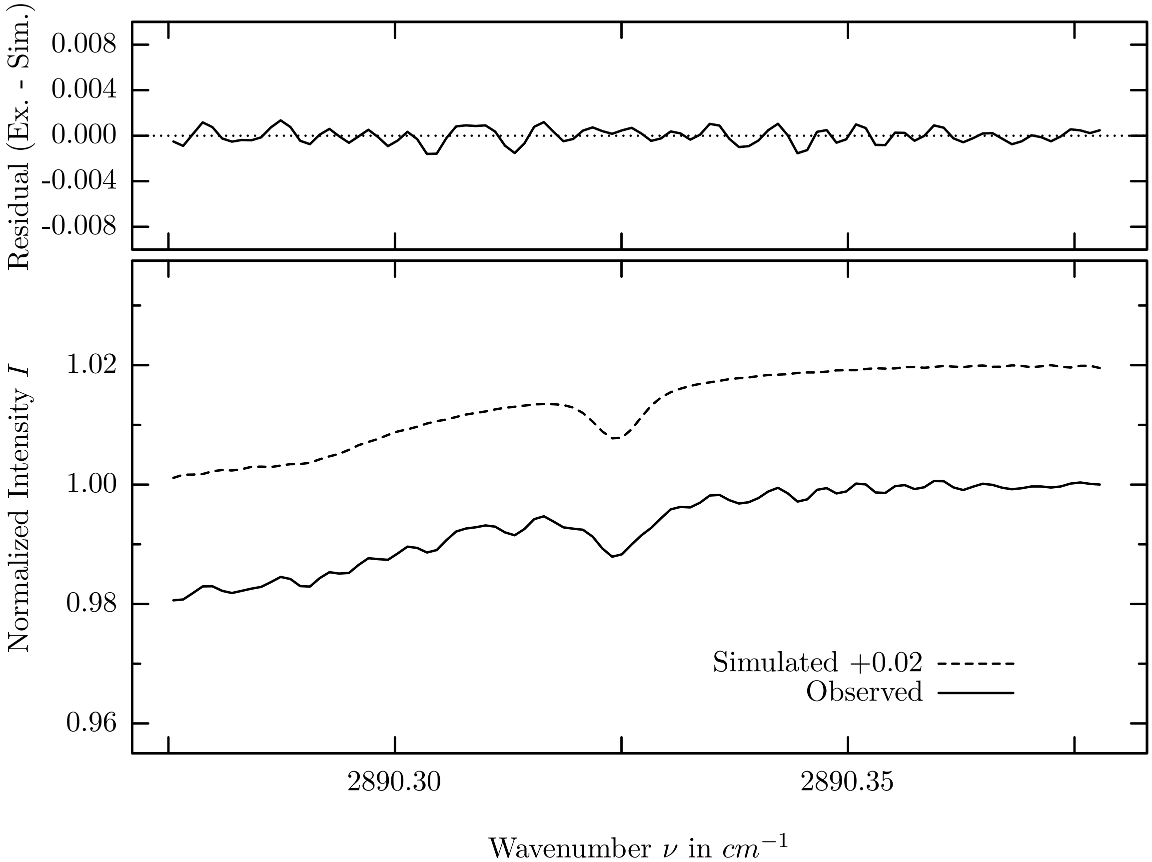

investigated species	:	NO_2
line position(s) ν_0	:	2890.3238, 2890.3241 cm^{-1}
lower state energy E''_{lst}	:	134.9, 134.9 cm^{-1}
retrieved TCA, information content	:	2.38E+15 $molec/cm^2$, 12.74
temperature dependence of the TCA	:	-0.050%/K (trop), +0.004%/K (strat)
location, date, solar zenith angle	:	Kiruna, 15/Mar/97, 69.87^o
spectral interval fitted	:	2890.275 – 2890.378 cm^{-1}

Molecule	iCode	Absorption	Molecule	iCode	Absorption
$H2O$	11	43.532%	$O3$	31	0.310%
$CH4$	61	15.203%	$H2CO$	201	0.137%
HDO	491	6.055%	OCS	191	0.068%
Solar(A)	—	3.011%	$NH3$	111	<0.001%
Solar-sim	—	0.002%	OH	131	<0.001%
$CH4$	6**2**	2.104%	HCl	151	<0.001%
NO2	101	1.416%	$H2S$	471	<0.001%

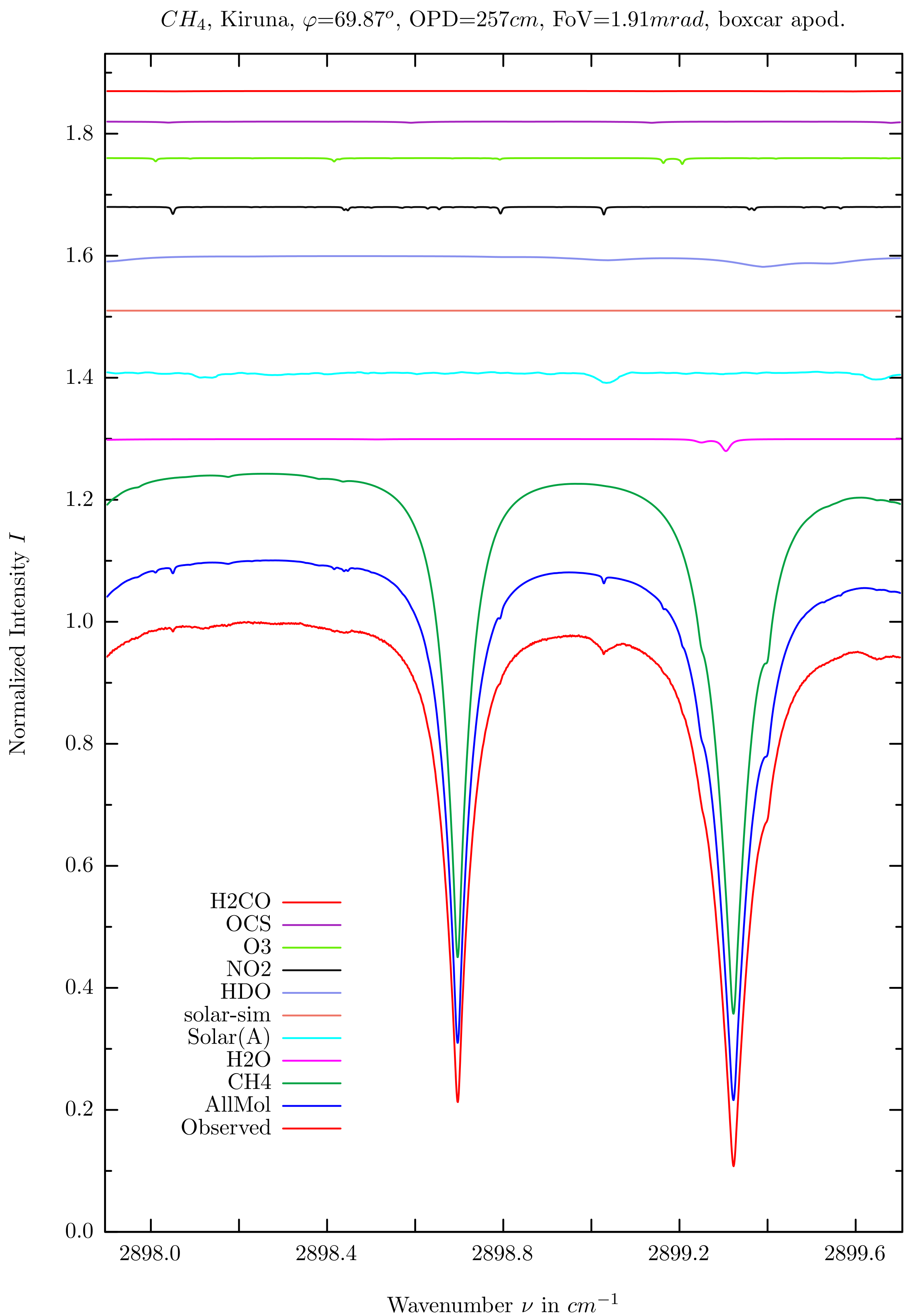

CH_4, Kiruna, φ=69.87^o, OPD=257cm, FoV=1.91$mrad$, boxcar apod.
Normalized Intensity I
Wavenumber ν in cm^{-1}
0.0
0.2
0.4
0.6
0.8
1.0
1.2
1.4
1.6
1.8
2898.0
2898.4
2898.8
2899.2
2899.6
H2CO
OCS
O3
NO2
HDO
solar-sim
Solar(A)
H2O
CH4
AllMol
Observed

σ=0.075%, 970315S3.90, φ=69.87^o, OPD=257cm, FoV=1.91$mrad$, Apod.=boxcar

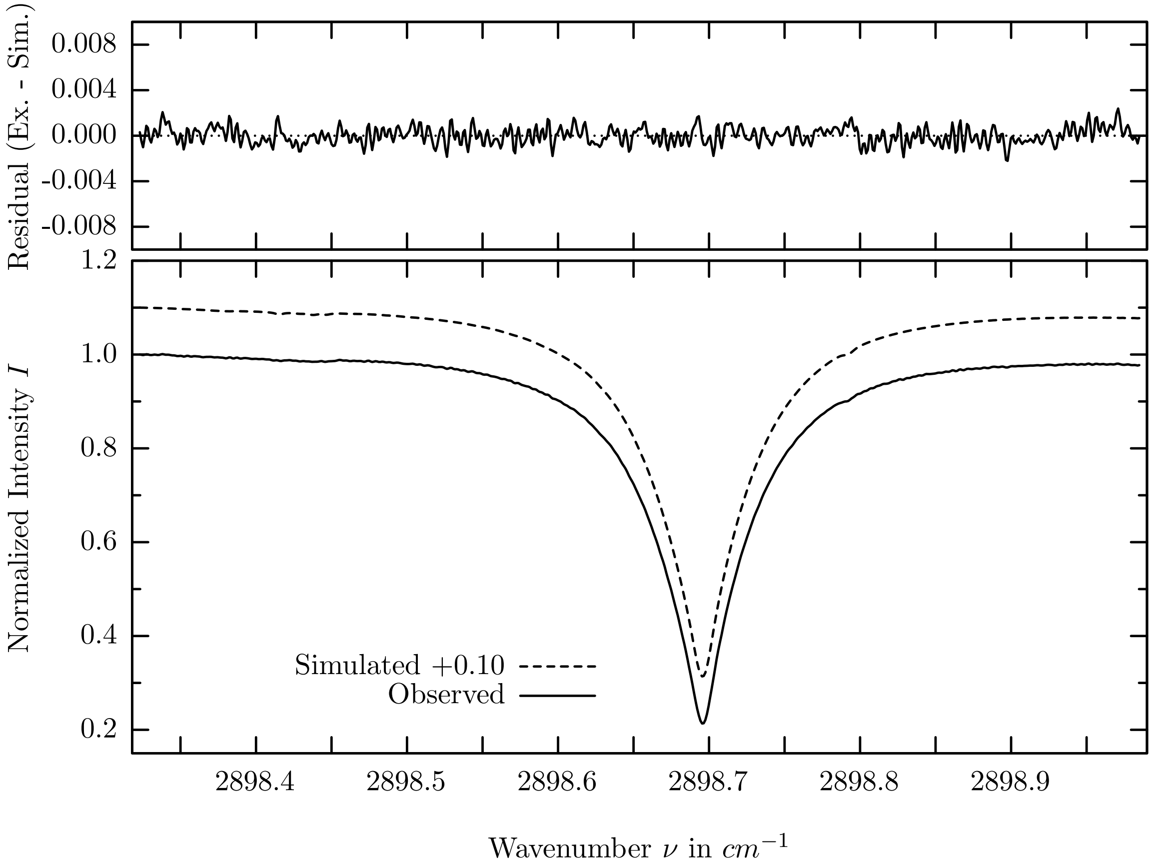

investigated species	:	CH_4
line position(s) ν_0	:	2898.6953 cm^{-1}
lower state energy E''_{lst}	:	157.1 cm^{-1}
retrieved TCA, information content	:	3.34E+19 $molec/cm^2$, 1051.6
temperature dependence of the TCA	:	+0.214%/K (trop), +0.003%/K (strat)
location, date, solar zenith angle	:	Kiruna, 15/Mar/97, 69.87^o
spectral interval fitted	:	2898.322 – 2898.985 cm^{-1}

Molecule	iCode	Absorption	Molecule	iCode	Absorption
CH4	61	91.293%	*OCS*	191	0.221%
H2O	11	2.020%	*H2CO*	201	0.070%
Solar(A)	—	1.840%	*NH*3	111	<0.001%
Solar-sim	—	<0.001%	*OH*	131	<0.001%
HDO	491	1.824%	*HCl*	151	<0.001%
*NO*2	101	1.272%	*H2S*	471	<0.001%
*O*3	31	0.984%			

CH_4, Kiruna, φ=69.87^o, OPD=257cm, FoV=1.91$mrad$, boxcar apod.

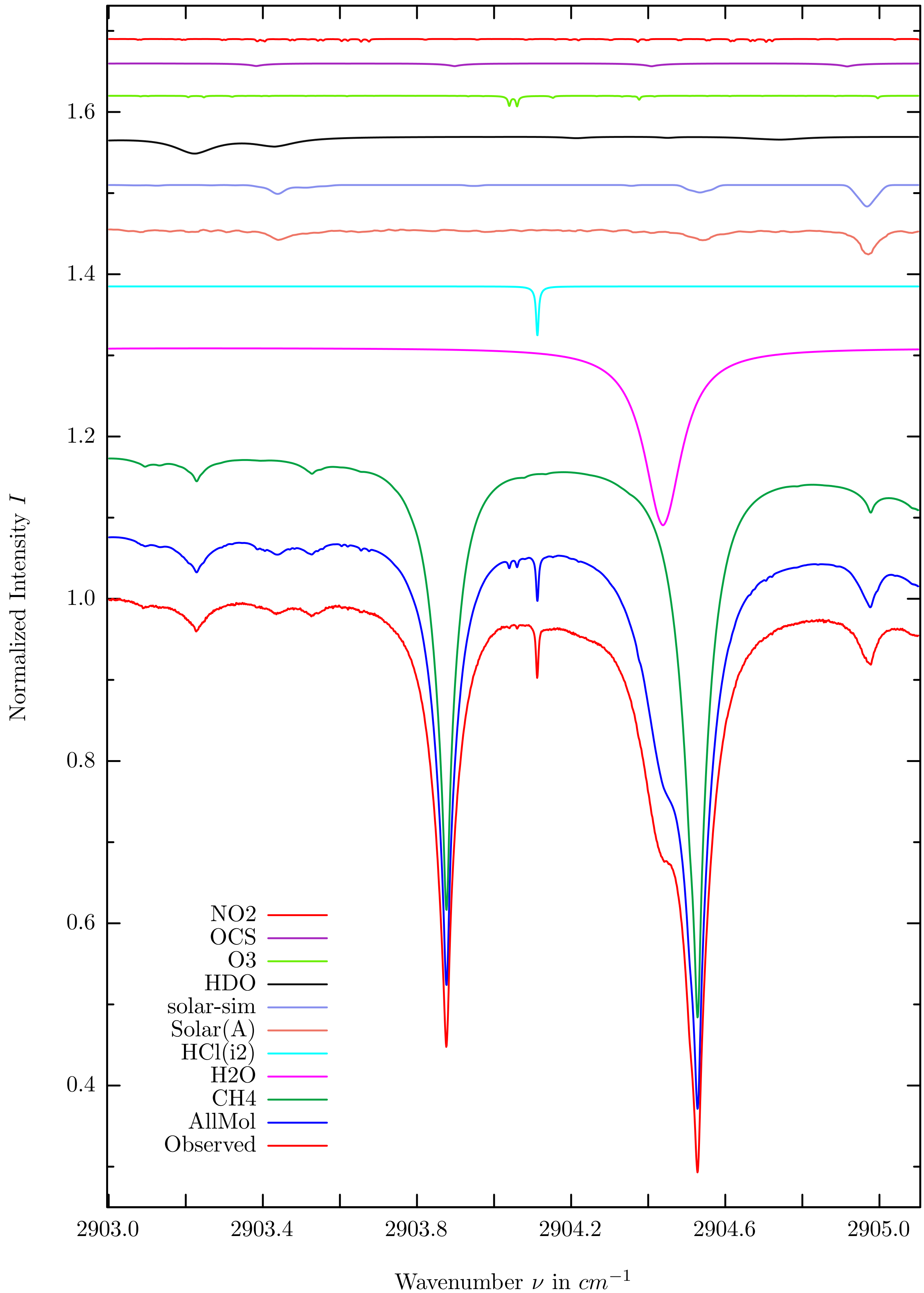

σ=0.074%, 970315S3.90, φ=69.87^o, OPD=257cm, FoV=1.91$mrad$, Apod.=boxcar

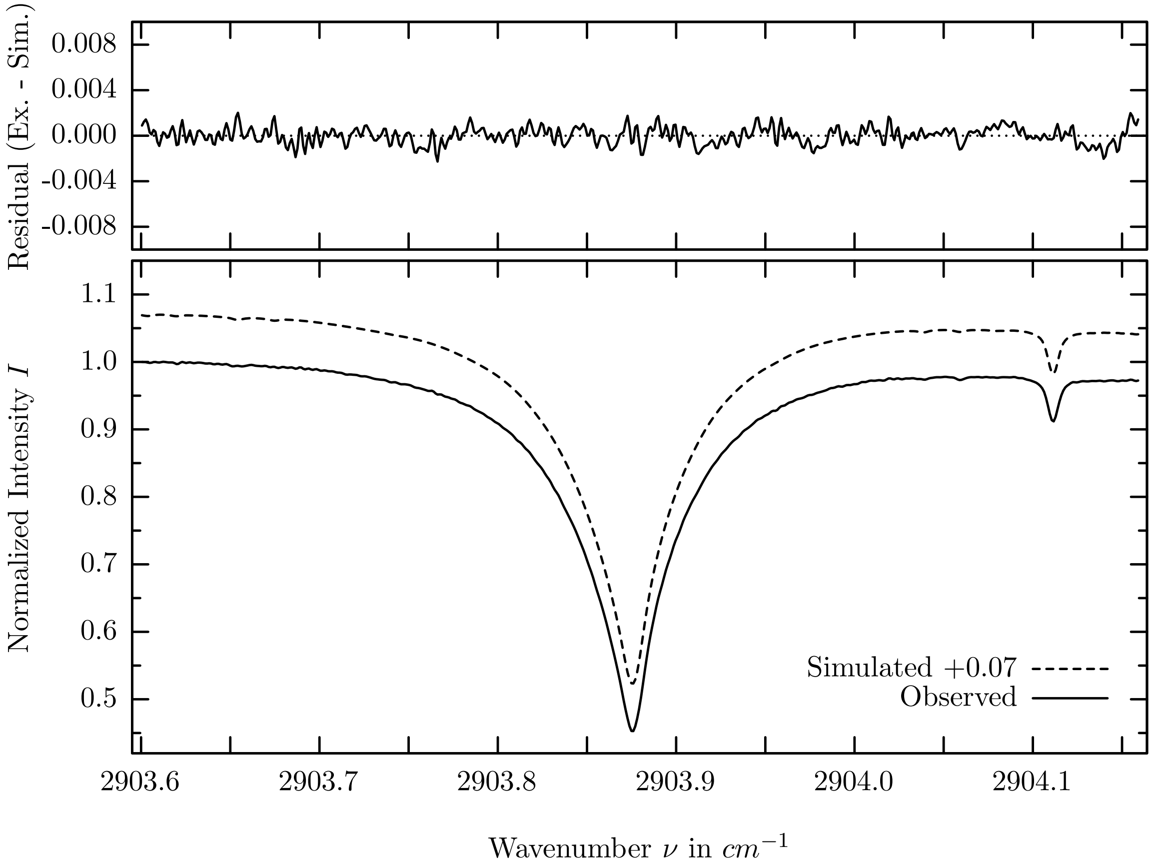

investigated species	:	$CH_4, (HCl(i2))$
line position(s) ν_0	:	2903.8757, (2904.1110) cm^{-1}
lower state energy E''_{lst}	:	219.9, (0.0) cm^{-1}
retrieved TCA, information content	:	3.38E+19, (3.19E+15) $molec/cm^2$, 734.4, (92.1)
temperature dependence of the TCA	:	-.087, (-.119)%/K (trop), -.019, (+.320)%/K (strat)
location, date, solar zenith angle	:	Kiruna, 15/Mar/97, 69.87^o
spectral interval fitted	:	2903.600 – 2904.160 cm^{-1}

Molecule	iCode	Absorption	Molecule	iCode	Absorption
CH4	61	70.652%	*NO2*	101	0.372%
H2O	11	21.937%	*H2CO*	201	0.041%
HCl	15**2**	6.128%	*HCl*	151	0.001%
Solar(A)	—	3.049%	*NH3*	111	<0.001%
Solar-sim	—	2.646%	*OH*	131	<0.001%
HDO	491	2.127%	*CH3Cl*	301	<0.001%
O3	31	1.329%	*H2S*	471	<0.001%
OCS	191	0.382%			

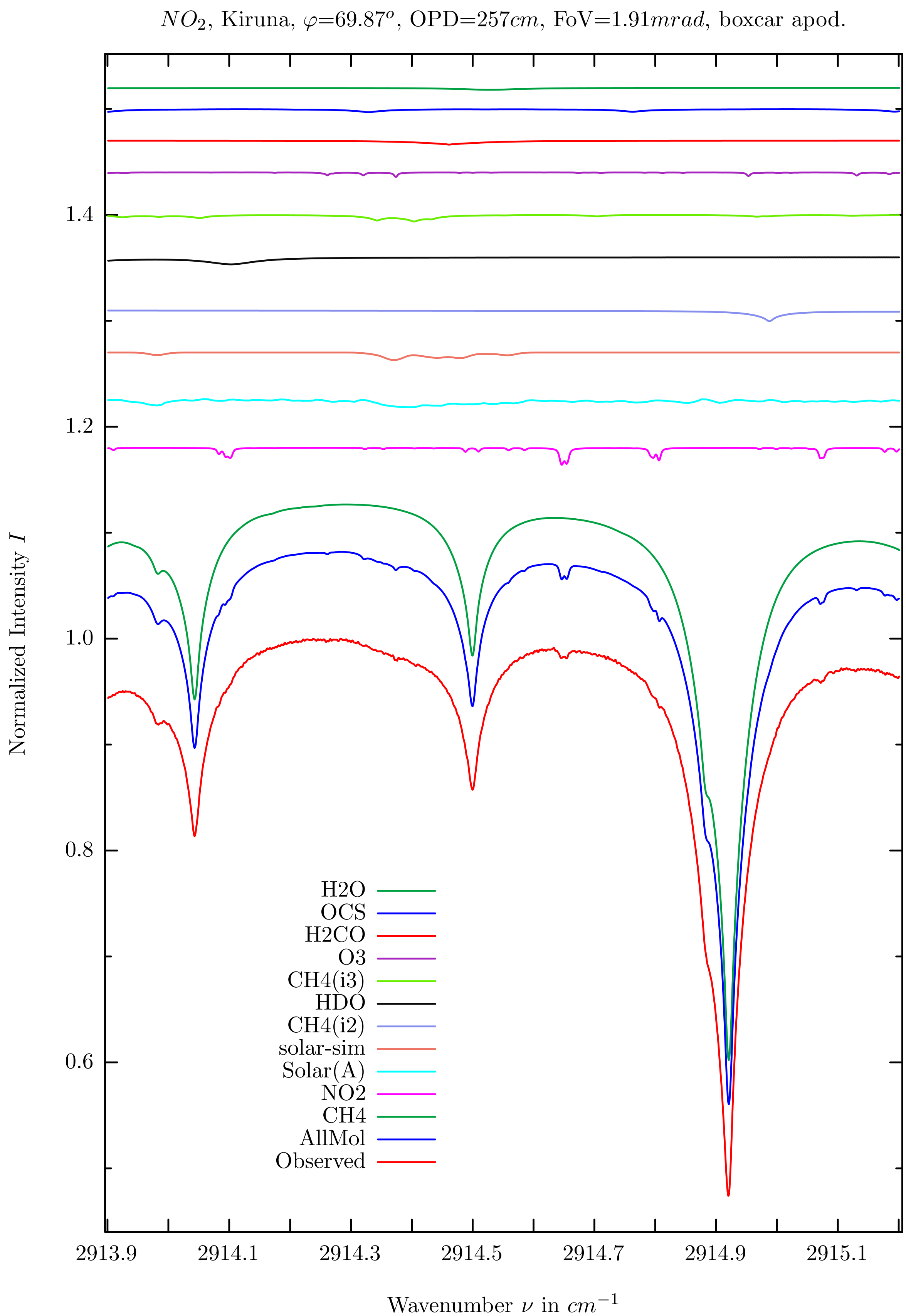
NO_2, Kiruna, φ=69.87^o, OPD=257cm, FoV=1.91$mrad$, boxcar apod.
Normalized Intensity I
1.4
1.2
1.0
0.8
0.6
2913.9
2914.1
2914.3
2914.5
2914.7
2914.9
2915.1
Wavenumber ν in cm^{-1}
H2O
OCS
H2CO
O3
CH4(i3)
HDO
CH4(i2)
solar-sim
Solar(A)
NO2
CH4
AllMol
Observed

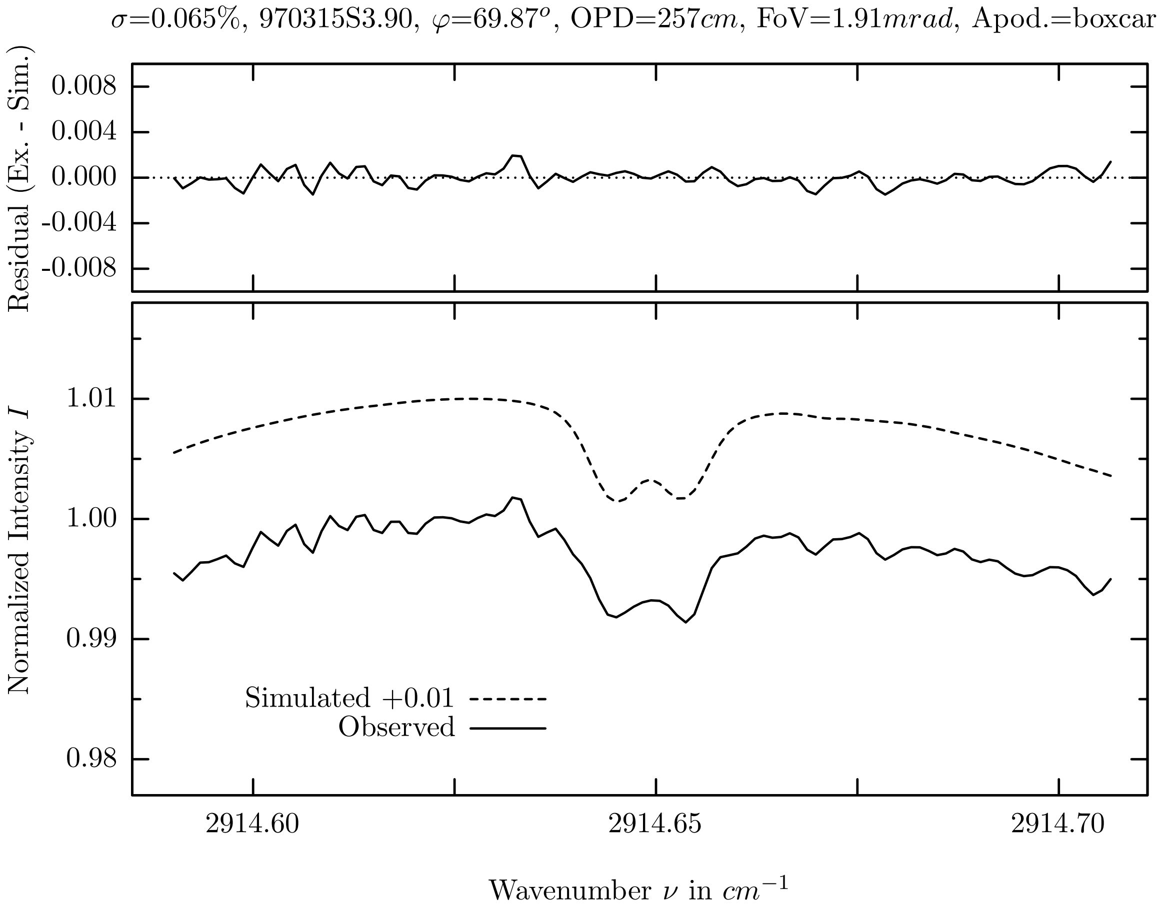

investigated species	:	NO_2
line position(s) ν_0	:	2914.6434*), 2914.6520*) cm^{-1}
lower state energy E''_{lst}	:	46.4, 54.6 cm^{-1}
retrieved TCA, information content	:	2.25E+15 $molec/cm^2$, 12.8, 11.74
temperature dependence of the TCA	:	-0.102%/K (trop), +0.282%/K (strat)
location, date, solar zenith angle	:	Kiruna, 15/Mar/97, 69.87^o
spectral interval fitted	:	2914.590 – 2914.707 cm^{-1}

Molecule	iCode	Absorption	Molecule	iCode	Absorption
$CH4$	61	55.816%	$H2CO$	201	0.372%
NO2	101	1.606%	OCS	191	0.314%
Solar(A)	—	1.160%	$H2O$	11	0.200%
Solar-sim	—	0.708%	$CH3Cl$	301	0.001%
$CH4$	6**2**	1.044%	OH	131	<0.001%
HDO	491	0.677%	HCl	151	<0.001%
$CH4$	6**3**	0.636%	$C2H4$	391	<0.001%
$O3$	31	0.428%	$H2S$	471	<0.001%

NO_2, Kiruna, φ=69.87^o, OPD=257cm, FoV=1.91$mrad$, boxcar apod.

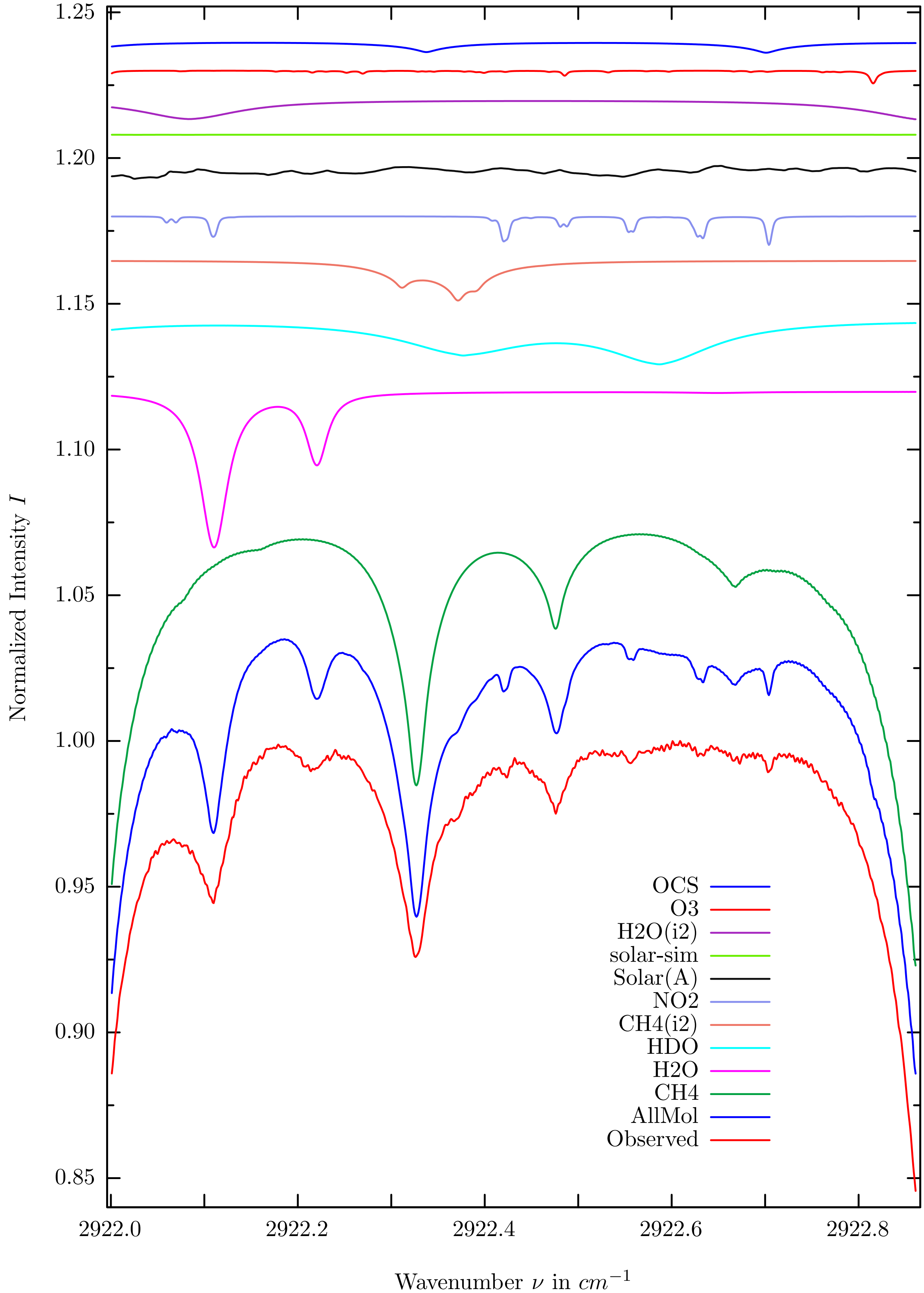

σ=0.065%, 970315S3.90, φ=69.87^o, OPD=257cm, FoV=1.91$mrad$, Apod.=boxcar

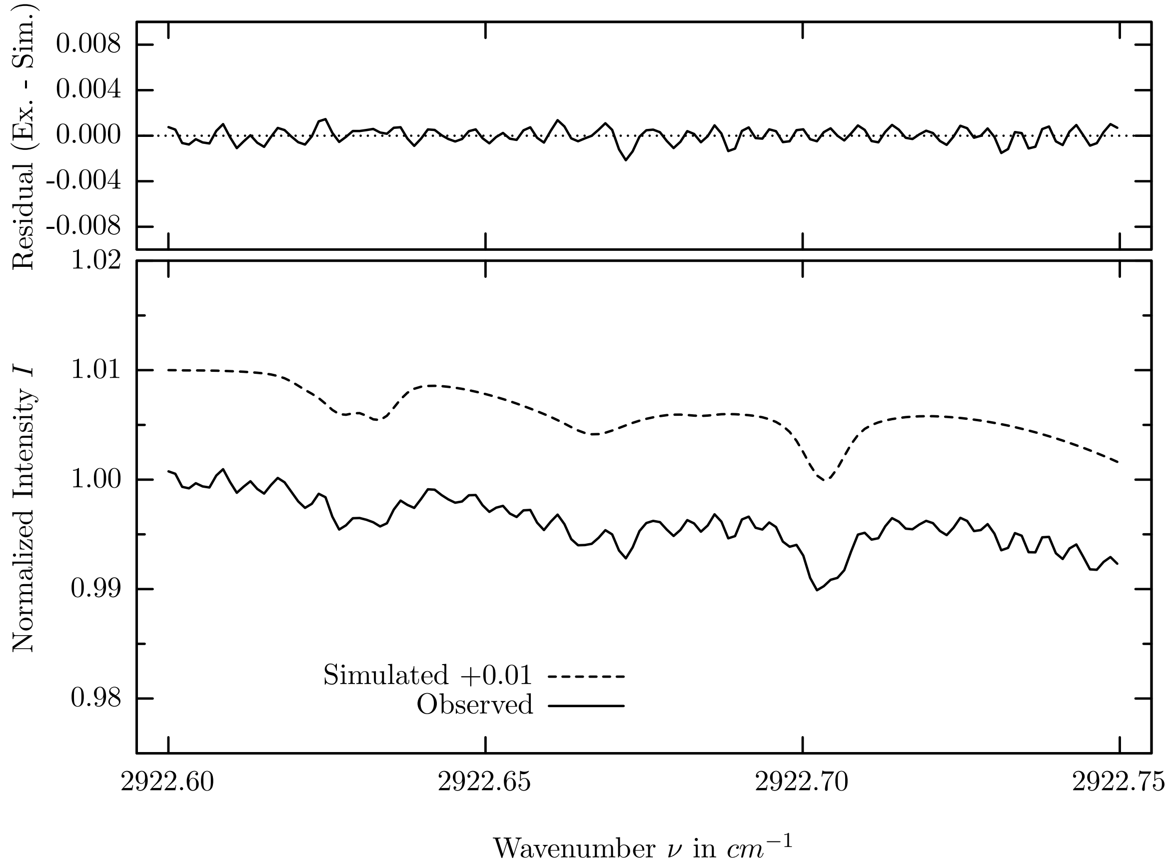

investigated species	:	NO_2
line position(s) ν_0	:	2922.6261, 2922.6327, 2922.7015 cm^{-1}
lower state energy E''_{lst}	:	237.1, 237.1, 233.9 cm^{-1}
retrieved TCA, information content	:	2.18E+15 $molec/cm^2$, 5.1, 5.8, 10.6
temperature dependence of the TCA	:	+0.099%/K (trop), -0.300%/K (strat)
location, date, solar zenith angle	:	Kiruna, 15/Mar/97, 69.87^o
spectral interval fitted	:	2922.599 – 2922.750 cm^{-1}

Molecule	iCode	Absorption	Molecule	iCode	Absorption
$CH4$	61	18.151%	OCS	191	0.384%
$H2O$	11	5.365%	$CH3Cl$	301	0.003%
HDO	491	1.578%	$H2CO$	201	0.002%
$CH4$	6**2**	1.391%	$C2H4$	391	0.001%
NO2	101	0.990%	$NH3$	111	<0.001%
Solar(A)	—	0.711%	OH	131	<0.001%
Solar-sim	—	0.003%	HCl	151	<0.001%
$H2O$	1**2**	0.674%	$H2S$	471	<0.001%
$O3$	31	0.443%			

HCl (i2), Kiruna, φ=69.87^o, OPD=257cm, FoV=1.91$mrad$, boxcar apod.

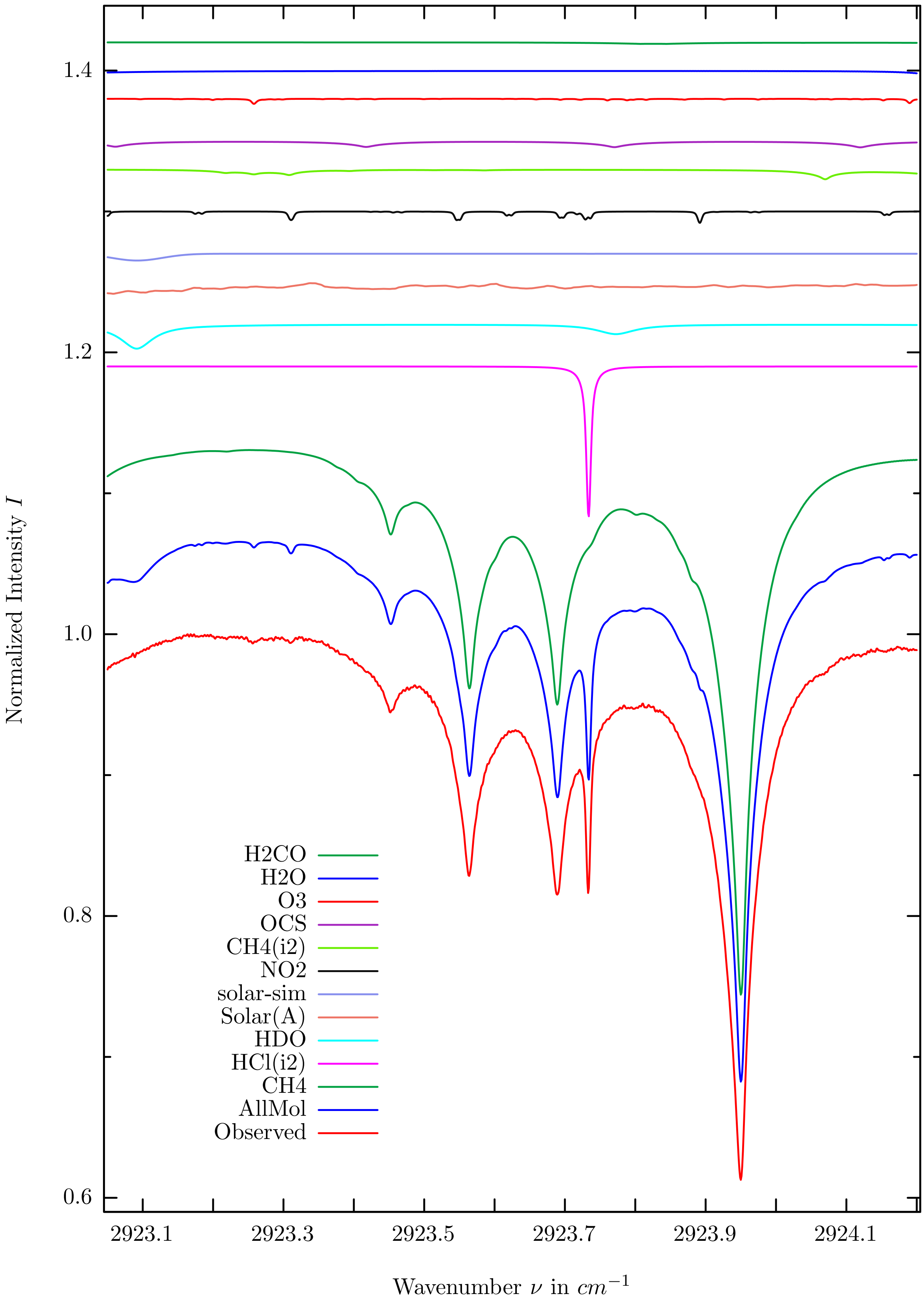

σ=0.071%, 970315S3.90, φ=69.87^o, OPD=257cm, FoV=1.91$mrad$, Apod.=boxcar

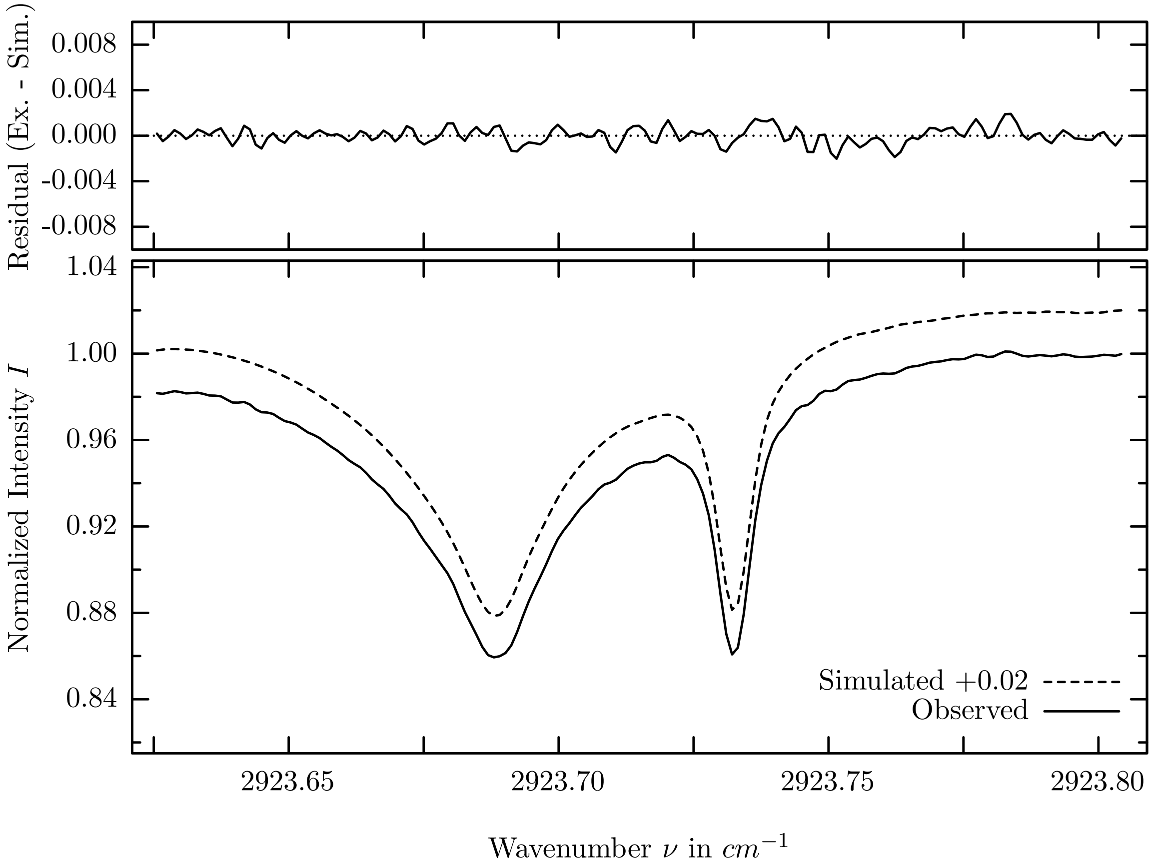

investigated species	:	$HCl(i2), (CH_4)$
line position(s) ν_0	:	2923.7322, (2923.6880) cm^{-1}
lower state energy E''_{lst}	:	20.8, (293.2) cm^{-1}
retrieved TCA, information content	:	2.78E+15, (3.26E+19) $molec/cm^2$, 159.3, (198.7)
temperature dependence of the TCA	:	-.933, (-.582)%/K (trop), -.095, (+.086)%/K (strat)
location, date, solar zenith angle	:	Kiruna, 15/Mar/97, 69.87^o
spectral interval fitted	:	2923.625 – 2923.805 cm^{-1}

Molecule	iCode	Absorption	Molecule	iCode	Absorption
$CH4$	61	41.536%	$H2O$	11	0.195%
HCl	15**2**	10.733%	$H2CO$	201	0.108%
HDO	491	1.737%	$CH3Cl$	301	0.003%
Solar(A)	—	0.840%	HCl	151	0.001%
Solar-sim	—	0.483%	$C2H4$	391	0.001%
NO2	101	0.819%	$NH3$	111	<0.001%
$CH4$	6**2**	0.715%	OH	131	<0.001%
OCS	191	0.450%	$H2S$	471	<0.001%
$O3$	31	0.367%			

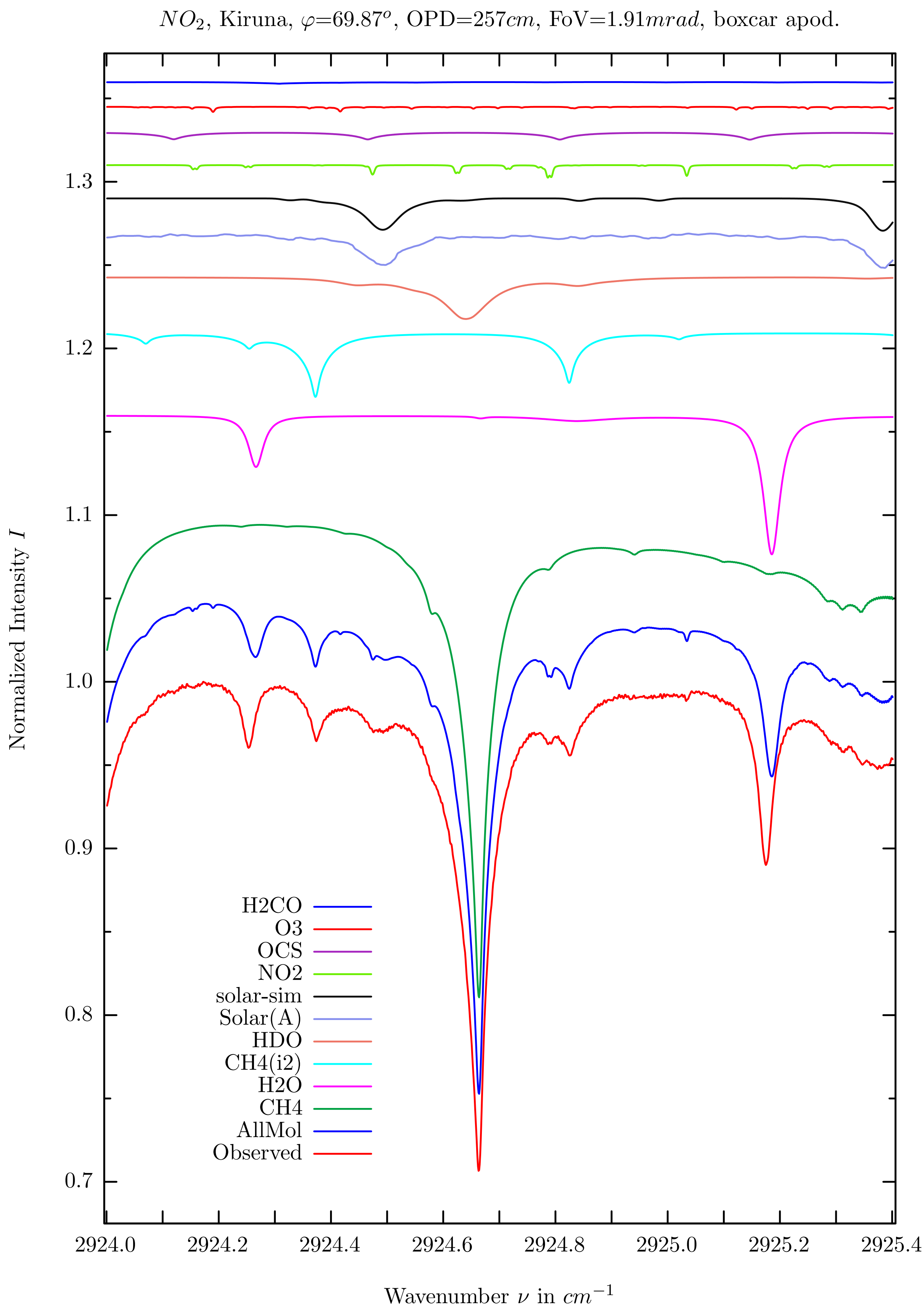

NO_2, Kiruna, φ=69.87^o, OPD=257cm, FoV=1.91$mrad$, boxcar apod.
Normalized Intensity I
1.3
1.2
1.1
1.0
0.9
0.8
0.7
H2CO
O3
OCS
NO2
solar-sim
Solar(A)
HDO
CH4(i2)
H2O
CH4
AllMol
Observed
2924.0
2924.2
2924.4
2924.6
2924.8
2925.0
2925.2
2925.4
Wavenumber ν in cm^{-1}

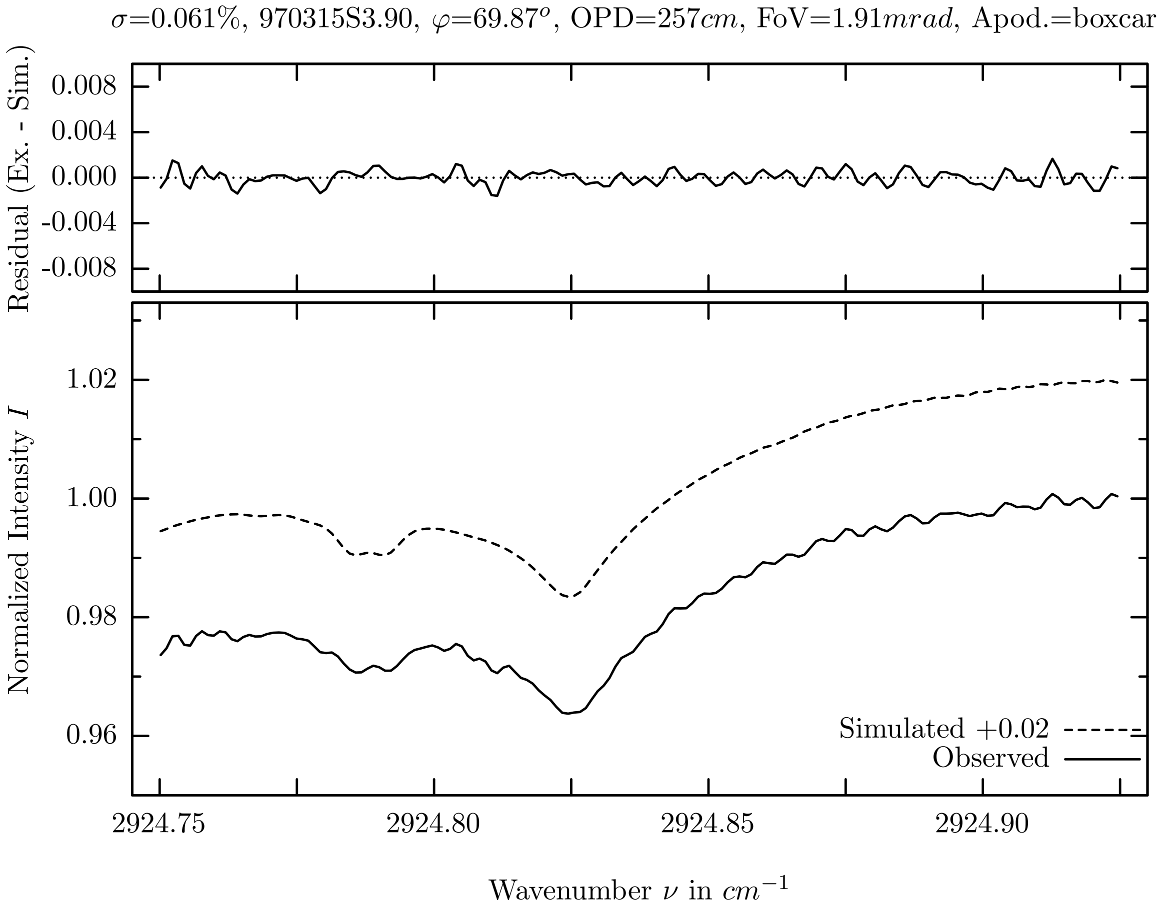

investigated species	:	$NO_2, (CH_4(i2))$
line position(s) ν_0	:	2924.7844, 2924.7917, (2924.8235) cm^{-1}
lower state energy E''_{lst}	:	321.8, 349.1, small (157.1) cm^{-1}
retrieved TCA, information content	:	2.61E+15, (3.07E+19) $molec/cm^2$, 11.9, 9.94, (59.5)
temperature dependence of the TCA	:	-1.010, (-.358)%/K (trop), -.924, (+.076)%/K (strat)
location, date, solar zenith angle	:	Kiruna, 15/Mar/97, 69.87^o
spectral interval fitted	:	2924.750 – 2924.925 cm^{-1}

Molecule	iCode	Absorption	Molecule	iCode	Absorption
CH4	61	31.876%	*O3*	31	0.313%
H2O	11	8.346%	*H2CO*	201	0.118%
CH4	6**2**	3.914%	*HCl*	151	0.003%
HDO	491	2.533%	*CH3Cl*	301	0.003%
Solar(A)	—	2.169%	*C2H4*	391	0.001%
Solar-sim	—	1.938%	*NH3*	111	<0.001%
NO2	101	0.765%	*OH*	131	<0.001%
OCS	191	0.474%	*H2S*	471	<0.001%

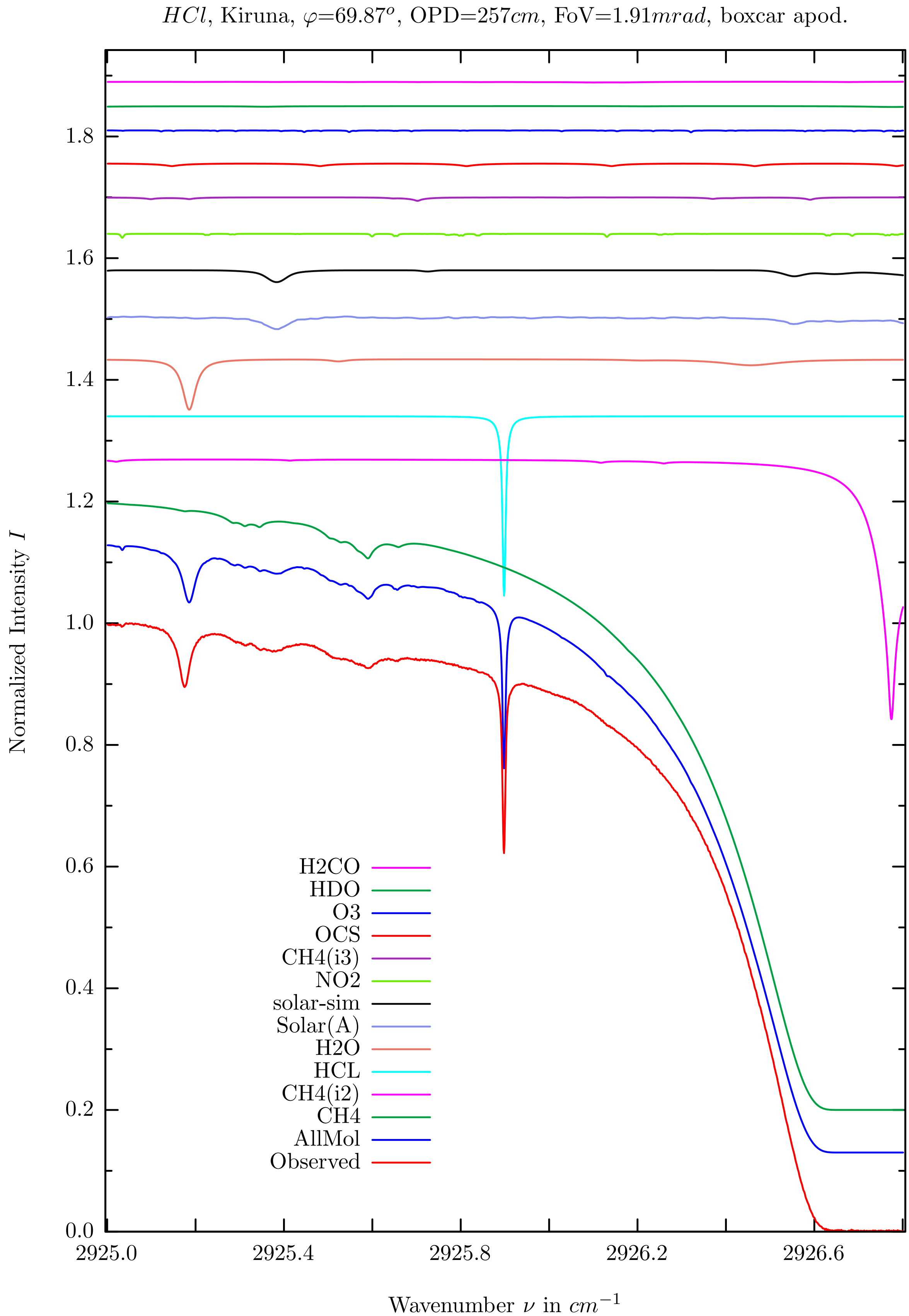

HCl, Kiruna, φ=69.87^o, OPD=257cm, FoV=1.91$mrad$, boxcar apod.
Normalized Intensity I
Wavenumber ν in cm^{-1}
0.0
0.2
0.4
0.6
0.8
1.0
1.2
1.4
1.6
1.8
2925.0
2925.4
2925.8
2926.2
2926.6
H2CO
HDO
O3
OCS
CH4(i3)
NO2
solar-sim
Solar(A)
H2O
HCL
CH4(i2)
CH4
AllMol
Observed

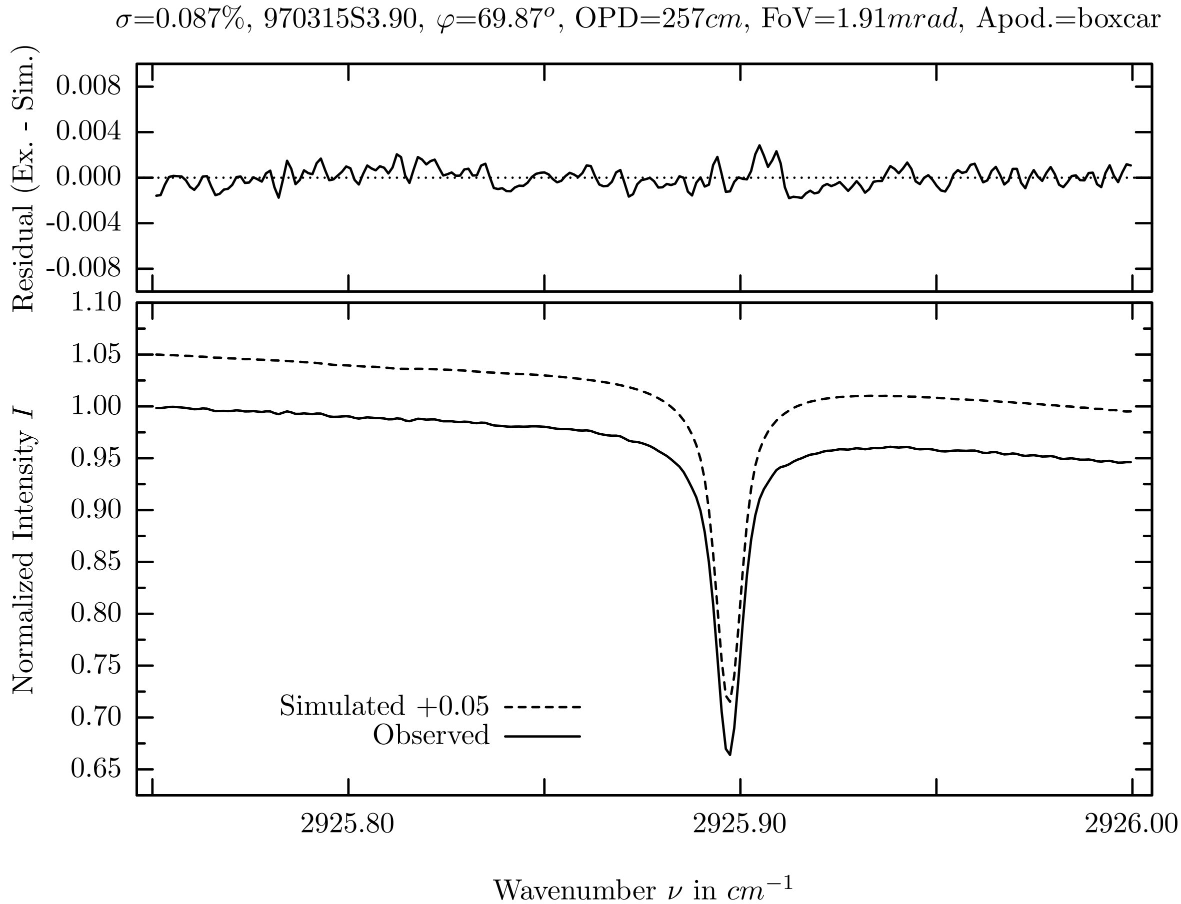

investigated species	:	HCl
line position(s) ν_0	:	2925.8967 cm^{-1}
lower state energy E''_{lst}	:	20.9 cm^{-1}
retrieved TCA, information content	:	3.14E+15 $molec/cm^2$, 355.9
temperature dependence of the TCA	:	-0.025%/K (trop), +0.303%/K (strat)
location, date, solar zenith angle	:	Kiruna, 15/Mar/97, 69.87^o
spectral interval fitted	:	2925.750 – 2926.000 cm^{-1}

Molecule	iCode	Absorption	Molecule	iCode	Absorption
$CH4$	61	100.000%	$O3$	31	0.320%
$CH4$	6**2**	42.856%	HDO	491	0.154%
HCL	151	29.654%	$H2CO$	201	0.128%
$H2O$	11	8.392%	$CH3Cl$	301	0.003%
Solar(A)	—	2.169%	$C2H4$	391	0.001%
Solar-sim	—	1.938%	$NH3$	111	<0.001%
$NO2$	101	0.656%	OH	131	<0.001%
$CH4$	6**3**	0.579%	$H2S$	471	<0.001%
OCS	191	0.476%			

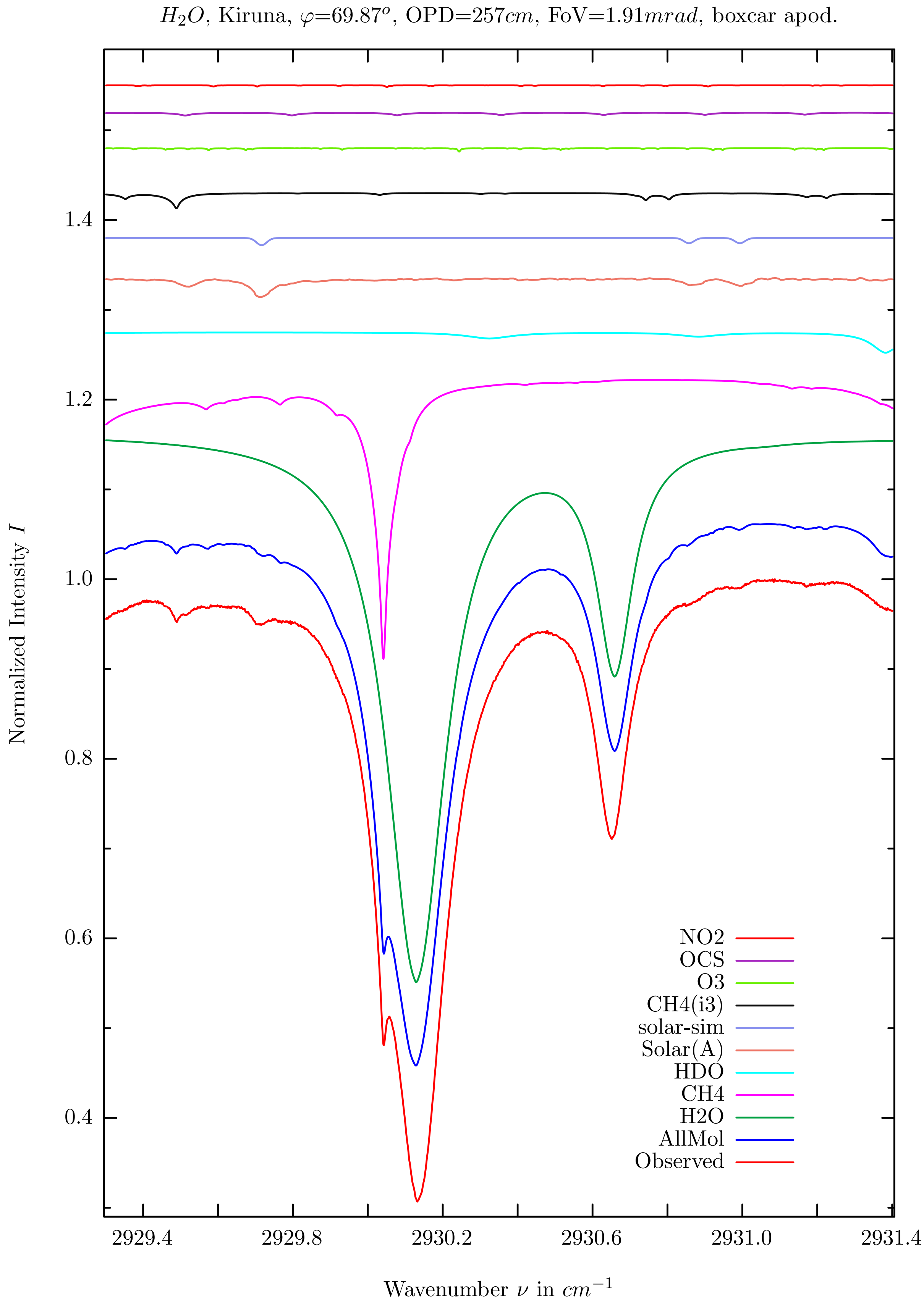
H_2O, Kiruna, φ=69.87^o, OPD=257cm, FoV=1.91$mrad$, boxcar apod.
Normalized Intensity I
Wavenumber ν in cm^{-1}
1.4
1.2
1.0
0.8
0.6
0.4
2929.4
2929.8
2930.2
2930.6
2931.0
2931.4
NO2
OCS
O3
CH4(i3)
solar-sim
Solar(A)
HDO
CH4
H2O
AllMol
Observed

σ=0.239%, 970315S3.90, φ=69.87°, OPD=257cm, FoV=1.91mrad, Apod.=boxcar

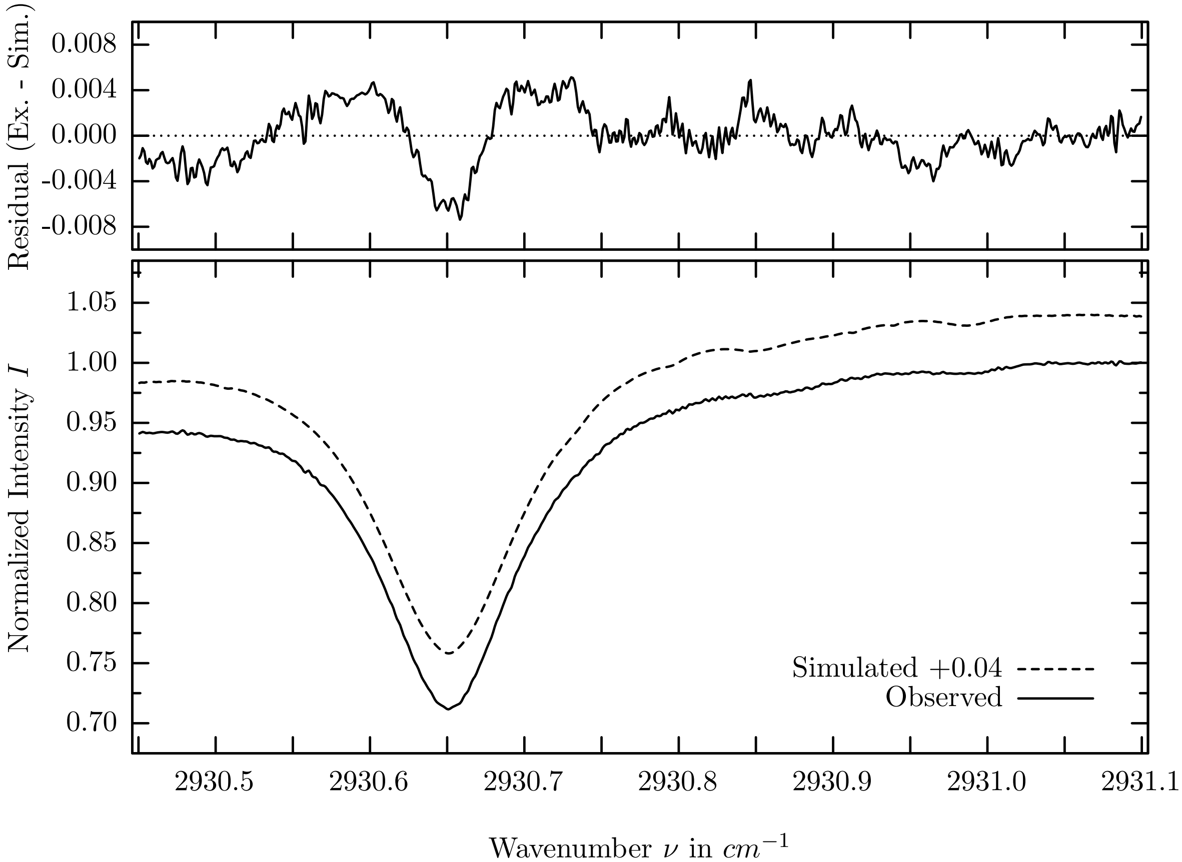

investigated species	:	H_2O
line position(s) ν_0	:	2930.6506 cm^{-1}
lower state energy E''_{lst}	:	1255.9 cm^{-1}
retrieved TCA, information content	:	6.10E+21 $molec/cm^2$, 107.8
temperature dependence of the TCA	:	-2.367%/K (trop), -0.014%/K (strat)
location, date, solar zenith angle	:	Kiruna, 15/Mar/97, 69.87^o
spectral interval fitted	:	2930.450 – 2931.100 cm^{-1}

Molecule	iCode	Absorption	Molecule	iCode	Absorption
H2O	11	61.382%	*NO*2	101	0.186%
*CH*4	61	33.875%	*H*2*CO*	201	0.049%
HDO	491	2.282%	*CH*3*Cl*	301	0.002%
Solar(A)	—	2.065%	*C*2*H*4	391	0.001%
Solar-sim	—	0.803%	*NH*3	111	<0.001%
*CH*4	6**3**	1.691%	*OH*	131	<0.001%
*O*3	31	0.382%	*HCl*	151	<0.001%
OCS	191	0.363%	*H*2*S*	471	<0.001%

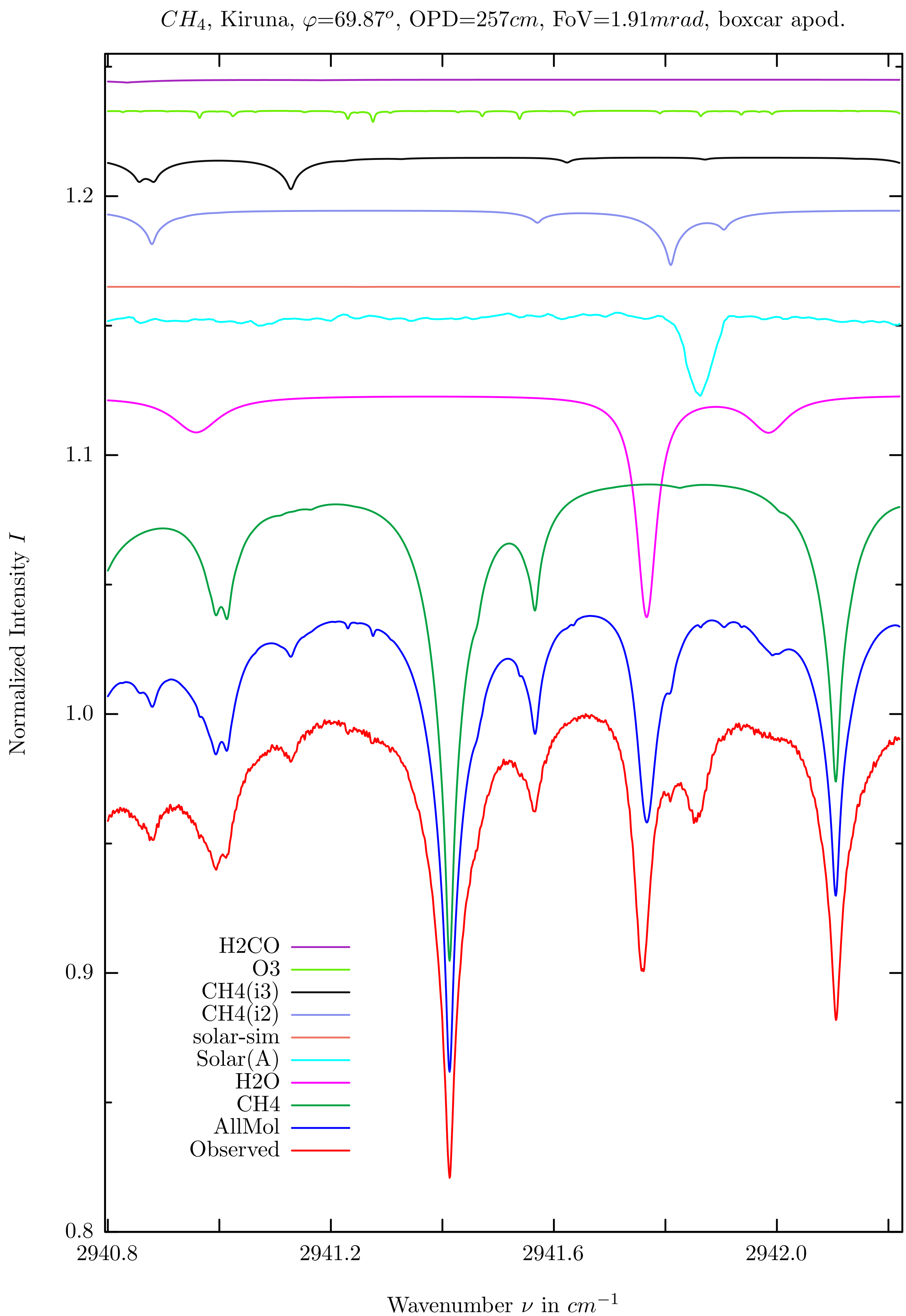
CH_4, Kiruna, φ=69.87^o, OPD=257cm, FoV=1.91$mrad$, boxcar apod.
Normalized Intensity I
1.2
1.1
1.0
0.9
0.8
2940.8
2941.2
2941.6
2942.0
Wavenumber ν in cm^{-1}
H2CO
O3
CH4(i3)
CH4(i2)
solar-sim
Solar(A)
H2O
CH4
AllMol
Observed

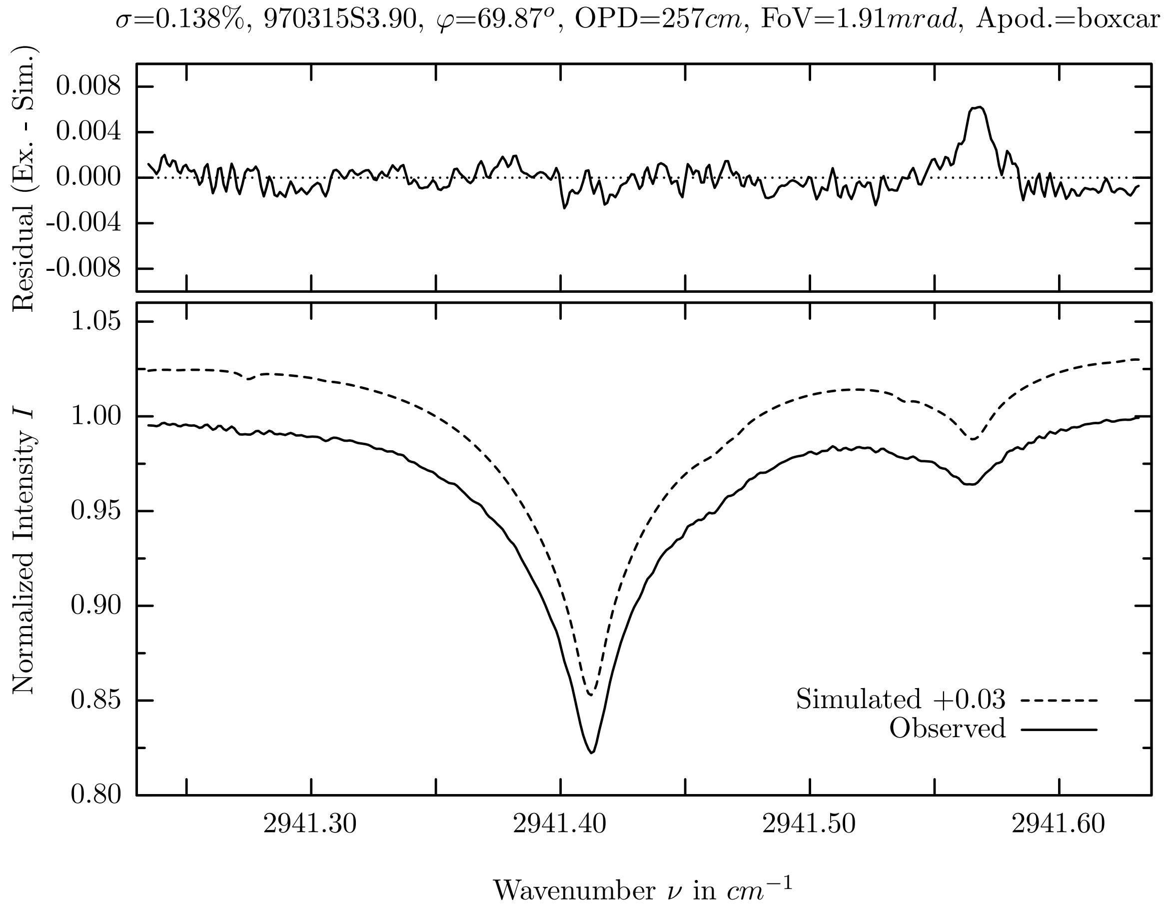

investigated species	:	CH_4
line position(s) ν_0	:	2941.4116, (2941.5652) cm^{-1}
lower state energy E''_{lst}	:	470.9, (219.9) cm^{-1}
retrieved TCA, information content	:	3.44E+00 $molec/cm^2$, 128.7
temperature dependence of the TCA	:	-1.519%/K (trop), -0.212%/K (strat)
location, date, solar zenith angle	:	Kiruna, 15/Mar/97, 69.87^o
spectral interval fitted	:	2941.234 – 2941.632 cm^{-1}

Molecule	iCode	Absorption	Molecule	iCode	Absorption
CH4	61	21.550%	*CH3Cl*	301	0.006%
H2O	11	8.762%	*C2H4*	391	0.005%
Solar(A)	—	3.210%	*OCS*	191	0.004%
Solar-sim	—	0.003%	*NO2*	101	<0.001%
CH4	6**2**	2.162%	*NH3*	111	<0.001%
CH4	6**3**	1.233%	*OH*	131	<0.001%
O3	31	0.440%	*HCl*	151	<0.001%
H2CO	201	0.112%	*H2S*	471	<0.001%
HDO	491	0.017%			

C_2H_6, Kiruna, φ=69.87^o, OPD=257cm, FoV=1.91$mrad$, boxcar apod.

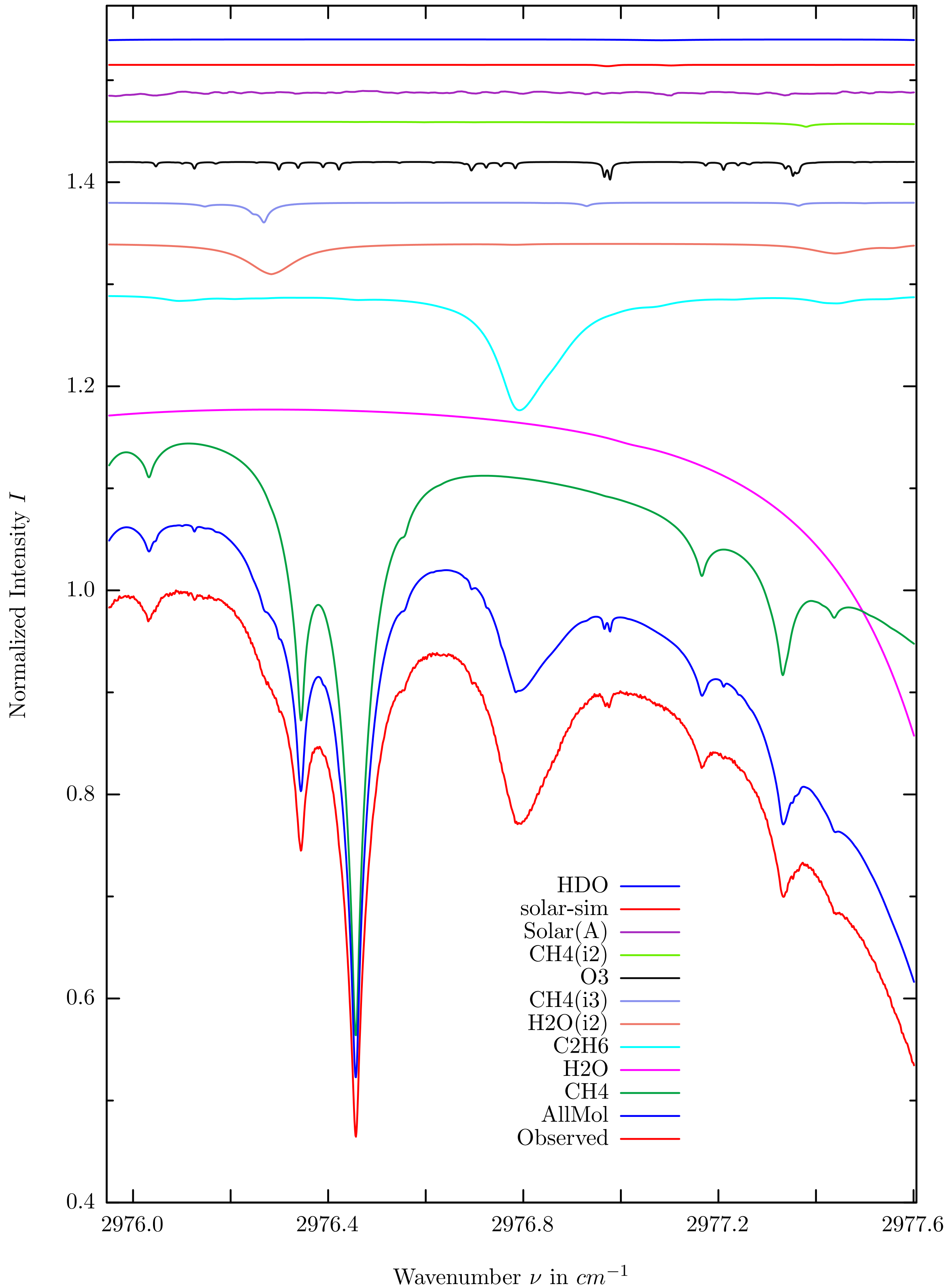

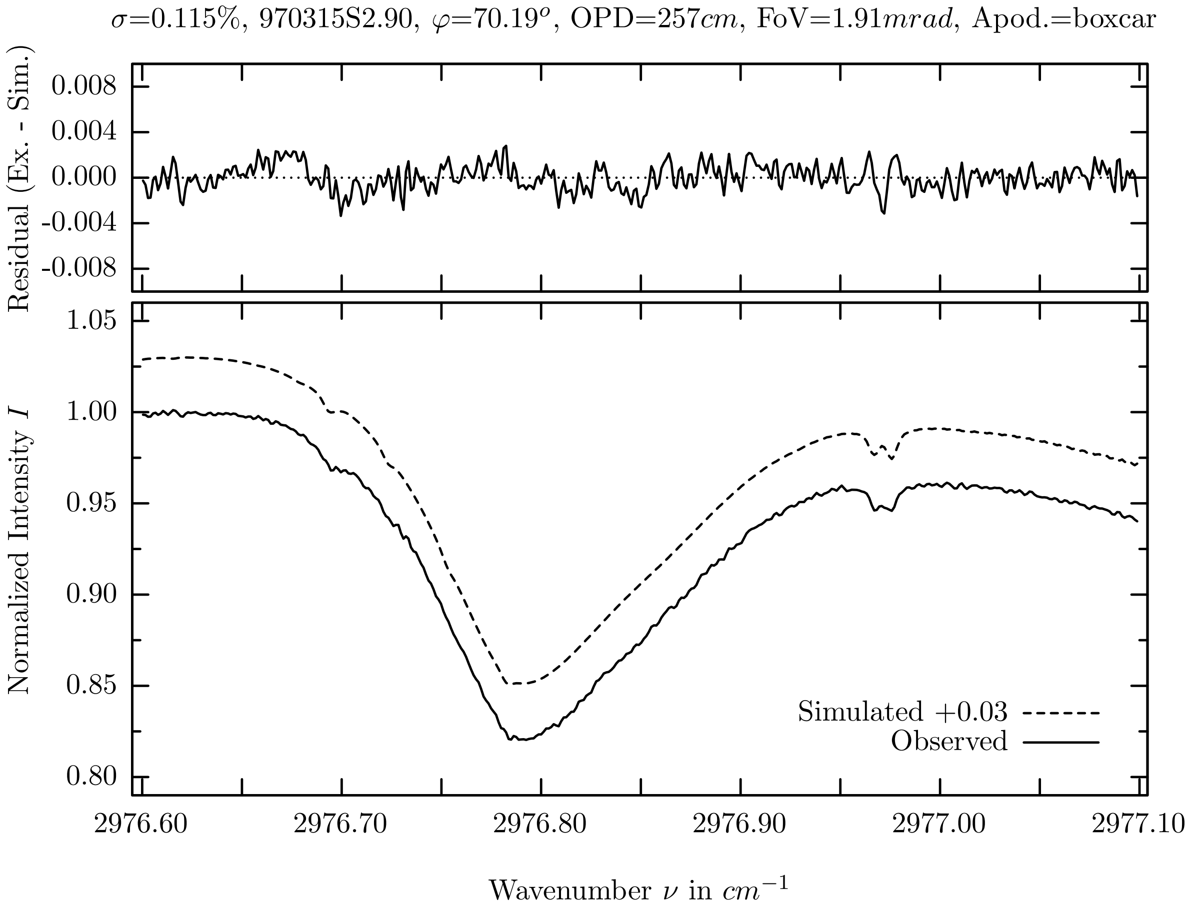

investigated species	:	C_2H_6
line position(s) ν_0	:	2976.7919*) cm^{-1}
lower state energy E''_{lst}	:	121.5 cm^{-1}
retrieved TCA, information content	:	3.62E+16 $molec/cm^2$, 150.5
temperature dependence of the TCA	:	+0.221%/K (trop), -0.025%/K (strat)
location, date, solar zenith angle	:	Kiruna, 15/Mar/97, 70.19^o
spectral interval fitted	:	2976.600 – 2977.100 cm^{-1}

Molecule	iCode	Absorption	Molecule	iCode	Absorption
CH4	61	58.874%	*HDO*	491	0.088%
H2O	11	36.546%	*CH3Cl*	301	0.044%
C2H6	381	10.318%	*C2H4*	391	0.042%
H2O	1**2**	3.543%	*H2CO*	201	0.017%
CH4	6**3**	1.951%	*NO2*	101	<0.001%
O3	31	1.764%	*NH3*	111	<0.001%
CH4	6**2**	0.565%	*OH*	131	<0.001%
Solar(A)	—	0.560%	*HCl*	151	<0.001%
Solar-sim	—	0.127%	*H2S*	471	<0.001%

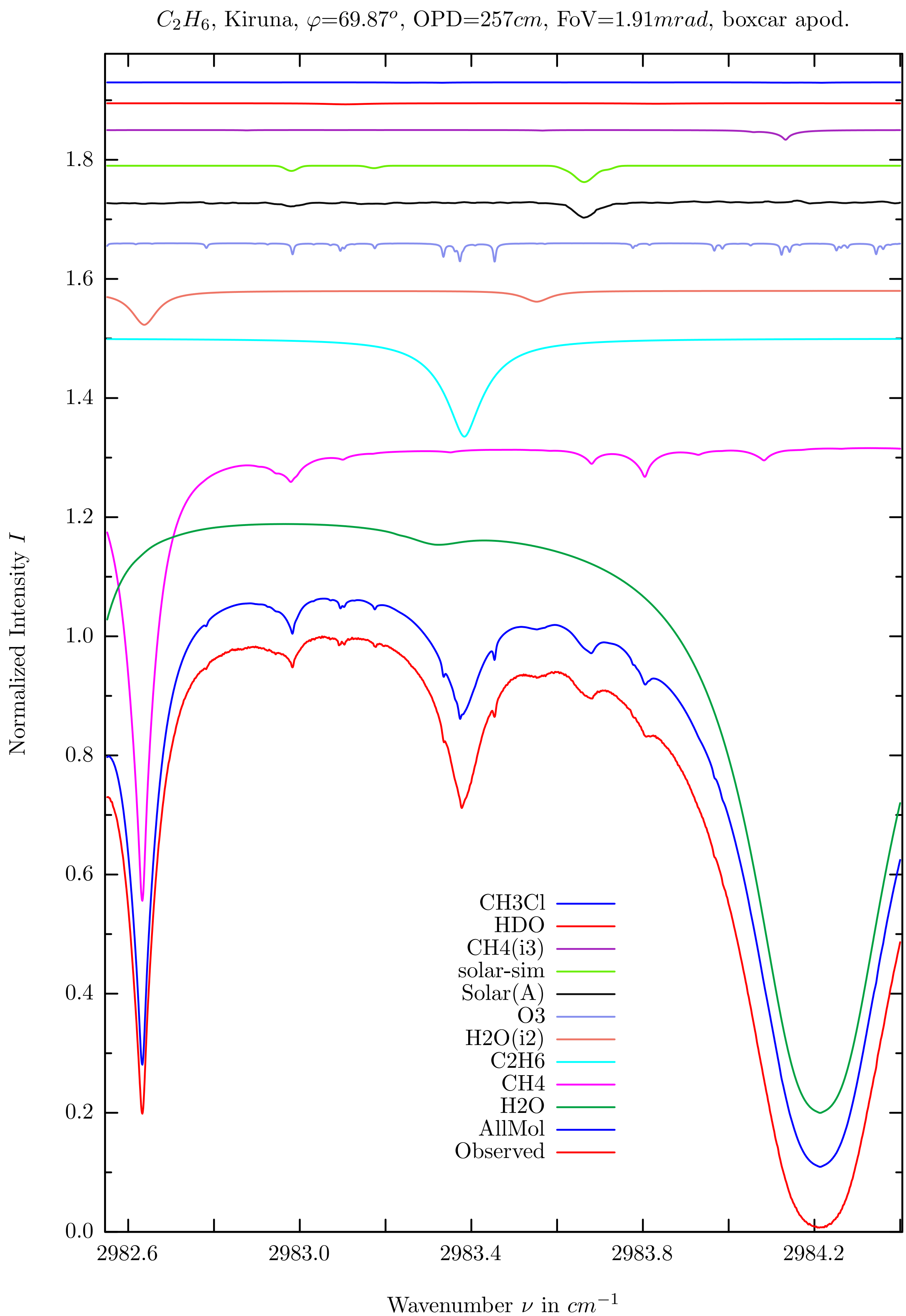

C_2H_6, Kiruna, φ=69.87^o, OPD=257cm, FoV=1.91$mrad$, boxcar apod.
Normalized Intensity I
Wavenumber ν in cm^{-1}
0.0
0.2
0.4
0.6
0.8
1.0
1.2
1.4
1.6
1.8
2982.6
2983.0
2983.4
2983.8
2984.2
CH3Cl
HDO
CH4(i3)
solar-sim
Solar(A)
O3
H2O(i2)
C2H6
CH4
H2O
AllMol
Observed

σ=0.119%, 970315S2.90, φ=70.19^o, OPD=257cm, FoV=1.91$mrad$, Apod.=boxcar

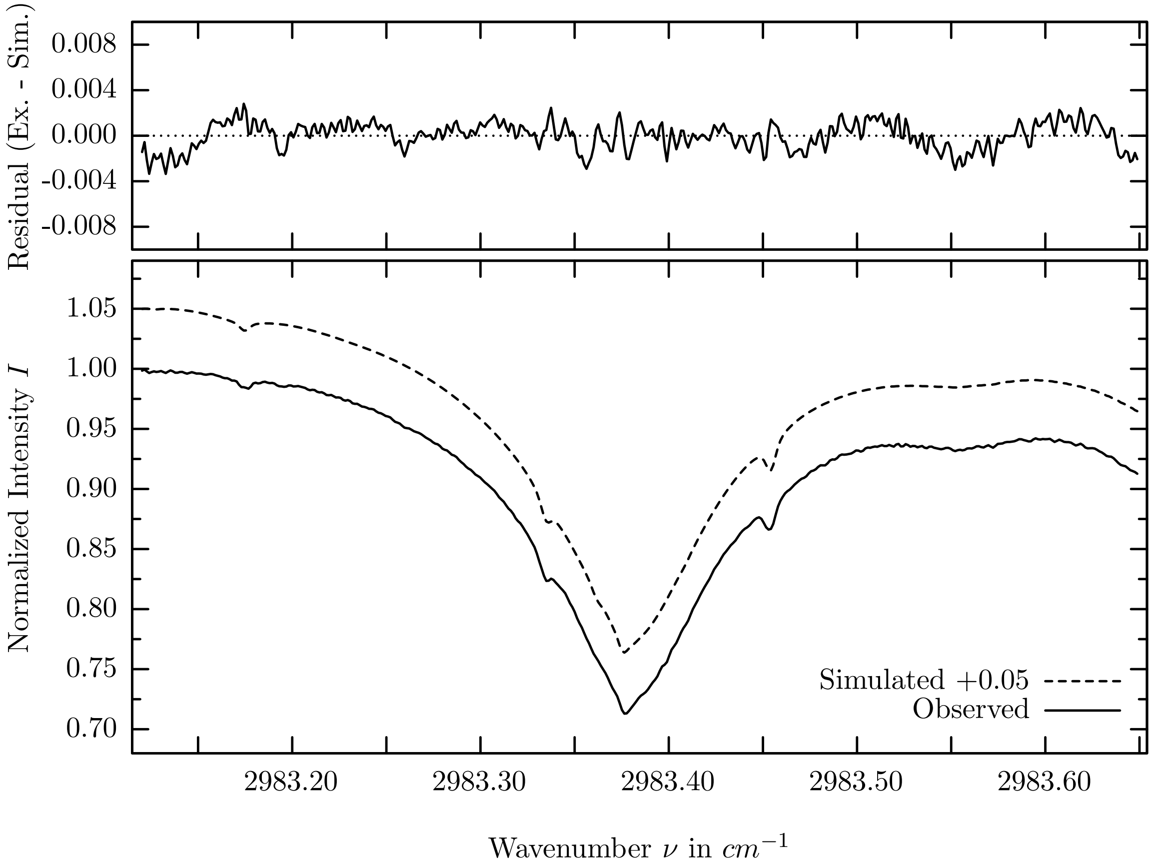

investigated species	:	C_2H_6
line position(s) ν_0	:	2983.3760$^{*)}$ cm^{-1}
lower state energy E''_{lst}	:	105.4 (15 to 930) cm^{-1}
retrieved TCA, information content	:	3.27E+16 $molec/cm^2$, 224.4
temperature dependence of the TCA	:	+0.040%/K (trop), +0.012%/K (strat)
location, date, solar zenith angle	:	Kiruna, 15/Mar/97, 70.19^o
spectral interval fitted	:	2983.120 – 2983.650 cm^{-1}

Molecule	iCode	Absorption	Molecule	iCode	Absorption
$H2O$	11	98.116%	$CH3Cl$	301	0.062%
$CH4$	61	79.434%	$C2H4$	391	0.018%
C2H6	381	12.979%	HCl	151	0.001%
$H2O$	1**2**	5.708%	$H2CO$	201	0.001%
$O3$	31	3.157%	$NO2$	101	<0.001%
Solar(A)	—	2.720%	$NH3$	111	<0.001%
Solar-sim	—	2.744%	OH	131	<0.001%
$CH4$	6**3**	1.632%	$H2S$	471	<0.001%
HDO	491	0.186%			

C_2H_6, Kiruna, φ=69.87^o, OPD=257cm, FoV=1.91$mrad$, boxcar apod.

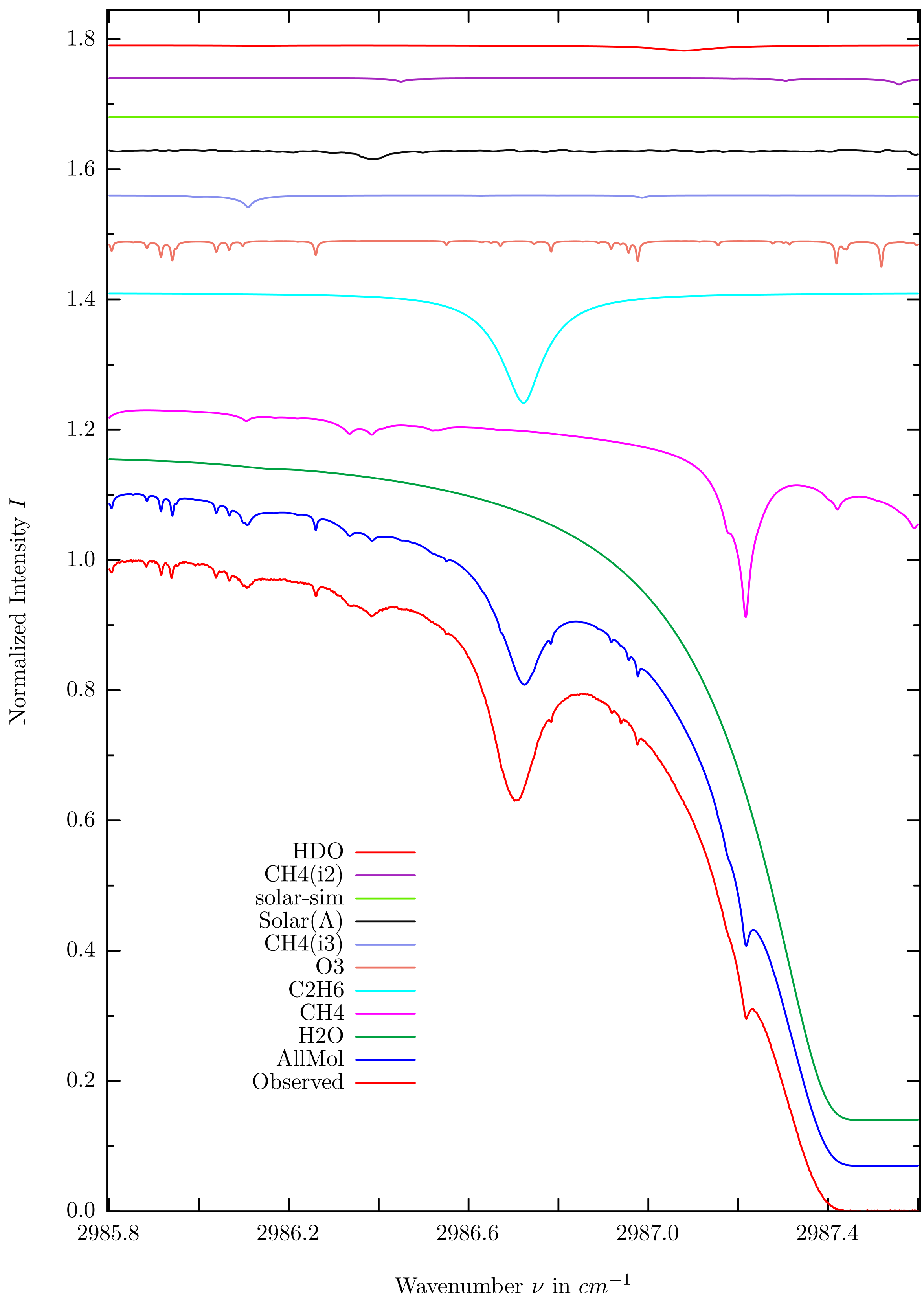

σ=0.191%, 970315S2.90, φ=70.19^o, OPD=257cm, FoV=1.91$mrad$, Apod.=boxcar

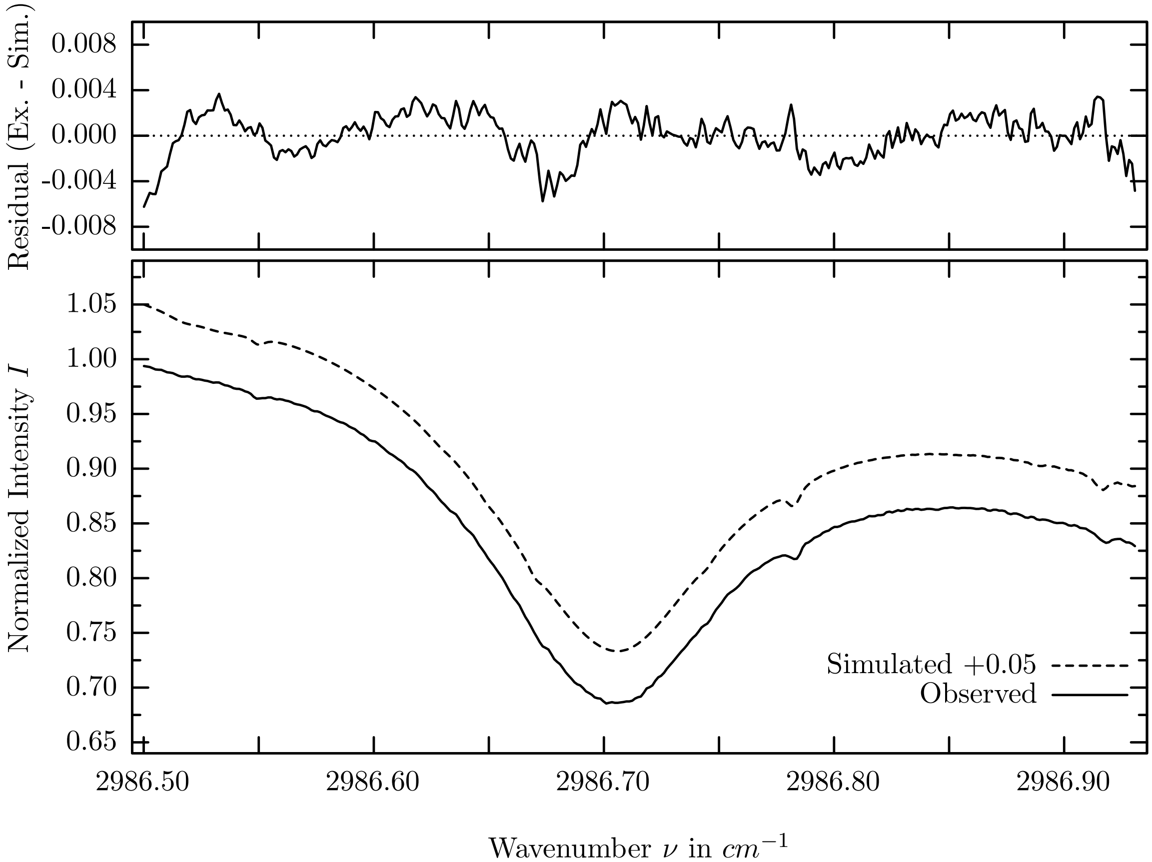

investigated species	:	C_2H_6
line position(s) ν_0	:	2986.7230$^{*)}$ cm^{-1}
lower state energy E''_{lst}	:	87.5 cm^{-1}
retrieved TCA, information content	:	3.55E+16 $molec/cm^2$, 133.4
temperature dependence of the TCA	:	+0.338%/K (trop), -0.027%/K (strat)
location, date, solar zenith angle	:	Kiruna, 15/Mar/97, 70.19^o
spectral interval fitted	:	2986.500 – 2986.932 cm^{-1}

Molecule	iCode	Absorption	Molecule	iCode	Absorption
$H2O$	11	100.000%	$C2H4$	391	0.041%
$CH4$	61	36.805%	$CH3Cl$	301	0.029%
C2H6	381	15.356%	$NO2$	101	<0.001%
$O3$	31	4.043%	$NH3$	111	<0.001%
$CH4$	6**3**	1.828%	OH	131	<0.001%
Solar(A)	—	1.451%	HCl	151	<0.001%
Solar-sim	—	0.005%	OCS	19**3**	<0.001%
$CH4$	6**2**	0.988%	$H2CO$	201	<0.001%
HDO	491	0.794%	$H2S$	471	<0.001%

$H_2{}^{18}O$, Kiruna, φ=69.87^o, OPD=257cm, FoV=1.91$mrad$, boxcar apod.

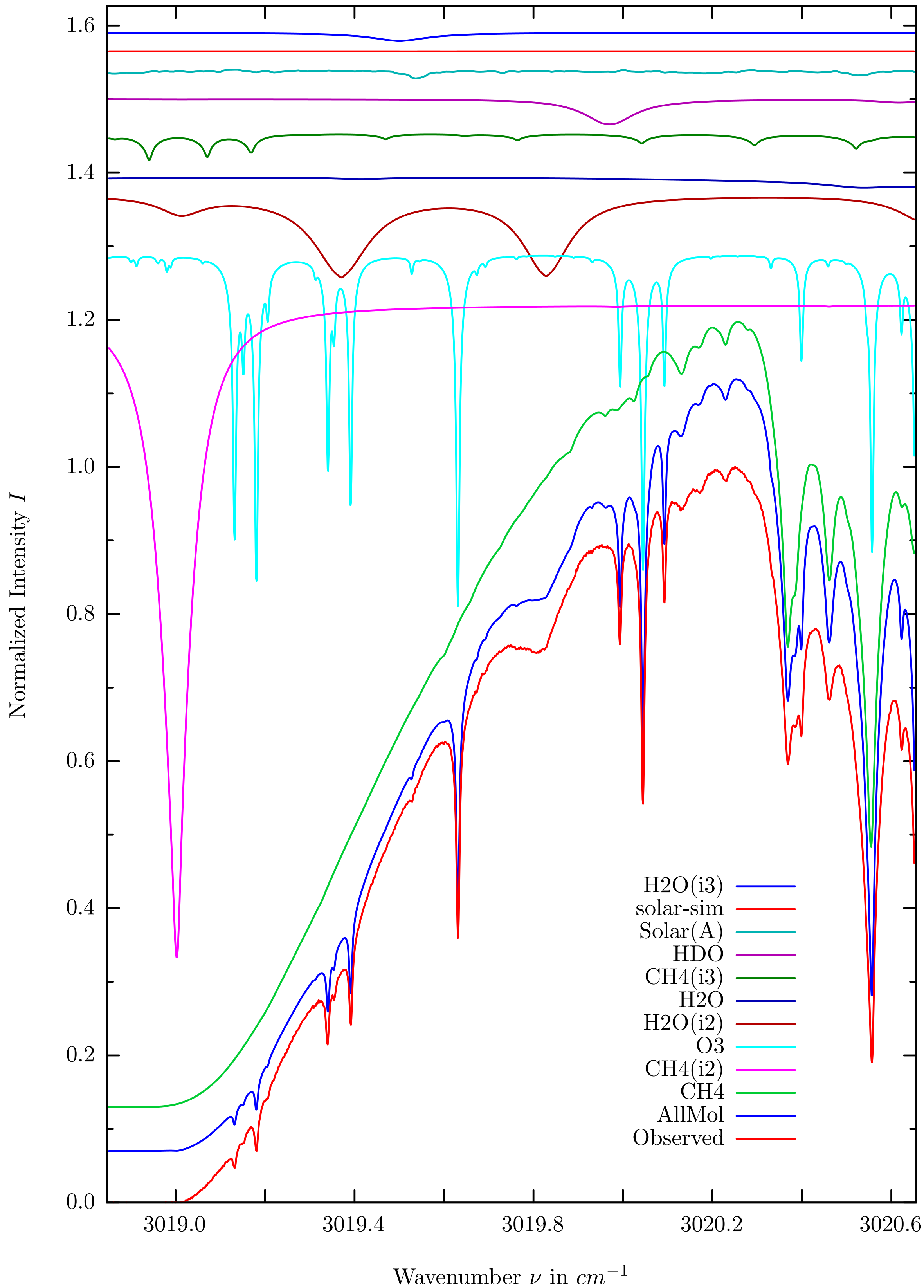

σ=0.181%, 970315S2.90, φ=70.19^o, OPD=257cm, FoV=1.91$mrad$, Apod.=boxcar

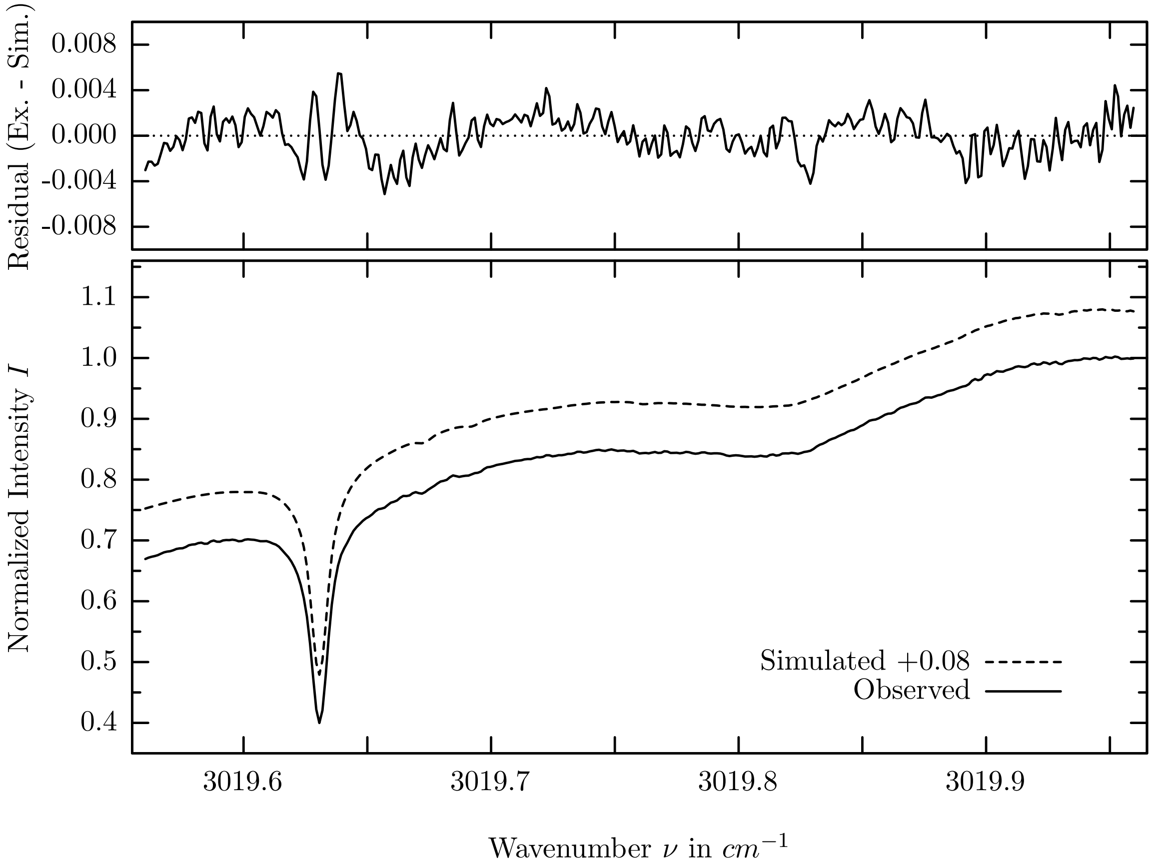

investigated species	:	$H_2O(i2{=}\ H_2\,^{18}O), (O_3)$
line position(s) ν_0	:	3019.8270, (3019.6297) cm^{-1}
lower state energy E''_{lst}	:	445.3, (226.5) cm^{-1}
retrieved TCA, information content	:	6.68E+21, (1.00E+19) $molec/cm^2$, 53.7, (191.0)
temperature dependence of the TCA	:	-.868, (-.521)%/K (trop), +.026, (+.067)%/K (strat)
location, date, solar zenith angle	:	Kiruna, 15/Mar/97, 70.19^o
spectral interval fitted	:	3019.560 – 3019.960 cm^{-1}

Molecule	iCode	Absorption	Molecule	iCode	Absorption
$CH4$	61	100.000%	$H2O$	1**3**	1.108%
$CH4$	6**2**	88.758%	$C2H4$	391	0.033%
$O3$	31	48.216%	$CH3Cl$	301	0.032%
H2O	1**2**	11.246%	OCS	19**3**	0.001%
$H2O$	11	4.036%	$NO2$	101	<0.001%
$CH4$	6**3**	3.584%	$NH3$	111	<0.001%
HDO	491	3.424%	OH	131	<0.001%
Solar(A)	—	1.181%	HCl	151	<0.001%
Solar-sim	—	0.006%	$H2S$	471	<0.001%

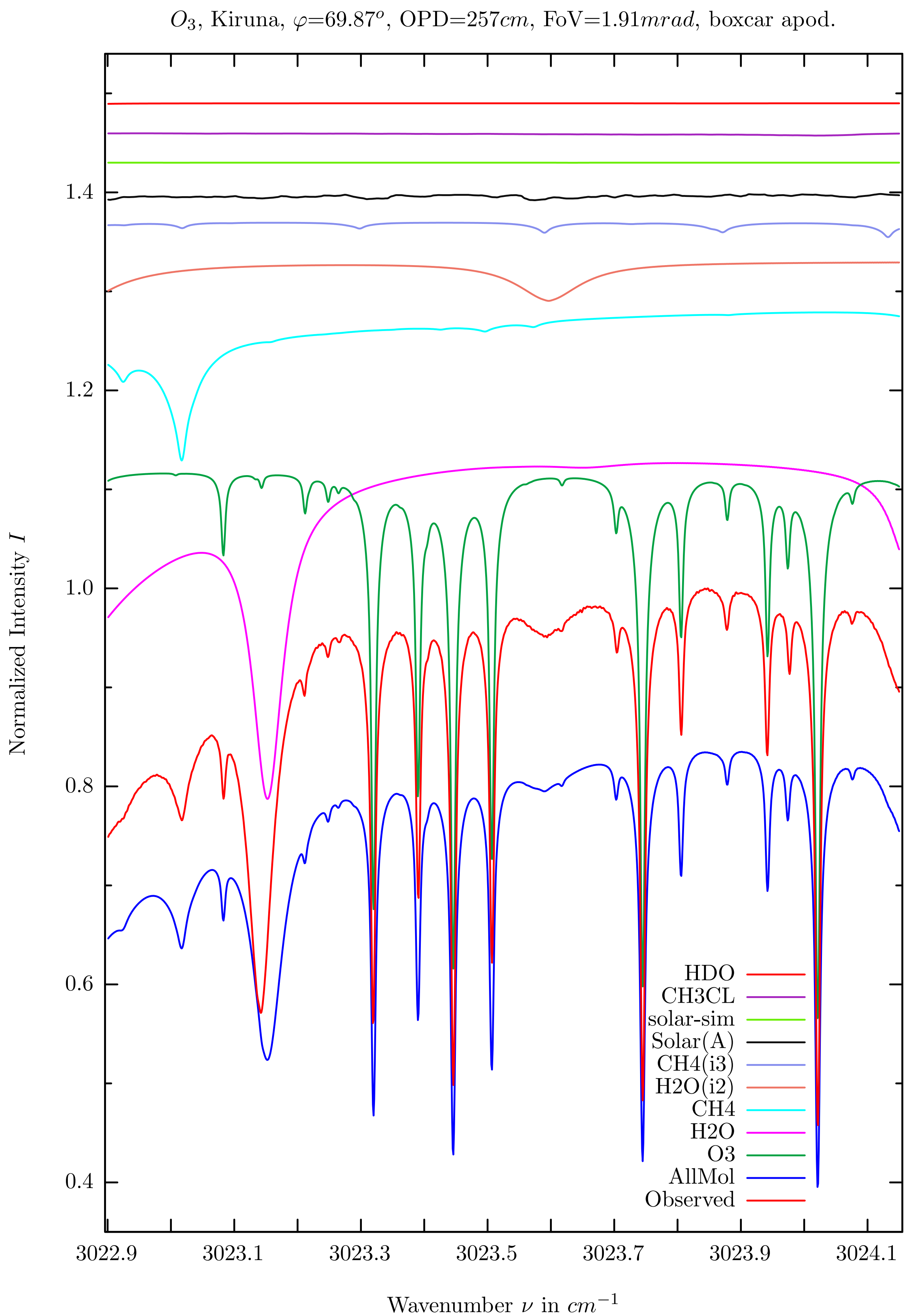
O_3, Kiruna, φ=69.87^o, OPD=257cm, FoV=1.91$mrad$, boxcar apod.
Normalized Intensity I
Wavenumber ν in cm^{-1}
1.4
1.2
1.0
0.8
0.6
0.4
3022.9
3023.1
3023.3
3023.5
3023.7
3023.9
3024.1
HDO
CH3CL
solar-sim
Solar(A)
CH4(i3)
H2O(i2)
CH4
H2O
O3
AllMol
Observed

σ=0.292%, 970315S2.90, φ=70.19^o, OPD=257cm, FoV=1.91$mrad$, Apod.=boxcar

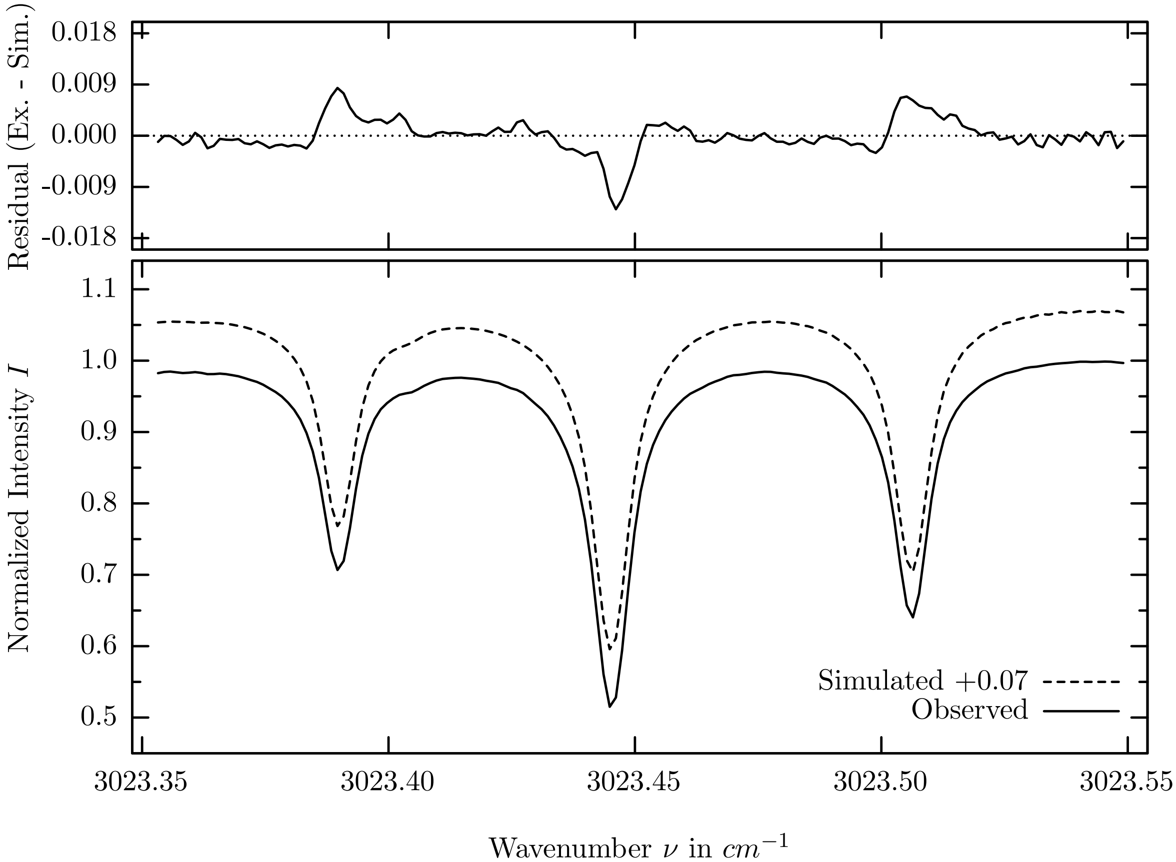

investigated species	:	O_3
line position(s) ν_0	:	3023.3887, 3023.4442, 3023.5052 cm^{-1}
lower state energy E''_{lst}	:	241.1, 191.7, 222.0 cm^{-1}
retrieved TCA, information content	:	1.00E+19 $molec/cm^2$, 103.3, 162.4, 125.3
temperature dependence of the TCA	:	-0.149%/K (trop), +0.125%/K (strat)
location, date, solar zenith angle	:	Kiruna, 15/Mar/97, 70.19^o
spectral interval fitted	:	3023.352 – 3023.550 cm^{-1}

Molecule	iCode	Absorption	Molecule	iCode	Absorption
O3	31	56.016%	HDO	491	0.055%
$H2O$	11	43.773%	$C2H4$	391	0.032%
$CH4$	61	23.884%	OCS	19**3**	0.001%
$H2O$	1**2**	3.959%	$NO2$	101	<0.001%
$CH4$	6**3**	1.521%	$NH3$	111	<0.001%
Solar(A)	—	0.790%	OH	131	<0.001%
Solar-sim	—	0.006%	HCl	151	<0.001%
$CH3Cl$	301	0.242%	$H2S$	471	<0.001%

O_3, Kiruna, φ=69.87^o, OPD=257cm, FoV=1.91$mrad$, boxcar apod.

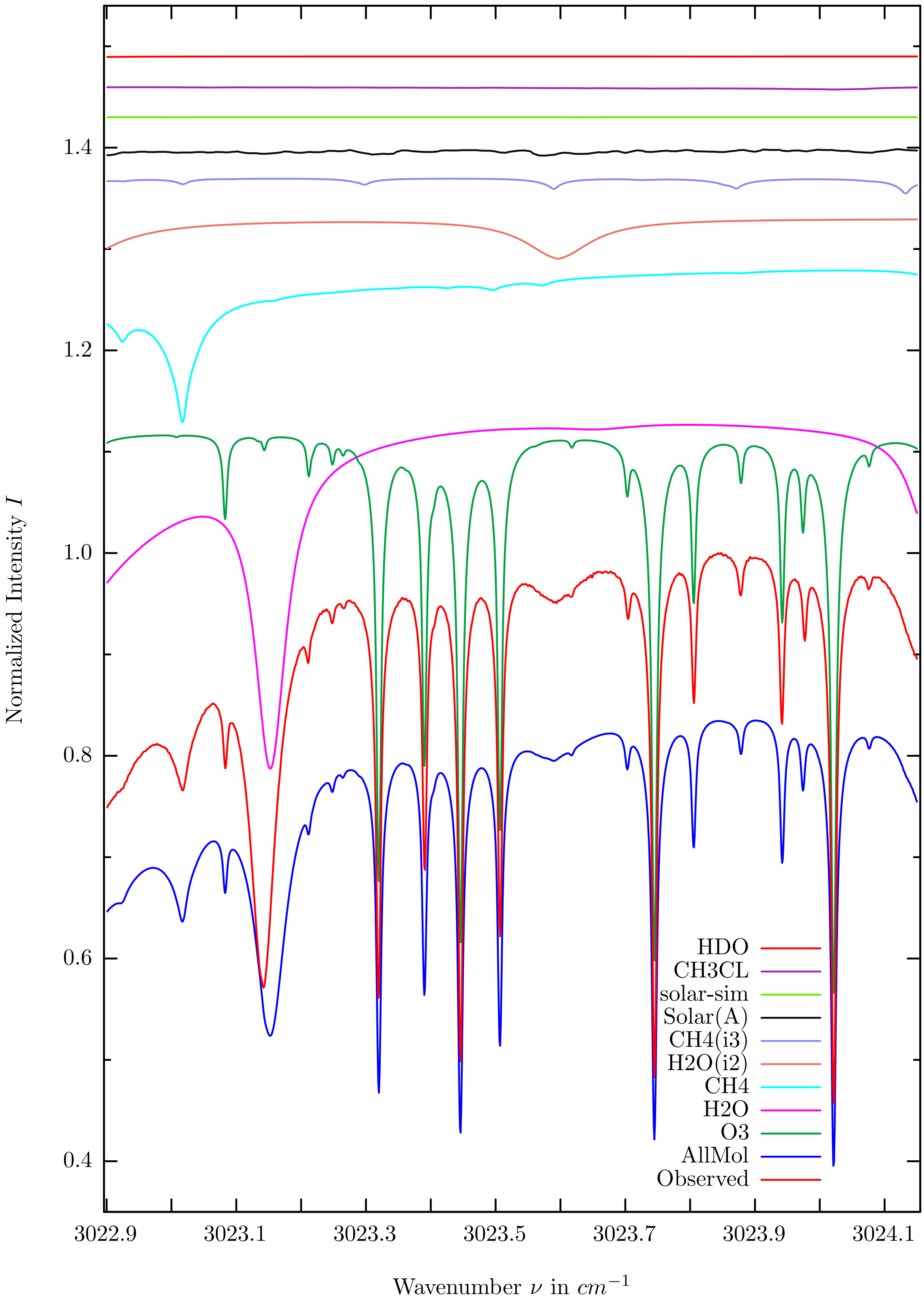

σ=0.180%, 970315S2.90, φ=70.19^o, OPD=257cm, FoV=1.91$mrad$, Apod.=boxcar

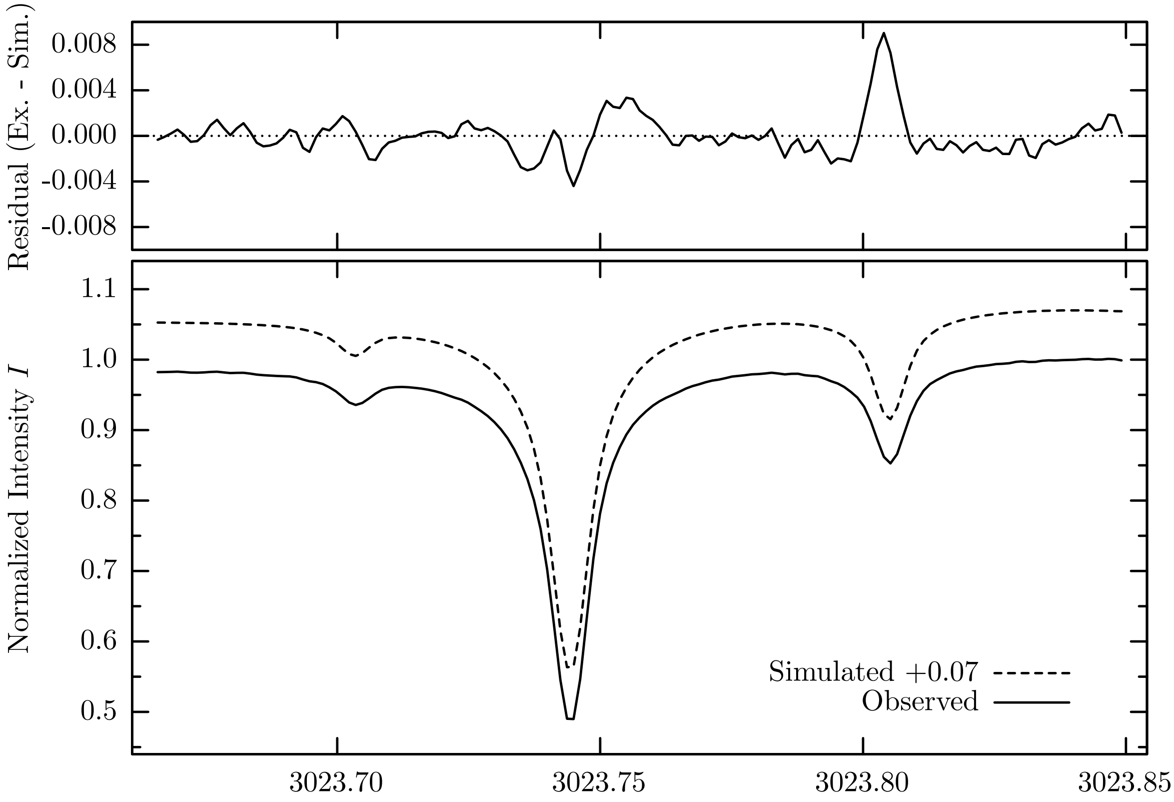

Wavenumber ν in cm^{-1}

investigated species	:	O_3
line position(s) ν_0	:	3023.7434, 3023.8041 cm^{-1}
lower state energy E''_{lst}	:	183.4, 287.9 cm^{-1}
retrieved TCA, information content	:	9.93E+18 $molec/cm^2$, 281.1, 85.74
temperature dependence of the TCA	:	-0.054%/K (trop), +0.286%/K (strat)
location, date, solar zenith angle	:	Kiruna, 15/Mar/97, 70.19^o
spectral interval fitted	:	3023.665 – 3023.850 cm^{-1}

Molecule	iCode	Absorption	Molecule	iCode	Absorption
O3	31	56.016%	HDO	491	0.055%
$H2O$	11	43.773%	$C2H4$	391	0.032%
$CH4$	61	23.884%	OCS	19**3**	0.001%
$H2O$	1**2**	3.959%	$NO2$	101	<0.001%
$CH4$	6**3**	1.521%	$NH3$	111	<0.001%
Solar(A)	—	0.790%	OH	131	<0.001%
Solar-sim	—	0.006%	HCl	151	<0.001%
$CH3Cl$	301	0.242%	$H2S$	471	<0.001%

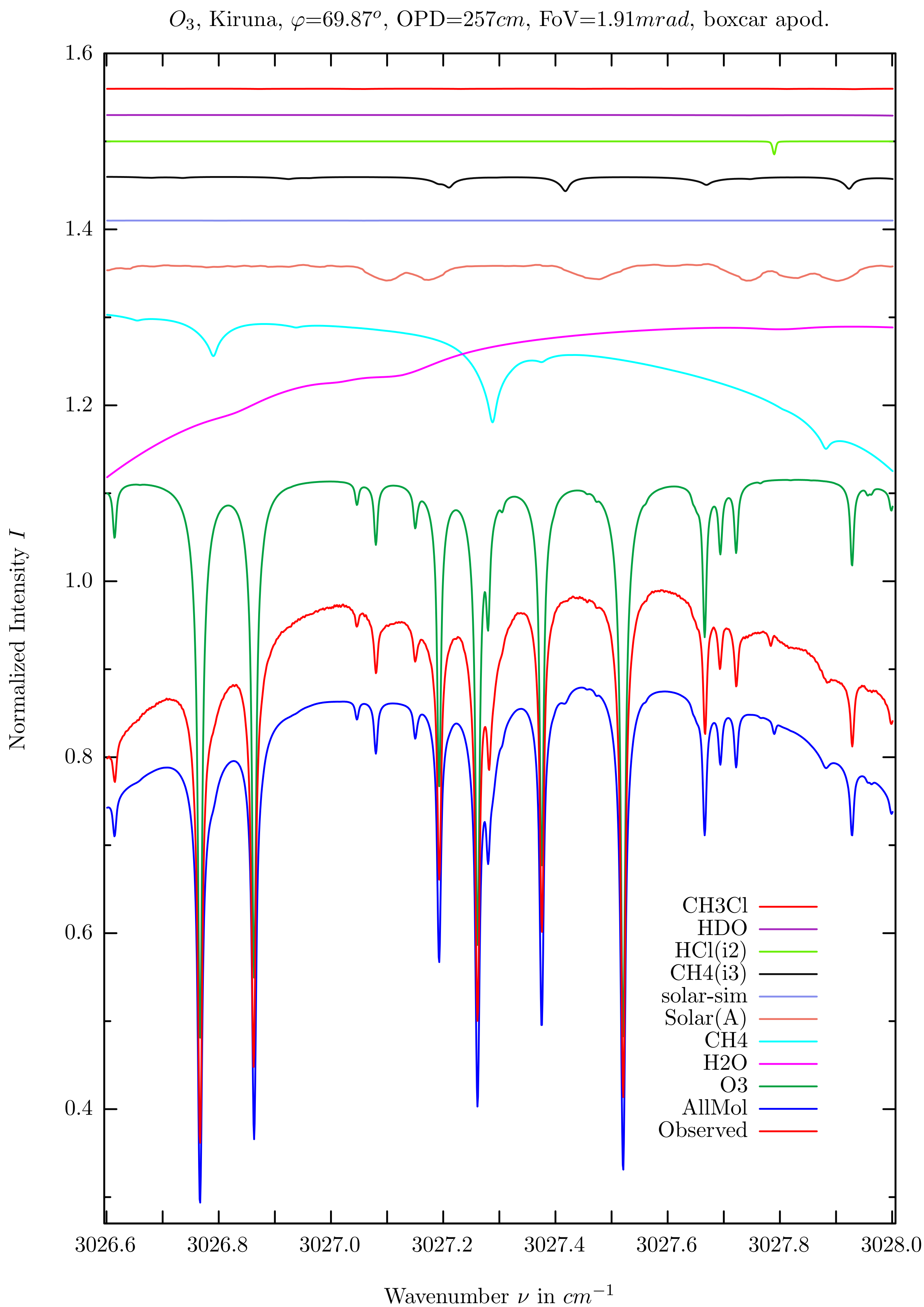
O_3, Kiruna, φ=69.87^o, OPD=257cm, FoV=1.91$mrad$, boxcar apod.
Normalized Intensity I
Wavenumber ν in cm^{-1}
CH3Cl
HDO
HCl(i2)
CH4(i3)
solar-sim
Solar(A)
CH4
H2O
O3
AllMol
Observed

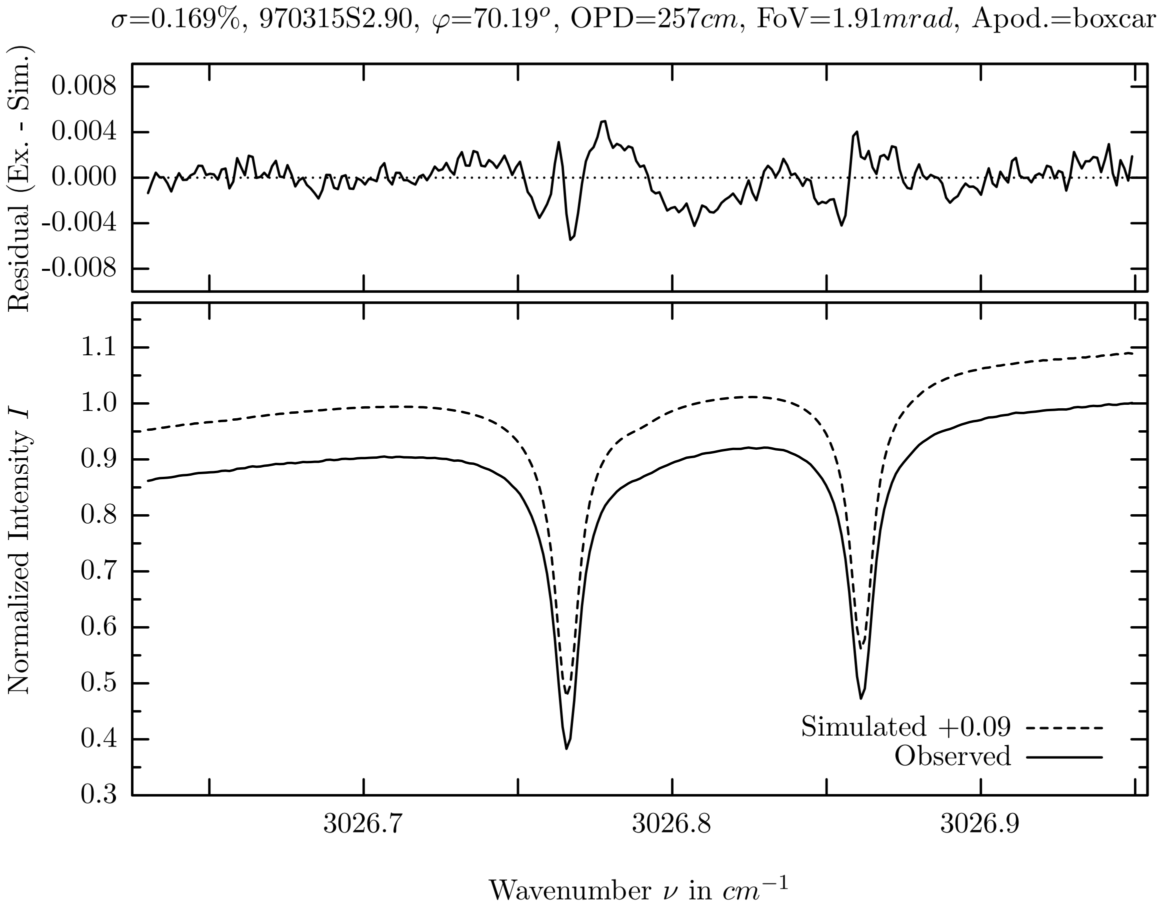

investigated species	:	O_3
line position(s) ν_0	:	3026.7651, 3026.8615 cm^{-1}
lower state energy E''_{lst}	:	141.1, 156.9 cm^{-1}
retrieved TCA, information content	:	1.01E+19 $molec/cm^2$, 326.5, 298.02
temperature dependence of the TCA	:	-0.194%/K (trop), +0.174%/K (strat)
location, date, solar zenith angle	:	Kiruna, 15/Mar/97, 70.19^o
spectral interval fitted	:	3026.630 – 3026.950 cm^{-1}

Molecule	iCode	Absorption	Molecule	iCode	Absorption
O3	31	59.741%	$CH3Cl$	301	0.057%
$H2O$	11	29.107%	$C2H4$	391	0.016%
$CH4$	61	21.404%	$NO2$	101	<0.001%
Solar(A)	—	1.857%	$NH3$	111	<0.001%
Solar-sim	—	0.007%	OH	131	<0.001%
$CH4$	6**3**	1.659%	HCl	151	<0.001%
HCl	15**2**	1.493%	OCS	19**3**	<0.001%
HDO	491	0.076%	$H2S$	471	<0.001%

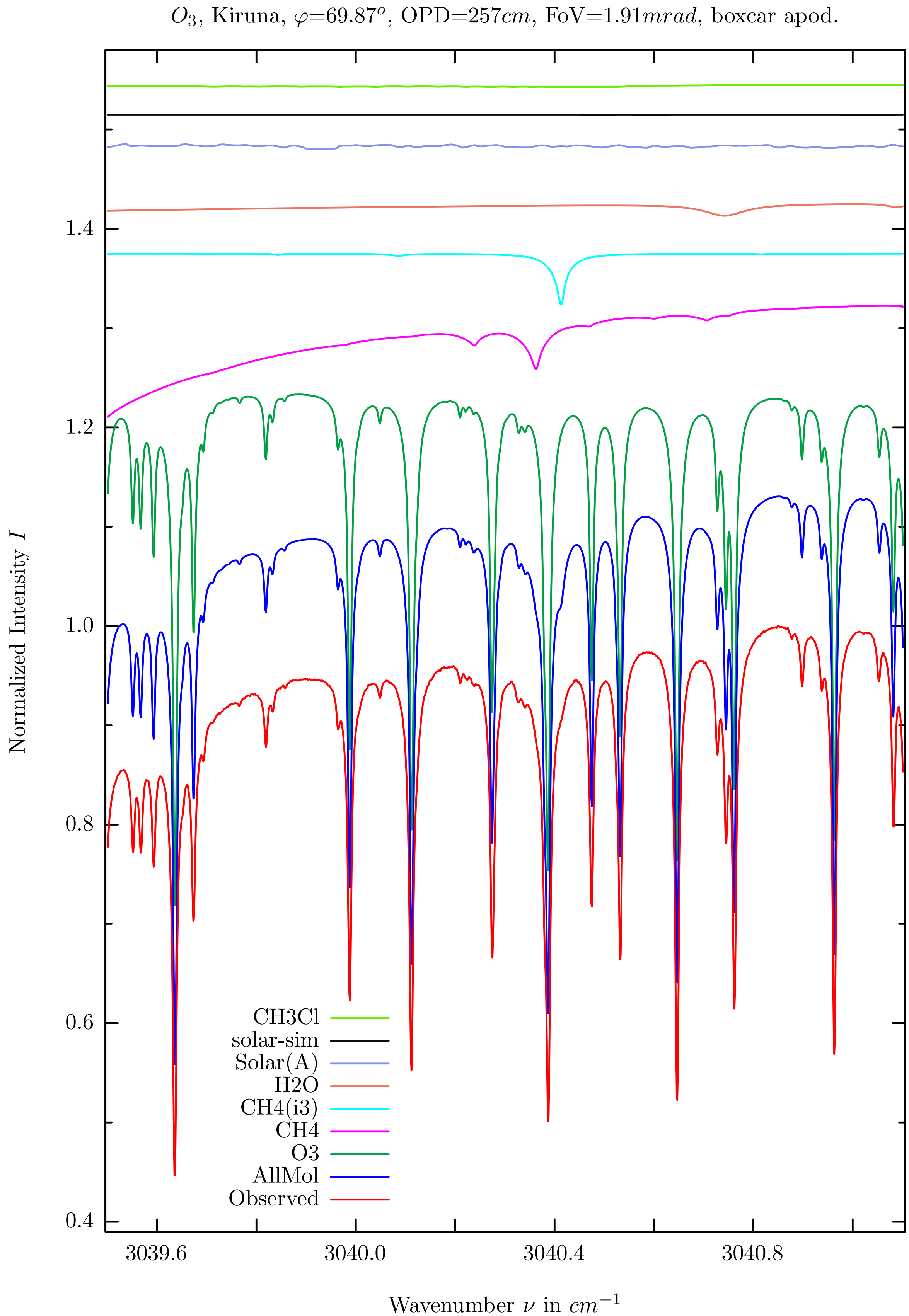

O_3, Kiruna, φ=69.87^o, OPD=257cm, FoV=1.91$mrad$, boxcar apod.
Normalized Intensity I
Wavenumber ν in cm^{-1}
0.4
0.6
0.8
1.0
1.2
1.4
3039.6
3040.0
3040.4
3040.8
CH3Cl
solar-sim
Solar(A)
H2O
CH4(i3)
CH4
O3
AllMol
Observed

σ=0.138%, 970315S2.90, φ=70.19^o, OPD=257cm, FoV=1.91$mrad$, Apod.=boxcar

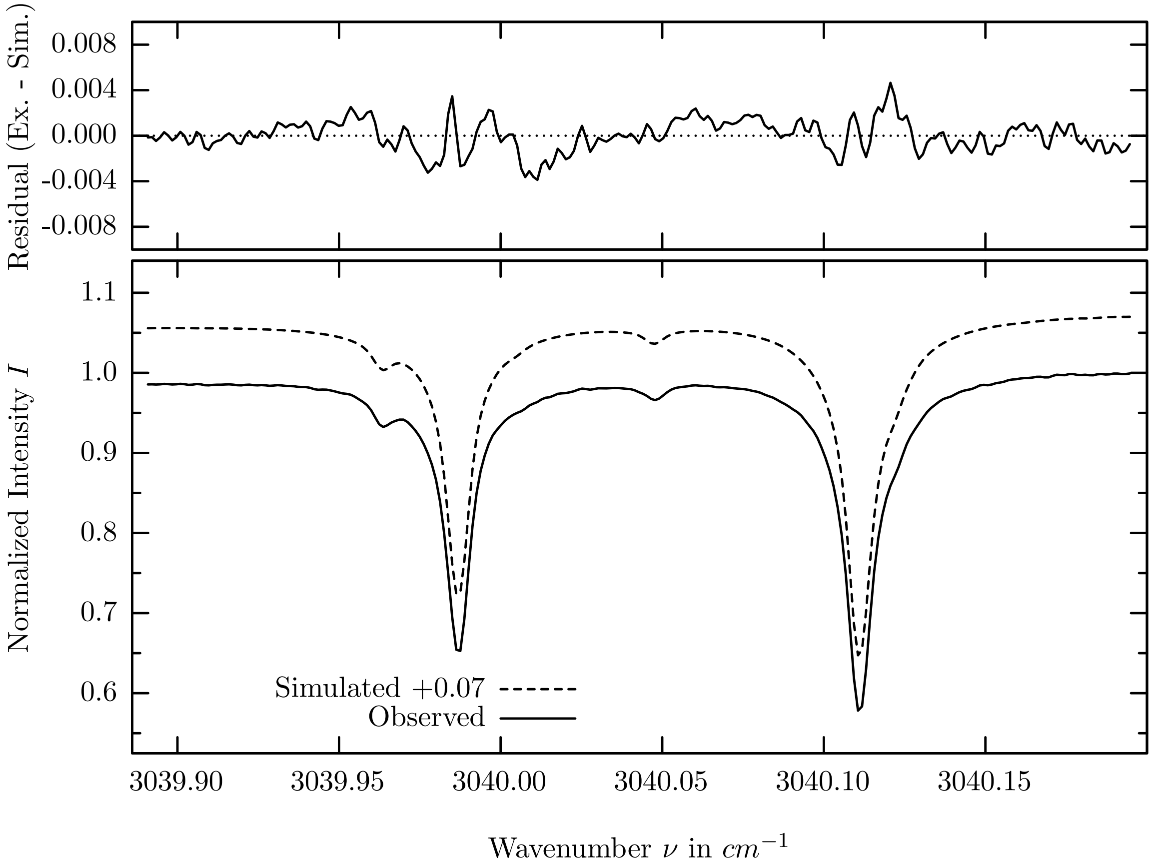

investigated species	:	O_3
line position(s) ν_0	:	3039.9866, 3040.1108 cm^{-1}
lower state energy E''_{lst}	:	158.8, 30.2 cm^{-1}
retrieved TCA, information content	:	9.90E+18 $molec/cm^2$, 249.8, 305.2
temperature dependence of the TCA	:	+0.015%/K (trop), +0.235%/K (strat)
location, date, solar zenith angle	:	Kiruna, 15/Mar/97, 70.19^o
spectral interval fitted	:	3039.890 – 3040.195 cm^{-1}

Molecule	iCode	Absorption	Molecule	iCode	Absorption
O3	31	52.367%	$C2H4$	391	0.018%
$CH4$	61	13.475%	$N2O$	41	<0.001%
$CH4$	6**3**	5.146%	$NO2$	101	<0.001%
$H2O$	11	3.166%	$NH3$	111	<0.001%
Solar(A)	—	0.481%	OH	131	<0.001%
Solar-sim	—	0.011%	HCl	151	<0.001%
$CH3Cl$	301	0.225%	$H2S$	471	<0.001%
HDO	491	0.039%			

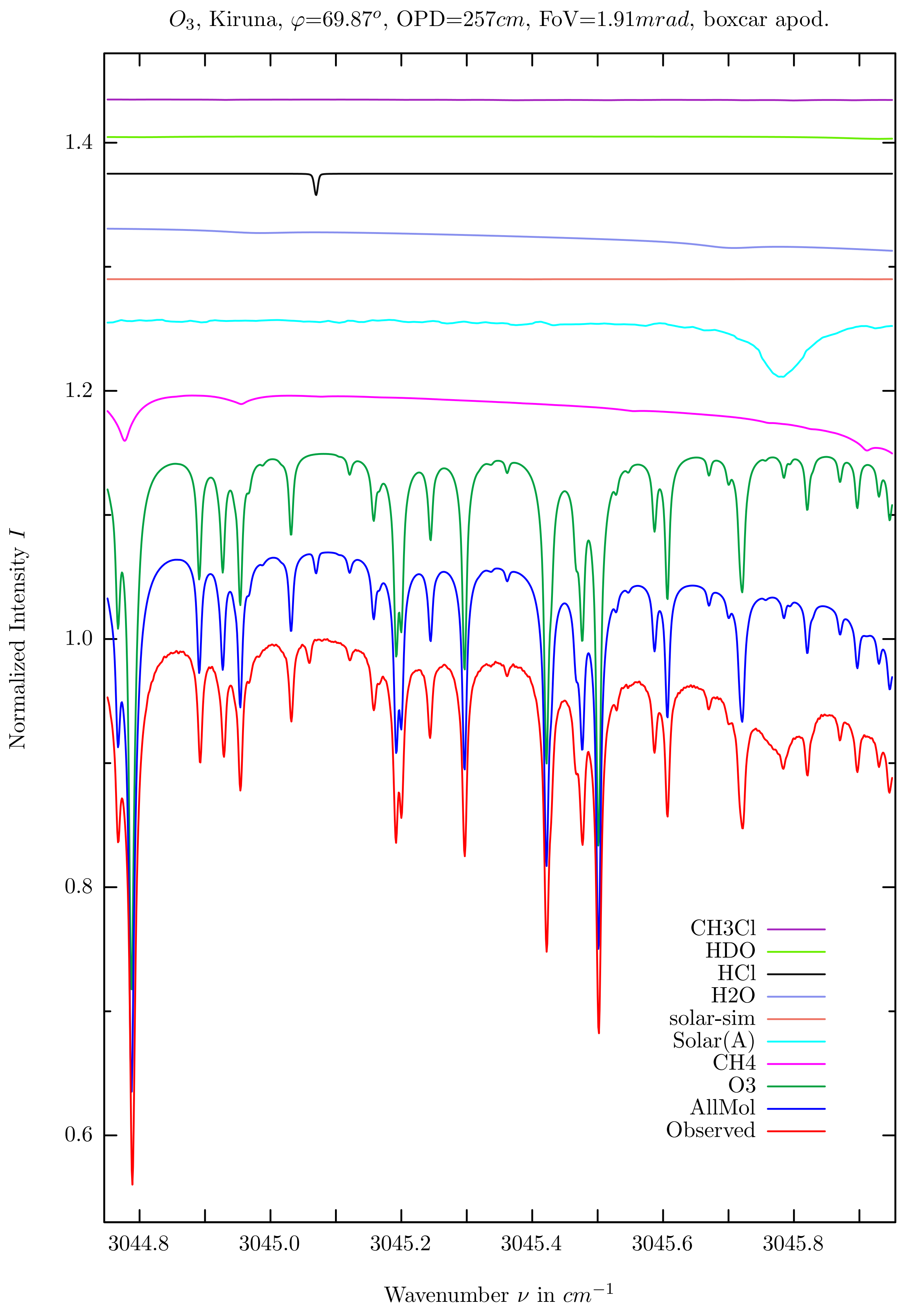
O_3, Kiruna, φ=69.87^o, OPD=257cm, FoV=1.91$mrad$, boxcar apod.
Normalized Intensity I
1.4
1.2
1.0
0.8
0.6
3044.8
3045.0
3045.2
3045.4
3045.6
3045.8
Wavenumber ν in cm^{-1}
CH3Cl
HDO
HCl
H2O
solar-sim
Solar(A)
CH4
O3
AllMol
Observed

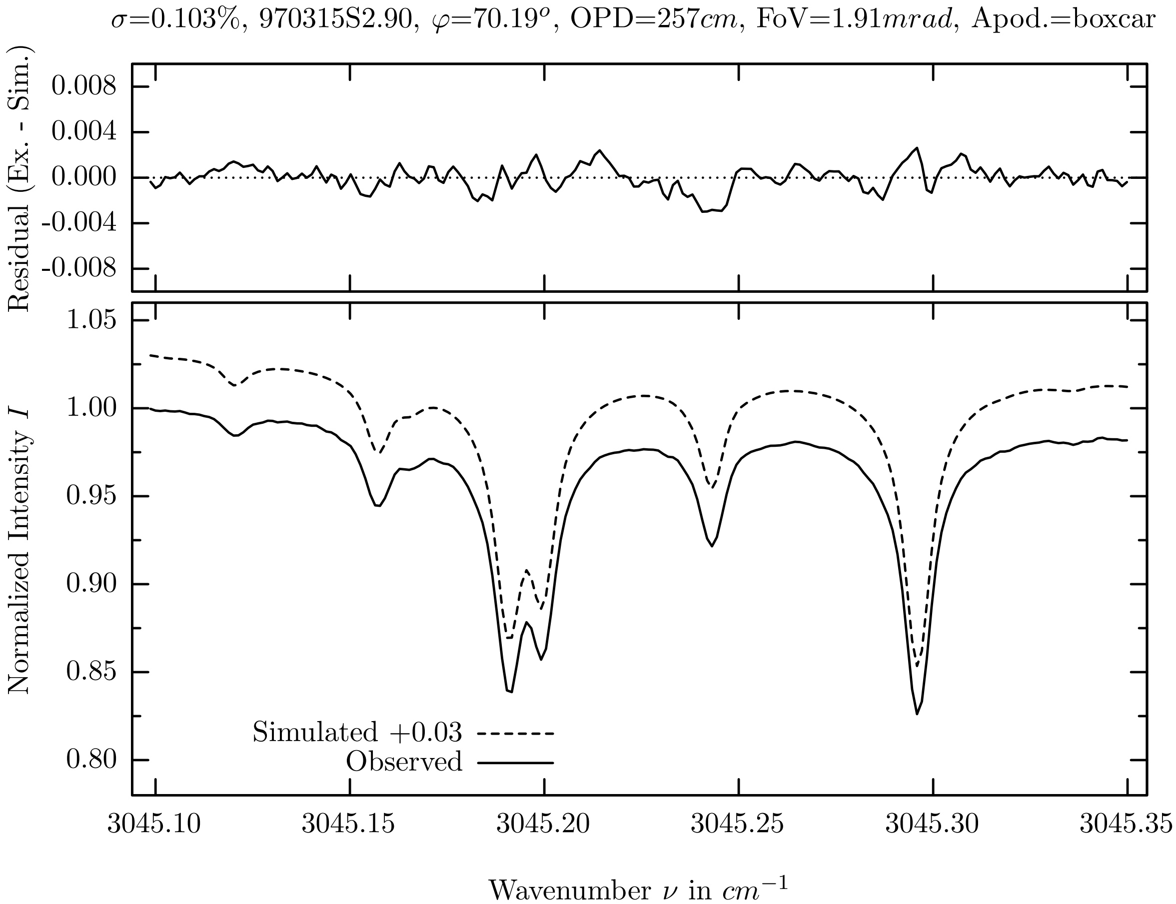

investigated species	:	O_3
line position(s) ν_0	:	3045.1987, 3045.2951 cm^{-1}
lower state energy E''_{lst}	:	340.7, 20.9 cm^{-1}
retrieved TCA, information content	:	1.01E+19 $molec/cm^2$, 155.3, 170.8
temperature dependence of the TCA	:	-0.020%/K (trop), +0.357%/K (strat)
location, date, solar zenith angle	:	Kiruna, 15/Mar/97, 70.19^o
spectral interval fitted	:	3045.097 – 3045.350 cm^{-1}

Molecule	iCode	Absorption	Molecule	iCode	Absorption
O3	31	44.344%	$CH3Cl$	301	0.073%
$CH4$	61	8.447%	$C2H4$	391	0.013%
Solar(A)	—	4.865%	$N2O$	41	0.012%
Solar-sim	—	0.007%	$NO2$	101	<0.001%
$H2O$	11	4.186%	$NH3$	111	<0.001%
HCl	151	1.750%	OH	131	<0.001%
HDO	491	0.192%			

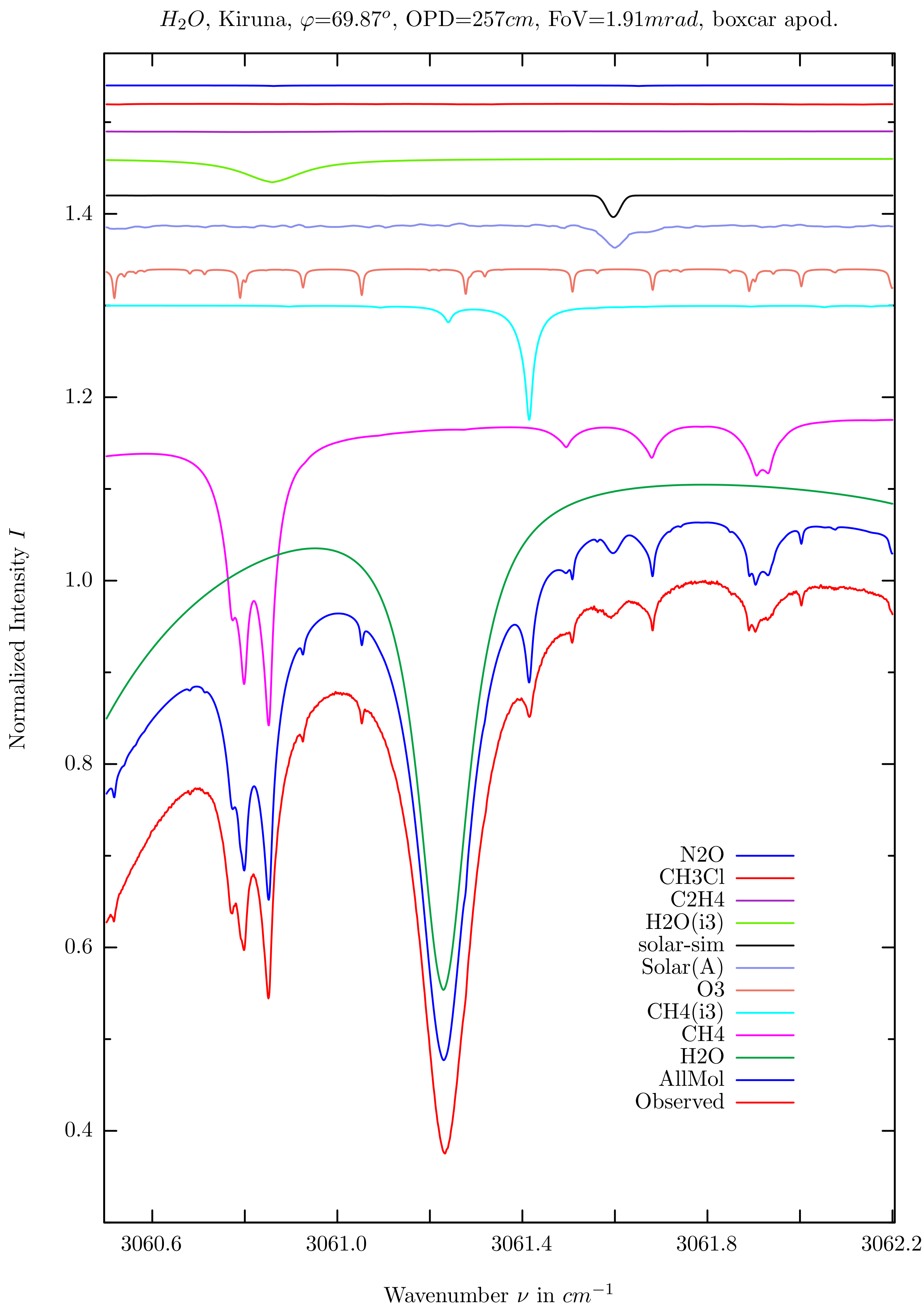

H_2O, Kiruna, φ=69.87^o, OPD=257cm, FoV=1.91$mrad$, boxcar apod.
Normalized Intensity I
Wavenumber ν in cm^{-1}
0.4
0.6
0.8
1.0
1.2
1.4
3060.6
3061.0
3061.4
3061.8
3062.2
N2O
CH3Cl
C2H4
H2O(i3)
solar-sim
Solar(A)
O3
CH4(i3)
CH4
H2O
AllMol
Observed

σ=0.187%, 970315S2.90, φ=70.19^o, OPD=257cm, FoV=1.91$mrad$, Apod.=boxcar

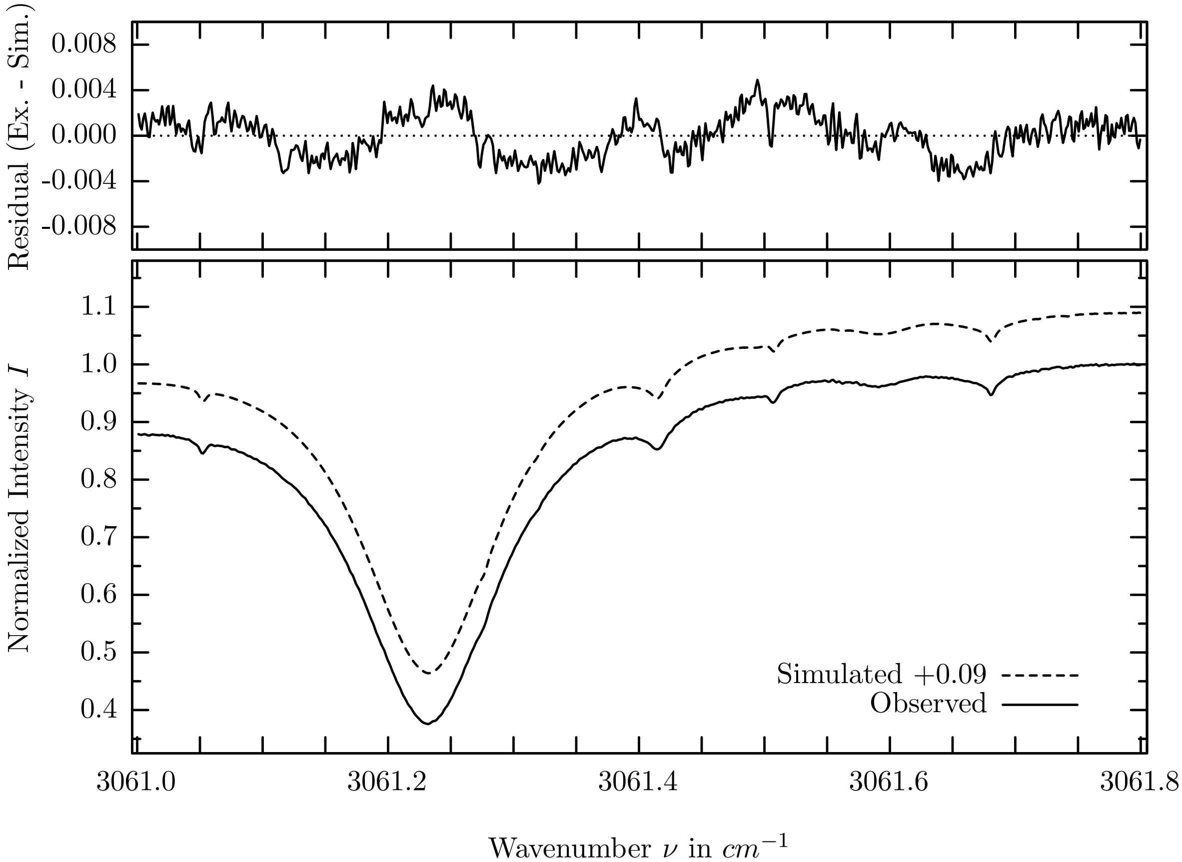

investigated species	:	H_2O
line position(s) ν_0	:	3061.2280 cm^{-1}
lower state energy E''_{lst}	:	1201.9 cm^{-1}
retrieved TCA, information content	:	5.66E+21 $molec/cm^2$, 333.5
temperature dependence of the TCA	:	-2.217%/K (trop), -0.015%/K (strat)
location, date, solar zenith angle	:	Kiruna, 15/Mar/97, 70.19^o
spectral interval fitted	:	3061.000 – 3061.800 cm^{-1}

Molecule	iCode	Absorption	Molecule	iCode	Absorption
H2O	11	66.023%	$CH3Cl$	301	0.067%
$CH4$	61	39.773%	$N2O$	41	0.060%
$CH4$	6**3**	12.496%	HDO	491	0.022%
$O3$	31	3.236%	$NH3$	111	<0.001%
Solar(A)	—	2.695%	OH	131	<0.001%
Solar-sim	—	2.352%	HCl	151	<0.001%
$H2O$	1**3**	2.558%	OCS	191	<0.001%
$C2H4$	391	0.075%			

CH_3D, Kiruna, φ=69.87^o, OPD=257cm, FoV=1.91$mrad$, boxcar apod.

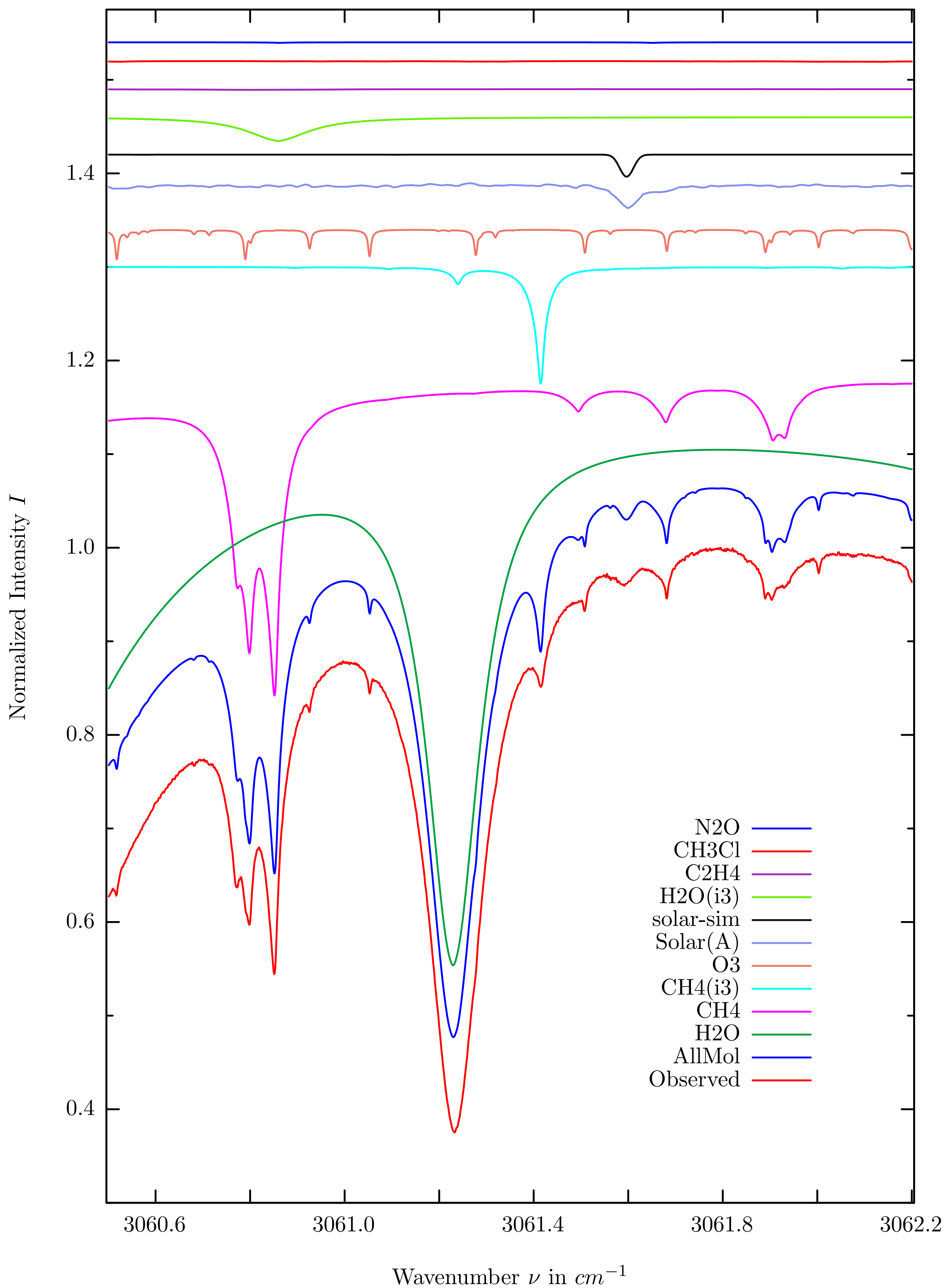

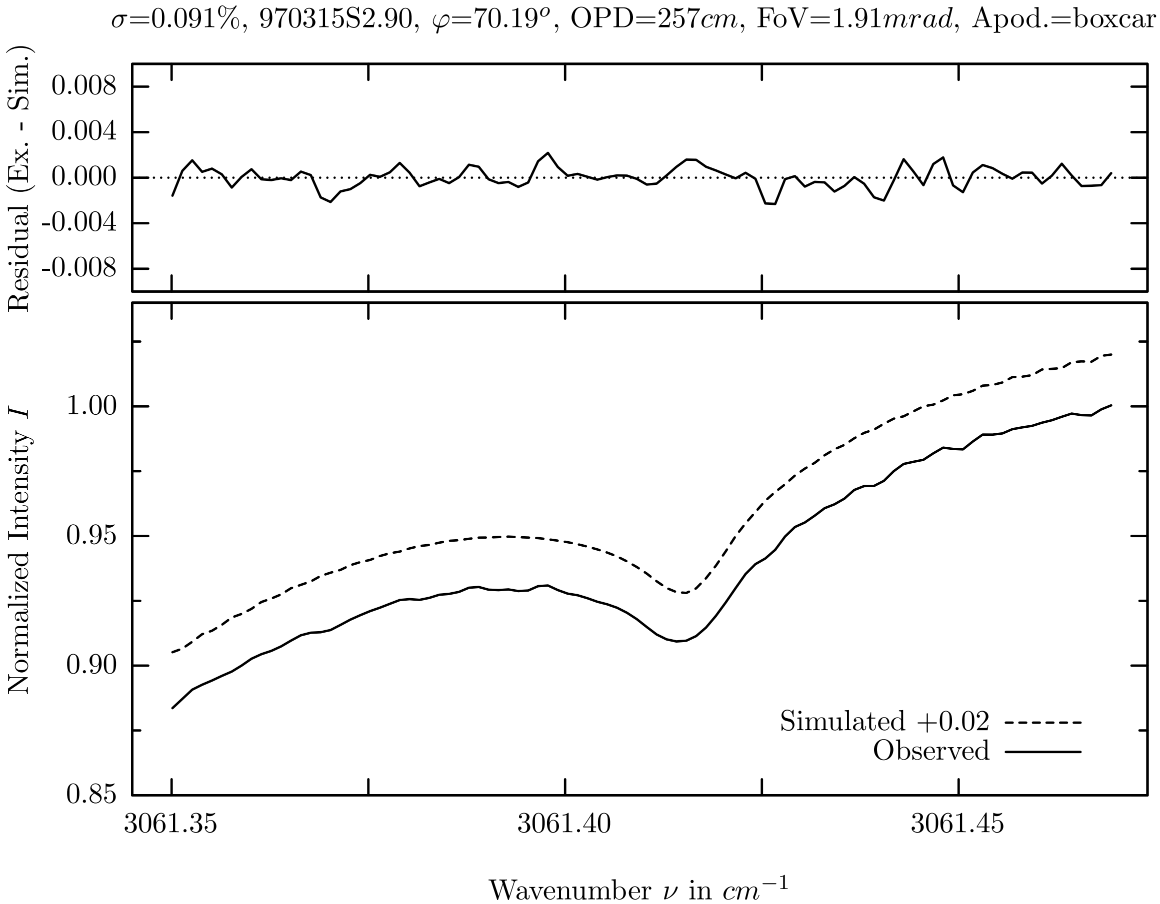

investigated species	:	CH_3D
line position(s) ν_0	:	3061.4140 cm^{-1}
lower state energy E''_{lst}	:	89.9 cm^{-1}
retrieved TCA, information content	:	2.09E+19 $molec/cm^2$, 62.1
temperature dependence of the TCA	:	-0.069%/K (trop), +0.029%/K (strat)
location, date, solar zenith angle	:	Kiruna, 15/Mar/97, 70.19^o
spectral interval fitted	:	3061.350 – 3061.470 cm^{-1}

Molecule	iCode	Absorption	Molecule	iCode	Absorption
$H2O$	11	66.023%	$CH3Cl$	301	0.067%
$CH4$	61	39.773%	$N2O$	41	0.060%
CH4	6**3**	12.496%	HDO	491	0.022%
$O3$	31	3.236%	$NH3$	111	<0.001%
Solar(A)	—	2.695%	OH	131	<0.001%
Solar-sim	—	2.352%	HCl	151	<0.001%
$H2O$	1**3**	2.558%	OCS	191	<0.001%
$C2H4$	391	0.075%			

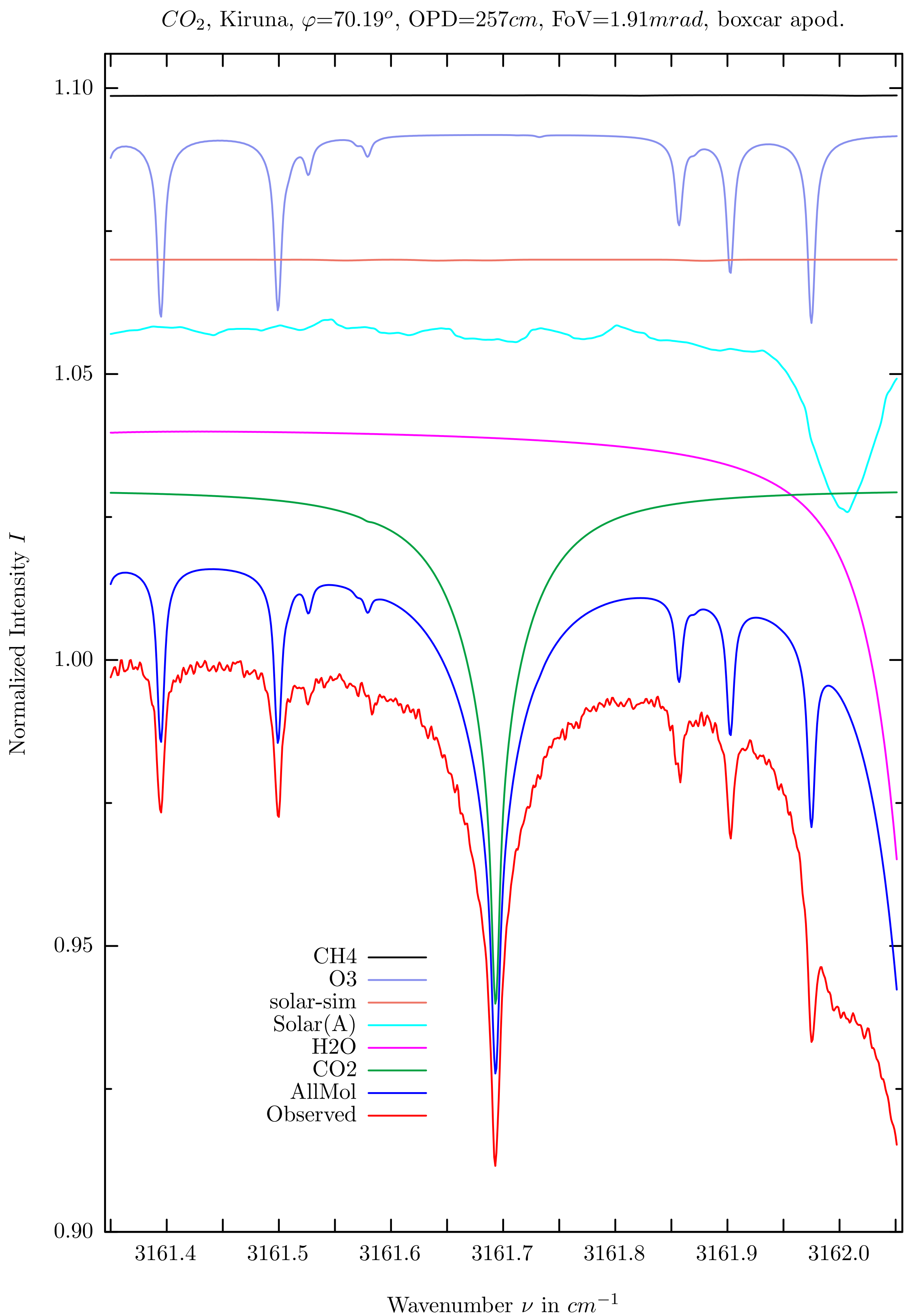
CO_2, Kiruna, φ=70.19^o, OPD=257cm, FoV=1.91$mrad$, boxcar apod.
Normalized Intensity I
Wavenumber ν in cm^{-1}
1.10
1.05
1.00
0.95
0.90
3161.4
3161.5
3161.6
3161.7
3161.8
3161.9
3162.0
CH4
O3
solar-sim
Solar(A)
H2O
CO2
AllMol
Observed

σ=0.077%, 970315S2.90, φ=70.19^o, OPD=257cm, FoV=1.91$mrad$, Apod.=boxcar

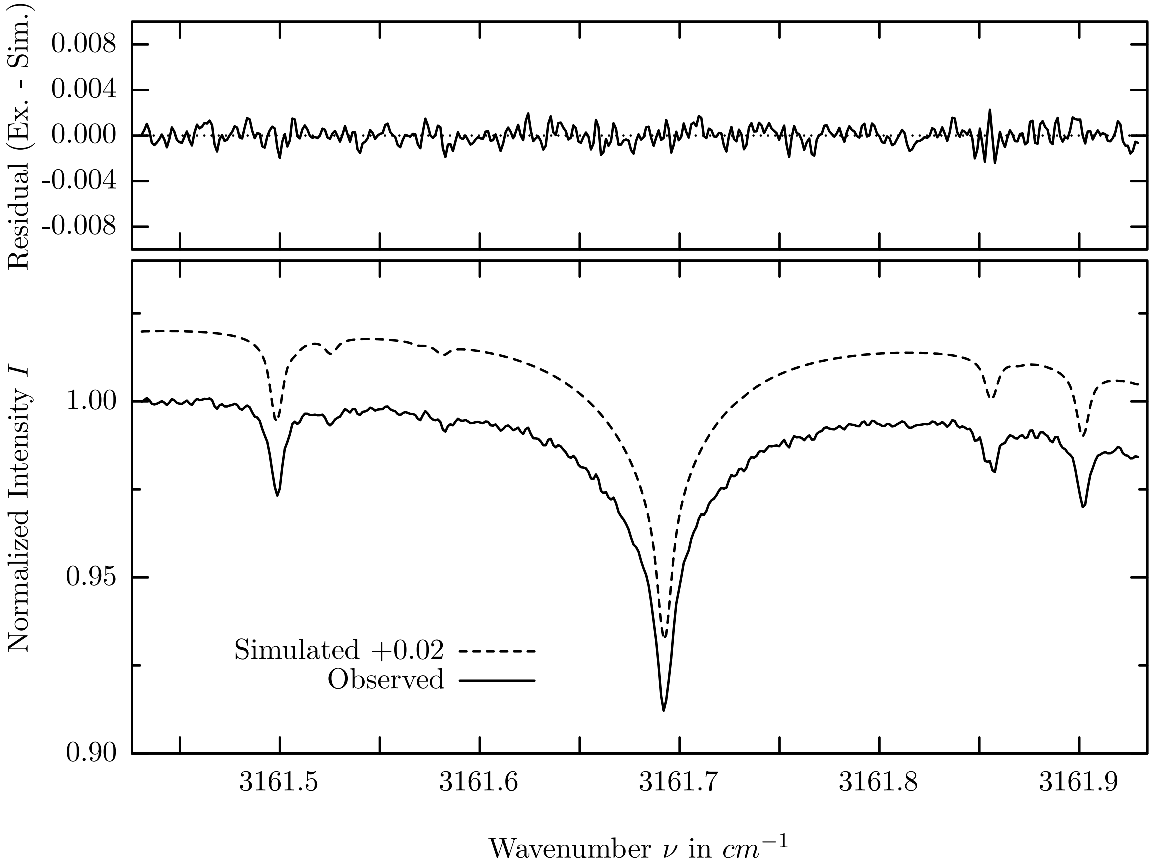

investigated species	:	$CO_2, (O_3)$
line position(s) ν_0	:	3161.6919, (3161.4977) cm^{-1}
lower state energy E''_{lst}	:	273.9, (260.4) cm^{-1}
retrieved TCA, information content	:	7.36E+21, (8.43E+18) $molec/cm^2$, 111.5, (33.5)
temperature dependence of the TCA	:	-.361, (-.162)%/K (trop), -.052, (-.228)%/K (strat)
location, date, solar zenith angle	:	Kiruna, 15/Mar/97, 70.19^o
spectral interval fitted	:	3161.430 – 3161.930 cm^{-1}

Molecule	iCode	Absorption	Molecule	iCode	Absorption
CO2	21	9.048%	$C2H4$	391	0.036%
$H2O$	11	8.404%	$CH3Cl$	301	0.002%
Solar(A)	—	3.415%	$N2O$	41	<0.001%
Solar-sim	—	0.020%	$NH3$	111	<0.001%
$O3$	31	3.337%	OH	131	<0.001%
$CH4$	61	0.137%	HCl	151	<0.001%
HDO	491	0.044%	HCN	281	<0.001%

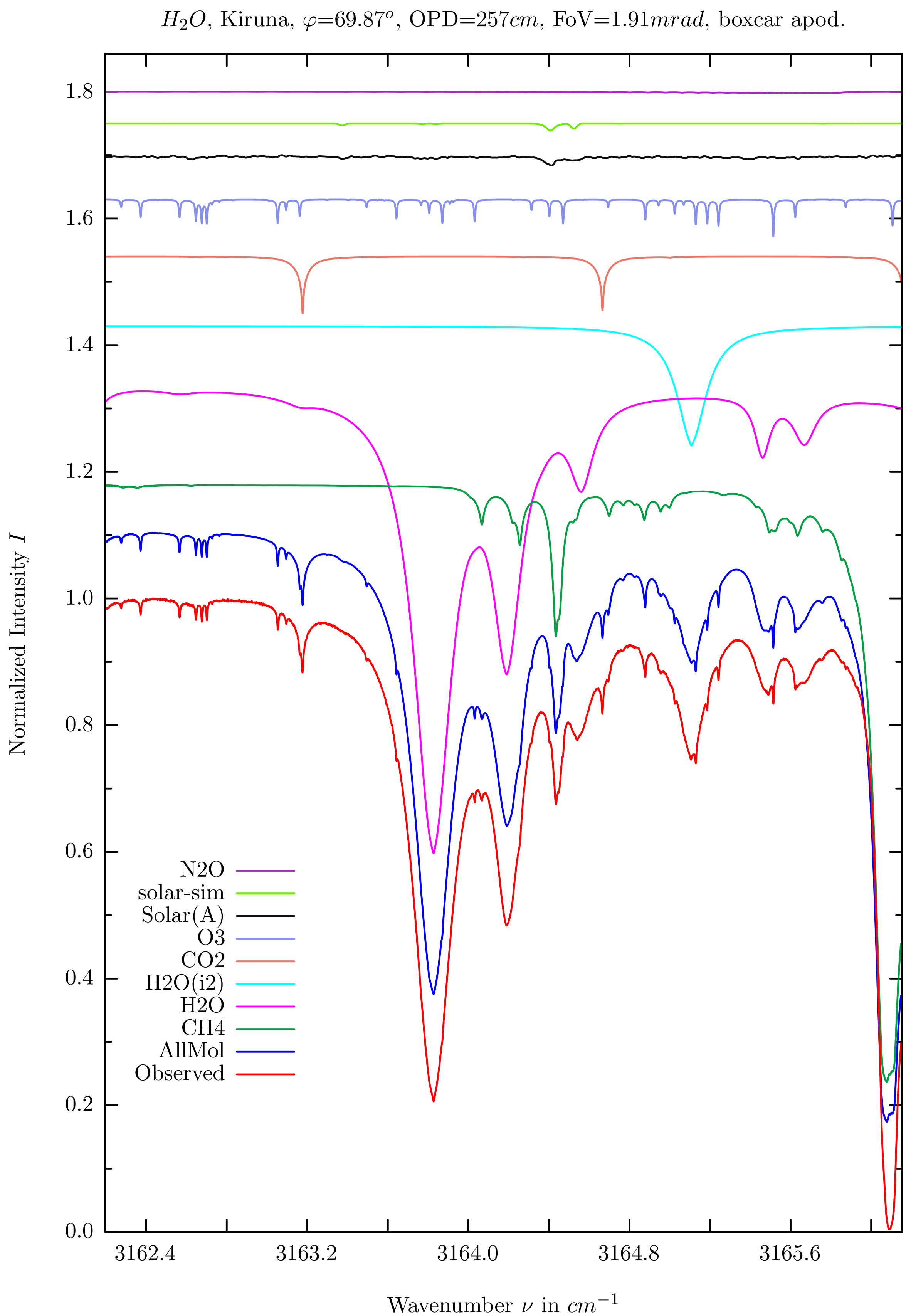
H_2O, Kiruna, φ=69.87^o, OPD=257cm, FoV=1.91$mrad$, boxcar apod.
1.8
1.6
1.4
1.2
1.0
0.8
0.6
0.4
0.2
0.0
Normalized Intensity I
N2O
solar-sim
Solar(A)
O3
CO2
H2O(i2)
H2O
CH4
AllMol
Observed
3162.4
3163.2
3164.0
3164.8
3165.6
Wavenumber ν in cm^{-1}

σ=0.460%, 970315S2.90, φ=70.19^o, OPD=257cm, FoV=1.91$mrad$, Apod.=boxcar

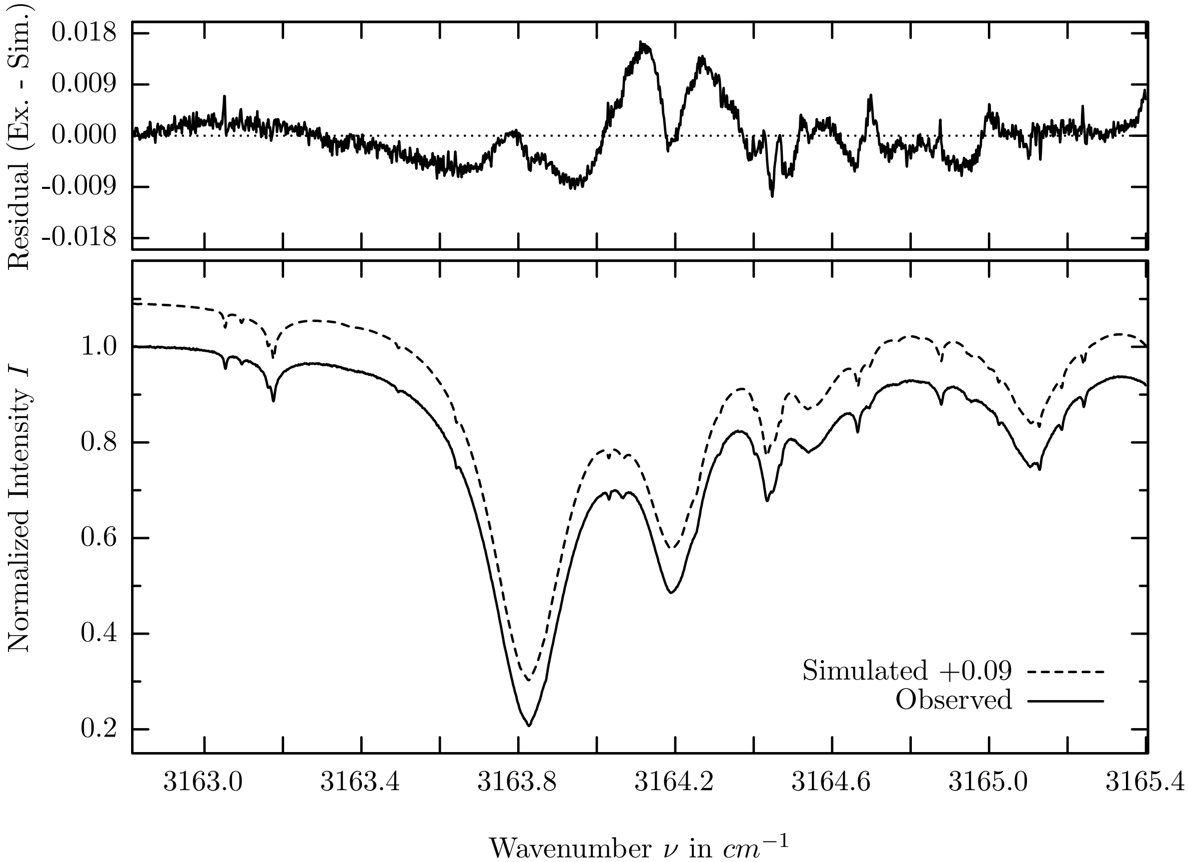

investigated species	:	$H_2O, (H_2O(i2))$
line position(s) ν_0	:	3163.8269, 3164.1851, (3165.1010) cm^{-1}
lower state energy E''_{lst}	:	136.2, 709.6, (23.8) cm^{-1}
retrieved TCA, information content	:	6.56e21, (6.83e21) $molec/cm^2$, 171.0, 111.5, (54.2)
temperature dependence of the TCA	:	-.146, (+.482)%/K (trop), -.009, (-.034)%/K (strat)
location, date, solar zenith angle	:	Kiruna, 15/Mar/97, 70.19^o
spectral interval fitted	:	3162.820 – 3165.400 cm^{-1}

Molecule	iCode	Absorption	Molecule	iCode	Absorption
$CH4$	61	94.317%	$C2H4$	391	0.027%
H2O	11	74.220%	HDO	491	0.009%
$H2O$	1**2**	18.865%	$CH3Cl$	301	0.002%
$CO2$	21	9.009%	$NH3$	111	0.001%
$O3$	31	5.915%	OH	131	<0.001%
Solar(A)	—	1.639%	HCl	151	<0.001%
Solar-sim	—	1.125%	HCN	281	<0.001%
$N2O$	41	0.219%			

H_2O, Kiruna, φ=70.19^o, OPD=257cm, FoV=1.91$mrad$, boxcar apod.

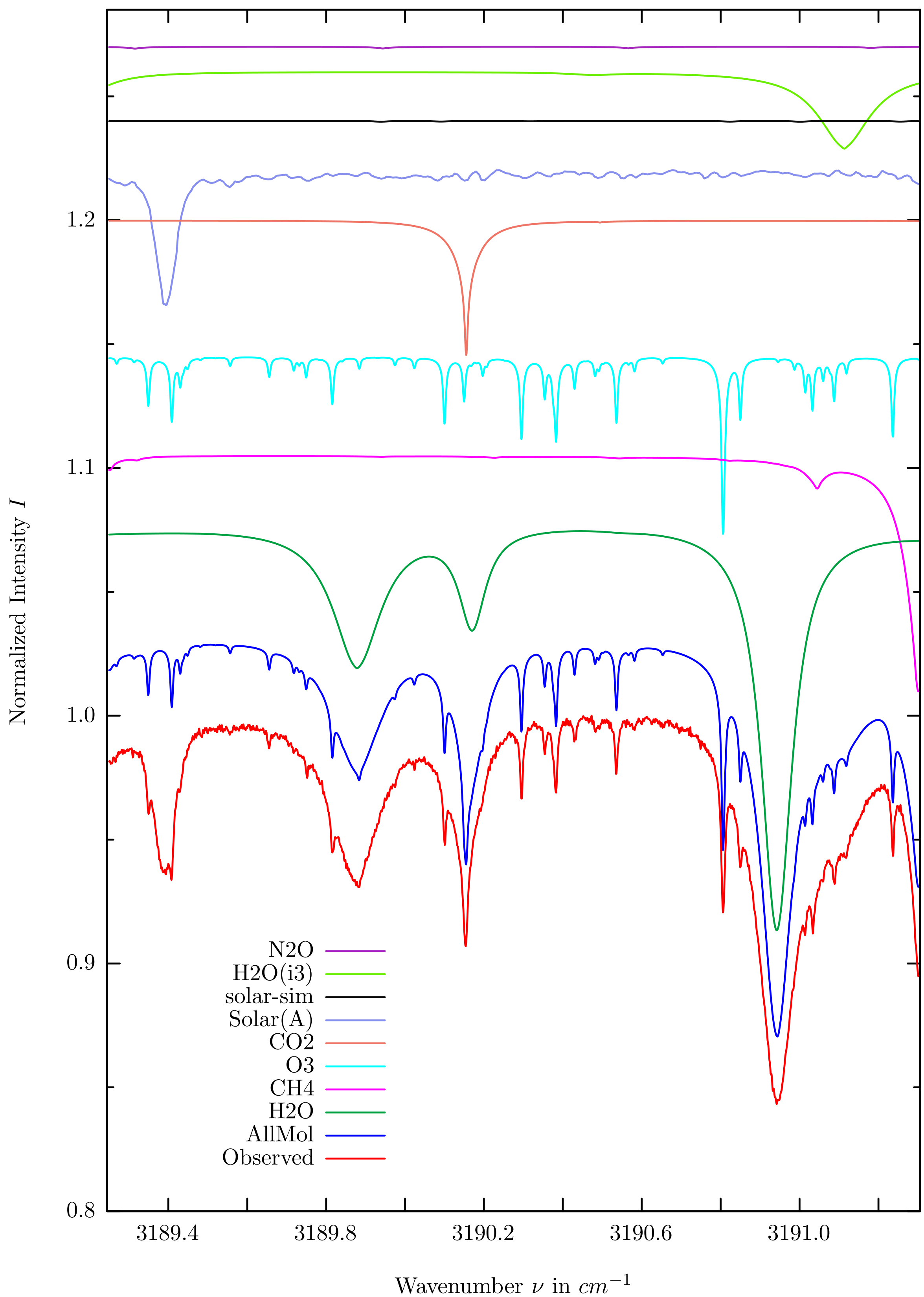

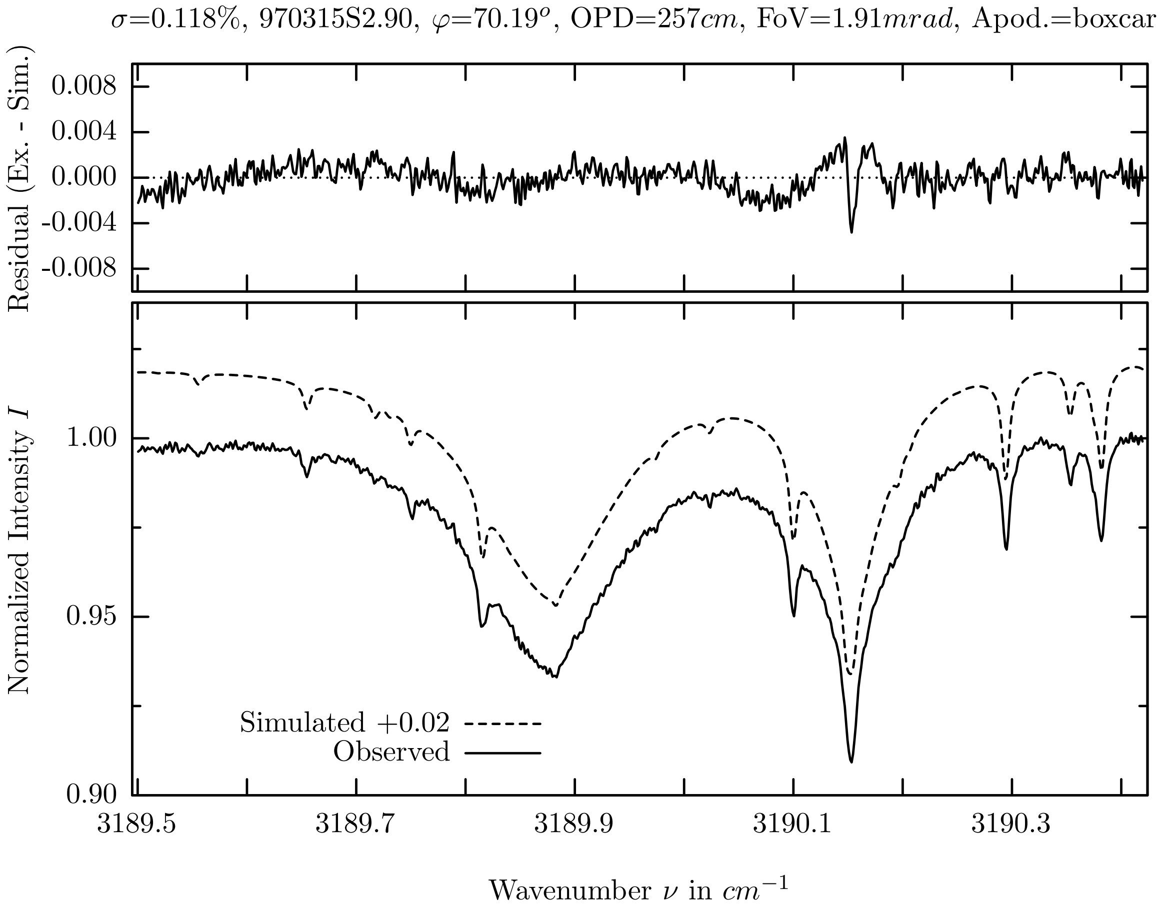

investigated species	:	H_2O
line position(s) ν_0	:	3189.8770 cm^{-1}
lower state energy E''_{lst}	:	1059.6 cm^{-1}
retrieved TCA, information content	:	5.53E+21 $molec/cm^2$, 56.8
temperature dependence of the TCA	:	-1.945%/K (trop), -0.018%/K (strat)
location, date, solar zenith angle	:	Kiruna, 15/Mar/97, 70.19^o
spectral interval fitted	:	3189.500 – 3190.420 cm^{-1}

Molecule	iCode	Absorption	Molecule	iCode	Absorption
H2O	11	21.729%	$C2H4$	391	0.020%
$CH4$	61	9.526%	$NH3$	111	0.001%
$O3$	31	7.233%	HDO	491	0.001%
$CO2$	21	5.459%	NO	81	<0.001%
Solar(A)	—	5.427%	OH	131	<0.001%
Solar-sim	—	0.023%	$HO2$	221	<0.001%
$H2O$	1**3**	3.111%	HCN	281	<0.001%
$N2O$	41	0.074%	$C2H2$	40**2**	<0.001%

CO_2, Kiruna, φ=70.19^o, OPD=257cm, FoV=1.91$mrad$, boxcar apod.

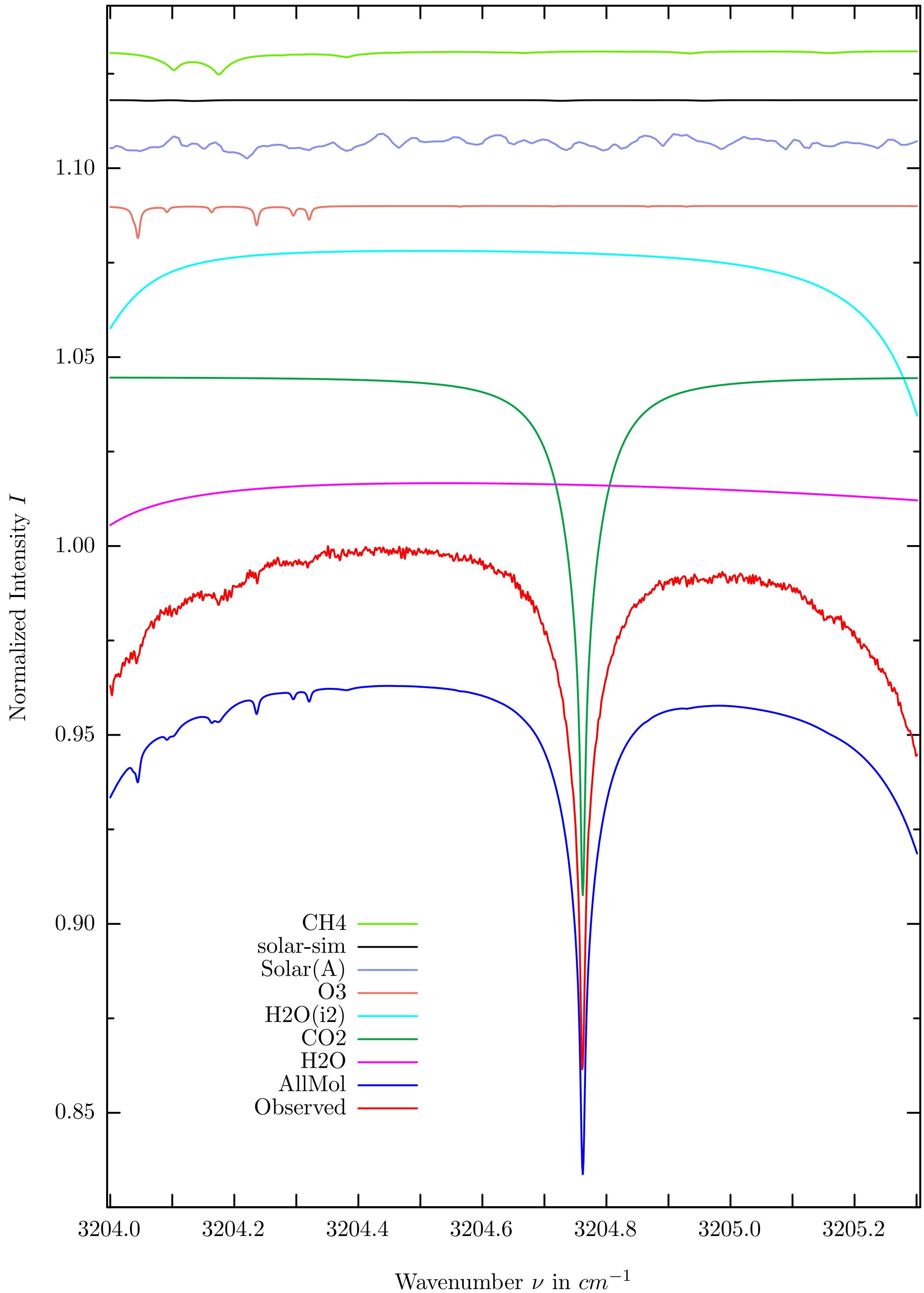

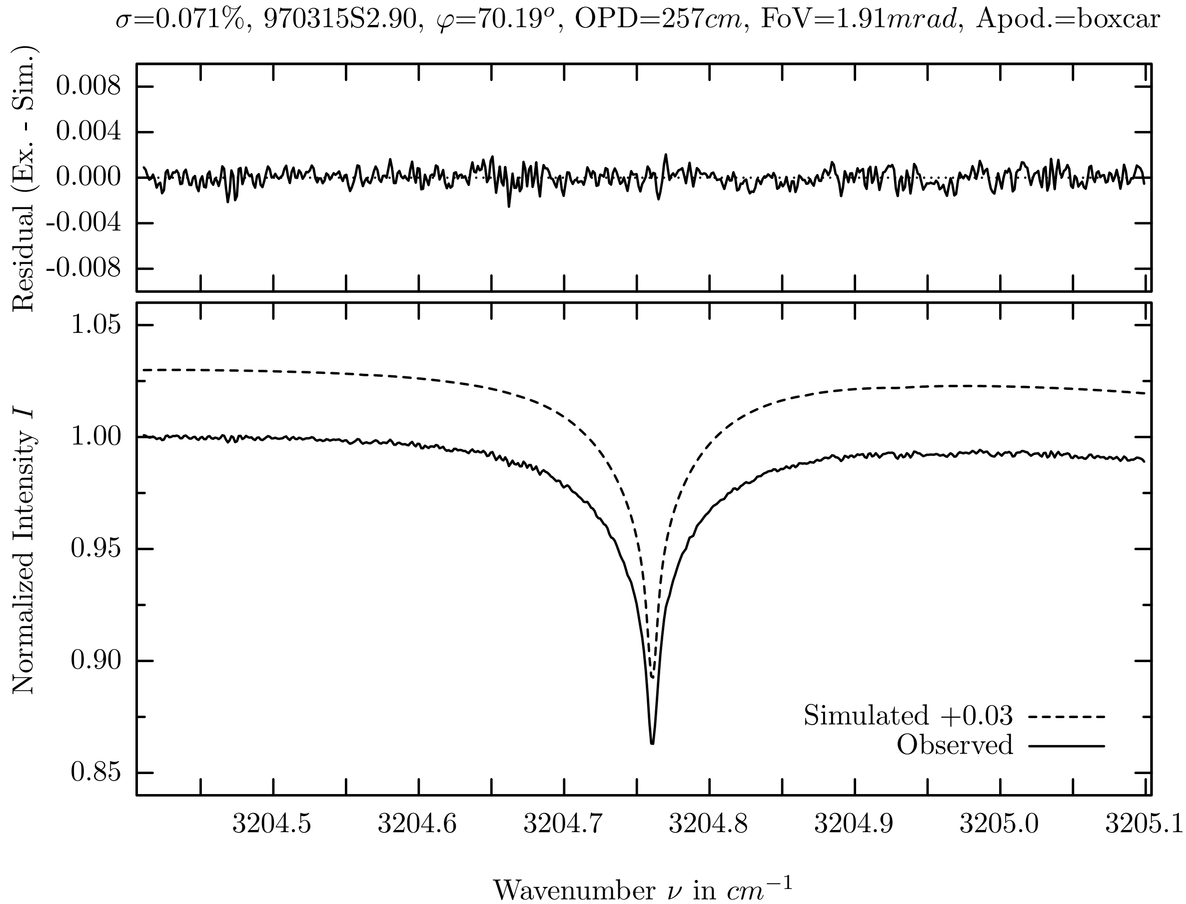

investigated species	:	CO_2
line position(s) ν_0	:	3204.7604 cm^{-1}
lower state energy E''_{lst}	:	316.8 cm^{-1}
retrieved TCA, information content	:	7.52E+21 $molec/cm^2$, 194.6
temperature dependence of the TCA	:	-0.439%/K (trop), -0.093%/K (strat)
location, date, solar zenith angle	:	Kiruna, 15/Mar/97, 70.19^o
spectral interval fitted	:	3204.410 – 3205.100 cm^{-1}

Molecule	iCode	Absorption	Molecule	iCode	Absorption
CO2	21	13.794%	$C2H4$	391	0.010%
$H2O$	11	6.407%	HDO	491	0.007%
$H2O$	1**2**	4.655%	$NH3$	111	0.001%
$O3$	31	0.864%	$N2O$	41	<0.001%
Solar(A)	—	0.640%	NO	81	<0.001%
Solar-sim	—	0.022%	OH	131	<0.001%
$CH4$	61	0.621%	$HO2$	221	<0.001%
$C2H2$	401	0.031%	HCN	281	<0.001%

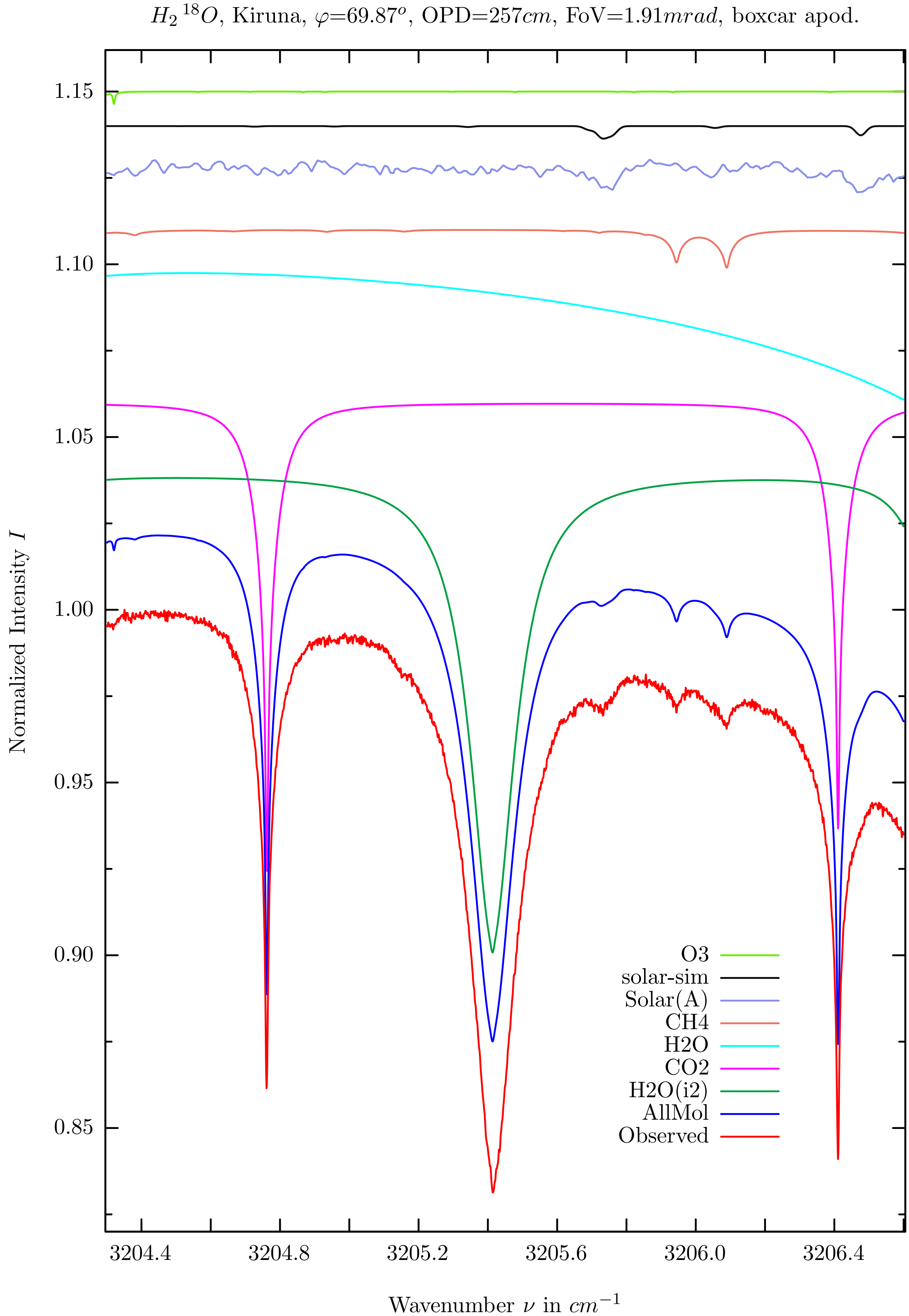
$H_2{}^{18}O$, Kiruna, φ=69.87^o, OPD=257cm, FoV=1.91$mrad$, boxcar apod.
Normalized Intensity I
1.15
1.10
1.05
1.00
0.95
0.90
0.85
3204.4
3204.8
3205.2
3205.6
3206.0
3206.4
Wavenumber ν in cm^{-1}
O3
solar-sim
Solar(A)
CH4
H2O
CO2
H2O(i2)
AllMol
Observed

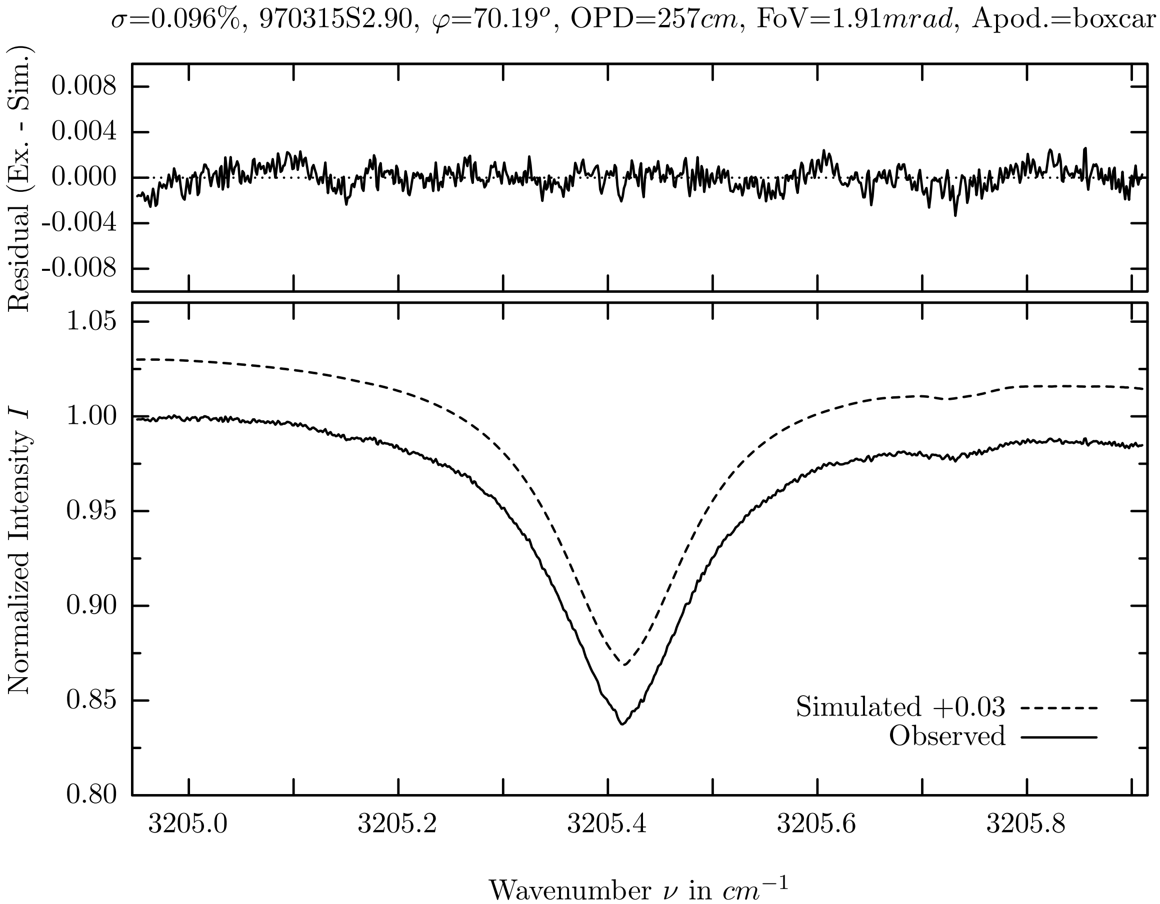

investigated species	:	$H_2O(i2)$
line position(s) ν_0	:	3205.4120 cm^{-1}
lower state energy E''_{lst}	:	172.9 cm^{-1}
retrieved TCA, information content	:	6.24E+21 $molec/cm^2$, 165.5
temperature dependence of the TCA	:	+0.222%/K (trop), -0.006%/K (strat)
location, date, solar zenith angle	:	Kiruna, 15/Mar/97, 70.19^o
spectral interval fitted	:	3204.950 – 3205.910 cm^{-1}

Molecule	iCode	Absorption	Molecule	iCode	Absorption
H2O	1**2**	13.923%	*C2H4*	391	0.010%
CO2	21	13.609%	*HDO*	491	0.007%
H2O	11	8.853%	*NH3*	111	0.001%
CH4	61	1.097%	*N2O*	41	<0.001%
Solar(A)	—	0.916%	*NO*	81	<0.001%
Solar-sim	—	0.365%	*OH*	131	<0.001%
O3	31	0.363%	*HO2*	221	<0.001%
C2H2	401	0.031%	*HCN*	281	<0.001%

H_2O, Kiruna, φ=69.87^o, OPD=257cm, FoV=1.91$mrad$, boxcar apod.

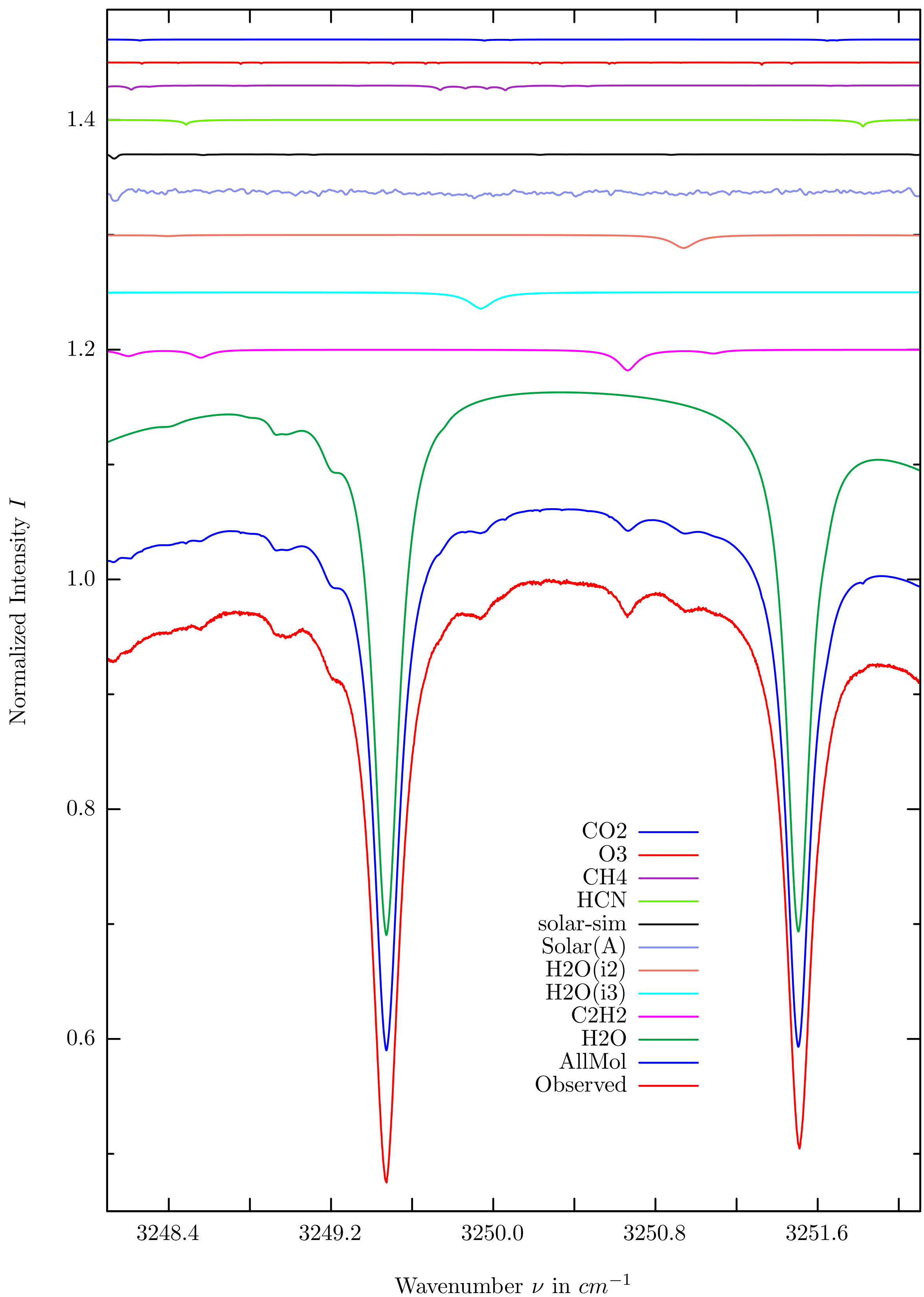

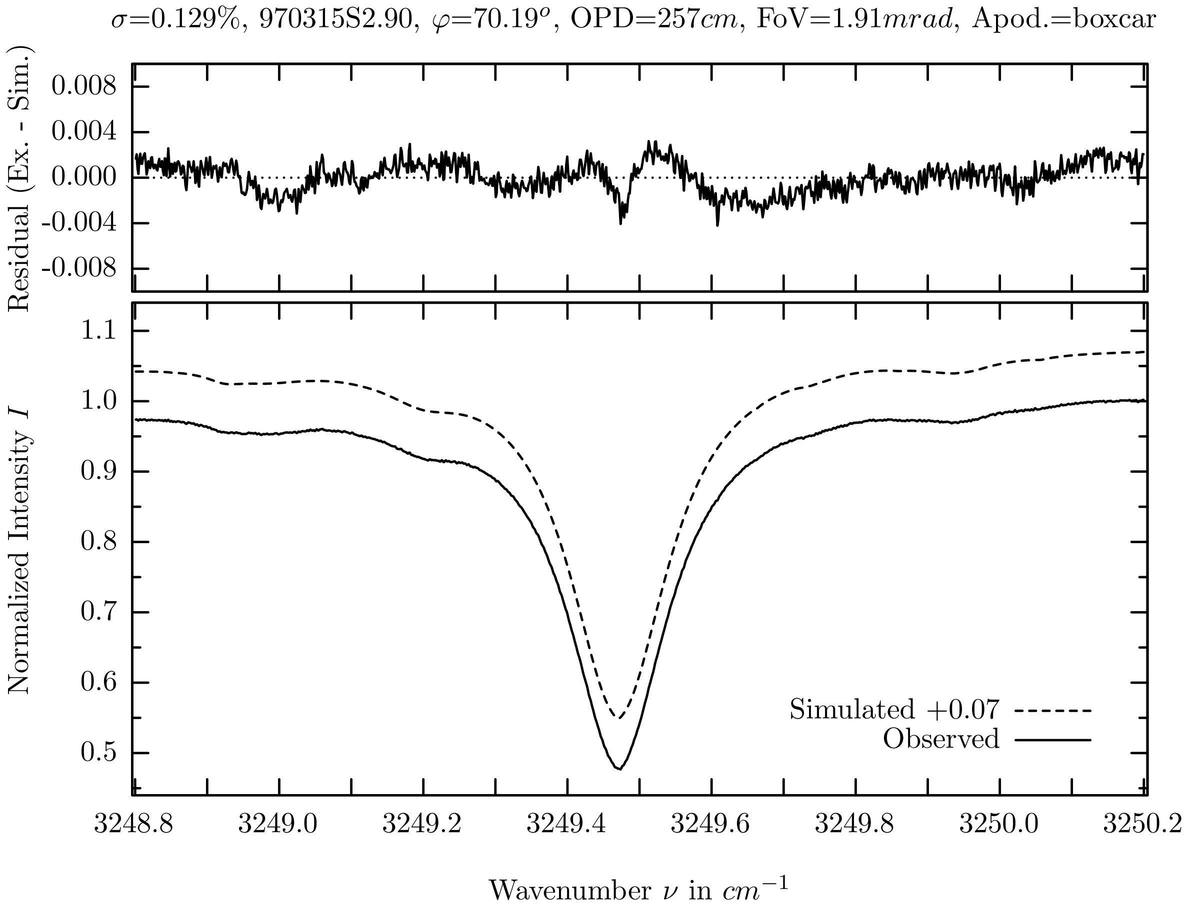

investigated species	:	$H_2O, (H_2O(i3))$
line position(s) ν_0	:	3249.4719, (3249.9380) cm^{-1}
lower state energy E''_{lst}	:	982.9, (224.3) cm^{-1}
retrieved TCA, information content	:	5.91E+21, (8.12E+21) $molec/cm^2$, 403.2, (12.7)
temperature dependence of the TCA	:	-1.769, (+.213)%/K (trop), -.013, (-.004)%/K (strat)
location, date, solar zenith angle	:	Kiruna, 15/Mar/97, 70.19^o
spectral interval fitted	:	3248.800 – 3250.200 cm^{-1}

Molecule	iCode	Absorption	Molecule	iCode	Absorption
H2O	11	54.966%	$O3$	31	0.201%
$C2H2$	401	1.800%	$CO2$	21	0.099%
$H2O$	1**3**	1.429%	HDO	491	0.032%
$H2O$	1**2**	1.151%	$NH3$	111	0.001%
Solar(A)	—	1.050%	NO	81	<0.001%
Solar-sim	—	0.367%	OH	131	<0.001%
HCN	281	0.570%	$HO2$	221	<0.001%
$CH4$	61	0.417%	$C2H4$	391	<0.001%

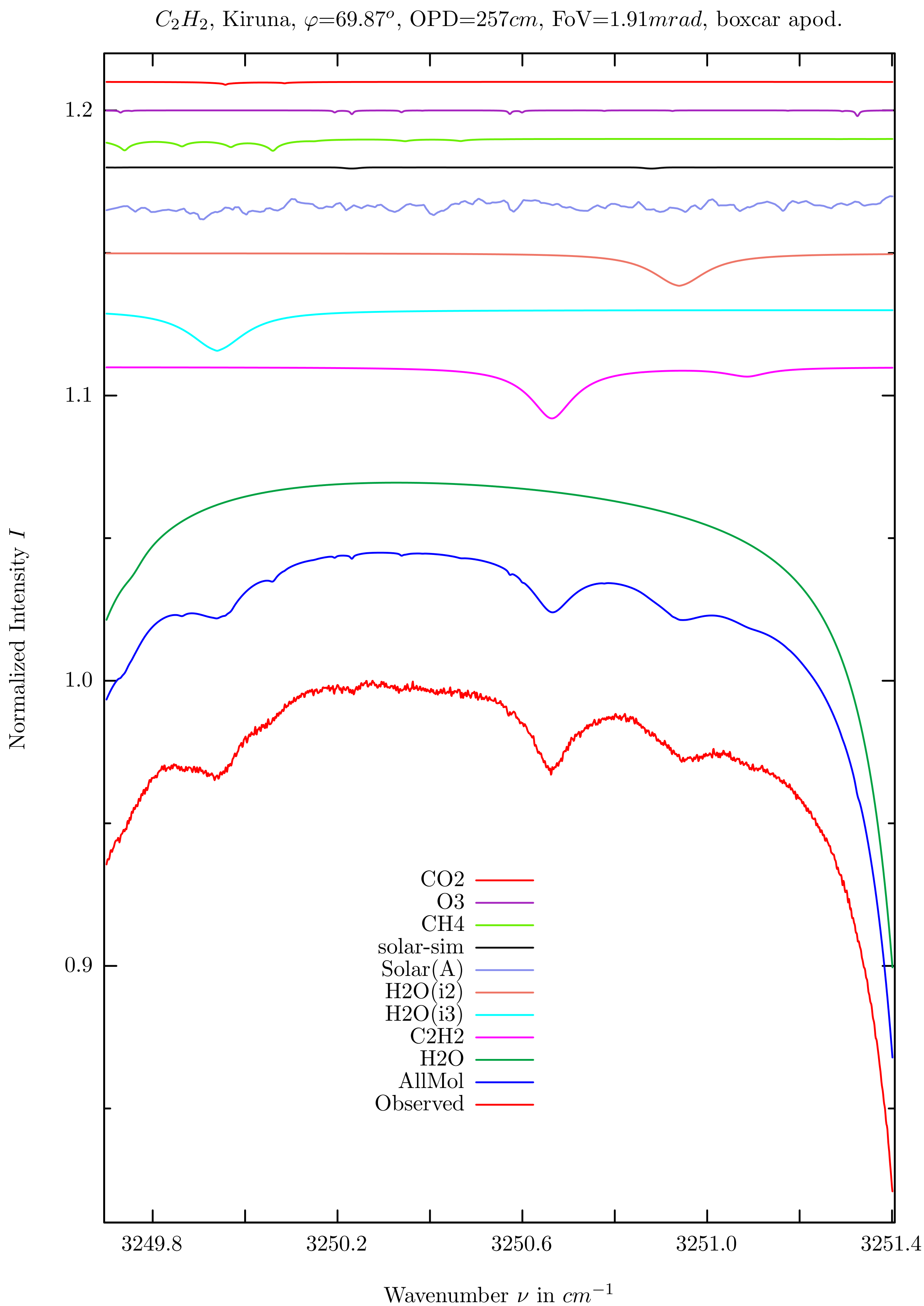

C_2H_2, Kiruna, φ=69.87^o, OPD=257cm, FoV=1.91$mrad$, boxcar apod.
Normalized Intensity I
Wavenumber ν in cm^{-1}
1.2
1.1
1.0
0.9
3249.8
3250.2
3250.6
3251.0
3251.4
CO2
O3
CH4
solar-sim
Solar(A)
H2O(i2)
H2O(i3)
C2H2
H2O
AllMol
Observed

σ=0.074%, 970315S2.90, φ=70.19^o, OPD=257cm, FoV=1.91$mrad$, Apod.=boxcar

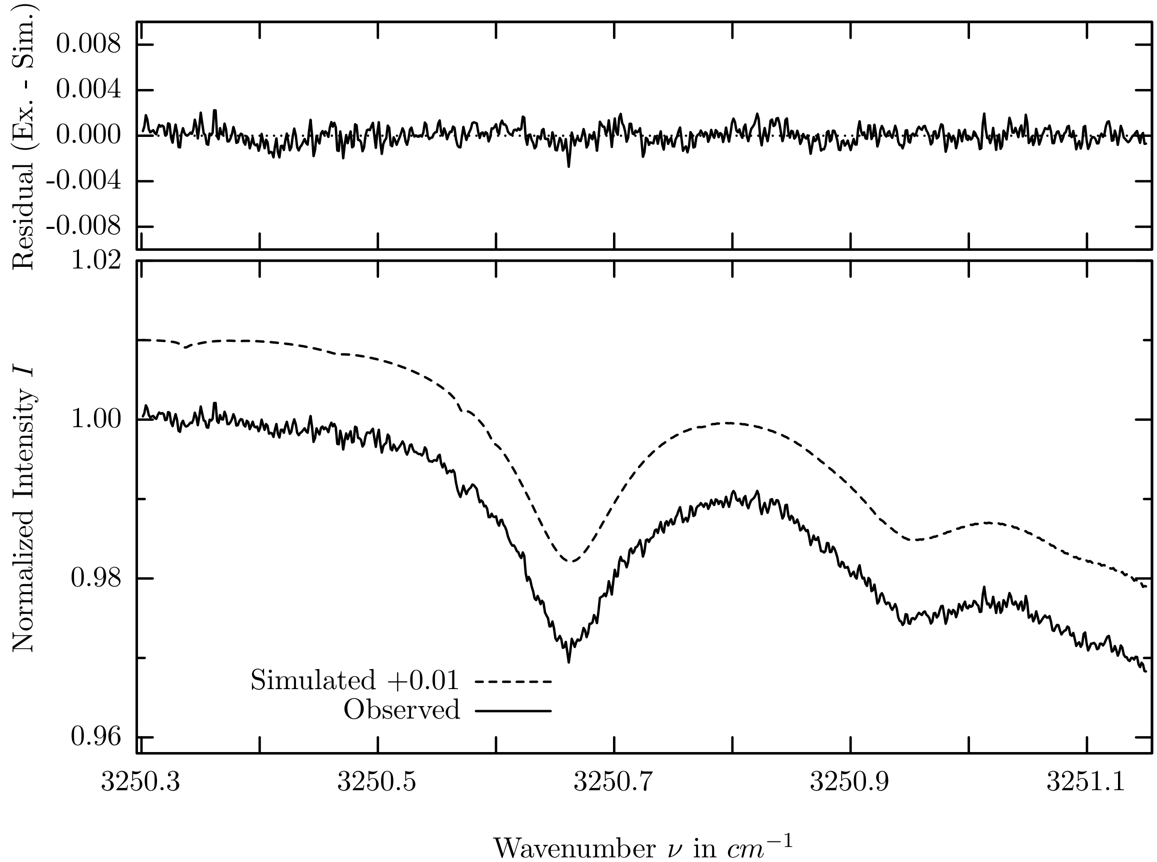

investigated species	:	C_2H_2
line position(s) ν_0	:	3250.6624 cm^{-1}
lower state energy E''_{lst}	:	214.1 cm^{-1}
retrieved TCA, information content	:	8.18E+15 $molec/cm^2$, 33.9
temperature dependence of the TCA	:	-0.270%/K (trop), -0.002%/K (strat)
location, date, solar zenith angle	:	Kiruna, 15/Mar/97, 70.19^o
spectral interval fitted	:	3250.300 – 3251.150 cm^{-1}

Molecule	iCode	Absorption	Molecule	iCode	Absorption
$H2O$	11	24.153%	$CO2$	21	0.099%
C2H2	401	1.800%	HDO	491	0.032%
$H2O$	1**3**	1.429%	HCN	281	0.006%
$H2O$	1**2**	1.150%	$NH3$	111	0.001%
Solar(A)	—	0.822%	NO	81	<0.001%
Solar-sim	—	0.040%	OH	131	<0.001%
$CH4$	61	0.417%	$HO2$	221	<0.001%
$O3$	31	0.201%	$C2H4$	391	<0.001%

HCN, Kiruna, φ=70.19^o, OPD=257cm, FoV=1.91$mrad$, boxcar apod.

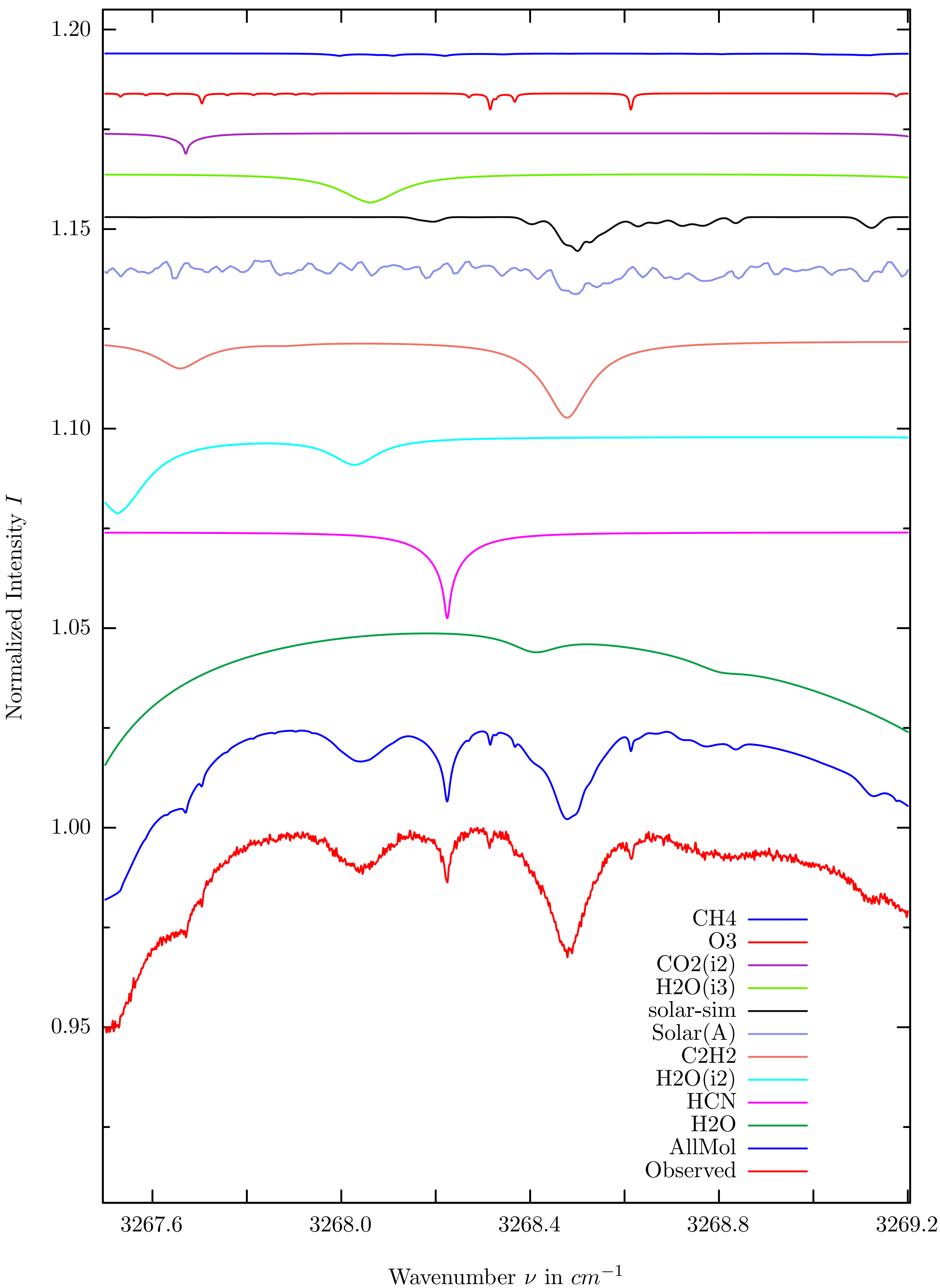

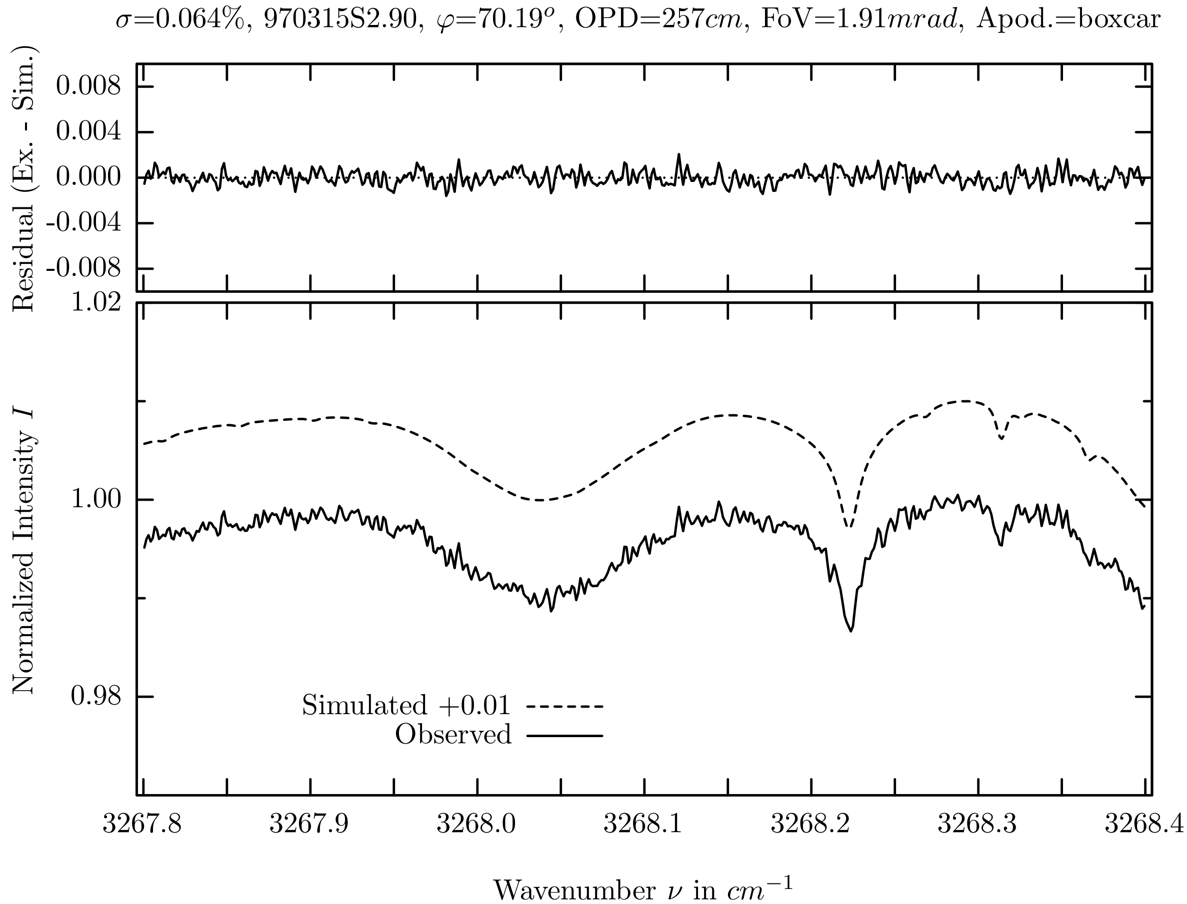

investigated species	:	HCN
line position(s) ν_0	:	3268.2229 cm^{-1}
lower state energy E''_{lst}	:	310.3 cm^{-1}
retrieved TCA, information content	:	2.91E+15 $molec/cm^2$, 20.3
temperature dependence of the TCA	:	-0.537%/K (trop), -0.122%/K (strat)
location, date, solar zenith angle	:	Kiruna, 15/Mar/97, 70.19^o
spectral interval fitted	:	3267.800 – 3268.400 cm^{-1}

Molecule	iCode	Absorption	Molecule	iCode	Absorption
$H2O$	11	10.187%	$CH4$	61	0.061%
HCN	281	2.156%	$N2O$	4**2**	0.020%
$H218O$	511	1.926%	HDO	491	0.012%
$C2H2$	401	1.925%	$NH3$	111	0.001%
Solar(A)	—	0.830%	$HO2$	221	0.001%
Solar-sim	—	0.850%	$CO2$	21	<0.001%
$H217O$	521	0.737%	NO	81	<0.001%
$CO2$	2**2**	0.515%	OH	131	<0.001%
$O3$	31	0.411%	HF	141	<0.001%

Note also the C_2H_2 line at 3268.5cm^{-1}. However, more favourable windows do exist for C_2H_2.

HCN, Kiruna, φ=69.87^o, OPD=257cm, FoV=1.91$mrad$, boxcar apod.

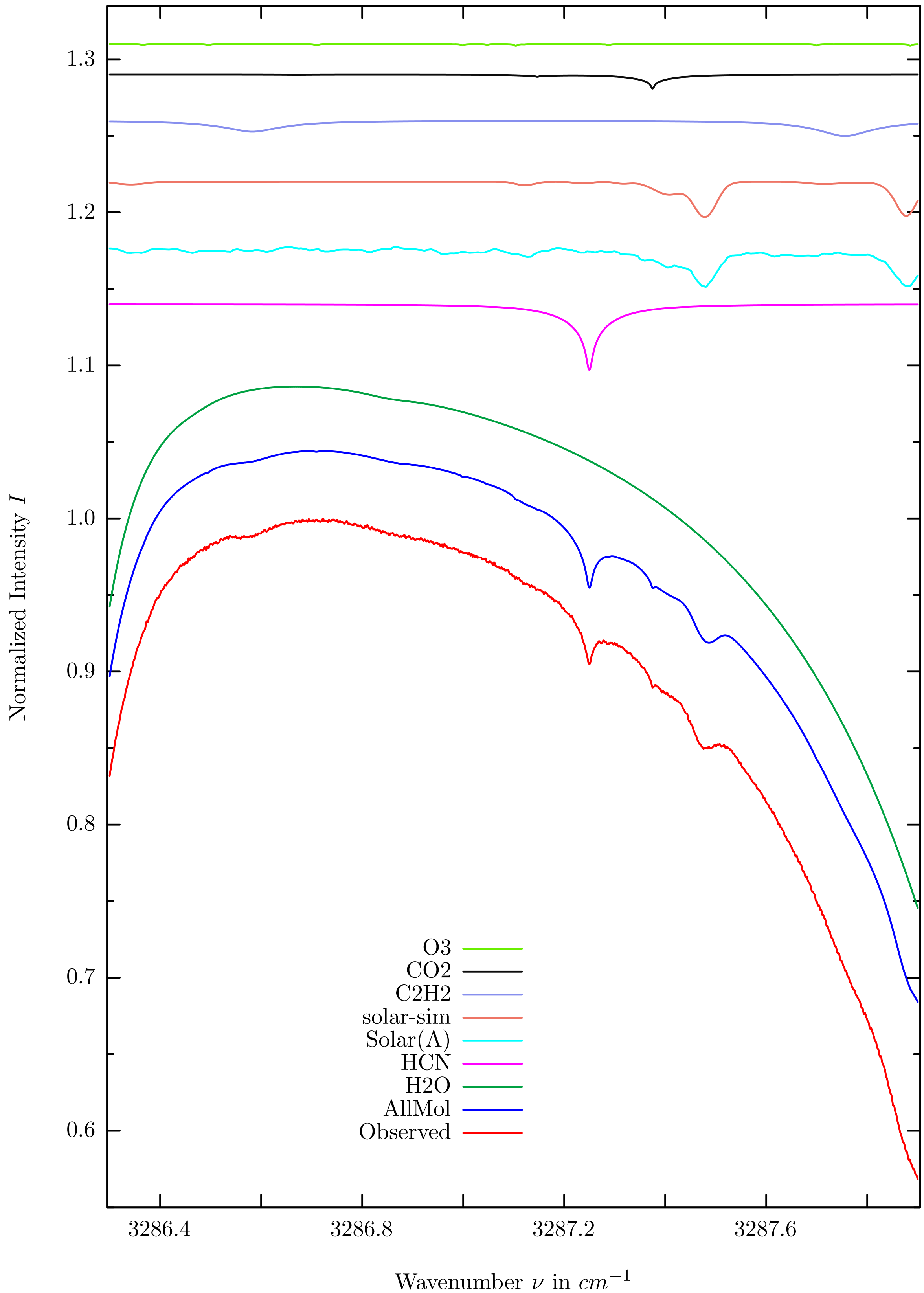

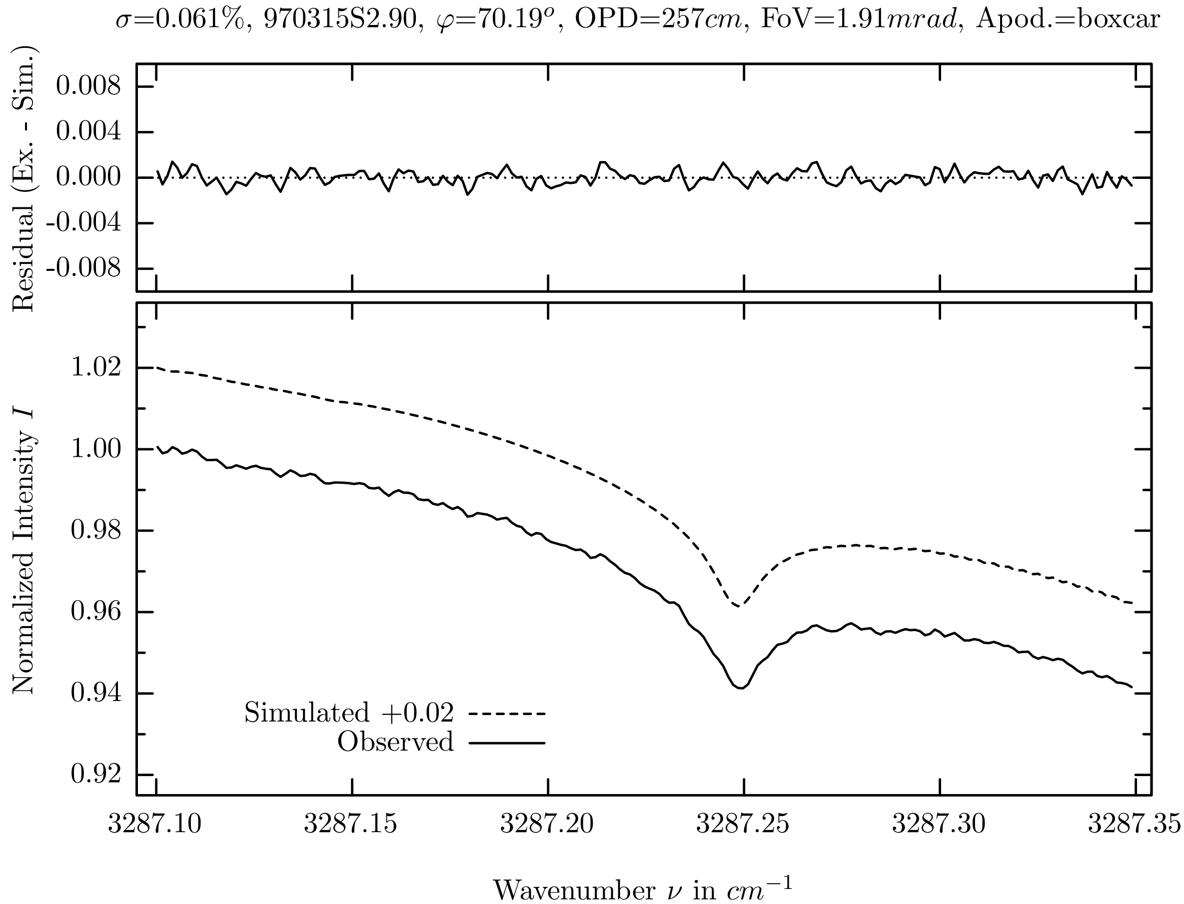

investigated species	:	HCN
line position(s) ν_0	:	3287.2483 cm^{-1}
lower state energy E''_{lst}	:	106.4 cm^{-1}
retrieved TCA, information content	:	3.29E+15 $molec/cm^2$, 48.6
temperature dependence of the TCA	:	-0.216%/K (trop), +0.005%/K (strat)
location, date, solar zenith angle	:	Kiruna, 15/Mar/97, 70.19^o
spectral interval fitted	:	3287.100 – 3287.350 cm^{-1}

Molecule	iCode	Absorption	Molecule	iCode	Absorption
$H2O$	11	42.576%	$CH4$	61	0.024%
HCN	281	4.299%	$N2O$	41	0.007%
Solar(A)	—	2.865%	$NH3$	111	0.001%
Solar-sim	—	2.310%	OH	131	0.001%
$C2H2$	401	1.020%	$HO2$	221	0.001%
$CO2$	21	0.918%	HDO	491	0.001%
$O3$	31	0.121%	NO	81	<0.001%

$H2O$, Kiruna, φ=70.19^o, OPD=257cm, FoV=1.91$mrad$, boxcar apod.

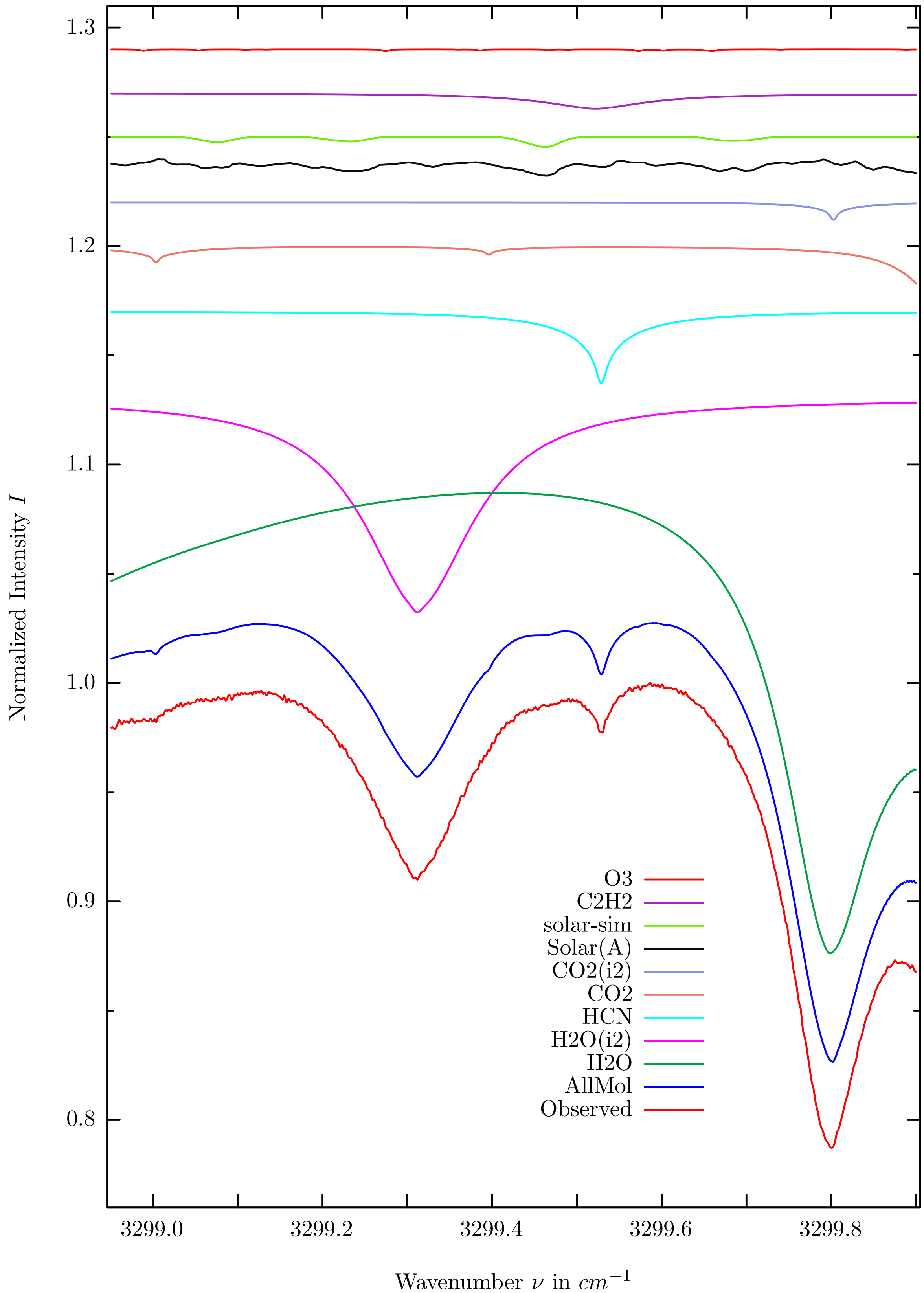

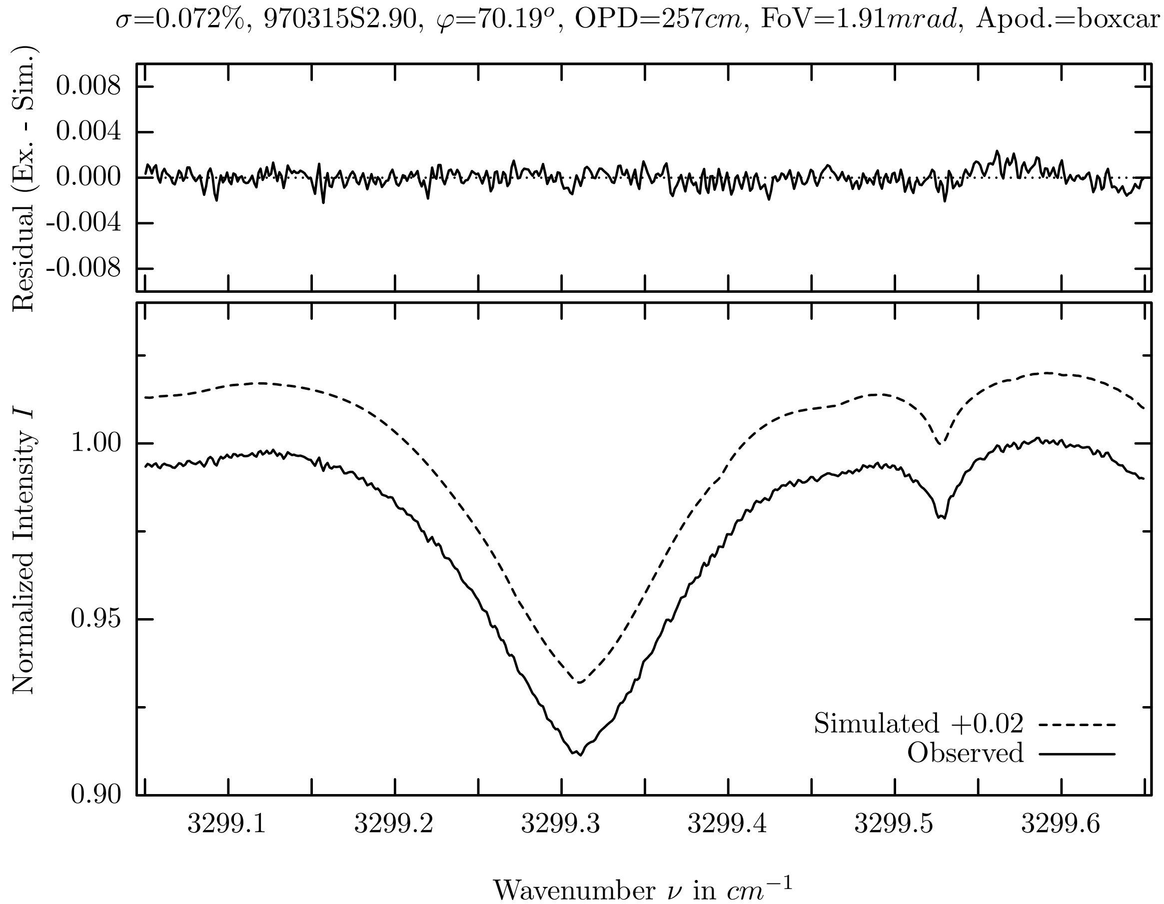

investigated species	:	$H_2O(i2)$
line position(s) ν_0	:	3299.3070 cm^{-1}
lower state energy E''_{lst}	:	79.0 cm^{-1}
retrieved TCA, information content	:	6.37E+21 $molec/cm^2$, 122.2
temperature dependence of the TCA	:	+0.024%/K (trop), +0.019%/K (strat)
location, date, solar zenith angle	:	Kiruna, 15/Mar/97, 70.19^o
spectral interval fitted	:	3299.050 – 3299.650 cm^{-1}

Molecule	iCode	Absorption	Molecule	iCode	Absorption
H2O	11	30.249%	*N2O*	41	0.032%
H2O	1**2**	9.769%	*CH4*	61	0.001%
HCN	281	3.278%	*NO*	81	<0.001%
CO2	21	1.783%	*NH3*	111	<0.001%
CO2	2**2**	0.806%	*OH*	131	<0.001%
Solar(A)	—	0.783%	*HO2*	221	<0.001%
Solar-sim	—	0.466%	*H2S*	471	<0.001%
C2H2	401	0.709%	*HDO*	491	<0.001%
O3	31	0.085%			

C_2H_2 was held constant during the retrieval. The a-priori profile of C_2H_2 had been replaced with the VMR profile retrieved in the 3250cm^{-1} interval prior to the analysis of this microwindow.

HCN, Kiruna, φ=70.19^o, OPD=257cm, FoV=1.91$mrad$, boxcar apod.

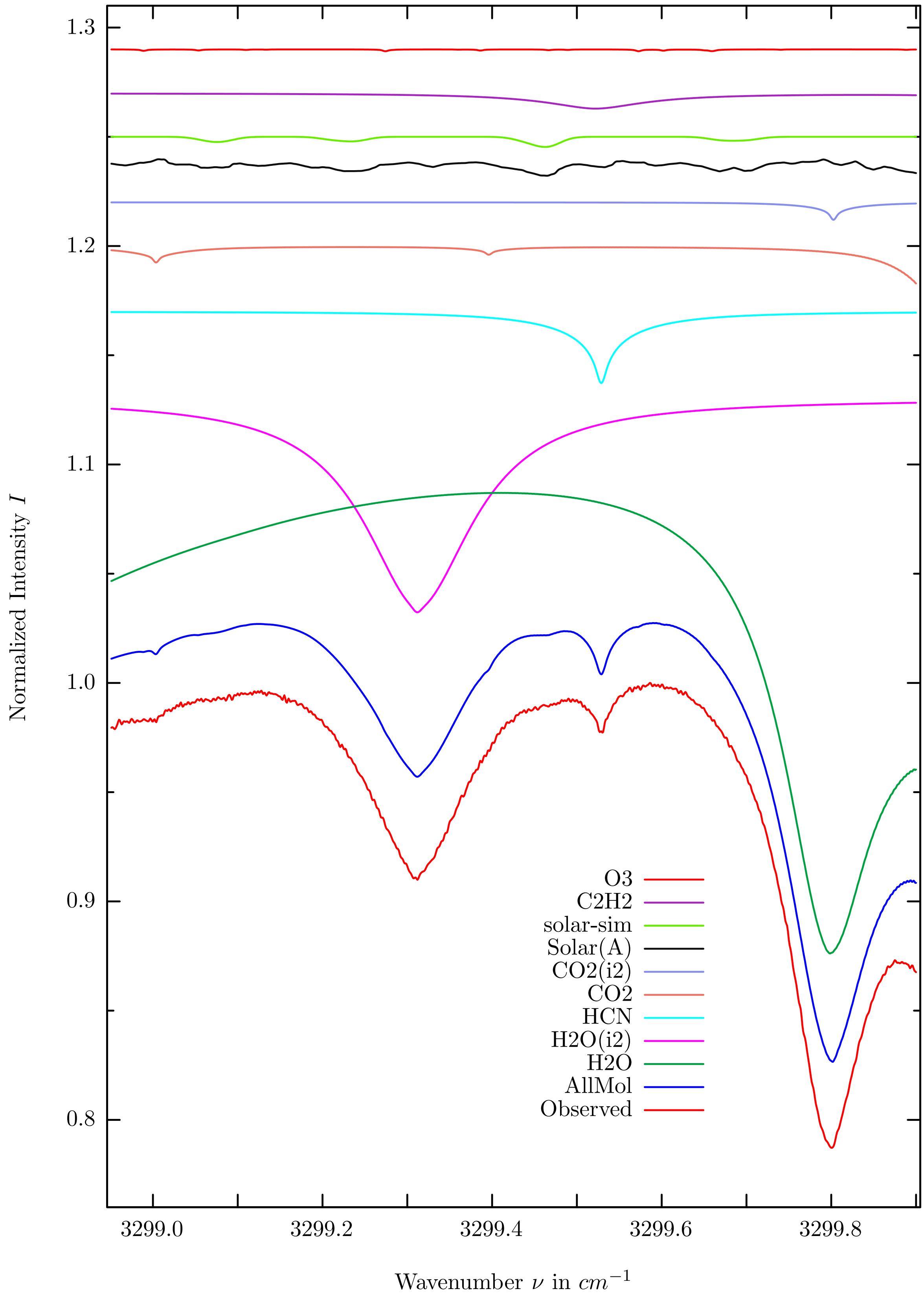

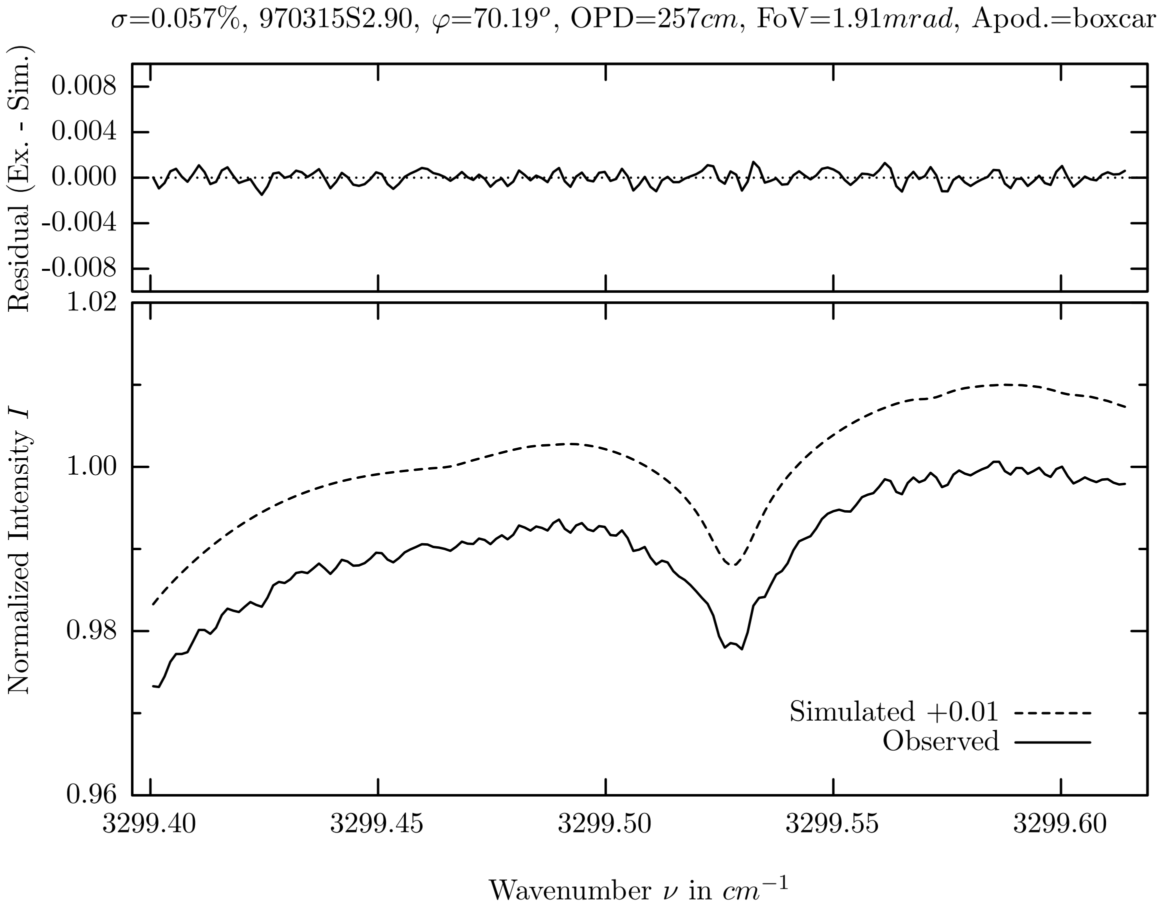

investigated species	:	HCN
line position(s) ν_0	:	3299.5273 cm^{-1}
lower state energy E''_{lst}	:	29.6 cm^{-1}
retrieved TCA, information content	:	3.53E+15 $molec/cm^2$, 34.6
temperature dependence of the TCA	:	-0.278%/K (trop), +0.055%/K (strat)
location, date, solar zenith angle	:	Kiruna, 15/Mar/97, 70.19^o
spectral interval fitted	:	3299.400 – 3299.615 cm^{-1}

Molecule	iCode	Absorption	Molecule	iCode	Absorption
$H2O$	11	30.249%	$N2O$	41	0.032%
$H2O$	1**2**	9.769%	$CH4$	61	0.001%
HCN	281	3.278%	NO	81	<0.001%
$CO2$	21	1.783%	$NH3$	111	<0.001%
$CO2$	2**2**	0.806%	OH	131	<0.001%
Solar(A)	—	0.783%	$HO2$	221	<0.001%
Solar-sim	—	0.466%	$H2S$	471	<0.001%
$C2H2$	401	0.709%	HDO	491	<0.001%
$O3$	31	0.085%			

C_2H_2 was held constant during the retrieval of HCN. The a-priori profile of C_2H_2 had been replaced with the VMR profile retrieved in the $3250 cm^{-1}$ interval prior to the analysis of this microwindow.

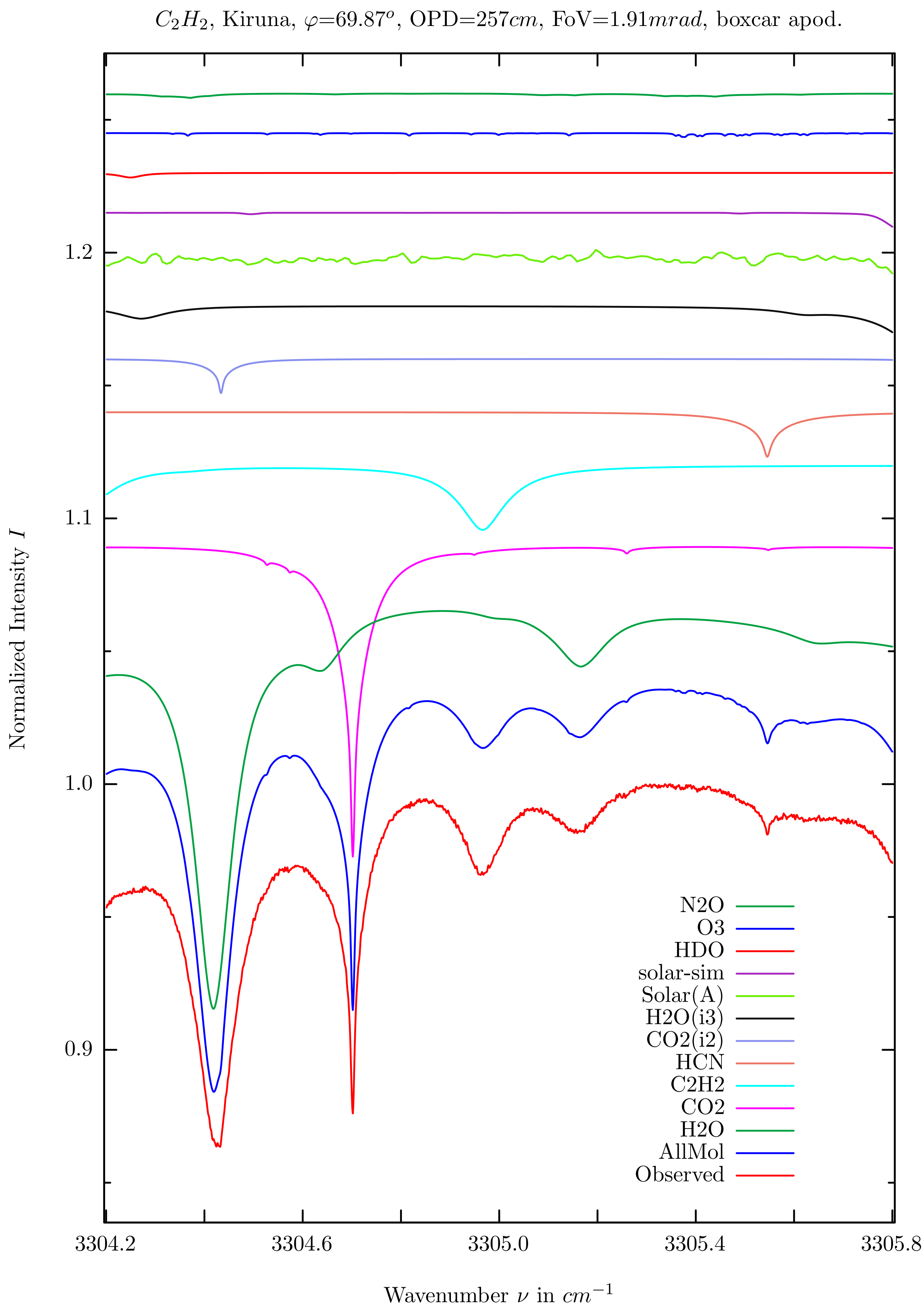

C_2H_2, Kiruna, φ=69.87^o, OPD=257cm, FoV=1.91$mrad$, boxcar apod.
Normalized Intensity I
1.2
1.1
1.0
0.9
3304.2
3304.6
3305.0
3305.4
3305.8
Wavenumber ν in cm^{-1}
N2O
O3
HDO
solar-sim
Solar(A)
H2O(i3)
CO2(i2)
HCN
C2H2
CO2
H2O
AllMol
Observed

σ=0.073%, 970315S2.90, φ=70.19^o, OPD=257cm, FoV=1.91$mrad$, Apod.=boxcar

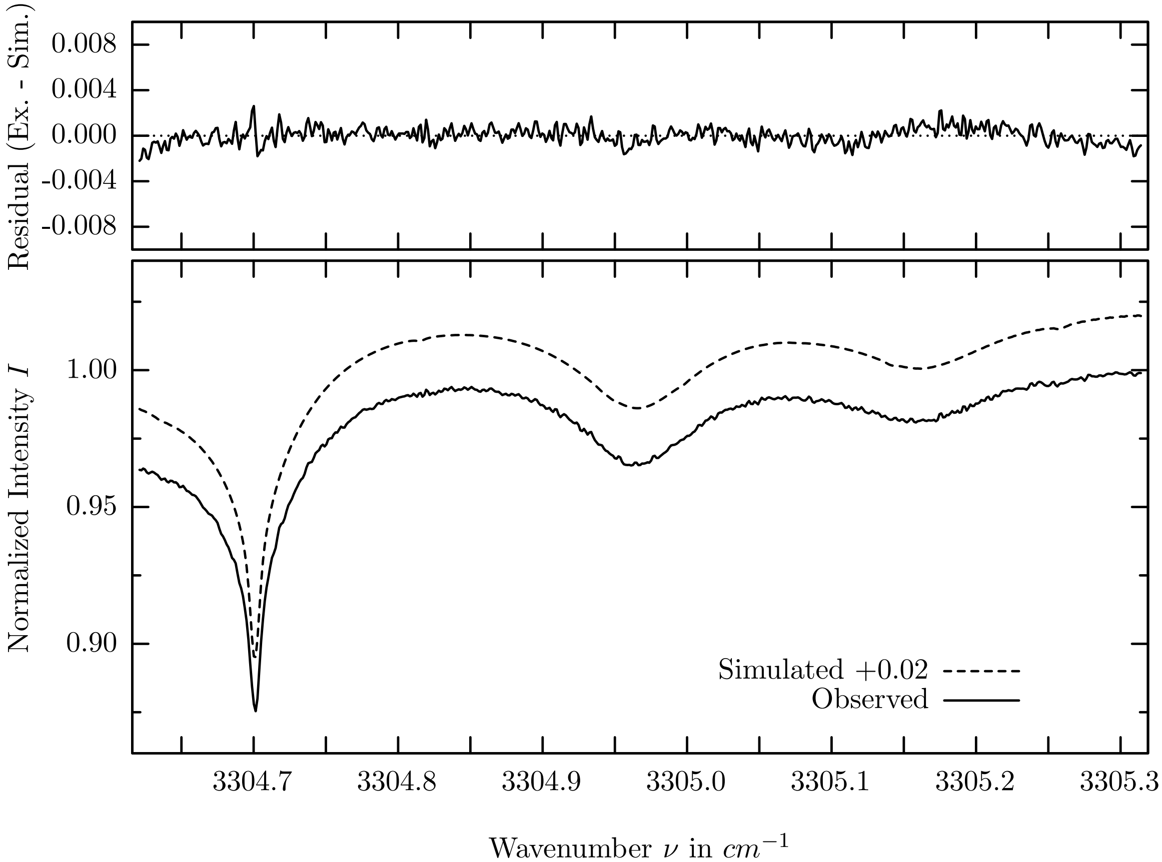

investigated species	:	C_2H_2
line position(s) ν_0	:	3304.9655 cm^{-1}
lower state energy E''_{lst}	:	105.9 cm^{-1}
retrieved TCA, information content	:	7.57E+15 $molec/cm^2$, 41.0
temperature dependence of the TCA	:	-1.135%/K (trop), -1.503%/K (strat)
location, date, solar zenith angle	:	Kiruna, 15/Mar/97, 70.19^o
spectral interval fitted	:	3304.620 – 3305.315 cm^{-1}

Molecule	iCode	Absorption	Molecule	iCode	Absorption
H2O	11	23.067%	*O3*	31	0.150%
CO2	21	11.767%	*N2O*	41	0.115%
C2H2	401	2.430%	*CH4*	61	0.010%
HCN	281	1.684%	*H218O*	511	0.003%
CO2	2**2**	1.292%	*NH3*	111	0.001%
H2O	1**3**	1.017%	*HO2*	221	0.001%
Solar(A)	—	0.801%	*NO*	81	<0.001%
Solar-sim	—	0.547%	*OH*	131	<0.001%
HDO	491	0.171%	*H2S*	471	<0.001%

HCN, Kiruna, φ=69.87^o, OPD=257cm, FoV=1.91$mrad$, boxcar apod.

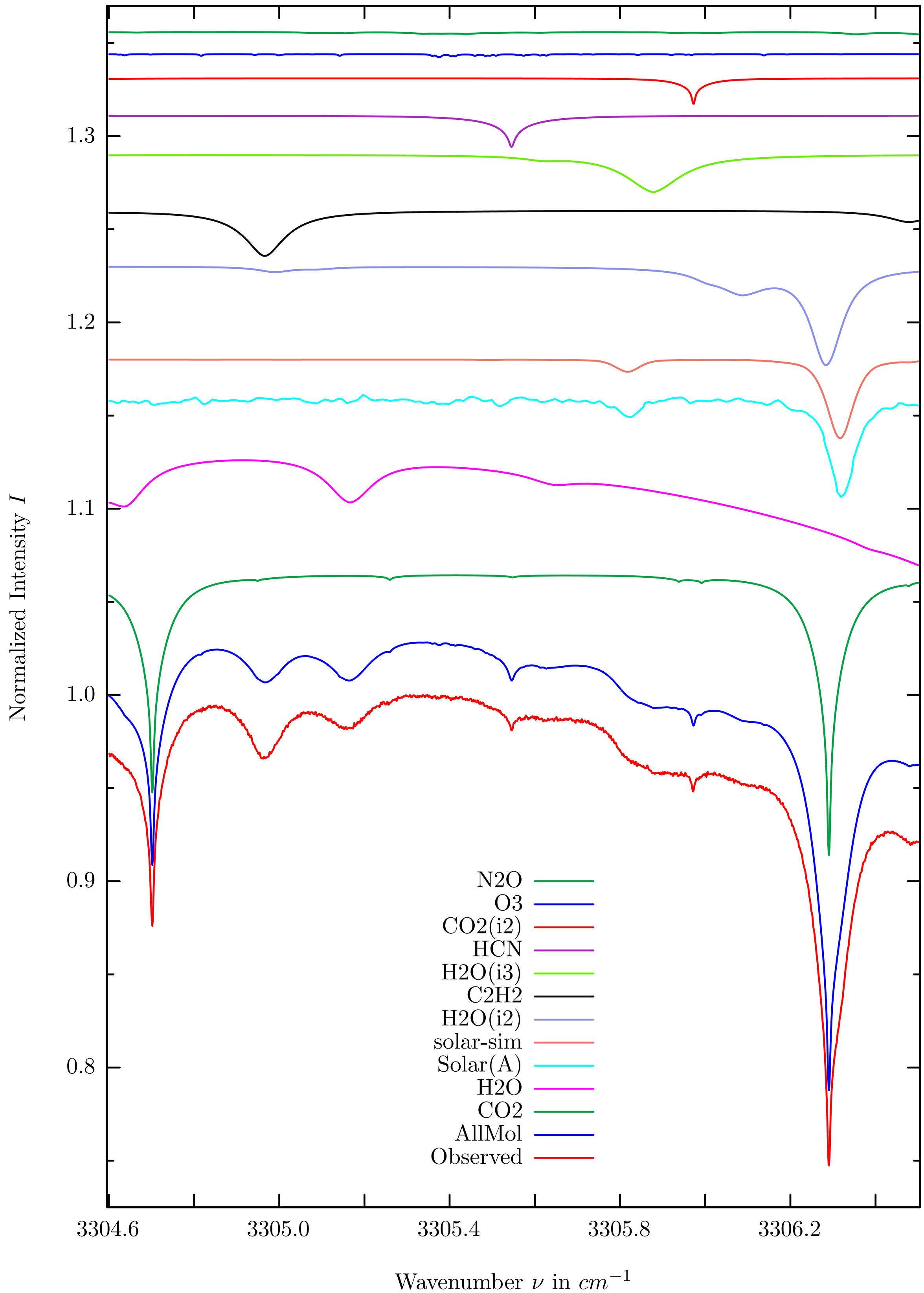

σ=0.055%, 970315S2.90, φ=70.19^o, OPD=257cm, FoV=1.91$mrad$, Apod.=boxcar

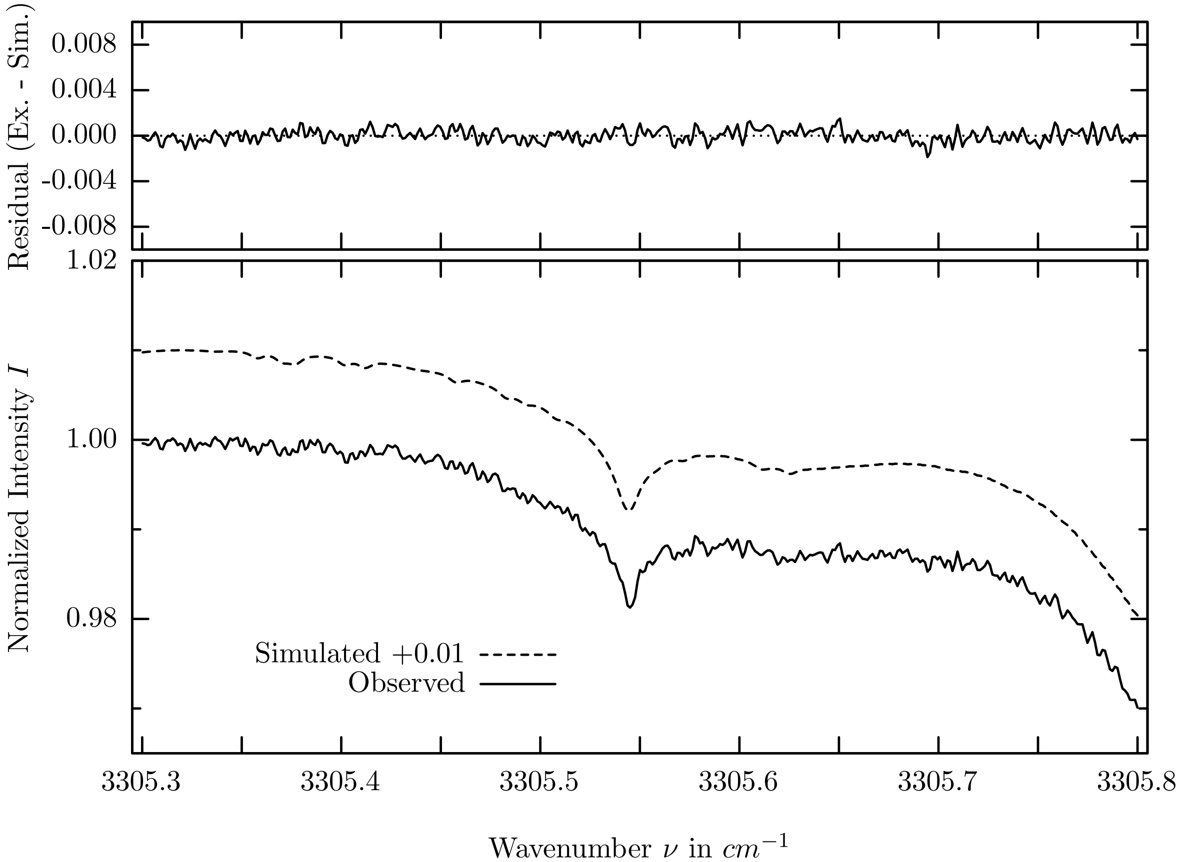

investigated species	:	HCN
line position(s) ν_0	:	3305.5440 cm^{-1}
lower state energy E''_{lst}	:	8.9 cm^{-1}
retrieved TCA, information content	:	2.87E+15 $molec/cm^2$, 17.9
temperature dependence of the TCA	:	-1.384%/K (trop), +0.167%/K (strat)
location, date, solar zenith angle	:	Kiruna, 15/Mar/97, 70.19^o
spectral interval fitted	:	3305.300 – 3305.800 cm^{-1}

Molecule	iCode	Absorption	Molecule	iCode	Absorption
$CO2$	21	15.177%	$N2O$	41	0.138%
$H2O$	11	12.550%	$CH4$	61	0.004%
Solar(A)	—	5.360%	$H218O$	511	0.002%
Solar-sim	—	4.216%	$NH3$	111	0.001%
$H2O$	1**2**	5.299%	$HO2$	221	0.001%
$C2H2$	401	2.430%	HDO	491	0.001%
$H2O$	1**3**	2.019%	NO	81	<0.001%
HCN	281	1.684%	OH	131	<0.001%
$CO2$	2**2**	1.377%	$H2S$	471	<0.001%
$O3$	31	0.150%			

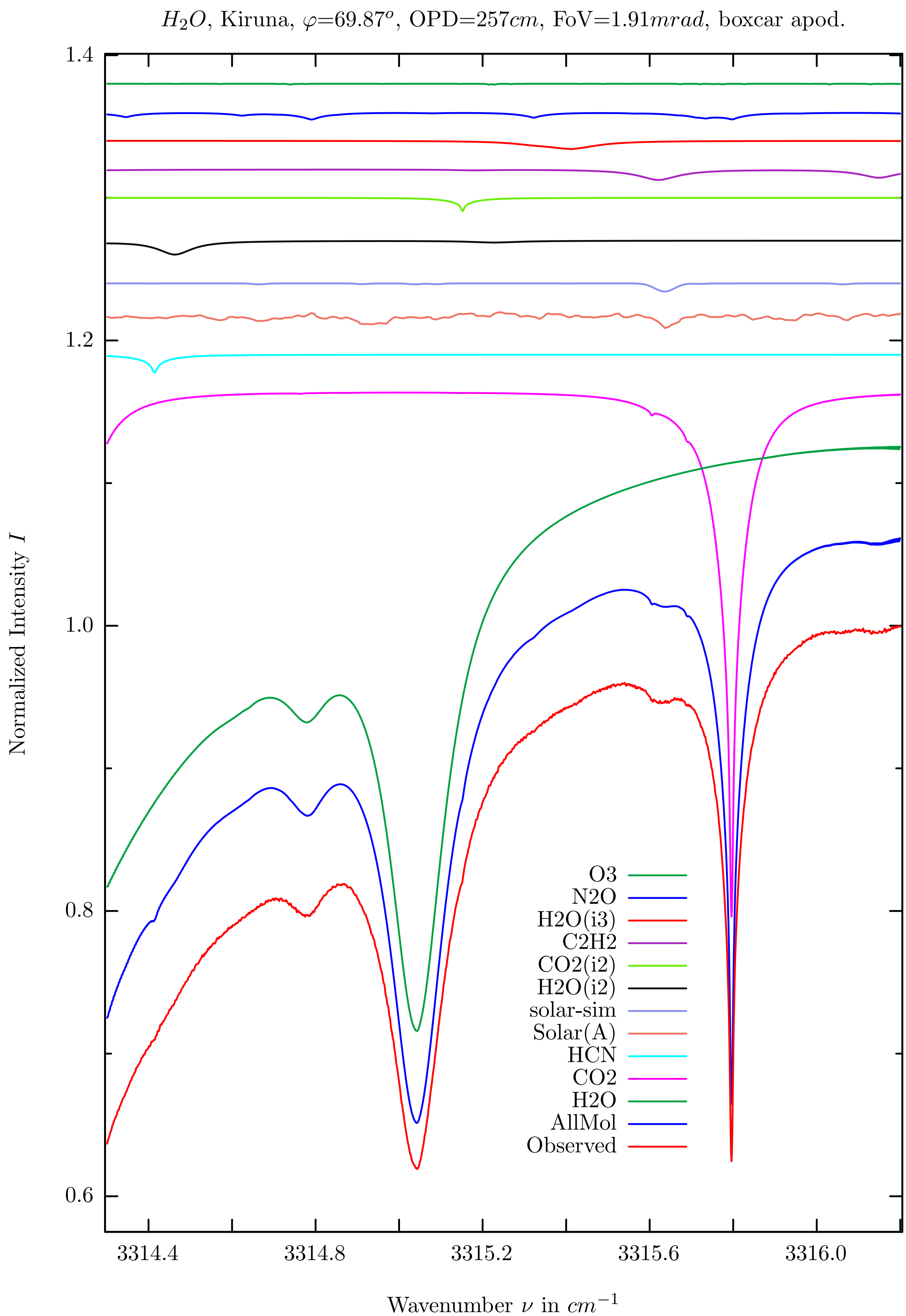

H_2O, Kiruna, φ=69.87^o, OPD=257cm, FoV=1.91$mrad$, boxcar apod.
1.4
1.2
1.0
0.8
0.6
Normalized Intensity I
3314.4
3314.8
3315.2
3315.6
3316.0
Wavenumber ν in cm^{-1}
O3
N2O
H2O(i3)
C2H2
CO2(i2)
H2O(i2)
solar-sim
Solar(A)
HCN
CO2
H2O
AllMol
Observed

σ=0.162%, 970315S2.90, φ=70.19^o, OPD=257cm, FoV=1.91$mrad$, Apod.=boxcar

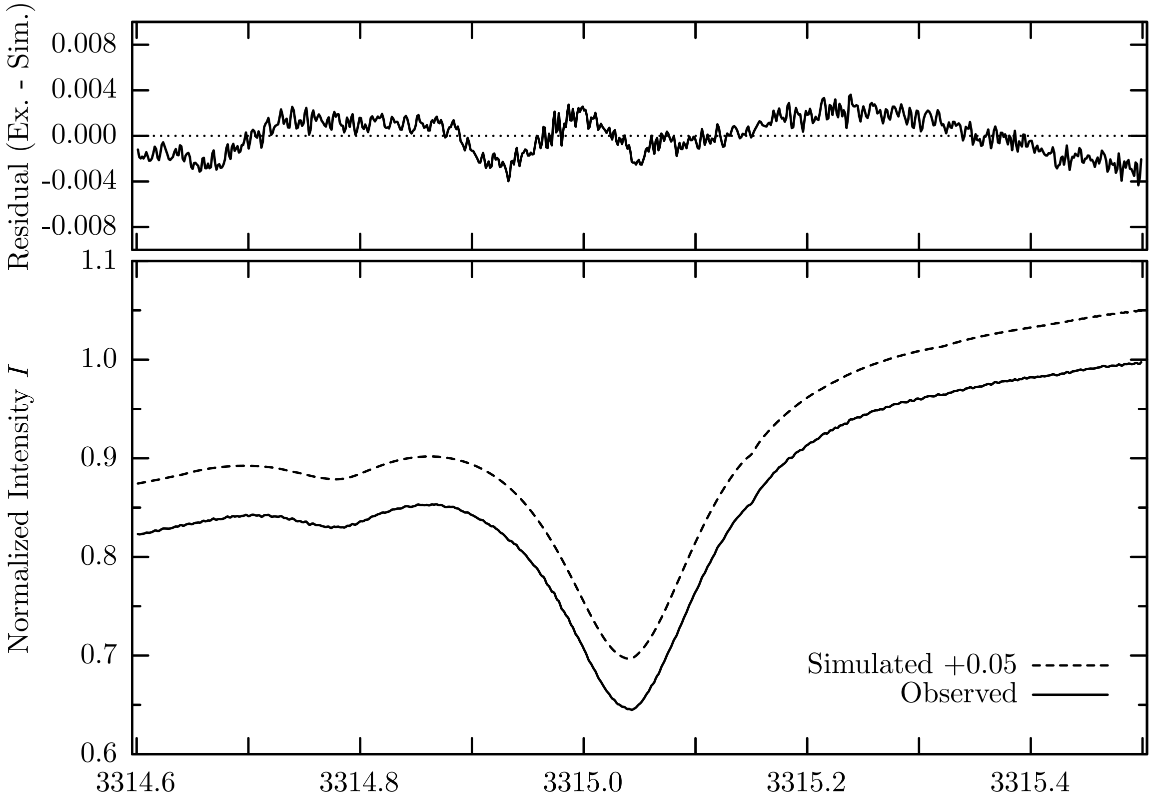

Wavenumber ν in cm^{-1}

investigated species	:	H_2O
line position(s) ν_0	:	3315.0430 cm^{-1}
lower state energy E''_{lst}	:	1477.3 cm^{-1}
retrieved TCA, information content	:	5.21E+21 $molec/cm^2$, 172.9
temperature dependence of the TCA	:	-2.919%/K (trop), -0.015%/K (strat)
location, date, solar zenith angle	:	Kiruna, 15/Mar/97, 70.19^o
spectral interval fitted	:	3314.600 – 3315.500 cm^{-1}

Molecule	iCode	Absorption	Molecule	iCode	Absorption
H2O	11	44.278%	$N2O$	41	0.487%
$CO2$	21	37.015%	$O3$	31	0.063%
HCN	281	1.239%	HDO	491	0.013%
Solar(A)	—	1.132%	$CH4$	61	0.001%
Solar-sim	—	0.568%	$NH3$	111	0.001%
$H2O$	1**2**	0.980%	$HO2$	221	0.001%
$CO2$	2**2**	0.930%	NO	81	<0.001%
$C2H2$	401	0.748%	OH	131	<0.001%
$H2O$	1**3**	0.579%	$H2S$	471	<0.001%

CO_2, Kiruna, φ=70.19^o, OPD=257cm, FoV=1.91$mrad$, boxcar apod.

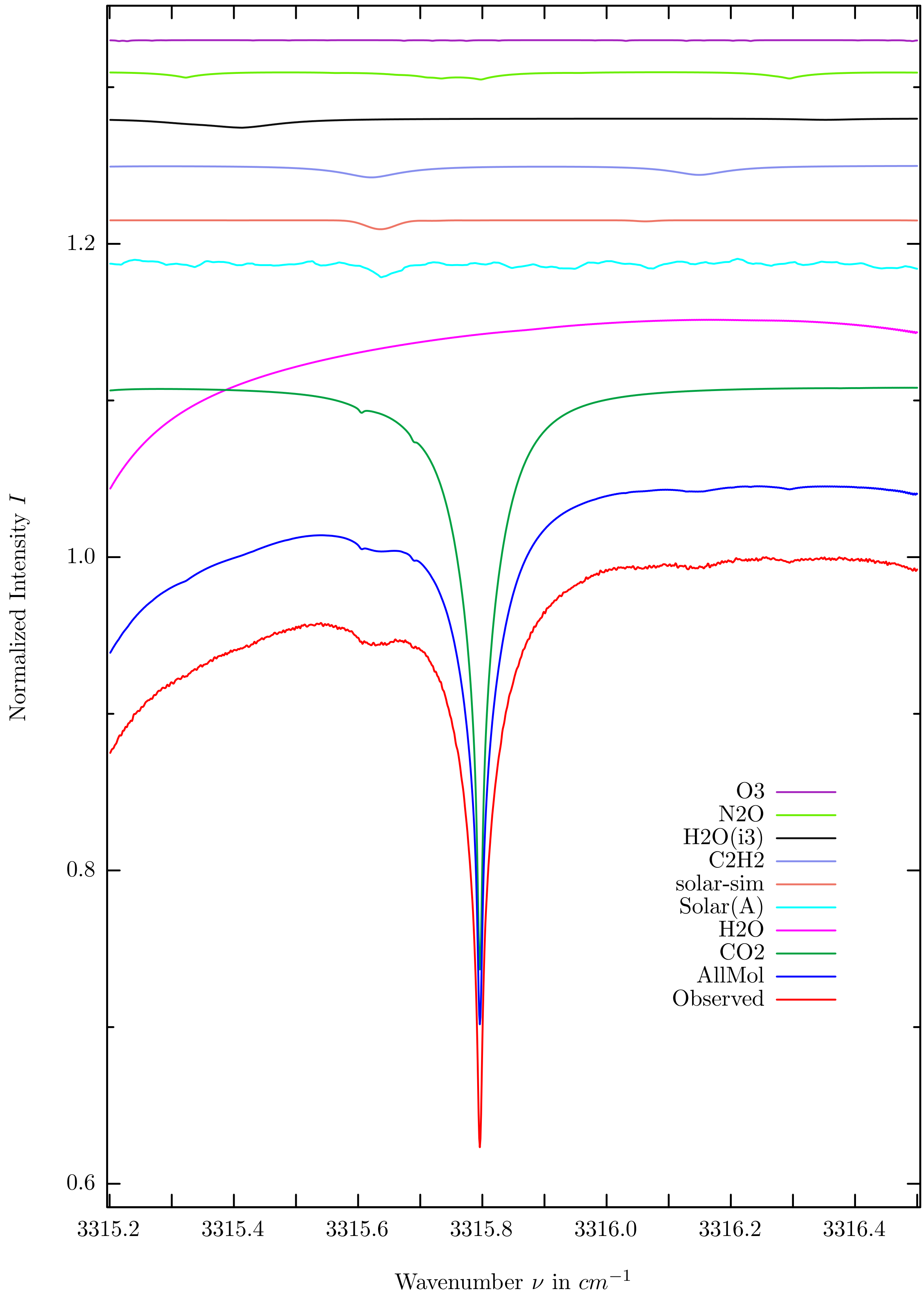

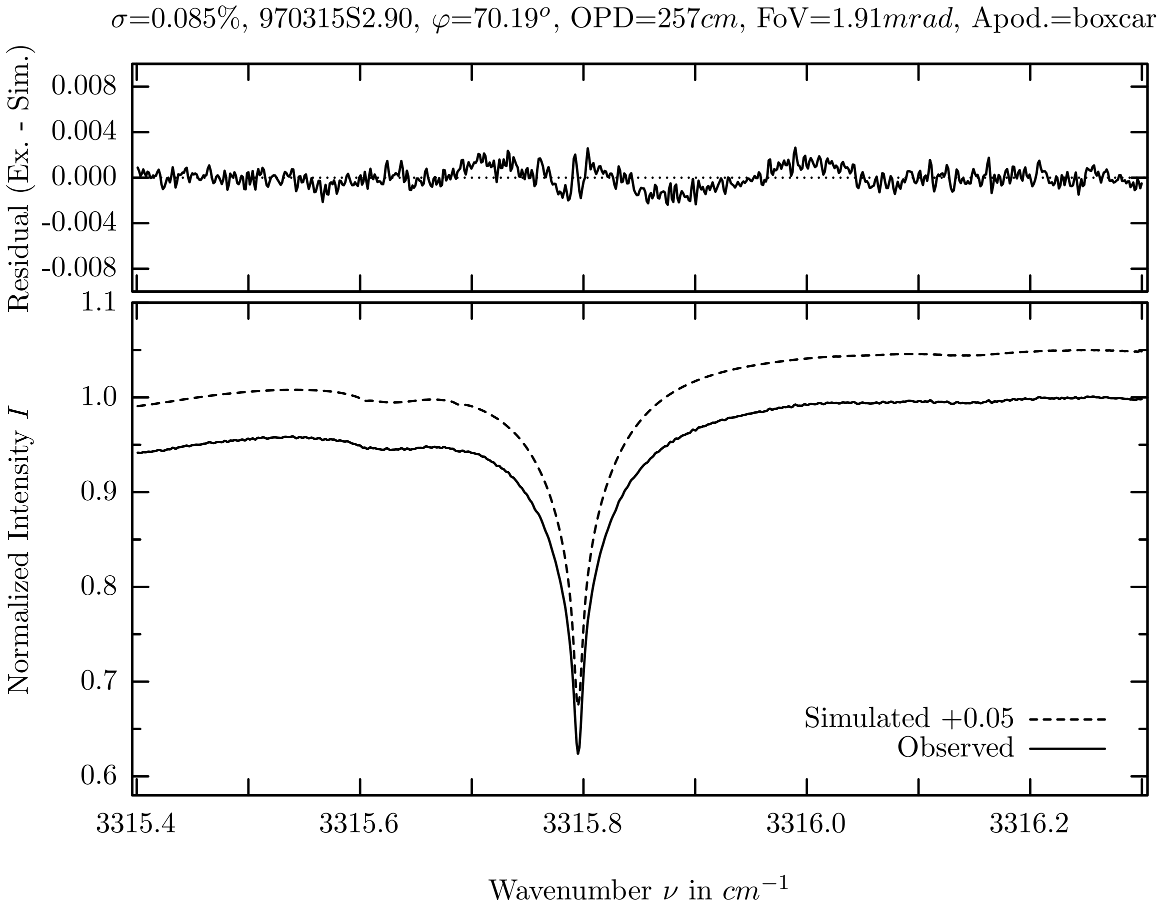

investigated species	:	CO_2
line position(s) ν_0	:	3315.7946 cm^{-1}
lower state energy E''_{lst}	:	362.8 cm^{-1}
retrieved TCA, information content	:	7.41E+21 $molec/cm^2$, 440.2
temperature dependence of the TCA	:	-0.591%/K (trop), -0.148%/K (strat)
location, date, solar zenith angle	:	Kiruna, 15/Mar/97, 70.19^o
spectral interval fitted	:	3315.400 – 3316.300 cm^{-1}

Molecule	iCode	Absorption	Molecule	iCode	Absorption
CO2	21	37.440%	*HCN*	281	0.008%
H2O	11	19.461%	*CH4*	61	0.001%
Solar(A)	—	1.132%	*NH3*	111	0.001%
Solar-sim	—	0.568%	*HO2*	221	0.001%
C2H2	401	0.759%	*HDO*	491	0.001%
H2O	1**3**	0.587%	*NO*	81	<0.001%
N2O	41	0.494%	*OH*	131	<0.001%
O3	31	0.064%	*H2S*	471	<0.001%

HF, Kiruna, φ=69.96^o, OPD=257cm, FoV=1.91$mrad$, boxcar apod.

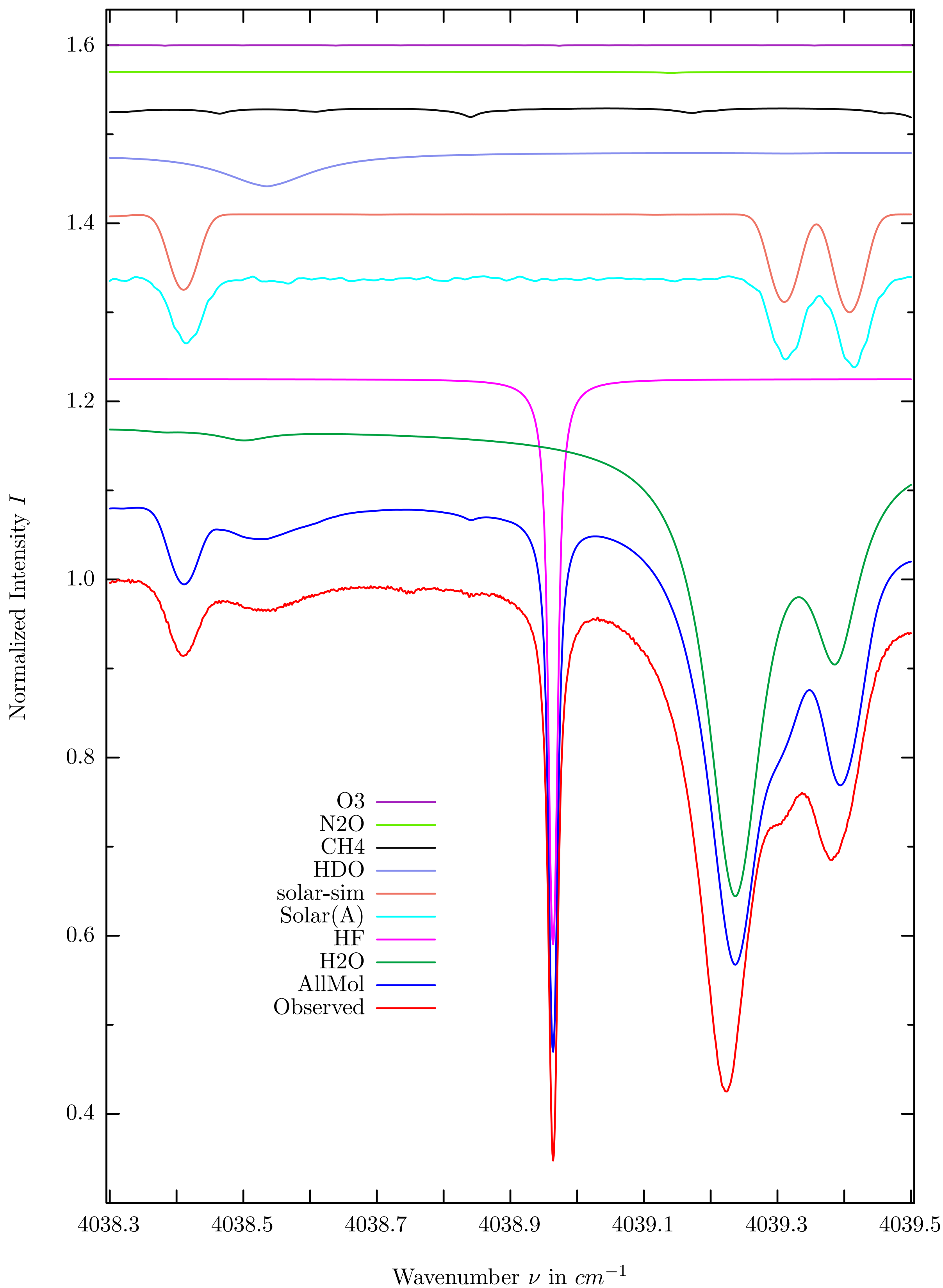

σ=0.219%, 970315S1.90, φ=69.96^o, OPD=257cm, FoV=1.91$mrad$, Apod.=boxcar

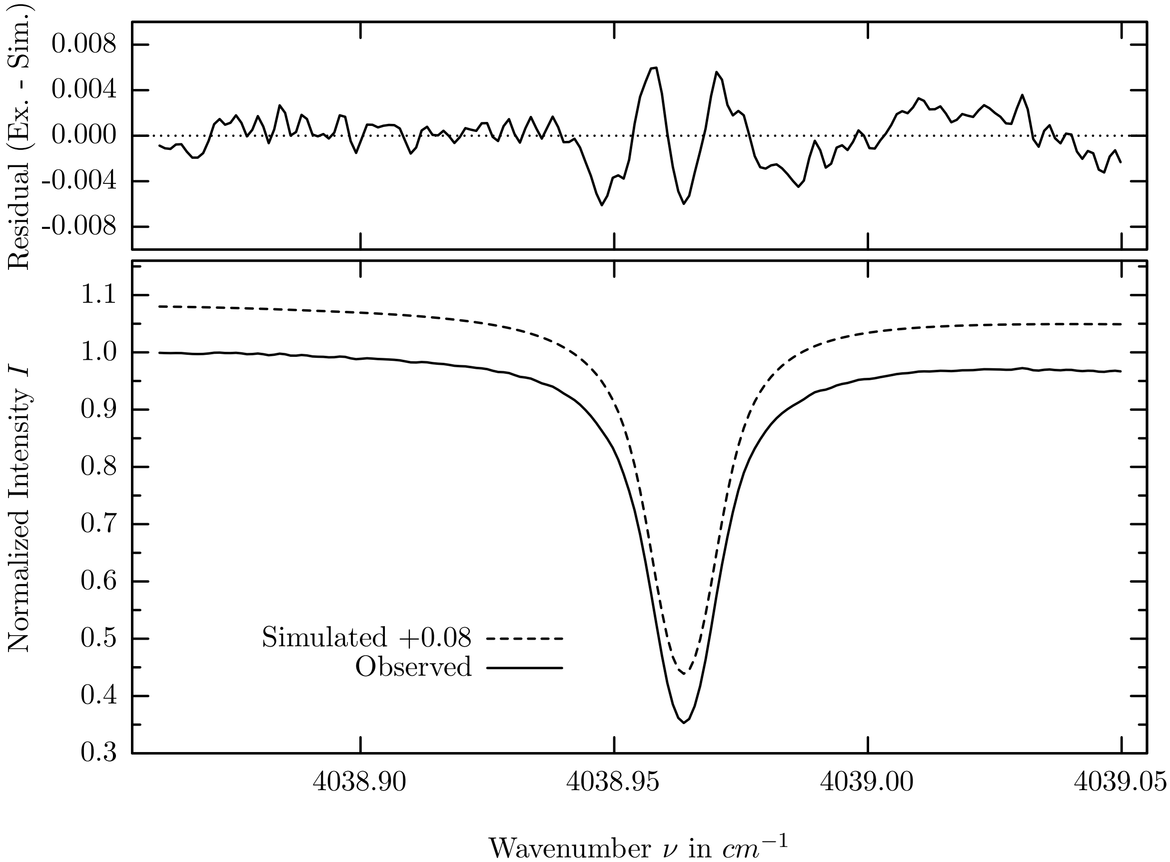

investigated species	:	HF
line position(s) ν_0	:	4038.9625 cm^{-1}
lower state energy E''_{lst}	:	41.1 cm^{-1}
retrieved TCA, information content	:	2.40E+15 $molec/cm^2$, 292.4
temperature dependence of the TCA	:	-0.785%/K (trop), -0.549%/K (strat)
location, date, solar zenith angle	:	Kiruna, 15/Mar/97, 69.96^o
spectral interval fitted	:	4038.860 – 4039.050 cm^{-1}

Molecule	iCode	Absorption	Molecule	iCode	Absorption
HF	141	63.636%	CO	51	<0.001%
$H2O$	11	55.590%	$SO2$	91	<0.001%
Solar(A)	—	10.167%	$NH3$	111	<0.001%
Solar-sim	—	10.998%	OH	131	<0.001%
HDO	491	3.860%	HI	171	<0.001%
$CH4$	61	1.163%	OCS	191	<0.001%
$N2O$	41	0.121%	$H2S$	471	<0.001%
$O3$	31	0.060%			

HF, Kiruna, φ=69.96^o, OPD=257cm, FoV=1.91$mrad$, boxcar apod.

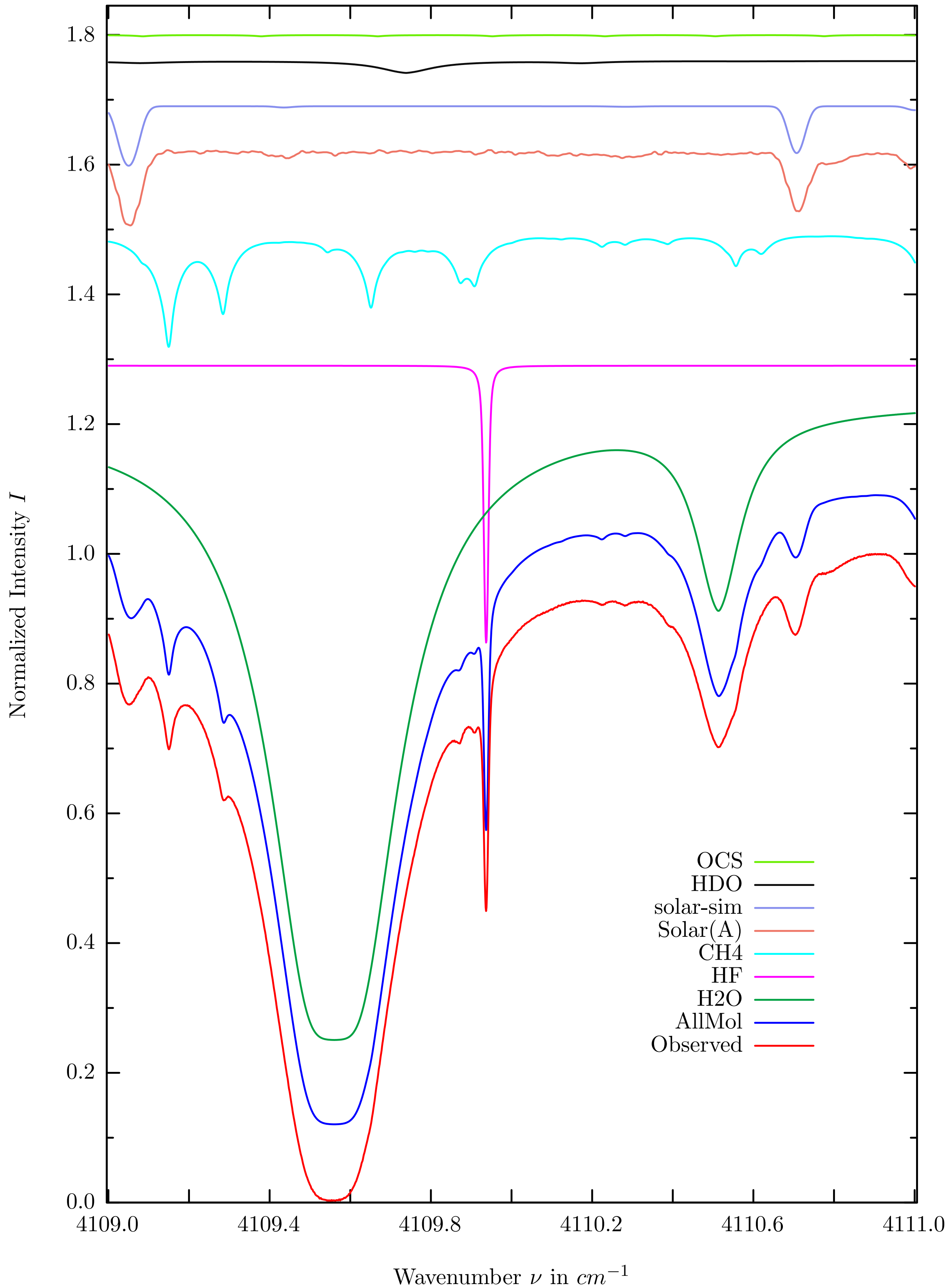

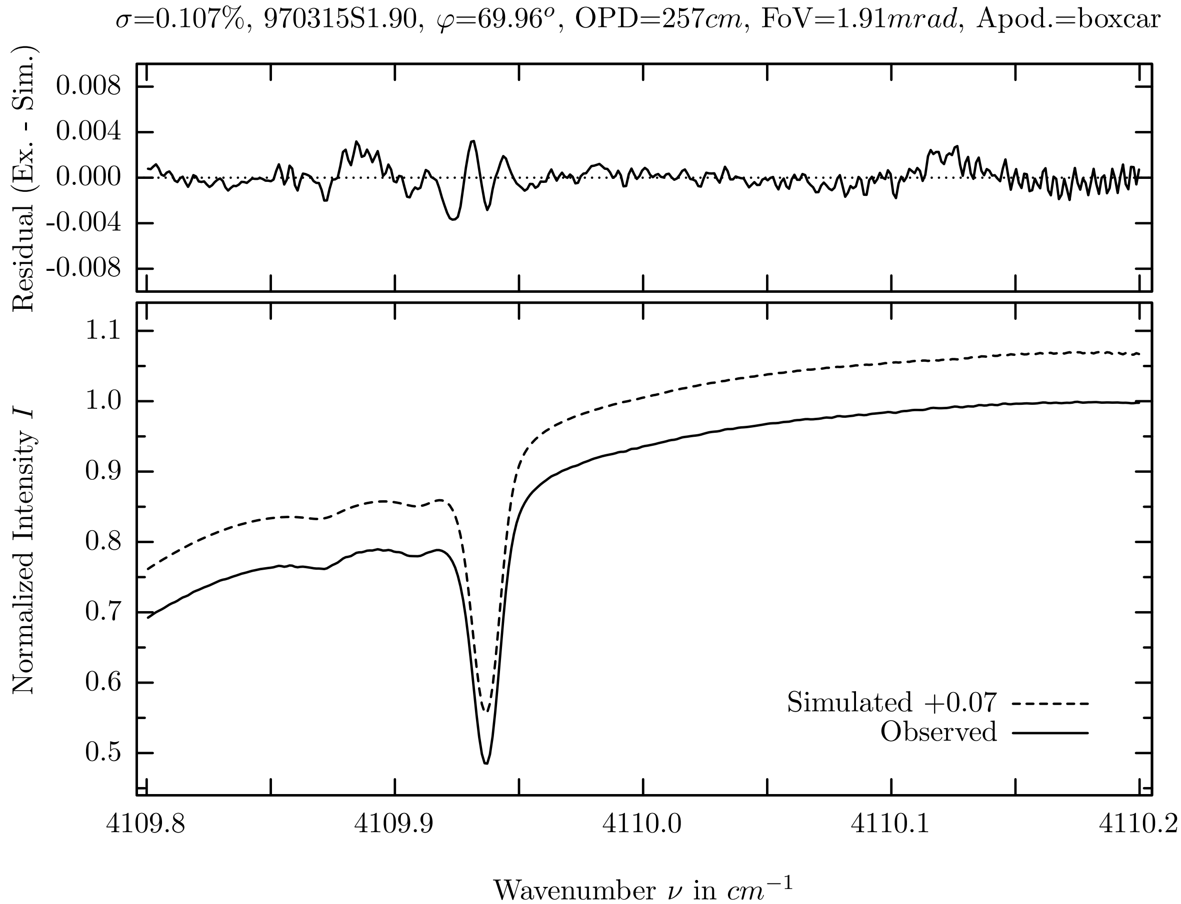

investigated species	:	HF
line position(s) ν_0	:	4109.9363 cm^{-1}
lower state energy E''_{lst}	:	246.4 cm^{-1}
retrieved TCA, information content	:	2.45E+15 $molec/cm^2$, 360.5
temperature dependence of the TCA	:	-0.338%/K (trop), -0.706%/K (strat)
location, date, solar zenith angle	:	Kiruna, 15/Mar/97, 69.96^o
spectral interval fitted	:	4109.800 – 4110.200 cm^{-1}

Molecule	iCode	Absorption	Molecule	iCode	Absorption
$H2O$	11	99.937%	CO	51	0.002%
HF	141	42.874%	$NO2$	101	<0.001%
$CH4$	61	17.618%	$NH3$	111	<0.001%
Solar(A)	—	11.374%	OH	131	<0.001%
Solar-sim	—	9.170%	HI	171	<0.001%
HDO	491	1.863%	$H2S$	471	<0.001%
OCS	191	0.219%			

The CH_4 line data near 4109.9cm^{-1} are inconsistent with observations. The position and air broadening coefficients of 2 methane lines have been changed to achieve a more acceptable (though still imperfect) fit.

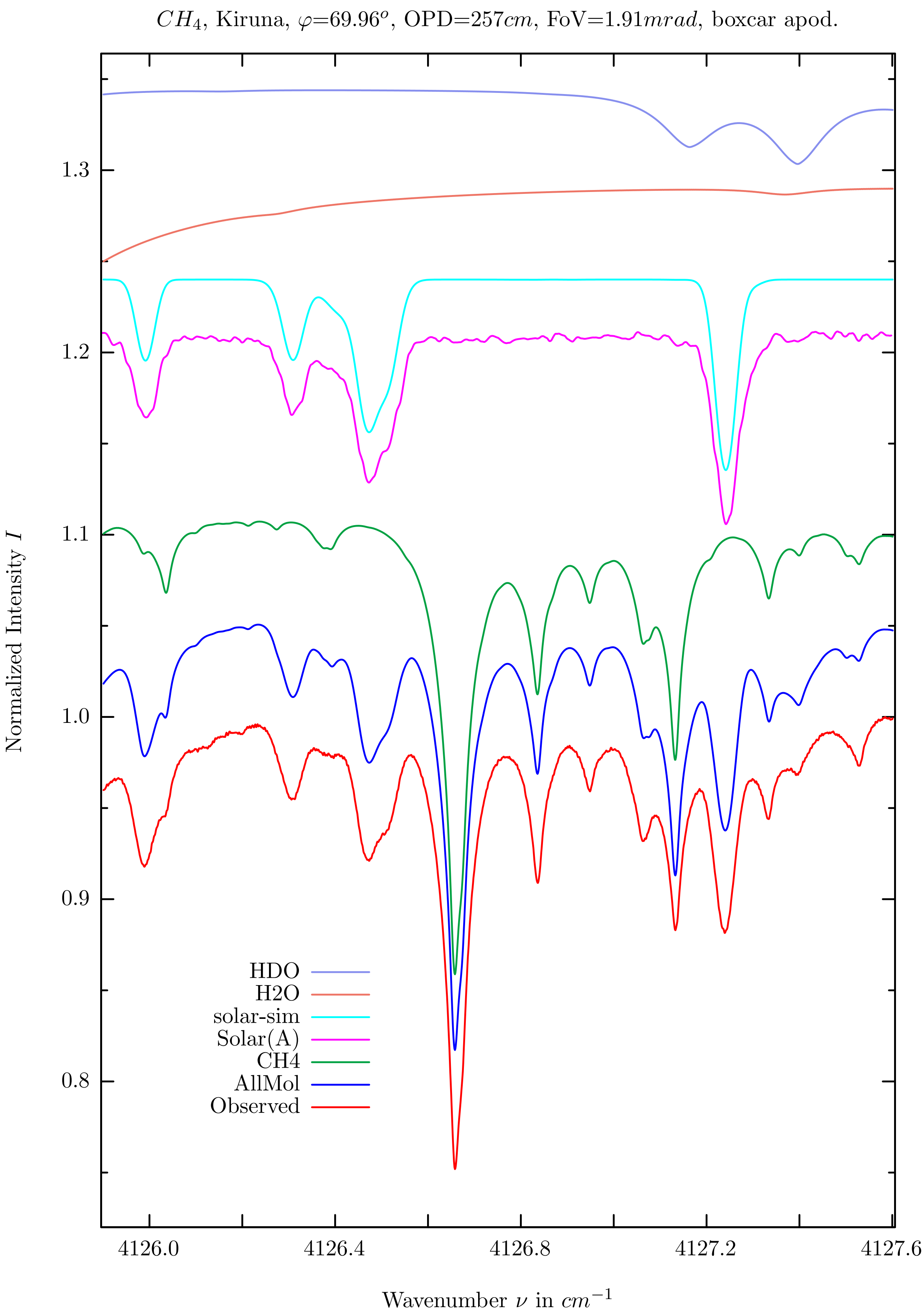
CH_4, Kiruna, φ=69.96^o, OPD=257cm, FoV=1.91$mrad$, boxcar apod.
1.3
1.2
1.1
1.0
0.9
0.8
Normalized Intensity I
4126.0
4126.4
4126.8
4127.2
4127.6
Wavenumber ν in cm^{-1}
HDO
H2O
solar-sim
Solar(A)
CH4
AllMol
Observed

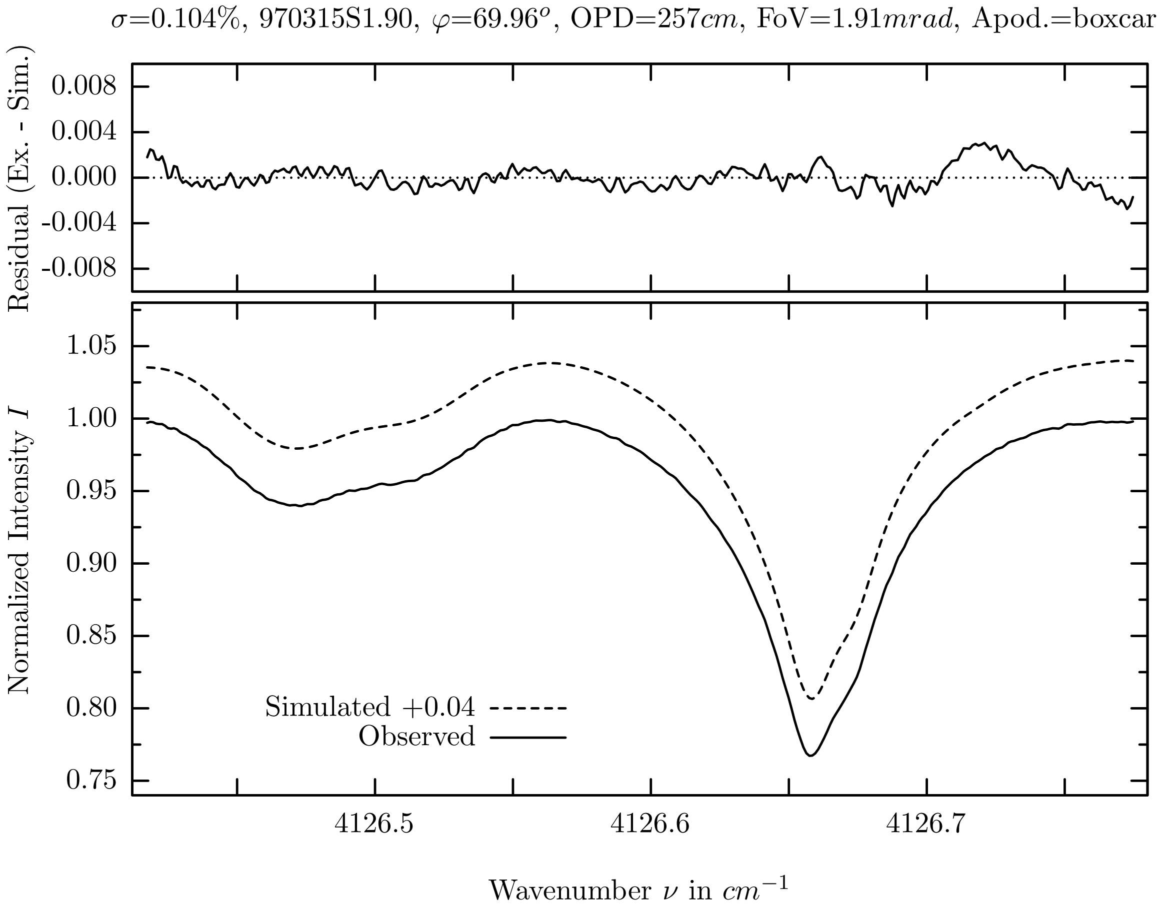

investigated species	:	CH_4
line position(s) ν_0	:	4126.6561, 4126.6724 cm^{-1}
lower state energy E''_{lst}	:	104.8, 104.8 cm^{-1}
retrieved TCA, information content	:	3.39E+19 $molec/cm^2$, 224.6, 178.4
temperature dependence of the TCA	:	+0.248%/K (trop), +0.027%/K (strat)
location, date, solar zenith angle	:	Kiruna, 15/Mar/97, 69.96^o
spectral interval fitted	:	4126.417 – 4126.775 cm^{-1}

Molecule	iCode	Absorption	Molecule	iCode	Absorption
CH4	61	26.143%	$NO2$	101	<0.001%
Solar(A)	—	10.421%	$NH3$	111	<0.001%
Solar-sim	—	10.460%	OH	131	<0.001%
$H2O$	11	4.943%	OCS	191	<0.001%
HDO	491	4.160%	$H2S$	471	<0.001%
CO	51	0.014%			

HDO, Kiruna, φ=69.96^o, OPD=257cm, FoV=1.91$mrad$, boxcar apod.

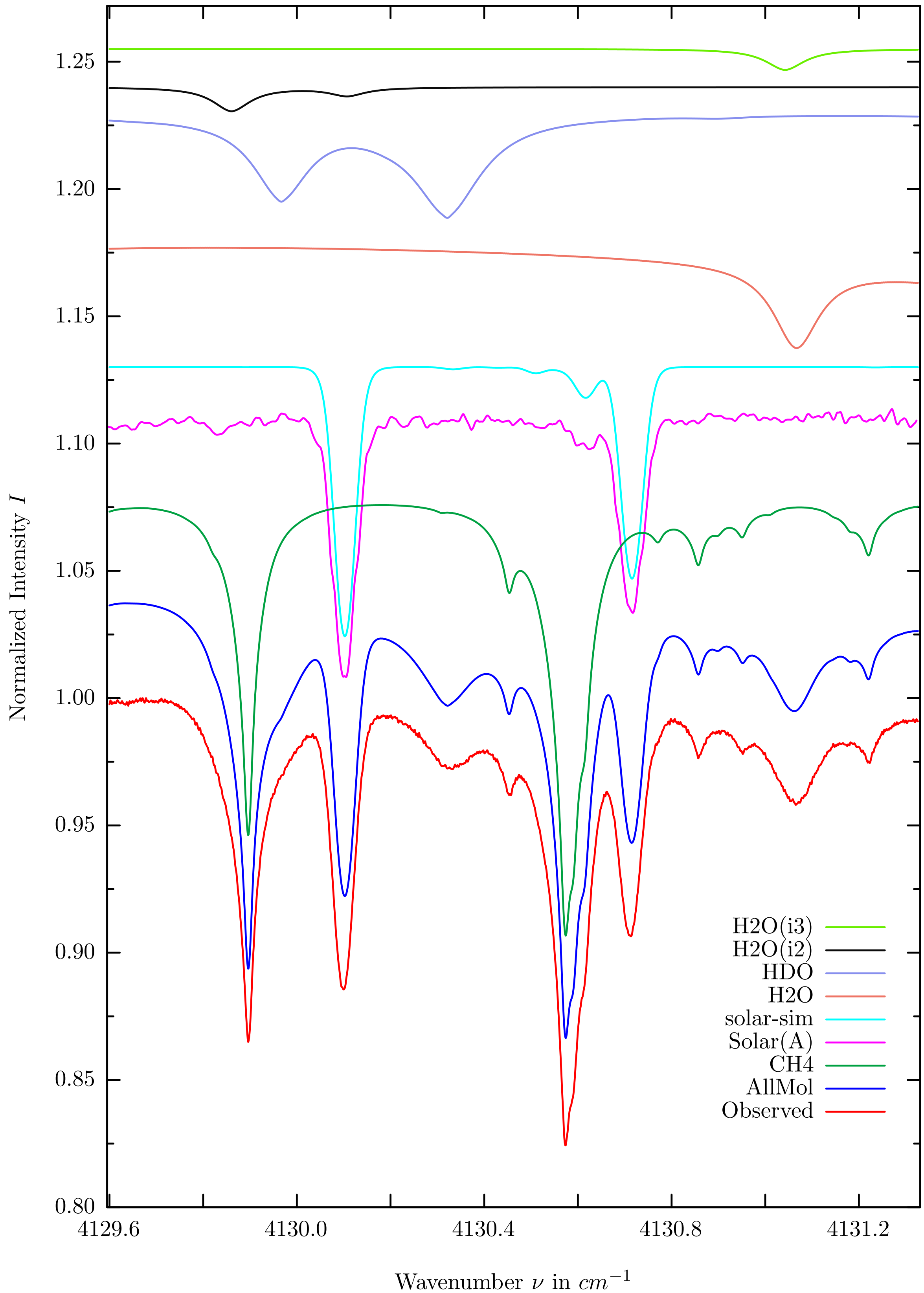

σ=0.085%, 970315S1.90, φ=69.96^o, OPD=257cm, FoV=1.91$mrad$, Apod.=boxcar

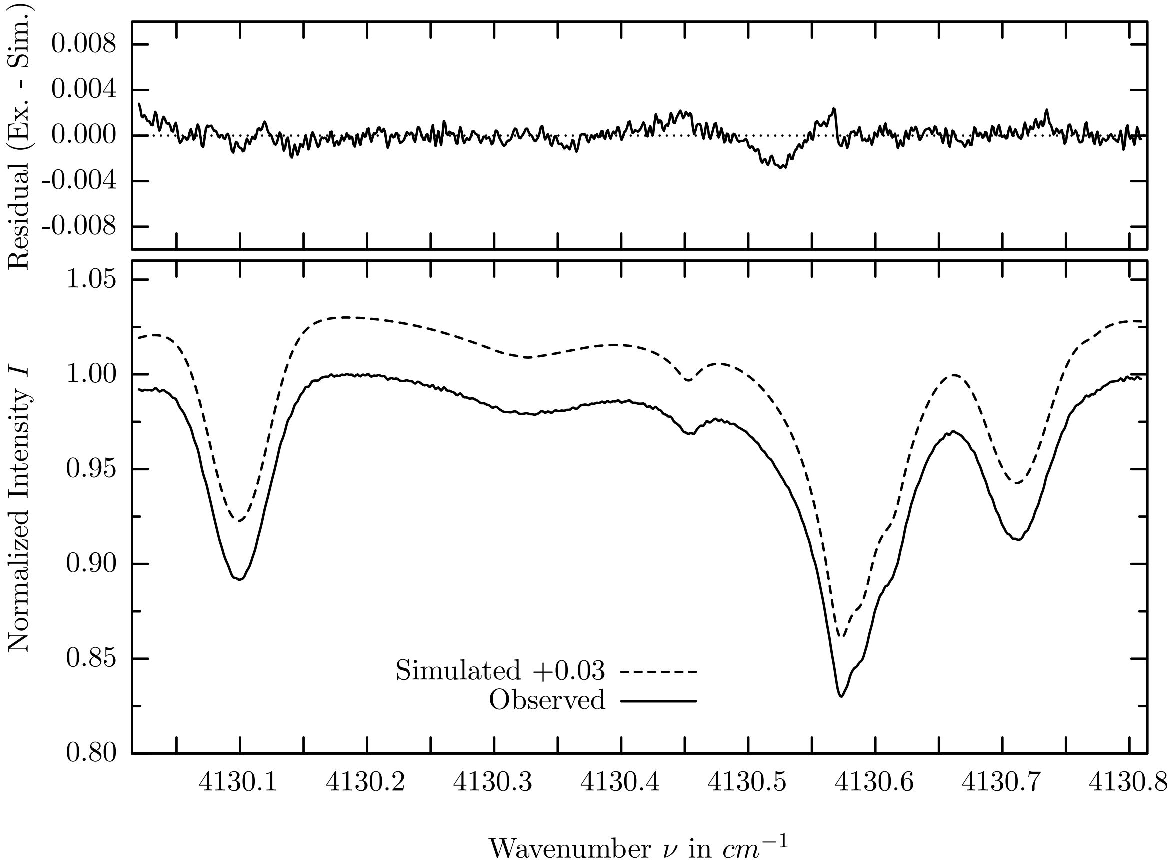

investigated species	:	HDO
line position(s) ν_0	:	4130.3200 cm^{-1}
lower state energy E''_{lst}	:	15.5 cm^{-1}
retrieved TCA, information content	:	3.94E+21 $molec/cm^2$, 24.2
temperature dependence of the TCA	:	-0.422%/K (trop), -0.094%/K (strat)
location, date, solar zenith angle	:	Kiruna, 15/Mar/97, 69.96^o
spectral interval fitted	:	4130.020 – 4130.810 cm^{-1}

Molecule	iCode	Absorption	Molecule	iCode	Absorption
$CH4$	61	17.343%	$NO2$	101	0.001%
Solar(A)	—	10.173%	CO	51	<0.001%
Solar-sim	—	10.575%	$NH3$	111	<0.001%
$H2O$	11	5.250%	OH	131	<0.001%
HDO	491	4.137%	HI	171	<0.001%
$H2O$	1**2**	0.948%	$H2S$	471	<0.001%
$H2O$	1**3**	0.824%			

HDO, Kiruna, φ=69.96^o, OPD=257cm, FoV=1.91$mrad$, boxcar apod.

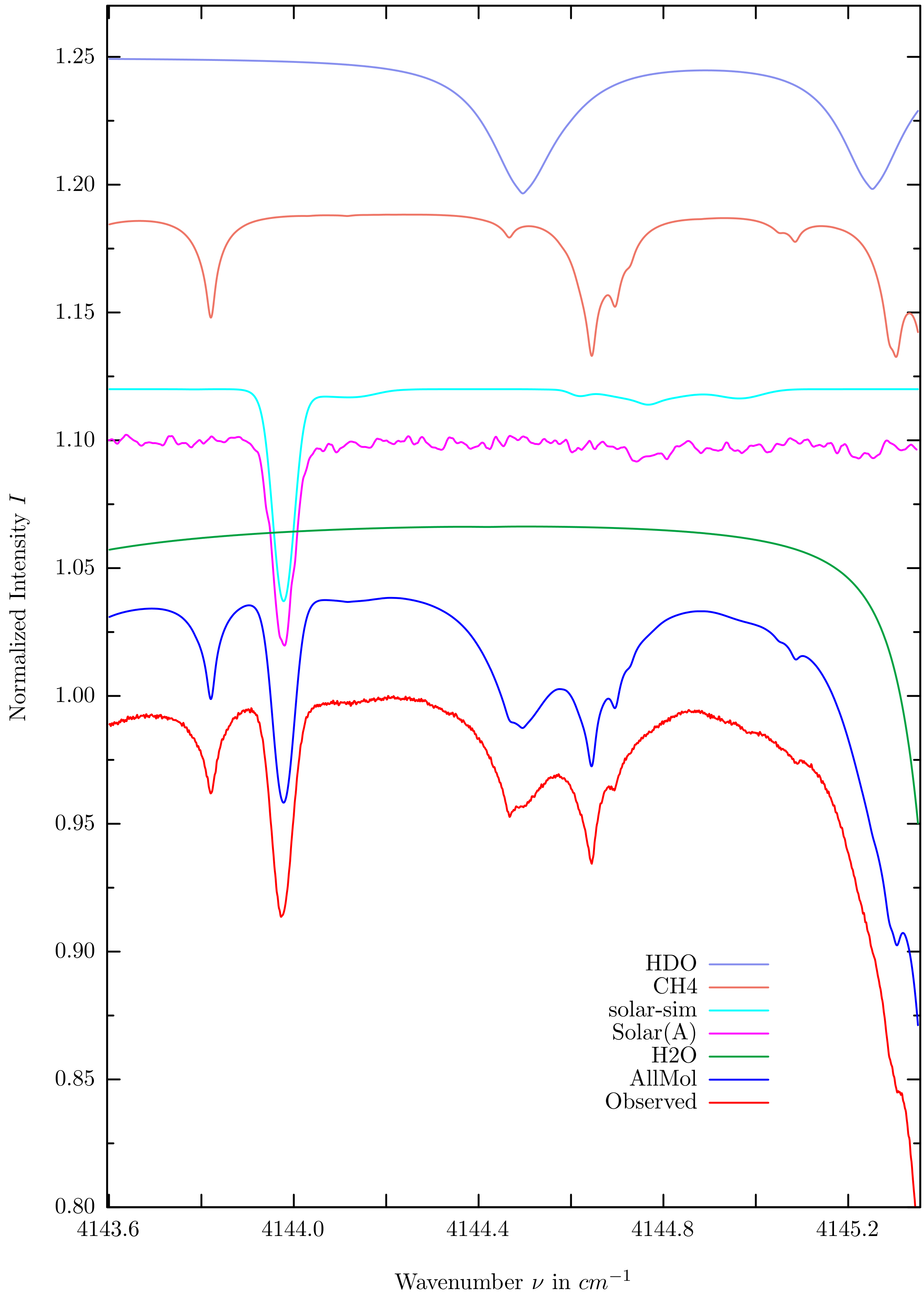

σ=0.063%, 970315S1.90, φ=69.96^o, OPD=257cm, FoV=1.91$mrad$, Apod.=boxcar

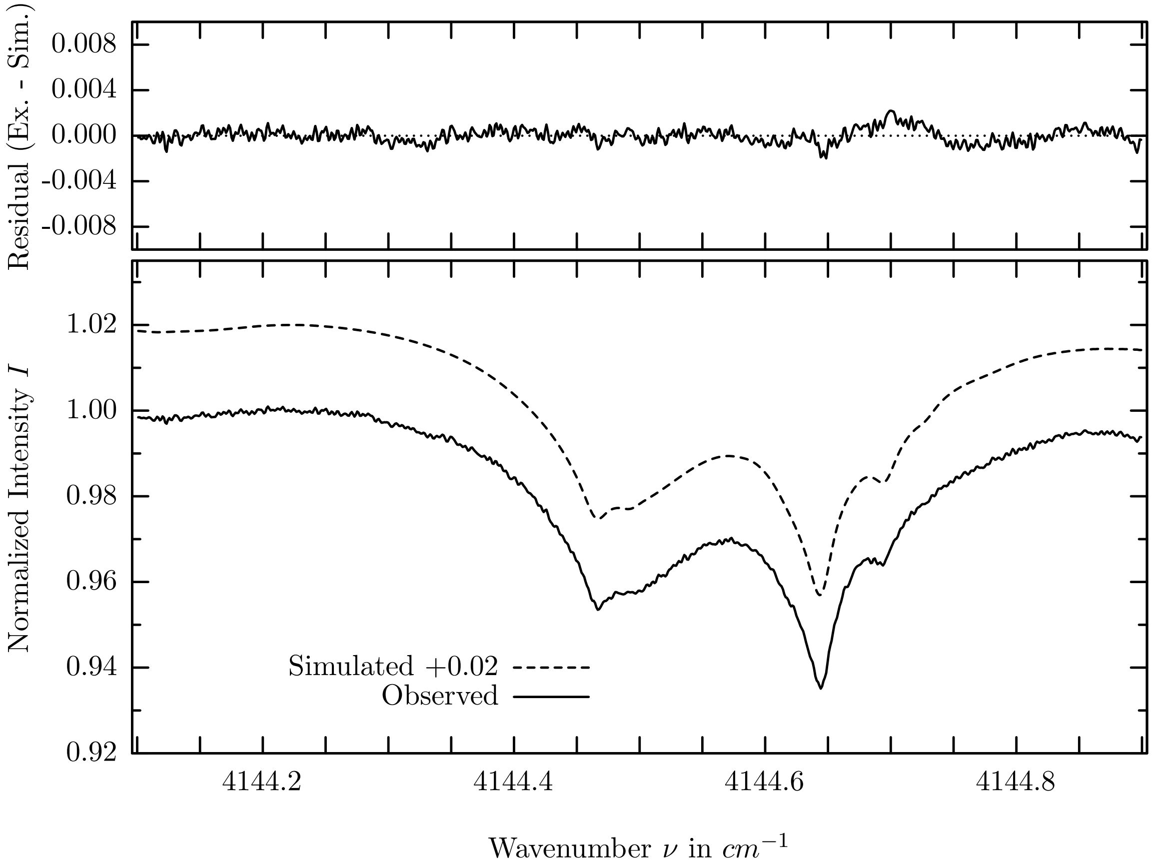

investigated species	:	HDO
line position(s) ν_0	:	4144.4940 cm^{-1}
lower state energy E''_{lst}	:	46.2 cm^{-1}
retrieved TCA, information content	:	4.45E+21 $molec/cm^2$, 68.3
temperature dependence of the TCA	:	+0.073%/K (trop), -0.034%/K (strat)
location, date, solar zenith angle	:	Kiruna, 15/Mar/97, 69.96^o
spectral interval fitted	:	4144.100 – 4144.900 cm^{-1}

Molecule	iCode	Absorption	Molecule	iCode	Absorption
$H2O$	11	13.286%	CO	51	0.001%
Solar(A)	—	8.030%	HF	141	0.001%
Solar-sim	—	8.297%	$NH3$	111	<0.001%
$CH4$	61	5.745%	OH	131	<0.001%
HDO	491	5.344%	HI	171	<0.001%
$NO2$	101	0.002%	$H2S$	471	<0.001%

H_2O, Kiruna, φ=69.96^o, OPD=257cm, FoV=1.91$mrad$, boxcar apod.

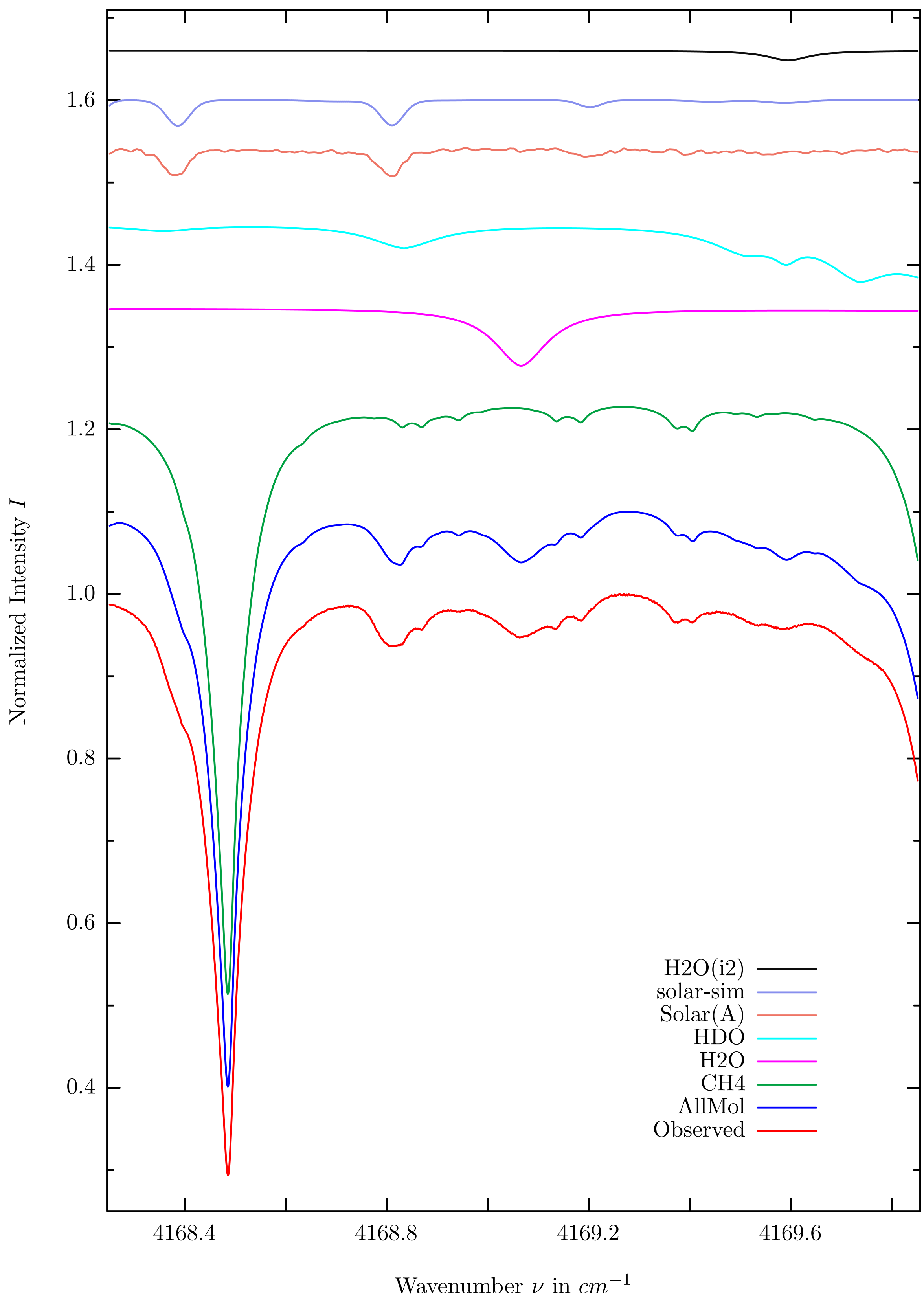

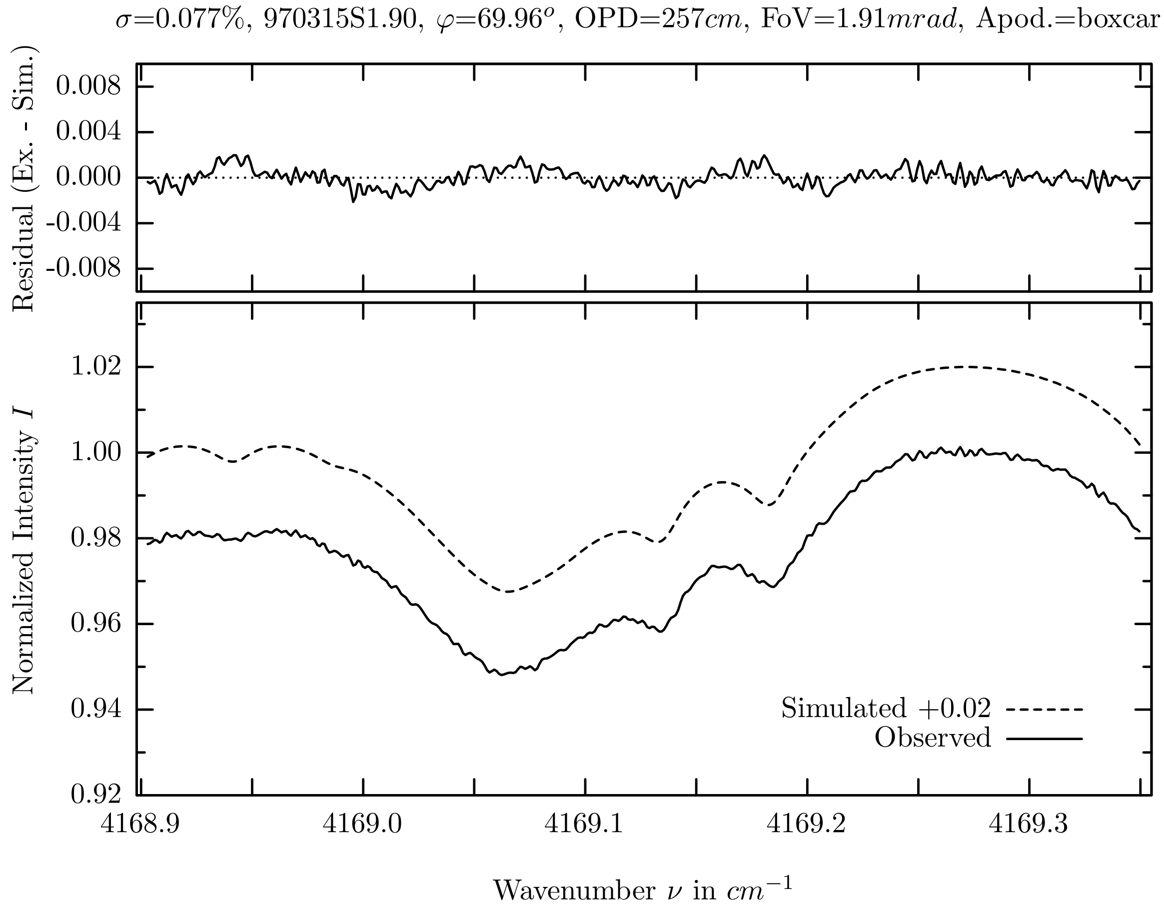

investigated species	:	H_2O
line position(s) ν_0	:	4169.0640 cm^{-1}
lower state energy E''_{lst}	:	508.8 cm^{-1}
retrieved TCA, information content	:	4.65E+21 $molec/cm^2$, 67.9
temperature dependence of the TCA	:	-0.920%/K (trop), -0.020%/K (strat)
location, date, solar zenith angle	:	Kiruna, 15/Mar/97, 69.96^o
spectral interval fitted	:	4168.902 – 4169.350 cm^{-1}

Molecule	iCode	Absorption	Molecule	iCode	Absorption
$CH4$	61	72.649%	$NO2$	101	0.011%
H2O	11	7.279%	$NH3$	111	<0.001%
HDO	491	7.124%	OH	131	<0.001%
Solar(A)	—	3.250%	HF	141	<0.001%
Solar-sim	—	3.105%	HI	171	<0.001%
$H2O$	1**2**	1.160%	$H2S$	471	<0.001%
CO	51	0.023%			

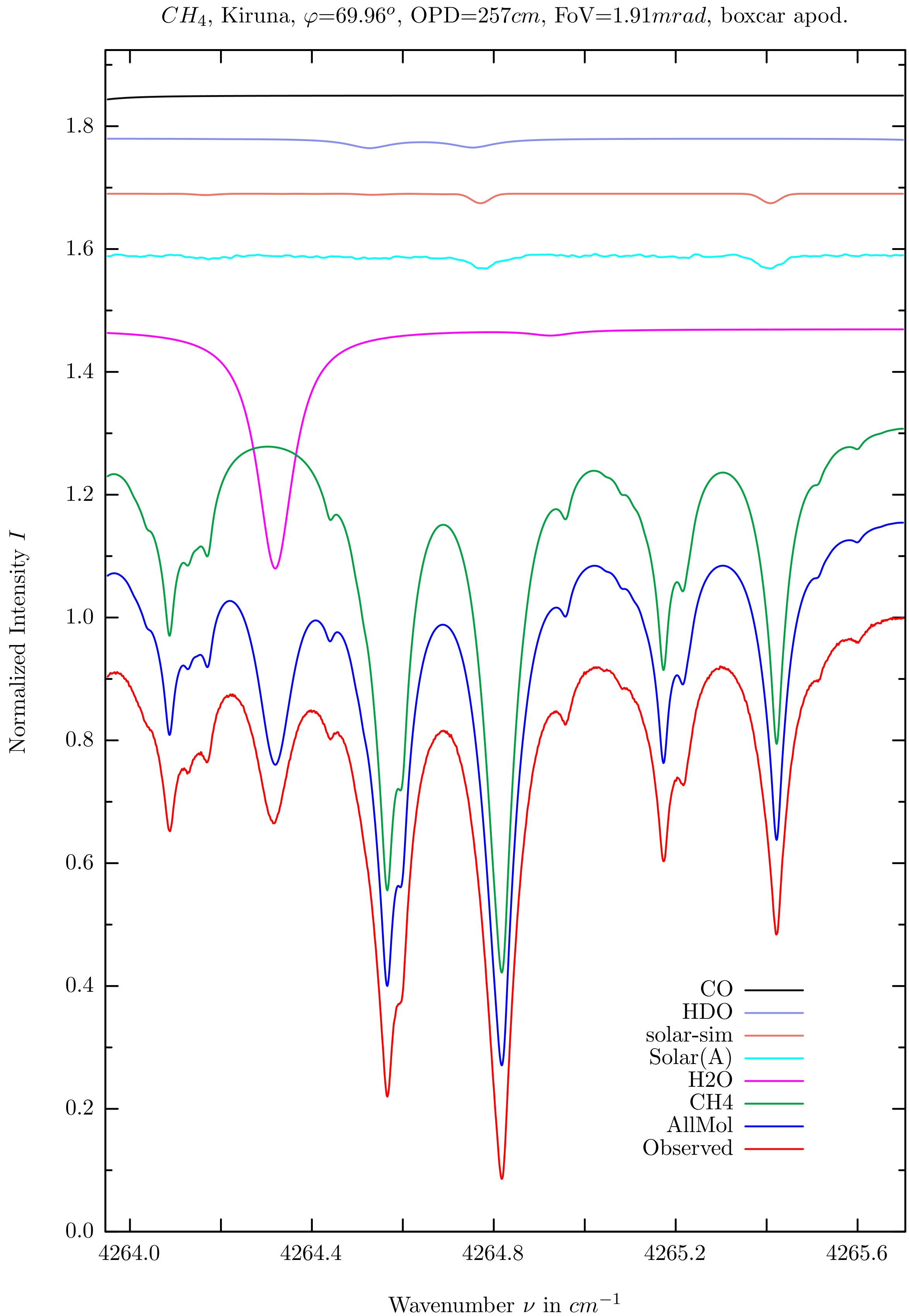
CH_4, Kiruna, φ=69.96^o, OPD=257cm, FoV=1.91$mrad$, boxcar apod.
Normalized Intensity I
Wavenumber ν in cm^{-1}
0.0
0.2
0.4
0.6
0.8
1.0
1.2
1.4
1.6
1.8
4264.0
4264.4
4264.8
4265.2
4265.6
CO
HDO
solar-sim
Solar(A)
H2O
CH4
AllMol
Observed

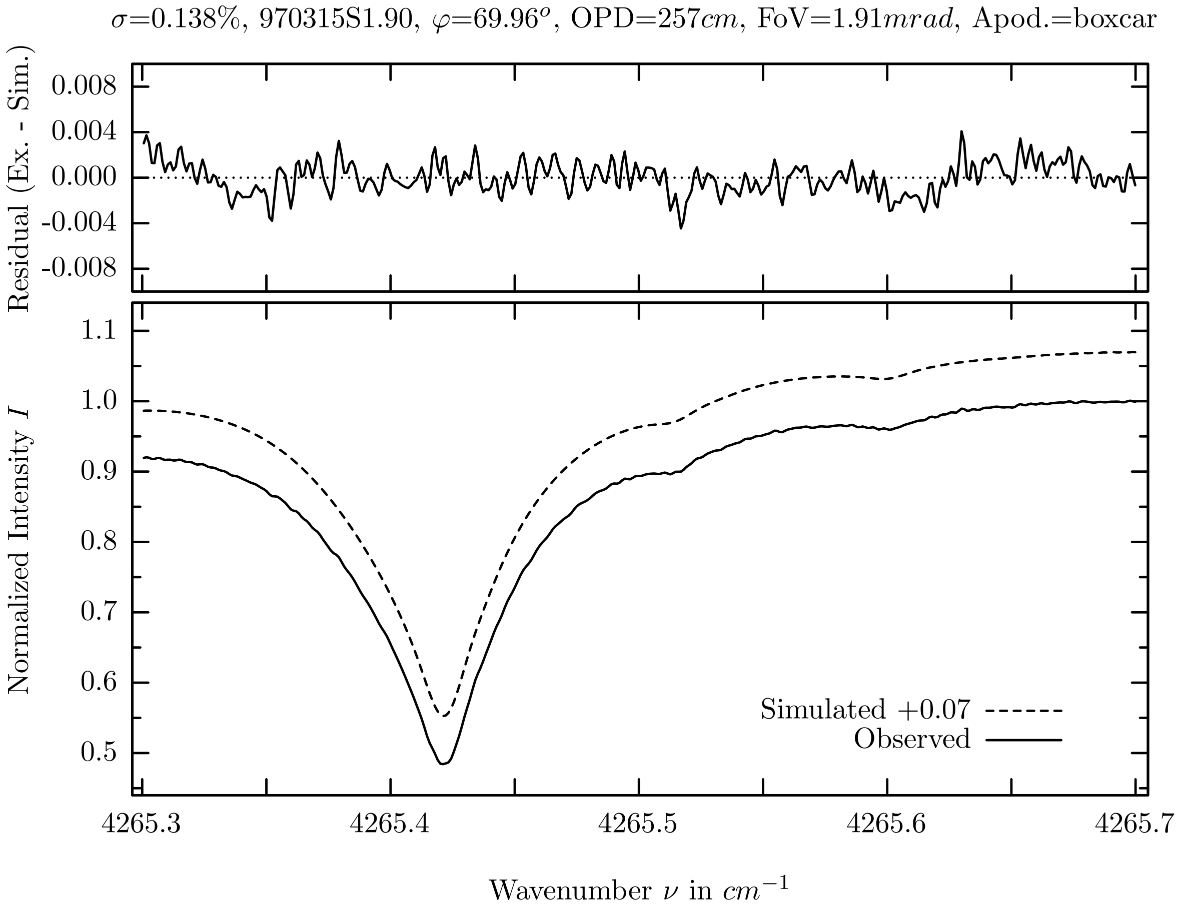

investigated species	:	CH_4
line position(s) ν_0	:	4265.4212 cm^{-1}
lower state energy E''_{lst}	:	157.1 cm^{-1}
retrieved TCA, information content	:	3.53E+19 $molec/cm^2$, 376.1
temperature dependence of the TCA	:	+0.004%/K (trop), -0.001%/K (strat)
location, date, solar zenith angle	:	Kiruna, 15/Mar/97, 69.96^o
spectral interval fitted	:	4265.300 – 4265.700 cm^{-1}

Molecule	iCode	Absorption	Molecule	iCode	Absorption
CH4	61	91.854%	$NH3$	111	<0.001%
$H2O$	11	39.037%	OH	131	<0.001%
Solar(A)	—	2.170%	HF	141	<0.001%
Solar-sim	—	1.540%	HI	171	<0.001%
HDO	491	1.575%	$H2S$	471	<0.001%
CO	51	0.623%			

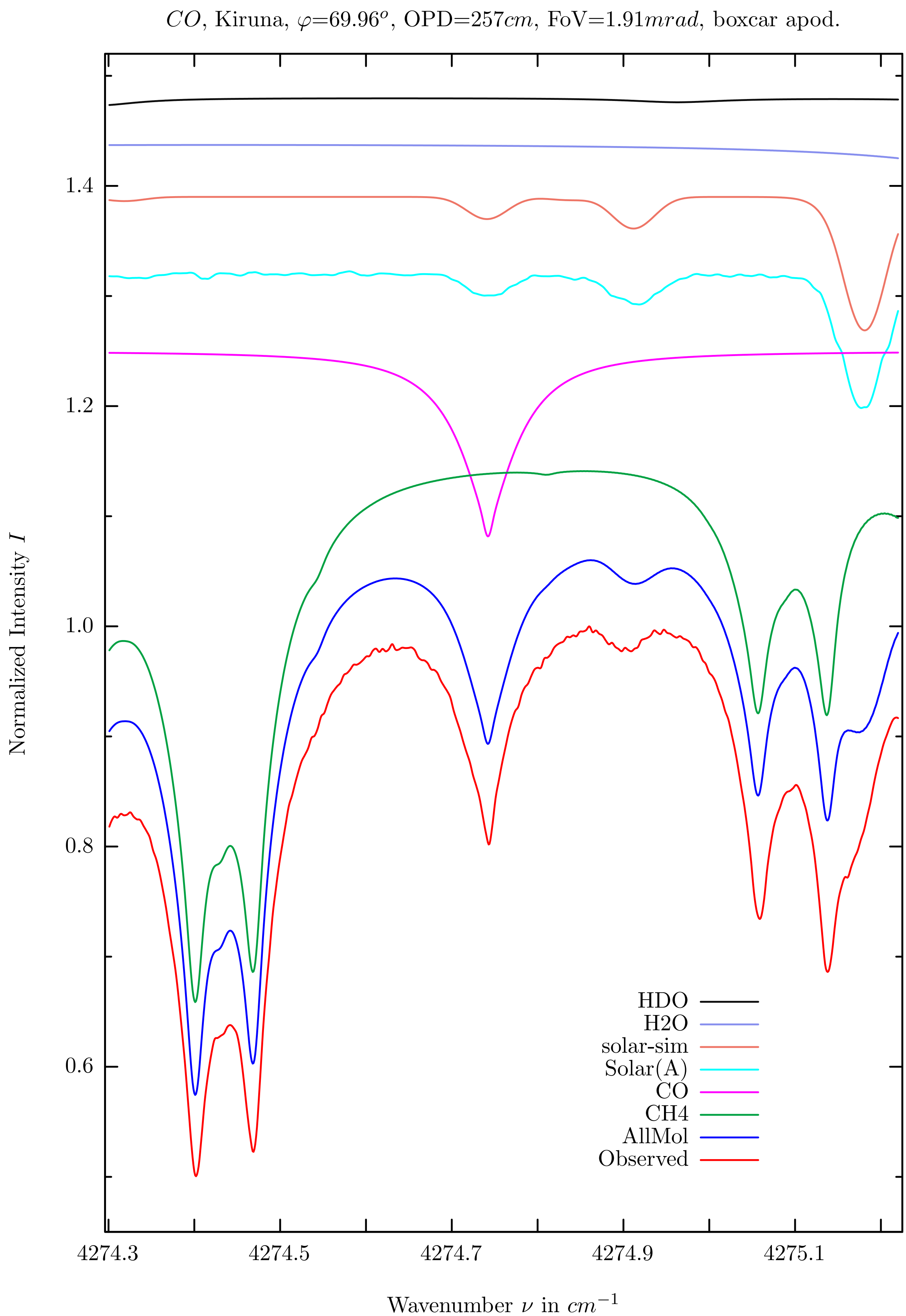
CO, Kiruna, φ=69.96^o, OPD=257cm, FoV=1.91$mrad$, boxcar apod.
Normalized Intensity I
1.4
1.2
1.0
0.8
0.6
4274.3
4274.5
4274.7
4274.9
4275.1
Wavenumber ν in cm^{-1}
HDO
H2O
solar-sim
Solar(A)
CO
CH4
AllMol
Observed

σ=0.154%, 970315S1.90, φ=69.96^o, OPD=257cm, FoV=1.91$mrad$, Apod.=boxcar

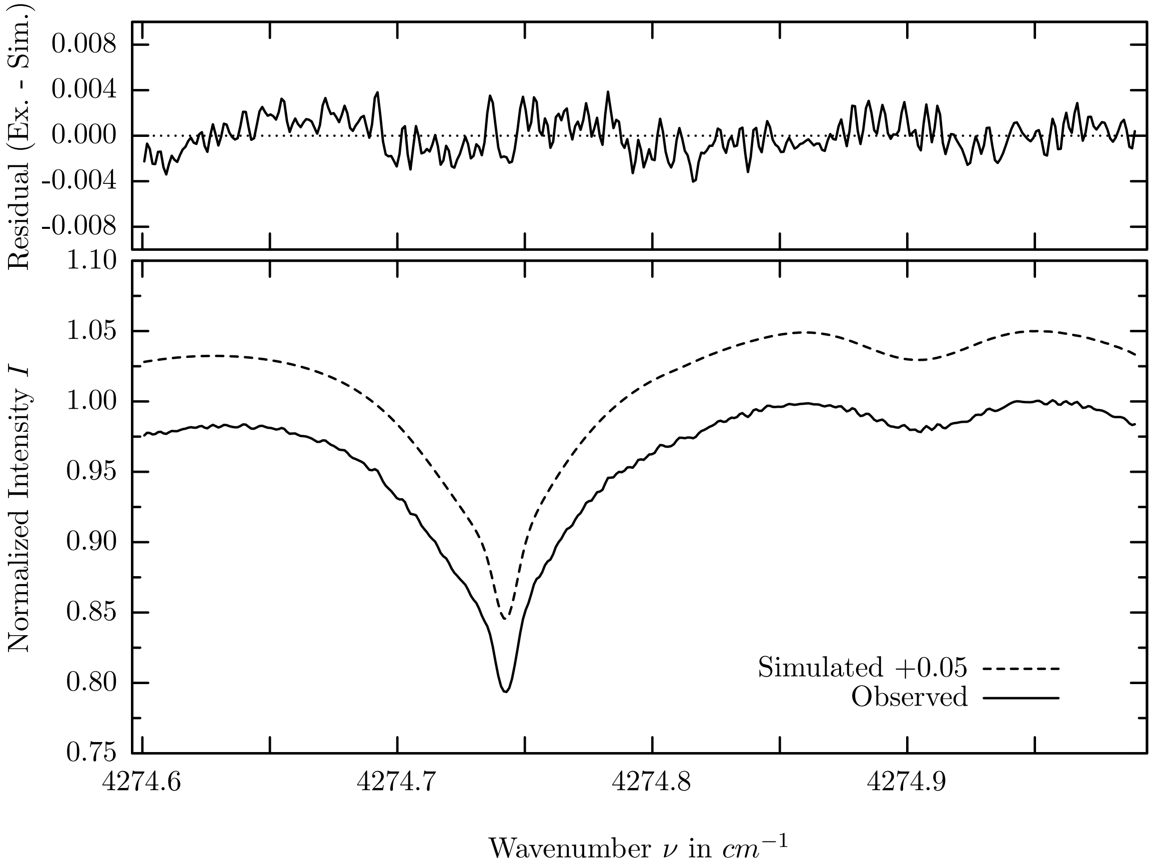

investigated species	:	CO
line position(s) ν_0	:	4274.7407 cm^{-1}
lower state energy E''_{lst}	:	23.1 cm^{-1}
retrieved TCA, information content	:	2.49E+18 $molec/cm^2$, 129.9
temperature dependence of the TCA	:	+0.135%/K (trop), +0.016%/K (strat)
location, date, solar zenith angle	:	Kiruna, 15/Mar/97, 69.96^o
spectral interval fitted	:	4274.600 – 4274.990 cm^{-1}

Molecule	iCode	Absorption	Molecule	iCode	Absorption
$CH4$	61	51.165%	HDO	491	0.648%
CO	51	16.854%	$NH3$	111	0.001%
Solar(A)	—	12.173%	OH	131	<0.001%
Solar-sim	—	12.125%	HF	141	<0.001%
$H2O$	11	1.502%	HI	171	<0.001%

CH_4, Kiruna, φ=69.96^o, OPD=257cm, FoV=1.91$mrad$, boxcar apod.

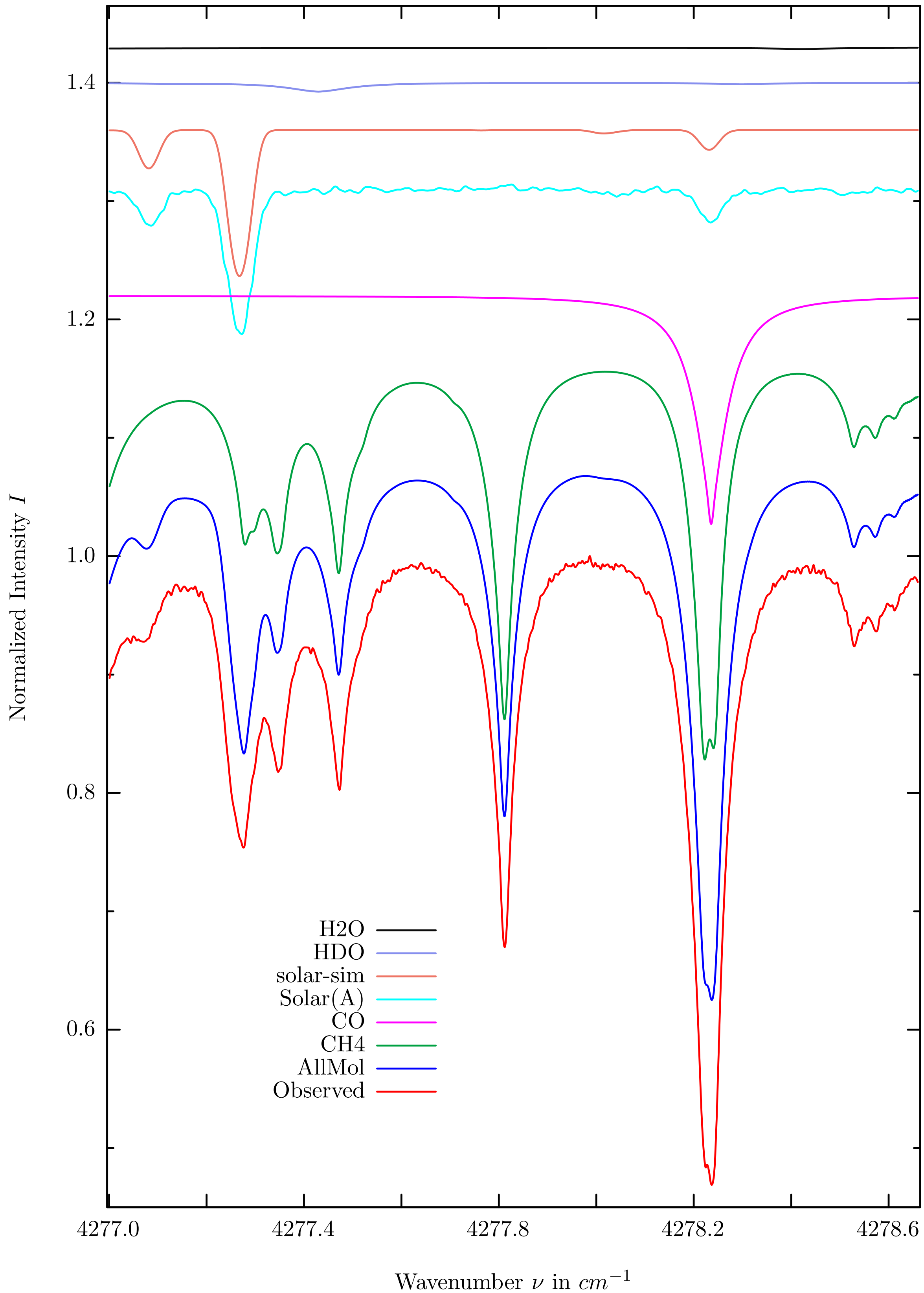

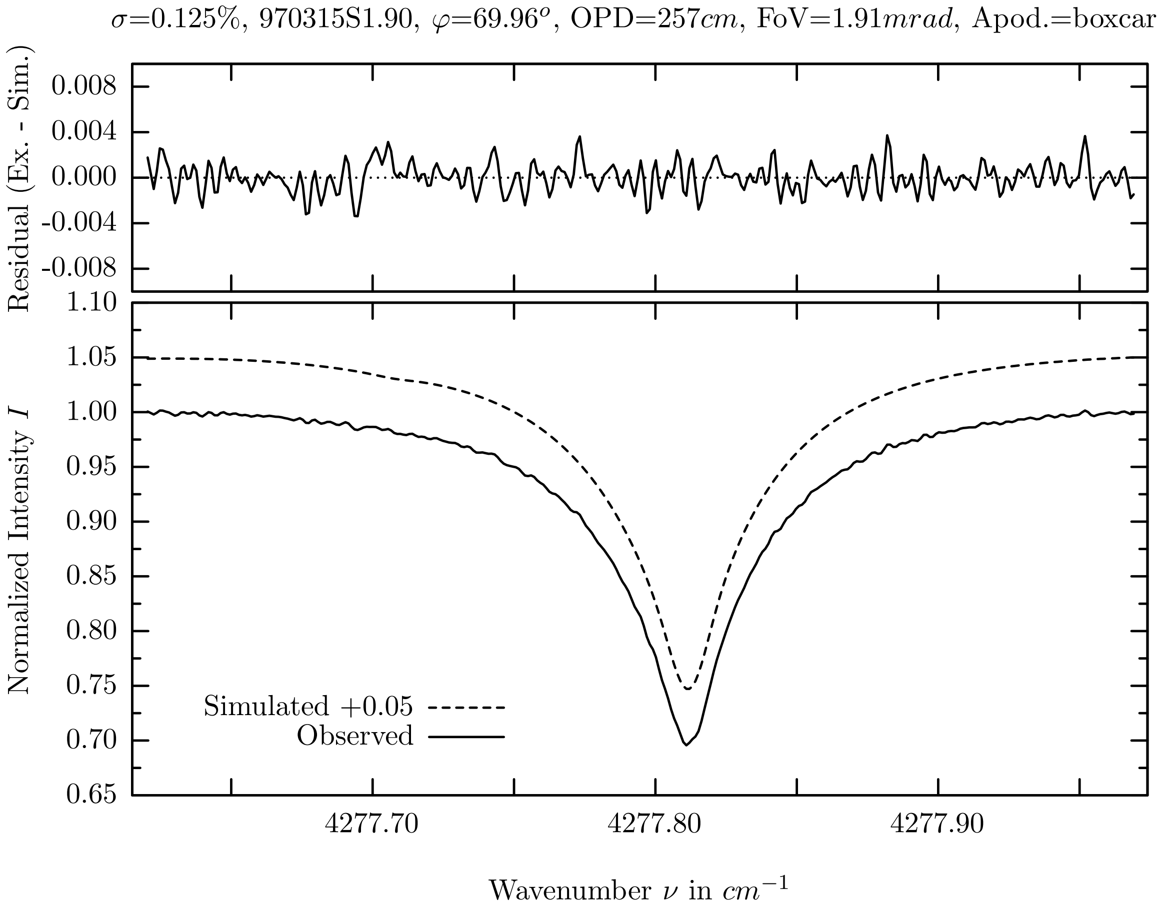

investigated species	:	CH_4
line position(s) ν_0	:	4277.8105 cm^{-1}
lower state energy E''_{lst}	:	293.2 cm^{-1}
retrieved TCA, information content	:	3.30E+19 $molec/cm^2$, 241.8
temperature dependence of the TCA	:	-0.204%/K (trop), -0.036%/K (strat)
location, date, solar zenith angle	:	Kiruna, 15/Mar/97, 69.96^o
spectral interval fitted	:	4277.620 – 4277.970 cm^{-1}

Molecule	iCode	Absorption	Molecule	iCode	Absorption
CH4	61	35.202%	*N2O*	4**2**	0.003%
CO	51	19.310%	*NH*3	111	0.001%
Solar(A)	—	12.238%	*OH*	131	<0.001%
Solar-sim	—	12.341%	*HF*	141	<0.001%
HDO	491	0.759%	*HI*	171	<0.001%
H2O	11	0.180%			

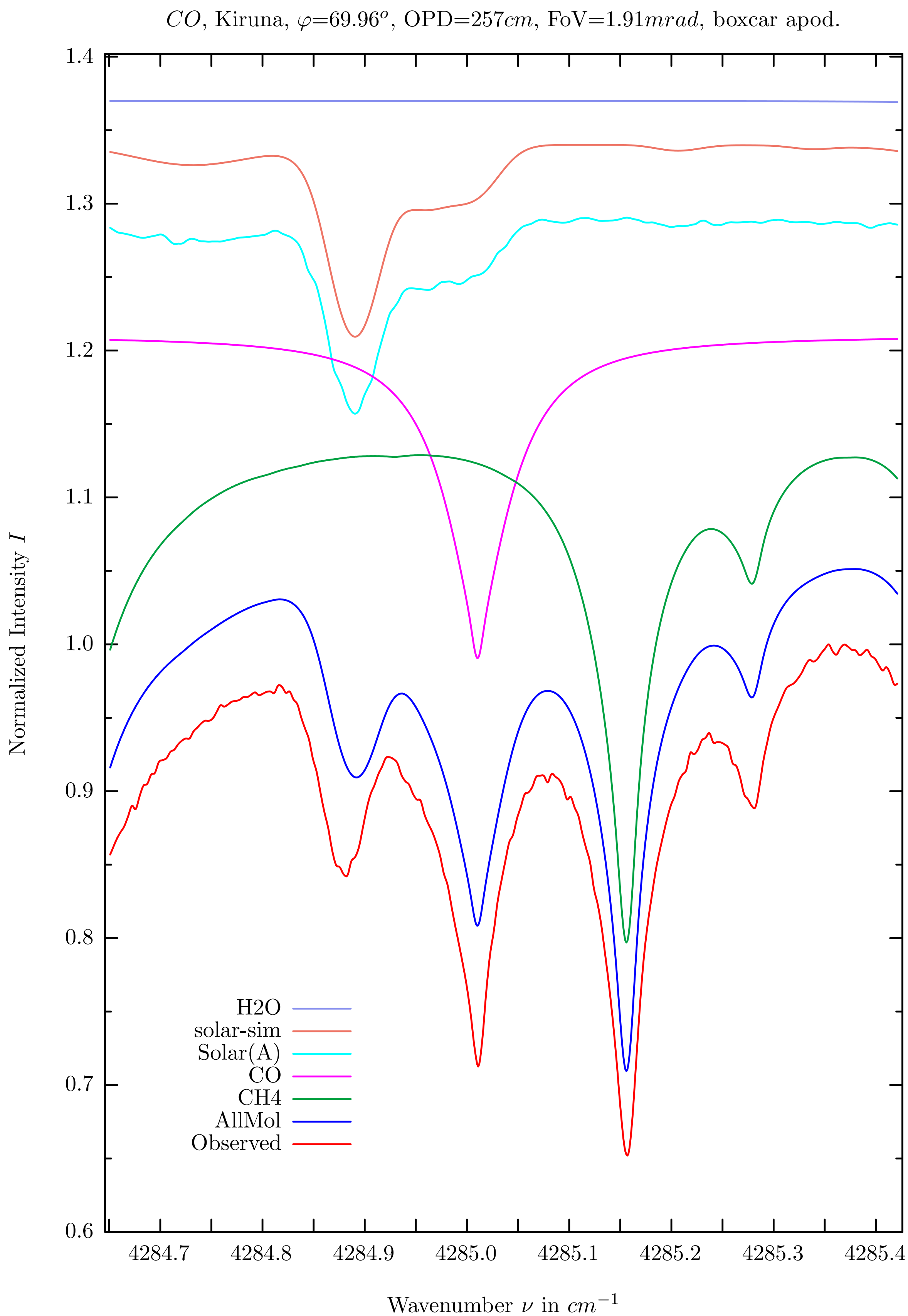

CO, Kiruna, φ=69.96^o, OPD=257cm, FoV=1.91$mrad$, boxcar apod.
Normalized Intensity I
Wavenumber ν in cm^{-1}
1.4
1.3
1.2
1.1
1.0
0.9
0.8
0.7
0.6
4284.7
4284.8
4284.9
4285.0
4285.1
4285.2
4285.3
4285.4
H2O
solar-sim
Solar(A)
CO
CH4
AllMol
Observed

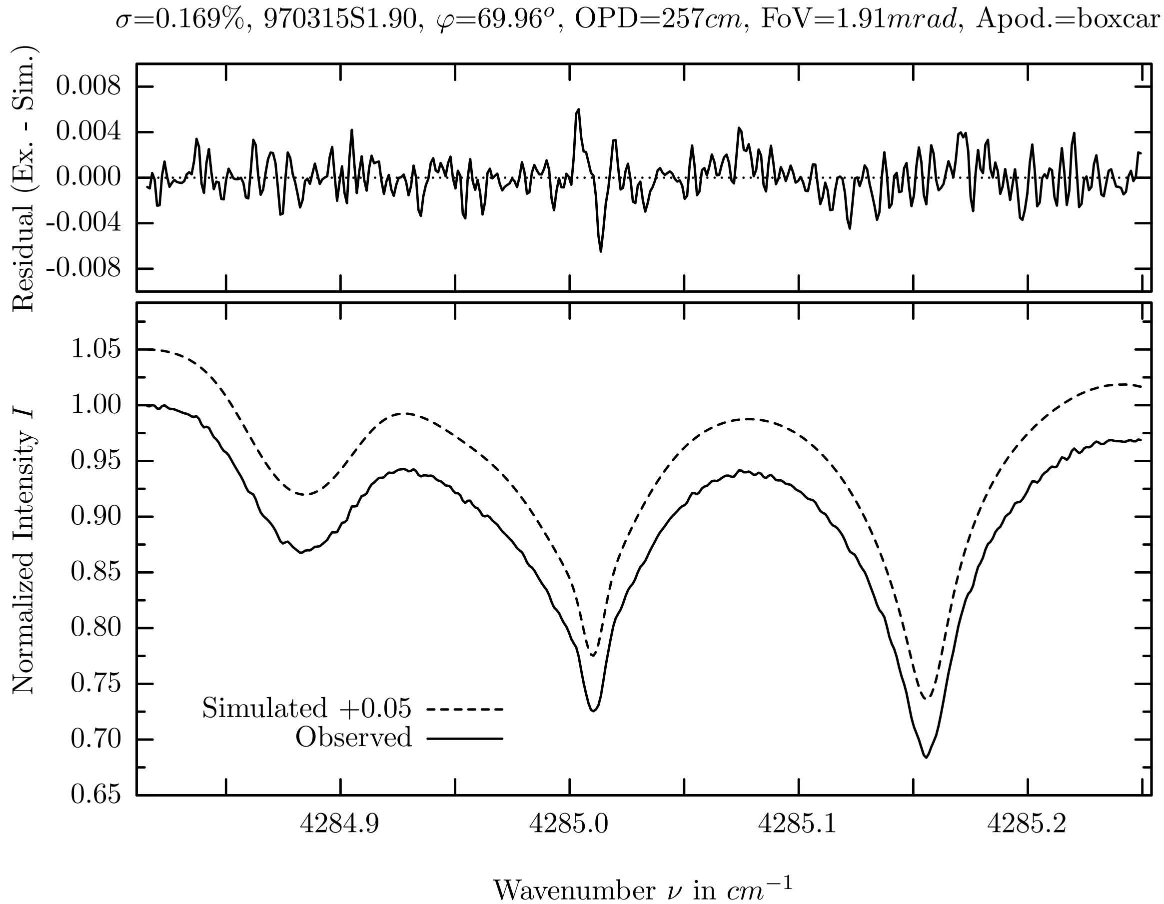

investigated species	:	$CO, (CH_4)$
line position(s) ν_0	:	4285.0089, (4285.1555) cm^{-1}
lower state energy E''_{lst}	:	80.7, (62.9) cm^{-1}
retrieved TCA, information content	:	2.30E+18, (3.26E+19) $molec/cm^2$, 140.5, (185.8)
temperature dependence of the TCA	:	+.508, (+.157)%/K (trop), +.080, (+.226)%/K (strat)
location, date, solar zenith angle	:	Kiruna, 15/Mar/97, 69.96^o
spectral interval fitted	:	4284.815 – 4285.250 cm^{-1}

Molecule	iCode	Absorption	Molecule	iCode	Absorption
$CH4$	61	36.342%	HDO	491	0.038%
CO	51	21.967%	$NH3$	111	0.001%
Solar(A)	—	13.296%	OH	131	<0.001%
Solar-sim	—	13.062%	HF	141	<0.001%
$H2O$	11	0.090%	HI	171	<0.001%

CH_4, Kiruna, φ=69.96^o, OPD=257cm, FoV=1.91$mrad$, boxcar apod.

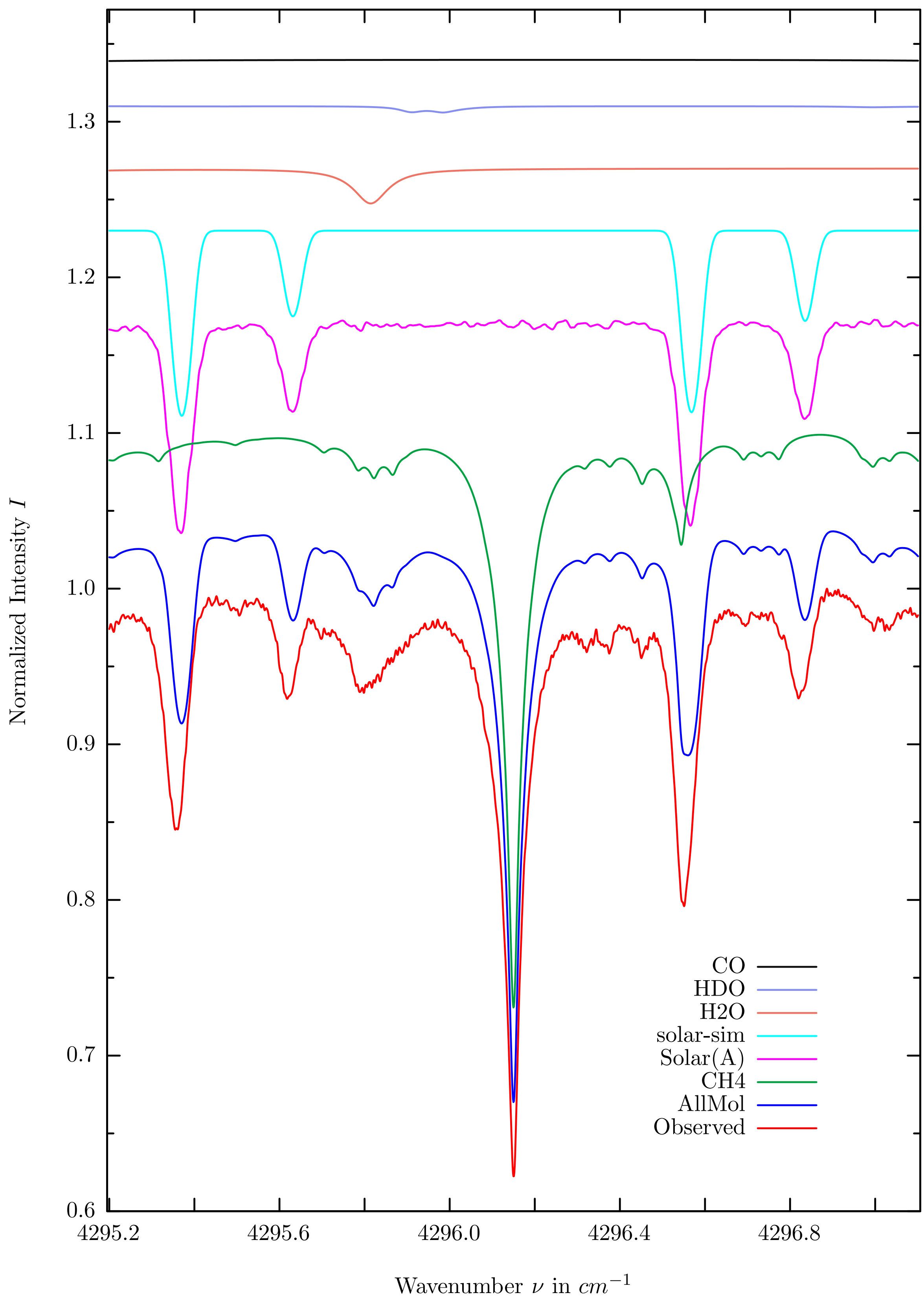

σ=0.258%, 970315S1.90, φ=69.96^o, OPD=257cm, FoV=1.91$mrad$, Apod.=boxcar

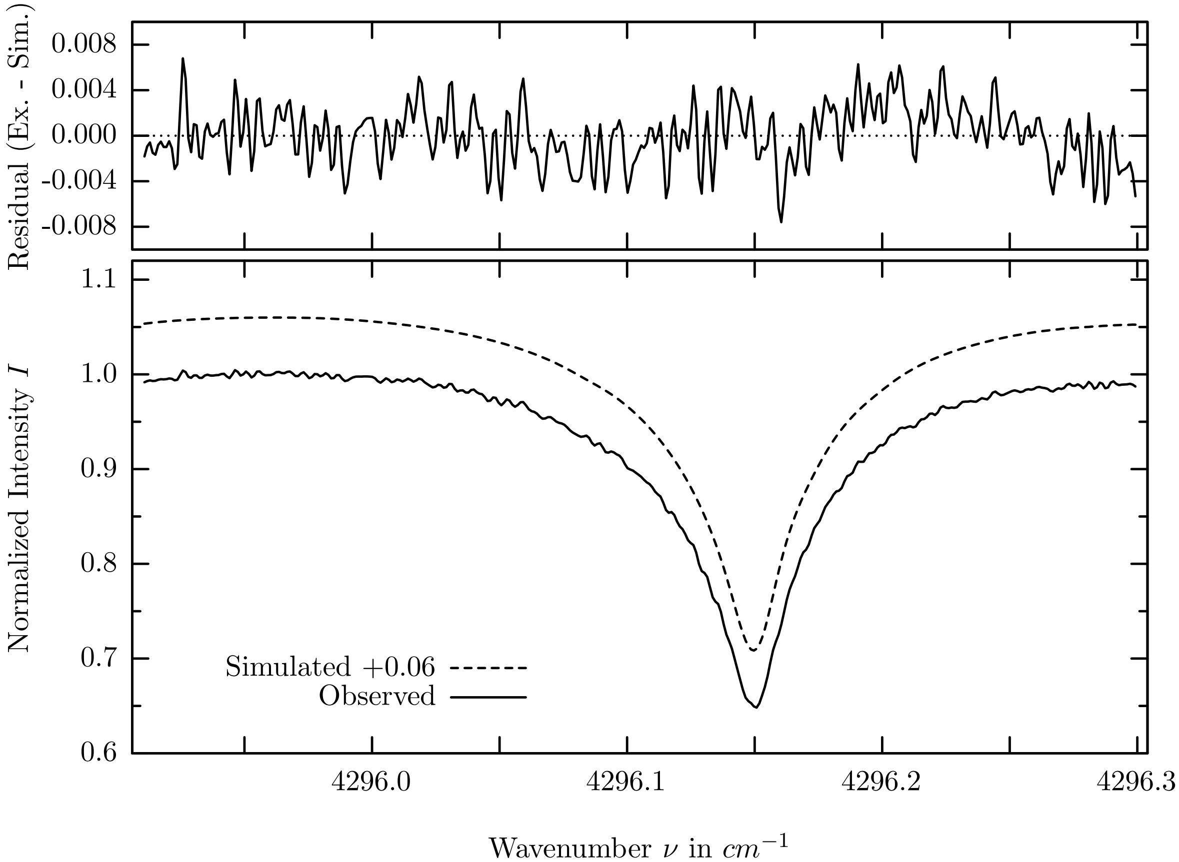

investigated species	:	CH_4
line position(s) ν_0	:	4296.1496 cm^{-1}
lower state energy E''_{lst}	:	31.4 cm^{-1}
retrieved TCA, information content	:	3.43E+19 $molec/cm^2$, 136.3
temperature dependence of the TCA	:	+0.275%/K (trop), +0.016%/K (strat)
location, date, solar zenith angle	:	Kiruna, 15/Mar/97, 69.96^o
spectral interval fitted	:	4295.910 – 4296.300 cm^{-1}

Molecule	iCode	Absorption	Molecule	iCode	Absorption
CH4	61	37.951%	CO	51	0.100%
Solar(A)	—	13.429%	$NH3$	111	0.001%
Solar-sim	—	11.898%	OH	131	<0.001%
$H2O$	11	2.253%	HF	141	<0.001%
HDO	491	0.409%	HI	171	<0.001%

H_2O, Kiruna, φ=65.02^o, OPD=120cm, FoV=1.91$mrad$, boxcar apod.

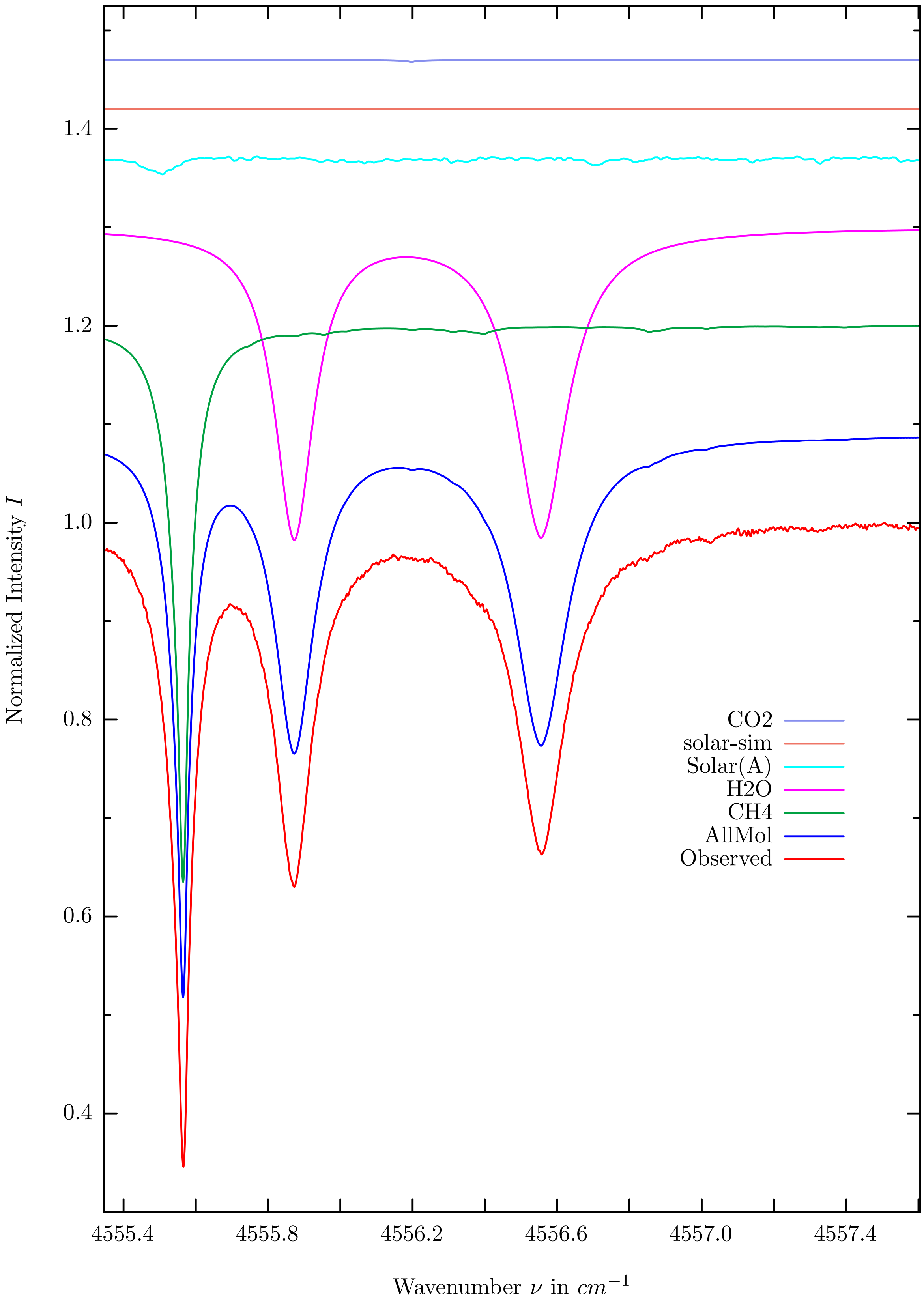

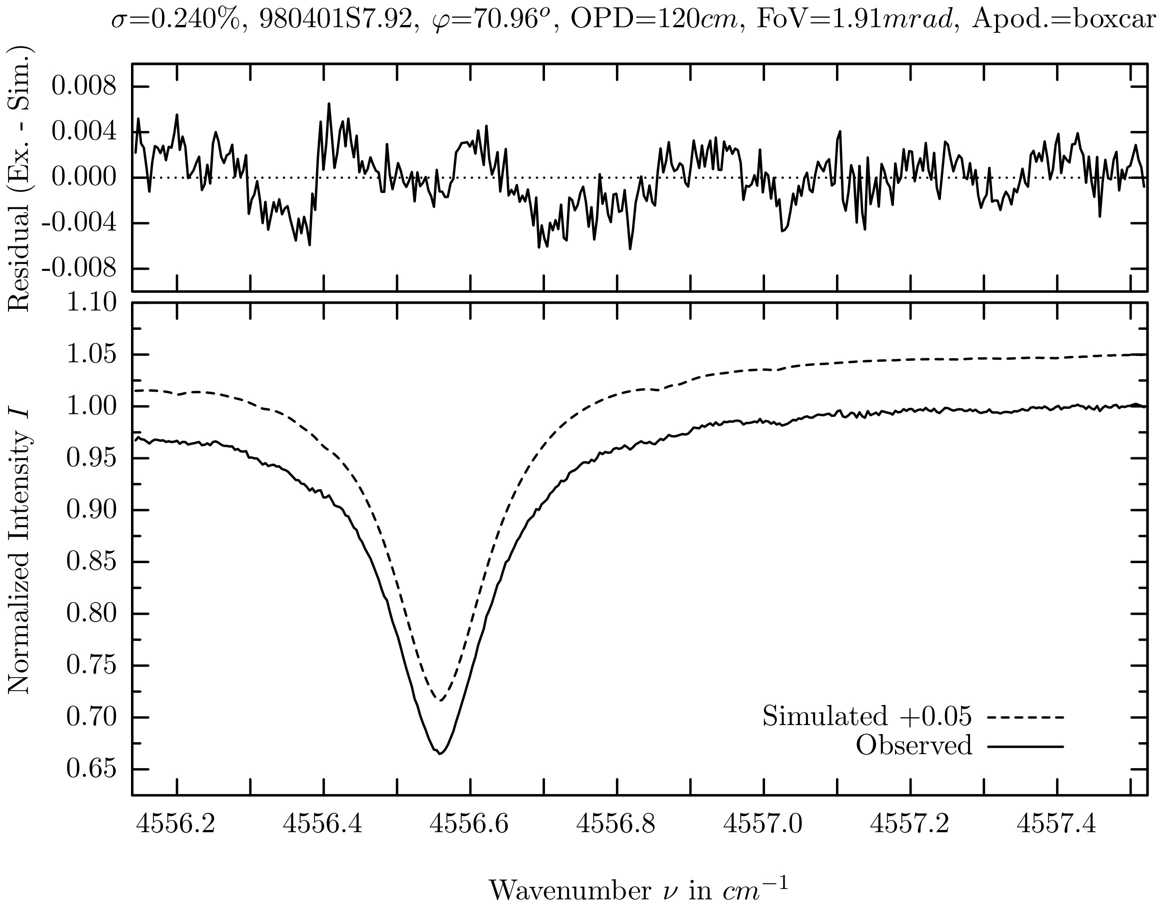

investigated species	:	H_2O
line position(s) ν_0	:	4556.5540 cm^{-1}
lower state energy E''_{lst}	:	300.4 cm^{-1}
retrieved TCA, information content	:	8.26E+21 $molec/cm^2$, 138.5
temperature dependence of the TCA	:	-0.090%/K (trop), -0.030%/K (strat)
location, date, solar zenith angle	:	Kiruna, 1/Apr/98, 70.96^o
spectral interval fitted	:	4556.140 – 4557.520 cm^{-1}

Molecule	iCode	Absorption	Molecule	iCode	Absorption
$CH4$	61	56.536%	$O3$	31	0.007%
H2O	11	31.760%	$NH3$	111	0.001%
Solar(A)	—	1.622%	$N2O$	41	<0.001%
Solar-sim	—	<0.001%	OH	131	<0.001%
$CO2$	21	0.228%	HDO	491	<0.001%

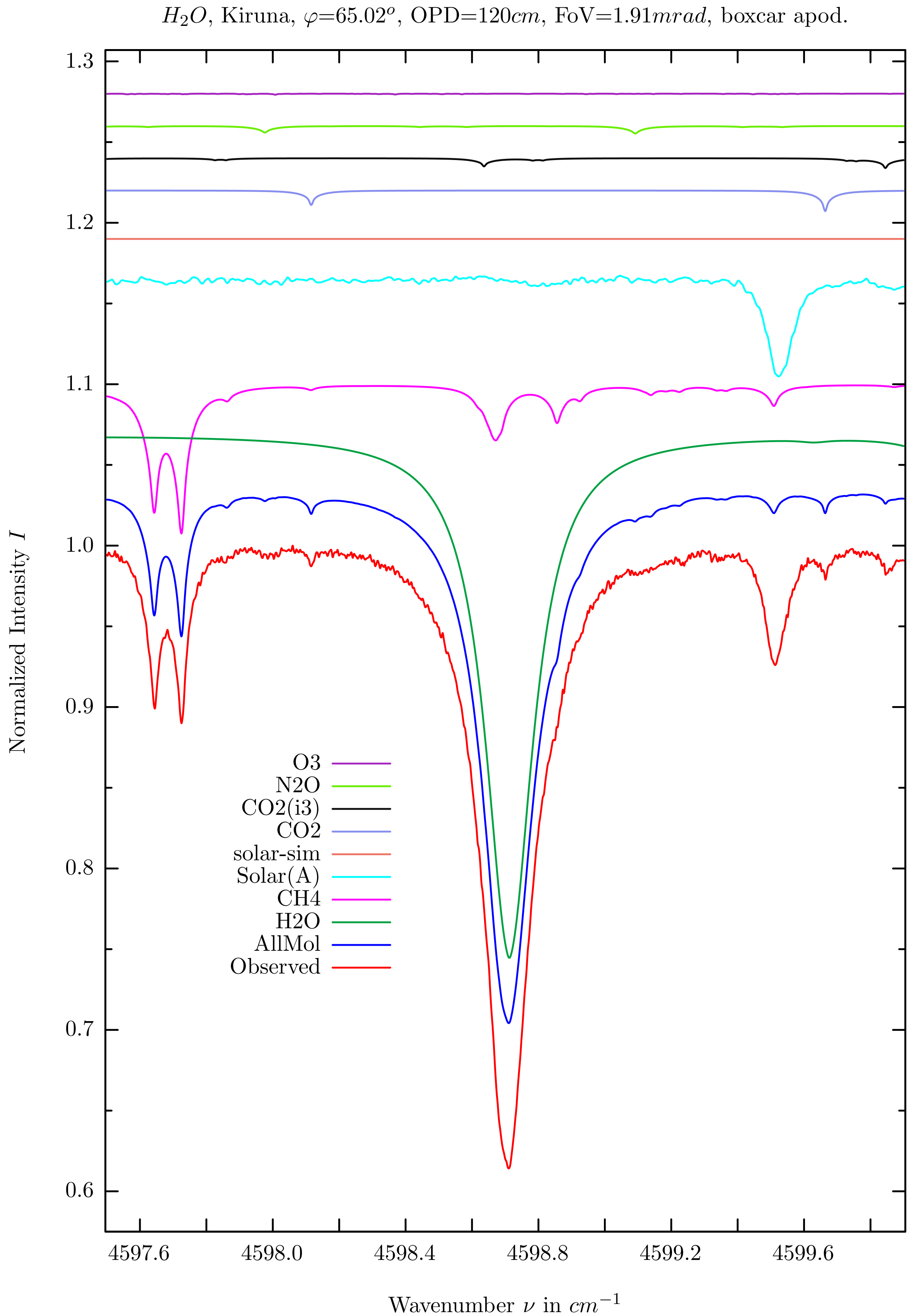

H_2O, Kiruna, φ=65.02^o, OPD=120cm, FoV=1.91$mrad$, boxcar apod.
Normalized Intensity I
Wavenumber ν in cm^{-1}
1.3
1.2
1.1
1.0
0.9
0.8
0.7
0.6
4597.6
4598.0
4598.4
4598.8
4599.2
4599.6
O3
N2O
CO2(i3)
CO2
solar-sim
Solar(A)
CH4
H2O
AllMol
Observed

σ=0.200%, 980401S7.92, φ=70.96^o, OPD=120cm, FoV=1.91$mrad$, Apod.=boxcar

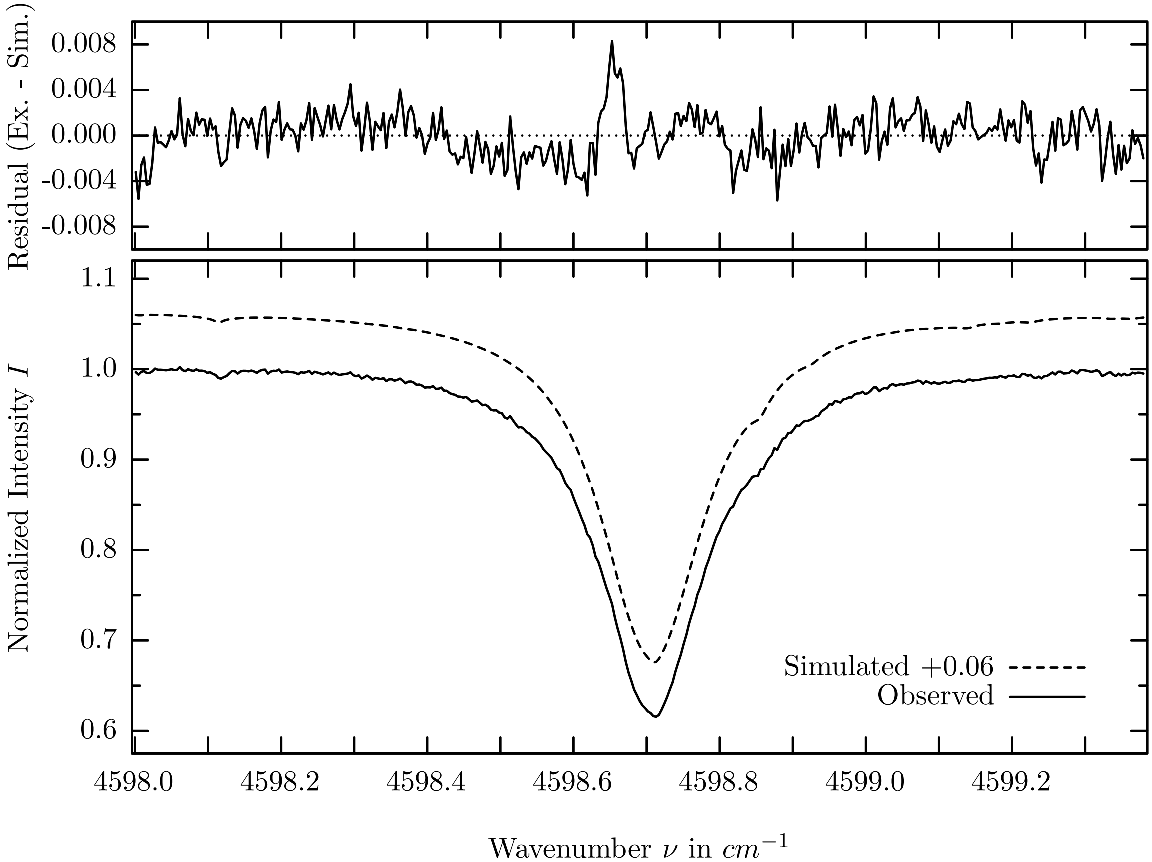

investigated species	:	H_2O
line position(s) ν_0	:	4598.7110 cm^{-1}
lower state energy E''_{lst}	:	222.1 cm^{-1}
retrieved TCA, information content	:	9.42E+21 $molec/cm^2$, 192.1
temperature dependence of the TCA	:	+0.180%/K (trop), -0.040%/K (strat)
location, date, solar zenith angle	:	Kiruna, 1/Apr/98, 70.96^o
spectral interval fitted	:	4598.000 – 4599.380 cm^{-1}

Molecule	iCode	Absorption	Molecule	iCode	Absorption
H2O	11	32.541%	$N2O$	41	0.474%
$CH4$	61	9.263%	$O3$	31	0.067%
Solar(A)	—	6.017%	$NH3$	111	<0.001%
Solar-sim	—	<0.001%	OH	131	<0.001%
$CO2$	21	1.286%	HBR	161	<0.001%
$CO2$	2**3**	0.613%			

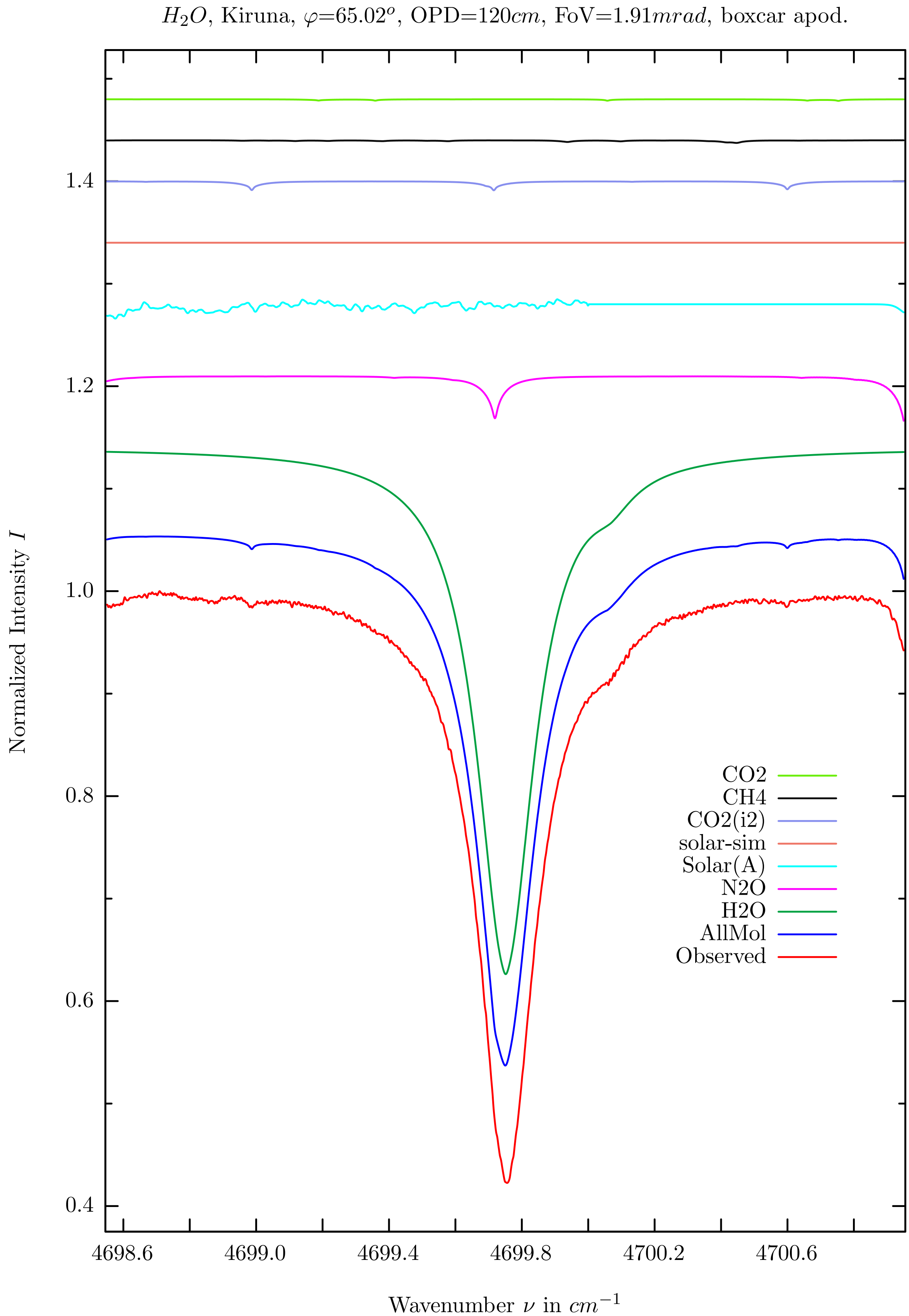

H_2O, Kiruna, φ=65.02^o, OPD=120cm, FoV=1.91$mrad$, boxcar apod.
Normalized Intensity I
1.4
1.2
1.0
0.8
0.6
0.4
4698.6
4699.0
4699.4
4699.8
4700.2
4700.6
Wavenumber ν in cm^{-1}
CO2
CH4
CO2(i2)
solar-sim
Solar(A)
N2O
H2O
AllMol
Observed

σ=0.226%, 980401S7.92, φ=70.96^o, OPD=120cm, FoV=1.91$mrad$, Apod.=boxcar

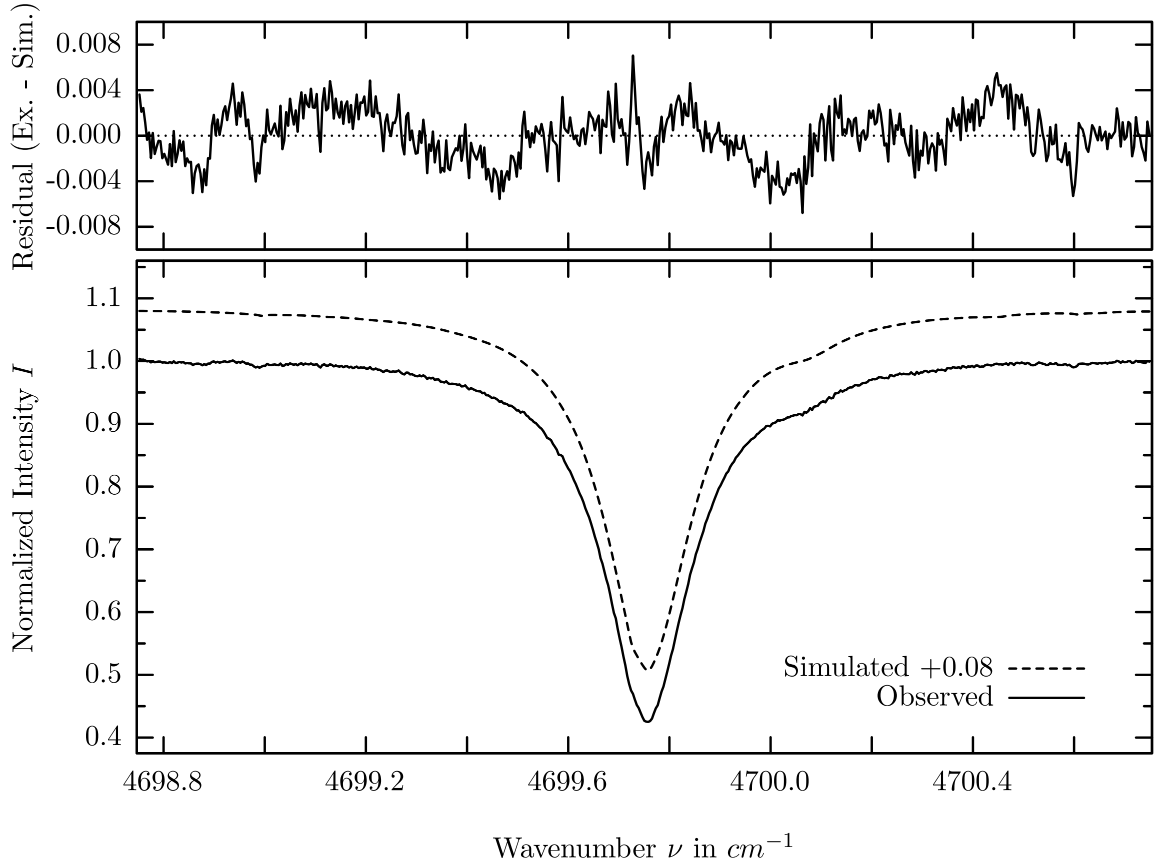

investigated species	:	H_2O
line position(s) ν_0	:	4699.7500 cm^{-1}
lower state energy E''_{lst}	:	23.8 cm^{-1}
retrieved TCA, information content	:	9.32E+21 $molec/cm^2$, 251.5
temperature dependence of the TCA	:	+0.542%/K (trop), -0.017%/K (strat)
location, date, solar zenith angle	:	Kiruna, 1/Apr/98, 70.96^o
spectral interval fitted	:	4698.750 – 4700.750 cm^{-1}

Molecule	iCode	Absorption	Molecule	iCode	Absorption
H2O	11	51.380%	$CH4$	61	0.260%
$N2O$	41	4.596%	$CO2$	21	0.121%
Solar(A)	—	1.399%	$O3$	31	0.007%
Solar-sim	—	<0.001%	$NH3$	111	<0.001%
$CO2$	**22**	0.889%	OH	131	<0.001%

N_2O, Kiruna, φ=70.96^o, OPD=120cm, FoV=1.91$mrad$, boxcar apod.

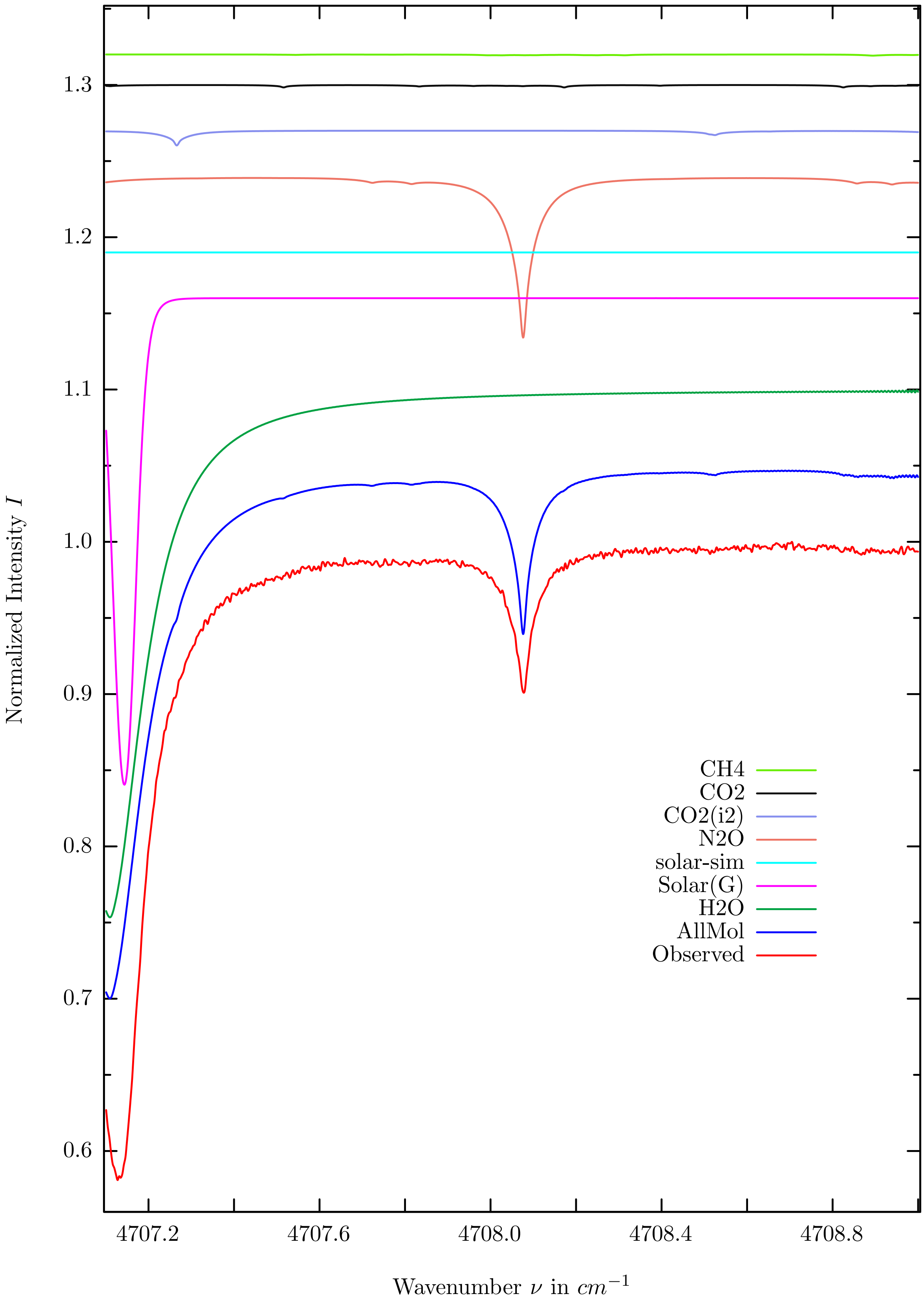

σ=0.124%, 980401S7.92, φ=70.96^o, OPD=120cm, FoV=1.91$mrad$, Apod.=boxcar

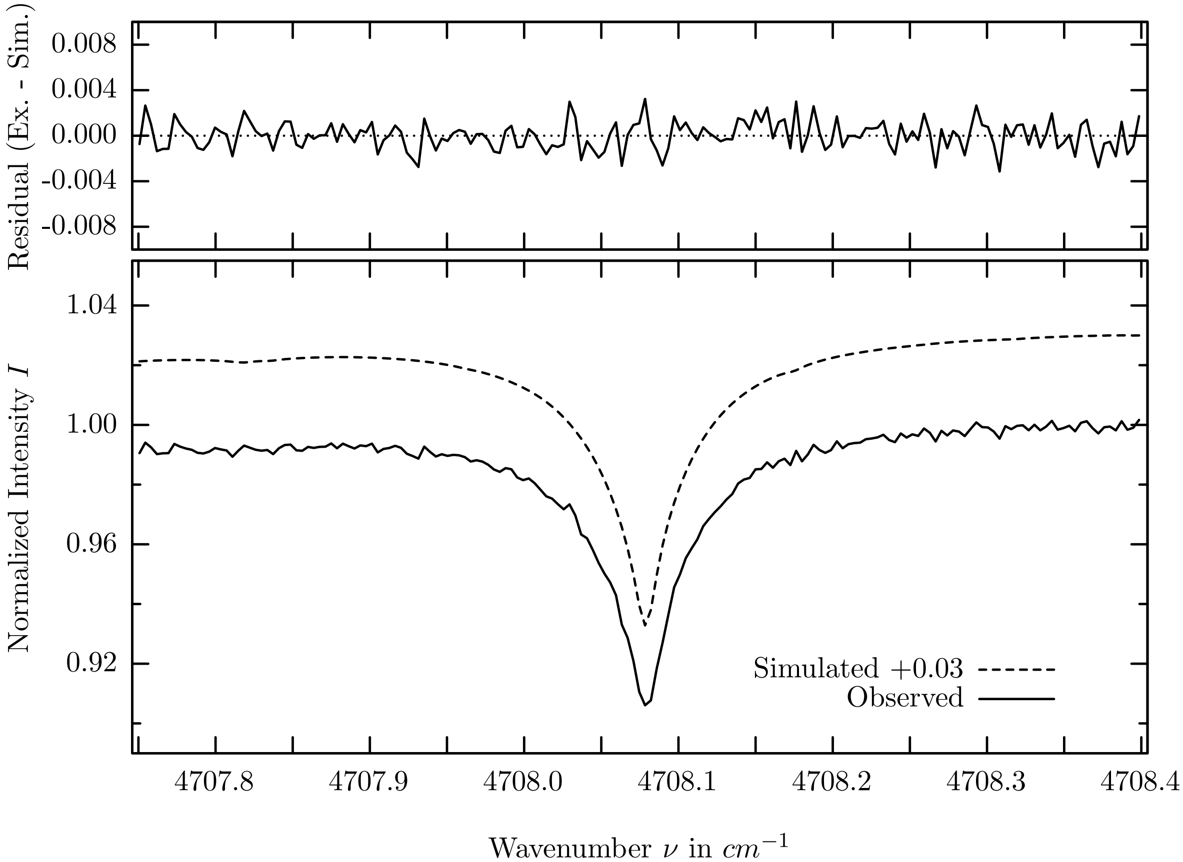

investigated species	:	N_2O
line position(s) ν_0	:	4708.0752 cm^{-1}
lower state energy E''_{lst}	:	231.2 cm^{-1}
retrieved TCA, information content	:	5.79E+18 $molec/cm^2$, 75.7
temperature dependence of the TCA	:	-0.205%/K (trop), -0.027%/K (strat)
location, date, solar zenith angle	:	Kiruna, 1/Apr/98, 70.96^o
spectral interval fitted	:	4707.750 – 4708.400 cm^{-1}

Molecule	iCode	Absorption	Molecule	iCode	Absorption
$H2O$	11	34.661%	$CH4$	61	0.077%
Solar(G)	—	31.948%	$O3$	31	<0.001%
Solar-sim	—	<0.001%	$NH3$	111	<0.001%
N2O	41	10.625%	OH	131	<0.001%
$CO2$	2**2**	0.981%	HBr	161	<0.001%
$CO2$	21	0.094%			

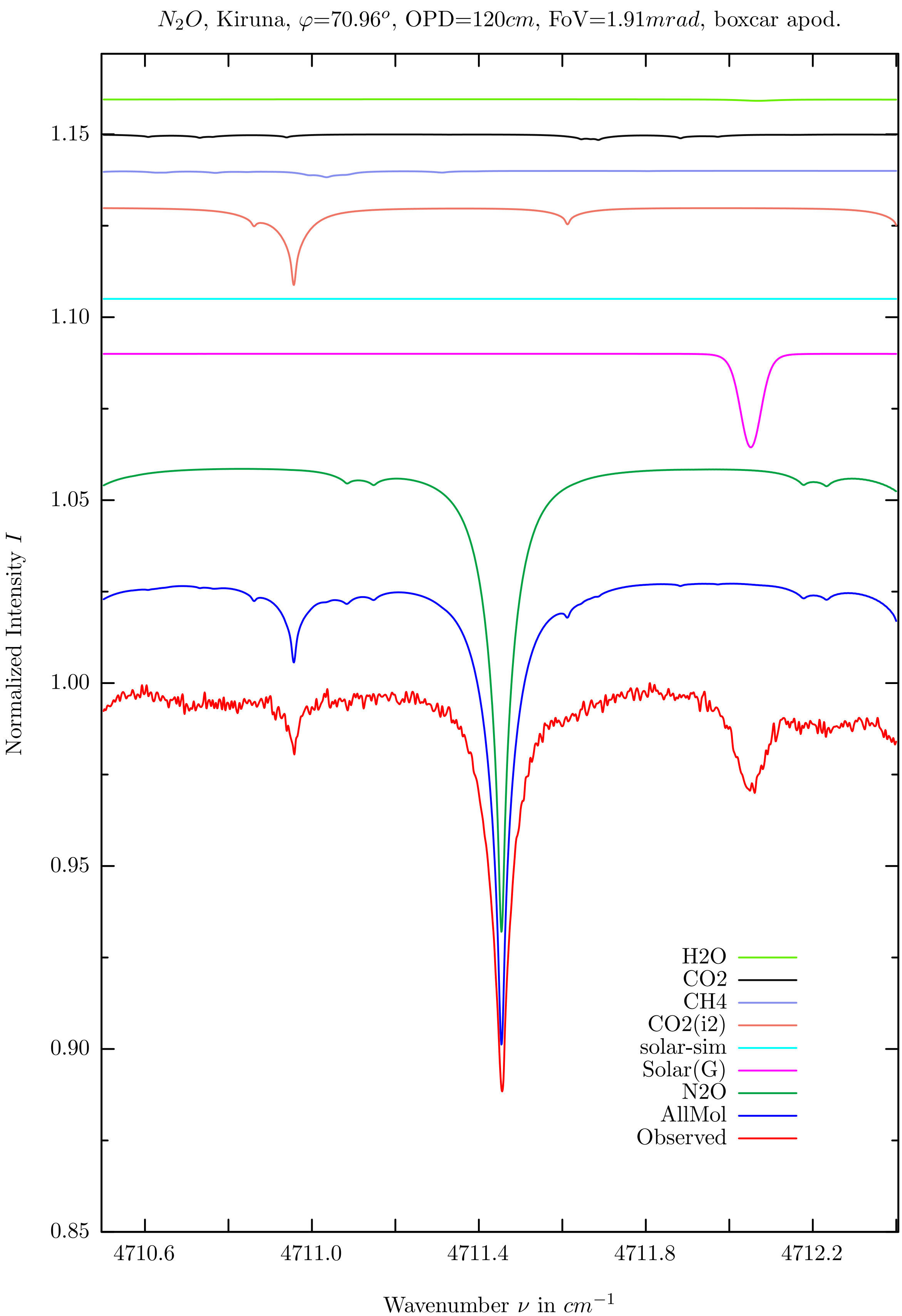

N_2O, Kiruna, φ=70.96^o, OPD=120cm, FoV=1.91$mrad$, boxcar apod.
Normalized Intensity I
1.15
1.10
1.05
1.00
0.95
0.90
0.85
4710.6
4711.0
4711.4
4711.8
4712.2
Wavenumber ν in cm^{-1}
H2O
CO2
CH4
CO2(i2)
solar-sim
Solar(G)
N2O
AllMol
Observed

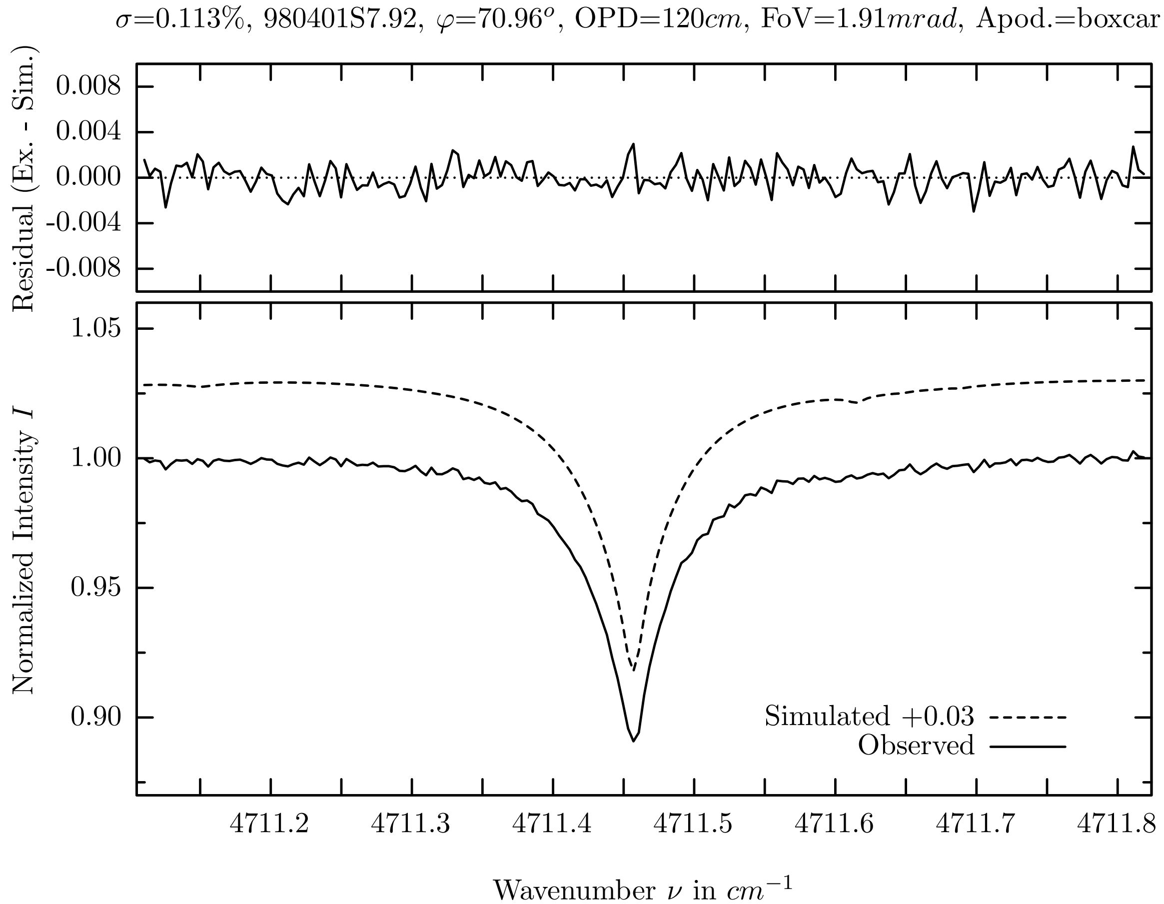

investigated species	:	N_2O
line position(s) ν_0	:	4711.4532 cm^{-1}
lower state energy E''_{lst}	:	176.0 cm^{-1}
retrieved TCA, information content	:	5.79E+18 $molec/cm^2$, 99.6
temperature dependence of the TCA	:	+0.036%/K (trop), -0.012%/K (strat)
location, date, solar zenith angle	:	Kiruna, 1/Apr/98, 70.96^o
spectral interval fitted	:	4711.110 – 4711.820 cm^{-1}

Molecule	iCode	Absorption	Molecule	iCode	Absorption
N2O	41	12.837%	$CO2$	21	0.128%
Solar(G)	—	2.556%	$H2O$	11	0.086%
Solar-sim	—	<0.001%	$NH3$	111	<0.001%
$CO2$	2**2**	2.133%	OH	131	<0.001%
$CH4$	61	0.174%	HBr	161	<0.001%

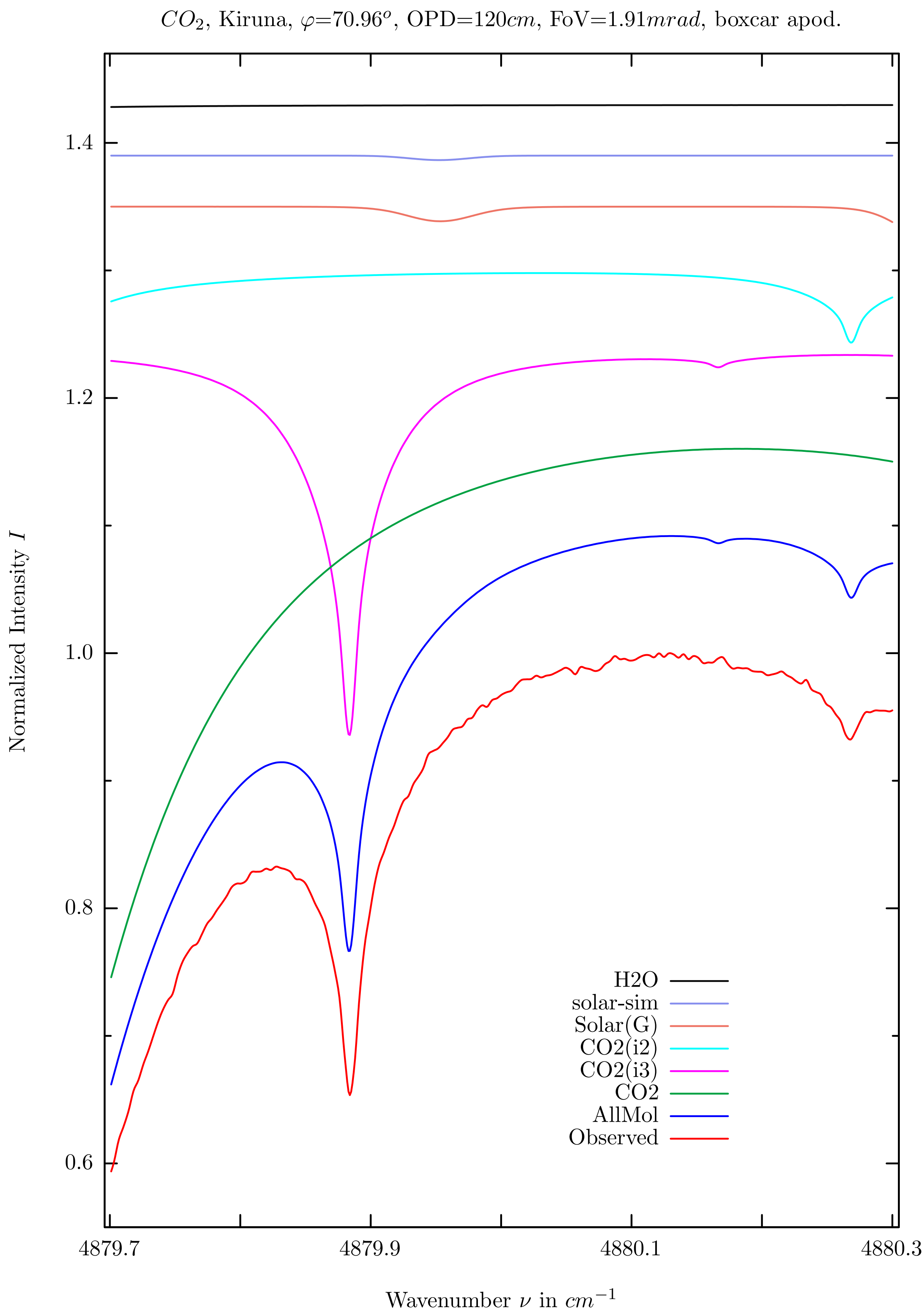
CO_2, Kiruna, φ=70.96^o, OPD=120cm, FoV=1.91$mrad$, boxcar apod.
Normalized Intensity I
Wavenumber ν in cm^{-1}
1.4
1.2
1.0
0.8
0.6
4879.7
4879.9
4880.1
4880.3
H2O
solar-sim
Solar(G)
CO2(i2)
CO2(i3)
CO2
AllMol
Observed

σ=0.216%, 980401S7.92, φ=70.96^o, OPD=120cm, FoV=1.91$mrad$, Apod.=boxcar

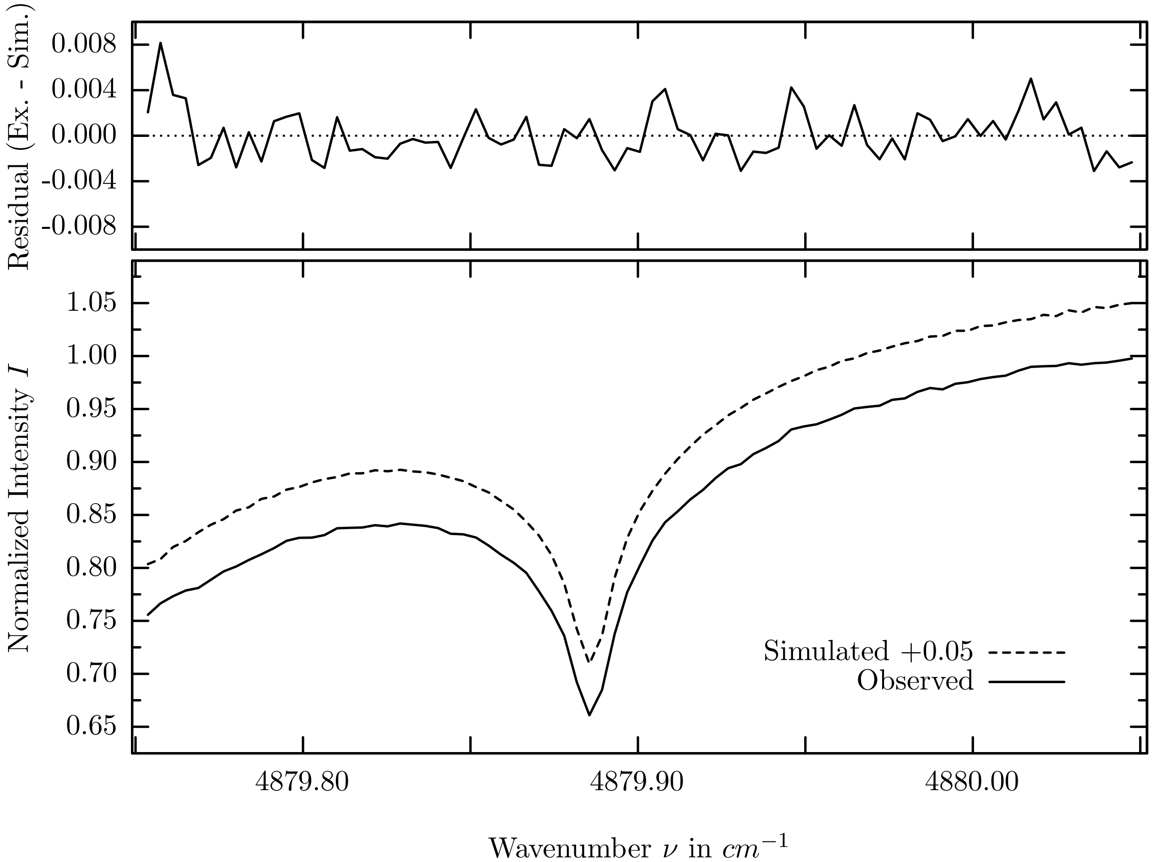

investigated species	:	$CO_2(i3)$
line position(s) ν_0	:	4879.8823 cm^{-1}
lower state energy E''_{lst}	:	342.3 cm^{-1}
retrieved TCA, information content	:	7.49E+21 $molec/cm^2$, 114.6
temperature dependence of the TCA	:	-0.576%/K (trop), -0.207%/K (strat)
location, date, solar zenith angle	:	Kiruna, 1/Apr/98, 70.96^o
spectral interval fitted	:	4879.750 – 4880.050 cm^{-1}

Molecule	iCode	Absorption	Molecule	iCode	Absorption
$CO2$	21	52.102%	$N2O$	41	0.045%
CO2	**23**	30.585%	HDO	491	0.042%
$CO2$	2**2**	6.691%	$CH4$	61	<0.001%
Solar(G)	—	2.695%	$NH3$	111	<0.001%
Solar-sim	—	0.349%	OH	131	<0.001%
$H2O$	11	0.187%			

CO_2, Kiruna, φ=70.96^o, OPD=120cm, FoV=1.91$mrad$, boxcar apod.

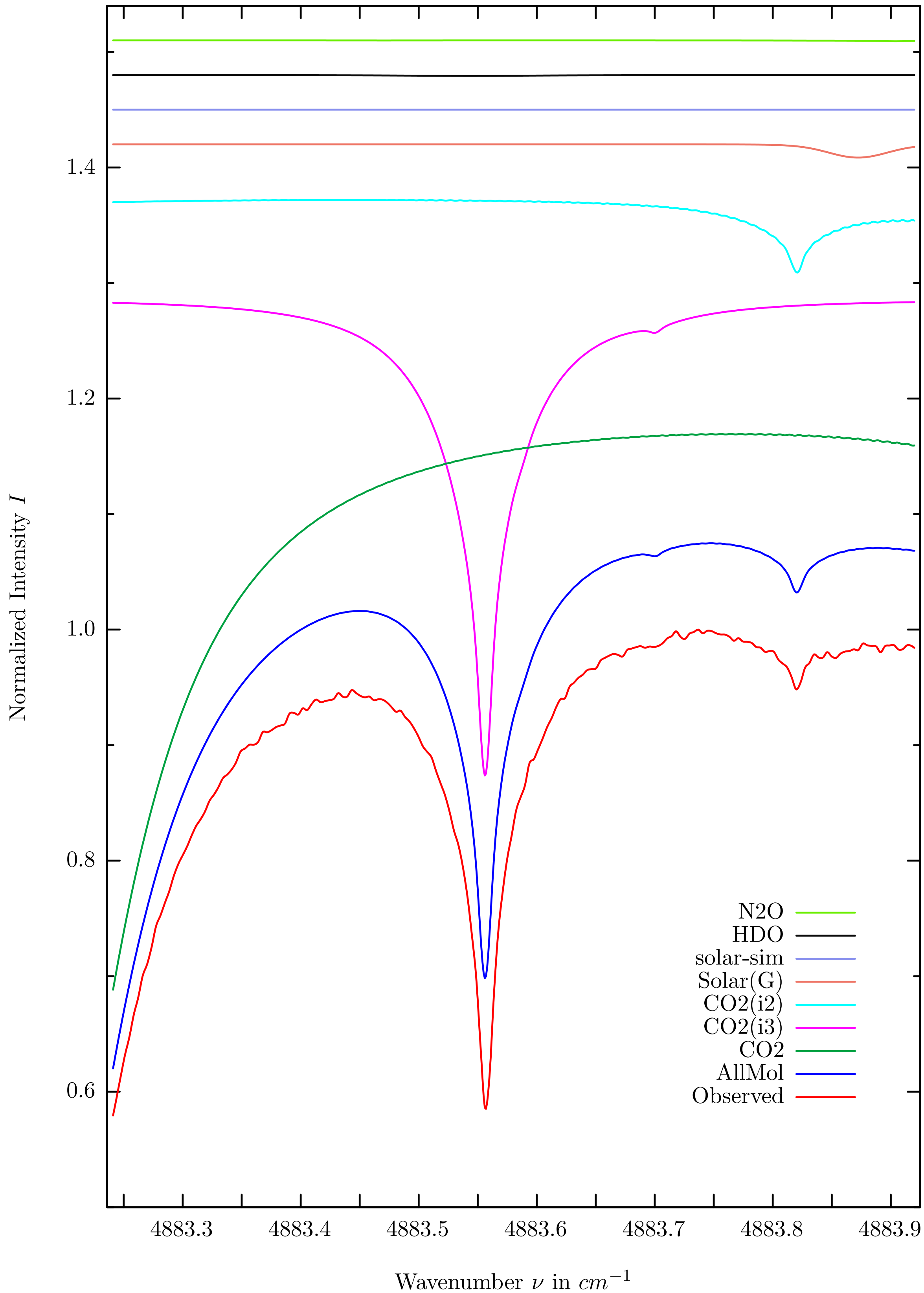

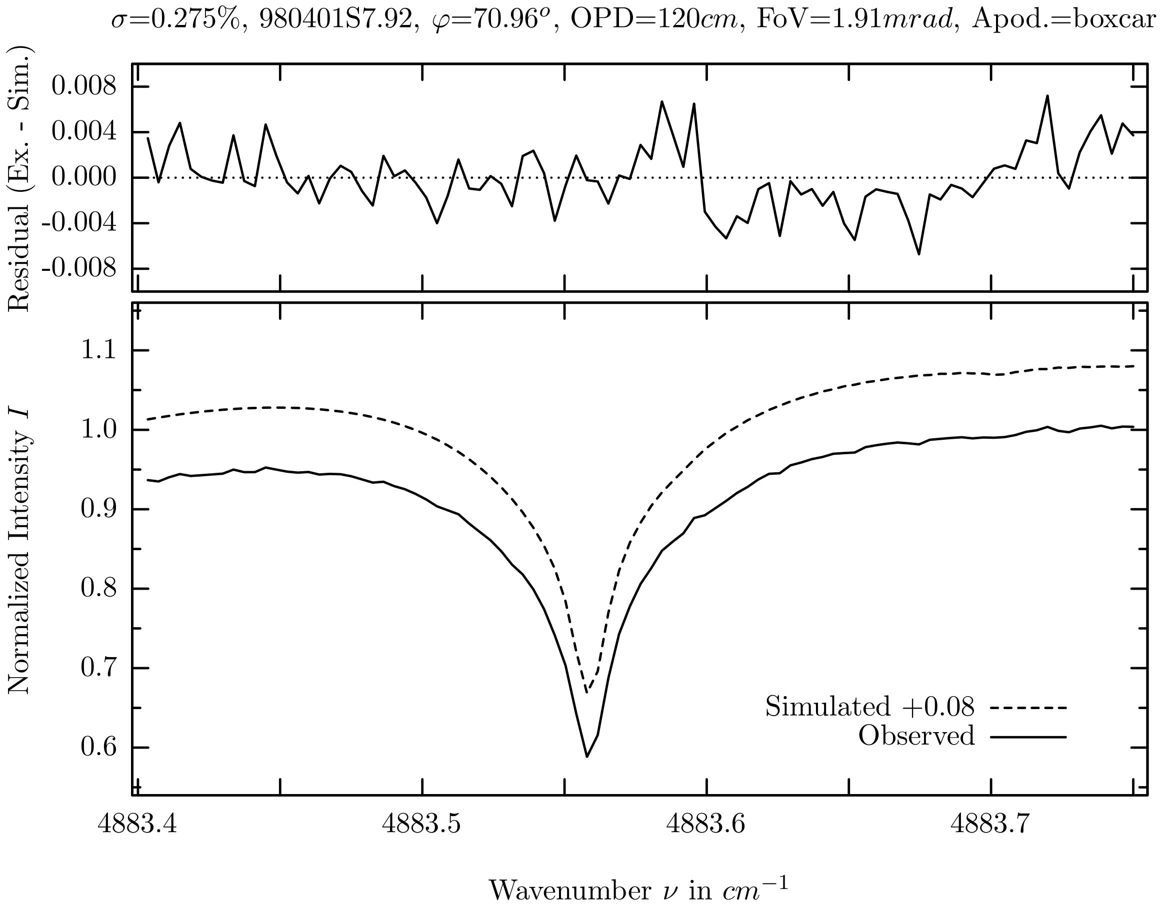

investigated species	:	$CO_2(i3)$
line position(s) ν_0	:	4883.5550 cm^{-1}
lower state energy E''_{lst}	:	258.4 cm^{-1}
retrieved TCA, information content	:	7.80E+21 $molec/cm^2$, 146.4
temperature dependence of the TCA	:	-0.339%/K (trop), -0.070%/K (strat)
location, date, solar zenith angle	:	Kiruna, 1/Apr/98, 70.96^o
spectral interval fitted	:	4883.400 – 4883.750 cm^{-1}

Molecule	iCode	Absorption	Molecule	iCode	Absorption
$CO2$	21	52.595%	$N2O$	41	0.069%
CO2	**23**	41.790%	$H2O$	11	0.013%
$CO2$	**22**	18.901%	$CH4$	61	<0.001%
Solar(G)	—	1.144%	$NH3$	111	<0.001%
Solar-sim	—	<0.001%	OH	131	<0.001%
HDO	491	0.077%	HBr	161	<0.001%

CO_2, Kiruna, φ=70.96^o, OPD=120cm, FoV=1.91$mrad$, boxcar apod.

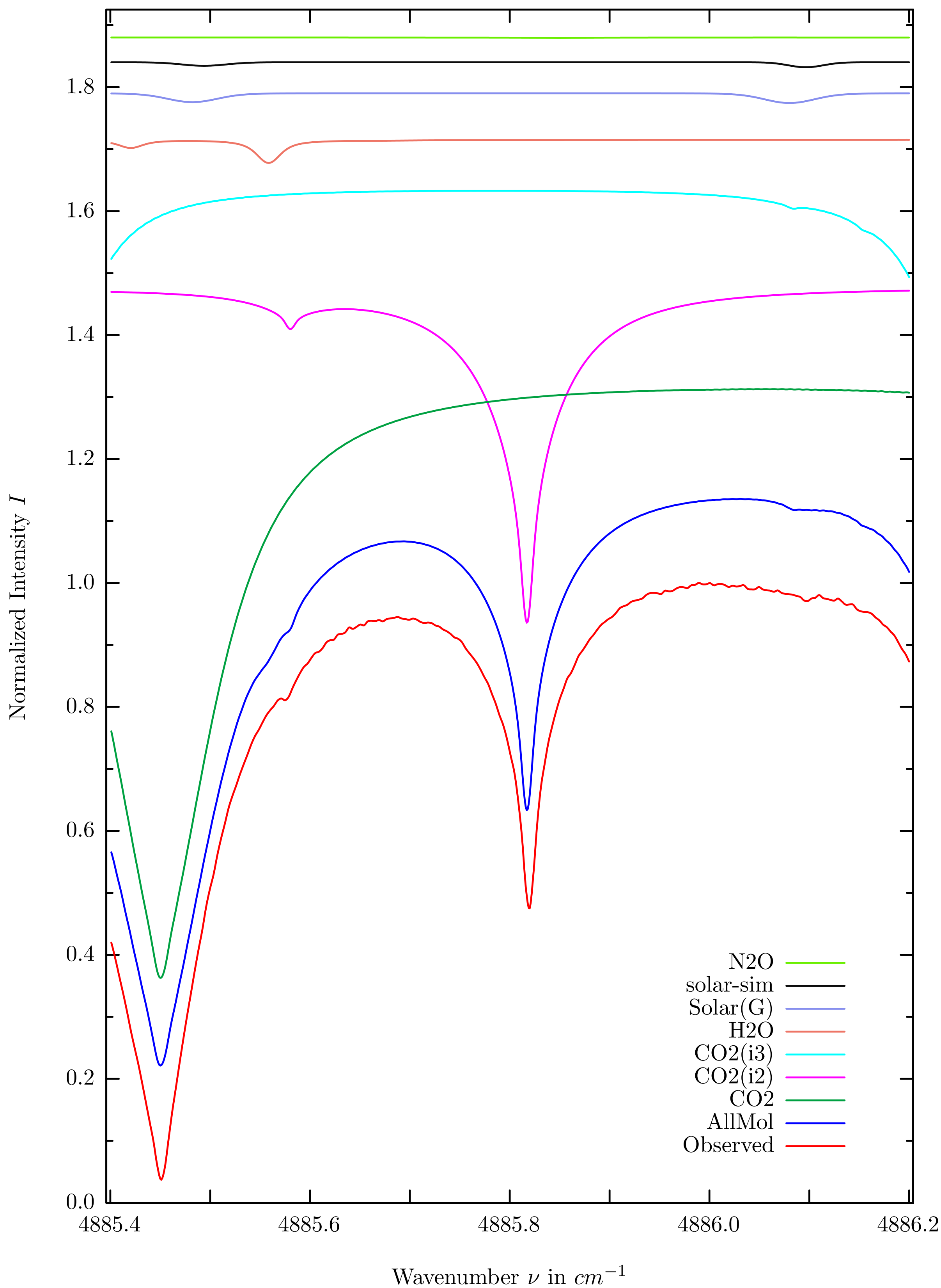

σ=0.209%, 980401S7.92, φ=70.96^o, OPD=120cm, FoV=1.91$mrad$, Apod.=boxcar

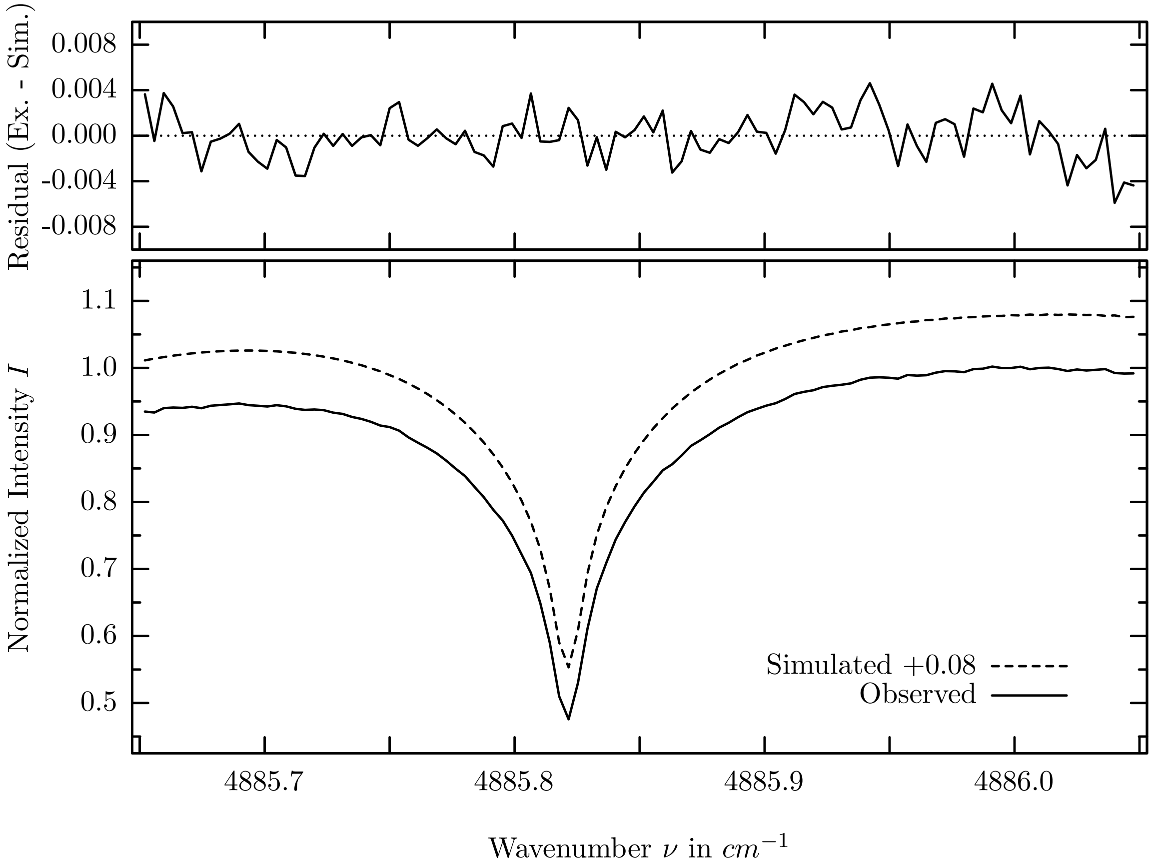

investigated species	:	$CO_2(i2)$
line position(s) ν_0	:	4885.8159 cm^{-1}
lower state energy E''_{lst}	:	2.3 cm^{-1}
retrieved TCA, information content	:	7.45E+21 $molec/cm^2$, 248.7
temperature dependence of the TCA	:	+0.096%/K (trop), +0.272%/K (strat)
location, date, solar zenith angle	:	Kiruna, 1/Apr/98, 70.96^o
spectral interval fitted	:	4885.650 – 4886.050 cm^{-1}

Molecule	iCode	Absorption	Molecule	iCode	Absorption
$CO2$	21	97.730%	$N2O$	41	0.086%
CO2	2**2**	54.593%	HDO	491	0.001%
$CO2$	2**3**	11.097%	$CH4$	61	<0.001%
$H2O$	11	3.733%	$NH3$	111	<0.001%
Solar(G)	—	1.569%	OH	131	<0.001%
Solar-sim	—	0.806%	HBr	161	<0.001%

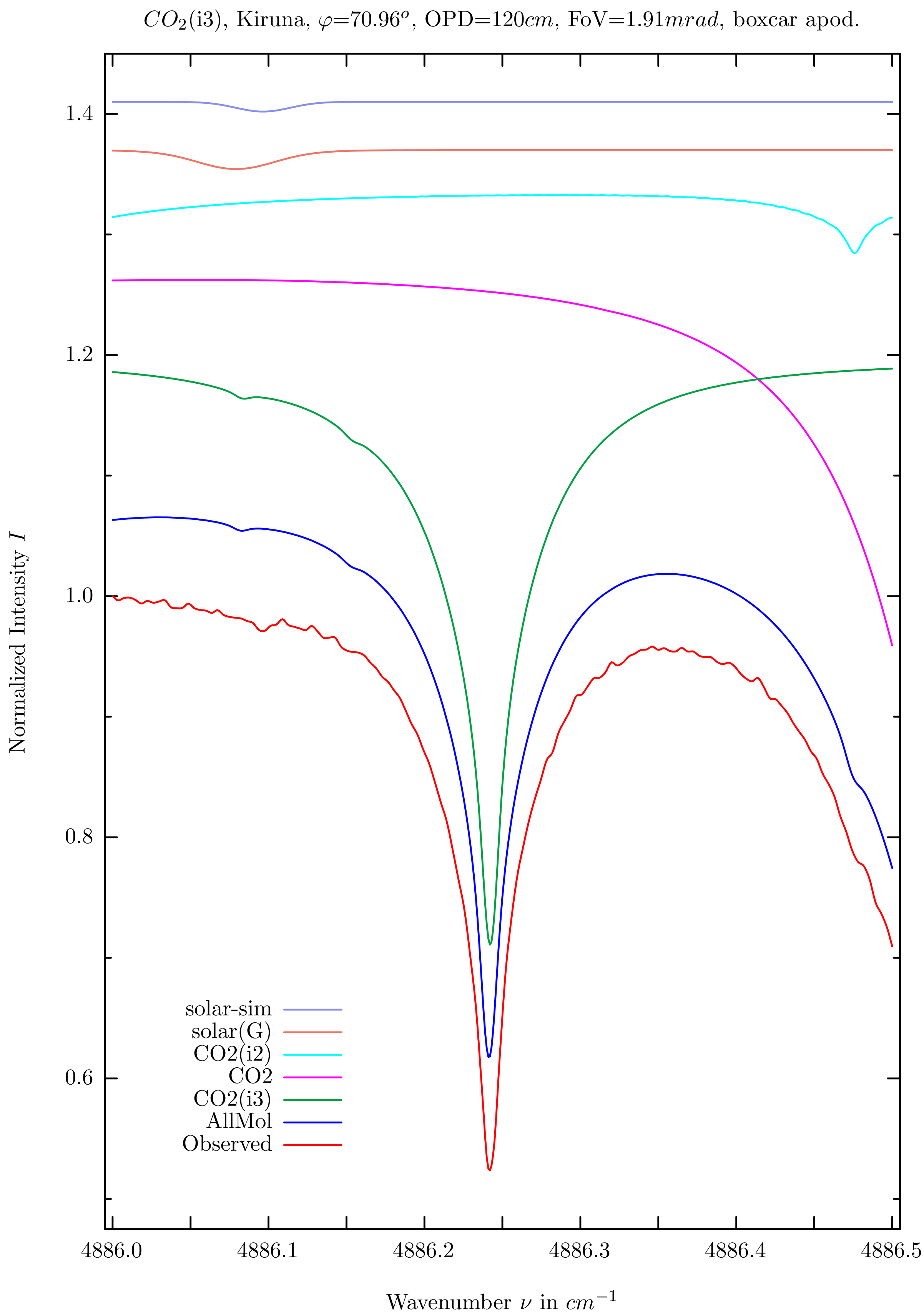
CO_2(i3), Kiruna, φ=70.96^o, OPD=120cm, FoV=1.91$mrad$, boxcar apod.
1.4
1.2
1.0
0.8
0.6
Normalized Intensity I
solar-sim
solar(G)
CO2(i2)
CO2
CO2(i3)
AllMol
Observed
4886.0
4886.1
4886.2
4886.3
4886.4
4886.5
Wavenumber ν in cm^{-1}

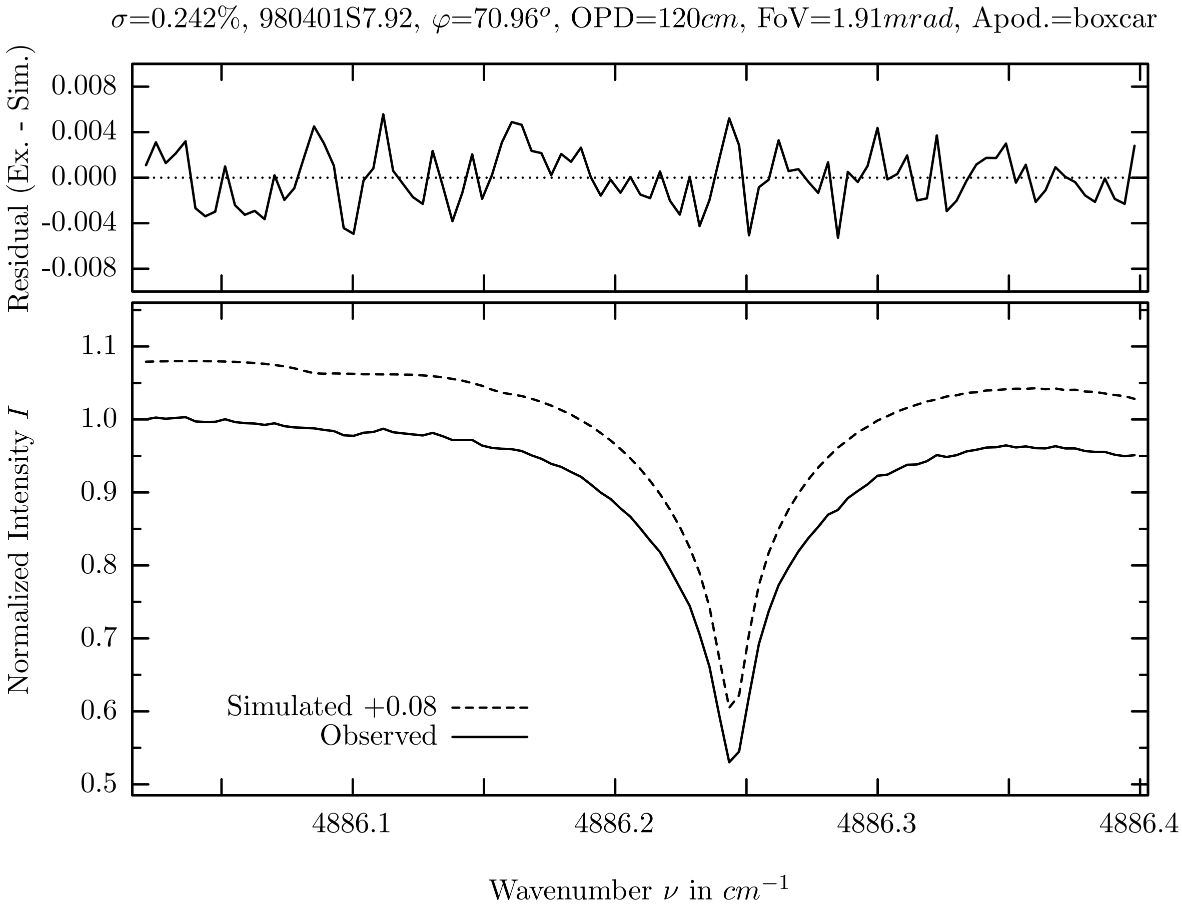

investigated species	:	$CO_2(i3)$
line position(s) ν_0	:	4886.2409 cm^{-1}
lower state energy E''_{lst}	:	203.2 cm^{-1}
retrieved TCA, information content	:	7.68E+21 $molec/cm^2$, 196.0
temperature dependence of the TCA	:	-0.236%/K (trop), +0.004%/K (strat)
location, date, solar zenith angle	:	Kiruna, 1/Apr/98, 70.96^o
spectral interval fitted	:	4886.020 – 4886.400 cm^{-1}

Molecule	iCode	Absorption	Molecule	iCode	Absorption
CO2	2**3**	49.077%	HDO	491	0.001%
$CO2$	21	33.611%	$CH4$	61	<0.001%
$CO2$	2**2**	4.855%	$NH3$	111	<0.001%
Solar(G)	—	1.569%	OH	131	<0.001%
Solar-sim	—	0.806%	HBr	161	<0.001%
$H2O$	11	0.028%			

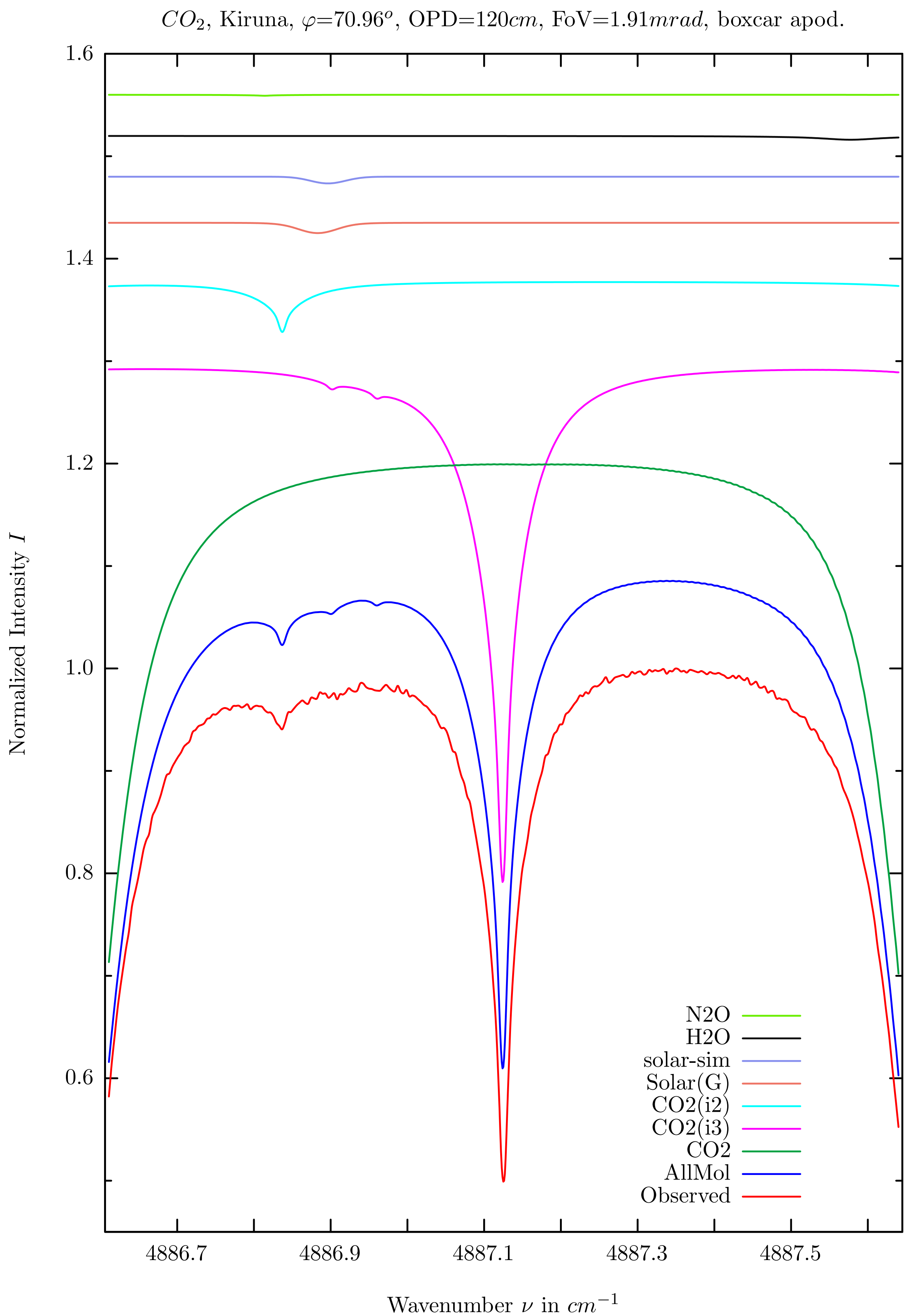

CO_2, Kiruna, φ=70.96^o, OPD=120cm, FoV=1.91$mrad$, boxcar apod.
1.6
1.4
1.2
1.0
0.8
0.6
Normalized Intensity I
4886.7
4886.9
4887.1
4887.3
4887.5
Wavenumber ν in cm^{-1}
N2O
H2O
solar-sim
Solar(G)
CO2(i2)
CO2(i3)
CO2
AllMol
Observed

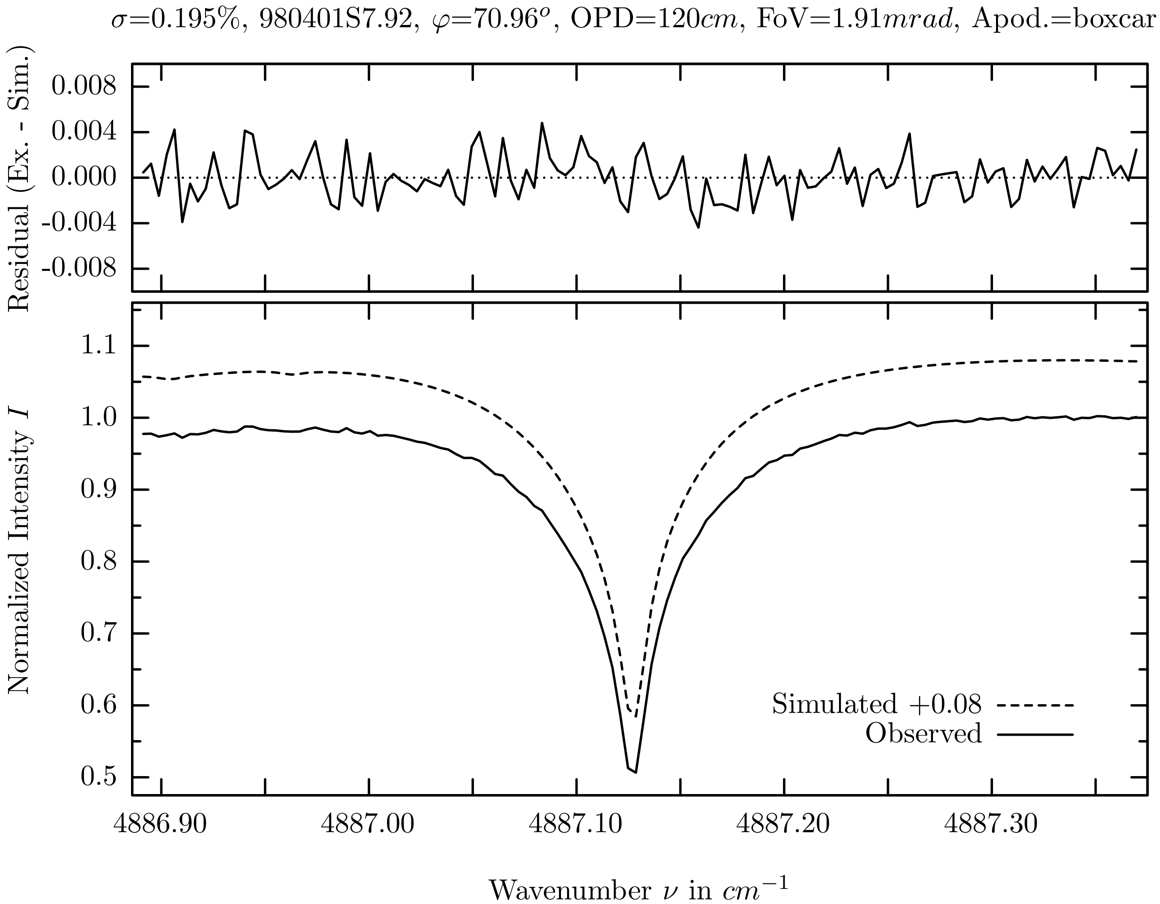

investigated species	:	$CO_2(i3)$
line position(s) ν_0	:	4887.1232 cm^{-1}
lower state energy E''_{lst}	:	186.3 cm^{-1}
retrieved TCA, information content	:	7.85E+21 $molec/cm^2$, 254.0
temperature dependence of the TCA	:	+0.060%/K (trop), -0.012%/K (strat)
location, date, solar zenith angle	:	Kiruna, 1/Apr/98, 70.96^o
spectral interval fitted	:	4886.890 – 4887.370 cm^{-1}

Molecule	iCode	Absorption	Molecule	iCode	Absorption
$CO2$	21	53.393%	$N2O$	41	0.096%
CO2	**23**	51.040%	HDO	491	0.003%
$CO2$	**22**	5.184%	$CH4$	61	<0.001%
Solar(G)	—	1.002%	$NH3$	111	<0.001%
Solar-sim	—	0.654%	OH	131	<0.001%
$H2O$	11	0.389%	HBr	161	<0.001%

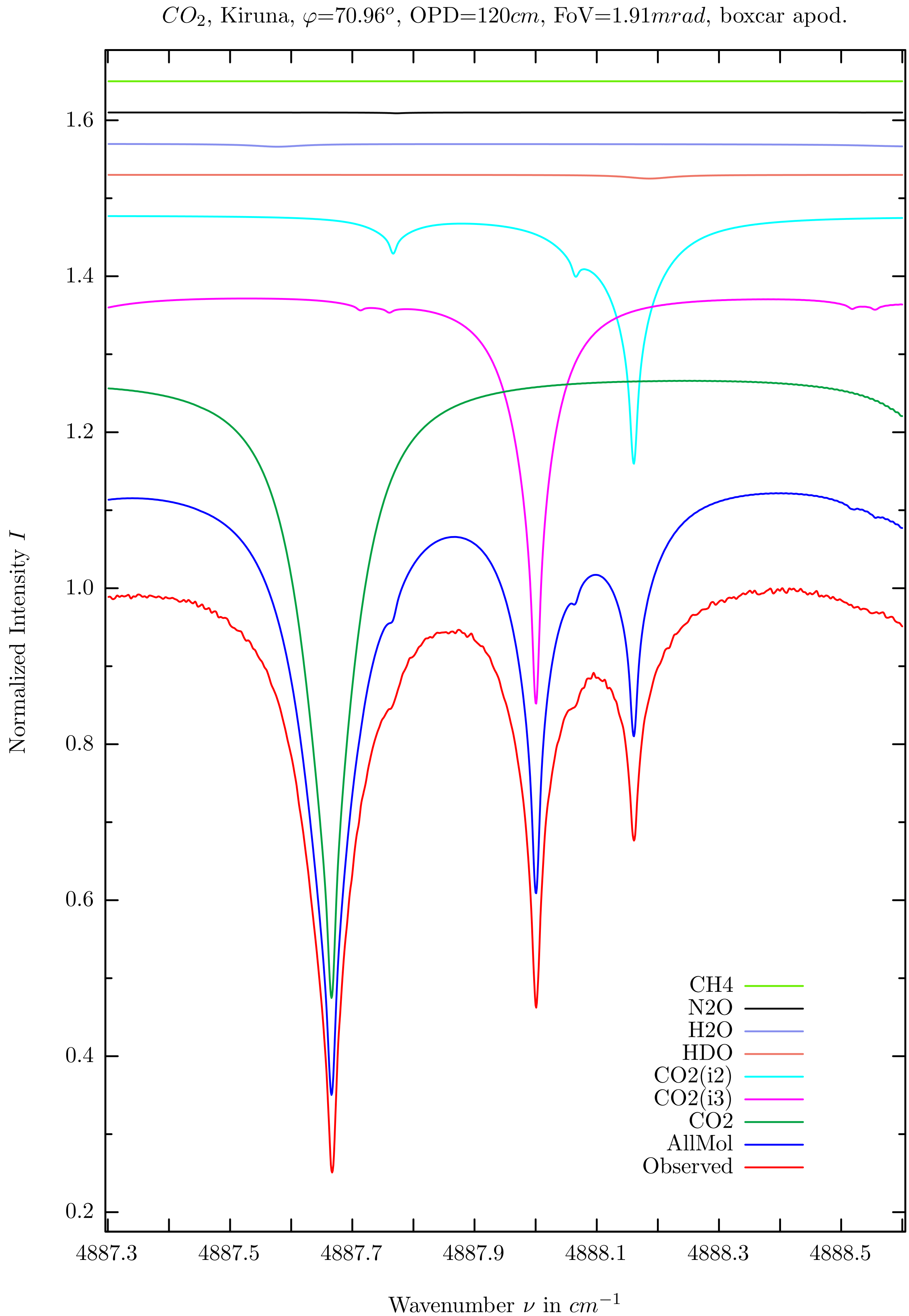

CO_2, Kiruna, φ=70.96^o, OPD=120cm, FoV=1.91$mrad$, boxcar apod.
Normalized Intensity I
Wavenumber ν in cm^{-1}
1.6
1.4
1.2
1.0
0.8
0.6
0.4
0.2
4887.3
4887.5
4887.7
4887.9
4888.1
4888.3
4888.5
CH4
N2O
H2O
HDO
CO2(i2)
CO2(i3)
CO2
AllMol
Observed

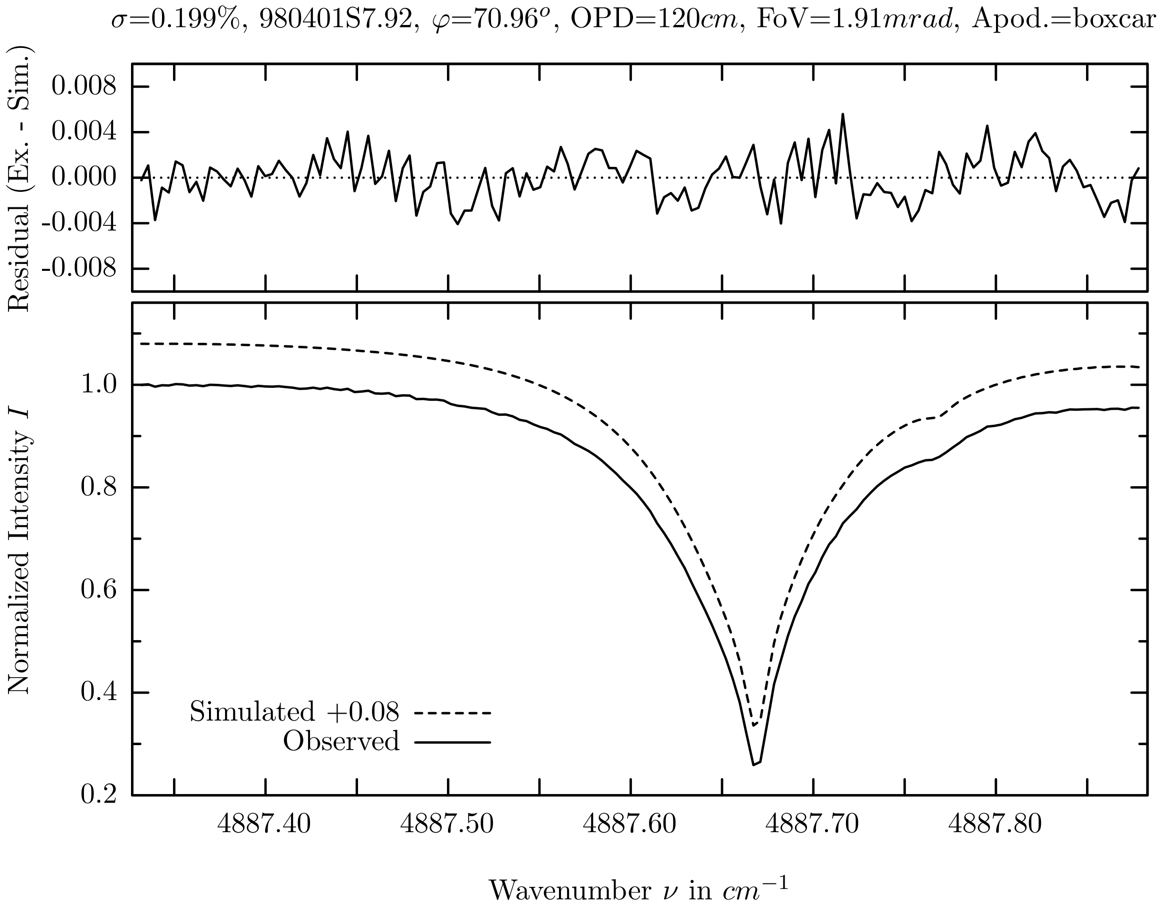

investigated species	:	CO_2
line position(s) ν_0	:	4887.6649 cm^{-1}
lower state energy E''_{lst}	:	994.2 cm^{-1}
retrieved TCA, information content	:	6.49E+21 $molec/cm^2$, 373.5
temperature dependence of the TCA	:	-1.853%/K (trop), -0.491%/K (strat)
location, date, solar zenith angle	:	Kiruna, 1/Apr/98, 70.96^o
spectral interval fitted	:	4887.330 – 4887.880 cm^{-1}

Molecule	iCode	Absorption	Molecule	iCode	Absorption
CO2	21	80.644%	$CH4$	61	<0.001%
$CO2$	2**3**	53.033%	$NH3$	111	<0.001%
$CO2$	2**2**	32.183%	OH	131	<0.001%
HDO	491	0.477%	HBr	161	<0.001%
$H2O$	11	0.389%	Solar(G)	—	<0.001%
$N2O$	41	0.106%	Solar-sim	—	<0.001%

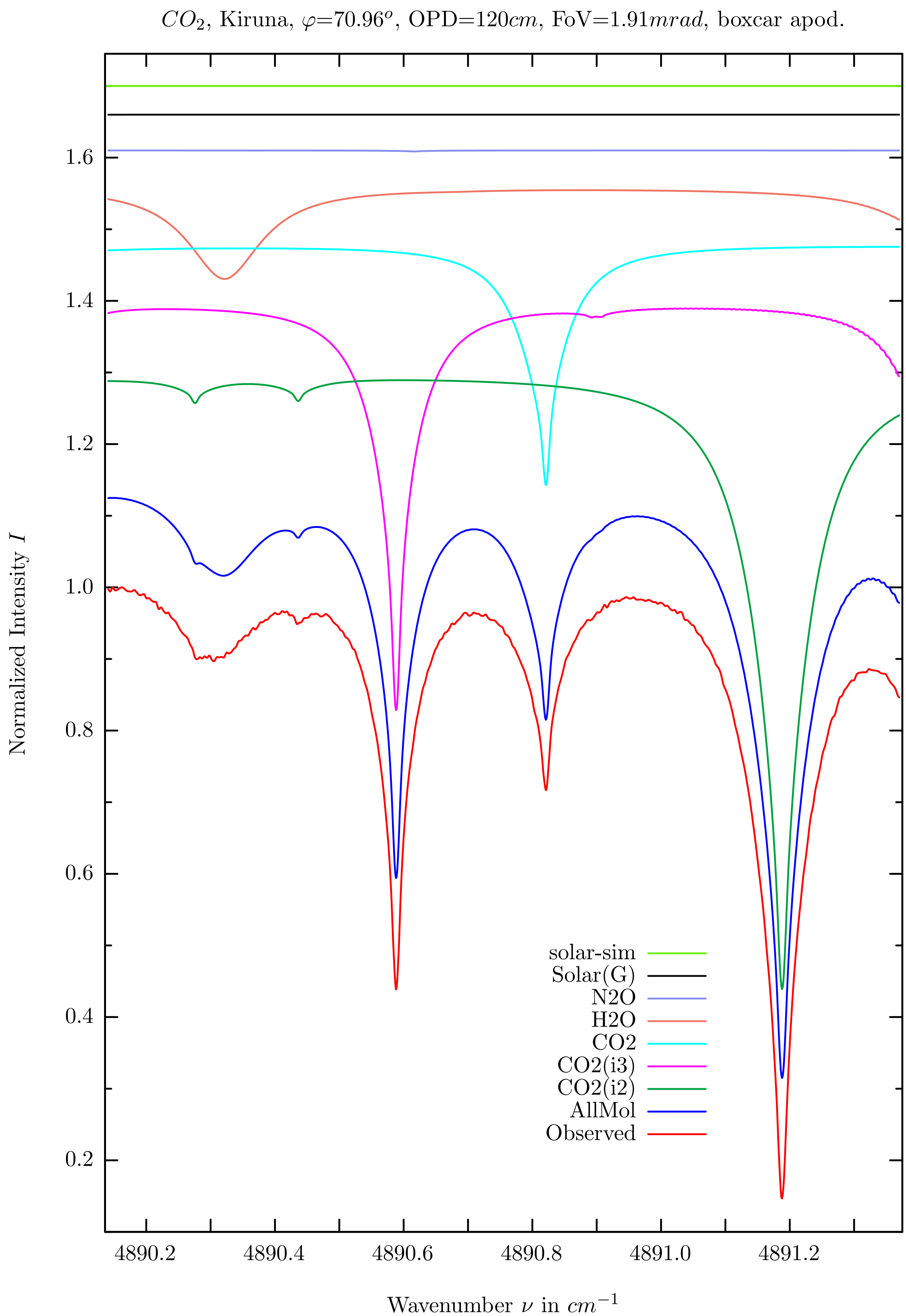

CO_2, Kiruna, φ=70.96^o, OPD=120cm, FoV=1.91$mrad$, boxcar apod.
Normalized Intensity I
Wavenumber ν in cm^{-1}
0.2
0.4
0.6
0.8
1.0
1.2
1.4
1.6
4890.2
4890.4
4890.6
4890.8
4891.0
4891.2
solar-sim
Solar(G)
N2O
H2O
CO2
CO2(i3)
CO2(i2)
AllMol
Observed

σ=0.232%, 980401S7.92, φ=70.96^o, OPD=120cm, FoV=1.91$mrad$, Apod.=boxcar

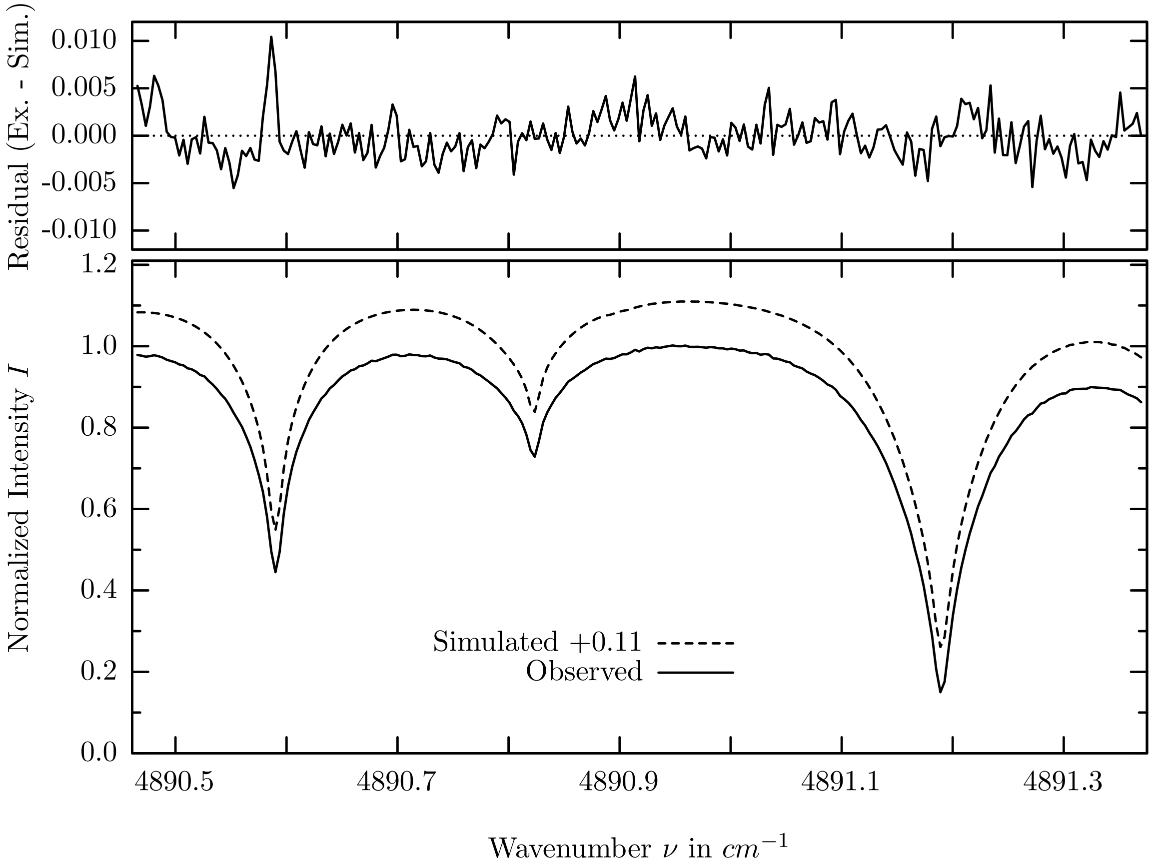

investigated species	:	$CO_2(i3)$, $(CO_2(i2))$
line position(s) ν_0	:	4890.5864, (4891.1846) cm^{-1}
lower state energy E''_{lst}	:	125.9, (7.8) cm^{-1}
retrieved TCA, information content	:	7.07E+21, (7.38E+21) $molec/cm^2$, 242.0, (365.5)
temperature dependence of the TCA	:	+.001, (+.176)%/K (trop), +.157, (+.140)%/K (strat)
investigated species, position	:	CO_2, 4890.8190cm^{-1}
lower state energy E''_{lst}	:	1244.2 cm^{-1}
retrieved TCA, information content	:	6.12e21 $molec/cm^2$, 116.8
temperature dependence of the TCA	:	-2.240%/K (trop), -0.545%/K (strat)
location, date, solar zenith angle	:	Kiruna, 1/Apr/98, 70.96^o
spectral interval fitted	:	4890.462 – 4891.370 cm^{-1}

Molecule	iCode	Absorption	Molecule	iCode	Absorption
CO2	**22**	86.196%	Solar-sim	—	<0.001%
CO2	**23**	57.370%	*HDO*	491	0.001%
CO2	21	33.780%	*CH4*	61	<0.001%
H2O	11	12.947%	*NH3*	111	<0.001%
N2O	41	0.139%	*OH*	131	<0.001%
Solar(G)	—	0.008%	*HBr*	161	<0.001%

CO_2, Kiruna, φ=70.96^o, OPD=120cm, FoV=1.91$mrad$, boxcar apod.

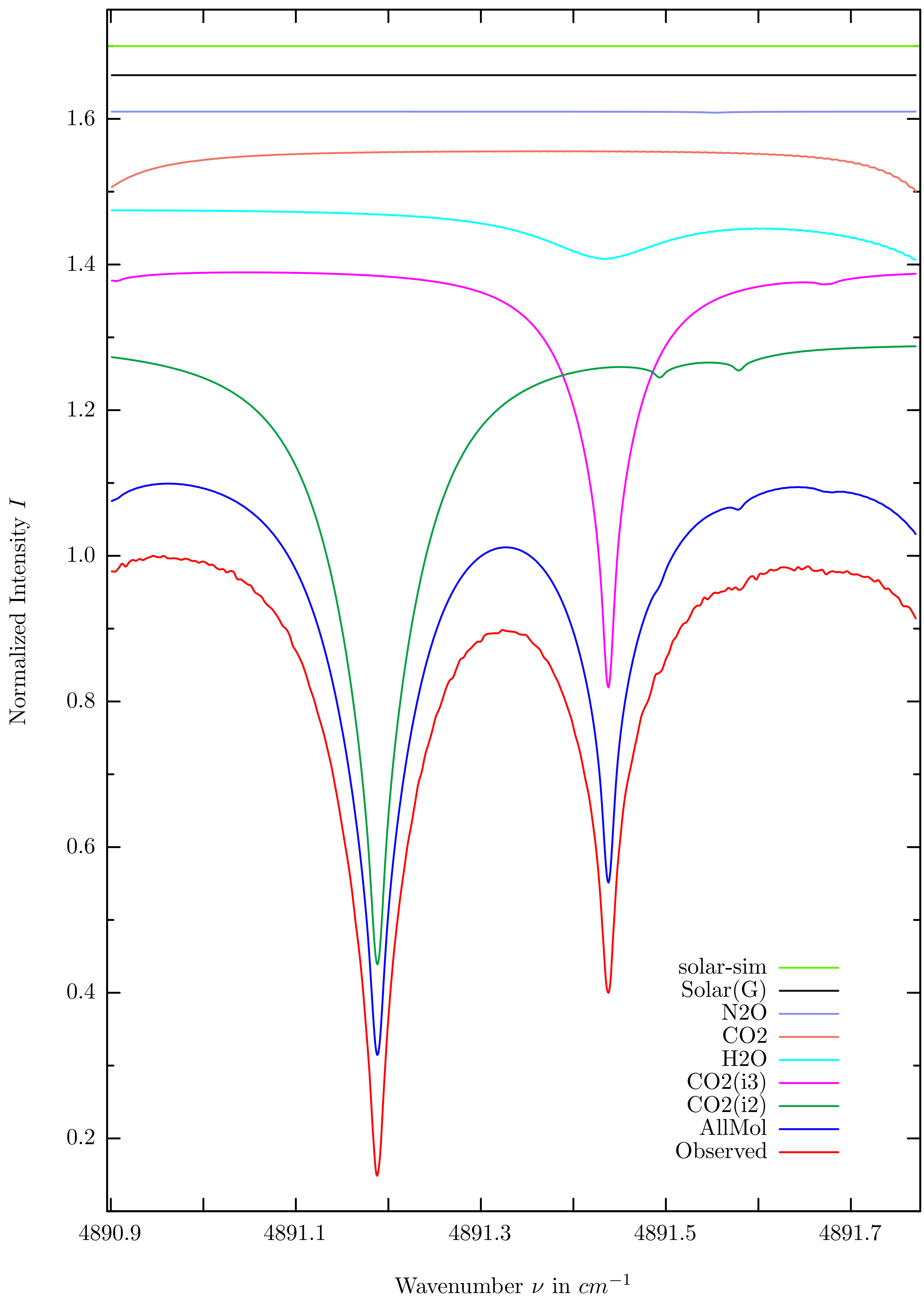

σ=0.212%, 980401S7.92, φ=70.96^o, OPD=120cm, FoV=1.91$mrad$, Apod.=boxcar

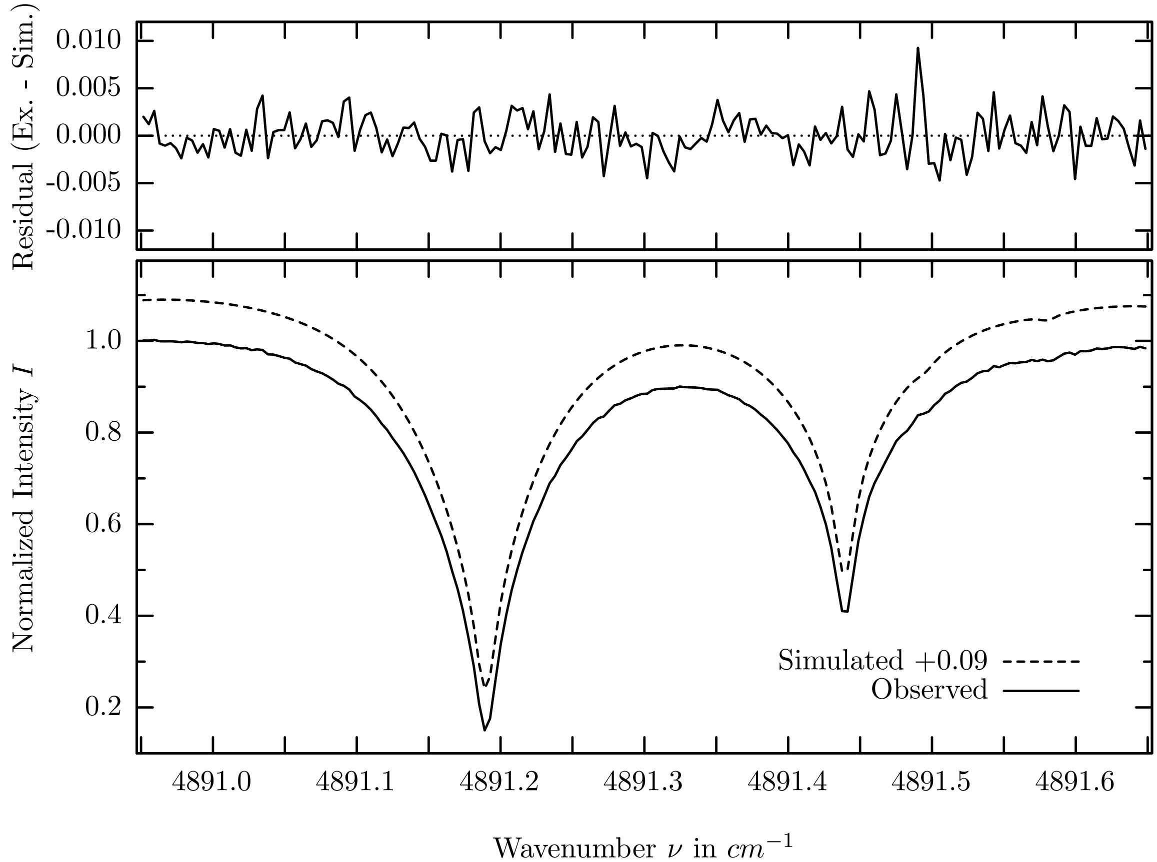

investigated species	:	$CO_2(i2), (CO_2(i3))$
line position(s) ν_0	:	4891.1846, (4891.4358) cm^{-1}
lower state energy E''_{lst}	:	7.8, (112.7) cm^{-1}
retrieved TCA, information content	:	7.50E+21, (6.76E+21) $molec/cm^2$, 399.9, (279.1)
temperature dependence of the TCA	:	+.547 (-1.14)%/K (trop), +.113 (-.466)%/K (strat)
location, date, solar zenith angle	:	Kiruna, 1/Apr/98, 70.96^o
spectral interval fitted	:	4890.950 – 4891.650 cm^{-1}

Molecule	iCode	Absorption	Molecule	iCode	Absorption
CO2	**22**	86.196%	Solar-sim	—	<0.001%
CO2	**23**	58.254%	HDO	491	0.001%
$H2O$	11	7.502%	$CH4$	61	<0.001%
$CO2$	21	6.149%	$NH3$	111	<0.001%
$N2O$	41	0.147%	OH	131	<0.001%
Solar(G)	—	0.001%	HBr	161	<0.001%

Comment: This is not a good retrieval window for CO_2(i3) because of the interference from water vapour. It is not so bad for CO_2(i2) though.

CO_2, Kiruna, φ=70.96^o, OPD=120cm, FoV=1.91$mrad$, boxcar apod.

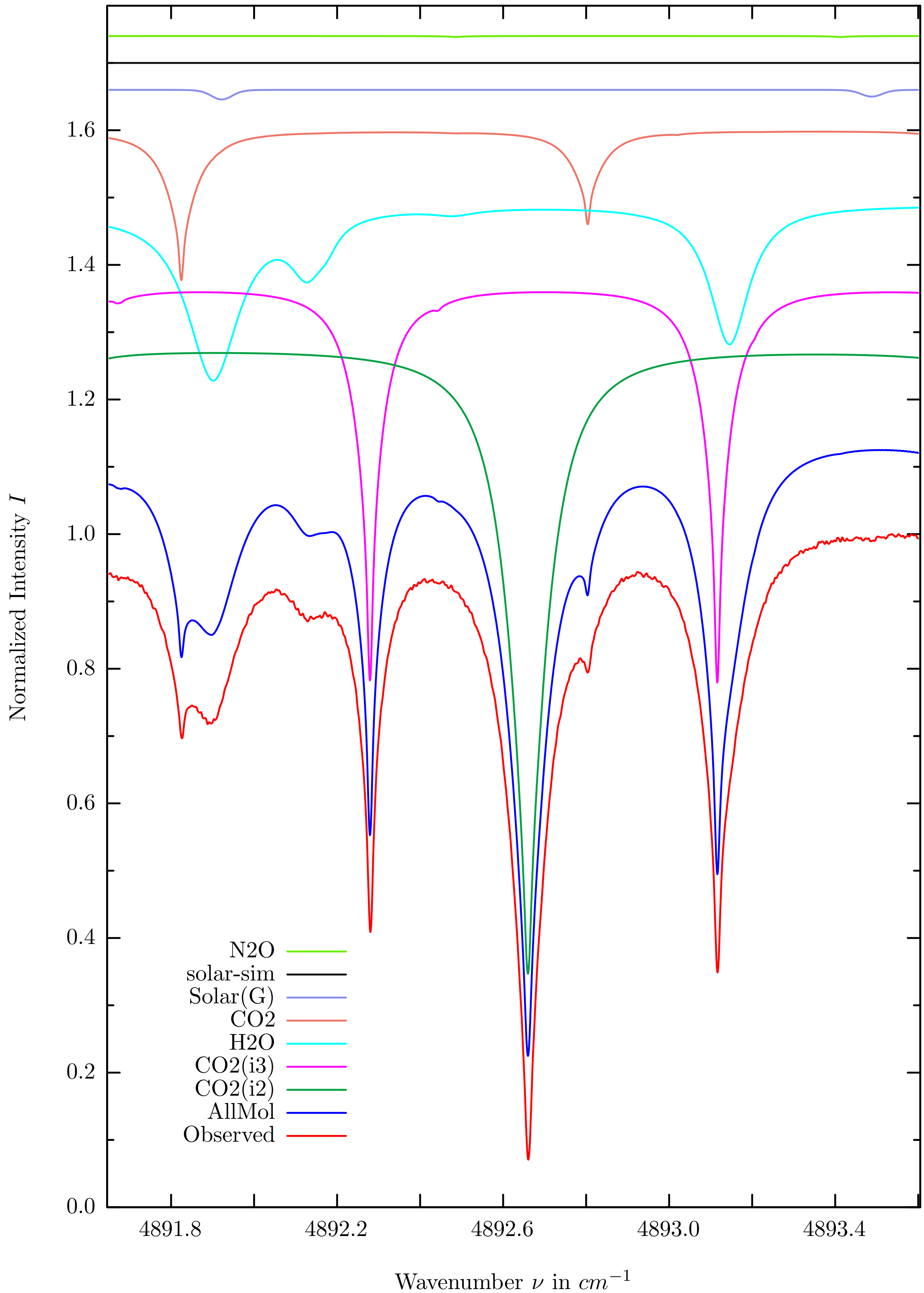

σ=0.296%, 980401S7.92, φ=70.96^o, OPD=120cm, FoV=1.91$mrad$, Apod.=boxcar

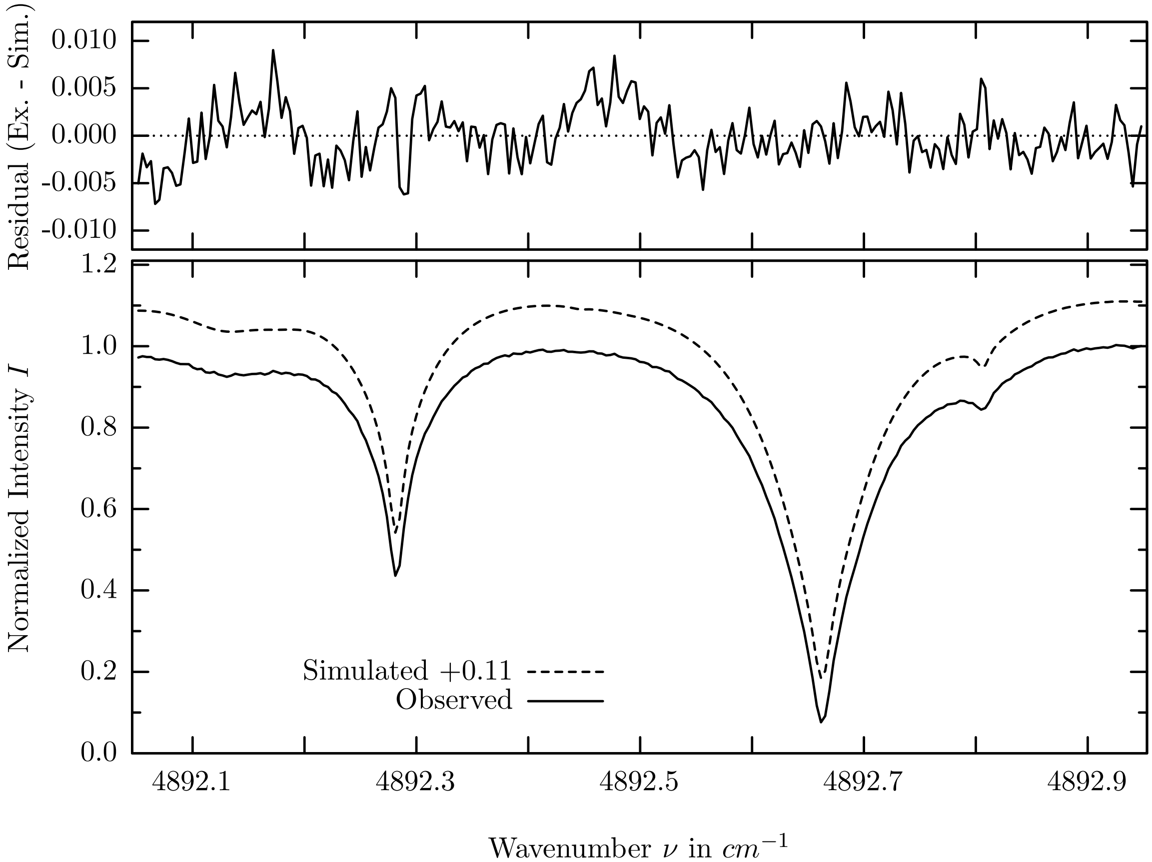

investigated species	:	$CO_2(i2), (CO_2(i3))$
line position(s) ν_0	:	4892.6575, (4892.2786) cm^{-1}
lower state energy E''_{lst}	:	16.4, (100.1) cm^{-1}
retrieved TCA, information content	:	7.47E+21, (7.32E+21) $molec/cm^2$, 312.6, (192.0)
temperature dependence of the TCA	:	+.270 (+.183)%/K (trop), +.088 (+.050)%/K (strat)
location, date, solar zenith angle	:	Kiruna, 1/Apr/98, 70.96^o
spectral interval fitted	:	4892.050 – 4892.950 cm^{-1}

Molecule	iCode	Absorption	Molecule	iCode	Absorption
CO2	2**2**	93.373%	*N2O*	41	0.165%
CO2	2**3**	59.225%	*HDO*	491	0.001%
H2O	11	26.219%	*CH4*	61	<0.001%
CO2	21	22.337%	*NH3*	111	<0.001%
Solar(G)	—	1.429%	*OH*	131	<0.001%
Solar-sim	—	<0.001%	*HBr*	161	<0.001%

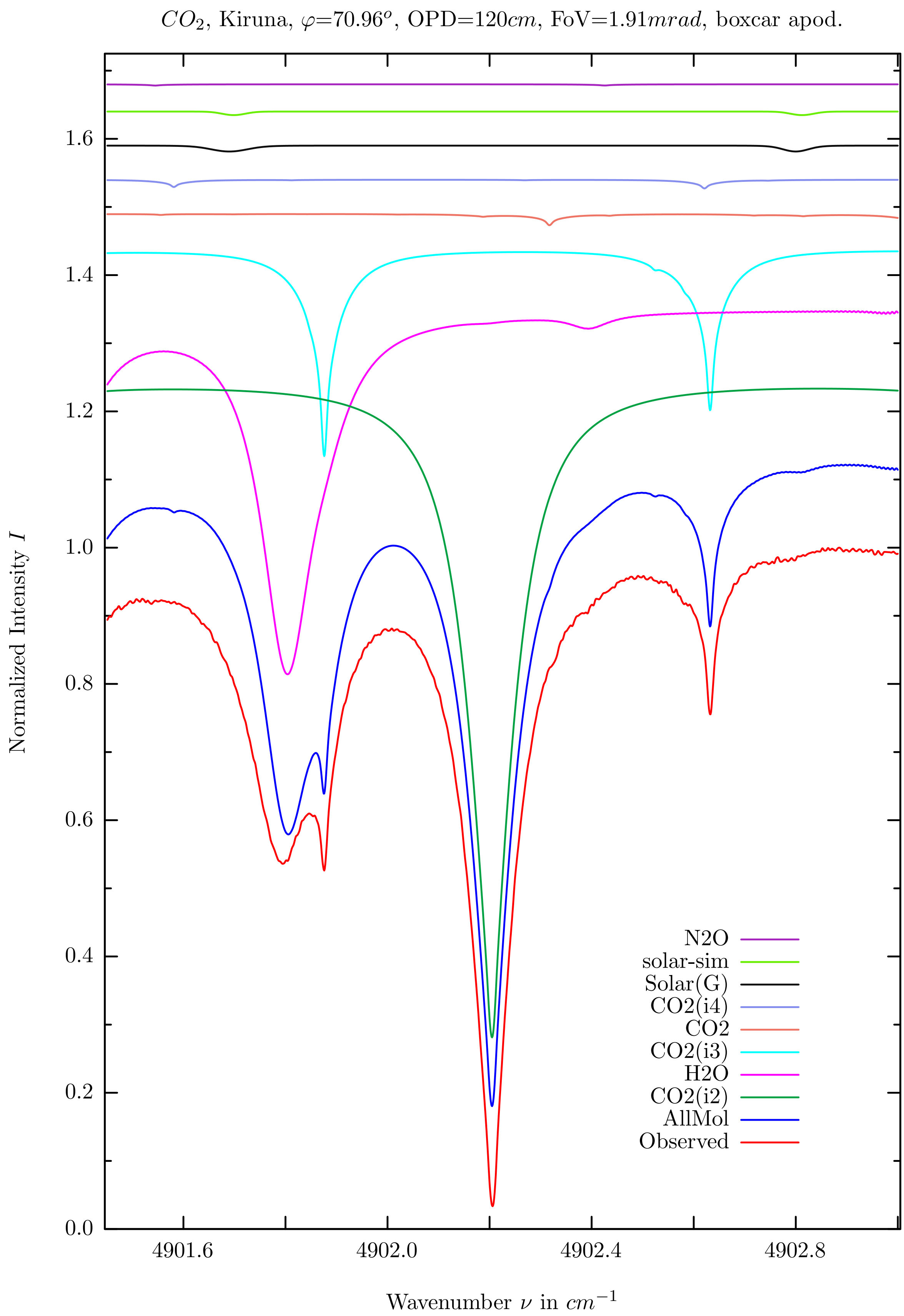
CO_2, Kiruna, φ=70.96^o, OPD=120cm, FoV=1.91$mrad$, boxcar apod.
Normalized Intensity I
Wavenumber ν in cm^{-1}
0.0
0.2
0.4
0.6
0.8
1.0
1.2
1.4
1.6
4901.6
4902.0
4902.4
4902.8
N2O
solar-sim
Solar(G)
CO2(i4)
CO2
CO2(i3)
H2O
CO2(i2)
AllMol
Observed

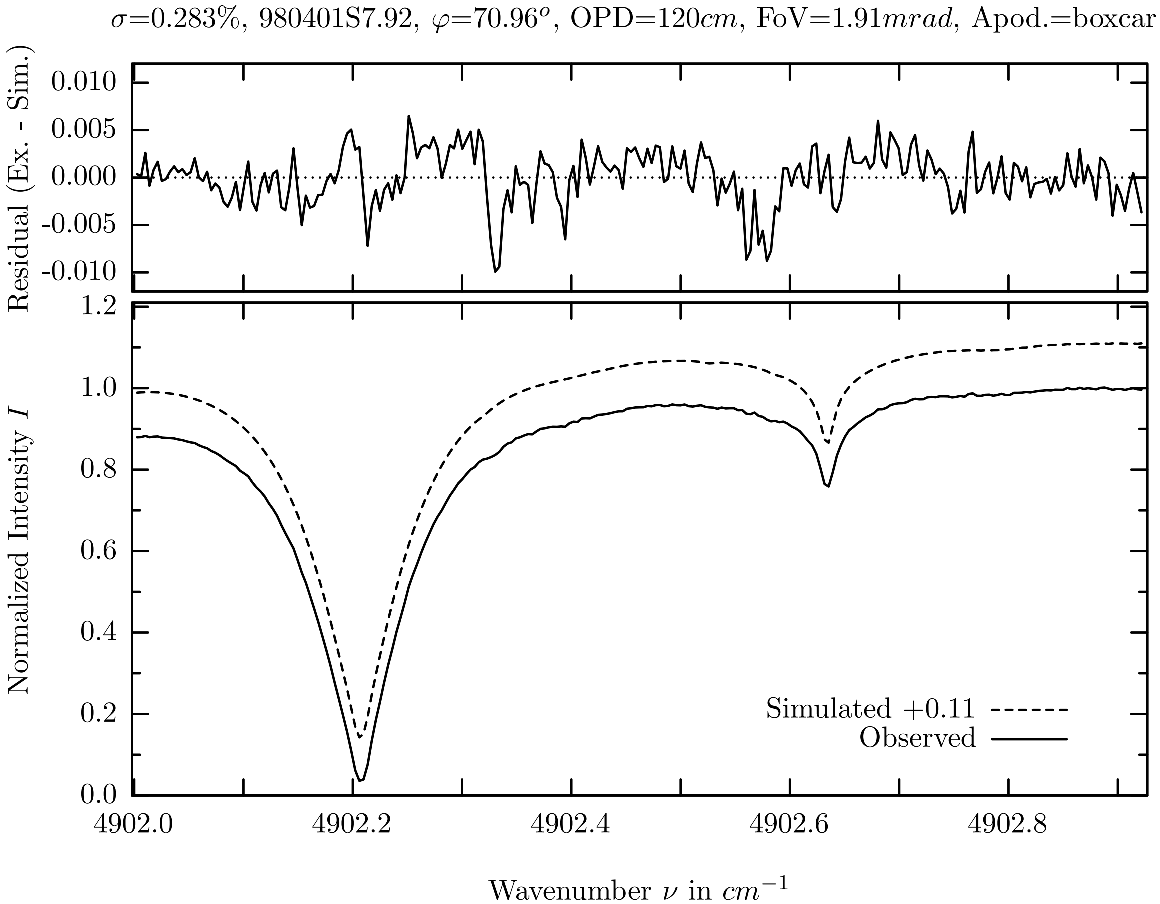

investigated species	:	$CO_2(i2), (CO_2(i3))$
line position(s) ν_0	:	4902.2035, (4902.6309) cm^{-1}
lower state energy E''_{lst}	:	163.9, (4.4) cm^{-1}
retrieved TCA, information content	:	7.52E+21, (7.29E+21) $molec/cm^2$, 341.4, (86.1)
temperature dependence of the TCA	:	+.044 (+.373)%/K (trop), -.015 (+.066)%/K (strat)
location, date, solar zenith angle	:	Kiruna, 1/Apr/98, 70.96^o
spectral interval fitted	:	4902.000 – 4902.925 cm^{-1}

Molecule	iCode	Absorption	Molecule	iCode	Absorption
CO2	**22**	96.896%	*N2O*	41	0.182%
H2O	11	53.595%	*NH3*	111	0.001%
CO2	**23**	30.697%	*CH4*	61	<0.001%
CO2	21	1.681%	*OH*	131	<0.001%
CO2	**24**	1.288%	*HBr*	161	<0.001%
Solar(G)	—	0.861%	*HDO*	491	<0.001%
Solar-sim	—	0.519%			

CO_2, Kiruna, φ=70.96^o, OPD=120cm, FoV=1.91$mrad$, boxcar apod.

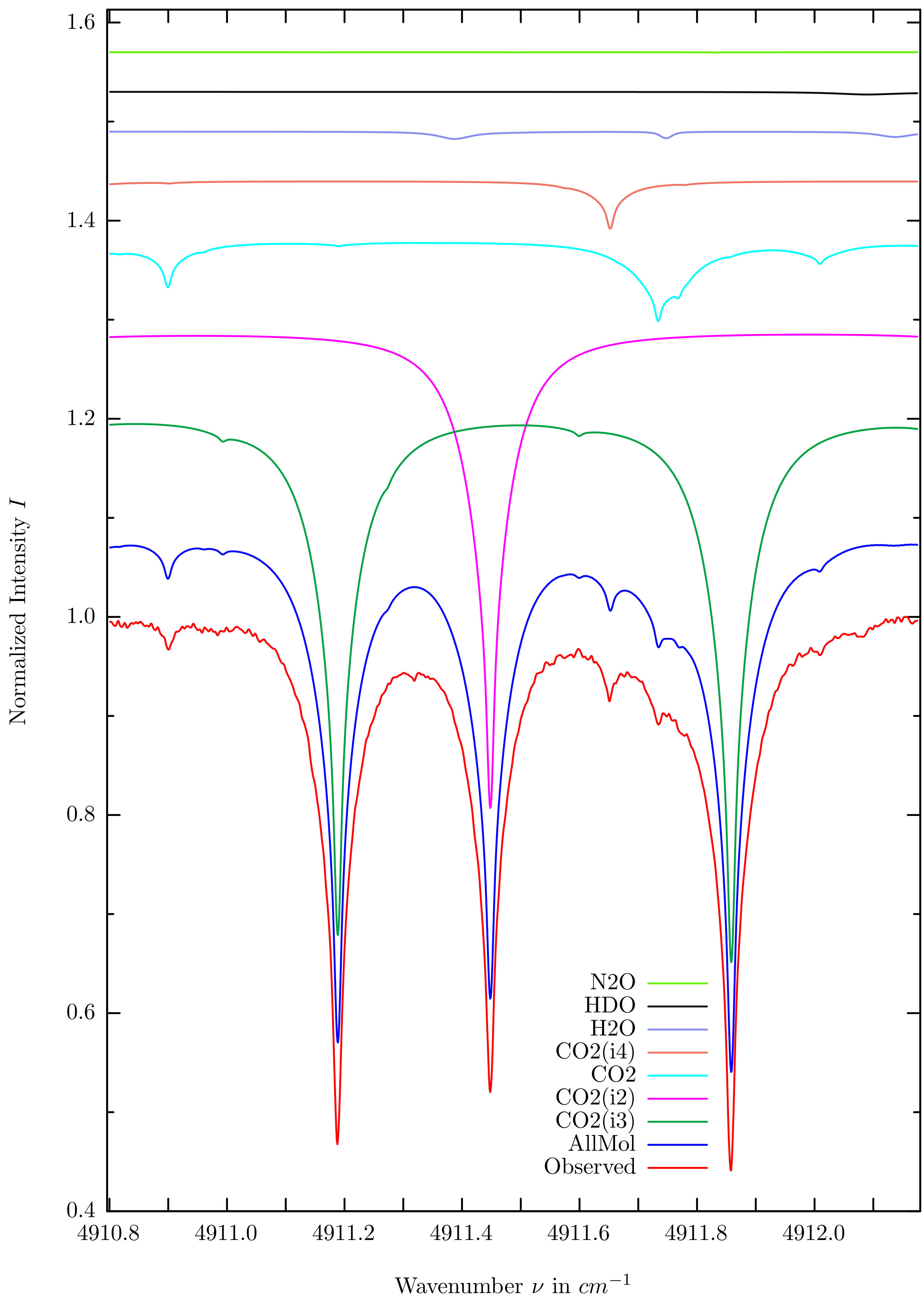

σ=0.335%, 980401S7.92, φ=70.96^o, OPD=120cm, FoV=1.91$mrad$, Apod.=boxcar

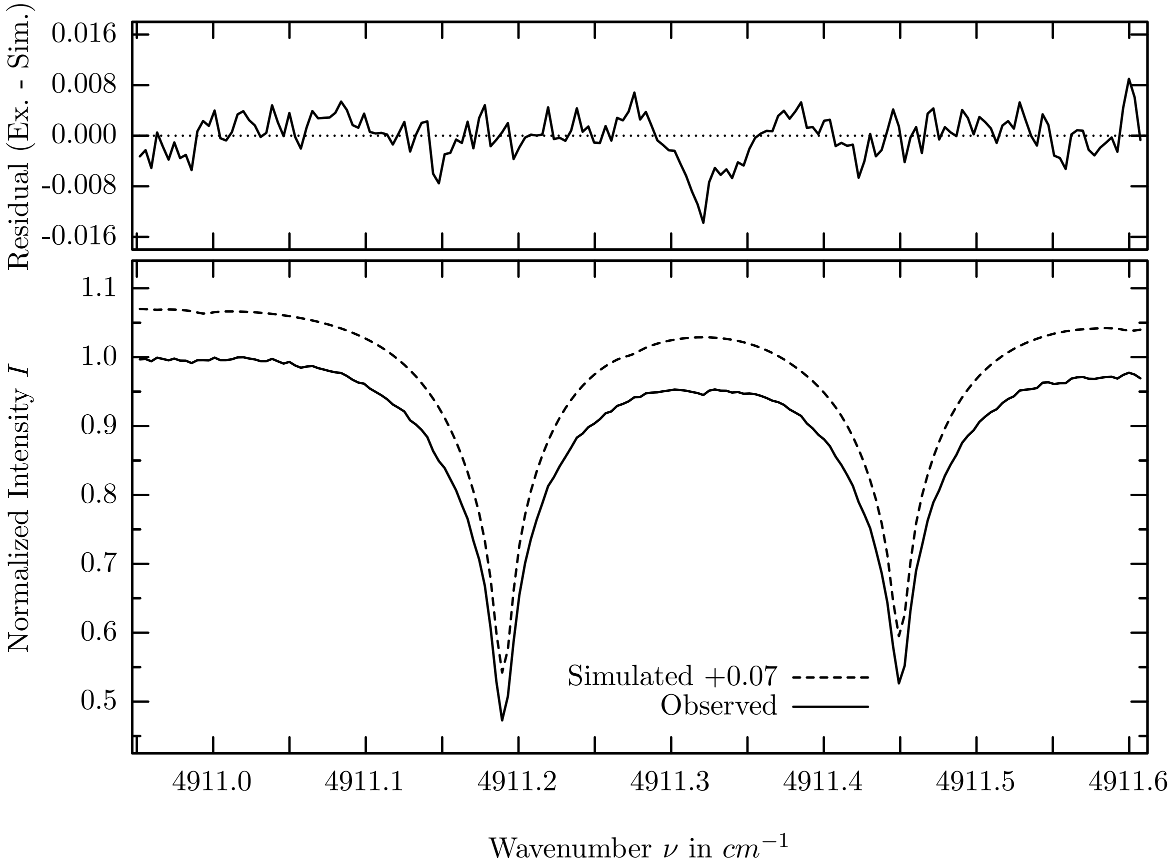

investigated species	:	$CO_2(i3), (CO_2(i2))$
line position(s) ν_0	:	4911.1863, (4911.4478) cm^{-1}
lower state energy E''_{lst}	:	26.5, (519.6) cm^{-1}
retrieved TCA, information content	:	7.13E+21, (7.45E+21) $molec/cm^2$, 157.8, (142.0)
temperature dependence of the TCA	:	+.377 (-.777)%/K (trop), +.082 (-.203)%/K (strat)
location, date, solar zenith angle	:	Kiruna, 1/Apr/98, 70.96^o
spectral interval fitted	:	4910.950 – 4911.610 cm^{-1}

Molecule	iCode	Absorption	Molecule	iCode	Absorption
CO2	**23**	56.075%	$CH4$	61	<0.001%
CO2	**22**	48.465%	$NH3$	111	<0.001%
$CO2$	21	8.115%	OH	131	<0.001%
$CO2$	24	4.852%	HBr	161	<0.001%
$H2O$	11	0.757%	Solar(G)	—	<0.001%
HDO	491	0.269%	Solar-sim	—	<0.001%
$N2O$	41	0.022%			

CO_2, Kiruna, φ=70.96^o, OPD=120cm, FoV=1.91$mrad$, boxcar apod.

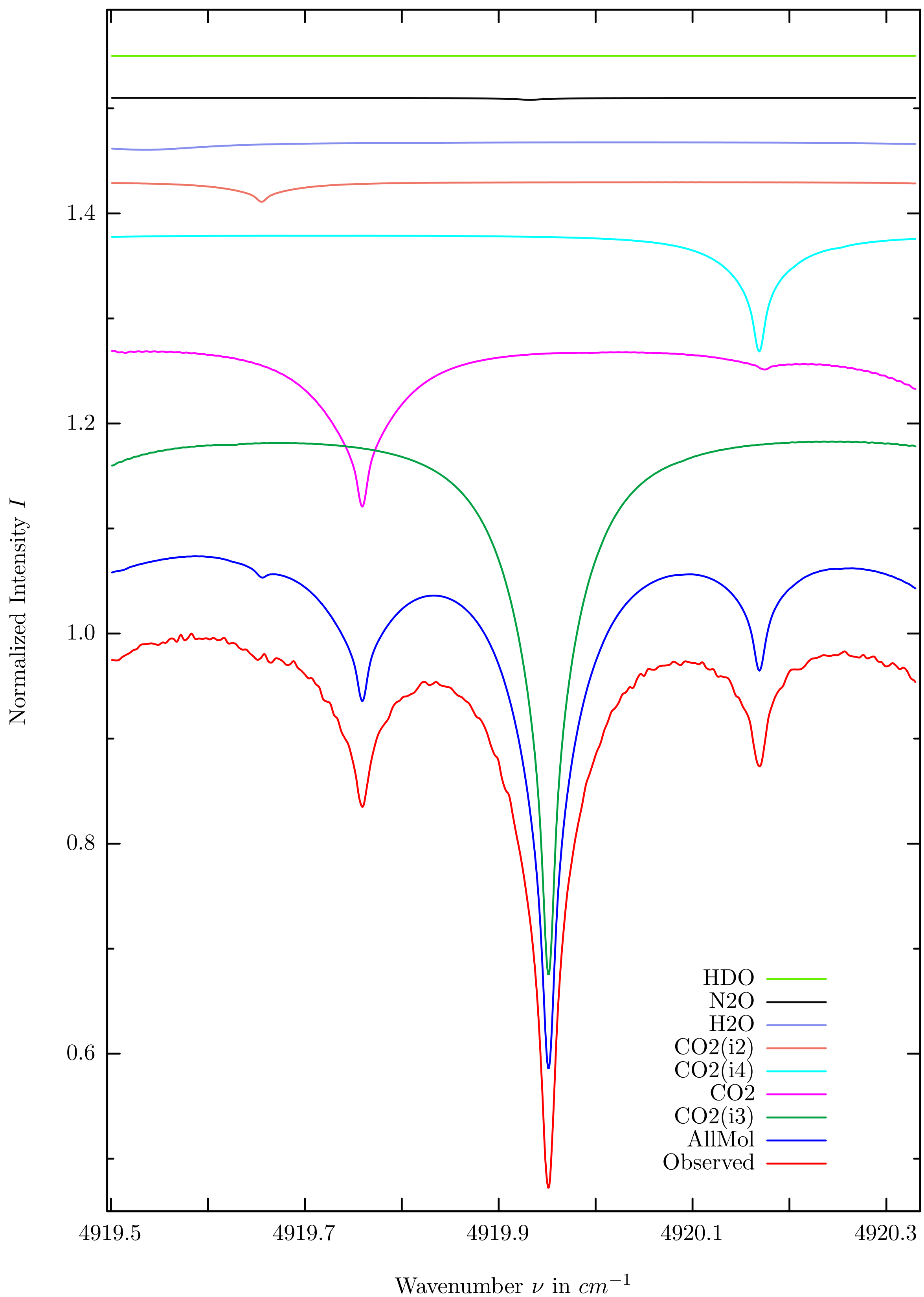

σ=0.217%, 980401S7.92, φ=70.96^o, OPD=120cm, FoV=1.91$mrad$, Apod.=boxcar

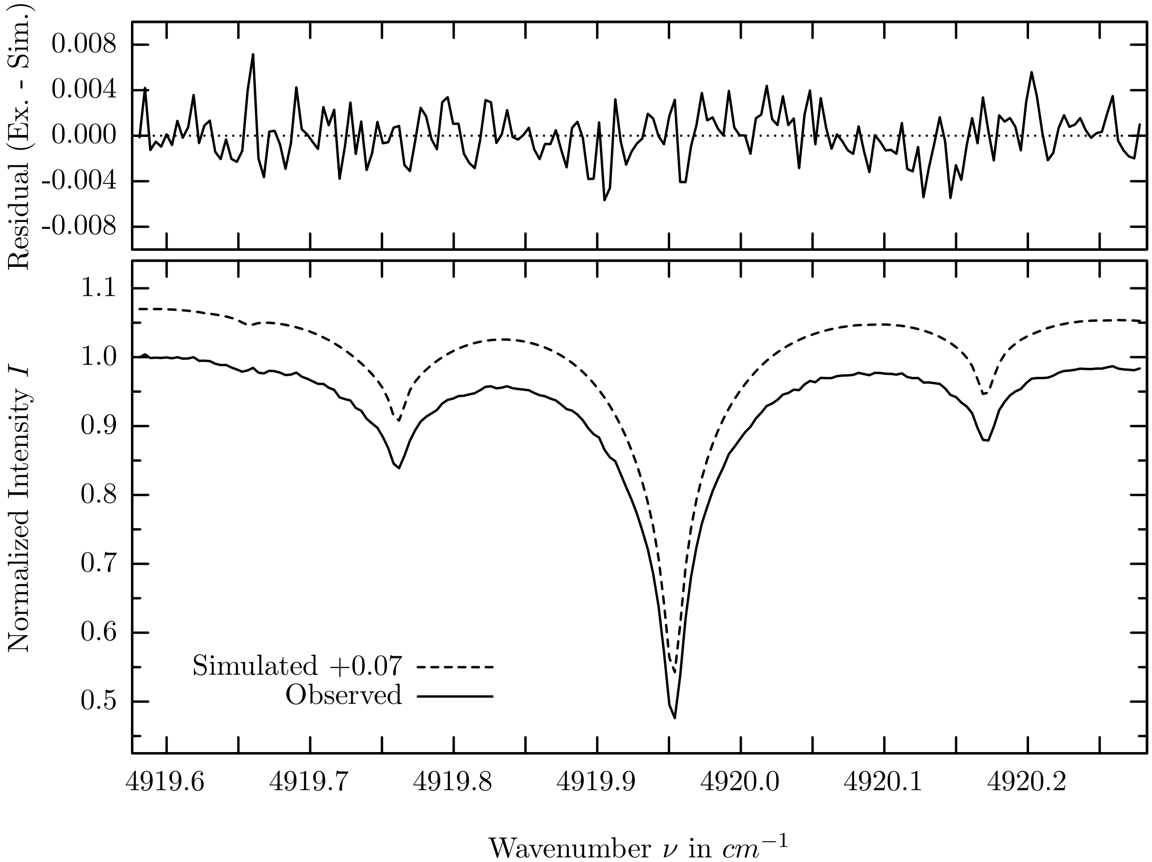

investigated species	:	$CO_2(i3), (CO_2(i4))$
line position(s) ν_0	:	4919.9492, (4920.1675) cm^{-1}
lower state energy E''_{lst}	:	186.3, (209.0) cm^{-1}
retrieved TCA, information content	:	7.57E+21, (8.19E+21) $molec/cm^2$, 243.1, (56.9)
temperature dependence of the TCA	:	+.132, (-.503)%/K (trop), +.022, (-.054)%/K (strat)
investigated species, position	:	CO_2, 4919.7575cm^{-1}
lower state energy E''_{lst}	:	1559.4 cm^{-1}
retrieved TCA, information content	:	8.03E+21 $molec/cm^2$, 74.7
temperature dependence of the TCA	:	-2.641%/K (trop), -0.867%/K (strat)
location, date, solar zenith angle	:	Kiruna, 1/Apr/98, 70.96^o
spectral interval fitted	:	4919.580 – 4920.280 cm^{-1}

Molecule	iCode	Absorption	Molecule	iCode	Absorption
CO2	**23**	52.701%	$CH4$	61	<0.001%
$CO2$	21	15.877%	$NH3$	111	<0.001%
CO2	**24**	11.202%	OH	131	<0.001%
$CO2$	**22**	1.906%	HBr	161	<0.001%
$H2O$	11	0.945%	Solar(G)	—	<0.001%
$N2O$	41	0.197%	Solar-sim	—	<0.001%
HDO	491	0.009%			

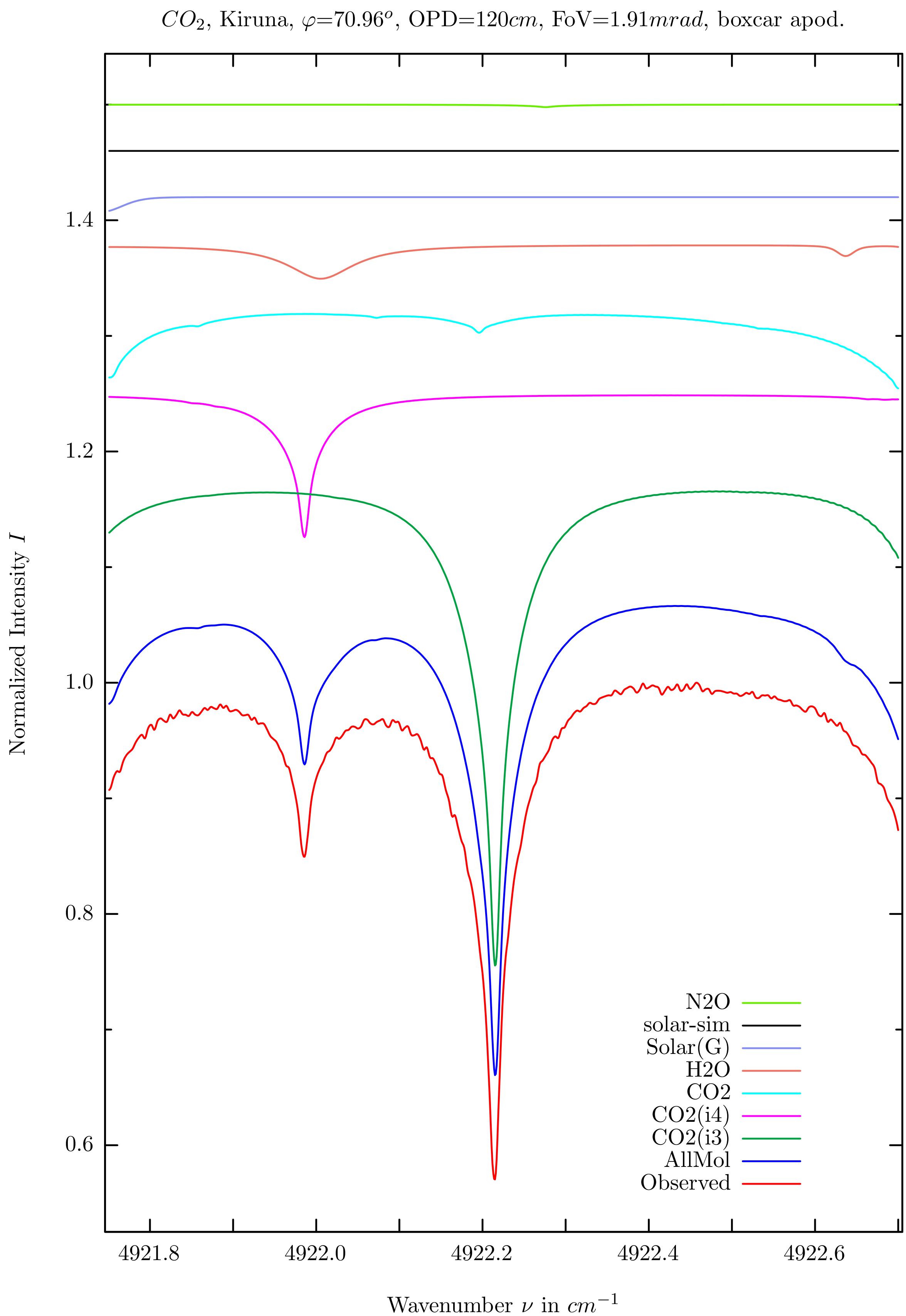
CO_2, Kiruna, φ=70.96^o, OPD=120cm, FoV=1.91$mrad$, boxcar apod.
Normalized Intensity I
1.4
1.2
1.0
0.8
0.6
4921.8
4922.0
4922.2
4922.4
4922.6
Wavenumber ν in cm^{-1}
N2O
solar-sim
Solar(G)
H2O
CO2
CO2(i4)
CO2(i3)
AllMol
Observed

σ=0.274%, 980401S7.92, φ=70.96^o, OPD=120cm, FoV=1.91$mrad$, Apod.=boxcar

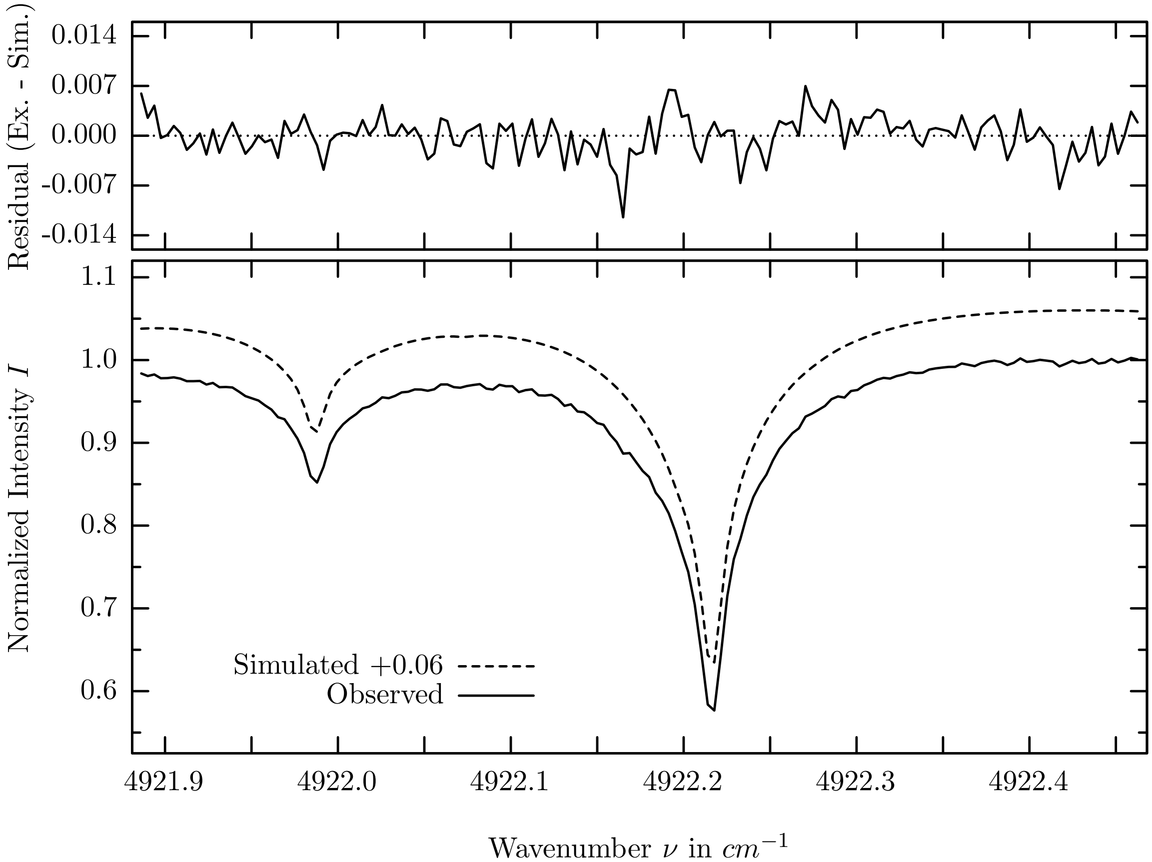

investigated species	:	$CO_2(i3), (CO_2(i4))$
line position(s) ν_0	:	4922.2122, (4921.9862) cm^{-1}
lower state energy E''_{lst}	:	258.4, (174.9) cm^{-1}
retrieved TCA, information content	:	7.27E+21, (8.28E+21) $molec/cm^2$, 155.5, (53.6)
temperature dependence of the TCA	:	-.162, (-.214)%/K (trop), -.001, (-.002)%/K (strat)
location, date, solar zenith angle	:	Kiruna, 1/Apr/98, 70.96^o
spectral interval fitted	:	4921.886 – 4922.465 cm^{-1}

Molecule	iCode	Absorption	Molecule	iCode	Absorption
CO2	**23**	42.670%	$N2O$	41	0.217%
CO2	**24**	12.467%	HDO	491	0.001%
$CO2$	21	7.620%	$CH4$	61	<0.001%
$H2O$	11	3.058%	$NH3$	111	<0.001%
Solar(G)	—	1.187%	OH	131	<0.001%
Solar-sim	—	<0.001%			

H_2O, Kiruna, φ=65.02^o, OPD=120cm, FoV=1.91$mrad$, boxcar apod.

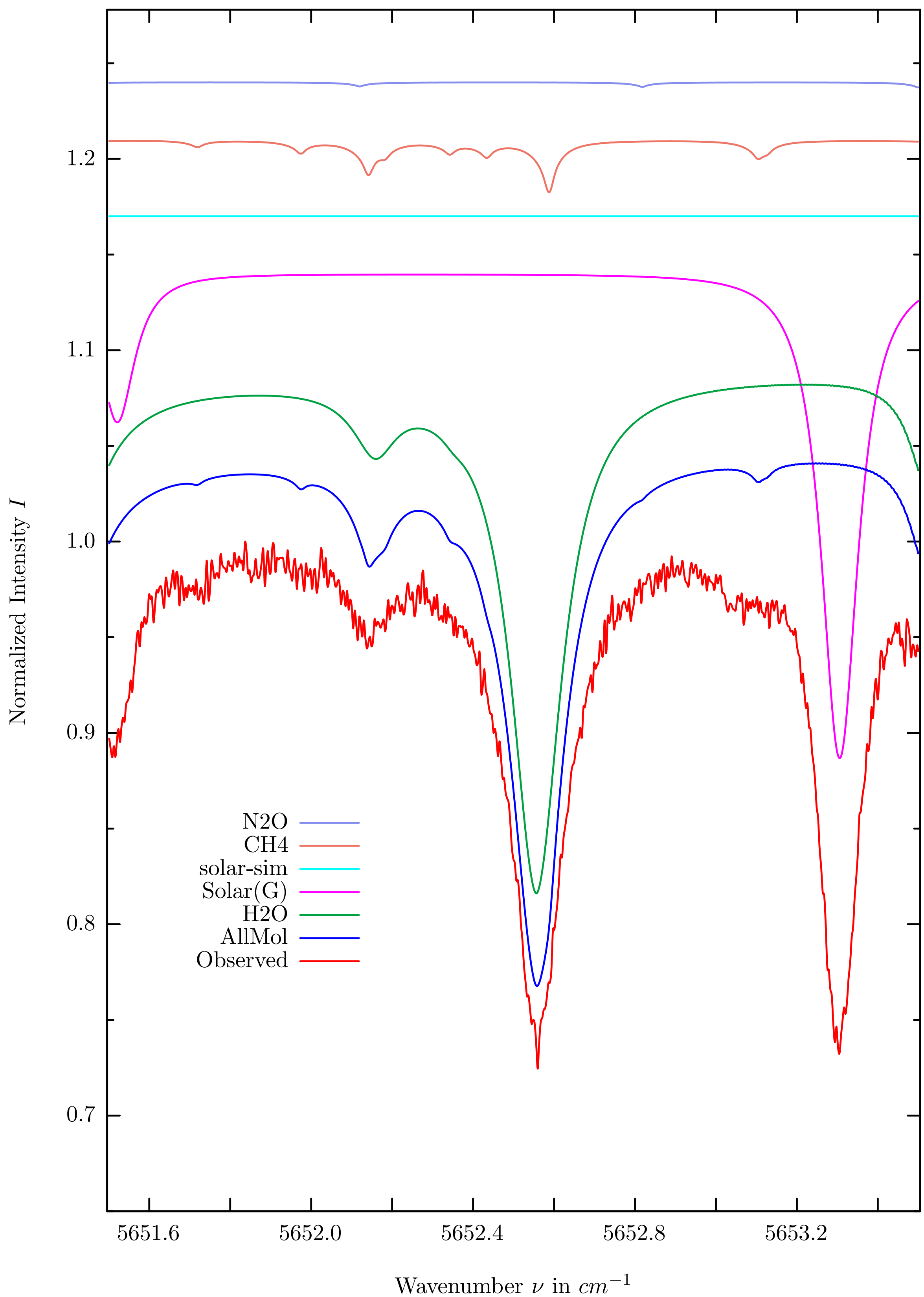

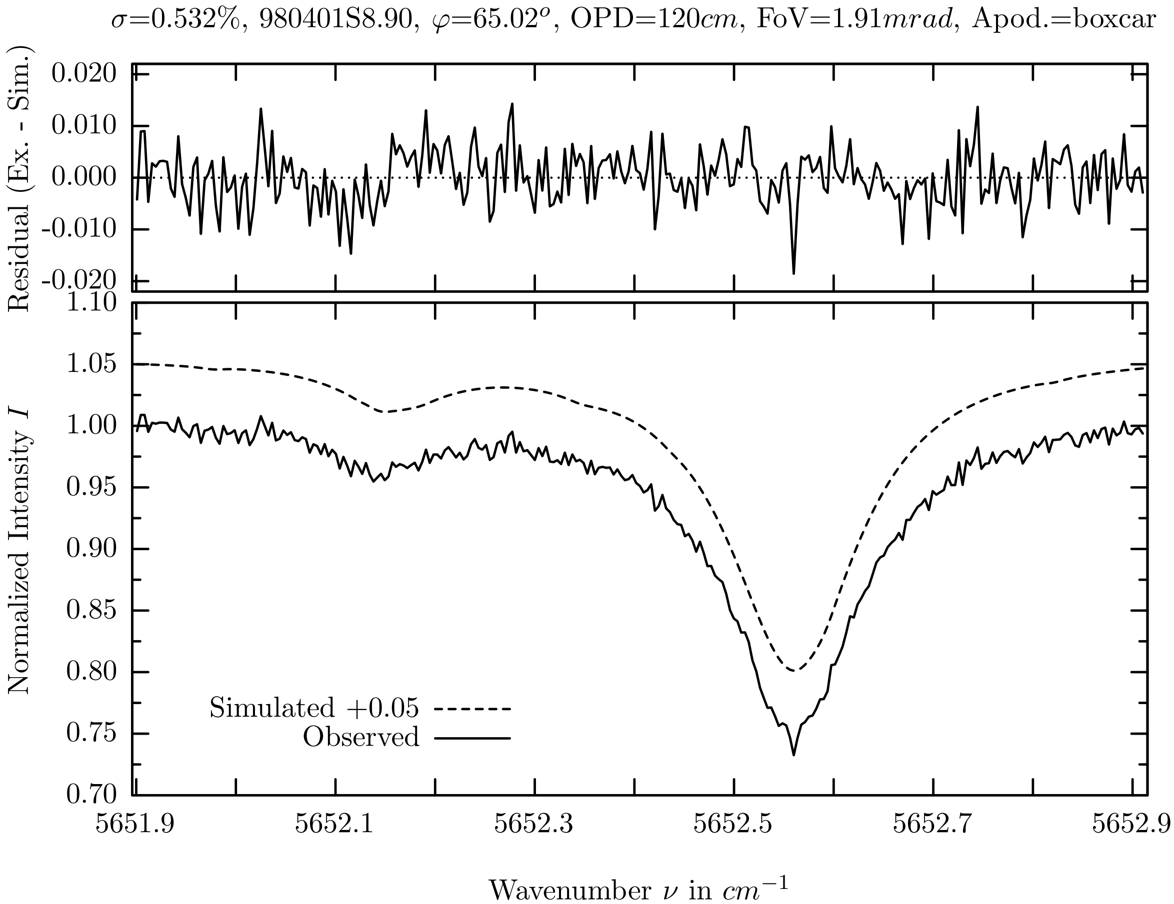

investigated species	:	H_2O
line position(s) ν_0	:	5652.5550 cm^{-1}
lower state energy E''_{lst}	:	224.8 cm^{-1}
retrieved TCA, information content	:	9.31E+21 $molec/cm^2$, 46.6
temperature dependence of the TCA	:	+0.347%/K (trop), +0.044%/K (strat)
location, date, solar zenith angle	:	Kiruna, 1/Apr/98, 65.02^o
spectral interval fitted	:	5651.900 – 5652.914 cm^{-1}

Molecule	iCode	Absorption	Molecule	iCode	Absorption
H2O	11	30.428%	*N2O*	41	0.263%
Solar(G)	—	25.321%	*CO2*	21	0.038%
Solar-sim	—	<0.001%	*OH*	131	<0.001%
CH4	61	2.751%	*HCL*	151	<0.001%

CH_4, Kiruna, φ=65.02^o, OPD=120cm, FoV=1.91$mrad$, boxcar apod.

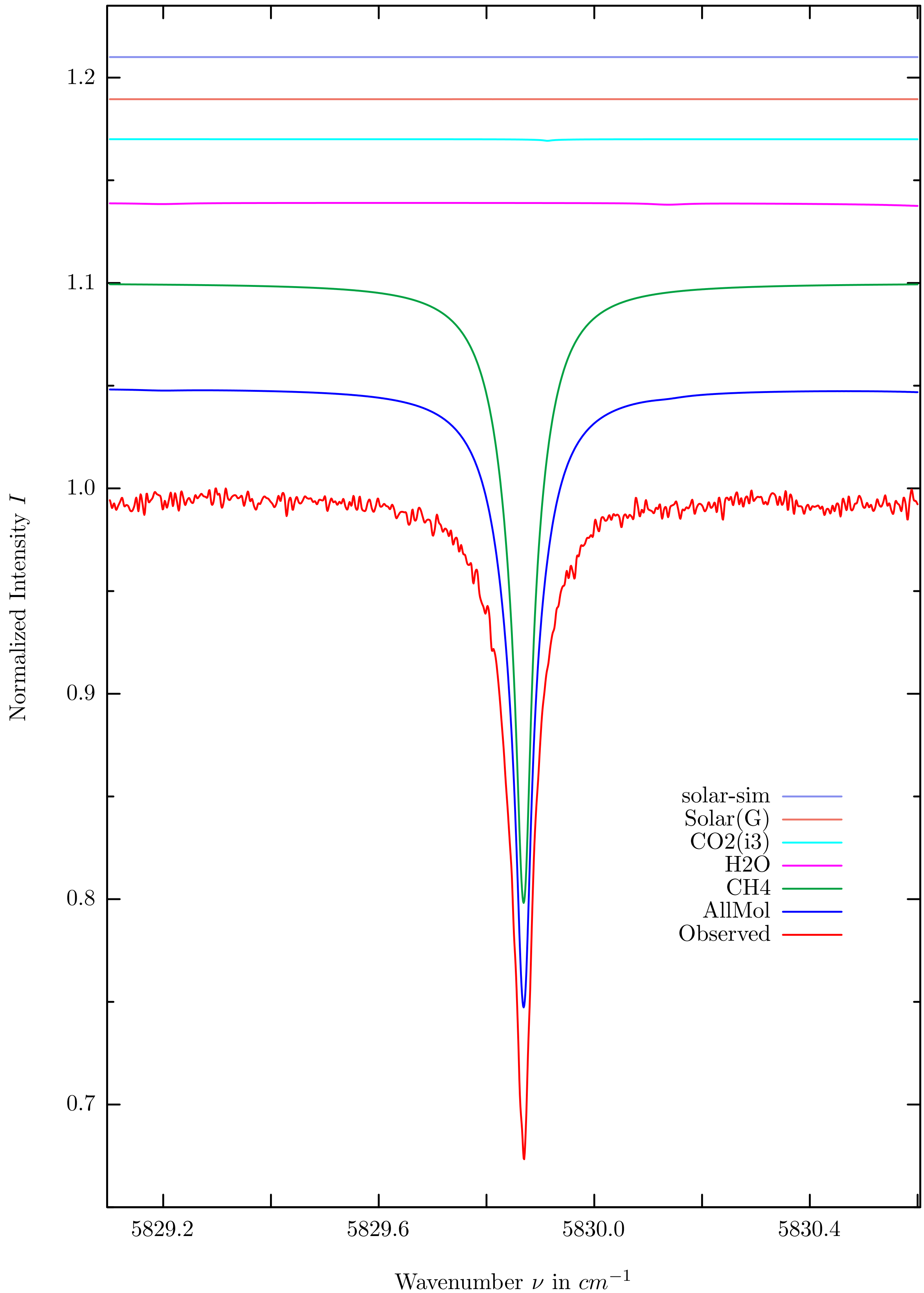

σ=0.286%, 980401S8.90, φ=65.02^o, OPD=120cm, FoV=1.91$mrad$, Apod.=boxcar

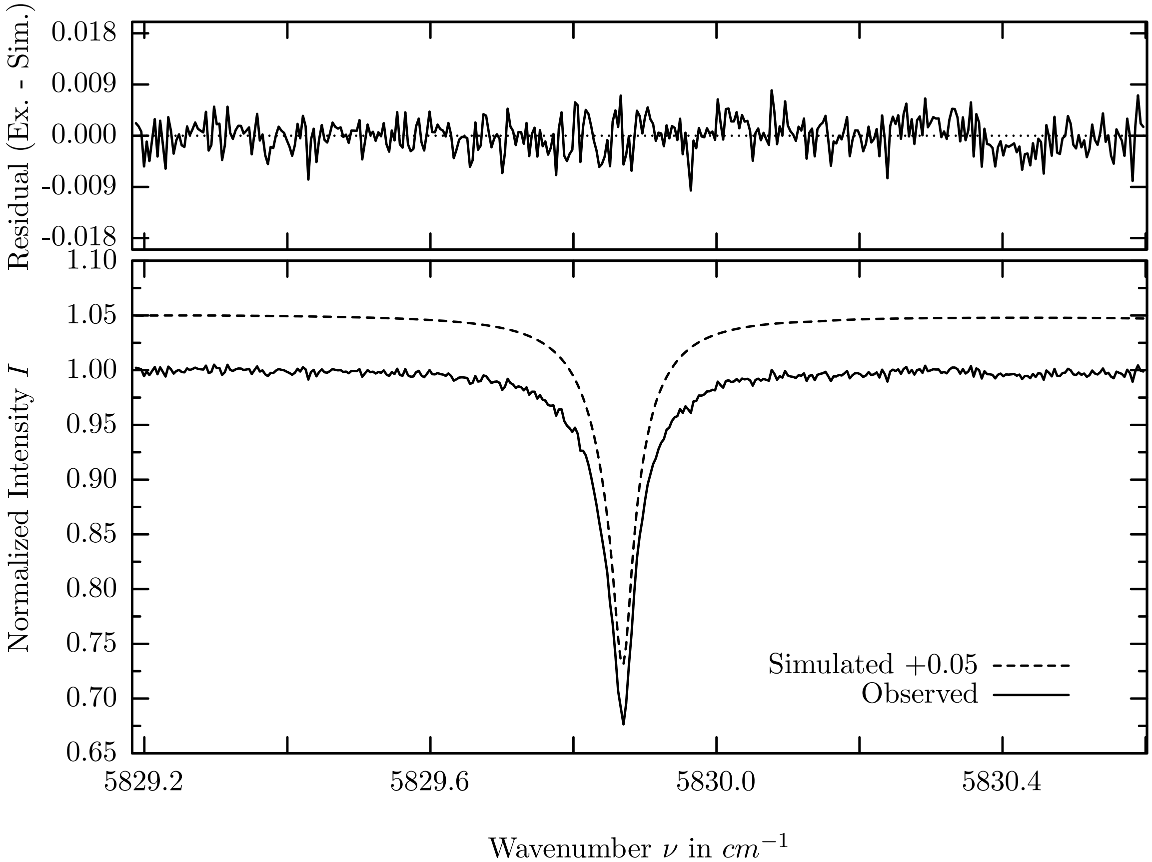

investigated species	:	CH_4
line position(s) ν_0	:	5829.8684 cm^{-1}
lower state energy E''_{lst}	:	10.5 cm^{-1}
retrieved TCA, information content	:	3.50E+19 $molec/cm^2$, 111.3
temperature dependence of the TCA	:	+0.552%/K (trop), +0.076%/K (strat)
location, date, solar zenith angle	:	Kiruna, 1/Apr/98, 65.02^o
spectral interval fitted	:	5829.185 – 5830.600 cm^{-1}

Molecule	iCode	Absorption	Molecule	iCode	Absorption
CH4	61	30.228%	$N2O$	41	<0.001%
$H2O$	11	0.250%	CO	5**5**	<0.001%
$CO2$	2**3**	0.078%	OH	131	<0.001%
Solar(G)	—	0.051%	HCl	151	<0.001%
Solar-sim	—	<0.001%			

CH_4, Kiruna, φ=65.02^o, OPD=120cm, FoV=1.91$mrad$, boxcar apod.

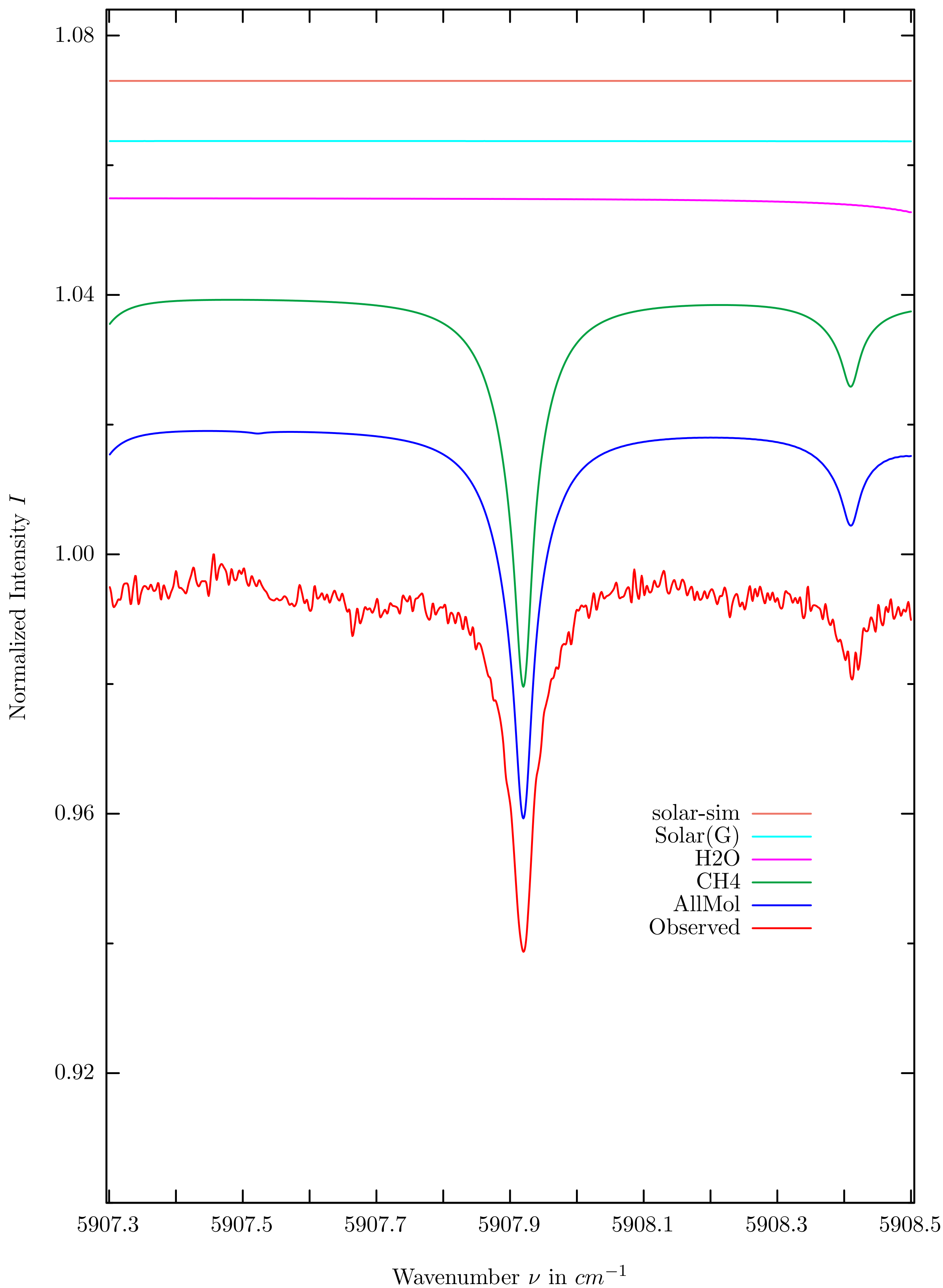

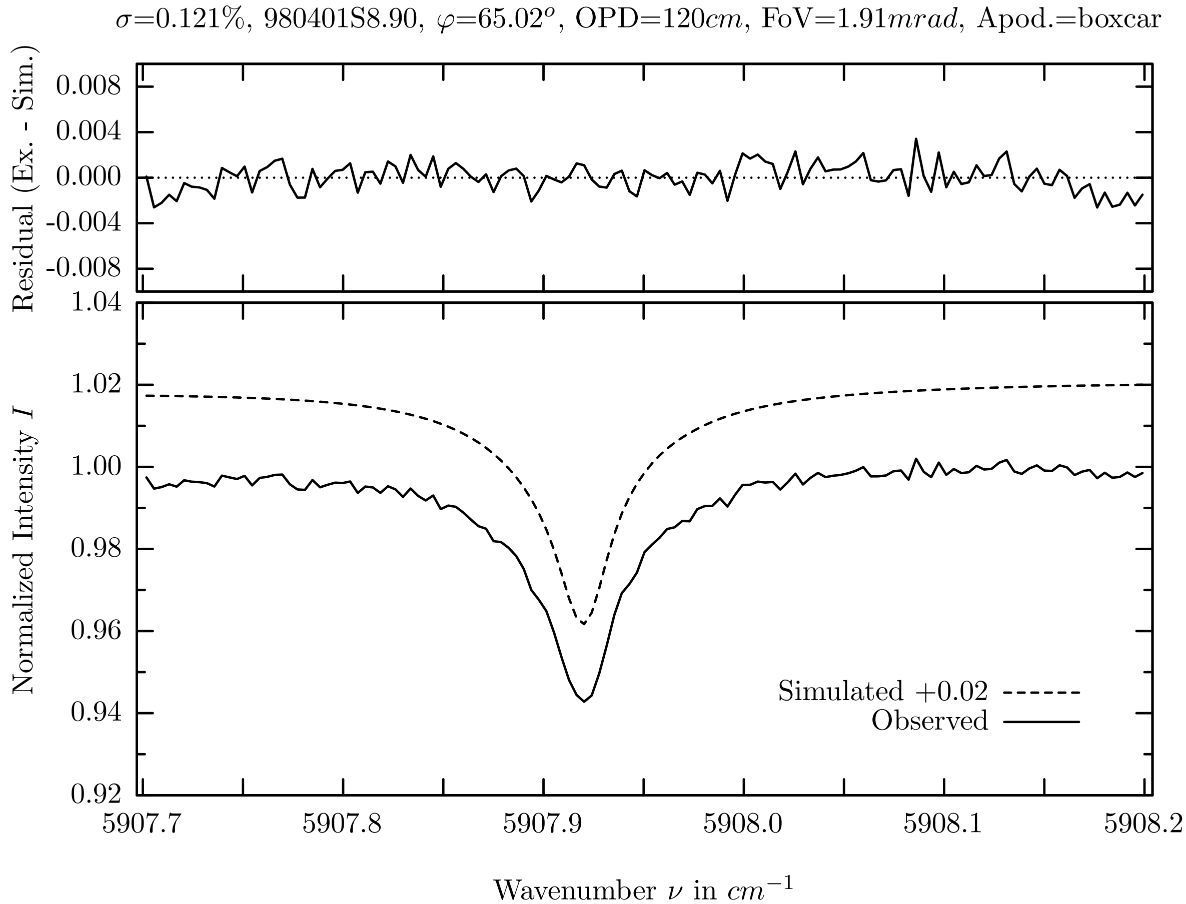

investigated species	:	CH_4
line position(s) ν_0	:	5907.9194 cm^{-1}
lower state energy E''_{lst}	:	104.7 cm^{-1}
retrieved TCA, information content	:	3.14E+19 $molec/cm^2$, 48.1
temperature dependence of the TCA	:	+0.188%/K (trop), +0.046%/K (strat)
location, date, solar zenith angle	:	Kiruna, 1/Apr/98, 65.02^o
spectral interval fitted	:	5907.700 – 5908.200 cm^{-1}

Molecule	iCode	Absorption	Molecule	iCode	Absorption
CH4	61	6.052%	*N2O*	41	0.048%
H2O	11	0.231%	*CO*	5**2**	<0.001%
Solar(G)	—	0.131%	*OH*	131	<0.001%
Solar-sim	—	<0.001%			

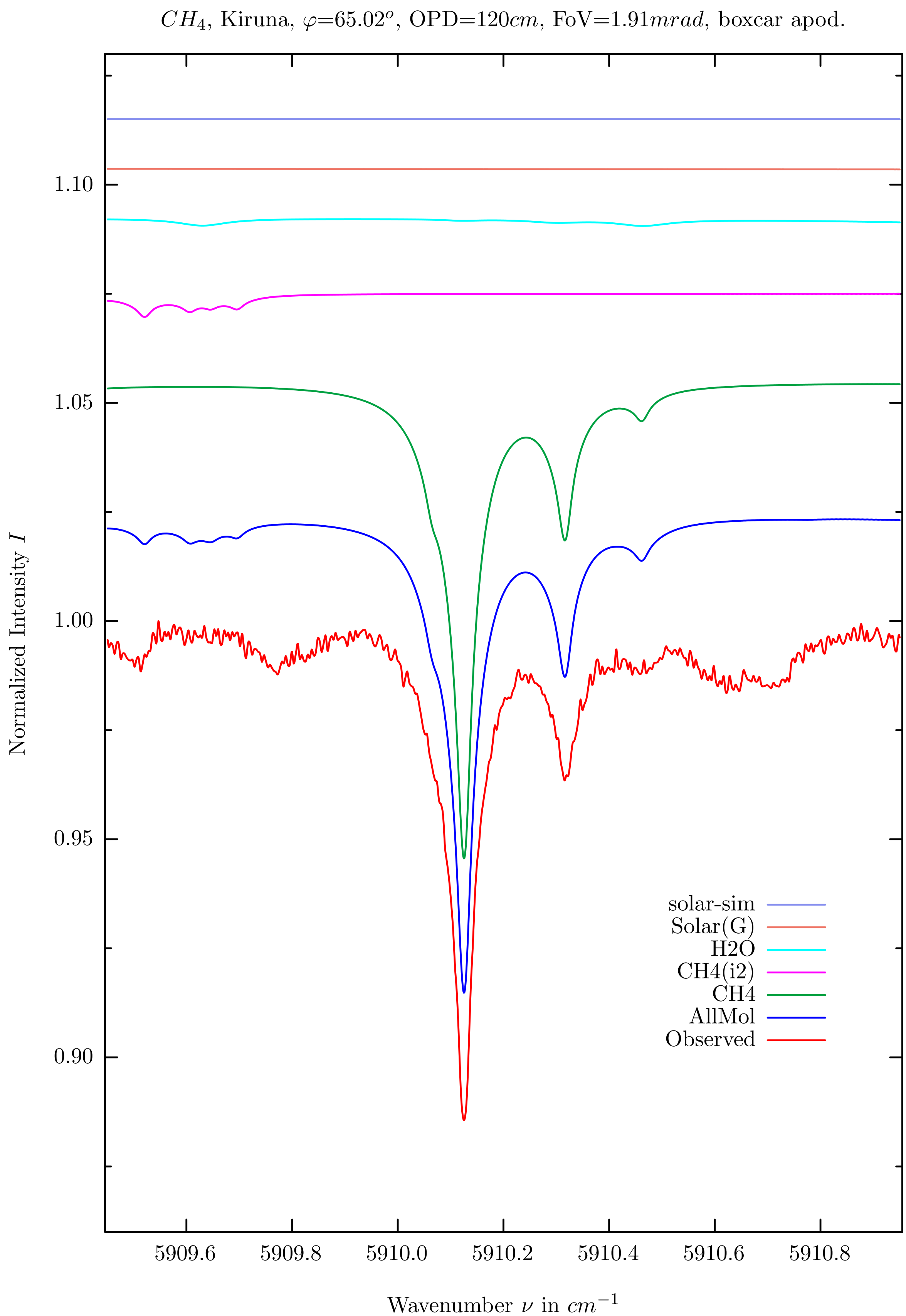

CH_4, Kiruna, φ=65.02^o, OPD=120cm, FoV=1.91$mrad$, boxcar apod.
1.10
1.05
1.00
0.95
0.90
Normalized Intensity I
5909.6
5909.8
5910.0
5910.2
5910.4
5910.6
5910.8
Wavenumber ν in cm^{-1}
solar-sim
Solar(G)
H2O
CH4(i2)
CH4
AllMol
Observed

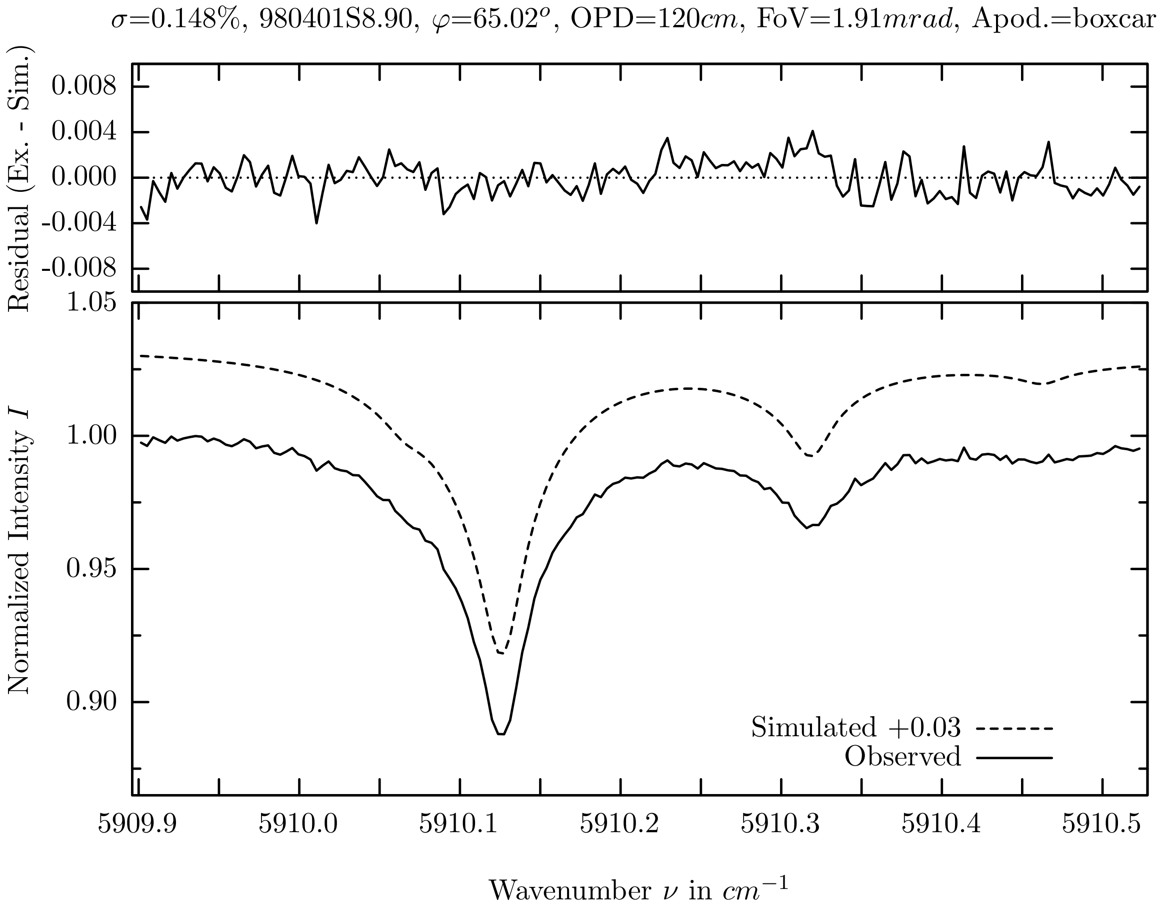

investigated species	:	CH_4
line position(s) ν_0	:	5910.1250 cm^{-1}
lower state energy E''_{lst}	:	293.1 cm^{-1}
retrieved TCA, information content	:	3.53E+19 $molec/cm^2$, 75.1
temperature dependence of the TCA	:	-0.151%/K (trop), -0.044%/K (strat)
location, date, solar zenith angle	:	Kiruna, 1/Apr/98, 65.02^o
spectral interval fitted	:	5909.900 – 5910.525 cm^{-1}

Molecule	iCode	Absorption	Molecule	iCode	Absorption
CH4	61	10.962%	olar-sim	980	<0.001%
CH4	6**2**	0.534%	*N2O*	41	0.025%
H2O	11	0.196%	*CO*	5**2**	<0.001%
Solar(G)	970	0.151%	*OH*	131	<0.001%

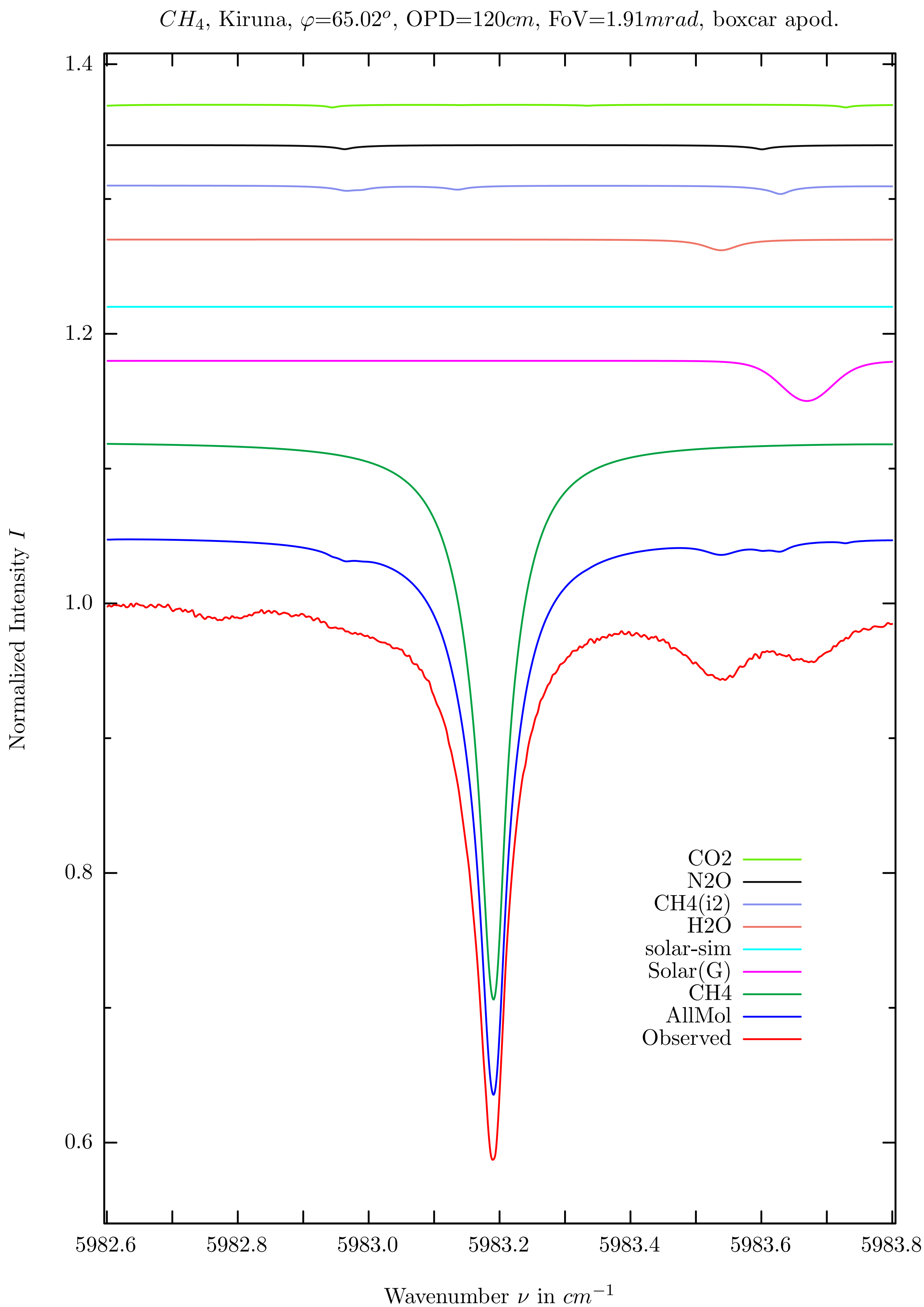

CH_4, Kiruna, φ=65.02^o, OPD=120cm, FoV=1.91$mrad$, boxcar apod.
1.4
1.2
1.0
0.8
0.6
Normalized Intensity I
CO2
N2O
CH4(i2)
H2O
solar-sim
Solar(G)
CH4
AllMol
Observed
5982.6
5982.8
5983.0
5983.2
5983.4
5983.6
5983.8
Wavenumber ν in cm^{-1}

σ=0.179%, 980401S8.90, φ=65.02^o, OPD=120cm, FoV=1.91$mrad$, Apod.=boxcar

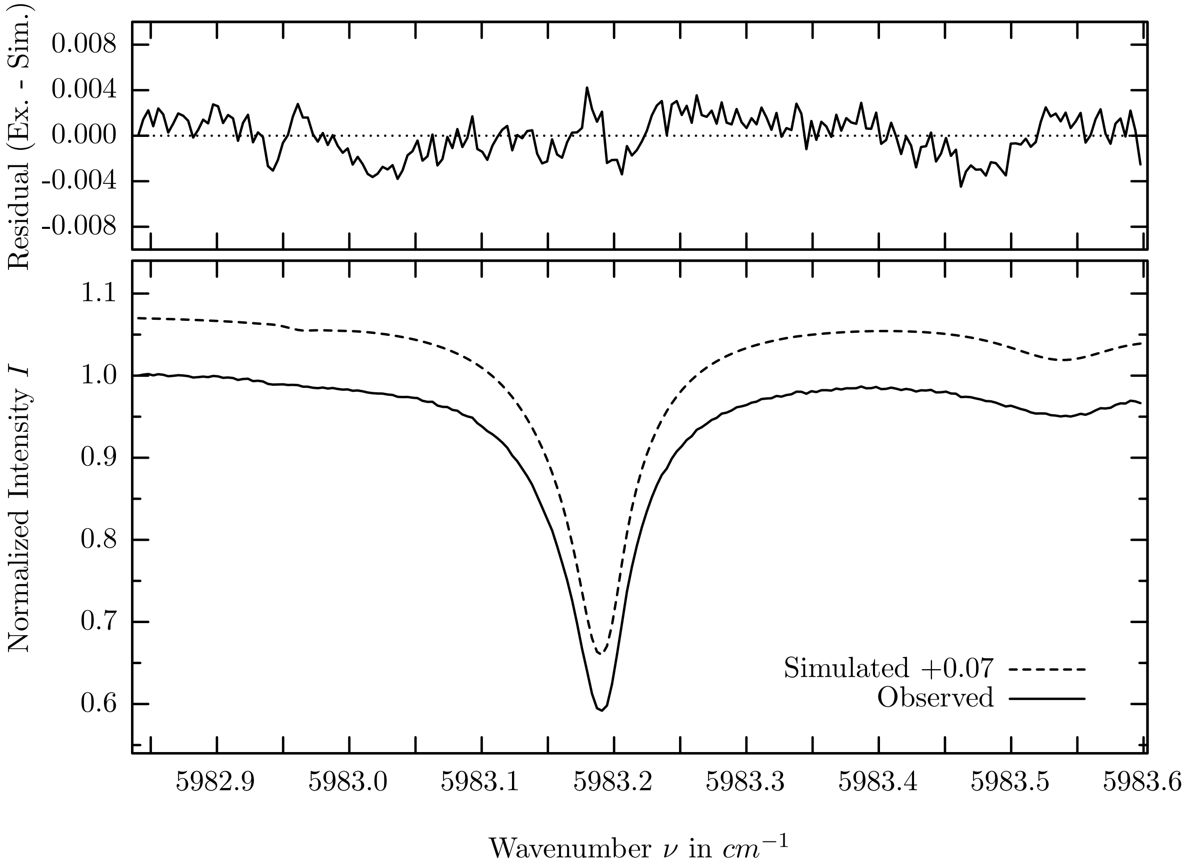

investigated species	:	CH_4
line position(s) ν_0	:	5983.1942 cm^{-1}
lower state energy E''_{lst}	:	31.4 cm^{-1}
retrieved TCA, information content	:	3.45E+19 $molec/cm^2$, 222.8
temperature dependence of the TCA	:	+0.449%/K (trop), +0.057%/K (strat)
location, date, solar zenith angle	:	Kiruna, 1/Apr/98, 65.02^o
spectral interval fitted	:	5982.840 – 5983.600 cm^{-1}

Molecule	iCode	Absorption	Molecule	iCode	Absorption
CH4	61	41.425%	$N2O$	41	0.317%
Solar(G)	—	2.985%	$CO2$	21	0.078%
Solar-sim	—	<0.001%	CO	51	<0.001%
$H2O$	11	0.804%	OH	131	<0.001%
$CH4$	6**2**	0.632%			

Comment: The spectroscopic data of the water line at 5983.54cm^{-1} is inconsistent with observations. This line was made stronger and broader for the fit shown.

H_2O, Kiruna, φ=65.02^o, OPD=120cm, FoV=1.91$mrad$, boxcar apod.

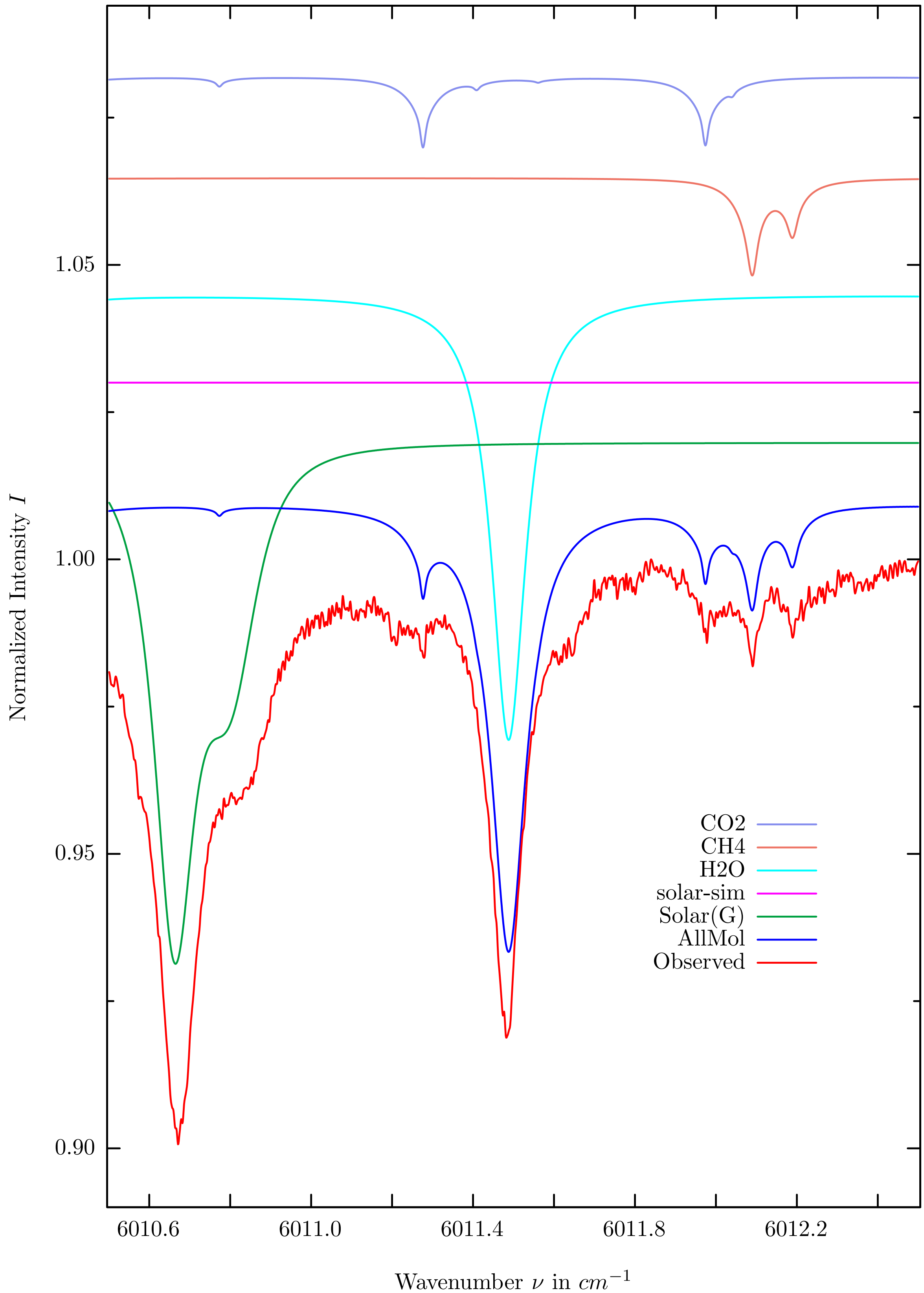

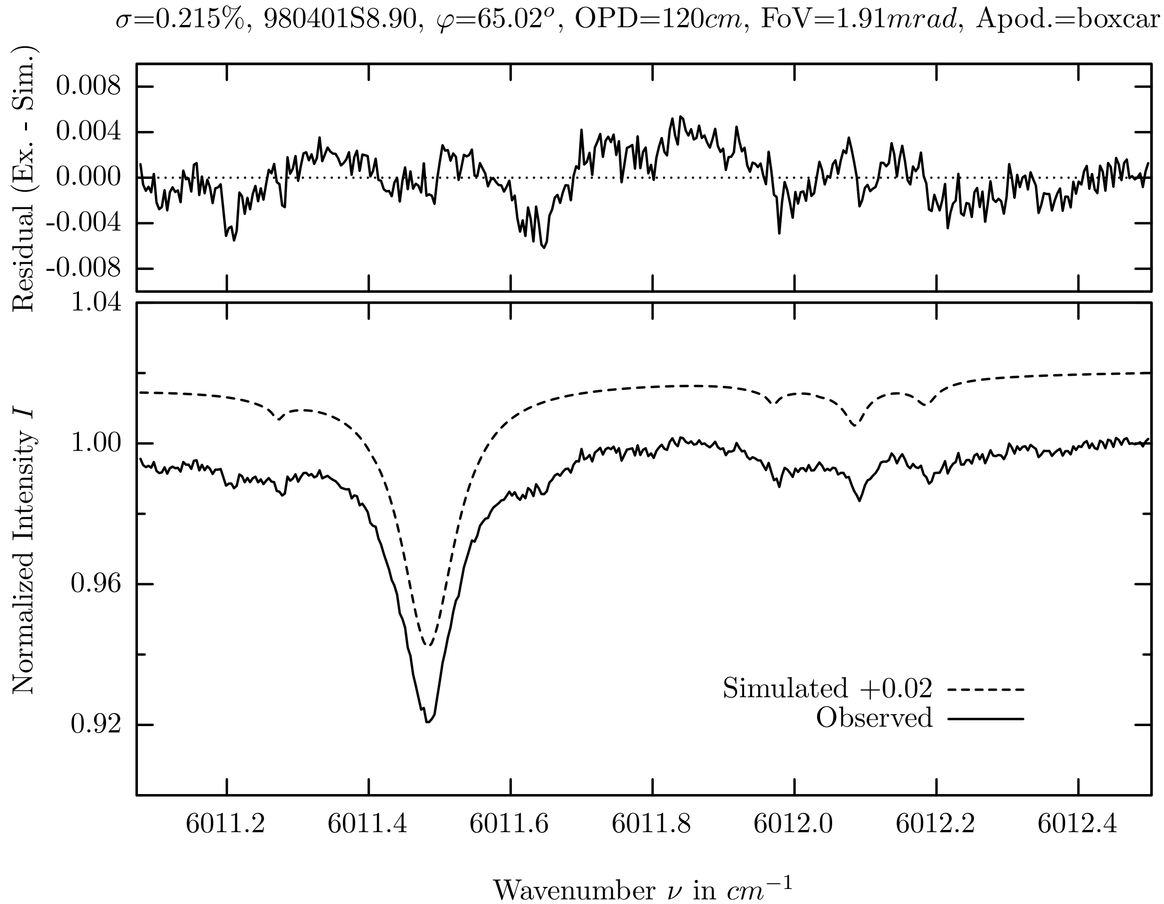

investigated species	:	H_2O
line position(s) ν_0	:	6011.4866 cm^{-1}
lower state energy E''_{lst}	:	586.2 cm^{-1}
retrieved TCA, information content	:	9.77E+21 $molec/cm^2$, 36.1
temperature dependence of the TCA	:	-1.125%/K (trop), -0.013%/K (strat)
location, date, solar zenith angle	:	Kiruna, 1/Apr/98, 65.02^o
spectral interval fitted	:	6011.078 – 6012.500 cm^{-1}

Molecule	iCode	Absorption	Molecule	iCode	Absorption
Solar(G)	—	8.868%	$CO2$	21	1.207%
Solar-sim	—	<0.001%	CO	51	<0.001%
H2O	11	7.569%	OH	131	<0.001%
$CH4$	61	1.684%			

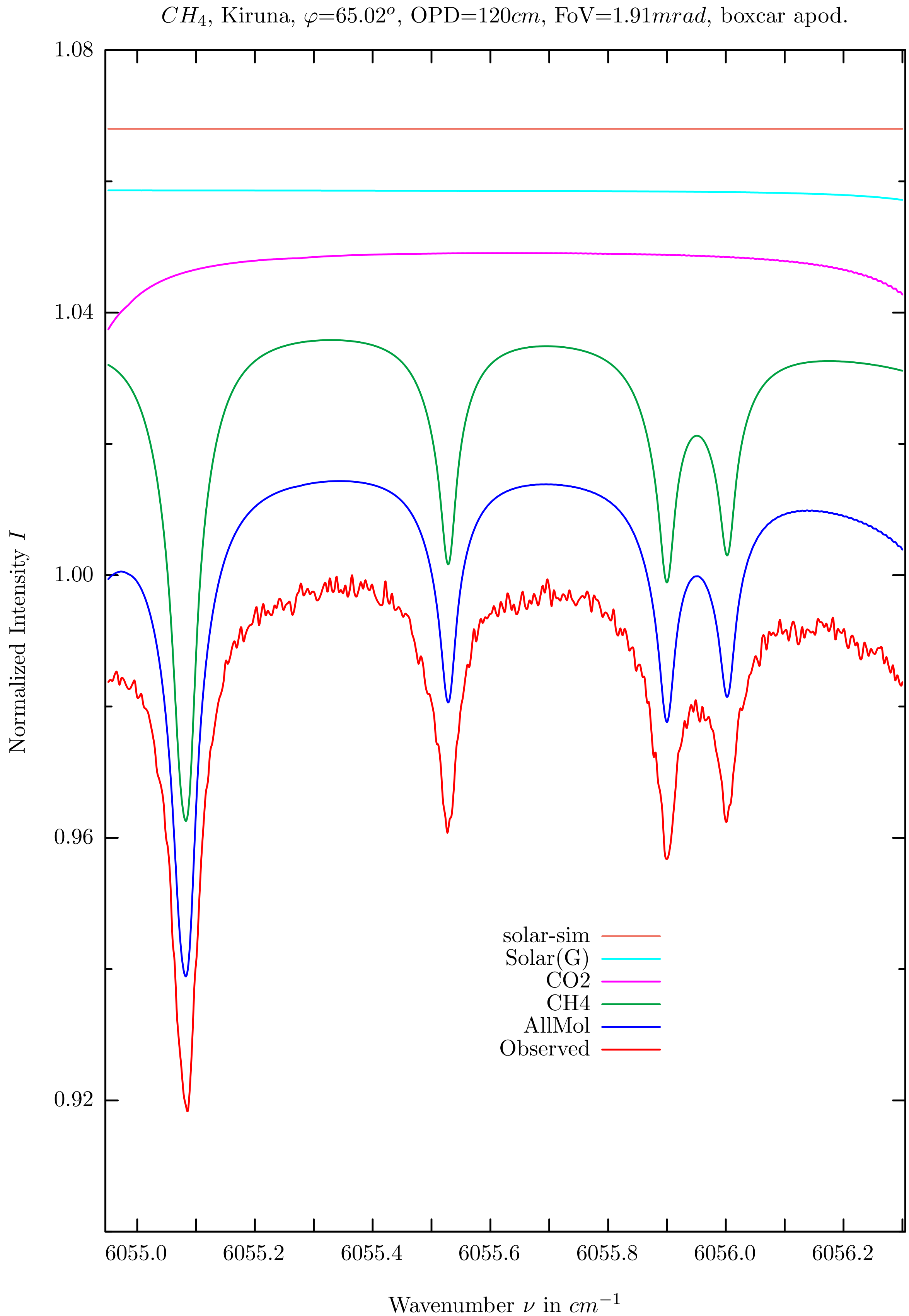

CH_4, Kiruna, φ=65.02^o, OPD=120cm, FoV=1.91$mrad$, boxcar apod.
1.08
1.04
1.00
0.96
0.92
Normalized Intensity I
6055.0
6055.2
6055.4
6055.6
6055.8
6056.0
6056.2
Wavenumber ν in cm^{-1}
solar-sim
Solar(G)
CO2
CH4
AllMol
Observed

σ=0.112%, 980401S8.90, φ=65.02^o, OPD=120cm, FoV=1.91$mrad$, Apod.=boxcar

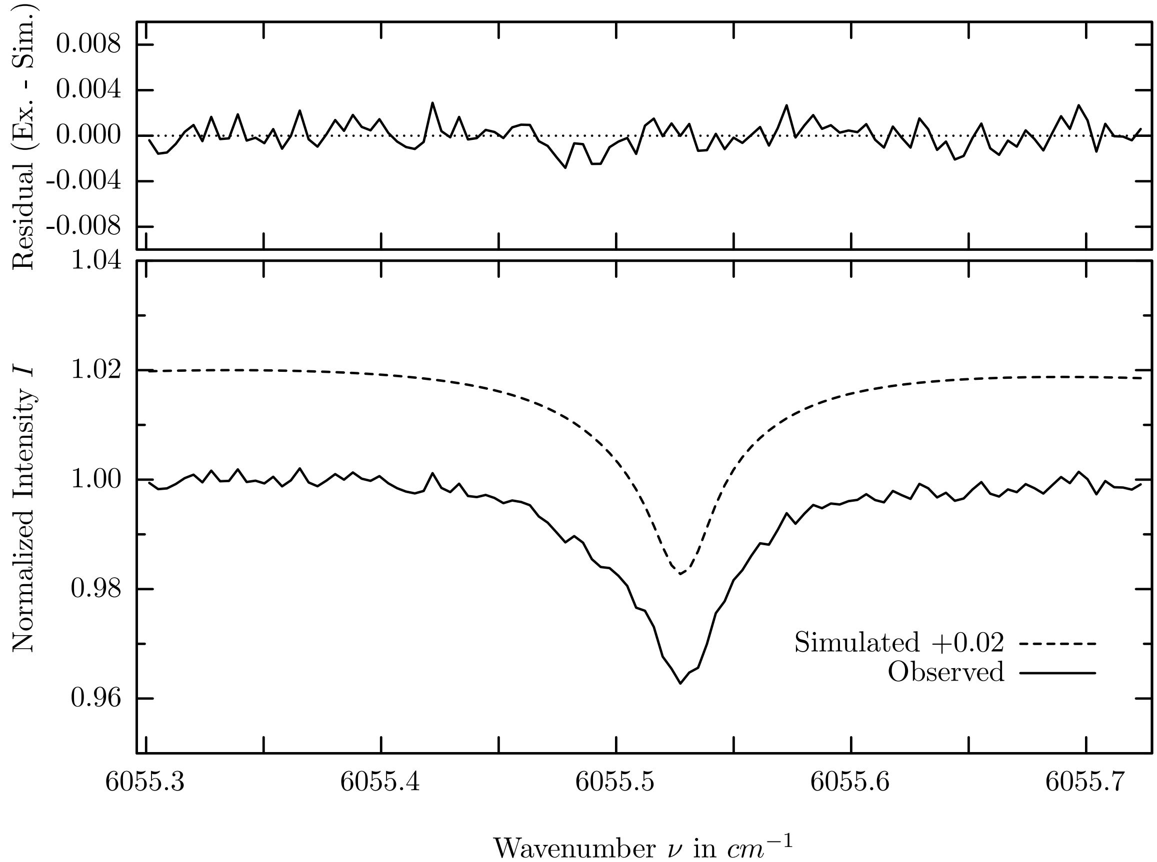

investigated species	:	CH_4
line position(s) ν_0	:	6055.5279 cm^{-1}
lower state energy E''_{lst}	:	62.7 cm^{-1}
retrieved TCA, information content	:	3.79E+19 $molec/cm^2$, 33.1
temperature dependence of the TCA	:	+0.096%/K (trop), +0.083%/K (strat)
location, date, solar zenith angle	:	Kiruna, 1/Apr/98, 65.02^o
spectral interval fitted	:	6055.300 – 6055.725 cm^{-1}

Molecule	iCode	Absorption	Molecule	iCode	Absorption
CH4	61	7.749%	$H2O$	11	0.019%
$CO2$	21	1.238%	CO	51	<0.001%
Solar(G)	—	0.284%	OH	131	<0.001%
Solar-sim	—	<0.001%	HI	171	<0.001%

CO_2, Kiruna, φ=65.02^o, OPD=120cm, FoV=1.91$mrad$, boxcar apod.

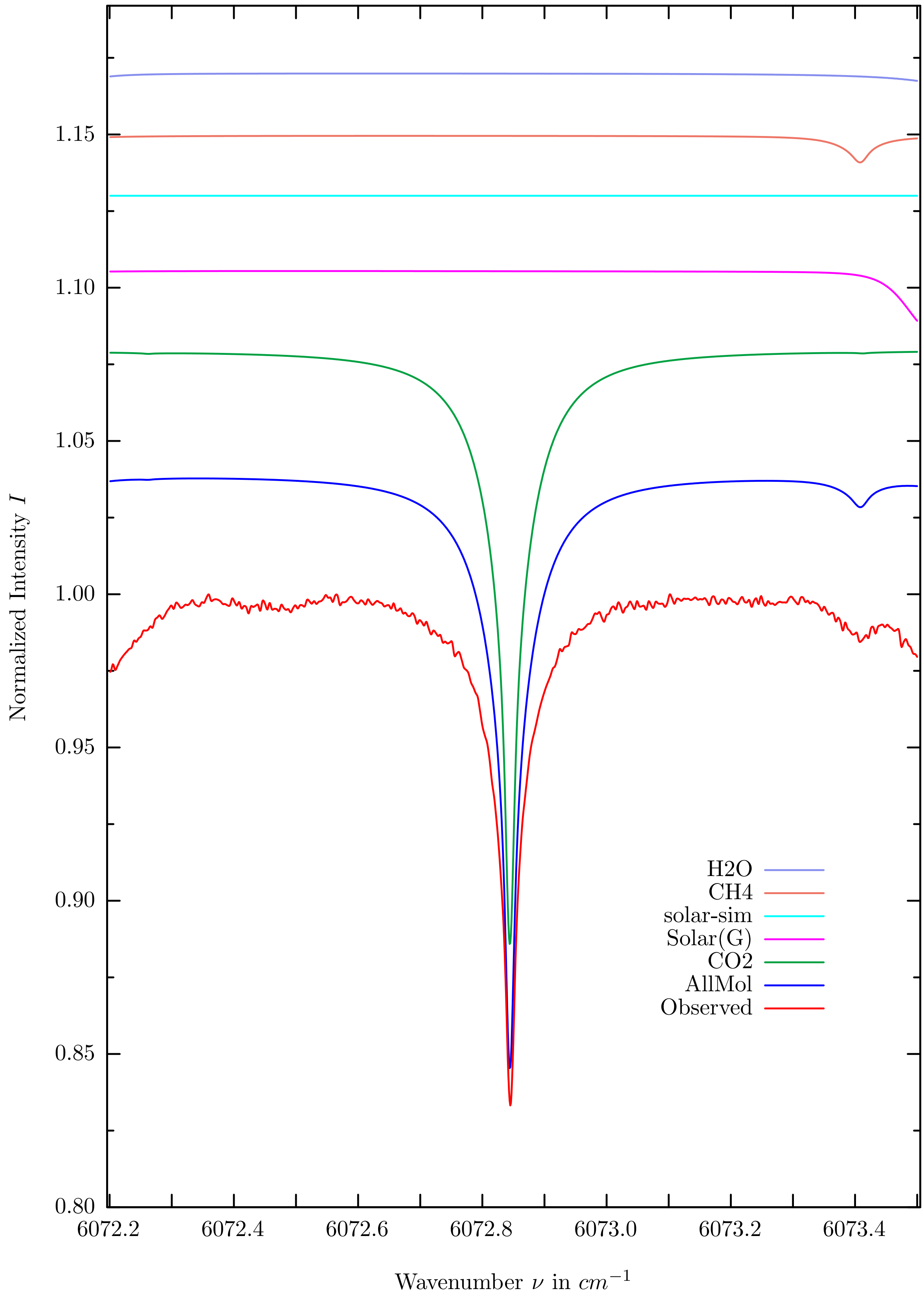

σ=0.110%, 980401S8.90, φ=65.02^o, OPD=120cm, FoV=1.91$mrad$, Apod.=boxcar

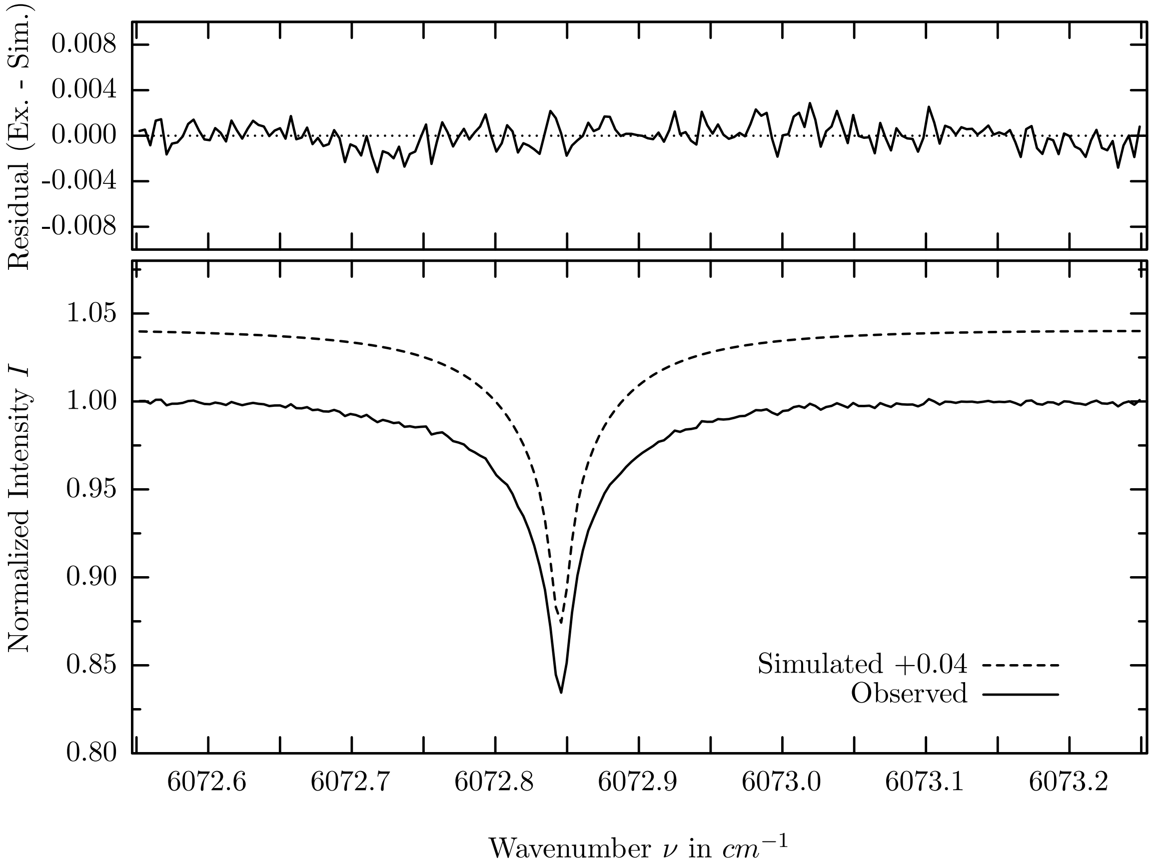

investigated species	:	CO_2
line position(s) ν_0	:	6072.8428 cm^{-1}
lower state energy E''_{lst}	:	7.8 cm^{-1}
retrieved TCA, information content	:	6.38E+21 $molec/cm^2$, 142.0
temperature dependence of the TCA	:	+0.331%/K (trop), +0.073%/K (strat)
location, date, solar zenith angle	:	Kiruna, 1/Apr/98, 65.02^o
spectral interval fitted	:	6072.550 – 6073.250 cm^{-1}

Molecule	iCode	Absorption	Molecule	iCode	Absorption
CO2	21	17.508%	$H2O$	11	0.258%
Solar(G)	—	2.104%	CO	51	<0.001%
Solar-sim	—	<0.001%	OH	131	<0.001%
$CH4$	61	0.914%			

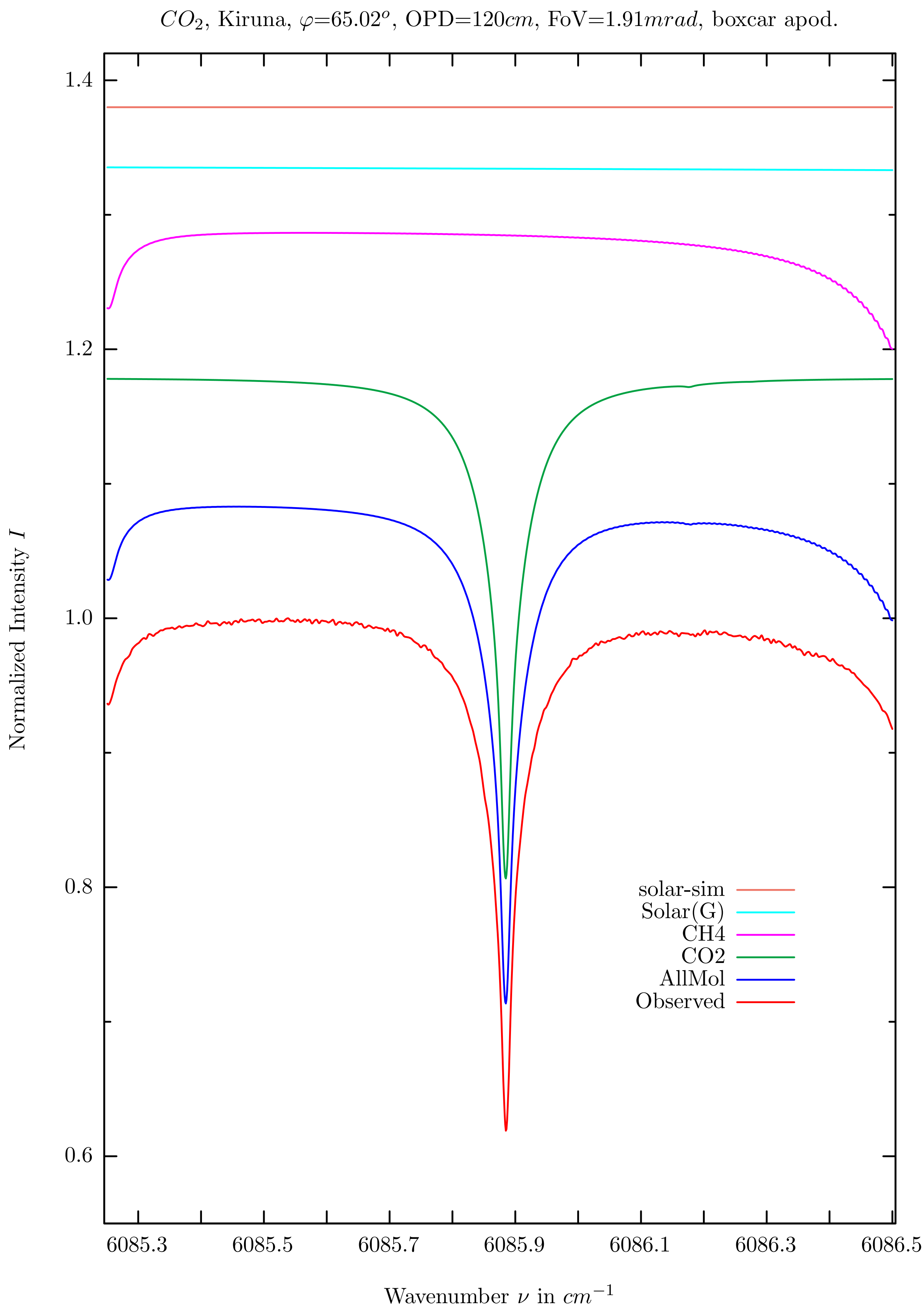

CO_2, Kiruna, φ=65.02^o, OPD=120cm, FoV=1.91$mrad$, boxcar apod.
1.4
1.2
1.0
0.8
0.6
Normalized Intensity I
6085.3
6085.5
6085.7
6085.9
6086.1
6086.3
6086.5
Wavenumber ν in cm^{-1}
solar-sim
Solar(G)
CH4
CO2
AllMol
Observed

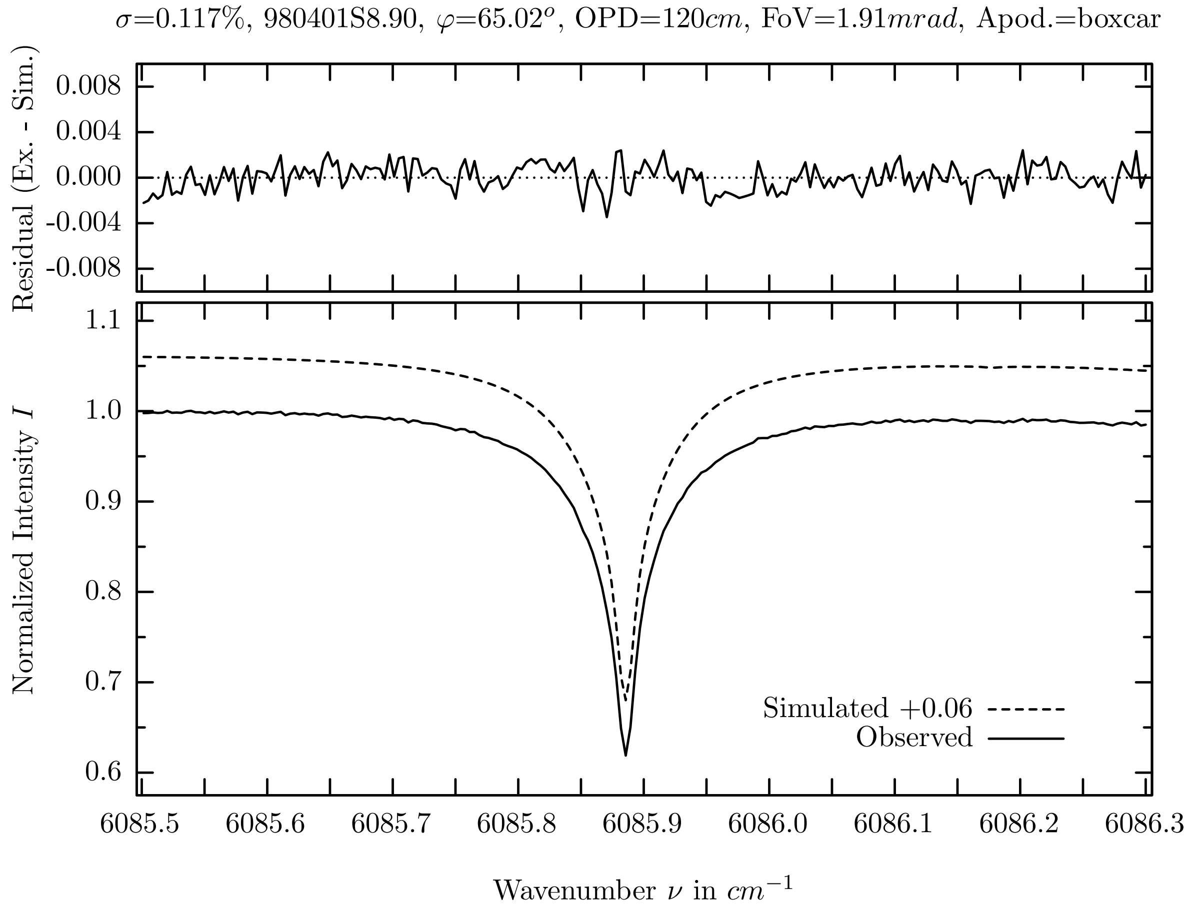

investigated species	:	CO_2
line position(s) ν_0	:	6085.8833 cm^{-1}
lower state energy E''_{lst}	:	60.9 cm^{-1}
retrieved TCA, information content	:	6.30E+21 $molec/cm^2$, 325.8
temperature dependence of the TCA	:	+0.256%/K (trop), +0.034%/K (strat)
location, date, solar zenith angle	:	Kiruna, 1/Apr/98, 65.02^o
spectral interval fitted	:	6085.500 – 6086.300 cm^{-1}

Molecule	iCode	Absorption	Molecule	iCode	Absorption
CO2	21	39.618%	$H2O$	11	0.001%
$CH4$	61	9.247%	CO	51	<0.001%
Solar(G)	—	1.680%	OH	131	<0.001%
Solar-sim	—	<0.001%	HI	171	<0.001%

CO_2, Kiruna, φ=65.02^o, OPD=120cm, FoV=1.91$mrad$, boxcar apod.

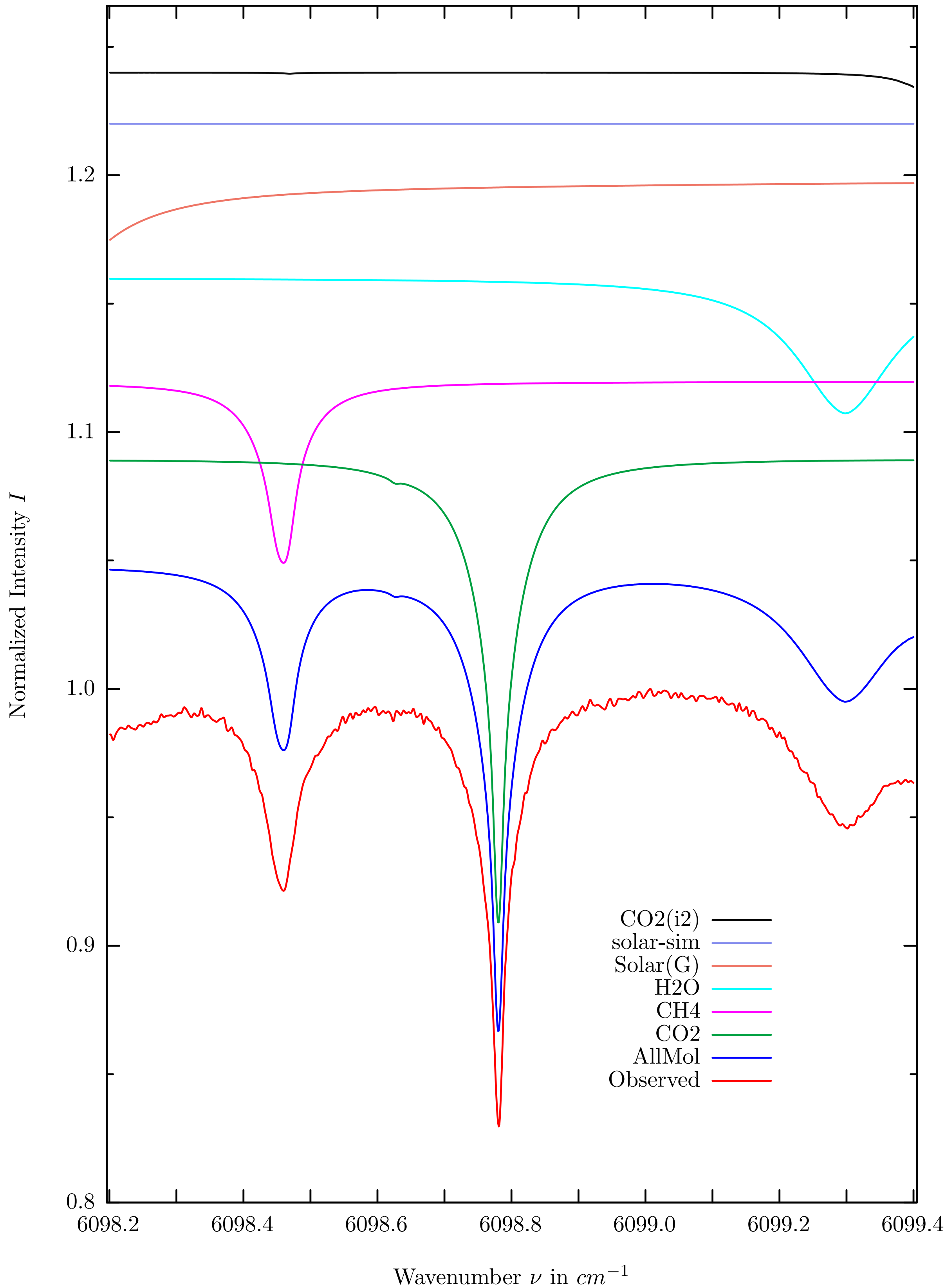

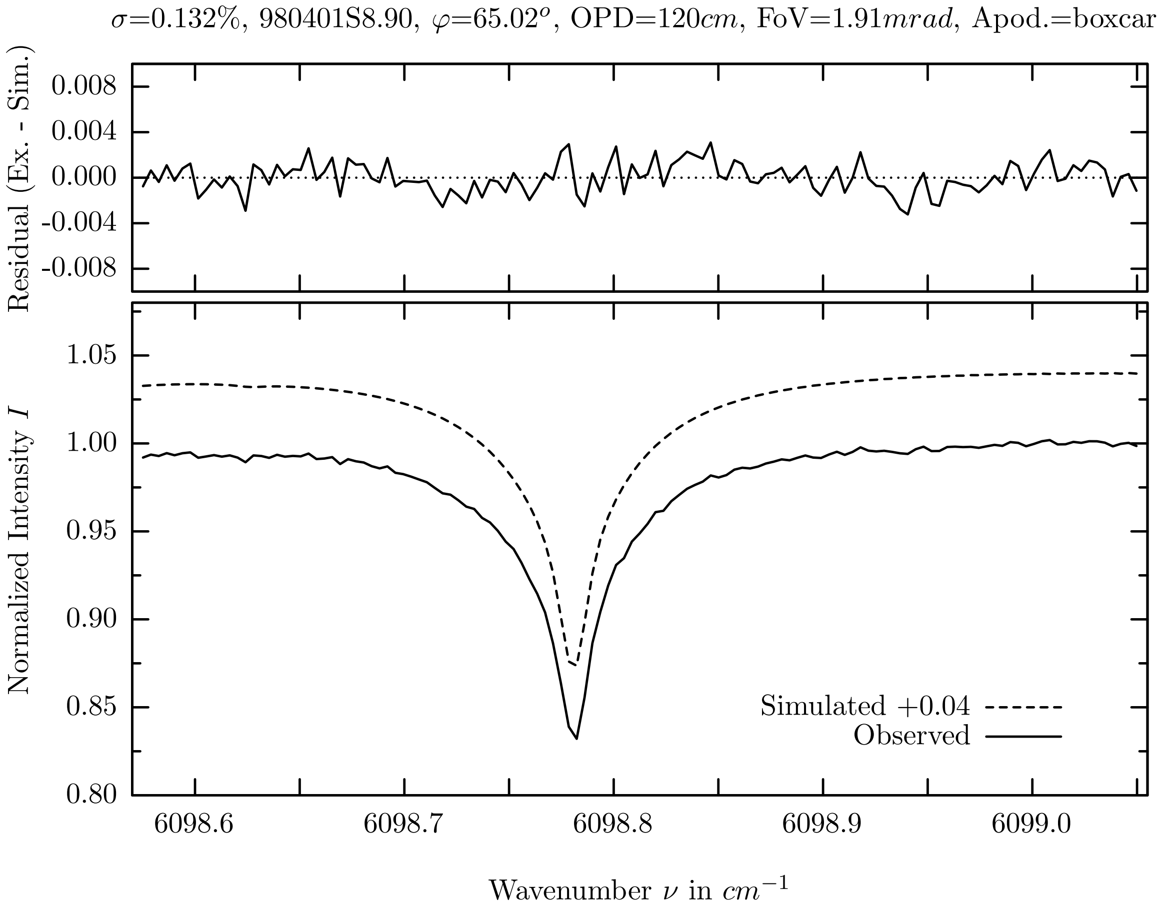

investigated species	:	CO_2
line position(s) ν_0	:	6098.7790 cm^{-1}
lower state energy E''_{lst}	:	362.8 cm^{-1}
retrieved TCA, information content	:	5.96E+21 $molec/cm^2$, 124.3
temperature dependence of the TCA	:	-0.484%/K (trop), -0.120%/K (strat)
location, date, solar zenith angle	:	Kiruna, 1/Apr/98, 65.02^o
spectral interval fitted	:	6098.575 – 6099.050 cm^{-1}

Molecule	iCode	Absorption	Molecule	iCode	Absorption
CO2	21	17.347%	$CO2$	**22**	0.597%
$CH4$	61	7.099%	CO	51	<0.001%
$H2O$	11	5.272%	OH	131	<0.001%
Solar(G)	—	4.017%	HI	171	<0.001%
Solar-sim	—	<0.001%			

H_2O, Kiruna, φ=65.02^o, OPD=120cm, FoV=1.91$mrad$, boxcar apod.

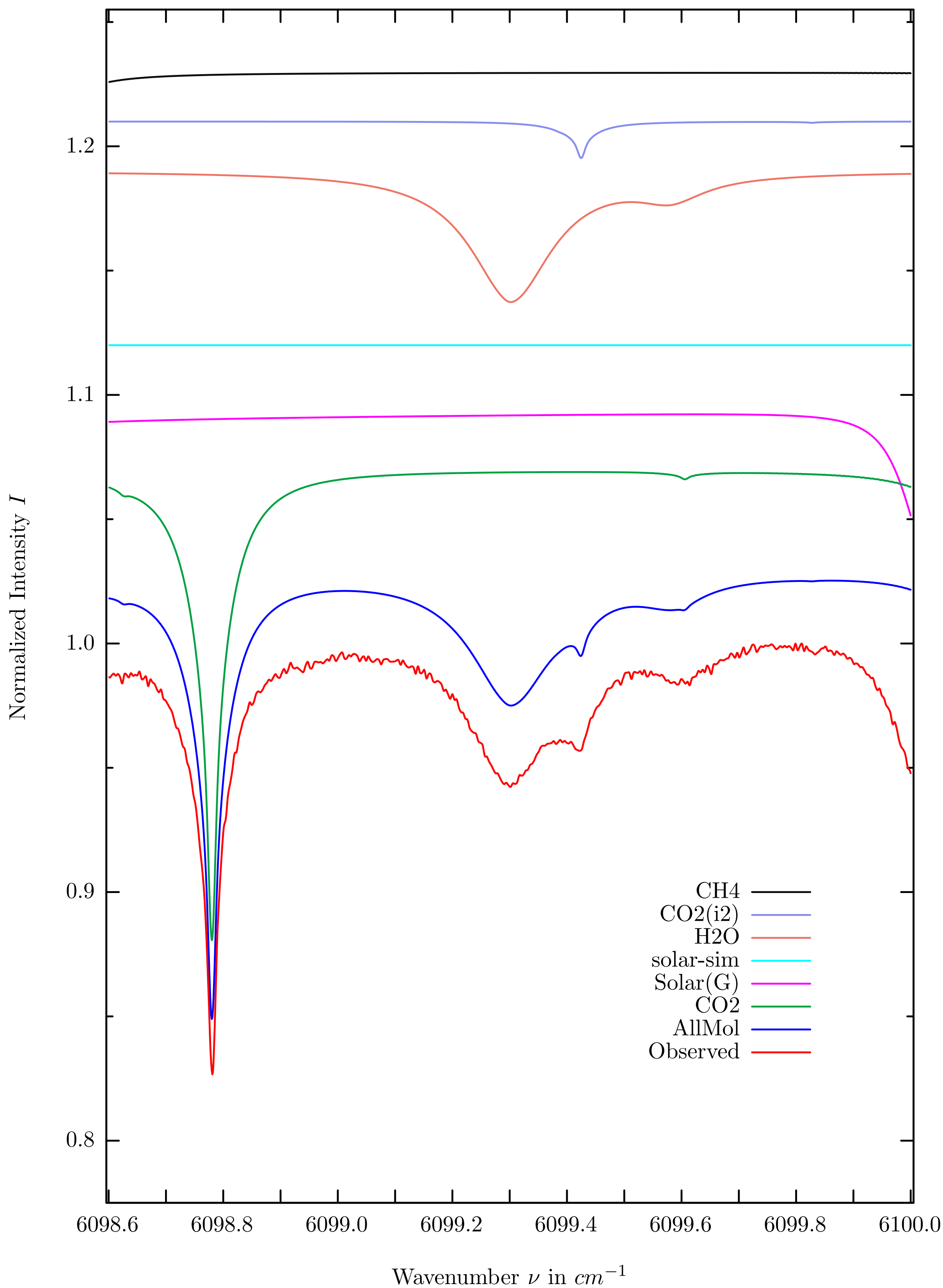

σ=0.158%, 980401S8.90, φ=65.02^o, OPD=120cm, FoV=1.91$mrad$, Apod.=boxcar

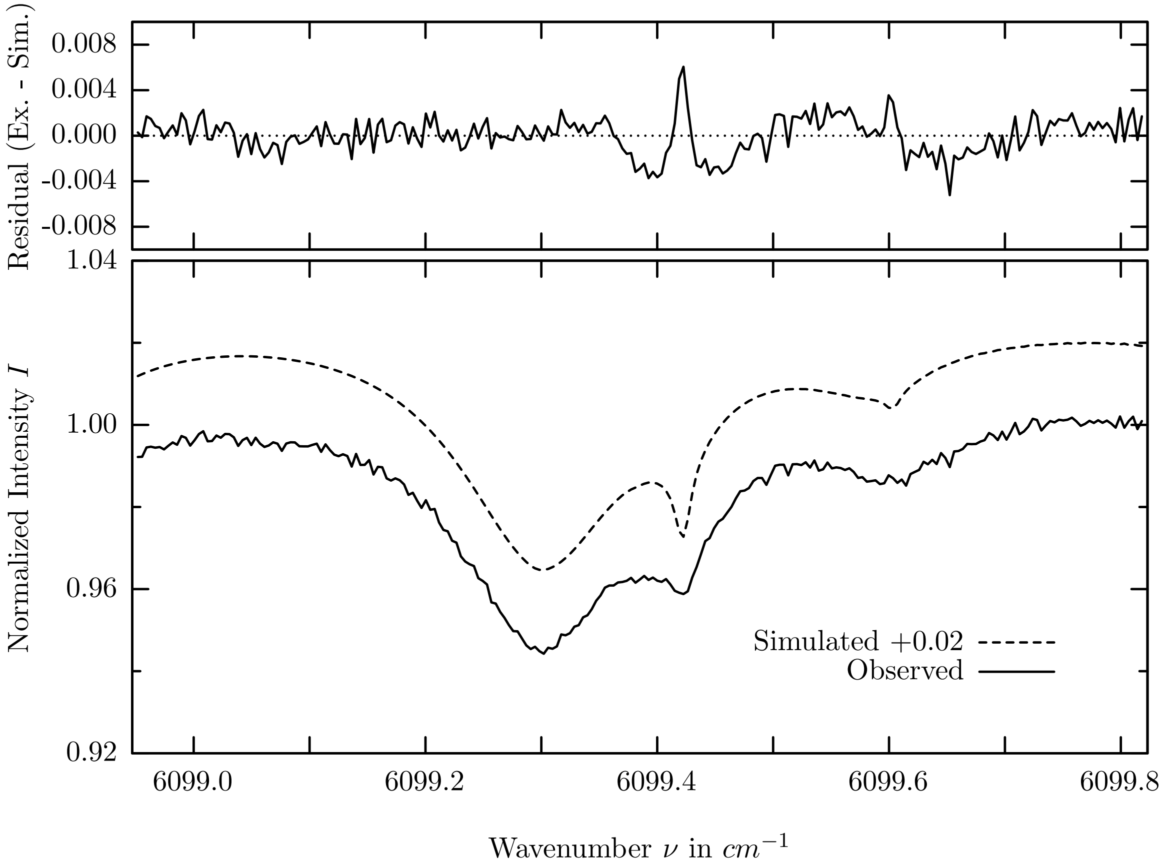

investigated species	:	H_2O
line position(s) ν_0	:	6099.2974 cm^{-1}
lower state energy E''_{lst}	:	136.8 cm^{-1}
retrieved TCA, information content	:	1.24E+22 $molec/cm^2$, 34.9
temperature dependence of the TCA	:	+0.056%/K (trop), -0.008%/K (strat)
location, date, solar zenith angle	:	Kiruna, 1/Apr/98, 65.02^o
spectral interval fitted	:	6098.950 – 6099.820 cm^{-1}

Molecule	iCode	Absorption	Molecule	iCode	Absorption
$CO2$	21	19.120%	$CH4$	61	0.408%
Solar(G)	—	5.929%	CO	51	<0.001%
Solar-sim	—	<0.001%	OH	131	<0.001%
H2O	11	5.268%	HI	171	<0.001%
$CO2$	**22**	1.480%			

CH_4, Kiruna, φ=65.02^o, OPD=120cm, FoV=1.91$mrad$, boxcar apod.

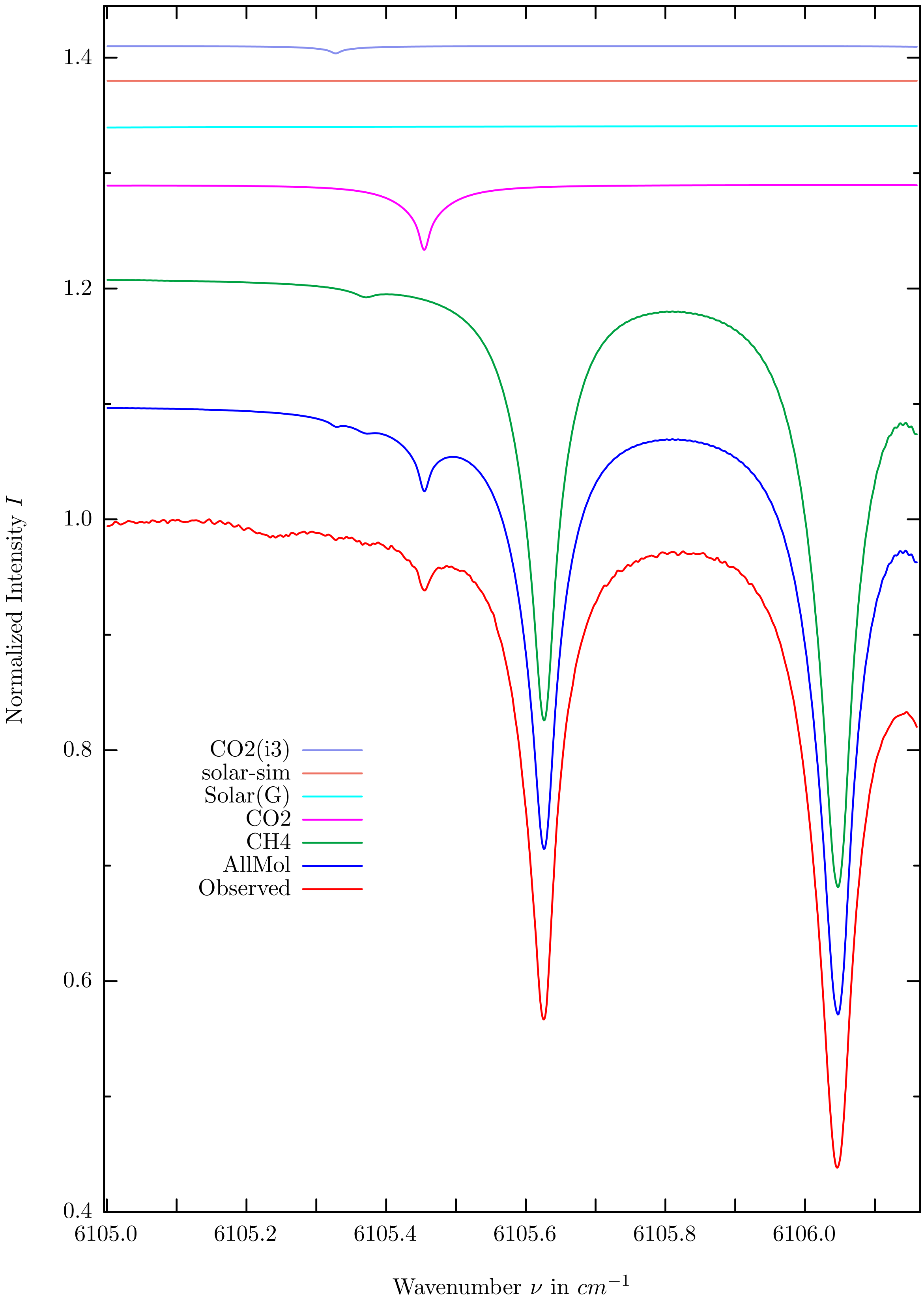

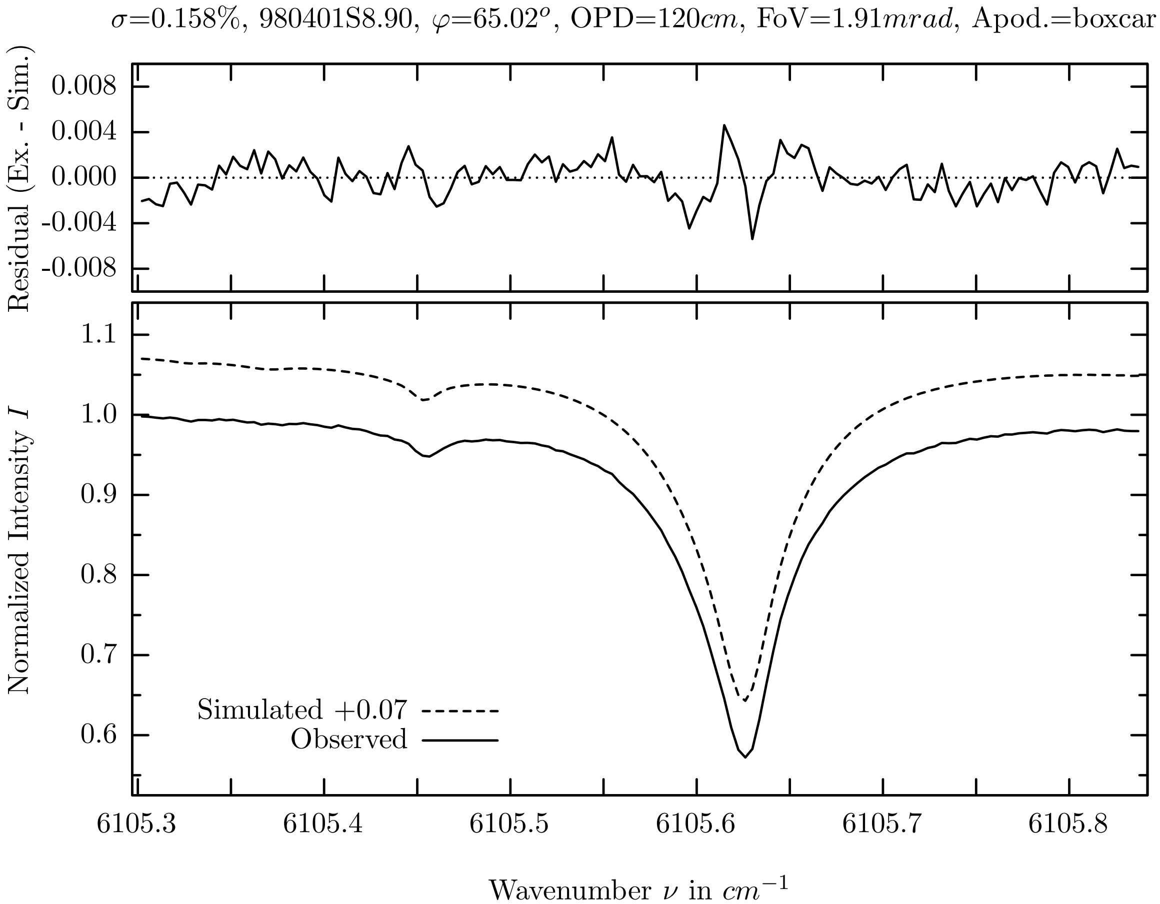

investigated species	:	CH_4
line position(s) ν_0	:	6105.6261 cm^{-1}
lower state energy E''_{lst}	:	470.7 cm^{-1}
retrieved TCA, information content	:	3.86E+19 $molec/cm^2$, 270.5
temperature dependence of the TCA	:	-0.579%/K (trop), -0.133%/K (strat)
location, date, solar zenith angle	:	Kiruna, 1/Apr/98, 65.02^o
spectral interval fitted	:	6105.300 – 6105.840 cm^{-1}

Molecule	iCode	Absorption	Molecule	iCode	Absorption
CH4	61	52.874%	$CO2$	2**3**	0.630%
$CO2$	21	5.674%	$H2O$	11	0.002%
Solar(G)	—	1.049%	CO	51	<0.001%
Solar-sim	—	<0.001%	OH	131	<0.001%

CO_2, Kiruna, φ=65.02^o, OPD=120cm, FoV=1.91$mrad$, boxcar apod.

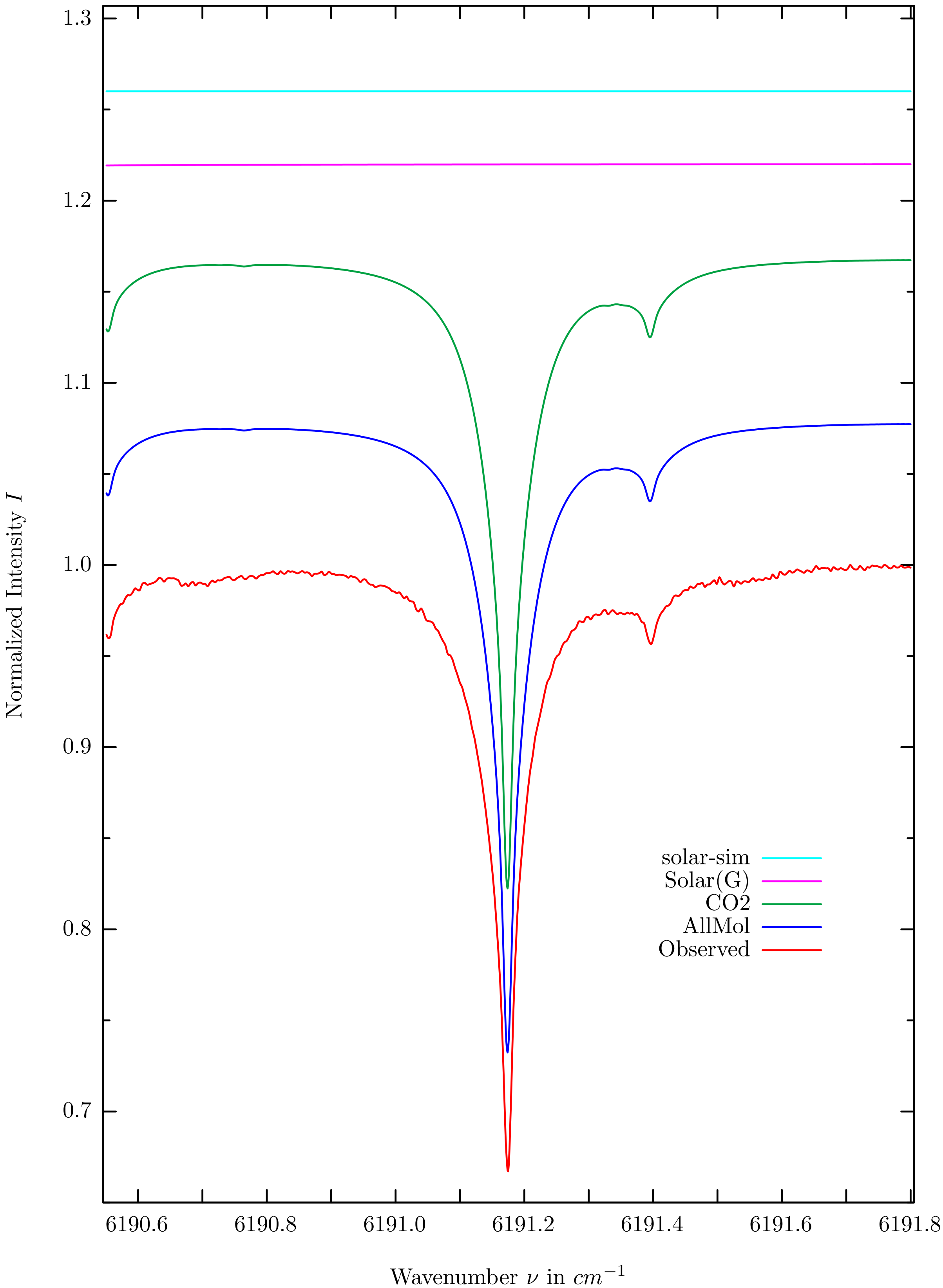

σ=0.113%, 980401S8.90, φ=65.02^o, OPD=120cm, FoV=1.91$mrad$, Apod.=boxcar

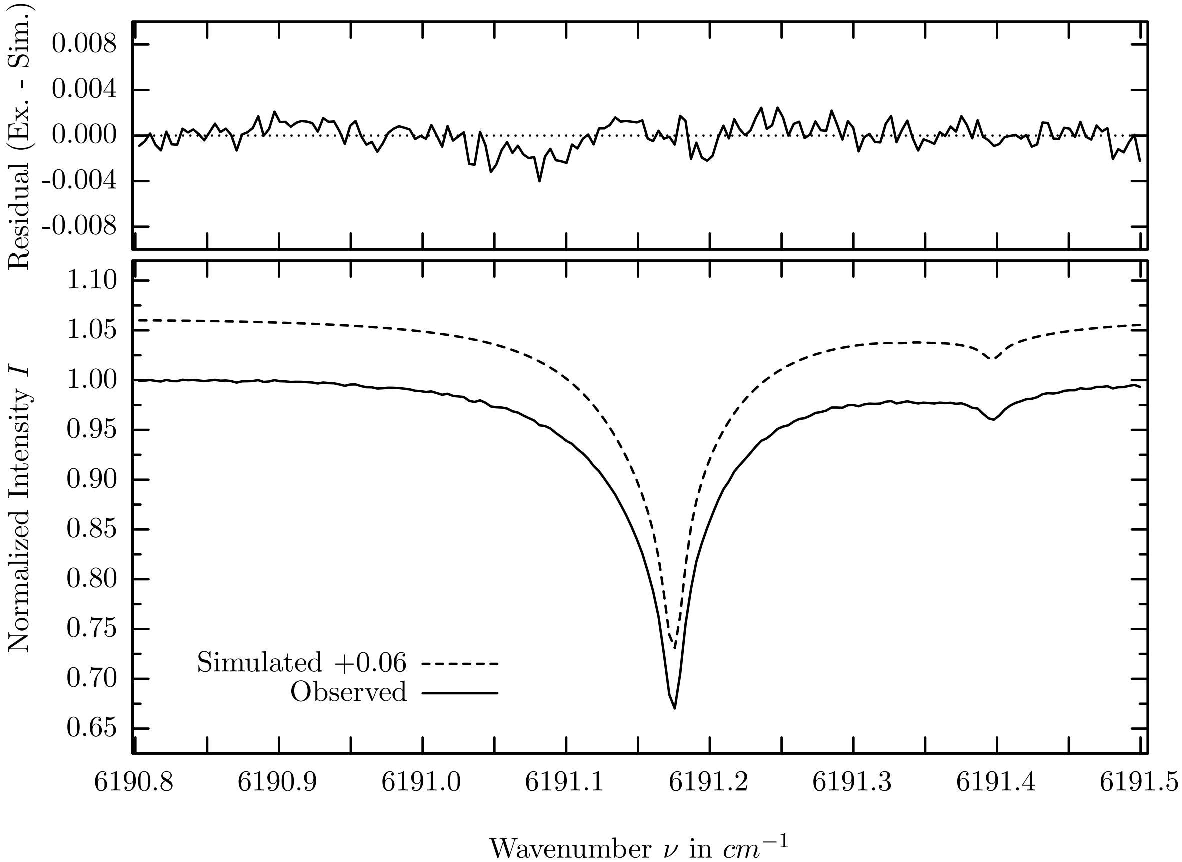

investigated species	:	CO_2
line position(s) ν_0	:	6191.1724 cm^{-1}
lower state energy E''_{lst}	:	639.6 cm^{-1}
retrieved TCA, information content	:	7.30E+21 $molec/cm^2$, 290.8
temperature dependence of the TCA	:	-1.008%/K (trop), -0.295%/K (strat)
location, date, solar zenith angle	:	Kiruna, 1/Apr/98, 65.02^o
spectral interval fitted	:	6190.800 – 6191.500 cm^{-1}

Molecule	iCode	Absorption	Molecule	iCode	Absorption
CO2	21	34.878%	*N2O*	41	<0.001%
Solar(G)	—	0.073%	*CO*	51	<0.001%
Solar-sim	—	<0.001%	*CH*4	61	<0.001%
H2O	11	0.002%	*OH*	131	<0.001%

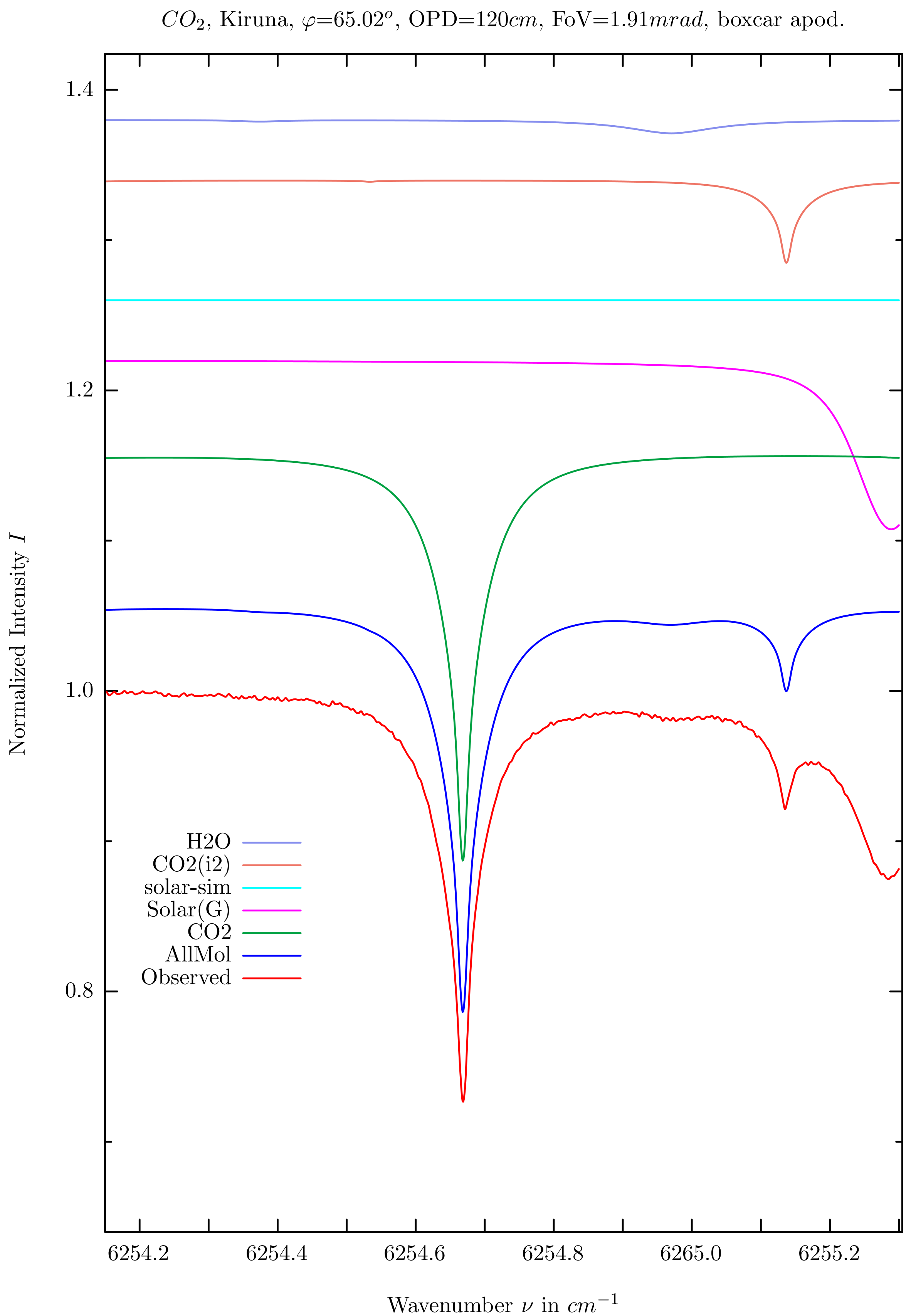
CO_2, Kiruna, φ=65.02^o, OPD=120cm, FoV=1.91$mrad$, boxcar apod.
1.4
1.2
1.0
0.8
Normalized Intensity I
H2O
CO2(i2)
solar-sim
Solar(G)
CO2
AllMol
Observed
6254.2
6254.4
6254.6
6254.8
6265.0
6255.2
Wavenumber ν in cm^{-1}

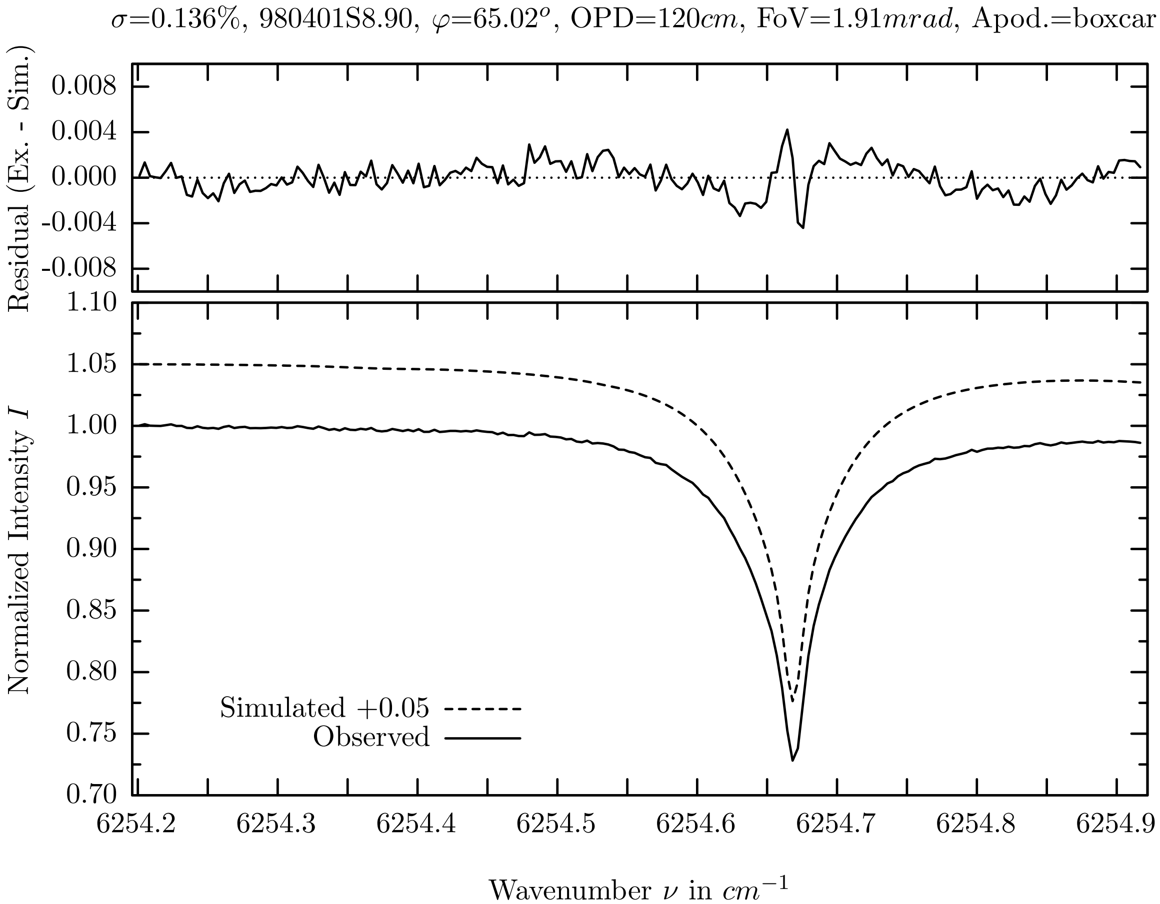

investigated species	:	CO_2
line position(s) ν_0	:	6254.6668 cm^{-1}
lower state energy E''_{lst}	:	704.3 cm^{-1}
retrieved TCA, information content	:	6.79E+21 $molec/cm^2$, 201.8
temperature dependence of the TCA	:	-1.233%/K (trop), -0.297%/K (strat)
location, date, solar zenith angle	:	Kiruna, 1/Apr/98, 65.02^o
spectral interval fitted	:	6254.200 – 6254.920 cm^{-1}

Molecule	iCode	Absorption	Molecule	iCode	Absorption
CO2	21	40.025%	*N2O*	41	0.005%
Solar(G)	—	11.248%	*CO*	51	0.004%
Solar-sim	—	<0.001%	*O2*	71	<0.001%
CO2	2**2**	5.819%	*OH*	131	<0.001%
H2O	11	0.895%	*HI*	171	<0.001%

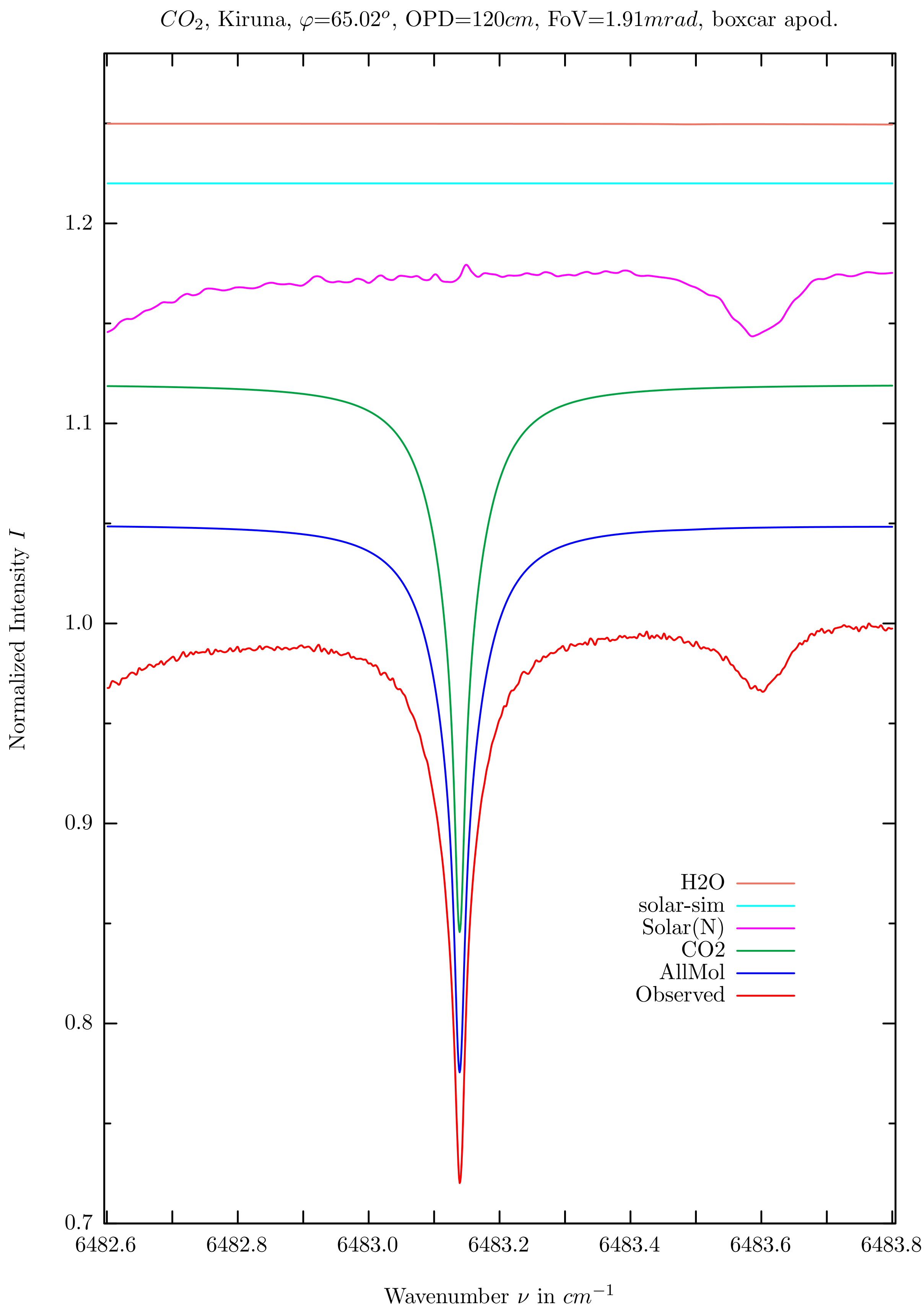

CO_2, Kiruna, φ=65.02^o, OPD=120cm, FoV=1.91$mrad$, boxcar apod.
Normalized Intensity I
Wavenumber ν in cm^{-1}
0.7
0.8
0.9
1.0
1.1
1.2
6482.6
6482.8
6483.0
6483.2
6483.4
6483.6
6483.8
H2O
solar-sim
Solar(N)
CO2
AllMol
Observed

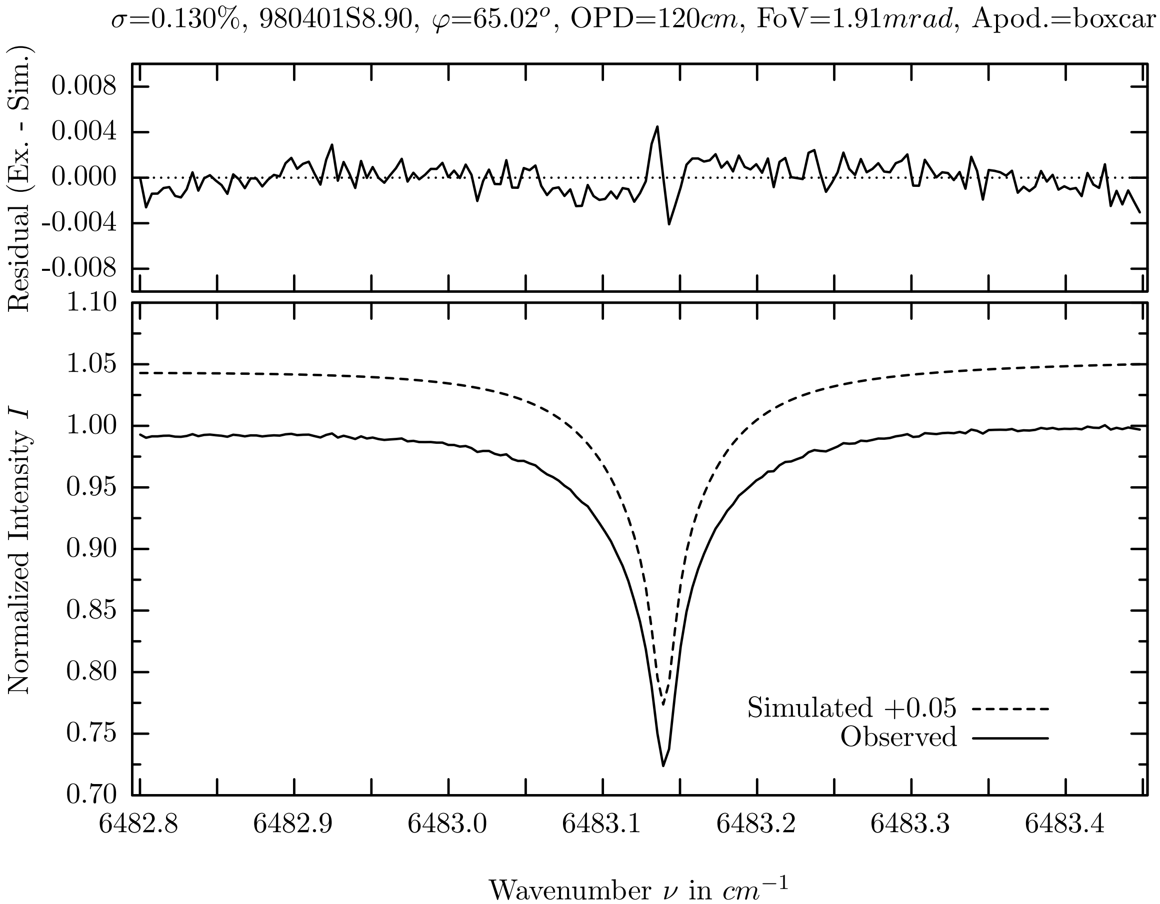

investigated species	:	CO_2
line position(s) ν_0	:	6483.1375 cm^{-1}
lower state energy E''_{lst}	:	234.1 cm^{-1}
retrieved TCA, information content	:	7.43E+21 $molec/cm^2$, 212.8
temperature dependence of the TCA	:	-0.139%/K (trop), -0.056%/K (strat)
location, date, solar zenith angle	:	Kiruna, 1/Apr/98, 65.02^o
spectral interval fitted	:	6482.800 – 6483.450 cm^{-1}

Molecule	iCode	Absorption	Molecule	iCode	Absorption
CO2	21	27.545%	$H2O$	11	0.057%
Solar(N)	—	3.646%	OH	131	<0.001%
Solar-sim	—	<0.001%	HI	171	<0.001%

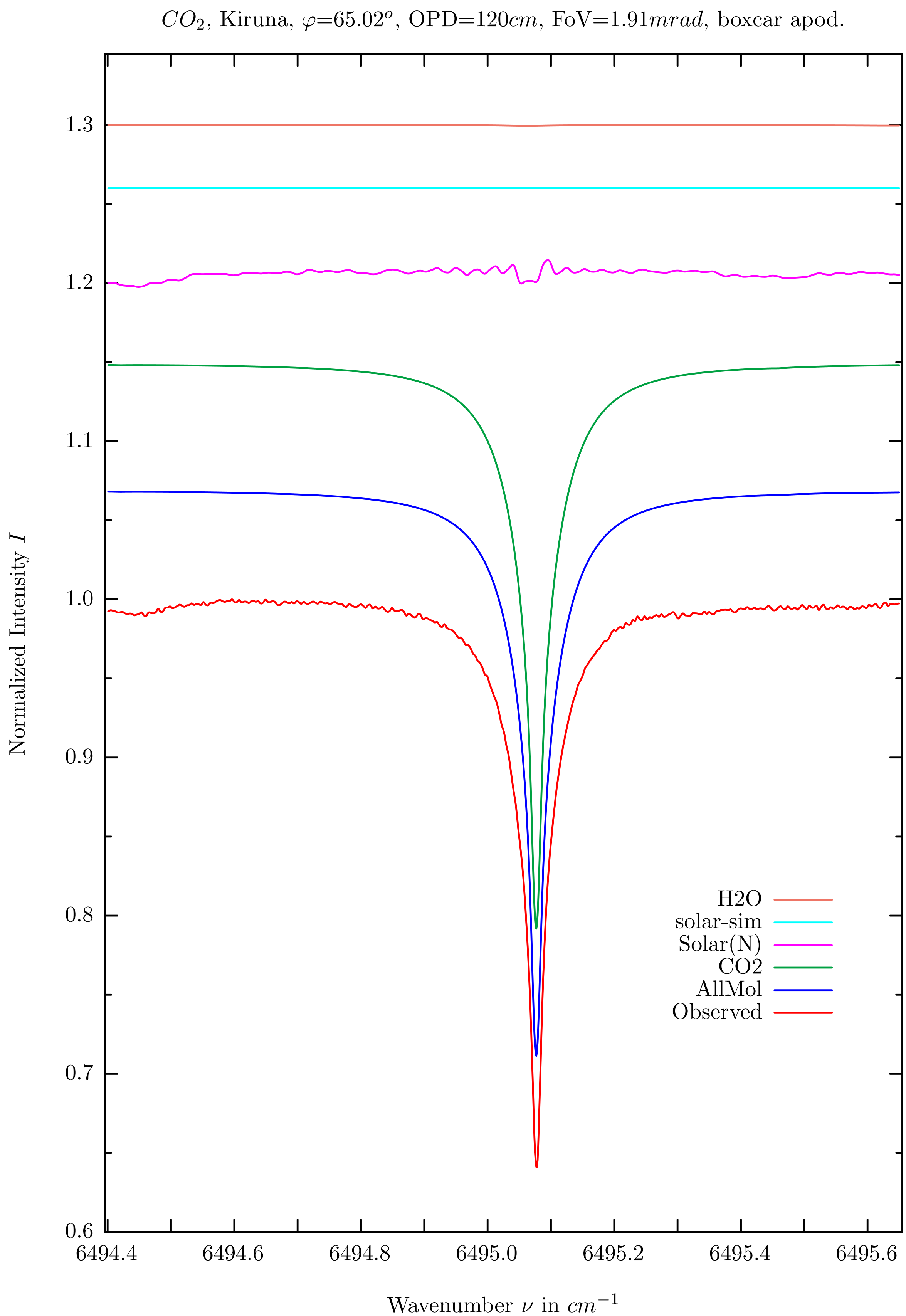

CO_2, Kiruna, φ=65.02^o, OPD=120cm, FoV=1.91$mrad$, boxcar apod.
1.3
1.2
1.1
1.0
0.9
0.8
0.7
0.6
Normalized Intensity I
6494.4
6494.6
6494.8
6495.0
6495.2
6495.4
6495.6
Wavenumber ν in cm^{-1}
H2O
solar-sim
Solar(N)
CO2
AllMol
Observed

σ=0.141%, 980401S8.90, φ=65.02^o, OPD=120cm, FoV=1.91$mrad$, Apod.=boxcar

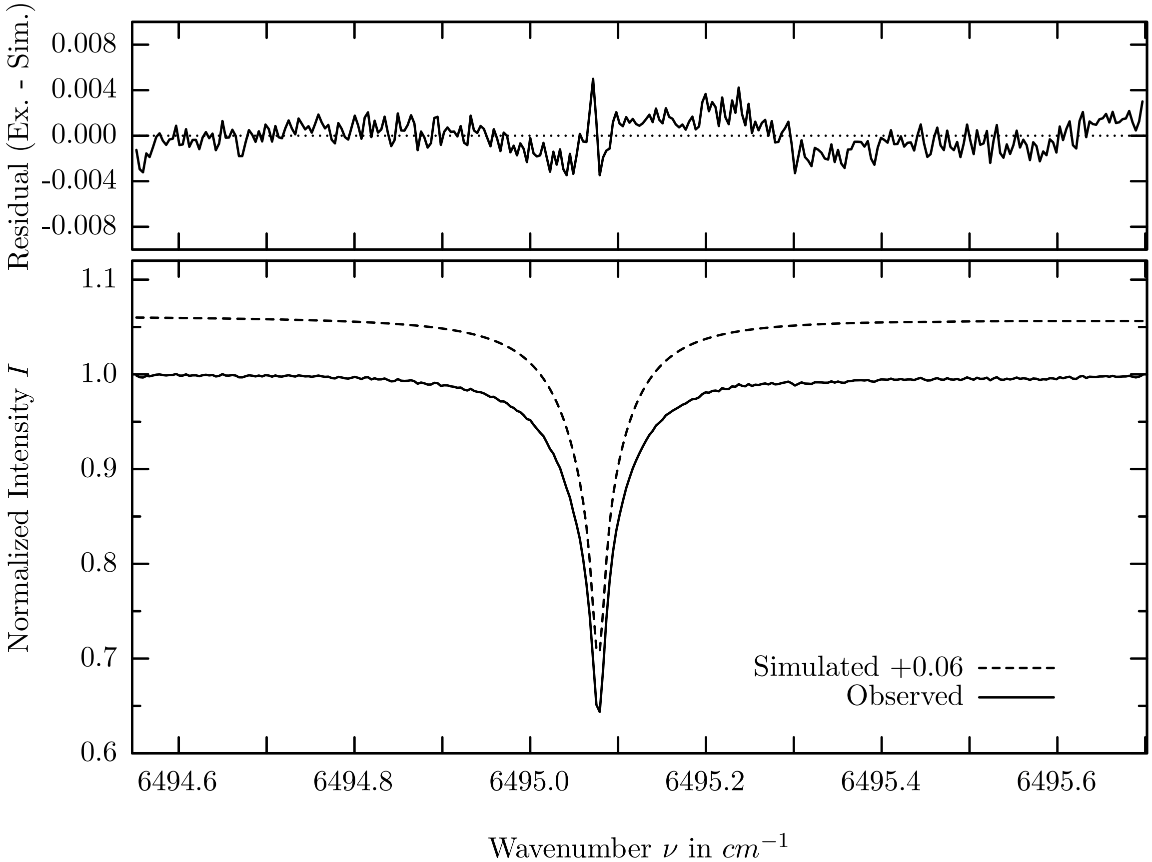

investigated species	:	CO_2
line position(s) ν_0	:	6495.0753 cm^{-1}
lower state energy E''_{lst}	:	42.9 cm^{-1}
retrieved TCA, information content	:	7.23E+21 $molec/cm^2$, 247.9
temperature dependence of the TCA	:	+0.319%/K (trop), +0.049%/K (strat)
location, date, solar zenith angle	:	Kiruna, 1/Apr/98, 65.02^o
spectral interval fitted	:	6494.550 – 6495.700 cm^{-1}

Molecule	iCode	Absorption	Molecule	iCode	Absorption
CO2	21	35.967%	*N2O*	41	<0.001%
Solar(N)	—	1.243%	*OH*	131	<0.001%
Solar-sim	—	<0.001%	*HI*	171	<0.001%
H2O	11	0.063%			

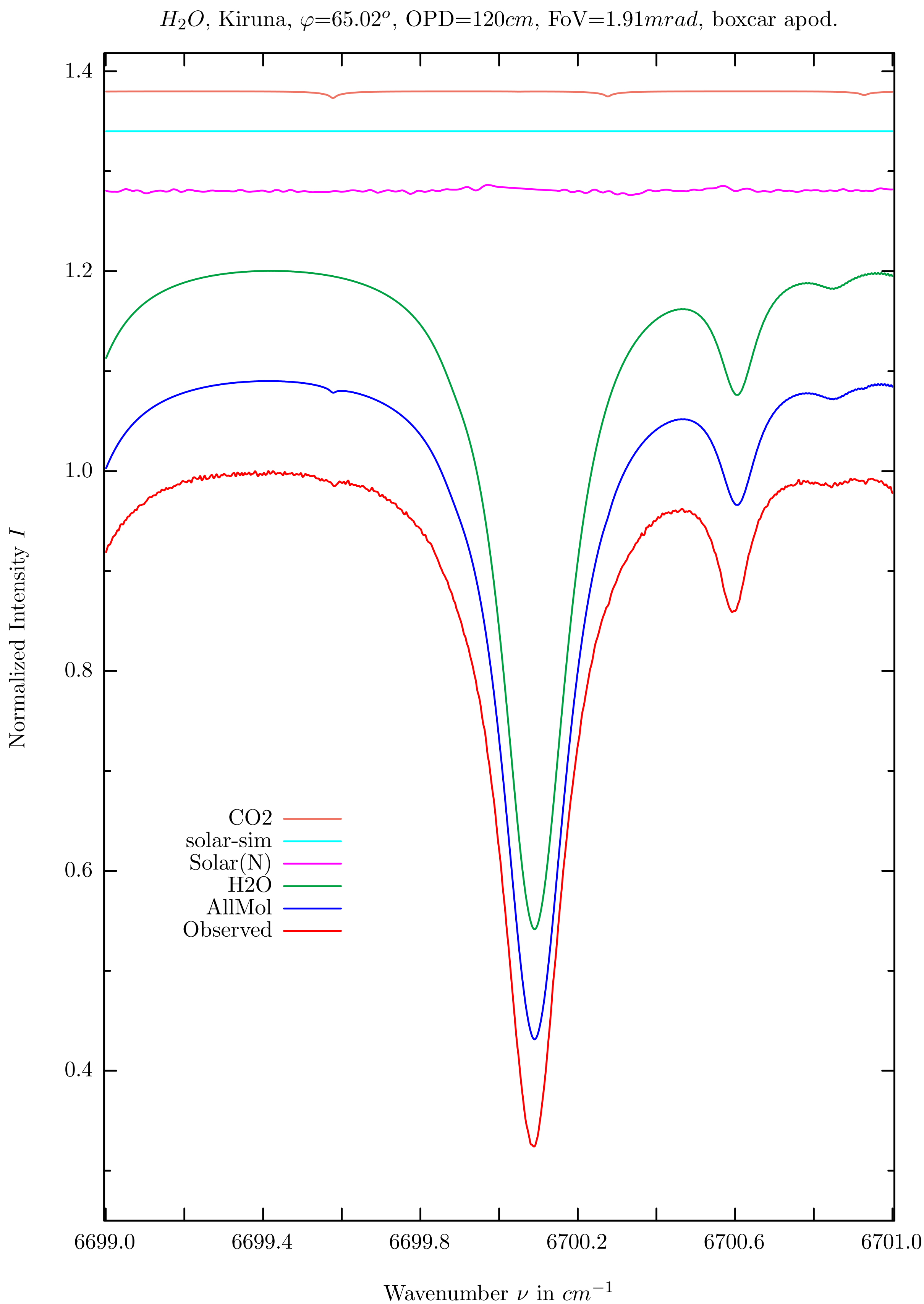

H_2O, Kiruna, φ=65.02^o, OPD=120cm, FoV=1.91$mrad$, boxcar apod.
Normalized Intensity I
Wavenumber ν in cm^{-1}
1.4
1.2
1.0
0.8
0.6
0.4
6699.0
6699.4
6699.8
6700.2
6700.6
6701.0
CO2
solar-sim
Solar(N)
H2O
AllMol
Observed

σ=0.310%, 980401S8.90, φ=65.02^o, OPD=120cm, FoV=1.91$mrad$, Apod.=boxcar

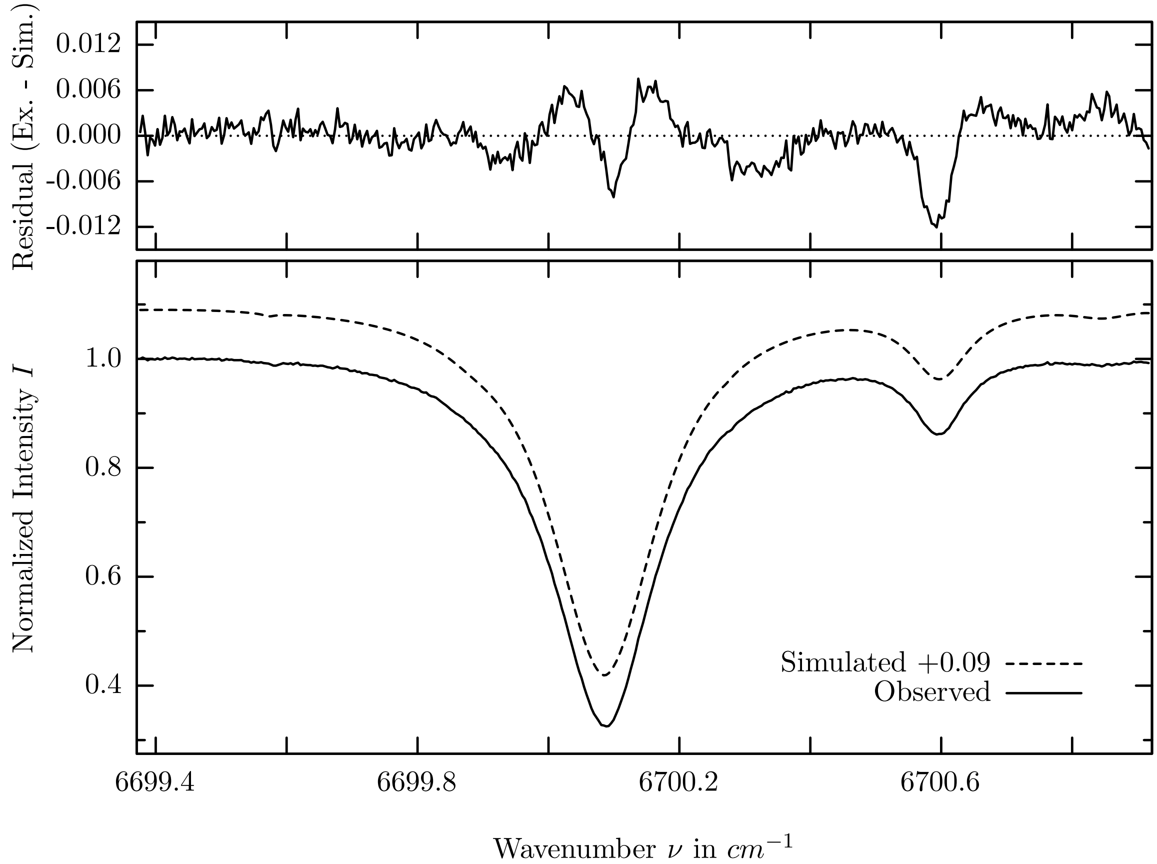

investigated species	:	H_2O
line position(s) ν_0	:	6700.0889 cm^{-1}
lower state energy E''_{lst}	:	300.4 cm^{-1}
retrieved TCA, information content	:	1.02E+22 $molec/cm^2$, 216.4
temperature dependence of the TCA	:	-0.118%/K (trop), -0.020%/K (strat)
location, date, solar zenith angle	:	Kiruna, 1/Apr/98, 65.02^o
spectral interval fitted	:	6699.375 – 6700.920 cm^{-1}

Molecule	iCode	Absorption	Molecule	iCode	Absorption
H2O	11	69.854%	$CO2$	21	0.678%
Solar(N)	—	1.394%	OH	131	<0.001%
Solar-sim	—	<0.001%			

End of Main section.

A Comparison of Kiruna spectra with other selected observation sites

The simulated spectra in the main section of this work depict only one particular observation geometry for one observation site for one particular day. It is beyond the scope of this work to provide complete scenarios for a full range of different observation locations, altitudes, seasons, etc, etc. This appendix tries to meet some of these shortcomings by comparing the observed Kiruna ground-based spectra in 5 selected micro-windows with comparable observations from a number of other well-established sites and mobile observation platforms.

Many colleagues have followed our call to provide us with sample spectra resulting in a near-complete list of scientific groups and observation sites that make up the NDSC-IRWG (Network for Detection of Stratospheric Change Infra-Red Working Group http://www.ndsc.ws). Volunteer participants were asked to provide one typical example spectrum each for the $ClONO_2$ window near $780.2cm^{-1}$, the HNO_3 windows from 865 to $875cm^{-1}$, the HCl window near $2925.9cm^{-1}$, the HF window near $4038.9cm^{-1}$ and one sample each for a humid and a dry day for the HDO window near $2612.5cm^{-1}$. Participants were also asked to match the spectral resolution of $0.004cm^{-1}$, an integration time of approximately 10 minutes and an astronomical solar zenith angle of close to 70^o where possible.

Additionally, participants were encouraged to provide unique spectra of particular interest. In this latter category we are able to present lunar spectra, spectra featuring the signatures of polar stratospheric ice clouds (PSCs), spectra recorded from aboard aircrafts, an event of tropospheric HCl pollution, solar spectra recorded through the plume of bush-fires, spectra taken more than 20 years apart, and ship-borne spectra recorded near the equator. Many thanks to everyone involved. This is to our knowledge the first time such an overview with global geographical coverage has been attempted.

A.1 Description of participating observation sites

In table A1.1 we give an overview over the locations and elevations of established NDSC or NDSC related observation sites, many of which provided sample spectra. The global network spans from pole to pole but is sparse in the tropical region. In the following paragraphs we provide some information on the sites and research groups that sent sample spectra followed by a graphical representation of their data. In some cases the sample spectra were subjected to a minor frequency re-calibration before plotting to ease direct comparison with the Kiruna spectra. The sites are discussed in order of latitude from north to south. For details on the stations and research groups, please consult the Literature list or visit the NDSC home-page at http://www.ndsc.ws.

A.1.1 Eureka, Canadian Arctic

Spectra from the Eureka site were provided by Hans Fast and Richard L. Mittermeier, Meteorological Service of Canada, 4905 Dufferin Street, Toronto, ON., M3H 5T4, Canada and their collaboration partner Yukio Makino, Japan Meteorological Agency, 1-3-4, Ote-Machi, Chiyoda-ku, Tokyo, 100-8122 Japan. The site in the high Canadian Arctic is equipped with a commercial Bomem DA-8 spectrometer typically operated at a maximum optical path difference (OPD) of 250cm. The instrument is one of the few instruments in the NDSC community capable of lunar observations – a valuable feature in a location where polar night lasts several months. For more details on the instrument and observation site see (Fast et al., 2000, Makino et al., 2000, Bell, 2001).

Table A1.1: List of established observation sites (most of which have NDSC status) and the location of 2 campaigns using mobile instruments (indicated by $^{*)}$). The observation sites are ordered by latitude.

Observation site	Latitude	Longitude	Elevation
Eureka, Canada	80.05 ^{o}N	86.42 ^{o}W	610m
Ny-Ålesund, Spitsbergen	78.92 ^{o}N	11.94 ^{o}E	20m
Kiruna, Sweden	67.84 ^{o}N	20.41 ^{o}E	419m
Poker Flat RR, Alaska	65.119^{o}N	147.433^{o}W	505m
Harestua, Norway	60.217^{o}N	10.753^{o}E	596m
Bremen, Germany	53.107^{o}N	8.854^{o}E	27m
Jetstream campaign (NPL)$^{*)}$	≈52.0^{o}N	≈1.0^{o}W	8000m
NPL Teddington, UK	51.424^{o}N	0.343^{o}W	30m
Zugspitze, German Alps	47.422^{o}N	10.987^{o}E	2964m
Jungfraujoch, Swiss Alps	46.549^{o}N	7.986^{o}E	3580m
Moshiri, Japan	44.367^{o}N	142.267^{o}E	280m
Toronto, Canada	43.66 ^{o}N	79.40 ^{o}W	174m
Rikubetsu, Japan	43.457^{o}N	143.766^{o}E	370m
Mt Bancroft, California	37.584^{o}N	118.235^{o}W	3801m
Denver, Colorado	36.673^{o}N	104.963^{o}W	1643m
Billings, Oklahoma	36.605^{o}N	97.485^{o}W	317m
Tsukuba, Japan	36.048^{o}N	140.116^{o}E	31m
Table Mountain, California	34.382^{o}N	117.677^{o}W	2258m
JPL Pasadena, California	34.200^{o}N	118.172^{o}W	350m
Kitt Peak, Arizona	31.90 ^{o}N	111.60 ^{o}W	2090m
Teneriffe, Canarian Islands	28.294^{o}N	16.490^{o}W	2367m
Mauna Loa, Hawaii	19.539^{o}N	155.578^{o}W	3398m
2.8 and 12.8^{o}S. Polarstern cruise (AWI)$^{*)}$	2.8–12.8^{o}S	25.5^{o}W	20m
Maido Summit, Reunion	21.071^{o}S	55.387^{o}E	2203m
Wollongong, Australia	34.45 ^{o}S	150.88 ^{o}E	30m
Lauder, New Zealand	45.045^{o}S	169.684^{o}E	370m
Arrival Heights, Antarctica	77.83 ^{o}S	166.67 ^{o}E	200m
South Pole, Antarctica	89.83 ^{o}S		2850m

In addition to this list NASA's space-borne ATMOS instrument that provided many of the solar spectra shown in the main part of the atlas ought to be mentioned.

A.1.2 Ny-Ålesund, Svalbard (European Arctic)

The Ny-Ålesund site is operated by the Alfred–Wegener Institute for Polar and Marine Research in Potsdam, Germany. Since March 1992 FTIR measurements are performed regularly using the sun as a light source (e.g. Notholt et al., 1993, 1994, 1995, 1997, and 2000). At the latitude of Ny-Ålesund the sun is below the horizon between the middle of October and the middle of March (the same applies to Eureka). In December 1992 the system has been modified to use additionally the moon as light source during the polar night, providing the first such measurements in the field (Notholt et al., 1993, 1994a, and 1995b, Meier 1997, Becker et al., 2000, Notholt and Lehman 2003).

The sample spectra were provided by two former staff: Justus Notholt, who recently took up a professorship with the Institute of Environmental Physics, University of Bremen - FB1, Postfach 330440, D-28334 Bremen, Germany and Arndt Meier, one of the authors. The current scientist in charge at Alfred-Wegener Institute is Astrid Schulz, Alfred-Wegener Institute, Telegrafenberg A43, D-14473 Potsdam, Germany. The total column amounts reported were retrieved by A. Meier. The 1995 solar spectra were recorded with a commercial Bruker 120M spectrometer and have been discussed in much detail as part of an NDSC instrumental inter-comparison (Paton-Walsh et al., 1997). The 1996 solar and lunar spectra were recorded with the new Bruker 120HR spectrometer that was deployed in late 1995. The existing 120M was re-fitted and has since been used as a mobile instrument, notably on the Polarstern cruises (see below).

A.1.3 Kiruna, Arctic Sweden

Measurements in Kiruna have been carried out on a regular basis since Mar 1996 and on a campaign basis since 1989. Early measurements were established by the *Institut für Meteorologie und Klimaforschung* (IMK, Institute of Meteorology and Climate Research), Forschungszentrum Karlsruhe, Germany, with a mobile Bruker IFS 120M instrument. In 1996 a formal collaboration between IMK Karlsruhe, the Swedish Institute of Space Physics (*Institutet för Rymdfysik* IRF), and the Japanese STELAB at University of Nagoya was established. The instrument was replaced with the more sophisticated 120HR model and given a new home at IRF Kiruna and has been in quasi-continuous operation since. Kiruna became the world's 2nd instrument to regularly record lunar spectra. Unlike the high arctic sites it offers 9 full moon phases a year where complete diurnal observations are possible by combining solar and lunar measurements (weather permitting).

The lunar spectra included in this appendix were recorded at a lower spectral resolution (45cm OPD) and integrated over a longer time (1 hour) to achieve an acceptable signal to noise ratio. The lunar absorption spectra were supplemented with two sets of emission spectra pointing the sun-tracker away from the moon at a high and a low zenith angle each and a set of spectra from an external hot blackbody using otherwise the same geometry and instrumental settings to obtain a high quality phase spectrum. The phase spectrum of the blackbody measurements was used to re-transform the interferograms from the emission measurements using the superior phase information from the hot blackbody (see Brault, 1987, for a detailed discussion on the advantages). A weighted combination of the phase corrected low and high zenith angle emission spectra matching the airmass-factor for the time of measurement of the absorption spectra was then calculated and subtracted from the lunar absorption spectrum for wavenumbers below $2000cm^{-1}$ resulting in the lunar absorption spectrum used for analysis (at higher wavenumbers the emission is negligible). This approach eliminates the need to take emission explicitly into account in the analysis allowing to use the same retrieval algorithms as for solar spectra at the price of adding some additional noise (from the emission spectra) and under the assumption that temperatures stayed fairly constant throughout the course of the measurements (which was a justified assumption in the given case). For a more in-depth discussion of lunar spectra see Meier, 1997.

The spectra shown were prepared by former IRF staff Arndt Meier. For recent observations and current activities in Kiruna please contact Thomas Blumenstock, IMK (see section Teneriffe).

The Kiruna solar spectra shown are the same as discussed throughout the main section of this book and the same ones as provided in electronic form on the supplemental DVD-ROM disk. All figures in this appendix feature the Kiruna spectra as the reference against which the sample spectra from other sites are being compared. The Kiruna spectra are shifted for clarity by either 0.1 or 0.2 relative intensity units for clarity and shown in a light grey shade. For more details please refer to previous chapters in this work and publications such as Meier et al., 1998, Blumenstock et al., 1997, 1998, and 2000, Höpfner et al., 2001.

A.1.4 Harestua, Norway

The Bruker 120M spectrometer at Harestua, located about 60km north of the Norwegian capital Oslo, is operated by Chalmers University, Gothenburg, Sweden. Operation as part of the NDSC was established in 1996 by the same group, then affiliated with *Institutet för Vatten och Luftvårdsforskning* IVL (Swedish Institute of Water and Clean Air Research), Gothenburg. The sample spectra were provided by Anders Strandberg, Johan Mellqvist and Bo Galle (contact: Anders.Strandberg@rss.chalmers.se). Observations and data analysis methods have been described e.g. in Galle et al., 1999 and 2000, Galle 1999, Mellqvist 1999, Mellqvist et al., 2002, Paton-Walsh et al., 1997.

A.1.5 NPL Teddington, UK (mobile instrument)

The FTIR group at the National Physics Laboratory headed by Peter Woods is well known for their key role in NDSC audited instrumental side-by-side intercomparisons in which their mobile Bruker IFS 120M has been used as a de facto comparison standard (e.g. Paton-Walsh, 1997, Goldman et al., 1999, Griffith et al., 2003, Bell et al, 2001). Although not carrying out continuous measurements at any fixed location, the group has undertaken a number of very interesting campaigns under often challenging conditions. Clare Murphy (formerly C. Paton-Walsh) has selected and made available spectra from 3 such campaigns. One set is discussed here, while the ClO Observations above Aberdeen and the tropospheric HCl pollution event are presented in Appendix B

Aircraft data:
Example solar absorption spectra recorded from a Jetstream aircraft at a cruising altitude of 8km. The 5 sample spectra Jethdo.0; jethcl.0; jethfcut.0; jethno3.0, and jetclno3.0 were taken on 8th March 1995 using a Bruker 120M at 180cm OPD with boxcar apodisation and with a field of view of 6.4 mrads (long wavelengths) and 5 mrads (shorter wavelengths). HF, HCl, and HDO use 7 co-added spectra; HNO3 and ClNO3 use 4 co-added spectra; all taken at a scan speed of 40kHz. The data were all taken at an approximate latitude of 52^{o}N with longitude varying from 0.5^{o}E to 2.5^{o}W. Measurements by Clare Paton-Walsh and William Bell, NPL.

For further information Peter Woods may be contacted at NPL, Queens Rd, Teddington, TW11 0LW, UK, peter.woods@npl.co.uk. Clare Murphy has since moved to Australia and is presently a member of the Wollongong FTIR group, email clarem@uow.edu.au.

A.1.6 Jungfraujoch, Swiss Alps

Since the early 1950s solar infrared spectra have been recorded regularly at the Jungfraujoch station, making it the longest record we have in this field to date. It provided direct evidence for the absence of freons during the early years of measurements at the Jungfraujoch, thus proving their man-made origin (see e.g. Brown et al., 1992). The high altitude makes it an excellent location for stratospheric research given the low amount of water vapour. What is more, interferences from tropospheric gases are reduced, because the lower ground pressure reduces the pressure-broadened line widths as compared to low altitude sites.

The University of Liège group of R. Zander, L. Delbouille, P. Demoulin, E. Mahieu, and co-workers operate 2 FTIR spectrometers at the site, a home-built instrument and (more recently) a customised Bruker IFS 120HR[6]. Both instruments are regularly operated simultaneously (for more than 10 years by now) to guarantee continuity of the measurement series. The list of publications featuring results from this site is long. The inclined reader may start with any of the works by any of the aforementioned group members (see Literature list for details). The sample spectra shown were recorded with the Bruker IFS 120 spectrometer and prepared by Philippe Demoulin, Institut d'Astrophysique et de Géophysique, Allée du VI Août, 17 - Bâtiment B5a, B-4000 Sart Tilman, Liège, Belgium, demoulin@astro.ulg.ac.be.

A.1.7 Toronto, Canada

The group of Kimberly Strong has begun regular observations on the University of Toronto campus only fairly recently (2002). As the data set is not as extensive yet, the zenith angles of the sample spectra sent for HCl and HF are only half that of the Kiruna spectra, resulting in a weaker absorption than one could expect for the same zenith angle at this location. Other members of this research group include Dmitri Yashkov and Aldona Wiacek with the latter kindly compiling the Toronto sample spectra shown here.

The Toronto site is one of few observation sites that is not in a remote location. It is located in the heart of a city with some 5 million inhabitants. It is probably fair to assume that there is a higher chance for local pollutants to show up in these spectra as compared to very remote sites.

For further questions please contact Kimberly Strong, Department of Physics, University of Toronto, 60 St. George Street Toronto, Ontario, M5S 1A7, Canada, strong@atmosp.-physics.utoronto.ca or Aldona Wiacek aldona@atmosp.physics.utoronto.ca

A.1.8 Tsukuba, Japan

According to the 2001 NDSC report there are 3 FTIR spectrometers operated at the Tsukuba site: a Bruker IFS 120HR run by H. Nakane and T. Nagahama (NIES, National Institute for Environmental Studies), a Bruker IFS 120M operated by H. Nakane and I. Murata (NIES/Tohoku University), and a Bomem DA-8 operated by Y. Makino and K. Shibata (MRI). The present sample spectra were recorded with the Bruker IFS 120M that has been in operation since 1998. The 120M has been earmarked to be moved to a new observation site near Irkutsk in Siberia with the newer 120HR in Tsukuba taking over as primary instrument for regular observations. The data shown here were kindly provided by Isao Murata, and his student Yahagi, Department of Geophysics, Graduate School of Science, Tohoku University, Aramaki-Aoba, Sendai, 980-8578, Japan, murata@pat.geophys.tohoku.ac.jp. Additional information may be found in Makino et al., 2000, Zhao et al, 2001.

[6] It is actually the first 120HR ever delivered by Bruker. Much knowledge from the Liège and IMK groups has gone into the design of the Bruker IFS 120 instruments.

A.1.9 Kitt Peak, Arizona

The sample spectra from Kitt Peak, Arizona, consist of sets of two spectra recorded about 20 years apart. The Kitt Peak instrument is a purpose-built instrument designed and built in the mid 1970s. The maximum optical path difference is 102*cm*, but many of the early spectra were recorded at a lower spectral resolution. The two to five times lower spectral resolution results in broader and shallower absorption features as compared to spectra from most other instruments including the Kiruna FTS. The sample spectra shown here were provided by Curtis P. Rinsland, and Linda Chiou, NASA Langley, Hampton VA. There are numerous publications describing the site, instrument and study results; e.g. Rinsland et al., 1982 to 2003.

A.1.10 Teneriffe, Canary Islands

Teneriffe hosts a high–altitude observatory equipped with a Bruker IFS 120M spectrometer. It is operational since Feb 1999 and well looked after by the Institute of Meteorology and Climate Research (IMK) of Forschungszentrum Karlsruhe, Germany. The spectra were provided by Thomas Blumenstock, Matthias Schneider, and Frank Hase, all from IMK. For more information on the instrument and the science undertaken please refer to Schneider et al., 2000, or contact thomas.blumenstock@imk.fzk.de.

A.1.11 Research vessel Polarstern, Atlantic shipcruise 1996

In addition to continuous observations on Spitsbergen the German Alfred-Wegener Institute for Polar and Marine Research (AWI) has ventured to study the latitudinal variabilities in atmospheric compostion during ship cruises on board the German research vessel Polarstern. The observation platform puts high demands on the suntracker device given the large and often unpredictable movements of the deck floor. This puts some constraints on the spectral resolution reasonably achievable as a function of sea swell. This pioneering work has provided the first solar FTIR spectra from truly tropical regions and has been described in detail in Notholt et al., 1995, 2000a, 2000b, and 2001.

The measurements on board the Polarstern have been performed using a mobile Bruker IFS 120M spectrometer. The instrument is installed in a thermostated container, mounted on the observation deck of the ship, 20 m above see level. Most trace gases commonly detected at higher latitudes could also be observed during the ship cruises. However, for a few compounds the interfering water vapour, caused by the high humidity, prevented their detection (e.g. NO in the tropics).

The sample spectra shown here were recorded at 25.5^{o}W and between 2.8 and 12.8^{o}S at spectral resolutions of 45cm OPD (HNO3, ClNO3), 128cm OPD (HF) and 180cm OPD (HCl) at zenith angles between 59.7 and 65.2^o. Spectra courtesy of Justus Notholt, Institute of Environmental Physics, University of Bremen - FB1, Postfach 330440, D-28334, Bremen, Germany.

A.1.12 Maido Summit, Réunion Island

Another fairly recent addition to the NDSC effort is Maido Summit on Ile de la Réunion, a subtropical, volcanic island in the Indian Ocean. Its geographical location, high altitude, and political stability make it a good choice for filling in the large observational gap between Hawaii (19^{o}N) and Wollongong (34^{o}S).

A campaign-style feasibility study at 2 sites, namely Maido Summit (2203m) and the local University campus near sea level, was carried out by a Belgian group headed by Martine De

Mazière in Oct 2002. The clear advantages in observation conditions at Maido Summit appear to justify the higher logistical expenses of operating a (highly automated) spectrometer on a routine basis at the higher altitude and we are looking forward to see more data from Maido Summit.

The sample spectra were recorded with a Bruker IFS 120M, equipped with the 6 standard NDSC bandpass optical filters and nitrogen-cooled InSb and MCT detectors. Data provided by Martine De Mazìere and Brice Barret, Belgian Institute for Space Aeronomy, Ringlaan 3, B-1180 Brussels, Martine.DeMaziere@bira-iasb.oma.be. For further details see De Mazière et al., 2003.

A.1.13 Wollongong, Australia

Regular observations at Wollongong on the Australian east coast have been carried out since 1995 (Griffith et al., 1998, Rinsland et al., 2001 and 2002). The team consists of David Griffith, Nicholas Jones (previously at Lauder), Clare Murphy (previously NPL), Arndt Meier (honorary, previously Kiruna), and Cirilo Bernardo (now at CSIRO). The site is equipped with a Bomem DA-8 spectrometer. The data acquisition system was recently replaced with a much more advanced delta-sigma system as theoretically suggested by James Brault (Brault, 1996) making it the first operational IR instrument of its kind (Bernardo, 2002, and unpublished material by DWT Griffith, C Bernardo, and A Meier, 2002).

The site is considered subtropical during a 3-months period in summer and mid-latitudinal throughout the rest of the year. Given its low elevation of 30m and a mere 2km distance from the Pacific ocean, it is probably the "wettest" site within the network (apart from ship cruises). The total column amount of water vapour on a humid day can be more than one hundred times higher than on a typical day at the Jungfraujoch.

Nevertheless, most molecules are well observable throughout the year, including NO near $1900cm^{-1}$. Splitting the 650 to $1350cm^{-1}$ regions into two optical filters in 1999 has markedly improved signal-to-noise ratios in low wavenumber regions hence boosting the quality of ClNO3 and HNO3 observations significantly (Rinsland et al., 2003). The sample spectra shown were prepared and analysed by Arndt Meier.

A.1.14 Lauder, New Zealand

A commercial Bruker IFS 120HR spectrometer has replaced the smaller IFS 120Ms at Lauder, New Zealand, in recent years. However, all but the HDO spectrum from December 2001 were taken with the older 120M instruments. The spectra shown have been prepared by Stephen Wood from NIWA, Lauder, New Zealand and former NIWA staff Nicholas B. Jones, now of Wollongong University, Australia. For more details, see Jones at al., 1994 and 2001, Connor et al., 1996 and 1997, Rinsland et al., 1994, 2001, 2002, and 2003, Bell et al., 2001, Griffith et al., 2003, or contact Stephen W. Wood, s.wood@niwa.co.nz, National Institute of Water and Atmospheric Research Ltd, Lauder, priv. bag 50061, Omakau, Central Otago, New Zealand.

A.1.15 Arrival Heights, Antarctica

The Arrival Heights site near McMurdo station is operated by the Lauder group in New Zealand with much commitment from Stephen Wood. The spectra were recorded with a commercial Bruker IFS 120M spectrometer. For further reading see also Connor et al., 1987, Jaramillo, 1988; Kreher 1996 and 1997, in addition to the Lauder references. Spectra for Arrival Heights have been provided by Stephen Wood from NIWA, Lauder, New Zealand (see contact details above).

A.2 Comparison of Chloronitrate

Table A1.2 lists the sites that provided sample spectra for the $780.2cm^{-1}$ microwindow for the retrieval of $ClONO_2$. Instrumental settings and the TCAs retrieved (where provided) are listed as well. The sample spectra from all sites listed are illustrated over the next few pages. Each in turn is compared to the Kiruna spectra used throughout the main section of this work. Kiruna spectra are in red or dashed and participating sites in blue or solid colour depending on whether you have the colour or monochrome edition.

Table A1.2: $ClONO_2$. *Details of the observation geometries and retrieved total column amounts for sample spectra featuring the Chloronitrate window near $780.2cm^{-1}$. Site locations and elevations are listed in the previous table. Zenith angles are solar or lunar astronomical zenith angles in degrees. Max. OPD is the maximum optical path difference or the reciprocal of the spectral resolution at which the spectra were recorded. FoV is the field of view defined as the diameter of the aperture stop divided by the focal length of the instrument. Duration is the total scanning time. Apodisation is the apodisation function applied in the Fourier Transform and sample name is the file name by which the individual investigators identify the sample data they sent. The total column amount (TCA) retrieved for the target molecule is listed where available, else the entry is marked 'not provided' (n.p.).*

Observation site	date of recording	zenith angle	OPD [cm]	FoV [mrad]	apodisation	Duration [s]	TCA molec/cm^2	sample name
Eureka	24/Apr/99	68.89	250	3.00	boxcar	1010	3.49e15	24a9904b.spc
Ny-Ålesund	28/May/95	63.24	180	3.86	boxcar	n.p.	1.76e15	95052876.s09
Ny-Ålesund	04/Apr/96	73.06	180	3.86	boxcar	736	3.47e15	96040404.s00
Ny-Ålesund lun	02/Feb/96	69.05	45	6.36	boxcar	3760	n.p.	96020218.s00
Kiruna, solar	15/Mar/97	71.68	257	4.07	boxcar	823	4.10e15	970315s6.s92
Kiruna, lunar	04/Dec/98	70.55	45	5.98	boxcar	4401	1.67e15	970323m6.s90
Harestua	20/Mar/01	70.44	180	3.86	boxcar	142	1.94e15	gb010320.25
Jet, 52^oN, 1^oW	08/Mar/96	68.55	180	6.36	boxcar	195	n.p.	b1920908.bnr
Jungfraujoch	15/Jan/01	69.62	125	4.78	boxcar	1715	$\leq$1.5e15$^{*)}$	r01115qk.moy
Toronto	20/Feb/03	56.62	250	2.46	boxcar	1010	n.p.	30220600.spc
Tsukuba	17/Feb/00	71.23	257	3.86	boxcar	308	n.p.	t048k6m0.770
Kitt Peak	26/Apr/81	84.53	102	n.p.	kpno10	n.p.	0.59e15	260d0775.bin
Kitt Peak	01/Aug/01	70.55	94	n.p.	kpno5	n.p.	n.p.	010j0775.bin
Teneriffe	27/May/02	64.0	250	2.50	boxcar	n.p.	0.38e15	clno3-020527
Polarstern, 4^oS	25/Oct/96	59.78	45	2.27	boxcar	n.p.	n.p.	96102539.08
Maido Summit	05/Oct/02	68.78	82	6.36	boxcar	102	n.p.	02a05001.sml
Wollongong	14/Jun/01	72.53	250	3.08	boxcar	565	0.92e15	010614f8.504
Lauder	11/Jul/01	69.55	257	3.86	boxcar	408	n.p.	b1920908.bnr
Arrival Heights	20/Dec/01	71.32	257	2.95	boxcar	256	n.p.	b3541807.mnr

Apodisation function kpno10 (kpno5) applies a squared cosine to the last 10% (5%) of the interferogram.

$^{*)}$ $ClONO_2$ is near the detection limit.

$ClONO_2$

Fig.A.1: Eureka, SZA 68.9^o, 24/Apr/1999

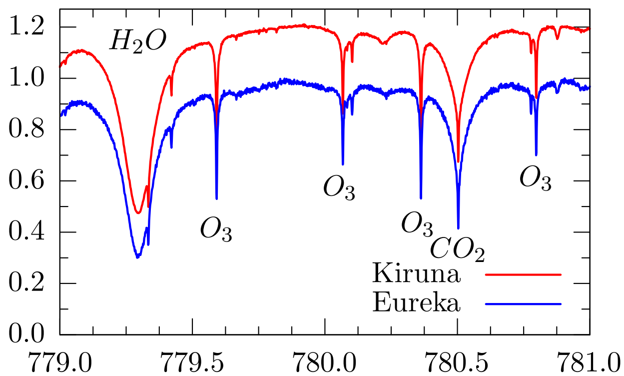

Fig.A.2: Eureka, SZA 68.89^o, 24/Apr/1999

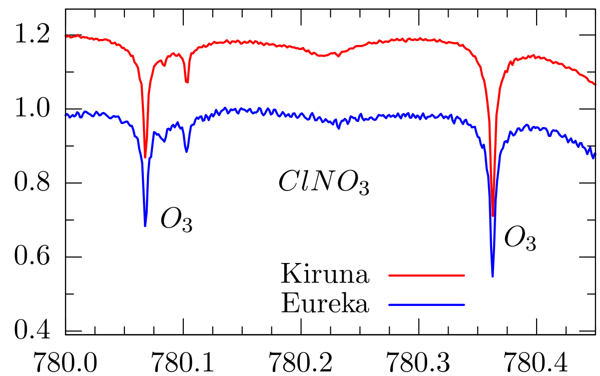

Fig.A.3: Ny-Åles., SZA 59/73^o, May 95 & Apr 96

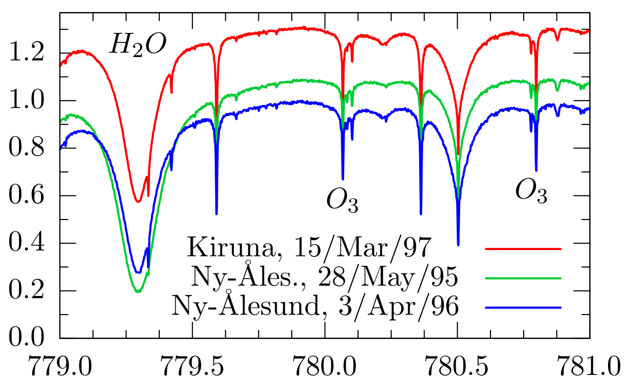

Fig.A.4: Ny-Åles., SZA 59/73^o, May 95 & Apr 96

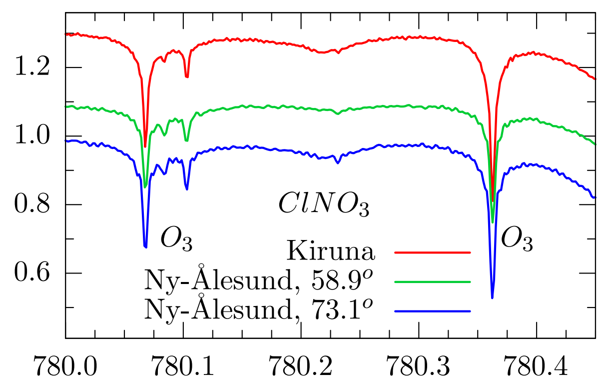

Fig.A.5: Ny-Ålesund, LunarZA 69^o, 2/Feb/96

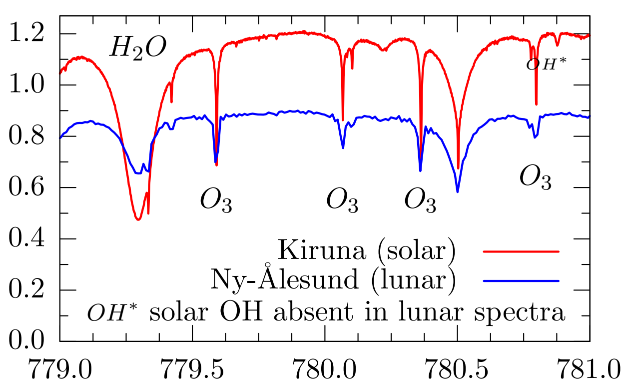

Fig.A.6: Ny-Åles., Lunar ZA 69^o, 2/Feb/96

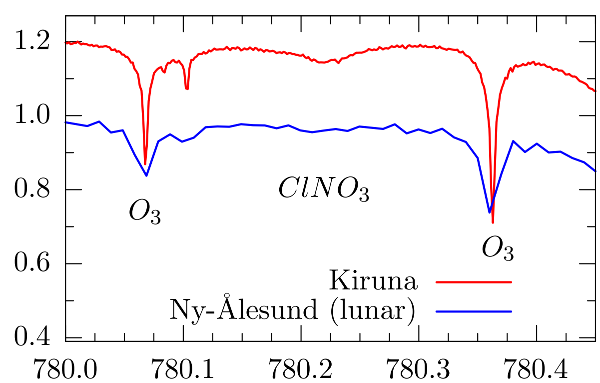

Note that the solar OH line near $780.875 cm^{-1}$ is absent in the lunar spectra.

$ClONO_2$

Fig.A.7: Kiruna, Lunar ZA 70.6^o, 4/Dec/98

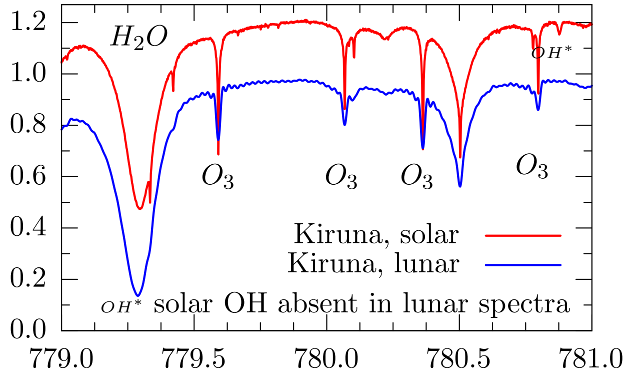

Fig.A.8: Kiruna, LunarZA 70.6^o, 4/Dec/98

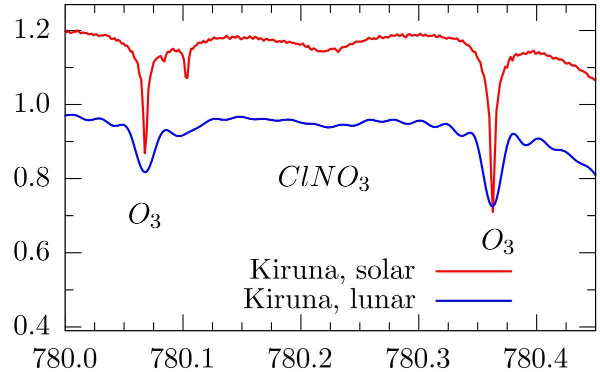

Fig.A.9: Harestua, SZA 70.4^o, 20/Mar/01

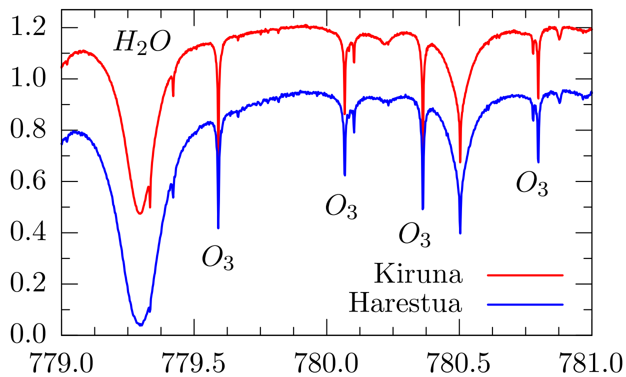

Fig.A.10: Harestua, SZA 70.4^o, 20/Mar/01

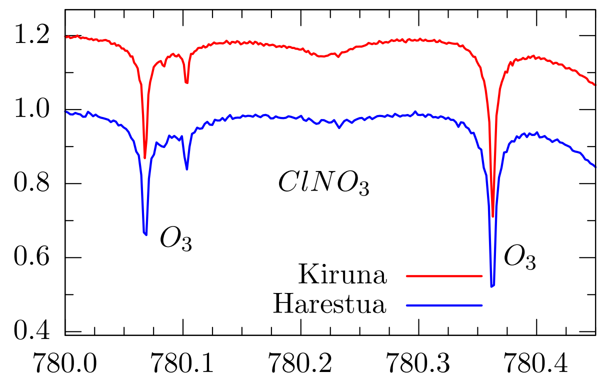

Fig.A.11: Jetstream camp., SZA 58^o, 8/Mar/96

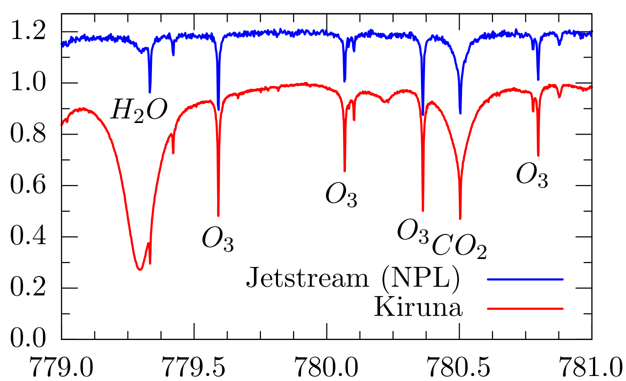

Fig.A.12: Jetstream camp., SZA 58^o, Mar 96

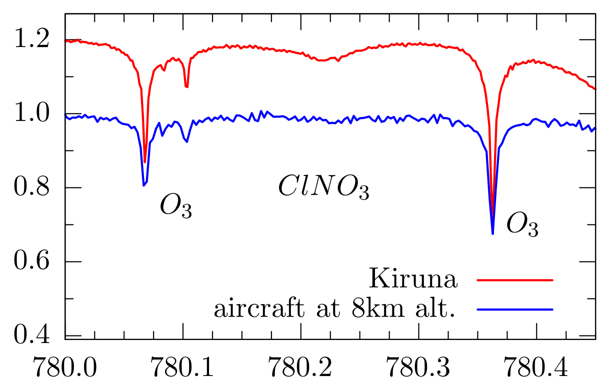

$ClONO_2$

Fig.A.13: Jungfraujoch, SZA 69.6^o, 15/Jan/01

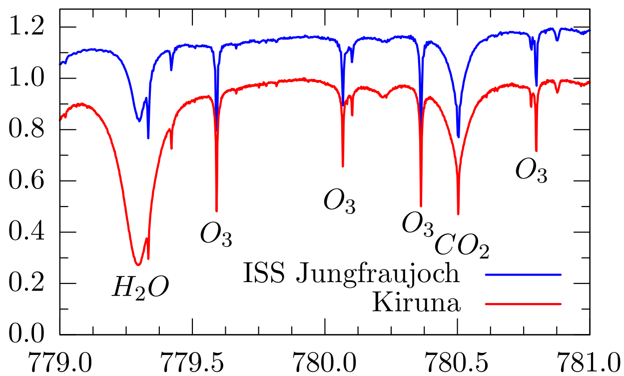

Fig.A.14: ISSJ, SZA 69.62^o, 15/Jan/01

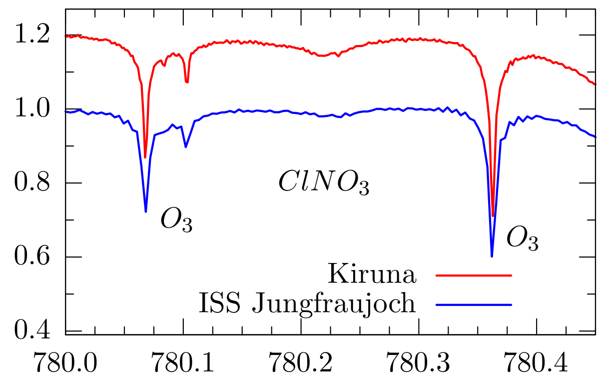

Fig.A.15: Toronto, SZA 56.62^o, 20/Feb/03

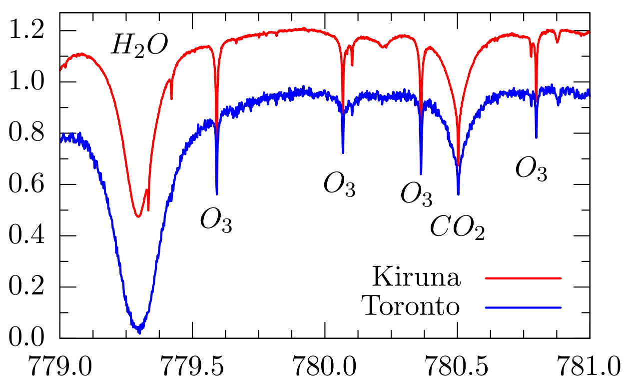

Fig.A.16: Toronto, SZA 56.62^o, 20/Feb/03

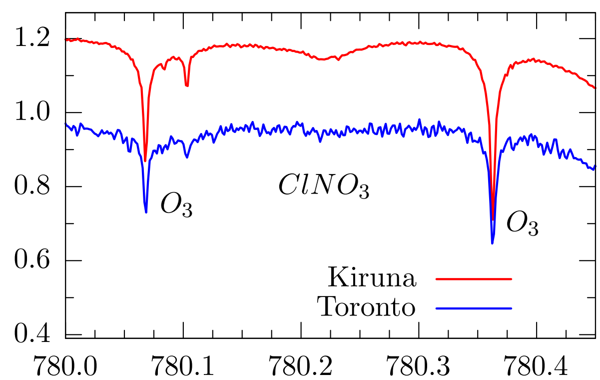

Fig.A.17: Tsukuba, SZA 71.2^o, 17/Feb/00

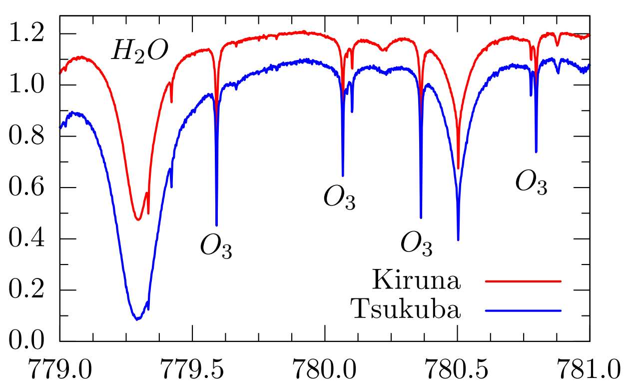

Fig.A.18: Tsukuba, SZA 71.2^o, 17/Feb/00

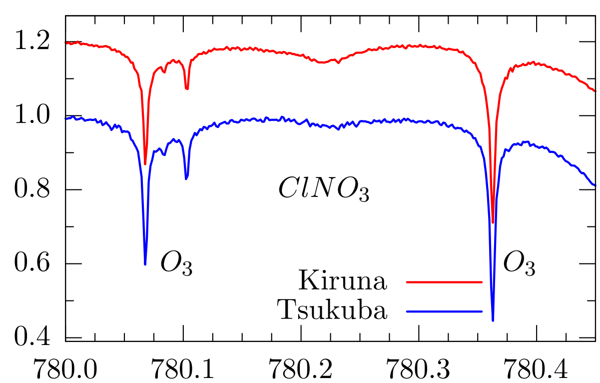

ClONO$_2$

Fig.A.19: Kitt Peak, Aug 1981 & Apr 2001

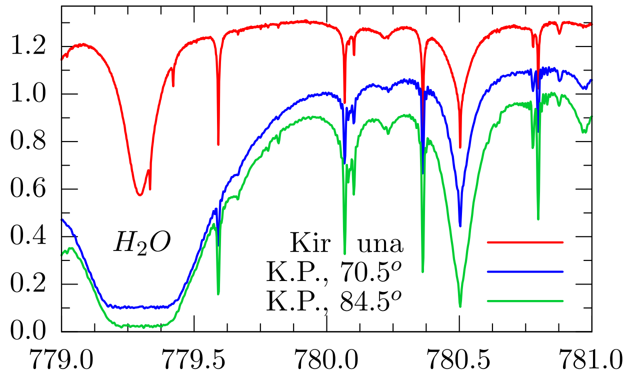

Fig.A.20: Kitt Peak, Aug 1981 & Apr 2001

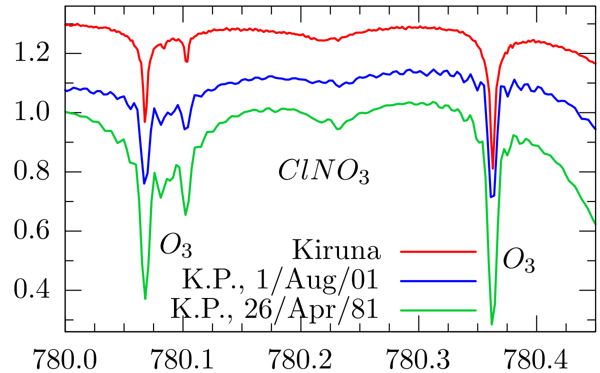

Fig.A.21: Teneriffe, SZA 64^o, 27/May/02

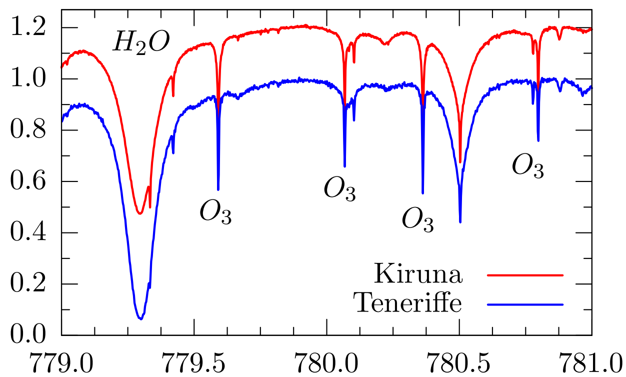

Fig.A.22: Teneriffe, SZA 64^o, 27/May/02

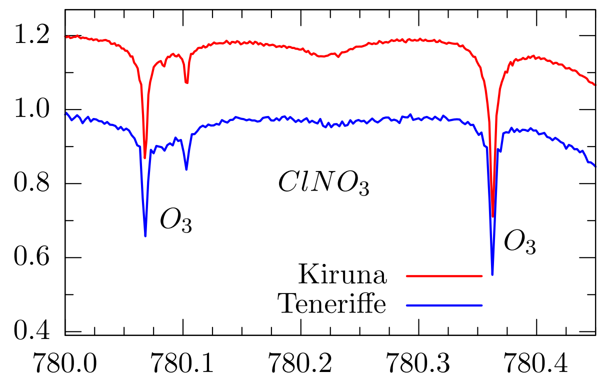

Fig.A.23: Equat.Atlantic, SZA 60^o, 25/Oct/96

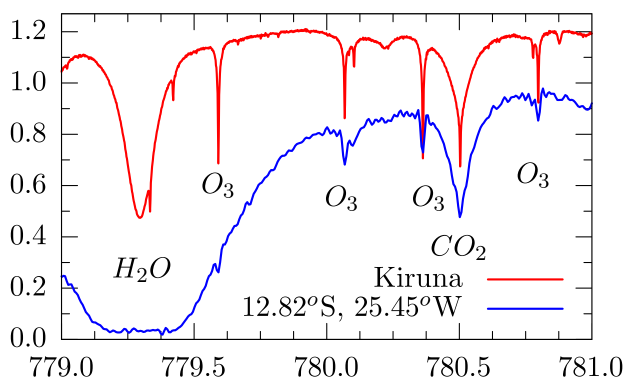

Fig.A.24: Equat.Atlantic, SZA 60^o, Oct/96

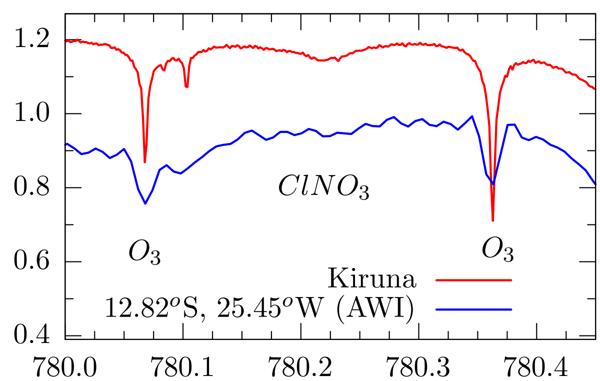

$ClONO_2$

Fig.A.25: Maido Summit, SZA 69^o, 5/Oct/02

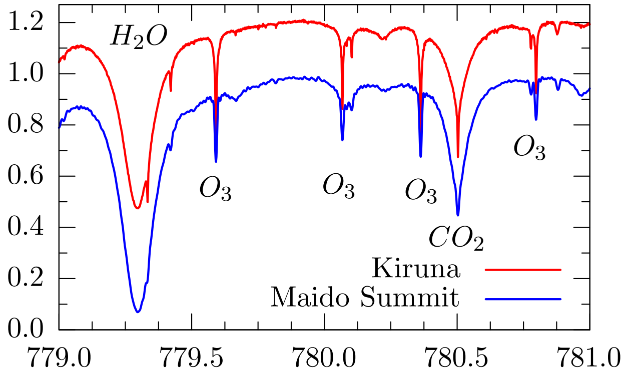

Fig.A.26: Maido Summit, SZA 69^o, 5/Oct/02

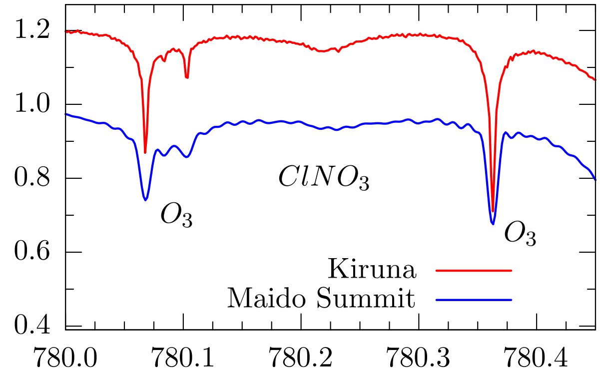

Fig.A.27: Wollongong, SZA 72.5^o, 14/Jun/01

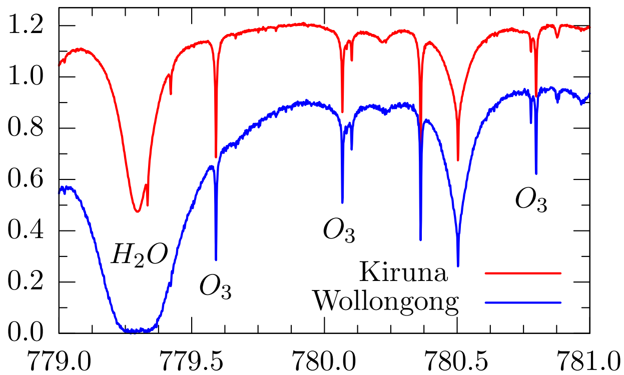

Fig.A.28: Wollongong, SZA 72.5^o, 14/Jun/01

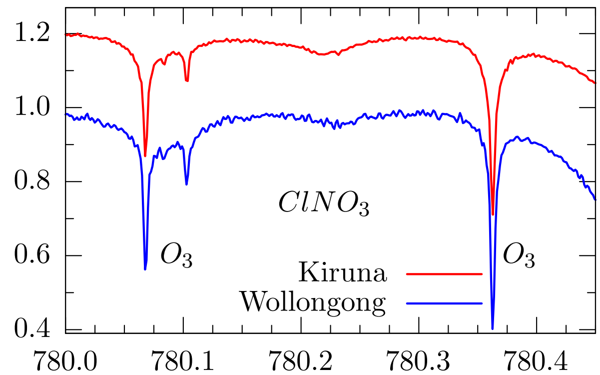

Fig.A.29: Lauder, SZA 69.55^o, 11/Jul/01

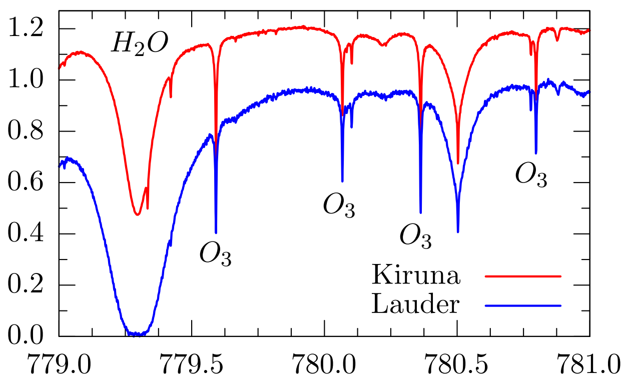

Fig.A.30: Lauder, SZA 69.55^o, 11/Jul/01

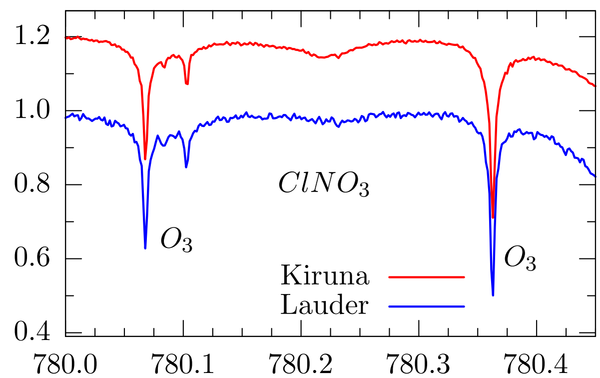

Fig.A.31: Antarctica, SZA 71.3^o, 20/Dec/01

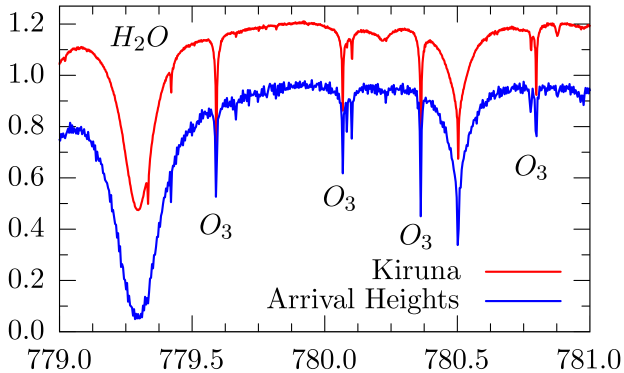

Fig.A.32: Antarctica, SZA 71.3^o, 20/Dec/01

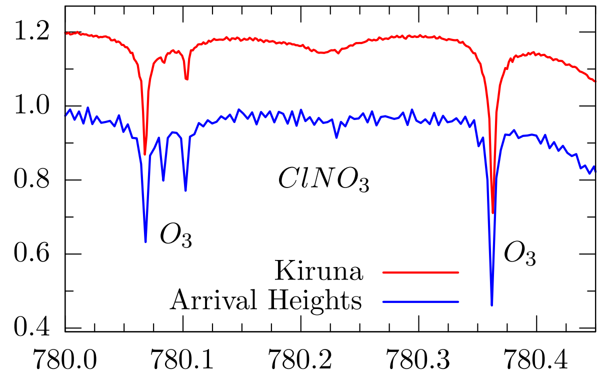

A.3 Comparison of Nitric Acid

Table A1.3 lists the sites that provided sample spectra for the 865–875cm^{-1} microwindows for the retrieval of HNO_3. Instrumental settings and the TCA retrieved (where provided) are listed as well. The sample spectra from all sites listed are illustrated over the next few pages.

Table A1.3: HNO_3 *Details of the observation geometries for the sample spectra featuring the nitric acid windows in the 865 to 875 cm^{-1} spectral interval. See Table A1.2 (page 518) for a description of the table items.*

Observation site	date of recording	zenith angle	OPD [cm]	FoV [mrad]	apodi-sation	Dura-tion[s]	TCA molec/cm^2	sample name
Eureka solar	24/Apr/99	68.89	250	3.00	boxcar	1010	2.22e16	24a9904b.spc
Eureka lunar	02/Mar/01	69.00	50	6.18	hamming	8096	2.38e16	l02m011c.spc
Ny-Ålesund	28/May/95	63.24	180	3.86	boxcar	n.p.	1.64e16	95052876.s09
Ny-Ålesund	04/Apr/96	73.06	180	3.86	boxcar	736	2.27e16	96040404.s00
Ny-Ålesund lun	02/Feb/96	69.05	45	6.36	boxcar	3760	n.p.	96020218.s00
Kiruna, solar	15/Mar/97	71.68	257	4.07	boxcar	823	2.67e16	970315s6.s92
Kiruna, lunar	04/Dec/98	70.55	45	5.98	boxcar	4401	2.51e16	970323m6.s90
Harestua	20/Mar/01	70.44	180	3.86	boxcar	142	2.72e16	ga010320.25
Jet, 52^{o}N, 1^{o}W	08/Mar/96	68.55	180	6.36	boxcar	195	n.p.	b1920908.bnr
Jungfraujoch	14/Aug/01	70.39	125	4.78	boxcar	539	1.16e16	r01814lj.moy
Toronto	20/Feb/03	56.62	250	2.46	boxcar	1010	n.p.	30220600.spc
Tsukuba	17/Feb/00	71.23	257	3.86	boxcar	308	1.57e16	t048k6m0.860
Kitt Peak	26/Apr/81	71.94	102	n.p.	kpno10	n.p.	1.10e16	260c0850.bin
Kitt Peak	01/Aug/01	70.55	94	n.p.	kpno5	n.p.	n.p.	010j0850.bin
Teneriffe	27/May/02	64.0	250	2.50	boxcar	n.p.	0.74e16	hno3-020527
Polarstern, 4^{o}S	25/Oct/96	59.78	45	2.27	boxcar	n.p.	n.p.	96102539.08
Maido Summit	05/Oct/02	68.78	82	6.36	boxcar	102	n.p.	02a05001.sml
Maido Summit	24/Oct/02	70.96	82	6.36	boxcar	102	n.p.	02a24001.sml
Wollongong	18/Oct/01	71.50	250	3.08	boxcar	565	1.25e16	011018f8.s06
Lauder	11/Jul/01	69.55	257	3.86	boxcar	408	n.p.	b1920908.bnr
Arrival Heights	20/Dec/01	71.32	257	2.95	boxcar	256	n.p.	b3541808.mnr

HNO_3

Fig.A.33: Eureka, SZA 68.89^o, 24/Apr/99

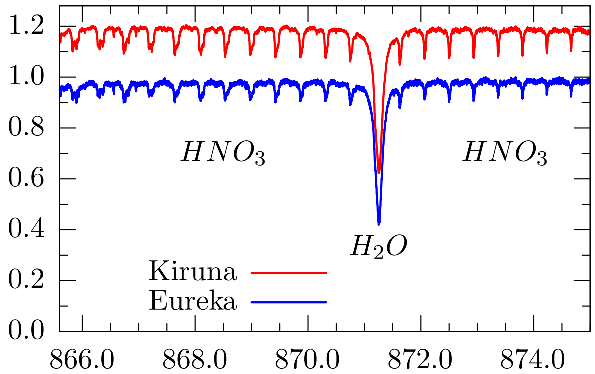

Fig.A.34: Eureka, SZA 68.89^o, 24/Apr/99

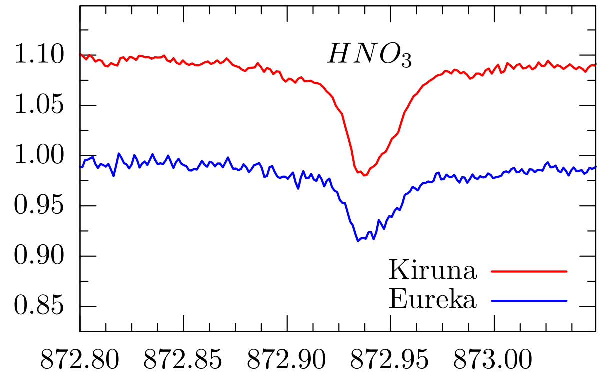

Fig.A.35: Eureka, lunar ZA 69.0^o, 2/Mar/01

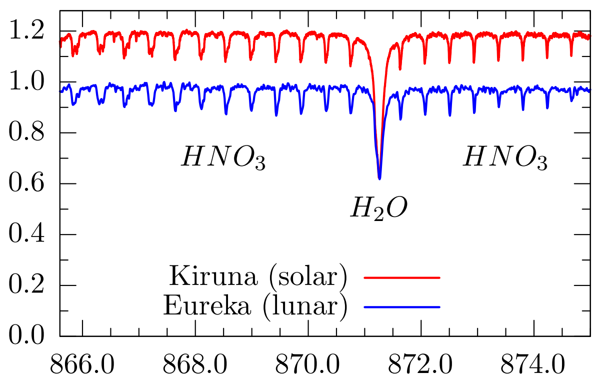

Fig.A.36: Eureka, lunar ZA 69.0^o, 2/Mar/01

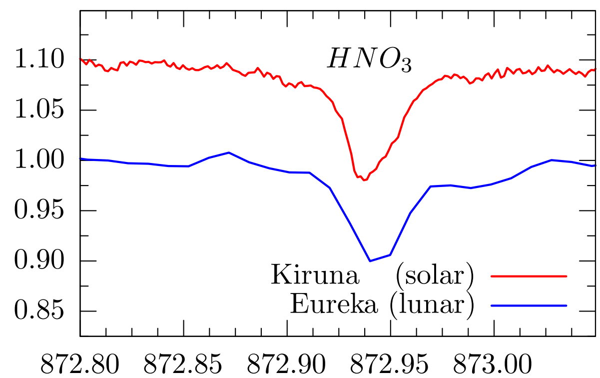

Fig.A.37: Ny-Ålesund, SZA 59/73^o, 5/95 & 4/96

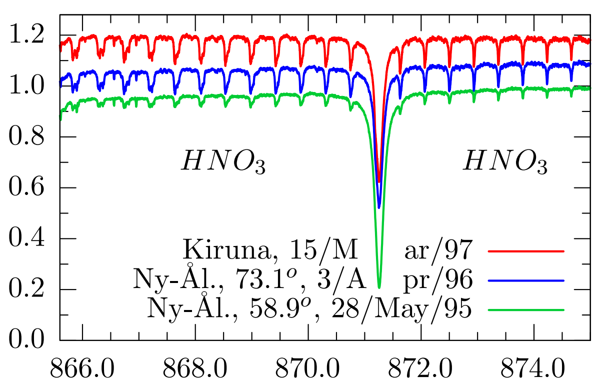

Fig.A.38: Ny-Ålesund, SZA 59/73^o, 5/95 & 4/96

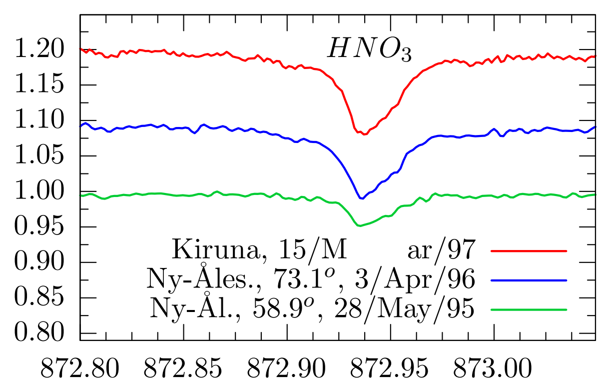

HNO_3

Fig.A.39: Ny-Ålesund, Lunar ZA 69^o, 2/2/96

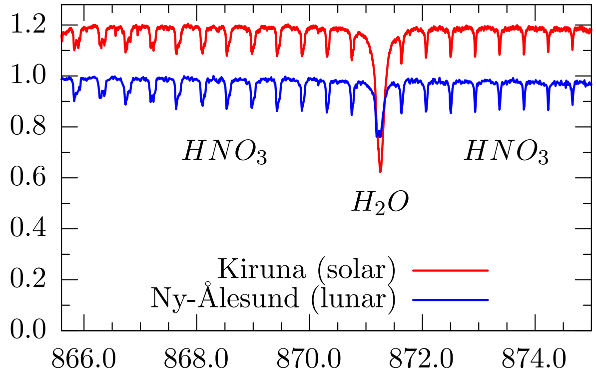

Fig.A.40: Ny-Ålesund, Lunar ZA 69^o, 2/2/96

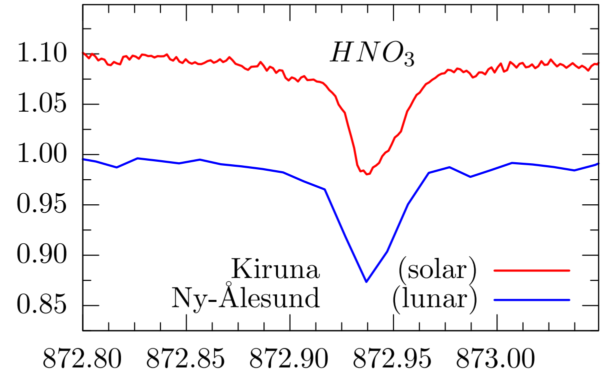

Fig.A.41: Kiruna, Lunar ZA 70.6^o, 4/Dec/98

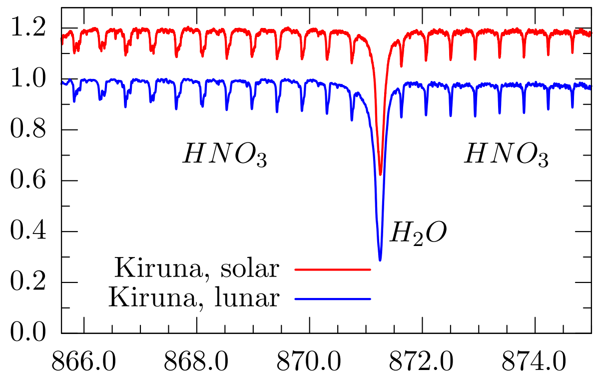

Fig.A.42: Kiruna, Lunar ZA 70.6^o, 4/Dec/98

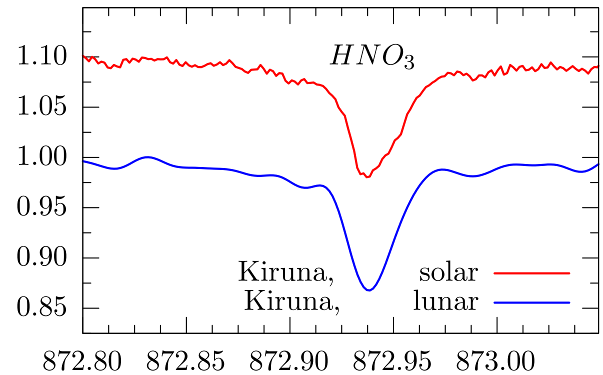

Fig.A.43: Harestua, SZA 70.4^o, 20/Mar/01

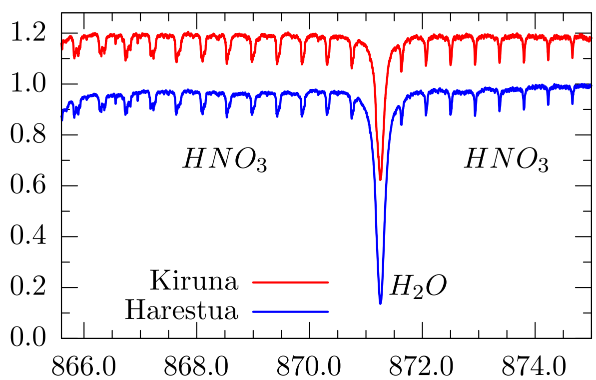

Fig.A.44: Harestua, SZA 70.4^o, 20/Mar/01

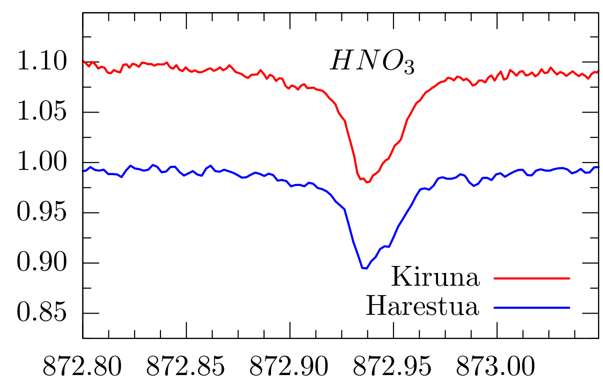

HNO_3

Fig.A.45: Jetstream, SZA 57.7^o, 8/Mar/96

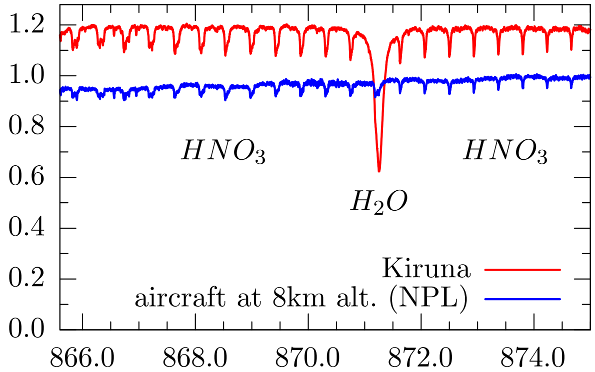

Fig.A.46: Jetstream, SZA 57.7^o, 8/Mar/96

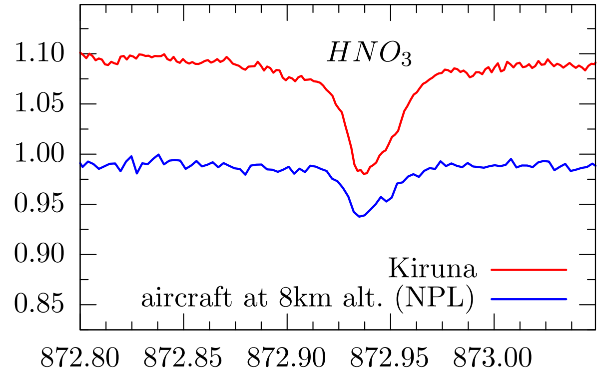

Fig.A.47: Jungfraujoch, SZA 70.4^o, 14/Aug/01

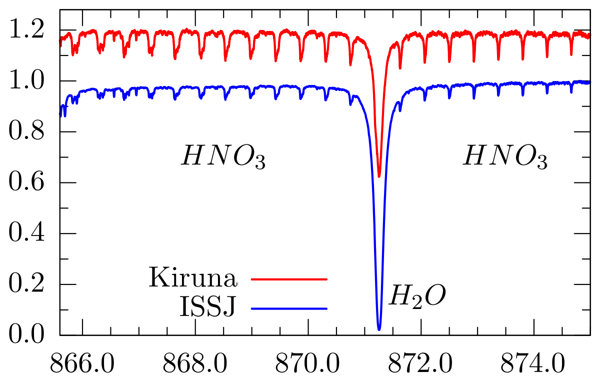

Fig.A.48: Jungfrauj., SZA 70.4^o, 14/Aug/01

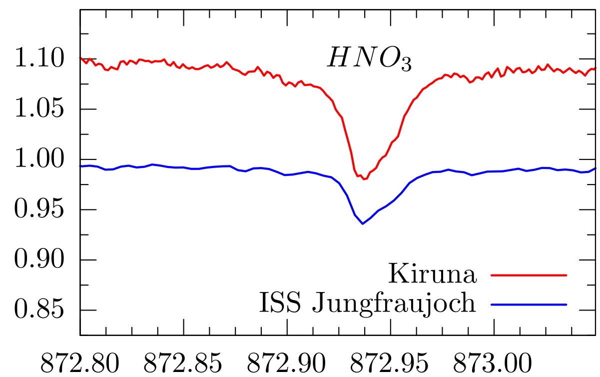

Fig.A.49: Toronto, SZA 56.62^o, 20/Feb/03

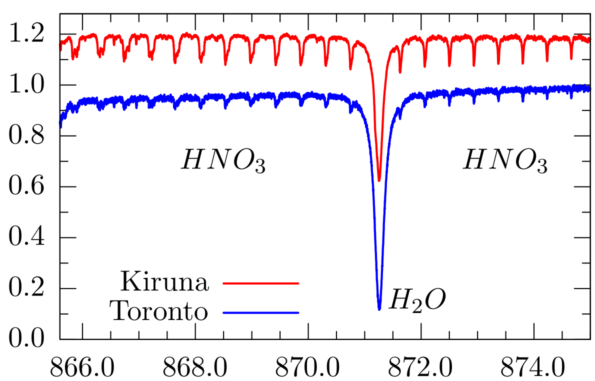

Fig.A.50: Toronto, SZA 56.62^o, 20/Feb/03

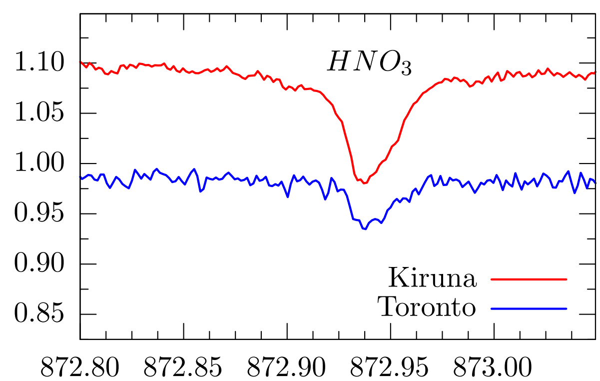

HNO_3

Fig.A.51: Tsukuba, SZA 71.23^o, 17/Feb/00

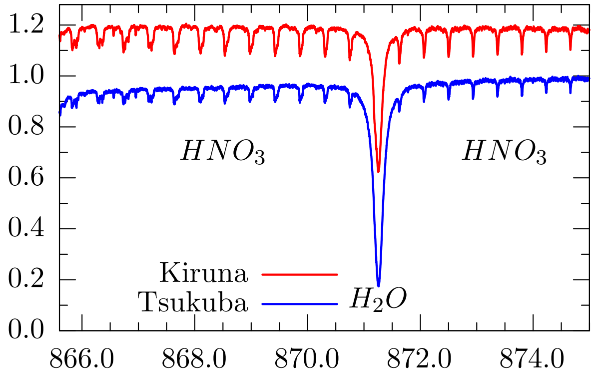

Fig.A.52: Tsukuba, SZA 71.23^o, 17/Feb/00

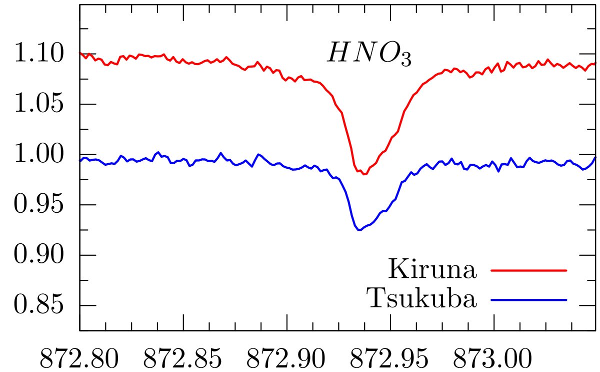

Fig.A.53: Kitt Peak, Aug 1981 & Apr 2001

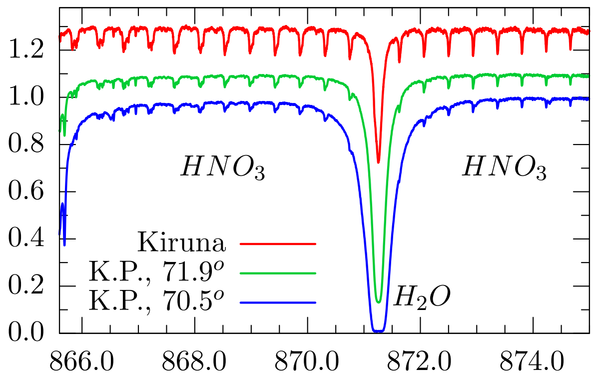

Fig.A.54: Kitt Peak, Aug 1981 & Apr 2001

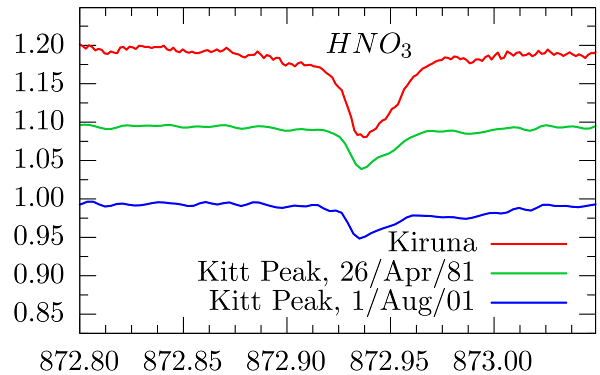

Fig.A.55: Teneriffe, SZA 64^o, 27/May/02

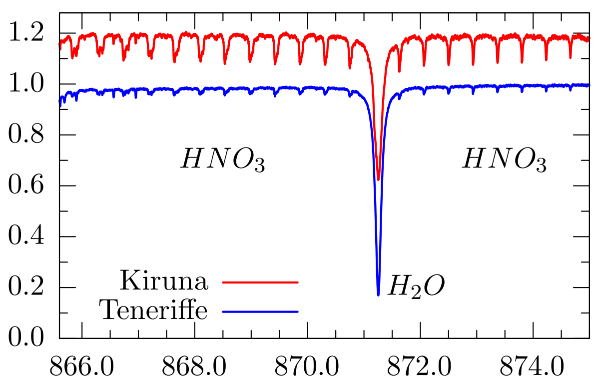

Fig.A.56: Teneriffe, SZA 64^o, 27/May/02

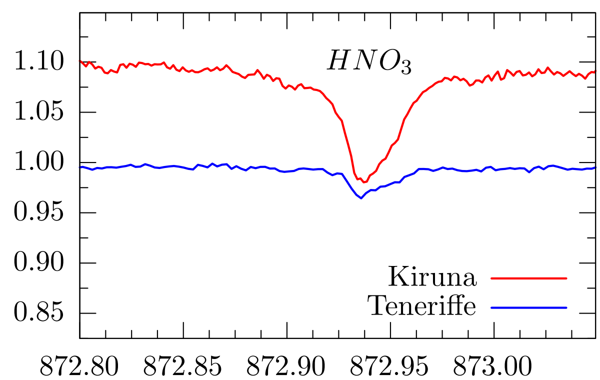

HNO_3

Fig.A.57: Equat. Atlantic, SZA 59.8^o, Oct/96

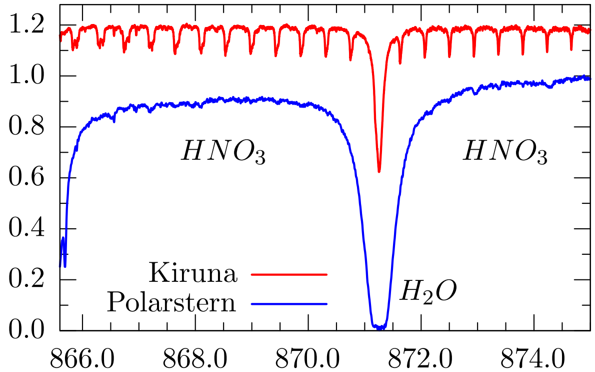

Fig.A.58: ship cruise, SZA 59.8^o, 25/Oct/96

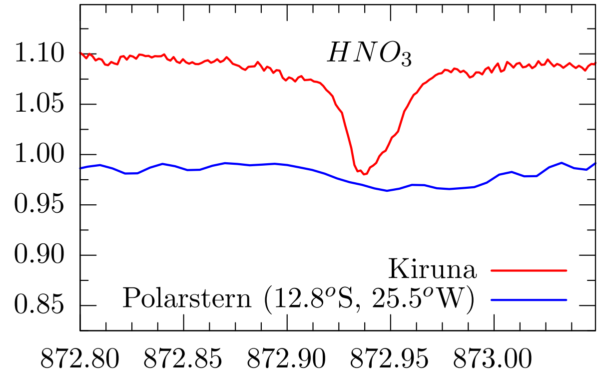

Fig.A.59: Maido Summit, SZA 71^o, 24/Oct/02

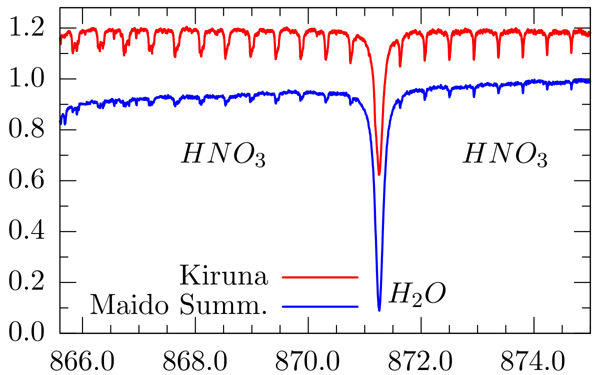

Fig.A.60: Maido Summit, SZA 71^o, Oct/02

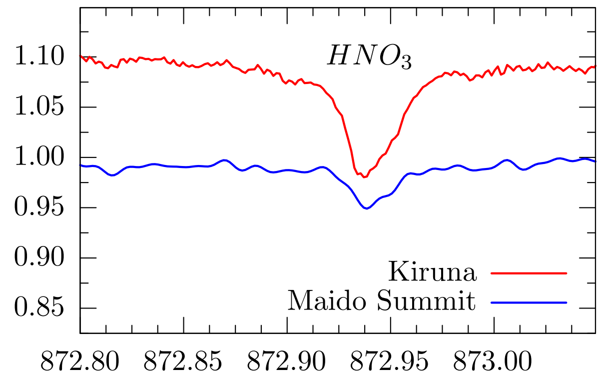

Fig.A.61: Wollongong, SZA 71.5^o, 18/Oct/01

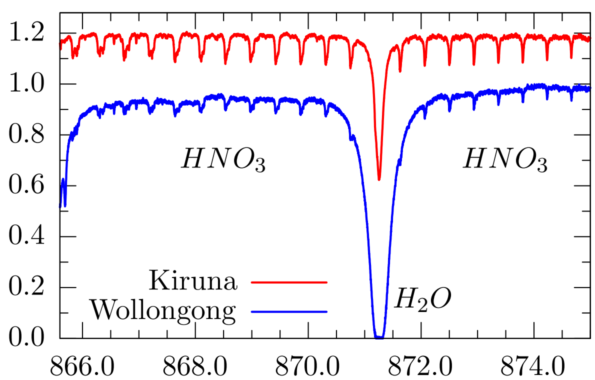

Fig.A.62: Wollongong, SZA 71.5^o, 18/Oct/01

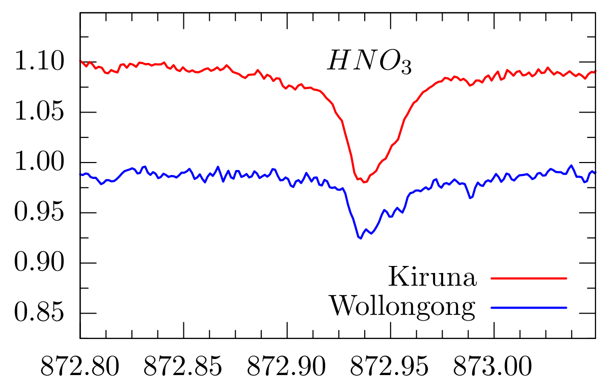

HNO_3

Fig.A.63: Lauder, SZA 69.6^o, 11/Jul/2001

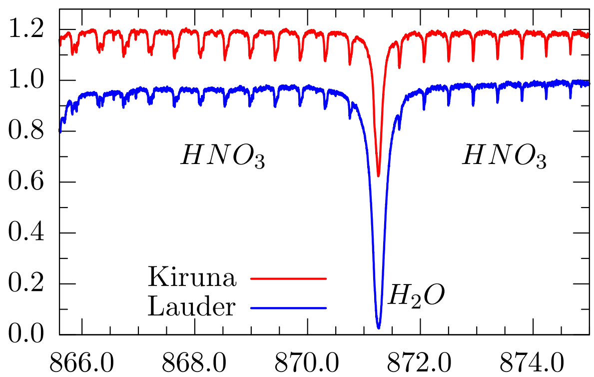

Fig.A.64: Lauder, SZA 69.6^o, 11/Jul/2001

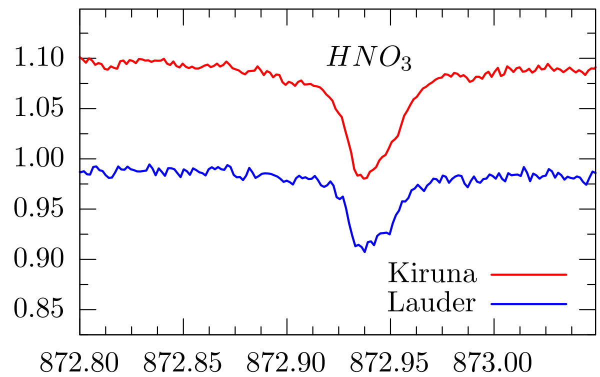

Fig.A.65: Antarctica, SZA 71.3^o, 20/Dec/01

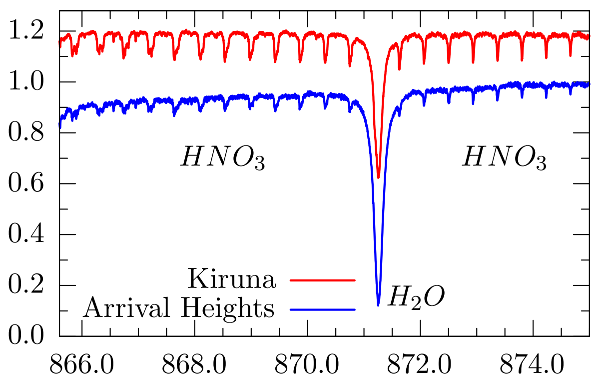

Fig.A.66: Antarctica, SZA 71.3^o, 20/Dec/01

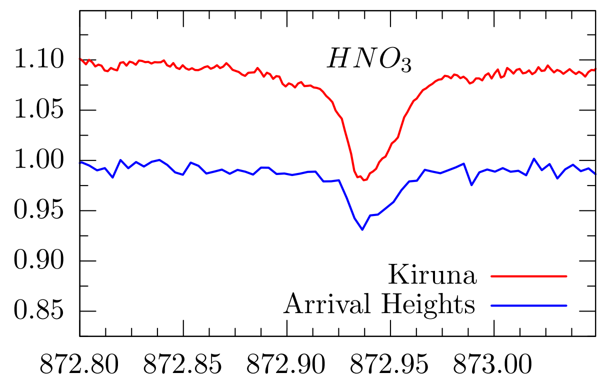

A.4 Comparison of Water Vapour

Table A1.4 lists the sites that provided sample spectra for the $2612cm^{-1}$ microwindow for the retrieval of HDO. Participants were asked to provide one example each for a dry and a humid day. Instrumental settings and the TCA retrieved (where provided) are listed as well. The TCA shown is the equivalent total water abundance under the assumption of the isotopic ratio of the HITRAN database – multiply the numbers with 3.10693e-04 if you are interested in HDO only (compare Table 2.3, page 19). The sample spectra from all sites listed are illustrated over the next few pages.

Table A1.4: HDO *Details of the observation geometries for the sample spectra featuring the heavy water vapour window near* $2612.5cm^{-1}$. *See Table A1.2 (page 518) for a description of the table items.*

Observation site	date of recording	zenith angle	OPD [cm]	FoV [mrad]	apodi-sation	Dura-tion/s	TCA molec/cm^2	sample name
Eureka 'dry'	24/Apr/99	73.68	250	1.69	hamming	1010	4.79e21	24a99011.spc
Eureka 'humid'	29/Aug/95	72.12	250	1.69	hamming	1010	11.00e21	29a95011.spc
Ny-Ålesund	03/Apr/96	74.13	180	1.36	boxcar	595	5.08e21	96040301.s00
Ny-Ålesund	28/May/95	59.32	180	2.27	boxcar	n.p.	10.55e21	95052808.s09
Kiruna, solar	15/Mar/97	71.02	257	2.39	boxcar	615	4.24e21	970315s4.s90
Harestua 'dry'	20/Mar/01	68.87	257	2.95	boxcar	203	n.p.	cc010320.01
Harestua 'humid'	20/Mar/01	68.00	257	2.95	boxcar	203	n.p.	cc010821.dpt
Jet, 52^oN, 1^oW	08/Mar/96	68.53	180	2.95	boxcar	186	n.p.	b1920908.bnr
Jungfraujoch 'dry'	08/Jun/98	72.53	101	2.63	boxcar	360	0.70e21	r98608km.moy
Jungfraujoch 'wet'	10/Jun/98	68.91	101	2.63	boxcar	200	1.30e21	r98610bf.moy
Toronto 'dry'	20/Jan/03	64.61	250	1.54	boxcar	1010	n.p.	30120300.spc
Toronto 'less dry'	09/Apr/03	38.77	250	1.54	boxcar	1010	n.p.	30409300.spc
Tsukuba 'dry'	17/Feb/99	70.57	257	2.27	boxcar	308	n.p.	t048j3m1.260
Tsukuba 'humid'	18/May/01	69.34	257	2.27	boxcar	308	n.p.	t138l3m0.260
Teneriffe 'dry'	27/May/02	59.0	250	1.14	boxcar	n.p.	4.83e21	hdo-020527
Teneriffe 'humid'	18/Jun/02	71.0	250	1.14	boxcar	n.p.	21.47e21	hdo-020618
Maido Summit	19/Oct/02	70.10	101	3.86	boxcar	123	n.p.	02a19001.shl
Wollongong 'dry'	09/Jul/98	72.05	250	2.46	boxcar	563	11.78e21	980709f4.501
Wollong. 'humid'	12/Jan/98	66.55	250	2.46	boxcar	563	102.90e21	980112f4.503
Lauder 'dry'	12/Sep/01	69.49	257	2.27	boxcar	408	n.p.	b2551326.bnr
Lauder 'humid'	21/Dec/01	68.75	257	2.75	boxcar	408	n.p.	b3552326.bnr
Arrival Hghts 'dry'	18/Oct/01	69.92	257	2.27	boxcar	102	n.p.	b2910326.mnr
Arrival Hghts 'wet'	25/Feb/01	68.87	257	2.27	boxcar	102	n.p.	b0560326.mnr

HDO

Fig.A.67: Eureka, SZA 73.7/72.1^o, 4/99 & 8/95

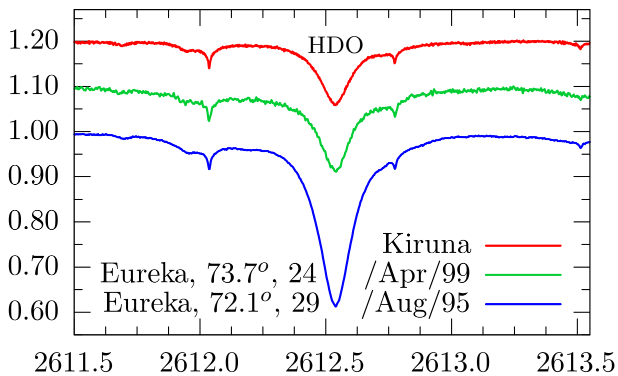

Fig.A.68: Ny-Ålesund, Lunar ZA 74^o, 2/96

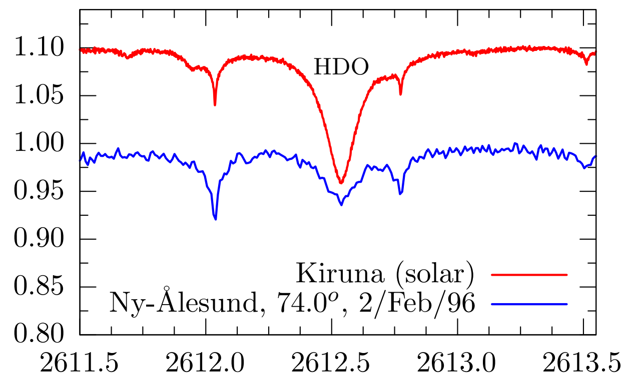

Fig.A.69: Ny-Ålesund, SZA 64/74^o, 5/95 & 4/96

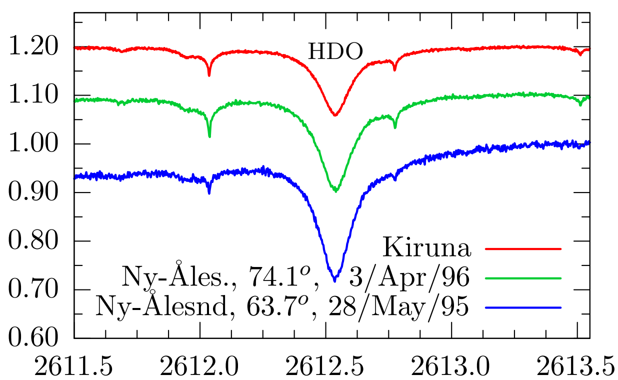

Fig.A.70: Harestua, 68.9/72.5^o, 3/01 & 3/03

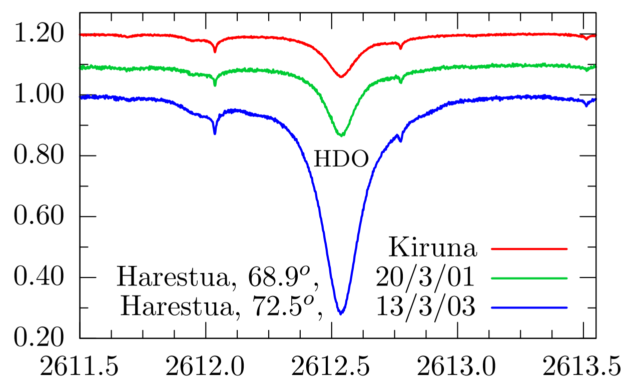

Fig.A.71: Jetstream camp., SZA 57^o, 8/Mar/96

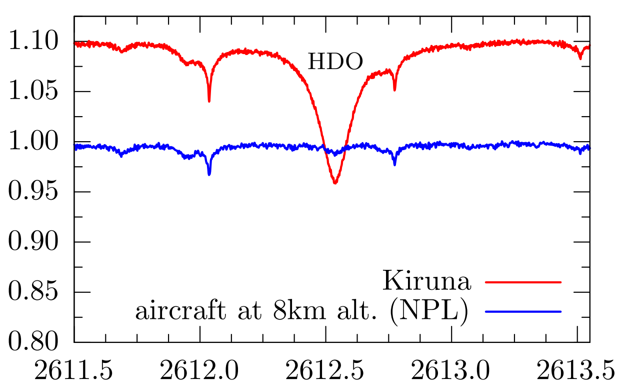

Fig.A.72: Jungfraujoch, SZA 72/69^o, Jun/98

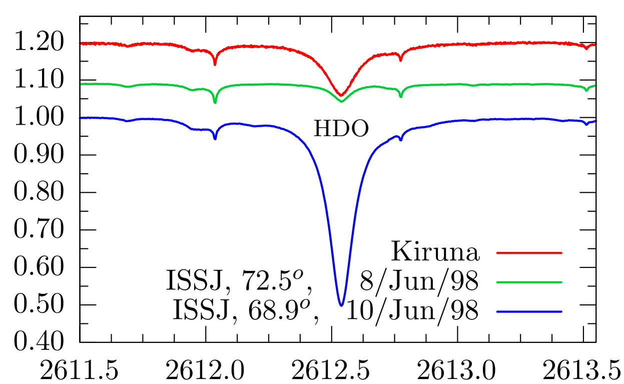

HDO

Fig.A.73: Toronto, SZA 65/37^o, 1/03 & 8/02

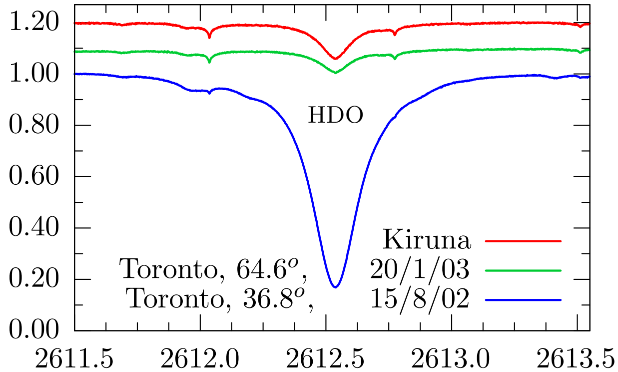

Fig.A.74: Tsukuba, 71/69^o, Feb/99 & May/01

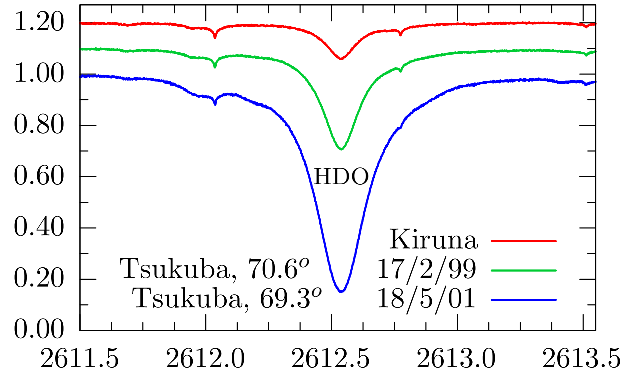

Fig.A.75: Teneriffe, 59/71^o, 27/5/02 & 18/6/02

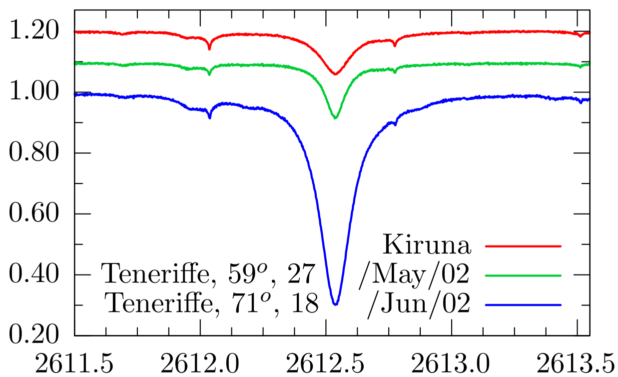

Fig.A.76: Wollongong, 72/67^o, 7/98 & 1/98

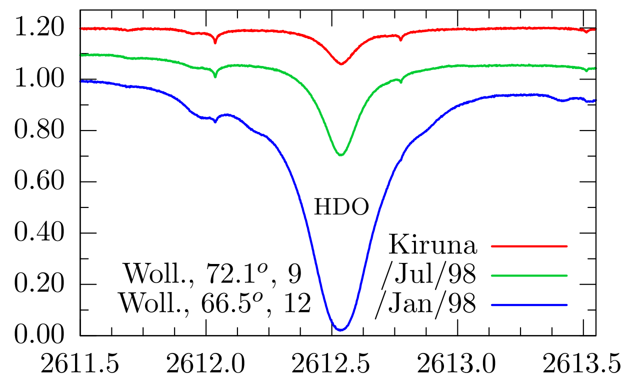

Fig.A.77: Lauder, 68.8/69.5^o, Sep/01 & Dec/01

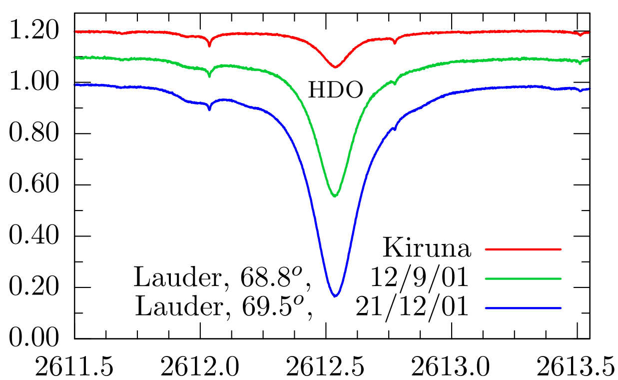

Fig.A.78: Antarctic, 70/69^o, Oct/01 & Feb/01

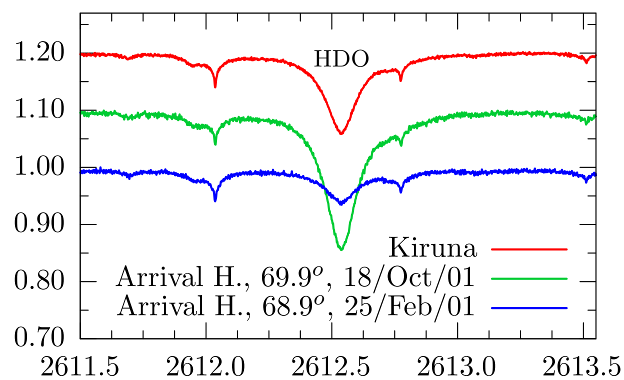

A.5 Comparison of Hydrogen Chloride

Table A1.5 lists the sites that provided sample spectra for the $2925.95cm^{-1}$ microwindow for the retrieval of HCl. Instrumental settings and the TCA retrieved (where provided) are listed as well. The sample spectra from all sites listed are illustrated over the next few pages.

Table A1.5: HCl Details of the observation geometries for the sample spectra featuring the hydrogen chloride window near $2925.9cm^{-1}$. See Table A1.2 (page 518) for a description of the table items.

Observation site	date of recording	zenith angle	OPD [cm]	FoV [mrad]	apodisation	Duration [s]	TCA molec/cm^2	sample name
Eureka	24/Apr/99	70.32	250	1.69	boxcar	1010	5.22e15	24a99006.spc
Ny-Ålesund	28/May/95	59.32	180	2.27	boxcar	n.p.	5.27e15	95052808.s09
Ny-Ålesund	03/Apr/96	74.13	180	1.36	boxcar	595	5.33e15	96040301.s00
Ny-Ålesund lun	02/Feb/96	73.97	45	6.36	boxcar	3760	n.p.	96020217.s00
Kiruna, solar	15/Mar/97	69.87	257	1.91	boxcar	615	3.12e15	970315s3.s90
Kiruna, lunar	04/Dec/98	68.81	45	5.98	boxcar	4401	3.74e15	970323m1.s40
Harestua	20/Mar/01	68.87	257	2.95	boxcar	203	6.37e15	cc010320.01
Jet, 52^{o}N, 1^{o}W	08/Mar/96	68.53	180	2.95	boxcar	186	n.p.	b1920908.bnr
Jungfraujoch	10/Dec/01	69.55	175	2.63	boxcar	1035	3.80e15	r01c10uw.moy
Toronto	15/Aug/02	36.78	250	1.54	boxcar	1010	n.p.	20815300.spc
Tsukuba	17/Feb/99	70.57	257	2.27	boxcar	308	10.33e15	t048j3m1.292
Tsukuba	18/May/01	69.34	257	2.27	boxcar	308	15.86e15	t138l3m0.292
Kitt Peak	14/May/78	69.75	48	n.p.	kpno10	n.p.	1.89e15	140a2925.bin
Kitt Peak	04/Jan/00	70.82	83	n.p.	kpno5	n.p.	n.p.	040m2925.bin
Teneriffe	27/May/02	59.0	250	1.14	boxcar	n.p.	2.41e15	hcl-020527
Polarstern, 2.8^{o}S	25/Oct/96	62.30	180	2.95	boxcar	n.p.	n.p.	96102512.09
Maido Summit	19/Oct/02	70.10	101	3.86	boxcar	123	n.p.	02a19001.shl
Wollongong	14/Sep/99	69.05	250	2.46	boxcar	563	3.80e15	990914f3.506
Lauder	12/Sep/01	69.49	257	2.27	boxcar	408	n.p.	b2551329.bnr
Arrival Heights	18/Oct/01	69.92	257	2.95	boxcar	102	n.p.	b2910329.mnr
Arrival Heights	06/Sep/01	84.53	257	2.95	boxcar	102	n.p.	b2490329.mnr

HCl

Fig.A.79: Eureka, SZA 70.32^o, 24/Apr/99

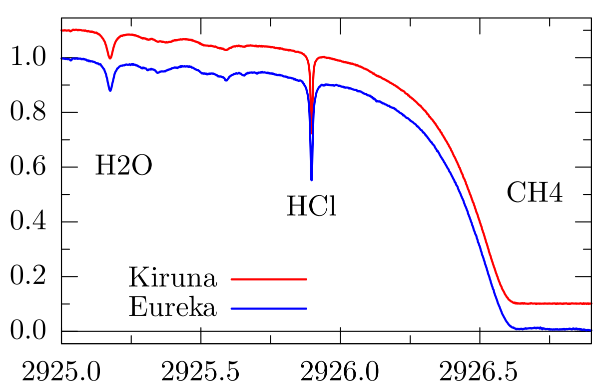

Fig.A.80: Eureka, SZA 70.32^o, 24/Apr/99

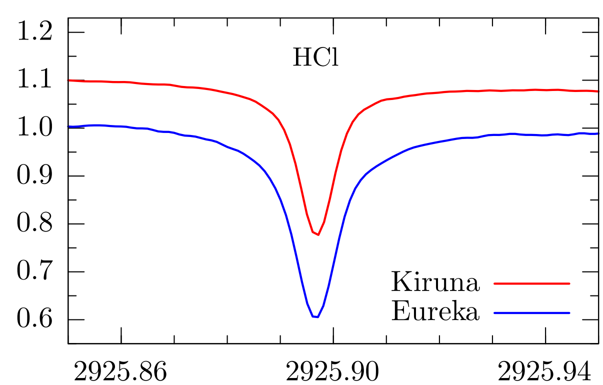

HCl

Fig.A.81: Ny-Ålesund, SZA 64/74^o, 5/95 & 4/96

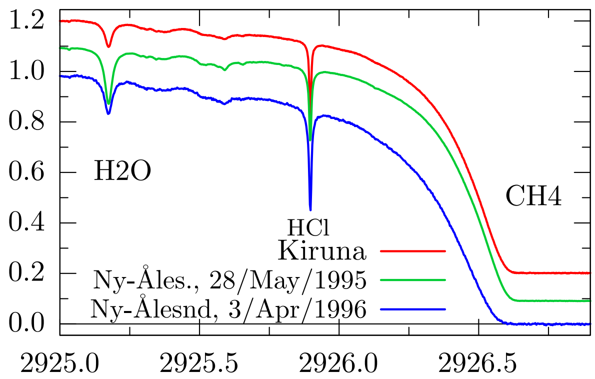

Fig.A.82: Ny-Ålesund, SZA 64/74^o, 5/95 & 4/96

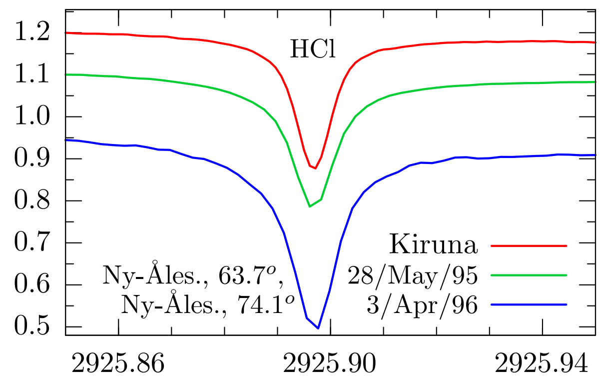

Fig.A.83: Ny-Ålesund, Lunar ZA 74^o, 2/2/96

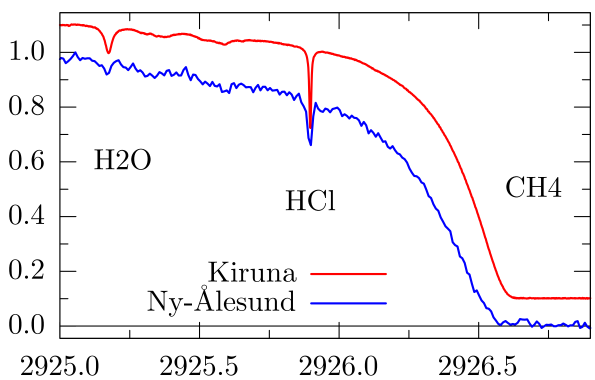

Fig.A.84: Ny-Ålesund, Lunar ZA 74^o, 2/2/96

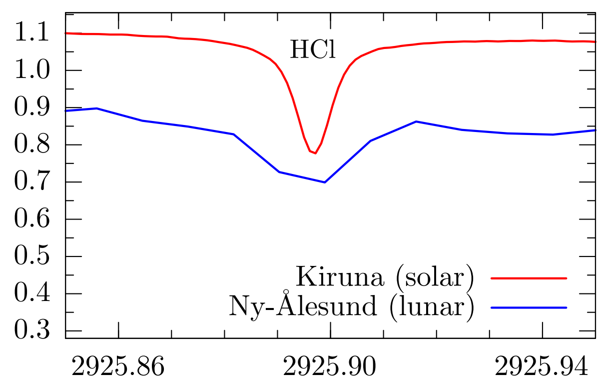

Fig.A.85: Kiruna, Lunar ZA 68.8^o, Mar/96

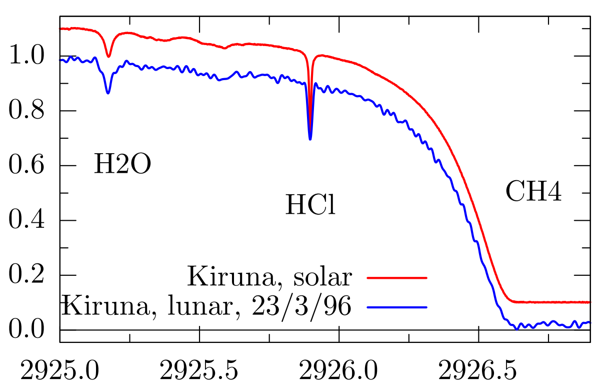

Fig.A.86: Kiruna, Lunar ZA 68.8^o, Mar/96

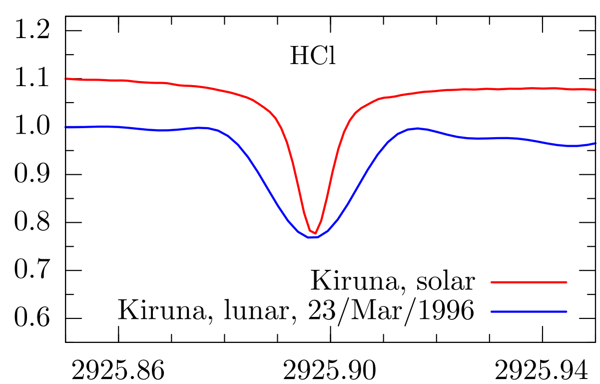

HCl

Fig.A.87: Harestua, SZA 68.9^o, 20/Mar/01

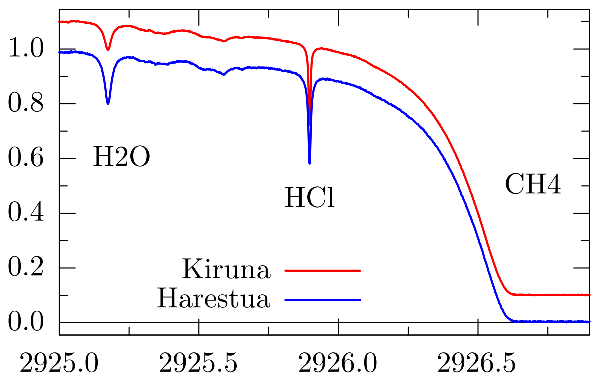

Fig.A.88: Harestua, SZA 68.9^o, 20/Mar/01

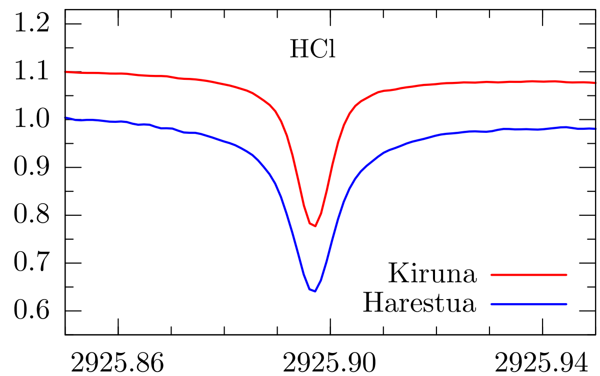

Fig.A.89: Jetstream camp., SZA 56.8^o, Mar/96

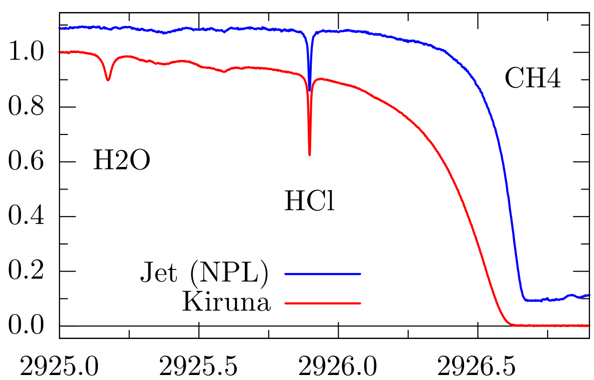

Fig.A.90: Jetstream, SZA 56.8^o, 8/Mar/96

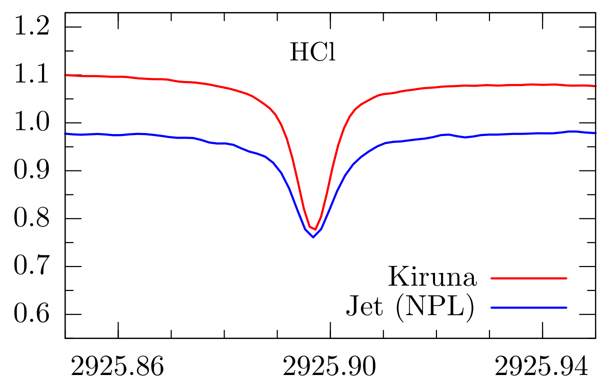

Fig.A.91: Jungfraujoch, SZA 70^o, 10/Dec/01

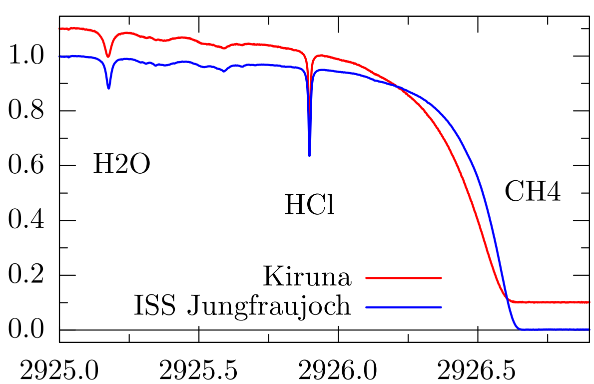

Fig.A.92: Jungfraujoch, SZA 70^o, 10/Dec/01

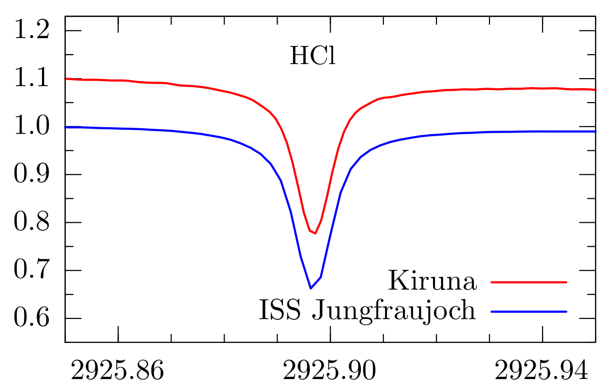

HCl

Fig.A.93: Toronto, SZA 38.8^o, 03/Apr/03

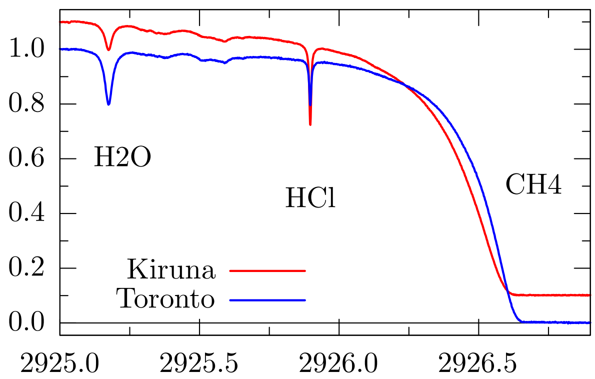

Fig.A.94: Toronto, SZA 38.8^o, 03/Apr/03

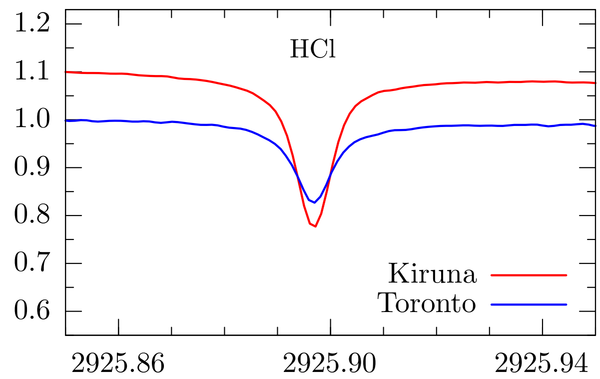

Fig.A.95: Tsukuba, SZA 70^o, Feb/99 & May/01

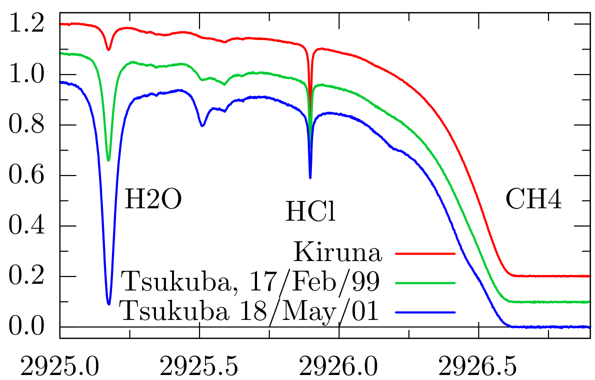

Fig.A.96: Tsukuba, SZA 70^o, Feb/99 & May/01

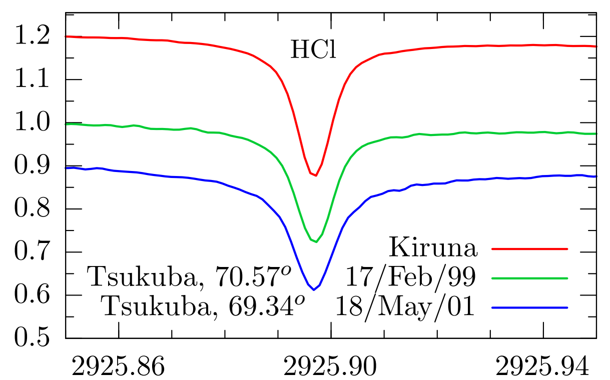

Fig.A.97: Kitt Peak, SZA 70^o, 5/1978 & 1/2000

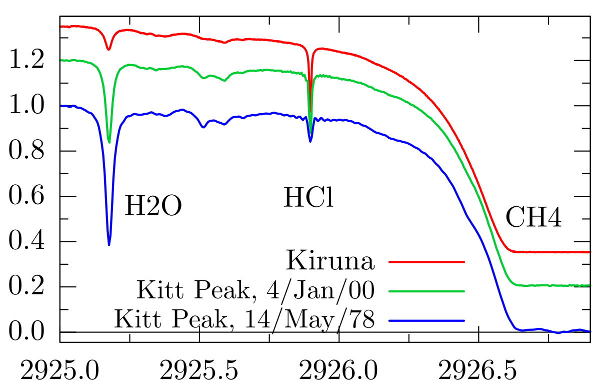

Fig.A.98: Kitt Peak, SZA 70^o, 5/78 & 1/2000

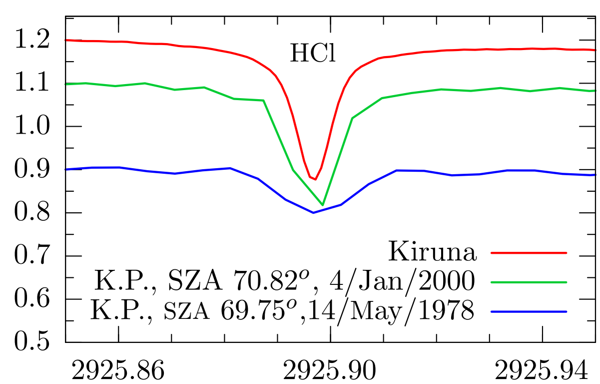

HCl

Fig.A.99: Teneriffe, SZA 59^o, 27/May/02

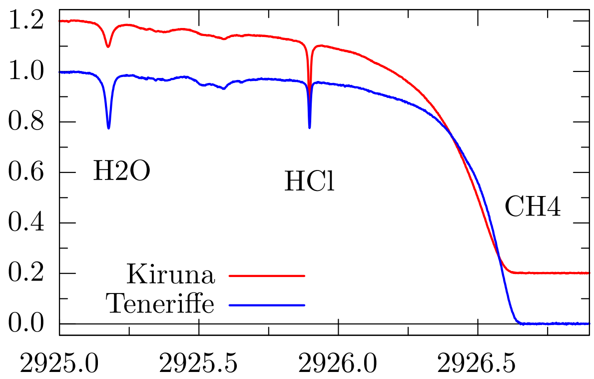

Fig.A.100: Teneriffe, SZA 59^o, 27/May/02

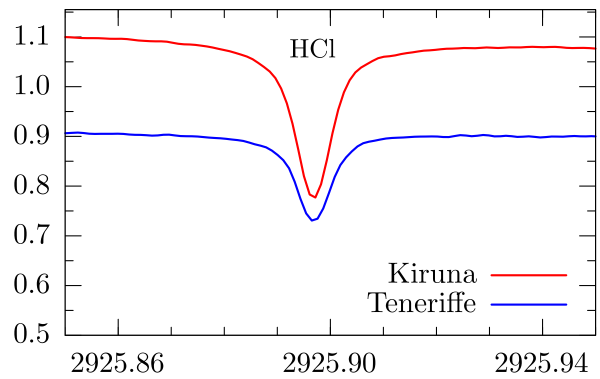

Fig.A.101: Equat. Atlantic, SZA 62^o, 25/10/96

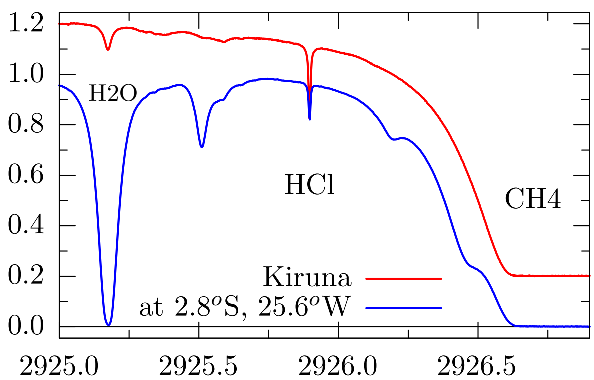

Fig.A.102: Equat. Atlantic, SZA 62^o, 25/10/96

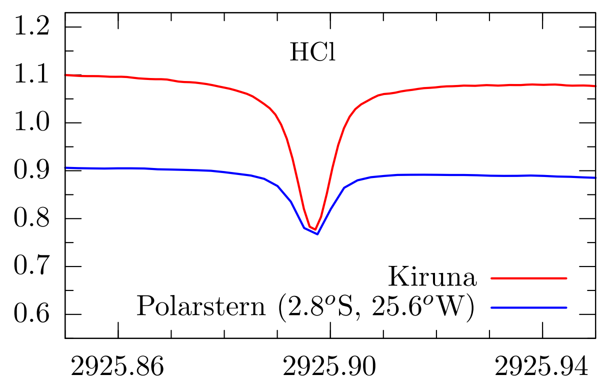

Fig.A.103: Maido Summit, SZA 70^o, 19/Oct/02

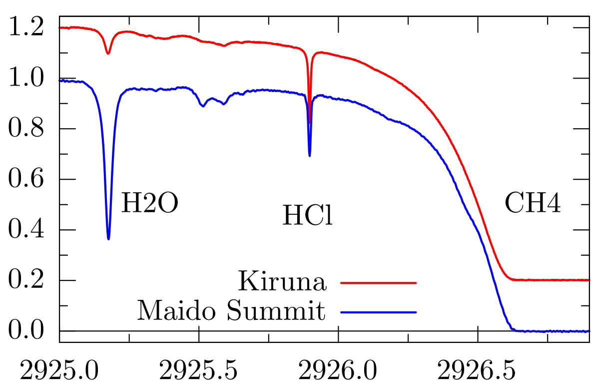

Fig.A.104: Maido Summit, SZA 70^o, 19/10/02

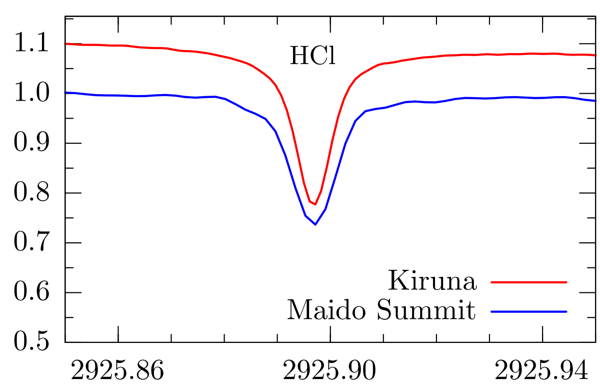

HCl

Fig.A.105: Wollongong, SZA 69^o, 14/Sep/99

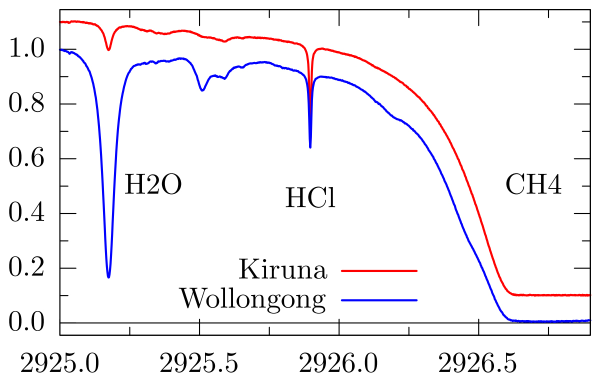

Fig.A.106: Wollongong, SZA 69^o, 14/Sep/99

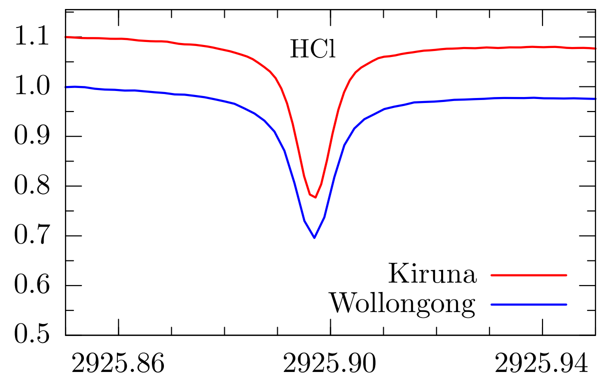

Fig.A.107: Lauder, SZA 69.5^o, 12/Sep/01

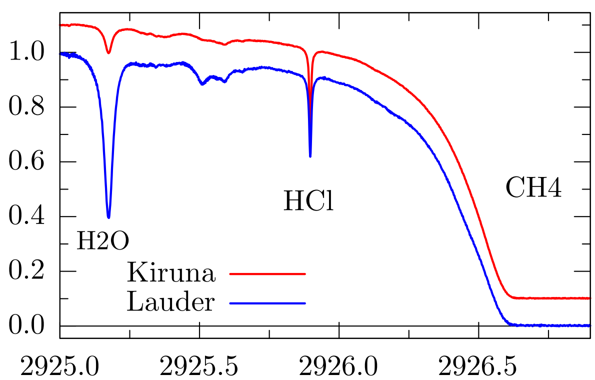

Fig.A.108: Lauder, SZA 69.5^o, 12/Sep/01

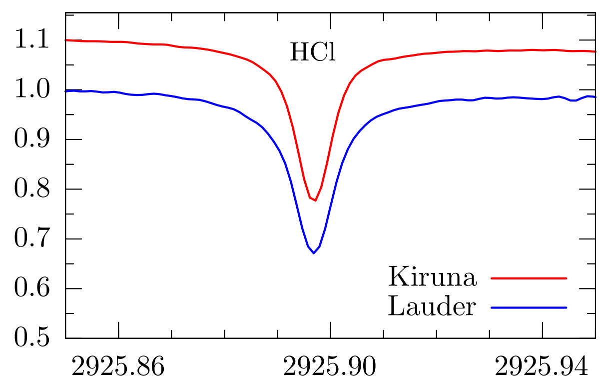

Fig.A.109: Antarctica, SZA 69.9^o, 18/Oct/01

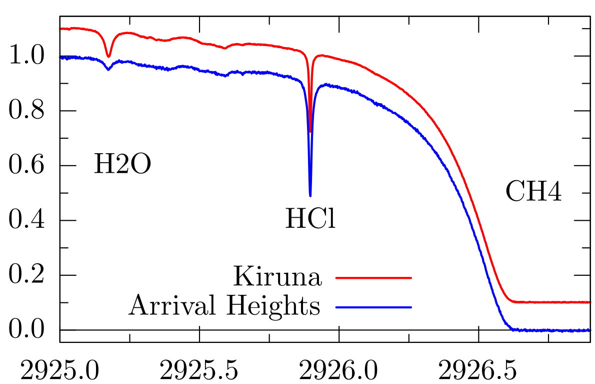

Fig.A.110: Antarctica, SZA 69.9^o, 18/Oct/01

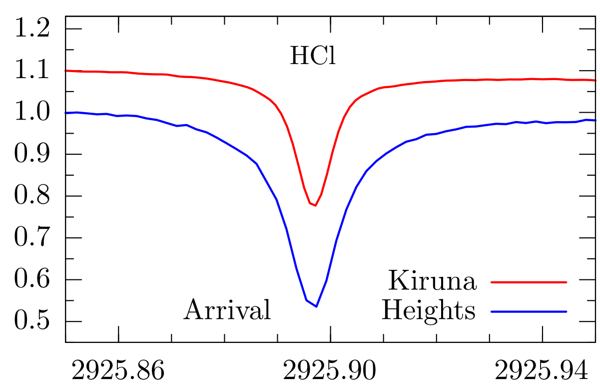

A.6 Comparison of Hydrogen Fluoride

Table A1.6 lists the sites that provided sample spectra for the 4038.9cm^{-1} microwindow for the retrieval of HF. Instrumental settings and the TCAs retrieved (where provided) are listed as well. The sample spectra from all sites listed are illustrated over the next few pages.

Table A1.6: HF Details of the observation geometries for the sample spectra featuring the hydrogen fluoride window near 4038.9cm^{-1}. See Table A1.2 (page 518) for a description of the table items.

Observation site	date of recording	zenith angle	OPD [cm]	FoV [mrad]	apodi-sation	Dura-tion [s]	TCA molec/cm^2	sample name
Eureka	24/Apr/99	70.96	250	1.69	boxcar	1010	1.96e15	24a99007.spc
Ny-Ålesund	28/May/95	57.88	128	2.27	boxcar	n.p.	1.45e15	95052846.s09
Ny-Ålesund	03/Apr/96	73.97	128	2.27	boxcar	595	2.84e15	96040302.s00
Ny-Ålesund lun	02/Feb/96	73.97	45	6.36	boxcar	3760	n.p.	96020217.s00
Kiruna, solar	15/Mar/97	69.97	257	1.91	boxcar	615	2.28e15	970315s1.s90
Kiruna, lunar	04/Dec/98	68.81	45	5.98	boxcar	4401	2.28e15	970323m1.s40
Harestua	20/Mar/01	68.10	180	2.95	boxcar	284	2.19e15	aa010320.23
Jet, 52^{o}N, 1^{o}W	08/Mar/96	68.54	128	2.95	boxcar	192	n.p.	b1920908.bnr
Jungfraujoch	14/Jan/01	70.38	114	2.63	boxcar	270	1.81e15	r01114on.moy
Toronto	24/Apr/03	35.80	250	1.54	boxcar	1010	n.p.	30424100.spc
Tsukuba	17/Feb/99	72.30	257	2.27	boxcar	308	1.02e15	t048j1m1.403
Tsukuba	18/May/01	70.99	257	2.27	boxcar	308	1.41e15	t138l1m1.403
Kitt Peak	02/Dec/79	78.74	35	n.p.	kpno10	n.p.	0.34e15	020b4025.bin
Kitt Peak	17/Jan/94	69.44	47	n.p.	kpno5	n.p.	n.p.	170j4025.bin
Teneriffe	27/May/02	52.0	180	1.14	boxcar	n.p.	0.87e15	hf020527.dpt
Polarstern, 13^{o}S	27/Oct/96	65.20	128	2.27	boxcar	n.p.	n.p.	96102722.09
Maido Summit	25/Oct/02	67.95	125	2.95	boxcar	303	n.p.	02a25007.shf
Wollongong	16/Jul/97	69.82	250	1.85	boxcar	563	1.01e15	970716f1.502
Lauder	25/May/01	70.85	257	2.27	boxcar	409	n.p.	b1453240.bnr
Arrival Heights	20/Dec/01	71.13	257	2.27	boxcar	102	n.p.	b3541240.mnr

HF

Fig.A.111: Eureka, SZA 70.96^o, 24/Apr/99

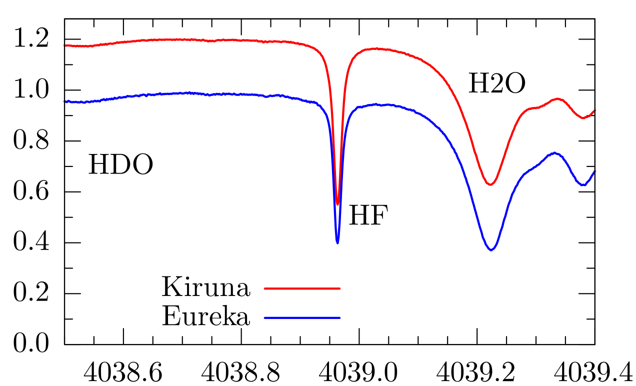

Fig.A.112: Eureka, SZA 70.96^o, 24/Apr/99

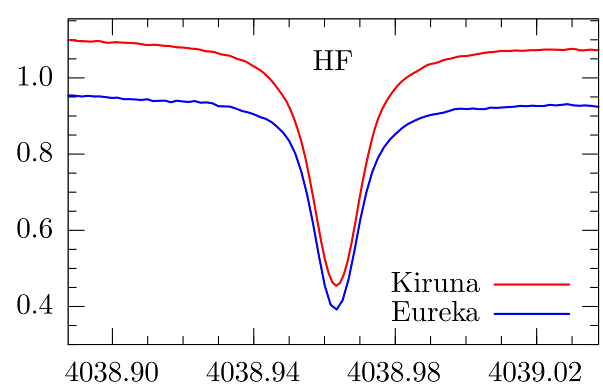

Fig.A.113: Ny-Ålesund, SZA 58/74^o, 5/95 & 4/96

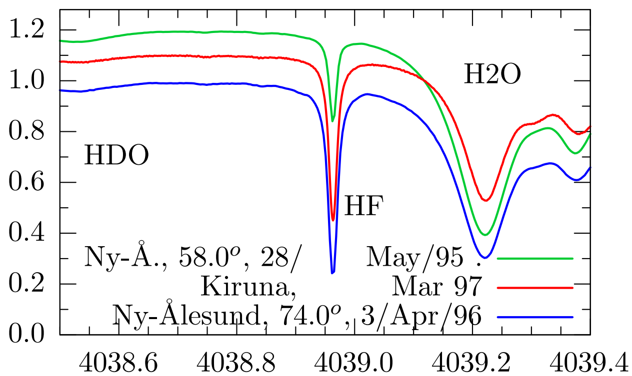

Fig.A.114: Ny-Ålesund, SZA 58/74^o, 5/95 & 4/96

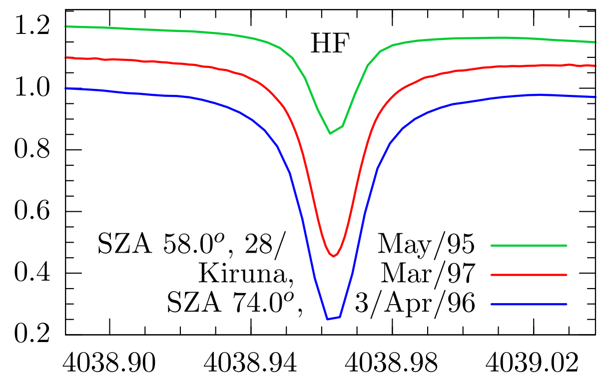

Fig.A.115: Ny-Ålesund, Lunar ZA 74^o, 2/2/96

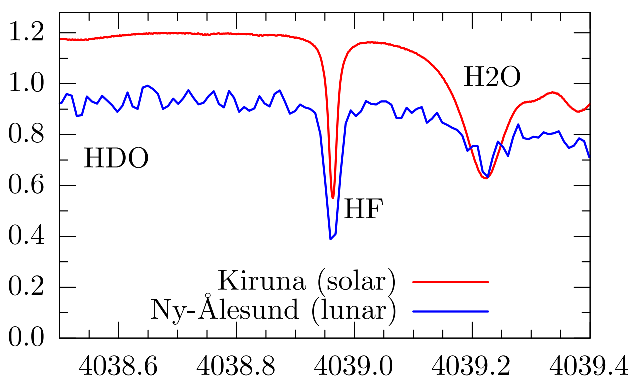

Fig.A.116: Ny-Ålesund, Lunar ZA 74^o, 2/2/96

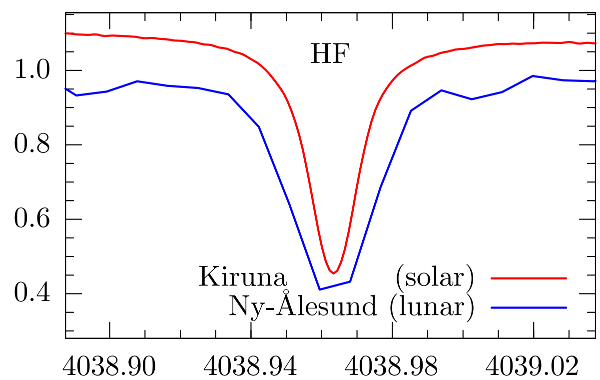

Fig.A.117: Kiruna, Lunar ZA 69^o, 23/3/96

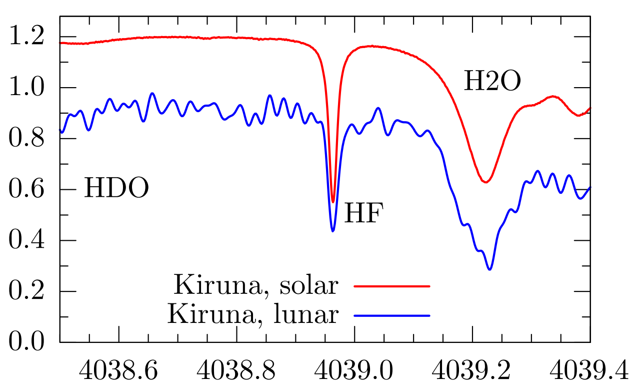

Fig.A.118: Kiruna, Lunar ZA 69^o, 23/3/96

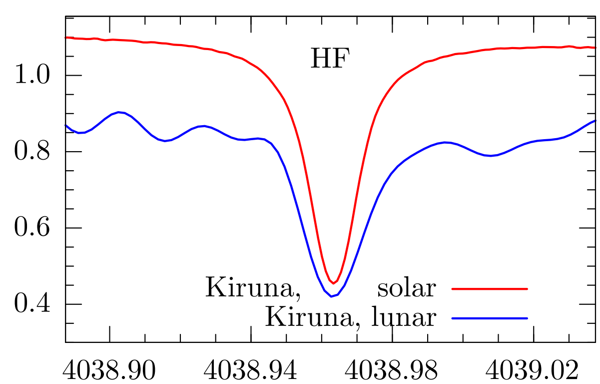

Fig.A.119: Harestua, SZA 68.1^o, 20/Mar/01

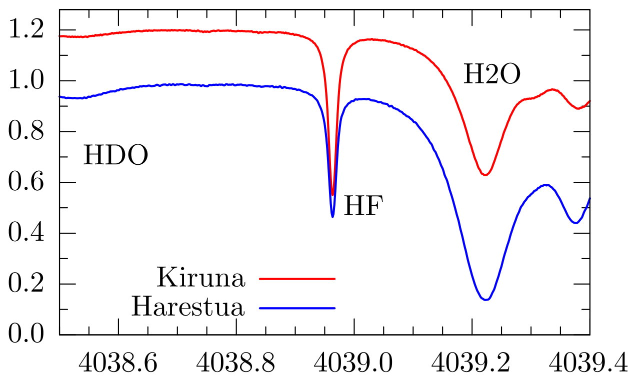

Fig.A.120: Harestua, SZA 68.1^o, 20/Mar/01

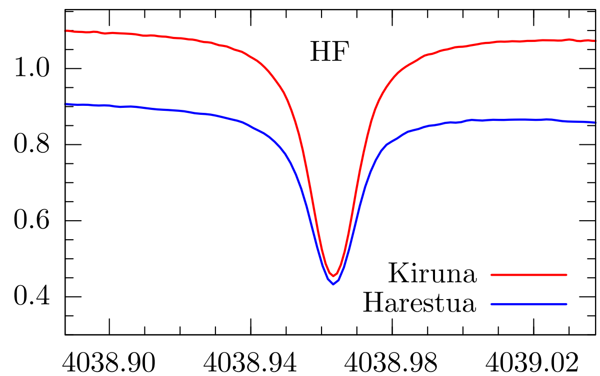

Fig.A.121: Jetstream camp., SZA 57^o, 8/Mar/96

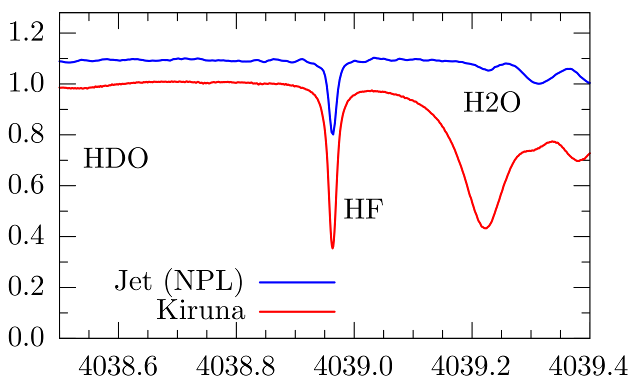

Fig.A.122: Jetstream, SZA 57^o, 8/Mar/96

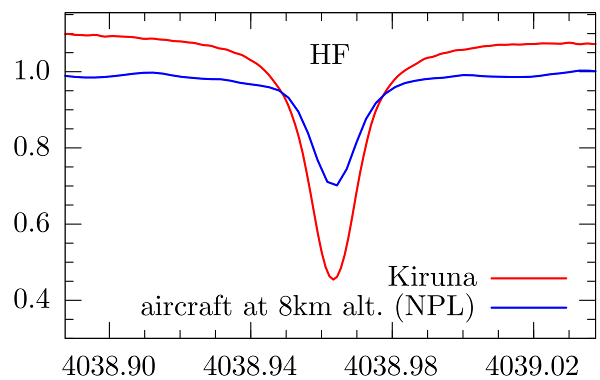

Fig.A.123: Jungfraujoch, SZA 70.4^o, 14/1/01

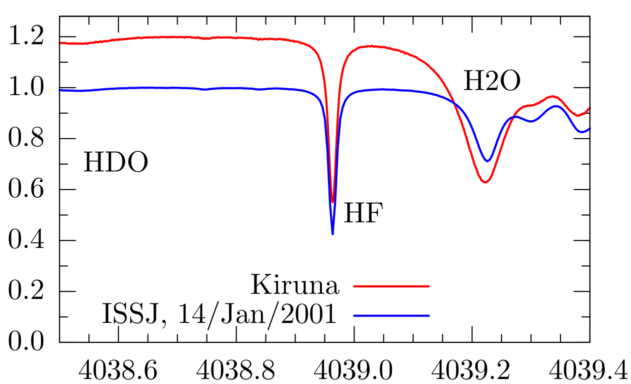

Fig.A.124: Jungfraujoch, SZA 70.4^o, 14/1/01

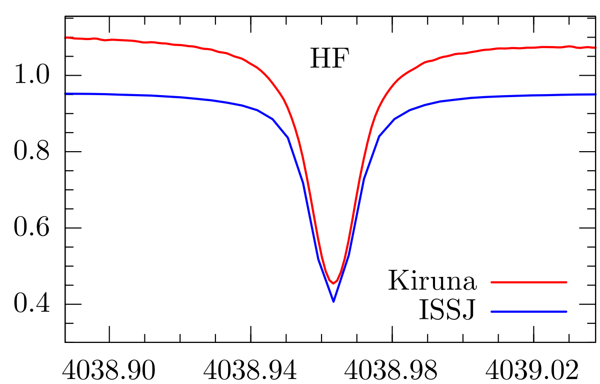

HF

Fig.A.125: Toronto, SZA 35.8^o, 24/Apr/03

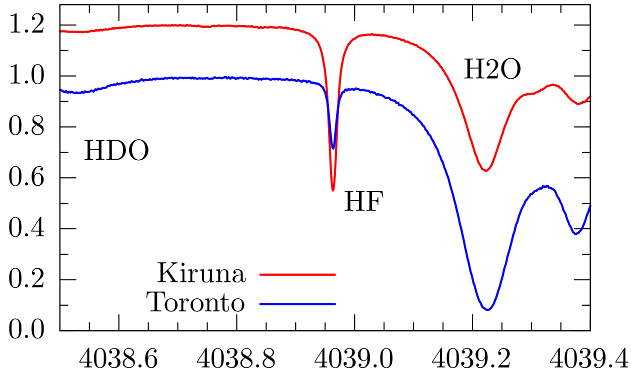

Fig.A.126: Toronto, SZA 35.8^o, 24/Apr/03

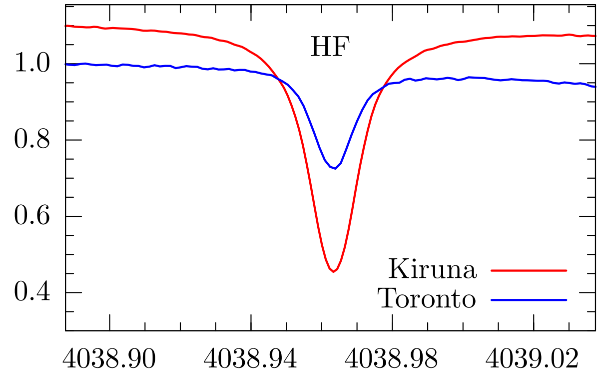

Fig.A.127: Tsukuba, SZA 70^o, 2/99 & 5/01

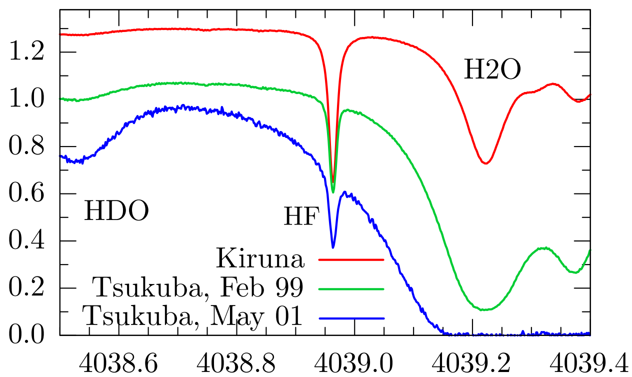

Fig.A.128: Tsukuba, SZA 70^o, 2/99 & 5/01

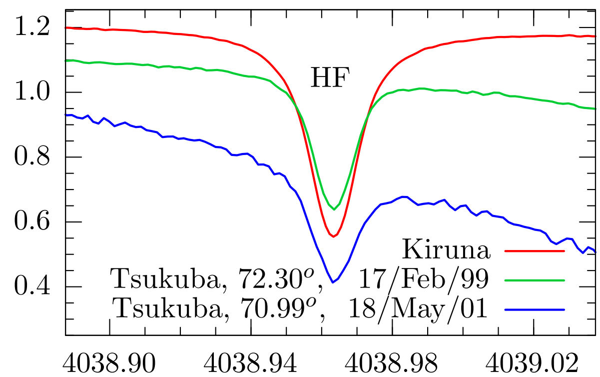

Fig.A.129: Kitt Peak, Dec 1979 & Jan 1994

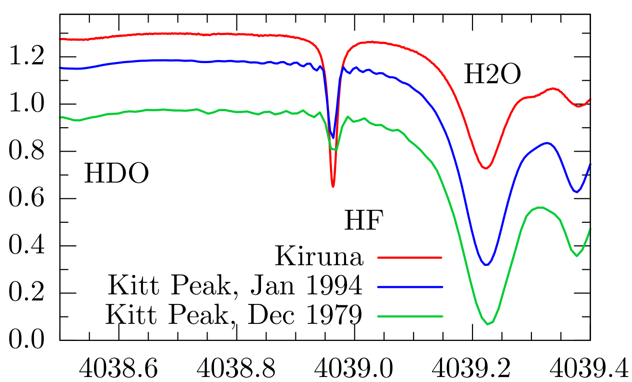

Fig.A.130: Kitt Peak, Dec 1979 & Jan 1994

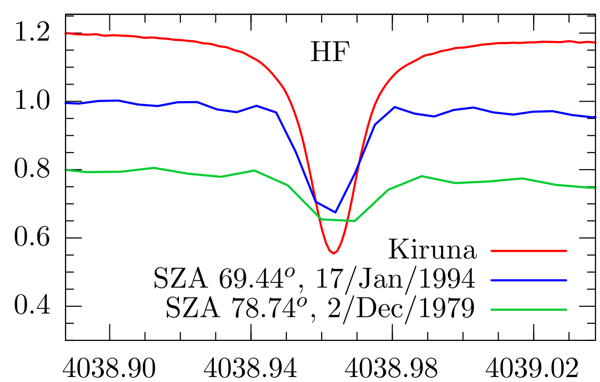

HF

Fig.A.131: Teneriffe, SZA 52^o, 27/May/02

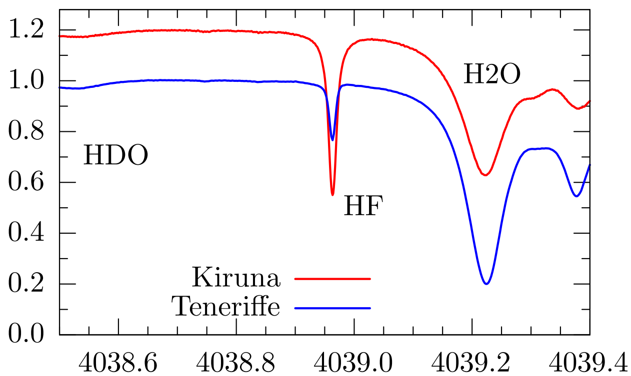

Fig.A.132: Teneriffe, SZA 52^o, 27/May/02

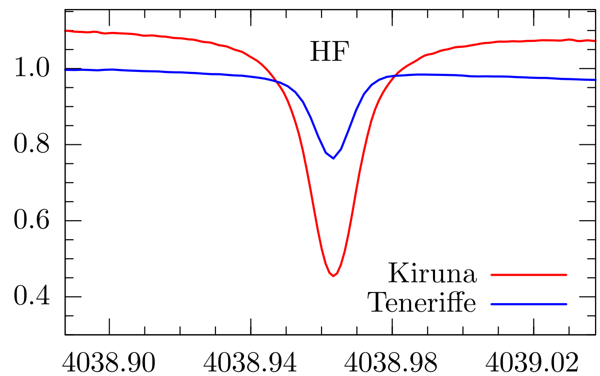

Fig.A.133: Equat. Atlantic, SZA 65^o, 27/10/96

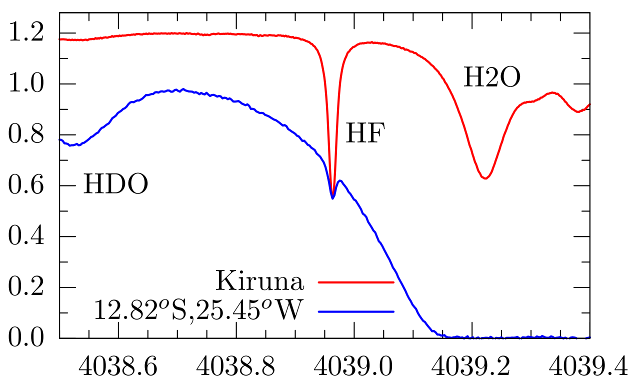

Fig.A.134: ship cruise, SZA 65^o, 27/10/96

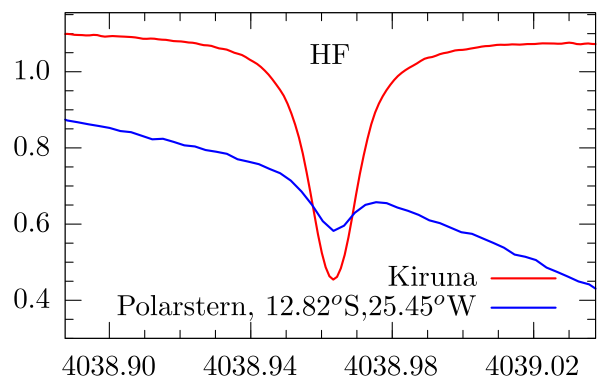

Fig.A.135: Maido Summit, SZA 68^o, 25/10/02

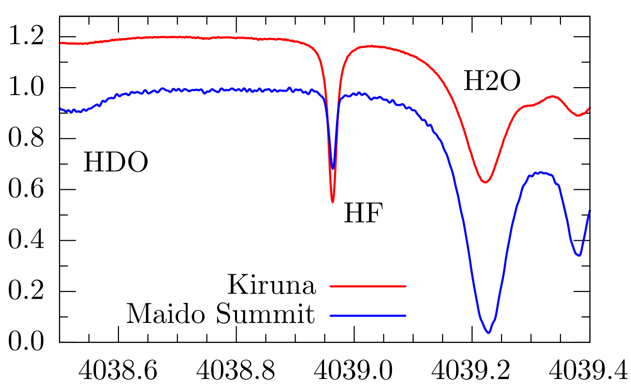

Fig.A.136: Maido Summit, SZA 68^o, 25/10/02

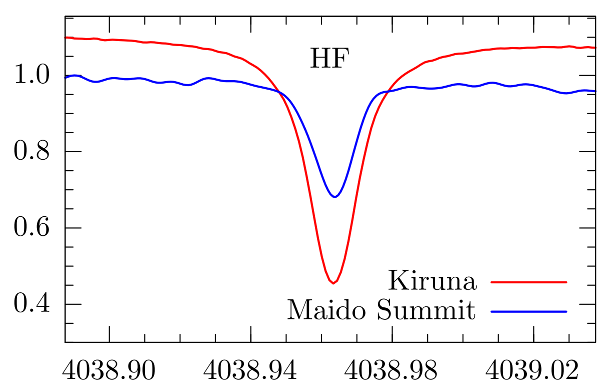

Fig.A.137: Wollongong, SZA 70^o, 16/Jul/97

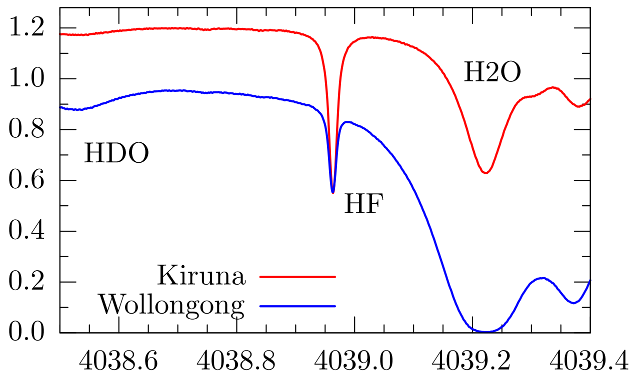

Fig.A.138: Wollongong, SZA 70^o, 16/Jul/97

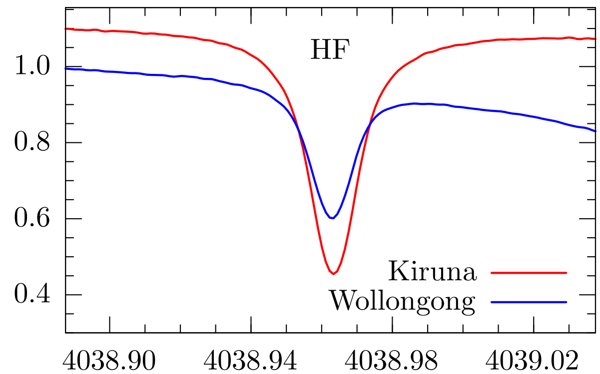

Fig.A.139: Lauder, SZA 70.9^o, 25/May/01

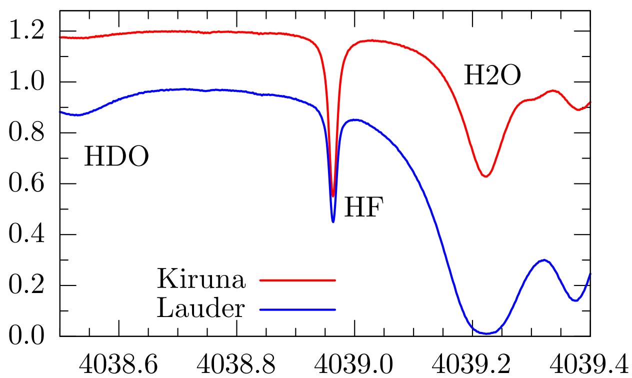

Fig.A.140: Lauder, SZA 70.9^o, 25/May/01

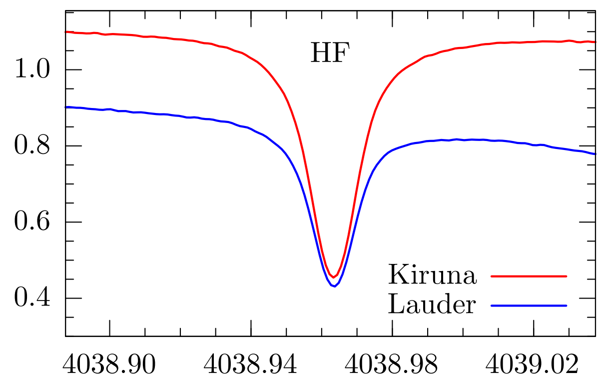

Fig.A.141: Antarctica, SZA 70^o, 20/Dec/01

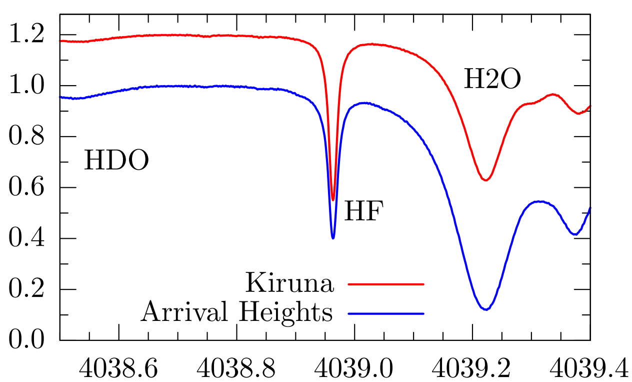

Fig.A.142: Antarctica, SZA 70^o, 20/Dec/01

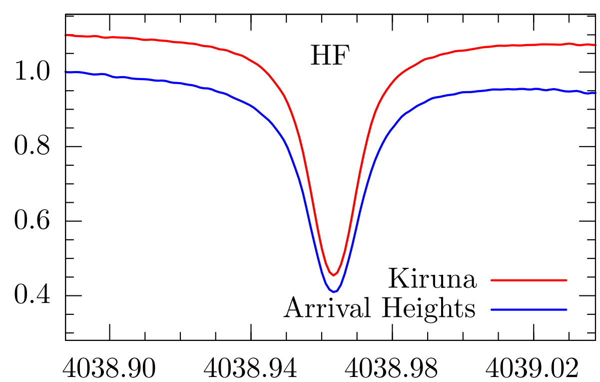

B Other spectra of special interest

Some of the *spectra of special interest* have already been included in the previous section. These include airborne observations from a cruising altitude of $8km$ (very low water vapour and narrow lines), spectra from the equatorial Atlantic (Polarstern ship-cruise), Kitt Peak spectra recorded some 20 years apart (note the significant increase in inorganic chlorine seen in Figures A.97 and A.98 over the time period), and lunar spectra from 3 Arctic locations (Ny-Ålesund, Kiruna, and Eureka).

This section gives additional examples of noteworthy spectra recorded under special conditions. This includes a closer look at lunar spectra, an event of tropospheric HCl pollution, an event of chlorine activation, the presence of polar stratospheric ice clouds, and spectra recorded during intense bushfires in Australia.

B.1 Tropospheric HCl pollution:

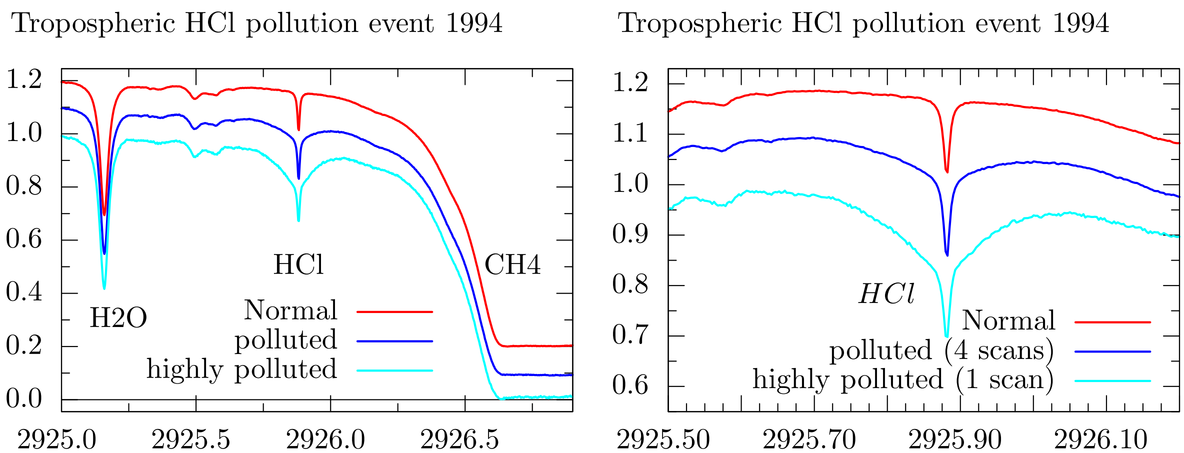

Fig. B.1: A local, tropospheric HCl pollution event recorded by the NPL team during an instrumental intercomparison in 1994.

Example of significant tropospheric HCl pollution measured in Oxfordshire, UK, 1994. The three spectra labelled "Normal", "polluted", and "highly polluted" show a co-add of 12 spectra from later the same day showing the HCl region as usual, a co-add of 4 spectra which all showed significant HCl pollution in the troposphere, and a single scan with very large HCl tropospheric pollution; respectively. The spectra were taken during an FTIR instrument intercomparison at Rutherford Appleton Laboratories 51.57^{o}N, 1.31^{o}W, 130m altitude on the 13th August, 1994, using 180cm OPD, boxcar apodisation and 5$mrad$ field of view on a Bruker 120M spectrometer run at scan speed 8 (40kHz). Measurements by Clare Paton-Walsh and William Bell, NPL.

B.2 ClO Observations above Aberdeen

Elevated levels of ClO measured from Aberdeen during the SESAME campaign. The 3 figures shown contain the regions of the p8.5, p10.5 and p11.5 lines. The regions are cut from co-added spectra (4 x 6 co-adds) taken between 13.10 and 13.25 UT on 20^{th} January 1995 from Aberdeen, UK (57^oN, 2^oW, $150m$ altitude) representing a solar zenith angle of 78.26^o. The ClO features are small but clearly identifyable at 833.3; 830.6 and $829.25cm^{-1}$, respectively (indicated by arrows). The maximum optical path difference was 180 cm with a field of view of 6.4 $mrad$ using boxcar apodisation on a Bruker IFS 120M spectrometer run at a scan speed of $40kHz$. Measurements by W. Bell, C. Paton-Walsh, and T.D. Gardiner, NPL.

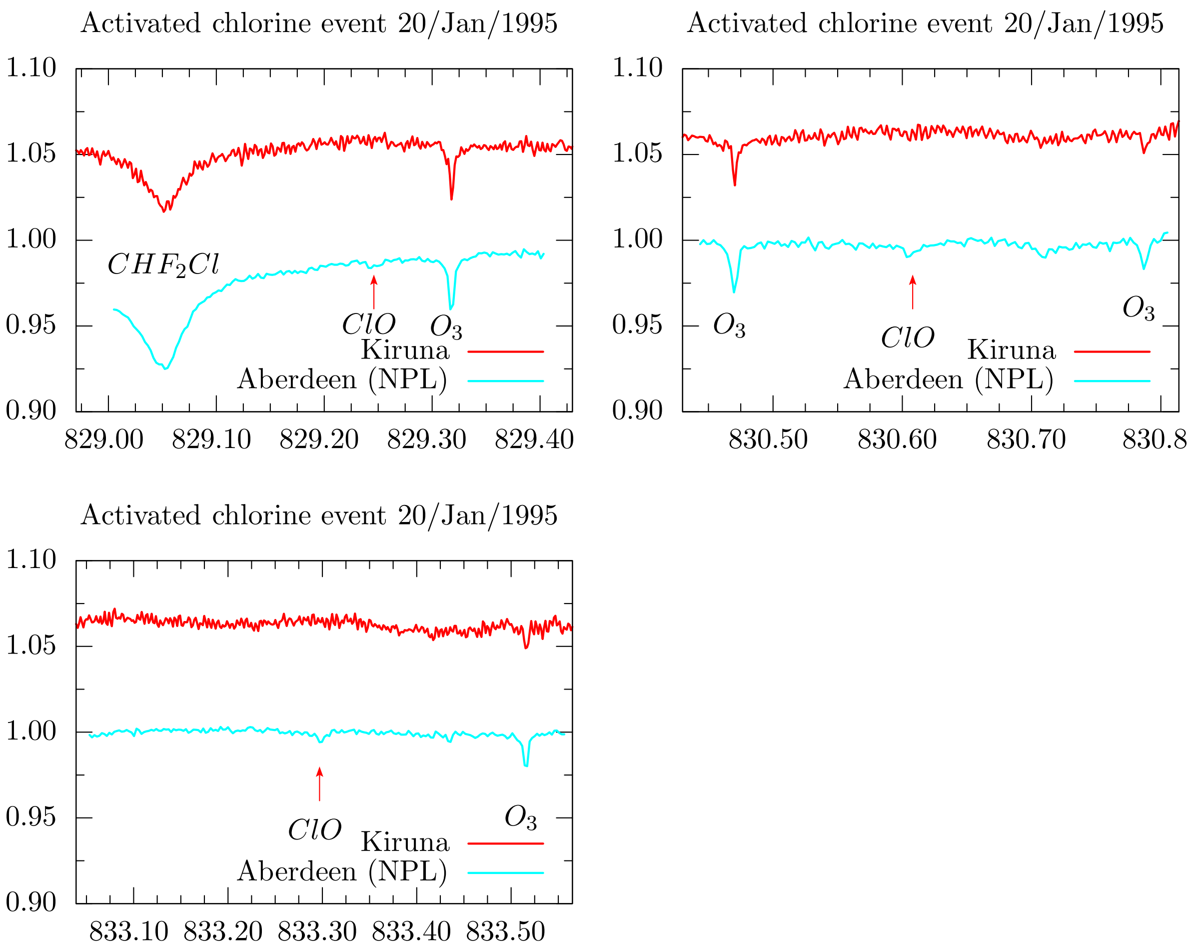

Fig. B.2: The three panels show the p8.5, p10.5 and p11.5 lines of ClO (indicated by arrows) as observed during the SESAME campaign and for comparison the Kiruna spectra in which the *ClO* features are below detection limit.

Analysis of 13 independent absorption features in the P and R branches of the (0–1) vibration-rotation band of ^{35}ClO in the 817–$855cm^{-1}$ spectral region yielded a total column amount of 3.42±0.47E15 molec/cm^2. These high values indicate that significant chlorine activation had occurred and that the airmasses sampled were of polar origin. A 3D chemical transport model employed in the studies suggested that most of the ClO was located between 16 and $22km$ altitude, which translates to a concentration of $2.6ppm$ to be consistent with the total column amount observed. Details of the measurements and their interpretation are found in (Bell, et al., 1996).

B.3 Lunar spectra

The following 5 figures illustrate lunar spectra recorded at the Kiruna site. Special attention is drawn to 2 important properties: The absence of undesired solar interferences and the important role of emission in lunar absorption spectra.

The moon is significantly cooler than the sun, reaching a typical temperature of 370K during full moon as opposed to an approximate 5600K for the source of solar spectra. A quick look at the Stefan–Boltzmann law that relates the radiation emitted by a blackbody to the 4^{th} power of its temperature translates into a difference in the radiation flux of 2 to 3 orders of magnitude in the spectral region of interest (Figure B.3, quoted from Meier, 1997). Consequently one may expect much a poorer singal–to–noise ratio for lunar spectra as compared to solar spectra under otherwise identical observation conditions. The anticipated lower flux can be compensated for to some extend through the use of a strong telescope in the suntracker optics, a larger aperture stop, more sensitive detectors, lower spectral resolution, and longer integration times. Except for an enhanced telescope all other measures were taken in the lunar spectra presented here (compare Table A1.2). The lunar spectra were recorded at an OPD of 45cm, a field of view of 6.36mrad, co-added over one hour, using dedicated high-sensitivity lunar MCT and InSb detectors.

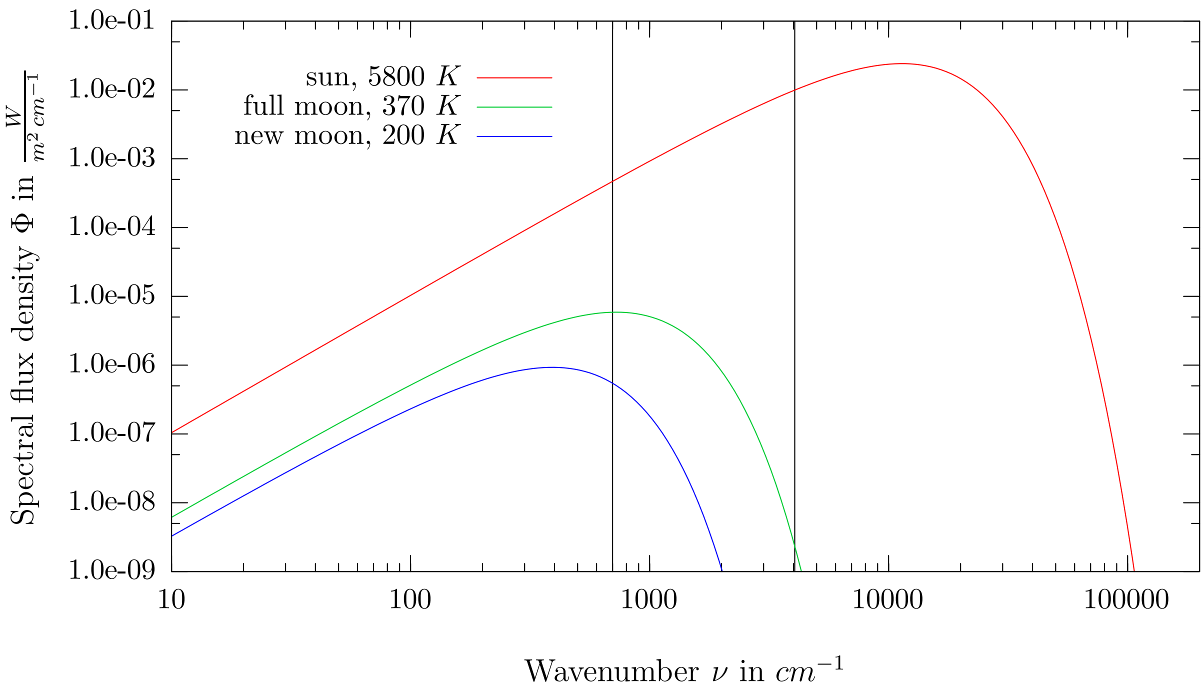

Fig. B.3: Comparison of the solar and lunar spectral flux density Φ incident on the terrestrial surface neglecting atmospheric interaction. In a simple approximation the sun and moon are treated as blackbodies of the temperatures given in the key. The maximum in radiation is found according to Wien's law near 12100 cm^{-1} (500 nm) for the solar spectrum and at 770 cm^{-1} (7.8 μm) for the full moon. The vertical lines indicate the mid-infrared region from 700 to 4050 cm^{-1}. (Figure quoted from Meier, 1997.)

Emission from the dark night sky and the instrument complicate the situation significantly and must be taken into account explicitly in the data analysis, because the typical temperature of the dark night sky (ca. 250K) and of the instrument itself (274K) is not dramatically

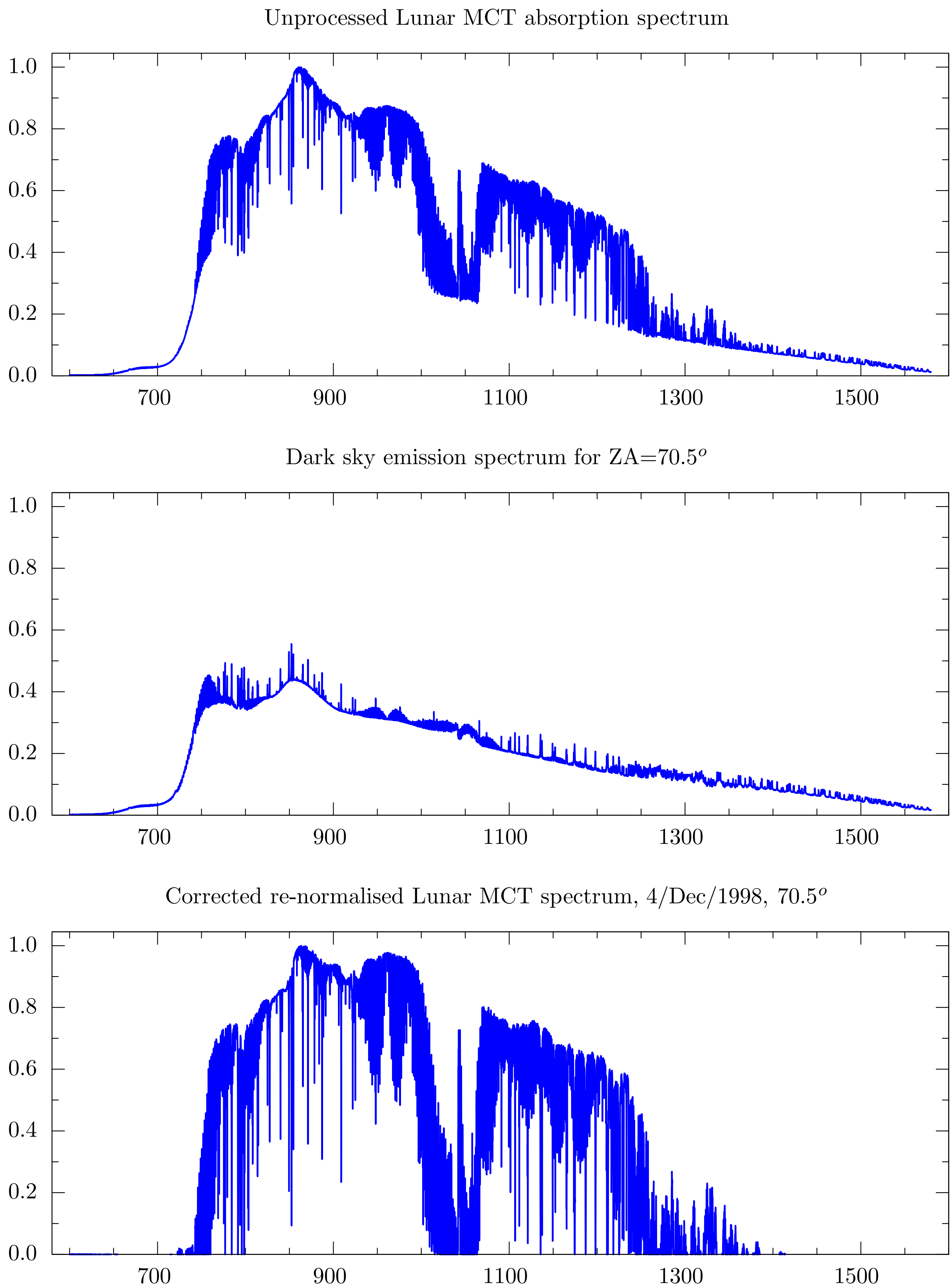

Fig. B.4: Illustration of the observed lunar spectrum (top) and its decomposition into emission contribution (center) and pure absorption spectrum (bottom).

lower than the temperature of the full moon (370K). Schreiber (1994) gives a very hands-on description of the pitfalls of self-emission in an FTS. In short, it is very advisable that the lunar detector does not see any parts of the spectrometer that are at room temperature – this is achieved by placing the aperture stop and the optical filter inside the detector dewar keeping them at the temperature of liquid nitrogen and avoidance of any external filters or lenses.

There is nothing we can do about the temperature of the sky though. However, this is only of importance below roughly $2000cm^{-1}$ as the emissivity of a blackbody at 250K drops sharply above $1500cm^{-1}$. The fact that we can still obtain an appreciable signal from the moon at higher wavenumbers is largely due to the fact that direct reflection takes over as the dominant source of light as opposed to blackbody radiation from the lunar surface dominating at lower wavenumbers (Notholt et al., 1994, 1995).

Figure B.4 illustrates a) the raw lunar MCT spectrum as recorded from the ground at Kiruna at a lunar zenith angle of 70.5^o on the evening of 4/Dec/1998. This is compared to b) a dark sky emission spectrum representative for the same zenith angle recorded the same night and c) the difference spectrum of a) - b). The emission spectrum was obtained by pointing the suntracker away from the moon (azimuth angle differs by greater than 30^o) and taking one emission spectrum each at a zenith angle of 40 and 80^o with otherwise identical instrumental settings. For each absorption spectrum recorded that night a matching emission spectrum was constructed by taking a weighted mean over the two emission spectra such that the required total air mass factor from the absorption spectrum was matched exactly. All interferograms were transformed using the phase information from a calibration spectrum recorded with the help of an external blackbody of 1000^oC – for a discussion of the advantages of using a stored phase for emission spectra see Brault (1987).

The resulting spectrum c) gives the lunar absorption spectrum after correcting for all emission contributions. This corrected lunar spectrum can be analysed just like any solar absorption spectrum except that solar absorption lines need not be taken into account. While lunar spectra require more diligence and result typically in lower spectral and temporal resolution, they add greatly to our observation capabilities during polar night and in the study of diurnal patterns. Given the nature of emission from the dark sky, this technique works best in cold nights. Note also that lunar observations are more susceptible to the distorting effects of clouds than solar spectra are; in particular if the clouds are "warm" tropospheric clouds,

Figure B.5 gives a close-up view of the emission spectrum and highlights the effects of a poor phase information. The emission spectrum (bottom, green) has been mirrored and stretched to superpose with the absorption spectrum. Absorbers in the relatively warm troposphere result in broad features in both the absorption and the emission spectrum, while the sharp features of ozone are practically absent from the emission spectrum. The stratosphere is much colder, thus very little emission from ozone is observed. Re-transforming the original emission interferogram with a stored phase results in a much better phase corrected spectrum (red) than compared to using the phase information from the low-intensity emission spectrum itself (blue) (see Brault, 1987, for an explanation). The stored phase was obtained with a blackbody spectrum taken immediately after the emission spectrum with identical instrumental settings except for a flat mirror in the parallel beam to switch from the suntracker to the blackbody source.

The next figure, B.6, compares the corrected and normalised lunar MCT spectrum (top) and the raw lunar InSb spectrum (bottom) to comparable spectra recorded with the sun. Note that the InSb solar spectra (lower panel), in contrast to the lunar spectra, are composite spectra, consisting of 4 solar spectra recorded with different optical filters that were normalised

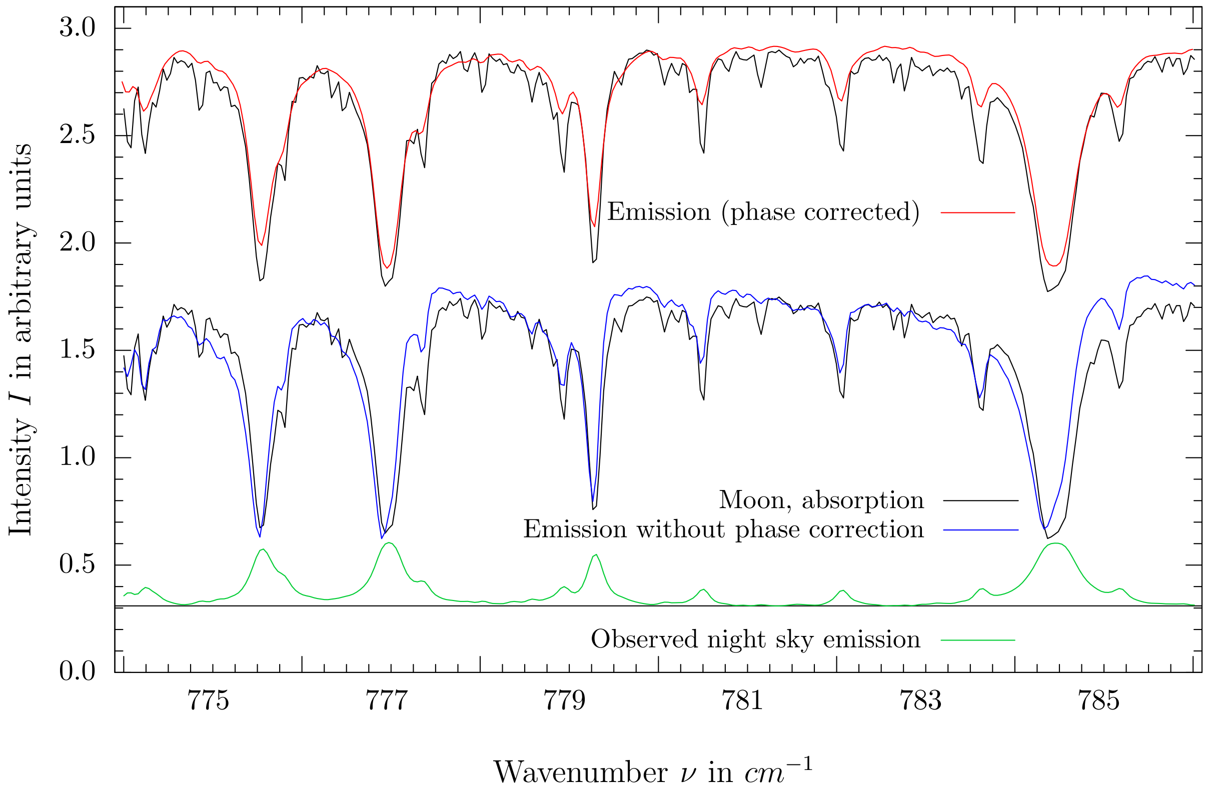

Fig. B.5: A more detailed comparison of the lunar absorption and the night sky emission spectrum is shown. The lowest curve (green or solid[7] line) gives the phase corrected night sky spectrum, with the blackbody portion indicated by the black or dashed line. Both the phase corrected (top red or solid line) and the not phase corrected emission spectrum (blue or broken line in the centre) have been projected onto the absorption spectrum (black or dotted line) by mirroring and stretching to illustrate the line shape distortion caused by the large phase errors common in emission spectra. Differences in the general lineshape between absorption and emission spectra are mostly due to differences in the location of signal formation. Most of the emission arises from the warmer lower troposphere. Thus, stratospheric gases like ozone are mostly absent in the emission spectra. (Figure quoted from Meier, 1997.)

individually before merging them. The solar spectra are the Kiruna solar spectra used as a reference throughout the microwindow atlas; i.e. they were recorded on 15/Mar/1997 (600 to $4370 cm^{-1}$) and and 1/Apr/1998 (3950 to $7140 cm^{-1}$).

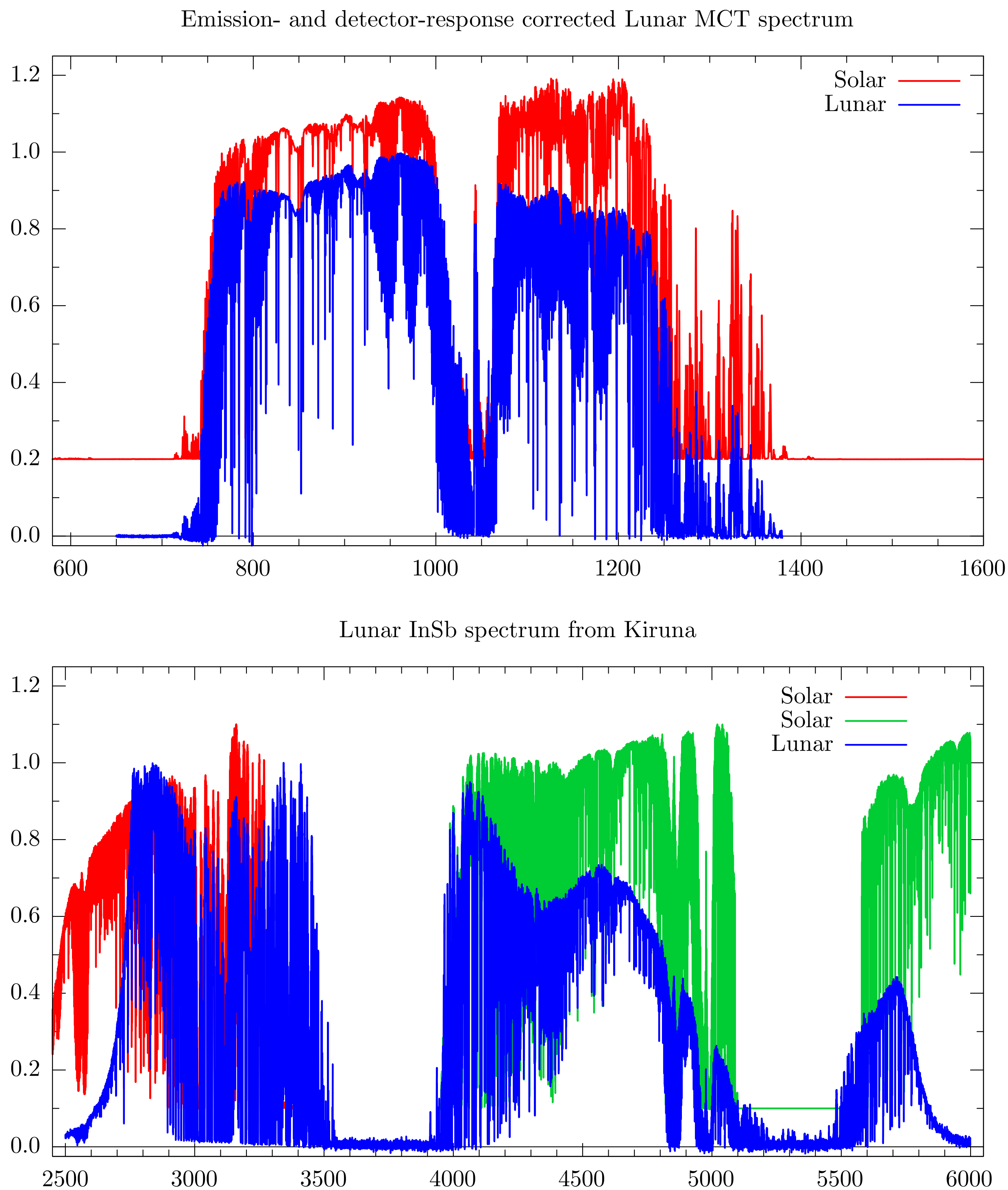

Fig. B.6: The corrected lunar absorption spectrum for the MCT detector (top) and for the InSb detector (bottom) are compared to solar spectra recorded at a similar zenith angle.

B.4 Polar stratospheric ice clouds

On 26^{th} Jan, 2000, around local noon and shortly after the end of polar night, solar absorption spectra were recorded from Kiruna in the presence of stratospheric ice clouds. These measurements coincided closely in time and space with lidar measurements from an aircraft. The measurements shown in Figure B.7 were kindly provided by Michael Höpfner, Thomas Blumenstock, and Frank Hase from FZ Karlsruhe.

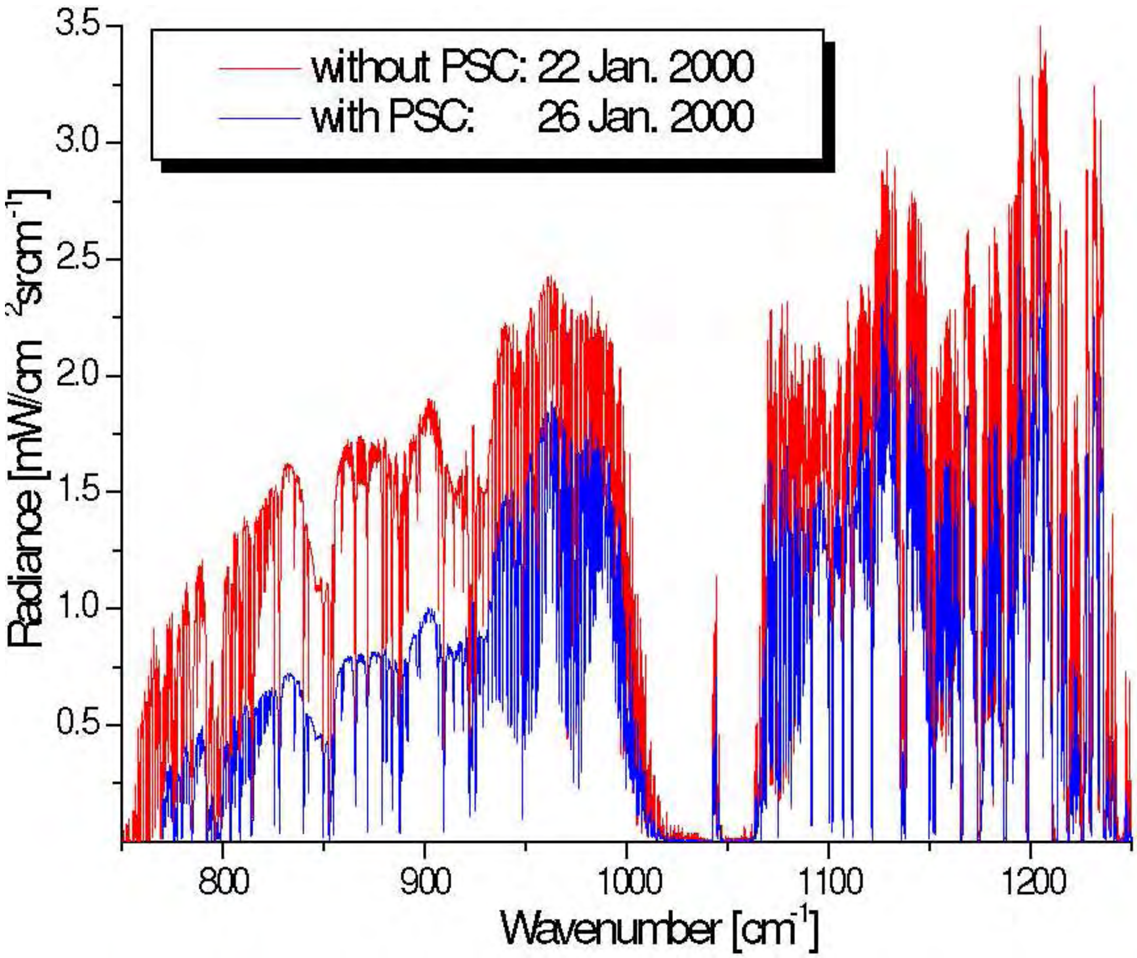

Fig. B.7: Solar absorption spectrum recorded through a thin polar stratospheric ice cloud at Kiruna on the 26^{th} Jan, 2000 and comparison with a clear-sky spectrum recorded 4 days earlier.

The measurements discussed represent the first report of ground-based solar FTIR techniques as a means of retrieving micro-physical parameters of ice clouds. The spectra were calibrated to absolute radiance with an external blackbody operated at $1273K$. The solar zenith angle was very high (88.3^o). However, zenith angle smearing can be neglected, because of the very slow change of the solar zenith angle at this latitude and season. Retrieval of the mean particle properties from the low resolution FTIR spectrum ($0.14cm^{-1}$) depends on the assumed width of the particle size distribution and range from 1.1 to $2.0\mu m$ radius and from 1.9 to $5.1cm^{-3}$ number density. The volume density determined is 60.2 to $63.8\mu m$ equivalent to $2.5ppmv$ of condensed water at $20hPa$. Simulations of lidar backscatter ratios based on the FTIR results are consistent with the lidar observations. For a full discussion of these spectra see Höpfner et al., 2001.

B.5 Intense bushfires in Australia

Wollongong is located on the Australian east coast, about 70km south of Sydney. It is surrounded by large areas of rainforests, except to the east where we find the Pacific ocean. Between 24/Dec/2001 and 5/Jan/2002 intense bushfires in the region destroyed about 500 000ha of forrest around the Wollongong observation site, some coming within a few kilometers. The FTS was operated daily, cloud cover permitting, resulting in more than 1000 solar spectra recorded during these 2 weeks. Visibility at the site dropped below 100m on the ground on several days due to the high levels of smoke.

On the 1st Jan, 2002, a particularly thick smoke plume was passing over the University campus. The plume was well developed and fairly stable between 10:30h and 13:30h local standard time, while the path of the solar beam cut a transect across the plume. Considerable amounts of charcoaled Eucalyptus leaves and ashes rained onto the roof, caused by a nearby fire, between 5 and 10 km to the southwest and west of the University Campus up on the escarpment and the far side of a small hill (Mt Keira). The signal on the suntracker quadrant diodes (which use visible light) had dropped to 1 to 2% of their clear-day values. However, the operation of the suntracker was not hampered as it switches automatically to calculating the solar position if the quadrant diode signals become too weak for active tracking.

Under these rather extreme conditions we recorded the highest levels of bushfire emitted combustion products recorded by high-resolution solar FTIR methods to date. Figures B.8 to B.14 illustrate some of the striking observations made. Shown in each figure are a spectrum recorded on the 01/Jan/2002 near midday and for comparison the same observation made 3 or 9 days later.

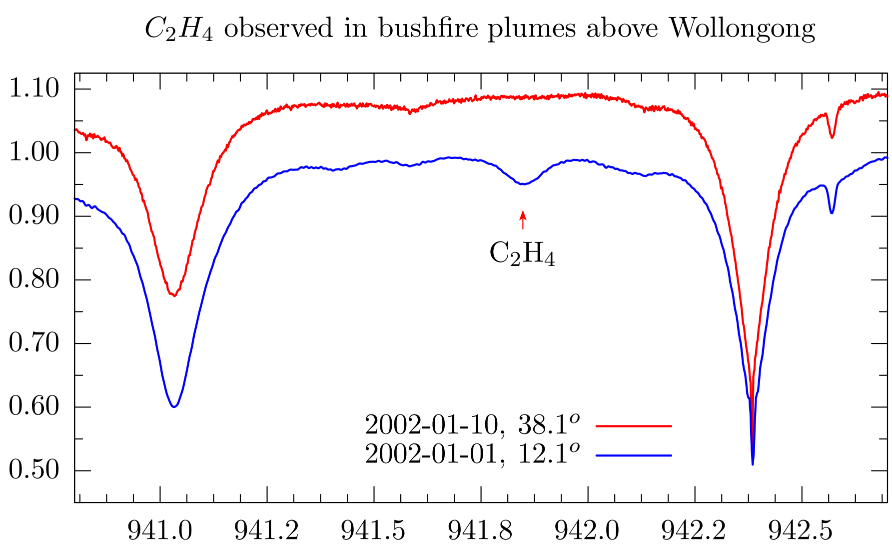

Fig. B.8: This figure illustrates the highest ethylene (C_2H_4) observation made from Wollongong between May 1995 and Feb 2002. The spectrum recorded on 01/Jan/2002 under a SZA of 38^o is compared to a similar spectrum recorded 9 days later with C_2H_4 dropped back to normal levels.

The total column amounts as well as the retrieved volume mixing ratios near ground are listed in Table B.1 and are compared to their corresponding 6–year mean values. Ethylene (C_2H_4) is a very short-lived combustion product that is usually near or below the detection limit at the Wollongong site. However, clear absorption features are visible in most of our

NH_3 observed in bushfire plumes above Wollongong

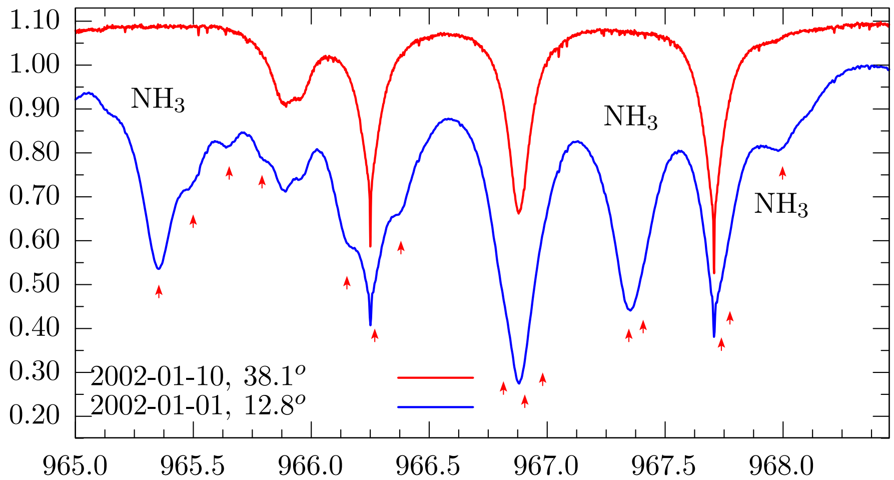

Fig. B.9: This figure illustrates the highest ammonia total column amount recorded above Wollongong between May 1995 and Feb 2002. The spectrum recorded on 01/Jan/2002 under a SZA of 38^o is compared to a similar spectrum recorded 9 days later with NH_3 showing normal levels.

HNO_3 & NH_3 observed in bushfire plumes above Wollongong

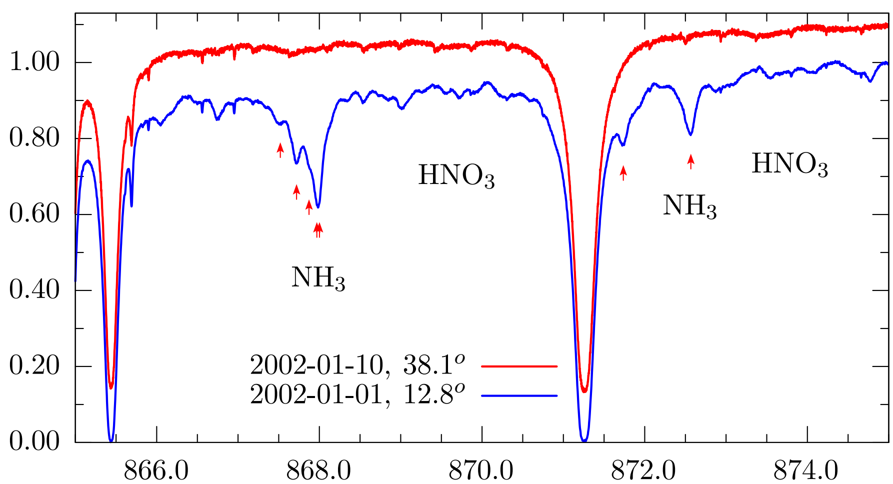

Fig. B.10: This figure illustrates the impact that high ammonia levels may have on the retrieval of nitric acid. This is admittedly an extreme case, but any enhanced levels of NH_3 must be taken into consideration when analysing HNO_3 in the $868cm^{-1}$ region.

CO observed in bushfire plumes above Wollongong

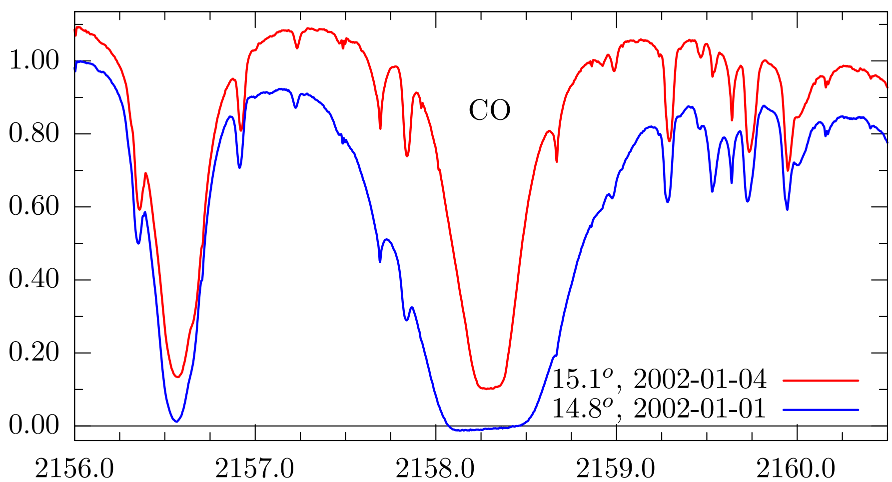

Fig. B.11: This figure illustrates the highest levels of carbon monoxide recorded above Wollongong between May 1995 and Feb 2002. The spectrum recorded on 01/Jan/2002 under a SZA of 15^o is compared to a similar spectrum recorded only 3 days later with *CO* showing almost normal levels.

CO observed in bushfire plumes above Wollongong

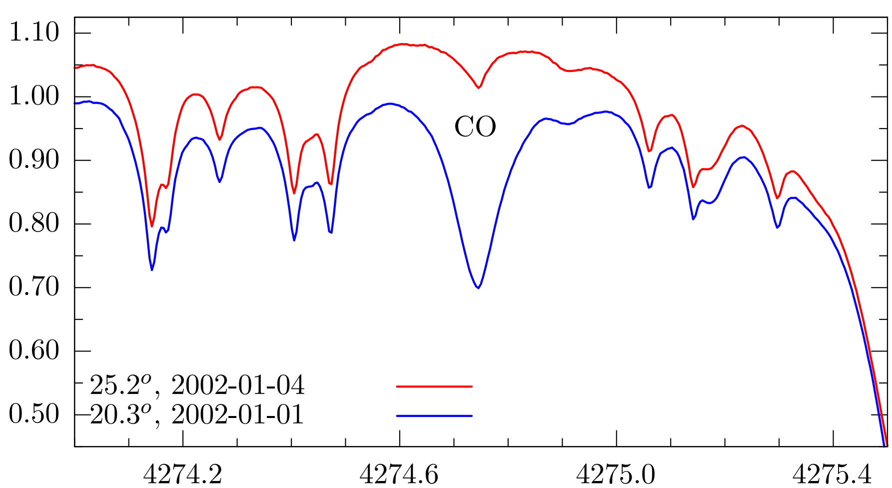

Fig. B.12: This figure shows similarly high levels of carbon monoxide later the same day but recorded in a different optical filter region . The spectrum recorded on 01/Jan/2002 under a SZA of 25^o is compared to a similar spectrum recorded only 3 days later with *CO* showing almost normal levels.

H2CO observed in bushfire plumes above Wollongong

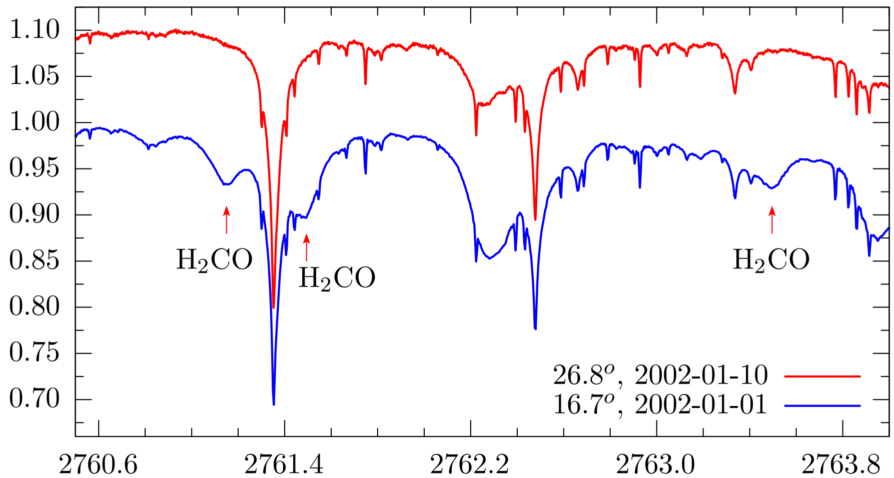

Fig. B.13: This figure illustrates the highest levels of H_2CO recorded above Wollongong between May 1995 and Feb 2002. The spectrum recorded on 01/Jan/2002 under a SZA of 27^o is compared to a similar spectrum recorded only 3 days later with H_2CO showing almost normal levels.

HCN observed in bushfire plumes above Wollongong

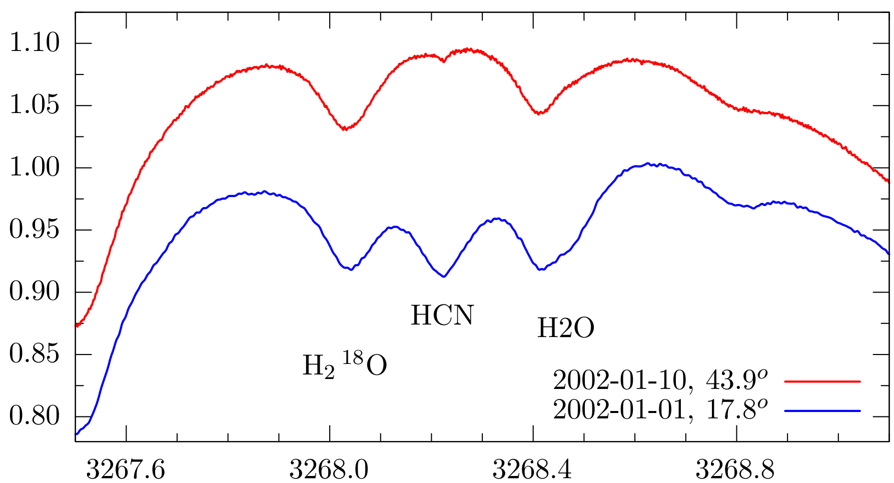

Fig. B.14: This figure illustrates the highest hydrogen cyanide levels recorded above Wollongong between May 1995 and Feb 2002. The spectrum recorded on 01/Jan/2002 under a SZA of 44^o is compared to a similar spectrum recorded 9 days later with HCN showing normal levels.

fire-affected spectra. An example is shown in Figure B.8 featuring a C_2H_4 line at 941.9 cm^{-1}.

The spectrometer was operated at a lower optical path difference than normal (50cm). This compromise was dictated by the expected higher variability of conditions in the optical path and somewhat lower total light fluxes in the infrared. The infrared signals available at the detectors were still fairly good because the smoke did not attenuate the infrared region as much as the visible region and the parallel beam from the solar tracker (60cm primary mirror) was allowed into the spectrometer in full by adjusting a manual iris.

The Nitric Acid windows shown in Figure B.10 are dominated by the much stronger Ammonia features present in the same interval. This illustrates the importance of handling Ammonia interference properly during HNO_3 retrievals, even in the absence of local fires. The 967cm^{-1} window that is often used for Ammonia retrieval is shown likewise in Figure B.9.

Carbon monoxide is one of the major combustion products and often used as a tracer to estimate the total amount of fuel burned. High levels of CO are known to harm the respirational and cardiovascular system in humans and animals. The CO observations illustrated in Figures B.11 and B.12 correspond to concentrations of 8$\pm$2ppm in the lowermost troposphere. These levels are high enough to cause health problems (compare *Li et al.,* 2000, *Paton-Walsh et al.,* 2004).

Formaldehyde (H2CO) is another weak absorber that is difficult to observe when abundances are at typical background levels. Several clear features are prominent in the 2760 to 2764cm^{-1} interval shown in Figure B.13 that correspond to abundances over 100 times above the 6-year mean value.

Hydrogen cyanide is illustrated in Figure B.14 and is the last trace gas discussed here. HCN, like the other bushfire tracers discussed, shows a massive enhancement over background values.

The profile retrieval performed indicates that most of the enhancement in all of the pollutants discussed here occur in the bottom few kilometers of the troposphere. This is in agreement with independent observations of the fire plume, fire locations and the general meteorological conditions.

Table B.1: Total column amounts (TCA) and near ground volume mixing ratios of combustion products observed above Wollongong during bush fires on 01/Jan/2002 and comparison with conditions 3 to 9 days later and with background levels. Measurements for carbon monoxide in the 2100cm^{-1} ($^{1)}$) and in the 4280cm^{-1} ($^{2)}$) spectral region were sampling different parts of the plume about 1 hour apart. Note that the VMRs listed are subject to considerable uncertainties (see text for details).

	01/Jan/2002		4 or 10/Jan/2002		6–year–mean	
	TCA	VMR	TCA	VMR	TCA	VMR
Molecule	molec/cm^2	30-730m	molec/cm^2	30-730m	molec/cm^2	30-730m
CO $^{1)}$	35.76e18	7.508ppm	5.462e18	0.840ppm	1.62e18	0.126ppm
CO $^{2)}$	23.95e18	9.248ppm	2.207e18	0.292ppm	1.62e18	0.126ppm
HCN	157.2e15	91.2ppb	4.557e15	0.197ppb	4.262e15	0.214ppb
H2CO	447.1e15	228.5ppb	1.39e15	0.126ppb	3.54e15	1.29ppb
NH3	310.0e15	111.3ppb	1.03e15	0.122ppb	3.39e15	0.40ppb
C2H4	33.23e16	87.22ppb	1.366e16	5.55ppb	N.A.	N.A.

A more detailed discussion of over 1700 solar spectra recorded under bush-fire affected conditions at the Wollongong station between Dec 2001 and Feb 2003 is found in Paton-Walsh et al. (2004). Table B.1 summarises the exceptionally high amounts of fire-enhanced trace gas levels observed in the spectra shown here. The spectra were analysed with SFIT2 V3.81 in profile retrieval mode. Meteorological data was based on a radio sonde launched $55km$ north from the site. Air mass calculations were performed with the enhanced FSCATM code (Meier et al, 2003) using a 205 layer model atmosphere. The atmosphere in the retrieval model was represented by 39 layers. Layer thickness was $700m$ at the ground increasing by 5% for every layer above. The retrieval parameters were adjusted such that it allowed for very large variability in the lower troposphere.

All Jan 1^{st} spectra showed very high values in the lowermost layer (0 to $700m$) dropping sharply with altitude and relaxing into near background conditions above $5km$ altitude. However, given the low sensitivity of the method to VMR changes near ground (as dictated by the averaging kernels) considerable uncertainties of 40% or more exist for the VMR values reported.

In summary, the enhancements in biomass burning tracers observed at Wollongong on the 1^{st}Jan, 2002, are very high and in many respects exceptional. Total column amounts of CO, HCN, H2CO, NH3, and C2H4 are 22, 37, 126, 91, and approximately 30 times larger than their respective annual mean values, respectively. It must be said in all fairness though that the uncertainties in the volume mixing ratios listed are very large. However, the enhancements in terms of total column amounts are very solid and it stands to reason that the enhancements were located in the lower troposphere given the fire dynamics and meteorological conditions such as they were.

C The infrared solar spectrum (by Frank Hase)

C.1 Introduction

For infrared ground-based high-resolution atmospheric measurements as e.g. performed in the framework of the NDSC (Network for the Detection of Stratospheric Change) the Sun serves as background source to allow for the observation of terrestrial absorption features with high signal to noise ratio. The solar radiation output can be approximated by a blackbody spectrum with brightness temperatures ranging between 4820 K (at 20μm) and 5730 K (at 5μm) [Cox, 2000]. Closer examination of the solar spectrum reveals various spectral features interfering with the terrestrial absorption signatures of interest. For this reason it is desirable to model the solar spectral features when simulating atmospheric transmission spectra in the analysis process.

C.2 Astrophysical background

C.2.1 The solar continuum

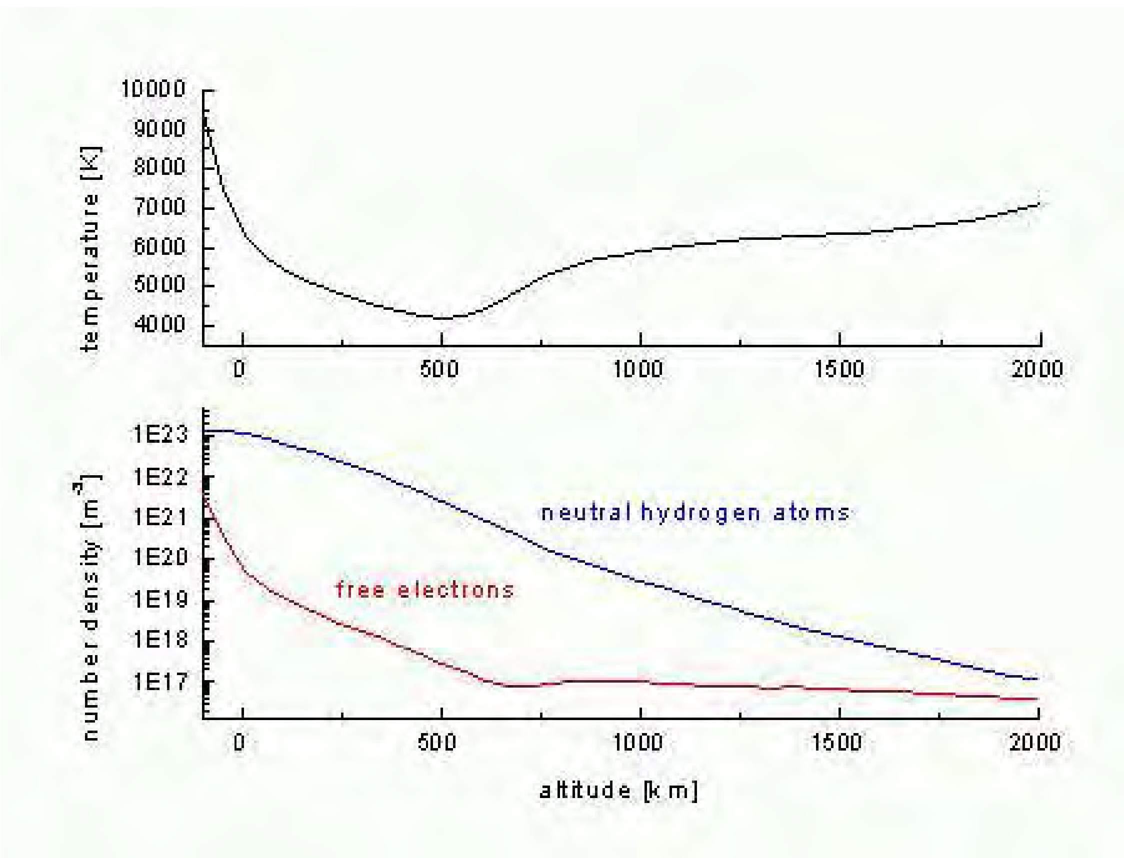

Fig. A3.1: Temperature and number density stratification in the quiet solar atmosphere according to [Vernazza et al., 1981].

The Sun appears as a sharp edged disk from the UV to the infrared. This is due to the fact, that the absorption coefficient steeply rises with depth, as does the density. In the visual region, the absorption is at a minimum, so the radiation leaves from the deepest layer accessible to observation, resulting in an observed brightness temperature of about 6400 K. The temperature stratification in the photosphere (ca. -100 to 500 km) and overlying chromosphere (ca. 500 to 2100 km) is shown in Fig. A3.1. As can be seen, a temperature minimum is found between photosphere and chromosphere.

The major source of opacity in the solar continuum is due to the overwhelmingly abundant hydrogen [Gray, 1992]. In Fig. A3.2 the absorption coefficient of solar material at a temperature of 5400 K is shown. In the near infrared, the bound-free transition of H^- dominates, whereas towards the mid-infrared the H^- free-free transition is the dominant mechanism. Most photons emerge from a height of about 170 km in the mid IR, where the temperature still decreases with altitude (see Fig. A3.1). Since the opacity rises towards the infrared, the brightness temperature decreases with wavelength. In the infrared, the opacity decreases steeply with altitude. Therefore, although the effective optical depth depends on the inclination of the observers line of sight, the centre-to-limb variation in the solar continuum is quite small [Cox, 2000].

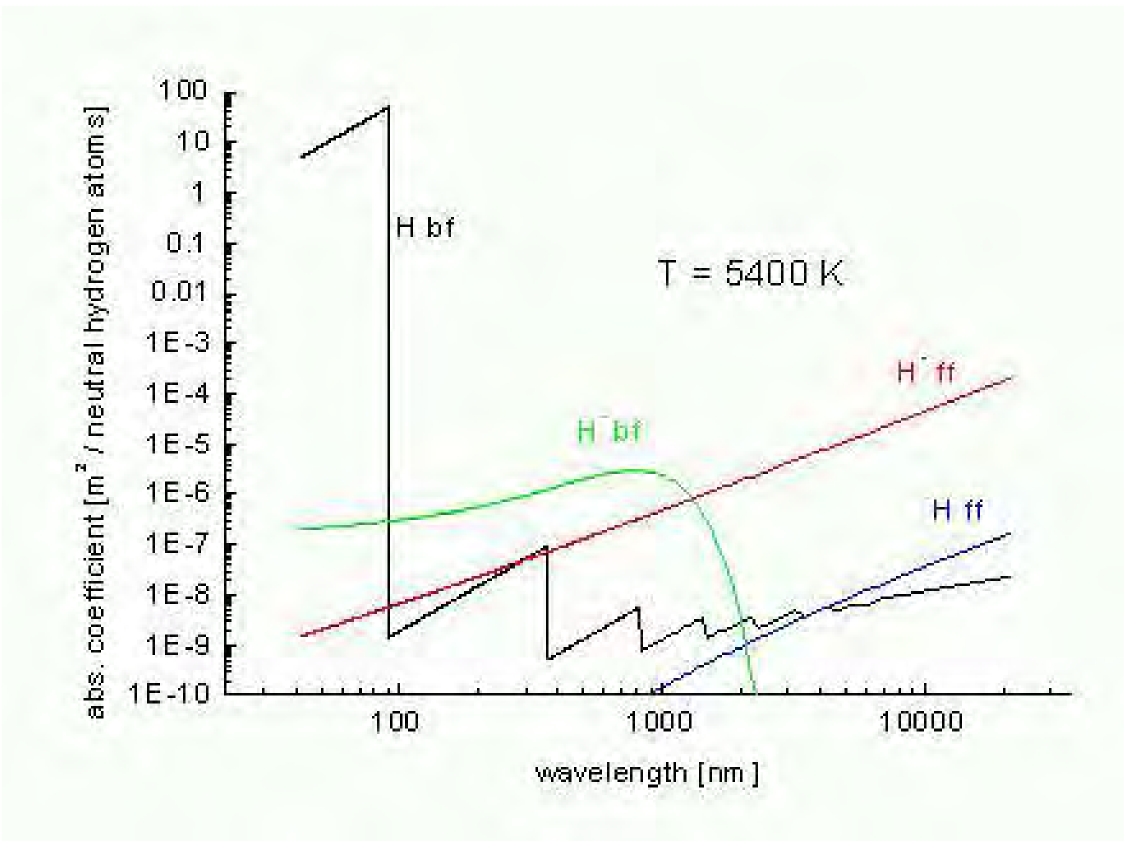

Fig. A3.2: Sources of the solar absorption coefficient due to hydrogen. According to [Gray, 1992]

C.2.2 Solar lines

In the case of a spectral line, the absorption coefficient is enhanced as compared to the adjacent continuum. Since the observed photons then emerge from higher layers where the temperature is lower, absorption lines are observed. In the case of excessive high absorption, the photons emerge from layers well above the temperature minimum, giving rise to some solar emission lines. The spectral lines are due to electronic transitions in atoms, e.g. Fe, as well as due to transitions in diatomic molecules, such as OH, CO, NH, etc. CO is the predominant absorber in the mid infrared with strong features in the regions ca. 1600 to 2300 cm^{-1} and 3700 to 4400 cm^{-1}. Since the effective optical depth and the effective partial columns of the absorbing species enclosed between two height levels depends upon the inclination of the observers line of sight, centre-to-limb variations in the area and width of solar lines are observed.

C.2.3 Solar rotation and microturbulence

The Sun is revolving within about 25 days with respect to the stars. The angular speed decreases towards the poles, the rotation period is about 31 days at 60^o heliographic latitude. The solar equatorial plane is inclined by 7^o with respect to Earth's orbital plane. With a solar radius of 696 000 km, the solar equatorial velocity seen from Earth is 1.85 km/s, which leads to an appreciable Doppler shift of solar lines versus telluric lines. If different positions on the solar disc are averaged, the rotation causes a smearing of the lines (Fig. A3.3). (In the case of a rigid rotating sphere with the rotation axis perpendicular to the line of sight, stripes of equal radial velocity increments are projected into straight bands of equal width on the observed disk.)

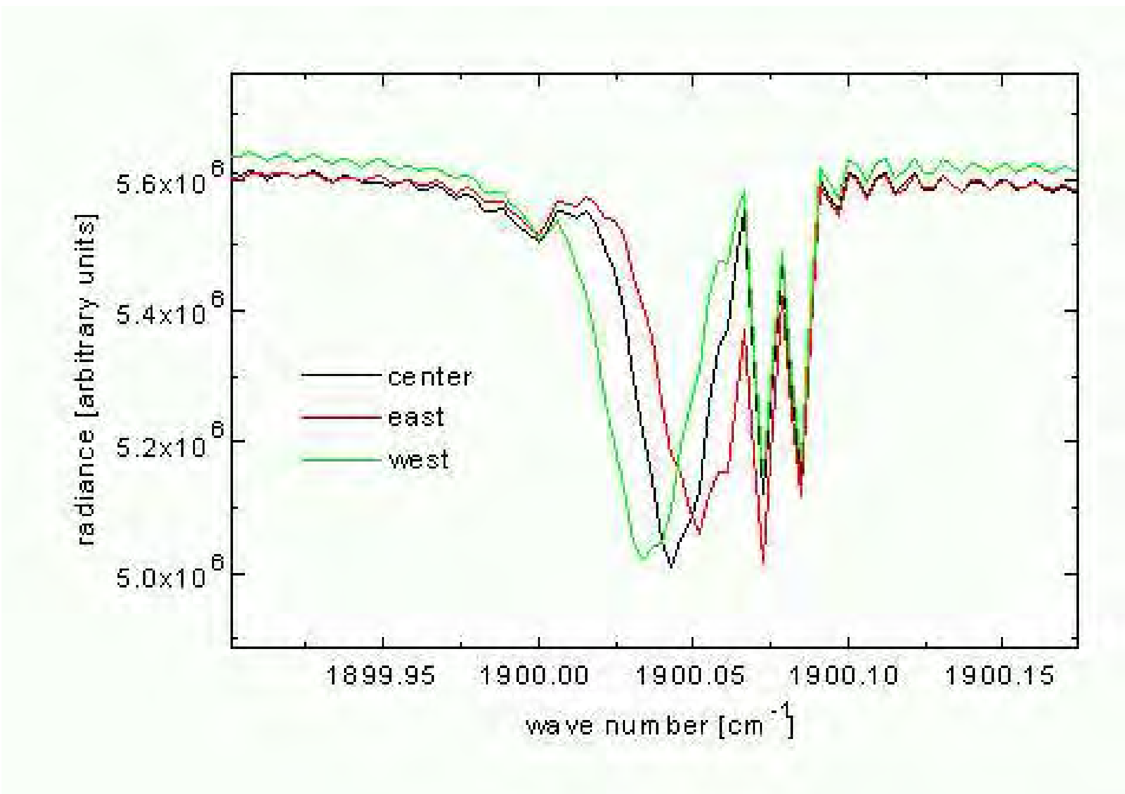

Fig. A3.3: Observations of the solar disc with a small de-centred field of view reveal the Doppler shifts due to the solar rotation. Measurements by [P. Demoulin, 2001].

In addition to this, energy transport by convection generates vertical motions in the photosphere, with rising hotter bubbles and cooler material sinking in between. The vertical velocities are in the order of 1 km/s. The associated granular structures seen in the photosphere are very small as compared to the size of the solar disk, typically in the order of 1 arcsecond. Thereby many volume elements are averaged in a typical field of view, and the observed linewidths are larger than calculated from the thermal motion alone. There are also slower horizontal flows associated with larger structures (supergranulation).

Radial motion of the observer with respect to the Sun

Due to the elliptical shape of the Earth's orbit, radial velocities up to ±0.5 km/s emerge in the course of the year. In case of an observer located at the equator, this amplitude equals the diurnal variation due to Earth's rotation (Fig. A3.4). This requires a scaling of the solar spectrum model abscissa.

C.2.4 Solar activity

The solar radiation output is not temporally constant, but shows variations connected with changes of the magnetic field penetrating the Sun's outer layers. There is an overall cycle of magnetic activity of about one decade, but strong variations on much shorter timescales are typical. The magnetic flux is not distributed smoothly over the surface, but forms well defined mostly bipolar magnetic regions. These active regions tend to develop cooler photospheric areas (sunspots), and are surrounded by networks of enhanced radiation output (faculae) (for pictures of the Sun, see http://www.bbso.njit.edu). The total area of sunspots, the effective number of sunspots, and the solar radio emission may serve as indicators for the solar activity (for recent data and links, see http://www.spaceweather.com). There is a much wider variety of phenomena connected to solar activity [Zirin, 1988], that cannot be described here. The variability in the visible and infrared continuum is negligible, but the spectral lines are affected by the solar activity to more or lesser extent, since the temperature stratification in the active regions is modified. Since the phenomena of solar activity are spatially structured, using a field of view that covers a considerable fraction of the solar disc tends to reduce the associated effects on the solar lines.

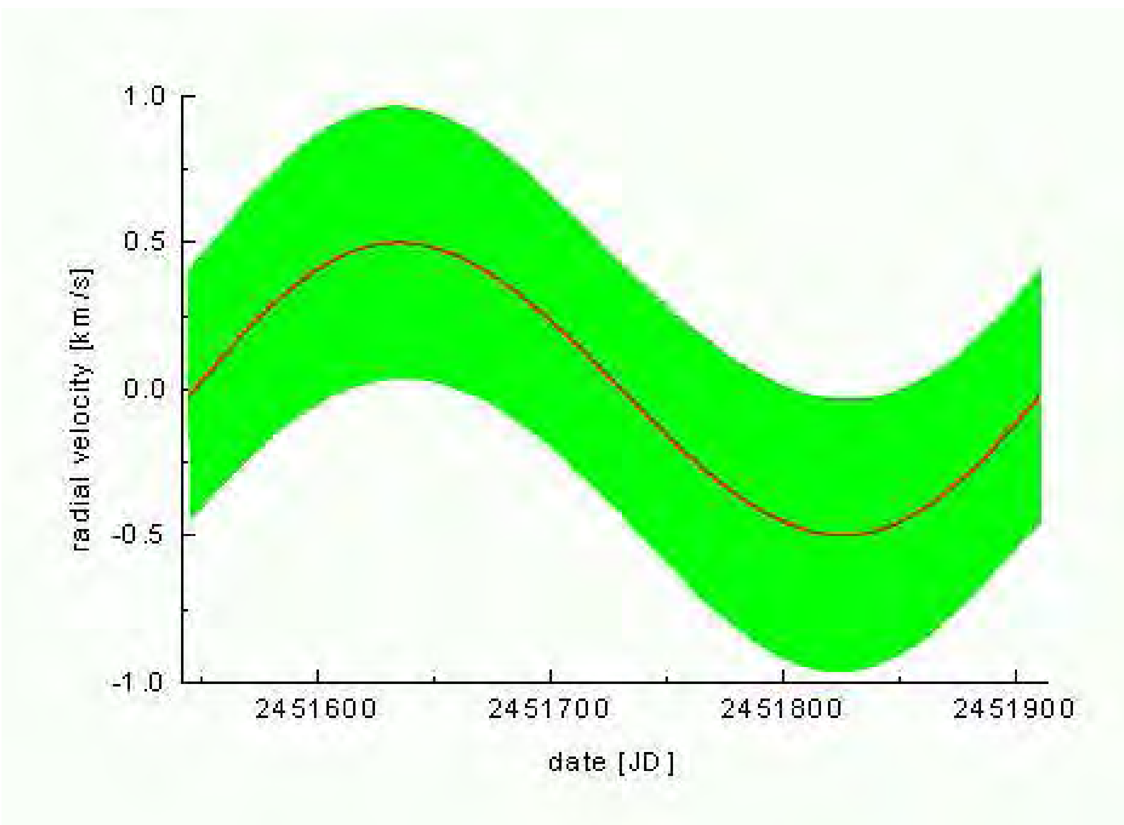

Fig. A3.4: Annual and diurnal variation of the Sun's radial velocity for an equatorial observer.

C.3 Observations

Considerable regions of the solar spectrum can be observed from high altitude sites such as Kitt Peak [Delbouille et al., 1981; Livingston & Wallace, 1991] and the Jungfraujoch [Farmer et al., 1994; Melen et al., 1995; Delbouille & Roland, 1995]. Balloon-borne measurements at high solar elevation angles suffer much less from telluric absorptions ([Goldman et al., 1996; Sen et al., 1996]). An outstanding reference to the solar absorption features are the sets of solar spectra taken by the ATMOS occultation spectrometer from Earth's orbit [Farmer & Norton, 1989; Geller, 1989; Abrams et al., 1996].

C.4 Modelling

A simple approach is to ratio the observed spectrum by an (appropriately frequency-scaled) ATMOS measurement of the solar spectrum. The drawback of this method lies in the limitations of the ATMOS spectra, which contain noise, some instrumental artifacts, suffering from nonlinearity, asynchronity in observation time and geometry with respect to ongoing ground-based observations, and are convolved with the ILS of the spectrometer. A line-by-line model can avoid some of these problems, and allows the introduction of further refinements, e.g. field of view dependent modelling of the spectrum.

Some current activities in modelling solar absorption features focus on formulating a mathematical description that allows an accurate representation of all aspects of the solar spectrum and its known variability over time and observation geometry with a limited set of adjustable parameters. Ideally, such a model provides *a-priori* knowledge of each parameter's exact value or value range, thereby minimising their impact on the analysis of ground-based high-resolution FTIR observations in the infrared. Amongst these modelling activities are:

- Based on the linelist of solar features deduced from ATMOS measurements [Toon, 2001], Geoffry C. Toon has determined lineshapes and widths of about 17500 lines using ATMOS and MkIV spectra in the 600 - 6000 cm^{-1} region and Kitt-Peak spectra up to 13000 cm^{-1}. The lineshape is approximated by a Gaussian profile with optional exponential wings. The smear due to the solar rotation is taken into account in an approximate way, by field of view dependent widening of the line's Gaussian core. The variable radial velocity between Sun and observer is also taken into account.

- Curtis P. Rinsland generated a list of solar CO lines starting from the work of [Goorvitch, 1994]. In the calculation of the linestrengths the presence of a layer containing all the CO at 4500 K was assumed [Rinsland et al., 1982; Rinsland et al., 1998]. Recently published improved positions and linestrengths for OH for solar temperatures [Goldman et al., 1998; Rinsland et al., 2002]. Based on Minnaert's approach to describe the profiles of saturated lines by assuming a residual intensity [Minnaert, 1935; Kilston, 1975], these models are incorporated into the SFIT retrieval code and tested on ATMOS spectra. The lineshape used is approximated by a Voigt profile. Various variables, like the shift of the solar spectrum, the value of the residual intensity, the solar column amount, and the widths of the lines can be fitted (by adjusting a microturbulence parameter). The smear due to the solar rotation and the variable radial velocity are not taken into account explicitly.

- In collaboration with P. Demoulin, A. Goldman, CP. Rinsland, and GC. Toon the author is working on a model of the solar lines in the mid-infrared. The model is based on the above mentioned compilations for CO and OH, complemented by GC. Toon's linelist to include features of other origins. For OH and CO, the predicted linestrengths by the single-layer models are matched to the observed linestrengths by modelling the radiative transfer in the solar atmosphere. This method, and the use of high-resolution ground based measurements pointing at -0.6/0.0/+0.6 solar radii [Demoulin, 2001], allow the estimation of centre-to-limb variations of the area and width of each line. The remaining features are readjusted according to MkIV, ATMOS, and ground-based spectra. The lineshapes are approximated by Voigtian profiles (including a residual intensity in case of OH and CO). The centre-to-limb variations in area and width are approximated by a parabola, and integration over the field of view is performed explicitly, taking into account the centre-to-limb variations as well as the nonrigid rotation of the Sun.

C.5 The solar spectra shown in this work (by A. Meier and F. Hase)

In the next few paragraphs a brief description of the solar spectra used in this work is given. Only some of them are actually shown in the contribution plots while others are included on the supplementary DVD. Please note that the ATMOS spectra were recorded at a 5 times lower spectral resolution as compared to all simulated spectra and the ground-based observations (257cm OPD). The solar spectra of NOAO, Kitt Peak, are also recorded at a lower resolution (100cm OPD) and the GGG simulations are ultimately based on observations with the MkIV FTIR spectrometer normally operated at the maximum 100cm OPD.

It is expected that there are larger differences in general between solar simulations created with Geoff Toon's GGG algorithm and with Frank Hases' new compilation on the one hand, and the SFIT Minneart formulae approach on the other hand, especially in the lineshape, which tends to be broader in the centres of strong lines with the SFIT model. Moreover, the first two spectra will in many cases contain weaker lines of other origin. Even if the differences between GGG simulated spectra and the work by F. Hase are smaller in general, it may be instructive for the reader to see, how much room for interpretation of the raw material involved is still left.

C.5.1 Simulated spectrum by Frank Hase

In the preceding section Frank Hase has given a comprehensive overview on the nature of solar spectra and the difficulties encountered when attempting to simulate realistic solar spectra. The simulation he ran for our specific case covers the spectral interval from 500 to 2350cm^{-1} at a point spacing of 0.004cm^{-1}. The geometry is for an observer in Kiruna (67.84^{o}N, 20.41^{o}E) at local noon. The idealised instrument observing the sun in absence of an atmosphere is said to have an effective field of view of 1.2$mrad$ and an optical path difference of 257cm (or a resolution of 0.004cm^{-1} if you prefer). In this case, the Doppler shift introduced by the earth rotating around its axis is negligibly small for all practical purposes, because of the high latitude. Further, it is assumed that the instrument is looking at the centre of the solar disk. This makes centre-to-edge differences across the solar disk negligible for the assumed field of view of 1.2$mrad$.

Please note that this is work in progress. We would have loved to include simulations up to 9000cm^{-1}, but decided not to delay the publication of this work unduly. However, you are welcome to contact Frank Hase at frank.hase@imk.fzk.de for obtaining an update that may extend the spectral range of the simulations we were able to include.

C.5.2 ATMOS spectra from space

In 1989 the first high-resolution FTIR went into space in the Atmospheric Trace Molecule Spectroscopy Experiment (ATMOS). The mission, data analysis, and some of the results are descried in Gunson et al., 1996, Abrams et al., 1996, Abbas et al., 1996, Irion et al., 2002. Of particular interest to this work are the high orbit solar spectra described by Farmer and Norton, 1989 and the complementing line identifications by Geller, 1989.

Robert L. Kurucz has compiled a "*grand mean*" over 20 observed solar spectra from the 1989 ATMOS mission that is available electronically via anonymous ftp (Kurucz, 2002). The spectrum represents the solar intensity integrated through a circular diaphragm centred on the disk and extending out to $\mu = 0.951$[8]. All instrumental and background features have been removed. Narrow telluric lines from outgassing in the instrument have not yet been removed. The spectral range is 605.6 to 4800 cm^{-1}.

We also had access to similar solar spectra from the November 1994 mission that are included on the supplemental DVD (file *atmos-11.94*). However, for the 1994 data we had no grand mean over all spectra plus the removal of instrumental artifacts is a difficult issue for someone not intimately familiar with the instrument and mission. All we did with the 1994 data available was a rough intensity normalisation and frequency calibration followed by the merging of 3 spectra across 3 different optical filters to obtain one continuous solar spectrum from the 1994 ATMOS mission.

The ATMOS spectra shown in the main section of this work always show the ATMOS spectrum compiled by Kurucz, because it has a superior signal to noise ratio and the better correction for instrumental artifacts.

C.5.3 Observations from NOAO, Kitt Peak

The NOAO spectra were obtained via anonymous ftp and are accompanied with the following 'restriction on use of these data': "*These data are freely available with one restriction: If you use the data or some product based on the data in a published paper, we ask that you include an acknowledgement as follows: NSO/Kitt Peak FTS data used here were produced by NSF/NOAO. For further information contact: F. Hill at fhill@noao.edu.*" The files are dated 29/Feb/1993. We are more than happy to acknowledge this great work. Our warm thanks to everyone involved in producing these solar spectra.

The NOAO spectra are accompanied by the following explanations and warnings: "*The composite solar NOAO spectrum included on the DVD was constructed from the original 25*cm^{-1} *wide spectra obtained with the Fourier Transform Spectrometer at the McMath/Pierce Solar Telescope situated on Kitt Peak, Arizona, and operated by the National Solar Observatory, a Division of the National Optical Astronomy Observatories. NOAO is adminstered by the Association of Universities for Research in Astronomy, Inc., under cooperative agreement with the National ScienceFoundation.*

The parameter "dg", which controlled the extent of the gaps in the original version of the solar component due to strong atmospheric absorption, replaces the last point in the "total". The user is warned that in this version there are no gaps. Instead, the regions where the solar component is undetermined are replaced by linear interpolations between the last "good" points on each side of the undetermined region. In order to identify these interpolated regions the user must either refer to the plots in the original version or use the parameter "dg" in the same way as the authors. This version of "An Atlas of the Solar Spectrum in the Infrared from 1850 to 9000 cm^{-1} (1.1 to 5.4 microns)" *(N.S.O. Technical Report #91-001,*

[8] There may be some inconsistencies in the diaphragm description that need to be cleared up.

July 1991) by W. Livingston and L. Wallace is meant to be used in conjunction with the original hard-copy version, and the caveats in the text of that version apply here equally.

Finally, the intensities of the spectra in each file have been adjusted to predetermined values. One result is that the intensities are not continuous from file to file. If continuity is required from one file to another, the intensities can be readjusted using the spectra in the overlap region" (end quote).

The original data was available in ASCII files covering 25 cm^{-1} wide intervals plus an overlap of 2 cm^{-1} at either side and were combined into a single composite spectrum by A. Meier after having normalised each spectrum individually prior to merging them. The point density of the original FTS spectra has been maintained with the result that 3061 points are contained in each 25 cm^{-1} interval.

C.5.4 GGG/GFIT solar spectra

The GGG (or GFIT) retrieval software developed at JPL Pasadena (*Sen et al.,* 1996 and *Toon et al.,* 1999) is a very powerful tool for analysing FTIR solar spectra both from high-altitude platforms (balloons) and ground-based sites. GGG can presently simulate much broader intervals than SFIT2 (100cm^{-1} and more) and does not use the Minneart formulae for simulating solar lines. Instead, GGG uses a pseudo-line approach with a linelist derived from both space-borne ATMOS and Mk-IV balloon-borne spectra, as described in section C.4 (page 565).

The solar simulations *'GGG-mir.00'* and *'GGG-nir.00'* were produced using GGG version 2.12.2. The frequency range is constrained to the available line parameter file, with significant gaps beyond 6000 cm^{-1}. The solar spectrum was calculated in approximately 600 cm^{-1} wide intervals and concatenated into a single spectrum afterwards.

The first file *'GGG-mir.00'* spans the middle infrared from 620 to 4380cm^{-1}. The instrumental settings assumed match the ground-based observations for the Kiruna spectra (OPD 257cm). The second file is *'GGG-nir.00'* and spans the near infrared from 3950 to 6420cm^{-1} and from 7580 to 9000cm^{-1}. The instrumental settings again match the corresponding Kiruna ground-based spectra (OPD 120cm). The simulations were carried out by Nicholas B. Jones from University of Wollongong (Thanks Nicholas!).

C.5.5 Other simulations

The following list briefly describes the remaining solar spectra found in the electronic supplement.

- *'solar-oh.00'* is a simulation carried out with SFIT2 based on the improved positions and linestrengths for OH for solar temperatures (*Goldman et al.,* 1998; *Rinsland et al.,* 2002). This data set is also refered to as the University of Denver solar OH linelist.

- *'cog-450.00'* is the solar CO simulation created with SFIT2 (Minneart formulae) and the *cog450.new* and *coog450.new* files that ship with SFIT1.09e.

- *'solar-am.00'* is a solar simulation carried out with SFIT2 and the *solar-am* linelist. The latter is a linelist prepared by Arndt Meier. It is based on a combination of the *solar-oh*, *cog450.new* and *coog450.new* linelists and a substantial number of pseudolines trained individually on ATMOS 1994 spectra. This linelist focuses on microwindows of interest to ground-based observations and achieves typically better residuals with SFIT2 than the original cog450 and solar-oh linelists. This is the **'solar-sim'** simulation that is shown in all contribution plots in the main section of this atlas.

- *'Composite.00'* and *'Composite.01'* are crude attempts to merge the different **observed** solar spectra to provide one solar spectrum covering the full spectral interval of interest. Given the limited availability of observed solar spectra from space, some compromises had to be made to fill observational gaps. The 'observed' spectra are constructed from the following solar spectra:
  - 500-631cm^{-1} solar-OH simulation from the Denver University linelist,
  - 631-4700cm^{-1} observed 1989 ATMOS spectrum (Kurucz),
  - 4700-6420cm^{-1} GGG pseudo-line simulation (based on observed spectra)
  - 6420-7584cm^{-1} NOAO Kitt Peak observed spectra,
  - 7584-8200cm^{-1} GGG pseudo-line simulation (based on observed spectra)
  - 8200-9000cm^{-1} NOAO Kitt Peak observed spectra.

  'Composite.00' covers the mid-IR interval from 500 to 4350cm^{-1} and *'Composite.01'* the near-IR interval from 3950 to 9000cm^{-1}.

D Derivation of pseudo-lines from laboratory cross-sections (by G.C. Toon and B. Sen)

D.1 Introduction

The problem of how best to interpolate/extrapolate laboratory cross- section spectra in temperature and pressure has no simple solution. We have chosen the approach of deriving "pseudo-linelists" to represent the absorption of heavy molecules (e.g. CCl4, CFC-11, CFC-12, CFC-113, HCFC-22, ClNO3, HCFC-142b, N2O5, CF4, SF6) for which only cross-section spectra exist. These pseudo-linelist have been successfully used in the analysis of MkIV balloon spectra (e.g. *Toon et al.,* 1999) and ATMOS Version 3 data (e.g. *Irion et al.,* 2002).

This compilation contains various pseudo-linelists which were derived at JPL by performing spectral fits to laboratory transmittance spectra. The lab spectra themselves were not measured at JPL. They were re-created from published temperature- and pressure-dependent cross-sections, together with information on the ILS, and cell length. These pseudo-linelists are in the HITRAN format and can be used to compute spectra in the same manner as any other linelist. The directory also contains the file, "isotopomer.dat", of molecular parameters (vibration frequencies, temperature-dependences of the rotational partition function) assumed in the derivation of the pseudo-linelists, along with a FORTRAN program "isotopomer.f" defining the parameters and illustrating how to read them.

Each pseudo-linelist was derived by fitting all of the relevant laboratory spectra simultaneously while solving for the 296K strength and the Ground State Energy (E") of each pseudo-line. The pressure-broadened half-width (PBHW) and its temperature dependence were determined "manually", by trying various values and selecting the ones that gave the best overall fit. Generally, for gases without sharp absorption features, the goodness of fit was insensitive to the choice of PBHW, whereas for gases like CFC-12 and HCFC-22 which have sharp Q-branches, the right choice of PBHW is important. Note that for some gases (e.g. CFC-12) the resulting value for the temperature-dependence of the PBHW (0.0) is well outside the normal range (0.5 to 0.8). All lines in a given absorption band were assumed to have the same PBHW and temperature dependence.

The idea of using pseudo-lines to represent broad featureless absorption bands is not new. However, whereas previously workers minimised the number of lines needed by ascribing them an exaggerated PBHW, we achieve the same goal by giving each pseudo-line an exaggerated Doppler width. The advantage of this latter approach is that it allows the correct PBHW to be employed, so that a realistic pressure-dependence can still be simulated, even in cases when all of the laboratory spectra were measured at low pressure (e.g. CF4).

D.2 Advantages of using pseudo-lines

These lists are not intended to supplant proper quantum-mechanically- based linelists. They were derived primarily as a convenient means of interpolating (and extrapolating) the laboratory cross-sections to temperatures and pressures where actual measurements are unavailable (I could not think of a realistic way of doing this directly from the cross-sections). However, in deriving and using these pseudo-linelists, several additional advantages became apparent:

1. Since the pseudo-linelists are in the HITRAN format, they can be accessed in exactly the same manner as all the regular gases, avoiding special code to read the raw cross-section spectra and interpolate them to the desired temperatures and pressures.

2. Fitting a physically-based function to the laboratory spectra also serves as a quality control measure: Since we are typically trying to determine just two unknowns (S & E")

from 4-30 spectra, the problem is over-determined and so performing the fit provides an assessment of the consistency of the various laboratory spectra. This makes it possible to identify and reject laboratory spectra which are inconsistent with the others, or even to quantify biases between different sets of laboratory spectra, perhaps measured under very different conditions. Furthermore, the retrieval of unphysical (i.e. -ve) values of S and E" provides a warning that serious problems exist.

3. Fitting the laboratory spectra provides an opportunity to remove instrumental artifacts. For example, the laboratory cross-sections will always be convolved with the Instrument Line Shape (ILS) of the laboratory spectrometer. In making a pseudo-linelist, the effects of this ILS is removed, since it is included in the forward model which calculates the cross-sections from the pseudo-lines. This is particularly important if the laboratory spectra are measured at a worse spectral resolution than the atmospheric spectra. Another example of removal of an instrumental artifact, is that of channel fringes in the laboratory spectra. If these can be properly fitted they will not be propagated into the pseudo-linelist.

4. Fitting the laboratory spectra provides an opportunity to remove absorption lines not belonging to the gas of interest. For example, laboratory spectra acquired over the 1300 to 1900 cm^{-1} region are often contaminated by H2O absorption lines. However, by fitting H2O along with the gas of interest, during the analysis of the laboratory transmittance spectra, propagation of H2O artifacts into the pseudo- linelist of the gas of interest will be greatly reduced.

5. Several different laboratory data-sets, even with widely different measurement conditions and spectral resolutions, can easily be assimilated into a single pseudo-linelist.

6. At the end of the fitting process, the pseudo list can be checked by comparing the forward model calculation (which uses the pseudo-lines) with the laboratory transmittance spectra. Of course, the agreement will not be perfect since the fit was overconstrained, but the differences are usually $<1\%$.

7. Absorption spectrum derived from the pseudolines are guaranteed to be continuous and differentiable functions of pressure and temperature (unlike some bivariate interpolation schemes), which helps minimise artifacts in the retrieved VMR profiles.

8. Since all the pseudo-lines in a given band are assumed to have the same PBHW and Doppler widths, only one evaluation of the Voigt lineshape per atmospheric level is necessary to compute the absorption spectrum resulting from all the pseudo-lines (provided that this lineshape is stored). Thus, the speed of using the pseudo- linelists is competitive with 2-D interpolation in the raw cross- sections (assuming one knew a good way of doing this).

D.3 Spacing of pseudo-lines

The choice of line spacing for the pseudo-lines was somewhat arbitrary. We tried to make it as wide as possible to minimise the total number of lines, yet still preserve any structure observed in the laboratory spectra that would also be apparent in an atmospheric spectrum.

Typically, the line spacing was chosen to be similar to the resolution of the laboratory spectra. Note that the positions and spacing of the pseudo-lines are completely independent of the spectral frequencies in the laboratory spectra. This fact makes it possible to simultaneously fit different sets of laboratory spectra.

Most of the pseudo-linelists are spaced at 0.01 cm^{-1}, which is ten times larger than an actual Doppler widths of most heavy gases. Although this would not be a problem in the troposphere where the pressure broadening would cause the pseudo-lines to overlap, in the upper stratosphere a high resolution computed spectrum would show narrow lines with large gaps between. To avoid this problem one must artificially increase the Doppler width until it approximately matches the line spacing. A convenient way of doing this is to set the molecular weight to an artificially small value (e.g. 1), however, this has drawbacks if one wants to use pseudo- lines, together with real quantum-mechanical lines, of the same gas in the same interval. Therefore, in all of the pseudo linelists, we have defined the isotope number to be zero. This allows pseudo lines to be easily distinguished from real lines (which have isotope numbers 1-9), and could allow the line-by-line code to explicitly set the Doppler width equal to the pseudo-line spacing whenever it encounters pseudo-lines, avoiding the need to fudge the molecular weight. This is especially helpful for gases like ClNO3 for which a proper quantum-mechanically derived linelist (requiring the actual molecular weight) exists for the region around the 780 cm^{-1} Q-branch, but pseudo lines must be used for other regions.

D.4 Line strength

The following expression for line strength was assumed in the derivation of the pseudo-linelists:

$$S(T) = S(296K) \cdot (296K/T)^{\beta} \cdot \frac{Qvib(T)}{Qvib(296K)} \cdot \frac{SE(T)}{SE(296K)} \cdot exp\left\{hcE" \cdot \left(\frac{1}{296K} - \frac{1}{T}\right)\right\}$$

where S(296) is the line strength (cm^{-1}/molec/cm-2) at 296K. β is the Temperature Dependence of the Rotational Partition Function.

$$Qvib(T) = II \cdot (1 - exp\{-h \cdot c \cdot Vj/kT\})^{-Gj}$$

is the vibrational partition function and the product is performed over all the vibrational frequencies, Vj, which are read from the file "isotopomer.dat", along with their degeneracies, Gj.

$$SE(T) = (1 - exp\{-h \cdot c \cdot Vi/kT\})$$

is the correction for the Stimulated Emission, Vi being the centre frequency (cm^{-1}) of the line in question. The term $(296K/T)^{\beta}$ is commonly known as the rotational partition function and β is usually (1.0, 1.5, or 2.0) The term $exp\{hcE"(1/296 - 1/T)\}$ is simply the Boltzmann factor, E" being the ground-state energy (cm^{-1}).

Most forward models should already have the code to compute the above expression because it is needed for the lighter gases. So it should be a simple matter to extend this capability to the heavy gases. Note that the same expression for S(T) was used for the fitting of the laboratory spectra, so the derived values of S(296) and E" values will only correctly reproduce the laboratory spectra provided that the user employs the same expressions.

Note that in the case of the O2 and N2 Collision Induced Absorption (CIA) bands, the absorption coefficients that are derived from the pseudolines must be multiplied by the atmospheric pressure (in atmospheres) before being used to calculate any optical thicknesses or transmittances. This is because of the pressure-squared dependence of the CIA.

Finally, we want to make it clear that one should not expect the forward calculation made using these pseudo-lines to agree perfectly with individual laboratory spectra, since the pseudo-lines were derived from an over- determined fit to ALL of the laboratory spectra. Differences will arise from noise on the laboratory spectra, and uncertainties in the measurement conditions (T,P,VMR), in addition to inadequacies in the pseudo-line approach.

Table D.1: *Molecules and spectral intervals for which pseudo-lines have been calculated.*

File	Molecule	Interval	Spacing	Lines	Error	Measurer
cf4.h92	CF4	1250 - 1290	0.0025	16093	4%	Nemtchinov & Varanasi
f12.h92	CFC-12	850 - 950	0.010	10000	2%	Varanasi
	CFC-12	1050 - 1200	0.010	15000	1%	Varanasi
f11.h92	CFC-11	810 - 880	0.010	7000	7%	Varanasi
	CFC-11	1050 - 1120	0.010	7000	6%	Varanasi
ccl4.h92	CCl4	750 - 812	0.010	6201	3%	Varanasi & Nemtchinov
f22.h92	CHF2Cl	776 - 850	0.00742	9977	5%	Varanasi & McDaniel
	CHF2Cl	1080 - 1150	0.010	7001	2%	McDaniel
	CHF2Cl	1290 - 1335	0.010	4501	2%	McDaniel
f113.h92	CFC-113	786 - 990	0.500	408	8%	McDaniel (omitted 203K)
sf6.h92	SF6	925 - 955	0.010	3001	2%	Varanasi
f142b.h92	HCFC-142b	870 - 1270	0.010	40000	4%	Newnham
clno3.h92	ClNO3	690 - 880	0.01	19000	2%	Birk & Wagner
	ClNO3	965 - 1005	0.01	4000	4%	Birk & Wagner
	ClNO3	1090 - 1130	0.01	4000	4%	Birk & Wagner
	ClNO3	1215 - 1330	0.01	11500	3%	Birk & Wagner
	ClNO3	1680 - 1790	0.07142	1540	?	Ballard (only 2 spectra)
n2o5.h92	N2O5	547 - 610	0.160	373	4%	NCAR
	N2O5	709 - 775	0.210	315	2%	NCAR
	N2O5	1194 - 1281	0.350	266	2%	NCAR
	N2O5	1663 - 1793	0.480	271	2%	NCAR
o2_cia.h92	O2	1275 - 1835	5.000	113	?	Thibault et al.(1997)
n2_cia.h92	N2	2030 - 2630	5.000	121	?	Lafferty et al.(1996)

D.5 Molecules and spectral intervals covered

In the table above (Table D.1) we summarise the gases and spectral intervals for which we have computed pseudo-linelists. We estimated the maximum error in absorber found in re-fitting the laboratory spectra using the final pseudo-linelist. Note that at specific frequencies, the error in the computed absorption coefficient may well exceed these tabulated values.

D.6 $ClONO_2$ pseudo-linelist

D.6.1 Introduction

This documents the ClONO2 pseudo-linelist derived at JPL in November 2000 from the laboratory spectra of Manfred Birk and Georg Wagner (Wagner and Birk, 2003), whose work was described at the 2000 HITRAN conference. The measurement conditions for each of these spectra are tabulated below. Each of these spectra covers the 690 to 1330 cm^{-1} region.

D.6.2 Description

First, the cross-sections were converted back into transmittance spectra from knowledge of the cell length and gas concentrations. In transmittance, the noise will be much more constant than in absorbance, especially considering that in some of the spectra, the depth of the 780 cm^{-1} Q-branch is over 80%. The resulting 25 transmittance spectra were then simultaneously fitted (using the GFIT algorithm) by iteratively adjusting the strengths and ground-state energies of the pseudo-lines.

Table D.2:*Measurement conditions for each of the laboratory spectra by Wagner and Birk. P_{tot} is the total pressure in mbar. P_{ClNO3} is the ClNO3 partial pressure in mbar.*

#	P_{tot}	P_{ClNO3}	Temp	Resn	Noise	File
1	1.068	1.0680	297.02	.0020	0.000	missing
2	0.558	0.5577	297.20	.0020	0.497	297_000.xy
3	95.08	1.0161	297.39	.0020	0.198	297_100.xy
4	44.76	1.0065	297.44	.0040	0.331	297_050.xy
5	23.91	1.0121	297.13	.0020	0.305	297_025.xy
6	1.013	1.0131	297.00	.00094	0.000	missing
7	0.321	0.3206	189.58	.0020	0.433	190_000.xy
8	96.24	0.6041	189.58	.0055	0.000	missing
9	94.59	0.3027	189.58	.0055	0.573	190_100.xy
10	44.96	0.3015	189.58	.0040	0.382	190_050.xy
11	24.57	0.3061	189.58	.0020	0.542	190_025.xy
12	75.73	0.3017	189.70	.0055	1.000	190_075.xy
13	12.74	0.2999	189.70	.0020	0.717	190_012.xy
14	155.8	0.3022	189.70	.0055	0.480	190_150.xy
15	0.603	0.6028	189.60	.00094	0.000	missing
16	95.42	0.6209	219.24	.0055	0.285	219_100.xy
17	0.303	0.3026	219.00	.0020	0.761	219_000.xy
18	154.2	0.3044	218.93	.0083	0.924	219_150.xy
19	53.40	0.3058	218.95	.0040	1.504	219_050.xy
20	26.10	0.3061	218.94	.0020	0.940	219_025.xy
21	12.83	0.3033	218.95	.0020	1.060	219_012.xy
22	5.225	0.3007	218.95	.0020	0.752	219_005.xy
23	147.8	0.3029	249.25	.0083	0.516	249_150.xy
24	98.30	0.6034	249.24	.0055	0.425	249_100.xy
25	25.59	0.3135	249.23	.0020	1.590	249_025.xy
26	53.53	0.6078	249.24	.0040	0.346	249_050.xy
27	12.72	0.3032	248.41	.0020	1.295	249_012.xy
28	0.303	0.3025	248.27	.0020	1.607	249_000.xy
29	13.86	0.3028	204.42	.0020	1.000	204_012.xy

D.6.3 Pseudo-line spacing

After trying various line spacings, an interval of 0.01 cm^{-1} was finally chosen. This difficult choice was a trade-off between:

1. minimising the number of ClNO3 pseudo lines,
2. adequately representing the ClNO3 spectral structure,
3. getting the correct slant column abundances of ClNO3.

Having more pseudolines (e.g. 0.002 cm^{-1} spacing) provides better representation of the spectral structure observed in the low pressure laboratory spectra, and gives slightly more accurate representation of their slant column abundances, but the differences were small (<1%).

But most of the atmospheric ClNO3 resides at pressures (25-75 mbar) where this fine structure is smeared by pressure-broadening. So in terms of correctly representing the ClNO3 absorption in spectra of the Earth's atmosphere, 0.01 cm^{-1} spacing seems to be adequate.

D.6.4 Discussion

Although the new laboratory ClNO3 measurements of Birk and Wagner are clearly the best to date, they are not perfect. Some minor deficiencies became apparent during the fitting of the laboratory spectra, that users of the raw cross-sections should be aware of:

1. Channel fringes of up to $\pm 1\%$ amplitude.
2. HNO3 absorptions of up to 2% depth are noticeable in the 1310- 1330 cm^{-1} region of spectrum #2 (297K; no air broadening).
3. H2O absorption lines are noticeable in the 1312-1321 cm^{-1} region of most spectra. # 16 (219K and 95 mbar) is especially prominant; the 1318.929 cm^{-1} H2O line attaining 8% in depth. Note that these H2O lines are formed at room temperature and at low pressure (inside the FTIR ?), not in the cell containing the ClNO3.

To minimise propagation of these artifacts into the ClNO3 pseudo- linelist, channel fringes, H2O, and HNO3 were all fitted during the pseudo-line iteration process. Otherwise, when analysing atmospheric spectra in the 1320 cm^{-1} region, H2O and HNO3 absorptions would be misidentified as ClNO3, and vice versa.

D.6.5 Implementation

To make best use of these pseudo-lines, the assumed ClNO3 Doppler width must be approximately equal to the 0.01 cm^{-1} pseudo-line spacing. Otherwise the ClNO3 spectrum will start to appear "spikey" in the upper stratosphere. If your analysis software calculates the Doppler width based on the molecular weight of ClNO3, I suggest reducing it from 97 to 1. Of course, this problem could have been completely avoided by having the ClNO3 pseudo-lines on a 0.001 grid, but then there would have been 40 Mbyte ClNO3 pseudo-linelist, rather than just 4 Mbyte.

D.6.6 Calculation of S and E"

At each line frequency, an effective strength and ground-state energy was derived by non-linear least squares fitting to the 25 spectra. Prior to this a PBHW of 0.078 cm^{-1}/atm had been chosen since it gave the best overall fits to the pressure dependence of the 780 cm^{-1} Q-branch region. As part of the fitting, the strengths and ground-state energies were both constrained to be +ve.

After deriving the pseudo-line strengths, we noticed that in certain spectral regions (880-965, 1005-1090 and 1130-1215 cm^{-1}) the strengths were all very small. We therefore deleted all the lines from these intervals to minimise the size of the pseudo-linelist and to save time when performing line-by-line calculations in those spectral regions.

Since the Birk laboratory spectra stop at 1330 cm^{-1}, the new ClNO3 pseudo-linelist still contains the old pseudo-lines for the 1680 to 1790 cm^{-1} region, which were based on the measurements of Ballard et al.(JGR, 93, 1659,1988). Note that the 1330–1340 cm^{-1} region, which was previously covered by Ballard's cross-section, is no longer represented in the new list. Table D.3 lists the spectral intervals covered by the new $ClNO_3$ pseudo-linelist.

Table D.3: *The spectral intervals covered by the new $ClNO_3$ pseudo-linelist.*

$V_{start} - V_{stop}$	N_{lines}	Δ_ν	Spectra
690 – 880 cm^{-1}	19000	0.01	Birk & Wagner
965 – 1005 cm^{-1}	4000	0.01	Birk & Wagner
1090 – 1130 cm^{-1}	4000	0.01	Birk & Wagner
1215 – 1330 cm^{-1}	11500	0.01	Birk & Wagner
1680 – 1790 cm^{-1}	1540	0.07142	Ballard et al.

Comparisons of ClNO3 retrievals from MkIV balloon spectra in the 780 cm^{-1} region, suggest that the new pseudo-linelist produces 5-10% smaller ClNO3 amounts than either the Bell linelist or the previous pseudo-linelist derived from the Ballard cross-sections. Furthermore, the new cross-sections of Birk and Wagner provide much better consistency between ClNO3 amounts derived from the 780 and 1290 cm^{-1} regions (previously the latter gave 15% smaller amounts).

Please direct any questions or comments regarding pseudo-lines to: Geoff Toon (Geoffrey.C.Toon@jpl.nasa.gov) or Bhaswar Sen (Bhaswar.Sen@jpl.nasa.gov)

E The spectroscopic data used in this work

In compiling the spectroscopic linelist for this work we carefully reviewed the latest data available freely and decided on HITRAN 2000 as the initial starting point, but included a number of updates and additions as listed in detail below.

HITRAN2000 is the HIgh TRANsmission Molecular Spectroscopic Database, released on 22/Dec/2000 (Rothmann et al., 2003, on-line access at: http://www.hitran.com). We included all official updates available by Aug 2002; i.e. the H2O, CH4, C2H2, NO, NO2, and O2 updates. The molecular indices have been changed to the ATMOS convention. The linelist was then subdivided into blocks of $20cm^{-1}$ as needed for the SFIT2 retrieval and SIMUL109 simulation codes and cover in total the spectral range from 480 to $9020cm^{-1}$. The official HITRAN updates included:

- Oxygen update (v11.0), 1/2001, a total replacement for all oxygen lines.

- Methane update, Linda Brown and Frank Hase, priv. comm. Jun to Aug 2002, supersedes the official HITRAN webpage update available at the time (v11.0), 2/2001, a total replacement for all methane lines. The 2/2001 data are taken from numerous studies of all three isotopes; the merging was performed by Linda R. Brown at the Jet Propulsion Laboratory (linda@regina.jpl.nasa.gov). The latest revision fixes problems in the pressure broadening pointed out by Frank Hase.

- Water-vapour update (v11.0), 4/2001, a total replacement for all water lines. This update makes a correction for some lines that were not part of the extensive update introduced with the Dec 2000 release, but were present on the previous HITRAN'96.

- Acetylene (C2H2) update (v11.0), 7/2001, a total replacement for all acetylene lines. The work is based on a joint effort between groups at the University Pierre et Marie Curie in Paris and the University of Reims (D. Jacquemart et al, submitted to JQSRT).

- Nitric Oxide (NO) update (v11.0), 7/2001, a total replacement for all nitric oxide lines. C. Chackerian et al, J.Mol.Spectrosc. 192, 215-219 (1998) M.N. Spencer et al, J.Mol.Spectrosc. 165, 506-524 (1994)

- Nitrogen Dioxide (NO2) update (v11.0), 9/2001, for the 3-μm region (J.-Y. Mandin et al, J.Mol.Spectrosc. 181, 379-388 (1997)).

The second source of line data are the pseudoline lists prepared by Geoff C. Toon and coworkers (Jet Propulsion Lab.). Details are described in the preceding chapter, Appendix D. Based on interpolations carried out at Denver University (Aaron Goldman), the pseudoline lists presented here are given with a finer point spacing than originally provided by GC Toon. Table E.1 lists all molecules contained in the linelist and the sources of information used.

Other spectroscopic data was obtained from the ATMOS linelist and from individual workers, namely Linda Brown (JPL), Jean-Marie Flaud & Agnes Perrin (University Marie and Pierre Curie, Paris), Robert Toth (JPL, Pasadena CA), Manfred Birk (DLR, Oberpfaffenhofen), Alain Barbe (Univ.Reims, France), and A.S. Pine (Alpine Technol., Germantown MD). Many thanks to these colleagues and to all the contributors of HITRAN.

Pseudo-lines are consistently given the isotopomer index of zero. Since pseudo-linelists are spaced at fairly large intervals, the retrieval code has to add artificial broadening – either by increasing the Doppler width artificially (GC Toon's GGG code) or by fudging the molecular mass to a small value of typically 1 or less (SFIT codes). An isotopomer code of zero flags

Table E.1: *Overview over all molecules contained in the linelist and their respective sources.*

Molecule	Source for the spectroscopic data
CCL2F2	GCT pseudolines (interpolated from Denver University)
CCL3F	GCT pseudolines (interpolated from Denver University)
CCL4	GCT pseudolines (interpolated from Denver University)
CF4	GCT pseudolines (interpolated from Denver University)
CFC113	GCT pseudolines (interpolated from Denver University)
CHF2CL	GCT pseudolines (interpolated from Denver University)
CLONO2	GCT pseudolines (interpolated from Denver University)
F142B	GCT pseudolines (interpolated from Denver University)
N2O5	GCT pseudolines (interpolated from Denver University)
SF6	GCT pseudolines (interpolated from Denver University)
COCL2	JPL linelist (G.C. Toon, priv. comm., 2001)
C2H2	HITRAN2000 with official update V11.0 7/2001
C2H4	HITRAN2000
C2H6	HITRAN2000, except 2975-2984cm^{-1} from Pine, 1999
CH3CL	HITRAN2000
CH4	HITRAN, Jun 2002 update by Linda Brown superseding the 'official' HITRAN update V11.0 (2/2001) on the HITRAN homepage. It fixes some erroneous air broadening parameters pointed out by Frank Hase (IMK).
CLO	HITRAN2000
CO	HITRAN2000
CO2	HITRAN2000
COCLF	ATMOS linelist, Brown et al.,1996
COF2	HITRAN2000
H2CO	HITRAN2000
H2O	HITRAN2000 with official update V11.0 4/2001 (based on R.Toth measurements) added 45 missing lines from R.Toth linelist between 750 and 2721cm^{-1} (see below)
HDO	HITRAN2000 with official update V11.0 4/2001 (based on R.Toth measurements) added 15 missing lines from R.Toth linelist between 1125 and 1288cm^{-1} (see below)
H2O2	Linelist from Agnes Perrin 1998
H2S	HITRAN2000
HBR	HITRAN2000
HCL	HITRAN2000
HCN	HITRAN2000
HCOOH	Linelist from Agnes Perrin 1999
HF	HITRAN2000
HI	HITRAN2000
HNO3	HITRAN2000
HO2	HITRAN2000
HO2NO2	ATMOS linelist, Brown et al.,1996
HOCL	HITRAN2000
N2	HITRAN2000
N2O	new measurements by Robert Toth (JPL) 2000
NH3	HITRAN2000
NO	HITRAN2000 with official update V11.0 7/2001
NO2	HITRAN2000 with official update V11.0 9/2001 extended from 4117 to 4203cm^{-1} with ATMOS linelist
O2	HITRAN2000 with official update V11.0 1/2001
O3	HITRAN2000, extended beyond 4500cm^{-1} with data from Barbe 2000 heavy isotopomers from new linelists by Flaud & Perrin
OCS	HITRAN2000, linewidth of numerous weaker lines updated according to GC Toon linelist
OH	HITRAN2000
SO2	HITRAN2000

the line as a pseudo-line to the retrieval code. Beware that the general distributions of SFIT1 and SFIT2 versions 3.81 and prior cannot handle isotopic codes of zero.

The line intensity of one water vapour line in the popular HNO3 window near $873 cm^{-1}$ has been changed from 1.4E-26 to 3.0E-27 as it is obviously inconsistent with observations. This inconsistency was confirmed by GC Toon. The change suggested here is within the measurement uncertainties (priv. comm. with the original H2O linelist author Bob Toth, 2002).

original HITRAN water vapour data line changed from

```
11 872.96946 1.432E-26 5.162E+00.0200.2000 4201.25290.350.020000 1 119 614 18 315 233251318
```

to

```
11 872.96946 3.000E-27 5.162E+00.0200.2000 4201.25290.350.020000 1 119 614 18 315 233251318
```

Some H2O and HDO lines that are listed in the original data from Bob Toth were absent in the HITRAN update largely based on the Toth data. A few of these lines are located in suitable windows and corresponding absorptions were seen in spectra recorded at the much wetter site of Wollongong that could be ascribed to the missing lines. Hence, it was decided to include these missing water lines in the present linelist:

The following 15 HDO lines were missing in the latest HITRAN files (taken from R. Toth linelist, priv.comm. Jun 2000):

```
491 1125.951700 1.391E-27 1.925E-04.0717.0000 1693.4442 .64 .000000 2 113 112 13 4 9 000 0 0 0
491 1151.427400 1.510E-27 3.510E-04.0681.0000 1804.8403 .64 .000000 2 113 211 13 5 8 000 0 0 0
491 1161.946100 1.410E-27 1.281E-03.0712.0000 2115.6558 .64 .000000 2 114 311 15 412 000 0 0 0
491 1181.763200 1.211E-27 4.074E-06.0785.0000 0818.0136 .64 .000000 2 1 7 3 5 07 5 2 000 0 0 0
491 1192.398700 1.071E-27 1.058E-05.0772.0000 1110.7600 .64 .000000 2 110 2 9 10 4 6 000 0 0 0
491 1192.522600 1.232E-27 6.637E-06.0848.0000 0942.5325 .64 .000000 2 1 8 3 5 08 5 4 000 0 0 0
491 1204.450200 2.581E-27 4.484E-06.0854.0000 0711.7954 .64 .000000 2 1 8 1 8 08 3 5 000 0 0 0
491 1204.818400 2.290E-27 1.142E-05.0764.0000 0951.6357 .64 .000000 2 1 9 2 8 09 4 5 000 0 0 0
491 1213.654900 3.915E-27 1.085E-05.0764.0000 0809.3933 .64 .000000 2 1 8 2 7 08 4 4 000 0 0 0
491 1227.665300 1.431E-27 3.918E-06.0725.0000 0809.3933 .64 .000000 2 1 9 1 9 08 4 4 000 0 0 0
491 1232.564900 1.347E-27 1.146E-06.0821.0000 0480.2589 .64 .000000 2 1 6 1 6 05 4 1 000 0 0 0
491 1260.979400 1.744E-27 4.211E-04.0715.0000 1846.4022 .64 .000000 2 113 410 14 311 000 0 0 0
491 1270.688400 1.496E-27 1.033E-06.0815.0000 0402.3292 .64 .000000 2 1 5 1 4 04 4 1 000 0 0 0
491 1276.151700 2.496E-27 1.465E-04.0514.0000 1543.2442 .64 .000000 2 113 112 13 311 000 0 0 0
491 1287.096000 2.257E-27 9.737E-05.0707.0000 1465.8299 .64 .000000 2 112 210 12 4 9 000 0 0 0
```

45 Lines found in Bob Toth's linelist (Jun 2000) but not in HITRAN V.11 4/2001

```
13 0751.406000 2.390E-26 3.407E-02.0137.0000 2322.7530 .64 .000000 1 115 312 14 213 000 0 0 0
11 0846.182703 2.020E-27 2.985E-02.0145.0000 4243.1620 .64 .000000 2 216 313 15 214 40016 0 0
11 0905.278373 1.710E-27 4.616E-03.0487.0000 3879.7200 .64 .000000 2 214 6 8 13 311 30016 0 0
11 0906.150200 3.850E-27 7.778E-09.0463.0000 0882.8910 .64 .000000 1 1 8 8 0 08 1 7 000 0 0 0
11 0907.046033 1.630E-27 1.692E-03.0416.0000 3650.5070 .64 .000000 2 212 8 4 11 5 7 30016 0 0
11 0918.821400 2.540E-27 5.375E-02.0117.0000 4608.2250 .64 .000000 1 120 615 19 316 000 0 0 0
11 0921.581800 5.420E-27 1.227E-05.0332.0000 2426.1950 .64 .000000 1 113 9 5 13 410 000 0 0 0
11 0973.828700 3.730E-27 3.909E-07.0564.0000 1998.9960 .64 .000000 1 11110 1 11 5 6 000 0 0 0
11 0991.388700 4.170E-27 1.512E-06.0341.0000 2275.3730 .64 .000000 1 11210 3 12 5 8 000 0 0 0
11 1038.913500 7.240E-27 6.579E-07.0316.0000 1774.6190 .64 .000000 1 112 8 4 12 111 000 0 0 0
11 1049.755100 7.360E-27 1.594E-07.0356.0000 1690.6650 .64 .000000 1 111 9 2 11 2 9 000 0 0 0
13 1052.528200 1.640E-27 3.225E-05.1000.4205 1405.1480 .68 .000000 2 1 7 3 4 08 6 3 002 5 514
13 1062.154600 1.780E-27 4.924E-05.0758.3283 1251.2910 .68 .000000 2 1 7 2 6 08 5 3 002 5 516
```

```
11 1085.550200 1.070E-26 1.054E-06.0296.0000 2042.3120 .64 .000000 1 113 8 5 13 112 000 0 0 0
11 1100.892400 4.350E-27 1.141E-06.0312.0000 2246.8880 .64 .000000 1 113 9 4 13 211 000 0 0 0
11 1129.673000 1.000E-26 3.441E-06.0683.3009 2009.8050 .68 .000000 2 1 9 5 5 09 8 2 002 0 016
13 1210.548800 1.840E-27 9.362E-03.0547.2991 2430.9250 .68 .000000 2 111 5 7 12 6 6 002 5 514
13 1223.007100 1.610E-27 1.643E-02.0502.2332 2802.2900 .68 .000000 2 111 7 4 12 8 5 002 5 514
11 1276.468000 1.800E-26 1.113E-07.0758.3283 1411.6120 .68 .000000 2 1 9 1 8 08 6 3 002 0 016
11 1299.444900 1.100E-26 4.390E-07.0617.2818 1616.4520 .68 .000000 2 111 111 10 4 6 002 0 016
13 1314.005000 1.790E-27 2.798E-02.0572.3230 2544.4340 .68 .000000 3 2 5 4 2 06 5 1 002 5 514
11 1335.796300 6.810E-27 2.295E-05.0306.0000 2586.5290 .64 .000000 1 11410 4 13 5 9 000 0 0 0
11 1885.152900 1.180E-26 1.959E-07.0504.2373 1774.7510 .68 .000000 2 111 5 6 12 211 002 5 516
13 1964.667700 2.120E-27 3.509E-03.0608.3397 2391.5670 .68 .000000 3 2 7 5 2 06 4 3 002 5 514
11 1966.615000 2.400E-26 1.972E-09.0644.3841 0586.2430 .68 .000000 2 1 6 5 2 07 0 7 002 0 016
13 1977.437600 1.600E-27 1.051E-06.0644.3841 0585.1620 .68 .000000 2 1 7 4 4 07 1 7 002 5 516
13 1995.039300 2.430E-27 4.824E-03.0406.2086 2397.7810 .68 .000000 3 2 6 6 1 05 5 0 002 5 514
13 2015.175100 1.600E-27 6.520E-07.0758.3283 0742.4910 .68 .000000 2 1 8 4 5 08 1 8 002 5 516
11 2077.502900 1.070E-26 8.135E-05.0737.0000 2998.7681 .64 .000000 4 210 3 8 09 4 5 000 0 0 0
11 2107.325900 1.130E-26 5.035E-04.0762.0000 3139.4771 .64 .000000 4 210 4 6 09 5 5 000 0 0 0
11 2142.495100 2.900E-26 2.249E-06.0844.4389 1908.0170 .68 .000000 3 2 5 5 0 04 2 3 002 0 016
13 2156.743800 1.600E-27 3.359E-04.0801.3967 2120.5160 .68 .000000 2 113 5 8 12 4 9 002 5 514
13 2178.402000 2.770E-27 6.795E-04.0547.3000 2137.4200 .68 .000000 2 112 7 6 11 6 5 002 5 514
11 2394.851100 1.400E-25 3.544E-07.0858.3304 1131.7760 .68 .000000 2 1 9 7 3 08 4 4 002 0 014
11 2395.413100 5.500E-26 2.114E-08.0758.3283 0744.0640 .68 .000000 2 1 9 5 5 08 0 8 002 0 016
11 2410.478000 2.300E-25 5.238E-07.0907.3513 1360.2360 .68 .000000 2 110 7 4 09 4 5 002 0 014
11 2421.903100 2.900E-26 6.199E-07.0918.3586 1616.4520 .68 .000000 2 111 7 5 10 4 6 002 0 014
11 2430.316900 2.300E-26 5.888E-07.0879.3914 1899.0080 .68 .000000 2 112 7 6 11 4 7 002 0 014
11 2430.532000 1.000E-26 2.850E-07.0558.2600 1695.0710 .68 .000000 2 112 6 6 11 3 9 002 0 016
11 2480.210900 2.300E-26 7.227E-07.0504.2373 1962.5080 .68 .000000 2 113 6 7 12 310 002 0 016
11 2507.137900 1.100E-26 2.659E-09.0710.4228 0602.7740 .68 .000000 2 1 7 7 1 06 2 4 002 0 016
11 2516.293900 1.300E-26 5.983E-08.0558.2600 1327.1190 .68 .000000 2 112 4 8 11 111 002 0 016
11 2688.601100 1.200E-26 2.504E-09.0644.3841 0842.3570 .68 .000000 2 1 8 8 1 07 3 4 002 0 016
11 2702.259000 1.100E-26 1.660E-08.0758.3283 1050.1580 .68 .000000 2 1 9 8 2 08 3 5 002 0 016
11 2720.053000 1.100E-26 6.533E-10.0644.3841 0586.2430 .68 .000000 2 1 8 7 2 07 0 7 002 0 016
```

Where pressure shifts were missing in the spectroscopic linelist, these were sometimes estimated for the example fit shown. The electronic supplement lists all spectroscopic lines of which the pressure shifts or line position were adjusted to be more consistent with observations. The resulting linelist can be found on the supplementary DVD in electronic from. It is identical to the linelist used throughout this work, except for heavy ozone isotopomers above $1800 cm^{-1}$ where we were not at liberty to pass on the latest spectroscopic line parameters.

References for the spectroscopic linelist used

Barbe, Alain; U.F.R. Sciences Exactes et Naturelles, Molecular Spectroscopy and Atmospheric Applications Group, Moulin de la Housse B.P., 1039, 51687 Reims Cedex, E-mail: alain.barbe@univ-reims.fr

Brown, L.R.; M.R. Gunson, R.A. Toth, F.W. Irion, C.P. Rinsland, and A. Goldman, "The 1995 Atmospheric Trace Molecule Spectroscopy (ATMOS) Linelist", Appl. Opt., **35**, 2828-2848, 1996.

Hase, Frank (frank.hase@imk.fzk.de) and Linda Brown (linda@regina.jpl.nasa.gov), the CH4 linelist used in this work superseding the ch4 update officially available from the HITRAN web pages at the time, priv. comm. May to Aug 2002.

Perrin A., Flaud J.-M., Valentin A., Camy-Peyret C., and Gbaguidi H., "The n1 and n2 bands of the $^{17}O\,^{16}O\,^{17}O$ isotopomer of ozone ", J. Mol. Spectrosc., **200**, 248-252, 2000.

Perrin, A.; C.P. Rinsland, & A. Goldman, "Spectral Parameters for the n6 Region of HCOOH and its Measurement in the Tropospheric Spectrum", J. Geophys. Res., **104**, 18661-18666, 1999.

Perrin, A.; J.-M. Flaud, F. Keller, et al., "The $\nu 1$ + $\nu 3$ bands of the $^{16}O\,^{17}O\,^{16}O$ and $^{16}O\,^{16}O\,^{17}O$ isotopomers of ozone", J. Molec. Spectrosc., in press, 2001.

Perrin, A.; J.-M. Flaud, P. Arcas, A. Goldman, R.D. Blatherwick, F.J. Murcray, A. Valentin, C. Camy-Peyret, J.-Y. Mandin, V. Dana, S. Klee, and M. Winnewisser, "New Line Position and (Absolute) Line Intensities for the Far Infrared and n6 bands of H_2O_2", Atmospheric Spectroscopy Applications (ASA) Conference, University of Reims, France, Sept. 1-3, 1999.

Pine A.S., Rinsland C.P., "The role of torsional hot bands in modeling atmospheric ethane", J. Quant. Spectrosc. Radiat. Transfer, **62** (4): 445-458, Jul 1999.

Rinsland C.P., Jones N.B., Connor B.J., Logan J.A., Pougatchev N.S., Goldman A., Murcray F.J., Stephen T.M., Pine A.S., Zander R., Mahieu E., and Demoulin P., "Northern and southern hemisphere ground-based infrared spectroscopic measurements of tropospheric carbon monoxide and ethane", J. Geophys. Res., **103** (D21): 28197-28217, Nov 20 1998.

Rothman, L.S.; A. Barbe, D.C. Benner, L.R. Brown, C. Camy-Peyret, M.R. Carleer, K. Chance, C. Clerbaux, V. Dana, V.M. Devi, A. Fayt, J.-M. Flaud, R.R. Gamache, A. Goldman, D. Jacquemart, K.W. Jucks, W.J. Lafferty, J.-Y. Mandin, S.T. Massie, V. Nemtchinov, D.A. Newnham, A. Perrin, C.P. Rinsland, J. Schroeder, K.M. Smith, M.A.H. Smith, K. Tang, R.A. Toth, J. Vander Auwera, P. Varanasi, and K. Yoshino, The HITRAN Molecular Spectroscopic Database: Edition of 2000 Including Updates of 2001; HITRAN Special Issue, J. Quant. Spectrosc. Radiat. Transfer, vol. **82**, numbers 1-4, 15 Nov to 15 Dec 2003.

Toon, G.C.; J.-F. Blavier, B. Sen, and B.J. Drouin, "Atmospheric COCl2 measured by solar occultation spectrometry", Geophys. Res. Let., **28**, 2835-2838, July 15, 2001.

Toth, Robert A.; "Air and N2 broadening parameters of HDO and D2O, 709 to 1936cm^{-1}", J. Molec. Spectrosc., **198**, 358-370, 1999.

Toth, Robert A.; "Air and N2 broadening parameters of water vapor: 604 to 2271cm^{-1}", J. Molec. Spectrosc., **201**, 218-243, 2000.

Toth, Robert A.; "HDO and D2O Low Pressure, Long Path Spectra in the 600 - 3100cm^{-1} Region", J. Molec. Spectrosc., **195**, 73-97, 1999.

Toth, Robert A.; "Line positions and strengths of N2O between 3515 and 7800cm^{-1}", J. Molec. Spectrosc., **197**, 158-187, 1999.

Toth, Robert A.; "Line strengths (900-3600cm^{-1}), self-broadened linewidths, and frequency shifts (1800-2360cm^{-1}) of N2O", Appl. Optics, **32**, 7326-7365, 1993.

Toth, Robert A.; "Line strengths of N2O in the 1120-1440cm^{-1} region", Appl.Optics, **23**, 1825-1836, 1984.

Toth, Robert A.; "Line-frequency measurements and analysis of N2O between 900 and 4700 cm^{-1}", Appl. Optics, 30, 5289-5315, 1991.

Toth, Robert A.; "N2- and air-broadened linewidths and frequency shifts of N2O", J. Quant. Spectrosc. Radiat. Transfer, **66**, 285-304, 2000.

Toth, Robert A.; "Water vapor measurements between 590 and 2582cm^{-1}: Line positions and strengths", J. Molec. Spectrosc., **190**, 379-396, 1998.

Acknowledgements

We like to thank all colleagues that sent us example spectra, lists of their favourite microwindows, spectroscopic linelists, or contributed to the discussion. Special thanks go to Nicholas Jones, University of Wollongong, for creating the solar simulations with the GFIT/GGG algorithm and to Clare Murphy, also University of Wollongong, for cross-reading the draft and making many useful suggestions for improvement. Our thanks also to Rick McGregor and Mats Luspa and everyone else from IRF that helped in getting this book into print. We also like to thank the developers of the SFIT2, FSCATM, GGG/GFIT and simul108 software that were used for the simulation and analysis of spectra, the authors of the freeware software Gnuplot and LaTeXthat were employed to create the figures and layout of this work and the large number of scientists that contributed to the spectroscopic linelists used. And last not least we thank our families and friends for their patience and support.

References

Abbas, M.M.; J. Guo, B. Carli, F. Mencaraglia, A. Bonetti, M. Carlotti, and I.G. Nolt, *"Stratospheric O3, H2O and HDO distributions from balloon-based far-infrared observations"*, J. Geophys. Res., **92**, 8354-8364, 1987.

Abbas, M.M.; J. Guo, B. Carli, F. Mencaraglia, M. Carlotti, and I.G. Nolt, *"Heavy ozone distribution in the stratosphere from far-infrared observations"*, J. Geophys. Res., **92**, 13231-13239, 1987.

Abbas, M.M.; J. Guo, B. Carli, F. Mencaraglia, M. Carlotti, and I.G. Nolt, *"Stratospheric distribution of HCN from far-infrared observations"*, Geophys. Res. Lett., **14**, 531-534, 1987.

Abbas, M.M.; M.J. Glenn, V.G. Kunde, J. Brasunas, B.J. Conrath, W.C. Maguire, and J.R. Herman, *"Simultaneous measurement of stratospheric O3, H2O, CH4 and N2O profiles from infrared limb thermal emissions"*, J. Geophys. Res. , **92**, 8343–8353, 1987.

Abbas, M.M.; M.J.Glenn, I.G. Nolt, B. Carli, F. Mencaraglia, and M. Carlotti, *"Far-infrared measurement of stratospheric carbon monoxide"*, Geophys. Res. Lett., **15**, 140-143, 1988.

Abbas, M.M.; V.G. Kunde, J.C. Brasunas, W.C. Maguire, J.R. Herman, M.J. Glenn, S.T. Massie, and W.A. Shaffer, *"Nighttime measurements of stratospheric NOx from balloonborne limb thermal emissions observations"*, Workshop on Tropospheric Ozone and Quadrennial Ozone Symposium, Abstracts, 151, 1988.

Abbas, M.M.; V.G. Kunde, J.C. Brasunas, J.R. Herman, and S.T. Massie, *"Nighttime reactive nitrogen measurements from stratospheric infrared thermal emission observations"*, J. Geophys. Res., **96**, 10885–10897, 1991.

Abbas, M.M.; H. A. Michelsen, M. R. Gunson, M. C. Abrams, M. J. Newchurch, R. J. Salawitch, A. Y. Chang, A. Goldman, F. W. Irion, G. L. Manney, E. J. Moyer, R. Nagaraju, C. P. Rinsland, G. P. Stiller, and R. Zander, *"Seasonal variations of water vapor in the lower stratosphere inferred from ATMOS/ATLAS-3 measurements of H2O and CH4"*, Geophys. Res. Lett. , **23**, 2401-2404, 1996.

Abbas, M.M.; M.G. Gunson,M.J. Newchurch, H.A. Michelsen, R.J. Salawitch, A. Allen, M.C. Abrams, A.Y. Chang, A. Goldman, F.W. Irion, E.J. Moyer, R. Nagaraju, C.P. Rinsland, G.P. Stiller, and R. Zander, *"The hydrogen budget of the stratosphere inferred from ATMOS measurements of H2O and CH4"*, Geophys. Res. Lett. , **23**, 2405-2408, 1996.

Abrams, M.C.; A. Goldman, M.R. Gunson, C.P. Rinsland, and R. Zander, *"Observations of the infrared solar spectrum from space by the ATMOS experiment"*, Applied Optics, Vol. **35**, No. 16, 2747-2751, 1996.

Abrams, M.C.; M.R. Gunson, A.Y. Chang, C.P. Rinsland, and R. Zander, *"Remote sensing of the Earth's atmosphere from space with high-resolution Fourier-transform spectroscopy: development and methodology of data processing for the Atmospheric Trace Molecule Spectroscopy experiment"*, Appl. Opt., **35**, 2774-2786, 1996.

Abrams, M.C.; M.R. Gunson, A.Y. Chang, G.L. Manney, M.M. Abbas, A. Goldman, F.W. Irion, H.A. Michelsen, M.J. Newchurch, C.P. Rinsland, R.J. Salawitch, G.P. Stiller, and R. Zander, *"ATMOS/ ATLAS–3 observations of long–lived tracers and descent in the Antarctic vortex in November 1994"*, Geophys. Res. Lett., **23**, 2345-2348, 1996.

Abrams, M.C.; M.R. Gunson, A.Y. Chang, G.L. Manney, M.M. Abbas, A. Goldman, F.W. Irion, H.A. Michelsen, M.J. Newchurch, C.P. Rinsland, R.J. Salawitch, G.P. Stiller, and R. Zander, *"ATMOS/ ATLAS-3 observations of trace gas transport in the Antarctic vortex in November 1994"*, Geophys. Res. Lett., **23**, 2345-2348, 1996.

Abrams, M.C.; M.R. Gunson, A.Y. Chang, M.M. Abbas, A.G. Goldman, F.W. Irion, H.A. Michelsen, M.J. Newchurch, C.P. Rinsland, G.P. Stiller, and R. Zander, *"On the assessment and uncertainty of atmospheric trace gas burden measurements with high-resolution infrared solar occultation spectra from space by the ATMOS experiment"*, Geophys. Res. Lett., **23**, 2337-2340, 1996.

Abrams, M.C.; M.R. Gunson, L.L. Lowes, C.P. Rinsland, and R. Zander, *"Pressure sounding of the middle atmosphere from ATMOS solar occultation measurements of atmospheric CO2 absorption lines"*, Appl. Opt., **35**, 2810-2820, 1996.

Adrian, G.P.; T. Blumenstock, H. Fischer, L. Gerhardt, T. Gulde, H. Oelhaf, P. Thomas, and O. Trieschmann, *"Column amounts of trace gases derived from ground-based measurements with MIPAS during CHEOPS III"*, Geophys. Res. Lett., **18**, 783–786, 1991.

Adrian, G.P.; T.v. Clarmann, H. Fischer, and H. Oelhaf, *"Trace gas measurements with the ground–based MIPAS experiment during the arctic winters 1990 to 1992"*, in *IRS'92: Current problems in atmospheric radiation*, edited by S. Keevallik and O. Kärner, Deepak Publishing, Hampton, Virginia, 359–362, 1993.

Adrian, G.P.; M. Baumann, T. Blumenstock, H. Fischer, A. Friedle, L. Gerhardt, G. Maucher, H. Oelhaf, W. Scheuerpflug, P. Thomas, O. Trieschmann, and A. Wegner, *"First results of ground-based FTIR measurements of atmospheric trace gases in north Sweden and Greenland during EASOE"*, Geophys. Res. Lett., **21**, 1343–1346, 1994.

Albrecht T.; J. Notholt, R. Wolke, S. Solberg, C. Dye, H. Malberg, *"Variations of CH2O and C2H2 determined from groundbased FTIR measurements and comparison with model results"*, Adv. Space Res. **29**, 1713-1718, 2002.

Amanatidis, G.; A. Bais, A. Kelesis, C. Zerefos, and J. Ziomas,*"Two years of regular stratospheric NO2 measurements in Greece using twilight photometry"*, Workshop on Tropospheric Ozone and Quadrennial Ozone Symposium, Abstracts, 162, 1988.

Arlander, D.W.; A. Barbe, M.T. Bourgeois, A. Hamdouni, J.-M. Flaud, C. Camy–Peyret, and P. Demoulin, *"The identification of $^{16}O^{18}O^{16}O$ and $^{16}O^{16}O^{18}O$ ozone isotopes in high resolution ground–based FTIR spectra"*, J. Quant. Spectrosc. Radiat. Transfer, **52**, 267–271, 1994.

Backer-Barilly, M.R. De; A. Barbe, S.A. Tashkun, V.G. Tyuterev, and A. Chichery, *"The 5ν3 Bands of ^{18}O Enriched Ozone: Line Positions of $^{16}O^{16}O^{18}O$, $^{16}O^{18}O^{18}O$ and $^{18}O^{16}O^{18}O$"*, Mol. Phys., **100**, 3499–3506, 2002.

Backer-Barilly, M.R. De; A. Barbe, V.G. Tyuterev, A. Chichery, and M.T. Bourgeois, *"High-Resolution Infrared Spectra of the $^{16}O^{18}O^{16}O$ Ozone Isotopomer in the Range 900-5000 cm^{-1}: Line Positions"*, J. Mol. Spectrosc., **216**, 454–464, 2002.

Backer-Barilly, M.R. De; A. Barbe, and V.G. Tyuterev, *"Infrared Spectrum of $^{16}O^{18}O^{16}O$ in the 5μm Range. Positions, Intensities, and Atmospheric Applications, Atmospheric and Oceanic Optics"*, **16**, 183–188, 2003.

Barbe, A.; L. Regalia, J.J. Plateaux, P. v.d. Heyden and X. Thomas, *"Temperature dependance of N_2 and O_2 broadening coefficients of ozone"*, J. Mol. Spectrosc., **180**, 175-180, 1996.

Barbe, A.; O. Sulakshina, J.J. Plateaux, V.G. Tyuterev and S. Bouazza, *"Line positions and intensities of the 3ν1+ν3 band ozone"*, J. Mol. Spectrosc., **175**, 296-302, 1996.

Barbe, A.; and J.J. Plateaux, *"Analysis of the 2ν1+2ν3 band of ozone: line positions and intensities"*, J. Quant. Spectrosc. Radiat. Transfer , **55**, 449-455, 1996.

Barbe, A.; *"High Resolution Infrared Spectroscopy of Ozone: A Support for Atmospheric Observations, Computational Technologies"*, **7**, 12–23, 2002.

Barret, B.; M. De Mazière, P. Demoulin, E. Mahieu, F. Mélen, B.J. Connor, and N.B. Jones, *"Investigation of height-resolved information in ground-based, high-resolution Fourier infrared solar spectra above the Jungfraujoch"*, in Proceedings of the "Quadrennial Ozone Symposium", Sapporo, Japan, July 3-8, 2000, 301-302, 2000.

Barret, B.; M. De Mazière, and P. Demoulin, *"Retrieval and characterisation of ozone profiles from solar infrared spectra at the Jungfraujoch"*, J. Geophys. Res. **107**, No. D24, 4788, 2002.

Barrett, J.; P. Solomon, M. Jaramillo, R.de Zafra, A. Parrish, and L. Emmons, *"Daytime ClO over McMurdo in September 1987: altitude profile retrieval accuracy"*, Polar Ozone Workshop, Session IV, May 1988.

Barrett, J.; P.M. Solomon, R.L.de Zafra, M. Jaramillo, L. Emmons, and A. Parrish, *"Formation of the Antarctic ozone hole by CO dimer formation"*, Nature, **336**, 455-458, 1988.

Becker, E.; J. Notholt, A. Herber, *"Tropospheric aerosol measurements in the Arctic by FTIR emission and Star photometer extinction spectroscopy"*, Geophys. Res. Lett. **26**, 1711-1714, 1999.

Becker, E.; J. Notholt, *"Intercomparison and validation of FTIR measurements with the sun, the moon and emission in the Arctic"*, J. Quant. Spec. Rad. Transfer, **65**, 779-786, 2000.

Bell, W.; N.A.Martin, T.D.Gardiner, N.R.Swann, P.T.Woods, P.F.Fogal, and J.W.Waters, *"Column measurements of stratospheric trace species over Are, Sweden in the winter of 1991-1992"*, Geophys. Res. Lett., **21**, 1347-1350, 1994.

Bell, W.; N.A. Martin, P.T. Woods, T.D. Gardiner, N.R. Swann, P.F. Fogal, and J.W. Waters, *"Column measurements of stratospheric trace species over Are, Sweden in the winter of 1991-1992"*, Geophys. Res. Lett. **21**, 1347–1350, 1994.

Bell, W.; C. Paton-Walsh, P.T. Woods, T.D.. Gardiner, N.R. Swann, N.A. Martin, L. Donohoe, M.P. Chipperfield, *"Measurements of Stratospheric Chlorine Monoxide (ClO) from Ground-based FTIR Observations", J. Atmos. Chem.}*, **24**, *285-297, 1996.*

Bell, W.; C. Paton-Walsh, P.T. Woods, T.D. Gardiner, L. Donohoe, A. Gould, D. Secker, S. Naughten, N.R. Swann, N.A. Martin, L.E. Page, M.P. Chipperfield, A.M. Lee, and S. Pullen, *"Ground-based FTIR Measurements of Stratospheric Trace Species from Aberdeen During Winter and Spring 1993/94 and 1994/95 and Comparison with a 3D Model"*, J. Atmos. Chem. **30**, 119-130, 1998.

Bell, W.; C. Paton-Walsh, P.T. Woods, T.D. Gardiner, M.P. Chipperfield, and A.M. Lee, *"Ground-based FTIR Measurements with High Temporal Resolution"*, J. Atmos. Chem. **30**, 131-140, 1998.

Bernardo, Cirilo; *"Measurement of Instrument Line Shape Functions of High-Resolution FTIR Spectrometers and their Application to the Analysis of Spectra"*, PhD Thesis, University of Wollongong, Australia, 2002.

Bièvre, P. de; M. Gallet, N.E. Holden, and I.L. Barnes, *"Isotopic abundances and atomic weights of the elements"*, J. Phys. Chem. Ref. Data **13**, 809–891, 1984.

Blatherwick, R.D.; D.G. Murcray, F.H. Murcray, F.J. Murcray, A. Goldman, G.A. Vanasse, S.T. Massie, and R.J. Cicerone, *"Infrared emission measurements of morning stratospheric N_2O_5"*, J. Geophys. Res., **94**, 18337–18340, 1989.

Blatherwick, R.D.; F.J. Murcray, X. Liu and J. Kosters, *"Measurements of HNO3, NO2, NO, O3, N2O5, N2O and CH4 From High Resolution Solar Occultation Spectra Before and After the Pinatubo Eruption"*, supplement to Eos, **77**(46), F121(A42A-2), 1996.

Blumenstock, T.; H. Fischer, A. Friedle, F. Hase, J. Schreiber, and P. Thomas, *"Column amounts of trace gases measured by ground-based FTIR spectroscopy near Kiruna, Sweden, during winter 1994/95"*, Proceedings of the third European workshop on Polar stratospheric ozone, Schliersee 1995, European Commission - Air pollution research report **56**, 340–343, 1996.

Blumenstock, T.; H. Fischer, A. Friedle, F. Hase, and P. Thomas, *"Column amounts of ClONO2, HCl, HNO3, and HF from ground-based FTIR measurements made near Kiruna, Sweden, in late winter 1994"*, J. Atmos. Chem. **26**, 311-321, 1997.

Blumenstock, T.; H. Fischer, A. Friedle, G.P. Stiller, P. Thomas, *"Column amounts of HCl, ClONO2 and HF measured by ground-based FTIR spectroscopy near Kiruna (S) during winter since 1990"*, Proceedings of the Quadrennial Ozone Symposium 1996, 469–472, 1998.

Blumenstock, T.; H. Fischer, S. Fietze, G.P. Stiller, M. Richter, P. Thomas, A. Meier, and H. Nakajima, *"Time Series of HNO3 Column Amounts Measured by Ground-Based FTIR Spectroscopy at Kiruna (Sweden) in Winter 1995/96 and 1996/97"*, Proceedings of the Fourth European Workshop on Polar Stratospheric Ozone, Schliersee 1997, European Commission - Air pollution research report **66**, 411–414, 1998.

Blumenstock, T.; H. Fischer, F. Hase, G.P. Stiller, R. Ruhnke, D. Yashcov, A. Meier, A. Steen, Y. Kondo, *"Ground Based FTIR Measurements of O3, HF, HCl, ClONO2, and HNO3 at Kiruna (Sweden) since Winter 1993/94"*, Proceedings of the Quadrennial Ozone Symposium, Sapporo 2000, 145–146, 2000.

Brasunas, J.C.; J.R. Herman, V.G. Kunde, W.C. Maguire, L.W. Herath, W.A. Shaffer, M.M. Abbas, and S.T. Massie, *"High resolution, balloonborne emission spectroscopy of trace species in the lower stratosphere: N_2O_5"*, Workshop on Tropospheric Ozone and Quadrennial Ozone Symposium, Abstracts, 151, 1988.

Brault, J.W.; *"High precision Fourier Transform Spectrometry: The critical role of phase corrections"*, Mikrochimica Acta, **III**, 215–227, 1987.

Brault, J.W.; *"New approach to high-precision Fourier-transform spectrometer design"*, Appl. Apt., **35**, June 1996.

Brown, L.R.; C.B. Farmer, C.P. Rinsland, and R.A. Toth, *"Molecular line parameters for the atmospheric trace molecule spectroscopy experiment"*, Appl. Opt. **26**, 5154–5179, 1987.

Brown, L.R.; C.B. Farmer, C.P. Rinsland, and R. Zander, *"Remote sensing of the atmosphere by high resolution infrared absorption spectroscopy"*, Chapter 2 in *"Spectroscopy of the Earth's Atmosphere and Interstellar Medium"*, pp. 97-151, K. Narahari Rao and A. Weber Eds. Academic Press, Inc. 1992.

Brown, L.R.; D.C. Benner, J.-P. Champion, V.M. Devi, L. Fejard, R.R. Gamache, T. Gabard, J.C. Hilico, B. Lavorel, M. Lonte, G.C. Mellau, A. Nikitin, A.S. Pine, A. Predoi-Cross, C.P. Rinsland, O. Robert, R.L. Sams, M.A.H. Smith, S.A. Tashkun, and V.G. Tyuterev, *"Methane Line Parameters in HITRAN"*; HITRAN Special Issue, J. Quant. Spectrosc. Radiat. Transfer, **82**, numbers 1-4, 2003.

Camy–Peyret C.; J.-M. Flaud, A. Perrin, V.M. Devi, C.P. Rinsland, and M.A.H. Smith, *"The hybrid–type Volumes ν_1 and ν_3 of $^{16}O^{16}O^{18}O$: Line positions and intensities"*, J. Mol. Spectrosc., **118**, 345–354, 1986.

Carli, B.; F. Mencaraglia, M. Carlotti, B.M.Dinelli and I.G. Nolt, *"Middle atmosphere composition and chemistry submillimeter measurement of stratospheric chlorine monoxide"*, J. Geophys. Res., **93**, 1063, 1988.

Carli, B. and J.H. Park, *"Simultaneous measurement of minor stratospheric constituents with emission far-infrared spectroscopy"*, J. Geophys. Res., **93**, 3851–3865, 1988.

Carlotti, M.; A. Barbis, B. Carli and S.Piccioli, *"Global fit analysis for the retrieval of O3 distribution from far-IR limb-scanning measurements"*, Workshop on Tropospheric Ozone and Quadrennial Ozone Symposium, Abstracts, 257, 1988.

Carlotti, M.; *"Global-fit approach to the analysis of limb-scanning atmospheric measurements"*, Appl. Opt., **27**, 3250-3254, 1988.

Carlotti, M.; A. Barbis, and B. Carli, *"Stratospheric ozone vertical distribution from far–infrared balloon spectra and statistical analysis of errors"*, J. Geophys. Res., **94**, D13, 16365–16372, 1989.

Cassam-Chena, Patrick; *"Ab Initio Predictions for the Q-branch of the Methane Vibrational Ground State"*; HITRAN Special Issue, J. Quant. Spectrosc. Radiat. Transfer, vol. 82, numbers 1-4, 2003.

Chackerian, C.; Jr, S.W. Sharpe, and T.A. Blake, *"Anhydrous Nitric Acid Integrated Absorption Cross Sections: 820 to 5300 cm^{-1}"*; HITRAN Special Issue, J. Quant. Spectrosc. Radiat. Transfer, vol. 82, numbers 1-4, 2003.

Chakrabarty, D.K.; G. Beig, and J.S. Sidhu, *"Winter variabilities of O_3 and NO_2 at low latitude"*, Workshop on Tropospheric Ozone and Quadrennial Ozone Symposium, Abstracts, 164, 1988.

Chance, K.V. and W.A.Traub, *"Evidence for stratospheric hydrogen peroxide"*, J. Geophys. Res., **92**, 3061, 1987.

Chance, K.V.; D.G. Johnson, and W.A. Traub, *"Measurement of stratospheric HOCl: Concentration profiles, including diurnal variation"*, J. Geophys. Res., **94**, 11059–11069, 1989.

Chance, K.V.; D.G. Johnson, W.A. Traub, and K.W. Jucks, *"Measurement of the stratospheric hydrogen peroxide concentration profile using far infrared thermal emission spectroscopy"*, Geophys. Res. Lett., **18**, 1003-1006, 1991.

Chichery, A.; A. Barbe, M.T. Bourgeois, P. Demoulin, and G. Tyuterev, *"The $3\nu3$ bands of isotopic ozone 668 and 686"*, in Proceedings of "Atmospheric Spectroscopy Applications 1999", Reims, France, September 1-3, 1999, 147–150, 1999.

Chipperfield, M.P.; M. Burton, W. Bell, C. Paton-Walsh, T. Blumenstock, M.T. Coffey, J.W. Hanningan, W.G. Mankin, B. Galle, J. Mellqvist, E. Mahieu, R. Zander, J. Notholt, B. Sen, and G.C. Toon, *"On the use of HF as a reference for the comparison of stratospheric observations and models"*, J. Geophys. Res., **102**, 12901–12919, 1997.

Coffey, M.T.; W.G. Mankin, A. Goldman, C.P. Rinsland, G.A. Harvey, V. Malathy Devi, and G.M. Stokes, *"Infrared measurements of atmospheric ethane (C_2H_6) from aircraft and groundbased solar absorption spectra in the 3000 cm^{-1} region"*,Geophys. Res. Lett., **12**, 199–202, 1985.

Coffey, M.T.; W.G. Mankin, and A. Goldman, *"Stratospheric NO2 retrieval from solar absorption spectra in the ν_3 and $\nu_1 + \nu_3$ infrared bands*, Appl. Opt., **25**, 2460–2462, 1986.

Coffey, M.T. and W.G. Mankin, *"Comparison of winter stratospheric chemistry in Arctic and Antarctic regions"*, Workshop on Tropospheric Ozone and Quadrennial Ozone Symposium, Abstracts, 75, 1988.

Coffey, M.T. and W.G. Mankin, *"Temporal and spatial distribution of stratospheric trace gases over Antarctica in August and September, 1987"*, Polar Ozone Workshop, Session IV, May 1988.

Coffey, M.T.; W.G. Mankin, and A. Goldman, *"Airborne measurements of stratospheric constituents over Antarctica in the Austral Spring, 1987", 2. "Halogen and nitrogen trace species"*, J. Geophys. Res., **94**, 16597–16613, 1989.

Coffey, M.T.; A. Goldman, J.W. Hannigan, W.G. Mankin, W.G. Schoenfeld, C.P. Rinsland, C. Bernardo, and D.W.T. Griffith, *"Improved vibration-rotation (0-1) HBr line parameters for validating high resolution infrared atmospheric spectra measurements"*, J. Quant. Spectrosc. Radiat. Transfer, **60**, 863–867, 1998.

Coheur, P.-F.; C. Clerbaux, M. Carleer, S. Fally, D. Hurtmans, R. Colin, C. Hermans, A.C. Vandaele, B. Barret, M. De Mazière, and H. De Backer, *"Retrieval of Atmospheric Water Vapor Columns from FT Visible Solar Absorption Spectra and Evaluation of Spectroscopic Databases"*; HITRAN Special Issue, J. Quant. Spectrosc. Radiat. Transfer, **82**, numbers 1-4, 2003.

Connor, B.J.; J.W. Barrett, A. Parrish, P.M. Solomon, R.L. de Zafra, and M. Jaramillo, *"Ozone over McMurdo station, Antarctica, Austral spring 1986: altitude profiles for the middle and upper stratosphere"*, J. Geophys. Res., **92**, 13221–13230, 1987.

Connor, B.J.; R.L. de Zafra, P.M. Solomon, A. Parrish, J.W. Barrett, and M. Jaramillo, *"Nitrous oxide in the tropical middle atmosphere observed by ground-based mm-wave spectrometry"*, Geophys. Res. Lett., **14**, 1254–1257, 1987.

Connor, B.J.; N.B. Jones, S.W. Wood, J.G. Keys, C.P. Rinsland, F.J. Murcray, *"Retrieval of HCl and HNO3 profiles from ground-based FTIR data using SFIT2"*; in: Bojkov, R.D.; Visconti, G. (eds). Atmospheric ozone; proceedings of the XVIII Quadrennial Ozone Symposium, L'Aquila, Italy, September 1996, vol. 2, 485–487. (Originally presented as a poster.) Parco Scientifico e Tecnologico d'Abruzzo, L'Aquila, 1998.

Cox, A.N.; *"Allen's Astrophysical Quantities"*, 4^{th} ed., Springer-Verlag New York, 2000.

Dang-Nhu, M. and A. Goldman, *"Line parameters for C_2H_6 in the 3000 cm^{-1} region"*, J. Quant. Spectrosc. Radiat. Transfer, **38**, 159–161, 1987.

Dang-Nhu, M.; R. Zander, A. Goldman, and C.P. Rinsland, *"Identification of magnetic dipole infrared transitions of the fundamental bend of oxygen"*, J. Mol. Spectrosc., **144**, 366–373, 1990.

David, S.J.; S.A. Beaton, M.H. Anderberg, and F.J. Murcray,*"Determination of total ozone over Mauna Loa using very high resolution infrared solar spectra"*, Geophys. Res. Lett., **20**, 2055–2058, 1993.

David, S.J.; F.J. Murcray, A. Goldman, C.P. Rinsland, and D.G. Murcray, *"The effect of the Mt. Pinatubo aerosol on the HNO_3 column over Mauna Loa, Hawaii"*, Geophys. Res. Lett., **21**, 1003–1006, 1994.

De Mazière, M.; C. Lippons, and C. Muller, *"Observations of stratospheric HCl: 1975-1985"*, in Proc. 28th Liège International Astrophysical Colloquium, *Our changing atmosphere*, edited by P.J. Crutzen, J.-C. Gerared, and R. Zander, University of Liège, Belgium, pp. 61–68, 1989.

De Mazière, M.; O. Hennen, M. van Roozendael, P.C. Simon, P. Demoulin, G. Roland, R. Zander, H. De Backer and R. Peter, *"Towards improved evaluations of total ozone at the Jungfraujoch, using vertical profile estimations based on auxiliary data"*, Proceedings of the "XXVIII Quadrennial Ozone Symposium", L'Aquila-Italy, September 12-21, 1996, R. Bojkov editor, 1997.

De Mazière, M.; M. Van Roozendael, C. Herman, P.C. Simon, P. Demoulin, G. Roland, and R. Zander, *"Quantitative evaluation of post-Pinatubo NO2 reduction and recovery, based on 10 years of FTIR and UV-visible spectroscopic measurements at the Jungfraujoch"*, J. Geophys. Res., **103**, 10849-10858, 1998.

De Mazière, M.; O. Hennen, M. van Roozendael, P. Demoulin, and H. De Backer, *"Daily ozone vertical profile model built on geophysical grounds, for column retrieval from atmospheric high-resolution infrared spectra"*, J. Geophys. Res., **104**, 23855-23869, 1999.

De Mazière, M.; and B. Barret, *"Retrieval of tropospheric information from ground-based FTIR observations, supported by synergistic exploitation of various ground-based and space-borne measurement techniques and data"*, in Annual Report 2001- TROPOSAT: The Use and Usability of Satellite Data for Tropospheric Research, EUROTRAC-2 International Scientific Secretariat (ISS), GSF-National Research Centre for Environment and Health, Munich, Germany, 146-150, May 2002.

De Mazière, M.; B. Barret, A.-C. Vandaele, E. Neefs, F. Scolas, T. Egerickx, C. Hermans, P.-F. Coheur, S. Fally, M. Carleer, and J. Leveau; *"Preliminary results from the FTIR campaign at Ile de la Réunion in September - October 2002"*, oral presentation at the NDSC IRWG meeting in Bremen, June 18-20, 2003.

De Mazière, M.; B. Barret, C. Hermans, E. Neefs, F. Scolas, A.-C. Vandaele, M. Carleer, S. Fally, P.-F. Coheur, J. Leveau, and J. Metzger, *"Ground-based FTIR atmospheric observations campaign at Ile de la Reunion"*; Poster presented at the Workshop on "Tropical Meteorology and Chemistry", Wessling, Pfarrstadl, Germany, 14-16 May, 2003.

Delbouille, L.; G. Roland, J. Brault, and L. Testerman, *"Photometric Atlas of the Solar Spectrum from 1,850 to 10,000 cm^{-1}"*, Kitt Peak National Observatory, Tucson, AZ, 1981.

Delbouille, L. and G. Roland, *"High-resolution solar and atmospheric spectroscopy from the Jungfraujoch high-altitude station"*, Optical Engineering, **34**, 2736–2739, 1995.

Demoulin, P.; C.B. Farmer, C.P. Rinsland, and R. Zander, *"Determination of absolute strengths of N2 quadrupole lines from high resolution ground based IR solar observations"*, J. Geophys. Res., **96**, 13003–13008, 1991.

Demoulin, P.; C.B. Farmer, C.P. Rinsland, and R. Zander, *"Determination of absolute strengths of N_2 quadrupole lines from high resolution ground based IR solar observations"*, J. Geophys. Res., **96**, 13003–13008, 1991.

Demoulin, P.; B. Schmid, G. Roland, and C. Servais, *"Vertical column abundance and profile retrievals of water vapor above the Jungfraujoch"*, in Proceedings of *"Atmospheric Spectroscopy Applications, ASA 96"*, Reims, September 4-6, 1996, 131–134, 1996.

Demoulin, P.; E. Mahieu, G. Roland, L. Delbouille, C. Servais, M. De Mazière and M. Van Roozendael, *"The Current Budget of NOy above the Jungfraujoch as derived from IR Solar Observations"*, in Proceedings of the "Fourth EuropeanSymposium on Polar Stratospheric Ozone Research", Schliersee, September 22–26, 1997.

Demoulin, P.; Université de Liège, e-mail: demoulin@astro.ulg.ac.be, priv. comm., 2001.

Denmead, O.T.; R. Leuning, D.W.T. Griffith, L.A. Harper, J.R. Freney, I.M. Jamie, and F. Turatti, *"Verifying current estimates of non-CO2 greenhouse gas emissions from animals, landfills and pastures with direct measurements"*, CSIRO Land and Water, Canberra, 1998.

Devi, V.M.; D.C. Benner, M.A.H. Smith, C.P. Rinsland, S.W. Sharpe, and R.L. Sams; *"A Multispectrum Analysis of the 1 Band of H12C14N: I. Intensities, Self-broadening and Self-shift Coefficients"*; HITRAN Special Issue, J. Quant. Spectrosc. Radiat. Transfer, **82**, numbers 1-4, 2003.

Dinelli, B.M.; B. Carli, M. Carlotti, and J.Park, *"Stratospheric distribution of hydroxyl radical from far-IR emission spectra"*, Workshop on Tropospheric Ozone and Quadrennial Ozone Symposium, Abstracts, 156, 1988.

Ehhalt, D.H.; U. Schmidt, R. Zander, Ph. Demoulin, and C.P. Rinsland, *"Seasonal cycle and secular trend of the total and tropospheric column abundance of ethane above the Jungfraujoch"*, J. Geophys. Res., **96**, 4985–4994, 1991.

Esler, M.B.; D.W.T. Griffith, S.R. Wilson, and L.P. Steele, *"Carbon monoxide, nitrous oxide, methane and carbon dioxide - trace gas analysis by FTIR spectroscopy"*, in Baseline Atmospheric Program Australia 1994-1995, edited by R.J. Francey, A.L. Dick, and N. Derek, Bureau of Meteorology, CSIRO Division of Atmospheric Research, 1996.

Esler, M.B.; S.R. Wilson, D.W.T. Griffith, and L.P. Steele, *"Baseline trace gas monitoring using Fourier Transform Infrared (FTIR) spectroscopy"*, in Baseline 96, edited by R.J. Francey, CSIRO Bureau of Meteorology, Melbourne, 1998.

Fally, S.; P.-F. Coheur, M. Carleer, C. Clerbaux, R. Colin, A. Jenouvrier, M.-F. Mérienne, C. Hermans, and A.C. Vandaele, *"Water Vapor Line Broadening and Shifting by Air in the 26000 - 13000 cm^{-1} Region"*; HITRAN Special Issue, J. Quant. Spectrosc. Radiat. Transfer, **82**, numbers 1-4, 2003.

Farmer, C.B.; G.C. Toon, P.W. Schaper, J.F. Blavier, and L.L. Lowes, *"Stratospheric trace gases in the spring 1986 Antarctic atmosphere"*, Nature, **329**, 126–130, 1987.

Farmer, C.B. and R.H. Norton, *"Atlas of the Infrared Spectrum of the Sun and the Earth Atmosphere from Space"*, Volume I, NASA Reference Publication 1224, 1989.

Farmer, C.B. and R.H. Norton; *"A High-Resolution Atlas of the Infrared Spectrum of the Sun and Earth Atmosphere from Space"*. NASA Reference Pub. 1224, in two volumes (volume 3, see Geller et al., 1992) , 1216 pp., 1989.

Farmer, C.B.; B. Carli, A. Bonetti, M. Carlotti, B.M. Dinelli, H. Fast, W.F.J. Evans, N. Louisnard, C. Alamichel, W. Mankin, M. Coffey, I.G. Nolt, D.G. Murcray, A. Goldman, G.M. Stokes, D.U. Johnson, W.A. Traub, K.V. Chance, G. Roland, and L. Delbouille, *Balloon Intercomparison campaigns: results of remote sensing measurements of HCl"*, J. Atmos. Chem., **10**, 237–272, 1990.

Farmer, C.B.; L. Delbouille, G. Roland, C. Servais, *"The Solar Spectrum between 16 and 40 microns"*, Publication of the San Juan Capistrano Research Institute (San Juan Capistrano, California 92675): SJI TECH. REPORT 94-2., 83 pages, 1994.

Farmer, C.B.; *"The ATMOS Solar Atlas"*, Infrared Solar Physics, 511–521, 1994.

Fast, H. and W.F.J. Evans, *"Stratospheric profiles of HCl and CH_4 at 32^o N obtained on project stratoprobe from 1978 to 1985"*, Adv. Space. Res., **7**, 127–131, 1987.

Fast, H.; R.L. Mittermeier, and Y. Makino, *"Arctic Trace Gas Measurements in the Winter of 1996/97 with the SOlar Interferometer at Eureka, Canada"*, Atmospheric Ozone, Proc. Quad. Ozone Symp., Sapporo, Japan, R.D. Bojkov and K. Shibasaki eds., 367–368, 2000.

Fischer, J.; R.R. Gamache, A. Goldman, L.S. Rothman, and A. Perrin, *"Total Internal Partition Sums for Molecular Species in the 2000 Edition of the HITRAN Database"*; HITRAN Special Issue, J. Quant. Spectrosc. Radiat. Transfer, **82**, numbers 1-4, 2003.

Flaud, J.-M.; C. Camy-Peyret, V.M. Devi, C. Rinsland, and M.A.H. Smith, *"The ν_1 and ν_3 Volumes of $^{16}O^{18}O^{16}O$: Line positions and intensities"*, J. Mol. Spectrosc., **118**, 334–344, 1986.

Flaud, J.-M.; C. Camy-Peyret, J.W. Brault, C.P. Rinsland, and D. Cariolle, *"Nighttime and daytime variation of atmospheric NO_2 from groundbased infrared measurements*, Geophys. Res. Lett., **15**, 261–264, 1988.

Galle B.; Mellqvist J., D.W. Arlander, I. Floisand, M.P. Chipperfield and A.M. Lee. *"Ground Based FTIR Measurements of Stratospheric Trace Species from Harestua, Norway during SESAME and Comparison with a 3-D Model"*, J. Atmos. Chem., **32**, 147–164, 1999.

Galle, Bo; *"Development and Application of Methods based on DOAS and FTIR Absorption Spectroscopy for Atmospheric Research"*, PhD thesis, Chalmeers University, School of Physics and Engineering Physics, Department of Experimental Physics, Gothenburg, Sweden, 1999.

Galle, B.; J. Mellqvist, J. Samuelsson, S. Magnusson, M. Van Roozendael, C. Fayt, C. Hermans, F. Hendrick, M.P. Chipperfield and A. Bjerke, *"FTIR and UV-Visible Measurements of Stratospheric Trace Species at Harestua, Norway during THESEO and Comparison with a 3-D Model"*, in: Proceedings of the 5th European Workshop on Stratospheric Ozone, Saint Jean de Luz, France, 27 Sept.-1 Oct. 1999. Air Pollution Research Report 73, European Commission - DG XII, Brussels, 2000.

Galle B.; C. Oppenheimer, A. Geyer, A. McGonigle, and M. Edmonds, *"A miniaturised ultraviolet spectrometer for remote sensing of SO2 fluxes: a new tool for volcano surveillance"*, J. Volcanology, accepted, 2002.

Gallery, W.O.; F.X. Kneizys, and S.A. Clough, *"Air mass computer program for atmospheric transmittance/radiance calculation: FSCATM"*, US Air Force Geophys. Lab., Environmental Research Paper No.828, AFGL–TR–83–0065, 145, 1983.

Gamache R.R.; and A. Goldman, *"Einstein-A Coefficient, Integrated Band Intensity, and Population Factors Application to the a^1Dg - X^3Sg^- (0,0)O2 Band"*, J. Quant. Spectrosc. Radiat. Transfer, **69**, 389–401, 2001.

Geller, M.; *"A high–resolution atlas of the infrared spectrum of the sun and the earth atmosphere from space – Volume III: Key to identification of solar features"*, (volumes 1+2, see Farmer and Norton, 1989), JPL CalTech, NASA ref. publication 1224, Washington D.C., 1992.

Gillis, J.R.; A. Goldman, G. Stark, and C.P. Rinsland, "Line parameters for the A^2S - X^2P bands of OH," J. Quant. Spectrosc. Radiat. Transfer, **68**, 225–230, 2001.

Goldman, A.; F.J. Murcray, R.D. Blatherwick, and D.G. Murcray, *"Quantification of HCl from high-resolution, ground-based, infrared solar spectra in the 3000cm^{-1} region"*, J. Quant. Sepctrosc. Radiat. Transfer, **36**, 385–387, 1986.

Goldman, A.; F.J. Murcray, R.D. Blatherwick, and D.G. Murcray, *"Quantification of HCl from highresolution, groundbased, infrared solar spectra in the 3000 cm−1 region"*, J. Quant. Spectrosc. Radiat. Transfer, **36**, 385–387, 1986.

Goldman, A.; F.J. Murcray, F.H. Murcray, and D.G. Murcray, *"Quantification of HCl from highresolution infrared solar spectra obtained at the south pole in December 1986"*, Geophys. Res. Lett., **14**, 622–623, 1987.

Goldman, A.; F.J. Murcray, F.H. Murcray, D.G. Murcray, and C.P. Rinsland, *"Measurements of several atmospheric gases above the south pole in December 1986 from highresolution 34 micron solar spectra"*, J. Geophys. Res., **93**, 7069–7074, 1988.

Goldman, A.; F.J. Murcray, D.G. Murcray, J.J. Kosters, C.P. Rinsland, J.-M. Flaud, C. Camy-Peyret, and A. Barbe, *"Isotopic abundances of stratospheric ozone from ballone-borne high-resolution infrared solar spectra"*, J. Geophys. Res., **94**, 8467–8473, 1989.

Goldman, A.; F.J. Murcray, R.D. Blatherwick, J.J. Kosters, F.H. Murcray, D.G. Murcray, and C.P. Rinsland, *"New spectral features of stratospheric trace gases identified from high resolution infrared balloon-borne and laboratory spectra"*, J. Geophys. Res., **94**, 14945–19955, 1989.

Goldman, A.; F.J. Murcray, R.D. Blatherwick, J.J. Kosters, F.H. Murcray, D.G. Murcray, and C.P. Rinsland, *"New spectral features of stratospheric trace gases identified from high resolution infrared balloon-borne and laboratory spectra"*, J. Geophys. Res., **94**, 14945–19955, 1989.

Goldman, A.; F.J. Murcray, C.P. Rinsland, R.D. Blatherwick, S.J. David, F.H. Murcray, and D.G. Murcray, *"Mt. Pinatubo SO_2 column measurements from Mauna Loa"*, Geophys. Res. Lett., **19**, 183–186, 1992.

Goldman, A.; F.J. Murcray, R.D. Blatherwick, J.J. Kosters, D.G. Murcray, C.P. Rinsland, J.-M. Flaud, and C. Camy-Peyret, *"Stratospheric HNO_3 measurements from 0.002 cm^{-1} resolution solar occultation spectra and improved line parameters in the 5.8 μm region"*, J. Geophys. Res.-A, **97**, (D2), 2561–2567, 20 Feb 1992.

Goldman, A.; R.D. Blatherwick, F. J. Murcray, and D. G. Murcray, *"University of Denver infrared spectral atlases"*, Applied Optics, **35**, No. 16, 2821–2827, 1996.

Goldman, A.; W.G. Schönfeld, D. Groovitch, C. Chackerian, H. Dothe, F. Mélen, M. C. Abrams, and J. E. A. Selby, *"Updated line parameters for OH X2II-X2II (u,u) transitions"*, Journal of Spectroscopy and Radiative Transfer, **59**, No. 3-5, 453–469, 1998.

Goldman, A.; C. Paton-Walsh, W. Bell, G.C. Toon, B. Sen, J.R. Blavier, M.T. Coffey, J.W. Hannigan, and W.G. Mankin, *"Network for the Detection of Stratospheric Change (NDSC) FTIR Intercomparison at Table Mountain Facility, November 1996"*, J. Geophys. Res., **104**, 30481–30503, 1999.

Goldman, A.; M.T. Coffey, T.M. Stephen, C.P. Rinsland, W.G. Mankin, and J.W. Hannigan, *"Isotopic OCS in the Troposphere and Lower Stratosphere Determined from High Resolution Infrared Solar Absorption Spectra"*, J. Quant. Spectrosc. Radiat. Transfer, **67**, 447–456, 2000.

Goldman, A.; R.R. Gamache, A. Perrin, J.-M. Flaud, C.P. Rinsland, and L.S. Rothman, *"HITRAN Partition Functions and Weighted Transition-Moments Squared"*, J. Quant. Spectrosc. Radiat. Transfer, **66**, 455–486, 2000.

Goldman, A.; C.P. Rinsland, A. Perrin, J.-M. Flaud, A. Barbe, C. Camy-Peyret, M.T. Coffey, W.G. Mankin, J.W. Hannigan, T.M. Stephen, V. Malathy Devi, M.A.H. Smith, *"Weak Ozone Isotopic Absorption in the 5 μm Region from High Resolution FTIR Solar Spectra"*, J. Quant. Spectrosc. Radiat. Transfer, **74**, 133–138, 2002.

Goldman, A.; M.T. Coffey, J.W. Hannigan, W.G. Mankin, K.V. Chance, and C.P. Rinsland, *"HBr and HI Line Parameters Update for Atmospheric Spectroscopy Databases"*, HITRAN Special Issue, J. Quant. Spectrosc. Radiat. Transfer, **82**, numbers 1-4, 2003.

Goldman, A.; T.M. Stephen, L.S. Rothman, L.P. Giver, J.-Y. Mandin, R.R. Gamache, C.P. Rinsland, and F.J. Murcray *"The 1-μm CO2 Bands and the O2(0-1) X/g - a/g and (1-0) X/g - b/g Bands in the Earth Atmosphere,"* HITRAN Special Issue, J. Quant. Spectrosc. Radiat. Transfer, **82**, numbers 1-4, 2003.

Goorvitch, D.; *"Infrared CO line list for the $X^1\Sigma^+$ state"*, The Astrophysical Journal Supplement Series, **95**, 535–552, 1994.

Goutail, F. and J.P. Pommereau, *"O4 and H2O atmospheric absorption measurements in the visible during the GLOBUS NOx campaign"*, Workshop on Tropospheric Ozone and Quadrennial Ozone Symposium, Abstracts, 161, 1988.

Gray, D.F.; *"The observation and analysis of stellar photospheres"*, Cambridge Univ. Press, 1992.

Griffith, D.W.T.; *"Synthetic calibration and quantitative analysis of gas phase infrared spectra"*, Appl. Spectrosc., **50**, 59–70, 1996.

Griffith, D.W.T.; N.B. Jones, and W.A. Matthews, *"Interhemispheric ratio and annual cycle of carbonyl sulfide (OCS) total column from ground based solar FTIR spectra"*, J. Geophys. Res., **103** (D7), 8447–8454, 1998.

Griffith, D.W.T.; G.C. Toon, B. Sen, and J.-F. Blavier, *"Vertical profiles of nitrous oxide isotopomer fractionation measured in the stratosphere"*, Geophysical Research Letters, **27**(16), 2485–2488, 2000.

Griffith, D.W.T.; N.B. Jones, B. McNamara, C. Paton-Walsh, W. Bell, and C. Bernardo, *"Intercomparison of ground-based solar FTIR measurements of atmospheric trace gases at Lauder"*, New Zealand, J. Ocean. Atmos. Tech., **20**(8), 1138–1153, 2003.

Gunson, M.R.; C.B. Farmer, R.H. Norton, R. Zander, C.P. Rinsland, J.H. Shaw, and B.-C. Gao, *"Measurements of CH_4, N_2O, CO, H_2O, and O_3 in the middle atmosphere by the atmospheric trace molecule spectroscopy experiment on Spacelab 3"*, J. Geophys. Res., **95**, 13867–13882, 1990.

Gunson, M.R.; M.M. Abbas, M.C. Abrams, M. Allen, L.R. Brown, T.L. Brown, A.Y. Chang, A. Goldman, F.W. Irion, L.L. Lowes, E. Mahieu, G.L. Manney, H.A. Michelsen, M.J. Newchurch, C.P. Rinsland, R.J. Salawitch, G.P. Stiller, G.C. Toon, Y. L. Yung, and R. Zander, *"The Atmospheric Trace Molecule Spectroscopy (ATMOS) experiment : deployment on the ATLAS Space Shuttle missions"*, Geophys. Res. Lett., **23**, 2333–2336, 1996.

Guo, J.; M.M. Abbas, and I.G. Nolt, *"Stratospheric $H_2^{18}O$ distribution from far infrared observations"*, Geophys. Res. Lett., **16**, 1989.

Hamdouni, A.; A. Barbe, P. Demoulin and R. Zander, *"Retrieval of ozone vertical column amounts from ground-based high resolution infrared solar spectra"*, J. Quant. Spectrosc. Radiat. Transfer, **57**, 11–22, 1997.

Hannigan, J.W.; M.T. Coffey, W.G. Mankin, A. Goldman, *"Column Observations of HNO3, N2O, HF, HCl, O3 at Sondre Stromfjord, Greenland During Winter 1994-'95"*, J. Atmos. Chem., **30**, 103–118, 1998.

Hase, F., T. Blumenstock, C. Paton-Walsh, *"Analysis of the instrumental line shape of high-resolution Fourier transform IR spectrometers with gas cell measurements and new retrieval software"*, Appl. Opt., **38**, 3417–3422, 1999.

Hase, F. and M. Höpfner, *"Atmospheric raypath modelling for radiative transfer algorithms"*, Appl. Opt., **38**, 3129–3133, 1999.

Hase, F.: *"Inversion von Spurengasprofilen aus hochaufgelösten bodengebundenen FTIR-Messungen in Absorption"*, Dissertation, FZK Report No. 6512, Forschungszentrum Karlsruhe, Germany, 2000.

Hase, F.; T. Blumenstock, H. Fischer, M. Höpfner, P. Thomas, A. Meier, A. Steen, Y. Kondo, *"Profiles of O3, HCl, and HF as retrieved from ground-based FTIR spectra recorded at Kiruna (Sweden) during winter 1997/98"*, Proceedings of the Fifth European Workshop on Polar Stratospheric Ozone, St. Jean Du Luz 1999, European Commission - Air pollution research report 73, 244–247, 2000.

Hurst, D.F.; D.W.T. Griffith, and G.D. Cook, *"Trace gas emissions from biomass burning in tropical Australian savannas"*, Journal of Geophysical Research, **99** (D8), 16441–16456, 1994.

Hurst, D.F.; D.W.T. Griffith, and G.D. Cook, *"Trace gas emissions from biomass burning in Australia, in Biomass Burning and Global Change, 2, Biomass Burning in South America, Southeast Asia, and Temperate and Boreal Ecosystems, and the Kuwait Oil Fires"*, edited by J.S. Levine, pp. 377, MIT Press, Cambridge, MA, 1996.

Höpfner, M., T. Blumenstock, F. Hase, A. Zimmermann, H. Flentje, S. Flueglistaler, *"Mountain polar stratospheric cloud measurement by ground-based FTIR solar absorption spectroscopy"*, Geophys. Res. Lett., **28**, 2189–2192, 2001.

Inngold, T.; B. Schmid, C. Mätzler, P. Demoulin, and N. Kämpfer, *"Modeled and empirical approaches for retrieving columnar water vapor from solar transmittance measurements in the 0.72, 0.82 and 0.94 μm absorption bands"*, J. Geophys. Res., **105**, 24327–24343, 2000.

Irion, F.W.; M. Brown, G.C. Toon, and M.R. Gunson, *"Increase in atmospheric CHF_2Cl (HCFC-22) over southern California from 1985-1990"*, Geophys. Res. Lett., **21**, 1723–1726, 1994.

Irion, F.W.; E.J. Moyer, M.R. Gunson, C.P. Rinsland, H.A. Michelsen, R.J. Salawitch, Y. L. Yung, A.Y. Chang, M .J. Newchurch, M.M. Abbas, M.C. Abrams, and R. Zander, *"Stratospheric observations of CH3D and HDO from ATMOS infrared solar spectra: enrichments of deuterium in methane and implications for HD"*, Geophys. Res. Lett., **23**, 2381–2384, 1996.

Irion, F.W.; M.R. Gunson, C.P. Rinsland, Y.L. Yung, M.C. Abrams, A.Y. Chang, and A. Goldman, *"Heavy ozone enrichment from ATMOS infrared solar spectra"*, Geophys. Res. Lett., **23**, 2377–2380, 1996.

Irion, F.W.; M.R. Gunson, G.C. Toon, L.R. Brown , A.Y. Chang, A. Eldering, E. Mahieu, G.L. Manney, H.A. Michelsen, E.J. Moyer, M.J. Newchurch, G.B. Osterman, C.P. Rinsland, R.J. Salawitch, B. Sen, Y. L. Yung, and R. Zander, *"The Atmospheric Trace Molecule Spectroscopy Experiment (ATMOS) version 3 data retrievals"*, Appl. Opt., **41** (33), 6968–6979, 2002.

Jacquemart, D.; J.-Y. Mandin, V. Dana, C. Claveau, J. Vander Auwera, M. Herman, L.S. Rothman, L. Régalia-Jarlot, and A. Barbe, *"The IR Acetylene Spectrum in HITRAN: Update and New Results"*, HITRAN Special Issue, J. Quant. Spectrosc. Radiat. Transfer, **82**, numbers 1-4, 2003.

Jacquinet-Husson, N.; E. Arié, A. Barbe, L.R. Brown, B. Bonnet, C. Camy-Peyret, J.P. Champion, A. Chédin, A. Chursin, C. Clerbaux, G. Duxbury, J.-M. Flaud, N. Fourrié, A. Fayt, G. Graner, R.R. Gamache, A. Goldman, Vl. Golovko, G. Guelachvilli, J.M. Hartmann, J.C. Hillico, G. Lefèvre, O.V.

Naumenko, V. Nemtchinov, D.A. Newnham, A. Nikitin, J. Orphal, A. Perrin, D.C. Reuter, L. Rosenmann, L.S. Rothman, N.A. Scott, J.E. Selby, L.N. Sinitsa, J.M. Sirota, A. Smith, K. Smith, R.H. Tipping, Vl.G. Tyuterev, S. Urban, P. Varanasi, and M. Weber, *"The 1997 Spectroscopic GEISA Databank"*, J. Quant. Spectrosc. Radiat. Transfer, **62**, 205–254, 1999.

Jaramillo, M.; R.L. de Zafra, J.W. Barrett, A. Parrish, and P.M. Solomon, *"MM-wave observations of stratospheric HCN at tropical latitudes"*, Geophys. Res. Lett., **15**, 265–268, 1988.

Jaramillo, M.; R.L. de Zafra, J. Barrett, L.K. Emmons, P.M. Solomon, and A. Parrish, *"A measured mixing ratio profile for HCN over McMurdo station during the Antarctic spring"*, Workshop on Tropospheric Ozone and Quadrennial Ozone Symposium, Abstracts, 69, 1988.

Jaramillo, M.; R.L. de Zafra, J. Barrett, and L.K. Emmons, *"Measurements of hydrogen cyanide as a tracer at stratospheric transport"*, Antarctic, J., xxiii, 158–159, 1988.

Johnston, P. V.; R.L. McKenzie; J.G. Keys, W.A. Matthews, *"Observations of depleted stratospheric NO2 following the Pinatubo volcanic eruption"*, Geophys. Res. Lett., **19**, 211–213, 1992.

Jones, N.B.; M. Koike, W.A. Matthews, and B.M. McNamara, *"Southern hemisphere mid-latitude seasonal cycle in total column nitric acid"*, Geophys. Res. Lett., **21**, 593–596, 1994.

Jones, N.B.; C.P. Rinsland, J. B. Liley, and J.M. Rosen, *"Correlation of Aerosol and Carbon Monoxide at $45^o S$, Evidence of Biomass burning Emissions"*, Geophys. Res. Lett., **28**, 709–712, 2001.

Karcher, F.; M. Amodei, G. Armand, C. Besson, B. Dufour, G. Froment, and J.P. Meyer, *"Simultaneous measurements of stratospheric HNO_3, NO_2, HCl, O_3, N_2O, CH_4, H_2O and CO from the STRATOZ3 flights"*, Workshop on Tropospheric Ozone and Quadrennial Ozone Symposium, Abstracts, 165, 1988.

Kaye, J.A.; A.R. Douglas, C.H. Jackman, R.S. Stolarski, R. Zander, and G. Roland, *"Two-dimensional model calculations of fluorine-containing reservoir species in the stratosphere"*, J. Geophys. Res., **96**, 12865–12881, 1991.

Kerr, J.B.; and W.F.J. Evans, *"Brewer spectrophotometer measurements in the Canadian Arctic"*, Polar Ozone Workshop, Session VII, May 1988.

Kerr, J.B.; *" Ground based measurements of nitrogen dioxide using the brewer spectrophotometer"*, Workshop on Tropospheric Ozone and Quadrennial Ozone Symposium, Abstracts, 163, 1988.

Kerridge, B.J. and H.K. Roscoe, *"Balloon-borne IR emission measurements of stratospheric nitrigen oxides and aerosol"*, Workshop on Tropospheric Ozone and Quadrennial Ozone Symposium, Abstracts, 152, 1988.

Keys, J.G.; and P.V. Johnston, *"Stratospheric column NO_2 measurements from three Antarctic sites"*, Polar Ozone Workshop, Session IV, May 1988.

Keys, J.G. and B.G. Gardiner, *"NO2 overnight decay and layer height at Halley Bay, Antarctica"*, Geophys. Res. Lett., **18**, 665–668, 1991.

Keys, J.G.; P.V. Johnston, R.D. Blatherwick, and F.J. Murcray, *"Evidence of heterogeneous reactions involving nitrogen compounds in the Antarctic stratosphere"*, Nature, **361**, 49–51, 1993.

Keys, J.G.; S.W. Wood, X. Liu, F.J. Murcray, and R.L. de Zafra, *"Partitioning of stratospheric chlorine during Antarctic spring as seen from ground-based infrared solar absorption and microwave observations"*, in Proceedings of the XVIII Quadrennial Ozone Symposium, L'Aquila, Italy, L'Aquila, Italy, accepted 1997.

Keys, J.G.; S.W. Wood, N.B. Jones, and F.J. Murcray, *"Spectral Measurements of HCl in the plume of the Antarctic volcano Mount Erebus"*, Geophys. Res. Lett., **25**, 2421–2424, 1998.

Kilston, S.; *"N-type carbon stars and the 3-alpha process"*, Pub. Astron. Soc. Pacific, **87**, 189–206, 1975.

Kleiner, I.; G. Tarrago, C. Cottaz, L. Sagui, L.R. Brown, R.L. Poynter, H.M. Pickett, P. Chen, J.C. Pearson, R.L. Sams, G.A. Blake, S. Matsuura, V. Nemtchinov, P. Varanasi, L. Fusina, and G. DiLonardo; *"NH3 and PH3 Line Parameters: 2000 HITRAN Update and New Results"*, HITRAN Special Issue, J. Quant. Spectrosc. Radiat. Transfer, **82**, numbers 1-4, 2003.

Koike, M.; N.B. Jones, W.A. Matthews, P.V. Johnston, R.L. McKenzie, D. Kinnison, and J. Rodriguez, *"Impact of Pinatubo aerosols on the partitioning between NO_2 and HNO_3*, Geophys. Res. Lett., **21**, 597–600, 1994.

Kondo, U.; et al, *"NOy correlation with N2O and CH4 in the midlatitude stratosphere"*, Geophys. Res. Lett., **23**, 2369–2372, 1996.

Kreher, K.; J.G. Keys, P.V. Johnston, U. Platt, and X. Liu, *"Ground-based measurements of OClO and HCl in austral spring 1993 at Arrival Heights, Antarctica"*, Geophys. Res. Lett., **23**, 1545–1548, 1996.

Kreher, K.; P.V. Johnston, S.W. Wood, B. Nardi, and U. Platt, *"Ground-based measurements of tropospheric and stratospheric BrO at Arrival Heights (78^{o}S), Antarctica"*, Geophys. Res. Lett., **24**, 3021–3024, 1997.

Kreher, K.; P.V. Johnston, S.W. Wood, and J.G. Keys, *"Ground-based observations of OClO, BrO and NO2 during 1995 at Arrival Heights (77.8^{o}S) Antarctica"*, in Proceedings of the XVIII Quadrennial Ozone Symposium, L'Aquila, Italy, L'Aquila, Italy, accepted 1997.

Kreher, K.; T. Wagner, U. Friess, U. Platt, S.W. Wood, P.V. Johnston, and B. Nardi, *"Observation of enhanced tropospheric bromine oxide in the Antarctic"*, in International Symposium on Atmospheric Chemistry and Future Global Environment, Nagoya, Japan, 78–81, 1997.

Kunde, V.G.; J.C. Brasunas, B.J. Conrath, R.A. Hanel, J.R. Herman, D.E. Jennings, W.C. Maguire, D.W. Walser, J.N. Annen, M.J. Silverstein, M.M. Abbas, L.H. Herath, H.L. Buijs, J.N. Berube, and J. McKinnon, *"Infrared spectroscopy of the lower stratosphere with a balloonborne cryogenic Fourier spectrometer"*, Appl. Opt., **26**, 545–553, 1987.

Kunde, V.G.; J.C. Brasunas, W.C. Maquire, J.R. Herman, S.T. Massie, M.M. Abbas, L.W. Herath, and W.A. Shaffer, *"Measurement of nighttime stratospheric N_2O_5 from infrared emission spectra"*, Geophys. Res. Lett., **15**, 1177–1180, 1988.

Kurucz, Robert L.; *"Electronic version of the ATMOS solar spectra reported by Farmer and Norton, 1989"*, reduced from 20 tapes and cleared from instrumental and background features; http://kurucz. harvard.edu/sun/ATMOS/, 2002.

Kurylo, M.J. and R. Zander, *"The NDSC-Its status after ten years of operation"*, in Proceedings of the "International Quadrennial Ozone Symposium", Sapporo, Japan, July 3-8, 2000, 167–168, 2000.

Kwabia Tchana, F.; J. Orphal, I. Kleiner, B. Redlich, D. Scheffler, R. Mbiake, and O. Bouba, *"The n2 band of BrNO2 around 792 cm-1 (12.7 mm)"*, J. Molec. Spectrosc., **216**, 292–296, 2002.

Leuning, R.; O.T. Denmead, D.W.T. Griffith, I.M. Jamie, P. Issacs, J. Hacker, C.P. Meyer, I.E. Galbally, H.A. Cleugh, M.R. Raupach, and M.B. Esler, *"Assessing biogenic sources and sinks of greenhouse gases at three interlinking scales"*, CSIRO Land & Water, Canberra, 1997.

Li, Q.; D.J. Jacob, I. Bey, R.M. Yantosca, Y. Zhao, Y. Kondo, J. Notholt, *"Atmospheric Hydrogen Cyanide (HCN): Biomass burning source, ocean sink?"* Geophys. Res. Lett., **27**, 357–360, 2000.

Liley, J.B.; J.M. Rosen, N.T. Kjome, N.B. Jones, and C.P. Rinsland, *"Springtime Enhancement of upper Tropospheric Aerosol at 45^{o}S"*, Geophys. Res. Lett., **28**, 1495–1498, 2001.

Liu, X.; R.D. Blatherwick, F.J. Murcray, J.G. Keys, and S. Solomon, *"Measurements and model calculations of HCl column amounts and related parameters over McMurdo during the austral spring in 1989"*, J. Geophys. Res., **97**, 20795–20804, 1992.

Liu, X.; and F.J. Murcary, *"N2O Vertical Profiles Retrieved From Ground-based Solar Absorption Taken at McMurdo Station During Austral Spring of 1989"*, Optical Remote Sensing of the Atmosphere, 6th Topical Meeting, Salt Lake City, Feb 6-10, 1995.

Liu, X.; and F.J. Murcary, *"Comparison Between the HALOE Measured HF and HCl VMR Profiles and the Profiles Obtained From Ground-based Very High Resolution FTIR Solar Spectra"*, J. Geophys. Res., **101**, 10175–10181, 1996.

Liu, X.; R. Blatherwick and F. J Murcray, *"Determination of a FTIR Instrument Line Shape Function from O3 3V3 lines Using Ozone Sondes for Improved Retrieval of HCl Altitude Profiles"*, supplement to Eos, **77**(46), F121(A42A-3), 1996.

Liu, X.; et al., *"Comparison of HF and HCl vertical profiles from ground-based high-resolution infrared solar spectra with Halogen Occultation Experiment observations"*, J. Geophys. Res., **101**, 10175–10181, 1996.

Livingston, W.; and L. Wallace *"An Atlas of the Solar Spectrum in the Infrared from 1850 to 9000 cm^{-1} (1.1 to 5.4 microns)"* (N.S.O. Technical Report #91-001, July 1991.

Mélen, F.; E. Mahieu, R. Zander, C.P. Rinsland, P. Demoulin, G. Roland, L. Delbouille, and C. Servais, *"Vertical column abundances of COF2 above the Jungfraujoch station derived from ground-based infrared solar observations"*, J. Atmos. Chem., **29**, 119–134, 1998.

Mélen, F.; N. Grevesse, L. Delbouille, G. Roland, Ch. Servais, A. J. Sauval, and C. B Farmer, *"A new analysis of the OH radical spectrum from solar infrared observations"*, in Proceedings of the Workshop on "Laboratory and Astronomical High Resolution Spectra", Brussels, August 29 - September 2, 1994, A.J. Sauval, R. Blomme, and N. Grevesse Eds., ASP Conference Series, **81**, 320–321, 1995.

Mérienne, M.-F.; A. Jenouvrier, C. Hermans, A.C. Vandaele, M. Carleer, C. Clerbaux, P.-F. Coheur, R. Colin, S. Fally, and M. Bach, *"Water Vapor Line Parameters in the 13000 - 9250 cm^{-1} Region"*, HITRAN Special Issue, J. Quant. Spectrosc. Radiat. Transfer, **82**, numbers 1-4, 2003.

Mahieu, E.; R. Zander, and P. Demoulin, *"Infrared remote monitoring of the vertical column abundance of CO above the Jungfraujoch between 1984 and 1993"*, Report (No. 98) of the WMO meeting of experts on global carbon monoxide measurements, Boulder, USA, February 7-11, 1994, WMO/TD-NO. 645, 52–55, 1994.

Mahieu, E.; C.P. Rinsland, R. Zander, P. Demoulin, L. Delbouille, and G. Roland, *"Vertical Column Abundances of HCN deduced from Ground-Based Infrared Solar Spectra: Long-Term Trend and Variability"*, J. Atmos. Chem., **20**, 299–310, 1995.

Mahieu, E.; R. Zander, M.R. Gunson, G.C. Toon, C.P. Rinsland, and P. Demoulin, *"Evaluation of the lifetime of SF6 in the Earth's atmosphere, based on ATMOS and Jungfraujoch IR solar observations, in Proceedings of "Atmospheric Spectroscopy Applications, ASA 96"*, Reims, September 4-6, 1996, 125–128, 1996.

Mahieu, E.; R. Zander, L. Delbouille, P. Demoulin, G. Roland and C. Servais, *"Observed Trends in Total Vertical Column Abundances of Atmospheric Gases from IR Solar Spectra Recorded at the Jungfraujoch"*, J. Atmos. Chem., **28**, 227–243, 1997.

Mahieu, E.; R. Zander, F. Mélen, P. Demoulin, C. Servais, L. Delbouille, and G. Roland, *"Recent Characteristic Budget of Inorganic Chlorine and Fluorine above the Jungfraujoch Station"*, in Proceedings of the Fourth European Symposium on Polar Stratospheric Ozone Research, Schliersee, Germany, September 22-26, 1997. European Commission, Air pollution research report **66**: 358–361, 1998.

Mahieu, E.; R. Zander, F. Mélen, P. Demoulin, C.P. Rinsland, and J.M. Russel-III, *"Monitoring the stratospheric chlorine budget during the past decades: the Montreal Protocol at work"*, in Proceedings of the International Quadrennial Ozone Symposium, Sapporo, Japan, 3-8 July 2000: 149–150, 2000.

Mahieu, E.; R. Zander, P. Demoulin, M. De Mazière, F. Mélen, C. Servais, G. Roland, L. Delbouille, J. Poels, and R. Blomme, *"Fifteen years-trend characteristics of key stratospheric constituents monitored by FTIR above the Jungfraujoch"*, in Proceedings of the Fifth European Symposium on Stratospheric Ozone, St. Jean de Luz, France, September 27-October 1, 1999. N. R. P. Harris, M. Guirlet and G. T. Amanatidis (Eds). Air pollution Research Report **73** - EUR 19340: 99-102, 2000.

Mahieu, E.; C.P. Rinsland, R. Zander, P. Duchatelet, C. Servais, and M. De Mazière, *"Tropospheric and stratospheric carbonyl sulphide (OCS): long-term trends and seasonal cycles above the Jungfraujoch station"*, in Proceedings of the "Sixth European Symposium on Stratospheric Ozone", Göteborg, Sweden, September 2-6, 2002.

Makino, Y.; H. Fast, R.L. Mittermeier, T. Sasaki, Y. Sawa, M. Hirota, and K. Kondo Miyagawa, *"IR-spectroscopic measurements of stratospheric minor constitutents over Tsukuba, Japan and Eurkea, Canadian Arctic"*, Atmospheric Ozone, Proc. Quad. Ozone Symp., Sapporo, Japan, R.D. Bojkov and K. Shibasaki eds., 531–532, 2000.

Mankin, W.G.; *"Airborne Fourier transform spectroscopy of the upper atmosphere"*, Opt. Engr., **17**, 39–43, 1978.

Mankin, W.G. and M.T. Coffey, *"Airborne observations of chemical constituents in the Antarctic winter stratosphere"*, Workshop on Tropospheric Ozone and Quadrennial Ozone Symposium, Abstracts, 54, 1988.

Mankin, W.G. and M.T. Coffey, *"Infrared measurements of column amounts of stratospheric constituents in the Antarctic winter"*, 1987, Polar Ozone Workshop, Session IV, May 1988.

Mankin, W.G.; M.T. Coffey, A. Goldman, M.R. Schoebrel, L.R. Lait, and P.A. Newman, *"Airborne measurements of stratospheric constituents over the arctic in the winter of 1989"*, Geophys. Res. Lett., **17**, 473–476, 1990.

Mankin, W.G.; M.T. Coffey, K.V. Chance, W.A. Traub, B. Carli, F. Mencaraglia, S. Piccioli, I.G. Nolt, J.V. Radostitz, R. Zander, G. Roland, D.W. Johnson, G.M. Stokes, C.B. Farmer, and R.K. Seals, *"Intercomparison of measurements of stratospheric hydrogen fluoride"*, J. Atmos. Chem., **10**, 219–236, 1990.

Massie, S.T.; J.A. Davidson, C.A. Cantrell, A.H. McDaniel, J.C. Gille, V.G. Kunde, J.C. Brasunas, B.J. Conrath, W.C. Maguire, A. Goldman, and M.M. Abbas, *"Atmospheric infrared emission of $ClONO_2$ observed by a balloonborne Fourier spectrometer"*, J. Geophys. Res., **92**, 14806–14814, 1987.

Massie, S.T. and A. Goldman, *"The Infrared Absorption Cross-section and Refractive-Index Data in HITRAN"*, HITRAN Special Issue, J. Quant. Spectrosc. Radiat. Transfer, **82**, numbers 1-4, 2003.

Matthews, W.A.; P.V. Johnston, D.G. Murcray, F.H. Murcray, and R.D. Blatherwick, *"Column abundance of hydrogen chloride above Lauder, New Zealand"*, in *Ozone in the Atmosphere*, 359–362, A. Deepak,Publishing, Hampton, VA, 1989.

May, R.D. and C.R. Webster, *"In-situ stratospheric measurements of HNO_3 and HCl near 30 km using the BLISS tunable laser spectrometer"*, J. Geophys. Res., **94**, 16343–16350, 1989.

McElroy, C.T.; A. Goldman, and D.G. Murcray, *"Tunable diode laser heterodyne spectrophotometry of ozone"*, Workshop on Tropospheric Ozone and Quadrennial Ozone Symposium, Abstracts, 247, 1988.

McElroy, C.T.; A. Goldman, and D.G. Murcray, *"Heterodyne spectrophotometry of ozone in the 9.6 micron band using a tunable diode laser"*, J. Geophys. Res., **95**, 5567–5575, 1990.

McKenzie, R.L.; W.A. Matthews, Y. Kondo, R. Zander, Ph. Demoulin, P. Fabian, D.G. Murcray, F.J. Murcray, O. Lado-Bordowsky, C. Camy-Peyret, H.K. Roscoe, J. A. Pyle, and R. D. McPeters, *"Intercomparison of NO column measurements during MAP/GLOBUS 1985"*, J. Atmos. Chem., **7**, 353–367, 1988.

Meier, A. and J. Notholt, *"Determination of the isotopic abundances of heavy ozone as observed in arctic ground–based FTIR–spectra"*, Geophys. Res. Lett., **23**, 551–554, 1996.

Meier, A.; *"Determination of atmospheric trace gas amounts and corresponding natural isotopic ratios by means of ground–based FTIR spectroscopy in the high arctic"*, AWI Verlag, 309 pp., Reports on Polar Research series, Vol. **236**, ISSN 0176-5027, 1997.

Meier, A.; T. Blumenstock, H. Nakajima, *"Regular isotopic observations of stratospheric ozone and its implication for the ozone formation theory"*, Proceedings of the Fourth European Workshop on Polar Stratospheric Ozone, Schliersee 1997, European Commission - Air pollution research report **66**, 216–219, 1998.

Meier, A.; A. Goldman, P.S. Manning, T.M. Stephen, C.P. Rinsland, N.B. Jones, and S.W. Wood, *"Improvements to Air Mass calculations for Ground-Based Infrared Measurements"*, J. Quant. Spectrosc. Radiat. Transfer, **83**, Electronic Supplement (full report), http://www.uow.edu.au/science/research/acrg/staff/fscatmf.pdf, 2003.

Meier, A.; A. Goldman, P.S. Manning, T.M. Stephen, C.P. Rinsland, N.B. Jones, and S.W. Wood, *"Improvements to Air Mass calculations for Ground-Based Infrared Measurements"*, J. Quant. Spectrosc. Radiat. Transfer, **83**, 109–113, (Summary Note), 2004.

Melen, F.; A.J. Sauval, N.Grevesse, C.B. Farmer, C. Servais, L. Delbouille, G. Roland, *"A New Analysis of the OH Radical Spectrum from Solar Infrared Observations"*, J.Mol.Spectroscopy, **174**, 490–509, 1995.

Mellqvist, J.; B. Galle and X. Liu, *"Retrieval of Height Information of Stratospheric Species from FTIR Spectra Measured in Norway During SESAME, XVII-Quadrennial ozone symposium"*, L'Aquila, Italy, 12-21, Nov., 1996.

Mellqvist, Johan; *"Application of Infrared and UV-Visible Remote Sensing Techniques for Studying the Stratosphere and for Estimating Antrophogenic Emissions"*, PhD thesis, Chalmeers University, School of Physics and Engineering Physics, Department of Experimental Physics, Gothenburg, Sweden, 1999.

Mellqvist, J; B. Galle and Strandberg, A., *"Groundbased FTIR measurements at Harestua Norway between 1996- 2001"*, NDSC 2001 Symposium celebrating 10 years of atmospheric research, 24-27 Sept. 2001, Arachon, France, 2001.

Mellqvist, J.; B. Galle, T. Blumenstock, F. Hase, D. Yaschov, J. Notholt, B. Sen, G.C. Toon, and M. Chipperfield, *"Ground-based FTIR observations of chlorine activation and ozone depletion inside the Arctic vortex during the winter of 1999/2000"*, J. Geophys. Res., **107**(D20), doi:10.1029/2001 JD001080, 2002.

Michelsen, H.A.; G.L. Manney, M.R. Gunson, C.P. Rinsland, and R. Zander, *"Correlations of stratospheric abundances of CH4 and N2O derived from ATMOS measurements"*, Geophys. Res. Lett., **25**, 2777–2780, 1998.

Michelsen, H.A.; G.L. Manney, M.R. Gunson, and R. Zander, *"Correlations of stratospheric abundances of NOy, O3, N2O and CH4 derived from ATMOS measurements"*, J.Geophys. Res., **103**, 28347–28359, 1998.

Mikhailenko, S.; A. Barbe, and V.G. Tyuterev, *"Extended Analysis of Line Positions and Intensities of Ozone Bands in the 2900-3400 cm^{-1} Region"*, J. Mol. Spectrosc., **215**, 29–41, 2002.

Mikhailenko, S.; Y. Babikov, V.G. Tyuterev, and A. Barbe, *"The DataBank of Ozone Spectroscopy on WEB (S&MPO)"*, Computational Technologies, **7**, 64–70, (in Russian), 2002.

Minnaert, M.; *"Die Profile der äußeren Teile der starken Fraunhoferschen Linien"*, Zeitschrift für Astrophysik, **10**, 40–51, 1935.

Mount, G. H.; R.W. Sanders, A.L. Schmeltekopf, and S. Solomon, *"Visible spectroscopy at McMurdo station, Antarctica, 1. overview and daily variations of NO_2 and O_3, Austral spring, 1986"*, J. Geophys. Res., **92**, 8320–8328, 1987.

Mount, G. H.; R.W. Sanders, R.O. Jakoubek, A.L. Schmeltekopf, and S. Solomon, *"Visible and near-ultraviolet spectroscopy at Thule AFB (76.5cm^{-1}N) from January 28 - February 15"*, 1988, Polar Ozone Workshop, Session VII, May 1988.

Murata, I.; Y. Kondo, H. Nakajima, M. Koike, Y. Zhao, W.A. Matthews, and K. Suzuki, *"Accuracy of total ozone columns observed with infrared solar spectroscopy"*, Geophys. Res. Lett., **24**, 77–80, 1997.

Murcray, D.G.; A. Goldman, J. Kosters, R. Zander, W. Evans, N. Louisnard, G. Alamichel, M. Bangham, S. Pollitt, B. Carli, B. Dinelli, S. Piccioli, A. Volboni, W. Traub, and K. Chance, *"Intercomparison of stratospheric water vapor profiles obtained during the balloon intercomparison campaign"*, J. Atmos. Chem., **10**, 159–179, 1990.

Murcray, F.J.; F.H. Murcray, A. Goldman, D.G. Murcray, and C.P. Rinsland, *"Infrared measurements of several nitrogen species above the south pole in December 1980 and November/December 1986"*, J. Geophys. Res., **92**, 13373–13376, 1987.

Murcray, F.J.; D.G. Murcray, A. Goldman, J.G. Keys, and W.A. Matthews, *"Infrared measurements in the spring 1987 ozone hole"*, Polar Ozone Workshop, Session IV, May 1988.

Murcray, F.J.; A. Goldman, R. Blatherwick, A. Matthews, and N. Jones, *"HNO_3 and HCl amounts over McMurdo during the spring of 1987"*, J. Geophys. Res., **94**, 16615–16618, 1989.

Murcray, F.J.; J.R. Starkey; W.J. Williams, W.A. Matthews, U. Schmidt, P. Aimedieu, C. Camy-Peyret, *"HNO3 profiles obtained during the EASOE campaign"*, Geophys. Res. Lett., **21**, 1223–1226, 1994.

Nakajima, H.; X. Liu, I. Murata, Y. Kondo, F.J. Murcray, M. Koike, Y. Zhao, and H. Nakane, *"Retrieval of vertical profiles of ozone from high resolution infrared solar spectra at Rikubetsu, Japan"*, J. Geophys. Res., **102**, 29981–29990, 1997.

Nemtchinov, Vassilii and Prasad Varanasi, *"Thermal Infrared Absorption Cross-sections of CCl4 Needed for Atmospheric Remote Sensing"*, HITRAN Special Issue, J. Quant. Spectrosc. Radiat. Transfer, **82**, numbers 1-4, 2003.

Nemtchinov, Vassilii and Prasad Varanasi, *"Thermal Infrared Absorption Cross-sections of CF4 for Atmospheric Applications"*, HITRAN Special Issue, J. Quant. Spectrosc. Radiat. Transfer, **82**, numbers 1-4, 2003.

Newchurch, M.J.; M. Allen, M.R. Gunson, R.J. Salawitch, G.B. Collins, K. H. Huston, M.M. Abbas, M.C. Abrams, A.Y. Chang, D.W. Fahey, R. S. Gao, F.W. Irion, M. Loewenstein, G. L. Manney, H.A. Michelsen, J. R. Podolske, C.P. Rinsland, and R. Zander, *"Stratospheric NO and NO2 abundances from ATMOS solar-occultation measurements"*, Geophys. Res. Lett., **23**, 2373–2376, 1996.

Nikitin, A.; J.-P. Champion, and V.G. Tyuterev, *"The MIRS Computer Package for Modeling the Rovibrational Spectra of Polyatomic Molecules"*, HITRAN Special Issue, J. Quant. Spectrosc. Radiat. Transfer, **82**, numbers 1-4, 2003.

Norton, R.H. and C.P. Rinsland, *"ATMOS data processing and science analysis methods"*, Appl. Opt., **30**, 389–400, 1991.

Notholt, J.; F. Cappellani, H. Roesdahl, G. Restelli, *"Absolute infrared band intensities and air broadening coefficient for spectroscopic measurements of formic acid in air"*, Spectrochim. Acta A, **47**A, No. 3/4, 477–483, 1991.

Notholt, J.; R. Neuber, O. Schrems, and T.v. Clarmann, *"Stratospheric trace gas concentrations in the Arctic polar night derived by FTIR–spectroscopy with the moon as light source"*, Geophys. Res. Lett., **20**, 2059–2062, 1993.

Notholt, J.; O. Schrems, *"Ground-based FTIR measurements of vertical column densities of several trace gases above Spitzbergen"*, Geophys. Res. Letters, **21**, 1355–1358, 1994.

Notholt, J.; T.v. Clarmann, G.P. Adrian, O. Schrems, *"Ground-based FTIR measurements of ClONO2 column amounts in the Arctic"*, Geophys. Res. Letters, **21**, 1359–1362, 1994.

Notholt, J.; *"FTIR measurements of HF, N_2O, and CFCs during the Arctic polar night with the moon as light source, subsidence during winter 1992/93"*, Geophys. Res. Lett., **21**, 2385–2388, 1994.

Notholt, J.; *"The Moon as a light source for FTIR measurements of stratospheric trace gases during the polar night: Application for HNO_3 in the Arctic"*, J. Geophys. Res., **99**, 3607–3614, 1994.

Notholt, J. and O. Schrems, *"Ground-based FTIR measurements of vertical column densities of several trace gases above Spitsbergen"*, Geophys. Res. Lett., **21**, 1355–1358, 1994.
Notholt, J. and O. Schrems," *Ground-based FTIR measurements of vertical column densities of several trace gases above Spitsbergen"*, Geophys. Res. Lett., **21**, 1355–1358, 1994.
Notholt, J.; A. Meier, and S. Peil, *"Total column densities of tropospheric and stratospheric trace gases in the undisturbed Arctic summer atmosphere"*, J. Atmosph. Chem., **20**, 311–332, 1995.

Notholt, J.; I. Beninga, O. Schrems, *"Shipborne FTIR measurements of atmospheric trace gases on a South ($33^o S$) to North ($53^o N$) Atlantic traverse"*, Applied Spectr., **49**, 1525–1527, 1995.

Notholt, J.; P.v.d. Gathen, and S. Peil, *"Heterogenous conversion of HCl and $CLONO_2$ during the arctic winter 1992/1993 initiating ozone depletion"*, J. Geophys. Res., **100**, 11269–11274, 1995.

Notholt, J. and O. Schrems, *"Ground-based FTIR spectroscopic absorption measurements of stratospheric trace gases with the sun and moon as light sources"*, J. Mol. Structure, **347**, 407–416, 1995.

Notholt, J.; K. Pfeilsticker, *"Stratospheric trace gas measurements in the near UV and visible spectral range with the sun as light source using a Fourier transform spectrometer"*, Applied Spectr., **50**, 583–587, 1996.

Notholt, J.; G.C. Toon, F. Stordal, S. Solberg, N. Schmidbauer, A. Meier, E. Becker, and B. Sen, *"Seasonal variations of atmospheric trace gases in the high arctic at 79^o N"*, J. Geophys. Res., **102**, 12855–12861, 1997.

Notholt, J.; G.C. Toon, R. Lehmann, B. Sen, J.-F. Blavier, *"Comparison of Arctic and Antarctic trace gas column abundances from ground-based FTIR spectrometry"*, J. Geophys. Res., **102**, 12863–12869, 1997.

Notholt, J.; H. Schütt, A. Keens, *"Solar absorption measurements of stratospheric OH in the UV with a Fourier-transform spectrometer"*, Appl. Optics, **78**, 833–841, 1997.

Notholt, J.; G.C. Toon, B. Sen, N.B. Jones, C.P. Rinsland, R. Lehmann, M. Rex, *"Variations in the tropical uplift following the Pinatubo eruption studied by infrared solar absorption spectrometry"*, Geophys. Res. Letters, **27**, 2609–2612, 2000.

Notholt, J.; G.C. Toon, C.P. Rinsland, N. Pougatchev, N.B. Jones, B.J. Conner, R. Weller, M. Gautrois, O. Schrems, *"Latitudinal variations of trace gas concentrations in the free troposphere measured by solar absorption spectroscopy during a ship cruise"*, J. Geophys. Res., **105**, 1337–1349, 2000.

Notholt, J.; T. Albrecht, M. Rex, J. Krieg, G.C. Toon, J. Russell-III, N. Jones, *"Measurements of atmospheric trace gases by solar absorption spectrometry between $80^o N$ and $70^o S$"*, in: Optical Remote Sensing of the Atmosphere, OSA Technical Digest, 167-169, 2001.

Notholt, J.; Z. Kuang, C.P. Rinsland, G.C. Toon, M. Rex, N. Jones, T. Albrecht, H. Deckelmann, J. Krieg, C. Weinzierl, H. Bingeme r, R. Weller, O. Schrems, *"Enhanced upper tropical tropospheric COS: Impact on the stratospheric aerosol layer"*, Science , **300**, 307–310, 2003.

Ogawa, T.; M. Koike, and K. Suzuki, *"Observation of vertical ozone profiles with the EXOSC backscattered UV spectrophotometer"*, Workshop on Tropospheric Ozone and Quadrennial Ozone Symposium, Abstracts, 131, 1988.

Orphal, J.; B. Redlich, H. Grothe, D. Scheffler, H. Willner, A. Frenzel, and C. Zetzsch, *"High-resolution spectra and rotational constants of the n4 band of BrNO2 (nitryl bromide)"*, J. Molec. Spectrosc., **191**, 88–92, 1998.

Orphal, J.; *"The n1 bands of 79BrNO2 and 81BrNO2"*, J. Molec. Struct., **517/518**, 181–186, 2000.

Park, J.H.; R. Zander, C.B. Farmer, C.P. Rinsland, J.M. Russell-III, R.H. Norton and O.F. Raper, *"Spectroscopic detection of CH_3Cl in the upper troposphere and lower stratosphere"*, Geophys. Res. Lett.,**13**, 765–768, 1986.

Park, J.H.; B. Carli, and A. Barbis, *"Stratospheric HBr mixing ratio obtained from far infrared emission spectra"*, Geophys. Res. Lett., **16**, 787–790, 1989.

Parrish, A.; R.L. de Zafra, M. Jaramillo, B. Connor, P.M. Solomon, and J.W. Barrett, *"Extremely low N_2O concentrations in the springtime stratosphere at McMurdo station, Antarctica"*, Nature, **332**, 53–55, 1988.

Parrish, A.; B.J. Connor, J.J. Tsou, I.S. McDermid, and W.P. Chu, *"Ground-based microwave monitoring of stratospheric ozone"*, J.Geophys, Res., **97**, 2541–2546, 1992.

Paton-Walsh, C.; W. Bell, T. Gardiner, N. Swann, P. Woods, J. Notholt, H. Schütt, B. Galle, W. Arlander, J. Mellqvist, *"An uncertainty budget for ground-based Fourier transform infrared column measurements of HCl, HF, N2O, and HNO3 deduced from results of side-by-side instrument intercomparisons"*, J. Geophys. Res., **102**, 8867–8873, 1997.

Paton-Walsh, C.; W. Bell, T. Blumenstock, M.P. Chipperfield, B. Galle, J. Mellqvist, J. Notholt, R. Zander, P. Demoulin, E. Mahieu, *"Ground-based FTIR Measurements from a Network of European sites during the Winter of 1995/96 and a Comparison with a 3D Chemical Transport Model: Evidence of Chlorine Activation and Ozone Depletion"*, Proceedings of the Fourth European Workshop on Polar Stratospheric Ozone, Schliersee 1997, European Commission - Air pollution research report **66**, 305–308, 1998.

Paton-Walsh, Clare; Nicholas B. Jones, Stephen Wilson, Arndt Meier, Nicholas Deutscher, David Griffith, Ross Mitchell and Susan Campbell, *"Trace gas emissions from biomass burning inferred from aerosol optical depth"*, Geophys. Res. Lett., **31**, in press, 2004.

Perner, D.; U. Parchatka, V. Wolf, and P.J. Crutzen, *"Ground based spectroscopic observations of the Arctic stratosphere, Polar Ozone Workshop"*, Session VII, May 1988.

Perner, D.; U. Parchatka, and V. Wolf, *"Spectroscopic observations in the springtime Arctic stratosphere"*, Workshop on Tropospheric Ozone and Quadrennial Ozone Symposium, Abstracts, 80, 1988.

Perrin, A.; C.P. Rinsland, and A. Goldman, *"Spectral Parameters for the n6 Region of HCOOH and its Measurement in the Tropospheric Spectrum"*, J. Geophys. Res., **104**, 18661–18666, 1999.

Perrin, A.; J.-M. Flaud, F. Keller, A. Goldman, R.D. Blatherwick, F.J. Murcray, and C.P. Rinsland, *"New Analysis of the n8+n9 Band of HNO3 Line Positions and Intensities, and Resonances Involving the v6=v7=1 Dark State"*, J. Molec. Spectrosc., **194**, 113–123, 1999.

Perrin, A.; J.-M. Flaud, F. Keller, M.A.H. Smith, C.P. Rinsland, V. Malathy Devi, D. Chris Benner, T.M. Stephen, and A. Goldman, *"The n1 + n3 Bands of the $^{16}O^{17}O^{16}O$ and $^{16}O^{16}O^{17}O$ Isotopomer of Ozone"*, J. Molec. Spectrosc., **200**, 248–252, 2000.

Perrin, A.; J.-M. Flaud, F. Keller, M.A.H. Smith, C.P. Rinsland, V. Malathy Devi, D. C. Benner, T. M. Stephen, and A. Goldman, *"The $\nu 1$ + $\nu 3$ Bands of the 16-O 17-O 16-O and 16-O 16-O 17-O Isotopomers of Ozone"*, J. Mol. Spectrosc., **207**, 54–59, 2001.

Peter, R.; K. Künzi, and G.K. Hartmann, *"Latitudinal survey of water vapor in the middle atmosphere using an airborne millimeter wave sensor"*, Geophys. Res. Lett.,**15**, 1173–1176, 1988.

Peterson, D.B. and J. M. Margitan (editors), *"Upper atmospheric research satellite correlative measurements program (UARS–CMP) balloon data atlas"*, NASA, Washington DC, 1995.

Podolske, J.R.; M. Loewenstein, S.E. Strahan, and T.E. Blackburn, *"ATLAS – an airborne tunable laser absorption spectrometer for rapid trace gas measurement from high altitude aircraft"*, Workshop on Tropospheric Ozone and Quadrennial Ozone Symposium, Abstracts, 175, 1988.

Pollitt, S.; D.G. Murcray, A. Goldman, J.J. Kosters, W.J. Williams, N. Louisnard, W.F.J. Evans, M.T. Coffey, W.G. Mankin, R. Zander, D.W. Johnson, G. Stokes, and R.K. Seals, *"BIC nitric acid intercomparison"*, J. Atmosph. Chem., *submitted*, 1990.

Pommereau, J.P. and F. Goutail, *"An ozone, nitrigen dioxide and chlorine dioxide permanent monitoring station at Dumont d'Urville, Antarctica (66 S, 134 E)"*, Workshop on Tropospheric Ozone and Quadrennial Ozone Symposium, Abstracts, 167, 1988.

Pommereau, J.P. and F. Goutail, *"Ozone and nitrogen dioxide ground based monitoring by zenith sky visible spectrometry in Artic and Antarctic"*, Polar Ozone Workshop, Session VII, May 1988.

Pougatchev, N.S.; A.G. Bessonov, and A.S. Smirnov,*Ground-based infrared measurements of the atmospheric ethane (C_2H_6) and acetylene (C_2H_2) from the high resolution solar absorption spectra"*, translation from *"Nazemnyye Izmereniya Soderzhaniya Etana (C_2H_6) I Atsetilena (C_2H_2) VO Vsey Tolshche Atmosfery Po Solnechnym Ik-Spectram Sysokogo Razresheniya"*, Optika Atmosfery,**3**, No. 2, 170–173, 1990.

Pougatchev, N.S. and C.P. Rinsland, *"Spectroscopic study of the seasonal variation of carbon monoxide distribution above Kitt Peak"*, J. Geophys. Res., **100**, 1409–1416, 1995.

Pougatchev, N.S.; B.J. Connor, and C.P. Rinsland,*"Infrared measurements of the ozone vertical distribution above Kitt Peak"*, J. Geophys. Res., **100**, 16689–16697, 1995.

Pougatchev, N.S.; B.J. Connor, N.B. Jones, C.P. Rinsland, *"Validation of ozone profile retrievals from infrared ground-based solar spectra"*, Geophys. Res. Lett., **23**(13), 1637–1640, 1996.

Pougatchev, N.S.; N.B. Jones, B.J. Connor, C.P. Rinsland, E. Becker, M.T. Coffey, V.S. Connors, P. Demoulin, A.V. Dzhola, H. Fast, E.I. Grechko, J.W. Hanningan, M. Koike, Y. Kondo, E. Mahieu, W.G. Mankin, R.L. Mittermeier, J. Norholt, H.G. Reichle Jr., B. Sen, L.P. Steele, G.C. Toon, L.N. Yurganov, R. Znader, and Y. Zhao, *"Ground-based infrared solar spectroscopic measurements of carbon monoxide during 1994 Measurement of Air Pollution From Space (MAPS) Flights"*, J. Geophys. Res., **103**, 19317–19325, 1998.

Raper, O.F.; C.B. Farmer, R. Zander, and J.H. Park,*" Infrared spectroscopic measurements of halogenated sink and reservoir gases in the stratosphere with the ATMOS instrument"*, J. Geophys. Res., **92**, 9851–9858, 1987.

Rathke, C.; J. Fischer, E. Becker, J. Notholt, *"Comparison of stratus cloud properties derived from coincident airborne visible and ground-based infrared spectrometer measurements"*, Geophys. Res. Lett., **27**, 2641–2644, 2000.

Reisinger, A.R.; N.B. Jones, W.A. Matthews, and C.P. Rinsland, *"Southern hemisphere ground based measurements of Carbonyl Fluoride (COF_2) and Hydrogen Fluoride (HF): Partitioning between Fluorine reservoire species"*, Geophys. Res. Lett., **21**, 797–800, 1994.

Reisinger, A.R.; N.B. Jones, W.A. Matthews, and C.P. Rinsland, *"Southern hemisphere midlatitude ground–based measurements of $ClONO_2$: Method of analysis, seasonal cycle, and long–term trend"*, J. Geophys. Res., **100**(D11), 23183–23193, 1995.

Rex, M.; N.R. Harris, P.v.d. Gathen, R. Lehmann, G.O. Braathen, E. Reimer, A. Beck, M.P. Chipperfield, R. Alfier, M. Allaart, F.O'Connor, H. Dier, V. Dorokhov, H. Fast, M. Gil, E. Kyrö, Z. Litynska, I. S. Mikkelsen, M. Molyneux, H. Nakane, J. Notholt, M. Rummukainen, P. Viatte, J. Wenger, *"Prolonged stratospheric ozone loss in the 1995/96 Arctic winter"*, Nature, **389**, 835–838, 1997.

Rex, M.; K. Dethloff, D. Handorf, A. Herber, R. Lehmann, R. Neuber, J. Notholt, A. Rinke, P. von der Gathen, A. Weisheimer, and H. Gernandt, *"Arctic and Antarctic ozone layer observations: chemical and dynamical aspects of variability and long-term changes in the polar stratosphere"*, Polar Research, **19**(2), 193–204, 2000.

Rinsland, C.P.; A. Goldman, F.J. Murcray, D.G. Murcray, M.A.H. Smith, R.K. Seals, Jr., J.C. Larsen, Jr., and P.L. Rinsland, *"Stratospheric N2O mixing ratio profile from high resolution balloon-borne solar absorption spectra and laboratory spectra near 1880 cm^{-1}"*, Appl. Opt., **21**, 4351–4355, 1982.

Rinsland, C.P.; M.A.H. Smith, P.L. Rinsland, A. Goldman, J.W. Brault, and G.M. Stokes, *"Ground-based infrared spectroscopic measurements of atmospheric hydrogen cyanide"*, J. Geophys. Res., **87**, 11119–11125, 1982.

Rinsland, C.P.; A. Goldman, V. Malathy Devi, B. Fridovich, D. Snyder, G.D. Jones, F.J. Murcray, M.A.H. Smith, R.K. Seals jr., M.T. Coffey, and W.G. Mankin, *"Simultaneous stratospheric measurements of H_2O, HDO, and CH_4 from balloon–borne and aircraft infrared solar absorption spectra and tunable diode laser laboratory spectra of HDO"*, J. Geophys. Res., **89**, 7259–7266, 1984.

Rinsland, C.P.; et al., *"Diurnal variation of atmospheric nitric oxide: Ground-based infrared spectroscopic measurements and their interpretation with time-dependent photochemical model calculations"*, J. Geophys. Res., **89**, 9613–9622, 1984.

Rinsland, C.P.; A. Goldman, and G.M. Stokes, *"Identification of atmospheric C2H2 lines in the 3230-3340 cm^{-1} region of high resolution solar absorption spectra recorded at the National Solar Observatory"*, Appl. Opt., **24**, 2044–2046, 1985.

Rinsland, C.P.; V. Malathy Devi, J.-M. Flaud, C. Camy–Peyret, M.A.H. Smith, and G.M. Stokes *"Identification of ^{18}O–Isotopic Lines of Ozone in Infrared Ground–Based Solar Absorption Spectra"*, J. Geophys. Res., **90**, 10719–10725, 1985.

Rinsland, C.P.; R. Zander, C.B. Farmer, R.H. Norton, L.R. Brown, J. M. Russell-III, and J.H. Park, *" Evidence for the presence of the 802.7 cm^{-1} band Qbranch of HO_2NO_2 in highresolution solar absorption spectra of the stratosphere"*, Geophys. Res. Lett.,**13**, 761–764, 1986.

Rinsland, C.P.; R. Zander, L.R. Brown, C.B. Farmer, J.H. Park, R.H. Norton, J.M. Russell-III, and O.F. Raper, *"Detection of carbonyl flouride in the stratosphere"*, Geophys. Res. Lett., **13**, 769–772, 1986.

Rinsland, C.P. and J.S. Levine, *"Identification and measurement of atmospheric ethane (C_2H_6) from a 1951 infrared solar spectrum*, Appl. Opt., **25**, 4522–4525, 1986.

Rinsland, C.P.; R. Zander, C.B. Farmer, R.H. Norton, and J. M. Russell-III, *"Concentrations of ethane (C_2H_6) in the lower stratosphere and upper troposphere and acetylene (C_2H_2) in the upper troposphere deduced from ATMOS/Spacelab 3 spectra"*, J. Geophys. Res., **92**, 11951–11964, 1987.

Rinsland, C.P.; A. Goldman, F.J. Murcray, F.H. Murcray, D.G. Murcray, and J.S. Levine,*"Infrared measurements of increased CF_2Cl_2 (CFC12) absorption above the south pole"*, Appl. Opt., **27**, 627–630, 1988.

Rinsland, C.P.; A. Goldman, F.J. Murcray, F.H. Murcray, R.D. Blatherwick, and D.G. Murcray, *"Infrared measurements of atmospheric gases above Mauna Loa, Hawaii, in February 1987"*, J. Geophys. Res., **93**, 12607–12626, 1988.

Rinsland, C.P.; D.W. Johnson, A. Goldman, and J.S. Levine, *"Evidence for a Decline in the Atmospheric Accumulation Rate of $CHClF_2$ (CFC-22)"*, Nature,**337**, 535–537, 1989.

Rinsland, C.P.; G.C. Toon, C.B. Farmer, R.H. Norton, and J.S. Namkung, *" Stratospheric N_2O_5 protiles at sunrise and sunset from further analysis of the ATMOS/Spacelab 3 solar spectra"*, J. Geophys. Res.,**94**, 18341–18349, 1989.

Rinsland, C.P.; R. Zander, J.S. Namkung, C.B. Farmer, and R.H. Norton, *"Stratospheric infrared continuum absorptions observed by the ATMOS instrument"*, J. Geophys. Res., **94**, 16303–16322, 1989.

Rinsland, C.P.; A. Goldman, F.J. Murcray, R.D. Blatherwick, J.J. Kosters, D.G. Murcray, N.D. Sze, and S.T. Massie, *"Long-term trends in the concentration of SF_6, $CHClF_2$, and COF_2 in the lower stratosphere from analysis of high-resolution infrared solar occultation spectra"*, J. Geophys. Res.,**95**, 16477–16490, 1990.

Rinsland, C.P.; L.R. Brown, and C.B. Farmer, *"Infrared spectroscopic detection of sulfur hexafluoride (SF_6) in the lower stratosphere and upper troposphere"*, J. Geophys. Res., **95**, 5577–5585, 1990.

Rinsland, C.P.; J.S. Levine, A. Goldman, N.D. Sze, M.K.W. Ko, and D.W. Johnson, *"Infrared measurements of HF and HCl total column abundances above Kitt Peak, 1977–1990: seasonal cycles, long–term increases, and comparison with model calculations"*, J. Geophys. Res., **96**, 15523–15540, 1991.

Rinsland, C.P.; M.R. Gunson, J.C. Foster, R.A. Toth, C.B. Farmer, and R. Zander, *"Stratospheric Profiles of Heavy Water Vapor Isotopes and CH_3D from Analysis of the ATMOS Spacelab 3 Infrared Solar Spectra"*, J. Geophys. Res., **96**, 1057–1068, 1991.

Rinsland, C.P.; R. Zander, A. Goldman, F.J. Murcray, D.G. Murcray, M.R. Gunson, and C.B. Farmer, *"The fundamental quadrupole band of $^{14}N_2$: line positions from high-resolution stratospheric solar absorption spectra"*, J. Mol. Spectrosc., **148**, 274–279, 1991.

Rinsland, C.P.; R. Zander, and P. Demoulin,*"Ground-based infrared measurements of HNO_3 total column abundances: Long–Term trend and variability"*, J. Geophys. Res., **96**, 9379–9389, 1991.

Rinsland, C.P.; M.R. Gunson, R. Zander, and M. Lopez–Puertas, *"Middle and upper atmosphere pressure–temperature profiles and the abundances of CO_2 and CO in the upper atmosphere from ATMOS/Spacelab 3 observations"*, J. Geophys. Res., **97**, 20479–20495, 1992.

Rinsland, C.P.; R. Zander, M. Mahieu, P. Demoulin, A. Goldman, D.H. Ehalt, and J. Rudolph,*"Ground–based infrared measurements of Carbonyl Sulfide total column abundances: Long-term trends and variability"*, J. Geophys. Res., **97**, 5995–6002, 1992.

Rinsland, C.P.; M.R. Gunson, M.C. Abrams, L.L. Lowes, R. Zander, and E. Mahieu, *"ATMOS/ATLAS 1 measurements of sulfur hexafluoride (SF6) in the lower stratosphere and upper troposphere"*, J. Geophys. Res., **98**, 20491–20494, 1993.

Rinsland, C.P.; A. Goldman, F.J. Murcray, S.J. David, R.D. Blatherwick, and D.G. Murcray, *"Infrared Spectroscopic measurements of the Ethane (C_2H_6) total column abundance above Mauna Loa, Hawaii – seasonal variations"*, J. Quant. Spectrosc. Radiative Transfer,**52**, 273–279, 1994.

Rinsland, C.P.; M.R. Gunson, M.C. Abrams, L.L. Lowes, R. Zander, E. Mahieu, A. Goldman, M.K.W. Ko, J.M. Rodriguez, and N. D. Sze, *"Heterogeneous conversion of N2O5 to HNO3 in the post-Mt. Pinatubo eruption stratosphere"*, J. Geophys. Res., **99**, 8213–8219, 1994.

Rinsland, C.P.; M.R. Gunson, M.C. Abrams, R. Zander, E. Mahieu, A. Goldman, M.K.W. Ko, J.M. Rodriguez, and N. D. Sze, *"Profiles of stratospheric chlorine nitrate (ClONO2) from atmospheric trace molecule spectroscopy/ATLAS-1 infrared solar occultation spectra"*, J. Geophys. Res., **99**, 18895–18900, 1994.

Rinsland, C.P.; N.B. Jones, and W.A. Matthews, *"Infrared Spectroscopic Measurements of the Total Column Abundance of Ethane (C2H6) above Lauder, New Zealand"*, J. Geophys. Res., **99**, 25941–25945, 1994.

Rinsland, C.P.; M.R. Gunson, M.C. Abrams, L.L. Lowes, R. Zander, E. Mahieu, A. Goldman, F.W. Irion, R. A. Salavitch, and H.A. Michelsen, *"April 1993 Arctic profiles of stratospheric HCl, ClONO2, and CCl2F2 from ATMOS/ATLAS 2 infrared solar occultation spectra"*, J. Geophys. Res., **100**, 14019–14027, 1995.

Rinsland, C.P.; B.J. Connor, N.B. Jones, I. Boyd, W.A. Matthews, A. Goldman, F.J. Murcray, D.G. Murcray, S.J. David, and N. S. Pugatchev, *"Comparison of infrared and Dobson total columns measured from Lauder, New Zealand"*, Geophys. Res. Lett., **23**, 1025–1028, 1996.

Rinsland, C.P.; E. Mahieu, R. Zander, M.R. Gunson, R.J. Salawitch, A.Y. Chang, A. Goldman, M.C. Abrams, H.A. Michelsen, M.M. Abbas, M.J. Newchurch, and F.W. Irion, *"Trends of OCS, HCN, SF6, and CHClF2 (HCFC-22) in the lower stratosphere from 1985 and 1994 Atmospheric Trace Molecule Spectroscopy experiment measurements near 30^{o}N latitude"*, Geophys. Res. Lett., **23**, 2349–2352, 1996.

Rinsland, C.P.; M.R. Gunson, R.J. Salawitch, H.A. Michelsen, R. Zander, M.J. Newchurch, M.M. Abbas, M.C. Abrams, G.L. Manney, A.Y. Chang, F.W. Irion, A. Goldman, and E. Mahieu, *"ATMOS/ATLAS-3 measurements of stratospheric chlorine and reactive nitrogen partitioning inside and outside the November 1994 Antarctic vortex"*, Geophys. Res. Lett., **23**, 2365–2368, 1996.

Rinsland, C.P.; M.R. Gunson, R.J. Salawitch, M.J. Newchurch, R. Zander, M.M. Abbas, M.C. Abrams, G.L. Manney, H.A. Michelsen, A.Y. Chang, and A. Goldman, *"ATMOS measurements of H2O+2CH4 and total reactive nitrogen in the November 1994 Antarctic stratosphere: dehydration and denitrification in the vortex"*, Geophys. Res. Lett., **23**, 2397–2400, 1996.

Rinsland, C.P.; R. Zander, P. Demoulin, and E. Mahieu, *"$ClONO_2$ total vertical column abundances above the Jungfraujoch station, 1986–1994: Long–term trend and winter–spring enhancements"*, J. Geophys. Res., **101**, 3891–3899, 1996.

Rinsland, C.P.; M.R. Gunson, P.H. Wang, R.F. Arduini, B.A. Baum, P. Minnis, A. Goldman, M.C. Abrams, R. Zander, E. Mahieu, R.J. Salawitch, H.A. Michelsen, F.W. Irion, and M.J. Newchurch, *"ATMOS/-ATLAS 3 infrared profile measurements of clouds in the tropical and subtropical upper troposphere"*, J. Quant. Spectrosc. Radiat. Transfer, **60**, 903–919, 1998.

Rinsland, C.P.; M.R. Gunson, P.H. Wang, R.F. Arduini, B.A. Baum, P. Minnis, A. Goldman, M.C. Abrams, R. Zander, E. Mahieu, R.J. Salawitch, H.A. Michelsen, F.W. Irion, and M.J. Newchurch, *"ATMOS/-ATLAS 3 infrared profile measurements of trace gases in the November 1994 tropical and subtropical upper troposphere"*, J. Quant. Spectrosc. Radiat. Transfer, **60**, 891–901, 1998.

Rinsland, C.P.; N.B. Jones, B.J. Connor, J.A. Logan, N.S. Pougatchev, A. Goldman, F.J. Murcray, T.M. Stephen, A.S. Pine, R. Zander, E. Mahieu, and P. Demoulin, *"Northern and southern hemisphere ground-based infrared spectroscopic measurements of tropospheric carbon monoxide and ethane"*, J. Geophys. Res., **103**, 28197–28218, 1998.

Rinsland, C.P.; A. Goldman, F.J. Murcray, T.M. Stephen, N.S. Pougatchev, J. Fishman, S.J. David, R.D. Baltherwick, P.C. Novelli, N.B. Jones, and B.J. Connor, *"Infrared solar spectroscopic measurements of free tropospheric CO, C2H6, and HCN above Mauna Loa, Hawaii: Seasonal variations and evidence for enhanced emissions from the Southeast Asian tropical fires of 1997-1998"*, J. Geophys. Res., **104**, 18667–18680, 1999.

Rinsland, C.P.; R.J. Salavitch, G.L. Manney, M.R. Gunson, H.A. Michelsen, S. Solomon, R. Zander, E. Mahieu, A. Goldman, M.J. Newchurch, and F.W. Irion, *"Polar Stratospheric Descent of NOy and CO and Arctic Denitrification during Winter 1992-1993"*, J. Geophys. Res., **104**, 1847–1861, 1999.

Rinsland, C.P.; A. Goldman, B.J. Connor, T.M. Stephen, N.B. Jones, S.W. Wood, F.J. Murcray, S.J. David, R.D. Blatherwick, R. Zander, E. Mahieu, and P. Demoulin, *"Correlation relationships of stratospheric molecular constituents from high spectral resolution, ground-based infrared solar absorption spectra"*, J. Geophys. Res., **105**, 14637–14652, 2000.

Rinsland, C.P.; E. Mahieu, R. Zander, P. Demoulin, J. Forrer, B. Buchmann, *"Free tropospheric CO, C2H6, and HCN above central Europe: Recent measurements from the Jungfraujoch station including the detection of elevated columns during 1998"*, J. Geophys. Res., **105** (D19), 24235–24249, 2000.

Rinsland, C.P.; N.B. Jones, B.J. Connor, J.A. Logan, N.S. Pougatchev, A. Goldman, F.J. Murcray, T.M. Stephen, A.S. Pine, R. Zander, E. Mahieu, P. Demoulin, C.P. Rinsland, J. Forrer, and B. Buchmann, *"Free tropospheric CO, C2H6 and HCN above central Europe: recent measurements from the Jungfraujoch station including the detection of elevated columns during 1998"*, J. Geophys. Res., **105**, 24235–24249, 2000.

Rinsland, C.P.; R.J. Salavitch, G.B. Osterman, F.W. Irion, B. Sen, R. Zander, E. Mahieu, and M.R. Gunson, *"Stratospheric CO at Tropical and Mid-Latitudes : ATMOS Measurements and Photochemical Steady-State Model Calculations"*, Geophys. Res. Lett., **27**, 1395–1398, 2000.

Rinsland, C.P.; A. Goldman, R. Zander, and E. Mahieu, *"Enhanced tropospheric HCN columns above Kitt Peak during the 1982-1983 and 1997-1998 El Nino warm phases"*, J. Quant. Spectrosc. Radiat. Transfer, **69**, 3–8, 2001.

Rinsland, C.P.; A. Meier, D.W.T. Griffith, and L.S. Chiou, *"Ground-based Measurements of Tropospheric CO, C2H6, and HCN from Australia at 34°S Latitude during 1997-1998"*, J. Geophys. Res., **106**, 20913–20924, 2001.

Rinsland, C.P.; R. Zander, E. Mahieu, L.S. Chiou, A. Goldman, and N.B. Jones, *"Stratospheric HF column abundances above Kitt Peak (31.9°N latitude) : Trends from 1977 to 2001 and correlations with stratospheric HCl columns"*, J. Quant. Spectrosc. Radiat. Transfer, **74**, 205–216, 2001.

Rinsland, C.P.; A. Goldman, E. Mahieu, R. Zander, J. Notholt, N. Jones, D.W.T. Griffith, T.M. Stephen, L.S. Chiou, *"Ground-based infrared spectroscopic measurements of carbonyl sulfide : Free tropospheric trends from a 24-year time series of solar absorption measurements"*, J. Geophys. Res., **107**, No. D22, 4657, doi: 10.1029/2002JD002522, 2002.

Rinsland, C.P.; N.B. Jones, B.J. Connor, S.W. Wood, A. Goldman, T.M. Stephen, F.J. Murcray, L.S. Chiou, R. Zander, and E. Mahieu, *"Multiyear infrared solar spectroscopic measurements of HCN, CO, C2H6 and C2H2 tropospheric columns above Lauder, New Zealand (45°S Latitude)"*, J. Geophys. Res., **107**, No. D14, doi: 10.1029/2001JD001150, 2002.

Rinsland, C.P.; R. Zander, E. Mahieu, L.S. Chiou, A. Goldman, and N.B. Jones, *"Stratospheric HF Column abundances above Kitt Peak (31.9°N Latitude): Trends from 1977 to 2001 and Correlations with HCl Stratospheric Columns"*, J. Quant. Spectrosc. Radiat. Transfer, **74**(2), 205–216, 2002.

Rinsland, C.P.; A. Goldman, T.M. Stephen, L.S. Chiou, E. Mahieu, and R. Zander, *"SF6 ground-based infrared solar absorption measurements : long-term trend, pollution events, and a search for SF5CF3 absorption"*, J. Quant. Spectrosc. Radiat. Transfer, **78**, 41–53, 2003.

Rinsland, C.P.; E. Mahieu, R. Zander, N.B. Jones, M.P. Chipperfield, A. Goldman, J. Anderson, J.M. Russell-III, P. Demoulin, J. Notholt, G.C. Toon, J.-F.Blavier, B. Sen, R. Sussmann, S.W. Wood, A. Meier, D.W.T. griffith, L.S. Chiou, F.J. Murcray, T.M. Stephen, F. Hase, S. Mikuteit, A. Schulz, and T. Blumenstock, *"Long-term trends of inorganic chlorine from ground-based infrared solar spectra: Past increases and evidence of stabilization"*, J. Geophys. Res., **108**(D8), 4252, doi:10.1029/2002JD003001, 2003.

Rinsland, C.P.; J.-M. Flaud, A. Perrin, M. Birk, G. Wagner, A. Goldman, A. Barbe, M.R. De Backer-Barilly, S.N. Mikhailenko, Vl.G. Tyuterev, M.A.H. Smith, V.M. Devi, D.C. Benner, F. Schreier, K.V. Chance, J. Orphal, and T.S. Stephen, *"Spectroscopic Parameters for Ozone and its Isotopes: Recent Measurements, Outstanding Issues, and Prospects for Improvements to HITRAN"*, HITRAN Special Issue, J. Quant. Spectrosc. Radiat. Transfer, **82**, numbers 1-4, 2003.

Rinsland, C.P.; S.W. Sharpe, and R.L. Sams, *"Temperature Dependent Absorption Cross-sections in the Thermal Infrared Bands of SF5CF3,"* HITRAN Special Issue, J. Quant. Spectrosc. Radiat. Transfer, **82**, numbers 1-4, 2003.

Rinsland, C.P.; V.M. Devi, M.A.H. Smith, D.C. Benner, S.W. Sharpe, and R.L. Sams, *"A Multispectrum Analysis of the 1 Band of H12C14N: II. Air- and N2-broadening, Shifts and their Temperature Dependences"*, HITRAN Special Issue, J. Quant. Spectrosc. Radiat. Transfer, **82**, numbers 1-4, 2003.

Rinsland, C.P.; D.W.T. Griffith, Nicholas B. Jones, Clare Paton-Walsh, Aaron Goldman, Stephen B. Wood, Linda Chiou, and Arndt Meier, *"High spectral Resolution Solar Absorption Measurements of Ethylene (C_2H_4)in a Forest Fire Smoke Plume using HITRAN 2000 Parameters: Tropospheric Vertical Profile Retrieval"*, submitted to J. Geophys. Res., 2004.

Rodgers, C.D.; *"Characterization and error analysis of profile retrieved from remotesounding measurements"*, J. Geophys. Res., **95**, 5587–5595, 1990.

Roscoe, H.K.; B.J. Kerridge, S. Pollitt, N. Louisnard, J.-M. Flaud, C. Camy–Peyret, C. Alamichel, J.-P. Pommereau, T. Ogawa, N. Iwagami, M.T. Coffey, W.G. Mankin, W.F.J. Evans, C.T. McElroy and J. Kerr, *"Intercomparison of remote measurements of stratospheric NO and NO_2*, J. Atmos. Chem., **10**, 111–144, 1990.

Rothman, L.S,; et al., *"The HITRAN molecular database: Edition of 1991 and 1992"*, J. Quant. Spectrosc. Radiat. Transfer, **48**, 469–507, 1992.

Rothman, L.S.; A. Goldman, and C.P. Rinsland (editors), *"HITRAN"*, special issue, J. Quant. Spectrosc. Radiat. Transfer, Vol **60**, 5/1998.

Rothman, L.S.; C.P. Rinsland, A. Goldman, S.T. Massie, D.P. Edwards, J.-M. Flaud, A. Perrin, C. Camy-Peyret, V. Dana, J.-Y. Mandin, J. Schroeder, A. McCann, R.R. Gamache, R.B. Wattson, K. Yoshino, K.V. Chance, K.W. Jucks, L.R. Brown, V. Nemtchinov, and P. Varanasi, *"The HITRAN Molecular Spectroscopic Database and HAWKS (HITRAN Atmospheric Workstation): 1996 Edition"*, J. Quant. Spectrosc. Radiat. Transfer, **60**, 665–710, 5/1998.

Rothman, L.S.; A. Barbe, D.C. Benner, L.R. Brown, C. Camy-Peyret, M.R. Carleer, K. Chance, C. Clerbaux, V. Dana, V.M. Devi, A. Fayt, J.-M. Flaud, R.R. Gamache, A. Goldman, D. Jacquemart, K.W. Jucks, W.J. Lafferty, J.-Y. Mandin, S.T. Massie, V. Nemtchinov, D.A. Newnham, A. Perrin, C.P. Rinsland, J. Schroeder, K.M. Smith, M.A.H. Smith, K. Tang, R.A. Toth, J. Vander Auwera, P. Varanasi, and K. Yoshino, *"The HITRAN Molecular Spectroscopic Database: Edition of 2000 Including Updates of 2001"*, HITRAN Special Issue, J. Quant. Spectrosc. Radiat. Transfer, **82**, numbers 1-4, 2003.

Russell-III, J. M.; C.B. Farmer, C.P. Rinsland, R. Zander, L. Froidevaux, G.C. Toon, B. Gao, J. Shaw and M. Gunson, *"Measurements of odd nitrogen compounds in the stratosphere by the ATMOS experiment on Spacelab 3"*, J. Geophys. Res.,**93**, 1718–1736, 1988.

Russell-III, J. M.; L.E. Deaver, M. Luo, R.J. Cicerone, J.H. Park, L.L. Gordley, G.C. Toon, M.R. Gunson, W.A. Traub, D.G. Johnson, K. W. Jucks, R. Zander, and I. G. Nolt, *"Validation of hydrogen fluoride measurements made by the Halogen Occultation Experiment from the UARS platform"*, J. Geophys. Res., **101**, 10162–10174, 1996.

Sanders, R.W.; S. Solomon, G.H. Mount, M.W. Bates, and A.L. Schmeltekopf, *"Visible spectroscopy at McMurdo station, Antarctica, 3. observations of NO3"*, J. Geophys. Res., **92**, 8339–8342, 1987.

Sanders, R.W.; S. Solomon, M.A. Carroll, and A.L. Schmeltekopf, *"Groundbased measurements of O_3, NO_2, OClO, and BrO during the 1987 Antarctic ozone depletion event"*, Workshop on Tropospheric Ozone and Quadrennial Ozone Symposium, Abstracts, 57, 1988.

Schiller, C.; U. Platt, and U. Schmidt, *"Measurements of column densities of NO2 and other species by visible and UV spectroscopy at 68^{o}N"*, Workshop on Tropospheric Ozone and Quadrennial Ozone Symposium, Abstracts, 163, 1988.

Schmid, B.; K.J. Thome, P. Demoulin, R. Peter, C. Matzler, and J. Sekler, *"Comparison of modeled and empirical approaches for retrieving columnar water vapor from solar transmittance measurements in the 0.94 micron region"*, J. Geophys. Res., **101**, 9345–9358, 1996.

Schmidt, U.; H.K. Roscoe, N.R.P. Harris, K. Künzi, L. Stefanutti, and R. Zander, *"Instrument Development and Deployment"*, pp. 201-241, in "European Research in the Stratosphere B The contribution of EASOE and SESAME to our current understanding of the ozone layer", European Commission B DGXII, Ref. EUR16986/ISBN 92-827-9719-8, 1997.

Schreiber, J., *"Untersuchung und Reduktion der Eigenstrahlung des Fourierspektrometers BOMEM-DA2"*, Diplomarbeit in physics (*Master's thesis*), Universität Karlsruhe, Germany, Institut für Meteorologie und Klimaforschung, 1994.

Schreiber, J., T. Blumenstock, and H. Fischer *"Effects of the self-emission of an IT Fourier-transfoem spectrometer on measured absorption spectra"*, Appl. Opt., **35**, 6203–6209, 1996.

Schreiber, J.; T. Blumenstock, and H. Fischer, *"Effects of the self-emission of an IR Fourier-transform spectrometer on measured absorption spectra"*, Appl. Opt., **35**, 6203–6209, 1996.

Schreiber, J.; T. Blumenstock, F. Hase, *"Application of a radiometric calibration method to Lunar Fourier transform IR spectra by using a liquid-nitrogen-cooled high-emissivity blackbody"*, Appl. Opt., **36**, 8168–8172, 1997.

Schneider, M.; T. Blumenstock, F. Hase, H. Fischer, M. Höpfner, P. Thomas, E. Cuevas, J. Sancho, A. Redondas, M. Yela, O. Puentedura, *"Ground-based FTIR measurements at Izana Observatory on Teneriffe in 1999"*, Proceedings of the Fifth European Workshop on Polar Stratospheric Ozone, St. Jean Du Luz 1999, European Commission - Air pollution research report **73**, 344–347, 2000.

Sen, B.; G.C. Toon, J.-F. Blavier, E.L. Fleming, and C.H. Jackman, *"Balloon-borne observations of mid-latitude fluorine abundance"*, J. Geophys. Res., **101**(D4), 9045–9054, 1996.

Shepard, M.W.; A. Goldman, S.A. Clough, and E.J. Mlawer, *"Spectroscopic Improvements Providing Evidence of Formic Acid in AERI-LBLRTM Validation Spectra"*, HITRAN Special Issue, J. Quant. Spectrosc. Radiat. Transfer, **82**, numbers 1-4, 2003.

Sherlock, V.J.; N.B. Jones, W.A. Matthews, F.J. Murcray, R.D. Blatherwick, D.G. Murcray, A. Goldman, C.P. Rinsland, C. Bernardo, and D.W.T. Griffith, *"Increase in the vertical column abundance of HCFC-22 (CHClF2) above Lauder, New Zealand, between 1985 and 1994"*, J. Geophys. Res., **102**, 8861–8865, 1997.

Smith J.P.; and S. Solomon,*"Atmospheric NO_3 3. sunrise disappearance and the stratospheric profile"*, J. Geophys. Res., **95** (D9), 13819–13827, 1990.

Smith, M.A.H.; V. Malathy Devi, D.C. Benner, and C.P. Rinsland, *"Absolute Intensities of $^{16}O_3$ Lines in the 9-11μm Region"*, J. Geophys. Res., **106**, 9909–9921, 2001.

Solomon, S.; A.L. Schmeltekopf and R.W. Sanders, *"On the interpretation of zenith sky absorption measurements"*, J. Geophys. Res., **92**, 8311–8319, 1987.

Solomon, S.; G.H. Mount, R.W. Sanders and A.L. Schmeltekopf, *"Visible spectroscopy at McMurdo station, Antarctica, 2. observations of OClO"*, J. Geophys. Res., **92**, 8329–8338, 1987.

Solomon, S.; R.W. Sanders, M.A. Carroll and A.L. Schmeltekopf, *"Observations of the diurnal variations of BrO and OClO at McMurdo Station, Antarctica (78^{o}S)"*, Polar Ozone Workshop, Session IV, May 1988.

Solomon, S.; and J.G. Keys, *"Seasonal variations in Antarctic NOx chemistry"*, J. Geophys. Res., **97**, 7971–7978, 1992.

Stephen, T.M.; A. Goldman, A. Perrin, J.-M. Flaud, F. Keller, and C.P. Rinsland, *"New high resolution analysis of the 3n3 and 2n1+n3 bands of nitrogen dioxide (NO2) by Fourier transform spectroscopy"*, J. Molec. Spectrosc., **201**, 134–142, 2000.

Stiller, G.P.; M.R. Gunson, L.L. Lowes, M.C. Abrams, O.F. Raper, C.B. Farmer, R. Zander, and C.P. Rinsland, *"Stratospheric and mesospheric pressure-temperature profiles from rotational analysis of CO2 lines in Atmospheric Trace Molecule Spectroscopy/ATLAS1 infrared solar occultation spectra"*, J. Geophys. Res., **100**, 3107–3117, 1995.

Stiller, G.P.; T. von Clarmann, A. Wegner, M. Baumann, E. Frank, and H. Oelhaf, *"Retrieval of tropospheric versus stratospheric partitioning of HCl from ground-based MIPAS FTIR spectra"*, J. Quant. Spectrosc. Radiat. Transfer, **54**, 899–912, 1995.

Strahan, S.E.; J.R. Podolske, T.E. Blackburn, and M. Loewenstein, *"CO mixing ratios over tropical Australia obtained with a new airborne laser spectrometer"*, Workshop on Tropospheric Ozone and Quadrennial Ozone Symposium, Abstracts, 175, 1988.

Strahan, S.E.; M. Loewenstein, J.R. Podolske, W.L. Starr, M.H. Proffitt, and K.K. Kelly, *"Correlation of N_2O and ozone in the southern polar vortex during the airborne Antarctic ozone experiment"*, Polar Ozone Workshop, Session V, May 1988.

Sussmann, R. et al., *"Infrared spectroscopy of tropospheric trace gases: combined analysis of horizontal and vertical column abundances"*, Appl. Opt., **36**, 735–741, 1997.

Sussmann, R.; *"Ground-based Fourier transform spectrometry at the NDSC site Zugspitze: Geophysical products for satellite validation"*, in Proceedings of the European Symposium on Atmospheric Measurements from Space, ESTEC, Noordwijk, The Netherlands, 18-22 Jan 1999, WPP-161, Vol. **2**, 661–664, 1999.

Toon, G.C.; C.B. Farmer, and R.H. Norton, *"Detection of stratospheric N_2O_5 by infrared remote sounding"*, Nature, **319**, 570–571, 1986.

Toon, G.C.; C.B. Farmer, L.L. Lowes, P.W. Schaper, J.F. Blavier, and R.H. Norton, *"Infrared aircraftmeasurements of stratospheric composition over Antarctica during September 1987"*, Polar Ozone Workshop, Session IV, May 1988., J. Geophys. Res., **94**, 16571–16596, 1989.

Toon, G.C.; C.B. Farmer, P.W. Schaper, J.-F. Blavier, and L.L. Lowes, *"Ground-based infrared measurements of tropospheric source gases over Antarctica during the 1986 austral spring"*, J. Geophys. Res., **94**(D9), 11613–11624, 1989.

Toon, G.C.; Jet Propulsion Laboratory, e-mail: toon@mark4sun.jpl.nasa.gov, priv. comm, 2001: the quoted linelist is a refined version of the linelist given by [Livingston & Wallace, 1991.

Toon, G.C.; *"The JPL MkIV Interferometer"*, Optics and Photonics News, **2**, 19–21, 1991.

Toon, G.C.; C.B. Farmer, P.W. Schaper, L.L. Lowes, and R.H. Norton, *"Composition measurements of the 1989 arctic winter stratosphere by airborne infrared solar absorption spectroscopy"*, J. Geophys. Res., **97**, 7939–7961, 1992.

Toon, G.C.; C.B. Farmer, P.W. Schaper, et al., *"Evidence for Subsidence in the 1989 Arctic Winter Stratosphere from Airborne Infrared Composition Measurements"*, J. Geophys. Res., **97**, 7963–7970, 1992.

Toon, G.C.; J.-F. Blavier and J.T. Szeto, Latitude variations of stratospheric trace gases, Geophys. Res. Lett., **21**, 2599–2602, 1994.

Toon, G.C.; J.-F. Blavier, B. Sen, R.J. Salawitch, G.B. Osterman, J. Notholt, M. Rex, C. T. McElroy, and J.M. Russell-III, *"Ground-based observations of Arctic ozone loss during spring and summer 1997"*, J. Geophys. Res., **104**, 26497–26510, 1999.

Torr, D.G.; M.R. Torr, W. Swift, J. Fennelly, and G. Liu, *"Measurements of OH (X2p) in the stratosphere by high-resolution UV spectroscopy"*, Geophys. Res. Lett., **14**, 937–940, 1987.

Torr, M.R. and D.G. Torr, *"Imaging spectrometer for high-resolution measurements of stratospheric trace constituents in the ultraviolet"*, Appl. Opt., **27**, 619–626, 1988.

Traub, W.A.; D.G. Johnson, and K.V. Chance, *"Stratospheric hydroxyl measurements"*, Science, **247**, 446–449, 1990.

Traub, W.A.; K.W. Jucks, D.G. Johnson, M.T. Coffey, W.G. Mankin and G.C. Toon, *"Comparison of column abundances from three infrared spectrometers during AASE2"*, Geophys. Res. Lett., **21**, 2591–2594, 1994.

Turatti, F.; D.W.T. Griffith, S.R. Wilson, M.B. Esler, T. Rahn, H. Zhang, G. Blake, and M. Wahlen, *"Positionally dependent ^{15}N fractionation factors in the photolysis of N2O determined by high resolution FTIR spectroscopy"*, Geophys. Res. Lett., **27**(16), 2489–2492, 2000.

Vercheval, J.; C. Lippens, C. Muller, M. Ackerman, M.P. Lemaitre, J. Besson, A. Girard, and J. Laurent, *"CO_2 and CO vertical distribution in the middle atmosphere and lower thermosphere deduced from infrared spectra"*, Annales Geophysicae,**4**, 161–164, 1986.

Vernazza, J.E.; E.H. Avrett, and R. Loeser, *"Structure of the solar chromosphere – Models of the EUV brightness components of the quiet-sun"*, The Astrophysical Journal Supplement Series, **45**, 635–725, 1981.

Wagner, G. and M. Birk, *"New Infrared Spectroscopic Database for Chlorine Nitrate"*, HITRAN Special Issue, J. Quant. Spectrosc. Radiat. Transfer, **82**, numbers 1-4, 2003.

Wahner, A.; R.O. Jakoubek, A.R. Ravishankara, G.H. Mount, and A.L. Schmeltekopf, *"Near UV atmospheric absorption measurements from the DC-8 aircraft during the 1987 airborne Antarctic ozone experiment"*, Polar Ozone Workshop, Session IV, May 1988.

Wallace, L. and W. Livingston, *"Spectroscopic observations of atmospheric trace gases over Kitt Peak 1. Carbon dioxide and methane from 1979 to 1985"*, J. Geophys. Res., **95**, 9823–9827, 1990.

Wallace, L. and W. Livingston, *"Spectroscopic observations of atmospheric trace gases over Kitt Peak 2. Nitrous oxide and carbon monoxide from 1979 to 1985*, J. Geophys. Res., **95**, 16383–16390, 1990.

Wallace, L. and W. Livingston, *"Spectroscopic observations of atmospheric trace gases over Kitt Peak. 3. The long-term trends of hydrogen chloride and hydrogen fluoride from 1978 to 1990"*, J. Geophys. Res., **96**, 15513–15522, 1991.

Wallace, L. and W. Livingston, *"The effect of the Pinatubo cloud on Hydrogen Chloride and Hydrogen Fluoride"*, Geophys. Res. Lett., **19**, 1209, 1992.

Waters, J.W.; R.A. Stachnik, J.C. Hardy, and R.F. Jarnot,*"ClO and O_3 stratospheric profiles: balloon microwave measurements"*, Geophys. Res. Lett., **15**, 780–783, 1988.

Webster, C.R. and R.D. May,*"Simultaneous in situ measurements and diurnal variations of NO, NO_2, O_3, NO_2, CH_4, H_2O and CO_2 in the 40 to 26km region using an open path tunable diode laser spectrometer"*, J. Geophys. Res., **92**, 11931–11950, 1987.

Webster, C.R.; R.D. May, R. Toumi, and J.A. Pyle,*"Active nitrogen partitioning and nighttime formation of N_2O_5 in the stratosphere: Simultaneous in situ measurements of NO, NO_2, HNO_3, O_3 and N_2O using the BLISS diode laser spectrometer"*, J. Geophys. Res., **95**, 13851–13866, 1990.

Wegner, A.; G.P. Stiller, T. von Clarmann, G. Maucher, T. Blumenstock, P. Thomas, *"Denitrification and chlorine activation as monitored by ground-based FTIR solar absorption measurements"*, J. Geophys. Res., **103**(D17), 22181–22200, 1998.

Yang, A.; G.C. Toon, J.S. Margolis, P.O. Wennberg, *"Atmospheric CO2 retrieved from ground-based near IR spectra"*, Geophys. Res. Lett., **29**(9), doi:10.1029/2001GL014537, 2002.

Yashcov, D.; A. Steen, T. Blumenstock, P. Thomas, *"Column Amounts of ClONO2, HCl, HNO3, and HF from Ground-Based FTIR Measurements at Kiruna (Sweden) during Winter 1999"*, Proceedings of the Fifth European Workshop on Polar Stratospheric Ozone, St. Jean Du Luz 1999, European Commission - Air pollution research report **73**, 396–399, 2000.

Yokelson, R.J.; D.W.T. Griffith, J.B. Burkholder, and D.E. Ward, *"Accuracy and advantages of synthetic calibration of smoke spectra"*, in Optical Remote Sensing for Environmental and Process Monitoring, pp. 365-376, Air & Waste Management Association, Pittsburgh, 1996.

Zafra, R.L. de; M. Jaramillo, A. Parrish, P. Solomon, B. Connor, and J. Barrett, *"High concentrations of chlorine monoxide at low altitudes in the antarctic spring stratosphere: diurnal variation"*, Nature, **328**, 408–411, 1987.

Zafra, R.L. de; M. Jaramillo, J. Barrett, L. Emmons, P. Solomon, and A. Parrish, *"Observed diurnal variation of anomalous ClO concentrations in the Antarctic spring stratosphere over McMurdo station"*, 1986 and 1987, Workshop on Tropospheric Ozone and Quadrennial Ozone Symposium, Abstracts, 56, 1988.

Zafra, R.L. de; M. Jaramillo, J. Barrett, L. Emmons, P. Solomon, and A. Parrish,*"Quantitative observations of the behavior of anomalous low altitude ClO in the Antarctic spring stratosphere, 1987"*, Polar OzoneWorkshop, Session IV, May 1988.

Zander, R.; C.P. Rinsland, C.B. Farmer, L.R. Brown, and R.H. Norton, *"Observation of several chlorine nitrate (ClONO2) bands in stratospheric infrared spectra"*, Geophys. Res. Lett., **13**, 757–760, 1986.

Zander, R.; C.P. Rinsland, C.B. Farmer, L.R. Brown, and R.H. Norton, *"Observation of several chlorine nitrate (ClONO2) bands in stratospheric infrared spectra"*, Geophys. Res. Lett., **13**, 757–760, 1986.

Zander, R.; C.P. Rinsland, C.B. Farmer, and R.H. Norton, *"Infrared spectroscopic measurements of halogenated source gases in the stratosphere with the ATMOS instrument"*, J. Geophys. Res., **92**, 9836–9850, 1987.

Zander, R.; C.P. Rinsland, C.B. Farmer, and R.H. Norton, *"Infrared spectroscopic measurements of halogenated source gases in the stratosphere with the ATMOS instrument"*, J. Geophys. Res., **92**, 9836–9850, 1987.

Zander, R.; G. Roland, L. Delbouille, A.J. Sauval, C.B. Farmer, and R.H. Norton, *"Column abundance and long-term trend of hydrogen chloride (HCl) above the Jungfraujoch station"*, J. Atmos. Chem., **5**, 395–404, 1987.

Zander, R.; G. Roland, L. Delbouille, A.J. Sauval, C.B. Farmer, and R.H. Norton, *"Monitoring of the integrated column of hydrogen fluoride above the Jungfraujoch station since 1977 - the HF/HCl column ratio"*, J. Atmos. Chem., **5**, 385–394, 1987.

Zander, R.; G. Roland, L. Delbouille, A.J. Sauval, P. Marché, F. Karcher, M. Amoudei, and B. Dufour, *"Concentration of hydrogen chloride and hydrogen fluoride measured during the MAP/GLOBUS campaign of September 1983"*, Planet. Space Sci., **35**, 665–672, 1987.

Zander, R.; C.P. Rinsland, C.B. Farmer, J. Namkung, R.H. Norton, and J.M. Russel III, *"Concentrations of Carbonyl Sulfide and Hydrogen Cyanide in the free upper troposphere and lower stratosphere deduced fromATMOS/Spacelab3 infrared solar occultation spectra"*, J. Geophys. Res., **93**(D2), 1669–1678, 1988.

Zander, R.; C.P. Rinsland, C.B. Farmer, J. Namkung, R.H. Norton, and J.M. Russell-III, *"Concentrations of carbonyl sulfide and hydrogen cyanide in the free upper troposphere and lower stratosphere deduced from ATMOS/Spacelab 3 infrared solar occultation spectra"*, J. Geophys. Res., **93**, 1663–1678, 1988.

Zander, R.; W.A. Matthews, J.P. Pommereau, and N. Iwagami, *"Measurements of column abundances of NO_2 from the ground during the GLOBUSNOx campaign"*, Workshop on Tropospheric Ozone and Quadrennial Ozone Symposium, Abstracts, 159, 1988.

Zander, R. and P. Demoulin,*"Spectroscopic evidence for the presence of the ν_4 Q-branch of chlorine nitrate ($ClONO_2$) in groundbased infrared solar spectra"*, J. Atmos. Chem., **6**, 191–200, 1988.

Zander, R.; P. Demoulin, D.H. Ehhalt, U. Schmidt, and C.P. Rinsland,*"Secular increase in the total vertical column abundance of carbon monoxide above central Europe since 1950"*, J. Geophys. Res., **94**, 11021–11028, 1989.

Zander, R.; M.R. Gunson, J.C. Foster, C.P. Rinsland, and J. Namkung, *"Stratospheric $ClONO_2$, HCl, and HF concentration profiles derived from ATMOS Spacelab 3 observations: An update"*, J. Geophys. Res., **95**, 20519–20525, 1990.

Zander, R.; C.P. Rinsland, D.H. Ehhalt, J. Rudolph, and P. Demoulin,*"Vertical column abundances and seasonal cycle of acetylene, C_2H_2, above the Jungfraujoch station, derived from IR solar observations*, J. Atmos. Chem., **13**, 359–372, 1991.

Zander, R.; C.P. Rinsland, and P. Demoulin, *"Infrared spectroscopic measurements of the vertical column abundance of sulfur hexafluoride, SF_6, from the ground"*, J. Geophys. Res., **96**, 15447–15454, 1991.

Zander, R.; M.R. Gunson, C.B. Farmer, C.P. Rinsland, F.W. Irion, and E. Mahieu, *"The 1985 chlorine and fluorine inventories in the stratosphere based on ATMOS observations at 30^o north latitudes"*, J. Atmos. Chem., **15**, 171–186, 1992.

Zander, R.; E. Mahieu, and P. Demoulin, *"Monitoring of stratospheric changes at the Jungfraujoch station by high-resolution IR solar observations in support of the Network for Detection of Stratospheric Change (NDSC)"*, in Proceedings of the colloquium "The Role of the Stratosphere in Global Change", Carqueiranne, France, September 14-25, 1992, NATO ASI Series, Vol. I 8, pp. 347-363, M.-L. Chanin Ed., Springer-Verlag Berlin Heidelberg, 1993.

Zander, R.; C.P. Rinsland, E. Mahieu, M.R. Gunson, C.B. Farmer, M.C. Abrams, and M.K.W. Ko, *"Increase of carbonyl fluoride (COF2) in the stratosphere and its contribution to the 1992 budget of inorganic fluorine in the upper stratosphere"*, J. Geophys. Res., **99**, 16737–16743, 1994.

Zander, R.; D.H. Ehhalt, C.P. Rinsland, U. Schmidt, E. Mahieu, J. Rudolph, P. Demoulin, G. Roland, L. Delbouille, and A.J. Sauval,*"Secular trend and seasonal variability of the column abundance of N_2O above the Jungfraujoch station determined from IR solar spectra"*, J. Geophys. Res. **99**, 16745–16756, 1994.

Zander, R.; E. Mahieu, P. Demoulin, C.P. Rinsland, D.K. Weisenstein, M.K.W. Ko, N.D. Sze, and M.R. Gunson, *"Secular Evolution of the Vertical Column Abundances of CHClF2 (HCFC-22) in the Earth's Atmosphere Inferred from Ground-Based IR Solar Observations at the Jungfraujoch and at Kitt Peak, and Comparison with Model Calculations"*, J. Atmos. Chem., **18**, 129–148, 1994.

Zander, R.; E. Mahieu, P. Demoulin, C.P. Rinsland, D.K. Weisenstein, M.K.W. Ko, N. D. Sze, and M.R. Gunson, *"Secular evolution of the vertical column abundances of CHClF2 (HCFC-22) in the Earth's atmosphere inferred from ground-based IR solar observations at the Jungfraujoch and at Kitt Peak, and comparison with model calculations"*, J. Atmos. Chem., **18**, 129–148, 1994.

Zander, R.; E. Mahieu, M.R. Gunson, M.C. Abrams, A. Y. Chang, M. Abbas, C. Aellig, A. Engel, A. Goldman, F.W. Irion, N. Kämpfer, H.A. Michelsen, M. J. Newchurch, C.P. Rinsland, R.J. Salawitch, G.P. Stiller, and G.C. Toon, *"The 1994 northern midlatitude budget of stratospheric chlorine derived from ATMOS/ATLAS-3 observations"*, Geophys. Res. Lett., **23**, 2357–2360, 1996.

Zander, R.; S. Solomon, E. Mahieu, A. Goldman, C.P. Rinsland, M.R. Gunson, M.C. Abrams, A.Y. Chang, R.J. Salawitch, H.A. Michelsen, M.J. Newchurch, and G.P. Stiller, *"Increase of stratospheric carbon tetrafluoride (CF4) based on ATMOS observations from space"*, Geophys. Res. Lett., **23**, 2353–2356, 1996.

Zander, R.; P. Demoulin, E. Mahieu, G. Roland, L. Delbouille, and C. Servais, *"Total Vertical Column Abundances of Atmospheric Gases Derived from IR Remote Solar Observations made at the Jungfraujoch Station"*, in A Transport and Chemical Transformation of pollutants in the Troposphere@, Vol. 6 - Tropospheric Ozone Research, Istein Hov Ed., Springer-Verlag, Berlin Heidelberg New York, 413–425, 1997.

Zander, R.; P. Demoulin, E. Mahieu, L. Delbouille, G. Roland, F. Mélen, C. Servais, M.De Mazière, and M.van Roozendael, *"An overview of NDSC-related activities at the Jungfraujoch through high-resolution infrared solar observations"*, in Proceedings of the XXVIII Quadrennial Ozone Symposium, L'Aquila, Italy, September 12-21, 1996. R. Bojkov and G. Visconti (Eds): 1005–1008, 1998.

Zander, R.; E. Mahieu, P. Demoulin, C. Servais, F. Mélen, G. Roland, and L. Delbouille, *"Spectrometric Solar Observations at the Jungfraujoch for Long-term Atmospheric Monitoring"*, Actes du Colloque "Ozone dans la Troposphère: la Recherche et la Politique", Bruxelles, 26 June 1998. SSTC-D/1999/1191/3 : 69–76, 1999.

Zander, R.; P.M. Midgley, and M.J. Kurylo, *"The NDSC in support of satellite data validation and calibration"*, in Proceedings of the ESA "European Symposium on Atmospheric Measurements from Space", ESTEC-Nordwijk, The Netherlands, January 18-22, 1999. WPP-161, Vol. **2**, 649–654, 1999.

Zander, R.; *"Experimental Studies of Atmospheric Changes and Contribution to the Study of the Earth's Atmosphere from Space (ATMOS)"*, Scientific Report Nr 2 to the OSTC Research Contract Nr. CG/DD/01D, 1–11, 1999.

Zander, R.; E. Mahieu, F. Mélen, and J. Elkins, *"An evaluation of the northern midlatitude tropopause heightening, based on N2O column abundance measurements above the Jungfraujoch"*, in Proceedings of the Fifth European Symposium on Stratospheric Ozone, St. Jean de Luz, France, September 27 - October 1, 1999. N. R. P. Harris, M. Guirlet and G. T. Amanatidis (Eds): 135–138, 2000.

Zander, R.; E. Mahieu, P. Demoulin, C. Servais, and F. Mélen, *"Long-term evolution of the loading of CH4, N2O, CO, CCl2F2, CHClF2 and SF6 above Central Europe during the last 15 years"*, in Proceedings of the Second International Symposium on Non-CO2 Greenhouse Gases - Scientific Understanding, Control and Implementation, Noordwijkerhout, The Netherlands, September 8-10, 1999. Sp. Vol. Environmental Monitoring and Assessment, 2000. Kluwer Academic Publishers: 211–216, 2000.

Zhao, Y.; Y. Kondo, F.J. Murcray, X. Liu, M. Koike, K. Kita, H. Nakajima, I. Murata, and K. Suzuki, *"Carbon monoxide column abundances and tropospheric concentrations retrieved from high resolution ground-based infrared solar spectra at 43.5^{o}N over Japan"*, J. Geophys. Res., **102**, 23403–23411, 1997.

Zhao, Y.; Y. Kondo, X. Liu, *"Carbon monoxide column abundance and tropospheric concentration retrieved from high resolution ground-based infrared solar spectra at 43.5^{o}N over Japan"*, J. Geophys. Res., **102**, 23403–23411, 1997.

Zhao, Y.; Y. Kondo, X. Liu, M. Koike, H.Nakajima, I. Murata, F.J. Murcray, and K. Suzuki, Proc. Quadren. Ozone Symp. 1996, *"Spectroscopic measurements of carbon monoxide at 34.5^{o}N and 43.5^{o}N in Japan"*, 643–646, 1998.

Zhao, Y.; Y. Kondo, F.J. Murcray, X. Liu, M. Koike, H. Irie, K. Strong, K. Suzuki, M Sera, and Y. Ikegami, *"Seasonal variations of HCN over northern Japan measured by ground-based infrared solar spectroscopy"*, Geophys. Res. Lett., **27**, 2085–2088, 2000.

Zhao, Y.; Y. Kondo, F.J. Murcray, X. Liu, M. Koike, H. Irie, K. Suzuki, M. Sera, and Y. Ikegami, *"Seasonal variations of HCN over northern Japan measured by ground-based infrared solar spectroscopy"*, Geophys. Res. Lett., **27**, 2085–2088, 2000.

Zhao, Y.; K. Strong, Y. Kondo, M. Koike, Y. Matsumi, H. Irie, C.P. Rinsland, N.B. Jones, K. Suzuki, H. Nakajima, H. Nakane, and I. Murata, *"Spectroscopic Measurements of Tropospheric CO, C2H6, C2H2, and HCN in Northern Japan"*, J. Geophys. Res., **107**(D18), 4343, doi: 10.1029/2001JD000748, 2002.

Zirin, H.; *"Astrophysics of the Sun"*, Cambridge Univ. Press, 1988.

Zou, Q. and P. Varanasi, *"Laboratory Measurement of the Spectroscopic Line Parameters of Water Vapor in the 610 - 2100 and 3000 - 4500 cm^{-1} Regions at Lower-Tropospheric Temperatures"*, HITRAN Special Issue, J. Quant. Spectrosc. Radiat. Transfer, **82**, numbers 1-4, 2003.

The electronic supplement[1]

The DVD-ROM contains the following data and software products:

- Simulated spectra from 500 to $4370 cm^{-1}$ at $257.14 cm$ OPD for the following 47 molecules: $BrNO_2$, CCl_2F_2, CCl_3F, CCl_4, CF_4, $CFC11_3$, CH_3Cl, CHF_2Cl, ClO, $ClONO_2$, $COCl_2$, $F142B$, H_2O_2, HO_2NO_2, O_2, $SF6$, C_2H_2, C_2H_4, C_2H6, CH_4, CO, CO_2, $COClF$, COF_2, H_2CO, H_2O, H_2S, HBr, HCl, HCN, $HCOOH$, HDO, HF, HI, HNO_3, HO_2, $HOCl$, N_2, N_2O, N_2O_5, NH_3, NO, NO_2, O_3, OCS, OH, and SO_2.
- Simulated spectra from 3950 to $9000 cm^{-1}$ at $120.0 cm$ OPD for the following 18 molecules: $CH4$, CO, CO_2, H_2O, H_2S, HBr, HCl, HDO, HF, HI, N_2O, NH_3, NO, NO_2, O_2, O_3, OCS, OH, SO_2.
- Simulated spectra for all isotopic forms of the molecules listed above.
- One spectrum each representing the sum of all single-molecule simulations for the 2 spectral intervals.
- Simulated spectra of CCl4, F134A, PAN, Acetone, C3H8, CCl2F2, CFC-113, and CH3COOH based on cross-sectional data.
- One set of full-resolution observed ground-based solar FTIR spectra from Kiruna.
- Observed and simulated spectra showing solar absorptions of non-terrestrial origin.
- Illustration of the effect of 14 different apodisation functions on a sharp ozone line.
- The OPUS-IR^{TM} free spectra viewer for Windows operating systems from *Bruker Optik GmbH*.
- The spectroscopic linelists used in SFIT format (HITRAN 2000 and supplements[2])
- The a-priori VMR profiles & model atmosphere used in the simulations and in the example retrievals.
- Executables of all specialised software used in the preparation of the atlas[2].
- The source code of selected software products[2].
- All spectra, observed and simulated, are provided in both the Bruker OPUS-IR^{TM} and the Bomem GRAMS^{TM} data formats.

[1] Please refer to the back cover whether you obtained a copy of the atlas with or without electronic supplement. Additional copies of the electronic supplement are available from the main author. See page 1 for contact details.

[2] Restrictions apply for some contents due to 3rd party consent requirement - please contact the main author for conditions and details of obtaining a decryption key.

☐ black and white edition.
☒ colour edition.
☒ does not contain the electronic supplement.
☐ contains the electronic supplement (1 DVD).

IRF Technical Report 048, April 2004, ISSN 0284-1738 (colour)